

तमसो मा ज्योतिर्गमय

VISVA BHARATI
LIBRARY
SANTINIKETAN

506

P.N.I.S.I

v. 20, 1954

189291

PROCEEDINGS
OF THE
NATIONAL INSTITUTE OF SCIENCES OF INDIA

VOL. XX
1954

NATIONAL INSTITUTE OF SCIENCES OF INDIA
NEW DELHI

INDEX
VOL. XX
1954

INDEX

	PAGE		PAGE
Absorption spectrum of BiBr (Sur and Majumdar) ..	235	Atmospheric oscillations at high altitudes and their relation to geomagnetic field variations (Pratap) ..	252
Absorption spectrum of 3-Chloro-Thionaphthene (Sreeramamurty and Haranath) ..	318	Atrioventricular conducting (connecting) system of the heart of human twins obtained from an aborted foetus. Observations (Prakash) ..	645
A.C. 'Silent' discharges. Origin of R.F. Oscillations (Khastgir and Srivastava) ..	290	Auxin content of the vernalised seed. Studies on the physiology of rice. (Sircar and Das)	673
African migratory locust. Its egg-wall (Roonwal) ..	361	Bacteria. The rôle of bacteria on the growth and viability of <i>Entamoeba histolytica</i> (Mukherjea) ..	660
Aggarwal, S. P.—Relation between maximum pressure and shot-start pressure ..	307	Bacteriology of inshore sea water and of mackerels off Telli-cherry, Malabar (Venkataraman and Sreenivasan) ..	651
Algal genera <i>Neomeris</i> and <i>Aci-cularia</i> from the Niniyur (Danian) beds of the Trichinopoly area (Varma) ..	298	Bambah, R. P.—Lattice coverings by spheres ..	25
Alkaline phosphatase and periodic acid-schiff reactions in the thymus of <i>Calotes versicolor</i> (Daud.) (Rao) ..	503	Bambah, R. P.—Polar reciprocal convex domains ..	119
Alkaline phosphatase in the vaginal smear of the rat during estrus cycle. Distribution and concentration. Effect of ovariectomy and replacement therapy (Roy, Kar and Karkun) ..	170	Bambah, R. P.—Polar reciprocal convex domains (addendum)	324
Aluminium molybdate and thorium arsenate gels: Intensity measurements. Light scattering from gel-forming systems during and after setting (Desai and Sundaram) ..	598	Band spectrum of Cl_2^+ . Emission band spectrum of Cl_2^+ (Rao) ..	70
Angelescus polynomials (Singh)	280	Banerjee, B. K.—Study of metal film on glass surface ..	241
Appell set of polynomials (Singh)	341	Banerjee, B. K.—Study on the state of dispersoid in the colloidal coloured glass ..	19
Argon-Neon mixture. Thermal conductivity (Srivastava and Madan) ..	587	Banerjee, T.—see Jacob, K. and Banerjee, T.	
<i>Ariophanta maderaspatana</i> . Studies on the reproductive tract (Gray) (Mollusca: Pulmonata). Histochemistry of the ammatatorial organ (Iyengar)	683	Bessel functions. Some infinite integrals involving Bessel functions (Rathie) ..	62
		BF_3 molecule. Force constants for BF_3 molecule (Santhamma) ..	245

	PAGE		PAGE
BiBr. Absorption spectrum (Sur and Majumdar) ..	235	multiple Compton scattering (Sen)	530
Biology of the grey mullet, <i>Mugil tade</i> Forskål, with notes on its fishery in Bengal (Pillay) ..	187	Convex domains. Polar reci- procal Convex domains (Bambah) ..	119; 324
Buch, K. P. and Sundaram, V.— Light scattering from gel- forming systems during and after setting. Sodium stear- ate in octyl alcohol and sodium stearate in decyl alcohol: Depolarization measurements	609	Crab. Some aspects of relative growth in the blue swimming crab <i>Neptunus pelagicus</i> (Linnaeus) (Prasad and Tampi)	218
Burman, U. R.—Existence of hydrogen atmospheres in red giant stars	620	Cytochemistry of hormone action	170; 428
<i>Calotes versicolor</i> . Alkaline phosphatase and periodic acid- schiff reactions in the thymus of <i>Calotes versicolor</i> (Daud.) (Rao)	503	D'Alembert's paradox and its resolution. A theory of resistance in potential flows (Ghosh)	74
Cantor Bendixon theorem. A generalization (Padmavally)	305	Das, T. M.—see Sircar, S. M. and Das, T. M.	
<i>Carchesium spectabile</i> . Nuclear apparatus (Dass) ..	174	Dass, C. M. S.—see Seshachar, B. R. and Dass, C. M. S.	
<i>Carcinus maenas</i> . Tyrosinase activity in relation to pheno- lic tanning of the cuticle in <i>Carcinus maenas</i> (Krishnan)	157	Dass, C. M. S.—Studies on the nuclear apparatus of peritri- chous ciliates. Nuclear appa- ratus of <i>Epistylis</i> sp. ..	703
Chaudhuri, R. N. —see Mukher- jee, K. L., Chaudhuri, R. N. and Werner, G.		Dass, C. M. S.—Studies on the nuclear apparatus of peritri- chous ciliates. The nuclear apparatus of <i>Carchesium</i> <i>spectabile</i> Ehrbg. ..	174
Chloro-thionaphthene. Absorp- tion spectrum of 3-Chloro- thionaphthene (Sreerama- murty and Haranath) ..	318	Desoxyribonucleic acid (DNA) synthesis in regenerating macronucleus of <i>Epistylis</i> <i>articulata</i> From. Photo- metric study (Seshachar and Dass)	656
Ciliates. Studies on the nuclear apparatus of peritrichous ciliates. The nuclear appa- ratus of <i>Epistylis</i> sp. (Dass) ..	703	Dissipation in potential motion. A theory of resistance in po- tential flows (Ghosh) ..	84
Closed wakes in two dimensions. A theory of resistance in potential flows (Ghosh) ..	88	Distribution and concentra- tion of alkaline phosphatase in the vaginal smear of the rat during estrus cycle: The effect of ovariectomy and re- placement therapy. Cyto- chemistry of hormone action. (Roy, Kar and Karkun) ..	170
Compton scattering. Radiation damping in Compton scattering (Roy) ..	524	Dependence of erosion ratio and rate of burning on position and time in a rocket motor (Gupta and Sodha) ..	634
Compton scattering in stellar atmospheres containing free- electrons. On the problem of softening of radiation by			

PAGE	PAGE
Desai, R. L. and Sundaram, V.— Light scattering from gel- forming systems during and after setting. Aluminium molybdate and thorium arsen- ate gels: Intensity measure- ments 598	Equilibrium phenomena: Activity coefficients (Dutta and Sengupta) 1
Detonation of condensed ex- plosives. An equation of state (Murgai) 548	E.M. radiation on the self- energy of free-electrons. Effect (Singh) 557
Dutta, M. and Sengupta, M.— A theory of strong electrolytes in solution based on a new statistics. Equilibrium phe- nomena: Activity coefficients 1	Embryological studies in mal- vaceae. Development of gametophytes (Rao) .. 127
Ecology of a brackishwater <i>bheri</i> with special reference to the fish-cultural practices and the biotic interaction (Pillay) .. 399	Embryological studies in meni- spermaceae. <i>Tiliacora race- mosa</i> Coleb. (Sastri) .. 494
Effect of adrenocorticotrophic hormone (ACTH) on alkaline phosphatase activity in the pars intermedia of the cat's hypophysis. Cytochemistry of hormone action. (Karkun and Kar) 428	Emission band spectrum of Cl_2^+ (Rao) 70
Effect of E. M. radiation on the self-energy of free-electrons (Singh) 557	<i>Entamoeba histolytica</i> . Rôle of bacteria on the growth and viability of <i>Entamoeba histo- lytica</i> (Mukherjea) .. 660
Effect of varying water levels on growth of rice in relation to nitrogen absorption. Studies on the physiology of rice (Ghosh) 371	<i>Entamoeba histolytica</i> . Rôle of culture medium and its con- stituents on the growth and viability of <i>Entamoeba histo- lytica</i> (Mukherjea) .. 437
Effect of vorticity on the specific heat ratio of a non-relativistic Fermi-Dirac gas (Vardya) .. 570	<i>Epistylis articulata</i> . Photo- metric study of desoxyribo- nucleic acid (DNA) synthesis in regenerating macronucleus of <i>Epistylis articulata</i> From. (Seshachar and Dass) .. 656
Eggs of the desert locust. Size, sculpturing, weight and mois- ture content of the developing eggs of the desert locust (Roonwal) 388	<i>Epistylis</i> sp. Nuclear appar- atus of <i>Epistylis</i> sp. Studies on the nuclear apparatus of peritrichous ciliates (Dass) 703
Egg-wall of the African migra- tory locust, <i>Locusta migratoria migratorioides</i> Reich. and Frm. (Roonwal) 361	Equation of state for the detona- tion of condensed explosives (Murgai) 548
Electrolytes. A theory of strong electrolytes in solution based on a new statistics.	Equilibrium phenomena: Acti- vity coefficients. A theory of strong electrolytes in solution based on a new statistics (Dutta and Sengupta) .. 1
	Erosion ratio and rate of burning and time in a rocket motor. Dependence (Gupta and Sodha) 634
	<i>Euphorbia hirta</i> Linn. Fertiliza- tion and the development of embryo and seed in <i>Euphorbia hirta</i> Linn. (Kajale) .. 35

	PAGE		PAGE
Existence of hydrogen atmospheres in red giant stars (Burman)	620	Free-electrons. Problem of softening of radiation by multiple Compton scattering in stellar atmospheres containing free-electrons (Sen) ..	530
Explosive charges. Target damages by explosive charges with lined conical cavities (Singh)	274	Gametophytes. Development. Embryological studies in malvaceae. (Rao)	127
Explosives. An equation of state for the detonation of condensed explosives (Murgai)	548	Gas. Effect of vorticity on the specific heat ratio of a non-relativistic Fermi-Dirac gas (Vardya)	570
Fermi-Dirac gas. Effect of vorticity on the specific heat ratio of a non-relativistic Fermi-Dirac gas (Vardya) ..	570	Gels. Aluminium molybdate and thorium arsenate gels: Intensity measurements (Desai and Sundaram) ..	598
Fertilization and the development of embryo and seed in <i>Euphorbia hirta</i> Linn. (Kajale)	353	Generalization of Cantor Bendixon theorem (Padmavally)	305
Fish. Bacteriology of inshore sea water and of mackerels off Tellicherry, Malabar (Venkataraman and Sreenivasan)	651	Generating function in partition theory (Gupta)	582
Fish. Biology of the grey mullet, <i>Mugil tade</i> Forskål, with notes on its fishery in Bengal (Pillay)	187	Geomagnetic field variations. Atmospheric oscillations at high altitudes and their relation (Pratap)	252
Fish. Ecology of a brackish-water <i>bheri</i> with special reference to the fish-cultural practices and the biotic interaction (Pillay)	399	Ghosh, B. N.—Studies on the physiology of rice. Effect of varying water levels on the growth of rice in relation to nitrogen absorption ..	371
Fish-cultural practices. Ecology of a brackishwater <i>bheri</i> with special references to the fish-cultural practices and the biotic interactions (Pillay) ..	399	Ghosh, B. N.—see Sircar, S. M. and Ghosh, B. N.	
Fish geography of the Himalayas (Menon)	467	Ghosh, K. M.—Karman's spectrum function of isotropic turbulence	336
Fishery in Bengal. Biology of the grey mullet, <i>Mugil tade</i> Forskål, with notes on its Fishery in Bengal (Pillay) ..	187	Ghosh, N. L.—Theory of resistance of potential flows ..	74
Force constants for 1, 3, 5 trimethyl benzene (Santhamma)	576	Ghosh, N. N.—Matrix treatment of four-dimensional rotation in hyperspace	542
Force constants for the BF ₃ molecule (Santhamma) ..	245	Glass surface. Metal film on glass surface (Banerjee) ..	241
Free-electrons. Effect of E.M. radiation on the self-energy of free-electrons (Singh) ..	557	<i>Glossopteris</i> fronds in the North-East Frontier tracts. Occurrence (Jacob and Banerjee) ..	53
		Gondwanas of North-Eastern India. A brief review (Jacob and Banerjee)	53
		Grey mullet, <i>Mugil tade</i> Forskål. Its biology with notes on its fishery in Bengal (Pillay) ..	187

	PAGE		PAGE
Gupta, H.—Generating function in partition theory ..	582	Integrals Some infinite integrals involving Bessel functions (Rathie) ..	62
Gupta, S. K. and Mehta, A. K.—Variation of pressure with time in rocket chamber ..	563	Irreducible representations of the Lie-Algebra of the orthogonal group with spin 3/2 • (Venkatachaliengar and Rao)	509
Gupta, S. K. and Sodha, M. S.—Dependence erosion ratio and rate of burning on position and time in a rocket motor ..	634	Isotropic turbulence. Karman's spectrum function (Ghosh) ..	336
Haranath, P. B. V.—see Sreeramamurthy, K. and Haranath, P. B. V.		Iron ores. Ore microscope studies of the vanadium-bearing titaniferous iron ores of Mayurbhanj with a detailed note on their texture (Roy) ..	691
Heart of human twins obtained from an aborted foetus. Observations on the atrioventricular conducting (connecting) system (Prakash) ..	645	Iyengar, V. K. S.—Reproductive tract of <i>Ariophanta maderaspatana</i> (Gray) (Mollusca: Pulmonata). Part I. Histochemistry of the ammatorial organ ..	683
Himalayas. Fish geography of the Himalayas (Menon) ..	467	Jacob, K. and Banerjee, T.—Occurrence of <i>Glossopteris</i> fronds in the North-East Frontier tracts, with a brief review of the Gondwanas of North-Eastern India ..	53
Histochemistry of the ammatorial organ. Studies on the reproductive tract of <i>Ariophanta maderaspatana</i> (Gray) (Mollusca: Pulmonata). Part I (Iyengar) ..	683	Jacob, K. and Narayanaswami, S.—Structural and drainage patterns of the Western Ghats in the vicinity of the Palghat Gap ..	104
Hormone action. Effect of adrenocorticotrophic hormone (ACTH) on alkaline phosphatase activity in the pars intermedia of the cat's hypophysis. Studies on cytochemistry of hormone action (Karkun and Kar) ..	428	Kajale, L. B.—Fertilization and the development of embryo and seed in <i>Euphorbia hirta</i> Linn. ..	353
Hormone action. Studies in the distribution and concentration of alkaline phosphatase in the vaginal smear of the rat during estrus cycle. The effect of ovariectomy and replacement therapy (Roy, Kar and Karkun) ..	170	Kar, A. B.—see Karkun, J. N. and Kar, A. B.	
Hydrogen atmospheres. Existence of hydrogen atmospheres in red giant stars (Burman) ..	620	Kar, A. B.—see Roy, S. K., Kar, A. B. and Karkun, J. N.	
Instability of non-radial oscillations of centrally condensed stars (Khare) ..	326	Karkun, J. N.—see Roy, S. K., Kar, A. B. and Karkun, J. N.	
		Karkun, J. N. and Kar, A. B.—Cytochemistry of hormone action. Effect of adrenocorticotrophic hormone (ACTH) on alkaline phosphatase activity in the pars intermedia of the cat's hypophysis ..	428

	PAGE		PAGE
Karman's spectrum function of isotropic turbulence (Ghosh)	336	development of gametophytes (Rao)	127
Khare, R. C.—Instability of non-radial oscillations of centrally condensed stars	326	Matrix treatment of four-dimensional rotation in hyperspace (Ghosh)	542
Khastgir, S. R. and Srivastava, C. M.—Origin of R.F. oscillations in A.C. 'Silent' discharges	290	Mayurbhanj. Ore microscopic studies of the vanadium-bearing titaniferous iron ores of Mayurbhanj with a detailed note on their texture (Roy)	691
Krishnan, G.—Tyrosinase activity in relation to phenolic tanning of the cuticle in <i>Carcinus maenas</i>	157	Mehta, A. K.—see Gupta, S. K.	
Lattice coverings by spheres (Bambah)	25	Menispermaceae. Embryological studies. <i>Tiliacora racemosa</i> Coleb. (Sastri)	494
Laud, B. B.—see Tawde, N. R. and Laud, B. B.		Menon, A. G. K.—Fish geography of the Himalayas	467
Lie-Algebra of the orthogonal group with spin 3/2. The irreducible representations (Venkatachaliengar and Rao)	509	Metal film on glass surface (Banerjee)	241
Locust. Size, sculpturing, weight and moisture content of the developing eggs of the desert locust (Roonwal)	388	<i>Mugil tade</i> Forskål. Biology of the grey mullet, <i>Mugil tade</i> Forskål (Pillay)	187
<i>Locusta migratoria migratorioides</i> Reich. Frm. (Orthoptera: Acrididae). Egg-wall of the African migratory locust (Roonwal)	361	Mukherjea, A. K.—Rôle of bacteria on the growth and viability of <i>Entamoeba histolytica</i>	660
Mackerels. Bacteriology of inshore sea water and of mackerels off Tellicherry, Malabar (Venkataraman and Sreenivasan)	651	Mukherjea, A. K.—Rôle of culture medium and its constituents on the growth and viability of <i>Entamoeba histolytica</i>	437
Madan, M. P.—see B. N. Srivastava and Madan, M. P.		Mukherjee, K. L., Chaudhuri, R. N. and Werner, G.—Plasma volume and thiocyanate space in nutritional oedema	151
Magnetographs and instantaneous values from recordings (Malurkar)	567	Murgai, M. P.—Equation of state for the detonation of condensed explosives	548
Majumdar, K.—see Sur, P. K. and Majumdar, K.		Narayanaswami, S.—see Jacob, K. and Narayanaswami, S.	
Malurkar, S. L.—Transients of magnetographs and instantaneous values from recordings	567	<i>Neomeris</i> and <i>Acicularia</i> .—Algal genera <i>Neomeris</i> and <i>Acicularia</i> from the Niniyur (Danian) beds of the Trichinopoly area (Varma)	298
Malvaceae. Embryological studies in malvaceae. I. De-		<i>Neptunus pelagicus</i> . Some aspects of relative growth in the blue swimming crab <i>Neptunus pelagicus</i> (Linnaeus) (Prasad and Tampi)	218

	PAGE		PAGE
Niniyur (Danian) beds of the Trichinopoly area. Algal genera <i>Neomeris</i> and <i>Acicularia</i> from the Niniyur beds (Varma) ..	298	Palghat Gap. Structural and drainage patterns of the Western Ghats in the vicinity of the Palghat Gap (Jacob and Narayanaswami) ..	104
North-East Frontier tracts. Occurrence of <i>Glossopteris</i> fronds (Jacob and Banerjee) ..	53	Partition theory. Generating function (Gupta) ..	582
Nuclear apparatus of peritrichous ciliates. Nuclear apparatus of <i>Carchesium spectabile</i> (Dass) ..	174	<i>Passiflora foetida</i> Linn. Pollination mechanism (Raju) ..	431
Nuclear apparatus of peritrichous ciliates. Nuclear apparatus of <i>Epistylis</i> sp. (Dass) ..	703	Pati, T.—Products of summability methods ..	348
Nutritional oedema. Plasma volume and thiocyanate space in nutritional oedema (Mukherjee, Chaudhuri and Werner) ..	151	Peierls, R. E.—Vibration spectrum of a crystal ..	121
Observations on the atrioventricular conducting (connecting) system of the heart of human twins obtained from an aborted foetus (Prakash) ..	645	Peritrichous ciliates. Nuclear apparatus (Dass) ..	174
Occurrence of <i>Glossopteris</i> fronds in the North-East Frontier tracts, with a brief review of the Gondwanas of North-Eastern India (Jacob and Banerjee) ..	53	Photometric study of desoxyribonucleic acid (DNA) synthesis in regenerating macronucleus of <i>Epistylis articulata</i> From. (Seshachar and Dass) ..	656
Origin of R. F. oscillations in A.C. 'Silent' discharges (Khastgir and Srivastava) ..	290	Physiology of rice. Effect of varying water levels on growth of rice in relation to nitrogen absorption (Ghosh) ..	371
Ore microscopic studies of the vanadium-bearing titaniferous iron ores of Mayurbhanj with a detailed note on their texture (Roy) ..	691	Physiology of rice. Studies. Auxin content of the vernalised seed (Sircar and Das) ..	673
Orthogonal group with spin $3/2$. The irreducible representations of the Lie-Algebra (Venkatachaliengar and Rao) ..	509	Physiology of rice. Effects of low and high temperature germination with or without short days on summer and winter varieties (Sircar and Ghosh) ..	452
Oscillations of centrally condensed stars. Instability of non-radial oscillations (Khare) ..	326	Pillay, T. V. R.—Biology of the grey mullet, <i>Mugil tade</i> Forskål, with notes on its fishery in Bengal ..	187
Padmavally, K.—Generalization of Cantor Bendixon theorem ..	305	Pillay, T. V. R.—Ecology of a brackishwater <i>bheri</i> with special reference to the fish-cultural practices and the biotic interaction ..	399
		Plasma volume and thiocyanate space in nutritional oedema (Mukherjee, Chaudhuri and Werner) ..	151
		Polar reciprocal convex domains (Bambah) ..	119; 324

	PAGE		PAGE
Pollination mechanism in <i>Passiflora foetida</i> Linn. (Raju) ..	431	Rao, C. Venkata.—Embryological studies in malvaceae. I. Development of gametophytes ..	127
Polynomials. Appell set (Singh) ..	341	Rao, P. Tiruvenganna.—Emission band spectrum of Cl_2^+ ..	70
Polynomials. Angelescus polynomials (Singh) ..	280	Rathie, C. B.—Some infinite integrals involving Bessel functions ..	62
Prakash, R.—Observations on the atrioventricular conducting (connecting) system of the heart of human twins obtained from an aborted foetus ..	645	Relation between maximum pressure and shot-start pressure (Aggarwal) ..	307
Pramanik, S. K. and Ramakrishnan, K. P.—Is salt in Sambhar lake wind-borne from the Rann of Cutch and the Arabian Sea? ..	265	Resistance and dissipation in motions with closed wakes. A theory of resistance in potential flows (Ghosh) ..	99
Prasad, R. R. and Tampi, P. R. S.—Some aspects of relative growth in the blue swimming crab <i>Neptunus pelagicus</i> (Linnaeus) ..	218	Resistance in potential flows. A theory (Ghosh) ..	74
Pratap, R.—Atmospheric oscillations at high altitudes and their relation to geomagnetic field variations ..	252	R. F. oscillations in A.C. 'Silent' discharges. Origin. (Khastgir and Srivastava) ..	290
Pressure. Relation between maximum pressure and shot-start pressure (Aggarwal) ..	307	Raju, M. V. S.—Pollination mechanism in <i>Passiflora foetida</i> Linn. ..	431
Problem of softening of radiation by multiple Compton scattering in stellar atmospheres containing free-electrons (Sen) ..	530	Ramakrishnan, K. P.—see Pramanik, S. K. and Ramakrishnan, K. P.	
Problem of transfer of radiation in a spherically symmetrical stellar atmosphere for the non-conservative case (Sen) ..	12	Rao, K. N. Srinivasa.—see Venkatachaliengar, K.	
Products of summability methods (Pati) ..	348	Rao, M. Appaswamy.—Alkaline phosphatase and periodic acid-schiff reactions in the thymus of <i>Calotes versicolor</i> (Daud.) ..	503
Radiation. Problem of transfer of radiation in a spherically symmetrical stellar atmosphere for the non-conservative case (Sen) ..	12	Rice. Studies on the physiology of rice. Auxin content of the vernalised seed (Sircar and Das) ..	673
Radiation by multiple Compton scattering in stellar atmospheres containing free-electrons. Problem of softening (Sen) ..	530	Rice. Studies on the physiology of rice. Effects of low and high temperature germination with or without short days on summer and winter varieties (Sircar and Ghosh) ..	452
Radiation damping in Compton scattering (Roy) ..	524	Rice. Studies on the physiology of rice. Effect of varying water levels on growth of rice in relation to nitrogen absorption (Ghosh) ..	371
		Rocket chamber. Variation of pressure in rocket chamber (Gupta and Mehta) ..	563

	PAGE		PAGE
Rocket motor. Dependence of erosion ratio and rate of burning on position and time in a rocket motor (Gupta and Sodha)	634	Sambhar lake. Is salt in Sambhar lake wind-borne from the Rann of Cutch and the Arabian Sea? (Pramanik and Ramakrishnan)	265
Rôle of bacteria on the growth and viability of <i>Entamoeba histolytica</i> (Mukherjea)	660	Santhamma, V.—Force constants for 1, 3, 5 trimethyl benzene	576
Rôle of culture medium and its constituents on the growth and viability of <i>Entamoeba histolytica</i> (Mukherjea)	437	Santhamma, V.—Force constants for the BF_3 molecule	245
Roonwal, M. L.—Egg-wall of the African migratory locust, <i>Locusta migratoria migratorioides</i> Reich. and Frm. (Orthoptera: Acrididae)	361	Sastri, R. L. N.—Embryological studies in menispermaceae. I. <i>Tiliacora racemosa</i> Coleb.	494
Roonwal, M. L.—Size, sculpturing, weight and moisture content of the developing eggs of the desert locust, <i>Schistocerca gregaria</i> (Forskål) (Orthoptera: Acrididae)	388	<i>Schistocerca gregaria</i> (Forskål) (Orthoptera: Acrididae). Size, sculpturing, weight and moisture content of the developing eggs of the desert locust (Roonwal)	388
Rotation in hyperspace. A matrix treatment of four-dimensional rotation in hyperspace (Ghosh)	542	Sen, K. K.—Problem of softening of radiation by multiple Compton scattering in stellar atmospheres containing free-electrons	530
Roy, S.—Ore microscopic studies of the vanadium-bearing titaniferous iron ores of Mayurbhanj with a detailed note on their texture.	691	Sen, K. K.—Problem of transfer of radiation in a spherically symmetrical stellar atmosphere for the non-conservative case	12
Roy, S. K., Kar, A. B. and Karkun, J. N.—Studies on cytochemistry of hormone action. Studies in the distribution and concentration of alkaline phosphatase in the vaginal smear of the rat during estrus cycle: The effect of ovariectomy and replacement therapy	170	Sengupta, M.—see Dutta, M. and Sengupta, M.	
Roy, T. C.—Radiation damping in Compton scattering	524	Seshachar, B. R. and Dass, C. M. S.—Photometric study of desoxyribonucleic acid (DNA) synthesis in regenerating macronucleus of <i>Epistylis articulata</i> From.	656
Salt in Sambhar lake. Is it wind-borne from the Rann of Cutch and the Arabian Sea? (Pramanik and Ramakrishnan)	265	Singh, I.—Effect of E.M. radiation on the self-energy of free-electrons	557
		Singh, Sampooran.—Target damages by explosive charges with lined conical cavities	274
		Singh, Vikramaditya.—Angelescus polynomials	280
		Singh, Vikramaditya.—Appell set of polynomials	341
		Sircar, S. M. and Das, T. M.—Physiology of rice. Auxin content of the vernalised seed	673

	PAGE		PAGE
Sircar, S. M. and Ghosh, B. N.— Studies on the physiology of rice. Effects of low and high temperature germination with or without short days on sum- mer and winter varieties ..	452	Stars. Instability of non-radial oscillations of centrally con- densed stars (Khare) ..	326
Size, sculpturing, weight and moisture content of the developing eggs of the desert locust, <i>Schistocerca gregaria</i> (Forskål) (Orthoptera: Acridi- didae) (Roonwal) ..	388	State of dispersoid. Study on the state of dispersoid in the colloidal coloured glass (Banerjee) ..	19
Sodha, M. S.—see Gupta, S. K. and Sodha, M. S. ..		Structural and drainage patterns of the Western Ghats in the vicinity of the Palghat Gap (Jacob and Narayanaswami) ..	104
Sodium stearate on octyl alco- hol and sodium stearate in decyl alcohol: Depolarization measurements (Buch and Sundaram) ..	609	Studies on the reproductive tract of <i>Ariophanta maderas- patana</i> (Gray) (Mollusca Pul- monata). Part I. Histo- chemistry of the animatorial organ (Iyengar) ..	683
Softening of radiation by mul- tiple Compton scattering in stellar atmospheres (Sen) ..	530	Study on the state of dispersoid in the colloidal coloured glass (Banerjee) ..	19
Some aspects of relative growth in the blue swimming crab <i>Neptunus pelagicus</i> (Linnaeus) (Prasad and Tampi) ..	218	Summability methods. Pro- ducts (Pati) ..	348
Some infinite integrals involving Bessel functions (Rathie) ..	62	Sundaram, V.—see Buch, K. P. and Sundaram, V.	
Spectrum. Emission band spectrum of Cl_2^+ (Rao) ..	70	Sundaram, V.—see Desai, R. L. and Sundaram, V.	
Spectrum. Vibration spectrum of a crystal (Peierls) ..	121	Sur, P. K. and Majumdar, K.— Absorption spectrum of BiBr ..	235
Spectrum of BiBr (Sur and Majumdar) ..	235	Tampi, P. R. S.—see Prasad, R. R. and Tampi, P. R. S.	
Spheres. Lattice coverings by spheres (Bambah) ..	25	Target damages by explosive charges with lined conical cavities (Singh) ..	274
Sreenivasan, A.—see Venkata- raman, R. and Sreenivasan, A.		Tawde, N. R. and Laud, B. B.— Working of some theories of vibrational transition prob- abilities ..	259
Sreeramamurty, K. and Hara- nath, P. B. V.—Absorption spectrum of 3-chloro-thio- naphthene ..	318	Tellicherry, Malabar. Bacterio- logy of inshore sea water and of mackerels off Tellicherry, Malabar (Venkataraman and Sreenivasan) ..	651
Srivastava, C. M.—see Khastgir, S. R. and Srivastava, C. M.		Theories of vibrational transition probabilities. On the work- ing of some theories (Tawde and Laud) ..	259
Srivastava, B. N. and Madan, M. P.—Thermal conductivity of Argon-Neon mixture ..	587	Theory of resistance in potential flows (Ghosh) ..	74
Stars. Existence of hydrogen atmospheres in red giant stars (Burman) ..	620		

	PAGE		PAGE
Theory of strong electrolytes in solution based on a new statistics. Equilibrium phenomena: Activity coefficients (Dutta and Sengupta)	1	the Niniyur (Danian) beds of the Trichinopoly area ..	298
Thermal conductivity of Argon-Neon mixture (Srivastava and Madan)	587	Vibration spectrum of a crystal. A note (Peierls)	121
<i>Tiliacora racemosa</i> Coleb. Embryological studies in menispermaceae (Sastri) ..	494	Vibrational transition probabilities. Working of some theories (Tawde and Laud) ..	259
Transients of magnetographs and instantaneous values from recordings (Malurkar) ..	567	Venkatachaliengar, K. and Rao, K. N. Srinivasa.—Irreducible representations of the Lie-Algebra of the orthogonal group with spin $3/2$..	509
Trimethyl benzene. Force constants for 1, 3, 5 trimethyl benzene (Santhamma) ..	576	Venkataraman, R. and Sreenivasan, A.—Bacteriology of inshore sea water and of mackerels off Tellicherry (Malabar)	651
Tyrosinase activity in relation to phenolic tanning of the cuticle in <i>Carcinus maenas</i> (Krishnan)	157	Vorticity on the specific heat ratio of a non-relativistic Fermi-Dirac gas. Effect (Vardya)	570
Vardya, M. S.—Effect of vorticity on the specific heat ratio of a non-relativistic Fermi-Dirac gas	570	Werner, G.—see Mukherjee, K. L., Chaudhuri, R. N. and Werner, G.	
Variation of pressure with time in rocket chamber (Gupta and Mehta)	563	Western Ghats. Structural and drainage patterns of the Western Ghats in the vicinity of the Palghat Gap (Jacob and Narayanaswami) ..	104
Varma, C. P.—Algal genera <i>Neomeris</i> and <i>Acicularia</i> from		Working of some theories of vibrational transition probabilities (Tawde and Laud) ..	259

CONTENTS

No. 1, January-February

	PAGE
A Theory of strong Electrolytes in Solution based on a new Statistics. Equilibrium Phenomena: Activity Coefficients <i>by</i> M. DUTTA and M. SENGUPTA	1
On the Problem of Transfer of Radiation in a spherically symmetrical stellar Atmosphere for the non-conservative Case <i>by</i> K. K. SEN	12
Study on the State of Dispersoid in the colloidal coloured Glass <i>by</i> B. K. BANERJEE	19
On Lattice Coverings by Spheres <i>by</i> R. P. BAMBAH	25
The Occurrence of <i>Glossopteris</i> Fronds in the North-East Frontier Tracts, with a brief Review of the Gondwanas of North-Eastern India <i>by</i> K. JACOB and T. BANERJEE	53
Some infinite Integrals involving Bessel Functions <i>by</i> C. B. RATHIE	62
The Emission Band Spectrum of Cl_2^+ <i>by</i> P. TIRUVENGANNA RAO	70
A Theory of Resistance in potential Flows (Parts I-IV) <i>by</i> N. L. GHOSH	74
The structural and drainage Patterns of the Western Ghats in the Vicinity of the Palghat Gap <i>by</i> K. JACOB and S. NARAYANASWAMI	104
On Polar reciprocal Convex Domains <i>by</i> R. P. BAMBAH	119
Note on the Vibration Spectrum of a Crystal <i>by</i> Sir R. E. PEIERLS	121

No. 2, March-April.

Embryological Studies in Malvaceae. I. Development of Gametophytes <i>by</i> C. VENKATA RAO	127
Plasma Volume and Thiocyanate Space in Nutritional Oedema <i>by</i> K. L. MUKHERJEE, R. N. CHAUDHURI and G. WERNER	151
Tyrosinase Activity in relation to Phenolic Tanning of the Cuticle in <i>Carcinus maenas</i> <i>by</i> G. KRISHNAN	157
Studies on Cytochemistry of Hormone Action. Part XIV. Studies in the Distribution and Concentration of Alkaline Phosphatase in the Vaginal Smear of the Rat during Estrus Cycle: The Effect of Ovariectomy and Replacement Therapy <i>by</i> S. K. ROY, A. B. KAR and J. N. KARKUN	170
Studies on the Nuclear Apparatus of Peritrichous Ciliates. Part II. The Nuclear Apparatus of <i>Carchesium spectabile</i> Ehrbg. <i>by</i> C. M. S. DASS	174
The Biology of the Grey Mullet, <i>Mugil tade</i> Forskål, with notes on its Fishery in Bengal <i>by</i> T. V. R. PILLAY	187
Some Aspects of relative growth in the Blue Swimming Crab <i>Neptunus pelagicus</i> (Linnaeus) <i>by</i> R. RAGHU PRASAD and P. R. S. TAMPI	218

No. 3, May-June.

The Absorption Spectrum of BiBr <i>by</i> P. K. SUR and K. MAJUMDAR	235
Study of Metal Film on Glass Surface <i>by</i> B. K. BANERJEE	241
Force Constants for the BF_3 Molecule <i>by</i> V. SANTHAMMA	245

Atmospheric Oscillations at high Altitudes and their Relation to Geomagnetic Field Variations <i>by</i> R. PRATAP	252
On the Working of some Theories of Vibrational Transition Probabilities <i>by</i> N. R. Tawde and B. B. LAUD	259
Is Salt in Sambhar Lake wind-borne from the Rann of Cutch and the Arabian Sea? <i>by</i> S. K. PRAMANIK and K. P. RAMAKRISHNAN	265
Target Damages by Explosive Charges with lined conical Cavities <i>by</i> SAMPOORAN SINGH	274
On Angelescus Polynomials <i>by</i> VIKRAMADITYA SINGH	280
Origin of R. F. Oscillations in A.C. 'Silent' Discharges <i>by</i> S. R. KHASTGIR and C. M. SRIVASTAVA	290
On the Algal Genera <i>Neomeris</i> and <i>Acicularia</i> from the Niniyur (Danian) Beds of the Trichinopoly Area (S. India) <i>by</i> C. P. VARMA	298
A Generalization of Cantor Bendixon Theorem <i>by</i> K. PADMAVALLY	305
Relation between maximum Pressure and shot-start Pressure <i>by</i> S. P. AGGARWAL	307
Absorption Spectrum of 3-Chloro-Thionaphthene <i>by</i> K. SREERAMAMURTY and P. B. V. HARANATH	318
On Polar Reciprocal Convex Domains. Addendum <i>by</i> R. P. BAMBAH	324
Instability of Non-radial Oscillations of centrally condensed Stars <i>by</i> R. C. KHARE	326
A note on the Karman's Spectrum Function of Isotropic Turbulence <i>by</i> K. M. GHOSH	336
Appell set of Polynomials <i>by</i> VIKRAMADITYA SINGH	341
Products of Summability Methods <i>by</i> T. PATI	348

No. 4, July-August.

Fertilization and the Development of Embryo and Seed in <i>Euphorbia hirta</i> Linn. <i>by</i> L. B. KAJALE	353
The Egg-wall of the African Migratory Locust, <i>Locusta Migratoria Migratorioides</i> Reich. and Frm. (Orthoptera, Acrididae) <i>by</i> M. L. ROONWAL	361
Studies on the Physiology of Rice. VII. Effect of varying Water Levels on Growth of Rice in relation to Nitrogen Absorption <i>by</i> B. N. GHOSH	371
Size, Sculpturing, Weight and Moisture Content of the Developing Eggs of the Desert Locust, <i>Schistocerca gregaria</i> (Forskål) (Orthoptera, Acrididae) <i>by</i> M. L. ROONWAL	388
The Ecology of a Brackishwater <i>Bheri</i> with special reference to the Fish-cultural Practices and the biotic Interaction <i>by</i> T. V. R. PILLAY	399
Studies on Cytochemistry of Hormone Action. Part XV. The Effect of Adrenocorticotrophic Hormone (ACTH) on Alkaline Phosphatase Activity in the pars intermedia of the Cat's Hypophysis <i>by</i> J. N. KARKUN and AMIYA B. KAR	428
Pollination Mechanism in <i>Passiflora foetida</i> Linn. <i>by</i> M. V. S. RAJU	431
The Rôle of Culture Medium and its Constituents on the Growth and Viability of <i>Entamoeba histolytica</i> <i>by</i> A. K. MUKHERJEA	437
Studies on the Physiology of Rice. VIII. The Effects of low and high Temperature Germination with or without Short Days on Summer and Winter Varieties <i>by</i> S. M. SIRCAR and B. N. GHOSH	452

	PAGE
Fish Geography of the Hinralayas <i>by</i> A. G. K. MENON	467
Embryological Studies in Menispermaceae. I. <i>Tiliacora racemosa</i> Coleb. <i>by</i> R. L. N. SASTRI	494
Alkaline Phosphatase and periodic Acid-Schiff Reactions in the Thymus of <i>Calotes versicolor</i> (Daud.) <i>by</i> M. APPASWAMY RAO	503

No. 5, September-October.

The irreducible Representations of the Lie-Algebra of the Orthogonal Group with Spin $3/2$ <i>by</i> K. VENKATACHALIENGAR and K. N. SRINIVASA RAO ..	509
Radiation Damping in Compton Scattering <i>by</i> T. C. ROY	524
On the Problem of Softening of Radiation by Multiple Compton Scattering in Stellar Atmospheres containing Free-Electrons <i>by</i> K. K. SEN ..	530
A Matrix Treatment of Four-Dimensional Rotation in Hyperspace <i>by</i> N. N. GHOSH	542
An Equation of State for the Detonation of condensed Explosives <i>by</i> M. P. MURGAI	548
Effect of E.M. Radiation on the Self-Energy of Free-Electrons—I. <i>by</i> INDERJIT SINGH	557
Variation of Pressure with Time in Rocket Chamber <i>by</i> S. K. GUPTA and A. K. MEHTA	563
Transients of Magnetographs and Instantaneous Values from Recordings <i>by</i> S. L. MALURKAR	567
The Effect of Vorticity on the Specific Heat Ratio of a Non-Relativistic Fermi-Dirac Gas <i>by</i> M. S. VARDYA	570
Force Constants for 1, 3, 5 Trimethyl Benzene <i>by</i> V. SANTHAMMA ..	576
On a Generating Function in Partition Theory <i>by</i> H. GUPTA	582
Thermal Conductivity of Argon-Neon Mixture <i>by</i> B. N. SRIVASTAVA and M. P. MADAN	587
Light Scattering from Gel-forming Systems during and after Setting— Part I. Aluminium Molybdate and Thorium Arsenate Gels: Intensity Measurements <i>by</i> R. L. DESAI and V. SUNDARAM	598
Part II. Sodium Stearate in Octyl Alcohol and Sodium Stearate in Decyl Alcohol: Depolarization Measurements <i>by</i> K. P. BUCH and V. SUNDARAM	609
On the Existence of Hydrogen Atmospheres in red Giant Stars <i>by</i> U. R. BURMAN	620
Dependence of Erosion Ratio and Rate of Burning on Position and Time in a Rocket Motor <i>by</i> S. K. GUPTA and M. S. SODHA	634

No. 6, November-December.

Observations on the atrioventricular conducting (connecting) System of the Heart of human Twins obtained from an aborted Foetus <i>by</i> R. PRAKASH	645
Bacteriology of inshore Sea Water and of Mackerels off Tellicherry (Malabar) <i>by</i> R. VENKATARAMAN and A. SREENIVASAN	651
Photometric Study of Desoxyribonucleic Acid (DNA). Synthesis in regenerating Macronucleus of <i>Epistylis articulata</i> From. <i>by</i> B. R. SESHACHAR and C. M. S. DASS	656

	PAGE
The Rôle of Bacteria on the Growth and Viability of <i>Entamoeba histolytica</i> by A. K. MUKHERJEA	660
Studies on the Physiology of Rice. IX. Auxin Content of the vernalised Seed by S. M. SIRCAR and T. M. DAS	673
Studies on the reproductive Tract of <i>Ariophanta maderaspatana</i> (Gray) (Mollusca: Pulmonata). Part I. Histochemistry of the Ammatorial Organ by V. K. S. IYENGAR	683
Ore microscopic Studies of the vanadium-bearing titaniferous Iron Ores of Mayurbhanj with a detailed note on their Texture by S. ROY	691
Studies on the Nuclear Apparatus of Peritrichous Ciliates. Part III. The Nuclear Apparatus of <i>Epistylis</i> sp. by C. M. S. DASS	703

A THEORY OF STRONG ELECTROLYTES IN SOLUTION BASED ON A NEW STATISTICS.

EQUILIBRIUM PHENOMENA: ACTIVITY COEFFICIENTS

by M. DUTTA and M. SENGUPTA, *University College of Science and Technology, Calcutta 9*

(Communicated by S. N. Bose, F.N.I.)

(Received February 23; read October 9, 1953)

INTRODUCTION

Following Milner (1912 and 1913), Ghosh (1918) has pointed out rightly that the deviations in the behaviour of solutions of strong electrolytes from that of ideal one are to be explained from the considerations of interionic fields existing in these solutions. But his calculations have been subsequently replaced by a method, generally accepted as more accurate, due to Debye and Hückel (1923). In their calculations, Debye and Hückel have assumed that in the atmosphere of an ion in solution other ions are distributed according to the Boltzmann statistics and have calculated the potential from an approximate evaluation of Poisson's equation for the field (assumed to be of electrostatic nature) for small values of ψ ($\epsilon\psi \ll kT$). They have also distinguished the available or free (electrical) energy from the total (electrical) potential energy of the assembly and have calculated the former by considering an ideal process of charging and discharging of the ions in the above field. The theoretical values of the mean activity coefficients (and other related quantities) of electrolytes obtained by the method of Debye and Hückel are generally admitted to be in good agreement with experimental results at low concentrations. But the method, as actually put forward by Debye and Hückel, has originally been the subject of criticisms mainly due to the following unsatisfactory features:

- (i) Firstly, the use of Poisson's equation in the present model, which admits fluctuations, requires a priori justifications.
- (ii) Secondly, unusual and sometimes inadmissible (i.e., negative) values are to be taken for the ionic radii in order to obtain a good fit with observations.
- (iii) Thirdly, for high concentrations and for ions of large-valency types, the deviations of the calculated values from those observed are considerably large.
- (iv) Fourthly, Sengupta (1952) has recently pointed out another very simple but fundamental inconsistency in the original calculations of Debye-Hückel. It has been shown that the value of $\epsilon\psi$ on the surface of ion, which only is of actual significance in calculations, is greater than that of kT and thus it contradicts the basic assumption of calculation that $\epsilon\psi \ll kT$.

Subsequently, Fowler (1927), Kramers (1927), Onsager (1933) and Kirkwood (1934) have justified the use of Poisson's equation in the model of Debye and Hückel from general considerations of statistical mechanics. Müller (1927) and Gronwall with his collaborators (1928) have shown that good fits with experimental values can be obtained with usual and admissible values of the ionic radii, if the Poisson

equation of the Debye-Hückel theory is evaluated more accurately. The question, raised recently by Sengupta, yet remains open.

Recently, Bagchi (1950) has remodelled the Debye-Hückel theory in a completely new line and has claimed to obtain good agreements with experimental values of activity coefficients for almost entire range of concentrations, especially in the case of uni-uni-valent electrolytes. Firstly, in his calculations in place of Boltzmann statistics the law of distribution of ions has been taken as

$$n_{i,r} = \frac{\sum n_i}{\frac{z_i \epsilon \psi_r}{e^{\alpha + \frac{\epsilon \psi_r}{kT}} + 1}}, \quad \dots \quad (1)$$

where

$n_{i,r}$ = number-density (i.e. number per c.c.) of ions of i -th type at a point in the solution, where the electrostatic potential energy is $z_i \epsilon \psi_r$, ϵ being the electronic charge, z_i the valency of ions of the i -th type, ψ_r the potential;

n_i = number-density (average) of ions in solution;

α = a parameter of distribution;

k = Boltzmann's constant;

T = temperature (absolute).

Secondly, the Poisson-equation has been evaluated * for small and large values of $\frac{\epsilon \psi}{kT}$ separately and the solution for large values has been used in calculations after fitting it with that for small values suitably. In other aspects, Bagchi's calculations are similar to those of Debye and Hückel.

As a theoretical support to the use of a formula different from that of Boltzmann in Bagchi's calculations, a general formula † for distribution of ions in solutions has been deduced (Dutta and Bagchi, 1950) by applying a general method of statistical mechanics, developed by Dutta (1947, 1948, 1951) in a series of papers on real gases, from the simple assumption that there is a minimum distance to which ions can approach one another, either due to finite size of ions or due to mutual repulsive reaction of like ions. The distribution formulae thus obtained, are

$$n_r^\pm \left(1 + n_r^\mp b_{+-}\right) = \frac{\frac{1}{b_\pm}}{e^{\nu_\pm + \frac{\epsilon_\pm \psi_r}{kT}} + 1}, \quad \dots \quad (2)$$

where

ϵ_\pm , k , T have their usual significance,

ν_\pm = assembly-parameters of distribution,

n_r^\pm = number-densities of positive and negative ions at a point in the solution with potential energy $\epsilon_\pm \psi_r$,

b_\pm = volumes of covering spheres (Deckungssphären) of positive or negative ions due to minimum approach amongst the like ions,

$b_{+-} = b_{-+}$ = the same for unlike ions.

* This method of evaluation has been originally suggested by Dr. G. Bandyopadhyay of Indian Institute of Technology, Kharagpur (India), to Bagchi and to Dutta, one of the present authors, and the present authors take this opportunity to express their thanks to him.

† This is the same as those obtained by Dutta for real gases (*loc. cit.*).

The formula (2) has recently been used by Bagchi (1952) in calculations of activity coefficients.

If one admits the assumption $b_{+-} < b_{\pm}$ which means that the distance of minimum approach of unlike ions is much smaller than those of like ion, and, which appears to be very plausible in the Coulombian field, then the formula (2) reduces to

$$n_{\pm} = \frac{1}{b_{\pm} \left(e^{v_{\pm} + \frac{e_{\pm} \psi_r}{kT}} + 1 \right)} \quad (3)$$

Subsequently Eigen and Wicke (1951) have obtained a good agreement between theoretical and observed values of activity coefficients by using in place of Boltzmann statistics, a distribution formula which they have claimed to be new and more general than formula (3). But as shown by Dutta (1952), the distribution formula used by Eigen and Wicke is practically the same as the formula (3), written in a different form with new symbols and with slightly different explanations for the parameters involved. Moreover, in reply to some misleading and confusing remarks * of Wicke and Eigen (1952) it has been further shown by Dutta (1953) that also the method by which Eigen and Wicke arrive at their distribution formula, is practically similar to that employed by Dutta and Bagchi (1950) in deducing formula (3). Still it is easy to see that the method used by Eigen and Wicke lacks the generality of that of Dutta, developed in the papers (Dutta, 1947, 1948, 1951, Dutta and Bagchi, 1950).

Thus up till now, no detailed calculations, based on the theoretically deduced distribution formula (3) in the original form and with original simple interpretations, has been made. In this paper, we propose to develop a complete scheme for the calculation of mean activity coefficients of electrolytes, starting from the formula (3) and to show clearly, as far as possible, the advantages and the disadvantages of the present method with other existing methods, such as those of Debye and Hückel (1923), Bagchi (1950), and of Eigen and Wicke (1951). For the sake of simplicity, the discussion here will be restricted to the case of uni-uni-valent electrolytes. The extension of the theory to the case of symmetrical electrolytes is obvious, the treatment of the case of non-symmetrical electrolytes is left over for future communications.

CHARGE-DENSITY IN ION-ATMOSPHERES

As in the Debye-Hückel theory, attention will be focussed on any one ion (say, of positive charge). The charge-density in the atmosphere of this ion will

* After the completion of this manuscript, the attention of the authors has been drawn to some further wrong and misleading remarks of Wicke and Eigen (cf. foot-note, *Zeit. f. Elektro. Chem.*, Bd. 56, No. 6, p. 558 (1952)). Here again Wicke and Eigen have wrongly chosen to identify (as they have done in their previous publications) the distribution formula (3) with the one originally used by Bagchi (1950). The essential difference between these two formulae has already been mentioned in previous publications of Dutta and also of Dutta and Bagchi and has been clearly shown in the present paper. Further to make the impression that formula (3) is the good old Fermi statistics, they have quoted some phrases from Bagchi's paper (1950), whereby it is obvious that they have failed to take proper notice of the relevant lines (at the end of first para) of the paper of Dutta and Bagchi (1950), where the difference of formula (3) from Fermi statistics has been clearly and unequivocally emphasised. For a clear understanding of these differences the papers of Dutta (III, 1951), of Dutta and Bagchi (1950) and a note by Dutta (1953) should be consulted. Again, that formula (3) does actually pass over to Boltzmann statistics, has already been shown in the paper (Dutta, 1951, communicated in 1949) and was therefore omitted in the paper (Dutta and Bagchi, 1950). Finally, the rôle of the very essential concept of the number of occupiable sites in the method of Dutta and Bagchi would have been clear to every one who has had a lance into the papers of Dutta, and of Dutta and Bagchi, which it is apprehended has not been done by Wicke and Eigen.

be calculated by using the formula (3) in place of the Boltzmann statistics. Then, the charge-density at the point in the atmosphere of the ion, where the potential is ψ_r , will be given by

$$\rho_r = \epsilon (n_r^+ - n_r^-), \quad \dots \quad (4)$$

$$= \epsilon \left\{ \frac{\frac{1}{b_+}}{e^{\nu_+ + \frac{\epsilon \psi_r}{kT}} + 1} - \frac{\frac{1}{b_-}}{e^{\nu_- - \frac{\epsilon \psi_r}{kT}} + 1} \right\}, \dots \quad (4)$$

where ϵ is the ionic charge.

$$\text{Therefore, as } \psi_r \rightarrow \infty, \rho \rightarrow -\frac{\epsilon}{b_-}. \quad \dots \quad (6)$$

The above result has a very elegant physical significance. Now $-\epsilon$ being the charge of negative ion and b_- , the volume exclusively under command of a single negative ion, $-\frac{\epsilon}{b_-}$ represents the density of negative charge, if the negative ions are distributed in close packing in the atmosphere of the positive ion under consideration. Again, b_- represents the crystallographic value (actual or after correcting for hydration), thus, for very large values of ψ , the distribution of ions is similar to that in crystals. This shows the plausibility of the quasi-lattice model proposed in a previous paper (Dutta, 1953).

Moreover, ρ as defined by the equation (4) is always bounded. In the Debye-Hückel theory, this is not the case. The unboundedness of ρ is devoid of physical significance, and so unsatisfactory, mainly due to the following reasons. An infinity of ρ means an infinite accumulation of negative charges in the close neighbourhood of the ion of positive charge. As soon as two or three negative ions come very near to the positive ion, there will be a shielding effect and the original Coulombian attractive field for negative ions will be transformed into a Coulombian repulsive field, and so, no further accumulation of negative ions is possible. So, the infinite accumulation of charges is unthinkable in the Coulomb field. Again, an infinite accumulation of ions in a certain neighbourhood of the central ion is in direct contradiction to the assumption, (which is simultaneously made in usual theories), that there exists a distance of minimum approach amongst the ions. This unsatisfactory self-contradictory feature of the theory has been easily avoided in the present theory simply by replacing the Boltzmann statistics by the formula (3).

Again, when $\psi_r \rightarrow 0$, the distribution is (on average) uniform, i.e.,

$$\frac{\frac{1}{b_+}}{e^{\nu_+ + 1}} = n_0^+ = n_0^- = \frac{\frac{1}{b_-}}{e^{\nu_- + 1}} = n_0 \text{ (say)}, \quad \dots \quad (7)$$

Then, for small values of ψ_r we have up to the first order

$$\rho = -\frac{2\epsilon^2}{kT} n_0 \left(1 - n_0 \frac{b_+ + b_-}{2} \right). \quad \dots \quad (8)$$

THE INTER-IONIC FIELD

Now, as in the theory of Debye and Hückel, the potential for the inter-ionic field will be taken to satisfy the Poisson equation,

$$\nabla^2 \psi = -\frac{4\pi}{D} \rho, \quad \dots \quad (9)$$

subject to boundary conditions.

$$\psi \rightarrow 0 \text{ as } r \rightarrow \infty, \quad \dots \quad (10)$$

and,
$$\int \left(\frac{d\psi}{dr} \right) dS = - \frac{4\pi}{D} \epsilon \text{ (Gauss' theorem).} \quad \dots \quad (11)$$

It is more convenient to introduce a dimensionless variable and we shall take

$$\lambda = \frac{\epsilon \psi}{kT}, \quad \dots \quad (12)$$

then (9) becomes

$$\nabla^2 \lambda = - \frac{4\pi \epsilon}{D kT} \rho. \quad \dots \quad (13)$$

Substituting the values of ρ we can write the differential equation in simpler forms for large and for small values of λ as follows:—

When $\lambda \sim 0$,
$$\nabla^2 \lambda = \kappa^2 \lambda, \quad \dots \quad (14)$$

and when $\lambda \sim \infty$,
$$\nabla^2 \lambda = \kappa^2 m_+, \quad \dots \quad (15)$$

where
$$\kappa^2 = \frac{8\pi \epsilon^2}{D kT} n_0 \left(1 - n_0 \frac{b_+ + b_-}{2} \right), \quad \dots \quad (16)$$

and
$$m_+ = \frac{1}{b_-(2n_0) \left(1 - n_0 \frac{b_+ + b_-}{2} \right)}. \quad \dots \quad (17)$$

One important point should be noted in this connection. As already mentioned after Sengupta (1953), it is known that the value of λ (when calculated from the expression for λ obtained by Debye and Hückel in their original calculations based on the assumption $\lambda \ll 1$) on the surface of the ion is in almost all cases greater than one. This inconsistency necessitates the approximate evaluation of the Poisson's equation for large values of λ , but this is not possible in Debye-Hückel theory as ρ is unbounded when $\psi \rightarrow \infty$. On the other hand, in the present development, as also in those of Bagchi, and of Eigen and Wicke, the evaluation of λ for large values is easy. This may be looked upon as an advantageous feature in these developments, entirely due to the replacing of Boltzmann formula by a new one, and may be looked upon as one of the main reason of their success.

Now, in Bagchi's original calculations, he writes the equations of the field as

$$\nabla^2 \lambda' = \kappa'^2 \lambda', \quad \dots \quad (14a)$$

and
$$\nabla^2 \lambda' = \kappa'^2 m'_+, \quad \dots \quad (15a)$$

where
$$\kappa'^2 = \frac{4\pi \epsilon^2}{D kT}, \quad \dots \quad (16a)$$

$$m'_+ = m'_-, \quad \dots \quad (17a)$$

$$\lambda' = \frac{\lambda}{2} = \frac{\epsilon \psi}{2kT}.$$

Thus, the material difference, between the equations in Bagchi's calculations and those in the present one, is in the factor

$$\left(1 - n_0 \frac{b_+ + b_-}{2} \right)$$

When $n_0 \frac{b_+ + b_-}{2}$ is $\ll 1$,

and so can be neglected, they become practically same. The omission of this factor in Bagechi's calculations may be the reason of the necessity of using large values of ionic radii.

SCHEME FOR EVALUATION OF λ

Here we shall take the approximate solution of the equation (9) subject to the boundary conditions (10) and (11) to be given by the integrals λ_1 and λ_2 of (13) and (14) respectively for different ranges of values of ψ , when the constants of integration have been determined from the following relations.

$$(\lambda_1)_{\xi_1} = m_+ = (\lambda_2)_{\xi_1}, \quad \dots \quad (18)$$

$$\left(\frac{d\lambda_1}{d\xi} \right)_{\xi_1} = \left(\frac{d\lambda_2}{d\xi} \right)_{\xi_1}, \quad \dots \quad (19)$$

$$\lambda \rightarrow 0 \text{ as } r \rightarrow \infty, \quad \dots \quad (20)$$

and also from the Gauss's theorem,

$$\int \left(\frac{d\psi}{dr} \right) dS = - \frac{4\pi}{D} \epsilon, \quad \dots \quad (21)$$

where

$$\xi = \kappa r. \quad \dots \quad (22)$$

Now, since $\lambda \rightarrow 0$ as $\xi \rightarrow \infty$ so λ_1 is given by

$$\lambda_1 = B \frac{e^{-\xi}}{\xi} \dots \quad (23)$$

The other solution is of the form

$$\lambda_2 = m_+ \left[\frac{\xi^2}{6} + C + \frac{H}{\xi} \right]. \quad \dots \quad (24)$$

Now, so far as the use of the condition (21) is concerned there will appear a practical difficulty. A priori there is nothing to decide from the beginning which of the integrals, λ_1 and λ_2 will represent λ close to the surface (i.e. at $r = a$) and so is to be used in the equation (21). Here, it is also to be remembered that in calculations of activity coefficients and other related thermodynamics quantities, the value of λ , close to the surface of the ion, is of actual importance. So, the actual procedure is a bit round-about and may be sketched as follows:—

Now, for sufficiently low concentrations, m_+ is a large number and the expression for κ^2 reduces to that of Debye-Hückel. Again from the finding of Sengupta (1952), it is known that the values of λ on the surface of ions, from (23), are not large. Then, since λ increases monotonically from 0 as r decreases from infinity, so the surface value of λ , being less than m_+ , will be reached before λ attains the value m_+ . Thus λ will be taken to be represented by λ_1 where B has been determined from (21). Thus, we get near the surface

$$\lambda = \lambda_1 = \frac{\epsilon^2}{DkT} \frac{e^{\kappa a_+}}{1 + \kappa a_+} \frac{e^{-\kappa r}}{r} \dots \quad (25)$$

Now, since the Poisson equation does not represent the field within the ion, which again is not of any interest for the present discussion, so, in the case under consideration λ is given by λ_1 , and λ_2 is devoid of any significance.

Thus the expression for potential is same as that in the original calculations of Debye and Hückel and so will yield the usually accepted limiting laws. For this reason, in this paper, calculations of activity coefficients for small concentrations have been omitted.

For comparatively high concentrations, m_+ is of the order of unity and may be less than the surface value of λ . Thus, λ reaches the value m_+ earlier, so λ near the surface is expected to be given by λ_2 and so

$$\lambda = \lambda_2 = m_+ \left[\frac{\xi^2}{6} + C + \frac{H}{\xi} \right], \quad \dots \quad (26)$$

where C , H , and ξ_1 (argument of λ corresponding to $\lambda = m_+$) are to be determined from the equations (17), (18) and (19). In a manner, similar to that of Bagchi, C and H are found to be

$$H = \frac{\epsilon^2 \kappa}{m_+ D k T} + \frac{\kappa^3 a_+^3}{3}, \quad \dots \quad (27)$$

$$= \frac{g_+}{3} \text{ (say)}, \quad \dots \quad (28)$$

$$\xi_1 = (1 + g_+)^{\frac{1}{2}} - 1, \quad \dots \quad (29)$$

$$C = \frac{1}{2} \{ 1 - (1 + g_+)^{\frac{1}{2}} \}. \quad \dots \quad (30)$$

CALCULATIONS OF AVAILABLE (OR FREE) ENERGY

Here, to calculate the free energy after Debye and Hückel, we shall consider the ideal process of charging and discharging. Of course, we shall think that the charge of the ion is on the surface of the ion, and so, the processes of charging and discharging are occurring on the surface of the ion instead of on the geometrical surface of the covering sphere (Deckungssphären) of the ion, as has been considered in the Debye-Hückel theory. Thus, for high concentrations,

$$\psi_2(a_+) = \frac{kT}{\epsilon} \lambda_2(a_+) = \frac{kT}{\epsilon} \frac{m_+ \kappa^2 a_+^2}{2} + \frac{\epsilon}{D a_+} + \frac{m_+ kT}{2\epsilon} \{ 1 - (1 + g_+)^{\frac{1}{2}} \}. \quad \dots \quad (31)$$

The potential due to the ion-atmosphere on the surface of ion is

$$\psi_2^*(a_+) = \frac{kT m_+}{2\epsilon} \left[\kappa^2 a_+^2 + \{ 1 - (1 + g_+)^{\frac{1}{2}} \} \right]. \quad \dots \quad (32)$$

The work done in charging

$$\begin{aligned} W_+ &= \int_0^1 \epsilon \left[\psi_2^*(a_+) \right]_{\epsilon x} dx \\ &= \frac{kT m_+}{2} \left\{ \kappa^2 a_+^2 \int_0^1 x dx + \int_0^1 \frac{1 - (1 + g_+ x^3)^{\frac{1}{2}}}{x} dx \right\} \\ &= \frac{kT m_+}{2} \left\{ \frac{1}{2} \kappa^2 a_+^2 + P + \phi_+(g_+) \right\}, \quad \dots \quad (33) \end{aligned}$$

where

$$P = \frac{1}{2} + \frac{1}{\sqrt{3}} \tan^{-1} \sqrt{3} - \frac{1}{2} \log_e 3 \approx 5551, \quad \dots \quad (34)$$

and,

$$\begin{aligned} \phi_+(g_+) = \frac{1}{2} \log \left[(1+g_+)^{\frac{1}{2}} + (1+g_+)^{\frac{1}{2}} + 1 \right] - \frac{1}{2}(1+g_+)^{\frac{1}{2}} \\ - \frac{1}{\sqrt{3}} \left(\tan^{-1} \frac{2(1+g_+)^{\frac{1}{2}} + 1}{\sqrt{3}} \right). \quad \dots \quad (35) \end{aligned}$$

A similar expression is obtained for W_- and the total work done in charging all the ions is given by:

$$\begin{aligned} W &= n_0 (W_+ + W_-) \\ &= \frac{kT}{2} n_0 \left[\frac{1}{2} (\kappa^2 m_+ a_+^2 + \kappa^2 m_- a_-^2) + P(m_+ + m_-) + (\phi_+ m_+ + \phi_- m_-) \right]. \quad \dots \quad (36) \end{aligned}$$

ACTIVITY COEFFICIENTS

Now, for convenience of calculations as in other theories we shall take

$$n_0^+ = n_0^- = n_0 = n_+ = n_-, \quad \dots \quad (37)$$

where n_+ and n_- are average number of positive and negative ions.

Then, on using the usual expression for the ionic activity coefficient, viz.,

$$\log f_+ = \frac{1}{kT} \frac{\partial W}{\partial n_+}, \quad \dots \quad (38)$$

we get from the equation (36)

$$\begin{aligned} \log f_+ &= \frac{m_+}{2} \left\{ \frac{1}{2} \kappa^2 a_+^2 + (P + \phi_+)(1 - n_+ D_+) + E_+(g_+) n_+ D_+ \right\} \\ &+ \frac{m_-}{2} \{ E_-(g_-) n_- D_+ - n_- D_+ (P + \phi_-) \}, \quad \dots \quad (39) \end{aligned}$$

where

$$D_+ = \frac{1 - 2n_0 b_+}{2n_0 \left(1 - n_0 \frac{b_+ + b_-}{2} \right)}, \quad \dots \quad (40)$$

and

$$\begin{aligned} E_+(g_+) &= \frac{1}{2} \frac{\frac{g_+}{(1+g_+)^{\frac{1}{2}}} + \frac{g_+}{2(1+g_+)^{\frac{1}{2}}}}{\frac{(1+g_+)^{\frac{1}{2}} + (1+g_+)^{\frac{1}{2}} + 1}{2}} - \frac{g_+}{2(1+g_+)^{\frac{1}{2}}} \\ &- \frac{g_+}{3(1+g_+)^{\frac{1}{2}} \left[1 + \frac{1}{3} \{ 2(1+g_+)^{\frac{1}{2}} + 1 \}^2 \right]} \quad \dots \quad (41) \\ &= \frac{1}{2} \{ 1 - (1+g_+)^{\frac{1}{2}} \}, \end{aligned}$$

A similar expression is also obtained for $\log f_-$.

Then, finally,

$$\log f_{\pm} = \frac{1}{2} \left[\frac{m_{+}}{2} \left\{ \frac{1}{2} \kappa^2 a_{+}^2 + (P + \phi_{+}) \left[1 - n_0(D_{+} + D_{-}) \right] + E_{+} n_0(D_{+} + D_{-}) \right\} \right. \\ \left. + \frac{m_{-}}{2} \left\{ \frac{1}{2} \kappa^2 a_{-}^2 + (P + \phi_{-}) \left[1 - n_0(D_{+} + D_{-}) \right] + E_{-} n_0(D_{+} + D_{-}) \right\} \right] \dots \quad (42)$$

COMPARISON WITH EXPERIMENTAL DATA

Consistent with our interpretation for b_{\pm} given in the papers (Dutta and Bagchi, 1950, Dutta, 1951-53) they will be taken as the volumes of exclusion (volumes of covering spheres, overlapping being neglected), i.e.,

$$b_{\pm} = \frac{4}{3} \pi (2a_{\pm})^3, \quad \dots \dots \dots (43)$$

where a_{\pm} are the ionic radii in the ordinary sense (i.e., either the crystallographic or the effective values due to hydration). Now, according to the accepted views, it is known that in the solutions, the effective ionic radii, on account of hydration are greater than the crystallographic values, and their differences are more and more prominent, the smaller the ionic radii (crystallographic), for ions of the same charge. So in this paper, for Cs^{+} we have taken the crystallographic value for the radius and for K^{+} and Na^{+} a value nearly equal to that due to hydration (Eucken, 1948). The values of the mean molar activity coefficients of the three electrolytes CsCl , KCl and NaCl at 25°C . as calculated according to the equation (42) are compared to the corresponding experimental values (molal).

TABLE I
Variation of activity coefficient* with concentration

		1 m.	1.5 m.	2 m.	2.5 m.	3 m.	3.5 m.	4 m.
CsCl	$a_{\text{Cs}^{+}} = 1.67 \text{ \AA}$..	Obs.	.543	.514	.495	.485	.480	.474
	$a_{\text{Cl}^{-}} = 1.81 \text{ \AA}$..	Cal.	.531	.484	.466	.459	.460	.480
KCl	$a_{\text{K}^{+}} = 2.15 \text{ \AA}$..	Obs.	.605	.585	.575	.572	.573	
	$a_{\text{Cl}^{-}} = 1.81 \text{ \AA}$..	Cal.	.554	.532	.532	.546	.579	
NaCl	$a_{\text{Na}^{+}} = 2.66 \text{ \AA}$..	Obs.	.658	.659	.671			
	$a_{\text{Cl}^{-}} = 1.81 \text{ \AA}$..	Cal.	.65	.65	.72			

Now it may be said that the fitting of a set of experimental data by suitable adjustment of an arbitrary parameter (the radius of the volume of exclusion), as it is done by Eigen and Wicke (1951), Bagchi (1950), is not conclusive. To avoid this criticism the calculated values for mean molar activity coefficients and the

* The experimental data given above are all taken from H. S. Harned and B. B. Owen Physical Chemistry of Electrolytic Solutions, Reinhold Publishing Corporation, New York, 1950 (2nd Ed.), p. 562.

corresponding observed values for molal activity coefficients for KCl at different temperatures with values of ionic radii used in the above fitting, have been tabulated in Table 2. The agreement in this case also is good.

TABLE 2
*Variation of activity coefficient * for KCl with temperature*

Temp. (°C)		0	5	10	15	20	25	30	35	40
5 m.	Obs.	·642	·646	·648	·650	·651	·651	·651	·648	·646
	Cal.	·615	·619	·626	·633	·640	·649	·658	·666	·675
3 m.	Obs.	·539	·549	·556	·562	·567	·571	·573	·574	·573
	Cal.	·538	·546	·555	·563	·571	·579	·586	·593	·601

CONCLUSION

In conclusion, the following features of the present theory may be stressed as satisfactory, new and important:

I. The distribution formula for ions in the electric field used in the paper has been deduced in a simple manner by a general statistical method from the plausible assumptions, viz.:

- (i) there is a distance of minimum approach between the ions (at least in average),
- (ii) the average gradient of the field is such that its change with distances of the order of ionic diameter can be neglected.

II. The charge-density ρ is always bounded as required for consistency with the assumptions of existence of the interionic Coulombian field and that of a distance of minimum approach.

III. Every quantity involved in the theory has a precise physical significance.

IV. As already mentioned in a note (Dutta, 1952), good agreement with experimental results have been obtained with usually accepted values of ionic radii, (in Bagchi's calculation large values are to be taken) and without using any quantity as adjustable arbitrary parameters (Eigen and Wicke have taken the number of occupiable sites suitably as a parameter).

V. For low concentrations, the method developed here yields the Debye-Hückel limiting laws.

The unsatisfactory feature of the theory, as it appears to the authors at present, is the approximate evaluation of Poisson's equation as it is done here.

In Table 1, the values of activity coefficients for KC and NaCl cannot be calculated at concentrations higher than 3 m. and 2 m. respectively, since then $n_0(b_+ + b_-) > 1$ so that $\kappa^2 < 0$, and so, the nature of the differential equations will be changed. This is so, as near about this concentration overlapping (which is neglected) is significant, and correction should be done for it, as it is done in (Dutta, 1952) for imperfect gases.

In the present paper, for large concentrations, we have used only the solution λ_2 corresponding to large values of λ . Consistency of calculations demand that $(\lambda)_a$ must be seen to be less than the corresponding m_i . If it is not satisfied then λ_1 , corresponding to small values of λ , is to be taken for λ and calculations are to

* Experimental values from Harned and Owen, *loc. cit.*, p. 558.

be made afresh. By this, some further betterments in the agreement between calculated and observed values are expected, and will be done in future communications.

SUMMARY

In this paper, a complete scheme of calculation of activity coefficients has been sketched based on the new statistics proposed in the papers of Dutta and in the paper of Dutta and Bagchi. The agreement of the observed and the calculated values of activity coefficients is found to be good. The values of the activity coefficients for different concentrations and for different temperatures have been calculated and have been given in two tables. Here some inconsistencies of the other existing theories, mainly, of the theory of Debye and Hückel, have been pointed out and how these can be avoided easily in the present development has been clearly shown.

ACKNOWLEDGEMENT

The authors desire to express their hearty thanks and deep gratitude to Prof. S. N. Bose, Prof. N. R. Sen, and Dr. S. C. Kar for the interest taken in this work.

REFERENCES

- Bagchi, S. N. (1950). A New Equation for Strong Electrolytes, Part I. *J. Ind. Chem. Soc.*, **27**, 199; Part II, 204.
- (1952). On Strong Electrolytes in Solutions. *Naturwiss.*, **39**, 209.
- Debye, P. and Hückel, E. (1923). Zur Theorie der Electrolyte. *Phys. Z.*, **24**, 185, 305.
- Dutta, M. (1947). On a Treatment of Imperfect Gases after Fermi's Model. *Proc. Nat. Inst. Sci. India*, **13**, 247.
- (1948). On a treatment of Imperfect Gases after Fermi's Model (II). *Ibid.*, **14**, 163.
- (1951). On a treatment of Imperfect Gas after Fermi's Model (III). *Ibid.*, **17**, 27.
- (1951). On a treatment of Imperfect Gas after Fermi's Model (IV). *Ibid.*, **17**, 445.
- (1952). On Equation of State of Real Gases. *Ibid.*, **18**, 81.
- (1952). On Strong Electrolytes in Solutions. *Naturwiss.*, **39**, 108.
- (1952). On Bagchi's Calculation of Activity-coefficients by the Method of Gronwall and his collaborators. *Naturwiss.*, **39**, 568.
- (1953). A Quasi-lattice Theory of Real Gases and Strong Electrolytes in Solution. *Proc. Nat. Inst. Sci. India*, **19**, 183-194.
- (1953). On the Distribution of Ions in Electrolytic Solutions. *Naturwiss.*, **40**, 51.
- Dutta, M. and Bagchi, S. N. (1950). On the Distribution of Ions in Solutions of Strong Electrolytes. *Ind. J. Phys.*, **24**, 61.
- Eigen, M., and Wicke, E. (1951). Zur Theorie der Starken Electrolyte. *Naturwiss.*, **38**, 453.
- Eucken, A. (1948). Ionenhydrate in Wässriger Lösung. *Z.f. Elektrochem.*, **51**, 6.
- Fowler, R. H. (1927). Strong Electrolytes in Relation to Statistical Theory, in Particular the Phase Integral of Gibbs. *Trans. Farad. Soc.*, **23**, 434.
- Ghosh, J. C. (1918). The Abnormality of strong Electrolytes, I. Electrical Conductivity of Aqueous Salt solutions. *J.C.S.*, **113**, 449.
- (1921). A General Theory of Electrolytic Solutions. *Z.f. Phys. Chem.*, **98**, 211.
- Gronwall, T. H., La Mer, V. K., and Sandved, K. (1928). Über den Einfluß der sogenannten höheren Glieder in der Debye-Hückelschen Theorie der Lösungen starker Elektrolyte. *Phys. Z.*, **29**, 358.
- Gronwall, T. H., La Mer V. K., and Grieff (1931). The Influence of Higher Terms of the Debye-Hückel Theory in the case of Unsymmetrical Valence Type Electrolytes. *J. Phys. Chem.*, **35**, 2345.
- Hückel, E. (1925). Zur Theorie Konzentrierteren Wässriger Lösungen Stärker Electrolyte. *Phys. Z.*, **25**, 93.
- Kirkwood, J. G. (1934). On the Theory of Strong Electrolyte Solutions. *J. Chem. Phys.*, **2**, 767.
- Kramers, H. A. (1927). Free Energy of a Mixture of Ions. *Proc. Roy. Acad. Sci. Amsterdam*, **30**, 145.
- Milner, S. R. (1912). The Virial of a Mixture of Ions. *Phil. Mag.*, **23**, 551.
- (1913). On the effect of Interionic Forces on the Osmotic Pressure of Electrolytes. *Phil. Mag.*, **25**, 742.
- Müller, H. (1927). Die Activitätskoeffizienten Kleiner Ionen. *Phys. Z.*, **28**, 324.
- Onsager, L. (1933). Theories of Concentrated Electrolytes. *Chem. Rev.*, **13**, 73.
- Sengupta, M. (1953). On a Consistency Test of the Theories of Strong Electrolytes in solution. *Ind. J. Phys.* (In press.)
- Wicke, E. and Eigen, M. (1952). Bemerkung zu der voranstehenden Mitteilung: 'On Strong Electrolytes in Solutions', *Naturwiss.*, **39**, 1108.

ON THE PROBLEM OF TRANSFER OF RADIATION IN A SPHERICALLY SYMMETRICAL STELLAR ATMOSPHERE FOR THE NON-CONSERVATIVE CASE

by K. K. SEN, *Chandernagore College, Chandernagore*

(Communicated by N. R. Sen, F.N.I.)

(Received April 27 ; read October 9, 1953)

1. The problem of transfer of radiation in the extended atmospheres of stars like supergiants in which the curvatures of the layers of the atmosphere have significant effect on the transfer problem has been considered by Kosirev (1934) and Chandrasekhar (1934). In recent years Chandrasekhar has developed a method of approximating the solution of the integro-differential equation of the transfer problem by a finite system of linear equations in which the Gaussian weights in the theory of evaluation of integrals play a prominent rôle. Chandrasekhar (1945) has given a first approximation solution of the problem of conservative isotropic scattering in an extended atmosphere by his method. In the present paper we have considered the solution of the problem for the non-conservative isotropic cases for an extended atmosphere with spherical symmetry by Chandrasekhar's method. The approximation is of the first order and two different sets of boundary conditions have been considered. In the first problem, the external boundary condition has been taken to be one of zero intensity both of incoming and outgoing radiation at the surface, while the internal boundary is a photospheric surface with a given outward flux of radiation (in comparison with which inward flux there, is considered negligible). In a second problem, the incoming radiation at the external boundary is supposed to be weak but not zero, so that the star is supposed to be embedded in a weak radiation bath with symmetry round the centre, while the inner boundary condition is the same as before. The external boundary in the second problem is artificially fixed by the condition that here the inward and outward intensities are equal. In the second case the external flux of radiation as a fraction of the flux at the internal boundary has been calculated and plotted against optical depth. It shows that when scattering is large, compared to absorption, large value of the ratio is attained by $\tau_1 = 2$ (and well below $\tau_1 = 2$ when scattering is very large) and for very large absorption a curve of entirely different character is obtained.

2. The equation of transfer appropriate to the problem of spherically symmetric atmosphere is given by

$$\mu \frac{\partial I(r, \mu)}{\partial r} + \frac{1 - \mu^2}{r} \frac{\partial I(r, \mu)}{\partial \mu} = -k\rho[I(r, \mu) - \mathcal{J}(r, \mu)] \quad \dots \quad (1)$$

where $\mathcal{J}(r, \mu)$ is the source-function and in the non-conservative isotropic case, it is given by

$$\mathcal{J}(r, \mu) = \frac{1}{2} \omega_0 \int_{-1}^{+1} I(r, \mu') d\mu' \quad \dots \quad (2)$$

where $\mu = \cos \vartheta$, ϑ being the inclination to the radius vector, and ω_0 , the albedo for single scattering, represents the fraction of light lost from the pencil by way

of scattering. Hence $(1-\omega_0)$ represents the remaining portion, which has been transformed into other forms of energy or of radiations of other wavelengths. Now replacing the integrals by Gaussian sums by the method suggested by Chandrasekhar (Radiative Transfer, p. 364), the equation of transfer (1) is reduced to an equivalent system of linear equations in a finite approximation, which can be combined into the equation given below.

$$\frac{d}{dr} \Sigma a_i \mu_i P_l'(\mu_i) I_i + \frac{l(l+1)}{r} \Sigma a_i P_l(\mu_i) I_i = -k\rho \Sigma a_i P_l'(\mu_i) I_i + \frac{1}{2} k\rho \omega_0 \Sigma a_i I_i \Sigma a_i P_l'(\mu_i) \quad \dots \quad (3)$$

where $(i = \pm 1, \pm 2, \dots, \pm n)$ and $(l = 1, 2, \dots, 2n)$.

Using known expressions for Legendre's polynomials, equation (3) for $l = 1$ and $l = 2$ becomes respectively

$$\frac{d}{dr} \Sigma a_i \mu_i I_i + \frac{2}{r} \Sigma a_i \mu_i I_i = -k\rho(1-\omega_0) \Sigma a_i I_i \quad \dots \quad (4)$$

and

$$\frac{d}{dr} \Sigma a_i \mu_i^2 I_i + \frac{1}{r} \Sigma a_i (3\mu_i^2 - 1) I_i = -k\rho \Sigma a_i \mu_i I_i \quad \dots \quad (5)$$

$$\text{Now putting } \frac{1}{2} \Sigma a_i I_i = J, \quad 2 \Sigma a_i \mu_i I_i = F, \text{ and } \frac{1}{2} \Sigma a_i \mu_i^2 I_i = K \quad \dots \quad (6)$$

and remembering that in the first approximation the radiation field is divided into an outward stream I_{+1} and an inward stream I_{-1} and that $a_{+1} = a_{-1} = 1$,

$$\mu_{+1} = -\mu_{-1} = \frac{1}{\sqrt{3}} \text{ and } \mu_i \text{'s are the zeros of } P_2(\mu_i) \quad \dots \quad (7)$$

$$\text{and } \therefore \Sigma a_i P_2(\mu_i) I_i = 0 \text{ or } 3K - J = 0 \text{ or } J = 3K \quad \dots \quad (8)$$

we see that the equations (4) and (5) take the forms

$$\frac{dF}{dr} + \frac{2F}{r} = -12k\rho(1-\omega_0)K \quad \dots \quad (9)$$

and

$$4 \frac{dK}{dr} = -k\rho F \quad \dots \quad (10)$$

It is well known that in the astrophysical contexts $k\rho$ varies as an inverse power of r (greater than unity)

$$\therefore k\rho = Cr^{-n}, \text{ where } C \text{ is a constant} \quad \dots \quad (11)$$

The optical thickness τ measured from $r = \infty$ inwards has the value

$$\tau = \int_r^\infty k\rho dr = \frac{Cr^{-n+1}}{n-1} \quad \dots \quad (12)$$

From (11) and (12)

$$k\rho r = (n-1)\tau \quad \dots \quad (13)$$

$$\text{and } d\tau = -k\rho dr \quad \dots \quad (14)$$

From (10)

$$4 \frac{dK}{d\tau} = F \quad \dots \quad (15)$$

Eliminating F from equation (9)

$$\frac{d^2 K}{d\tau^2} - \frac{2}{(n-1)\tau} \cdot \frac{dK}{d\tau} - 3(1-\omega_0)K = 0 \quad \dots \quad (16)$$

Putting $K = z^\nu f(z)$, where $z = q\tau$, $q = \sqrt{3(1-\omega_0)}$ and $\nu = \frac{n+1}{2(n-1)}$.. (17)

and substituting in equation (16), we get

$$z^2 \frac{d^2 f}{dz^2} + z \frac{df}{dz} - (z^2 + \nu^2)f = 0 \quad \dots \quad (18)$$

This is Bessel's equation for imaginary arguments and its solutions are known. The fundamental solutions are $I_\nu(z)$ and $K_\nu(z)$. The general solution is

$$f(z) = C_1 I_\nu(z) + C_2 K_\nu(z) \quad \dots \quad (19)$$

3. If the atmosphere is supposed to extend to $r = \infty$, C_1 and C_2 can be evaluated under the following boundary conditions:

(i) Vanishing of both outward and inward intensities and hence of both flux and K -integral at the outer boundary of the atmosphere denoted by $\tau = 0$, $z = 0$;

(ii) the existence of a definite outward flux at the lower bound of the photosphere, denoted by $\tau = \tau_1$, $z = z_1$.

That is, from the inner bound is emerging a given flux and overlying this boundary, there exists an envelope scattering according to a constant albedo for single scattering ($\omega_0 = \text{Constant}$), whose value is less than unity. The atmosphere is supposed to be so extensive that the flux and the K -integral simultaneously vanish at the outer boundary of the atmosphere.

In order that K -integral may vanish at $\tau = 0$ or $z = 0$, $z^\nu f(z) \rightarrow 0$ as $z \rightarrow 0$ by (17). But it is found that while $z^\nu I_\nu(z) \rightarrow 0$ for $z \rightarrow 0$, $z^\nu K_\nu(z)$ tends to a limiting value (not equal to zero) as $z \rightarrow 0$. Hence for K to be zero at $z = 0$, we put $C_2 = 0$ and

$$f(z) = C_1 I_\nu(z) \quad \dots \quad (20)$$

At $\tau = \tau_1$ or $z = z_1$, the intensity of the inward radiation is negligible in comparison with the intensity of the outward radiation. Let the outward flux at this surface be $F(z_1)$.

The flux and the K -integral at the inner boundary are given in the first approximation by the well-known relations

$$F(z) = \frac{2}{\sqrt{3}} I_{+1}(z) \quad \dots \quad (21)$$

and
$$K(z_1) = \frac{I_{+1}(z_1)}{6} = \frac{1}{4\sqrt{3}} F(z_1) \quad \dots \quad (22)$$

[The present $I_{+1}(z_1)$ and $K(z_1)$ are not to be confused with $I_\nu(z)$ and $K_\nu(z)$, the solutions of Bessel Equation in (19)]

But from (17),

$$f(z_1) = \frac{K(z_1)}{z_1^\nu} = \frac{F(z_1)}{4\sqrt{3} z_1^\nu} \quad \dots \quad (23)$$

$$\therefore C_1 = \frac{f(z_1)}{I_\nu(z_1)} = \frac{F(z_1)}{4\sqrt{3} I_\nu(z_1) z_1^\nu} \quad \dots \quad (24)$$

$$\therefore f(z) = \frac{F(z_1)}{4\sqrt{3} I_\nu(z_1) z_1} I_\nu(z) \quad \dots \quad (25)$$

Hence at any depth z .

$$K(z) = z^\nu f(z) \quad \dots \quad (26)$$

$$J(z) = \frac{1}{3} K(z)$$

The source function

$$\tilde{f}(z) = \frac{\omega_0}{3} z^\nu f(z) \quad \dots \quad (27)$$

$$F(z) = 4q \frac{dK(z)}{dz} = q \frac{F(z_1)}{\sqrt{3} z_1^\nu I_\nu(z_1)} z^\nu I_{\nu+1}(z) \quad \dots \quad (28)$$

Thus for given values of q , z_1 and $F(z_1)$ the K -integral, the flux, the energy density and the source-function can be evaluated.

4. A special case may now be considered, where the outer boundary is taken to be the surface, which looks equally bright from both sides. On this surface the net flux is zero, not because the inward and outward intensities simultaneously vanish, but because the inward and outward intensities are equal. The atmosphere under this circumstance is finite but yet sufficiently large to validate the approximation

$$\tau = \int_r^R k\rho dr \approx \frac{Cr^{n+1}}{n-1}$$

($r = R$ denoting the outer boundary is extremely large) and hence

$$k\rho r = (n-1)\tau \text{ and } d\tau = -k\rho dr$$

To realise the above conditions for this configuration the measurement of optical depth is made from a surface somewhat lower than the boundary fixed in the previous case, where the above condition is supposed to obtain. Or, as an alternative, we can consider the star to be in a weak radiation bath. The boundary is defined as the surface on which outward flow of radiation is balanced by the inward stream due to the surrounding field. As the atmosphere is very extensive, both the intensities will be very feeble. So the term containing reduced incident radiation in the transfer equation can be ignored and the original equation of transfer adapted to the present case.

Under the circumstances mentioned above, the constants in the general equation (19) may be evaluated under the following boundary conditions:—

(i) at the outer boundary denoted by $\tau = 0$, $z = 0$, $K = K(0) = \text{Constant}$ and $F = F(0) = 0$.

(ii) at the inner boundary denoted by $\tau = \tau_1$, $z = z_1$, flux $F(z) = F(z_1)$. This flux is always outwards as the inward flux at the lower bound of the photosphere may be neglected in comparison with the outward one.

From (17) and (19)

$$K(z) = z^\nu f(z) = C_1 z^\nu I_\nu(z) + C_2 z^\nu K_\nu(z) \quad \dots \quad (30)$$

Applying the first boundary condition, the K -integral at $\tau = 0$ or $z = 0$ is given by

$$K(0) = C_2 \times \lim_{z \rightarrow 0} (z^\nu K_\nu(z)) \quad \dots \quad (31)$$

If n is taken to be equal to 2,

$$\nu = \frac{n+1}{2(n-1)} = \frac{3}{2} \quad \dots \quad \dots \quad \dots \quad \dots \quad (32)$$

$$\lim_{z \rightarrow 0} z^{\frac{1}{2}} K_{\frac{3}{2}}(z) = \sqrt{\frac{\pi}{2}} \quad \dots \quad \dots \quad \dots \quad \dots \quad (33)$$

$$C_2^* = K(0) \left(\frac{2}{\pi} \right)^{\frac{1}{2}} \quad \dots \quad \dots \quad \dots \quad \dots \quad (34)$$

Using the second boundary condition, C_1 can be evaluated. If at the lower boundary given by $\tau = \tau_1$ or $z = z_1$, $K(z) = K(z_1)$

$$C_1 = \frac{K(z_1)}{z_1^{\nu} I_{\nu}(z_1)} - \left(\frac{2}{\pi} \right)^{\frac{1}{2}} K(0) \frac{K_{\nu}(z_1)}{I_{\nu}(z_1)} \quad \dots \quad \dots \quad \dots \quad (35)$$

Hence

$$f(z) = \left\{ \frac{K(z_1)}{z_1^{\nu} I_{\nu}(z_1)} - \left(\frac{2}{\pi} \right)^{\frac{1}{2}} K(0) \frac{K_{\nu}(z_1)}{I_{\nu}(z_1)} \right\} I_{\nu}(z) + \left(\frac{2}{\pi} \right)^{\frac{1}{2}} K(0) K_{\nu}(z) \quad \dots \quad (36)$$

The value of K -integral at any depth is given by

$$\frac{K(z)}{K(0)} = \left\{ \frac{K(z_1)}{K(0)} \cdot \frac{1}{z_1^{\nu} I_{\nu}(z_1)} - \left(\frac{2}{\pi} \right)^{\frac{1}{2}} \frac{K_{\nu}(z_1)}{I_{\nu}(z_1)} \right\} z^{\nu} I_{\nu}(z) + \left(\frac{2}{\pi} \right)^{\frac{1}{2}} K_{\nu}(z) z^{\nu} \quad \dots \quad (37)$$

$$\therefore \frac{K(z)}{K(0)} = A z^{\nu} I_{\nu}(z) + \left(\frac{2}{\pi} \right)^{\frac{1}{2}} K_{\nu}(z) z^{\nu} \quad \dots \quad \dots \quad \dots \quad (38)$$

where

$$A = \frac{K(z_1)}{K(0)} \cdot \frac{1}{z_1^{\nu} I_{\nu}(z_1)} - \left(\frac{2}{\pi} \right)^{\frac{1}{2}} \frac{K_{\nu}(z_1)}{I_{\nu}(z_1)} \quad \dots \quad \dots \quad (39)$$

and

$$J(z) = \frac{1}{3} K(z), \quad \mathcal{F}(z) = \frac{\omega_0}{3} K(z) \quad \dots \quad \dots \quad \dots \quad (40)$$

And $F(z)$ at any depth is given by

$$\frac{F(z)}{K(0)} = 4q \frac{d}{dz} \left(\frac{K(z)}{K(0)} \right) = 4q \left[A z^{\nu} I_{\nu-1}(z) - \left(\frac{2}{\pi} \right)^{\frac{1}{2}} z^{\nu} K_{\nu-1}(z) \right] \quad \dots \quad (41)$$

Thus knowing the values of ω_0 , z_1 , and $\frac{K(z_1)}{K(0)}$, we can evaluate $\frac{K(z)}{K(0)}$, $\frac{F(z)}{K(0)}$

$\frac{J(z)}{K(0)}$ and $\frac{\mathcal{F}(z)}{K(0)}$ in the present case.

5. The boundary condition at the outer boundary allows us to divide the total flux there into two equal fluxes $F_{+1}(0)$ and $F_{-1}(0)$ meaning the outward and inward fluxes respectively at $\tau = 0$ and $z = 0$. Now, expressing the K -integrals and fluxes at the inner and outer boundary in terms of inward and outward intensities, it is possible for us to find out an expression for the ratio of the outward fluxes at the inner and outer surface in terms of q and z_1 . Fixing the value of q , it is possible to draw up a table showing the relation between $\frac{F(z_1)}{F_{+1}(0)}$ and z_1 and plot $\frac{F(z_1)}{F_{+1}(0)}$ against z_1 in a curve.

We know that

$$K(z_1) = \frac{1}{2} \Sigma a_i \mu_i^2 I_i = \frac{1}{6} (I_{+1}(z_1) + I_{-1}(z_1)) \approx \frac{1}{6} I_{+1}(z_1) \quad \dots \quad \dots \quad (42)$$

$$F(z_1) = 2 \Sigma a_i \mu_i I_i = \frac{2}{\sqrt{3}} (I_{+1}(z_1) - I_{-1}(z_1)) \approx \frac{2}{\sqrt{3}} I_{+1}(z_1) \quad \dots \quad (43)$$

as at the inner boundary inward intensity is negligible in comparison with the outward.

$$\therefore K(z_1) = \frac{\sqrt{3}}{12} F(z_1) \quad \dots \quad (44)$$

At the outer boundary total flux is equal to zero, and the K -integral is $K(0)$.

$$\therefore \left. \begin{aligned} F(0) &= \frac{2}{\sqrt{3}} (I_{+1}(0) - I_{-1}(0)) = 0 \\ \therefore I_{+1}(0) &= I_{-1}(0) \end{aligned} \right\} \quad \dots \quad (45)$$

$$K(0) = \frac{1}{6} (I_{+1}(0) + I_{-1}(0)) = \frac{1}{3} I_{+1}(0) \quad \dots \quad (46)$$

$$\text{and } F_{+1}(0) = \frac{2}{\sqrt{3}} I_{+1}(0), \quad K(0) = \frac{F_{+1}(0)}{2\sqrt{3}} \quad \dots \quad (47)$$

$$\therefore \frac{K(z_1)}{K(0)} = \frac{1}{2} \frac{F(z_1)}{F_{+1}(0)}, \quad \text{and } \frac{F(z_1)}{K(0)} = 2\sqrt{3} \frac{F(z_1)}{F_{+1}(0)} \quad \dots \quad (48)$$

Now putting $z = z_1$ in equation (41)

$$\frac{F(z_1)}{F_{+1}(0)} = \frac{4qz_1^{\nu-1}}{(2\pi)^{\frac{1}{2}} [qI_{\nu-1}(z_1) - \sqrt{3} I_{\nu}(z_1)]} \quad \dots \quad (49)$$

The values of this ratio for different values of τ_1 and hence z_1 are shown in the following table for different values of ω_0 . Three cases have been considered, namely $\omega_0 = 90\%$, $\omega_0 = 67\%$, $\omega_0 = 10\%$

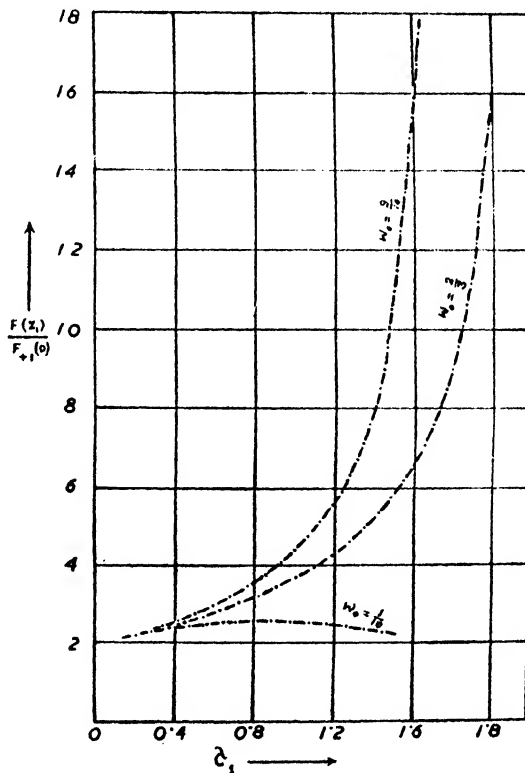


Fig. 4.

TABLE

z_1	$\omega_0 = 90\%$		$\omega_0 = 67\%$		$\omega_0 = 10\%$	
	τ_1	$\frac{F(z_1)}{F_{+1}(0)}$	τ_1	$\frac{F(z_1)}{F_{+1}(0)}$	τ_1	$\frac{F(z_1)}{F_{+1}(0)}$
0.2	0.36	2.49	0.2	2.25	0.12	2.13
0.3	0.55	2.86	0.3	2.38	0.18	2.20
0.4	0.73	3.32	0.4	2.52	0.24	2.26
0.5	0.91	4.00	0.5	2.68	0.30	2.32
0.6	1.10	4.94	0.6	2.85	0.36	2.38
0.7	1.28	6.44	0.7	3.02	0.43	2.42
0.8	1.46	9.42	0.8	3.24	0.49	2.47
0.9	1.64	17.61	0.9	3.46	0.55	2.51
1.0	1.83	156.5	1.0	3.71	0.61	2.54
1.1	1.1	3.98	0.67	2.56
1.2	1.2	4.33	0.73	2.59
1.3	1.3	4.74	0.79	2.60
1.4	1.4	5.23	0.85	2.62
1.5	1.5	5.86	0.91	2.62
1.6	1.6	6.62	0.97	2.62
1.7	1.7	7.62	1.03	2.60
1.8	1.8	9.26	1.10	2.59
1.9	1.9	11.66	1.16	2.57
2.0	2.0	15.81	1.22	2.54
2.14	1.30	2.49
2.30	1.40	2.43
2.46	1.50	2.36

The variation of the ratio of the outward fluxes of radiation at the inner and outer boundaries of an atmosphere with a surface slowly merging into an external radiation field, with optical depth has been plotted in Fig. 1. The atmosphere considered is an extensive one. So that the flux ratios obtained for small z_1 are unreliable. For $\omega_0 = 90\%$, beyond $z_1 = 1.1$, the value of the flux ratio increases very fast (tending to infinity). The curves for $\omega_0 = 90\%$ and $\omega_0 = 67\%$ show remarkable similarity of behaviour. But for $\omega_0 = 10\%$, i.e. for small scattering, the curve behaves in a different manner. According to the present theory, the curve in this case is very flat and gradually approaches a limiting value, a large value of flux ratio never being attained in this case.

It is a pleasure to acknowledge my indebtedness to Prof. N. R. Sen for his constant advice and helpful discussions, during the preparation of this work.

ABSTRACT

The equation of transfer of radiation in spherically symmetric atmosphere for non-conservative isotropic scattering has been solved by the method of Chandrasekhar in which integrals are replaced by corresponding Gaussian sums, and first approximation results have been fitted to two boundary conditions, one of no incident radiation and the other of a very weak radiation field penetrating from outside. In the second case the variation of outward flux with optical depth for very large, moderate and weak scattering has been worked out and the results shown in a diagram.

REFERENCES

- Chandrasekhar, S. (1934). Radiative equilibrium of Extended Stellar Atmospheres. *Monthly Notices, Roy. Astro. Soc., London*, **94**, 444-457.
 Chandrasekhar, S. (1945). On the Radiative Equilibrium of a stellar Atmosphere—V. *Astrophysical Journal*, **101**, 95-107.
 Kosirev, N. A. (1934). Radiative Equilibrium of Extended Stellar Photospheres. *Monthly Notices, Roy. Astro. Soc., London*, **94**, 430-443.

STUDY ON THE STATE OF DISPERSOID IN THE COLLOIDAL COLOURED GLASS

by B. K. BANERJEE, *I.C.I. Research Fellow, N.I.S.I., Indian Association for the Cultivation of Science, Calcutta 32*

(Communicated by K. Banerjee, F.N.I.)

(Received August; 1 read October 9, 1953.)

INTRODUCTION

The understanding of the correct mechanism of the coloration of the ruby glass is a long-standing problem. The ruby glass covers the whole type of colloidal coloured glasses such as gold ruby, copper ruby, etc. Along with that the glasses coloured by Ag and Pt need be studied because they belong to the same class of ruby glass but they are of different colours. In course of the preparations of the above glasses, two operations are required: (1) preparation of colourless transparent glass, and (2) development of colour by heat-treatment.

All workers are unanimous that the coloration of the glass is due to the fine suspension of the metal. But there is much controversy regarding the state of existence of metal in colourless glass. Zsigmondy (1909), Weyl (1945), etc., believe that metals like Au and Pt exist in atomic form or in a form of nucleus in the colourless glass while Silverman (1931), Stookey (1949), etc., believe that the metal exists in oxidised state in the above glass. In the present paper the above problem about the state of existence of the metal in the colourless glass has been studied in borate and sodasilica glass where the solubility of metal is appreciable in comparison with usual silicate glass. Along with that the effect of concentration of the dispersed phase and heat-treatment on the size of the metal particle has been studied. It is worthwhile to mention here that as the size of the particle increases, the scattering of the incident light comes into prominence. Although some works have been done in the above direction, yet it is expected that the above investigation will give some valuable information about the different stages of the dispersed phase during the development of colour in above glass specimens. Use has been made of both chemical and physical methods so as to study the following problems: (1) the state of existence of the dispersoid in colourless glass specimen, (2) to study the effect of heat-treatment on the colour and the size of the suspensoid, (3) the relation between the concentration and the size of the suspensoid in the glassy matrix, (4) to determine the size of the suspensoid by the X-ray method, (5) to study the effect of concentration of the dispersoid on the characteristic diffraction pattern of the original glass base.

CHEMICAL STUDY OF COLOURLESS GLASS SPECIMEN

Glass specimens of $M\text{-B}_2\text{O}_3$, M-borax and M-Lindemann and M-soda-silica glass (where M stands for Au, Pt or Ag) were prepared in the Pt-crucible in an electric furnace and in complete absence of any reducing agent. In all these glass samples M can be dispersed to an appreciable extent as for example, Au can be dispersed in borate and soda-silica glass with 25% soda content to the extent

of 2.45% and 0.20% respectively. Colourless transparent glass was obtained by rapidly quenching the melt in a low temperature, but in course of that operation it is observed that some high M (especially Au) content specimens exhibit coloration even when rapidly quenched. However, some colourless specimens of each series were prepared. All the borate glass specimens are moderately soluble in water and the solubility of soda-silicate glass in water is quite appreciable. In colourless specimens in order to find out whether M can exist in atomic or ionic form or can form a compound with the glass-solvent, the aqueous solution of 2 gm. of 0.5% M content borax and B_2O_3 glass and that of 4 gm. of 0.1% M content of soda-silica glass were subjected to the following chemical reaction.

With NaCl solution, a precipitate of AgCl was obtained from a clear solution of silver glass and that indicated the presence of Ag ion in solution. Again with the addition of dil. HNO_3 to the filtrate after the separation of AgCl, a further precipitate of AgCl although very small in amount was obtained and that indicated the presence of Ag in the elemental state. Whereas in a clear solution of gold and Pt-glass no evidence of metal in the ionic state was found when the respective solution was treated with specific test for Au^{+++} ion such as alkali iodide in alkaline solution and the above operation indicated absence of metal in the oxidised state. But in the solution of Au or Pt-glass in aqua regia, when treated similarly as above, evidence of metal in the ionic state was obtained and that indicated the presence of elemental metal in glass. Thus it is obvious from the above operation that Ag remains in the glass in both elemental and ionic state whereas Au and Pt exist only in the elemental state in glass. Further it has been corroborated by the fact that up to this time any borate or silicate of Au and Pt is not known, while Ag can form both borate and silicate.

THE EFFECT OF HEAT-TREATMENT ON THE SIZE OF THE DISPERSOID

It has been stated before that during the heat-treatment of colourless specimen, the coloration of glass takes place. The duration of heating and temperature of heat-treatment vary with the nature of glass composition. It has been suggested by Zsigmondy that the development of coloration in glass is controlled by the relative rate of two distinct processes: (1) nucleus formation, (2) the speed of crystal growth where nucleus is a colourless discrete particle containing a number of atoms just sufficient for the thermodynamic stability and the crystal growth is a process in which additional material deposits on this particle causing it to increase in size. These two functions are independent of changes of temperature, both of them having maxima, more or less pronounced at different temperatures, and they cause crystallisation of the dispersed phase. The above process of crystallisation of the dispersed phase is quite distinct from the devitrification.

The relation between the concentration and the size of the suspensoid

In connection with the size of the dispersoid of different coloured glasses, having the same or different metallic colourant, of different glass compositions, but of same or different thermal history, the size of the dispersoid has been determined by the X-ray method. The present investigation also includes some specimens of AgCl-borax glass. During the course of our study of different glass specimens, we have found that the width of the line of the dispersed phase in the X-ray picture decreases gradually with the rise of concentration of the dispersed phase, and that is due to the increase of particle size and the details of the particle size measurement have been discussed in the following sections.

Particle size of suspensoids in colloidal coloured glass

The relation between the particle size and the width of the diffraction line at half maximum intensity was proposed by Scherrer (1920) on the assumption that the radiation was parallel and the sample was transparent by the following equation—

$\beta = \frac{k\lambda}{L \cos \theta} + b$, where β = the breadth of diffraction interference at points of half-maximum intensity, expressed in radians.

λ = wavelength of X-rays.

L = the edge length of the crystal considered as cubic.

θ = the angle of diffraction.

b = the natural breadth of the Debye-Scherrer diffraction line which is a constant depending upon the particular apparatus, size, and absorption of the specimen.

k = a constant, the value of which is 0.9. It must be pointed out that the above two assumptions of Scherrer are difficult to realise in practice.

An equation similar to Scherrer was derived by Seljakov, Bragg, Laue (1926), etc. Laue derived an equation which in its most general form permits the size evaluation in different directions on the assumption that the radiation was purely divergent. The general form of that equation is as follows:—

$$\beta = \frac{\pi n \left(\frac{r}{R} \right)^2 \cos^3 \theta}{\sqrt{1 + \left(\frac{wr}{nR} \cos^2 \theta \right)^2} - 1}$$

β = absolute corrected value of the breadth in angular measure.

θ = angle of reflection.

w = a constant (0.55).

r = specimen radius.

R = radius of camera.

n is a quantity related to the particle size by a complex expression which, for cubic crystals, reduces to

$$n = \frac{\lambda}{4\pi\Delta}$$

where Δ = edge length of the particle. Later on Brill (1928), Brill and Pelzer (1931) and a few other workers published some interesting accounts of the limitation of the above equations and suggestions of some new equations and procedure considering the nature of the experimental specimen.

It is worth while to mention here that in the case of colloidal coloured glass specimens, we are confronted with some difficulties such as weak lines, the presence of diffuse bands of glass which in some cases superimpose on strong lines, absorption factor of glass base, etc., and some of the details of X-ray photographs have been given in our previous paper (1953). The particle size of the dispersoids of some glass specimens has been measured in the usual process. The X-ray pictures were photometered on a Moll's recording microphotometer. The angular width at half-maximum intensity is measured from the curves after converting the above curves into densities with the help of a standard wedge in the usual process. Again, in the evaluation of the particle size, broadening due to instrumental factor has

been considered. The average particle size of some dispersoids is* given in the following table :—

TABLE I

Glass composition.	Sample No.	Concentration of dispersoids.	Average particle size.
Pt-borax ..	1	0.75%	89 A
Pt-borax ..	2	0.975%	120 A
Pt-borax ..	3	1.63%	228 A
Pt-B ₂ O ₃ ..	4	0.80%	124 A
Pt-B ₂ O ₃ ..	5	1.62%	243 A
Pt-Lindemann ..	6	0.61	60 A
Pt-Lindemann ..	7	0.75%	100 A
Pt-Lindemann ..	8	1.75%	243 A
Ag-borax ..	9*	0.50%
Ag-borax ..	10	1.50%	115 A
Ag-borax ..	11	3.50%	275 A
AgCl-borax ..	12*	0.45%
AgCl-borax ..	13	1.20%	86 A
AgCl-borax ..	14	3.20%	139 A

* Lines of the dispersoid are too weak for the correct evaluation of half-width.

Thus it is quite evident from the table that the concentration of the dispersed phase decides the ultimate size of the particle and the size of the particle increases with concentration in the same series, when other factors such as glass composition, thermal history, etc., are the same. The average size of the particle lies within the range of colloidal particle. We may mention here that in transparent coloured glass the amount of colloidal particle does not represent the whole of the dispersed phase, because along with the colloidal form, there is a possibility of existence of atomic form or nucleus form in the glassy matrix. However, the size and the number of colloidal particles will be increased by the diffusion process at the cost of atomic form of the dispersed metal, ultimately by prolonged heat-treatment, the whole of the dispersed phase is precipitated thereby causing a drastic change in colour and transparency of the glass. That has been amply demonstrated by X-ray study of a transparent Ag-borax glass which initially did not reveal the presence of crystalline Ag, but after prolonged heat-treatment for six hours at 550°C. that particular specimen revealed the presence of big crystallites of Ag which was indicated by the discontinuous lines of Ag in the diffraction photograph of glass specimen.

NATURE OF THE GLASS BAND

It is well known that the X-ray diffraction pattern of oxide glass consists of bands only and from the analysis of the diffraction pattern, valuable informations concerning the interatomic distance between the atoms and the co-ordination number of cation are known. In connection with that work the rôle of different cations in the glass composition has been understood with considerable success. Warren and his associates (1938, 1942) have done a considerable amount of work on the above problem. But the colloidal coloured glass deviates from the usual oxide glass by the existence of fine suspensoid of metal in the glassy matrix. During the course of investigation comprising several coloured glasses, it is found that the characteristics of the diffuse band of pure glass remain unchanged in coloured silicate, B₂O₃, borax and Lindemann glass. Only with the rise of concentration of the dispersed phase, there is an increase of diffuseness and lowering of intensity

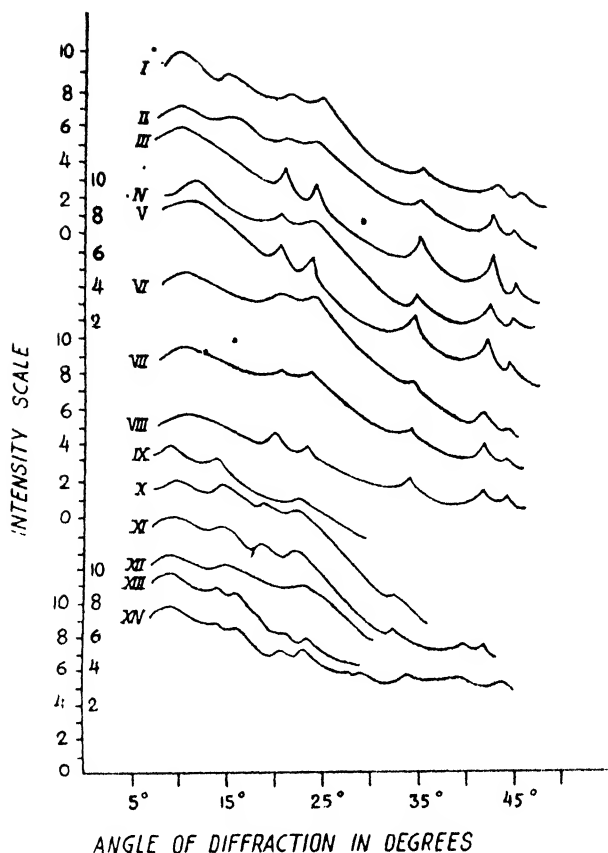


FIG. 1.

Maximum of every curve is taken as 10 units. Photometric curves of samples I, IV, VII, XIII and XIV with intensity Units have been shown in the above figure. Details of each sample have been given in Table I.

of the bands (*vide* photometric curves of samples of the same glass base with increasing concentration of solute, for example, Sp. 1, 2, 3; Sp. 4, 5; Sp. 6, 7, 8; Sp. 9, 10, 11; and Sp. 12, 13, 14, in Fig. I) and that is due to the increase of randomness in the respective glass structure in addition to the high absorption coefficient factor of the dispersed phase. The photometric curves of X-ray diffraction pattern of some glass series are given in Fig. I.

ABSTRACT

This paper comprises the information about the different stages of the dispersed phase during the development of colour in the colloidal coloured glass samples. The nature of the dispersed phase, the relation between the size of the dispersoid with concentration as well as with heat-treatment and the influence of the dispersoid on the characteristics of the diffuse band of the original glass base have been studied. It is found that Ag remains in both elemental and ionic state in glassy matrix while Au and Pt exist mainly in the elemental state.

ACKNOWLEDGEMENTS

I am thankful to Prof. K. Banerjee for his keen interest and guidance throughout the progress of the work. Thanks are also due to Dr. A. Bose for his keen interest in the work. I am also thankful to the Council of National

Institute of Sciences of India for the award of an I.C.I. Research Fellowship to me and also to the authorities of the Indian Association for the Cultivation of Science for laboratory and other facilities.

REFERENCES

- Banerjee, B. K. (1953). X-ray study of Colloidal coloured glasses. *Proc. Nat. Inst. Sci.*, **19**, 291.
- Banerjee, B. K. (1953). Colloidal coloured silica glass. *Proc. Nat. Inst. Sci.*, **19**, 491.
- Banerjee, B. K. (1953). Colloidal coloured silver glasses. *Proc. Nat. Inst. Sci.*, **19**, 495.
- Brill, R. (1928). Teilchengrossen-bestimmungen mit Hilfe von Rontgenstrahlen. *Z. Krist.*, **68**, 387.
- Brill, R. and Pelzer (1931). Rontgenographische Teilchengrossen-bestimmung. *Ibid.*, **72**, 398.
- Lau, M. V. (1926). Lorentz-Faktor and Intensitatsverteilung in Debye-Scherrer-Ringen. *Ibid.*, **64**, 115.
- Scherrer, P. (1920). Bestimmung der innern Struktur and der Grosse von Kolloidteilchen mittels Rontgenstrahlen. *Kolloid-Chemie*, **3**, 387.
- Silverman, A. (1931). Colloid Chemistry, Vol. 3, 283.
- Stokey, S. D. (1949). Coloration of glass by gold, silver and copper. *J. Am. Ceram. Soc.*, **32**, 246.
- Warren, B. E. and Biscoc, J. (1938). Structure of soda-boric oxide glass. *J. Am. Ceram. Soc.*, **21**, 287.
- Warren, B. E. (1942). Basic principles involved in glassy state. *J. Applied Physics*, **13**, 602.
- Weyl, W. A. (1945). Coloured glasses - IV. *J. Soc. Glass Tech.*, **29**, 291.
- Zsigmondy, R. (1909). Colloids and Ultramicroscope, 1st edition. Translated by Jerome Alexander, p. 245.

Issued January 29, 1954.

ON LATTICE COVERINGS BY SPHERES

by R. P. BAMBAH, *The Institute for Advanced Study, Princeton, U.S.A. and Punjab University College, Hoshiarpur.*

(Communicated by H. Gupta, F.N.I.)

(Received January 13; read October 9, 1953.)

1. The object of this paper is to obtain the most economical lattice coverings of the three-dimensional Euclidean space by equal spheres.

Let K be a body in n dimensions and Λ a lattice such that every point of the n -dimensional space lies in one at least of the bodies obtained from K by applying to it all possible lattice translations. Then we say that Λ is a *covering lattice* for K . If K is bounded, the ratio of the total volume of the bodies K to whole space (in the obvious * sense) is $V(K)/d(\Lambda)$, where $V(K)$ is the volume of K and $d(\Lambda)$ the determinant of Λ . This ratio $V(K)/d(\Lambda)$ is called the density of the lattice covering by K provided by Λ . The lower bound $\theta(K)$ of $V(K)/d(\Lambda)$ taken over all covering lattices Λ for K is called the *density of the most economical coverings by K* and the coverings with this density are called the most economical lattice coverings. Their existence for convex bodies was proved by Hlawka.†

The problem of most economical or thinnest lattice coverings is connected with an interesting type of Diophantine inequalities, an example of which is provided by Theorem 2.

The analogous problem of closed lattice packings has been studied for a long time mainly because of its connection with another type of Diophantine inequalities. But the problem of thinnest coverings has only recently started attracting the attention it deserves and within the last few years a number of interesting results have been obtained. However, the value of $\theta(K)$ is known only for convex bodies in two dimensions, where the problem is equivalent to finding the largest symmetrical hexagon contained in K .‡ The results of this paper seem to be the first § exact results in dimensions higher than the second.

For spheres in n -dimensions Davenport || has proved that for large n ,

$$\theta(K) < (1.15)^n,$$

and Bambah and Davenport ¶ have shown that

$$\theta(K) > 4/3 - \epsilon_n, \quad \epsilon_n \rightarrow 0 \text{ as } n \rightarrow \infty.$$

Our results can be stated as

THEOREM 1:—Let K be a sphere in three-dimensional Euclidean space and $\theta(K)$, the density of the most economical lattice covering by K .

* Let X be a cube of side L and N , the number of bodies K having a point in common with X . Then the ratio is defined as $\lim_{L \rightarrow \infty} NV(K)/L^n$, where $V(K)$ is the volume of K .

† *Monat. Math.*, 53 (1949), 81–131.

‡ See Fáry, I., *Bull. de la Société Math. de France*, 78 (1950), 152–161.

§ Except, of course, for a number of space filling polyhedra.

|| *Rend. di Palermo*, Ser. II, vol. 1 (1952), 1–16.

¶ *Jour. Lond. Math. Soc.*, 27 (1952), 224–229.

Then

$$\theta(K) = J_3 \frac{5\sqrt{5}}{32}, \quad \dots \quad (1)$$

where $J_3 = \frac{4}{3}\pi$ is the volume of a unit sphere.

Further, a lattice Λ provides the most economical lattice covering* by K if and only if by a suitable choice of orthogonal axes, Λ is generated by the points

$$\frac{2r}{\sqrt{5}}(-1, 1, 1), \frac{2r}{\sqrt{5}}(1, -1, 1), \frac{2r}{\sqrt{5}}(1, 1, -1).$$

and K has the equation

$$x^2 + y^2 + z^2 = r^2.$$

It can be easily shown † that Theorem 1 is equivalent to

THEOREM 2:—Let $f(x, y, z) = ax^2 + by^2 + cz^2 + 2ryz + 2syz + 2txy$ be a positive definite quadratic form with real coefficients and determinant $D > 0$. Then there exist real numbers x_0, y_0, z_0 , such that for all integers x, y, z , we have

$$f(x+x_0, y+y_0, z+z_0) \geq \left(\frac{125}{1024} D\right)^{\frac{1}{3}}, \quad \dots \quad (2)$$

the sign of equality being necessary if and only if

$$f \sim \rho(3x^2 + 3y^2 + 3z^2 - 2yz - 2zx - 2xy), \quad \dots \quad (3)$$

and $\rho > 0$ is any real number.‡

It will follow from our proof that

THEOREM 3:—Let Π be the largest convex space-filling§ polyhedron that is contained in K . Then Π has seven pairs of opposite faces and all the vertices of Π lie on the surface of K .

I am grateful to Professor H. Davenport for a very useful correspondence. I am also indebted to Prof. H. S. M. Coxeter for useful comments.

2. Let $f(x, y, z) = ax^2 + by^2 + cz^2 + 2ryz + 2syz + 2txy$ be a positive definite form. We shall denote its determinant by D_f or by D , when there is no danger of confusion. Let (ξ, η, ζ) be any set of real numbers. Denote by $m_f(\xi, \eta, \zeta)$ the minimum of $f(\xi-x, \eta-y, \zeta-z)$ for integers x, y, z . Let m_f be the upper bound of $m_f(\xi, \eta, \zeta)$ for all sets (ξ, η, ζ) . Then Theorem 2 is equivalent to saying that

$$m = \underline{bd} M_f = \underline{bd} \left(\frac{m_f}{D_f^{\frac{1}{3}}}\right) = \left(\frac{125}{1024}\right)^{\frac{1}{3}} \quad \dots \quad (4)$$

the lower bound being taken over all forms f , and that m is attained by those forms and those alone which are equivalent to $\rho(3x^2 - 2yz)$.

* Prof. Coxeter points out that this lattice is the 'body centred' cubic lattice of crystallographers and that its Dirichlet region is the truncated octahedron (so named by Kepler in 1619).

† See, e.g., Davenport, loc. cit.

‡ It is interesting to remark that the critical forms here are reciprocal to the form $\mu(x^2 + yz)$, which are critical in the packing case.

§ I.e., $\theta(\Pi) = 1$.

·OUTLINE OF PROOF

3. We first observe that the expression $M_f = \frac{m_f}{D_f^{\frac{1}{2}}}$ is invariant under integral uni-modular linear substitutions on the variables x, y, z . Consequently we can suppose, without loss of generality, that f is reduced in the sense of Seeber*, i.e. the coefficients a, b, c, r, s, t satisfy the relations

$$0 < a \leq b \leq c, \quad \dots \dots \dots (6)$$

$$2|s|, 2|t| \leq a, \quad 2|r| \leq b \quad \dots \dots \dots (7)$$

$$r, s, t \text{ are all negative or all non-negative,} \quad \dots \dots \dots (8)$$

$$\text{and} \quad a+b+2r+2s+2t \geq 0. \quad \dots \dots \dots (9)$$

We denote by Λ_0 the fundamental lattice of points with integer co-ordinates.

We shall also denote by Π_f the set of all points $X = (x, y, z)$ for which $f(X) \leq f(X-A)$, for all points A of Λ_0 . Then it is clear that the bodies obtained by giving all possible lattice translations to Π_f together fill the whole space without gaps or overlappings. Also Π_f being the intersection (common part) of all half spaces $f(X) \leq f(X-A)$ is convex. Consequently, by a well-known theorem of Minkowski, Π_f is a symmetrical convex polyhedron with at most seven pairs of opposite faces. By the definition of Π_f it is clear that

$$m_f = \max_{X \in \Pi_f} f(X) = \max_{X \text{ a vertex of } \Pi_f} f(X), \quad \dots \dots \dots (10)$$

since the ellipsoid $f(x, y, z) \leq m_f$ is convex and Π_f is the convex cover of its vertices

As we know that every convex body has at least one lattice which provides a covering with the least density, it follows that $\underline{bd} \, m_f/D_f^{\frac{1}{2}}$ is actually attained for at least one form $\Sigma(ax^2+2ryz)$.

Our proof will run as follows:

We shall first construct the polyhedron Π_f for the form $3\Sigma x^2-2\Sigma yz$ and show that for all vertices V of Π_f , $f(V) \equiv \frac{5}{4}$ from which it easily follows that for

$$f = 3\Sigma x^2-2\Sigma yz, \quad M_f = m_f/D_f^{\frac{1}{2}} = \left(\frac{125}{1024}\right)^{\frac{1}{2}}.$$

We then divide the reduced positive definite quadratic forms into a number of types. For each f in every type we show that either at a point P of Π_f , $f(P)/D_f^{\frac{1}{2}}$ is greater than $(125/1024)^{\frac{1}{2}}$ or we show that by suitable variations in the coefficients a, b, c, r, s, t , we get a neighbouring form f' of f with $m_{f'}/D_{f'}^{\frac{1}{2}}$ smaller than $m_f/D_f^{\frac{1}{2}}$ unless $f = 3\Sigma x^2-2\Sigma yz$. In the first case we often proceed as follows: We first establish that for forms of a certain set \mathcal{E} , that contains f , and for P , a point of Π_f defined in a certain way in \mathcal{E} , the minimum of $f(P)/D_f^{\frac{1}{2}}$ for all $f \in \mathcal{E}$ is actually attained at some form of \mathcal{E} . Then for any f in \mathcal{E} we show that for a suitable neighbour-

* See, e.g., Dickson, L. E., Studies in the Theory of Numbers, Chicago (1930), pp. 163-165, noting that if $rst=0$, we can take r, s, t non-negative by a transformation $x = \mathcal{E}_1x, y = \mathcal{E}_2y, z = \mathcal{E}_3z, \mathcal{E}_i = \pm 1$.

ing form $f' \in \Sigma$, $f'(P)/D_f^{\frac{1}{2}}$ is smaller than $f(P)/D_f^{\frac{1}{2}}$ unless f satisfies certain conditions. After obtaining a sufficient number of such conditions we show that for f satisfying these conditions $f(P)/D_f^{\frac{1}{2}}$ is greater than $(125/1024)^{\frac{1}{2}}$. In short the whole method can be described as that of variation of parameters a, b, c, r, s, t .

PROOF OF THE THEOREM

4. As explained earlier, the polyhedra Π_f play an important rôle in our investigation. It will be convenient to state certain properties of Π_f which are of use in their construction.

Some Properties of Π_f : The equation of any face of Π_f is of the type $f(X) = f(X-A)$, where A is a suitable point of A_0 , the fundamental lattice.* If $f(X) = f(X-A)$ is a face of Π_f , then so also is $f(X) = f(X+A)$. Further, $\frac{1}{2}A$ is an inner point of the face $f(X) = f(X-A)$. If we denote the infinite strip bounded by planes $f(X) = f(X-A)$ and $f(X) = f(X+A)$ by S_A , then Π_f is the intersection of a finite number of these strips S_A where A are points of A_0 . Also if A and B are any two points of A_0 and $\frac{1}{2}B$ is not an inner point of S_A , then S_B does not play any part in the construction of Π_f , i.e. Π_f can be regarded as the intersection of a number of S_A , all different from S_B .

5. We shall first dispose of the fact that for $f = 3\Sigma x^2 - 2\Sigma yz$, M_f has the value $(125/1024)^{\frac{1}{2}}$.

The polyhedron Π_f can be easily seen to be the intersection of strips S_A for different A in the following set †:

$$(1, 0, 0), (0, 1, 0), (0, 0, 1), (0, 1, 1), (1, 0, 1), (1, 1, 0), (1, 1, 1).$$

The fourteen faces of Π_f have the following equations †:

$$6x - 2y - 2z = \pm 3$$

$$-2x + 6y - 2z = \pm 3$$

$$-2x - 2y + 6z = \pm 3$$

$$-4x + 4y + 4z = \pm 4$$

$$4x - 4y + 4z = \pm 4$$

$$4x + 4y - 4z = \pm 4$$

$$2x + 2y + 2z = \pm 3.$$

The twenty-four vertices ‡ of Π_f are the following together with their images in the origin:

$$\left(\frac{1}{2}, -\frac{1}{2}, \frac{1}{2}\right), \left(\frac{1}{2}, \frac{1}{2}, -\frac{1}{2}\right), \left(-\frac{1}{2}, \frac{1}{2}, \frac{1}{2}\right), \left(\frac{1}{2}, \frac{1}{2}, -\frac{1}{2}\right), \left(-\frac{1}{2}, \frac{1}{2}, \frac{1}{2}\right), \left(\frac{1}{2}, -\frac{1}{2}, \frac{1}{2}\right), \left(\frac{3}{2}, \frac{1}{2}, \frac{1}{2}\right), \left(\frac{1}{2}, \frac{3}{2}, \frac{1}{2}\right), \left(\frac{1}{2}, \frac{1}{2}, \frac{3}{2}\right), \left(\frac{3}{2}, \frac{1}{2}, \frac{1}{2}\right), \left(\frac{1}{2}, \frac{3}{2}, \frac{1}{2}\right), \left(\frac{1}{2}, \frac{1}{2}, \frac{3}{2}\right).$$

It can be easily verified that the value of f at each of these points is $5/4$. (In fact one has to verify it only for two points, one from the first six and one from the rest.) Since the determinant $D_f = 16$, it follows that

$$M_f = (125/1024)^{\frac{1}{2}}.$$

We now divide our proof into two main parts. In the first part we deal with form f with non-negative r, s, t , and in the second with forms of negative r, s, t .

* The lattice of points with integer co-ordinates.

† For fuller explanation see § 13.

PART I

6. In this part we shall throughout suppose that the coefficients a, b, c, r, s, t of f satisfy the following conditions:

$$0 < a \leq b \leq c; \dots \dots \dots (11)$$

$$0 \leq 2s, \quad 2t \leq a; \quad 0 \leq 2r \leq b. \dots \dots \dots (12)$$

We shall very often denote f by the symbol (a, b, c, r, s, t) .

In the following table we write down the equations of a number of faces $f(X) = f(X - A)$ of strips S_A . These S_A will be enough to define Π_f .

TABLE I

A	Faces of S_A	Symbols for faces
$\pm(1, 0, 0)$	$2ax + 2ty + 2sz = \pm a$	$\pm F_1$
$\pm(0, 1, 0)$	$2tx + 2by + 2rz = \pm b$	$\pm F_2$
$\pm(0, 0, 1)$	$2sx + 2ry + 2cz = \pm c$	$\pm F_3$
$\pm(1, -1, 0)$	$2(a-t)x - 2(b-t)y - 2(r-s)z = \pm(a+b-2t)$	$\pm F_4$
$\pm(0, 1, -1)$	$-2(s-t)x + 2(b-r)y - 2(c-r)z = \pm(b+c-2r)$	$\pm F_5$
$\pm(-1, 0, 1)$	$-2(a-s)x - 2(t-r)y + 2(c-s)z = \pm(c+a-2s)$	$\pm F_6$
$\pm(1, 1, -1)$	$2(a+t-s)x + 2(b+t-r)y - 2(c-r-s)z =$ $\pm(a+b+c+2t-2r-2s)$	$\pm F_7$
$\pm(-1, 1, 1)$	$-2(a-s-t)x + 2(b+r-t)y + 2(c+r-s)z =$ $\pm(a+b+c+2r-2s-2t)$	$\pm F_8$
$\pm(1, -1, 1)$	$2(a+s-t)x - 2(b-t-r)y + 2(c+s-r)z =$ $\pm(a+b+c+2s-2t-2r)$	$\pm F_9$

We shall in future refer to these faces by the symbols in the last column.

With the help of (11) and (12) it is easy to verify that for any B of A_0 which does not appear in the first column the point $\frac{1}{2}B$ is not an inner point of one at least of the strips S_A corresponding to the A of Table I, e.g. for integers $p, q, r > 0$, $\frac{1}{2}(-p, q, r)$ is not an inner point of S_A bounded by $\pm F_8$, etc. Consequently Π_f is the intersection of the nine strips S_A bounded by the planes $\pm F_i, i = 1, \dots, 9$.

We shall now divide these forms f into three types, (i), (ii), and (iii) according to the relative magnitude of r, s, t which shall be studied separately.

$$(i) \quad 0 \leq t \leq s, r,$$

$$(ii) \quad 0 \leq s \leq t, r,$$

$$(iii) \quad 0 \leq r \leq s, t.$$

Forms of type (i)

7. Let P be the point of intersection of planes F_1, F_2 and F_3 and Q_1 that of F_1, F_3 and $-F_5$. Then it can be easily verified that both P and Q_1 lie in each of the nine S_A appearing in Table I. Consequently both P and Q_1 are points of Π_f and

$$m_f \geq \max.(f(P), f(Q_1)).$$

Now

$$f(x, y, z) = \frac{1}{c} (cz + sx + ry)^2 + \frac{1}{c(ac - s^2)} \left\{ c(ax + ty + sz) - s(cz + sx + ry) \right\}^2 + \frac{D^2 y^2}{(ac - s^2)D}, \quad \dots \dots \dots (13)$$

where $D = D_f$ is the determinant of f .

Therefore,

$$\begin{aligned} 4(ac - s^2)D \{ f(Q_1) - f(P) \} &= \begin{vmatrix} a & a & s \\ t & -b + 2r & r \\ s & c & c \end{vmatrix}^2 - \begin{vmatrix} a & a & s \\ t & b & r \\ s & c & c \end{vmatrix}^2 \\ &= \begin{vmatrix} a & 0 & s \\ t & 2(-b + r) & r \\ s & 0 & c \end{vmatrix}^2 - \begin{vmatrix} a & 2a & s \\ t & 2r & r \\ s & 2c & c \end{vmatrix}^2 \\ &= 4(b - r)(a - s)(ac - s^2)(ct - rs) \end{aligned}$$

and consequently,

$$\text{if } ct = rs, \text{ then } f(P) = f(Q_1). \quad \dots \dots \dots (14)$$

8. Define the number m_1 as

$$m_1 = \underline{bd} f(P) / D_f^{\frac{1}{2}} \quad \dots \dots \dots (15)$$

where the \underline{bd} is taken over all forms (a, b, c, r, s, t) of type (i) with the additional property

$$ct = rs. \quad \dots \dots \dots (16)$$

Then we prove, for all f of type (i),

$$\text{LEMMA 1.} \quad M_f = m_f / D_f^{\frac{1}{2}} \geq m_1. \quad \dots \dots \dots (17)$$

Proof: We distinguish three cases:—

$$(i) \ ct > rs, \quad (ii) \ ct = rs, \quad (iii) \ ct < rs.$$

$$(i) \text{ Suppose } ct > rs. \quad \dots \dots \dots (18)$$

Then, by (13), we have

$$m_f \geq f(Q_1) = \frac{c}{4} + \frac{c(a-s)^2}{4(ac-s^2)} + \frac{\Phi_1^2}{4(ac-s^2)D_f}, \quad \dots \dots \dots (19)$$

where

$$\begin{aligned} \Phi_1 &= \begin{vmatrix} a & -a & s \\ t & b-2r & r \\ s & -c & c \end{vmatrix} \\ &= abc - acr + act - ars - cst - bs^2 + 2rs^2 > 0, \quad \dots \dots \dots (20) \end{aligned}$$

(since $bs^2 + cst + arc \leq \frac{1}{4}abc + \frac{1}{4}abc + \frac{1}{4}abc = abc$ and $ct > rs$), and

$$D_f = abc + 2rst - ar^2 - bs^2 - ct^2. \quad \dots \dots \dots (21)$$

Now
$$\frac{\partial \Phi_1}{\partial t} = c(a-s) > 0, \quad \dots \dots \dots (22)$$

and

$$\frac{\partial D_f}{\partial t} = 2(rs-ct) < 0. \quad \dots \dots \dots (23)$$

Therefore, by (19), (20), (22) and (23) we can decrease $f(Q_1)/D_f^{\frac{1}{2}}$ by decreasing t until $ct = rs$, so that for $f' = (a, b, c, r, s, t')$ with $ct' = rs$, we have, using (14),

$$M_f \geq f(Q_1)/D_f^{\frac{1}{2}} \geq f'(Q_1)/D_{f'}^{\frac{1}{2}} = f'(P)/D_{f'}^{\frac{1}{2}} \geq m_1 \quad \dots \dots (24)$$

(ii) Obvious.

(iii) Suppose $ct < rs$. $\dots \dots \dots (25)$

By (13), we have

$$m_f \geq f(P) = \frac{c}{4} + \frac{c(a-s)^2}{4(ac-s^2)} + \frac{\Psi_1^2}{4(ac-s^2)D_f}, \quad \dots \dots (26)$$

where

$$\begin{aligned} \Psi_1 &= \begin{vmatrix} a & a & s \\ t & b & r \\ s & c & c \end{vmatrix} \\ &= abc - acr - act + ars + cst - bs^2 \\ &> 0 \quad \dots \dots \dots (27) \end{aligned}$$

(since $abc - acr - act + ars + cst - bs^2$

$$\begin{aligned} &= \frac{1}{2}c(b-2t)(a-2s) + \frac{1}{2}ca(b-2r) + \frac{1}{2}bs(c-2s) + ars \\ &\geq ars > act \geq 0). \end{aligned}$$

Now

$$\frac{\partial \psi_1}{\partial t} = -c(a-s) < 0. \quad \dots \dots \dots (28)$$

and

$$\frac{\partial D}{\partial t} = 2(rs-ct) > 0. \quad \dots \dots \dots (29)$$

Therefore, by (26)–(29) we can decrease $f(P)/D_f^{\frac{1}{2}}$ by increasing t until $ct = rs$, so that writing $f' = (a, b, c, r, s, t')$ where $ct' = rs$ we get

$$M_f \geq f(P)/D_f^{\frac{1}{2}} \geq f'(P)/D_{f'}^{\frac{1}{2}} \geq m_1. \quad \dots \dots \dots (30)$$

9. After Lemma 1, in order to prove Theorem 2 for forms of type (i) it will suffice to show that

$$m_1 > \left(\frac{125}{1024} \right)^{\frac{1}{2}} \quad \dots \dots \dots (31)$$

By (26) and (27) it is easy to see that for forms f with $ct = rs$,

$$\begin{aligned} F_1(P) &= 4D_f \cdot f(P) = abc(\Sigma a - 2\Sigma r) - \Sigma a^2 r^2 + 2\Sigma bcst \\ &= abc(a+b+c-2r-2s) - a^2 r^2 - b^2 s^2 - r^2 s^2 + 2brs^2 + 2ar^2 s, \quad \dots \quad (32) \end{aligned}$$

and

$$\begin{aligned} D_f &= abc + 2rst - ar^2 - bs^2 - ct^2 \\ &= abc + \frac{s^2 r^2}{c} - ar^2 - bs^2. \quad \dots \quad \dots \quad \dots \quad (33) \end{aligned}$$

Further, using the expressions for $F_1(P)$ and D_f free of t , we obtain

$$m_1 = bd \cdot F_1(P)/4D_f^{\frac{1}{2}}, \quad \dots \quad \dots \quad \dots \quad (34)$$

where the bd is taken over all sets of real numbers (a, b, c, r, s) satisfying *

$$0 \leq a \leq b \leq c; \quad 0 \leq 2s \leq a; \quad 0 \leq 2r \leq b. \quad \dots \quad \dots \quad (35)$$

If there is no danger of confusion we shall often use the symbol f for the set (a, b, c, r, s) in the following section.

$$\text{Since } f(P) > \frac{c}{4} \geq \frac{1}{4}(abc)^{\frac{1}{3}} \geq \frac{1}{4}D_f^{\frac{1}{2}}, \text{ and } a \geq \frac{1}{bc}D_f \geq \frac{1}{16f^2(P)}D_f,$$

it can be shown easily by using Mahler's theorem on bounded lattices (*P.R.S.*, 187, 151-187, Th. 2) that m_1 is attained for some sets (a, b, c, r, s) satisfying (35). We shall call such sets m_1 -sets.

10. We now prove a number of lemmas leading to the proof of Theorem 2 for all forms of type (i).

LEMMA 2: *For an m_1 -set we must have $a = 2s$.*

Proof: If not, let $f: (a, b, c, r, s)$ be an m_1 -set with $a > 2s$.

Then for small $\delta s > 0$, $\delta c \geq 0$, the neighbouring set $f' = f + \delta f$ satisfies (35). Let δs and δc satisfy

$$\left(ab - \frac{r^2 s^2}{c^2}\right) \delta c - 2s \left(b - \frac{r^2}{c}\right) \delta s = 0. \quad \dots \quad \dots \quad (36)$$

Then (32), (33) and (36) give

$$\delta D_f = 0,$$

and

$$\begin{aligned} \delta F_1(P) &= \delta c(a^2 b + ab^2 + 2abc - 2abr - 2abs) + \delta s(-2abc - 2b^2 s - 2r^2 s + ar^2 + 4brs) \\ &= -\frac{2}{abc^2 - r^2 s^2} \delta s \{ -abc(bc - r^2)(a - 2s)(c - s) - ar^2 s(c - s)(bc - r^2) \\ &\quad - r^2 s(b - r)^2(ac - s^2) \} \\ &< 0, \end{aligned}$$

so that f' has smaller $F_1(P)/4D_f^{\frac{1}{2}}$ than f and we get a contradiction that proves the lemma.

LEMMA 3: *An m_1 -set must have $b = 2r$.*

Proof: Suppose f is an m_1 -set with $b > 2r$.

* Since $c \geq 2r$, $2s$, the conditions $t \leq r$, s ; $0 \leq 2t \leq a$ are contained in $ct = rs$, $0 \leq 2s \leq a$.

Then for small $\delta c \geq 0$, $\delta r > 0$, the neighbouring set $f' = f + \delta f$ satisfies (35). Let δc and δr be related by

$$\left(ab - \frac{r^2 s^2}{c^2}\right) \delta c - \frac{2r}{c} (ac - s^2) \delta r = 0.$$

Then

$$\delta D_f = 0,$$

and

$$\begin{aligned} \delta F_1(P) &= \delta c(a^2b + ab^2 + 2abc - 2abr - abs) + \delta r(-2abc - 2a^2r - 2rs^2 + 4ars + 2bs^2) \\ &= -\frac{2}{abc^2 - r^2s^2} \delta r \{abc(ac - s^2)(c - r)(b - 2r) + brs^2(ac - s^2)(c - r) \\ &\quad + rs^2(bc - r^2)(a - s)^2\} \\ &< 0, \end{aligned}$$

and we easily obtain a contradiction that proves the lemma.

LEMMA 4: $m_1 > \left(\frac{125}{1024}\right)^{\frac{1}{3}}$, and Theorem 2 is true for all forms of type (i).

Proof: From Lemmas 2, 3 for an m_1 -form we have

$$F_1(P) = abc^2 - \frac{a^2b^2}{16},$$

and

$$\begin{aligned} D_f &= abc + \frac{a^2b^2}{16c} - \frac{ab}{4}(a+b) \\ &\leq abc + \frac{a^2b^2}{16c} - \frac{1}{2}ab\sqrt{ab} \\ &= \frac{ab}{16c}(4c - \sqrt{ab})^2. \end{aligned}$$

Therefore, writing $\xi = c/\sqrt{ab}$, we have

$$\frac{F_1(P)}{4D_f^{4/3}} = \left(\frac{1}{4}\right)^{\frac{1}{3}} \frac{\xi^{4/3}(4\xi + 1)}{(4\xi - 1)^{5/3}} = K(\xi) \text{ say,}$$

and

$$m_1 = \min_{\xi \geq 1} K(\xi).$$

Differentiating logarithmically

$$\frac{1}{K} \frac{dK}{d\xi} = \frac{4(8\xi^2 - 8\xi - 1)}{3(16\xi^2 - 1)} = 0 \text{ for } \xi = \frac{2 + \sqrt{6}}{4} = \xi_0 > 1.$$

Since $\frac{dK}{d\xi} < 0$ for $1 \leq \xi < \xi_0$ and $\frac{dK}{d\xi} > 0$ for $\xi > \xi_0$, it follows that

$$m_1 = K(\xi_0),$$

so that

$$m_1^3 = \frac{1}{1024} (2 + \sqrt{6})^4 (3 + \sqrt{6})^3 (1 + \sqrt{6})^{-5} > \frac{125}{1024}$$

since

$$(2 + \sqrt{6})^4(3 + \sqrt{6})^3 = 31,716 + 12,948\sqrt{6},$$

and

$$125(\sqrt{6} + 1)^5 = 30,125 + 12,625\sqrt{6}.$$

Forms of type (ii)

11. We now consider forms of type (ii). For these forms we have

$$0 \leq a \leq b \leq c; \quad 0 \leq 2s, \quad 2t \leq a; \quad 0 \leq 2r \leq b; \quad s \leq t, r. \quad \dots (37)$$

It can be verified easily that points P and Q_2 defined as the intersections of planes F_1, F_2, F_3 and F_2, F_3, F_4 respectively lie in each of the nine S_A in Table I and hence are points of Π_f .

By repeating word by word the discussion in §§ 7, 8 replacing (a, b, c) , (r, s, t) , (x, y, z) , and Q_1 by (c, a, b) , (t, r, s) , (z, x, y) and Q_2 respectively wherever they occur it is possible to prove

LEMMA 5: Let $f: (a, b, c, r, s, t)$ be a form which satisfies conditions (37). Let f' be the form (a, b, c, r, s', t) , where $bs' = rt$. Then

$$m_f/D_f^{\frac{1}{2}} \geq f'(P)/D_{f'}^{\frac{1}{2}}.$$

We next prove

LEMMA 6: Let f be a form (a, b, c, r, s, t) , which satisfies (37) and for which $bs = rt$. Let f' be the form $(a, b, c, r', s', t') = \left(a, b, c, r, t, \frac{b}{c}s\right)$. Then

$$f(P)/D_f^{\frac{1}{2}} \geq f'(P)/D_{f'}^{\frac{1}{2}} \geq m_1.$$

Proof: Since P is the intersection of planes F_1, F_2 , and F_3 it is easy to verify (by permuting (a, b, c) to (c, a, b) in (26), (27) for example), that

$$f(P) = \frac{b}{4} + \frac{b(c-r)^2}{4(bc-r^2)} + \frac{\Psi^2}{4(bc-r^2)D_f}, \quad \dots \dots \dots (38)$$

where

$$\Psi = abc - bct - bcs + ctr + brs - ar^2. \quad \dots \dots \dots (39)$$

Also

$$f'(P) = \frac{b}{4} + \frac{b(c-r)^2}{4(bc-r^2)} + \frac{\Psi'^2}{4(bc-r^2)D_{f'}}, \quad \dots \dots \dots (40)$$

where

$$\begin{aligned} \Psi' &= abc - bct' - bcs' + ct'r' + br's' - ar'^2 \\ &= abc - b^2s - bct + brs + brt - ar^2. \quad \dots \dots \dots (41) \end{aligned}$$

Since

$$\begin{aligned} D_{f'} - D_f &= abc + 2r's't' - ar'^2 - bs'^2 - ct'^2 - (abc + 2rst - ar^2 - bs^2 - ct^2) \\ &= 2\frac{b}{c}rst - bt^2 - \frac{b^2}{c}s^2 - 2rst + bs^2 + ct^2 \\ &= \frac{1}{c}(c-b)(ct^2 + bs^2 - 2rst) \\ &\geq 0 \end{aligned}$$

(Since $bs = rt$ and $rst \leq rt^2 < ct^2$),

and

$$\begin{aligned}\Psi - \Psi' &= b^2s - bcs + crt - brt \\ &= (b-c)(bs - rt) = 0,\end{aligned}$$

it follows from (38)–(41) that

$$f'(P)/D_{f'}^{\frac{1}{2}} \leq f(P)/D_f^{\frac{1}{2}}.$$

As $ct' = bs = rt = r's'$, the second inequality also follows.

Lemmas 4, 5 and 6 together give a proof of Theorem 2 for forms of type (ii) also.

Forms of type (iii)

12. We now consider forms of type (iii), namely those forms (a, b, c, r, s, t) which satisfy

$$0 \leq a \leq b \leq c; \quad 0 \leq 2s, 2t \leq a; \quad 0 \leq 2r \leq b; \quad r \leq s, t. \quad \dots \quad (42)$$

It can be verified that points P and Q_3 defined as the intersections of planes F_1, F_2, F_3 and F_1, F_2, F_6 respectively are vertices of Π_f .

By repeating word by word the discussion in §§ 7-8 replacing (a, b, c) , (r, s, t) , (x, y, z) and Q_1 by (b, c, a) , (s, t, r) , (y, z, x) and Q_3 respectively one can prove

LEMMA 7: Let $f: (a, b, c, r, s, t)$ be a form of type (iii). Let f' be the form (a, b, c, r', s, t) where $ar' = st$. Then

$$m_j/D_f^{\frac{1}{2}} \geq f'(P)/D_{f'}^{\frac{1}{2}}.$$

We next prove

LEMMA 8: Let f be a form (a, b, c, r, s, t) of type (iii) which satisfies the further condition $ar = st$. Let f' be the form $(a, b, c, r', s', t') = (a, b, c, s, \frac{a}{b}r, t)$. Then

$$f(P)/D_f^{\frac{1}{2}} \geq f'(P)/D_{f'}^{\frac{1}{2}} \geq m_1.$$

Proof: One can easily verify that

$$f(P) = \frac{a}{4} + \frac{a(b-t)^2}{4(ab-t^2)} + \frac{\Phi^2}{4(ab-t^2)D_f}, \dots \dots \dots (43)$$

where

$$\Phi = abc - abs - abr + bst + art - ct^2, \dots \dots \dots (44)$$

and

$$f'(P) = \frac{a}{4} + \frac{a(b-t)^2}{4(ab-t^2)} + \frac{\Phi'^2}{4(ab-t^2)D_{f'}}, \dots \dots \dots (45)$$

where

$$\Phi' = abc - a^2r - abs + art + ast - ct^2. \dots \dots \dots (46)$$

As in Lemma 6, it is easily verified that $D_{f'} \geq D_f$, and $\Phi' = \Phi$, and the first inequality follows from (43)–(46). The second inequality follows easily from Lemma 6.

Lemmas 7 and 8 together prove Theorem 2 for forms of this type also. This completes the proof of Theorem 2 for all forms with non-negative r, s, t .

PART II

13. Let f be a form for which $M_f = m$ (see (4)). Then we shall call f an ' m -form'.

Theorem 2 is obviously equivalent to the statement 'All reduced m -forms are multiples of $3\Sigma x^2 - 2\Sigma yz$.' We have seen in Part I that the reduced forms with non-negative r, s, t cannot be m -forms. Therefore, we have only to establish that if a reduced form with negative r, s, t is an m -form, then it must be a multiple of $3\Sigma x^2 - 2\Sigma yz$. This we proceed to do in this part.

It will be convenient to write

$$r = -\rho, \quad s = -\sigma, \quad \text{and} \quad t = -\tau, \quad \text{where } \rho, \sigma, \tau > 0,$$

and to use the symbol $(a, b, c, \rho, \sigma, \tau)$ for the form $(a, b, c, -\rho, -\sigma, -\tau)$. We note that the real numbers $a, b, c, \rho, \sigma, \tau$ satisfy the following:

$$0 < a \leq b \leq c; \quad 0 < 2\sigma, 2\tau \leq a; \quad 0 < 2\rho \leq b;$$

and

$$a + b - 2\rho - 2\sigma - 2\tau \geq 0. \quad \dots \dots \dots (47)$$

Our first object is to obtain an expression for m_f in terms of the values of f at a finite number of points. For this purpose we have to distinguish between two cases (i) $a > \sigma + \tau$, (ii) $a = \sigma + \tau$; we will be able to drop this distinction later.

(i) Suppose $a > \sigma + \tau$. Then we shall show that Π_f has fourteen faces whose equations are given in the following table. As we know, every face of Π_f has an equation of the form $f(X) = f(X - A)$, $A \in A_0$. In the first column we give the points A , corresponding to the faces of Π_f given in column 2 and in the third column we give symbols $\pm F_i$, by which we shall refer to these faces.

TABLE II

A	Face	Symbol
$\pm (1, 0, 0)$	$2ax - 2\tau y - 2\sigma z = \pm a$	$\pm F_1$
$\pm (0, 1, 0)$	$-2\tau x + 2by - 2\rho z = \pm b$	$\pm F_2$
$\pm (0, 0, 1)$	$-2\sigma x - 2\rho y + 2cz = \pm c$	$\pm F_3$
$\pm (1, 1, 0)$	$2(a - \tau)x + 2(b - \tau)y - 2(\rho + \sigma)z = \pm (a + b - 2\tau)$	$\pm F_{10}$
$\pm (0, 1, 1)$	$-2(\sigma + \tau)x + 2(b - \rho)y + 2(c - \rho)z = \pm (b + c - 2\rho)$	$\pm F_{11}$
$\pm (1, 0, 1)$	$2(a - \sigma)x - 2(\tau + \rho)y + 2(c - \sigma)z = \pm (c + a - 2\sigma)$	$\pm F_{12}$
$\pm (1, 1, 1)$	$2(a - \sigma - \tau)x + 2(b - \tau - \rho)y + 2(c - \rho - \sigma)z = \pm (a + b + c - 2\Sigma\rho)$	$\pm F_{13}$

With the help of inequalities (47) it is easy to verify that for any $B \in A_0$ which does not appear in the first column of the above table, the point $\frac{1}{2}B$ is not an inner point of at least one S_A bounded by the planes $\pm F_i$, $i = 1, 2, 3, 10, 11, 12, 13$. Also for each A' of the above table $\frac{1}{2}A'$ lies in the interior of all the S_A with $A \neq A'$. From this it easily follows that Π_f is bounded by the planes occurring in the above table.

In the next table we list the vertices of Π_f . In the first column we write symbols by which we shall refer to these vertices, in the second the planes on which these vertices lie and in the third the values at the vertex of the expressions

$$2\xi_1 = 2(ax - \tau y - \sigma z), \quad 2\xi_2 = 2(-\tau x + by - \rho z) \quad \text{and} \quad 2\xi_3 = 2(-\sigma x - \rho y + cz).$$

TABLE III

<i>Vertex</i>	<i>Faces</i>	<i>Values of $2\xi_1, 2\xi_2, 2\xi_3$</i>
$\pm V_1^{(1)}$	$\pm F_1, \mp F_2, \pm F_{12}$	$\pm a, \mp b, \pm (c-2\sigma)$
$\pm V_1^{(2)}$	$\pm F_1, \mp F_3, \pm F_{10}$	$\pm a, \pm (b-2\tau), \mp c$
$\pm V_1^{(3)}$	$\pm F_3, \pm F_{12}, \pm F_{13}$	$\pm (a-2\sigma), \pm (b-2\rho-2\tau), \pm c$
$\pm V_1^{(4)}$	$\pm F_2, \pm F_{10}, \pm F_{13}$	$\pm (a-2\tau), \pm b, \pm (c-2\rho-2\sigma)$
$\pm V_2^{(1)}$	$\pm F_2, \mp F_3, \pm F_{10}$	$\pm (a-2\tau), \pm b, \mp c$
$\pm V_2^{(2)}$	$\pm F_2, \mp F_1, \pm F_{11}$	$\mp a, \pm b, \pm (c-2\rho)$
$\pm V_2^{(3)}$	$\pm F_1, \pm F_{10}, \pm F_{13}$	$\pm a, \pm (b-2\tau), \pm (c-2\rho-2\sigma)$
$\pm V_2^{(4)}$	$\pm F_3, \pm F_{11}, \pm F_{13}$	$\pm (a-2\sigma-2\tau), \pm (b-2\rho), \pm c$
$\pm V_3^{(1)}$	$\pm F_3, \mp F_1, \pm F_{11}$	$\mp a, \pm (b-2\rho), \pm c$
$\pm V_3^{(2)}$	$\pm F_3, \mp F_2, \pm F_{12}$	$\pm (a-2\sigma), \mp b, \pm c$
$\pm V_3^{(3)}$	$\pm F_2, \pm F_{11}, \pm F_{13}$	$\pm (a-2\sigma-2\tau), \pm b, \pm (c-2\rho)$
$\pm V_3^{(4)}$	$\pm F_1, \pm F_{12}, \pm F_{13}$	$\pm a, \pm (b-2\tau-2\rho), \pm (c-2\sigma).$

It is easy to see, either by using the symmetry about the point $\frac{1}{2}A$ of any face $f(X) = f(X-A)$, or by direct calculations that the values of $f(x, y, z)$ at vertices with the same subscript are the same. Consequently, writing

$$\left. \begin{aligned} f_1 &= f(\pm V_1^{(i)}) \\ f_2 &= f(\pm V_2^{(i)}) \\ f_3 &= f(\pm V_3^{(i)}) \end{aligned} \right\} i = 1, 2, 3, 4.$$

and

we obtain

$$m_f = \max(f_1, f_2, f_3). \quad \dots \quad (48)$$

Next suppose $a = \sigma + \tau$. Then it can be verified that Π_f is bounded by six pairs of planes, namely $\pm F_1, \pm F_2, \pm F_3, \pm F_{10}, \pm F_{12}$, and $\pm F_{13}$. Also Π_f has sixteen vertices, namely those of Table III except for $\pm V_2^{(2)}, \pm V_2^{(4)}, \pm V_3^{(1)}$ and $\pm V_3^{(3)}$. But the equation (48) continues to hold.

Therefore, we can throughout suppose that

$$m_f = \max(f_1, f_2, f_3)$$

and f_1, f_2, f_3 are defined by the points of Table III.

By straightforward calculations we obtain

$$F_1 = 4D_f \cdot f_1 = abc(\Sigma a - 2\Sigma \rho) - \Sigma a^2 \rho^2 + 2\Sigma bc\sigma\tau - 4bc\sigma\tau + 4b\sigma^2\tau + 4c\sigma\tau^2 - 4a\rho\sigma\tau - 4\sigma^2\tau^2, \quad \dots \quad (49)$$

$$F_2 = 4D_f \cdot f_2 = abc(\Sigma a - 2\Sigma \rho) - \Sigma a^2 \rho^2 + 2\Sigma bc\sigma\tau - 4ca\tau\rho + 4c\tau^2\rho + 4a\tau\rho^2 - 4b\rho\sigma\tau - 4\tau^2\rho^2, \quad \dots \quad (50)$$

and

$$F_3 = 4D_f \cdot f_3 = abc(\Sigma a - 2\Sigma \rho) - \Sigma a^2 \rho^2 + 2\Sigma bc\sigma\tau - 4ab\rho\sigma + 4a\rho^2\sigma + 4b\rho\sigma^2 - 4c\rho\sigma\tau - 4\rho^2\sigma^2. \quad \dots \quad (51)$$

We next observe

$$F_1 - F_2 = 4\tau(c - \rho - \sigma)(a\rho + \sigma\tau - b\sigma - \rho\tau), \quad \dots \quad (52)$$

$$F_2 - F_3 = 4\rho(a - \sigma - \tau)(b\sigma + \rho\tau - c\tau - \rho\sigma), \quad \dots \quad (53)$$

and

$$F_3 - F_1 = 4\sigma(b - \tau - \rho)(c\tau + \rho\sigma - a\rho - \sigma\tau). \quad \dots \quad (54)$$

14. In this section we prove a number of lemmas to show that for an m -form we must have m_f equal to at least two of f_1, f_2 and f_3 .

LEMMA 9. For an m -form we cannot have

$$f_1 > f_2, f_3.$$

Proof. Suppose $f: (a, b, c, \rho, \sigma, \tau)$ is an m -form with $f_1 > f_2, f_3$. Then we must also have $F_1 > F_2, F_3$, and therefore, by (52)–(54), observing that

$$c \geq \rho + \sigma, \quad b \geq \tau + \rho, \quad a \geq \sigma + \tau$$

we get

$$a\rho + \sigma\tau > b\sigma + \rho\tau, \quad c\tau + \rho\sigma.$$

In particular

$$\sigma(b - \tau) < \rho(a - \tau),$$

and therefore, $\sigma < \rho$.

Also

$$\sigma < \frac{a\rho}{b} + \frac{\tau}{b}(\sigma - \rho) < \frac{a\rho}{b} \leq \frac{1}{2}a.$$

Therefore, $a > 2\sigma$.

In view of the above for small $\delta\sigma > 0$, $\delta\rho < 0$, $\delta\rho + \delta\sigma = 0$, the neighbouring form $f' = f + \delta f$ satisfies inequalities (47).

Now

$$m_f = f_1 > f_2, f_3.$$

Therefore, for small $\delta\sigma, \delta\rho$

$$m_{f'} = f_1' > f_2', f_3'.$$

As

$$\begin{aligned} f(x, y, z) &= ax^2 + by^2 + cz^2 - 2pyz - 2\sigma zx - 2\tau xy \\ &= \frac{1}{a}(ax - \tau y - \sigma z)^2 + \frac{1}{a(ab - \tau^2)}\{(ab - \tau^2)y - (a\rho + \sigma\tau)z\}^2 + \frac{D_f z^2}{(ab - \tau^2)} \\ &= \frac{1}{a}\xi_1^2 + \frac{1}{a(ab - \tau^2)}(a\xi_2 + \tau\xi_1)^2 + \frac{1}{4(ab - \tau^2)D_f}(2D_f z)^2, \end{aligned}$$

it follows that

$$m_f = f_1 = f(V_1^{(1)}) = \frac{a}{4} + \frac{a(b - \tau)^2}{4(ab - \tau^2)} + \frac{\Phi_1^2}{4(ab - \tau^2)D_f}, \quad \dots \quad (55)$$

where

$$\begin{aligned} \Phi_1 &= \begin{vmatrix} a & -\tau & a \\ -\tau & b & -b \\ -\sigma & -\rho & c - 2\sigma \end{vmatrix} = (abc - ab\sigma - ab\rho - b\sigma\tau + a\rho\tau + 2\tau^2\sigma - c\tau^2) \\ &= (ab - \tau^2)(c - \rho - \sigma) + \tau(a\rho + \sigma\tau - b\sigma - \rho\tau) > 0, \quad \dots \quad (56) \end{aligned}$$

and

$$D_f = abc - 2\rho\sigma\tau - a\rho^2 - b\sigma^2 - c\tau^2 > 0. \quad \dots \dots \dots (57)$$

Now

$$\begin{aligned} \delta\Phi_1 &= (2\tau^2 - ab - b\tau)\delta\sigma + (a\tau - ab)\delta\rho \\ &= -\tau(a+b-2\tau)\delta\sigma < 0 \quad \dots \dots \dots (58) \end{aligned}$$

and

$$\begin{aligned} \delta D_f &= -2(\rho\tau + b\sigma)\delta\sigma - 2(\sigma\tau + a\rho)\delta\rho \\ &= 2(a\rho + \sigma\tau - b\sigma - \rho\tau)\delta\sigma > 0. \quad \dots \dots \dots (59) \end{aligned}$$

Therefore f' has a smaller $m_{f'}/D_{f'}^{\frac{1}{2}}$ than f and we get a contradiction that proves the lemma.

LEMMA 10: For an m -form we cannot have

$$f_2 > f_3, f_1.$$

Proof: Suppose f is an m -form with

$$f_2 > f_3, f_1.$$

Then $F_2 > F_3, F_1$ and by (53), we have

$$b\sigma + \rho\tau > c\tau + \rho\sigma,$$

and

$$\tau < \frac{\sigma(b-\rho)}{c-\rho} \leq \sigma \leq \frac{1}{2}a,$$

i.e. $a > 2\tau$.

Now the proof follows by applying a cyclic permutation* to the proof of Lemma 9 from the sentence 'In view of the above for small $\delta\sigma > 0, \delta\rho < 0, \dots$ ' onwards.

LEMMA 11: For an m -form we cannot have

$$f_3 > f_1, f_2.$$

Proof: Suppose f is an m -form with

$$f_3 > f_1, f_2.$$

Then

$$c\tau + \rho\sigma > a\rho + \sigma\tau, b\sigma + \rho\tau.$$

We distinguish between the following two cases:

$$(i) \quad b > 2\rho,$$

$$(ii) \quad b = 2\rho.$$

(i) We get a contradiction by applying a cyclic permutation to the proof of Lemma 10 from the step $a > 2\tau$ onwards.

(ii) $b = 2\rho$. Since $a+b \geq 2\rho+2\sigma+2\tau$, it follows that $a > 2\sigma$. Consequently, for small $\delta\sigma > 0, \delta\tau < 0, \delta\sigma+\delta\tau=0$, the form $f': (a, b, c, \rho, \sigma+\delta\sigma, \tau+\delta\tau)$ satisfies (47). Also

$$m_{f'} = f'_3 > f'_1, f'_2.$$

* I.e. by replacing in the proof $(a, b, c), (\rho, \sigma, \tau), (f_1, f_2, f_3), (F_1, F_2, F_3)$ and (x, y, z) by $(b, c, a), (\sigma, \tau, \rho), (f_2, f_3, f_1), (F_2, F_3, F_1)$ and (y, z, x) respectively.

Now

$$\begin{aligned} f(x, y, z) &= \frac{1}{c} (cz - \sigma x - \rho y)^2 + \frac{1}{(bc - \rho^2)c} \{ (bc - \rho^2)y - (c\tau + \rho\sigma)x \}^2 + \frac{D_f x^2}{(bc - \rho^2)} \\ &= \frac{1}{c} \xi_3^2 + \frac{1}{c(bc - \rho^2)} (c\xi_2 + \rho\xi_3)^2 + \frac{1}{4D_f(bc - \rho^2)} (2D_f x)^2. \end{aligned}$$

Therefore,

$$f_3 = f(V_3^{(2)}) = \frac{c}{4} + \frac{c(b - \rho)^2}{4(bc - \rho^2)} + \frac{\Phi^2}{4D_f(bc - \rho^2)},$$

where

$$\begin{aligned} \Phi &= \begin{vmatrix} a - 2\sigma & -\tau & -\sigma \\ -b & b & -\rho \\ c & -\rho & c \end{vmatrix} = (abc - bc\sigma - bc\tau + c\rho\tau - b\rho\sigma - a\rho^2 + 2\rho^2\sigma) \\ &= (bc - \rho^2)(a - \sigma - \tau) + \rho(c\tau + \rho\sigma - b\sigma - \rho\tau) > 0, \quad \dots \quad \dots \quad \dots \quad (60) \end{aligned}$$

and

$$D_f = abc - 2\rho\sigma\tau - a\rho^2 - b\sigma^2 - c\tau^2 > 0. \quad \dots \quad \dots \quad \dots \quad (61)$$

As

$$\begin{aligned} \delta\Phi &= \delta\sigma(-bc - b\rho + 2\rho^2) + \delta\tau(-bc + c\rho) \\ &= -\delta\sigma(b + c - 2\rho) \\ &< 0, \end{aligned}$$

and

$$\begin{aligned} \delta D_f &= \delta\sigma(-2\rho\tau - 2b\sigma) + \delta\tau(-2\rho\sigma - 2c\tau) \\ &= 2\delta\sigma(c\tau + \rho\sigma - b\sigma - \rho\tau) \\ &> 0, \end{aligned}$$

it follows that f' has a smaller $m_f/D_f^{\frac{1}{2}}$ than f , which is a contradiction that leads to the lemma.

From Lemmas 9-11 it follows that for an m -form m_f is equal to at least two of f_1, f_2 and f_3 . The object of the next three sections will be to prove that for an m -form we must have $f_1 = f_2 = f_3$.

15. The object of this section will be to prove that an m -form cannot have

$$f_1 = f_2 > f_3.$$

We shall throughout this section suppose that $f: (a, b, c, \rho, \sigma, \tau)$ is an m -form with $f_1 = f_2 > f_3$ and get a contradiction.

LEMMA 12: *The form f must have*

$$a = 2\sigma + \tau, \quad b = 2\rho + \tau. \quad \dots \quad \dots \quad \dots \quad (62)$$

Proof: Since $f_1 = f_2 > f_3$, we clearly have

$$F_1 = F_2 > F_3,$$

and it follows from (52) and (53) that

$$a\rho + \sigma\tau = b\sigma + \rho\tau > c\tau + \rho\sigma. \quad \dots \quad \dots \quad \dots \quad (63)$$

We now observe that

$$b \geq 2\rho + \tau. \quad \dots \quad \dots \quad \dots \quad (64)$$

If not, suppose

$$b < 2\rho + \tau.$$

Then,

$$a > 2\sigma + \tau$$

and

$$\sigma(2\rho + \tau) + \rho\tau > b\sigma + \rho\tau = a\rho + \sigma\tau > \rho(2\sigma + \tau) + \sigma\tau,$$

which is a contradiction that proves (64).

From (63) and (64) it follows that

$$a \geq 2\sigma + \tau \dots \dots \dots (65)$$

Also the signs of equality and inequality in (64) and (65) go together.

Now suppose

$$a > 2\sigma + \tau, b > 2\rho + \tau \dots \dots \dots (66)$$

Then

$$a + b > 2\rho + 2\sigma + 2\tau,$$

so that for small $\delta\rho > 0$, $\delta\sigma > 0$, and $\delta c > 0$, the neighbouring form f' : $(a, b, c + \delta c, \rho + \delta\rho, \sigma + \delta\sigma, \tau)$ satisfies the inequalities (47). Let $\delta\sigma$, $\delta\rho$, and δc be connected by the relations

$$(a - \tau)\delta\rho = (b - \tau)\delta\sigma, \dots \dots \dots (67)$$

and

$$(ab - \tau^2)\delta c = 2(a\rho + \sigma\tau)(\delta\rho + \delta\sigma) \dots \dots \dots (68)$$

Now,

$$a(\rho + \delta\rho) + (\sigma + \delta\sigma)\tau - b(\sigma + \delta\sigma) - (\rho + \delta\rho)\tau = 0.$$

Therefore,

$$m_{f'} = f'_1 = f'_2 > f'_3.$$

By giving cyclic permutation twice to the expression for f_3 in Lemma 11, (part ii), or by direct computation,

$$f_2 = (V_2^{(2)}) = \frac{b}{4} + \frac{b(a - \tau)^2}{4(ab - \tau^2)} + \frac{\Phi^2}{4D_f(ab - \tau^2)}$$

where

$$\begin{aligned} \Phi &= (abc - ab\rho - ab\sigma + b\sigma\tau - a\rho\tau - c\tau^2 + 2\rho\tau^2) \\ &= (ab - \tau^2)(c - \rho - \sigma) + \tau(b\sigma + \rho\tau - a\rho - \sigma\tau) \\ &> 0, \dots \dots \dots (69) \end{aligned}$$

since

$$c \geq \frac{1}{2}(a + b) > \rho + \sigma + \tau.$$

Now

$$\begin{aligned} \delta\Phi &= (ab - \tau^2)\delta c - (ab + a\tau - 2\tau^2)\delta\rho - (ab - b\tau)\delta\sigma \\ &= \frac{1}{(a - \tau)}\delta\sigma \{ 2(a\rho + \sigma\tau)(a + b - 2\tau) - (ab + a\tau - 2\tau^2)(b - \tau) - b(a - \tau)^2 \} \\ &= \frac{1}{(a - \tau)}\delta\sigma(a + b - 2\tau)(2a\rho + 2\sigma\tau - ab + \tau^2) \\ &< 0, \end{aligned}$$

since, by (66),

$$ab - 2a\rho - 2\sigma\tau - \tau^2 = a(b - 2\rho) - \tau(2\sigma + \tau) > 0.$$

Also

$$\begin{aligned}\delta D_f &= (ab - \tau^2)\delta c - 2(a\rho + \sigma\tau)\delta\rho - 2(b\sigma + \rho\tau)\delta\sigma \\ &= (ab - \tau^2)\delta c - 2(a\rho + \sigma\tau)(\delta\rho + \delta\sigma) \\ &= 0.\end{aligned}$$

Therefore, f' has a smaller $m_f/D_f^{\frac{1}{2}}$ than f which is a contradiction that disproves (66) and the lemma follows from (64), (65) and the remark before (66).

LEMMA 13. *The form f cannot have*

$$b = 2\rho + \tau, \quad a = 2\sigma + \tau. \quad \dots \quad (67)$$

Proof: Suppose f satisfies (67). Since $f_1 = f_2 > f_3$, we have

$$a\rho + \sigma\tau = b\sigma + \rho\tau > c\tau + \rho\sigma. \quad \dots \quad (68)$$

In particular,

$$\sigma(b - \rho) > \tau(c - \rho),$$

so that

$$\tau < \sigma \leq \frac{1}{2}a.$$

Consequently for small $\delta\tau > 0$, $\delta\rho < 0$, $\delta\sigma < 0$ and

$$\delta\tau = -2\delta\rho = -2\delta\sigma, \quad \dots \quad (69)$$

the form f' : $(a, b, c, \rho + \delta\rho, \sigma + \delta\sigma, \tau + \delta\tau)$ satisfies conditions (47). As

$$\begin{aligned}&a(\rho + \delta\rho) + (\sigma + \delta\sigma)(\tau + \delta\tau) - b(\sigma + \delta\sigma) - (\rho + \delta\rho)(\tau + \delta\tau) \\ &= \delta\rho(a - 2\sigma + \tau - b + 2\rho - \tau) \quad (\text{by } 69), \\ &= 0, \quad (\text{by } 67),\end{aligned}$$

it follows that

$$m_{f'} = f_1' = f_2' > f_3'.$$

Now, by (49),

$$\begin{aligned}4D_f f_1 = F_1 &= abc(a + b + c - 2\rho - 2\sigma - 2\tau) - a^2\rho^2 - b^2\sigma^2 - c^2\tau^2 + 2bc\sigma\tau \\ &\quad + 2ca\tau\rho + 2ab\rho\sigma - 4bc\sigma\tau + 4b\sigma^2\tau + 4c\tau^2\sigma - 4a\rho\sigma\tau - 4\sigma^2\tau^2. \quad \dots \quad (71)\end{aligned}$$

Therefore, substituting for $\delta\rho$ and $\delta\sigma$ from (69) and simplifying, we get

$$\delta F_1 = \delta\tau(b - a - 2c + 4\sigma - 2\tau)(b\sigma + c\tau - 2\sigma\tau - a\rho). \quad \dots \quad (72)$$

On substituting for a and b from (67) in the above, we obtain

$$\delta F_1 = -2\tau(c - \rho - \sigma + \tau)(c - \rho - \sigma)\delta\tau < 0. \quad \dots \quad (72.1)$$

Also

$$\delta D_f = \delta\tau(a\rho + \sigma\tau + b\sigma + \rho\tau - 2c\tau - 2\rho\sigma) > 0. \quad \dots \quad (73)$$

From (70)–(73) it follows that f' has a smaller $m_f/D_f^{\frac{1}{2}}$ than f which is a contradiction that proves the lemma.

Since Lemmas 12 and 13 contradict each other, it follows that

LEMMA 14: *For an m -form we cannot have*

$$f_1 = f_2 > f_3.$$

16. In this section we shall prove by reductio ad absurdum that an m -form cannot have

$$f_2 = f_3 > f_1.$$

We assume the contrary, i.e. that $f: (a, b, c, \rho, \sigma, \tau)$ is an m -form for which

$$f_2 = f_3 > f_1,$$

and so also

$$F_2 = F_3 > F_1.$$

Then from (53) and (54) it follows that we have

$$\text{either} \quad (i) \quad a = 2\sigma = 2\tau, \quad c\tau + \rho\sigma \geq b\sigma + \rho\tau > a\rho + \sigma\tau, \quad \dots \quad \therefore (74)$$

$$\text{or} \quad (ii) \quad a > \sigma + \tau, \quad c\tau + \rho\sigma = b\sigma + \rho\tau > a\rho + \sigma\tau. \quad \dots \quad \therefore (75)$$

We now prove a number of lemmas which will lead to a contradiction and hence prove that m -forms cannot have $f_2 = f_3 > f_1$.

LEMMA 15: *The form f cannot have*

$$a = 2\sigma = 2\tau, \quad c\tau + \rho\sigma > b\sigma + \rho\tau > a\rho + \sigma\tau. \quad \dots \quad (76)$$

Proof: Suppose f satisfies (76). Since $a = 2\sigma = 2\tau$ and $a + b \geq 2\rho + 2\sigma + 2\tau$, it follows that $b > 2\rho$. Consequently for small $\delta\rho > 0$, $\delta\tau < 0$, $\delta\rho + \delta\tau = 0$, the form $f': (a, b, c, \rho + \delta\rho, \sigma, \tau + \delta\tau)$ satisfies the inequalities (47). Also for f' ,

$$m_{f'} = f'_3 > f'_2 > f'_1.$$

Now applying two 'cyclic permutations' to the proof of Lemma 9 from the relation (55) onwards we get a contradiction that gives the lemma.

LEMMA 16: *We cannot have*

$$a = 2\sigma = 2\tau, \quad c\tau + \rho\sigma = b\sigma + \rho\tau > a\rho + \sigma\tau. \quad \dots \quad (77)$$

Proof: Suppose f satisfies (77). Then it follows from $\sigma = \tau$ that $b = c$. Also, as before, $b > 2\rho$. Therefore, for small $\delta\rho > 0$, $\delta\tau < 0$, $\delta\sigma < 0$, and

$$\delta\rho = -2\delta\sigma = -2\delta\tau, \quad \dots \quad (78)$$

the neighbouring form $f': (a, b, c, \rho + \delta\rho, \sigma + \delta\sigma, \tau + \delta\tau)$ satisfies (47).

Since

$$c(\tau + \delta\tau) + (\rho + \delta\rho)(\sigma + \delta\sigma) - b(\sigma + \delta\sigma) - (\rho + \delta\rho)(\tau + \delta\tau) = 0,$$

it follows that

$$m_{f'} = f'_3 = f'_2 > f'_1.$$

Applying a cyclic permutation to the proof of Lemma 13 from (70) to (72) we have

$$\delta F_2 = (c - b - 2a + 4\tau - 2\rho)(c\tau + a\rho - 2\rho\tau - b\sigma)\delta\rho.$$

On substituting $a = 2\tau$, $c = b$ and $\tau = \sigma$, the above gives

$$\delta F_2 = 0. \quad \dots \quad (79)$$

Also, by (78) and (77),

$$\delta D_f = \delta\rho(b\sigma + \rho\tau + c\tau + \rho\sigma - 2a\rho - 2\sigma\tau) > 0. \quad \dots \quad (80)$$

From (79) and (80) we obtain a contradiction that proves the lemma.

After Lemmas 15 and 16 we can suppose that f satisfies inequalities (75).

LEMMA 17: *We cannot have*

$$a = 2\tau.$$

Proof: Since $b\sigma + \rho\tau = c\tau + \rho\sigma$ and $b \leq c$, it follows that $\tau \leq \sigma$, and since $2\sigma \leq a$, $a = 2\tau$ would imply $a = \sigma + \tau$, which contradicts (75).

LEMMA 18: *If $b > a$ and $a + b > 2\rho + 2\sigma + 2\tau$, then $a > 2\sigma$.*

Proof: Suppose $a = 2\sigma$, so that $b > 2\rho + 2\tau$. By Lemma 17, $a > 2\tau$. Therefore, for small $\delta a > 0$, $\delta\tau > 0$, the form f' : $(a + \delta a, b, c, \rho, \sigma, \tau + \delta\tau)$ satisfies (47). Let δa and $\delta\tau$ be connected by

$$(bc - \rho^2) \delta a = 2(c\tau + \rho\sigma) \delta\tau. \quad \dots \quad (81)$$

Now

$$\delta(c\tau + \rho\sigma - b\sigma - \rho\tau) = (c - \rho) \delta\tau > 0.$$

Therefore,

$$m_{f'} = f'_3 > f'_2 > f'_1.$$

By applying a cyclic permutation to (69) or by direct calculation we obtain

$$f_3 = f(V_3^{(2)}) = \frac{c}{4} + \frac{c(b - \rho)^2}{4(bc - \rho^2)} + \frac{\Phi^2}{4D_f(bc - \rho^2)}$$

where

$$\begin{aligned} \Phi &= (abc - bc\sigma - bc\tau + c\rho\tau - b\rho\sigma - a\rho^2 + 2\sigma\rho^2) \\ &= (bc - \rho^2)(a - \sigma - \tau) + \rho(c\tau + \rho\sigma - b\sigma - \rho\tau) \\ &> 0. \end{aligned} \quad \dots \quad (82)$$

Since $b - \rho - 2\tau > \rho$ and $c \geq a \geq 2\sigma$, it is clear that

$$\begin{aligned} \delta\Phi &= (bc - \rho^2)\delta a + (c\rho - cb)\delta\tau \\ &= -\{c(b - \rho - 2\tau) - 2\rho\sigma\}\delta\tau \\ &< 0, \end{aligned} \quad \dots \quad (83)$$

Also

$$\delta D_f = (bc - \rho^2)\delta a - 2(c\tau + \rho\sigma)\delta\tau = 0. \quad \dots \quad (84)$$

From (83) and (84) we obtain a contradiction to f having smallest $m_f/D_f^{\frac{1}{3}}$ and that proves the lemma.

LEMMA 19: *We must have one at least of the following:*

- (i) $a = b$,
- (ii) $a + b = 2\rho + 2\sigma + 2\tau$.

Proof: Suppose $a < b$ and $a + b > 2\rho + 2\sigma + 2\tau$.

Then by Lemmas 18 and 17, we have $a > 2\sigma$, 2τ . Therefore, for small $\delta a > 0$, $\delta\sigma > 0$, $\delta\tau > 0$, the form f' : $(a + \delta a, b, c, \rho, \sigma + \delta\sigma, \tau + \delta\tau)$ satisfies (47). Let δa , $\delta\sigma$ and $\delta\tau$ be connected by the relations

$$(c - \rho)\delta\tau = (b - \rho)\delta\sigma, \quad \dots \quad (85)$$

and

$$(bc - \rho^2)\delta a = 2(b\sigma + \rho\tau)(\delta\sigma + \delta\tau). \quad \dots \quad (86)$$

From

$$c\tau + \rho\sigma = b\sigma + \rho\tau > a\rho + \sigma\tau,$$

it is easy to prove that $c > 2\sigma + \rho$, $b > 2\tau + \rho$,

($c \leq 2\sigma + \rho \Rightarrow b \geq a > 2\tau + \rho$ and a contradiction) and the proof can be completed by giving a cyclic permutation to the proof of Lemma 12 from (69) onwards.

LEMMA 20: *We must have*

$$a + b = 2\rho + 2\sigma + 2\tau.$$

Proof: Suppose $a + b > 2\rho + 2\sigma + 2\tau$.

Then, by Lemma 19, $a = b$. Since $a\rho + \sigma\tau < b\sigma + \rho\tau$, and $a = b$ it follows that $\rho < \sigma$, and $b > \rho + \sigma + \tau > 2\rho$. Consequently for small $\delta\rho > 0$, $\delta\sigma < 0$, $f': (a, b, c, \rho + \delta\rho, \sigma + \delta\sigma, \tau)$ satisfies (47). Let $\delta\rho$ and $\delta\sigma$ satisfy the equation

$$(a\rho + \sigma\tau)\delta\rho + (b\sigma + \rho\tau)\delta\sigma = 0. \quad \dots \dots \dots (87)$$

As $c\tau + \rho\sigma = b\sigma + \rho\tau$, it follows that $\sigma \geq \tau$, and

$$\delta(c\tau + \rho\sigma - b\sigma - \rho\tau) = (\sigma - \tau)\delta\rho - (b - \rho)\delta\sigma > 0,$$

so that

$$m_{f'} = f'_3 > f'_2, f'_1.$$

By (51) we have

$$4D_f. f_3 = F_3 = abc(\Sigma a - 2\Sigma\rho) - \Sigma a^2\rho^2 + 2\Sigma bc\sigma\tau - 4ab\rho\sigma + 4a\rho^2\sigma + 4b\rho\sigma^2 - 4c\rho\sigma\tau - 4\rho^2\sigma^2.$$

Using (87), we get

$$\begin{aligned} (b\sigma + \rho\tau)\delta F_3 &= -2\delta\rho\{(\sigma - \rho)(a - \tau)(a^2c + a^2\rho + a\rho\sigma - a\rho\tau - 4a\rho\sigma) - 2a\rho\sigma\tau(\sigma - \rho) \\ &\quad - 2a^2(\sigma - \rho)(\sigma^2 + \rho^2 + \sigma\rho) + 2a(\sigma^2 - \rho^2)(a\sigma + \rho\tau + \rho\sigma)\} \\ &= -2\delta\rho(\sigma - \rho)\Psi, \end{aligned}$$

where, using $a = b > \rho + \sigma + \tau$, we have

$$\begin{aligned} \Psi &> (\rho + \sigma)(a^2c + a^2\rho + a\rho\sigma - a\rho\tau - 4a\rho\sigma) - 2a\rho\sigma\tau - 2a^2(\sigma + \rho)^2 \\ &\quad + 2a^2\rho\sigma + 2a(\sigma + \rho)(a\sigma + \rho\tau + \rho\sigma) \\ &= (\rho + \sigma)(a^2c - a^2\rho + a\rho\tau - a\rho\sigma) + 2a\rho\sigma(a - \tau) \\ &> (\rho + \sigma)(a^2c + a\rho\sigma + a\rho\tau - a^2\rho) \\ &> 0. \end{aligned}$$

Therefore

$$\delta F_3 < 0, \quad \dots \dots \dots (88)$$

Also, by (81),

$$\delta D_f = 0$$

and, as before, we obtain a contradiction that proves the lemma.

LEMMA 21: *We must have $b = c$.*

Proof: We remark that

$$b > 2\rho + \tau.$$

LEMMA 22: *We cannot have $b = c$.*

Proof: Suppose $b = c$. Then $\sigma = \tau$ and $a > 2\sigma = 2\tau$. As we saw in Lemma 21, $b > 2\rho$. Therefore, for small $\delta\rho > 0$, $\delta\sigma < 0$, $\delta\tau < 0$ and $\delta\rho = -2\delta\sigma = -2\delta\tau$, the form $f' = f + \delta f$ satisfies (47).

Since

$$c(\tau + \delta\tau) + (\rho + \delta\rho)(\sigma + \delta\sigma) - b(\sigma + \delta\sigma) - (\rho + \delta\rho)(\tau + \delta\tau) = 0,$$

it follows that

$$m_{f'} = f_3 = f'_2 > f'_1.$$

Then, as in Lemma 16, equation (78), we get on writing $b = c$, $\sigma = \tau$,

$$\begin{aligned}\delta F_2 &= (c - b - 2a + 4\tau - 2\rho)(c\tau + a\rho - 2\rho\tau - b\sigma)\delta\rho \\ &= -2\rho(a + \rho - 2\tau)(a - 2\tau)\delta\rho \\ &< 0\end{aligned}$$

and

$$\delta D_f = \delta\rho(c\tau + \rho\sigma + b\sigma + \rho\tau - 2a\rho - 2\sigma\tau) > 0,$$

and we obtain in the usual way a contradiction that proves the lemma.

Since Lemmas 21 and 22 contradict each other, we achieve our object in this section, i.e.

LEMMA 23: *For an m -form, we cannot have*

$$f_2 = f_3 > f_1.$$

17. In this section our object is to prove that an m -form cannot have

$$f_3 = f_1 > f_2,$$

or what is equivalent,

$$c\tau + \rho\sigma = a\rho + \sigma\tau > b\sigma + \rho\tau. \quad \dots \dots \dots (91)$$

As usual, we assume the contrary, i.e. assume that the form $f: (a, b, c, \rho, \sigma, \tau)$ is an m -form which satisfies (91). Then on this assumption prove a number of lemmas that lead to a contradiction.

LEMMA 24: *We must have one at least of the following:*

$$\left. \begin{array}{l} \text{(i) } b = 2\rho, \\ \text{(ii) } b = c, \text{ and} \\ \text{(iii) } a + b = 2\rho + 2\sigma + 2\tau. \end{array} \right\} \dots \dots \dots (92)$$

Proof: Suppose f does not satisfy any of the relations (92). Then for small $\delta b > 0$, $\delta\rho > 0$, $\delta\tau > 0$, $f' = f + \delta f$ satisfies (47). We can also show that $a > 2\tau + \sigma$, $c > 2\rho + \sigma$ and then the proof of the lemma follows by applying a 'cyclic permutation' twice* to the proof of Lemma 12 from (67) onwards or once to the proof of Lemma 19.

* I.e., by replacing in the proof (x, y, z) , (a, b, c) , (ρ, σ, τ) , (f_1, f_2, f_3) and (F_1, F_2, F_3) by (z, x, y) , (c, a, b) , (τ, ρ, σ) , (f_3, f_1, f_2) and (F_3, F_1, F_2) respectively.

LEMMA 25: We must have $b = c$.

Proof: We first remark that from

$$a\rho + \sigma\tau = c\tau + \rho\sigma > b\sigma + \rho\tau, \quad a+b \geq 2\rho + 2\sigma + 2\tau,$$

it is easy to deduce that

$$a > 2\sigma + \tau, \quad a \geq \sigma + 2\tau, \quad c \geq 2\rho + \sigma.$$

Suppose $b < c$. Then for small $\delta c < 0$, $\delta\rho < 0$, $f' = f + \delta f$ satisfies (47). Let δc and $\delta\rho$ satisfy

$$(ab - \tau^2)\delta c = 2(a\rho + \sigma\tau)\delta\rho. \quad \dots \dots \dots (93)$$

Then

$$\begin{aligned} (ab - \tau^2)\delta(c\tau + \rho\sigma - a\rho - \sigma\tau) &= -\delta\rho\{ab(a - \sigma) - a\tau(2\rho + \tau) - \sigma\tau^2\} \\ &\geq -\delta\rho\{a\tau(2b - 2\rho - \tau) - \sigma\tau^2\} \\ &> 0, \end{aligned}$$

and

$$m_{f'} = f'_3 > f'_1 > f'_2.$$

Now

$$f_3 = f(V_3^{(2)}) = \frac{b}{4} + \frac{b(a - 2\sigma - \tau)^2}{4(ab - \tau^2)} + \frac{\Phi^2}{4(ab - \tau^2)D_f},$$

where

$$\begin{aligned} \Phi &= \begin{vmatrix} a & -\tau & a - 2\sigma \\ -\tau & b & -\sigma \\ -\sigma & -\rho & c \end{vmatrix} \\ &= (abc - ab\rho - c\tau^2 - b\sigma\tau + a\rho\tau + ab\sigma - 2\rho\sigma\tau - 2b\sigma^2) \\ &= ab(c - \rho) + b\sigma(a - \tau - 2\sigma) + \tau(a\rho - c\tau - 2\rho\sigma) \\ &= ab(c - \rho) + b\sigma(a - \tau - 2\sigma) - \tau\sigma(\rho + \tau) \\ &> 0 \end{aligned}$$

since $c > \rho + \tau$, $b > \rho + \tau$, $a > 2\sigma + \tau$.

Again

$$\begin{aligned} \delta\Phi &= (ab - \tau^2)\delta c + (-ab + a\tau - 2\sigma\tau)\delta\rho \\ &= -a(b - \tau - 2\rho)\delta\rho. \end{aligned}$$

Since $b \neq c$, Lemma 24 gives

$$\text{either } b = 2\rho \text{ or } a + b = 2\rho + 2\sigma + 2\tau,$$

so that in both cases since $a > 2\sigma + \tau$, we have $b < 2\rho + \tau$. Consequently,

$$\delta\Phi < 0.$$

Combined with

$$\delta D_f = 0,$$

the above gives a contradiction in the usual way and the lemma follows.

LEMMA 26: We cannot have $b = c$.

Proof: We first observe that

$$c\tau + \rho\sigma = a\rho + \sigma\tau \quad \dots \quad (94)$$

implies that $\tau \leq \rho$. Also we have seen in the beginning of Lemma 25 that

$$a = 2\tau + \sigma + k, \quad c = 2\rho + \sigma + k', \quad \dots \quad (95)$$

with $k \geq 0$, $k' \geq 0$. Substituting from (95) in (94), we have

$$\rho k = \tau k',$$

and since $\tau \leq \rho$, it follows that

$$k' \geq k. \quad \dots \quad (96)$$

Now suppose f satisfies the condition

$$b = c.$$

As $a > 2\sigma + \tau > 2\sigma$, it is clear that for small $\delta\sigma > 0$, $\delta\tau < 0$, $\delta\rho < 0$, $\delta\sigma = -2\delta\tau = -2\delta\rho$, $f' = f + \delta f$ satisfies (47).

Now

$$\begin{aligned} & c(\tau + \delta\tau) + (\rho + \delta\rho)(\sigma + \delta\sigma) - a(\rho + \delta\rho) - (\sigma + \delta\sigma)(\tau + \delta\tau) \\ &= \frac{1}{2}\delta\sigma \{ a - (2\tau + \sigma) \} - \{ c - (2\rho + \sigma) \} \\ &= \frac{1}{2}\delta\sigma(k - k') \\ &\leq 0, \end{aligned}$$

therefore,

$$m_{f'} = f'_1 > f'_3 > f'_2.$$

Since

$$\begin{aligned} 4D_f \cdot f_1 = F_1 = & abc(\Sigma a - 2\Sigma\rho) - \Sigma a^2\rho^2 + 2\Sigma bca\sigma\tau - 4bca\sigma\tau + 4b\sigma^2\tau \\ & + 4c\tau^2\sigma - 4a\rho\sigma\tau - 4\sigma^2\tau^2, \end{aligned}$$

it follows, on putting $\delta\tau = \delta\rho = -\frac{1}{2}\delta\sigma$, that

$$\delta F_1 = \delta\sigma(a\rho - b\sigma - c\tau + 2\sigma\tau)(a + 2b - c - 4\tau + 2\sigma).$$

On putting $c = b$ and $a\rho - c\tau = \rho\sigma - \sigma\tau$, we get

$$\delta F_1 = -\delta\sigma(a + b + 2\sigma - 4\tau)(b - \rho - \tau)\sigma < 0.$$

Combining the above with

$$\delta D_f = \delta\sigma(a\rho + \sigma\tau + c\tau + \rho\sigma - 2b\sigma - 2\rho\tau) > 0,$$

we get a contradiction which proves the lemma.

Since Lemmas 25 and 26 contradict each other we obtain

LEMMA 27: An m -form cannot have

$$f_3 = f_1 > f_2.$$

18. It follows from the discussion in § 14–§ 17 that if $f = (a, b, c, \rho, \sigma, \tau)$ is an m -form, then we must have

$$a\rho + \sigma\tau = b\sigma + \rho\tau = c\tau + \rho\sigma. \quad \dots \quad (97)$$

It is easy to prove with the help of $a+b \geq 2\rho+2\sigma+2\tau$, $c \geq b \geq a$, that

$$a \geq 2\sigma+\tau, \quad b \geq 2\rho+\tau, \quad a \geq 2\tau+\sigma. \quad \dots \quad \dots \quad \dots \quad (98)$$

We suppose f is an m -form. Then

LEMMA 28: $a+b = 2\rho+2\sigma+2\tau$.

Proof: Suppose $a+b > 2\rho+2\sigma+2\tau$. Then

$$a > 2\sigma+\tau, \quad b > 2\rho+\tau,$$

and for small $\delta c > 0$, $\delta\rho > 0$, $\delta\sigma > 0$, the form $f' = f + \delta f$ satisfies conditions (77). Now let δc , $\delta\rho$, $\delta\sigma$ satisfy the relations

$$(a-\tau) \delta\rho = (b-\tau) \delta\sigma \quad \dots \quad \dots \quad \dots \quad (99)$$

and

$$\bullet (ab-\tau^2) \delta c = 2(b\sigma+\rho\tau) (\delta\rho+\delta\sigma). \quad \dots \quad \dots \quad \dots \quad (100)$$

Then, using (99) and (100),

$$\begin{aligned} & (ab-\tau^2) (a-\tau) \delta \{ (a\rho+\sigma\tau) - (c\tau+\rho\sigma) \} \\ &= (ab-\tau^2) (a-\tau) \{ (a-\sigma) \delta\rho + (\tau-\rho) \delta\sigma - \tau \delta c \} \\ &= (ab-\tau^2) \{ (a-\sigma) (b-\tau) + (\tau-\rho) (a-\tau) \} \delta\sigma \\ & \quad - \tau \{ 2(b\sigma+\rho\tau) (a+b-2\tau) \} \delta\sigma \\ &= \delta\sigma \{ (ab-\tau^2)^2 - 2(ab-\tau^2) (a\rho-\rho\tau) - 2\tau(b\sigma+\rho\tau) (a+b-2\tau) \} \\ & \quad (\text{since } a\rho-\rho\tau = b\sigma-\sigma\tau) \\ &= \delta\sigma \{ (ab-\tau^2)^2 - 2(ab-\tau^2) (a\rho-\rho\tau) - 2\tau(b\sigma+\rho\tau) (a+b-2\tau) \\ & \quad + 2\tau^2(a\rho+\sigma\tau-b\sigma-\rho\tau) \} \\ &= \delta\sigma \{ (b-2\rho-\tau) (a^2b-a\tau^2-2b\sigma\tau) + \tau(a-2\sigma-\tau) (ab-\tau^2+2b\rho) \} \\ &> 0. \end{aligned}$$

Also

$$a(\rho+\delta\rho) + (\sigma+\delta\sigma)\tau - b(\sigma+\delta\sigma) - (\rho+\delta\rho)\tau = 0.$$

Therefore,

$$m_{j'} = f'_2 = f'_1 > f'_3.$$

Repeating the proof of Lemma 12 from (67) onwards we get a contradiction which proves the lemma.

From Lemma 28 it follows that

$$a = 2\sigma+\tau, \quad b = 2\rho+\tau. \quad \dots \quad \dots \quad \dots \quad (101)$$

Consequently from (97) we get

$$c = \rho + \sigma + \frac{\rho\sigma}{\tau}. \quad \dots \quad \dots \quad \dots \quad (102)$$

We now observe that any form $f = (a, b, c, \rho, \sigma, \tau)$ which satisfies (101), (102), and

$$\rho \geq \sigma \geq \tau > 0 \quad \dots \dots \dots (103)$$

automatically satisfies conditions (47). Consequently we can say that m -forms are those forms which satisfy (101)–(103) and for which $m_f/D^{\frac{1}{2}}$ is minimum.

In other words, we can define m -forms in terms of sets of real numbers ρ, σ, τ which satisfy (103) and for which the expression $F/4D^{\frac{1}{2}}$, with F and D as defined below, takes its minimum value.

$$\begin{aligned} F &= 4D_f \cdot f_1 = 4D_f \cdot f_2 = 4D_f \cdot f_3 \\ &= abc(\Sigma a - 2\Sigma \rho) - \Sigma a^2 \rho^2 + 2\Sigma bc\sigma\tau - 4ab\rho\sigma + 4\rho\sigma(a\rho + b\sigma - c\tau) - 4\rho^2\sigma^2 \\ &= abc^2 - (a\rho + b\sigma - c\tau)^2 + 4\rho\sigma(a\rho + b\sigma - c\tau) - 4\rho^2\sigma^2 \\ &= (2\sigma + \tau)(2\rho + \tau) \left(\rho + \sigma + \frac{\rho\sigma}{\tau} \right)^2 - \rho^2\sigma^2 \\ &= 2\tau(\rho + \sigma)^3 + \tau^2(\rho + \sigma)^2 + 8\rho\sigma(\rho + \sigma)^2 + (\rho + \sigma) \left(2\rho\sigma\tau + \frac{10\rho^2\sigma^2}{\tau} \right) + \frac{4\rho^3\sigma^3}{\tau^2} \end{aligned} \quad \dots (104)$$

and

$$\begin{aligned} D &= abc - 2\rho\sigma\tau - a\rho^2 - b\sigma^2 - c\tau^2 \\ &= \frac{1}{\tau} \{ \tau(\rho + \sigma) + 2\rho\sigma \}^2. \quad \dots \dots \dots (105) \end{aligned}$$

We shall now refer to the sets ρ, σ, τ corresponding to the m -forms as m -sets.

LEMMA 29: For an m -set $\rho = \sigma$.

Proof: Suppose $\rho > \sigma$.

Then for small $\delta\rho < 0$, $\delta\sigma > 0$, the set $\rho + \delta\rho, \sigma + \delta\sigma, \tau$ satisfies (103). Let $\delta\rho$ and $\delta\sigma$ satisfy

$$(2\sigma + \tau)\delta\rho = -(2\rho + \tau)\delta\sigma. \quad \dots \dots \dots (106)$$

Then

$$\begin{aligned} (2\sigma + \tau)\delta F &= \delta\sigma \left\{ 12\tau(\rho + \sigma)^2(\sigma - \rho) + 4\tau^2(\rho + \sigma)(\sigma - \rho) + 32\rho\sigma(\rho + \sigma)(\sigma - \rho) \right. \\ &\quad - 8(\rho + \sigma)^2(\sigma - \rho)\tau + 2(\sigma - \rho) \left(2\rho\sigma\tau + \frac{10\rho^2\sigma^2}{\tau} \right) + 2(\rho + \sigma)(\rho - \sigma)\tau^2 \\ &\quad \left. + 20(\rho + \sigma)\rho\sigma(\rho - \sigma) + \frac{12\rho^2\sigma^2}{\tau}(\rho - \sigma) \right\} \\ &= (\sigma - \rho) \left(12\rho^2\sigma + 12\rho\sigma^2 + 4\rho^2\tau + 4\sigma^2\tau + 12\rho\sigma\tau + 2\rho\tau^2 + 2\sigma\tau^2 + \frac{8\rho^2\sigma^2}{\tau} \right) \delta\sigma \\ &< 0, \end{aligned}$$

and

$$\delta D = 0,$$

so that the set $\rho + \delta\rho, \sigma + \delta\sigma, \tau$ has a smaller $F/4D^{\frac{1}{2}}$ which is a contradiction that proves the lemma.

After the last lemma we can say that the only m -sets are ρ, ρ, τ for which ρ/τ is the value of x in the range $x \geq 1$, where

$$\begin{aligned} A(x) &= \frac{16\rho^3\tau + 4\rho^2\tau^2 + 32\rho^4 + 4\rho^3\tau + \frac{20\rho^5}{\tau} + \frac{4\rho^6}{\tau^2}}{\left(1 + \frac{4\rho^2}{\tau}(\rho + \tau)^2\right)^{\frac{1}{2}}} \\ &= \frac{4x^6 + 20x^5 + 32x^4 + 20x^3 + 4x^2}{4\{4x^2(1+x)^2\}^{\frac{1}{2}}} \\ &= \frac{1}{4} \cdot \frac{x^2 + 3x + 1}{x^{\frac{1}{2}}(1+x)^{\frac{1}{2}}} \end{aligned}$$

attains its minimum value.

Differentiating logarithmically we have

$$\frac{1}{A} \cdot \frac{dA}{dx} = \frac{2x+3}{x^2+3x+1} - \frac{2}{3x} - \frac{2}{3(1+x)} = \frac{(x-1)(2x^2+3x+2)}{3x(x+1)(x^2+3x+1)}$$

and it is easy to see that $x = 1$ gives the minimum. From this it follows that the only m -sets are ρ, ρ, ρ and therefore the only m -forms are $\rho(3, 3, 3, 1, 1, 1)$ which completes the proof of the theorem.

A large part of the work on this paper was done during the tenure of a senior Research Fellowship of the National Institute of Sciences of India, which is gratefully acknowledged.

Issued February 5, 1954.

THE OCCURRENCE OF *GLOSSOPTERIS* FRONDS IN THE NORTH-EAST FRONTIER TRACTS, WITH A BRIEF REVIEW OF THE GONDWANAS OF NORTH-EASTERN INDIA *

by K. JACOB, *F.N.I.* and T. BANERJEE, *Geological Survey of India*

(Received September 9 ; read October 9, 1953)

CONTENTS

	<i>Page</i>
Introduction	53
Geology	53
Description of Fossils	54
Gondwana Sediments in other parts of North-Eastern India ..	
Darjeeling Area	54
Sikkim	54
Subansiri Gorge	56
Abor Hills	56
Bhutan	57
Aka Hills	57
Dikrang Valley	57
Garo Hills and Tripura	57
Conclusions	57
Summary	60
References	61

INTRODUCTION

During the field season of 1952-53, two specimens of *Glossopteris* were collected by one of us (T. Banerjee) from certain slaty beds in a road section below Flat Two, in the Sela Sub-Agency, N.-E. Frontier, Assam. The presence of these fronds firmly establishes the Lower Gondwana age of these sediments, and this record now forms the easternmost extent of this genus in the Indian sub-continent. A careful search of these slates (believed to be the Damudas), further to the north-east, is likely to yield fruitful results.

GEOLOGY

In the submontane tracts of the Assam Himalaya lying immediately to the east of the Bhutan border, a strip of Damuda beds (Permian in age), nearly four miles in width, overlies the Upper Tertiary Tipam rocks in an extensively inverted sequence with the Damudas apparently overlain by the older Dalings to the north. The beds strike parallel to the grain of the hill ranges and, as shown below, extend laterally as a more or less continuous formation along the foot of the Himalaya for considerable distances to the east and to the west, where similar rocks were previously observed by Mallet (1874), La Touche (1885), Pilgrim (1906) and others.

The area from where the fossils were obtained has been examined in recent years. The rocks comprise hard, gray, coarse, and pebbly to medium grained, well cemented, jointed and fractured quartzitic sandstones, inter-stratified with black carbonaceous slaty shales and thin coal seams. The beds have suffered much disturbance and have been somewhat metamorphosed. The sandstone is intimately

* Published by permission of the Director, Geological Survey of India.

veined with quartz; the coal has been rendered flaky and powdery and the beds sometimes show local acutely overturned folds.

DESCRIPTION OF FOSSILS

Only two specimens were obtained from the slaty shales in the Sela area, of which one is fairly well preserved. The better preserved, but incomplete frond (Figs. 1, 1A), measures about 8.5 cm. in length, and it is at least 3 cm. broad with a clearly marked, comparatively thin, persistent midrib from which bifurcating and freely anastomosing secondary veins arise at acute angles arching slightly outwards a short distance from the midrib. The tip of the leaf is not clearly seen, but it would appear that it was somewhat blunt. The base is not preserved. The secondary veins are numerous, crowded, and more or less parallel with narrow, elongate meshes which are longer near the midrib, but contracting towards the margin.

In our opinion this specimen which is undoubtedly a *Glossopteris*, may be accommodated with some hesitation in the species *Glossopteris indica*. Owing to its fragmentary nature, we are at present inclined to refer it as *Glossopteris* cf. *G. indica*.

The second specimen figured here (Fig. 2) is a rather poorly preserved, comparatively narrow frond about 2.5 cm. broad and more than 10 cm. long. A distinct midrib is present; the anastomosing secondary veins are hardly visible; but there are sufficient indications to justify its inclusion in *Glossopteris*, although specific determination is difficult. It may probably belong to the same species as the one described above.

Beyond indicating that the sediments are undoubtedly Lower Gondwanas, the specimens are not helpful for closer age determination. But the narrow strip of the Gondwanas of the north-east Himalayan foot-hills, stretching more or less continuously from Abor Hills in the east to Nepal, and further to the west, are generally believed to be the Damudas.

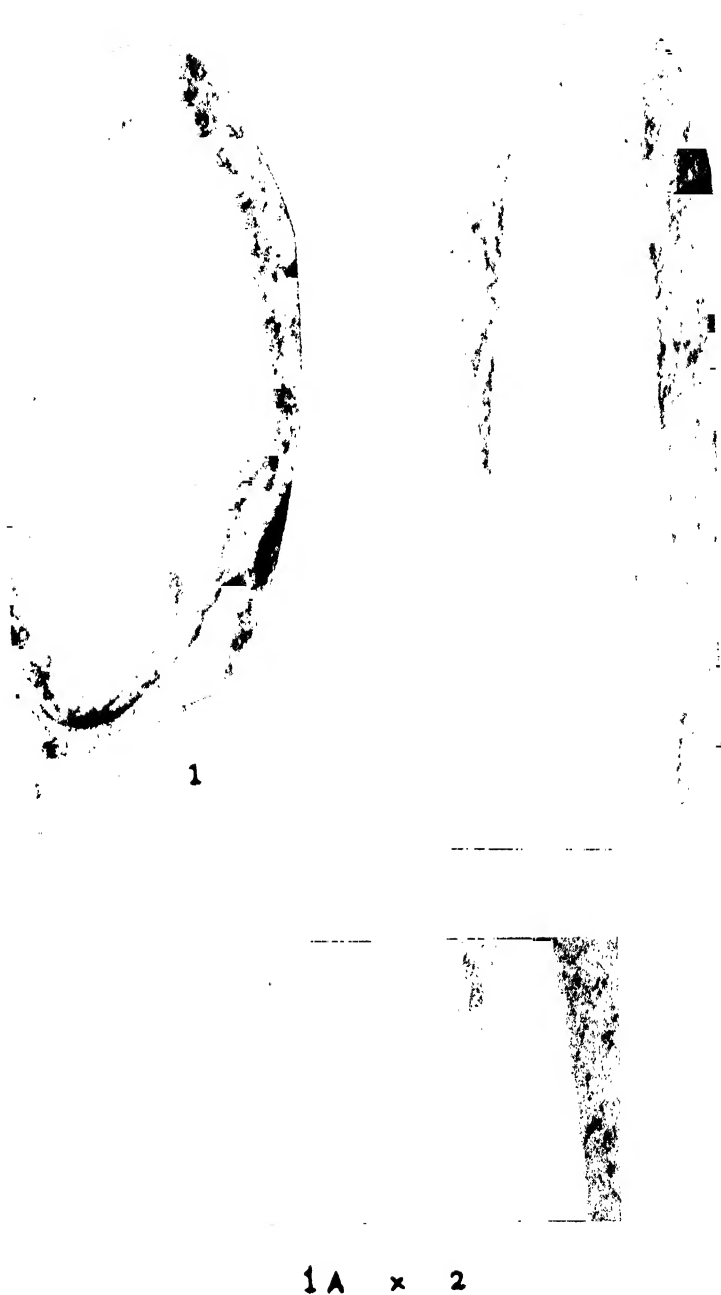
GONDWANA SEDIMENTS IN OTHER PARTS OF NORTH-EASTERN INDIA

Opportunity is taken to review briefly our knowledge of the known fresh-water Gondwana sediments and the marine intercalations in Assam and the adjoining territories in north-eastern India the distribution of which is of importance in Gondwana palaeogeography.

Darjeeling Area.—At Pankabari, on the Darjeeling Gondwanas, Hooker (1854) and Mallet (1874) reported the occurrence of *Glossopteris* sp., *Vertebraria indica*, *Phyllothea* sp. and *Sphenophyllum speciosum*. The Lower Gondwanas in this area are composed mostly of highly disturbed and crushed, grayish, massive-bedded, felspathic, and occasionally calcareous sandstones and sandy micaceous shales which are sometimes carbonaceous with occasional coal seams (Mallet, 1877; Bose, 1890; Ray, 1947). A glacial boulder bed has been reported by Fox (1934, p. 9) and Auden (1935) above Tindharia station occupying a position at the base of the Gondwanas. This discovery, according to Fox (1934, p. 9), has rendered uncertain the correlation of the Darjeeling and the Eastern Himalayan Gondwanas with the Raniganj and he suggests the possibility of the Himalayan Gondwanas belonging to the Barakars. As shown elsewhere in this paper, the question of their age cannot be considered as settled and needs careful re-examination.

Sediments believed to be the Damudas have been recognized in a narrow, more or less continuous belt further to the east of Darjeeling up to the region of the Abor Hills; but till now undoubted plant fossils have not been found in these sediments. The present discovery is therefore of some significance.

Sikkim.—Quite recently G. N. Dutt and S. N. Sen of the Geological Survey of India, located plant-bearing Gondwana beds in the Rangit valley in Western Sikkim,



- FIG. 1. *Glossopteris* cf. *G. indica*. — Nat. size.
 FIG. 1A. *Glossopteris* cf. *G. indica*. Same specimen as above, enlarged to show venation. $\times 2$.
 FIG. 2. *Glossopteris* sp. A poorly preserved specimen, probably belonging to the same species as the one figured above. — Nat. size.

The specimens are preserved in the Museum of the Geological Survey of India.

situated some distance to the north of the fossil locality Pankabari in the Darjeeling area. The poorly preserved plant remains were collected by Dutt from a locality, about two miles west of Asangthang from slightly altered sandstones a few hundred feet above certain 'pebble beds' (believed to be the equivalents of the Talchir boulder bed) which, apparently, occupy a basal position in the series and are well developed near Khandasangphu and Khemgaon. The plants include *Schizoneura*, *Vertebraria indica* and a doubtful *Glossopteris* (? *Gangamopteris*). Sen's specimens come from a locality about two miles north-east of the junction of the Rangit and the Roathak Khola, north of Naya Bazar, and include an imperfect specimen of *Glossopteris*, probably *G. indica*. These recent fossil finds in Western Sikkim conclusively prove that this series of sediments (at one time thought to be a part of the Dalings), occurring isolated from the Gondwana exposures of the southern foot-hills of the Darjeeling Himalaya, is also undoubtedly Lower Gondwana.

The Gondwanas are particularly well exposed in the form of a 'window' in the Rangit valley, 12 miles north of Darjeeling (Ghosh, 1952, 1953) and contain a few thin seams of semi-anthracitic coal (see also La Touche, 1910; Mallet, 1874). The sediments which have been traced for about 14 miles along the bridle path from Naya Bazar nearly to the base of the descent from Rinchinpong, consist mainly of grey, gritty and felspathic sandstones and carbonaceous slates 'and have at their base tillite and varved slates....' (Ghosh, 1952). The tillite recalls the glacial boulder bed of the Himalayan foot-hills reported by Fox (1934, p. 9) and Auden (1935) at Tindharia, in the Darjeeling foot-hills, and the pebble beds noticed at the base of the Gondwanas in the Lish valley south of Kalimpong, the Balipara frontier area, the Abor Hills and in the Kosi valley in Nepal. The Lachi pebble bed of North Sikkim mentioned below may also represent a contemporaneous stratigraphical horizon of glacial origin.

North of Namchi near Khemgaon in W. Sikkim, A. M. N. Ghosh (1952, 1953) and T. Banerjee found *Spirifer* (? *Neospirifer* cf. *moosakhailensis*) and fragments of other 'Permo-Carboniferous' marine brachiopods and bivalves in a loose block. G. N. Dutt informs us that he re-visited the area and located the source bed of the fossiliferous rocks, and in exposures of these marine beds between the Tista and the Rangit rivers, he collected many more fossils including, species of *Spirifer* (? *Neospirifer*), *Productus*, *Fenestella* (? *Fenestrellina*), etc.

Wager (1939) collected Carboniferous and Permian marine shells from the Lachi ridge in N. Sikkim. Based on the study of these fossils Muir-Wood and Oakley (1941) have recognised two fossiliferous horizons, namely, a Middle or Upper Carboniferous consisting of limestones and shales and an Upper Permian* mostly of sandstones. The former contain *Productus* sp., *Athyris* sp., *Spirigerella* sp., *Straparollus* sp., and *Ellipsellipsopa* sp. In the Upper Permian horizon of fossiliferous sandstones were recognised *Waagenoconcha purdoni* (Dav.), *Cumaroataechia* sp., *Uncinunellina jabiensis* (Waag.), *Syringothyris lydekkeri* (Dien.), *Batostomella* sp., *Fenestrellina* aff. *fossula* (Lons.), *Nuculana* sp., *Parallelodon* aff. *tenuistriatum* (Meek and Worthen), *Pleurophorus* sp., *Aviculopecten hyemalis* (Salt.), *A.* aff. *leniusculus* (Dana) and *Pleurotomaria* aff. *orientalis* (Roem.). Between these two fossiliferous horizons occur certain 'pebble beds' about 600 ft. in thickness. The 'pebble bed' is a grit composed of ungraded angular quartz grains and felspar set in a very fine paste of quartz and mica with sparsely scattered pebbles consisting of dark quartzites and pinkish limestone. The beds are suspected to be the equivalents of the uppermost Carboniferous Talchir boulder bed of the Peninsula and the Blaini boulder bed of the Simla region (Muir-Wood and Oakley, 1941; Auden, 1935).

There is also a slightly higher horizon in the sandstones overlying the 'pebble beds', containing *Orthotetid*, *Chonetes wageri* Muir-Wood, *Dictyoclostus* cf. *gratiosus* (Waag.), *D.* cf. *subcostatus* (Waag.), *Linoproductus* cf. *cora* (d'Orb.), *Marginifera*

* The possibility of this horizon being Lower Permian should also be borne in mind.

himalayensis Dien., *Pustula* sp., *Neospirifer moosakhailensis* (Dav.), *Spiriferella rajah* (Salter), *Goniocladia* sp. and *Rhombopora* cf. *circumcincta* Reed.

According to Muir-Wood and Oakley (1941, p. 66) the two upper Lachi fossil beds overlying the glacial 'pebble beds' are of 'Upper Permian, Kazanian age (= *Productus* shales and Zewan beds)'. The underlying lower fossiliferous bed, in their view, would be Middle or Upper Carboniferous and may belong to the Mount Everest Limestone. The Lower Permian is probably missing in this sequence.

Subansiri Gorge.—The above occurrences of marine fossils at the base of the Gondwana in Sikkim recalls Maclaren's (1904) find of boulders of fossiliferous Permo-Carboniferous limestone at the mouth of the Subansiri gorge about 350 miles to the west of the above locality. About 20 boulders and pebbles of fossiliferous limestone, some arenaceous and the others argillaceous, were picked up by him, and these revealed the following genera and species (Diener, 1905):—from the arenaceous limestone boulders: *Productus* cf. *pustulosus* Phill., *Spirifer* sp., *Spiriferina* sp., *Reticularia* cf. *inaequilateralis* Gemm., *Dielasma* aff. *uralica* Krot., *D.* aff. *biflex* Waag., *Dielasma* sp.; from the hard, bluish argillaceous limestone boulders: *Chonetes* cf. *carbonifera* Keys., *Mylina* sp., *Monopteris subansirica* Dien., *Laxonema* sp., *Pleurotomaria* aff. *punjabica* Waag., *Bellerophon* sp., *Fenestella* sp. and impressions of Crinoidea. According to Diener these fossils recall the Kuling shales of Lilang and Spiti which are generally rich in *Chonetes carbonifera*. Maclaren correlated this horizon with the Lower *Productus* limestone of the Salt Range and suggested a close connection with similar beds in Spiti and China, and 'possibly of Tenasserim and Southern Shan States'. Muir-Wood and Oakley (1941), however, correlate the fauna with that of the Upper *Productus* limestone. The correct horizon needs future verification.

Although the specimens were not obtained from beds *in situ*, there is not much doubt, 'from the lithological characters of the boulders, that they could not have travelled for any great distances' (Holland, 1905). Maclaren (1904) himself suggested that the locus may possibly be looked for at the base of the Damuda series 'at no very great distance from the Assam plain'. Alternatively, he suggested that the original beds might occur at the edge of the Tibetan plateau. But from the nature of the boulders which we have examined, it appears to us that the first suggestion is more plausible. In recent years B. Laskar of the Geological Survey of India again found two or three boulders from the Subansiri, composed of hard, bluish, argillaceous limestone in which the only fossil identifiable was a poorly preserved *Chonetes* cf. *carbonifera* Keys. It is, therefore, of prime importance to search for the original beds from which these boulders have been derived, most probably at no great distance from the belt of Tertiary sediments.*

Abor Hills.—Rolled limestone boulders which are slightly arenaceous containing badly preserved crinoid ossicles have also been reported in the upper course of the Sireng river in the Abor Hills (Coggin Brown, 1912). 'These rocks undoubtedly belong to the base of the Gondwana series, and must occur somewhere in the steep jungle-covered ravine slopes of the upper Sireng' (Coggin Brown, 1912). According to Muir-Wood and Oakley (1941, p. 60) the Subansiri fauna and the Abor Hills marine limestone boulders with the poorly preserved fossils providing very meagre data for correlation, may be of the same age as the upper Lachi fossil horizons overlying the glacial 'pebble beds'. The fossiliferous beds of the Rangit-Tista area in south-western Sikkim may also be of the same age (Upper Permian).

With regard to the fresh-water sediments in the Abor Hills, near Rammidumbang contorted black carbonaceous shales (coaly in places), believed to belong to the Lower

* Early in 1953, Laskar again visited the area and he informs us that he located the bed composed of the hard, bluish, fossiliferous limestone in the Ranganadi basin, about 20 miles south-west of the Subansiri (Maclaren's locality) and only a few hundred feet from the Tertiary belt lying to the south.

Gondwana, have been recognised. Hard, white sandstones, contorted grey slates and reddish brown shales are well exposed in the Sirpu stream. There are also quartzites, carbonaceous shales interbedded with quartzites, and a 4'-5' thick coal seam. Gondwanas are also exposed in the upper Sireng valley to the south-west of Kalak where sandstones and shales are prominent.

Bhutan.—In Bhutan (Pilgrim, 1906; 1906a) the Gondwanas are well exposed in the Kala Pani where soft sandstones interbedded with crushed coal seams occur. The upper bands of sandstone are quartzitic with thin intercalations of carbonaceous shales. Similar sediments also occur in the Bor Naddi, 12 miles to the west and in the Nunai Naddi, four miles to the east.

Aka Hills.—La Touche (1885) recognised Lower Gondwana sediments in the Aka Hills in the Lower Himalaya to the north of Tezpur in Assam. The geological features are similar to those of the Gondwanas in Sikkim to the west and the Daphla to the east.

In the upper waters of the Bhareli river, Damuda rocks are found as narrow contorted bands of hard quartzitic sandstones interstratified with carbonaceous shales and seams of coal, dipping at high angles to the south.

Dikrang Valley.—Further east on the Dikrang river, south-west of the Subansiri and the Ranganadi, are found clay shales, often carbonaceous and interstratified with thin bands of sandstone. The carbonaceous shales occasionally pass into a crushed splintery coal.*

Garo Hills and Tripura.—The only other undoubted occurrence of Lower Gondwana sediments in the north-eastern parts of India, is in the western extremity of the Garo Hills at Singrimari where Fox (1934, p. 29) discovered a small patch of carbonaceous shales containing specimens of *Vertebraria indica*.

In 1952, S. N. Sen of the Geological Survey of India handed over two specimens of plant impressions on carbonaceous shales from Tripura State which proved to be *Vertebraria indica*. But the true provenance of these undoubted *Vertebraria* requires confirmation before anything further could be stated on the significance of the occurrence of Gondwana sediments so far east in a major basin of Tertiary sediments.

CONCLUSIONS

The distribution of the fresh-water Gondwana sediments with the marine Permo-Carboniferous deposits at the base in the eastern Himalayan region, although still not fully known, gives us some idea of the trend of the northern coast line of Gondwanaland. Holland (1905, p. 135) expressed the opinion that 'the Crystalline axis of the Himalayas has been a long persistent land-mark in the physical history of Central Asia, marking approximately the northern boundary line of the great Gondwana continent, and forming the southern shore of the...Tethys'. While it may be partly true, it should be remembered that the 'Crystalline axis' or the 'Central gneiss' of the Himalaya, is apparently a mixture of rocks of different ages, mainly granitic in composition, some of them pre-Tertiary and some Tertiary in age.

In the Lachi area in North Sikkim, as shown above, there was a marine phase in the Middle or Upper Carboniferous times. This sea did not apparently reach the Darjeeling-Subansiri-Abor Hills region in the Himalayan foot-hills. But it should be remembered that we have as yet no satisfactory data available indicating the definite age of the Dalings or the Baxas. Parts of the Carboniferous might be represented by the former. But it is not unreasonable to hope for future dis-

* The marine fossiliferous band recently located by B. Laskar in the Ranganadi (verbal communication), may most probably extend south-eastwards in the vicinity of the Dikrang valley and should also be searched further south-westwards at the base of the Gondwanas. It is most likely that this marine band may be traced from Abor Hills (where fossiliferous limestone boulders have been found in the upper Sireng valley), to the Dikrang and perhaps even further westwards along the foot-hills within a short distance of the Tertiary sediments.

coveries of organic remains which may throw considerable light on the age and the palaeogeography of these regions.

The later retreat of the Middle or Upper Carboniferous sea northwards was followed by the spread of ice-sheets during the uppermost Carboniferous. The extension of the Gondwana ice-sheet from the south as far north as, and probably beyond, Lachi is suggested by the glacial bed ('pebble bed') in northern Sikkim. The tillites with varved slates in Western Sikkim (Ghosh, 1952) clearly suggest glacial conditions on land, for varved clays are seldom, if at all, formed by the action of ice drifting into shallow seas from glaciated continental margin. It would therefore appear that Gondwanaland extended over most of Nepal, Sikkim, Bhutan and to the north of the Dafia and Abor Hills. If we accept the views of Muir-Wood and Oakley, the Lower Permian in the north-eastern parts of India is apparently not represented due to non-deposition, unless, of course, parts of the Baxas are proved to occupy that position. During the Upper Permian, shallow marine conditions again prevailed in most parts of Sikkim extending westward to Kumaon, Garhwal and Kashmir, and eastward up to the Subansiri river and Abor Hills regions lying to the south of the 'Crystalline complex'.

It is possible, as Fox (1934, p. ii) has stated, that the Gondwana sediments were deposited widely over north-western Assam and north-eastern Bengal as part of the Damudas of the Bengal and Bihar coalfields, and the present discontinuity is due to 'dislocations by faulting and mountain uplift and to enormous erosions of exposed surfaces since the close of the Palaeozoic era'. 'Furthermore, there are now cogent reasons for believing that a line of faulting trends up the Brahmaputra side of the alluvium from the delta above Barisal NNW into Cooch Behar towards the western border of Bhutan. The upthrow side of the fault is the Garo Hills of Assam (where a small patch of Lower Gondwana sediments is seen in the western extremity), so that the movements tend to drop the coal measures, if any (between the Garo Hills and the Bengal-Bihar coal measures) deeper under the alluvium' (Fox, 1934, p. 30). Mallet (1874, pp. 32-33) has also suggested that the coal-bearing Damudas may underlie the alluvium between the Darjeeling Himalaya and the Rajmahal Hills. In the Brahmaputra Valley, in northern Assam, the evidence of gneissic inliers and other factors suggests probable severe overthrusting in the Himalayan region and extensive erosion of the areas to the south of it before the Gangetic alluvium was laid down, so that except close to the Himalayan foot-hills in the valley where the thickness of the alluvium is likely to be great, the Gondwanas are not likely to be present.

The Gondwana sediments in Sikkim and the southern foot-hills of the Himalaya, as mentioned above, are believed by some to be Upper Permian, probably representing the upper part of the Damudas; but *Glossopteris* and certain other elements of the Gondwana flora (*Noeggerathiopsis hislopi*, *Palaeovittaria kurzi*, etc.) have been reported to occur in younger rocks (? Rhaetic) in Tongkin beyond the Shan States (Zeiller, 1903), and if this is correct their likely path of eastward migration across the marine barrier of the Tethys at some period before the end of the Triassic, probably by means of a land-bridge or an island chain, might have lain in the north-eastern parts of Assam, possibly in the vicinity of the north-eastern syntaxis and the adjoining territories to the north. Jongmans (1937, 1937a), Sahni (1938), Halle, Just (1952) and some others, however, believe that Zeiller's *Glossopteris* from Tonkin may not be true *Glossopteris* and that the southern flora never invaded the Cathaysia flora (see also Holland, 1943-44). Nevertheless, some minor resemblances are there which demand an explanation. Detailed field investigations in the difficult parts of the country in N.E. India may throw some light on this aspect of Gondwana palaeogeography, in addition to bringing to light a more representative fossil flora from that region which may show the presence of eastern elements as well.

In this connection the discovery by Fox (1931, p. ii) in the lower Barakars (Lower Permian) of the Jharia coalfield, of calamitean shoots which are closely

related to, if not identical with *Lobatannularia* sp. (Kawasaki, 1927; Halle, 1927; Seward, 1931, pp. 235, 236) characteristic of the Lower Permian Shansi flora of China (Upper Shihhotse series), is of considerable interest. The Shansi flora, as in the case of the Russian Kusnezsk flora both of which are essentially Permian, shows a large number of plants of Mesozoic type, and *Lobatannularia*, among others in the Shansi flora, is of further significance as forming a connecting link, according to Seward (1931, p. 329), between the Palaeozoic and the Mesozoic floras.

The Indian specimens occur in the floor shales of the IX seam near Barwabera. This solitary report which has nearly been lost sight of in a large memoir by Fox (1931), requires emphasis and a detailed illustrated account of these interesting specimens is now under preparation by the senior author, who has recently re-examined the specimens. Although this form is very poorly represented at the only locality known in India and no other forms characteristic of the eastern Permian flora have been found so far, it will, nevertheless, be unwise not to bear in mind the possibility of intermigration between the Chinese Shansi flora (*Gigantopteris* flora) and the Indian Gondwana flora across the marine barrier. Evidence at present available is no doubt too meagre to draw far reaching conclusions. It is all the more important, therefore, to search for possible traces of the eastern Shansi flora in the Gondwana sediments particularly of the north-eastern parts of India which probably lay in the path of migration. Hsü (1952, p. 260) considers it hardly possible that there was an early Permian land connection between Gondwanaland and Cathaysia, but the possibility of such a connection should not be easily discarded on grounds which are not entirely convincing.

A noteworthy feature of the generally metamorphosed Gondwana sediments of the Himalayan region in North-East India, is the rarity of fossil finds. While a careful search may bring to light megafossil impressions in more satisfactory numbers, it is most unlikely that microfossils like spores may be met with in altered sediments, as these microscopic remnants of actual cutinous vegetable substance (and not impressions or casts) are usually destroyed by metamorphism because they are generally smaller than the average size of the newly formed minerals and have a tendency to volatilise easily during the process of sediment alteration. Numerous samples of somewhat metamorphosed Gondwana rocks including coal have been examined in the Survey laboratories during the past few years without satisfactory results. But we could certainly expect future finds of megafossils in the Himalayan Gondwanas which were deposited in the marginal areas of the ancient continent and have not suffered a high metamorphism.

Digressing from the main topic of this paper, it is suggested that search should also be made for traces of organic matter (a) in the metamorphosed Dalings (Nepal, Sikkim and Darjeeling areas), consisting predominantly of slates and phyllites passing into mica-schists where they merge with the Darjeeling gneiss; (b) the Baxas (Bhutan area), mostly composed of slates, phyllites, quartzites, mica-schists, limestones and dolomites; (c) and other argillaceous schists and gneisses of the Himalayan region in the north-eastern parts of India, where they all apparently overlie the Gondwanas in inverted sequence. Although their respective ages have not been proved, it has been suggested by Wager (1939) that the Dalings, once a thick dominantly argillaceous deposit, now largely chlorite schists, may be Carboniferous or somewhat earlier in age, while the Baxas may represent metamorphosed (Permo-) Carboniferous sediments.

We may also recall the independent suggestion put forward by Auden, and Heron (Auden, 1935, p. 162) that 'the pelitic component of the Darjeeling gneiss may be the same as the Daling series... If the above correlations are correct this would mean that the sedimentary part of Darjeeling gneiss is the same as the Mount Everest pelitic series' (Carboniferous or somewhat earlier) (Wager, 1939, p. 186). Ray (1935, pp. 29, 41, 44; 1947) also thinks that the Darjeeling gneiss and the Daling series may represent different metamorphic facies of one continuous

sedimentary succession, and suggests the 'increasing possibility' of the Dalings and the Darjeeling gneiss being Palaeozoic. That the Gondwanas and the Dalings may perhaps be considered as constituting one continuous formation showing different grades of metamorphism is also suspected by him (Ray, 1947, p. 118). This suggestion has been questioned by Ghosh (1952, p. 197). However, it should be remembered that some of the sediments in Western Sikkim previously referred to the Daling series, have now been proved to be Gondwanas.

However shapeless one's present ideas may be on the age of the Dalings and the Baxas, the important point is to remember that organic remains have been found in the past in highly altered Palaeozoic and later sediments, and if Wager's suggestion as to the age of the above series is anywhere near the truth, a serious search for fossils in the metamorphic rocks of the Himalaya should be made which, if successful, may help to fix their age with a greater degree of certainty, and will go a long way in understanding more fully the processes of metamorphism and the nature of deformation in the region of metamorphism in orogenic belts. It may be of interest to recall that fossils such as the ammonite *Ariatites* have been known to occur in zoisite-biotite-schist (Liassic Bündner Schiefer, Switzerland), the lamellibranch *Gryphea* in marble (Bündner Schiefer), the anthozoans *Halysites* and *Favosites* in marble (Silurian, New Hampshire), the lamellibranch *Cardinia* in zoisite-garnet-mica-schist (Bündner Schiefer), the brachiopod *Spirifer* in quartz-plagioclase-garnet-biotite-gneiss (Silurian, New Hampshire), the lamellibranch *Halobia* in solid garnet rock (Triassic, Nevada), etc. (Bucher, 1953).

As Bucher (1953, p. 292) explains the preservation of fossils in such highly altered sediments, '... typical metamorphic rocks, such as chlorite and mica schists, can form as a result of re-crystallization alone, with or without introduction of atoms or ions, in the presence of pressure differences that give direction to crystal growth, but need not produce differential movements. This does not mean that in many, perhaps most, cases mechanical effects did not play a rôle also, at least on the microscopic scale. But they are incidental, not essential to the production of schistosity in metamorphism. That is why fossils are not destroyed by metamorphism, provided they are much larger than the average size of the newly formed minerals.'

As regards the Dalings and the Baxas, however, the possibility should be borne in mind that parts of these were originally sediments which occupied the deeper parts of the Himalayan geosyncline, and generally benthonic fossils are found to be rare in such sediments. 'A careful analysis, ... leaves little doubt that, of all possible factors, considerable depth of water is the one that will reduce the benthonic fauna drastically, no matter what sediment accumulates on the sea floor.' In such areas a marine depression of sufficient depth was produced to prevent the occupation by a normal benthonic fauna. This aspect has also been discussed in some detail by one of us (Jacob, *in the press*) in a paper on the radiolarian cherts found associated with ultramafics in the Andaman geosynclinal belt. However, attempts should be made to look for fossils in the metamorphosed sediments in the Himalaya which, at first appearance, may be most unpromising. The extreme hardness of these rocks which prevents easy accessibility to the usually poorly preserved and comparatively rare fossils in them and the general unpreparedness to expect remains in highly metamorphosed rocks, might have contributed, in part, to the scarcity of fossil finds in them.

We are grateful to Dr. M. S. Krishnan, Director, Geological Survey of India, for his valuable suggestions.

SUMMARY

In this paper is described a few fronds of *Glossopteris* recently found in the Sela Sub-Agency in the North-East Frontier tracts of Assam. The discovery conclusively proves that the fresh-water sediments which yielded these fossils undoubtedly belong to the Lower Gondwana. These sediments run in a more or less continuous belt along the foot-hills of the Himalaya from Nepal

to the Abor Hills in the east. *Glossopteris* and certain other genera were previously known from the Darjeeling area and the present record now forms the easternmost extent of this flora in the Indian sub-continent.

Our knowledge of the known fresh-water Gondwana sediments, and the marine intercalations, in Assam and the adjoining territories in north-eastern India, of importance in Gondwana palaeogeography, is also reviewed. The recent finds of *Glossopteris*, *Schizoneura* and *Vertebraria* and an underlying marine Permian in the Rangit valley in Western Sikkim, and the location of a definite fossiliferous Permian bed in the Subansiri-Ranganadi area in the foot-hills of the Assam Himalaya are briefly mentioned. The age of the Gondwana sediments of the Himalayan region in the north-eastern parts of India and the probable palaeogeographical conditions that prevailed at the time are also discussed.

REFERENCES

- Auden, J. B. (1935). Traverses in the Himalayas. *Rec. Geol. Surv. Ind.*, **69**, Pt. 2.
- Bose, P. N. (1890). The Darjeeling coal between the Lisu and the Ramthi rivers. *Rec. Geol. Surv. Ind.*, **23**, Pt. 4.
- Brown, J. Coggin (1912). A geological reconnaissance through the Dibong Valley, being the geological results of the Abor Expedition, 1911-12. *Rec. Geol. Surv. Ind.*, **42**, Pt. 4.
- Bucher, W. H. (1953). Fossils in metamorphic rocks. *Bull. Geol. Soc. Amer.*, **64**, No. 3.
- Diener, C. (1905). Notes on an Anthracolithic fauna from the mouth of the Subansiri gorge, Assam. *Rec. Geol. Surv. Ind.*, **32**, Pt. 3.
- Fox, C. S. (1931). The Gondwana system and related formations. *Mem. Geol. Surv. Ind.*, **58**.
- (1934). The Lower Gondwana coalfields of India. *Mem. Geol. Surv. Ind.*, **59**.
- Ghosh, A. M. N. (1952). A new coalfield in the Sikkim Himalaya. *Current Science*, **21**, No. 7.
- (1953). Preliminary notes on the Rangit Valley Coalfield, Western Sikkim. *Ind. Min.*, **6**, No. 3.
- Halle, T. G. (1927). Palaeozoic plants from Central Shansi. *Pal. Sinica*, Ser. A, **2**, Fasc. 1.
- Holland, T. H. (1905). General Report of Geological Survey of India for the period April, 1903 to 1904. *Rec. Geol. Surv. Ind.*, **32**, Pt. 2.
- (1943-44). The theory of continental drift. *Proc. Linn. Soc. Lond.*, **155**, Pt. 2.
- Hooker, J. D. (1854). Himalayan Journals, **1**, London.
- Hsu, J. (1952). Fossil plants from the K'ungshanch'ang coal series of North-Eastern Yunnan, China. *Palaeobotanist*, **1**.
- Jacob, K. The occurrence of radiolarian cherts in association with ultra-mafic intrusives in the Andaman Islands and its significance in sedimentary tectonics. *Rec. Geol. Surv. Ind.*, **83**, Pt. 2 (*in the press*).
- Jongmans, W. J. (1937). The flora of the Upper Carboniferous of Djambi (Sumatra, Netherl. India) and its possible bearing on the palaeogeography of the Carboniferous. *Compt. Rend., Duz. Congr. l'avanc. etud. strat. Carbon., Heerlen*.
- (1937a). Synchronismus und stratigraphie. *Compt. Rend., Duz. Congr. l'avanc. etud. strat. Carbon., Heerlen*, **1**.
- Just, T. (1952). Fossil floras of the Southern Hemisphere and their phytogeographical significance. *Bull. Amer. Mus. Nat. Hist.*, **99**, Art. 3.
- Kawasaki, S. (1927). The flora of the Heian system. Pt. 1. *Bull. Geol. Soc. Chosen (Korea)*, **6**.
- La Touche, T. H. D. (1885). Notes on the Geology of the Aka Hills, Assam. *Rec. Geol. Surv. Ind.*, **18**, Pt. 2.
- (1910). General Report of Geological Survey of India for 1909. *Rec. Geol. Surv. Ind.*, **40**.
- Maclaren, J. M. (1904). The geology of Upper Assam. *Rec. Geol. Surv. Ind.*, **31**, Pt. 4.
- Mallet, F. R. (1874). On the geology and mineral resources of the Darjeeling district and the Western Duars. *Mem. Geol. Surv. Ind.*, **11**, Pt. 1.
- (1877). On recent coal explorations in the Darjeeling district. *Rec. Geol. Surv. Ind.*, **10**, Pt. 3.
- Muir-Wood, H. M. and Oakley, K. P. (1941). Upper Palaeozoic faunas of North Sikkim. *Pal. Ind.*, **31**, Mem. 1.
- Pilgrim, G. E. (1906). Notes on the geology of a portion of Bhutan. *Rec. Geol. Surv. Ind.*, **34**, Pt. 1.
- (1906a). Report on the coal occurrences in the foot-hills of Bhutan. *Ibid.*, Pt. 3.
- Ray, S. (1935). The gneissic complex of the Darjeeling district, Bengal. *Quart. Journ. Geol. Min. Met. Soc. Ind.*, **7**, No. 1.
- (1947). Zonal metamorphism in the Eastern Himalaya and some aspects of local geology. *Quart. Journ. Geol. Min. Met. Soc. Ind.*, **19**, No. 4.
- Sahni, B. (1938). Recent advances in Indian palaeobotany. *Lucknow Univ. Studies*, **2**.
- Seward, A. C. (1931). Plant life through the ages. *Cambridge*.
- Wager, L. R. (1939). The Lachi series of North Sikkim and the age of the rocks forming Mount Everest. *Rec. Geol. Surv. Ind.*, **74**, Pt. 2.
- Zeiller, R. (1903). Flora fossile des Gites de Charbon du Tonkin. *Paris*. (Plates, 1902.)

SOME INFINITE INTEGRALS INVOLVING BESSEL FUNCTIONS

by C. B. RATHIE, *Professor of Mathematics, M.B. College, Udaipur.*

(Communicated by R. S. Varma, F.N.I.)

(Received January 16; read October 9, 1953)

1. The object of this paper is to evaluate a few infinite integrals involving modified Bessel functions of the second kind by the methods of Operational Calculus. Some of the results obtained are believed to be new and interesting.

As usual, the notation $\phi(p) \doteq f(x)$ means that

$$\phi(p) = p \int_0^\infty e^{-px} f(x) dx$$

when the integral is convergent and $R(p) > 0$.

We shall use the following

THEOREM. If

$$f(x) \doteq \phi(p) \text{ and } p^{2-2\nu} e^{\frac{a}{p}} f(p) \doteq g(x)$$

then

$$\phi(p) = 2p^\nu \int_0^\infty (p+x)^{-\nu} K_{2\nu} \{2\sqrt{a(p+x)}\} g(x) dx \quad \dots \quad (1)$$

provided that $g(x) = O(x^\mu)$ for small x , where $R(\mu) > -1$, and for large x , $g(x)$ may utmost be of the order of $x^\lambda e^{2\sqrt{ax}}$ if $R(\nu - \lambda - \frac{3}{2}) > 0$, $R(p) > 0$, $R(a) > 0$.

PROOF. Since

$$p^{2-2\nu} e^{\frac{a}{p}} f(p) \doteq g(x)$$

and (McLachlan and Humbert, 1950, p. 16)

$$e^{-kx - \frac{a}{x}} x^{2\nu-1} \doteq 2p \left(\frac{p+k}{a} \right)^{-\nu} K_{2\nu} \{2\sqrt{a(p+k)}\}, \quad R(k) > 0, R(a) > 0$$

we have, on applying Parseval-Goldstein theorem (Goldstein, 1932)

$$\int_0^\infty e^{-kx} f(x) dx = 2a^\nu \int_0^\infty (x+k)^{-\nu} K_{2\nu} \{2\sqrt{a(x+k)}\} g(x) dx.$$

Hence, on replacing k by p , the theorem follows immediately.

2. (i) Taking (McLachlan and Humbert, 1950, p. 35)

$$g(x) = x^{\frac{1}{2}\lambda} I_\lambda (2\sqrt{ax})$$

$$\doteq a^{\frac{1}{2}\lambda} p^{-\lambda} e^{\frac{a}{p}}, \quad R(\lambda) > -1$$

we have

$$\begin{aligned} f(x) &= a^{i\lambda} x^{2\nu-\lambda-2} \\ &\doteq \Gamma(2\nu-\lambda-1) a^{i\lambda} p^{2+\lambda-2\nu} \\ &= \phi(p), \quad R(2\nu-\lambda-1) > 0, \quad R(p) > 0. \end{aligned}$$

Applying the theorem we get

$$p^{1+\lambda-2\nu} = \frac{2a^{\nu-i\lambda}}{\Gamma(2\nu-\lambda-1)} \int_0^\infty x^{i\lambda} (p+x)^{-\nu} I_\lambda(2\sqrt{ax}) K_{2\nu}\{2\sqrt{a(p+x)}\} dx \quad \dots (2)$$

valid, by A.C. (analytic continuation), for $R(\lambda) > -1$, $R(2\nu-\lambda-1) > 0$, $|\arg p| < \pi$, $|\arg a| < \pi$, $a \neq 0$, $p \neq 0$.

(ii) Starting with (Mitra, 1933)

$$\begin{aligned} \phi(p) &= 2pK_\mu(\sqrt{2pa}) I_\mu(\sqrt{2pa}) \\ &\doteq x^{-1} e^{-\frac{a}{x}} I_\mu\left(\frac{a}{x}\right) = f(x), \end{aligned}$$

we have on term by term interpretation,

$$\begin{aligned} p^{2-2\nu} e^{\frac{a}{p}} f(p) &= \frac{(\frac{1}{2}a)^\mu p^{1-\mu-2\nu}}{\Gamma(\mu+1)} {}_0F_1\left(\mu+1; \frac{a^2}{4p^2}\right) \\ &\doteq \frac{(\frac{1}{2}a)^\mu x^{2\nu+\mu-1}}{\Gamma(\mu+1) \Gamma(2\nu+\mu)} {}_0F_3\left(\mu+1, \frac{2\nu+\mu}{2}, \frac{2\nu+\mu+1}{2}; \frac{a^2x^2}{16}\right) \\ &= g(x), \quad R(2\nu+\mu) > 0. \end{aligned}$$

Therefore, by the theorem, we have

$$\begin{aligned} K_\mu(\sqrt{2pa}) I_\mu(\sqrt{2pa}) &= \frac{2^{-\mu} a^{\mu+\nu}}{\Gamma(\mu+1) \Gamma(2\nu+\mu)} \int_0^\infty (p+x)^{-\nu} x^{2\nu+\mu-1} \\ &\quad \times K_{2\nu}\{2\sqrt{a(p+x)}\} {}_0F_3\left(\mu+1, \frac{2\nu+\mu}{2}, \frac{2\nu+\mu+1}{2}; \frac{a^2x^2}{16}\right) dx \quad \dots (3) \end{aligned}$$

valid, by A.C., for $R(2\nu+\mu) > 0$, $|\arg p| < \pi$, $|\arg a| < \pi$, $p \neq 0$, $a \neq 0$.

Since

$$ber_\nu^2(\sqrt{2x}) + bei_\nu^2(\sqrt{2x}) = \frac{(\frac{1}{2}x)^\nu}{\Gamma^2(\nu+1)} {}_0F_3\left(\nu+1, \frac{\nu+2}{2}, \frac{\nu+1}{2}; \frac{x^2}{16}\right) \quad \dots (4)$$

we have on taking $\nu = \frac{1}{2}$ in (3),

$$\begin{aligned} K_\mu(\sqrt{2pa}) I_\mu(\sqrt{2pa}) &= \sqrt{a} \int_0^\infty (p+x)^{-\frac{1}{2}} K_1\{2\sqrt{a(p+x)}\} \\ &\quad \times \left\{ ber_\mu^2(\sqrt{2ax}) + bei_\mu^2(\sqrt{2ax}) \right\} dx \quad \dots (5) \end{aligned}$$

where $R(\mu) > -1$, $|\arg p| < \pi$, $|\arg a| < \pi$, $p \neq 0$, $a \neq 0$.

(iii) Next taking (McLachlan and Humbert, 1950, p. 51)

$$f(x) = x^{-k} e^{-\frac{a}{2x}} W_{k,m} \left(\frac{a}{x} \right) \\ \doteq 2\sqrt{a} p^{k+\frac{1}{2}} K_{2m}(2\sqrt{ap}) = \phi(p), \quad R(p) > 0,$$

we have

$$p^{2-2\nu} e^{\frac{a}{p}} f(p) = p^{2-2\nu-k} e^{\frac{a}{2p}} W_{k,m} \left(\frac{a}{p} \right) \\ \doteq x^{k+2\nu} {}_2F_2 \left\{ \frac{\Gamma(-2m)(ax)^{m+\frac{1}{2}}}{\Gamma(\frac{1}{2}-m-k)\Gamma(k+2\nu+m-\frac{1}{2})} \right. \\ \left. \times {}_1F_2(\frac{1}{2}+m-k; 1+2m, k+2\nu+m-\frac{1}{2}; ax) \right\} \\ = g(x), \quad R(k+2\nu \pm m - \frac{1}{2}) > 0 \text{ and } 2m \text{ not an integer.}$$

The theorem then gives

$$K_{2m}(2\sqrt{ap}) = a^{\nu-\frac{1}{2}} p^{\frac{1}{2}-k} \int_0^{\infty} (p+x)^{-\nu} x^{k+2\nu-2} K_{2\nu} \{2\sqrt{a(p+x)}\} \\ \times \left\{ \sum_{m, -m} \frac{\Gamma(-2m)(ax)^{m+\frac{1}{2}}}{\Gamma(\frac{1}{2}-m-k)\Gamma(k+2\nu+m-\frac{1}{2})} \right. \\ \left. \times {}_1F_2(\frac{1}{2}+m-k; 1+2m, 2\nu+k+m-\frac{1}{2}; ax) \right\} dx \dots \quad (6)$$

valid, by A.C., for $R(k+2\nu \pm m - \frac{1}{2}) > 0$, $|\arg p| < \pi$, $|\arg a| < \pi$, $a \neq 0$, $p \neq 0$.

A few special cases of (6) are worth mentioning:

(a) When $k = m + \frac{1}{2}$, we get

$$K_{2m}(2\sqrt{ap}) = \frac{a^{\nu+m} p^{-m}}{\Gamma(2m+2\nu)} \int_0^{\infty} (p+x)^{-\nu} x^{2m+2\nu-1} K_{2\nu} \{2\sqrt{a(p+x)}\} dx \dots \quad (7)$$

$$R(m+\nu) > 0, \quad |\arg p| < \pi, |\arg a| < \pi, p \neq 0, a \neq 0.$$

(b) If we take $\nu = \frac{1}{2} - k$, and use the relation

$$2K_{\nu}(2\sqrt{z}) = \sum_{\nu, -\nu} \Gamma(-\nu) z^{\frac{1}{2}\nu} {}_0F_1(1+\nu; z) \dots \dots \dots \quad (8)$$

we have

$$K_{2m}(2\sqrt{ap}) = \frac{2(ap)^{\frac{1}{2}-k}}{\Gamma(\frac{1}{2}-k+m)\Gamma(\frac{1}{2}-k-m)} \int_0^{\infty} (p+x)^{k-\frac{1}{2}} x^{-k-\frac{1}{2}} \\ \times K_{2k-1} \{2\sqrt{a(p+x)}\} K_{2m}(2\sqrt{ax}) dx \dots \dots \dots \quad (9)$$

$$R(\frac{1}{2}-k \pm m) > 0, \quad |\arg p| < \pi, |\arg a| < \pi, p \neq 0, a \neq 0.$$

(c) Finally, we take $\nu = 2m + \frac{3}{4}$ and $k = -m$ and use the relation

$$2\Gamma(\mu+1)I_{\mu}(z)K_{\mu}(z) = \Gamma(\mu) {}_1F_2(\frac{1}{2}; 1+\mu, 1-\mu; z^2) \\ + (\frac{1}{2}z)^{2\mu} \Gamma(-\mu) {}_1F_2(\frac{1}{2}+\mu; 1+\mu, 1+2\mu; z^2) \quad (10)$$

we then get

$$K_{2m}(\sqrt{ap}) = \frac{2a^{m+\frac{1}{2}} p^{m+\frac{1}{2}}}{\Gamma(2m+\frac{1}{2})} \int_0^\infty (p+x)^{-2m-\frac{1}{2}} x^{2m} \\ \times K_{4m+\frac{3}{2}}\{2\sqrt{a(p+x)}\} I_{2m}(\sqrt{ax}) K_{2m}(\sqrt{ax}) dx \quad \dots \quad (11)$$

$R(m) > -\frac{1}{4}, |\arg p| < \pi, |\arg a| < \pi, p \neq 0, a \neq 0.$

(iv) Now taking (Meijer, 1936, p. 18)

$$f(x) = x^{-3\mu-\frac{1}{2}} e^{-\frac{a}{2x}} W_{\mu, \mu} \left(\frac{a}{x} \right) \\ = \frac{2}{\sqrt{\pi}} a^{\frac{1}{2}-\mu} p^{2\mu+1} K_{2\mu}^2(\sqrt{ap}) \\ = \phi(p), \quad R(p) > 0, \quad R(a) > 0,$$

we have

$$p^{2-2\nu} e^{\frac{a}{p}} f(p) = p^{\frac{3}{2}-2\nu-3\mu} e^{\frac{a}{2p}} W_{\mu, \mu} \left(\frac{a}{p} \right) \\ = x^{3\mu+2\nu-\frac{3}{2}} \left\{ \frac{\Gamma(-2\mu)(ax)^{\mu+\frac{1}{2}}}{\Gamma(\frac{1}{2}-2\mu)\Gamma(4\mu+2\nu)} {}_1F_2(\frac{1}{2}; 1+2\mu, 4\mu+2\nu; ax) \right. \\ \left. + \frac{\Gamma(2\mu)(ax)^{-\mu+\frac{1}{2}}}{\Gamma(\frac{1}{2})\Gamma(2\mu+2\nu)} {}_1F_2(\frac{1}{2}-2\mu; 1-2\mu, 2\mu+2\nu; ax) \right\} \\ = g(x), \quad R(\mu+\nu) > 0, \quad R(2\mu+\nu) > 0.$$

Applying the theorem we have

$$K_{2\mu}^2(\sqrt{ap}) = \sqrt{\pi} p^{-2\mu} a^{\nu+\mu} \int_0^\infty (p+x)^{-\nu} x^{3\mu+2\nu-1} K_{2\nu} \{2\sqrt{a(p+x)}\} \\ \times \left\{ \frac{\Gamma(-2\mu)(ax)^\mu}{\Gamma(\frac{1}{2}-2\mu)\Gamma(4\mu+2\nu)} {}_1F_2(\frac{1}{2}; 1+2\mu, 4\mu+2\nu; ax) \right. \\ \left. + \frac{\Gamma(2\mu)(ax)^{-\mu}}{\Gamma(\frac{1}{2})\Gamma(2\mu+2\nu)} {}_1F_2(\frac{1}{2}-2\mu; 1-2\mu, 2\mu+2\nu; ax) \right\} dx \quad (12)$$

valid, by A.C., for $R(\mu+\nu) > 0, R(2\mu+\nu) > 0, |\arg p| < \pi, |\arg a| < \pi, p \neq 0, a \neq 0.$

In particular, taking $2\mu+\nu = \frac{1}{4}$ and using (8), we get

$$K_{2\mu}^2(\sqrt{ap}) = \frac{2p^{-2\mu} a^{\frac{1}{4}-\mu}}{\Gamma(\frac{1}{2}-2\mu)} \int_0^\infty (p+x)^{2\mu-\frac{1}{4}} x^{-\mu-\frac{1}{4}} K_{2\mu}(2\sqrt{ax}) \\ \times K_{4\mu-\frac{1}{4}}\{2\sqrt{a(p+x)}\} dx \quad \dots \quad (13)$$

$$R(\mu) < \frac{1}{4}, |\arg p| < \pi, |\arg a| < \pi, p \neq 0, a \neq 0.$$

On the other hand, if we take $\nu = \frac{1}{2}-3\mu$ and use (10), we have

$$K_{2\mu}^2(\sqrt{ap}) = \frac{2\sqrt{\pi} p^{-2\mu} a^{\frac{1}{2}-\mu}}{\Gamma(\frac{1}{2}-2\mu)} \int_\infty^\infty (p+x)^{3\mu-\frac{1}{2}} x^{-2\mu} \\ \times K_{6\mu-1}\{2\sqrt{a(p+x)}\} I_{-2\mu}(\sqrt{ax}) K_{2\mu}(\sqrt{ax}) dx \quad \dots \quad (14)$$

$$R(\mu) < \frac{1}{4}, |\arg p| < \pi, |\arg a| < \pi, p \neq 0, a \neq 0.$$

(v) Next taking (Meijer, 1936, p. 19)

$$\begin{aligned} f(x) &= x^{-1} e^{-\frac{a}{2x}} W_{\frac{1}{2}, \mu} \left(\frac{a}{x} \right) \\ &\doteq 2p^{3/2} \sqrt{\frac{a}{\pi}} K_{\mu+\frac{1}{2}}(\sqrt{ap}) K_{\mu-\frac{1}{2}}(\sqrt{ap}) \\ &= \phi(p), \quad R(p) > 0, \quad R(a) > 0, \end{aligned}$$

we have

$$\begin{aligned} p^{2-2\nu} e^{\frac{a}{p}} f(p) &= p^{1-2\nu} e^{\frac{2p}{a}} W_{\frac{1}{2}, \mu} \left(\frac{a}{p} \right) \\ &\doteq x^{2\nu-1} \sum_{\mu, -\mu} \left\{ \frac{\Gamma(-2\mu)(ax)^{\mu+\frac{1}{2}}}{\Gamma(-\mu)\Gamma(\frac{1}{2}+\mu+2\nu)} {}_1F_2(\mu; 1+2\mu, 2\nu+\mu+\frac{1}{2}; ax) \right\} \\ &= g(x), \quad R(2\nu \pm \mu + \frac{1}{2}) > 0. \end{aligned}$$

Hence, by the theorem we get

$$\begin{aligned} K_{\mu+\frac{1}{2}}(\sqrt{ap}) K_{\mu-\frac{1}{2}}(\sqrt{ap}) &= a^\nu \sqrt{\frac{\pi}{p}} \int_0^\infty (p+x)^{-\nu} K_{2\nu} \left\{ 2\sqrt{a(p+x)} \right\} x^{2\nu-1} \\ &\quad \times \left\{ \sum_{\mu, -\mu} \frac{\Gamma(-2\mu)(ax)^\mu}{\Gamma(-\mu)\Gamma(2\nu+\mu+\frac{1}{2})} {}_1F_2(\mu; 1+2\mu, 2\nu+\mu+\frac{1}{2}; ax) \right\} dx \quad \dots \quad (15) \end{aligned}$$

valid, by A.C., for

$$R(2\nu \pm \mu + \frac{1}{2}) > 0, \quad |\arg p| < \pi, \quad |\arg a| < \pi, \quad p \neq 0, \quad a \neq 0.$$

(vi) Lastly, taking (Watson, 1944, p. 439)

$$\begin{aligned} f(x) &= \frac{1}{x} e^{-\frac{\alpha+\beta}{x}} K_\mu \left(\frac{2\sqrt{\alpha\beta}}{x} \right) \\ &\doteq 2p K_\mu(2\sqrt{\alpha p}) K_\mu(2\sqrt{\beta p}) \\ &= \phi(p), \quad R(\alpha) > 0, \quad R(\beta) > 0, \quad R(p) > 0 \end{aligned}$$

we have, on taking $a = (\sqrt{\alpha} + \sqrt{\beta})^2$ in the theorem

$$\begin{aligned} p^{2-2\nu} e^{\frac{(\sqrt{\alpha} + \sqrt{\beta})^2}{p}} f(p) &= p^{1-2\nu} e^{\frac{2\sqrt{\alpha\beta}}{p}} K_\mu \left(\frac{2\sqrt{\alpha\beta}}{p} \right) \\ &= \frac{1}{2} p^{1-2\nu} e^{\frac{2\sqrt{\alpha\beta}}{p}} \sum_{\mu, -\mu} \left\{ \Gamma(-\mu) \left(\frac{\sqrt{\alpha\beta}}{p} \right)^\mu {}_0F_1 \left(1+\mu; \frac{\alpha\beta}{p^2} \right) \right\} \\ &= \frac{1}{2} p^{1-2\nu} \sum_{\mu, -\mu} \left\{ \Gamma(-\mu) \left(\frac{\sqrt{\alpha\beta}}{p} \right)^\mu {}_1F_1 \left(\mu + \frac{1}{2}; 2\mu + 1; \frac{4\sqrt{\alpha\beta}}{p} \right) \right\} \end{aligned}$$

by virtue of the relation

$${}_1F_1(\alpha; 2\alpha; 2z) = e^z {}_0F_1(\alpha + \frac{1}{2}; \frac{1}{2}z^2). \quad \dots \quad \dots \quad \dots \quad (16)$$

On finding the original function, we have

$$g(x) = \frac{1}{2} x^{2\nu-1} \sum_{\mu, -\mu} \left\{ \frac{\Gamma(-\mu)}{\Gamma(2\nu+\mu)} (\sqrt{\alpha\beta} x)^\mu {}_1F_2\left(\mu+\frac{1}{2}; 2\mu+1, 2\nu+\mu; 4\sqrt{\alpha\beta} x\right) \right\}$$

$$R(2\nu \pm \mu) > 0.$$

Thus the theorem gives

$$2K_\mu(2\sqrt{\alpha p})K_\mu(2\sqrt{\beta p}) = (\sqrt{\alpha} + \sqrt{\beta})^{2\nu} \int_0^\infty (p+x)^{-\nu} K_{2\nu}\{2(\sqrt{\alpha} + \sqrt{\beta})\sqrt{p+x}\}$$

$$\times x^{2\nu-1} \left\{ \sum_{\mu, -\mu} \frac{\Gamma(-\mu)}{\Gamma(2\nu+\mu)} (\sqrt{\alpha\beta} x)^\mu {}_1F_2\left(\mu+\frac{1}{2}; 2\mu+1, 2\nu+\mu; 4\sqrt{\alpha\beta} x\right) \right\} dx \quad (17)$$

valid, by A.C., for

$$R(2\nu \pm \mu) > 0, |\arg p| < \pi, |\arg \alpha| < \pi, |\arg \beta| < \pi, p \neq 0, \alpha \neq 0, \beta \neq 0.$$

In particular, when $\nu = \frac{1}{2}$, this result simplifies with the help of the relations

$$K_{\frac{1}{2}}(z) = \sqrt{\frac{\pi}{2z}} e^{-z} \quad \dots \quad (18)$$

$$\Gamma\left(\frac{1}{2}+z\right)\Gamma\left(\frac{1}{2}-z\right) = \pi \sec \pi z \quad \dots \quad (19)$$

and

$$\sqrt{\pi} \Gamma(2z) = 2^{2z-1} \Gamma(z) \Gamma\left(z+\frac{1}{2}\right) \quad \dots \quad (20)$$

to

$$K_\mu(2\sqrt{\alpha p})K_\mu(2\sqrt{\beta p}) = \cos(\mu\pi) \int_0^\infty (px+x^2)^{-\frac{1}{2}} e^{-2(\sqrt{\alpha} + \sqrt{\beta})\sqrt{p+x}}$$

$$\times K_{2\mu}(4\sqrt{\alpha\beta}x) dx \quad \dots \quad (21)$$

$$|R(\mu)| < \frac{1}{2}, |\arg p| < \pi, |\arg \alpha| < \pi, |\arg \beta| < \pi, p \neq 0, \alpha \neq 0, \beta \neq 0.$$

3. It is possible to transform the theorem into another form which involves Whittaker function. For example, if we use the integral (Goldstein, 1932)

$$2K_{2\nu}(2\sqrt{x}) = x^{\frac{1}{2}-\nu} \int_0^\infty e^{-\frac{x}{u}-\frac{1}{2}u} u^{l-2} W_{l,\nu}(u) du \quad \dots \quad (22)$$

in (1), taking $a = 1$, we have

$$\phi(p) = p \int_0^\infty (p+x)^{\frac{1}{2}-\nu} g(x) dx \int_0^\infty e^{-\frac{p+x}{u}-\frac{1}{2}u} u^{l-2} W_{l,\nu}(u) du$$

$$= p \int_0^\infty e^{-\frac{p}{u}-\frac{1}{2}u} u^{l-2} W_{l,\nu}(u) du \int_0^\infty (p+x)^{\frac{1}{2}-\nu} e^{-\frac{x}{u}} g(x) dx$$

on reversing the order of integration, a process which can easily be justified if, for small x , $g(x) = o(x^\mu)$ where $R(\mu) > -1$, and $g(x) = o(x^\lambda)$ for large x .

The result may then be stated in the following form: If

$$f(x) \doteq \phi(p) \text{ and } p^{2-2\nu} e^{\frac{1}{p}} f(p) \doteq g(x)$$

then

$$\phi(p) = p \int_0^{\infty} e^{-\frac{p}{u} - \frac{1}{u}} u^{l-2} W_{l, \nu}(u) F(p, u) du \quad \dots \quad (23)$$

where

$$F(p, u) = \int_0^{\infty} (p+x)^{l-\nu-l} e^{-\frac{x}{u}} g(x) dx$$

provided that the integrals are convergent.

As an illustration, we take (McLachlan and Humbert, 1950, p. 16)

$$f(x) = e^{-\frac{1}{x}} x^{-m-1} \\ \doteq 2p^{l+m+1} K_m(2\sqrt{p}) = \phi(p)$$

we then have

$$p^{2-2\nu} e^{\frac{1}{p}} f(p) = p^{-m-2\nu+1} \\ \doteq \frac{x^{2\nu+m-1}}{\Gamma(2\nu+m)} = g(x), \quad R(2\nu+m) > 0$$

and

$$F(p, u) = \frac{1}{\Gamma(2\nu+m)} \int_0^{\infty} (p+x)^{l-\nu-l} x^{2\nu+m-1} e^{-\frac{x}{u}} dx \\ = e^{\frac{p}{u}} (pu)^{l(\nu+m-l-\frac{1}{2})} u W_{-\frac{1}{2}(3\nu+l+m-\frac{3}{2}), \frac{1}{2}(\nu+m-l+\frac{1}{2})} \left(\frac{p}{u}\right) \\ R(2\nu+m) > 0,$$

on using the integral (Whittaker and Watson, 1935, p. 340)

$$\int_0^{\infty} t^{\alpha}(t+z)^{\beta} e^{-kt} dt = \Gamma(\alpha+1) e^{\frac{1}{2}kz} z^{\frac{1}{2}(\alpha+\beta)} \\ \times k^{-\frac{1}{2}(\alpha+\beta+2)} W_{\frac{1}{2}(\beta-\alpha), \frac{1}{2}(\alpha+\beta+1)}(kz), \quad R(\alpha+1) > 0.$$

On applying (23), we get

$$2K_m(2\sqrt{p}) = p^{l(\nu-l-\frac{1}{2})} \int_0^{\infty} e^{-\frac{1}{u} \left(u + \frac{p}{u}\right)} u^{l(\nu+m+l-\frac{5}{2})} \\ \times W_{l, \nu}(u) W_{-\frac{1}{2}(3\nu+l+m-\frac{3}{2}), \frac{1}{2}(\nu+m-l+\frac{1}{2})} \left(\frac{p}{u}\right) du \quad (24)$$

The restriction $R(2\nu+m) > 0$ may now be removed by A.C. When $m = -2\nu$, this yields (22).

I am grateful to Dr. R. S. Varma for his guidance and interest in the preparation of this paper.

REFERENCES

- Goldstein, S. (1932). Operational Representations of Whittaker's Confluent Hypergeometric Function and Weber's Parabolic Cylinder Functions. *Proc. Lond. Math. Soc.*, (2), **34**, 103-125.
- McLachlan, N. W. and Humbert, P. (1950). Formulaire pour le Calcul symbolique. *Memorial des Sci. Math.*, Fasc. 100.
- Meijer, C. S. (1936). Über Whittakersche Bezw. Besselsche Funktionen und deren Produkte. *Nieuw Archief voor Wiskunde*, Amsterdam, (2), **18**, 4tes Heft, 10-39.
- Mitra, S. C. (1933). On certain Integrals and Expansions involving Bessel Functions. *Bull. Cal. Math. Soc.*, **25**, 81.
- Watson, G. N. (1944). *Theory of Bessel Functions* (Camb. Univ. Press).
- Whittaker, E. T. and Watson, G. N. (1935). *Modern Analysis*.

Issued February 10, 1954.

THE EMISSION BAND SPECTRUM OF Cl_2^+

by P. TIRUVENGANNA RAO, *I.C.I. Research Fellow, N.I.S.I., Department of Physics, Andhra University, Waltair*

(Communicated by K. R. Rao, F.N.I.)

(Received August 1; read October 9, 1953)

INTRODUCTION

During the course of an attempt to excite the band spectrum of CbCl in a high frequency discharge through CbCl_5 vapour, the author has obtained an extensive band spectrum of chlorine, part of which has been analysed and attributed to the Cl_2^+ molecule by Elliott and Cameron (1937 and 1938). Of about 90 bands recorded by them in the visible region, 45 bands were arranged into two sub-systems on the basis of a $^2II-^2II$ electronic transition. Though they confess that their vibrational arrays of both the systems were rather meagre, their assignment of vibrational quantum numbers was extensively supported by the observed chlorine isotope effect in both the systems. Further confirmation of the vibrational assignment was obtained by the rotational analysis of some of the bands belonging to a common level in a progression. In conclusion, Elliott and Cameron suggest that the remaining unclassified bands might belong to another doublet system or that the whole spectrum might consist of four sub-systems arising from a $^4\Delta-^4\Delta$ transition. In view of this, the author felt that there is need for further investigation on the emission spectrum of chlorine.

DESCRIPTION AND ANALYSIS OF THE BANDS

Owing to the free decomposition of the CbCl_5 into free chlorine and other products, the set-up of a high frequency discharge through low-pressure vapour proved a suitable method of excitation. The spectrum was photographed both

TABLE I
Vibrational analysis of Sub-system I of Cl_2^+ bands

$\nu'' \backslash \nu'$	0	1	2	3	4	5	6	7
0		20120.7		18859.2				
1	21324.7							
2	21872.7		20595.0*	19971.7	19349.7			
3			21139.3	20509.2				
4		22302.4	21668.7	21040.9	20418.9		19192.3	18587.7
5	23457.7	22820.5	22186.2	21559.0		20320.8		
6	23967.1	23327.7	22694.0		21440.4	20827.9		
7			23184.6	22556.9	21936.2		20713.5	
8	24947.9	24308.4						20595.0*
9		24788.3	24148.2		22893.7			
10	25883.5	25242.2	24600.6		23354.7			

* Occurs twice in the system.

TABLE II
Isotopic Separations of the new Cl_2^+ bands

Wave-number.	Classification.	Isotopic separations.	
		Calc.	Obs.
20509.2 20514.7 i	3, 3	3.7	5.5
20595.0	• 2, 2	2.7	*
21132.6 i 21139.3	3, 2	4.6	6.7
21315.1 i 21324.7	1, 0	7.1	9.6
21433.5 i 21440.4	6, 4	6.9	6.9
21919.9 i 21936.2	7, 4	12.7	16.3
22168.5 i 22186.2	5, 2	17.3	17.7
22537.0 i 22556.9	7, 3	20.9	19.9
22868.0 i 22893.7	9, 4	23.5	25.7
23155.6 i 23184.6	7, 2	29.3	29.0
23327.4 i 23354.7	10, 4	28.3	27.3
23420.9 i 23457.7	5, 0	34.7	36.8
24554.1 i 24600.6	10, 2	45.1	46.5
24735.1 i 24788.3	9, 1	48.7	53.2
25184.4 i 25242.2	10, 1	53.6	57.8

* Too small to be measured accurately.

on a Fuess Glass Instrument and on the higher dispersion of a three prism Glass Littrow spectrograph. Plate II(a) and II(b) which are reproductions of plates taken on the latter, show the well-resolved rotational structure of most of the bands. For a detailed rotational analysis of the bands, still higher dispersion such as the first order of a 10 ft. grating is necessary. However, the dispersion of the Glass Littrow instrument was quite sufficient for a vibrational analysis of the bands.

A close scrutiny of the reproductions shown here with those published by Elliott and Cameron (1937) revealed the existence of many bands newly obtained

in the present investigation. Owing to the fact that the development of the vibrational schemes given by them is rather meagre, the author's first attempt was to see whether these new bands could form part of the two sub-systems. It was found that 30 new bands could be fitted into the vibrational scheme of sub-system I as shown in Table I. Half of these bands were due to the less abundant molecule $\text{Cl}^{35}\text{Cl}^{37+}$. The correctness of the assignment is proved not only by the fit of the bands in the band head formula

$$\nu = 20797.3 + [572.3 (v' + \frac{1}{2}) - 5.32 (v' + \frac{1}{2})^2 - 0.013 (v' + \frac{1}{2})^3] \\ - [645.3 (v'' + \frac{1}{2}) - 2.91 (v'' + \frac{1}{2})^2]$$

but also by the extensive agreement between the calculated and observed isotopic separations shown in Table II. Some of the prominent isotopic pairs newly assigned were shown in the reproductions II(a) and II(b). No new bands belonging to sub-system II were observed.

The intensity distribution in the bands (including those analysed in the present work) on a scale of 10 is shown in Table III. It can be seen that the distribution corresponds to a Franck-Condon parabola type to be expected for a system with such ω_e values as given above.

TABLE III
Intensity Distribution in Sub-system I

	0	1	2	3	4	5	6	7
0	..	2	..	3
1	8
2	4	..	6	4	2
3	5	4
4	..	2	7	8	4	..	1	1
5	4	8	6	5	..	4
6	3	7	6	..	6	7
7	5	6	6	..	5	..
8	3	4	6
9	..	6	7	..	2
10	3	5	4	..	7

For establishing the electronic transition of both the sub-systems a detailed study of the rotational analysis of some of the new bands using the higher dispersion of a 10 ft. grating is necessary. An attempt should also be made to interpret the origin of the large number of unclassified bands some of which are very intense. They may probably belong to the neutral molecule Cl_2 . Further study of the spectrum in the visible and the near infra-red is still in progress.

The emission spectrum of bromine was also photographed in the visible region and further study in the near infra-red is in progress.

ABSTRACT

The emission spectrum of chlorine has been excited in a high frequency discharge tube containing a small quantity of CbCl_5 using a three prism glass Littrow spectrograph. An examination of the spectrum revealed the existence of about 30 new bands attributable to Cl_2^+ in addition to those reported earlier by Elliott and Cameron. A vibrational analysis of these bands has shown that they belong to sub-system I of Cl_2^+ bands analysed by them on the basis of a ${}^2\Pi - {}^2\Pi$ transition. About 15 bands have been newly classified, the remaining being the isotopic heads due to the less abundant molecule $\text{Cl}^{35}\text{Cl}^{37+}$.

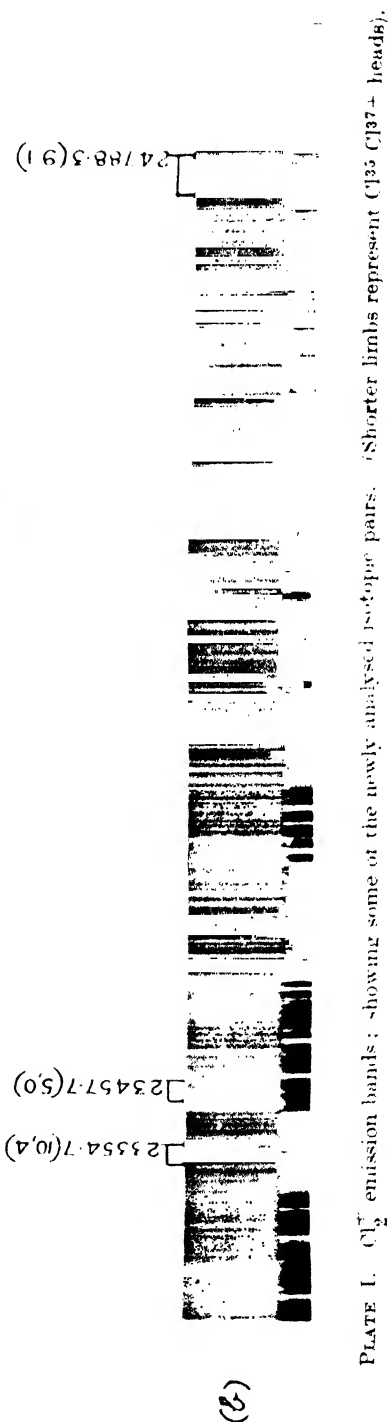
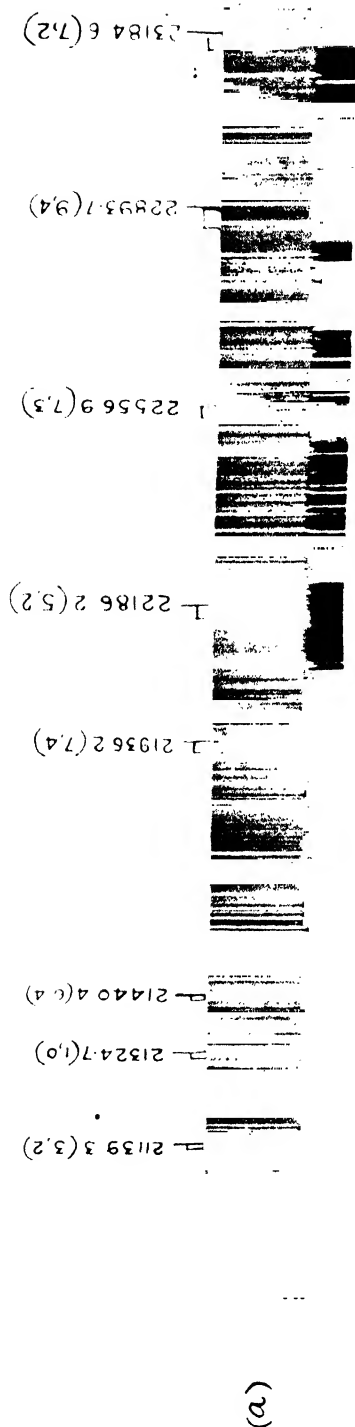


PLATE I. $C_{15} C_{137}^+$ emission bands: showing some of the newly analysed isotope pairs. (Shorter limbs represent $C_{15} C_{137}^+$ heads).

The vibrational assignment of each one of the bands is well supported by the observed isotope effect.

Further work to know the origin of the remaining unclassified bands in the emission spectrum of chlorine is in progress.

ACKNOWLEDGEMENTS

The author desires to express his grateful thanks to Prof. K. R. Rao for his interest in the work and to the National Institute of Sciences of India for the award of an I.C.I. Fellowship.

REFERENCES

- Elliott, A. and Cameron, W. H. B. (1937). The emission band spectrum of chlorine— I. *Proc. Roy. Soc. Lond.*, **158**, 681–691.
- (1938). The emission band spectrum of chlorine (Cl_2^+)— II. *Ibid.*, **164**, 531–546.

Issued February 10, 1954.

A THEORY OF RESISTANCE IN P~~O~~TENTIAL FLOWS

(PARTS I-IV)

by N. L. GHOSH, *Senior Professor of Mathematics, Presidency College, Calcutta*

(Communicated by N. R. Sen, F.N.I.)

(Received August 25; read October 9, 1953)

PART I

D'ALEMBERT'S PARADOX AND ITS RESOLUTION

SEC. A

Introduction

1. *A Brief Survey of the Problem*

D'Alembert proved, as is well known, that when a perfect fluid flows past a solid body in potential motion the total pressure thrust of the fluid on the body (excluding buoyancy) vanishes. In actual experience it has always been found that a body moving through air or water does experience a resistance. The treatment of air and water as perfect fluids yielded, in Hydrostatics, results remarkably in accord with experience. The flow past solid bodies was actually observed to be very largely a potential flow. It was therefore expected that the theory of potential flows should account for at least a major part of the resistance experienced by solids. D'Alembert's results pointed to the contrary and were therefore regarded as paradoxical. They seemed to provide a proof of the inadequacy of the classical theory of fluid flows. (Durand, 1935; Goldstein, 1938; Prandtl-Tietjens, 1934; Birkhoff, 1950).

Helmholtz's attempts to obtain resistance in potential flows by means of the theory of free-stream-lines and wakes is well known. (Helmholtz, 1868; Kirchhoff, 1869.) The basic principles of his approach were founded on the observed fact that when a body moves through a fluid it is usually followed by a dead-water region relatively at rest with the body, called the wake, and the observed potential flow is outside the system formed by the body and the wake. If any resistance is experienced by the body in uniform motion it should be the total reaction of the fluid on the body-wake system upon which D'Alembert's paradox would again apply. To avoid this difficulty, known as Brillouin paradox (Villat, 1929), the wake had to be extended to infinity, which resulted in the outside potential flow being delimited by the so-called free-streamlines where the velocity was everywhere the same. These specifications were, however, sufficient to determine the flow uniquely (Riabouchinsky, 1930) and further application of this theory was made in the study of several problems (Leray, 1935). As for resistance, it was applied to the case of a flat plate moving at right angles to itself; a positive result was obtained but it was nearly about half the observed value. (Goldstein, 1938, Vol. I, p. 37.) The work of Levi-civita (1907) and Cisotti (1922) extended the applicability of the theory to the case of curved boundaries and some solutions for circular boundaries have been obtained. (Rosenhead, 1928; Brodetzky, 1926; Wenistein, 1933.)

But the essential objection to Helmholtz theory lies in the admission that the introduction of the body should modify the flow at infinity, i.e., the wake should extend to infinity—a contradiction to observed facts. Besides, when the body is moving the wake must have an infinite energy.

Another phenomenon that observation records, in addition to closed wakes, is the formation of vortices inside the wake. On the basis of this observation a theory of calculation of the *form drag* was constructed and gave much better results. It was, however, found that a symmetrical system of vortex filaments (in two-dimensional flow) could not be stable. The stable arrangement, known as the 'Karman vortex street' would introduce asymmetry and thereby disturb the steady character of the flow (Lamb, 1932; Milne Thomson, 1949; Durand, 1935; Goldstein, 1938.)

Meanwhile it was contended that a real fluid like air or water has an appreciable coefficient of viscosity and that D'Alembert's paradox was possibly a consequence of the neglect of viscosity. Attempts to introduce viscosity into the theory of fluid flows resulted in the modification of Euler's equations of motion into the Navier-Stokes equations. The order of the equation was raised and consequently additional boundary conditions were looked for. After a long and protracted controversy (Goldstein, 1938, Vol. II, Appendix) it was finally decided that in the case of viscous fluids there should be no tangential component of the velocity on the surface of a body; in other words 'there should be no slip'.

The intractability of the Navier-Stokes equations thwarted all attempts at exact solutions except in a few simple cases, and perhaps the Hagen-Poiseuille flow in capillary tubes is the strongest available evidence in favour of the no-slip hypothesis. Motions past spheres or cylinders were solved under highly restrictive conditions as in Stokes or Oseen's solutions. (Lamb, 1932.)

Prandtl (1904) effected a sort of compromise between observation and theory in what is known as the Boundary Layer Theory. The main arguments of the theory are as follows:—'Let us admit the fact that the flow of a real fluid past a solid body is mainly a potential flow except in a thin layer round the body and possibly the wake, where only viscosity comes into play. There should be no slip on the boundary but, instead of a sudden discontinuity into the main-stream potential flow, let us conceive of a thin layer of fluid where a quick transition from the no-velocity on the surface to the main-stream velocity takes place.' The theory explained the separation of the flow and the formation of vortices but its mathematical aspects were never regarded as too satisfactory (Krzywoblocki, 1953). It provides, however, the only basic method for the calculation of the skin-friction drag at present.

In practical aeronautics to-day, calculations are carried out in parts. The form-drag is calculated from the theory of vortices and the skin-friction-drag is calculated in an approximate manner by means of the Boundary Layer Theory. (Goldstein, 1938; Durand, 1935.)

Thus the problem of fluid-resistance cannot yet be said to be in all too happy a state.

2. *The physical background and the justification for a new outlook.*

Let us turn for a moment to the basic facts of experience and observations as recorded in the photographs taken at various laboratories. (Goldstein, 1938; Durand, 1935; Birkhoff, 1950.) These have been very ably summarised by Goldstein, 1938 (Vol. I, Chaps. I and II). They are as follows:—

- (i) A real fluid like air or water has an appreciable amount of viscosity.
- (ii) A resistance is experienced when a body moves steadily through a real fluid.

- (iii) At start, the flow is practically wholly potential without wakes.
(We shall henceforth characterise this as the *Primary Potential* flow.)
- (iv) When a steady state is attained, the relative-flow picture (i.e. when the camera is fixed to the body) reveals usually a wake of finite dimensions and a potential flow outside the body-wake system. Inside the wake vortices are seen to exist. Separation takes place at some point wherefrom starts the boundary of the wake as in Fig. 1 (after

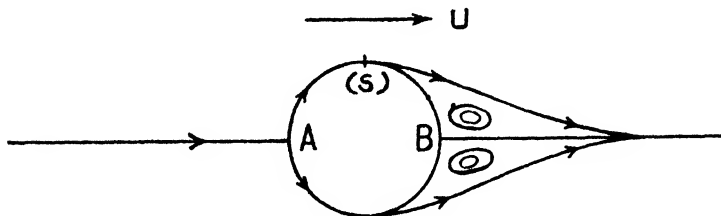


FIG. 1.

- (Goldstein, 1938, Vol. I, p. 64.) The separation point S , changes position and approaches the forward stagnation point A closer and closer as the velocity of the main flow is increased.
- (v) Pressure measurements round circular cylinders and spheres even in flows with little wakes reveal a higher pressure in the foreparts than at the back. (See Goldstein, Vol. I, p. 24, Figs. 4, 5.)
 - (vi) The flow, a little away from the body, has been shown by computation to agree very closely with the theoretically calculated potential flow (Goldstein, 1938, Vol. II, p. 551).
 - (vii) By appropriate sucking at points of the body-surface it is possible to retard the separation of the flow and make it coincide very nearly with the primary potential flow, so that the non-zero surface-velocity of the potential flow shows itself almost immediately beside the surface.

Before proceeding further, it is necessary to remember that Jeffreys (1930) had given a theoretical proof that the only potential motion possible under the no-slip condition is a rigid body motion where the fluid and the solid move as a whole. It has been our convention, so far, that for $\mu \neq 0$ we must impose the no-slip condition on the boundary. This contradicts the possibility of potential flows when viscosity is taken into account.

Nature, however, reveals that in the case of real fluids where viscosity is not of a negligible order, potential motions with or without wakes do take place. Possibly Nature avoids Jeffreys's condition by forming an indefinitely thin layer of sticking fluid over which slipping takes place—as is generally envisaged in the Boundary Layer Theory. We shall see, as we proceed, that it is possible to resolve some of the long-standing paradoxes of fluid mechanics by discarding the 'hypothesis of no slip' on the surface in the case of real fluids.

3. The New Approach and its Consequences

With the above in view, we start with the assumptions—

- (i) that in real fluids, in motion, $\mu \neq 0$.
- (ii) that, despite (i), the fluid may have a tangential velocity on the body-surface.

We know that the general equations of motion for a viscous fluid are represented by the Navier-Stokes equations*. It is easy to see that all potential flows ($\nabla^2\psi = 0$) are solutions of these equations. This whole set of solutions stand barred when the no-slip hypothesis is brought in. Hence when the no-slip condition is no longer adhered to, potential flows of viscous fluids become possible. We shall develop our results on the basis of this possibility.

Consequences

As a consequence of the above we shall show without further assumptions or approximations that:—

1. A solid moving in a real fluid does experience a positive resistance, even when the flow has no circulation or vortices. This resolves D'Alembert's paradox.
2. The resolution of D'Alembert's paradox removes all objections to the possibility of *finite wakes* and hence resolves Brillouin's paradox.
3. Even in a primary potential flow, i.e., a flow without wakes, vortices, or circulation, the thrust in the foreparts of the obstacle does exceed the same in the hind parts.
4. That the form-drag and the skin-friction drag both exist in a definite way in every case of primary potential flow.
5. That it is possible to construct a general formula for the total drag on a cylinder in every case of flow, with or without wakes.

These constitute the major achievements of our approach.

Normal Thrust and Pressure

The usual concept of pressure in a fluid holds only when the fluid is assumed to be perfect or is at rest if viscous. With the introduction of viscosity and the fluid in motion we must replace the simple pressure concept by that of the normal and tangential tractions across a surface which may change with the orientation of the surface. The symbol ' p ' used in the Navier-Stokes equations can no longer be interpreted as the normal thrust per unit area in every direction; it will merely represent the average normal stress across three orthogonal surfaces through a point of the fluid.

In the case of two-dimensions, ' p ', therefore, no longer represents the normal action per unit length. That will, in general, be different from ' p ' and we shall denote it by p_n .

In all pressure measurements with airfilled tubes like the Pitot tubes, the effective pressure on the gas is the normal thrust per unit area and hence must be a measure of p_n instead of p . Hence, all actual records of 'pressure' measurements will be interpreted to measure p_n and not p .

In section B, Part I, we shall work out a few results in support of our conclusions.

SEC. B

The Resolution of D'Alembert's Paradox

4. General Formulae.

Let us consider a primary two-dimensional potential flow past any fixed cylinder. We assume that the flow takes place in the x - y plane and that ϕ_1 , ψ_1

* In two dimensions it is

$$\frac{\partial}{\partial t} \nabla^2 \psi + \psi_y \nabla^2 \psi_x - \psi_x \nabla^2 \psi_y = \nu \nabla^4 \psi$$

where ψ represents the stream-function.

represent the velocity-potential and the stream-function respectively for the same, and that, ψ_1 vanishes on the surface S of the body. If

$$W_1 \equiv \phi_1 + i\psi_1 \quad \dots \quad \dots \quad \dots \quad \dots \quad (4.1)$$

represents the complex potential, the whole of the x - y plane with the exception of the area occupied by the body is mapped into the W_1 plane with a slit on the ϕ_1 -axis and any point in the x - y plane outside the body or on it can be represented by a pair of orthogonal curvilinear co-ordinates (ϕ_1, ψ_1) . Let us assume that ϕ_1 increases from left to right and ψ_1 increases from below upwards.

If ds_1, ds_2 be the elements of length normal to $\phi_1 = \text{constant}$ and $\psi_1 = \text{constant}$, respectively, at (ϕ_1, ψ_1) we have

$$\left. \begin{aligned} ds_1 &= \frac{1}{q_1} d\phi_1 \\ ds_2 &= \frac{1}{q_1} d\psi_1 \end{aligned} \right\} \quad \dots \quad \dots \quad \dots \quad \dots \quad (4.2)$$

where q_1 represents the speed of flow at (ϕ_1, ψ_1) .

Stresses.

In the general orthogonal system $\alpha = \text{const.}$, $\beta = \text{const.}$, $\gamma = \text{const.}$ in three dimensions, the stress components are given by

$$\left. \begin{aligned} p_{\alpha\alpha} &= -p + 2\mu e_{\alpha\alpha} \\ p_{\beta\beta} &= -p + 2\mu e_{\beta\beta} \\ p_{\alpha\beta} &= p_{\beta\alpha} = \mu e_{\alpha\beta} \\ &\text{etc.} \dots \end{aligned} \right\} \quad \dots \quad \dots \quad \dots \quad \dots \quad (4.3)$$

where

$$\left. \begin{aligned} e_{\alpha\alpha} &= \frac{1}{h_1} \frac{\partial u}{\partial \alpha} + \frac{v}{h_1 h_2} \frac{\partial h_1}{\partial \beta} + \frac{w}{h_3 h_1} \frac{\partial h_1}{\partial \gamma} \\ e_{\beta\beta} &= \frac{1}{h_2} \frac{\partial v}{\partial \beta} + \frac{w}{h_2 h_3} \frac{\partial h_2}{\partial \gamma} + \frac{u}{h_1 h_2} \frac{\partial h_2}{\partial \alpha} \\ e_{\alpha\beta} &= \frac{h_2}{h_1} \frac{\partial}{\partial \alpha} \left(\frac{v}{h_2} \right) + \left(\frac{h_1}{h_2} \right) \frac{\partial}{\partial \beta} \left(\frac{u}{h_1} \right) \\ &\text{etc.} \dots \end{aligned} \right\} \quad \dots \quad \dots \quad (4.4a)$$

u, v, w representing the velocity components normal to the surfaces $\alpha = \text{const.}$, $\beta = \text{const.}$ and $\gamma = \text{const.}$ respectively and where

$$ds^2 = (h_1 d\alpha)^2 + (h_2 d\beta)^2 + (h_3 d\gamma)^2 \quad \dots \quad \dots \quad \dots \quad (4.4b)$$

Hence for the two-dimensional ϕ_1, ψ_1 system where $\phi_1 \equiv \alpha$, $\psi_1 \equiv \beta$, $\gamma \equiv z$,

$\left(\frac{\partial}{\partial z} = 0 \right)$ we have

$$\left. \begin{aligned} h_1 &= h_2 = \frac{1}{q_1}, h_3 = 1 \\ u &= q_1, v = 0, w = 0 \end{aligned} \right\} \quad \dots \quad \dots \quad \dots \quad (4.5)$$

and consequently

$$\left. \begin{aligned} p_{xx} &\equiv p_{\phi_1\phi_1} = -p + \mu \frac{\partial q_1^2}{\partial \phi_1} \\ p_{\beta\beta} &\equiv p_{\psi_1\psi_1} = -p - \mu \frac{\partial q_1^2}{\partial \psi_1} \\ p_{x\beta} &\equiv p_{\phi_1\psi_1} = \mu \frac{\partial q_1^2}{\partial \psi_1} \end{aligned} \right\} \dots \dots \dots (4.6)$$

On the surface of the body $\psi_1 = \text{const.}$ and hence the components of the stress exerted by the fluid on the body are (Fig. 2).

- (i) a normal stress $-p_{\psi_1\psi_1}$ per unit length towards the body;
- (ii) a tangential stress $-p_{\phi_1\phi_1}$ per unit length in the positive sense of flow.

Denoting these two components of the surface action by p_n and p_t respectively, we have,

$$p_n = -p_{\psi_1\psi_1} = p + \mu \frac{\partial q_1^2}{\partial \phi_1} \dots \dots \dots (4.7)$$

$$p_t = -p_{\phi_1\phi_1} = -\mu \frac{\partial q_1^2}{\partial \psi_1} \dots \dots \dots (4.8)$$

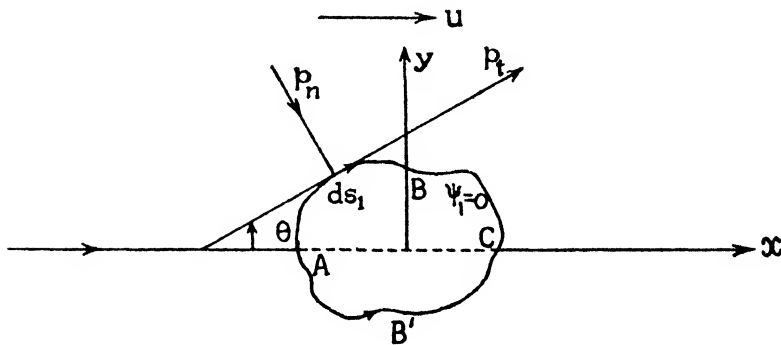


FIG. 2.

If now X and Y denote the x - and y -components of the total reaction we have (Fig. 2)

$$X = \int_{ACB'A} (p_t \cos \theta + p_n \sin \theta) ds_1; \quad Y = \int_{ACB'A} (p_t \sin \theta - p_n \cos \theta) ds_1.$$

Now,

$$\frac{dx}{ds_1} = \cos \theta, \quad \frac{dy}{ds_1} = \sin \theta.$$

Hence substituting from (4.7) and (4.8) and remembering that

$$\int p dy = \int p dx = 0 \dots \dots \dots (4.9)$$

by D'Alembert's paradox, we have

$$\begin{aligned} X &= \mu \oint \left\{ \frac{\partial q_1^2}{\partial \phi_1} dy - \frac{\partial q_1^2}{\partial \psi_1} dx \right\} \\ Y &= -\mu \oint \left\{ \frac{\partial q_1^2}{\partial \psi_1} dy + \frac{\partial q_1^2}{\partial \phi_1} dx \right\} \end{aligned} \quad \dots \dots \dots (4.10)$$

where the integrals are taken round the contour of the body in the clockwise sense in each case.

Modification of Blasius' Theorem.

Equations (4.10) provide the corresponding modification of the Blasius' theorem. In the general case where (4.9) is not assumed to hold, we have, in fact,

$$X - iY = -\frac{1}{2} \rho i \oint \left| \frac{dW_1}{dz} \right|^2 dz + 2\mu i \oint \frac{\partial q_1^2}{\partial \bar{W}_1} d\bar{z}, \quad \dots \dots (4.11)$$

$W_1 = \bar{W}_1$

where \bar{W}_1 and \bar{z} represent the complex conjugates of W_1 and z .

Form-drag and Skin-friction-drag.

In every symmetrical case where the flow is parallel to the x -axis, $Y = 0$ and the total resistance X (per unit length of the cylinder) is contributed by both p_n and p_t . These two contributions are technically known as the *form-drag* and the *skin-friction-drag* respectively. Denoting them by X_N and X_t we have

$$X_N = \mu \oint \frac{\partial q_1^2}{\partial \phi_1} dy \quad \dots \dots \dots (4.12)$$

$$X_t = -\mu \oint \frac{\partial q_1^2}{\partial \psi_1} dx \quad \dots \dots \dots (4.13)$$

where (4.9) is assumed to hold. Of course,

$$X = X_N + X_t \quad \dots \dots \dots (4.14)$$

5. Particular Cases.

A. Circular Cylinder (radius = a)

$$W_1 = U \left(z + \frac{a^2}{z} \right) \quad \dots \dots \dots (5.1)$$

$$q_1^2 = U^2 \left\{ 1 - \frac{2a^2}{r^2} \cos 2\theta + \frac{a^4}{r^4} \right\} \quad \dots \dots \dots (5.1a)$$

On $r = a$,

$$\begin{aligned} q_1 \frac{\partial}{\partial \psi_1} &= \frac{\partial}{\partial r} \\ q_1 \frac{\partial}{\partial \phi_1} &= -\frac{1}{a} \frac{\partial}{\partial \theta} \quad (\text{as } \theta \text{ decreases with } s_1) \end{aligned}$$

hence from (4.10), (4.12) and (4.13) we have,

$$\left. \begin{aligned} X &= 8\pi\mu U (\neq 0) \\ X_N &= 4\pi\mu U \\ X_t &= 4\pi\mu U \\ Y &= 0. \end{aligned} \right\} \quad \dots \quad \dots \quad \dots \quad (5.2)$$

Besides, from (4.7) and (4.8)

$$p_n = p - \frac{4\mu U}{a} \cos \theta \quad \dots \quad \dots \quad \dots \quad (5.2a)$$

$$p_t = \frac{4\mu U}{a} \sin \theta \quad \dots \quad \dots \quad \dots \quad (5.2b)$$

where p is given by Bernoulli's equation, so that

$$p = \Pi - \frac{1}{2}\rho q_1^2 \quad \dots \quad \dots \quad \dots \quad (5.2c)$$

Π denoting the stagnation pressure (Fig. 3).

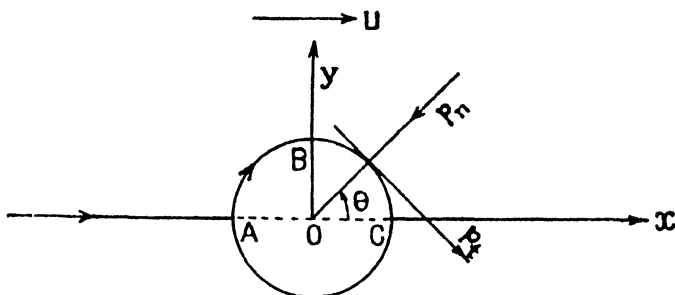


FIG. 3.

Observations

(i) From (5.2) it is clear that a circular cylinder in a primary potential flow without wakes or vortices will actually experience a force towards the direction of the flow. There is a positive form-drag and a skin-friction drag and the two are equal.

(ii) (5.2a) shows obviously (Fig. 3) that the normal thrust at the foreparts of the cylinder where $\frac{\pi}{2} \leq \theta \leq \pi$ exceeds the same at corresponding points on the hind parts where $0 \leq \theta < \frac{\pi}{2}$. This verifies a well-known item of experience without bringing in wakes.

B. Elliptic Cylinder: Flow parallel to the major axis

In this case, the primary potential flow is represented by

$$W_1 = U \left[b \sqrt{\frac{a+b}{a-b}} e^{-\zeta} + cz \right] \quad \dots \quad \dots \quad \dots \quad (5.3)$$

where

$$z = c \cosh \zeta = c \cosh (\xi + i\eta). \quad \dots \quad \dots \quad \dots \quad (5.4)$$

The surface of the body is the ellipse

$$\frac{x^2}{a^2} + \frac{y^2}{b^2} = 1 \quad \dots \dots \dots (5.4a)$$

where

$$\left. \begin{aligned} \xi &= \alpha \text{ (const.)} \\ a &= c \cosh \alpha, \quad b = c \sinh \alpha, \quad c^2 = a^2 - b^2 \end{aligned} \right\} \dots \dots (5.4b)$$

Now, on a $\xi = \text{const.}$

$$\frac{\partial}{\partial n} = \frac{1}{h} \frac{\partial}{\partial \xi}, \quad \frac{\partial}{\partial s} = \frac{1}{h} \frac{\partial}{\partial \eta}$$

s being measured from left to right, so that

$$h^2 = c^2 (\sinh^2 \xi + \sin^2 \eta) \quad \dots \dots \dots (5.4c)$$

Now for such a flow

$$q_1^2 = \frac{U^2}{h^2} \left[h^2 + ab \left(\frac{a+b}{a-b} \right) e^{-2\xi - b(a+b)} \cos 2\eta \right] \dots \dots (5.5)$$

but, in general,

$$\left. \begin{aligned} q_1 \frac{\partial}{\partial \psi_1} &= \frac{\partial}{\partial n}, \quad q_1 \frac{\partial}{\partial \phi_1} = \frac{\partial}{\partial s} \\ \psi_1 &= \text{const.} \end{aligned} \right\} \dots \dots \dots (5.6)$$

Hence,

$$X = -\mu \oint \frac{1}{q_1 h} \left[\frac{\partial q_1^2}{\partial \xi} dx + \frac{\partial q_1^2}{\partial \eta} dy \right]$$

which gives on simplification (for $b \neq 0$)

$$X = 4\pi\mu U \left(1 + \frac{b}{a} \right) \dots \dots \dots (5.7)$$

Also, from (4.12), (4.13), we have

$$\left. \begin{aligned} X_N &= 2\pi\mu U \left(1 + \frac{b}{a} \right) \\ X_t &= 2\pi\mu U \left(1 + \frac{b}{a} \right) \end{aligned} \right\} \dots \dots \dots (5.7a)$$

We notice that there is again a positive resistance and the form and skin-friction drags are equal in this case also.

In the limiting case when $b \rightarrow a$ either $\alpha \rightarrow \infty$ or $c \rightarrow 0$, but the ellipse becomes a circle and the result agrees with those for a circular cylinder for which the drags are independent of the radius (as is expected from dimensional considerations).

6. Solid Sphere

When a sphere moves through a fluid with uniform velocity the motion is three-dimensional but has an axis of symmetry. Calculations for the total resistance etc. can be carried out in a manner similar to the above as the primary potential motion for such a body is known; and the stress components can be

calculated from (4.3), (4.4) without difficulty. Measuring θ from the back stagnation point in an anticlockwise sense we have the following results :—

$$\left. \begin{aligned} \phi_1 &= Ur \sin \theta + \frac{1}{2} U \frac{a^3}{r^2} \cos \theta \\ u &= \frac{\partial \phi_1}{\partial r} = U \cos \theta \left(1 - \frac{a^3}{r^3} \right) \\ v &= \frac{1}{r} \frac{\partial \phi_1}{\partial \theta} = -U \sin \theta \left(1 + \frac{1}{2} \frac{a^3}{r^3} \right) \end{aligned} \right\} \quad \dots \quad (6.1)$$

$$q_1^2 = U^2 \left[\cos^2 \theta \left(1 - \frac{a^3}{r^3} \right)^2 + \sin^2 \theta \left(1 + \frac{1}{2} \frac{a^3}{r^3} \right)^2 \right] \quad \dots \quad (6.1a)$$

$$p_n = p - \frac{6\mu U}{a} \cos \theta \quad \dots \quad (6.2a)$$

$$p_t = \frac{3\mu U}{a} \sin \theta \quad \dots \quad (6.2b)$$

$$X_N = - \int_S p_n \cos \theta \, dS = 8\pi\mu Ua \quad \dots \quad (6.3a)$$

$$X_t = \int_S p_t \sin \theta \, dS = 8\pi\mu Ua \quad \dots \quad (6.3b)$$

$$X = X_N + X_t = 16\pi\mu Ua \quad \dots \quad (6.4)$$

Observations

(i) The remarks made on the results for a circular cylinder hold here also though the results are not quantitatively the same.

(ii) It should be remembered that Stokes' famous formula for the resistance on a sphere gives the value $6\pi\mu Ua$. Thus there is an agreement in order though not in value. There is, however, every reason why the two results should differ. Stokes' formula was derived on the assumption that the motion is very slow so that the inertia terms were neglected and, further, the no-slip condition on the boundary was also imposed. In our case, there is no approximation, but the existence of the potential flow is assumed (and consequently the no-slip condition discarded). A primary potential flow round a sphere is unlikely to be stable, as we shall see in Part II, but if such a flow holds at any time there is hardly any escape from the resistance being $16\pi\mu Ua$.

7. Further possibilities

(I) *Flows with circulation or vortices.*—It is obviously quite an easy matter to extend the calculations to those cases where the potential flow is attended with a circulation or vortices. We have merely to modify the complex potential W_1 but the general formulae derived in Art. 4 hold *mutatis mutandis*. The singularities of the field do not create any difficulty as integration on the body surface only is involved.

(II) *Potential flows in three-dimensions.*—For any three-dimensional system for which the primary potential flow is known the stress components on the body surface can always be calculated from (4.3), (4.4a) by a suitable choice of orthogonal co-ordinates or even in a Cartesian system. Hence it is always possible to calculate either the form-drag or the skin-friction drag for any body whatsoever, under any

type of general motion, provided the primary potential flow round it is solved. I believe the procedure is direct enough to need no illustration.

Besides, it appears that the method opens up an extensive field of investigation specially to the advantage of aeronautical practice, where the flow round the aerofoil is supposed to be very nearly a potential flow. If the flow is not primary potential (with or without isolated vortices) it should be followed by a wake and we shall see in Part IV how the calculations can be extended to the cases of flows with wakes.

ABSTRACT

This paper is divided into Sections A and B. Section A contains a critical survey of the existing theories of fluid resistance and pointing out some of the major inconsistencies explains that the age-old paradoxes of the Classical theory really arise out of a neglect of viscosity coupled with the hypothesis of no slip on the boundary. It further, points out that a change of outlook more in agreement with the facts of observation brings in a remarkable simplification into the whole problem and at the same time resolves effectively D'Alembert's paradox and Brillouin's paradox.

Section B gives a general formula—a modification of Blasius' formula—for the calculation of the resistance on any cylinder moving in a real incompressible fluid with uniform velocity and the results thereof, for the resistance of a circular cylinder, an elliptic cylinder and a sphere.

REFERENCES

- Brodetzky, S. (1926). Discontinuous fluid motions past curved Barriers. *Proc. II. Congress for Appl. Maths. Zurich*.
- Cisotti, U. (1921-22). *Idromeccanica piana*, Milan.
- Durand, W. F. (1935). *Aerodynamic Theory*, Julius Springer, 6 vols.
- Goldstein, S. (1938). *Modern Developments in Fluid Dynamics*, Oxford. 2 vols.
- Helmholtz, H. von (1868). Über discontinuierliche Flüssigkeitsbewegungen. *Phil. Mag.*, Nov.
- Jeffreys, H. (1930). *Proc. Roy. Soc. A*, **128**, 376.
- Kirchhoff, G. (1869). Zur Feier Flüssigkeitsstrahlen. *Crelle's journals, für Math.* **70**, 289-298.
- Krzywoblocki, M. Z. (1953). On the fundamentals of the Boundary Layer Theory. *Jour. Franklin Inst.*, April.
- Lamb, H. (1932). *Hydrodynamics*.
- Leray, J. (1935). Les problèmes de représentation conforme de Helmholtz théorie des sillages et des pous. *Commentarii Math. Helv.*, **8**.
- Levi-Civita, T. (1907). Scie e leggi di resistenza. *Rendiconti Circolo Mat., Palermo*, **23**, 1-37.
- Milne-Thomson, L. M. (1950). *Theoretical Hydrodynamics*, Oxford.
- Prandtl, L. and Tietjens, O. G. (1934). *Hydro and Aeromechanics*, McGraw-Hill, 2 vols.
- Prandtl, L. (1904). Verhandlungen des dritten internationalen Mathematiker Kongresses, Heidelberg, 484-491.
- (1938). *Mechanics of viscous Fluids in Aerodynamic Theory* (edited by Durand), **3**.
- Riabouchinsky, D. (1930). Sur quelques problèmes généraux relatif au mouvement et à la résistance des fluides. *Proc. Int. Cong. Appl. Math. III*, I, Stockholm.
- Rosenhead, L. (1928). Resistance of a Barrier in the shape of an arc of a circle. *Proc. Roy. Soc. A*, **117**, 417.
- Villat, H. (1911). Sur la résistance des fluides, Paris.
- Weinstein, A. (1933). Sur les sillages provoques par des arcs circulaires. *Acc. dei Lincei*, **17**, 83.

PART II

DISSIPATION IN POTENTIAL MOTION

1. It is well known that the total rate of dissipation, i.e., the rate at which mechanical energy is disappearing, is given by (Lamb, 1932, pp. 379-381).

$$D = \mu \int (\xi^2 + \eta^2 + \zeta^2) dv - \mu \int \frac{\partial q^2}{\partial n} dS + 2\mu \int \left| \begin{array}{ccc} l, m, n \\ u, v, w \\ \xi, \eta, \zeta \end{array} \right| dS. \quad \dots (1.1)$$

where

D = the total rate of dissipation,

u, v, w = the components of velocity,

ξ, η, ζ = the components of vorticity,

q = the speed of motion,

the first integral is taken over the entire range of the fluid, the second and third integrals are taken over all finite boundaries S (irrespective of slip or no slip on the surface) and l, m, n denote the direction-cosines of the normal drawn at a point of S into the fluid.

In the particular case where the flow is purely potential ξ, η, ζ vanish everywhere and the equation (1.1) reduces to

$$D = -\mu \int \frac{\partial q^2}{\partial n} \cdot dS \quad \dots \quad \dots \quad \dots \quad (1.2)$$

$\frac{\partial}{\partial n}$ denoting the derivative taken along the normal drawn into the fluid.

If slipping is not permitted on the surface the dissipation given by (1.2) will vanish. But it is well known that D in general, can be written as (Lamb, *ibid.*, p. 381).

$$\mu \int [2(a^2 + b^2 + c^2) + f^2 + g^2 + h^2] dv \quad \dots \quad \dots \quad \dots \quad (1.3)$$

where a, b, c, f, g, h denote the components of strain and the integration is taken over the whole volume of the fluid. Now the integrand in (1.3) is an essentially positive quantity and hence D can vanish only if

$$a = b = c = f = g = h = 0 \quad \dots \quad \dots \quad \dots \quad (1.4)$$

that is, only if the motion reduces to a purely rigid-body motion. This is consistent with Jeffreys' result (Jeffreys, 1930). Hence in a potential flow, which is not merely one of rigid translation, *dissipation must exist* and can never be equal to zero. As potential flow of a real fluid past a solid obstacle is a fact, dissipation must be a necessary feature of such flows and, hence, the integral (1.2) never vanishes—in conformity with our rejection of the no-slip condition (Part I). Thus having allowed slip on the surface for the potential flow of a *real* fluid, we must admit that such a flow will always be attended with a dissipation given by (1.2).

It must be noted that (1.1) or for the matter of that (1.2), has been actually arrived at by converting the volume integral (1.3) into the surface integrals in parts. Hence any singularities in the flow will modify (1.1) and hence also (1.2) and the corresponding corrections must be introduced.

2. Dissipation in primary potential flows past cylindrical boundaries.

Let us suppose that we are considering the potential flow of a real fluid past a solid cylinder and that the motion is defined by the complex potential $W_1 = \phi_1 + i\psi_1$ as in Art. 4, Part I. As the surface of the body in a potential flow must be a streamline, and for such a surface (cf. Eqns. (4.2), I)

$$q_1 \frac{\partial}{\partial \psi_1} = \frac{\partial}{\partial n}$$

$$\frac{1}{q_1} d\phi_1 = ds,$$

we can write (1.2) in the form

$$D = -\mu \oint \frac{\partial q_1^2}{\partial \psi_1} \cdot d\phi_1 \quad \dots \quad \dots \quad \dots \quad \dots \quad (2.1)$$

where q_1 represents the speed and the integral is taken round the entire contour of the body.

The quantity D given by (1.2) or (2.1) can be easily evaluated for a sphere, a circular cylinder or an elliptic cylinder as the stream-functions for such flows are known.

We have the following results:

I. Circular cylinder (radius a)

$$D = 8\pi\mu U^2 \quad \dots \quad \dots \quad \dots \quad \dots \quad (2.2)$$

II. Elliptic cylinder (axes $2a$, $2b$)

$$D = 2\pi\mu U^2 \left(1 + \frac{b}{a}\right)^2 \quad \dots \quad \dots \quad \dots \quad \dots \quad (2.3)$$

III. Sphere (radius a)

$$D = 12\pi\mu a U^2 \quad \dots \quad \dots \quad \dots \quad \dots \quad (2.4)$$

where U represents the velocity of the fluid at infinity parallel to the axis of x .

3. Maintenance of Steady Relative Motion.

When a body moves through an otherwise still fluid with uniform speed U , the fluid in the neighbourhood of the body is thrown into motion and at any instant the body is followed by a field of disturbed fluid surrounding it, the disturbance dying away at an infinite distance from the body. Now, for a real fluid ($\mu \neq 0$) the motion will entail a dissipation of energy. The picture relative to the body cannot become steady unless the rate of supply of energy to the fluid just balances the rate of dissipation and in that case the rate of change of kinetic energy with the motion will vanish. This result can be established in the following general manner:

Let Γ_{vx} , Γ_{vy} , Γ_{vz} be the components of the stress per unit area at any point of a surface bounding the fluid exerted by the surface on the fluid. Then the total work done on the fluid per unit time is, in general, given by

$$\int_{S+\Sigma} (\Gamma_{vx} \cdot u + \Gamma_{vy} \cdot v + \Gamma_{vz} \cdot w) dS \quad \dots \quad \dots \quad \dots \quad (3.1)$$

the integral being taken over the finite body surface S as well as the surfaces Σ at infinity. Following the principle that the fluid at infinity remains undisturbed when the body moves through it, the integral over Σ vanishes and hence (3.1) reduces to

$$\int_S (\Gamma_{vx} \cdot u + \Gamma_{vy} \cdot v + \Gamma_{vz} \cdot w) dS \quad \dots \quad \dots \quad \dots \quad (3.2)$$

the integral being now taken over the body-surface only.

Now, (3.2) can be written as

$$\sum_{u, v, w} \int u \left(\frac{\partial \Gamma_{xx}}{\partial x} + \frac{\partial \Gamma_{xy}}{\partial y} + \frac{\partial \Gamma_{xz}}{\partial z} \right) dv + \int \Phi dv$$

where Φ represents the rate of dissipation per unit volume. Hence, substituting in the first term from the Navier-Stokes equations we have

$$\int_S (\Gamma_{vx} \cdot u + \Gamma_{vy} \cdot v + \Gamma_{vz} \cdot w) dS = \frac{1}{2} \rho \frac{D}{Dt} \int q^2 dv + D$$

where D is given by (1.3) and $\frac{1}{2} \rho q^2$ represents the kinetic energy per unit volume.

For a steady relative picture we must have

$$\frac{D}{Dt} \int \frac{1}{2} \rho q^2 \cdot dv = 0$$

and hence

$$\int (\Gamma_{vx} \cdot u + \Gamma_{vy} \cdot v + \Gamma_{vz} \cdot w) dS = D \quad \dots \quad (3.3)$$

Now, if R be the resistance experienced by a body moving with uniform velocity U , the rate of work done on the fluid is $R.U$ and hence, finally, we must have

$$R.U = D \quad \dots \quad (3.4)$$

Equation (3.4) must be regarded as very fundamental for the maintenance of a steady relative picture and we shall impose this as a necessary condition for the preservation of a steady flow.

In Part I, Art. 5, we have calculated the total resistance R in a few symmetrical cases of primary potential flow and represented the same by X . Also equations (2.2), (2.3), (2.4) give us the corresponding values of D . The results are shown in the following table:—

Body	RU	D
1. Circular cylinder	$8\pi\mu U^2$	$8\pi\mu U^2$
2. Elliptic cylinder	$4\pi\mu U^2 \left(1 + \frac{b}{a}\right)$	$2\pi\mu U^2 \left(1 + \frac{b}{a}\right)^2$
3. Sphere	$16\pi\mu a U^2$	$12\pi\mu a U^2$

From the above table it becomes clear that whereas equation (3.4) is obeyed for a circular cylinder, it is not so for either an elliptic cylinder or a sphere. Hence, on the assumption of the primary potential motion, the flow round a circular cylinder only can be maintained steadily. That round a sphere or an elliptic cylinder cannot be so maintained and if started at any time it will change soon. The additional energy supply to the fluid by the work of the body-forces in the two latter cases will, it appears, tend to create a wake and enlarge it until the two rates just balance and equation (3.4) is satisfied for the altered motion. Our next enquiry therefore will be to look for such a situation. With a view to that we shall develop the theory of closed wakes bounded by potential flows in Part III of this work.

ABSTRACT

This paper contains a discussion of the dissipation in potential flow of a real incompressible fluid and establishes the condition for the maintenance of a steady flow. Calculations show that the classical potential flow round a circular cylinder can be maintained steadily but that round an elliptic cylinder or a sphere cannot be so maintained. This result is interpreted to indicate the formation of wakes.

REFERENCES

- Jeffreys, H. (1930). Wake in fluid flow past a Solid. *Proc. Roy. Soc. A*, 128, 376-393.
 Lamb, H. (1932). *Hydrodynamics*.

PART III

CLOSED WAKES IN TWO DIMENSIONS.

1. Introduction

The Classical wake or the Helmholtz wake being supposed to extend to infinity the position was never regarded as satisfactory as was observed in Part I. Closed wakes are a reality that could hardly be denied. For a long time there seemed to have developed a sort of resignation to the situation for lack of new light. Recently, however, the question seems to have been reopened and several attempts have already been made to introduce and discuss the question of closed wakes. (Klose, 1941; Kolscher, 1940; Southwell and Vasey, 1946; Manarini, 1948; Allen, 1949; Lighthill, 1949; Kármán, 1949).

So long, however, as D'Alembert's paradox remained unresolved objections against closed wakes could not be overridden—so far, at least, as motion with uniform velocity is concerned. In Part I of our present theory we have resolved D'Alembert's paradox and so the chief argument *against* closed wakes has already been removed. We shall therefore proceed with the analysis of closed wakes in potential flows.

2. The Requirements.

Let us consider a two-dimensional primary potential flow past a fixed cylinder and let W_1 represent the complex potential for the flow. The character of the primary potential flow is that the stream-line $\psi_1 = 0$ where

$$W_1 = \phi_1 + i\psi_1 \quad \dots \quad \dots \quad \dots \quad (2.1)$$

enclasps the body surface completely, meeting at the front stagnation point A and leaving it at the back stagnation point B as shown by the thick line Fig. 1. The

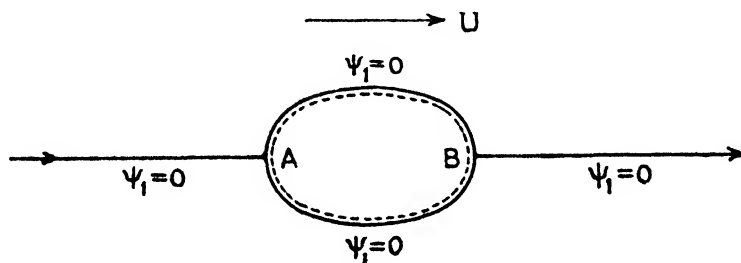


FIG. 1

dotted line, inside, indicates the body surface. In the case of motion with a wake we would look for a flow where one stream-line should usually meet the body surface at the front stagnation point A , separate and run along the surface of the body for some distance (AC , AC'), leave the body surface at two points C , C' on the two sides

and meet again at a distance from the body, say at D . The whole area enclosed in the loop thereby formed, will then contain the body and the wake (Fig. 2).

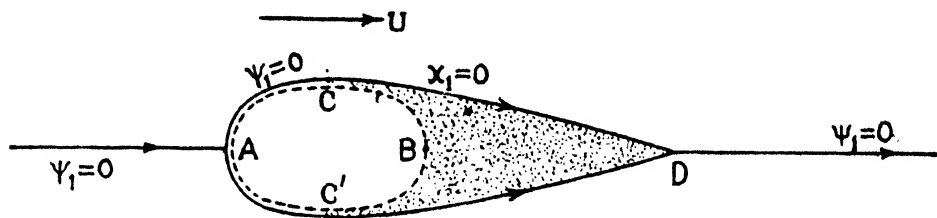


Fig. 2

These requirements will be readily satisfied if the stream-function ψ is of the form

$$\psi = \psi_1 \chi_1, \quad \dots \quad \dots \quad \dots \quad \dots \quad (2.2)$$

For, then, $\psi = 0$ will be satisfied by $\psi_1 = 0$ as well as $\chi_1 = 0$ so that when χ_1 is suitably chosen the wake boundary CD or $C'D$ will be represented by

$$\chi_1 = 0 \quad \dots \quad \dots \quad \dots \quad \dots \quad \dots \quad (2.3)$$

The points C and D can then be easily obtained as the intersections of

$$\text{with } \left. \begin{array}{l} \psi_1 = 0 \\ \chi_1 = 0 \end{array} \right\} \quad \dots \quad \dots \quad \dots \quad \dots \quad (2.4)$$

Now, by our *assumption* the motion outside is to be a purely potential motion and if there be any vortices they may lie inside the loop, i.e., in the wake. For a steady motion outside, it is enough that the wake boundary remains fixed.

Thus the requirements for the altered, i.e., the wake-flow are:—

- (1) It should be a potential flow without singularities outside the body-wake system.
- (2) It should reduce itself to the primary potential flow at large distances from the body (observational result mentioned in Part 1).
- (3) Its stream-function should be of the form (2.2).
- (4) The equations (2.4) should (for a closed wake) have at least, one real solution within the range AB and one real finite solution on the right of B .

3. The Complex Potential in Symmetrical Flows

We shall designate the new wake-flow the 'secondary' flow and denote its complex potential by W_2 . Further, we shall confine ourselves only to the consideration of flows symmetrical about the axis of x .

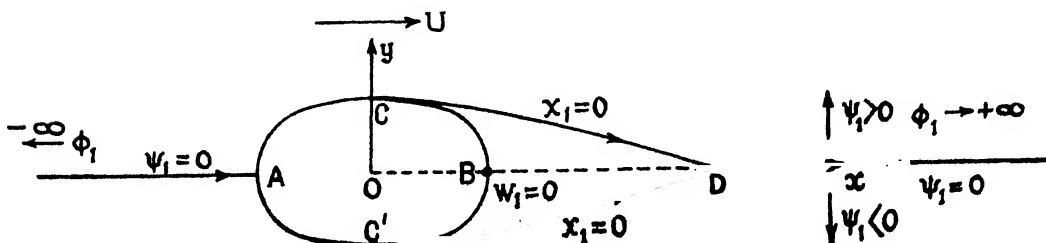


Fig. 3

As before, we assume that the primary potential flow is represented by (2.1) and that the flow has symmetry about the x -axis in the real, i.e., the flow plane. Thus ψ_1 vanishes on the axis of X as well as on the body-surface and ϕ_1 may vary from $-\infty$ on the extreme left to $+\infty$ on the extreme right, ψ_1 being positive above and negative below the x -axis. If, now, the points in the flow plane be expressed in curvilinear co-ordinates (ϕ_1, ψ_1) this symmetry will be disturbed unless the origin of W_1 (i.e., the point $\phi_1 = 0, \psi_1 = 0$) is situate on the axis of x . The most convenient point for such a choice for $W_1 = 0$ is, however, the rear stagnation point B , for the primary flow. We shall therefore suppose, in all our subsequent analysis, that

$$\phi_1 = \psi_1 = 0 \quad \text{at } B. \quad \dots \quad (3.1)$$

Now, to satisfy requirement (1) it is enough to have W_2 as a function of W_1 . To satisfy (2) this function of W_1 must $\rightarrow W_1$ as $|W_1| \rightarrow \infty$. Hence we assume, generally,

$$W_2 = W_1 + \sum_0^r \frac{\alpha_r}{W_1^r} \quad \dots \quad (3.2)$$

the quantities α_r being constants or at least independent of co-ordinates (x, y) .

Now, W_1 being an analytic function, W_2 is also so, outside $W_1 = 0$. But $W_1 = 0$ at the rear stagnation point B . So, W_2 given by (3.2) will be analytic everywhere outside a small area surrounding B . As under condition (4) B will be safely enclosed inside the wake, W_2 will be analytic everywhere outside the loop. In fact, W_2 , given by (3.2), can be made to satisfy all necessary requirements for a *finite wake*.

Let us put

$$W_2 = \phi_2 + i\psi_2 \quad \dots \quad (3.3)$$

and by (2.1)

$$W_1 = \phi_1 + i\psi_1 \equiv \rho e^{i\sigma}, \quad \text{say}; \quad \dots \quad (3.4)$$

so that

$$\phi_1 = \rho \cos \sigma, \quad \psi_1 = \rho \sin \sigma. \quad \dots \quad (3.4a)$$

To cover all points in the W_1 plane we shall take

$$\left. \begin{array}{l} \rho > 0, \quad W_1 \neq 0 \\ \rho = 0, \quad W_1 = 0 \end{array} \right\} \quad \dots \quad (3.5)$$

so that σ may vary between 0 and 2π . Besides, on

$$\left. \begin{array}{l} \psi_1 = 0 \\ \sigma = 0, \quad \phi_1 > 0 \\ \sigma = \pi, \quad \phi_1 < 0 \end{array} \right\} \quad \dots \quad (3.5a)$$

Further, owing to the assumed symmetry it will be enough to consider the upper half of the W_1 -plane (including the origin) and for this domain

$$\left. \begin{array}{l} 0 \leq \sigma \leq \pi, \quad \rho > 0 \\ \rho = 0, \quad W_1 = 0 \end{array} \right\} \quad \dots \quad (3.5b)$$

is sufficient for our analysis, conditions being exactly the same on the other side of the ϕ_1 -axis.

4. The Wake Boundary

With (3.3), (3.4), (3.4a) we have from (3.2)

$$\phi_2 = \alpha_0 + \rho \cos \sigma \left\{ 1 + \sum_1^{\infty} \frac{\alpha_r \cdot \cos r\sigma}{\rho^{r+1} \cdot \cos \sigma} \right\} \quad \dots \quad (4.1)$$

$$\psi_2 = \rho \sin \sigma \left\{ 1 - \sum_1^{\infty} \frac{\alpha_r \cdot \sin r\sigma}{\rho^{r+1} \cdot \sin \sigma} \right\} \quad \dots \quad (4.2)$$

$$= \psi_1 \left\{ 1 - \sum_1^{\infty} \frac{\alpha_r}{\rho^{r+1}} \cdot \frac{\sin r\sigma}{\sin \sigma} \right\} \quad \dots \quad (4.2a)$$

Comparing with (2.2), where ψ_2 takes the place of ψ , we have

$$\chi_1 \equiv \left\{ 1 - \sum_1^{\infty} \frac{\alpha_r \cdot \sin r\sigma}{\rho^{r+1} \cdot \sin \sigma} \right\} \quad \dots \quad (4.3)$$

Hence, the equation of the wake-boundary is given, in general, by

$$1 - \sum_1^{\infty} \frac{\alpha_r \cdot \sin r\sigma}{\rho^{r+1} \cdot \sin \sigma} = 0 \quad \dots \quad (4.4)$$

where, of course, ρ and σ are as defined by (3.4a). The intersection of the wake-boundary with $\psi_1 = 0$ is therefore given by the roots of the equation

$$\begin{aligned} \text{Lt.}_{\substack{\psi_1 \rightarrow 0 \\ \rho \rightarrow \phi_1}} \left\{ 1 - \sum_1^{\infty} \frac{\alpha_r \cdot \sin r\sigma}{\rho^{r+1} \cdot \sin \sigma} \right\} &\equiv \text{Lt.}_{\substack{\sigma \rightarrow 0 \\ \rho \rightarrow \phi_1}} \left\{ 1 - \sum_1^{\infty} \frac{\alpha_r \cdot \sin r\sigma}{\rho^{r+1} \cdot \sin \sigma} \right\} \\ &= 0, \end{aligned}$$

that is, by the real roots of

$$1 - \sum_1^{\infty} \frac{r\alpha_r}{\phi_1^{r+1}} = 0, \quad \dots \quad (4.5)$$

in general.

It is obvious that when a finite number of terms are considered the sum of the roots must vanish in every case. Besides, it is important to note that every real intersection of $\chi_1 = 0$ with $\psi_1 = 0$ and hence every real root of (4.5) *must be a stagnation point*. This can be shown quite easily.

For by (2.2)

$$\psi_2 = \psi_1 \chi_1.$$

Therefore

$$\nabla \psi_2 = \psi_1 \nabla \chi_1 + \chi_1 \nabla \psi_1. \quad \dots \quad (4.6)$$

But, at a point of intersection, $\psi_1 = 0$ and $\chi_1 = 0$, hence

$$\nabla \psi_2 = 0 \quad \dots \quad (4.7)$$

which proves the result.

5. *Points of Separation and Reunion of the Flow*

As the rear stagnation point has been chosen as the origin $W_1 = 0$, the front stagnation point A will be given by $\psi_1 = 0$ and a negative value for ϕ_1 , for ϕ_1 is supposed to increase in the direction of the flow. Let this value be ϕ_{1A} . Then, for a real separation of the flow from the body surface equation (4.5) must have at least one negative root lying in the range -

$$\phi_{1A} < \phi_1 < 0. \quad \dots \quad (5.1)$$

For two or more coincident negative roots within the range the separation will take place tangentially. In the absence of any real positive root of (4.5) the flow does not unite. For only one real positive root the union or confluence takes place at an angle. For two or more coincident positive roots the confluence takes place in the form of a *cusp*.

Thus it is clear that the coefficients α_r determine the pattern of the wake. Given any specified pattern it is possible to choose the coefficients suitably. In general, however, there doesn't seem to exist any definite physical principle which may specify the constants uniquely. It is possible that flows for all values of α_r are permitted but only some of them are stable. This is a mere surmise and does not presume to be a proof. Experimental photographs show the existence of different types of wake-boundaries for the same obstacle when subjected to flows with different Reynolds numbers, i.e., for different velocities of the undisturbed flow. All these patterns of the wake boundary must obviously belong to the same topological group so that one can be transformed into another by a continuous deformation—and physical intuition suggests that the sole parameter of this deformation must be the speed U or to be exact the corresponding Reynolds number.

Speaking of experimental results, it may be observed that photographs (Goldstein, 1938, Vol. I, plates 7, 8) actually reveal the existence of what looks like stagnation areas near the points of separation and reunion.

6. *Angle of Separation and Angle of Reunion or Confluence*

It is possible to construct a general result which will give the angle at which the separation from the body-surface or at which reunion of the flow on the x -axis takes place.

At any point let q_2, θ_2 denote the speed and direction of the secondary flow in the real plane (z -plane); let q', θ' denote the same in the W_1 -plane and let q_1, θ_1 denote the speed and direction of the primary flow in the actual flow plane (i.e., z -plane). Then,

$$\begin{aligned} \frac{dW_1}{dz} &= u_1 - iv_1 = q_1 e^{-i\theta_1} \\ \frac{dW_2}{dz} &= u_2 - iv_2 = q_2 e^{-i\theta_2} \} \quad \dots \quad (6.1) \\ \frac{dW_2}{dW_1} &= u' - iv' = q' e^{-i\theta'} \end{aligned}$$

and

where the suffix 1 refers to the primary flow, 2 to the secondary flow, both in the z -plane and the dash (') refers to the secondary flow in the W_1 -plane. But

$$\frac{dW_2}{dz} = \frac{dW_2}{dW_1} \cdot \frac{dW_1}{dz} \quad \dots \quad (6.2)$$

Hence,

$$q_2 e^{-i\theta_2} = q' q_1 e^{-i(\theta' + \theta_1)}$$

which shows

$$q_2 = q' q_1 \quad \dots \quad \dots \quad \dots \quad \dots \quad (6.3)$$

$$\theta_2 = \theta' + \theta_1 \quad \dots \quad \dots \quad \dots \quad \dots \quad (6.4)$$

But $\theta_2 - \theta_1$ is the angle between the directions of the primary and the secondary flow in the real (i.e., z) plane. Hence by (6.4) the angle through which the velocity at any point is turned in passing from the primary to the secondary flow is given by

$$\theta' = \theta_2 - \theta_1 \quad \dots \quad \dots \quad \dots \quad \dots \quad (6.5)$$

so that the angle θ of separation or confluence which means the angle of turning of the flow at either point is given by

$$\tan \theta = \tan \theta' = \frac{v'}{u'} \quad \dots \quad \dots \quad \dots \quad \dots \quad (6.6)$$

At a stagnation point $v' = u' = 0$, because $q = 0$ but $q_1 \neq 0$. Hence for such points we have

$$\tan \theta = \text{Lt. } \frac{v'}{u'} \quad \dots \quad \dots \quad \dots \quad \dots \quad (6.7)$$

But

$$u' = \frac{\partial \psi_2}{\partial \phi_1}, \quad v' = -\frac{\partial \psi_2}{\partial \phi_1}$$

so that, for separation or confluence

$$\tan \theta = -\text{Lt. } \left[\frac{\frac{\partial \psi_2}{\partial \phi_1}}{\frac{\partial \psi_2}{\partial \phi_1}} \right]_{\substack{\psi_1 \rightarrow 0 \\ \chi_1 \rightarrow 0}} \quad \dots \quad \dots \quad \dots \quad (6.8)$$

$$\left. \begin{array}{l} \text{For a point of separation, } \chi_1 \rightarrow 0 \text{ and } \sigma \rightarrow \pi \\ \text{for a point of reunion, } \chi_1 \rightarrow 0 \text{ and } \sigma \rightarrow 0 \end{array} \right\} \quad \dots \quad \dots \quad (6.8a)$$

We shall distinguish between these two angles by the suffixes s and m , so that

$$\left. \begin{array}{l} \theta_s = \text{angle of separation} \\ \theta_m = \text{angle of reunion} \end{array} \right\} \quad \dots \quad \dots \quad \dots \quad (6.8b)$$

With (2.2) and (6.8b), equation (6.8) can be written as

$$\tan \theta_s = -\text{Lt. } \left[\frac{\frac{\partial \chi_1}{\partial \phi_1}}{\frac{\partial \chi_1}{\partial \phi_1}} \right]_{\sigma \rightarrow \pi} \quad \dots \quad \dots \quad \dots \quad (6.9a)$$

$$\tan \theta_m = -\text{Lt. } \left[\frac{\frac{\partial \chi_1}{\partial \phi_1}}{\frac{\partial \chi_1}{\partial \phi_1}} \right]_{\sigma \rightarrow 0} \quad \dots \quad \dots \quad \dots \quad (6.9b)$$

Alternatively, it is easy to see from the principles of conformal transformations that θ_m or θ_s are the angles at which the curve $\chi_1 = 0$ in the W_1 -plane meets the ϕ_1 axis. Hence, if $\chi_1 = 0$ is expressed in polar co-ordinates (ρ, σ) in the W_1 -plane,

$$\text{and} \quad \left. \begin{aligned} \tan \theta_m &= \text{Lt.}_{\sigma \rightarrow 0} \left(\rho \frac{d\sigma}{d\rho} \right) \\ \tan \theta_s &= \text{Lt.}_{\sigma \rightarrow \pi} \left(\rho \frac{d\sigma}{d\rho} \right) \end{aligned} \right\} \dots \dots \dots (6.10)$$

Referring to the general equation (4.4) for $\chi_1 = 0$ it becomes obvious that the last two formulae are most convenient for the calculation of θ_m and θ_s .

7. *Special Types of Wake-flows*

We shall now describe a few simple types of closed wakes, as particular cases of the general results established above.

Type I. $[\alpha_r \neq 0, r < 1; \alpha_r = 0, r > 1.]$

In this case

$$W_2 = \alpha_0 + W_1 + \frac{\lambda^2}{W_1} \dots \dots \dots (7.1)$$

(where λ^2 has been put for α_1)

$$\phi_2 = \alpha_0 + \phi_1 \left(1 + \frac{\lambda^2}{\rho^2} \right) \dots \dots \dots (7.2)$$

(α_0 being supposed real),

$$\psi_2 = \psi_1 \left(1 - \frac{\lambda^2}{\rho^2} \right) \dots \dots \dots (7.3)$$

where

$$\rho^2 = \phi_1^2 + \psi_1^2; \dots \dots \dots (7.4)$$

$$\chi_1 = \left(1 - \frac{\lambda^2}{\rho^2} \right), \dots \dots \dots (7.5)$$

so that the equation to the wake boundary in the W_1 -plane is

$$\rho = \lambda \dots \dots \dots (7.5a)$$

This circle will necessarily have real intersections with $\psi_1 = 0$, so that the corresponding wake in the z -plane must be closed. The intersections are given by

$$\phi_1 = \pm \lambda \dots \dots \dots (7.6)$$

and by (6.10), or obviously

$$\theta_m = \theta_s = \frac{\pi}{2} \quad (\text{signs being omitted}) \dots \dots \dots (7.7)$$

Thus in this case the flow separates from the body surface normally and meets on the x -axis again normally.

(Photographic plates actually record cases where the reunion appears to be normal. For example, Durand (1935), Vol. III, plate III, fig. 30.)

Type II. $[\alpha_r \neq 0, r < 2, \alpha_r = 0, r > 2]$

In this case,

$$W_2 = \alpha_0 + W_1 + \frac{\alpha_1}{W_1} + \frac{\alpha_2}{W_1^2} \quad \dots \quad (7.8)$$

$$\chi_1 = 1 - \frac{\alpha_1}{\rho^2} - \frac{2\alpha_2 \cos \sigma}{\rho^3} \quad \dots \quad (7.9)$$

The wake boundary $\chi_1 = 0$ is given by

$$\rho^3 - \rho\alpha_1 - 2\alpha_2 \cos \sigma = 0 \quad \dots \quad (7.10)$$

The points of separation and reunion are given by the roots of

$$\phi_1^3 - \alpha_1 \phi_1 - 2\alpha_2 = 0 \quad \dots \quad (7.11)$$

For a closed wake, there must be at least two real roots one positive and one negative. Hence all the roots must be real. For a physically interpretable case (only one separation point and one confluence point) two of the roots must be equal. If $\lambda_1, \lambda_2, \lambda_3$ be the three roots we must have

$$\lambda_1 + \lambda_2 + \lambda_3 = 0 \quad \dots \quad (7.11a)$$

Besides, say,

$$\lambda_1 = \lambda_2 \quad \dots \quad (7.11b)$$

then (7.11a) becomes

$$2\lambda_1 + \lambda_3 = 0 \quad \dots \quad (7.12)$$

Comparing with

$$(\phi_1 - \lambda_1)^2 (\phi_1 - \lambda_3) = 0$$

we have, besides (7.12),

$$\left. \begin{aligned} \lambda_1^2 + 2\lambda_1\lambda_3 &= -\alpha_1 \\ \lambda_1^2\lambda_3 &= 2\alpha_2 \end{aligned} \right\} \quad \dots \quad (7.12a)$$

Hence eliminating λ_1, λ_3 from (7.12) and (7.12a) we have

$$\alpha_1^3 = 27\alpha_2^2, \quad \dots \quad (7.13)$$

(The result could be obtained from the discriminant for a cubic) so that it is necessary that

$$\alpha_1 > 0 \quad \dots \quad (7.14)$$

$$\alpha_2 = \pm \left(\frac{\alpha_1}{3} \right)^{\frac{2}{3}} \quad \dots \quad (7.15)$$

Thus two cases are possible, viz.,

$$\left. \begin{aligned} \lambda_3 < 0, \lambda_1 > 0, \alpha_2 < 0 \\ \lambda_3 > 0, \lambda_1 < 0, \alpha_2 > 0 \end{aligned} \right\} \quad \dots \quad (7.16)$$

Hence

(i) When the last coefficient α_2 is negative there is one negative root and two equal positive roots. The flow leaves the surface at an angle and meets back in a cusp.

(ii) When the last coefficient is positive, there are two negative equal roots and one positive root. In this case separation takes place tangentially and the confluence takes place at an angle.

Both the above cases are possible. But in either, equations (7.14) and (7.15) must be obeyed. Thus out of the two constants α_1 and α_2 only one becomes independent.

Putting

$$\alpha_1 = 3\lambda^2 \quad \dots \dots \dots (7.17a)$$

we have from (7.15)

$$\alpha_2 = \mp \lambda^3, \quad \dots \dots \dots (7.17b)$$

the upper and the lower sign corresponding to the cases (i) and (ii) respectively. Now, (7.11) can be put in the form

$$\phi_1^3 - 3\lambda^2\phi_1 \pm 2\lambda^3 = 0 \quad \dots \dots \dots (7.18)$$

so that the roots in the two cases are

$$\left. \begin{array}{l} -2\lambda, \lambda, \lambda \\ -\lambda, -\lambda, 2\lambda \end{array} \right\} \quad \dots \dots \dots (7.18a)$$

respectively.

Correspondingly,

$$W_2 = \alpha_0 + W_1 + \frac{3\lambda^2}{W_1} \mp \frac{\lambda^3}{W_1^2} \quad \dots \dots \dots (7.19)$$

$$\phi_2 = \alpha_0 + \rho \cos \sigma \left\{ 1 + \frac{3\lambda^2}{\rho^2} \mp \frac{\lambda^3}{\rho^3} \cdot \frac{\cos 2\sigma}{\cos \sigma} \right\} \quad \dots \dots (7.19a)$$

$$\psi_2 = \rho \sin \sigma \left\{ 1 - \frac{3\lambda^2}{\rho^2} \pm \frac{2\lambda^3}{\rho^3} \cos \sigma \right\} \quad \dots \dots (7.19b)$$

$$\chi_1 = 1 - \frac{3\lambda^2}{\rho^2} \pm \frac{2\lambda^3 \cos \sigma}{\rho^3} \quad \dots \dots \dots (7.19c)$$

and for case (i)

$$\left. \begin{array}{l} \theta_s = \frac{\pi}{2}, \theta_m = 0 \\ \theta_s = 0, \theta_m = -\frac{\pi}{2} \end{array} \right\} \quad \dots \dots \dots (7.20)$$

for case (ii)

Thus in case (i) the separation is orthogonal and union is in cusp and in case (ii) the separation is tangential but union is orthogonal.

Type III. *Separation tangential, Union in a cusp.*

Retaining only four terms in the expansion (3.2) we have

$$W_2 = \alpha_0 + W_1 + \frac{\alpha_1}{W_1} + \frac{\alpha_2}{W_1^2} + \frac{\alpha_3}{W_1^3} \quad \dots \dots \dots (7.21)$$

Then,

$$\left. \begin{array}{l} \phi_2 = \alpha_0 + \rho \cos \sigma \left\{ 1 + \frac{\alpha_1}{\rho^2} + \frac{\alpha_2 \cos 2\sigma}{\rho^3 \cos \sigma} + \frac{\alpha_3}{\rho^4} \cdot \frac{\cos 3\sigma}{\cos \sigma} \right\} \\ \psi_2 = \rho \sin \sigma \left\{ 1 - \frac{\alpha_1}{\rho^2} - \frac{\alpha_2 \cdot 2 \cos \sigma}{\rho^3} - \frac{\alpha_3}{\rho^4} (3 - 4 \sin^2 \sigma) \right\} \end{array} \right\} \quad \dots (7.21a)$$

so that

$$\chi_1 = 1 - \frac{\alpha_1}{\rho^2} - \frac{\alpha_2 \cdot 2 \cos \sigma}{\rho^3} - \frac{\alpha_3}{\rho^4} (3 - 4 \sin^2 \sigma) \quad \dots \dots (7.22)$$

The points of intersection are given by

$$\phi_1^4 - \alpha_1 \phi_1^2 - 2\alpha_2 \phi_1 - 3\alpha_3 = 0 \quad \dots \dots (7.22a)$$

We shall consider only that case where the separation and the union are both tangential, i.e., where $\theta_m = \theta_s = 0$. For this it is necessary that (7.22a) should have two distinct pairs of equal roots and since the sum of the roots always vanishes two of these must be negative and two positive. Applying the necessary conditions from the theory of biquadratics, we have

$$\left. \begin{aligned} \alpha_1 &> 0 \\ \alpha_2 &= 0 \\ -3\alpha_3 &= \frac{\alpha_1^2}{4} \end{aligned} \right\} \dots \dots \dots (7.23)$$

Hence putting

$$\alpha_1 = 2\lambda^2 \dots \dots \dots (7.24)$$

we have from (7.22a)

$$\phi_1^4 - 2\lambda^2 \phi_1^2 + \lambda^4 = (\phi_1^2 - \lambda^2)^2 = 0$$

so that the points of intersection of the wake-boundary with $\psi_1 = 0$ are given by

$$\phi_1 = -\lambda, -\lambda, \lambda, \lambda$$

furnishing the necessary pairs of coincident roots. It should be noted that the points of separation and reunion are at equal distances from the back stagnation point in the W_1 -plane. In this case, as expected, $\theta_s = \theta_m = 0$ and,

$$\phi_2 = \alpha_0 + \rho \cos \sigma \left\{ 1 + \frac{2\lambda^2}{\rho^2} - \frac{1}{3} \frac{\lambda^4}{\rho^4} (4 \cos^2 \sigma - 3) \right\} \dots \dots (7.25a)$$

$$\psi_2 = \rho \sin \sigma \left\{ 1 - \frac{2\lambda^2}{\rho^2} + \frac{1}{3} \frac{\lambda^4}{\rho^4} (3 - 4 \sin^2 \sigma) \right\} \dots \dots (7.25b)$$

$$\chi_1 = 1 - \frac{2\lambda^2}{\rho^2} + \frac{1}{3} \frac{\lambda^4}{\rho^4} (3 - 4 \sin^2 \sigma) \dots \dots \dots (7.25c)$$

α_0 , of course, being arbitrary.

8. Application to Circular and Elliptic Cylinders

To calculate the wake-flow past any cylinder we have merely to substitute the appropriate expression for W_1 as a function of z , so adjusted that the origin for W_1 is transferred to the back stagnation point. Thus, for

(1) the Circular Cylinder

$$W_1 = -2aU + Uz \left(1 + \frac{a^2}{z^2} \right) \dots \dots \dots (8.1)$$

which makes

$$\phi_1 = -2aU + Ux \left(1 + \frac{a^2}{r^2} \right) \dots \dots \dots (8.1a)$$

$$\psi_1 = Uy \left(1 - \frac{a^2}{r^2} \right) \dots \dots \dots (8.1b)$$

so that ϕ_1, ψ_1 vanish at the back stagnation point $(a, 0)$.

Further,

$$\phi_{1A} = \left(\phi_1 \right)_{\substack{x=-a \\ y=0}} = -4aU \dots \dots \dots (8.2)$$

so that for flows of the different types enumerated before, we must have the following limitations on the parameter λ in order that the separation may remain between the stagnation points A and B for the primary flow.

$$\text{Type I} \quad 0 < \lambda < 4aU \quad \dots \dots \dots (8.2a)$$

$$\text{Type II (i)} \quad 0 < 2\lambda < 4aU \quad \dots \dots \dots (8.2b)$$

$$\text{Type II (ii)} \quad 0 < \lambda < 4aU \quad \dots \dots \dots (8.2c)$$

$$\text{Type III} \quad 0 < \lambda < 4aU \quad \dots \dots \dots (8.2d)$$

(II) For an Elliptic Cylinder

$$W_1 = -U(a+b) + U \left[b \sqrt{\frac{a+b}{a-b}} e^{-\zeta} + \sqrt{a^2-b^2} \cosh \zeta \right] \left. \vphantom{\begin{matrix} W_1 \\ \zeta \end{matrix}} \right\} \dots (8.3)$$

$$z = c \cosh \zeta \equiv c \cosh (\xi + i\eta)$$

so that

$$\phi_1 = -U(a+b) + U \left[b \sqrt{\frac{a+b}{a-b}} e^{-\xi} + \sqrt{a^2-b^2} \cosh \xi \right] \cos \eta \dots (8.4a)$$

$$\psi_1 = -U \left[b \sqrt{\frac{a+b}{a-b}} e^{-\xi} - \sqrt{a^2-b^2} \sinh \xi \right] \sin \eta \quad \dots \dots (8.4b)$$

and

$$\phi_{1,1} = -2U(a+b) \dots \dots \dots (8.4c)$$

In the subsequent part (Part IV) of this paper we shall discuss the question of resistance and dissipation in wake flows.

ABSTRACT

The resolution of D'Alembert's paradox removes the objection to closed wakes—a difficulty met by Helmholtz by the free-streamline theory. In this part, therefore, the author develops the Theory of closed wakes in potential flow. A general formula for the wake flow in two dimensions past any cylinder is established and by an analysis of the wake-boundary several types of closed wakes are demonstrated.

REFERENCES

- De G. Allen, D. N. (1949). The formation of closed wakes in Fluid Motions. *Qly. J. of Mech. and Applied Math.*, **2**, 64-72.
- Karman, T. (1949). Accelerated flow of an incompressible fluid with wake formation. *Ann. Mat. Pura. Appl.* (4) **29**, 247-249.
- Klose Alfred (1941). Theorie der Luftkrafte bei verswindender Reibung. *Abh. Preuss. Akad. Wiss. Math. Nat. kl.*, **9**, 50.
- Kolscher, M. (1940). Unstetige Stromungen mit endlichen Totwasser. *Luftfahrtforschung*, **17**, 154-160.
- Discontinuous solutions of the equations of motion of fluid flow. Ministry of Aircraft Production, (Lond.) R.T.P. (Translation No. 2403).
- Leghthill, M. J. (1949). A note on cusped cavities. *Aeronaut. Res. Council Rep. and Memo.*, 2328.
- Manarini, M. (1948). Sui paradossi di D'Alembert e di Brillouin nella dinamica dei fluidi. *Atti. Accad. Naz. Lincei. Rend. Cl. Sci. Fis. Mat. Nat.* (8) **4**, 427-433.
- Southwell, R. V. and Vasey, G. (1946). *Phil. Trans. A*, **240**, 117.

PART IV

RESISTANCE AND DISSIPATION IN MOTIONS WITH CLOSED WAKES

1. *Introduction*

In Part I of this paper we have resolved D'Alembert's paradox and calculated the resistance in the primary potential flow of a real incompressible fluid on obstacles of different shapes. In Part II we have seen that the energy supplied to the fluid by the work of the body forces exceeds, in some cases, the amount of mechanical energy necessary to maintain a steady flow, proving thereby, that the primary potential flows concerned could not be maintained steadily in such cases without modification. We interpreted this result as leading to the formation of wakes behind those obstacles. But wakes must necessarily be closed. With the resolution of D'Alembert's paradox objections to the existence of closed wakes were removed and in Part III we formulated the theory of potential flows with closed wakes—in contrast to the Helmholtz theory of infinite wakes. In the few simple cases discussed in Art. 7, Part III, it could be noted that the parameter λ (which really determines the point of separation of the flow and the end of the wake, in every case considered) was left arbitrary. By the application of the Principle of Maintenance enunciated in Art. 3, Part II, we shall be in a position to determine this parameter.

With this in view we shall first indicate how the Resistance and the Dissipation in potential flows with closed wakes can be obtained. The expressions for both will involve the unknown parameter λ and the equation expressing the condition for maintenance will be the one determining λ . The result in every case will conceivably depend on the primary flow chosen, i.e., on the nature of the cylindrical obstacle selected for study. With the writing down of the equation of maintenance, however, the theoretical part of the present investigations is brought to its completion.

2. *Resistance in motion with closed wakes*

We have indicated previously in the introduction to Part I that we conceive of the wake as a mass of dead-water following the body and relatively at rest with it in the sense that the velocity of the centre of mass of the particles constituting the wake is the same as that of the body and hence U , by assumption, although the elements of the fluid may be executing vortex motions inside the region bounded by the body-surface and the wake-boundary between the points of separation and confluence as shown in Fig. 1, Part I. Thus the total linear momentum of the fluid in the wake remains invariable when the motion becomes steady. Consequently the resultant of the stresses acting on the wake alone across its bounding surfaces must vanish. If now, a force P is necessary to drive the body steadily through the fluid, since the body also is supposed to move with the uniform velocity U , Newton's Second Law applied to the system of the body and the wake taken as a whole gives P as merely balancing the total reaction of the outside fluid on the body-wake system exerted across the boundary of the combined system, i.e., across the boundary of the loop inside $\psi_2 = 0$, mentioned in Art. 2, Part III (see Fig. 3, Part III). The above argument, however, applies equally well to any three-dimensional problem and hence we can say generally that—

'When a body moves steadily through a fluid and a closed wake of finite dimensions forms behind it, the total resistance experienced by the body can be calculated merely as the resultant effect of the surface stresses exerted by the rest of the fluid across the boundary of the body-wake system.'

This result is independent of the nature of the fluid motion outside the body-wake system and also independent of the internal motions executed by the fluid particles inside the wake so long as the wake maintains its boundary and its total linear momentum invariable.

In our present discussion the flow outside the body-wake system is potential by assumption. Hence by a reference to Art. 4, Part I, we notice that the total resistance can be calculated from formula (4.10), Part I (by merely replacing ϕ_1 , ψ_1 by ϕ_2 , ψ_2 and integrating over the boundary of the body-wake system $ACDC'A$ (Fig. 3, Part III) instead of that of the body surface alone. Thus we have, (for a two-dimensional flow only)—

$$X = \mu \oint \left\{ \frac{\partial q^2}{\partial \phi_2} dy - \frac{\partial q^2}{\partial \psi_2} dx \right\} \quad \dots \quad (2.1)$$

$$Y = -\mu \oint \left\{ \frac{\partial q^2}{\partial \phi_2} dx + \frac{\partial q^2}{\partial \psi_2} dy \right\} \quad \dots \quad (2.2)$$

q representing the speed in the secondary flow $W_2 (= \phi_2 + i\psi_2)$ and the integrals being taken round the body-wake contour $ACDC'A$ (Fig. 3, Part III), in a clockwise sense.

For motions with symmetry about the x -axis, Y vanishes as before and then (2.1) can be written as

$$X = 2\mu \int_A^D \left\{ \frac{\partial q^2}{\partial \phi_2} dy - \frac{\partial q^2}{\partial \psi_2} dx \right\} \quad \dots \quad (2.3)$$

the path of integration being the half-contour ACD .

An alternative form.

It would sometimes be more convenient to put (2.1) in a more readily adaptable form. For this we see that, in general, q^2 may be regarded as a function of the complex conjugate variables W_2 and \bar{W}_2 where

$$\begin{aligned} W_2 &= \phi_2 + i\psi_2 \\ \bar{W}_2 &= \phi_2 - i\psi_2 \end{aligned} \quad \dots \quad (2.4)$$

and as

$$\left. \begin{aligned} \frac{\partial}{\partial \phi_2} &= \frac{\partial}{\partial W_2} + \frac{\partial}{\partial \bar{W}_2} \\ \frac{\partial}{\partial \psi_2} &= i \left(\frac{\partial}{\partial W_2} - \frac{\partial}{\partial \bar{W}_2} \right) \end{aligned} \right\} \quad \dots \quad (2.5)$$

we have

$$\left. \begin{aligned} \frac{\partial}{\partial \phi_2} + i \frac{\partial}{\partial \psi_2} &= 2 \frac{\partial}{\partial \bar{W}_2} \\ dx - idy &= d\bar{z} \end{aligned} \right\} \quad \dots \quad (2.6)$$

also

With these (2.1) becomes

$$X = -2\mu I \oint \frac{\partial q^2}{\partial \bar{W}_2} d\bar{z} \quad \dots \quad (2.7)$$

where I stands for the imaginary part and, of course,

$$q^2 = \left| \frac{dW_2}{dz} \right|^2 \quad \dots \quad (2.8)$$

the integration being taken round the whole contour in a clockwise sense. The equation of the path of integration ($W_2 = \bar{W}_2$) is given by

$$W_1 = \bar{W}_1, \quad z \neq \bar{z} \quad \dots \quad (2.9)$$

for the parts AC , AC' (Fig. 3, Part III) and

$$W_2 = \bar{W}_2, \quad W_1 \neq \bar{W}_1 \quad \dots \quad (2.10)$$

for the remaining parts CD , $C'D$.

The formula (2.7) becomes most convenient where the inverse transformation

$$z \equiv z(W_2)$$

for the flow is easily obtained. For in that case the whole path of integration can merely be taken as

$$W_2 = \bar{W}_2 \quad \dots \quad (2.10a)$$

and Cauchy's theorem can be directly applied for the evaluation of X . For such a procedure we shall obviously be carrying out the integration in the W_2 -plane instead of the real (i.e., z) plane.

In the types of flow discussed previously, however, the inverse transformation merely adds to the complication instead of simplifying it. It is therefore useful to investigate the possibilities of integration in the real or z -plane. For this we see that

$$q^2 = \frac{dW_2}{dz} \cdot \frac{d\bar{W}_2}{d\bar{z}} \quad \dots \quad (2.11)$$

$$\begin{aligned} \therefore \frac{\partial q^2}{\partial \bar{W}_2} &= \frac{dW_2}{dz} \cdot \frac{d^2 \bar{W}_2}{d\bar{z}^2} \cdot \frac{d\bar{z}}{d\bar{W}_2} \\ &= \frac{\frac{dW_2}{dz}}{\frac{d\bar{W}_2}{d\bar{z}}} \cdot \frac{d^2 \bar{W}_2}{d\bar{z}^2} \quad \dots \quad (2.12) \end{aligned}$$

and for the path of integration (2.10a)

$$\frac{dW_2}{dz} = \frac{d\bar{W}_2}{d\bar{z}} \cdot \frac{d\bar{z}}{dz} \quad \dots \quad (2.13)$$

so that we have

$$\frac{\partial q^2}{\partial \bar{W}_2} = \frac{d^2 \bar{W}_2}{d\bar{z}^2} \cdot \frac{d\bar{z}}{dz} \quad \dots \quad (2.14)$$

and so (2.7) gives

$$X = -2\mu I \oint \frac{d^2 \bar{W}_2}{d\bar{z}^2} \cdot \frac{d\bar{z}}{dz} \cdot d\bar{z} \quad \dots \quad (2.15)$$

The disadvantage of this form is that Cauchy's formula for integration cannot be directly applied. For, the equation of the two parts of the path CAC' and CDC'

in the z -plane are given by different equations as shown in (2.9) and (2.10); so working with (2.15) we have to split up the integral into two parts and assuming symmetry we have

$$X = -2\mu I \left[2 \int_A^C \frac{d^2 \bar{W}_2}{d\bar{z}^2} \cdot \frac{d\bar{z}}{dz} \cdot d\bar{z} + 2 \int_C^D \frac{d^2 \bar{W}_2}{d\bar{z}^2} \cdot \frac{d\bar{z}}{dz} \cdot d\bar{z} \right] \quad \dots \quad (2.16)$$

$$\left(\begin{matrix} w_1 = \bar{w}_1 \\ z \neq \bar{z} \end{matrix} \right) \qquad \left(\begin{matrix} w_2 = \bar{w}_2 \\ w_1 \neq \bar{w}_1 \end{matrix} \right)$$

The correctness of these formulae can be verified from the fact that these give back our previous results of Part I when W_2 is replaced by W_1 and C and D coincide.

In the more general case, where no symmetry is assumed the modified Blasius's formula for the wake-flow can be at once written down in the same way in which (2.7) was obtained. We shall thereby obtain:

$$X - iY = -\frac{1}{2} \rho i \oint \left| \frac{dW_2}{dz} \right|^2 dz + 2\mu i \oint \frac{\partial q^2}{\partial \bar{W}_2} dz \quad \dots \quad (2.17)$$

with q^2 given by (2.8) and the path of integration being the entire contour of the body-wake system in a clockwise sense.

3. The Rate of Dissipation and the Maintenance of the Flow

The rate of dissipation in the potential flow outside the body-wake system must for the same reasons as in Part II be totally compensated for by the work of the body-wake system on the fluid outside, for a steady motion. Besides, the dissipation in the potential flow outside can be obtained from eqn. (2.1), Part II, in the manner indicated in the preceding article. We thus have in this case,

$$D = -\mu \oint \frac{\partial q^2}{\partial \phi_2} \cdot d\phi_2 \quad \dots \quad (3.1)$$

where q^2 is given by (2.8), as before.

With (2.4) and (2.5), this can be written as

$$D = -\mu i \oint \left\{ \frac{\partial q^2}{\partial W_2} - \frac{\partial q^2}{\partial \bar{W}_2} \right\} dW_2 \quad \dots \quad (3.2)$$

provided (2.10a) is taken into account as defining the path of integration.

Alternatively, with (2.14) and a similar relation we can write (3.2) in the form

$$D = \mu i \oint \left\{ \frac{d^2 W_2}{dz^2} \cdot \frac{dz}{d\bar{z}} - \frac{d^2 \bar{W}_2}{d\bar{z}^2} \cdot \frac{d\bar{z}}{dz} \right\} \frac{dW_2}{dz} \cdot dz \quad \dots \quad (3.3)$$

for integration in the z -plane, the integral being taken round the whole body wake contour in an *anti-clockwise* sense.

Maintenance of the Flow

From what has been said above and from the discussion in Art. 3, Part II, it is clear that the motion relative to the moving body-wake will remain steady if

$$X \cdot U = D \quad \dots \quad (3.4)$$

in the case of flows with symmetry, X and D being now given by (2.1) and (3.1) respectively. In other words, for a steady symmetrical flow past a cylinder we must have

$$\mu \oint \left\{ \frac{\partial q^2}{\partial \phi_2} dy - \frac{\partial q^2}{\partial \psi_2} dx \right\} = - \frac{\mu}{\Gamma} \oint \frac{\partial q^2}{\partial \psi_2} d\phi_2 \quad \dots \quad (3.5)$$

The importance of equation (3.5),* as mentioned in the introduction to this part, lies in the fact that it provides us with the tool for the determination of the arbitrary parameter λ which characterises the different types of flow discussed in Art. 7, Part III. Having chosen a particular cylinder for study, the first thing we have to do is to determine W_1 , the primary potential flow round it--by the means made available by well-known classical theories. Having obtained W_1 we next choose a particular type of the closed wake, like the cases shown in Art. 7, Part III, for study. The character of the wake boundary being sufficiently restricted to leave only one parameter open, we can apply equation (3.5) to test if the chosen type of wake is possible for the cylinder under consideration. For a real value of the parameter satisfying (3.5) we can safely say that the type of flow chosen may be exhibited when the particular cylinder is in motion in a real fluid steadily. Besides, the value of the parameter thus obtained will fix up the position of the wake boundary in relation to the body and for the types of closed wakes detailed in Part III such a value of the parameter will fix up the position of the separation point as well as the end of the wake represented by the 'confluence' or the 'union' as we have called it.

Conclusion

This brings to a completion the theoretical formulations of our present investigations.

The investigation of possible closed-wake flows round a circular or an elliptic cylinder is a matter of detail and we prefer to postpone it for a future communication on the subject.

Finally, I must thank the authorities of the National Institute of Sciences of India who by selecting me a Senior Research Fellow of the Institute gave me leisure and opportunity to complete this theory the rudiments of which had been hanging around my mind for some time past. Lastly I take this opportunity to express my most sincere gratefulness to Prof. N. R. Sen, in whose laboratory this work was pursued and to whose constant encouragement and untiring watchfulness I owe the major part of my success in completing this theory.

ABSTRACT

This part obtains a general formula for resistance in Potential flows with wakes past any cylinder and also the condition for the maintenance of such a flow.

Issued February 15, 1954.

THE STRUCTURAL AND DRAINAGE PATTERNS OF THE WESTERN GHATS IN THE VICINITY OF THE PALGHAT GAP¹

by K. JACOB, F.N.I. and S. NARAYANASWAMI, *Geological Survey of India, Calcutta*

(Received September 9; read October 9, 1953)

CONTENTS

	<i>Pages</i>
I. Introduction	104
II. Physiography of the Area	104
III. Climate	106
IV. General Drainage	106
V. Geological Formations	107
VI. Geological Structure	107
VII. Drainage pattern in the Hill Tracts adjoining the Palghat Gap and its possible explanation	109
VIII. The Evolution of the Palghat Gap	113
IX. Bathymetric contours in the Arabian Sea west of the Palghat Gap	115
X. Period of formation of the present West Coast and the probable age of the Palghat Gap	116
XI. References	118

I. INTRODUCTION

The Palghat Gap which lies across the Western Ghats in Malabar, forming the only major break in the continuity of the high hills and connecting the West Coast with the rest of the Madras State, is a noteworthy feature in the physiography of southern India. The nature and the mode of origin of the gap is an interesting problem in the geology of southern India which has hardly received any serious attention. No detailed geological mapping of the area of the gap and the adjoining high hills has been carried out till now.

A study of the one-inch and quarter-inch topographic maps of the region has brought to light the remarkably interesting drainage pattern in the hills immediately to the south of the Palghat Gap. The alignment of certain streams and groups of streams with intervening cols along two or three lines forming straight linear patterns of some considerable extent, would seem to indicate possible lines of shearing or faulting. A careful study of the trend lines in relation to the physiography, drainage and geology of the area reveals many striking facts and has enabled us to arrive at certain tentative conclusions regarding the evolution of the drainage pattern of the area and also the possible origin and the age of the Palghat Gap.

II. PHYSIOGRAPHY OF THE AREA

Physiographically the peninsular area south of Mangalore, with which we are concerned, may be divided into three broad natural divisions, (1) the narrow strip

¹ Published by permission of the Director, Geological Survey of India.

Dr. S. L. Hora, Director, Zoological Survey of India, after studying the fish fauna of the hill streams of the Western Ghats, has arrived at certain interesting conclusions regarding their distribution on either side of the Palghat Gap. On discussing with him the geological aspects implied in the distribution of the hill stream fauna, we were stimulated to search for evidence which may throw some light on the structure and the possible age of the Gap.

of coastal plains of South Kanara, Malabar, Cochin and Travancore, (2) the high ranges of the Western Ghats with a narrow gap at Palghat, and (3) the broad undulating plains of South Madras comprising the districts of Coimbatore, Salem, Madura, Trichinopoly, Ramnad and Tinnevely.

(1) *Coastal Plains*.—The plains along the West Coast extend continuously from Bhatkal port north of Mangalore as far as Cape Comorin at the southern tip of the Peninsula. In the Mangalore region, the coastal plain is 5–8 miles in width, but it narrows down to a strip of only 2 miles near Kasargod. South of Cannanore the plain broadens out and in the region between Calicut and Quilon, reaches a width of nearly 15–20 miles. Between Trivandrum and Nagercoil in the south, it again narrows down to 6 or 8 miles. A section across the coastal plain from east to west reveals four sub-divisions, (a) a steeply sloping, partially forested country formed of hills and ridges immediately at the foot of the ghats, followed by, (b) an undulating tract with water-logged paddy fields interspersed with low hillocks and mounds of laterite, succeeded by, (c) a flat raised tract (3–6 miles) capped with laterite and underlain by sub-recent sediments towards the coast, (d) the regions between Ponnani and Cochin, and between the latter and Quilon are marked by the backwaters parallel to the coast.

(2) *Western Ghats*.—The Western Ghats extend as a range of high hills, 15–30 miles in width, over a distance of nearly 450 miles in a NNW-SSE direction from near Karwar on the Bombay border to Cape Comorin in the south. The highest peaks are the following:—

South Kanara: Kodachadri (4,402) and Kudremukha (6,207).

Coorg: Pushpagiri (5,620).

Nilgiri: Vavulmala (7,673), Doddabetta (8,640), Kolarbetta (5,624).

Nilgiri-Malabar border: Gulkal (8,090), Anginda (7,817), etc.

Cochin: Karimalai Gopuram (4,721).

Anaimalai hills: Anaimudi (8,841), Tanakamalai (8,244), etc.

Kodaikanal hills: Ibex Peak (8,663), Vembadi Shola Peak (8,221), Kodai-kanal Peak (7,664).

Andippatti-Varshanad hills: Surulimalai (5,680), Suruliparai (6,221).

North Travancore-Tinnevely border: Kottaimalai (6,624), Sivagirimalai (5,723) and Devarmalai (6,307).

South Travancore-Tinnevely border: Vairattimotti (5,237). Agastiyamalai (6,132) and Mahendragiri (5,427).

The general trend of the ghats is NNW-SSE and there are three more or less arcuate projections extending eastward into the South Madras plains: (a) the Nilgiri range running ENE between the Coimbatore plains and the Mysore plateau, and continued northward into the Satyamangalam-Kollegal hills of Madras and Biligirirangan Hills of Mysore, (b) the Palni range (Kodaikanal hills) running also ENE and continued east and ESE, after a narrow pass at Dindigul, into the Sirumalai-Ammayanayakkanur-Ayyalur hills, and (c) the low Varshanad-Andippatti range running NE towards the Vaigai valley. Lying between the arcuate projections of the Nilgiri range and the Anaimalai-Palni range is the Palghat Gap, with an elevation of 250–1,000 ft., the highest point in the gap being a little over 1,000 ft. near Pollachi.

(3) *Plains of South Madras*.—The plains to the east of the ghats comprising the districts of Coimbatore, Salem, Trichinopoly, Madura, Ramnad and Tinnevely, form a broad undulating region sloping gently to the east and south-east towards the Bay of Bengal and the Gulf of Manaar. These fall into two divisions, (a) the Coimbatore-Salem-Trichinopoly region lying between the Nilgiri-Satyamangalam hills in the north and the Palni hills to the south, and (b) the Madura-Ramnad-Tinnevely region to the south, separated from the northern region by the projection of the Palni-Varshanad-Andippatti ranges. Between the Palni and the Andippatti

hills lies the narrow Kambam valley. The general elevation of the northern plain is between 500 and 1,000 ft., while that of the southern is between 250 and 500 ft.

III. CLIMATE

The area has an equable temperature ranging between 75° and 100°, the mean for the year being 80°-90°. February to May is the hot season when the temperature rises to 90°-100°; between December and January is the cold season with a temperature range of 70°-77°. With regard to rainfall, there is great contrast between the West Coast and the plains to the east of the ghats. The south-west monsoon breaks on the West Coast at the end of May and, for three or four months the region is in the full grip of the monsoon. The annual rainfall, which is mostly received during this period, goes up to 200 inches. The South Madras plains, being on the leeward side of the ghats, receive practically no rainfall during the south-west monsoon except around the Palghat Gap and the high passes as in the Kambam valley and around Shencottah. Only strong dry westerly winds prevail here during this period which lower the summer temperature considerably. The rainfall on this side is around 35 inches, the greater portion of which is received during the north-east monsoon in October, November and December. During this period, the coastal region immediately adjoining the Palghat Gap is subjected to dry easterly winds and dust storms.

IV. GENERAL DRAINAGE

The drainage of the region is in conformity with the three physiographic divisions, with the summit of the Western Ghats forming the natural divide between the drainage systems of the West Coast plains and the South Madras plains.

The rivers and streams along the western slope of the ghats flow west and north-west and, on emerging into the coastal plains, run west or south-west into the Arabian Sea within a short distance from their source in the hills. The most important of these rivers are the Netravati and Payaswani in South Kanara, the Valarpattanam, Beypore and Ponnani (Bharata Puzha) in Malabar, the Chalakkudi Ar and Periyar in the Cochin region, and the Manimalai Ar (Pamba Ar), Achankovil Ar and Kodayar in Travancore. Owing to the heavy rainfall along the western slopes of the ghats, the rivers and streams on the West Coast are perennial. Their course from the hill slopes to the sea is short and steep, and they flow rapidly into the sea cutting steep valleys.

The rivers and streams of the South Madras plains have their sources on the steep eastern slopes of the ghats and they flow east or south-east towards the Bay of Bengal, Palk Strait or the Gulf of Manaar. They flow with only moderate currents and have developed long broad valleys. Having their source on the leeward side of the ghats which receives only a low rainfall, the majority of the rivers and streams, except the Cauvery, are dry during the greater part of the year and are flooded only during the monsoon.

In relation to the two sub-divisions of the region, the drainage systems are also quite separable. The chief rivers of northern region are the Bhavani from the Nilgiri hills, the Noyyal from the Coimbatore hills and the Amravati from the Anaimalai hills. These flow east or north-east into the Cauvery which enters this region from the Mysore plateau after cutting through the Kollegal hills and flows south, south-east and east between the districts of Salem, Coimbatore and Trichinopoly.

The important rivers of the southern region are the Vaigai from the Cardamom hills, the Vaippar from the Sivagiri hills, the Chittar from the Tenkasi hills and the Tambraparni from the Papanasam hills. All of them flow south-east into the Gulf of Manaar. The Vaigai is the longest river in the area. Rising from the Periyar

lake on the eastern slopes of the Cardamom hills, as the Suruli Ar, it flows north-east through the Kambam valley for nearly 50 miles and then turns south-east as the Vaigai river flowing through Madura and entering the sea not far from Rannad town. The details of drainage of the area adjoining the Palghat Gap are given in Sections VII and IX below.

V. GEOLOGICAL FORMATIONS

The geological formations of the area belong to the Pre-Cambrian metamorphic complex with a narrow belt of sedimentaries along the coastal region. The Pre-Cambrian rocks consist of granitoid mica-gneisses and garnetiferous gneisses, with broad massive bands of charnockitic rocks, and thin bands and lenses of hornblende and biotite schists, granular quartzites, crystalline limestones and calc-granulites, and metamorphosed rocks of igneous or sedimentary origin including pyroxene granulites, epidiorites, etc. The northern part of the region, comprising the districts of South Kanara, Malabar, Cochin, Nilgiris, Coimbatore, Salem, Trichinopoly and Madura, shows a more predominant development of granitoid biotite-gneisses, while the area to the south is chiefly composed of garnetiferous gneisses. A few lenses and masses of ultrabasic rocks like pyroxenites, amphibolites and dunites are also found. Pink granites and granitic gneisses of a late age (equivalent to the Closepet granites of Mysore) occur amidst the gneisses of both the regions, but more commonly in the north. With these granites are associated some younger pegmatites and quartz veins which carry at places mica, gemstones and rare-earth minerals like allanite and columbite-tantalite.

The sedimentary formations along the West Coast are of small thickness and of Recent and sub-Recent age, except for the Miocene Warkalai and Quilon beds. The lignites of Bepore and Cannanore are probably also of the same age.

The rocks of the South Madras plains are not weathered to any considerable extent and the country commonly displays good outcrops. The soil and alluvial mantle, except along the river valleys, is very thin, ranging up to 10 feet in thickness. The summits of the Western Ghats and the steep eastern slopes of the range are also composed of barren precipitous rocks with only a thin capping of soil.

Conditions are different on the West Coast and on the western slopes of the ghats, owing to the heavy rainfall and thick vegetation. The soil cover in the West Coast plains is on an average 50 ft. in thickness and there is also a thick capping of laterite in many places, especially on the western slopes of the ghats, the higher regions of the ghats being composed of barren unweathered rocks.

VI. GEOLOGICAL STRUCTURE

(Text-figs. 1 and 2)

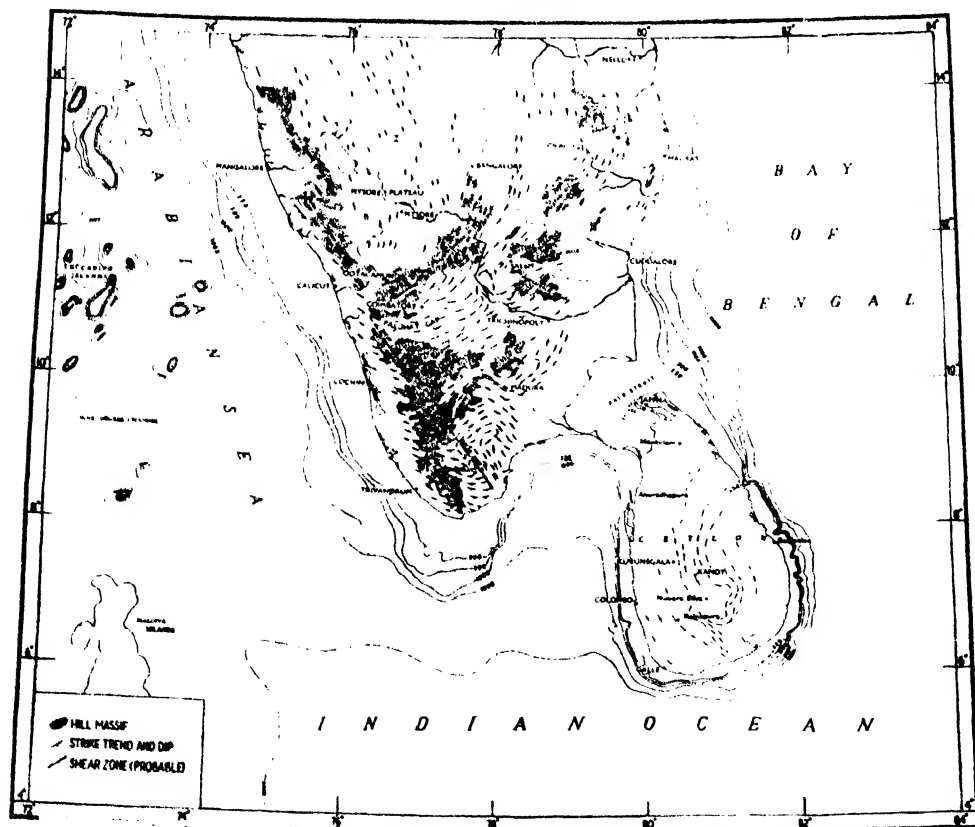
The trend lines of the rocks together with the broad physiographic features and geology are shown in the accompanying sketch map (Text-fig. 1).

The strike of the rocks in the coastal plains and along the western slopes of the ghats is generally NW-SE, varying between NNW-SSE in North Kanara and Coorg, NW-SE in Malabar and North Travancore, and WNW-ESE in the South Travancore region. About a NNW-SSE imaginary line passing through the summit of the Western Ghats, through Coorg, Wynaad, Anaimalai hills, Periyar lake and Tenkasi town, there is a sudden change in the trend of the rocks due to folding about a north-south axis. From a NNW-SSE or NW-SE trend on the western side of the ghats, the strike veers round to the east, ENE and finally to NE on the eastern side. The strike of the North Malabar-Coorg rocks continues into the Nilgiri range in a ENE direction. This is continued further on into the NNE (and occasional

northerly strikes) of the Satyamangalam-Biligirirangan-Kollegal hills along the Mysore border. The rocks of the Palghat Gap region continue similarly into the Coimbatore plains and turn gradually with a NE strike into the Salem region. This north-easterly trend extends from the Shevaroy-Kalrayan hill tracts of Salem into the Javadi-Yelagiri hills of South Arcot and is continued into the neighbourhood of Chingleput and Madras city. Similarly the NW-SE strike of the South Malabar-Cochin rocks continues east and ENE into the Anaimalai and Palni hills and further up into the Trichinopoly-North Madura region in a NE directions, beyond which it is concealed by younger rocks. The NW-SE strike of the North Travancore rocks turns round to the NE into the Kambam valley, Andippatti-Varshanad hills and West Ramnad plains beyond which the Archaeans are covered by Tertiary sediments. The NW-SE and WNW-ESE trends of South Travancore extend into the South Tinnevely plains and gradually curve round to an easterly direction towards the coast where they become concealed underneath the sub-recent coastal deposits.

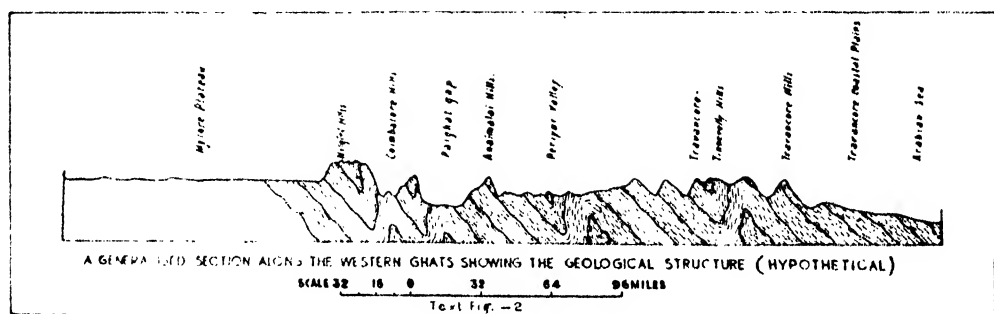
The general regional trend of the rocks in South Madras plains some distance east of the Western Ghats is thus NE-SW. But about a roughly north-south irregular line passing through Erode, Dindigal, Madura city, Virudhunagar and Kovilpatti, there is a northerly loop in the strike of the rocks due to folding of the strata about a north-south axis, similar to the one noticed along the Western Ghats (Text-fig. 1).

TEXT FIG. 1-PROVISIONAL TECTONIC MAP (PRE-CAMBRIAN) OF PARTS OF
PENINSULAR INDIA AND CEYLON
SCALE IN MILES 0 20 40 60 80 100 120 140 160



The general regional dip of the rocks is to the WSW, SW and SSW in the West Coast region, which changes to south, SSE and SE in the South Madras plains. Opposing northerly dips, i.e., to the NW, NNW, north, NE and ENE, are often found along certain areas as a result of local folding. Along the north-south fold axis in the region of Erode-Madura-Kovilpatti, the dips are rather confusing due to the variations in the nature of the folding at different places. The dip is generally steep to moderate. In the West Coast region, it varies from 80° – 60° in South Kanara, Coorg and Malabar to 60° – 50° in Travancore. In the South Madras plains the dip ranges from nearly vertical to about 50° – 60° , and as in the West Coast region, there appears to be slight flattening of the dips as we proceed southward.

The rocks of the Mysore Plateau on the northern side of this region strike NNW-SSE. The Dharwarian schists form linear belts amidst the gneissic and granitic rocks as north-pitching synclinal folds with the intervening anticlinals eroded away. Structurally this region appears to represent the eroded portion of a main anticlinorium.



A careful study of the map seems to indicate that the strike trends of the rocks of South Madras closely follow those of the Dharwar schist belts. The schistose formations thus seem to form the basal portion of the Dharwar schists which may probably rest on older formations. The general structure of the region is that of a series of major anticlines and synclines with minor folds on the limbs of the major ones. In conformity with the Dharwar synclines, these folds should also plunge to the north. The southerly loop in the strike of the rocks about the Western Ghats and in the vicinity of the Palghat Gap thus appears to be a north pitching synclinal fold and the northerly loop about Erode, Madurai and Kovilpatti is a north-pitching anticlinal.

VII. DRAINAGE PATTERN IN THE HILL TRACTS ADJOINING THE PALGHAT GAP AND ITS POSSIBLE EXPLANATION

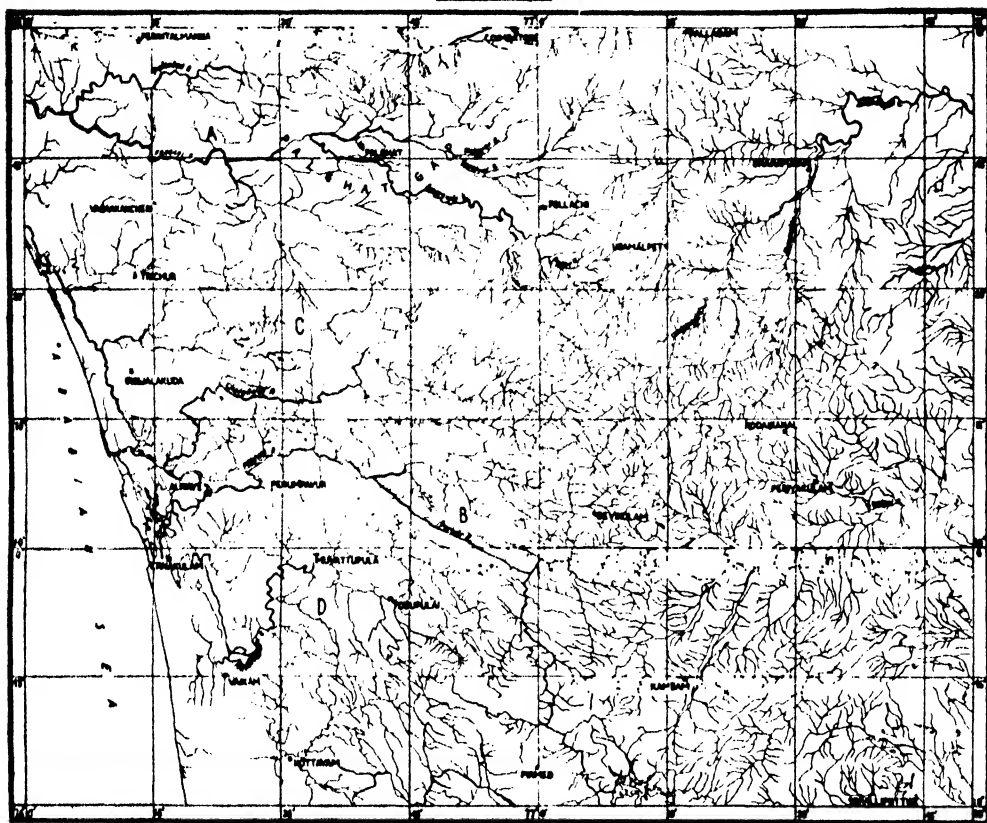
(Text-figs. 3–6)

A study of the topographic maps of the West Coast and the western slopes of the ghats of this region reveals that the majority of the rivers and the larger streams flow in a general westerly and north-westerly direction in their course through the hills following the strike of the rocks. In the coastal plains which are covered with a thick mantle of alluvium and laterite and sub-Recent formations, the streams have a low gradient towards the sea, preferring no particular directions.

In contrast with the general direction of flow of these main streams, are other smaller streams and tributaries which join the main drainage at high angles cutting across the general trend of the hills and the direction of strike of the rocks. The hill tracts of South Malabar and Cochin lying immediately to the south of the Palghat Gap are of interest in this respect (Text-fig. 3).

TEXT FIG. 3—DRAINAGE PATTERN OF THE AREA AROUND PALGHAT GAP.

SCALE 1:10 000 000



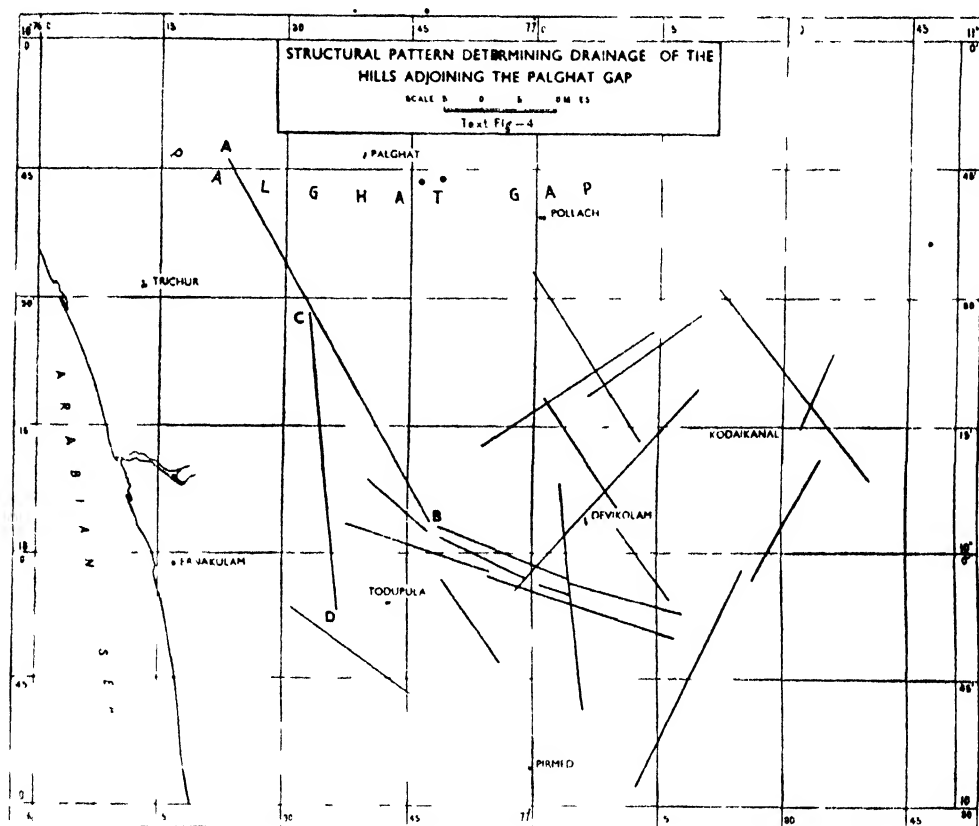
The main streams in this region running west and north-west are (1) the Bharata Puzha in the Palghat Gap, (2) the Mappili Puzha and Parambikolam Ar (along the sides of which the government timber tram line runs), (3) the Chalakkudi Ar, (4) the Yedamalai Ar, (5) the Puyankutti Ar and (6) the Periyar.

Meeting these rivers at fairly wide angles are two sets of prominent tributaries, (1) the Gavitri Puzha, the Karappara Ar, the connecting streams between Parambikolam Ar and the Chalakkudi Ar and between the northern and southern sections of the Yedamalai Ar and a few others extending in a NW-SE line between the Bharata Puzha and the Periyar; (2) the Kannankuzhi Todu, Perum Todu, Kottapara Todu and a few others running in a N-S line. The courses of the main streams are also marked occasionally by sharp bends which offset the streams for short distances. Groups of waterfalls and cascades are found not only along the main streams but also in the tributaries, particularly near their junctions.

The remarkably straight alignment of the tributary streams (A-B, C-D; in Text-figs. 3, 4) mentioned above is very striking. These are streams (with intervening cols) which take part in the linear patterns. One set lies in a NW-SE direction extending for nearly 64 miles (A-B, Text-figs. 3, 4) and the other in a N-S direction running for a distance of 32 miles (C-D, Text-figs. 3, 4). The two sets converge at the western end of the Palghat Gap area. They probably represent certain well defined structural features.

The northern ends of both may be traced to the actual gap where the height above mean sea-level is only 500 ft. As the straight river patterns are developed between altitudes of 500 ft. and 5,000 ft. above sea-level, it is not improbable, as

Auden (1951, p. 35) pointed out, that the structural features are of great lateral extent, and are developed through a considerable vertical range. In the case of a NE-SW linear pattern extending for nearly 40 miles and which passes near Mattupatti dam site in Travancore, Auden estimates a vertical range of 6,200 ft.



Similar straight alignments, but less striking, are also noticed in the upper reaches of the Yedamalai Ar and Puyankutti Ar, and also at places in the Anaimalai-Devikolam hills. As seen in Text-figure 4, four major directions may be recognized in the linear stream patterns developed in the region to the south of the Gap.

The first impression conveyed by these linear patterns is that they are possibly fault planes. A careful examination of the valleys along the Mappili Puzha and Parambikolam Ar during a traverse along the timber tram line has, however, not indicated the presence of such later faulting. The rocks here are foliated and banded gneisses with charnockitic bands, and have a general WNW-ESE, E-W and ENE-WSW trend with low dips of about 20° - 30° generally to the south. The gneissic and charnockitic bands are clearly seen traversing the beds of these tributaries without any lateral shifting or other signs of disturbance. No indication of any fault could be noticed in the vicinity of Ottappalam along the Bharata Puzha west of Palghat where the NW-SE line appears to terminate.

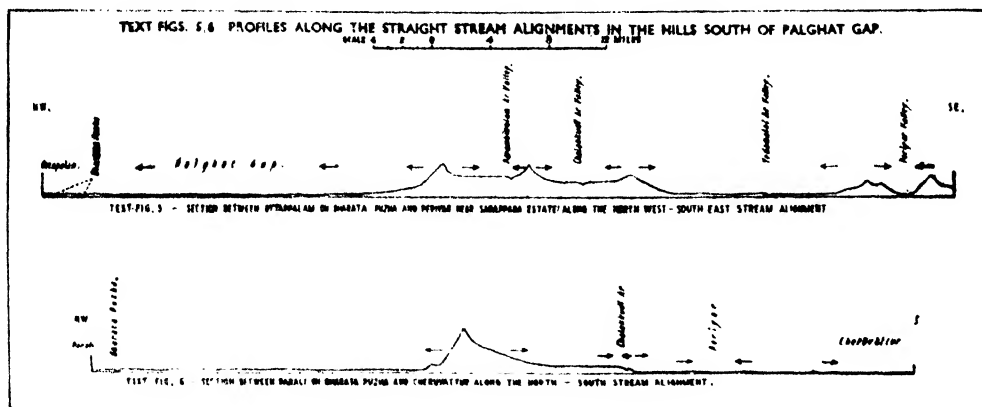
Auden (51) had, however, observed a shear zone about 70 ft. in width near the Mattupatti dam site through which a NE-SW linear pattern runs. He could not find any convincing evidence of major fault offsets having taken place along this zone.

A careful study of the map reveals that the linear patterns (A-B, CD, in Text-figs. 3, 4) are more or less at right angles to the strike directions of the rocks and they occur in greater numbers at the north-pitching synclinal fold, where the strike of the rocks changes from NW-SE and WNW-ESE to E-W and ENE-WSW. It is possible, therefore, that the linear patterns may be the result of shearing.

Shearing may occur more or less uniformly along a straight boundary for considerable length. It may also follow the easiest planes of weakness in the rocks which, in this case, are at right angles to the strike. Such shear fractures most probably determined the straight courses of the tributaries in contract with the courses of the main streams which follow the strike of the rocks. Elsewhere, these fractures might have encouraged block-faulting, so that one may reasonably expect to find them indicated by long straight segments of streams begun or ended by abrupt bends. If one examines carefully the other parts of the Western Ghats, more examples may come to light. In this connection the recent papers by Radhakrishna (1952) and Radhakrishna and Ghose (1951) may be seen. An extended study of the stream patterns, particularly of the region south of the gap, should be worthwhile.

It may be pointed out here that during the course of systematic mapping in the Tinnevely district, a 'thrust' zone of presumably Pre-Cambrian age has been recognized by one of us (S.N.) running in a NW-SE direction for a distance of over 120 miles (Text-fig. 1). This zone is traced from the Tambraparni river near Srivaikuntam up to the foot of the Western Ghats north of Srivilliputhur. Except for a slight lateral shift in its alignment in the hills near the Periyar lake region, the 'thrust' zone recognized here apparently extends in continuation of the major shear line (Text-fig. 4, A-B; Text-fig. 1) noticed in the Palghat Gap region.

To our mind an alternative explanation of the linear stream patterns immediately to the south of the Gap is to consider them as remnants of an original drainage much older than the main streams. The present west and north-west flowing streams like the Periyar, Chalakkudi Ar, Bharata Puzha, etc. are apparently subsequent to the faulting of the West Coast region and these have followed the strike directions of the rocks. The direction of flow of the tributaries which make the straight line patterns appears to have no definite relation to the main streams which they join. The sections shown in Text-figs. 5, 6 are drawn along the lines of tributaries extending south-east



and south from the Bharata Puzha to the Periyar. A study of these profiles shows that the divides between the opposing pairs of tributaries gradually decrease in elevation as one proceeds southward, and the south-flowing tributaries are much longer than the north-flowing ones. These features perhaps indicate the possible existence in the past of south-east and south flowing main streams which occupied

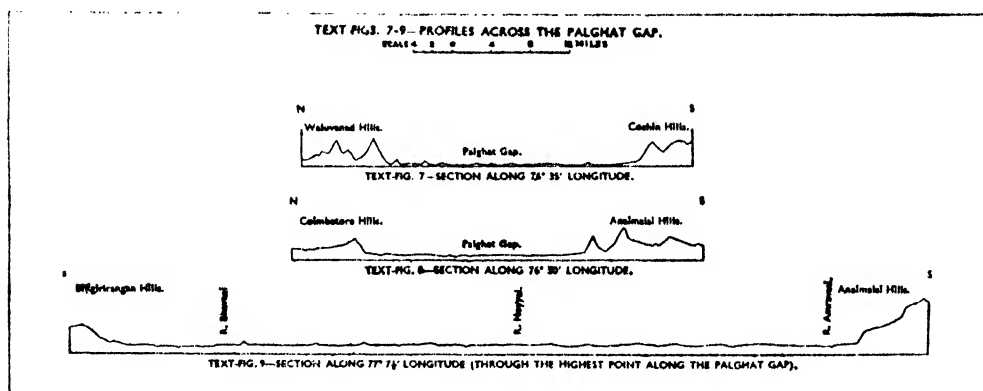
these valleys at a much higher elevation than at present. They were consequent upon the original slope of the terrain. Subsequent to the faulting and tilting of the West Coast region, these streams might have considerably dwindled in size, probably because the sea encroached upon the area to the west stimulating the development of west-flowing streams. They now occupy the position of the old valleys as tributaries meeting the west and north-west flowing main streams formed at a later period.

A recent paper by West (1951) has come to our notice wherein the author mentions having recognized paired shear fractures *en echelon* over a wide area in Alaska, which at times determine straight stream directions. The author has also attempted to determine the direction of inferred force. In the case of the shear fractures recognized in parts of South India we are at present not in a position to determine the direction of force without additional data.

VIII. THE EVOLUTION OF THE PALGHAT GAP

(Text-figs. 1, 4, 7-9)

As mentioned in an earlier section, the Palghat Gap is a fairly undulating pass extending east to west with an average width of eight miles (Text-figs. 1, 7-9). The elevation of the gap ranges from 250 ft. near Palghat to a little over 1,000 ft. at Pollachi (Text-figs. 7-9). The hills on either side rise abruptly as steep precipitous scarps reaching to heights of over 3,000 ft. The almost straight direction of the



hills and their steepness on either side of the gap, especially to the south, might suggest that faulting in an E-W or NE-SW line was responsible for the formation of the gap. A study of the strike trends and other features apparently does not support such a suggestion for the origin of the Palghat Gap. No trace of faulting has been noticed in the rocks of the Coimbatore region immediately to the east of the gap. From a NW-SE trend on the West Coast the rocks turn eastwards through the gap and run east and ENE into the Coimbatore region. It appears, therefore, that evidence for the evolution of the gap has to be searched for in the physiography and the drainage features of the area.

The river Cauvery which forms the main drainage basin here, flows to the south-east and east through the Coimbatore-Trichinopoly plains, between the Nilgiri-Satyamangalam-Salem hill tracts in the north and the Palni-Dindigal hills to the south. The rivers Bhavani, Noyyal and Amravati are the main tributaries which enter the Cauvery from the western side after draining the Coimbatore plains. The combined basin of these tributaries is a broad undulating peneplain.

The major portion of the area receives a low rainfall and the rivers are flooded only for a short period during the rainy season. It is really difficult to conceive of such a broad penepplain developed by denudation by these rivers alone. The shape and size of the basin and its general slope towards the east seem to suggest that it was once occupied by a larger stream flowing eastwards right from the Palghat Gap and receiving a much greater flow of water from the hills to the west.

A study of the contours also indicates that this stream probably occupied the course of the present Amravati river between Karur and Dharapuram, and the Uppar Odai between Dharapuram and Pollachi. The course of the stream further west was probably through the centre of the Palghat Gap with a gradual northerly turn towards its source just above the region of Anangamalai (Δ 1291). The Bhavani and the Noyyal were probably its tributaries which entered the main river from the north.

After the faulting and the subsequent tilting of the West Coast region resulting in the diminution of the water supply from the hills to the west, this Ur-Cauvery might have become considerably dried up. Depending on the degree and direction of tilting, the ancient Cauvery appears to have captured the present stream from the Mysore plateau after cutting its way through the Kollegal-Biligirirangan hills.

The existence of deep gorges like the Mekedatu and waterfalls like Sivasamudram and Hoganakal seems to point to the still youthful stage of the Cauvery in this region. The alternate straight courses of the river following the strike of the rocks, followed by sharp bends cutting across the strikes with deep gorges and waterfalls, apparently indicate a subsequent drainage.

The original east flowing river might have gradually dwindled in size leaving only a steep-sided wind gap in the Palghat region. The profile section across the gap (Text-figs. 7-9) reveals steep and almost precipitous slopes on either side down to 1,000 ft., below which occurs the almost flat valley of the Bharata Puzha.

In addition to the easterly drainage, the probable presence of a large westerly flowing drainage system with its source very close to the Palghat region is indicated by the landward curvature of the bathymetric contours in the region of the Arabian Sea opposite to the gap and continued WSW to a deep channel, 'the Nine-Degree Channel', between the Laccadive and the Maldive groups of islands (Text-fig. 1). The significance of this submarine depression which may possibly indicate a submerged river valley is discussed in Section IX below. Medicott and Blanford (1893, p. 495) had postulated the possible existence of a large westerly flowing river running through the Palghat Gap area, its main drainage having been reversed by earth movements which 'raised' the Western Ghats. They suggested that probably these movements considerably reduced the former westerly flowing river into the much smaller stream, the present Bharata Puzha, while the major part of the drainage was diverted to the east.

In explaining the accumulation of the ancient alluvium in the plains of the Nerbada, of Berar and of the upper Godavari, Vredenburg (1906, pp. 38, 39), on the other hand, postulates the formation of a shallow anticlinal ridge running west of the western termination of the Nerbada and Purna plains with a strike slightly east of north, instead of a general tilting of the western side of the Peninsula. Warping, as suggested here by Vredenburg, cannot explain many other remarkable features on the West Coast. No doubt there are evidences of warping in the western half of the Peninsula, but we feel that tilting has also taken place to some extent. In our opinion tilting and warping of the western parts of the Peninsula followed the block faulting.

The drainage systems mentioned above followed the general slope of the land, and their direction had, therefore, been to the east, south and west. Subsequent to the faulting on the West Coast, a new set of west-flowing streams developed from the steep western slopes of the ghats. These streams followed the weak planes of the rocks which now naturally lie along the strike, viz., to the west and NW.

The Bharata Puzha is one such subsequent stream which has developed along the old gap in the Palghat region. It is now cutting headward into the gap and on to the Coimbatore plains, and its tributaries have their origin from the slopes of the Anaimalai hills south of Pollachi. As may be seen from the section in Text-fig. 9, the only remnants of the original east-sloping valley floor which have withstood erosion and occur as isolated stumps are: (1) the 1,250 ft. high-ground ENE of Pollachi, and probably (2) the ridge Anangamalai (1,500 ft.) to the NE of Shoranur.

In a recent contribution by King (1950, pp. 109-111) on the study of the world's plainlands, the author suggests the existence of three cyclic erosion surfaces in the Indian Peninsular region. In southern India he recognizes a 'Gondwana Cycle' of levelled residuals of Gondwana age in parts of the Nilgiri and Cardamom hills, rising above the general plateau ('Indian Cycle') which he considers to be younger. According to him, the 'Gondwana' land surface is pre-Cretaceous, while the 'Indian' land surface is Cretaceous-Middle Tertiary. The Palghat Gap area is shown in his map as 'post-Indian' land surface of late Tertiary-Recent age. In our opinion, King's views require scrutiny before they can be accepted. However, it is of interest to note that the N-S and NW-SE linear drainage patterns observed in the Palghat Gap area cut across the 'Indian' (Cretaceous-Middle Tertiary) and 'post-Indian' (late Tertiary-Recent) land surfaces. To those who find King's views acceptable, it may appear that any shearing that might have been responsible for these linear patterns, probably took place not earlier than the late Tertiary. On the other hand, it is not unlikely that a more ancient feature of the land was rejuvenated in comparatively recent time.

IX. BATHYMETRIC CONTOURS IN THE ARABIAN SEA WEST OF THE PALGHAT GAP

(Text-fig 1)

It is noteworthy that in the region due west of the Palghat Gap in the Arabian Sea, the 200, 500, 1,000 and 5,000 ft. bathymetric contours take a more or less sharp bend towards the coast, thereby suggesting that in this region a submarine valley exists (Text-fig. 1). Further west, between the Laccadives and the Maldives this valley probably extends in a WSW direction as the 'Nine-Degree Channel'. The alignment of this channel and the prominent deflection of the bathymetric contours towards the region of the coast west of the gap, is approximately in the ENE-WSW direction.

This interesting feature may at first suggest the existence of a submerged valley formed by a large river which once took its course through the gap (as postulated in an earlier chapter) in a WSW direction and extending into the region of the Arabian Sea.

It would appear that the Pleistocene changes of sea-level owing to the repeated formation on land of thick ice sheets and their melting, would only account for an oscillation of sea-level of about 300 ft. It is possible that during the low sea-levels of the Pleistocene Ice Age the upper parts of the submarine valley were incised when the shelf surface was largely situated at or above sea-level.

According to Bourcart (1938), continental flexure has apparently taken place along their margins causing periodical marginal flexure or bowing upwards of the borders of the continents, accompanied by submergence of the margins resulting in rejuvenation of the continental border relief. Jessen (1934) has also supported this idea. Such rejuvenation has been a characteristic feature of comparatively recent geological times. But these movements caused by subsidence of the shelf areas and the uplift of the coastal regions can only be small in amplitude.

On the other hand, if we assume a N-S coastal block faulting with crustal subsidence from a normal level, we shall have to postulate a downthrow of at least

5,000 ft. magnitude to account for an erosion base at that depth. It may be that the theories based on sub-aerial origin alone, explaining the present level of the submarine valley, will have to be abandoned.

In a subsequent section, we have attempted to adduce evidence for the Lower Miocene faulting of the West Coast, although some hold the view that this event took place in the Pliocene or Pleistocene times which may be true of only the Mekran Coast.

Though the faulting is of Miocene age, it would seem that the submerged land had preserved some of its erosional features such as the postulated ENE-WSW drowned river valley extending from the Palghat Gap area towards the 'Nine-Degree Channel'. In the present state of our knowledge, it is difficult to decide whether to consider this feature as a mere submerged river valley or as something else. However, as Kuenen (1950) has pointed out, 'Conditions under water may possibly tend to encourage the development of forms that are destroyed on land. The absence of weathering and to a large degree of the creep of surface layers on the sea floor should allow bold forms to persist almost indefinitely that would soon crumble away under the influence of atmospheric attack'. It is therefore quite possible that gullies and valleys of a former land surface may persist under submarine conditions for a much longer period than similar features on the land. Hence the submarine surface features now seen may reflect those present on the land surface in the Miocene just before the land was faulted down.

The Laccadives and the Maldives which for the most part arise from two separate plateaus (Sewell, 1935, p. 42) with the former at a depth of about 1,000 fathoms and the latter about 1,900 fathoms (Gardiner, 1902, p. 296), are not exactly in the same alignment; the latter group of islands lie slightly displaced to the east from a perfect N-S alignment. The 'Nine-Degree Channel' between the two groups of islands may possibly represent a drowned valley occupying a zone of an ancient fault line, the displacement extending ENE opposite to the Palghat Gap area. It has also been suggested by Davis (1928, p. 525) that the Laccadive and the Maldive atolls and reefs are perched on the tops of fault blocks (Sewell, 1935, p. 435).

In our opinion, major changes in sea-levels on the West Coast were caused by several factors including subsidence of land after the block faulting, eustatic changes during the Pleistocene as a result of the formation and melting of large sheets of land ice mostly in the northern continents, and possibly also continental flexure.

X. PERIOD OF FORMATION OF THE PRESENT WEST COAST AND THE PROBABLE AGE OF THE PALGHAT GAP

Subsequent to the faulting along the West Coast of the Peninsula, subsidence took place accompanied by brief incursions of the sea into the land. At that time the present West Coast region was worn back and a wave-cut platform resulted with the formation of wave-built terrace in front. If this surmise is correct the present plains lying immediately at the foot of the ghats represent the wave-cut platform and the laterite uplands towards the coast underlain by the marine sediments, the wave-built terrace. As the trend lines of the rocks are nearly transverse to the coast, drowning and marine denudation have resulted in long promontories alternating with narrow estuaries. This may be seen from the projecting ridges of harder rocks alternating with low narrow valleys at the foot of the ghats. As already pointed out by Medlicott and Blanford (1893, p. 11), the sea probably extended as a bay into the Palghat Gap thus augmenting the steepening of the walls of the gap.

These events were followed by the emergence of the West Coast which then began to expose the sediments deposited in the previous period.

From fossil evidence, the age of the Quilon beds on the West Coast is believed to be Burdigalian (Lower Miocene; Jacob and Sastri, 1951; Eames, 1950). The

characteristic Lower Miocene foraminifer, *Austrotrillina houchini* recently found in the Quilon beds (Jacob and Sastri, 1951) also occur in the Miocene of Broach on the Bombay coast (Rao, 1941). It is believed that the two patches are most probably of the same age (Lower Miocene). Near Ratnagiri also, between Quilon and Broach, marine Miocene sediments have been reported although their exact horizon is not definitely known. It would appear, therefore, that the faulting along the West Coast took place before the Burdigalian followed by marine incursion. The later emergence of the coast was in all probability post-Burdigalian.

Profiles drawn at intervals (1) from north to south across the Palghat Gap, and (2) from east to west along the West Coast plains from the sea to the Western Ghats seem to indicate some minor accordance of levels below 2,000 ft. altitude (Text-figs. 5, 6). These levels roughly correspond to elevations of 1,000 ft., 750 ft., 400 ft., and at intervals of 100 ft., between 400 ft. and the sea-level. The possibility cannot be overlooked that these levels may indicate different stages of emergence of the coast. The presence of groups of waterfalls along certain intermittent elevations inside the ghats also seems to have some relation with the suggested emergence in stages (Text-figs. 7-9). Further detailed study in the field will be necessary before any definite views may be expressed on the periods of emergence and other related phenomena.

In the preceding pages we have discussed at some length the possible significance of linear drainage patterns noticed in the Palghat Gap area, in the hope that it may focus attention on the desirability of taking up similar studies in other parts of India. Much of this paper is somewhat speculative. If, however, the views put forward, right or wrong, serve as a stimulus for further observations its purpose has been fulfilled.

ACKNOWLEDGEMENT

We are grateful to Dr. M. S. Krishnan, Director, Geological Survey of India, for going through the paper and making valuable suggestions. We are also deeply indebted to Dr. J. B. Auden, Geological Survey of India, and to Mr. R. Tirunaranan, Madras Educational Service, for useful suggestions on various occasions.

SUMMARY

The Palghat Gap which lies across the Western Ghats in Malabar, forming the only major break in the continuity of the high hills and connecting the West Coast with the rest of the Madras State, is a noteworthy feature in the physiography of southern India.

The physiography, general drainage, climate and the degree of weathering of the region are first described.

The geological formations of the area belong chiefly to the Pre-Cambrian metamorphic complex with a narrow belt of sedimentaries along the coastal region. The Pre-Cambrian rocks consist of granitoid mica-gneisses and garnetiferous gneisses traversed by broad massive bands and lenses of hornblende and biotite schists, granular quartzites, crystalline limestones and calc-granulites, all of which represent intensely folded granitized and metamorphosed remnants of original sediments and basic intrusive and effusive rocks.

The strike and dip of the rocks of south Madras closely follow the trend lines of the Dharwarian schist belts. The gneissic and charnockitic formations with the associated highly metamorphic rocks probably rest on older formation and have suffered the same degree of deformation as the latter. The general geological structure of the region is that of a series of major compressed anticlines and synclines, with minor folds on the limbs of the major ones. In conformity with the Dharwarian rocks, the synclinal folds in these rocks also plunge to the north. The southerly loop in the strike of the rocks about the Western Ghats in the vicinity of the Palghat Gap thus appears to be a north-pitching synclinal fold and the northerly loop about Erode, Madura and Kovilpatti is a north-pitching anticlinal.

In regard to the drainage pattern, the remarkably straight alignment of the tributary streams immediately to the south of the Palghat Gap area with associated waterfalls is very striking. One set of these lines lies in a NW-SE direction extending for nearly 64 miles and the other in a N-S direction running for a distance of 32 miles. They run more or less at right angles to the strike direction of the rocks at each place, and occur in greater numbers in the

north-pitching synclinal fold where the strike of the rocks changes from NW-SE and WNW-ESE to E-W and ENE-WSW direction. The two sets converge at the western end of the Palghat Gap area. It is surmised that there existed south-east and south flowing main streams which occupied these valleys at a much higher elevation than at present. They were probably consequent upon the original slope of the terrain. Subsequent to the faulting and tilting of the West Coast region, these streams might have considerably dwindled in size, probably because the sea encroached upon the area to the west. They now occupy the position of what are thought to be the old valleys of tributaries meeting the west and north-west flowing main streams formed at a later period.

It is suggested that the combined basin of the Bhavani, Noyyal and Amravati which join the Cauvery, is a broad undulating peneplain, once occupied by a larger stream flowing eastwards from the Palghat Gap and receiving a much greater flow of water from the hills to the west. After the faulting and the subsequent tilting of the West Coast region there was a diminution in the supply of water to this Ur-Cauvery. The original east-flowing river probably left only a steep-sided wind gap. In addition to the pronounced easterly drainage, the probable presence of a large westerly flowing drainage system with its source very close to the Palghat region seems to be indicated by the landward curvature of the bathymetric contours in the region of the Arabian Sea opposite to the gap and continued WSW to a deep channel, 'the Nine-Degree Channel', between the Laccadive and the Maldive groups of islands. This submarine depression may therefore indicate a submerged river valley. The combined head erosion of these two opposite flowing streams in the Palghat Gap region might have augmented the formation of the low saddle in the gap.

The evolution of the Palghat Gap may be said to have commenced from the time of block faulting of the West Coast and the possible incursion of the sea into the region. This, in all likelihood, took place earlier than the Middle Miocene, and if this surmise is correct, the age of the gap is not later than the Lower Miocene.

Much of this paper is somewhat speculative. If, however, the views put forward, right or wrong, serve as a stimulus for further observations its purpose has been fulfilled.

XI. REFERENCES

- Auden, J. B. (1947). Geological Report on the Mattupatti dam site and Sengulam Project, Travancore State (unpublished).
- (1949). Dykes in Western India. A study of their relationships with the Deccan Traps. *Trans. Nat. Inst. Sci. Ind.*, **3**, 123-157.
- (1951). The bearing of geology on multipurpose projects. *Presid. Addr., Geology and Geography, 38th Ind. Sci. Congr.*, 1951, 1-45.
- Bourcart, J. (1938). La marge continentale. *Bull. Soc. Geol. France*, **8**.
- Davis, W. M. (1928). The coral reef problem. *Sp. Publ. No. 9, Amer. Geogr. Soc.*
- Eames, F. E. (1950). On the ages of certain Upper Tertiary beds of Peninsular India and Ceylon. *Geol. Mag.*, **87**, No. 4.
- Gardiner, J. S. (1902). The formation of the Maldives. *Geogr. Journ.*, **19**, No. 3, 277-96.
- Jacob, K. and Sastri, V. V. (1951). The occurrence of *Austrotrillina* in the Quilon limestone, South India. *Science and Culture*, **16**, No. 7, 326-327.
- Jessen, O. (1943). Die Randschwellen der Kontinente. *Peterm. Geogr. Mitt. Erg.*, **241**.
- King, L. C. (1950). The study of the World's plainlands: A new approach in geomorphology. *Quart. Journ. Geol. Soc. Lond.*, **106**, Pt. 1, 101-131.
- Krishnan, M. S. (1953). Structural and Tectonic history of India. *Mem. Geol. Surv. Ind.*, **81**.
- Kuenen, P. H. (1950). Marine Geology. *New York and London*.
- Medlicott, H. B. and Blandford, W. T. (1893). A manual of the geology of India. 2nd Ed. revised by R. D. Oldham. *Calcutta*.
- Radhakrishna, B. P. (1952). The Mysore Plateau. Its structural and physiographical evolution. *Bull. Mysore Geol. Assoc.*, No. 3, 1-56.
- Radhakrishna, B. P. and Ghose, M. (1951). On the recognition of faults in the granite terrain in Mysore. *Current Science*, **20**, 203-204.
- Rao, S. R. N. (1941). The Tertiary sequence near Surat and Broach (Western India) with description of foraminifera of the genus *Pellatispira* from the Upper Eocene of this region. *Journ. Mys. Univ.*, **2**, 5-17.
- Sewell, R. B. S. (1935). Geographic and Oceanographic research in Indian waters. Pt. VII. The topography and bottom deposits of the Laccadive sea. *Mem. As. Soc. Bengal*, **9**, No. 7, 425-480.
- Vredenburg, E. (1906). Pleistocene movement as indicated by irregularities of gradient of the Nerbada and other rivers in the Indian Peninsula. *Rec. Geol. Surv. Ind.*, **33**, Pt. 1, 33-45.
- West, S. S. (1951). Major shear fractures of Alaska and adjacent regions. *Trans. Amer. Geophys. Union*, **32**, No. 1, 81-86.
- Wiseman, J. D. H. and Sewell, R. B. S. (1937). The floor of the Arabian Sea. *Geol. Mag.*, **74**, 219-230.

ON POLAR RECIPROCAL CONVEX DOMAINS

by R. P. BAMBAH, *Institute for Advanced Study, Princeton, N.J., U.S.A., and Punjab University College, Hoshiarpur.*

(Communicated by H. Gupta, F.N.I.)

(Received September 4; read December 4, 1953.)

1. Let k and K be two symmetrical convex domains in the plane with centres at the origin. Suppose k and K are polar reciprocal with respect to the unit circle C centred at the origin.

Let $\Delta(K)$ be the critical determinant* of K and $c(k)$ the covering constant of k , i.e. the upper bound of the determinants of the covering lattices for k , where a lattice A is called a covering lattice for k if every point in the plane lies in one at least of the bodies obtained from k by applying to it all possible lattice translations.

Mahler (1948) proved that

$$\frac{1}{2} \leq \Delta(K) \Delta(k) \leq \frac{3}{4}, \quad \dots \dots \dots (A)$$

and that both the inequalities are best possible.

It seems worth noticing that

$$2 \leq \Delta(K) c(k) \leq \frac{3}{4}, \quad \dots \dots \dots (1)$$

and that both inequalities here again are best possible.

2. In this section we prove (1).

Write $H_s(K)$ for the area of the smallest symmetrical convex hexagon† circumscribed to K and $h_s(k)$ for the area of the largest symmetrical convex hexagon† inscribed in k . Then it is known that

$$\Delta(K) = \frac{1}{4} H_s(K), \quad \dots \dots \dots (2)$$

and

$$c(k) = h_s(k); \quad \dots \dots \dots (3)$$

(2) follows from Theorem 1 of Mahler (1948) and Theorem 3 of Dowker (1944) while (3) is lemma 8 of Bambah and Rogers (1952).

Let H be the symmetrical convex hexagon circumscribed to K with area $a(H) = H_s(K)$. Then H' , the polar reciprocal of H , is a symmetrical convex hexagon inscribed in k so that

$$c(k) = h_s(k) \geq a(H'),$$

where $a(H')$ is the area of H' . Consequently

$$\Delta(K) c(k) = \frac{1}{4} H_s(K) h_s(k) \geq \frac{1}{4} a(H) a(H') \geq 2; \quad \dots \dots (4)$$

the last inequality following from inequalities A of Mahler (1948).

* For definition see e.g., K. Mahler, *Proc. Royal Soc., A*, 187 (1946), 151.

† By a hexagon we mean a polygon with at most six sides.

Now suppose h is the convex symmetrical hexagon of area $a(h) = h_s(k)$ inscribed in k . Then h' , its polar reciprocal, is a convex symmetrical hexagon circumscribed to K , so that

$$\Delta(K) = \frac{1}{4} H_s(K) \leq \frac{1}{4} a(h'),$$

where $a(h')$ is the area of h' . Therefore we have

$$\Delta(K) c(k) = \frac{1}{4} H_s(K) h_s(k) \leq \frac{1}{4} a(h') a(h) \leq \frac{9}{4}, \quad \dots \quad (5)$$

the last inequality following from inequalities *A* of Mahler (1948).

(4) and (5) together prove (1).

Let k and K be the squares:

$$k: |x| \leq 1; |y| \leq 1; K: |x| + |y| \leq 1.$$

Then

$$c(k) = 4, \Delta(K) = \frac{1}{2} \text{ and } c(k) \Delta(K) = 2. \quad \dots \quad (6)$$

If k and K become the unit circle or the regular hexagon inscribed in the unit circle and its polar reciprocal, then

$$c(k) = \frac{3\sqrt{3}}{2}, \Delta(K) = \frac{\sqrt{3}}{2},$$

and

$$c(k) \Delta(K) = \frac{9}{4}, \quad \dots \quad (7)$$

which together with (6) shows that the inequalities (1) are best possible.

3. From the well-known results

$$3^{-n+1} V(K) \leq c(K) \leq V(K) \text{ (Rogers),}$$

$$2^{-n} V(k) \leq \Delta(k) \leq \frac{1}{a_n} V(k), \quad a_n \rightarrow 4.921 \text{ as } n \rightarrow \infty$$

(Minkowski and Davenport-Rogers)

and

$$\frac{2^n J_n}{(n! n^n)^{\frac{1}{2}}} \leq V(k) V(K) \leq J_n^2$$

(Dvoretzky Rogers and Santalo)

(where J_n is the volume of the unit sphere in n dimensions), one can find analogous inequalities for $c(k) \Delta(K)$ and $c(k) c(K)$ for polar reciprocal symmetrical convex bodies k and K in n dimensions but they appear to be far from best possible.

REFERENCES

- Bambah, R. P. and Rogers, C. A. (1952). *Jour. London Math. Soc.*, **23**, 304-314.
 Dowker, C. H. (1944). *Bull. Amer. Math. Soc.*, **50**, 120-122.
 Mahler, K. (1948). *Proc. Kon. Ned. Akad. V Wet.*, Amsterdam, **51**, 482-485.

Issued February 20, 1954.

NOTE ON THE VIBRATION SPECTRUM OF A CRYSTAL

by R. E. PEIERLS, *Professor of Mathematical Physics, University of Birmingham.*

(Communicated by D. S. Kothari, F.N.I.)

(Received November 26 ; read December 4, 1953)

The purpose of this note is to present a simple proof of the rule usually given for obtaining the spectrum of normal frequencies of a crystal. The rule is that the distribution of frequencies is the same as those of a hypothetical crystal satisfying the 'cyclic boundary condition'. We shall in the following refer to the hypothetical case as the 'mathematical crystal'.

Arguments for this rule have been given in many contexts, the most complete proof being probably that given by Ledermann (1944) but, in view of the fact that there is still some controversy about it, it may be useful to give yet another proof, based on a more physical reasoning.

For our purpose 'spectrum' refers merely to the position of the characteristic frequencies. No statement is implied about their occurrence in the omission, absorption or scattering of light.

The rule must be understood with the following limitations: (a) it is not claimed that the normal *modes* of the mathematical crystal are identical with those of the real crystal. (b) It is not claimed that the exact values of the frequencies are the same in both cases, but merely that the distribution, i.e. the average number in a frequency interval $\Delta\omega$ large enough to contain many frequencies is the same in the two cases to the leading order in N , where N is the linear dimension of the crystal in terms of the lattice spacing. Our argument will be formulated to cover three dimensions and the presence of several atoms in the unit cell. This will make our notation somewhat cumbersome; to avoid adding to the formal complications we assume the lattice to be of cubic symmetry and take a unit cell of cubic shape. We also assume the crystal to be a cube with its edges along the crystal axes. The argument could easily be freed also from these restrictions, at the expense of some slight further complexity of notation.

The idea of the proof is to show a connection between the frequency distribution and the propagation of disturbances through the crystal. In particular, from the knowledge of the propagation of disturbances over times up to a certain time τ , we can uniquely determine the frequency distribution except for its fine structure which concerns frequency intervals less than $1/\tau$. Now for a disturbance starting from a point distant l from the nearest surface, the propagation will be the same as in an infinite crystal for a time less than l/c , where c is the maximum velocity of sound. Hence, for a crystal dimension of 1 cm., and with $c \sim 10^5$, l/c will be of the order of 10^{-5} sec., and larger than say, 10^{-10} sec., for practically all the crystal. It follows therefore that over such times the propagation of disturbances is the same in the mathematical and the real crystal, and hence that the frequency distribution for the two is the same except for oscillations in frequency intervals of the order of 10^{10} sec. $^{-1}$, (corresponding in spectroscopic terminology to about 0.05 cm. $^{-1}$).

A very similar reasoning was used in an earlier paper (Peierls, 1936) concerned with justifying the cyclic boundary condition in the derivation of the equation of state of a relativistic gas. There are, however, some minor differences between the two problems, the crystal problem being, on the whole, the simpler one, and it is

therefore easiest to explain the method anew, rather than to rely on the results of the earlier paper.

We assume our crystal to be a cube, each side containing N cells, so that each cell can be enumerated by three integers,

$$1 \leq n_1, n_2, n_3 \leq N \quad \dots \quad \dots \quad \dots \quad \dots \quad (1)$$

We label the position of an atom within the cell by s ,

$$1 \leq s \leq p \quad \dots \quad \dots \quad \dots \quad \dots \quad (2)$$

The three co-ordinates will be distinguished by a suffix ρ

$$\rho = x, y, z \quad \dots \quad \dots \quad \dots \quad \dots \quad (3)$$

Then, if the ρ -th co-ordinate of the s -th atom in cell \underline{n} at time t is denoted by $x_{\rho s}(\underline{n}, t)$, a normal vibration is given by

$$x_{\rho s}(\underline{n}, t) = a_{\rho s}^{\alpha}(\underline{n}) \cos(\omega_{\alpha} t - \gamma_{\alpha}) \quad \dots \quad \dots \quad \dots \quad (4)$$

Here α labels the normal modes

$$1 \leq \alpha \leq 3pN \quad \dots \quad \dots \quad \dots \quad \dots \quad (5)$$

ω_{α} is the corresponding (circular) frequency; γ_{α} is a phase. The coefficients and the frequencies are, in principle, to be found from the equations of motion and the boundary conditions.

It is known from general theory that the amplitudes a are orthogonal in the sense that

$$\sum_{\rho} \sum_s \sum_{\underline{n}} a_{\rho s}^{\alpha}(\underline{n}) a_{\rho s}^{\beta}(\underline{n}) m_s = 0, \quad \alpha \neq \beta$$

m_s being the mass of the s -th atom. They can be normalized so as to make the sum equal to unity when $\alpha = \beta$; with that convention we have

$$\sum_{\rho} \sum_s \sum_{\underline{n}} a_{\rho s}^{\alpha}(\underline{n}) a_{\rho s}^{\beta}(\underline{n}) m_s = \delta_{\alpha\beta} \quad \dots \quad \dots \quad \dots \quad (6)$$

$\delta_{\alpha\beta}$ being the Kronecker symbol, as usual.

Conversely it follows that

$$\sum_{\alpha} a_{\rho s}^{\alpha}(\underline{n}) a_{\rho' s'}^{\alpha}(\underline{n}') = \frac{1}{m_s} \delta_{\rho\rho'} \delta_{ss'} \delta_{\underline{n}\underline{n}'} \quad \dots \quad \dots \quad \dots \quad (7)$$

We now want to consider the distribution of frequencies ω_{α} . To find the number of frequencies within the interval $\omega + \frac{1}{2}\Delta$, $\omega - \frac{1}{2}\Delta$, we should obtain the quantity

$$F(\omega) = \sum_{\alpha} D(\omega_{\alpha} - \omega) \quad \dots \quad \dots \quad \dots \quad (8)$$

where

$$D(x) = \begin{cases} 1, & |x| < \frac{\Delta}{2} \\ 0, & |x| > \frac{\Delta}{2} \end{cases}$$

However, this definition is not convenient, because of the discontinuity, which means that whether a certain frequency is counted or not depends on its precise value. It is therefore more convenient to use a smooth weight function for D to which we give the following properties :

$$\int_{-\infty}^{\infty} D(x) dx = \Delta \quad \dots \quad \dots \quad \dots \quad (9)$$

$$D(x) \ll 1 \text{ if } x \gg \Delta \quad \dots \quad \dots \quad \dots \quad (10)$$

In addition, $D(x)$ is to be a smooth function so that its Fourier transform converges rapidly ; if

$$g(\tau) = \frac{1}{2\pi} \int_{-\infty}^{\infty} e^{-i\tau\omega} D(\omega) d\omega; \quad D(\omega) = \int_{-\infty}^{\infty} e^{+i\tau\omega} g(\tau) d\tau \dots \quad (11)$$

the condition

$$g(\tau) \ll \Delta \text{ if } \tau \gg \frac{1}{\Delta} \quad \dots \quad \dots \quad \dots \quad (12)$$

is compatible with (9) and (10). For instance, a possible choice of D is

$$D(x) = \frac{1}{\sqrt{2\pi}} e^{-x^2/2\Delta^2}; \quad g(\tau) = \frac{\Delta}{2\pi} e^{-\Delta^2\tau^2/2}$$

It is clear that, with this definition of D , the expression (8) represents the spectrum of vibrations except for the fine structure, provided Δ is small compared to the maximum frequency ω_{\max} .

It will be convenient in the following to replace $F(\omega)$ by

$$\begin{aligned} G(\omega) &= F(\omega) + F(-\omega) \\ &= \sum_{\alpha} \left[D(\omega_{\alpha} - \omega) + D(\omega_{\alpha} + \omega) \right] \quad \dots \quad \dots \quad \dots \quad (13) \end{aligned}$$

Because of (10) the extra term vanishes in fact, unless we are concerned with the very low-frequency end of the spectrum, where $\omega \sim \Delta$, otherwise, since the ω_{α} are positive, $\omega + \omega_{\alpha}$ will certainly appreciably exceed Δ .

Now insert the Fourier transform (11)

$$\begin{aligned} G(\omega) &= \sum_{\alpha} \int d\tau g(\tau) \left[e^{i\omega_{\alpha}\tau} e^{-i\omega\tau} + e^{i\omega_{\alpha}\tau} e^{+i\omega\tau} \right] \\ &= \int d\tau 2g(\tau) \cos \omega\tau \sum_{\alpha} e^{i\omega_{\alpha}\tau} \quad \dots \quad \dots \quad \dots \quad (14) \end{aligned}$$

If $D(x)$ is an even function, $g(\tau)$ will also be even, so that (14) can also be written as

$$G(\omega) = 4 \int_0^{\infty} d\tau g(\tau) \cos \omega\tau \sum_{\alpha} \cos \omega_{\alpha}\tau \quad \dots \quad \dots \quad \dots \quad (15)$$

However, because of (12) it is sufficient to include Fourier components belonging to values of τ not much greater than $1/\Delta$, say up to ϵ/Δ , where ϵ is a numerical constant. We write

$$G(\omega) = 4 \int_0^{\epsilon/\Delta} d\tau g(\tau) \cos \omega\tau \Phi(\tau) \quad \dots \quad \dots \quad \dots \quad (16)$$

where

$$\Phi(\tau) = \sum_{\alpha} \cos \omega_{\alpha}\tau, \quad \tau < \epsilon/\Delta \quad \dots \quad \dots \quad \dots \quad (17)$$

Now we show that $\Phi(\tau)$ has a simple physical significance. For this purpose use the identity (6) to write (17) as

$$\begin{aligned} \Phi(\tau) &= \sum_{\alpha} \sum_{\rho, s, \underline{n}} m_s a_{\rho s}^{\alpha}(\underline{n}) a_{\rho s}^{\alpha}(\underline{n}) \cos \omega_{\alpha}\tau \\ &= \sum_{\rho s \underline{n}} \phi_{\rho s \underline{n}}(\tau) \quad \dots \quad \dots \quad \dots \quad \dots \quad \dots \quad (18) \end{aligned}$$

with

$$\phi_{\rho s \underline{n}}(\tau) = \sum_{\alpha} m_s a_{\rho s}^{\alpha}(\underline{n}) a_{\rho s}^{\alpha}(\underline{n}) \cos \omega_{\alpha}\tau \quad \dots \quad \dots \quad \dots \quad (19)$$

This quantity has the following meaning: Let at $t=0$ all atoms be in their equilibrium positions except that the s -th atom in cell \underline{n} is displaced by an infinitesimal amount δ in the ρ direction, and is there released from rest. Then the value of the ρ -th co-ordinate of this atom at time τ is exactly $\delta \cdot \phi_{\rho s \underline{n}}(\tau)$.

To see this, remember that the general solution of the equation of the motion is given by

$$x_{\rho s}(\underline{n}, t) = \sum_{\alpha} c_{\alpha} a_{\rho s}^{\alpha}(\underline{n}) \cos (\omega_{\alpha}t - \gamma_{\alpha}) \quad \dots \quad \dots \quad \dots \quad (20)$$

the c_{α} and γ_{α} being arbitrary.

We require that solution for which all atoms are at rest at $t=0$, which requires that all $\gamma_{\alpha} = 0$.

Furthermore, to satisfy given initial values $x_{\rho s}(\underline{n}, 0)$

$$x_{\rho s}(\underline{n}, 0) = \sum_{\alpha} c_{\alpha} a_{\rho s}^{\alpha}(\underline{n}) \quad \dots \quad \dots \quad \dots \quad (21)$$

We can solve this for c_{α} in the usual way using the orthogonality relation (6). Multiply (21) by a particular $a_{\rho s}^{\alpha}(\underline{n})$ and by m_s and sum:

$$c_{\alpha} = \sum_{\rho, s, \underline{n}} m_s a_{\rho s}^{\alpha}(\underline{n}) x_{\rho s}(\underline{n}, 0) \quad \dots \quad \dots \quad \dots \quad (22)$$

Insert in (20)

$$x_{\rho s}(\underline{n}, t) = \sum_{\rho' s' \underline{n}'} x_{\rho' s'}(\underline{n}', 0) \sum_{\alpha} m_{s'} a_{\rho s}^{\alpha}(\underline{n}) a_{\rho' s'}^{\alpha}(\underline{n}') \cos \omega_{\alpha}t \quad \dots \quad (23)$$

(23) expresses generally the co-ordinates of any atom at time t in terms of those of all atoms at time 0. If at time 0 only one co-ordinate is disturbed, the sum on the right contains only one term, and the same co-ordinate at time t becomes then

$$x_{\rho s}(\underline{n}, t) = x_{\rho s}(\underline{n}, 0) \sum_{\alpha} m_s a_{\rho s}^{\alpha}(\underline{n}) a_{\rho s}^{\alpha}(\underline{n}) \cos \omega_{\alpha} t$$

which by comparison with (19) is

$$x_{\rho s}(\underline{n}, 0) \phi_{\rho s \underline{n}}(t)$$

This proves our statement about the $\phi_{\rho s \underline{n}}$.

Now it is known that a disturbance will propagate in the main with the group velocity, and that at time t a disturbance starting from cell \underline{n} will be negligible at all points in the lattice distant more than ct from \underline{n} , where c is the greatest value of the group velocity (for either the 'acoustic' or 'optical' branches). Its order of magnitude is the same as that of ordinary sound velocity.

To be precise one should remember that in a dispersive medium there exist 'precursor' signals preceding the main front, which advances with maximum group velocity. However, their amplitude diminishes exponentially with the distance from the front.

Now compare the value of $\phi_{\rho s \underline{n}}(t)$ with the same quantity for an infinite crystal. Let the distance of cell from the boundary of the actual crystal be l_n . Then the solution of the time-dependent equations for the infinite crystal will *almost* satisfy the boundary conditions if $l_n > ct$. The amplitude at the boundary will depend exponentially on l_n . To satisfy the boundary conditions exactly we must add a reflected wave of similar amplitude, and its amplitude at cell \underline{n} will, in fact, vary exponentially with $2l_n - ct$. Hence the difference between ϕ and ϕ^{∞} decreases exponentially with $2l_n - ct$.

Now divide the crystal into an interior and a surface part, the 'surface' part extending to a depth βN , where β is a suitable small number. The total contribution from the 'surface' terms to the sum (18) is then of the order of $6\beta N^3$ compared to a total of N^3 and their omission represents a relative error of the order 6β . On the other hand, the remaining 'internal' terms belong to points distant from the surface by more than βN atoms and their contribution is therefore equal to those of an infinite crystal except for corrections decreasing exponentially with

$$2\beta Na - ct \quad \dots \quad \dots \quad \dots \quad \dots \quad (24)$$

Except for these errors, the ϕ functions are the same as for an infinite crystal and also the same as for the 'mathematical' crystal with the cyclic boundary condition for which it is easy to write down the spectrum explicitly.

(It is equally easy to write down expressions for the $\phi_{\rho s}^{\infty}(\underline{n})$ for the infinite crystal directly and thus evaluate the spectrum of a finite crystal without using the cyclic boundary condition at all; the answer is, of course, just the same.)

To illustrate the quantitative side, assume a crystal of 1 cm. thickness ($N \sim 10^8$). Choose $\beta = 10^{-4}$ and $\tau = 10^{-10}$ sec. assuming c to be about 10^6 cm./sec.

Then the omission of surface atoms in the sum (18) causes a relative error of $6\beta \sim 0.6\%$. The boundary correction for the ϕ for an internal point is an exponential function of (24) in which the positive term is at least 10^{-4} and the negative at most 10^{-5} . Hence we get an exponential function of an argument 10^{-4} cm. or 10^4 lattice constants. Both these errors are therefore negligible for practical purposes.

On the other hand, our choice of τ means that in the Fourier integral (16) we lose components with $\tau > 10^{-10}$ sec. and therefore the fine structure of the spectrum $G(\omega)$ over frequency ranges less than $\Delta \sim \frac{1}{\tau} \sim 10^{10} \text{ sec.}^{-1}$. In spectroscopic language this corresponds to about $10^{10}/2\pi c_L \sim 0.5 \text{ cm.}^{-1}$, (c_L being the light velocity) a fine structure which would not normally be resolved if it existed. Clearly these numbers represent generous limits and much closer estimates could be obtained.

REFERENCES

- Lodermann, W. (1944). Asymptotic formulae relating to the physical theory of Crystals. *Proc. Roy. Soc., A* **182**, 362.
 Peierls, R. E. (1936). Note on the derivation of the equation of state for a degenerate relativistic gas. *Monthly Notices, R.A.S.*, **96**, 780.

Issued February 22, 1954.

EMBRYOLOGICAL STUDIES IN MALVACEAE.

I. DEVELOPMENT OF GAMETOPHYTES

by C. VENKATA RAO, *Department of Botany, Andhra University, Waltair*

(Communicated by A. C. Joshi, F.N.I.)

(Received November 11, 1952 ; after revision August 12 ; read October 9, 1953)

INTRODUCTION

The family Malvaceae comprising 50 genera and about 1,000 species (Rendle, 1938), is better known embryologically than the remaining families of Malvales or Columniferae. The observations of the previous investigators like Warming (1873), Jonsson (1879), Strasburger (1884), Hegelmaier (1885), Hofmeister (1849), Guignard (1893, 1900, 1904), Byxbee (1900), Lantis (1912), Woyciecki (1911, etc.), Yamaha (1926), Youngman (1927) and others, have been summarized by Schnarf (1931). Stenar's (1925) work is the most extensive and covers about 25 species distributed over a dozen genera. On account of its economic importance, the genus *Gossypium* has received the special attention of morphologists, cytologists as well as embryologists like Cannon (1903), Balls (1906), Denham (1924a, 1924b), Kearney and Harrison (1924), Beal (1928), Banerji (1929), Singh (1931), Baritt (1932), Gore (1932), Harland (1932), Ayyar and Ayyangar (1933), Longley (1933), Skovsted (1933), Gulati (1934), Jacob (1942), etc. The cytology of several other members of the family was studied by Youngman (1931), Burkett (1932), Kessler (1932), Latter (1932), Davie (1933) and L. N. Rao (1941). The pollen grains are especially large and suitable for intensive study; Lang (1937) investigated their morphology and cell inclusions and Iyengar (1938) studied the pollen tubes of *Gossypium*. Reeves (1936) made a special study of the seed anatomy of several members of the family.

In all species investigated, the cells of the anther tapetum which are sometimes multinucleate, form a periplasmodium. In some members like *Malva* species, *Lavatera trimestris*, *Anoda cristata*, *Sidalcea candida* and *Gossypium herbaceum*, the pollen mother cells stand in a uniseriate manner in the anther loculus while in others like *Malvastrum capense*, *Sida napacea*, *Abutilon Theophrasti*, they undergo a secondary increase and stand in a multiseriate manner. In the last named species, Lantis (1912) described that every primary sporogenous cell gives rise to four microsporogenous cells. Cytokinesis takes place by furrowing. Though usually the pollen grains are shed at the 2-nucleate stage, Woyciecki (1911) found that in *Malva silvestris*, *M. rotundifolia* and *Althaea officinalis* 10–20% of the grains become 3-nucleate. Guignard (1904) noticed the division of generative nucleus in the pollen tube in *Althaea*, *Hibiscus* and *Lavatera*.

The ovules are bitegmic, crassinucellate and slightly or markedly campylo-tropous. In *Gossypium* species (*G. peruvianum*, *G. barbadense* and *G. hirsutum*, Gore, 1932), and *Thespesia* (Reeves, 1936), the ovules are anatropous. Stenar (1925) as well as the previous investigators reported that the archesporium of the ovule consists of a single sub-epidermal cell. The primary parietal cell cut off to the outside gives rise to several layers of parietal cells, while the epidermis itself forms a massive nucellar cap. Stenar (1925) drew attention to one interesting feature which occurs in several Malvaceae namely one or more parietal cells

secondarily assume the characters of sporogenous cells. These are distinguished as 'accessory sporogenous cells' from those which function from the beginning which are termed 'definitive cells'. These cells function till the tetrad stage or early embryo sacs. The occurrence of these cells, however, is variable even within a genus like *Malva*. Both linear and T-shaped tetrads occur and the chalazal megaspore develops into the embryo sac according to the *Normal*-type. The report of Balls (1906) that in cotton the micropylar megaspore functions, was contradicted by Gore (1932) who found that in all the three species of *Gossypium* investigated by him only the chalazal megaspore functioned. Since there was only one megaspore mother cell to start with, Gore (1932) attributed the occasional occurrence of two embryo sacs in one ovule of cotton, to the functioning of two megaspores of the same tetrad. The synergids are reported to show a filiform apparatus only in cotton (Gore, 1932). Usually the polar nuclei fuse only at the time of fertilization, though in *Lavatera thuringiaca* (Stenar, 1925), they were found to fuse earlier. Super-numerary and binucleate antipodals were recorded in *Lavatera thuringiaca*, *Anoda hastata* and *A. crispa*. Starch grains are absent from the embryo sac (Stenar, 1925) but present in the cells of placenta, chalaza and integument of cotton (Gore, 1932).

The emergence of pollen tubes is polysiphonous. Stenar (1925) counted up to 14 pollen tubes in pollen grains of *Malva neglecta* germinating on the stigma, while Lang (1937) counted 20-30 tubes from a single grain of *Anoda hastata* and *Lavatera* species germinating in artificial medium. The tubes traverse endotropically through the transmitting tissue of the style which is richly supplied with starch grains. The distal part of the tube is closed off with callose plugs and usually the vegetative nucleus disintegrates *in situ* (Iyengar, 1938). More than one pollen tube was seen to enter an ovule, though polyspermy was not noticed. Guignard (1904) as well as Stenar (1925) observed that the pollen tube branches in the region of the nucellus.

Endosperm is nuclear and cell wall formation commences after a large number of nuclei are formed.

A perusal of the previous literature shows that while the development of the gametophytes and fertilization were studied in some detail, comparatively little attention was paid to the study of the embryogeny. The only complete account of this phase is that of Souèges (1922) in *Malva rotundifolia*. The embryo in this species develops according to the *Asterad* Type and resembles closely that in *Urtica pilulifera* (Souèges, 1921); Johansen (1950) classed it in the *Urtica* variation of the *Asterad* Type.

This paper deals with the development and structure of the anther, pollen, ovule and embryo sac in the following 15 species of Malvaceae distributed in 11 genera.

MALVEAE: *Sida cordifolia* L., *S. carpinifolia* L., *S. veronicaefolia* L. (= *S. humilis* Willd.), *Abutilon indicum* G. Don., *Althaea rosea* Cav., and *Kydia calycina* Roxb.

URENEAE: *Urena lobata* L., *Malvaviscus arboreus* Cav., *Pavonia zeylanica* L., *Malachra capitata* L.

HIBISCEAE: *Hibiscus solandra* L. Herit., *H. micranthus* L., *H. hirtus* L., *Ablemoschus esculentus* (L.) Moench. (= *Hibiscus esculentus* in older system of nomenclature cf. Pal, Singh and Vishnu Swarup, 1952) and *Thespesia populnea* Corr.

MATERIALS AND METHODS

Malvaviscus arboreus and *Hibiscus hirtus* are grown commonly as garden plants in S. India and *Thespesia populnea* as an avenue tree. The material of *Kydia*

calycina was collected from Anantagiri hills, Visakhapatnam district, where the plants grow wild. The materials of *Urena lobata* and *Malachra capitata* were collected from Kakinada and the rest locally. Formalin-acetic-alcohol was used as the fixative. After following the customary methods of dehydration and infiltration, the material was embedded in paraffin wax. Delafield's and Heidenhain's haematoxylin were used as stains, of which the former gave more satisfactory results. Addition of a pinch of safranin powder to material in 1 : 1 alcohol xylol mixture proved useful in locating the tannin bearing and starch containing cells and also in bringing out more prominently the pollen tubes.

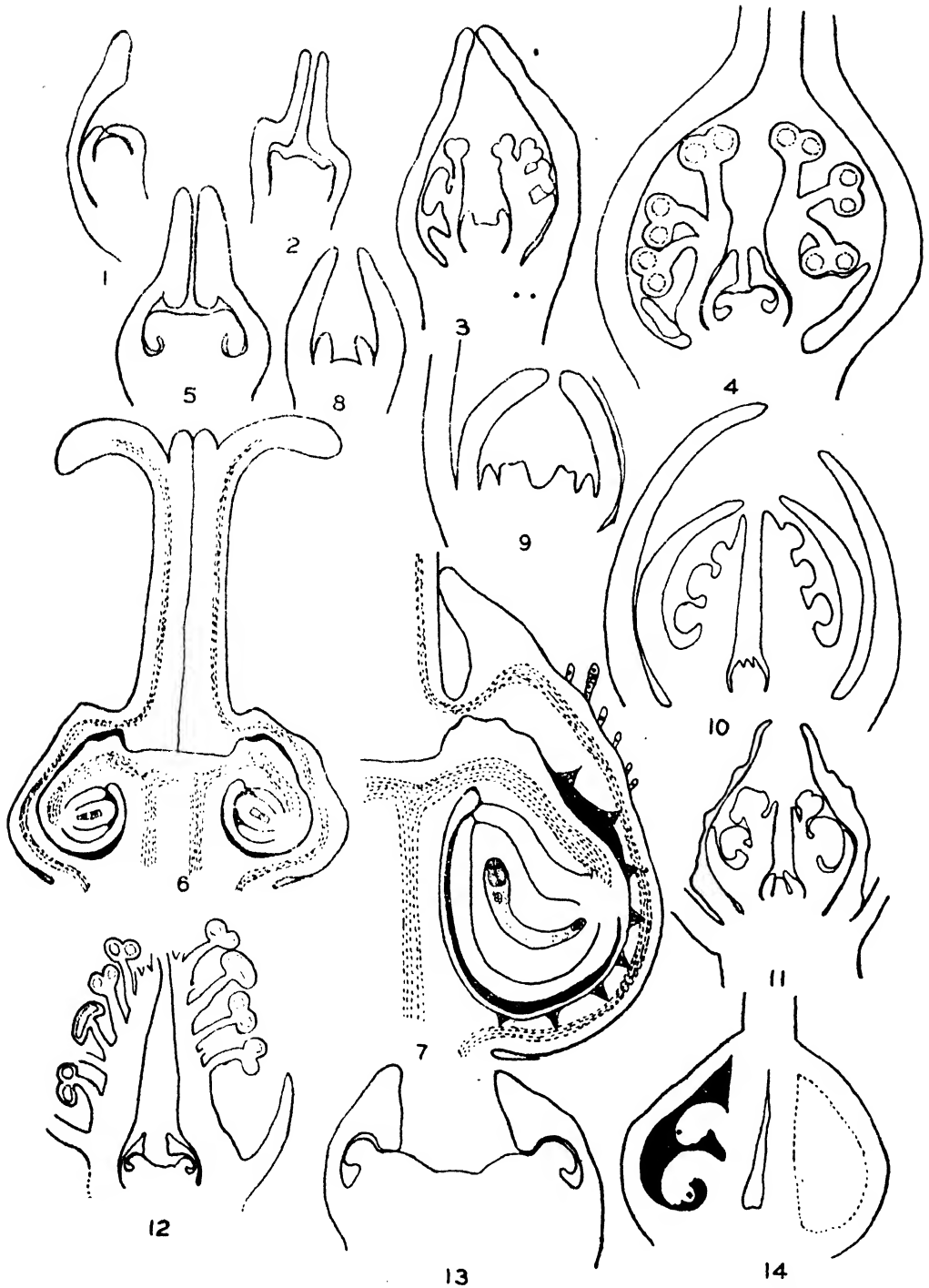
. FLOWERS

The flowers present typical malvaceous features. The flowers of *Kydia calycina* are polygamous. The staminodes of the female flowers show abortive pollen grains. The ovules of pistillode degenerate after the embryo sac is fully formed. Unlike in the bisexual and female flowers, the style in the male flowers remains included in the staminal tube (Figs. 65, 66). In *Kydia*, there are 3 carpels; in the different species of *Sida* studied they range from 5-10; in *Abutilon* and *Althaea* they are numerous and in the rest five. Multicellular hairs are present on sepals, bases of petals, staminal tube and ovary wall.

ORGANOGENY

The sequence in the development of floral organs is: epicalyx (where present), calyx, corolla plus androecium and lastly gynoecium. In *Malvaviscus arboreus* (Figs. 8-10) which has epicalyx, the bracteoles arise on the convex floral primordium and reach a considerable size before the appearance of the sepals. To the inside of the latter arises an annular zone which represents the common primordium of the corolla and androecium. In *Sida cordifolia* (Figs. 1-7) which has no epicalyx, the sepals attain a considerable size before the primordia of petals and stamens arise. In *Malvaviscus arboreus* when the common corolla androecium primordium has attained the height of sepals, the primordia of the five petals appear on its outer surface (Fig. 9), while the inner zone continues to grow up and gives rise to the stamen primordia later (Fig. 10). As in Sterculiaceae, the petals grow in a tardy manner initially; they do not cover up the essential organs, protection being given by calyx and epicalyx (Figs. 4, 11, 12). After the sporogenous cells are organised in the anthers, the apex of the floral axis which is still convex, becomes cup-shaped and develops into the ovary. It becomes lobed and the infolded carpellary margins later develop into septa, while the rim of the cup closes and grows up to form the style. The style is hollow to start with in all species; in *Abutilon* and *Althaea*, it remains hollow even in the open flower while in others it becomes solid.

There are two kinds of styles in Malvaceae which show interesting features of development; terminal as in *Hibiscus* and gynobasic as in *Sida*, *Althaea* and *Abutilon*. In *Hibiscus*, the rim of the cup-shaped ovary primordium grows upwards without bending and cleaves at the top into the stigmatic branches. The ovules arise on the inner margins of carpellary wall (Fig. 14). In *Sida cordifolia* (Figs. 5-7) and *Althaea rosea* (Fig. 13), the central part of the ovarian cup grows to form a lobed column simultaneously as the rim of the cup grows to form the style. From the apex of the central column the ovule primordia arise and bend into the loculus so that the ovules are pendulous. The basal part of the styler region bends inwards so as to touch the placental column (Figs. 5, 13). The line of contact between the two can be clearly seen even in the mature ovary of *Sida* (Fig. 7). In this genus, the top of each carpel grows to form two spinescent processes making the style in the open flowers relatively more deep seated. So the gynobasic style is also terminal in origin but establishes contact with the base of the ovary by bending inwards at



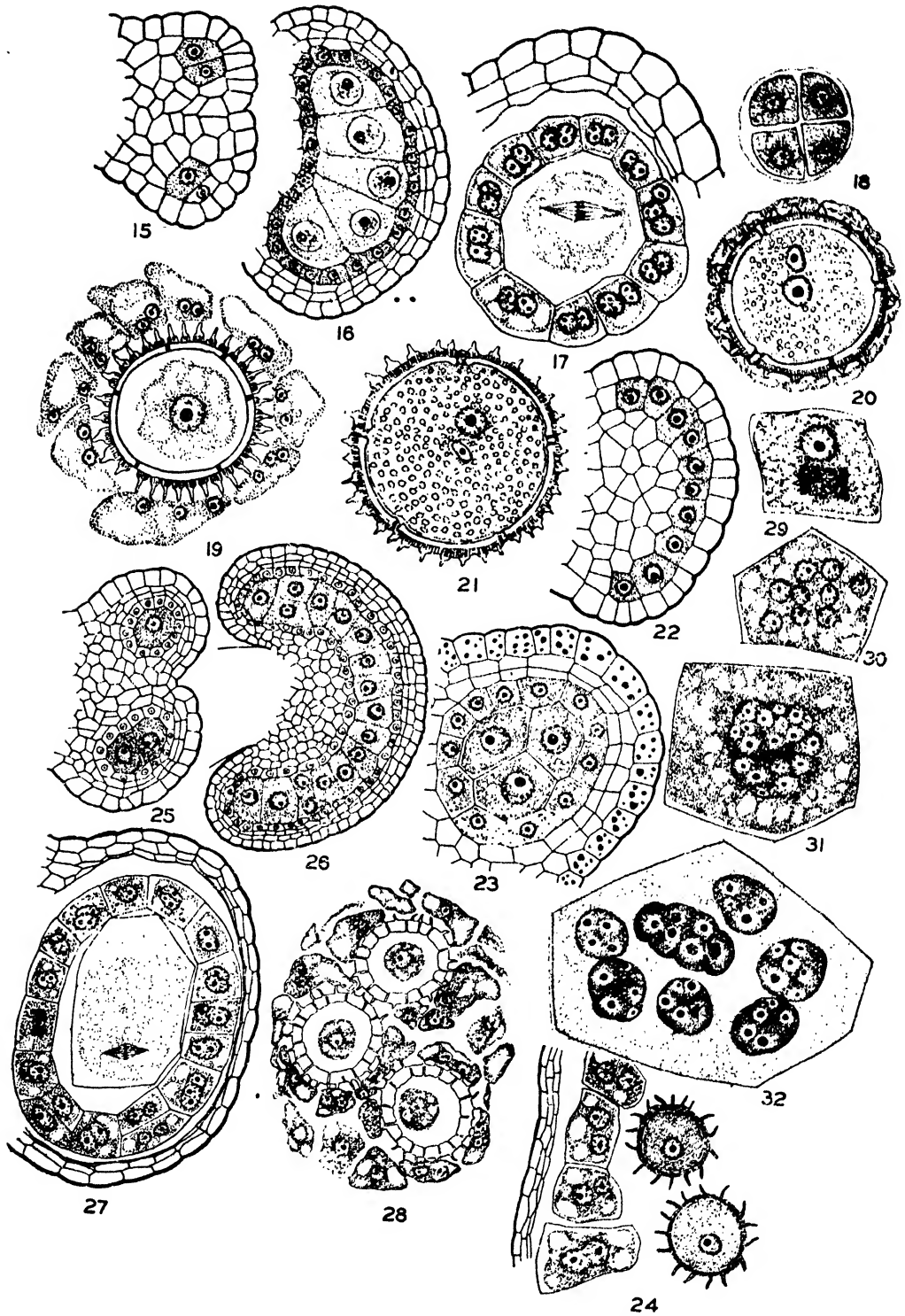
FIGS. 1-7. Organogeny of flower and development of ovary and ovule of *Sidu cordifolia*.
Figs. 1-3, $\times 45$; Figs. 4-7, $\times 30$.

FIGS. 8-10. Organogeny of flower of *Malvaviscus arboreus*. $\times 30$.

FIG. 11. L.s. of flower of *Paronia zeylanica*. $\times 30$.

FIGS. 12 and 13. L.s. of flower and ovary of *Althaea rosea*. $\times 10$ and $\times 45$ respectively.

FIG. 14. L.s. of ovary of *Hibiscus hirtus*. $\times 35$.



FIGS. 15-32. Microsporogenesis and male gametophyte in Malvaceae. Fig. 15. T.s. of young anther of *Sida cordifolia*. $\times 400$. Fig. 16. L.s. of anther of *Sida carpinifolia*. $\times 400$. Fig. 17. T.s. of older anther lobe of *S. cordifolia*. $\times 400$. Fig. 18. A bilateral tetrad of
(Continued at foot of next page.)

base. In *Malachra capitata*, the style is terminal as in *Hibiscus* to start with, but becomes slightly gynobasic in the open flower not by bending of the base of style but due to the growth of the apex of each carpel (Figs. 109, 110). The gynoecium in *Abutilon indicum* is interesting since in each loculus occur ovules which are pendulous (as in *Sida* and *Althaea*) as well as horizontal and descending (as in *Hibiscus*). The reason for this becomes evident by a study of the development of the ovary. As in *Sida* and *Althaea* the style is gynobasic. The axial part of the ovary grows slightly not in the form of a solid column as in the above genera but as a cup, and bears one tier of ovules which are pendulous. In addition to these, the margins of each carpel bear two ovules which are variously inclined. The rim of the ovarian primordium bends inwards and again grows up to form the open style. In the early stages, there is a large space between the placental column and base of the style, which becomes smaller in the open flower. Several multicellular hairs arise from the base of the style and project into this cavity and function as obturator (Figs. 88, 89).

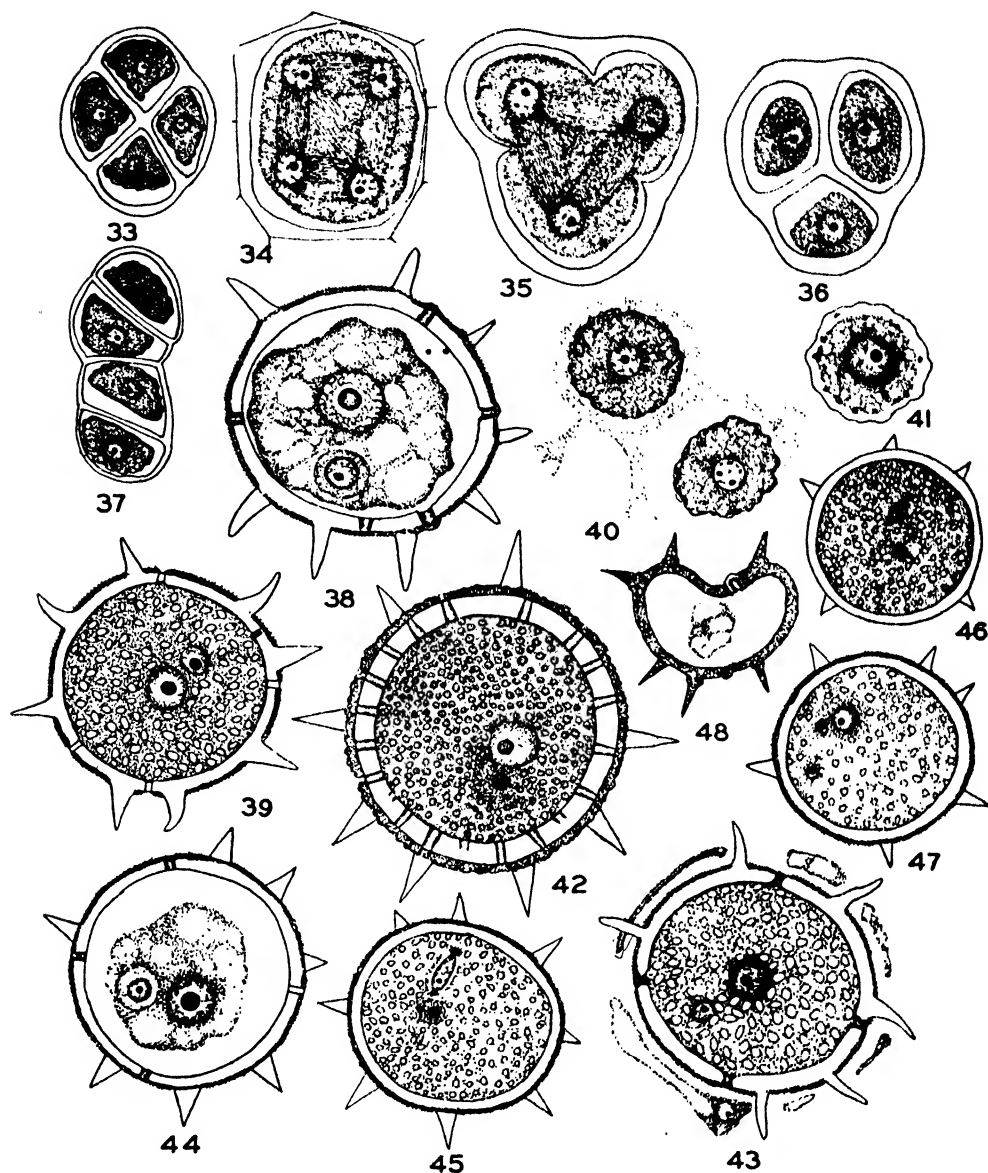
MICROSPOROGENESIS AND MALE GAMETOPHYTE

As the anthers are monotheous, the archesporium differentiates only at two places in the anther primordium. At each place there are one or two rows of cells (Figs. 15, 25). The number of cells in a row varies with the size of the anther; in *Sida cordifolia* (Fig. 16) there are about five cells; in *Abutilon indicum* (Fig. 22) about 10 cells and in *Pavonia zeylanica* (Fig. 26), about 15 cells in a row. The cells divide periclinally and give rise to the primary parietal cells to the outside and the primary sporogenous cells to the inside (Fig. 15). Divisions in the primary parietal cells and their derivatives result usually in the formation of three layers of wall cells below the epidermis (Figs. 16, 17, 24-27). The epidermal cells become tangentially stretched and accumulate some deep-staining contents probably tannin (Fig. 23). The hypodermal layer develops into the fibrous endothecium and the innermost wall layer forms the tapetum while the middle layers ultimately get crushed. Some of the cells of the tapetum divide periclinally and make it two-layered at places (Fig. 27).

In all species investigated, the tapetum is of the plasmodial type, a feature reported in all the previously investigated members (Schnarf, 1931). The tapetal cells enlarge considerably and take deeper stain at all stages of development, than the sporocytes. Their nuclei undergo the first mitotic division when the microsporocytes are in prophase I and most of the cells remain binucleate. In a few cells, however, mitotic divisions continue (Fig. 29), as a result of which they become 3-20 nucleate. Such cells are more frequently met with in *Hibiscus solandra* (Fig. 30) and *Malvaniscus arboreus* (Fig. 32). In some cells, the nuclei again fuse to form large multinucleolate polyploid nuclei (Fig. 31). As the meiotic divisions proceed in the sporocytes, the tapetal cells separate out as a layer from the wall cells (Figs. 17, 27). After the pollen grains grow to some extent and produce the exine with its spinescent outgrowths, the walls of the tapetal cells break down and the protoplasts which remain intact, wander into the loculus and closely surround the pollen grains

(Continued from foot of previous page.)

S. cordifolia. ×400. Fig. 19. One nucleate pollen grain of *S. cordifolia* surrounded by periplasmodium. ×335. Fig. 20. Two-nucleate pollen grain of *S. carpinifolia* with remnants of periplasmodium. ×220. Fig. 21. Mature pollen grain of *S. veronicaefolia*. ×220. Figs. 22 and 23. L.s. and t.s. of anther lobe of *Abutilon indicum*. Fig. 22, ×400; Fig. 23, ×335. Fig. 24. Older anther of *Abutilon indicum* showing 1-nucleate pollen grains and periplasmodium. ×220. Figs. 25 and 26. T.s. and l.s. of anther lobe of *Pavonia zeylanica*. Fig. 25, ×335; Fig. 26, ×195. Fig. 27. T.s. of young anther of *Althaea rosea*. ×335. Fig. 28. Pollen grains of *Althaea rosea* surrounded by periplasmodium. ×335. Figs. 29 and 30. Tapetal cells of *Hibiscus hirtus*. ×400. Figs. 31 and 32. Tapetal cells of *Malvaniscus arboreus*. ×400.



Figs. 33-48. Microsporogenesis and male gametophyte in Malvaceae. Figs. 33-36. Bilateral and tetrahedral tetrads in *Hibiscus hirtus*. $\times 425$. Fig. 37. A linear tetrad of *Hibiscus hirtus*. $\times 355$. Fig. 38. Two nucleate pollen grain of *Hibiscus micranthus*, note generative cytoplasm. $\times 425$. Fig. 39. Two nucleate pollen grain of *H. hirtus*. $\times 285$. Fig. 40. Microspores of *Urena lobata* being liberated from special wall. $\times 425$. Figs. 41 and 42. Young and mature pollen grains of *Malachra capitata*. $\times 285$. Fig. 43. Two nucleate pollen grain of *Pavonia zeylanica*. $\times 285$. Figs. 44-47. Pollen grains of *Kydia calycina*. $\times 285$. Fig. 48. Abortive pollen grain of *Hibiscus solandra*. $\times 285$.

(Figs. 24, 28). It is evident from this that the tapetum does not initiate the sculpturing of the exine. The exine and the rudiments of the spines and pores are already apparent on the microspores even before the latter are liberated from the special wall (Figs. 40, 41). It is possible, however, that the periplasmodium may hasten the further growth of the exine because both the exine and pollen grains are seen to show sudden and considerable growth after this stage (Figs. 19, 28). This

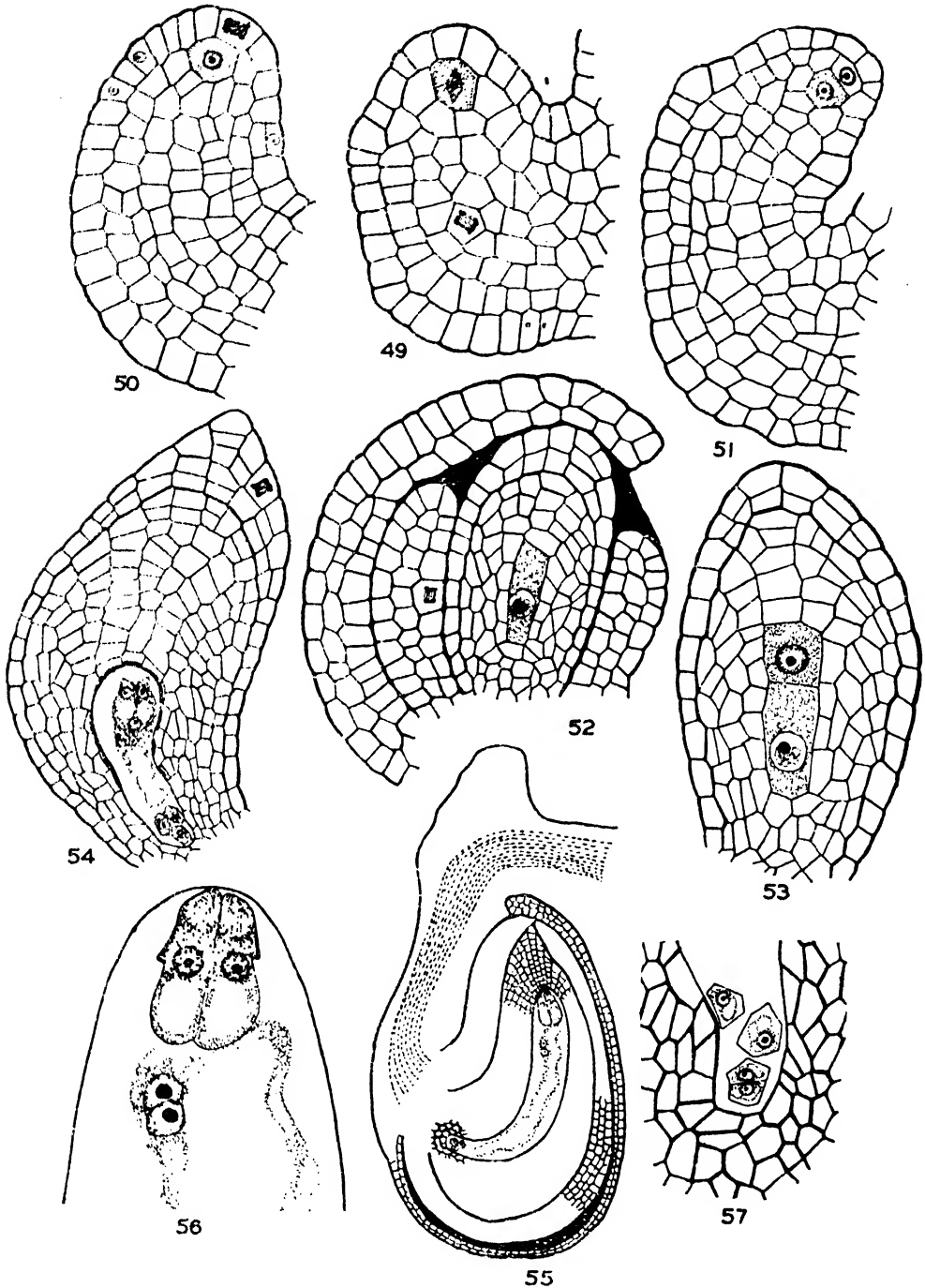


FIG. 49. Ovule primordium of *Sida carpinifolia*. $\times 390$.

FIGS. 50-52. Various stages in the development of megaspore mother cell and parietal tissue in the ovule of *S. cordifolia*. Figs. 50 and 51, $\times 390$; Fig. 52, $\times 260$.

FIG. 53. Nucellus of *S. cordifolia* showing megaspore mother cell and accessory sporogenous cell. $\times 390$.

FIG. 54. Nucellus with young embryo sac of *S. cordifolia*. $\times 125$.

FIG. 55. Mature ovule of *S. carpinifolia*. $\times 70$.

FIGS. 56 and 57. Micropylar and antipodal parts of embryo sac of *S. cordifolia*; note filiform apparatus in fig. 56; one antipodal cell has divided in fig. 57. $\times 390$.

becomes clear on comparing the pollen grains of the two loculi of the same anther. As the microspores enlarge, the protoplasts of the tapetal cells which still retain their individuality, become smaller and smaller and ultimately they get absorbed (Figs. 19–21). They may disappear even before the microspore nucleus has divided as in *Urena lobata*, or their remnants may persist till the pollen grains have become 2-nucleate and nearly mature as in *Sida carpinifolia* (Fig. 20) and *Pavonia zeylanica* (Fig. 43).

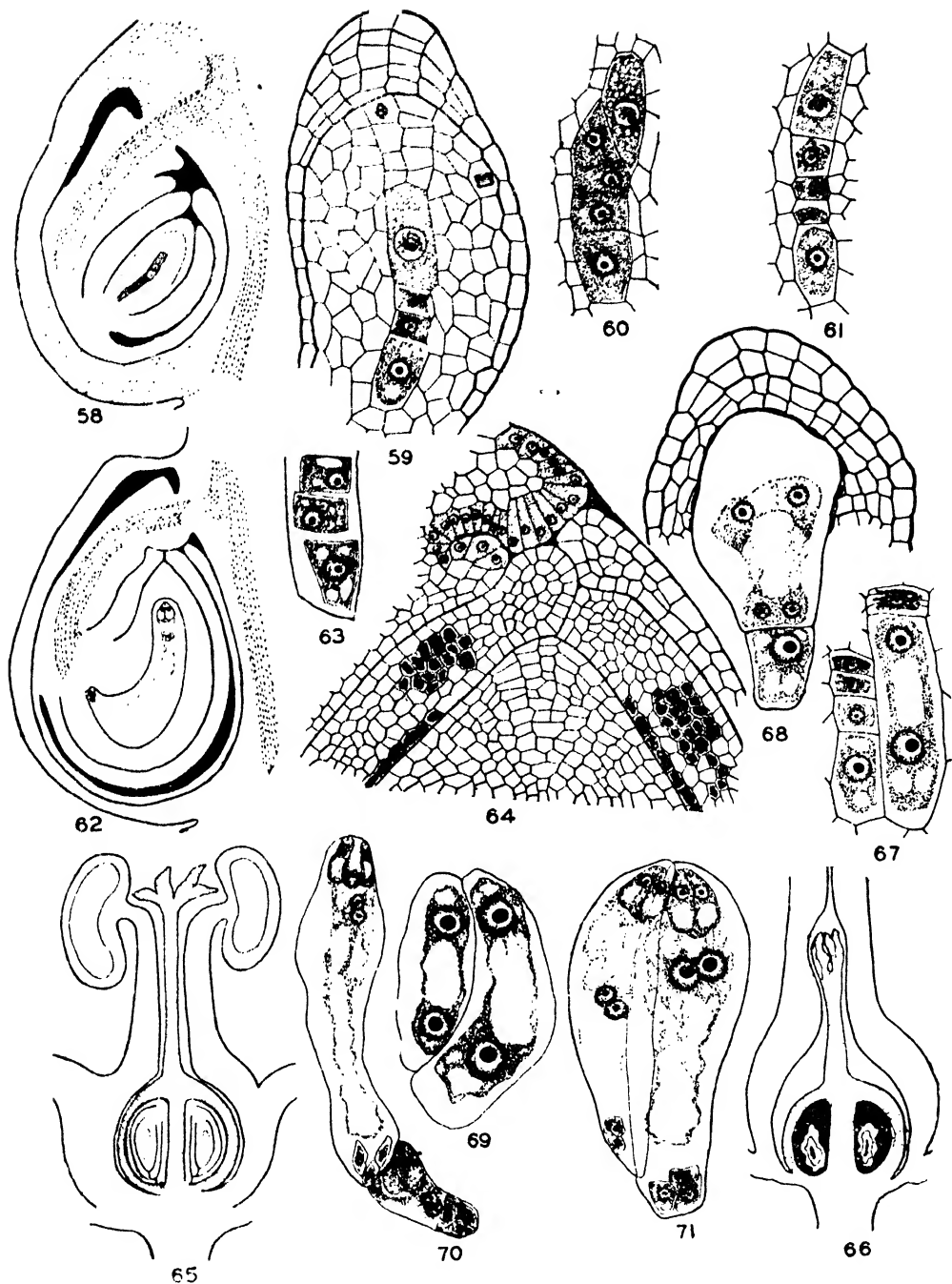
In some species like *Althaea rosea*, *Pavonia zeylanica* and *Sida cordifolia*, the primary sporogenous cells function directly as microspore mother cells, while in others like *Abutilon indicum* they undergo a few mitotic divisions to increase the number of sporogenous cells. In the latter case, the sporogenous cells are arranged in several rows (Fig. 23). In any case, the number of sporogenous cells per loculus is much smaller than in other families of the order and their size larger. Their nucleoli show densely chromatic peripheral and a vacuole like central region inside which there may be a crystalline body as also reported by L. N. Rao (1941) in *Hibiscus trionum*. Usually the microspores are arranged in a tetrahedral manner (Figs. 35, 36), bilateral tetrads being noticed occasionally (Figs. 18, 33, 34). One case of linear tetrad was found in *Hibiscus solandra* (Fig. 37). The wall of the microsporocyte lasts till telophase II and before this has broken down, the protoplast gets invested by a special wall of callose (Fig. 33). The secondary spindle fibres which connect the tetrad of nuclei play no part in cytokinesis; even before they disappear, furrows develop in the periphery of the cytoplasm and wedges of special wall follow them till they meet at the centre and encircle the microspores completely (Figs. 35, 36). L. N. Rao (1941) believes that the special wall plays some part in the formation of the spore coat since its transparency increases as the exine and the sculpturing become more and more prominent.

The nucleus of the microspore undergoes division while the cytoplasm is still vacuolated. Within a short time of its formation, the partition between the two cells gives way and the generative cell migrates into the vegetative cytoplasm. In the early stages, the generative cytoplasm can be seen as a relatively hyaline sheath around the nucleus (Figs. 38, 44), which is brought out more clearly in preparations stained in Delafield's haematoxylin. In course of time, it becomes obscure due to the accumulation of numerous starch grains and protein granules in the vegetative cytoplasm.

Various kinds of cell inclusions are noticed in the cytoplasm of the pollen grain, namely fat, proteins and starch grains of which the last are most abundant. They vary in their size and shape, being irregular, dumb-bell shaped, circular and lenticular. Sometimes an oily matter is secreted by the protoplast which accumulates on the exine in the shape of droplets and makes the pollen grains stick together.

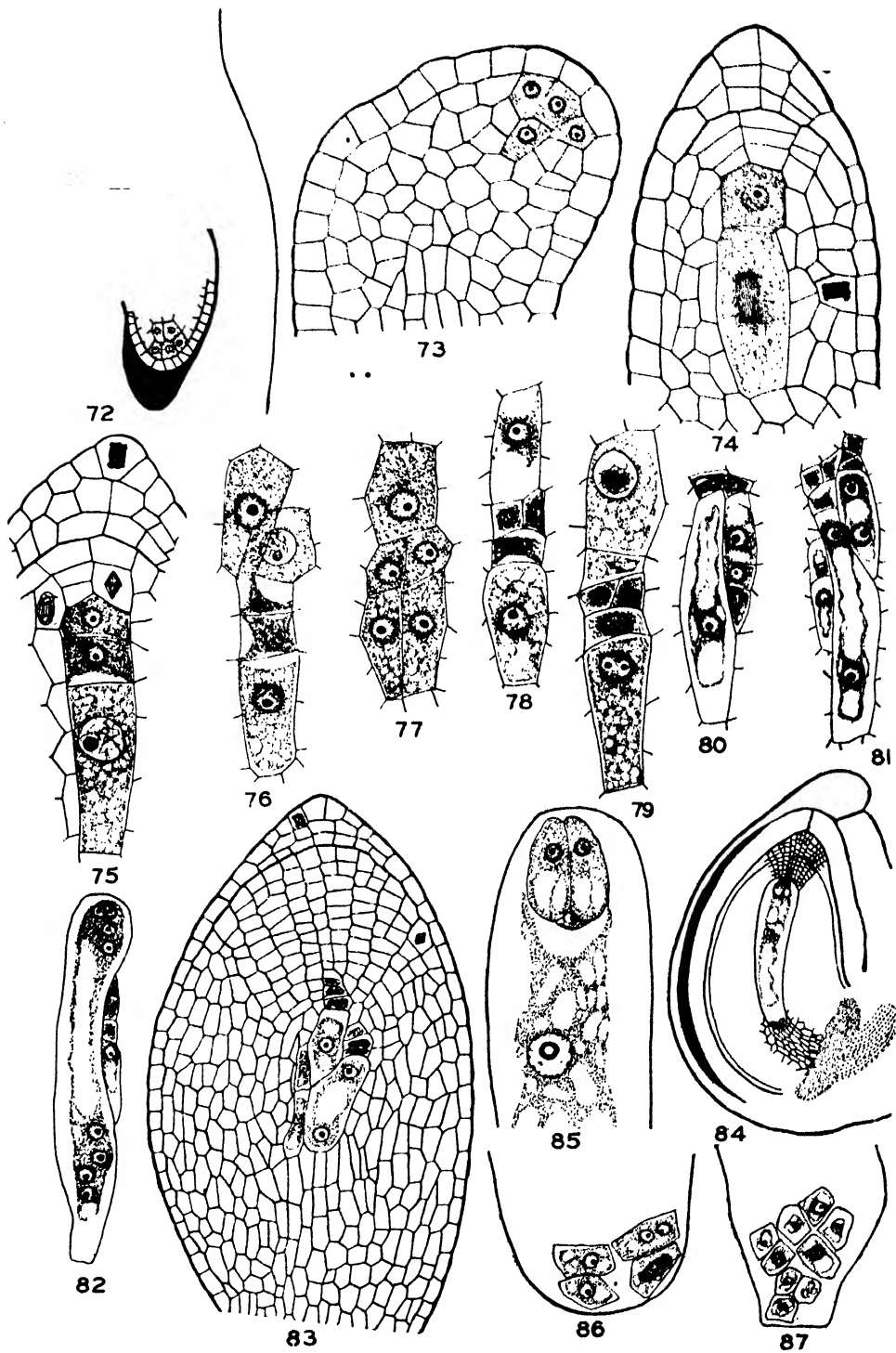
Usually the pollen grains are shed at the 2-nucleate stage (Figs. 39, 42). In the mature pollen grains of *Sida veronicaefolia* (Fig. 21) and *Kydia calycina* (Fig. 45), the generative nucleus becomes ellipsoidal and attains the prometaphase stage. It is surrounded at the sides by the hyaline generative cytoplasm; at the two ends are seen conical caps of relatively deep staining cytoplasm (Fig. 45), thus presenting a structure closely similar to what was observed in *Triumfetta rhomboidea* (C. V. Rao and K. V. S. Rao, 1952). In a few pollen grains of *Kydia calycina*, the generative nucleus divided and formed 2 spherical male nuclei (Figs. 46, 47). The pollen grains are relatively large and range from 60 μ as in *Abutilon indicum* to 120 μ as in *Hibiscus solandra*. In several species, some degenerating pollen grains which are probably formed as a result of irregular meiotic divisions, are found associated with normal ones (Fig. 48).

The pollen grains are spinescent and multiporate. The spines may be long, tapering and sparse as in *Hibiscus*, or short, somewhat blunt, broad based and closely set as in *Sida*. The exine is thick, ranging from 5 μ as in *Sida* to 10–12 μ as in *Malachra capitata*. In general, it shows two layers: an inner thicker, homogeneous,



FIGS. 58-64. *Sula veronicaefolia*. Fig. 58. Young ovule with definitive and accessory megaspore mother cells; note development of obturator. $\times 105$. Fig. 59. Nucellus showing T-shaped tetrad (of which one megaspore is out of focus) and an accessory sporogenous cell. $\times 400$. Figs. 60 and 61. Linear tetrads and accessory sporogenous cells. $\times 400$. Fig. 62. Mature ovule with obturator. $\times 55$. Fig. 63. Antipodals. $\times 665$. Fig. 64. Micropylar part of the ovule magnified to show the obturator and micropyle. $\times 265$.

FIGS. 65-71. *Kydia calycina*. Figs. 65 and 66. L.s. of bisexual and male flowers. $\times 10$. Fig. 67. Two collaterally placed tetrads from one ovule, of which the lowest megaspores have formed 1- and 2-nucleate embryo sacs. $\times 400$. Fig. 68. Nucellus with 2 embryo sacs. $\times 265$. Fig. 69. Two 2-nucleate embryo sacs from one ovule. $\times 400$. Fig. 70. Two superposed 8-nucleate embryo sacs from one ovule. $\times 265$. Fig. 71. Two collaterally placed mature embryo sacs from one ovule. $\times 400$.

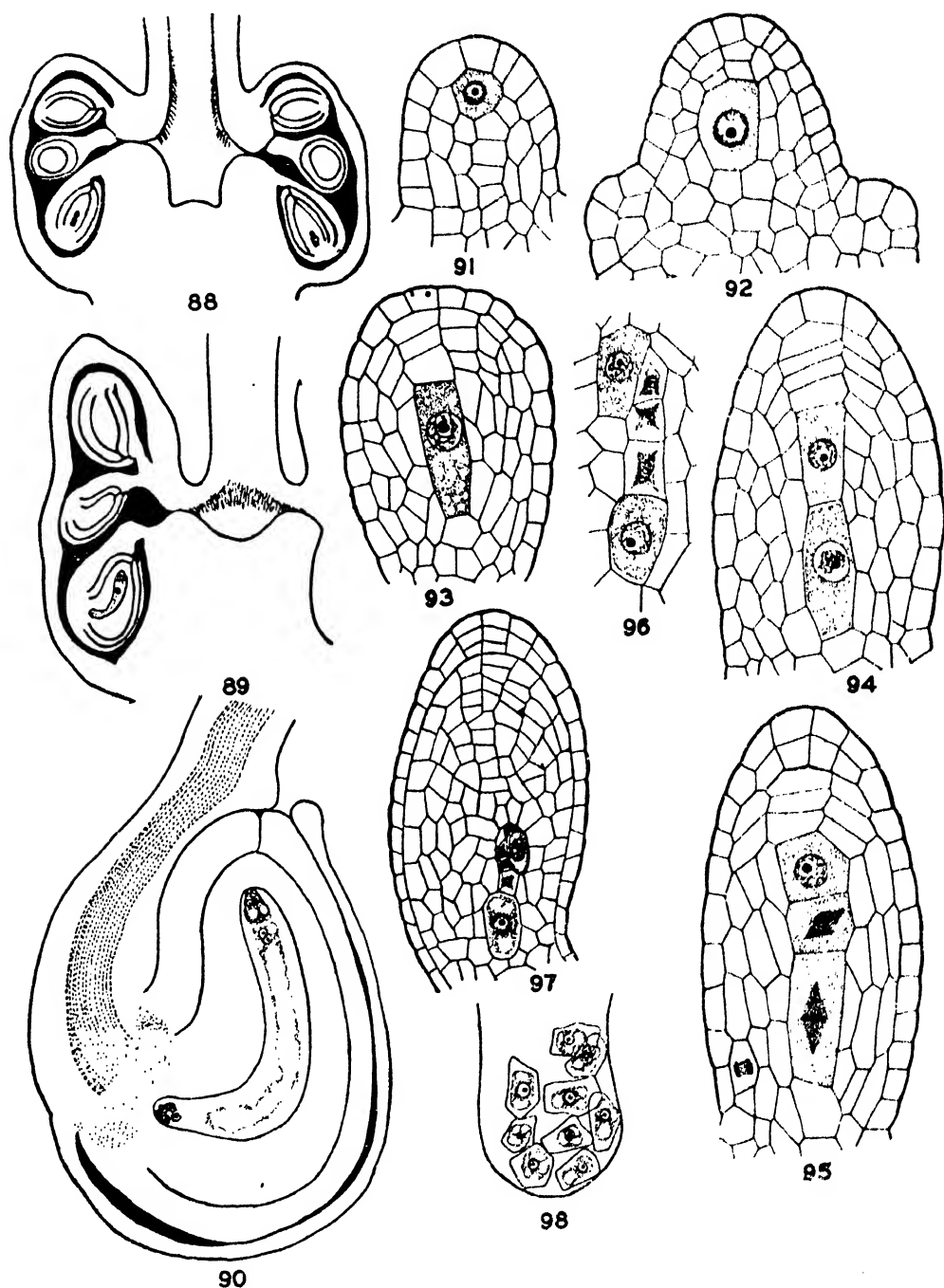


FIGS. 72-87. *Althaea rosea*. Fig. 72. L.s. loculus of ovary showing ovule primordium. $\times 140$. Fig. 73. Ovule primordium showing multicellular archesporium. $\times 425$. Figs. 74 and 75. Nucelli showing definitive megaspore mother cell and development of accessory sporogenous cells. $\times 425$. Figs. 76-79. Formation of dyads and tetrads by the definitive megaspore mother cells. $\times 425$. Figs. 80-82. Development of embryo sacs. $\times 285$. Fig. 83. Nucellus with 1- and 2- nucleate embryo sacs and degenerating cells. $\times 285$. Fig. 84. L.s. of ovule with embryo sac. $\times 30$. Fig. 85. Micropylar part of embryo sac. $\times 165$. Figs. 86 and 87. Antipodals. $\times 715$.

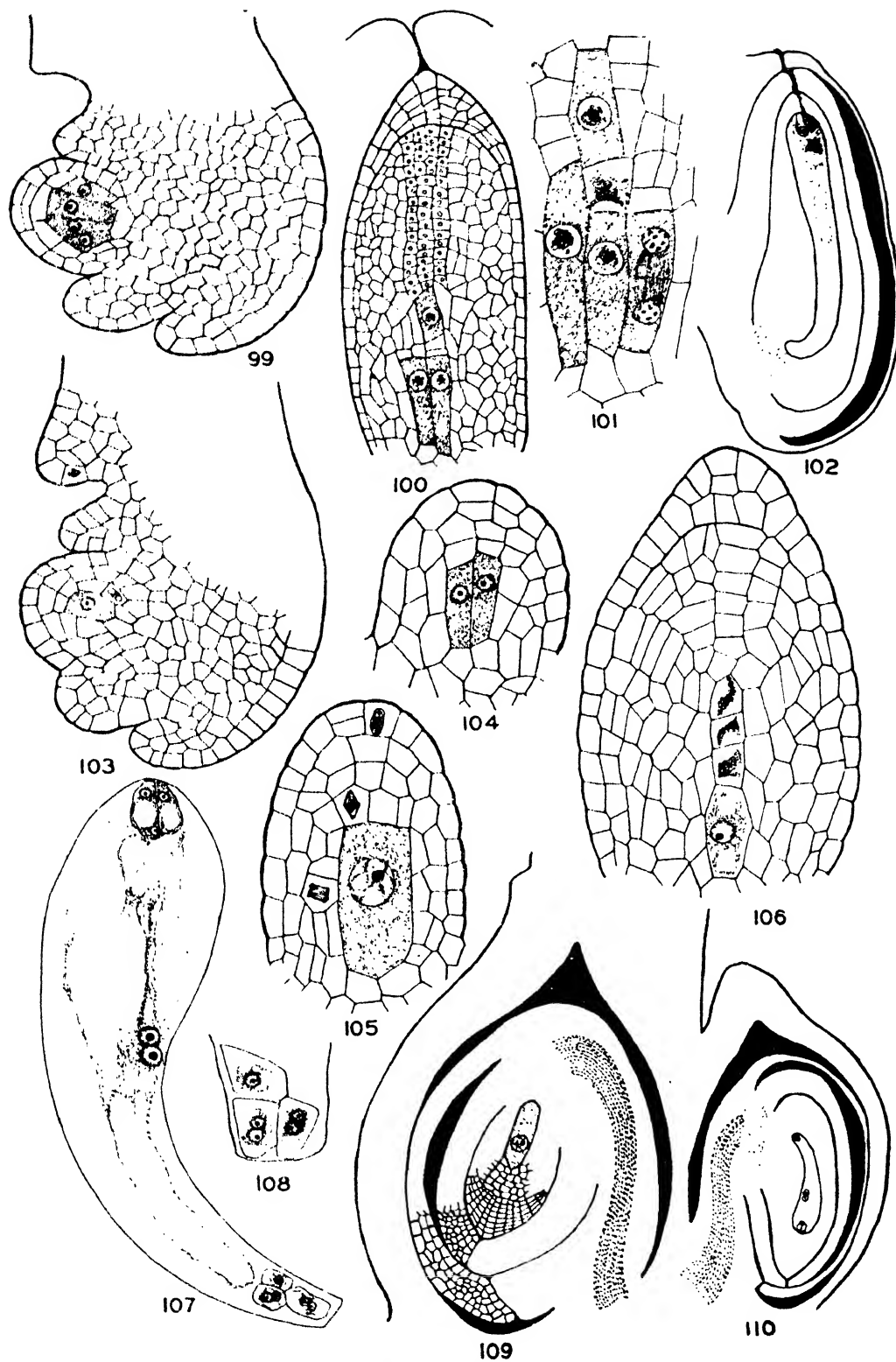
non-stainable zone and an outer thinner stainable one in which bar-like striations are clearly seen. These project to the outside and present a granular or reticulate pattern to the surface view. Like the spines, the germ pores are distributed uniformly on the exine. Applying the theory put forward by Wodehouse (1935) in case of *Chenopodiaceae* and *Polygonaceae*, Lang (1937) concluded that the pores in *Malvaceae* are morphologically equivalent to furrows which have become so shortened as to coincide in extent with their enclosed germ pores. Evidence for this was found in pollen grains of *Hibiscus vitaeifolius* in which the pore was surrounded by a circular depression. From an intensive study of pollen grain characters, Lang (1937) believes that the length of spines and their shape, their distance apart, number, size and distribution of the germ pores, the relation they bear to the spines and the nature of starch grains stored within, are useful characters for distinguishing genera and even species.

OVULE

In all species studied, the ovules are bitegmic and crassinucellate. In *Kydia calycina* (Fig. 65) and *Thespesia populnea* (Figs. 133, 136), they are anatropous and in the rest slightly or markedly campylotropous. The integuments arise when the archesporium differentiates in the ovule (Figs. 49, 50, 73, 111), or a little later (Fig. 144). The outer integument grows faster than the inner and covers up the nucellus by the time the megaspore mother cell is full grown (Figs. 52, 58, 109, 113, 137). In *Urena lobata* (Fig. 100), and *Thespesia populnea* (Fig. 131), the inner also closes by this time. In most genera the outer integument is 2-3 layered while the inner is 4-8 cells thick. In *Thespesia populnea*, on the other hand, the outer integument is 5-6 cells thick and the inner 10-12 layered (Fig. 131). This genus and also *Gossypium* and *Ingenhousia* (Reeves, 1936), differ from the rest of the family in showing integumentary vascular bundles (Figs. 133, 135, 136). The vascular bundle of the funicle gives off from its chalazal end, 6-9 branches which traverse the outer integument nearly to the micropyle, branching on the way. The outer integument of *Thespesia*, when cleared in chloral hydrate shows a number of druses, the significance of which is doubtful. The cells of the epidermis of the ovule lose their cytoplasmic contents and accumulate tannin. The inner epidermis of the inner integument also accumulates tannin, except in a cap-like region around the micropyle (Figs. 64, 148), as in some members of *Sterculiaceae* like *Melochia corchorifolia* (C. V. Rao, 1951). Tannin and starch grains are stored also in the median layers of the inner integument in the region of micropyle (Fig. 64). An air space develops between the integuments on the side opposite to the funicle (Figs. 84, 90) or allround (Fig. 135). In *Sida cordifolia* (Fig. 6), *S. veronicaefolia* (Fig. 58), *S. carpinifolia*, *Urena lobata* and *Malachra capitata* (Fig. 109), the outer integument gets separated from the inner very early and becomes attached to the inside of the ovary wall in which condition it remains even in the fertilisable ovary (Figs. 7, 55, 62, 102, 110). The micropyle which is formed by both the integuments, has the usual zigzag form (Fig. 64). In *Sida veronicaefolia*, a knob-like outgrowth of radially elongated richly protoplasmic cells develops at the base of the funicle even before the megaspore mother cell has divided (Fig. 58). In the fertilisable ovule it presses against the integuments and functions as the obturator (Figs. 62, 64). Other species of *Sida* studied, namely *S. cordifolia* and *S. carpinifolia* do not show such a structure. The position of the micropyle varies in different species according to placentation. In *Pavonia zeylanica*, *Malachra capitata*, *Urena lobata*, *Malvaviscus arboreus* and *Althaea rosea*, it faces the base of the ovary, the raphe being ventral. In *Sida* species, it is directed towards the top of the loculus, the raphe being dorsal. In *Ablemoschus esculentus*, the ovules are slightly inclined and the micropyles point towards the ovarian axis. In *Abutilon indicum*, *Hibiscus micranthus*, and *H. hirtus*, the ovules are variously inclined and the micropyles point towards the axis of the ovary, top or base of the loculus (Fig. 143).



Figs. 88-98. *Abutilon indicum*. Figs. 88 and 89. I.s. of young and mature ovaries showing placentation, gynobasic style and development of obturator. Fig. 88, $\times 25$; Fig. 89, $\times 10$. Fig. 90. A mature ovule. $\times 75$. Figs. 91-93. Ovule primordia with archesporium and megaspore mother cells. $\times 425$. Fig. 94. Nucellus showing definitive and accessory sporogenous cells. $\times 425$. Figs. 95 and 96. Formation of tetrads by definitive sporogenous cells. $\times 425$. Fig. 97. Nucellus with 1- and 2-nucleate embryo sacs. $\times 285$. Fig. 98. Antipodals. $\times 715$.



FIGS. 99-110.—Explanation at foot of next page.

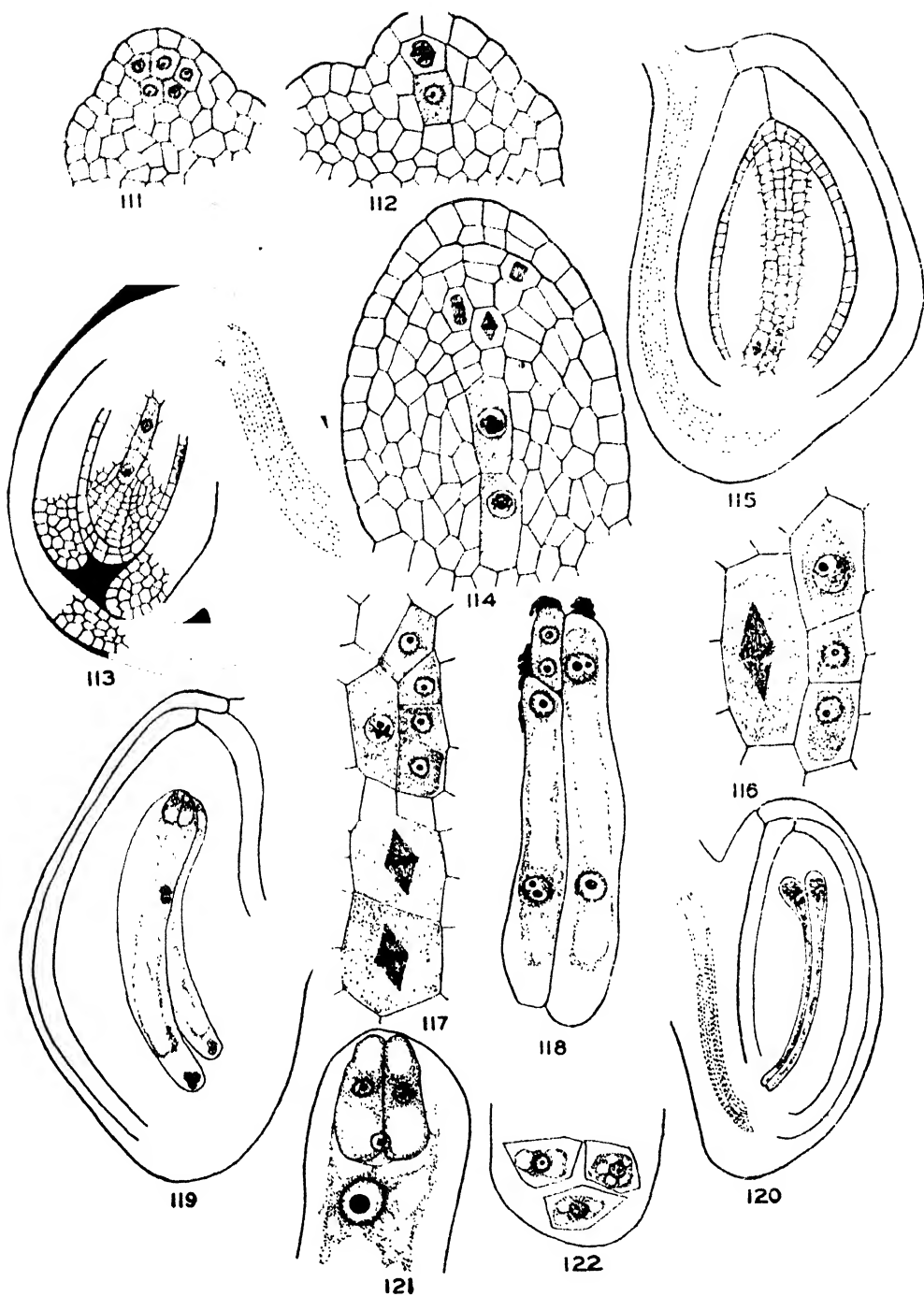
The nucellus may be straight as in *Kydia calycina* (Fig. 65) and *Thespesia populnea* (Fig. 133) or slightly bent as in *Urena lobata* (Fig. 102), *Malachra capitata* (Fig. 110) and *Pavonia zeylanica* or markedly curved as in *Sida* species (Figs. 7, 55, 62), *Abutilon indicum* (Fig. 90) and *Hibiscus solandra* (Fig. 148). Accordingly the embryo sac also may be straight or curved to a varying degree. The micropylar part of the nucellus consists of partly the several layered epidermal cap and partly the tissue derived from one or more primary parietal cells cut off by the hypodermally situated archesporial cells. Periclinal divisions of the cells of the nucellar epidermis occur at a very early stage (Figs. 99, 125). In *Urena lobata* (Fig. 100) and *Thespesia populnea* (Fig. 132) in which the parietal tissue is more extensive than in the rest, the cells stand out prominently by their richer deep-staining protoplasm and form a sort of 'epistase'. The whole of the parietal tissue gets crushed by the enlarging embryo sac and only the epidermal cap or a part of it persists in the fertilisable ovule. Laterally the embryo sac is surrounded by several layers of cells which are more on the side of the funicle in campylotropous ovules. In *Urena lobata* (Fig. 100), *Malvaviscus arboreus* (Figs. 113, 115), *Sida* species (Figs. 6, 52, 58, 59), *Abutilon indicum* (Fig. 93), *Pavonia zeylanica* (Fig. 137), *Hibiscus hirtus* (Fig. 145), *H. solandra* (Fig. 147) and *H. micranthus* (Fig. 149), the megaspore mother cells have their lower ends extending to the chalaza. In these species the antipodal end of the embryo sac reaches the tannin and starch bearing cells of the chalaza (Figs. 7, 54, 62, 102, 119, 148). Two or three layers of cells surrounding the extreme end of the sac become thick-walled (Fig. 57). In other species like *Althaea rosea* (Fig. 83) and *Thespesia populnea* (Fig. 132) there are several layers of nucellar cells below the group of megaspore mother cells. These cells later become elongated and thick-walled and form a hypostase (Figs. 133, 134). As the cells stand more or less in regular rows and connect the embryo sac and the vascular bundle in the chalaza, they seem to facilitate the conduction of food materials into the sac. In this feature, these species resemble some members of Sterculiaceae and Tiliaceae.

MEGASPOROGENESIS

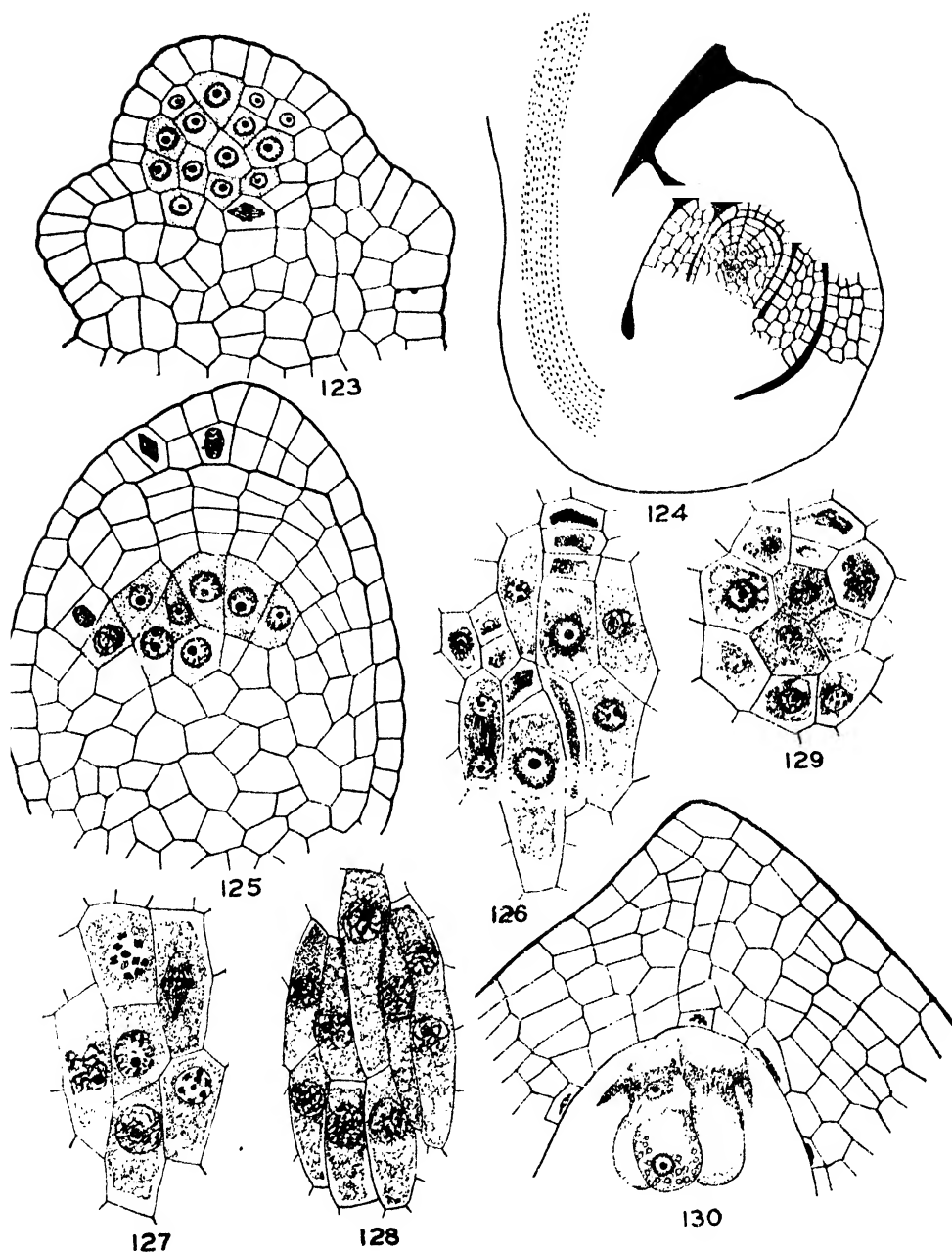
The archesporium of the ovule may consist of a single hypodermal cell as in *Sida carpinifolia* (Fig. 49), *S. cordifolia* (Figs. 50, 51), *Abutilon indicum* (Figs. 91, 92), *Hibiscus hirtus* (Fig. 144) and *Hibiscus solandra* (Fig. 146) or a group of hypodermal and sub-hypodermal cells as in *Althaea rosea* (Figs. 72, 73), *Urena lobata* (Fig. 99), *Malvaviscus arboreus* (Fig. 111) and *Thespesia populnea* (Figs. 123, 129). In the latter case, there are two types: in some like *Althaea rosea*, *Malachra capitata* (Figs. 103, 105, 109), *Malvaviscus arboreus* (Fig. 112) *Pavonia zeylanica* (Figs. 137, 138), only one hypodermally placed cell continues to function while the rest merge into the nucellus. Only occasionally two cells may function till megaspore mother cell stage (Fig. 104) or more rarely till embryo sacs are formed (Figs. 67, 69, 71). In others like *Urena lobata* (Figs. 100, 101) and *Thespesia populnea* (Figs. 124-128) several cells continue to function and form tetrads or embryo sacs. None of the

Explanation of Figs. 99-110 (p. 14).

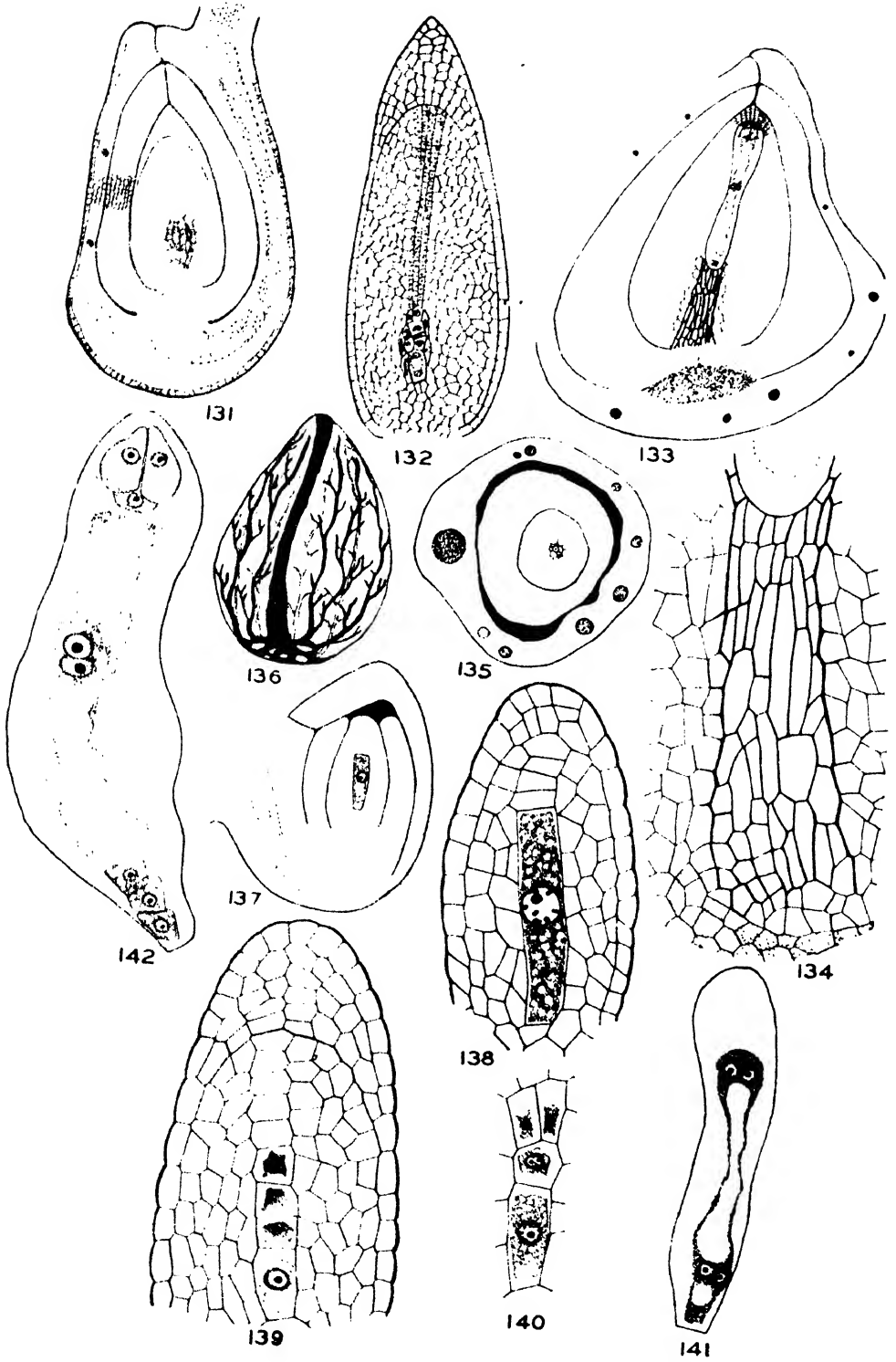
- Figs. 99-102. *Urena lobata*. Fig. 99. Young ovule with several megaspore mother cells; note periclinal divisions in nucellar epidermis. $\times 285$. Fig. 100. Nucellus with full grown megaspore mother cells and accessory sporogenous cell; note epistase like structure. $\times 230$. Fig. 101. A group of sporogenous cells in meiosis; note degeneration of one of the sporogenous cells. $\times 425$. Fig. 102. Ovule showing entry of pollen tube. $\times 45$.
Figs. 103-110. *Malachra capitata*. Figs. 103 and 104. Ovules with 1- and 2- functional megaspore mother cells. $\times 285$ and $\times 425$ respectively. Fig. 105. Nucellus with megaspore mother cell showing formation of nucellar cap. $\times 425$. Fig. 106. Nucellus with linear tetrad of which the lowest megaspore is enlarging. $\times 425$. Fig. 107. Mature embryo sac. $\times 285$. Fig. 108. Antipodals; note two-nucleate condition in two of them. $\times 425$. Figs. 109 and 110. Loculi of young and old ovaries; note development of 'gynobasic' style. $\times 135$ and $\times 45$ respectively.



FIGS. 111-122. *Mulaviscus arboreus*. Fig. 111. Ovule primordium with multicellular archesporium. $\times 420$. Fig. 112. Ovule showing divisions in primary parietal cell. $\times 420$. Fig. 113. Ovule with definitive and accessory sporogenous cells. $\times 115$. Fig. 114. Nucellus showing megaspore mother cell and development of accessory sporogenous cell and parietal layers. $\times 420$. Fig. 115. Ovule with megaspore mother cell in meiosis I. $\times 115$. Fig. 116. Sporogenous cells from the above magnified. $\times 445$. Fig. 117. Formation of tetrads by definitive and accessory sporogenous cells. $\times 445$. Fig. 118. Three 2-nucleate embryo sacs derived from different tetrads. $\times 420$. Fig. 119. Ovule with two mature embryo sacs. $\times 65$. Fig. 120. Ovule showing degeneration of embryo sacs. $\times 45$. Fig. 121. Micropylar part of embryo sac. $\times 255$. Fig. 122. Antipodals. $\times 445$.



FIGS. 123-130. *Thespesia populnea*. Fig. 123. Ovule primordium with multicellular archesporium. $\times 425$. Fig. 124. Young ovule showing development and structure of integuments and parietal tissue. $\times 135$. Fig. 125. Nucellus showing sporogenous cells and development of parietal layers and nucellar cap. $\times 255$. Figs. 126-128. Group of sporogenous cells in meiosis. $\times 425$. Fig. 129. T.s. through a group of sporogenous cells. $\times 425$. Fig. 130. Micropylar part of an embryo sac; note hooked synergids and starch grains in egg cytoplasm. $\times 285$.



Figs. 131-142.—Explanation at foot of next page.

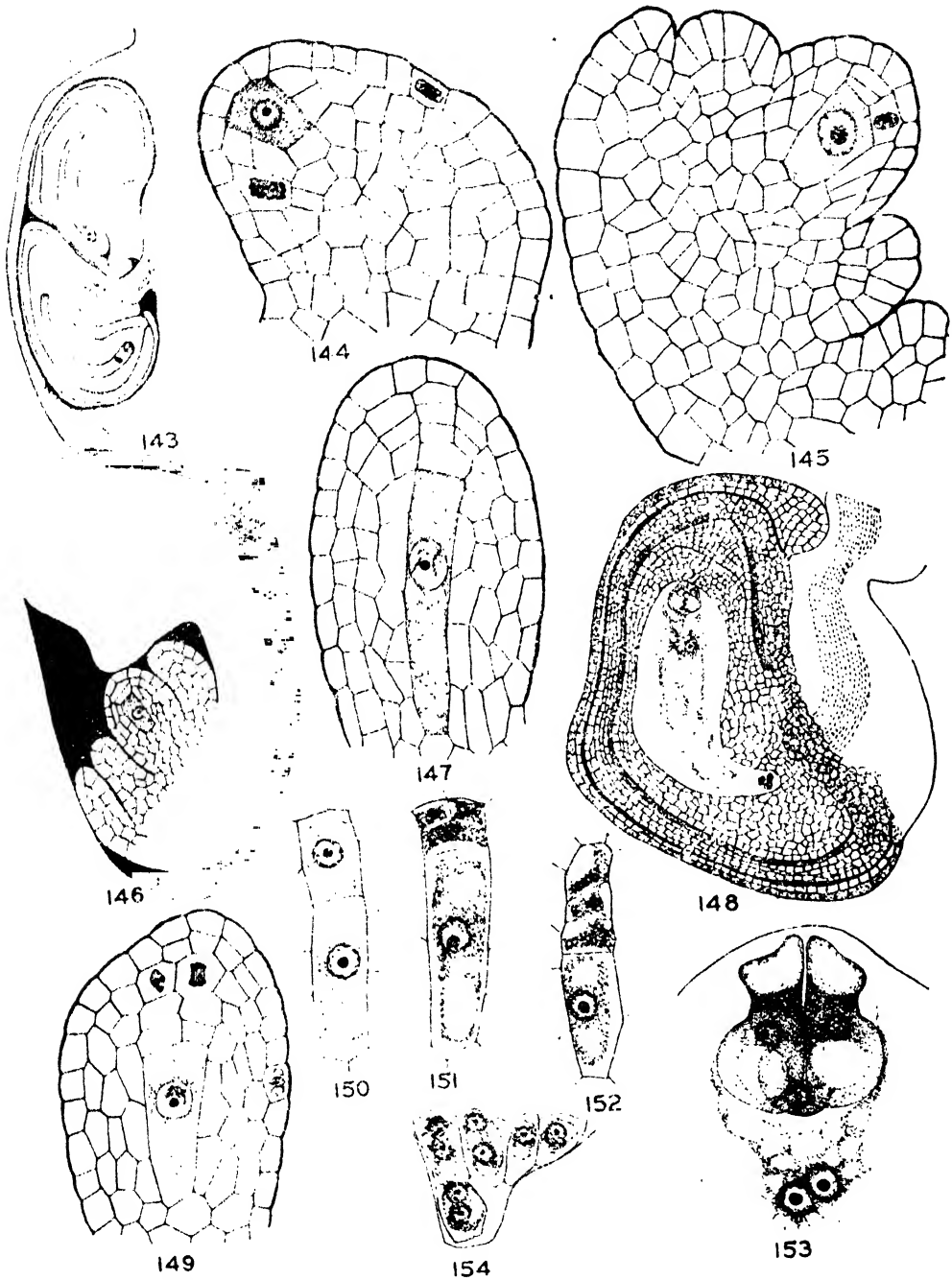
previous investigators reported such typically multicellular archesporium with several functional cells in Malvaceae. The archesporium in these species resembles that in *Pterospermum* species, e.g. *P. suberifolium* (C. V. Rao, 1952) and *Triumfetta rhomboidea* (C. V. Rao and K. V. S. Rao, 1952). In several species with a single functional cell, accessory sporogenous cells develop from one or more cells of parietal tissue, a feature to which Stenar (1925) has already drawn attention, e.g., *Sida cordifolia* (Fig. 53), *S. veronicaefolia* (Figs. 58–61), *Althaea rosea* (Figs. 74–79), *Abutilon indicum* (94–96), *Urena lobata* (Figs. 100, 101) and *Malvaviscus arboreus* (Figs. 113–117). The accessory sporogenous cells become demarcated at the time of meiosis of the definitive cells. In this connection Stenar (1925) makes a significant remark: 'in order to make sure whether accessory sporogenous cells are present or not, it is not enough to observe the early stages of ovules in which only a few cover cells are present, but such ovules in which the definitive sporogenous cells are undergoing divisions'.

The megaspore mother cells have an elongated and tapering form (Figs. 52, 93, 138, 147, 149). Due to the position of the nucleus nearer to the micropylar end of the cell at prophase I, the upper dyad cell is always smaller than the lower (Fig. 150). In the second division the cell wall may be laid in a horizontal (Figs. 60, 61, 106, 139, 152) or oblique (Figs. 95, 117) or in a vertical manner (Figs. 78, 79, 140, 151) so that megaspore tetrads are not always linear. T-shaped tetrads are commonly formed by the deep seated cells probably due to spatial relations. Normally the chalazal megaspore functions (Figs. 59, 61, 67, 80–83, 97, 106, 139, 140). In *Althaea rosea*, in one case (Fig. 80) the second megaspore from the micropylar side was seen to be enlarging. The case sketched in fig. 68 of *Kydia calycina* appears to be due to the functioning of two megaspores of the same tetrad. The third megaspore from the micropylar side is more precocious and has formed a 4-nucleate embryo sac while the lowest is still in the uninucleate stage. In another case (Fig. 70), two superposed 8-nucleate embryo sacs are seen which also appear to be derived from two megaspores of the same tetrad. Similar development of two megaspores of a tetrad was reported by Gore (1932) in cotton.

Usually the accessory sporogenous cells degenerate before undergoing the meiotic divisions. The more favourably placed sporogenous cells complete the meiotic divisions earlier (Figs. 59, 61, 77–79, 95, 96, 117) and one or more megaspores derived from them enlarge and crush out the nonfunctional cells (Figs. 80–82). Only rarely the accessory sporogenous cells divide earlier (Figs. 97, 117) in which case the megaspores derived from them have greater chances of functioning. Also when the accessory or definitive cells are collaterally placed, the megaspores derived from them have equal chances of functioning since they have equal nutritive facilities and the enlargement of one sac does not result in immediate crushing of the other as happens when the two are superposed. The embryo sacs in such cases reach maturity (Figs. 71, 118–120). In embryo sacs which are superposed, usually the enlargement of one results in crushing out the other (Fig. 70).

Explanation of Figs. 131–142 (p. 144).

- Figs. 131–136. *Thespesia populnea*. Fig. 131. Ovule with several megaspore mother cells. $\times 125$. Fig. 132. Nucellus with megaspore tetrads; note 'epistase' like group of parietal cells. $\times 70$. Fig. 133. L.s. mature ovule; note integumentary vascular bundles and hypostase. $\times 70$. Fig. 134. Hypostase magnified. $\times 155$. Fig. 135. T.s. ovule showing integumentary vascular bundles. $\times 35$. Fig. 136. Seed with its vascular supply. $\times 3$.
- Figs. 137–142. *Pavonia zeylanica*. Fig. 137. Young ovule with megaspore mother cell. $\times 110$. Figs. 138 and 139. Nucelli with megaspore mother cell and linear tetrad respectively. $\times 400$. Fig. 140. A T-shaped tetrad. $\times 400$. Fig. 141. Four nucleate embryo sac which has begun to curve. $\times 265$. Fig. 142. Mature embryo sac. $\times 310$.



FIGS. 143-145. *Hibiscus hirtus*. Fig. 143. L.s. loculus of ovary. $\times 45$. Fig. 144. Ovule primordium with one archesporial cell. $\times 400$. Fig. 145. Ovule showing formation of parietal layers. $\times 400$.
 FIGS. 146-148. *Hibiscus solandra*. Fig. 146. Young ovule. $\times 185$. Fig. 147. Nucellus with full grown megaspore mother cell. $\times 400$. Fig. 148. Mature ovule. $\times 280$.
 FIGS. 149-154. *Hibiscus micranthus*. Fig. 149. Nucellus with full grown megaspore mother cell. $\times 400$. Figs. 150-152. Dyads, T-shaped and linear tetrads respectively. $\times 400$. Figs. 153 and 154. Micropylar and antipodal parts of embryo sac; Fig. 153, $\times 400$; Fig. 154, $\times 665$.

EMBRYO SAC

By three successive free nuclear divisions of the megaspore nucleus, the 8-nucleate embryo sac is derived. In campylotropous ovules, the embryo sac begins to curve at the 2- or 4-nucleate stage (Fig. 141) and the curvature increases with the growth of the sac (Fig. 142). The nuclei of the synergids are derived from one parent nucleus and those of the egg and upper polar nucleus from another (Fig. 82). In *Sida cordifolia* (Fig. 56), *S. carpinifolia*, *S. veronicaefolia*, and *Thespesia populnea* (Fig. 130) the synergids show prominent hooks. In the rest they are pear-shaped without hooks (Fig. 153). The synergids and egg show normal vacuolation. In *Sida carpinifolia* and *S. cordifolia* (Fig. 56), the synergids show filiform apparatus. In *Thespesia populnea*, starch grains are seen not only in the embryo sac but also in the cytoplasm of the egg (Fig. 130); these are absent from the embryo sacs of other species. The polar nuclei meet at about the middle of the sac and travel together upwards and remain in proximity to the egg apparatus. Only in *Althaea rosea* (Fig. 85) and *Malva viscus arboreus* (Fig. 121) they were seen to fuse before fertilization. The antipodals show much variation. In *Sida veronicaefolia* (Fig. 63), *Kydia calycina* (Figs. 70, 71), *Malva viscus arboreus* (Fig. 122) and *Hibiscus solandra* (Fig. 148), they are three in number and 1-nucleate. In *Sida carpinifolia* (Fig. 57) in one case, one of the cells divided and formed two cells. In *Althaea rosea* (Figs. 86, 87), *Abutilon indicum* (Fig. 98), *Malachra capitata* (Fig. 108), and *Hibiscus micranthus* (Fig. 154) either the antipodal nuclei divide in free nuclear manner or a cell wall is formed after the division so that binucleate and supernumerary antipodals are formed. In *Hibiscus micranthus* they increased still further in number after fertilization and persisted till the embryo became a large globular mass.

DISCUSSION

A comparative study of the embryological features of the various species investigated shows that while the characters of the microsporangium and male gametophyte are fairly uniform, there is some variation in the development and structure of the archesporium, embryo sac and ovule.

The microspore mother cells in several species form a single row in the anther. The tapetum is of plasmodial type. The pollen grains are multiporate and spinescent and distinctly differ from those of other families of the order in which they are predominantly smooth walled and triporate. Wodehouse (1936) is of the opinion that spinescent multiporate pollen is more evolved than the smooth walled and triporate pollen. On the basis of pollen grain characters, Malvaceae seems to be the most evolved family of the order. The campylotropous ovules which are common in Malvaceae are also not met with in other families of Malvales. In *Adansonia digitata* (Bombacaceae), the ovule is anatropous but the seed becomes campylotropous. The presence of epistase, hypostase, synergids with filiform apparatus, well defined transmitting tissue in the style and obturator are again features of a specialised nature. In the presence of super-numerary, sometimes binucleate and persistent antipodals, Malvaceae differs from other families of the order and resembles highly evolved families like Rubiaceae, Compositae and Gramineae. Their persistence till a comparatively late stage in the development of the seed and their position between the endosperm and the food bearing cells of the chalaza suggest that they might assist in the transport of food materials into the embryo sac, a function which the persistent pollen tube seems to subserve in the micropylar part of the ovule (C. V. Rao, 1952a). From the above, it can be inferred that embryologically Malvaceae is the most advanced family among the Malvales.

Malvaceae is divided into four tribes (Schuman in Engler and Prantl, 1895), based on the disposition of carpels, nature of fruit, number of stylar branches, etc.

1. MALOPEAE: Carpels in vertical rows.
2. MALVEAE: Fruit schizocarp; stigmas as many as carpels. *Sida*, *Abutilon*, *Althaea*, *Kydia*.
3. URENEAE: Fruit schizocarp; stigmas twice as many as carpels. *Urena*, *Malvariscus*, *Pavonia* and *Malachra*.
4. HIBISCEAE: Fruit capsule; stigmas equal to the number of carpels. *Gossypium*, *Thespesia* and *Hibiscus*.

A comparison of the embryological features shows that there is much overlapping. Genera belonging to different tribes may show similar embryological features like the formation of accessory sporogenous cells in the ovules (*Sida*, *Malvariscus*) or typical multicellular archesporium with several functional cells (*Urena*, *Thespesia*). Similarly genera belonging to the same tribe may differ markedly in their embryological features. This point becomes clear on comparing the embryological features of the three genera of the tribe of Hibisceae, namely, *Gossypium*, *Thespesia* and *Hibiscus*. *Gossypium* and *Thespesia* resemble each other in their anatropous ovules, massive integuments, integumentary vascular bundles, and differ from *Hibiscus* which shows campylotropous ovules and no integumentary vascular supply. On the other hand, *Thespesia* differs from *Gossypium* in the presence of epistase and hypostase, multicellular archesporium with several functional cells in the ovule, hooked synergids without filiform apparatus and presence of starch grains in the embryo sac. Though Edlin (1935) considered on the basis of capsular fruits, that the tribe Hibisceae is the most primitive among Malvaceae and transitional between Bombacaceae and Malvaceae, it seems to be the most evolved on embryological grounds, a conclusion reached by Reeves (1936) also on study of seed anatomy. They show features of specialisation like organisation like epistase, hypostase, filiform apparatus in synergids, massive integuments and integumentary vascular bundles, epidermal hairs and resin glands in the testa and non-endospermic seeds with food reserve in the embryo.

SUMMARY

Organogeny, development of the male and female gametophytes, and structure of the ovules were studied in the following 15 species of Malvaceae belonging to eleven genera: *Sida cordifolia* L., *S. veronicaefolia* L. (= *S. humilis* Willd.), *S. carpinifolia* L., *Abutilon indicum* G. Don., *Althaea rosea* Cav., *Kydia calycina* Roxb., *Urena lobata* L., *Malvariscus arboreus* Cav., *Pavonia zeylanica* L., *Malachra capitata* L., *Hibiscus solandra* L. Herit., *H. micranthus* L., *H. hirtus* L., *Ablemoschus esculentus* (L.) Moench., and *Thespesia populnea* Corr.

Of the four layered anther-wall, the sub-epidermal layer develops into the fibrous endothecium and the innermost into the tapetum of the plasmodial type. The tapetum seems only to hasten the growth of the sculpturing of the exine but not initiate it. In some species like *Pavonia zeylanica*, the primary sporogenous cells of the anther function as the microspore mother cells directly while in others like *Abutilon indicum*, they undergo a secondary increase. Microspore tetrads are usually tetrahedral bilateral and linear tetrads being noticed occasionally. Cytokinesis is by furrowing. The pollen grains are spinescent and multiporate and are shed mostly in the 2-nucleate condition, though in *Kydia* a few 3-nucleate grains were met with. The generative cytoplasm forms a hyaline sheath around the nucleus in the initial stages and is later obscured by the starch grains, protein and fat that accumulate in the cytoplasm of the vegetative cell.

The ovules are bitegmic, crassinucellate, anatropous or more commonly campylotropous. The inner integument is more massive than the outer. Some cells of the integuments and chalaza accumulate tannin and starch grains. *Thespesia* shows integumentary vascular bundles. 'Epistase' occurs in the nucellus of *Urena* and *Thespesia* and also a hypostase in the latter.

The archesporium is typically one-celled in some members like *Hibiscus* species while it is multicellular with several functional cells in *Urena* and *Thespesia*. In several genera like *Sida*, *Malvariscus*, *Abutilon*, and *Althaea*, some of the parietal cells later assume characters of sporogenous cells and function as such till the formation of tetrads or embryo sacs. In *Kydia*, some-

times two megaspores of the same tetrad function and develop into 8-nucleate embryo sacs. Megaspore tetrads are linear as well as T-shaped, and embryo sac develops according to *Normal-type*. Synergids are hooked in *Sida* and *Thespesia*; they show filiform apparatus in *Sida cordifolia* and *S. carpinifolia*. Polar nuclei fuse only at the time of fertilization except in *Althaea rosea* and *Malvaviscus arboreus* in which they fuse earlier. In some like *Abutilon indicum*, *Hibiscus hirtus* and *H. micranthus*, supernumerary and sometimes binucleate antipodals occur. In *Hibiscus micranthus* and *H. hirtus* they persist till a late stage in the development of the seed and seem to assist in transport of food materials from the starch bearing cells of the chalaza into the embryo sac. Starch grains are seen in the cytoplasm of the embryo sac and egg of *Thespesia populnea*.

ACKNOWLEDGEMENTS

The writer wishes to express his grateful thanks to Prof. J. Venkateswarlu and Prof. A. C. Joshi for their kind interest in the work and encouragement. His thanks are also due to Prof. P. Maheshwari for the article of Stenar which he kindly lent and also for some valuable suggestions.

REFERENCES

- Ayyar, V. R. and Ayyangar, G. S. (1933). Differentiation of hairs on the seed of cotton. *Emp. Cotton Growing Rev.*, **10**, 21-23.
- Balls, W. L. (1906). The sexuality of cotton. *Yearbook Khediv. Agric. Soc.*, Cairo.
- Banerji, I. (1929). The chromosome numbers of Indian cottons. *Ann. Bot.*, **43**, 603-607.
- Baritt, N. W. (1932). The differentiation of the epidermal layer in the cotton seed and its relation to ginning outturn. *Emp. cotton Growing Rev.*, **9**, 126-131.
- Beal, J. M. (1928). A study of the heterotypic prophase in the microsporogenesis of cotton. *La Cellule*, **38**, 245-268.
- Burkett, G. W. (1932). Chromosome numbers in *Althaea rosea*. *Science*, **75**, 488.
- Byxbee, E. S. (1900). The development of the karyokinetic spindle in pollen mother cells of *Lavatera*. *Proc. Calif. ac. sci. Ser. Bot.*, **2**, nr. 2.
- Cannon, W. A. (1903). Studies in plant hybrids: The spermatogenesis of a hybrid cotton. *Bull. Torr. Bot. Club.*, **30**, 133-172.
- Denham, H. J. (1924a). The cytology of the Cotton plant. Microspore formation of Sea Island cotton. *Ann. Bot.*, **38**, 407-432.
- (1924b). The cytology of Cotton plant. Chromosome numbers in old and new world cottons. *Ibid.*, **38**, 433-438.
- Davie, H. (1933). Cytological studies in the Malvaceae and certain related families. *Jour. Genet.*, **28**, 33-67.
- Edlin, H. L. (1935). A critical revision of certain taxonomic groups of the Malvales. *New Phyt.*, **34**, 1-20; 122-143.
- Engler, A. and Prantl, K. (1895). *Natürlichen Pflanzenfamilien*, Leipzig.
- Gore, U. R. (1932). The development of the female gametophyte in cotton. *Amer. Jour. Bot.*, **19**, 795-807.
- Guignard, L. (1893). Recherches sur le développement de la graine et en particulier du tegument seminal. *Jour. de bot.*, **7**, 1-14, etc.
- (1900). Nouvelles recherches sur la double fecundation chez les végétaux angiospermes. *C.R. Acad. Paris*, **131**, 153-160.
- (1904). La double fecundation chez les Malvacees. *Jour. Bot.*, **18**, 296-308.
- Gulati, A. N. (1934). A note on the differentiation of hairs from epidermis of cotton seeds. *Indian Jour. Agric. Sci.*, **4**, 471-474.
- Harland, S. C. (1932). The genetics of *Gossypium*. *Bibliographia genetica*, **9**, 108-182.
- Hegelmair, F. (1885). Untersuchungen über die Morphologie des Dicotyledon-Endosperms. *Nova acta Leop. Car. Acad. Naturf.*, **49**, nr. 1.
- Hofmeister, W. (1849). Die Entstehung des Embryo der Phanerogamen. Leipzig.
- Iyengar, N. K. (1938). Pollen tube studies in *Gossypium*. *Jour. Genet.*, **37**, 69-106.
- Johansen, D. A. (1950). *Plant embryology*. Chronica Botanica.
- Jonsson, B. (1879). Om embryosäckens utveckling hos Angiospermena. *Lunds Univ. Årsskr.*, **16**.
- Jacob, K. T. (1942). Nuclear changes in the lint primordial cells of *Gossypium herbaceum* var. *typicum*. *Science and Culture*, **7**, 512-513.
- Kearney, T. H. and Harrison, G. H. (1924). Selective fertilisation in cotton. *Jour. Agric. Res.*, **27**, 329-340.
- Kessler, E. von. (1932). Observations in chromosome numbers of *Althaea rosea*, *Callirhoe involucrata* and *Hibiscus coccineus*. *Amer. Jour. Bot.*, **19**, 129-130.

- Lang, C. H. (1937). Investigations of the pollen of the Malvaceae with special reference to the inclusions. *Jour. Royal Microsc. Soc.*, **58**, 75-102.
- Lantini, V. (1912). Development of the microsporangia and microspores of *Abutilon theophrasti*. *Bot. Gaz.*, **54**, 330-335.
- Lauter, M. J. (1932). The meiotic divisions in the pollen mother cells of *Malva silvestris*. *Ann. Bot.*, **46**, 1-10.
- Longley, A. E. (1933). Chromosome numbers in *Gossypium* and related genera. *Jour. Agric. Res.*, **46**, 217-227.
- Pal, B. P., Singh, H. B. and Vishnu Swarup (1952). Taxonomic relationships and breeding possibilities of *Ablmoschus* related to OKRA (*A. esculentus*). *Bot. Gaz.*, **113**, 455-464.
- Rao, C. V. (1951). Contributions to the embryology of Sterculiaceae—III. *Melochia corchori-folia* L. *J. Indian Bot. Soc.*, **30**, 122-131.
- (1952). Contributions to the embryology of Sterculiaceae—IV. *Pterospermum suberifolium*. *Ibid.*, **31**, 250-260.
- (1952a). Occurrence of persistent pollen tubes in Malvaceae. *Curr. Sci.*, **21**, 49-50.
- Rao, C. V. and Rao, K. V. S. (1952). A contribution to the embryology of *Triumfetta rhomboidea* and *Corchorus acutangulus*. *J. Indian Bot. Soc.*, **31**, 56-68.
- Rao, L. N. (1941). Cytology of *Hibiscus trionum*. *New Phyt.*, **40**, 326-335.
- Rendle, A. B. (1938). *Classification of flowering plants*. Vol. II. Cambridge.
- Reeves, R. G. (1936). Comparative anatomy of the seeds of cottons and other Malvaceous plants. *Amer. Jour. Bot.*, **23**, 291-296; 394-405.
- Schnarf, K. (1931). *Vergleichende Embryologie der Angiospermen*. Berlin.
- Singh, T. C. N. (1931). Notes on the early stages in the development of the cotton fibre and structure of the boll and seed. *Ann. Bot.*, **45**, 378-380.
- Skovsted, A. (1933). Cytological studies in cotton. The mitosis and meiosis in diploid and triploid Asiatic cotton. *Ibid.*, **47**, 227-251.
- Souèges, R. (1921). Developpement de l'embryon chez l'*Urtica pilulifera*. *Bull. Soc. bot., France*, **68**, 172-188.
- (1922). Developpement de l'embryon chez le *Malva rotundifolia*. *C.R. ac. Paris*, **175**, 1435-1436.
- Stenar, H. (1925). Embryologische studien. I. Zur Embryologie einiger Columniferen. *Akad. Abh. Uppsala*.
- Strasburger, E. (1884). Neuere Untersuchungen über den Befruchtungsvorgang bei den Phanerogamen als Grundlage für eine Theorie der Zeugung. Jena.
- Warming, E. (1873). Untersuchungen über pollenbildende Phyllome und Kaulome. *Bot. Abh. herausg. von Hanstein*, **2**, 1-90.
- Wodehouse, R. P. (1935). Pollen grains. MacGraw Hill. N.Y.
- (1936). Evolution of pollen grains. *Bot. Rev.*, **2**, 67-86.
- Woycieki, Z. (1911). Zur Frage der Entstehung der Pollenhaut bei *Malva silvestris*. *Ber. d. deutsch bot. Ges.*, **29**, 636-646, etc.
- Yamaha, G. (1926). Über die Zytokinese bei der Pollen-tetradenbildung, zugleich weitere Belege zur Kenntnis der Zytokinese im Pflanzenreiche. *Jap. Jour. Bot.*, **3**, 139-162.
- Youngman, W. (1927). Studies in the cytology of the Hibisceae—I. *Ann. Bot.*, **41**, 755-778.
- (1931). Studies in the cytology of the Hibisceae—II. The behaviour of the nucleus during cell division in the root tip of *Thespesia populnea* and comparative observations of the phenomenon in some related plants. *Ibid.*, **45**, 49-72.

PLASMA VOLUME AND THIOCYANATE SPACE IN NUTRITIONAL OEDEMA

by K. L. MUKHERJEE *, R. N. CHAUDHURI, F.N.I. and G. WERNER,
School of Tropical Medicine, Calcutta

Received June 25; read October 9, 1953)

Oedema is a common feature^{1,2} observed in patients exposed to malnutrition or suffering from conditioned nutritional deficiency. The distribution of body water over the various fluid compartments in such oedematous patients has been studied by a number of workers (Perera, 1946; Mollison, 1946; Beattie *et al.*, 1948; Walters *et al.*, 1947; and Keys *et al.*, 1950). As regards the extracellular space, all the investigators agree upon its increase which even outlasts the disappearance of the clinically recognisable oedema during the recovery period. The plasma volume per kg. of body weight of such patients is reported either within the normal range given by Gibson and Evans (1937) or increased. Some of these investigations were carried out in patients with hypoproteinemia, others in persons having a more or less normal serum protein concentration. Well controlled animal experiments (Metcoff *et al.*, 1945; Weech *et al.*, 1937) have shown a contraction of circulating plasma volume as a result of dietary protein deficiency which has caused hypoproteinemia.

To clarify the situation it appears appropriate to consider the cases with hypoproteinemia separate from those having normal serum proteins. Such a distinction permits correlation of clinical observations on hypoproteinemic patients with the condition in experimental animals mentioned above. The investigations reported here are therefore restricted to such cases having lowered serum proteins.

There is another point which deserves consideration: it is common experience with patients suffering from nutritional oedema that they very often lose their swelling within a short time after admission to the hospital by diuresis. It is obvious that the relative size of the fluid compartments undergoes considerable changes during this period so that the plasma volume will alter in relation to the time of measurement. The significance of this point will be illustrated by the results of repeated estimations of the plasma volume in each individual patient in different stages of the disease as reported in this paper.

MATERIALS AND METHODS

Eighty-three patients were subjected to the investigations. The diagnosis was arrived at by considering the following points:—

- (1) History of poor dietary intake or conditioned nutritional deficiency.
- (2) Presence of oedema, being generalised from the start or starting from the lower extremities.
- (3) Absence of signs of portal obstruction, cardiac failure or albuminuria.
- (4) Absence of marked anaemia.
- (5) Absence of any congenital abnormalities like Milroy's disease, etc.

Cases in which malnutrition was secondary to other diseases like tuberculosis, malignant tumour, etc., were not included.

After admission to hospital, the patients were simply put under observation, the daily weight (under standard conditions) and urinary output charted. If

* Indian Council of Medical Research Fellow: May and Baker Fellow from 2-4-1953.

during a period of two days following admission to the hospital, the weight remained steady or was on the increase and the urinary output was less than 500 ml. on an unrestricted fluid intake, the patients were placed under group A. Out of the 83 patients investigated 25 belonged to this group according to the criteria given. If, however, they manifested diminution of weight, decrease of oedema and polyuria they were placed under group B which consisted of the remaining 58 patients. On the third day after admission the plasma volume, thiocyanate space, total serum protein, albumin and globulin were estimated. The tests were repeated at an interval of 1-2 weeks.

The plasma volume and thiocyanate space (C.N.S.) were determined simultaneously by the method of Gregersen and Stewart (1939). The total serum proteins, albumin and globulin were estimated by the microkjeldahl technique and later on in the course of the investigations by the method of Greenberg (1929).

The following results were obtained in the first series of estimations following admission (mean and standard deviations are given in each case):—

No. of cases	Plasma vol. (ml.)	Plasma vol. (ml./kg.)	Cell vol. (%)	C.N.S. space (ml./kg.)	Total serum protein (g.%)	Serum albumin (g.%)
GROUP A:						
25	1849 ± 266	43.7 ± 2.2	28 ± 1.0	398 ± 18	4.8 ± 0.3	1.9 ± 0.4
GROUP B:						
58	2876 ± 216	71.9 ± 4.4	22.5 ± 1.3	376 ± 44	4.9 ± 0.2	1.7 ± 0.8
Normal controls (figs. taken from Chaudhuri <i>et al.</i> (1951 a, b.))						
	1591 ± 180	47.7 ± 8.1		236.3 ± 30.8		

It is obvious that the mean plasma vol./kg. in the patients in group A is much less than that in group B, the difference being statistically significant at 0.01% level; it is even lower than that in the average normal persons found by Chaudhuri *et al.* (1951a) for Indians and as also found in our normal controls. So long as the patients in group A did not develop diuresis and lose weight, their plasma vol./kg. did not show any significant change as found by repeated estimations. When as a result of treatment (high caloric protein rich diet, plasma infusion, amino acid administrations and supplements of vitamin concentrates *) these patients developed diuresis and started losing weight and oedema, their plasma volume became markedly increased. It is interesting to note here that not only the relative plasma volume (per kg. body weight) was increased but there was an increase of absolute plasma volume as well which means that the loss of weight could not simply account for the relative increase of plasma volume/kg. The average values shown by these patients during the period of recovery were as follows:—

No. of cases	Plasma vol. (ml.)	Plasma vol. (ml./kg.)	Cell vol. (%)	C.N.S. space (ml./kg.)	Total serum protein (g.%)	Serum Albumin (g.%)
GROUP A:						
25	2808 ± 358	70.7 ± 4.4	23.5 ± 1.2	336 ± 26	4.9 ± 0.2	1.8 ± 0.5

* Litrison, Hoffmann La Roche.

It can be further observed that these changes in body fluid distribution are not accompanied by any significant change in total serum protein concentration. It is only some time after the patients lost their oedema, that the serum protein level went up.

Seven seriously ill patients, on admission belonging to group A, had moderate to severe oedema, profuse diarrhoea and very low blood pressure. They were particularly interesting because they had clinical signs of dehydration, i.e., a dry tongue, pinched features and circles around the eyes in spite of their oedema. Their weight remained steady, urine varied from 180–240 ml./24 hours, their anaemia was not marked, cell volume was about normal, erythrocyte sedimentation rate (E.S.R.) was 1–4 mm. with the Westergren scale; plasma volume was between 41–44 ml./kg., C.N.S. space was 398–422 ml./kg. They remained like this, critically ill, with the signs of dehydration persisting so long as the diarrhoea continued. When the number of stools became reduced and they started to improve, the signs of dehydration cleared up. But the weight increased and oliguria persisted. The haemoglobin concentration (per 100 c.c. blood) now was about half of that observed on admission, cell volume decreased, E.S.R. rose markedly (60–110 on the Westergren scale) and plasma volume became increased. Strikingly enough, the thiocyanate space at this period showed diminution to the extent of 2–4 litres though there was no diuresis and loss of weight. Shortly afterwards these patients developed increased urinary output and followed the usual pattern of recovery as in the other patients belonging to group A.

The further course undergone by the patients in group A, once the diuresis started, followed closely the pattern in group B. Gradually the patients lost weight and oedema, the plasma volume remained high for some time and then started to return to normal. But though the oedema could no longer be detected clinically, the thiocyanate space was still high. There was a lag period when, although there was no gain or loss of weight and the patients were not clinically oedematous, the thiocyanate space became progressively reduced and it is only after that, that the serum proteins increased.

Two patients belonging to group A deserve special mention because they redeveloped oedema during the progress of the investigation. On admission they had reduced plasma volume, increased C.N.S. space and normal E.S.R.; however after a few weeks' stay they started diuresis, lost weight and their oedema subsided. During this recovery period the same change in the body fluid distribution occurred as mentioned before, i.e., the plasma volume increased, C.N.S. space diminished, there was hemodilution and increased sedimentation rate. Then, for no apparent reason, the patients suddenly gained weight and became oedematous. At that stage, the plasma volume again diminished, C.N.S. space slightly increased and there was the same diminution of sedimentation rate as originally.

In six patients belonging to group A mercurial diuretics were administered intramuscularly being preceded by ammonium chloride. There was diuresis during the next 24 hours. The plasma volume, however, showed no significant change.

DISCUSSION

From these investigations it becomes clear that two phases can be distinguished in the course of the nutritional oedema. As the oedema develops the plasma volume becomes reduced on a weight basis as well as on an absolute scale, whereas it appears increased during the recovery phase. The question now arises whether the initial reduction of the circulation plasma volume can be regarded simply as one of the features of the disease or whether it is a primary event in the course of the disease leading to a reduced glomerular filtration rate (Cort, 1952) and 'glomerulo-tubular imbalance'—a condition, which, under appropriate circumstances, will lead to sodium retention. In any case, this initial phase of the disease is markedly different

from the oedema due to cardiac failure or hepatic cirrhosis, since in both cases an increased plasma volume has been repeatedly observed (Gibson and Evans, 1937; Perera, 1946). The suggestion that the reduction of serum albumen gives rise to the decrease of plasma volume (Weech, 1938) is not supported by the observations of Mollison (1946) and Beattie *et al.* (1948) and by our own data, since we regularly observed that the return of the body fluid distribution to normal is not linked up with a concomitant alteration of the serum protein concentration.

Although there is oedema and expansion of the thiocyanate space, the patients appear dehydrated considering their reduced plasma volume—a fact which is even confirmed by the presence of clinical signs of dehydration in some of them; an excess production of antidiuretic hormone could, therefore, be assumed. Gopalan (1950) seemed to have succeeded to demonstrate an increased amount of antidiuretic substances in the urine of such patients, but other workers (Saha and Sengupta, 1952), have failed to confirm it.

On the basis of these observations, it does not seem justified to attribute to the decrease of the serum protein level a primary rôle in the genesis of the oedema as assumed in the Starling hypothesis (Starling, 1908). However, the possibility exists as shown by Ayer, Schiess and Pitts (1947) in experiments on dogs and by Dicker (1948) on rats, that the glomerular filtration rate is decreased in the presence of hypoproteinemia. Besides, the glomerular filtration rate is no longer independent of the rate of urine flow in the presence of hypoproteinemia (Dicker, 1949). It is furthermore known that an artificial alteration of plasma colloid content by means of infusion of albumin (Welt and Orloff, 1949) exerts a considerable influence on the excretion of water and salts, infusion of hyperoncotic solutions causing a reduction of sodium excretion, that of iso-oncotic solutions producing increased excretion of water; but both the hyperoncotic as well as the iso-oncotic infusion cause increase of the circulating blood volume. Rapid administration of albumin causes in addition a marked increase of the total renal plasma flow, possibly by opening previously closed arterio venous anastomosis (Michie *et al.*, 1949; Barker *et al.*, 1949). These facts indicate that the balance of at least two forces, namely the colloid osmotic pressure and the plasma volume, determine in some way the excretory function of the kidney. Possibly the size of the extracellular fluid compartment also influences the urinary output, since in oedematous subjects even hyperoncotic solutions have diuretic effect (Orloff, Welt and Stowe, 1949). If the decrease of the serum protein level is the primary cause at all for the water retention, then it appears to be so because of the colloid osmotic pressure being one of the conditioning factors for water and salt excretion through the kidney and not because of the disturbance of the Starling equilibrium.

During the development and the height of the disease a paradoxical state exists where the plasma volume is reduced but the thiocyanate space is increased. The disturbance of the fluid compartments seems, however, to be even more complicated than already mentioned. During the recovery phase in these patients a stage was observed in which the thiocyanate space became reduced, though there was no alteration in weight and urinary output. A transfer of water from extracellular into intracellular space must have taken place as the simultaneous increase of plasma volume cannot account for more than a small fraction of the diminution of the extracellular fluid. We do not know to what extent a potassium depletion arising from the associated diarrhoea contributes to the observed disturbance of the fluid distribution. Eliel *et al.* (1950) have recently shown that, in such a condition, intracellular dehydration can occur concurrently with expansion of the extracellular fluid compartment. Possibly as the patients recover, their tissue protein content increases towards normal thus accounting for a water movement from outside into the intracellular space. Of course, we do not know the degree of protein depletion in the tissues, however, the reduced serum protein level certainly indicates that some degree of tissue protein depletion must be present. Besides there is evidence

that the proportion of osmotically inactive base within the cells may vary under certain circumstances (Elkinton *et al.*, 1948) and malnutrition might represent an instance which alters that proportion.

One particular fact noticed in the patients of group B is the lack of any correlation between the circulating plasma volume with total serum protein concentration. In this respect and in the subsequent course of the disease, they resemble the patients of group A during the recovery period. There is no reason to assume that a basic difference of the pathological process exists between the patients of group A and group B; they simply represent different stages of one and the same disease.

The possible part played by the proteins in the development of the nutritional oedema has been considered before. Unfortunately no data are yet available to ascertain the significance of sodium, the main ionic constituent of the extracellular fluid, in that condition. Based on the well-supported observation that in most instances isotonicity is more carefully guarded by the body than the constancy of the fluid volume (Peters, 1947), we would expect sodium retention at the onset of the oedema; but Schroeder (1949) has demonstrated that oedema is also compatible with the presence of a 'low salt syndrome'. Particularly the clinical signs of dehydration observed in some patients together with the reduction of the plasma volume at the initial stage of the disease might reflect a chronic sodium depletion (Black, 1953). The constantly observed diarrhoea certainly gives sufficient reason to suspect such a condition. Besides, salt depletion is known to impair the elimination of water through the kidney (McCance and Widdowson, 1937; Baldes and Smirk, 1934) and the existence of such a markedly impaired water excretion was repeatedly demonstrated in our patients of group A by administering a water load by mouth: no significant amount of extra urine was produced in such tests; moreover the urine maintained its hypertonicity with respect to the osmotic pressure of serum. Leaf and Mamby (1952) have recently shown, that conditions exist which cause conservation of water irrespective of serum solute levels; those authors believe that the constancy of the extracellular fluid tonicity is sacrificed in these cases and water is retained to maintain the fluid volume high: low salt intake or salt loss combined with ad libitum water intake seems to trigger this volume conserving antidiuretic mechanism which, together with the hypoproteinemia, appears to determine the symptomatology of nutritional oedema.

SUMMARY

Plasma volume, thiocyanate space, total serum proteins and albumin concentration were determined in 83 patients suffering from nutritional oedema. The patients could be divided into two groups (A and B) according as they were gaining or losing oedema on rest in bed. The plasma volume/kg. in group A (43.7 ± 2.2 ml./kg.) was significantly lower than that in group B (71.9 ± 4.4 ml./kg.). This lowered plasma volume persisted in the patients in group A till they developed diuresis and commenced losing oedema. They had signs of haemoconcentration as well and seven patients manifested clinical signs of dehydration. When they started to lose the oedema their plasma volume increased (70.7 ± 4.4 ml./kg.) and approached that in group B. The thiocyanate space was increased considerably at the start but remained higher than normal, even when there was no clinically detectable oedema in both groups. No correlation was found between the serum protein concentration and the changes in the distribution of the body fluid.

REFERENCES

- Ayer, J. L., Schiess, W. A. and Pitts, R. F. (1947). Independence of phosphate reabsorption and glomerular filtration in the dog. *Am. J. Physiol.*, **151**, 169.
Baldes, E. J. and Smirk, F. H. (1934). The effect of water drinking, mineral starvation and salt administration on the total osmotic pressure of the blood in man, chiefly in relation to problems of water absorption and water diuresis. *J. Physiol.*, **82**, 62.
Barker, H. G., Clark, J. K., Crosby, A. P. and Cummins, A. J. (1949). The effect of salt poor human albumin on renal oxygen consumption. *Am. J. Med. Sc.*, **218**, 715.

- Beattie, J., Herbert, P. H. and Bell, D. J. (1948). Famine Oedema. *British Journal of Nutrition*, **2**, 47.
- Black, D. A. K. (1953). Body fluid depletion. *Lancet*, **1**, 305 and 353.
- Chaudhuri, R. N., Chakrabarti, H. and Dutta, B. N. (1951a). Blood volume in healthy Indians. *Ind. Jour. Med. Res.*, **39**, 237.
- Chaudhuri, R. N., Chakravarti, H. and Dutta, B. N. (1951b). Estimation of extracellular fluid by thiocyanate in healthy Indians. *Ibid.*, **39**, 553.
- Cort, J. H. (1952). The renal response to extra renal depletion of the blood volume. *J. Physiol.*, **116**, 307.
- Dicker, S. E. (1948). Diuresis in hypoproteinaemic animals. *Biochem. J.*, **43**, 453.
- Dicker, S. E. (1949). Effect of the protein content of the diet on the glomerular filtration rate of young and adult rats. *J. Physiol.*, **108**, 197.
- Elliel, L. P., Pearson, O. H. and Rawson, R. W. (1950). Post-operative potassium deficit and metabolic alkalosis. *New England J. Med.*, **243**, 471.
- Elkinton, J. R., Winkler, A. W. and Danowski, T. S. (1948). Transfer of cell sodium and potassium in experimental and clinical conditions. *J. Clin. Invest.*, **27**, 74.
- Gibson, J. G. and Evans, W. A. (Jr.) (1937). Clinical studies of blood volume. *J. Clin. Invest.*, **16**, 317.
- Gibson, J. G. and Evans, W. A. (Jr.) (1937). Clinical studies of blood volume. *Ibid.*, **16**, 851.
- Greenberg, D. M. (1929). The colorimetric determination of the serum proteins. *J. Biol. Chem.*, **82**, 545.
- Gregersen, M. I. and Stewart, J. D. (1939). Simultaneous determination of plasma volume with T-1824 and the available fluid volume with sodium thiocyanate. *Am. J. Physiol.*, **125**, 142.
- Gopalan, C. (1950). Antidiuretic factor in urine of patients with nutritional oedema. *Lancet*, **1**, 304.
- Keys, A., Brozek, J., Henschel, A., Mickelsen, O. and Taylor, H. L. (1950). The Biology of Human starvation. Minneapolis University of Minnesota Press, p. 2777.
- Leaf, A. and Mamby, A. R. (1952). An antidiuretic mechanism not regulated by extracellular fluid toxicity. *J. Clin. Invest.*, **31**, 60.
- McCance, R. A. and Widdowson, E. M. (1937). The secretion of urine in man during experimental salt deficiency. *J. Physiol.*, **91**, 222.
- Metcalf, J., Favour, G. B. and Stare, P. J. (1945). Plasma protein and Haemoglobin in protein deficient rats. *J. Clin. Invest.*, **24**, 82.
- Michie, A. J., Gimbel, N. S. and Riegel, C. (1949). Renal hemodynamics during short and long periods of salt poor albumin administration. *Fed. Proc.*, **8**, 110.
- Mollison, P. L. (1946). Observations on cases of starvation at Belsen. *British Med. J.*, **1**, 4.
- Orloff, J., Welt, L. G. and Stowe, L. (1949). The effects of salt poor albumin on the excretion of water and electrolytes in oedematous patients. *J. Clin. Invest.*, **28**, 802.
- Perera, G. A. (1946). The effect of significant weight change on the predicted plasma volume. *Ibid.*, **25**, 491.
- Perera, G. A. (1946). Plasma volume in Laennec's cirrhosis of liver. *Ann. Int. Med.*, **24**, 643.
- Peters, J. P. (1947). Water balance in Health and Disease. In: G. Duncan, Diseases of Metabolism. Saunders.
- Saha, H. L. and Sengupta, K. (1952). Body fluid distribution and anti-diuretic hormone in urine in different types of oedema. *J. Ind. Med. Ass.*, **22**, 1.
- Watters, J. H., Rossiter, R. J. and Lehmann, H. (1947). Blood volume changes in protein deficiency. *Lancet*, **1**, 244.
- Starling, E. H. (1908). The fluids of the body. The Herter Lectures, New York.
- Weech, A. A., Wollstein, A. and Goettsch, E. (1927). Nutritional, oedema in dogs. *J. Clin. Invest.*, **16**, 719.
- Weech, A. A. (1938-39). The Harvey Lecture Series, 34, 57, William and Wilkins Co., Baltimore.
- Welt, L. G. and Orloff, J. (1949). Effects of infusion of albumin on the excretion of water and electrolytes in normal subjects. *J. Clin. Invest.*, **28**, 818.

TYROSINASE ACTIVITY IN RELATION TO PHENOLIC TANNING OF THE CUTICLE IN *CARCINUS MAENAS*

by G. KRISHNAN, Department of Zoology, University of Madras

(Communicated by S. L. Hora, F.N.I.)

(Received May 10; read October 9, 1953)

CONTENTS

	Page
1. Introduction	157
2. Material and Methods	157
3. Tyrosine and Tyrosinase in the Blood	158
4. Redox Potential of the Blood and Tyrosinase Activity	159
5. Cyanide-Insensitive Respiration and Redox Potentials	161
6. Hormonal control of Tyrosinase Activity	163
7. Discussion	166
8. Summary	167
9. Acknowledgements	168
10. References	168

I. INTRODUCTION

It has been suggested that the mechanism of tanning of the cuticle in Crustacea may be similar to that in insects (Dennell, 1947*b*) but very little is known of the processes resulting in the formation of polyphenols involved in tanning. However, evidence of the existence of the necessary polyphenol-producing mechanism is given by the occurrence of a tyrosine-tyrosinase system in crustacean blood (Pinhey, 1930). A fluctuation in tyrosinase activity noted by Pinhey in *Maia squinado* and *Cancer pagurus* is probably significant in relation to tanning of the cuticle (Dennell, 1947*b*). But the factors responsible for this variability and the nature of the regulation of the formation of polyphenols are unknown. A suggestive line of approach to this problem may be found in the observation of Dennell (1949) that in *Calliphora erythrocephala* a factor holding in check the oxidative activity of tyrosinase may result from the presence of a dehydrogenase system showing a fluctuation correlated with tyrosine oxidation. A balance between tyrosinase activity and a dehydrogenase system both controlled by hormones appears to exist in blowfly larva. The hormonal control of pupation in the blowfly larva first suggested by Fraenkel (1935) and later shown to occur in other Diptera is exercised by Weismann's ring (Hadorn, 1937; Burt, 1938) which is homologous with the corpora allata and corpora cardiaca of other insects (Burt, 1937; Day, 1943). It has been pointed out that the hormones secreted by the corpus cardiacum-allatum system show physiological effects similar to those of the sinus gland located in the eyestalks of decapod Crustacea (see Hanstrom, 1949). It is therefore of interest to examine what part, if any, the sinus gland hormone plays in relation to tanning of the cuticle and how far the mechanism of control of tanning in Crustacea corresponds to that in insects. A preliminary account of the findings has been given elsewhere (Krishnan, 1950).

2. MATERIAL AND METHODS

This work has been carried out in *Carcinus maenas* Pennant obtained living from Plymouth and Millport laboratories and on material collected while working

at the Marine Biological Laboratory, Plymouth. For the estimation of tyrosine in the blood, the colorimetric method of Folin and Denis (1912) was used. The fructose determinations were made by the method elaborated by Roe (1934) based on the Selivanoff reaction. An evaluation of the reducing power of blood in different stages of the moult cycle was made by measurement of electrode potentials using a Cambridge pH meter as a voltmeter. The cyanide-insensitive respiration of blood and soft parts which showed significant variations in the course of the moult cycle was estimated under various experimental conditions using a Barcroft differential respirometer and the values obtained were taken to indicate the activity of an enzyme system. The rôle of the eyestalk hormone in relation to phenolic tanning was studied by noting the effects of eyestalk extirpation on the enzyme system involved as indicated by the cyanide-insensitive oxygen uptake.

3. TYROSINE AND TYROSINASE IN THE BLOOD

Tyrosine which appears to be the precursor of polyphenols in insects, is known to occur also in crustacean blood which blackens on exposure, a feature recognised as indicating the oxidation of tyrosine to form melanic pigments (Heim, 1892; Hemmingsen, 1924; Pinhey, 1930). A further similarity to the condition observed in insects is suggested by a fluctuation in the discoloration of the blood in different individuals and in the same individual at different periods (Pinhey, 1930). Such variations in insects have been shown to be significant as indicating a regulation of tyrosinase activity in relation to tanning of the cuticle (Dennell, 1947a). The occurrence of similar variations in crustaceans such as *Maia* and *Cancer* might suggest, as has been pointed out by Dennell (1947b) a relationship to the elaboration of polyphenols. But it is not known whether there occurs as in insects a rhythm in tyrosinase activity, whether the variations if present are due to quantitative changes in the enzyme or the substrate or both and if when both tyrosine and tyrosinase are present the internal environment has a determining influence on tyrosinase activity.

With this object in view the blood of *Carcinus* was examined in different stages of the moult cycle. As the crabs kept in the laboratory tanks moulted only infrequently, the various stages in the moult cycle were collected fresh from their natural environment. To minimise discrepancies arising from the difficulty of fixing the time interval since moulting the averages of two or more evaluations made in similar stages have been taken for purposes of comparison. The phases in the moult cycle recognised in the following study are those described by Baumberger and Olmsted (1928) which are (a) the hard crab stage (b) the 'pillans' stage representing the condition a few days before ecdysis, (c) the moulting stage in which the crab is in the process of emerging from the old shell, (d) the soft crab characterised by a soft cuticle, and (e) the paper shell stage in which the cuticle is only very slightly hardened. Blood from all stages exposed on filter paper turned black, but marked gradations were shown in the intensity of blackness as may be seen from Table I.

TABLE I

	Moulting stage.	Soft crab.	Paper shell crab.	Hard crab.	Pillans.
Blood (untreated)	++	+	++	++	++++
Blood + KCN	---	---	---	---	---
Blood + methyl alcohol	+	+	+++	++++	++++

If the degree of intensity of blackness is an indication of the extent of enzyme activity as may be inferred from the lack of darkening in the presence of cyanide it may appear that tyrosinase shows fluctuations in activity in different periods of the moult cycle. An additional indication that an enzyme present in the blood is responsible for the blackening of shed blood is provided by the positive reaction with the 'NADI' reagent which has been extensively used to detect tyrosinase and polyphenol oxidases on account of the oxidation it undergoes in their presence.

The feeble darkening of exposed blood of crabs soon after moulting is probably due to a reduction of tyrosinase in the blood. This may be inferred from the suggestion of Pinhey (1930) that tyrosinase is contained in the haematocytes which as observed by Baumberger and Olmsted (1928) are fewer in number at the time of moulting when the blood is much diluted due to a marked absorption of water. If the tyrosinase of the blood is involved in tanning of the cuticle, only very little of it may be expected to be found in the blood at this stage since phenolic hardening is complete immediately after moulting. In the stages following there is a noticeable upward trend in the blackening effect which is most marked in the pillans stage when the new cuticle is being laid down and tanned before its exposure at the time of moulting. Such variations may be attributable to quantitative changes in tyrosinase or to changes in the tyrosine content of the blood. It also appears likely that variations in the inhibition of tyrosinase activity may account for the above observations. Qualitative tests for tyrosine in the blood of *Carcinus maenas* using Morner's reagent and α -nitroso- β -naphthol gave positive reactions indicating the presence of tyrosine (Feigl, 1947) at all stages of the moult cycle. With a view to determine whether the amount of tyrosine varies in different stages, a colorimetric estimation of tyrosine was made using the 'phenol reagent' (Folin and Denis, 1912). It was found that the amount of tyrosine present in the blood was approximately constant, the average value being 0.003%. Pinhey (1930) obtained for *Cancer pagurus* an average value of 0.004%. She found that tyrosine is always present in the blood and is in excess of requirements for oxidase activity, as seen by the fact that when to the blood which has ceased to blacken a small amount of blood which does show blackening is added, discoloration at once appears showing that the blood must have contained the substrate as the 'blackening is very much more intense than that which could be produced from the action of the added enzyme on the small amount of substrate necessarily added with it'. From the observations made on *Carcinus* it may be inferred that tyrosine and tyrosinase are present at all stages of the moult cycle but it is the enzyme which shows a variation in activity.

4. THE REDOX POTENTIAL OF THE BLOOD AND TYROSINASE ACTIVITY

In spite of the presence of both tyrosine and tyrosinase there is no evidence of tyrosinase activity in the blood of intact animals as may be inferred from the absence of a positive ferric chloride test in the blood drawn from the animal in the different stages of the moult cycle. Possibly the elaboration of dihydroxyphenols is confined to a very brief period when they may occur in a concentration too low to be revealed by colour tests. Such a condition is explicable in view of the short duration of the tanning process in this animal. If the above assumption is valid it would appear that the oxidation of tyrosine is held in check by some inhibiting factor probably present in the blood.

Previous authors have emphasized the importance of the oxidation-reduction potentials of the medium in determining biological oxidations. Graubard (1933) observed that tyrosinase activity in *Drosophila melanogaster* is dependent on the state of the environment which enables the enzyme present to be involved in the reaction. Similarly Figge (1940) showed that tyrosinase is active only within a certain range of redox potentials and that any shift of potential from the optimum

either to the negative or positive side would inactivate the enzyme. That this holds good not only in vitro but also in vivo is shown by the observations of this author that phenol-indophenol with an E^0 value of $+0.227$ at pH 7 produces palor in amphibian larvae by inhibiting tyrosinase in melanophores although it stimulates melanogenesis in the connective tissue cells. The differential reaction of cells to the same substance is explained in the light of the view mentioned above that tyrosinase is active at an optimum potential. It has been pointed out that the melanophores maintain a more positive and connective tissue cells a more negative potential so that with the addition of phenol-indophenol there is a shift of potential away from the optimum in the melanophores and towards the optimum in the connective tissue cells thus accounting for the opposite responses observed. Further Dennell (1947a) suggested that the oxidation of tyrosine in the third larval instar of *Sarcophaga* before puparium formation is prevented by the low redox potential of the blood.

In the light of the above observations the redox potential of the blood of *Carcinus* was studied. It is realized that blood may contain a complex mixture of reducing substances whose proportion may affect the redox potentials of the blood. But it is known from the work of Kuwana (1937) that the reducing power of the blood of silkworm shows a stable and unstable part the latter disappearing on exposure concurrently with the darkening of the blood. That this unstable reducing power may be due to a dehydrogenase which is diminished on exposure, has been suggested by Dennell (1949) as a result of observations in the larva of *Calliphora erythrocephala*. In the following study an attempt has been made to estimate the unstable reducing power of the blood (see Dennell, 1947b) whose disappearance or diminution on exposure is accompanied by melanosis. For this purpose the electrode potentials of the blood as soon as drawn, in the different stages of the moult cycle was determined using the Cambridge pH meter, with a saturated KCl-calomel electrode of potential of $+0.250$ V at 20°C . ($+0.076$ MV for 1°C .) as a reference electrode.

TABLE II

No.	Moulting stage.	Soft crab.	Paper shell crab.	Hard crab.	Pillans.
1	$+0.283$ V	$+0.320$ V	$+0.272$ V	$+0.260$ V	$+0.355$ V
2	$+0.295$ V	$+0.308$ V	$+0.270$ V	$+0.250$ V	$+0.318$ V
3	$+0.286$ V	$+0.304$ V	$+0.280$ V	$+0.218$ V	$+0.333$ V
4	$+0.292$ V	$+0.290$ V	$+0.286$ V	$+0.242$ V	$+0.320$ V
5	..	$+0.296$ V	$+0.288$ V	$+0.216$ V	$+0.332$ V
6	..	$+0.302$ V	$+0.276$ V	$+0.242$ V	$+0.322$ V
Average ..	$+0.289$ V ± 0.006	$+0.303$ V ± 0.017	$+0.279$ V ± 0.009	$+0.238$ V ± 0.022	$+0.330$ V ± 0.025

Table II and fig. 1 show the average values of redox potentials of the blood of *Carcinus* in different stages of the moult cycle. It is seen that the values show a rise sometime before moulting and at the time of shedding the exuvium the potential falls below the level before and after the process. The oxidation-reduction characteristics of the blood indicate a correlation with the active and inactive periods of tyrosinase activity of the blood in the course of the moult cycle, the potentials being high at the pillans stage when tyrosinase activity as seen by the blackening of blood is most marked.

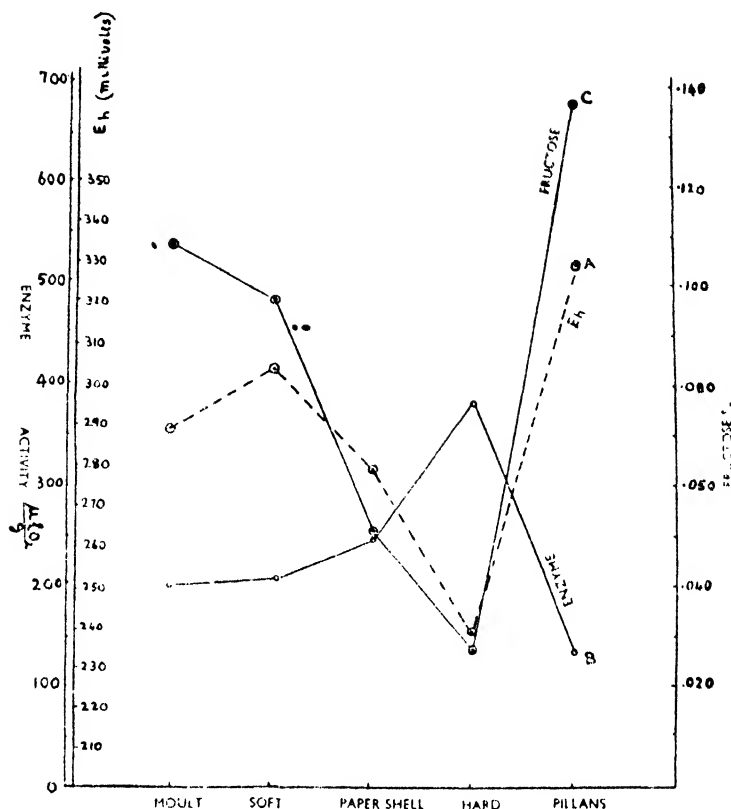


FIG. 1.—Variations in redox potentials of the blood, enzyme activity and fructose values in the course of the moulting cycle of *Carcinus maenas*.

Abscissae, Stages in moulting cycle; Ordinates: (i) Redox potentials of the blood in millivolts; (ii) Enzyme activity expressed as O_2 uptake $\left\{ \frac{\mu_1 \cdot \text{O}_2}{g. \text{ tissue}} \right\}$; (iii) Fructose as gm. % of tissue. Curve A—Redox potentials. Curve B—Enzyme. Curve C—Fructose content.

5. CYANIDE-INSENSITIVE RESPIRATION AND REDOX POTENTIALS

Discussing the causes of the reducing power of insect blood Dennell (1947a) observed that the mere presence of reducing substances such as glucose, uric acid or ascorbic acid cannot by themselves account for the reducing power, which as noted by Kuwana (1937) shows a stable and unstable fraction, the latter disappearing on exposure. From the observation that this unstable reducing power may be removed by treatment with narcotics such as urethane, chloroform (Graubard, 1933; Dennell, 1947a) it is inferred that the agency responsible may be of the nature of dehydrogenases which are known to be susceptible to the action of narcotics. Further in *Calliphora erythrocephala* a study of the cyanide-insensitive respiration revealed variations apparently correlated with tyrosinase activity and it has been suggested that the cyanide-insensitive respiration may reflect the activity of a dehydrogenase system (Dennell, 1949). With this possibility in view the blood of *Carcinus* was treated with thymol, urethane and other narcotics but these substances did not produce any appreciable effect on tyrosinase activity. However, it has been observed that the blood of hard crabs darkens more intensely in the presence of methyl alcohol indicating an increase in tyrosinase activity. It has been suggested that the above reaction may be due to the removal of an inhibiting enzyme probably

susceptible to methyl alcohol (see Dennell, 1947a; Fraenkel and Rudall, 1947). The action of methyl alcohol was found to have varying effects in the different stages of the moult cycle. Blood from soft crabs did not blacken as markedly in the presence of methyl alcohol as that of crabs in the middle stages of the inter-moult period, suggesting a fluctuation in the activity of the enzyme concerned. A correlation between such a fluctuation of enzyme activity and the oxygen uptake of blood and soft parts of the crab in the presence of cyanide suggested that the enzyme-system indicated thereby may be involved in tyrosine oxidation. To determine whether this is indeed correlated with tyrosine oxidation a detailed study of the cyanide-insensitive respiration in different periods of the moult cycle was made.

Enzyme activity though indicated when blood only was used, the values obtained were low compared to those recorded with extracts of muscles. In the following experiments muscle extracts were used. The tissues were ground well with sand in distilled water and the ground tissue after several washings was suspended in 5 ml. of $M/15$ K_2HPO_4 and shaken for about forty minutes. After centrifugation the supernatant fluid was used. 2.5 ml. of the extract and 2.5 ml. of 1% KCN were taken together in the right hand flask of the respirometer and an equal quantity of phosphate buffer and KCN added to the left hand flask. Under these conditions the extract did not show any oxygen uptake. However, the addition of either glucose or fructose to the extract caused an immediate oxygen uptake indicating the presence of an enzyme system capable of catalysing the oxidation of these substrates. It is to be noted that the addition of fructose caused a greater uptake than the addition of glucose. The enzymic nature of the reaction was indicated by the absence of an oxygen uptake when the extract was previously boiled. With fructose as the added substrate marked fluctuations in the oxygen uptake were noted in the different stages of the moult cycle. Therefore a detailed study of the cyanide-insensitive oxygen uptake in the course of the moult cycle was made. The oxygen uptakes were referred to the dry weight of the tissues after extraction and the values expressed as $\frac{\mu l. O_2}{g. \text{ tissue}}$ during thirty minutes. The

experimental temperature was maintained at 20°C. In referring the oxygen uptakes to the dry weight of tissues, it is realized that marked changes in the composition of tissues in the course of the moult cycle (Hoet and Kerridge, 1926) render the values as obtained above not strictly comparable. But such an anomaly could not be overcome by using wet weights as the water content of the crabs is subject to very wide fluctuations (Maluf, 1939). However, since the object of these estimations is to note the fluctuations in enzyme activity in relation to moulting rather than the determination of absolute values, a certain exaggeration of the values in the early stages after moulting may not vitiate the overall trend of events. The values obtained in the course of the moult cycle are given in Table III.

It should be pointed out that in the above experiments when tissue extracts were used without addition of fructose there was no oxygen uptake. Possibly the naturally occurring substrate of the enzyme was lost in the process of extraction described above or more likely was soon metabolized in this preparation and the added fructose served as a substitute. It was therefore of interest to find whether fructose normally occurs in the tissues and the body fluid and if so whether it shows quantitative changes which may be related to enzyme activity noted above. A quantitative estimation of fructose in the tissues and blood was made by the method of Roe (1934). While the fructose content of the blood was low, with extracts of muscles quite appreciable quantities were indicated. For estimating fructose in the muscles the aqueous extracts of tissues were treated in the same way as for blood and the values obtained were referred to the dry weight of the tissue used for extraction and expressed as gm. % of tissue. Care was taken to see that the stages in which the fructose estimations were made were identical with those used

TABLE III

Enzyme Activity expressed as $\frac{\mu_1 \cdot O_2}{g. \text{ tissue}}$ (with added fructose).

No.	Moulting stage.	Soft crab.	Paper shell.	Hard crab.	Pillans.
1	159	171	200	413	111
2	216	181	236	318	120
3	196	188	187	427	148
4	214	193	289	385	113
5	..	188	222	315	127
6	..	278	282	450	204
Average ..	196	200	236	385	137

for enzyme estimation. The variations in the fructose values in the course of the moult cycle are shown in Table IV and fig. 1.

TABLE IV

Fructose in gm. %.

No.	Moulting stage.	Soft crab.	Paper shell crab.	Hard crab.	Pillans.
1	0.117	0.088	0.051	0.026	0.167
2	0.094	0.089	0.053	0.036	0.113
3	0.083	0.109	0.053	0.029	0.170
4	0.132	0.112	0.057	0.024	0.173
5	..	0.085	0.055	0.019	0.095
6	..	0.091	0.043	0.021	0.094
Average ..	0.107	0.096	0.052	0.026	0.135

A correspondence is apparent between the values for fructose and those for enzyme activity, the latter varying inversely with the former (fig. 1). It is noteworthy that the lowest values for enzyme activity as determined by the above experiments and the highest electrode potentials occur at the pillans stage when the crab is preparing for moult. This is also the stage at which tyrosinase activity as judged by the darkening of the exposed blood is most evident. It may be suggested that in *Carcinus*, during the intermoult period chiefly represented by the hard crab stage, tyrosinase activity is held in check by the low redox potential which does not permit of the oxidation of tyrosine. Just before moulting at the pillans stage, the potential rises and the consequent oxidation of tyrosine due to tyrosinase activity leads to the production of phenols responsible for the tanning of the new cuticle which will be exposed at the time of moulting.

6. HORMONAL CONTROL OF TYROSINASE ACTIVITY

Although moulting in decapod Crustacea is a comparatively brief process, preparatory changes antecedent to this, extend over several days and involve physiological changes affecting many aspects of the metabolism of the animal.

For several days previous to moulting calcium is withdrawn from the exoskeleton and stored in the hepatopancreas in crabs (Paul and Sharpe, 1916; Robertson, 1937) or in gastroliths in the crayfish (Kyer, 1942; Scudamore, 1947). Changes in the glycogen content of the hepatopancreas have been noted in relation to moulting in *Callinectes sapidus* (Baumberger and Dill, 1928) and in *Carcinus maenas* (Schonborn, 1910). Similarly the blood glucose in *Maia squinado* shows a rise preceding moulting and a fall succeeding it (Drillhon, 1933). Changes in water content and oxidative metabolism have been shown to commence several days before the onset of moulting (Scudamore, 1947). It is now well established that moulting in decapod Crustacea is hormonally regulated by the endocrine activity of the neurosecretory organs located in the eyestalks (Brown, 1944; Scudamore, 1947). Further considerable evidence exists to show that many features associated with moulting such as changes in water content, oxygen consumption, resorption of materials from the cuticle, are also under hormonal control (Kyer, 1942; Scudamore, 1947). In the light of the above observations it is of interest to discover whether the tyrosinase of the blood, the activity of which seems related to ecdysis and hardening of the new cuticle, may also be regulated by the hormones of the eyestalk.

To elucidate the problem whether or not the hormones of the eyestalk control the process of tanning, normal animals have been compared with those in which the eyestalks have been removed, with reference to the cyanide-insensitive respiration, fructose content and tyrosinase activity. For these experiments hard crabs of the same carapace breadth and of similar stage in relation to the moult cycle were chosen to ensure similarity of members of a batch used for experiments. Animals in very early stages of the hard crab phase as indicated by the nature and appearance of the shell were selected. The suitability of such a stage for purposes of these experiments lies in the fact that the hard crab stage represents the longest phase in the moult cycle when it may be presumed that some uniformity of general metabolic features may be established so enabling comparative experimental observations over several days to be made.

For each set of experiments twenty-four male crabs were divided into two groups of twelve each. In one group both eyestalks were extirpated. Caution was not applied as haemorrhage was little and the wound was soon closed by a blood clot. The operated crabs were segregated in individual jars. The remaining twelve animals were used as controls and similarly segregated in individual jars. Each set of experiments was continued for nearly three weeks. During this period a test animal was killed every third day and enzyme activity as indicated by the cyanide-insensitive oxygen uptake with added fructose was estimated. The method followed was the same as in previous experiments. At the same time the fructose values of the muscles were also determined. Tyrosinase activity was estimated by

TABLE V

Days after eyestalk extirpation.	Normal animals.		Operated animals.	
	$\frac{\mu_1 \cdot O_2}{g. \text{ tissue.}}$	Fructose gm. %	$\frac{\mu_1 \cdot O_2}{g. \text{ tissue.}}$	Fructose gm. %.
3 days	318	0.045	118	0.136
6 days	242	0.055	120	0.087
9 days	113	0.173	155	0.102
12 days	127	0.095	180	0.115
15 days	192	0.117	171	0.114
18 days	188	0.160	219	0.107

the observation of the extent of darkening of exposed blood. The values obtained were compared with those of the control animals in the corresponding periods of the experiment. Table V gives the average values of enzyme activity and fructose in control and operated animals.

It was seen that three days after the operation, the eyestalkless animals showed a marked reduction of enzyme activity compared with the control animals (fig. 2). In the later stages of the experiment an increase in enzyme values of the operated animals was noted. From the absence of a uniform decrease of enzyme activity following the eyestalk removal, it would appear that the relation between them may not be a simple and direct one. Experimental animals killed about fifteen days after the eyestalk extirpation showed evidence of an incipient moult but died before completing it. At the corresponding period none of the control animals showed signs of an impending moult. It seemed clear that the eyestalk extirpation in the test animals had hastened the onset of moulting and the reduction of enzyme activity noted above is consistent with this feature. In view of the trends in enzyme

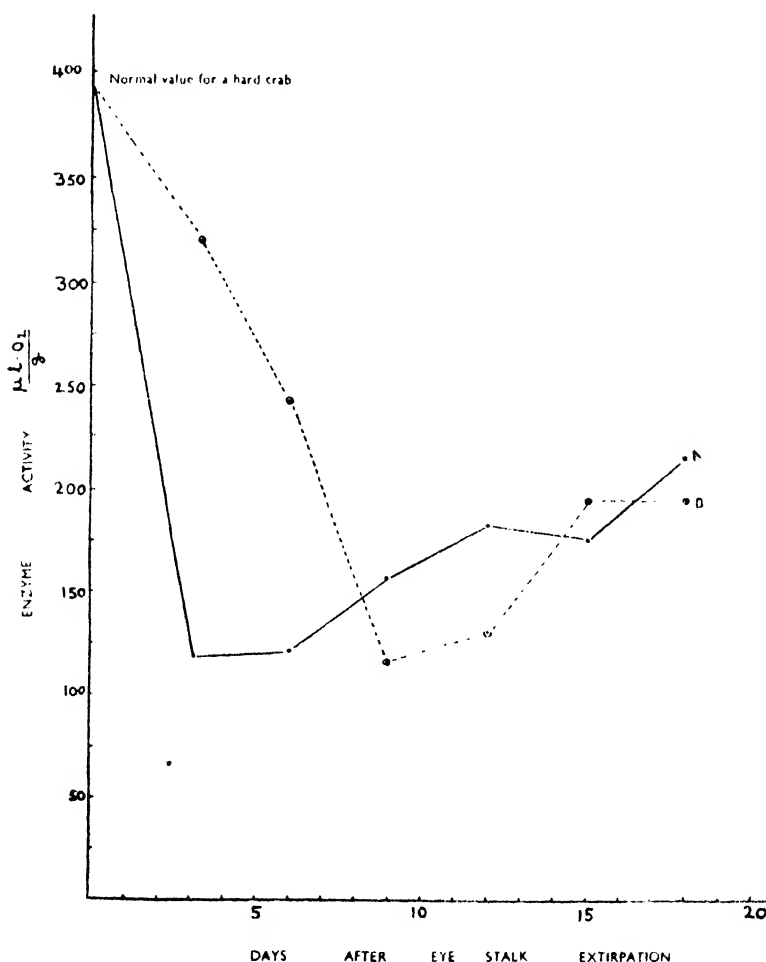


FIG. 2.—Changes in enzyme activity as a result of eyestalk removal. Abscissae, days after eyestalk extirpation; ordinates, enzyme activity expressed as O_2 uptake $\left\{ \frac{\mu_1 \cdot \text{O}_2}{\text{g. tissue}} \right\}$; Curve A changes in experimental animals; Curve B controls in corresponding periods as in the experimental animals.

activity in relation to moult cycle already noted and the effect produced on it by the eyestalk extirpation it may be reasonable to infer that the enzyme activity noted above constitutes only a part of a system controlled by the hormone of the eyestalk. This hormone in normal animals has been shown to have an inhibiting effect on moulting and its elimination seems not only to hasten moulting but also to set in train all the events associated with moulting in advance of their normal occurrence (Seudamore, 1947). It may be inferred from fig. 2 on which a parallel may be seen between Curve B, showing the variations in enzyme activity in the control animals and the Curve A, representing the values in experimental animals, that in the latter the fall and subsequent rise of enzyme activity is advanced in point of time.

In another set of similar experiments paper shell crabs were used instead of hard crabs and over a period of fifteen days the cyanide-insensitive respiration and fructose values were determined. Differing from the effect of eyestalk extirpation in hard crabs there was an irregular rise of oxygen uptake in the experimental animals. The effect of the removal of eyestalks on the enzyme activity at this stage was different from that at a later stage.

Additional experiments to throw light on the relation between eyestalk extirpation and enzyme activity in question have been performed in which the operated animals without eyestalks were at different periods injected with saline extracts of eyestalks of animals in stages corresponding to those of the experimental animals. The amount of extract injected was equivalent to one eyestalk per animal (*see* Brown and Seudamore, 1940). The enzyme activity as indicated by the cyanide-insensitive oxygen uptake was estimated one hour after injection. But in the eyestalkless crabs subsequently injected, the enzyme activity gave anomalous values. In the above experiments it has been noted that a rise in enzyme activity in the test animals appeared to affect tyrosine oxidation, the blood on exposure blackening less intensely than before eyestalk injection.

7. DISCUSSION

With the recording of tyrosinase activity in the blood of *Maia squinado* and *Cancer pagurus* (Pinhey, 1930) and the suggestion that it may be related to the tanning of the cuticle in decapod Crustacea (Dennell, 1947*b*) it may be reasonable to expect a mechanism of tanning similar to that in insects. The observations recorded in the foregoing study of *Carcinus maenas* support such a view. Not only the oxidation products of tyrosine appear to be utilized for tanning of the cuticle as may be inferred from the occurrence of maximum tyrosinase activity at the pillans stage when the new cuticle is laid and tanned, but also the mechanism by which tyrosine oxidation is held in check till the appropriate period, appears to show a close parallel to that in insects. Dennell (1947*a*, 1949) from a study of cyclorhaphous Diptera suggested that the activity of an enzyme system having an influence on the redox potentials of the blood so controls the internal environment affecting tyrosine oxidation, that the polyphenols are formed only at the time of tanning of the cuticle. In *Carcinus maenas* a striking correlation seen between the fluctuations in the cyanide-insensitive oxygen uptake in different stages of the moult cycle and tyrosinase activity may suggest as in insects, a causal relation between the two processes. However, the precise nature of the enzyme or enzymes involved and the mechanism of enzyme action as well as the rôle of fructose in the intermediary metabolism are not known and constitute a problem in enzyme chemistry.

From the observations made on the effect of eyestalk extirpation in relation to the cyanide-insensitive oxygen uptake, it may appear that the hormone of the eyestalk has a controlling influence on the enzymes regulating tyrosinase activity in that a removal of the source of this hormone in the hard crab stage brings about a

reduction in enzyme activity which seems to characterise animals preparing for moult. This is explicable in view of the fact that the eyestalk hormone is known to have an inhibiting effect on moulting and its removal accelerates the onset of moulting. The relationship between the enzyme activity noted above and the hormone of the eyestalk suggests a striking parallel to that between certain metabolic processes accompanying moulting and the sinus gland hormone noted by Scudamore (1947). It has been pointed out that, in the crayfish, the formation of gastroliths, increase in oxygen consumption and in water content, commence some days before the moult and that these changes could be induced to take place much earlier than in normal animals by bilateral eyestalk extirpation or sinus gland removal. The suggestion made by the above author that these metabolic changes may not be separately controlled by hormones but are associated to form a single functional system controlled by the eyestalk hormone, supports the inference that could be made from the results obtained for the regulation of tyrosinase activity in *Carcinus maenas*. It appears reasonable to suggest that tyrosine oxidation as a precursor to the tanning of the newly formed cuticle at the time of moulting may be only a part of a series of metabolic processes associated with moulting and that any change in the timing of the moulting process may bring about corresponding changes in the processes linked up with moulting.

In this connection it is of interest to compare the hormonal regulation of moulting in Crustacea and insects. It has been shown that in insects a dualistic control is exercised by two hormones, a juvenile hormone responsible for the development of nymphal characteristics and a moulting hormone inducing adult traits, the effect produced at any stage being the result of the two hormones exerting their influence in varying degrees (Wigglesworth, 1940). In Crustacea it is known that a moult-inhibiting hormone is produced by the sinus gland or as has been recently observed secreted by the neurosecretory centres in the eyestalk and stored in sinus gland (Bliss and Welsh, 1952). The physiological effects of this hormone suggest a similarity to the juvenile hormone of insects, produced by the corpus allatum or its homologue the Weismann's ring of Diptera. But it is not known whether in Crustacea there is evidence of a moult-inducing hormone comparable to that secreted by the intercerebralis-cardiacum system of insects (see Scharrer and Scharrer, 1944). In this connection the observations of Scudamore (1947) are suggestive. He noted that injections of extracts of brain or thoracic ganglia in crayfish result in an increased oxygen consumption and stimulate gastrolith formation, which characterise animals preparing for moult. If this is an indication of a moult-inducing hormone in Crustacea, a very striking parallel would seem to exist with the condition described in insects in regard to a dualistic hormonal control of moulting.

8. SUMMARY

1. Tyrosine and tyrosinase occur in the blood of *Carcinus maenas*. Tyrosinase activity shows variations in different stages of the moult cycle, while tyrosine content is more or less unchanged.

2. The fluctuations in tyrosinase activity appear to be related to the changing redox potentials of the blood estimated electrometrically. The potentials show a fall in the stages following moulting and a rise before the onset of moulting. The rise of potential coincides with the period of most intense tyrosinase activity.

3. It is suggested that low redox potential of the blood may be due among other factors to the activity of an enzyme system, indicated by the cyanide-insensitive oxygen uptake in different periods of the moult cycle, showing a depression in the period before moult and a rise after the moult.

4. The fructose content of the muscles shows variations in the course of the moult cycle and it appears suggestive that such variations may be related to the enzyme activity as estimated by the cyanide-insensitive oxygen uptake.

5. From the observations made it is suggested that the tyrosinase activity is kept in check for a greater part of the intermoult period by the low redox potential of the blood arising from the activity of an enzyme system, the depression of which sometime before moulting raises the

redox potential so as to make possible tyrosinase activity and the elaboration of polyphenols involved in tanning.

6. The control of moulting by a hormone elaborated in the neurosecretory organs of the eyestalk has been studied in relation to the enzyme system noted above. Experimental evidence is adduced that the removal of the eyestalks accelerates the normal course of rise and fall in the activity of the enzyme in relation to moulting. It is suggested that the eyestalk hormone has a controlling influence on the enzyme system in question as a part of the physiological system related to moulting.

9. ACKNOWLEDGEMENTS

This work was carried out in the Zoology Department of the University of Manchester. I am indebted to Prof. R. Dennell, for his suggestion of the problem and help during the course of the work, and to Prof. H. Graham Cannon, F.R.S., for his continued interest and permission to occupy the Manchester Table at the Marine Biological Laboratory, Plymouth. My thanks are also due to Mr. F. S. Russell, F.R.S., the Director of the Plymouth Laboratory, and his colleagues for generous facilities afforded to me. I am thankful to the Government of Madras for the grant of an Overseas Fellowship.

10. REFERENCES

- Baunberger, J. P. and Dill, D. B. (1928). A study of the glycogen and sugar content and osmotic pressure of crabs during the moult cycle. *Physiol. Zool.*, **1**, 545.
- Baunberger, J. P. and Olmsted, J. M. D. (1928). Changes in osmotic pressure and water content of crabs during moult cycle. *Ibid.*, **1**, 531.
- Bliss, D. E. and Welsh, J. H. (1952). The neurosecretory system of brachyuran Crustacea. *Biol. Bull.*, **103**, 157.
- Brown, F. A. (Jr.) (1944). Hormones in Crustacea. *Quart. Rev. Biol.*, **19**, 32 and 188.
- Brown, F. A. (Jr.) and Seudamore, H. H. (1940). Differentiation of two principles from the crustacean sinus gland. *J. cell. comp. Physiol.*, **18**, 339.
- Burt, E. T. (1937). On the corpora allata of dipterous insects—I. *Proc. Roy. Soc. B*, **124**, 13.
- Burt, E. T. (1938). On the corpora allata of dipterous insects—II. *Ibid.*, **126**, 210.
- Day, M. F. (1943). The homologues of the ring gland of Diptera Brachycera. *Ann. Ent. Soc. Amer.*, **36**, 1.
- Dennell, R. (1947a). A study of an insect ecdyle: the formation of the puparium of *Sarcophaga falcularia* Pand (Diptera). *Proc. Roy. Soc. B.*, **134**, 79.
- Dennell, R. (1947b). The occurrence and significance of phenolic tanning in the newly formed cuticle of Crustacea Decapoda. *Ibid.*, **134**, 485.
- Dennell, R. (1949). Weismann's ring and the control of tyrosinase activity in the larva of *Calliphora erythrocephala*. *Ibid.*, **136**, 94.
- Drillhon, A. (1933). Le glucose et la mue des Crustacés. *C. R. Acad. Sci. Paris*, **196**, 506.
- Feigl, F. (1947). Qualitative analysis by spot tests. Elsevier Publishing Company, New York.
- Figge, F. H. J. (1940). Pigment metabolism studies. The regulation of tyrosinase melanin formation by oxidation-reduction systems. *J. cell. comp. Physiol.*, **15**, 245.
- Follin, O. and Denis, W. (1912). Tyrosine in proteins as determined by a new colorimetric method. *J. biol. Chem.*, **12**, 245.
- Fraenkel, G. (1935). A hormone causing pupation in the blowfly *Calliphora erythrocephala*. *Proc. Roy. Soc. B*, **118**, 1.
- Fraenkel, G. and Rudall, K. M. (1947). The structure of insect cuticles. *Ibid.*, **134**, 111.
- Graubard, M. A. (1933). Tyrosinase in mutants of *Drosophila melanogaster*. *J. Genet.*, **27**, 199.
- Hudon, E. (1937). An accelerating effect of normal 'ring glands' on puparium formation in lethal larva of *Drosophila melanogaster*. *Proc. Nat. Acad. Sci. Wash.*, **23**, 478.
- Hanstrom, B. (1949). Endocrinologie des Arthropodes. Centre National de la Recherche Scientifique, Paris.
- Heim, F. (1892). Sur la matière colorante bleue du sang des Crustacés. *C. R. Acad. Sci. Paris*, **114**, 771.
- Hemmingsen, A. M. (1924). The blood sugar of some invertebrates. *Skand. Arch. Physiol.*, **45**, 204.
- Hoet, J. P. and Kerridge, P. M. T. (1926). Observations on the muscles of normal and moulting Crustacea. *Proc. Roy. Soc. B*, **100**, 116.
- Krishnan, G. (1950). Sinus gland and tyrosinase activity in *Carcinus maenas*. *Nature*, **165**, 364.
- Kuwana, Z. (1937). Reducing power of the body fluid of the silkworm. *Jap. J. Zool.*, **7**, 273.
- Kyer, D. L. (1942). The influence of sinus glands on gastrolith formation in the crayfish. *Biol. Bull.*, **82**, 68.

- Maluf, N. S. R. (1939). The blood of Arthropods. *Quart. Rev. Biol.*, **14**, 149.
- Paul, J. H. and Sharpe, J. S (1916). Studies on calcium metabolism. (I) The deposition of lime salts in the integument of decapod Crustacea. *J. Physiol.*, **50**, 183.
- Pinhey, K. G. (1930). Tyrosinase in crustacean blood. *J. exp. Biol.*, **7**, 19.
- Robertson, J. D. (1937). Some features of the calcium metabolism of the shore crab *Carcinus maenas*. *Proc. Roy. Soc. B*, **124**, 162.
- Roe, J. H. (1934). A colorimetric method for the determination of fructose in blood and urine. *J. biol. Chem.*, **107**, 15.
- Scharrer, B. and Scharrer, E. (1944). Neurosecretion--VI. A comparison between the inter-cerebralis-cardiacum allatum system of the insects and the hypothalamo-hypophyseal system of the vertebrates. *Biol. Bull.*, **87**, 242.
- Schonborn, E. (1910). Beiträge zur kenntnis des kohle hydrate toff wechels bei *Carcinus maenas*. *Z. Biol.*, **55**, 70.
- Scudamore, H. H. (1947). The influence of sinus glands upon molting and associated changes in crayfish. *Physiol. Zool.*, **20**, 187.
- Wigglesworth, V. B. (1940). The determination of characters at metamorphosis in *Rhodnius prolixus* (Hemiptera). *J. exp. Biol.*, **17**, 201.

Issued March 22, 1954.

STUDIES ON CYTOCHEMISTRY OF HORMONE ACTION

PART XIV.—STUDIES IN THE DISTRIBUTION AND CONCENTRATION OF ALKALINE PHOSPHATASE IN THE VAGINAL SMEAR OF THE RAT DURING ESTRUS CYCLE: THE EFFECT OF OVARIECTOMY AND REPLACEMENT THERAPY

by S. K. ROY, AMIYA B. KAR and J. N. KARKUN, *Central Drug Research Institute, Lucknow*

(Communicated by B. Mukerji, F.N.I.)

(Received August 10; read October 9, 1953)

THE PROBLEM

Thibault and Soulairac (1948) reported pronounced alkaline phosphatase activity in the vaginal mucosa of rats. Ovariectomy caused a total disappearance of the enzyme from the vagina which, however, was restored on replacement therapy with estrogen. Kamell and Atkinson (1948) made similar observations on mice. Recently, Ring (1950) noted a correlation between phosphatase activity in the vaginal epithelium of rats and the different stages of estrus cycle. He pointed out that the concentration of the enzyme was maximum in the proestrus and minimum in the metaestrus or diestrus stages. These findings were based solely on histological sections of the vagina and consequently do not provide a detailed picture of phosphatase distribution in the different cellular elements of the mucosa. The vaginal smear preparations, on the other hand, allow a much clearer elucidation of the enzyme pattern as the mucosal elements can be studied individually and with better precision.

In view of the above, an attempt has been made to investigate the distribution and concentration of alkaline phosphatase in the vaginal smear of the rat during different stages of estrus cycle. Attention has also been paid in this study to the responses evoked by ovariectomy and replacement therapy on the distribution of this enzyme in the vaginal smear elements.

EXPERIMENTAL PROCEDURE.

Albino rats, weighing 114.4 ± 10.6 gms., were used in this study. A total of 22 animals were used of which 12 were ovariectomized and the remaining 10 served as the normal controls. A group of 6 operated rats were injected intramuscularly with 1 mg. of estradiol dipropionate (in 0.2 c.c. of sterile sesame oil) daily for 6 days. The hormone therapy commenced 24 hours after the operation. An equal number of overiectomized animals were treated with sesame oil alone in a similar manner. All the animals were maintained under uniform husbandry conditions throughout the experimental period.

Daily examination of vaginal smears of the normal rats was made till each animal of the group completed all the four stages of the estrus cycle. In the overiectomized animals, however, the smears were taken from the 7th day after the operation in order to ensure a response of the genital accessories to the operative procedure and estrogen therapy.

The vaginal smears were fixed in chilled 80% ethyl alcohol and processed according to the technique of Gomori (1941) for the demonstration of alkaline

phosphatase. The sites of enzyme activity in the cellular elements are marked by the deposition of cobalt sulfide in fine black granules. In order to allow critical observation of these black granular deposits no counterstain was used. The smears were dehydrated and mounted in the usual manner. For comparison, parallel smears from each animal were stained with Ehrlich's hematoxylin followed by alcoholic eosin after ethyl alcohol fixation.

RESULTS

The cellular picture of vaginal smear of the rat during different stages of oestrus cycle, is too well known to merit a repetition. No attempt is, therefore, necessary for a cytological characterisation of the vaginal smears. It would be quite appropriate to restrict our attention to the changes in the distribution of alkaline phosphatase in the cellular elements contained in the smears.

Diestrus stage.—The nucleus of the leucocytes stains positively for the phosphatase but the cytoplasm reacts in a somewhat diffuse manner. The epithelial cells, however, show considerable phosphatase activity both in the nucleus and in the cytoplasm. The overall picture at this stage is one of pronounced enzyme activity (Pl. III, fig. 1, table I).

Proestrus stage.—As in the diestrus condition, the nucleus of the leucocytes stains positively for the phosphatase but the cytoplasm is virtually negative for the enzyme. A more or less similar pattern is noticeable in the epithelial cells but in some of these, the enzyme also occurs in the cytoplasm.

Different stages of cornification are seen in the epithelial cells. Some are slightly cornified and show a normal nucleus but in others the nucleus is degenerated and the entire cell is relatively more keratinized. A fully cornified cell, however, is scale-like and is conspicuous by the absence of a nucleus.

In the cornified cells with a normal nucleus an intense phosphatase activity is visible both in the nucleus and in the cytoplasm but those with a degenerated nucleus stain only faintly. The fully cornified cells, however, are devoid of any phosphatase activity (Pl. III, fig. 2).

Estrus stage.—Only the enucleated type of cornified cells are encountered at this stage. These cells stain negatively for the phosphatase (Pl. III, fig. 3).

TABLE I

The distribution of alkaline phosphatase in the vaginal smear elements of normal and experimental rats.

	Diestrus.	Proestrus.	Estrus.	Metaestrus.	Ovariectomized.	Ovariectomized plus estrogen.
<i>Leucocytes</i> ..	++ ⁿ	++ ⁿ	..	++ ⁿ	++ ⁿ	..
<i>Epithelial cells</i> ..	++	++	++	..
<i>Cornified cells</i> —						
(a) With normal nucleus	++
(b) With degenerated nucleus	+	..	+
(c) Without nucleus	—	—	—	—	—

Legend:— ++ⁿ = Strong phosphatase activity only in the nucleus.
 ++ = Strong activity throughout the cell.
 + = Faint reactions.
 — = Negative reactions.

Metaestrus stage.—The nucleus of the leucocytes gives positive reactions for the phosphatase but the cytoplasm reacts only in a faint manner. The enzyme is completely absent in the enucleated cornified cells but a diffuse reaction is given by those with a degenerated nucleus (Pl. III, fig. 4).

Ovariectomized rats.—The vaginal smears of ovariectomized rats show a typical diestrus condition with an overall high concentration of phosphatase in the cellular elements. As in the normal rats, only the nucleus of the leucocytes stains positively for the enzyme but the cytoplasm shows a diffuse distribution. The epithelial cells give a positive reaction in the nucleus but the cytoplasm reacts intensely. The isolated cornified cells, however, show only negligible amounts of the enzyme.

Estrogen therapy.—Only enucleated cornified cells are visible in the vaginal smears of the ovariectomized rats treated with estrogen. These cells stain negatively for the phosphatase.

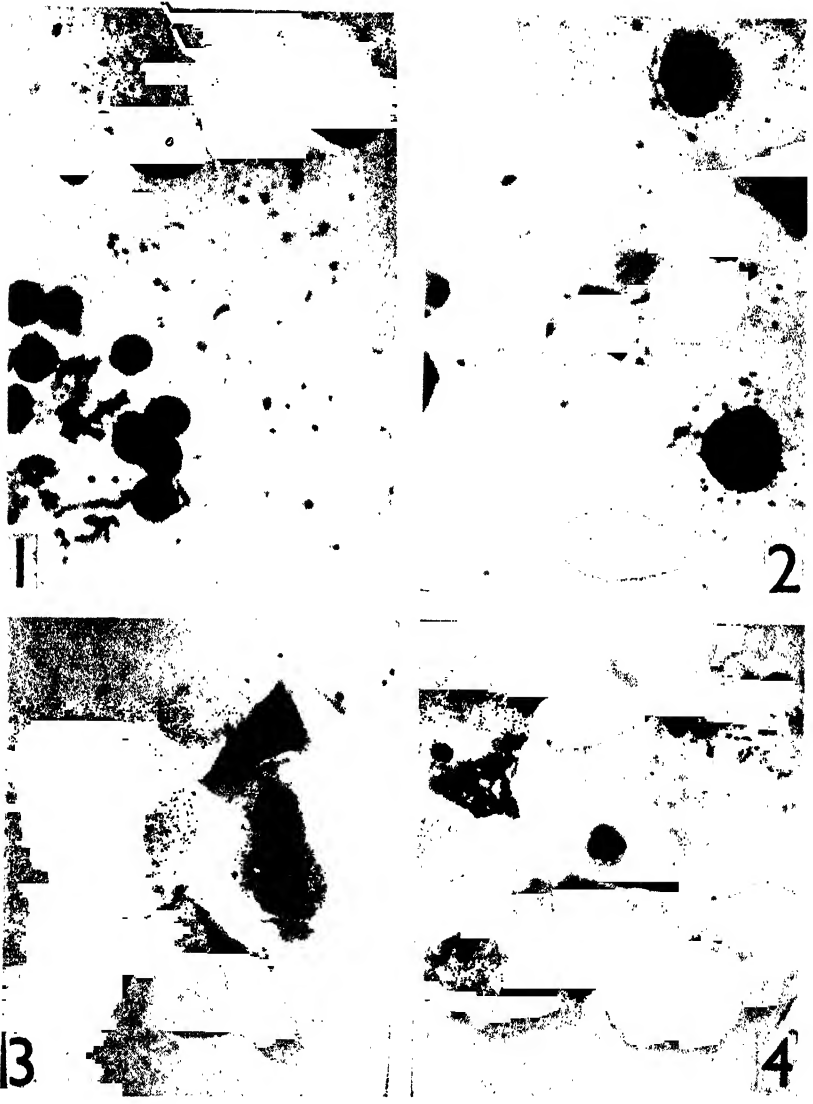
DISCUSSION

The present studies indicate clearly that there is pronounced phosphatase activity in the vaginal smear elements during the diestrus and the proestrus stages. However, the activity of the enzyme is considerably lowered during the estrus but reappears from the metaestrus stage. The ovariectomized rats exhibit a typical diestrus pattern and estrogen therapy is associated with a lowered activity of the enzyme as in the estrus condition.

Ring (1950) reported that phosphatase activity is maximum during the proestrus and minimum in the metaestrus or early diestrus stages. He added that the concentration of the enzyme is considerably less in the estrus condition. Our findings on the distribution of alkaline phosphatase in the vaginal smears are in general agreement with those of Ring. It may, however, be recalled that we observed a recurrence of enzyme activity in the metaestrus stage which is significantly enhanced during the diestrus. These apparently discrepant results could be ascribed to the fact that Ring focussed his entire attention on the epithelial cells but did not take into account the leucocytes which are found in large numbers during the diestrus and the metaestrus stages. As these cells exhibit fairly high enzyme activity, their contribution to the total phosphatase picture of the vaginal mucosa has to be taken into due consideration.

Thibault and Soullairac (1948) noted that ovariectomy causes a total disappearance of alkaline phosphatase from the vaginal mucosa which is adequately restored after replacement therapy with estrogen. Similar observations are reported by Kamell and Atkinson (1948) on mice. Ring (1950), on the other hand, described a marked concentration of the enzyme in the vaginal epithelium of the ovariectomized rats. Estrogen therapy produces a typical estrus picture of phosphatase distribution. The present studies on vaginal smear preparations lend support to Ring's findings and show that the activity of the enzyme in ovariectomized rats is similar to that of the normal diestrus condition and that estrogen therapy simulates the phosphatase pattern of the estrus stage. It may be recalled that the enzyme activity is considerably high in the diestrus stage but goes down markedly in the estrus.

A question may now be raised as to the physiological significance of the cyclic fluctuations in vaginal phosphatase activity during the estrus cycle. Ring (1950) suggested that the enzyme is concerned with the formation of keratin in the epithelial cells. The present findings also subscribe to such a concept. In this connection, reference may be made to our observation that there are three stages in the cornification of epithelial cells which are clearly discernible by the condition of the nucleus. In the initial stage when the formation of keratin has just commenced, the nucleus presents a normal appearance. With rapid progress in the process of keratinization, the nucleus becomes degenerated whereas in a completely keratinized cell it is absent. Concomitantly, the phosphatase activity is very high in the initial stage



of keratinization but is considerably reduced as keratinization progresses and is practically absent in a fully cornified cell. Apart from this, it is also probable that the enzyme is concerned with the proliferation of the epithelial cells, particularly during the proestrus stage when the vaginal mucosa thickens appreciably and numerous mitoses appear in the basal epithelial layers (Turner, 1948).

SUMMARY

1. Pronounced alkaline phosphatase activity is visible in the vaginal smears of the rat during the diestrus and the proestrus stages. The activity of the enzyme is considerably reduced during the estrus but there is a recurrence from the metaestrus stage.

2. Ovariectomy induces typical diestrus pattern of phosphatase distribution but replacement therapy with estrogen is associated with a low enzyme concentration as in the estrus.

3. The phosphatase is probably concerned with the keratinization and proliferation of the epithelial cells of the vaginal mucosa.

ACKNOWLEDGEMENTS

Authors wish to express their gratitude to Dr. B. Mukerji for the keen interest he has taken in this study. Thanks are due to Dr. O. Wenger of Messrs. Ciba Pharma, Ltd., Bombay, for the generous distribution of estradiol dipropionate (Ovocyclin P.) used in this investigation.

REFERENCES

- Gomori, G. (1941). The distribution of alkaline phosphatase in normal organs and tissues. *J. Cell. and Comp. Physiol.*, **17**, 71-83.
- Kamell, S. A. and Atkinson, W. B. (1948). Effects of ovarian hormone on certain cytoplasmic reactions in the vaginal epithelium. *Proc. Soc. Exp. Biol. and Med.*, **68**, 537-540.
- Ring, J. R. (1950). Changes in alkaline phosphatase activity of rat vaginal epithelium during estrus cycle. *Anat. Rec.*, **107**, 121-131.
- Thibault, C. and Soulaire, A. (1948). L'activité phosphatasique du tractus génital des mammifères. Modifications expérimentales chez le rat femelle. *Ann. Endocrinol.*, **9**, 555-557.
- Turner, C. D. (1948). *General Endocrinology*, W. B. Saunders Co., London.

EXPLANATION OF PLATE III

(All figures are photomicrographs and are magnified $\times 400$.)

- FIG. 1. Vaginal smear elements of a rat in diestrus condition. Note pronounced phosphatase activity in the large epithelial cells.
- FIG. 2. Vaginal smear picture of a rat in proestrus stage. Note the distribution of alkaline phosphatase in the epithelial cells which are in different stages of cornification. Leucocytes are not shown in the figure.
- FIG. 3. Vaginal smear elements of a rat in estrus. Phosphatase is absent from the scale-like cornified cells.
- FIG. 4. Vaginal smear picture of a rat in metaestrus condition. Note the distribution of the enzyme in the different elements.

STUDIES ON THE NUCLEAR APPARATUS OF PERITRICHOUS CILIATES.

PART II. THE NUCLEAR APPARATUS OF *CARCHESIUM SPECTABILE* EHRBG.

by C. M. S. DASS, *I.C.I. Research Fellow, N.I.S.I., Department of Zoology, Central College, Bangalore.*

(Communicated by B. R. Seshachar, F.N.I.)

(Received July 2; read October 9, 1953.)

CONTENTS

	Page
Introduction	174
Material and Methods	175
Observations:	
The vegetative individual	175
Binary fission	175
Conjugation:	
(a) Formation of the conjugants	175
(b) Fusion of conjugants and formation of synkaryon	176
(c) Formation of the nuclear anlagen	177
(d) Reorganization fissions	177
Discussion:	
Nuclear apparatus	179
Binary fission	179
Micronuclear variation	180
Conjugation:	
(a) Formation of conjugants	180
(b) Fusion of conjugants	181
(c) Formation of nuclear anlagen	183
(d) Reorganization fissions	184
Summary	184
Acknowledgement	185
References	185
Explanation of photomicrographs	186

INTRODUCTION

The only work on the cytology of the nuclear apparatus of the genus *Carchesium* is that by Popoff (1908) on *C. polypinum*. Recent studies on allied genera of Peritricha, e.g., *Trichodina* sp. (Diller, 1928), *Zoothamnium arbuscula* (Furssenko, 1929), *Vorticella microstoma* (Finley, 1943), *Urceolaria synaptae* (?) (Colwin, 1944), *Lagenophrys tattersalli* (Willis, 1948), *Vorticella convallaria* (Seshachar and Dass, 1951), *Rhabdostyla vernalis* (Finley, 1952) and *Epistylis articulata* (Dass, 1953) have shown a number of interesting features in the cytology of this group, viz., variation in the number of micronuclei, form and shape of the macronucleus, behaviour of the macronucleus during binary fission, difference in the number of progamic divisions of the micronucleus in the two conjugants and behaviour of the macronucleus during conjugation. The present study is an attempt to interpret the condition in *Carchesium spectabile* in consonance with these recent findings.

MATERIAL AND METHODS

The colonies of *Carchesium spectabile* are found attached to weeds and rocks in running sewage water. Pillai and collaborators (1942) have shown that among the dominant organisms met with when raw sewage is aerated, are peritrichous ciliates of the genera *Vorticella*, *Epistylis*, *Carchesium*, *Zoothamnium* and *Opercularia*. This fact was made use of in obtaining large supplies of material. The material was collected from flowing sewage waters about six miles out of Bangalore and while some of it was fixed on the spot, large quantities were brought to the laboratory for further examination and treatment. The material was fixed in hot Schaudinn's, Carnoy's and San Felice's fluids and stained in Feulgen-light green.

OBSERVATIONS

The vegetative individual.

The nuclear apparatus, as in other euciliates, comprises two entities, the macronucleus and the micronucleus. The macronucleus is a greatly elongated, cylindrical body. It has no definite shape and can best be described as an irregularly bent cylinder. It exhibits a fine granular appearance and gives an intense Feulgen reaction. During the height of trophic activity a number of Feulgen negative areas are seen in the macronucleus (Pl. IV, fig. 1). They are not seen during binary fission nor do they occur in conjugating animals. The micronucleus, on the other hand, is a spherical body averaging about $5\ \mu$ in diameter. It is faintly stained, compared with the macronucleus. One micronucleus is generally found in each animal. However, instances are abundant where multimicronucleate individuals occur. Animals with two, three and even four micronuclei are found in my material (Text-fig. I, figs. *a*, *b* and *c*; Pl. IV, fig. 4). The future behaviour of such multimicronucleate animals indicates that once the variation is introduced, it becomes perpetuated in a colony for a considerable time, all the micronuclei taking part in division.

Binary fission.

This is the common method of asexual reproduction. The division activity is heralded by changes in the micronucleus. It loses its uniform appearance and thread-like chromosomes are faintly discernible. The nucleus increases in size and later assumes a spindle shape. The chromosomes move to the poles and the daughter nuclei are pushed far apart by the central spindle that develops between the two anaphase chromosome sets. As the two daughter micronuclei separate the cleavage furrow starts from the oral end and the macronucleus stretches across it. Eventually the macronucleus is cut into two almost equal halves (Pl. IV, fig. 2). This sequence of events takes place in quick succession.

In some members of the colony, another type of binary fission, where the macronucleus condenses into a deeply staining polymorphic body prior to its splitting, is also noticed (Pl. IV, fig. 3). Such a phenomenon was found in *Epistylis articulata* (Dass, 1953) but the fine filamentar processes produced by the macronucleus into the cytoplasm in *Epistylis* were not seen in *Carchesium*.

Conjugation.

The process of conjugation can be divided into four phases: (a) formation of conjugants, (b) fusion of the conjugants and formation of synkaryon, (c) formation of nuclear anlagen, and (d) reorganization fissions.

(a) *Formation of conjugants*

As in all Peritrichous ciliates, the two individuals participating in conjugation differ in size. The smaller microconjugant is produced earlier than the macro-

conjugant. At certain periods one notices the production, in very large numbers, of the microconjugants in the colony; it would seem the stimulus for their formation pervades the whole colony. Microconjugants are produced by normal individuals of a colony by a series of fissions. The first division gives rise to two animals which appear to pause for a while until each develops a stalk. Two divisions follow this successively,—each stalk bearing four small animals (Text-fig. I, fig. *d*). All the four microconjugants detach themselves soon and swim about in search of macroconjugants.

The formation of the macroconjugant appears to involve no preparatory division. Any vegetative individual of the colony seems capable of acting as the macroconjugant. However, I have noticed a slight change in the nuclear apparatus of potential macroconjugant. The macronucleus ~~exhibits~~ a tendency to be drawn out into a skein, while the micronucleus increases in size and becomes fainter.

(b) *Fusion of conjugants and formation of synkaryon*

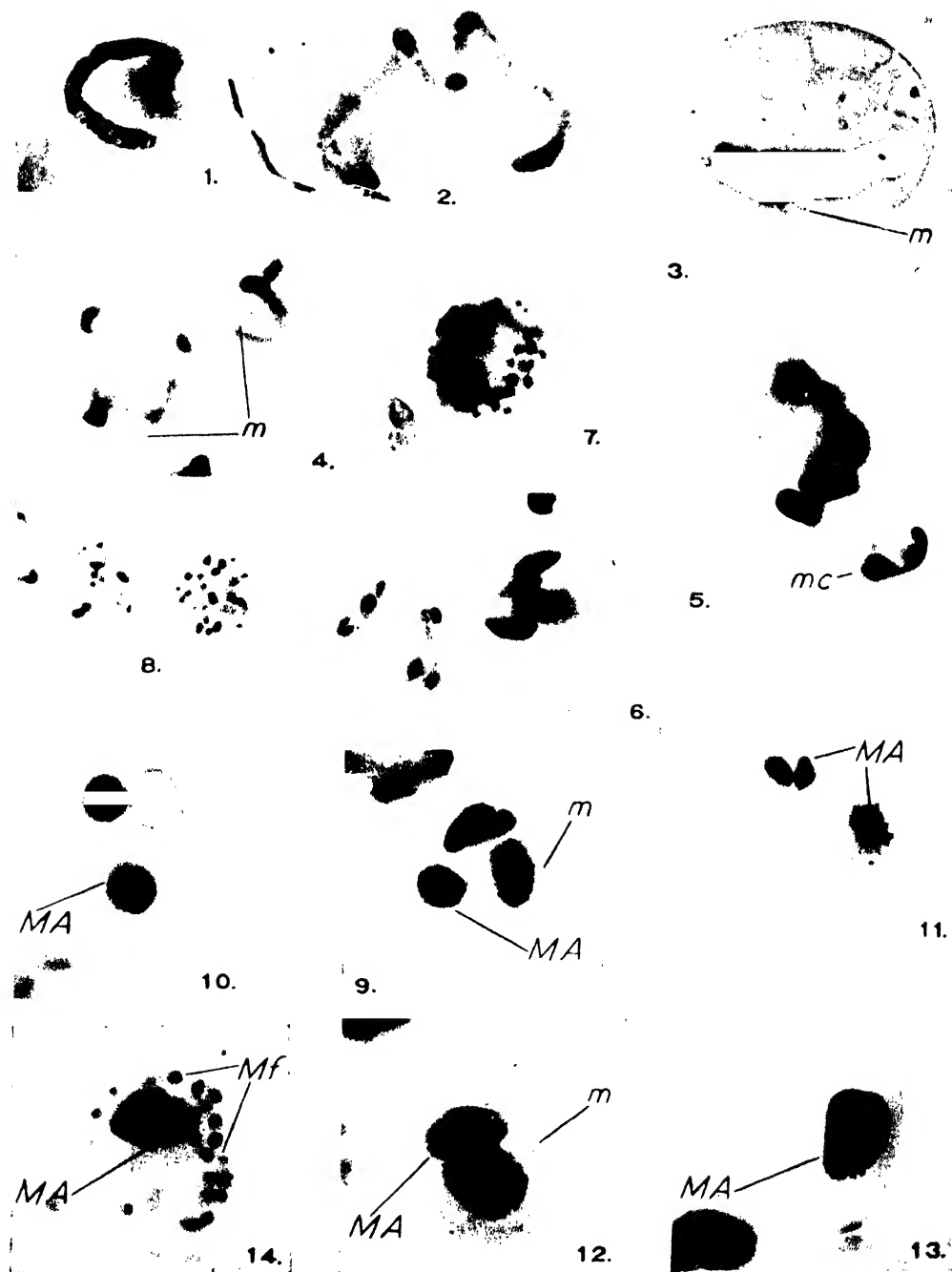
When the microconjugant comes in contact with the macroconjugant, it spins on its surface for a while and attaches firmly. The position on the body of the macroconjugant where it attaches is highly variable and perhaps the entire surface of the body is receptive to it. But the most common sites of fusion are at the base, on either side of the stalk (Pl. IV, fig. 5), and on the sides of the body. More than one microconjugant is often seen in association with a macroconjugant. It is also seen, in some instances, that one microconjugant is attached to another which is in association with a macroconjugant (Pl. IV, fig. 6).

The nuclear changes in the two conjugants can be treated under two heads: (a) the micronucleus and (b) the macronucleus.

(a) *The micronucleus*.—The beginnings of micronuclear activity in the microconjugant are seen even before its attachment with the macroconjugant. The micronucleus starts the first division, and if the time spent by the microconjugant in search of a macroconjugant is long enough, this division is completed. As a consequence, at the time of contact, the microconjugant has two micronuclei, while the macroconjugant has only one (Text-fig. I, fig. *e*). In those instances where the microconjugant comes in contact with the macroconjugant immediately after the former's release, it is seen that the micronucleus of the macroconjugant waits for the completion of the first division of the micronucleus of the microconjugant. The first and second divisions of the micronucleus of the macroconjugant are completed along with the second and third divisions of the micronucleus of the microconjugant (Text-fig. I, figs. *f* and *g*). Consequently, eight progamic nuclei are found in the microconjugant while only four are seen in the macroconjugant. One progamic nucleus of each of the conjugants becomes the pronucleus; the rest are absorbed in the cytoplasm.

(b) *The macronucleus*.—The meeting of the conjugants brings attendant changes in their macronuclei also. The macronucleus of the microconjugant splits into three or four bodies which later break up into 15–20 rounded bodies. The behaviour of the macronucleus of the macroconjugant, however, is interesting. It is thrown out into a skein, as in other peritrichous forms. A number of small deeply stained bodies are extruded from it and these are absorbed in the cytoplasm (Text-fig. I, fig. *e*). A little later, the macronucleus breaks up into a number of elongate bodies, which gradually fragment into spherical bodies numbering about 150–200. The fragments average 2.3 μ in diameter.

The fusion of the pronuclei takes place almost immediately after the boundary between the two conjugants breaks down and in the earliest synconjugant, the pale large and spherical synkaryon can be easily differentiated from the many macronuclear fragments derived from both conjugants that literally fill the cytoplasm.



(c) Formation of the nuclear anlagen

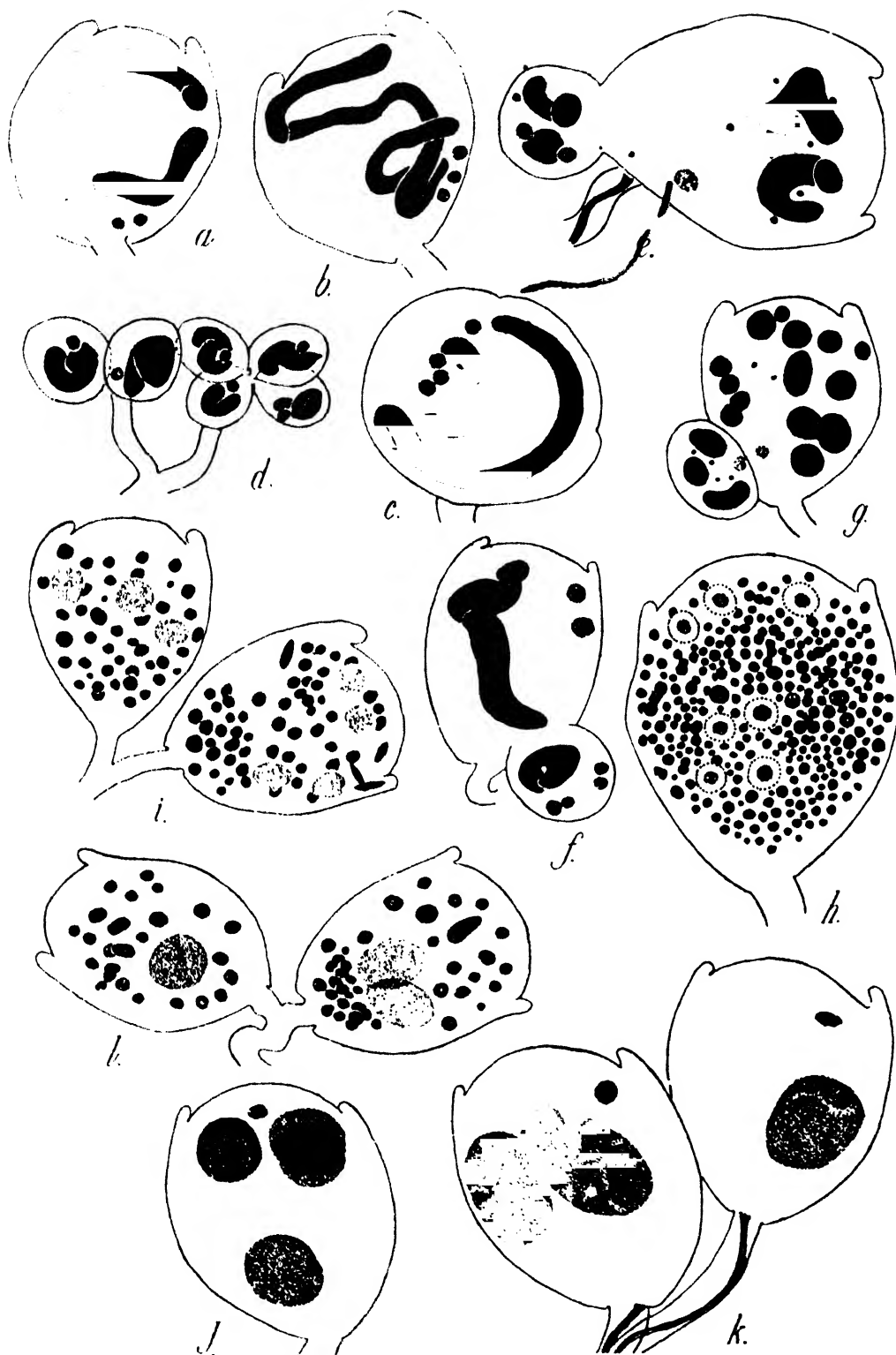
Immediately after its formation, the synkaryon divides successively thrice giving rise to eight nuclei; each is about $5\ \mu$ in diameter and a faint indication of a granular network-like structure can be seen in it. Soon, seven of them enlarge in size to about $15\ \mu$ in diameter while the other shrinks in size to about $3\ \mu$ (Text-fig. I, fig. *h*). The seven enlarged bodies are the macronuclear anlagen while the eighth is the micronuclear anlage. The macronuclear anlagen can be distinguished from the micronuclear anlage not only from their larger size but also from the fact that while in the former, the network-like appearance is seen clearly, the latter presents a homogeneous appearance characteristic of the definitive micronucleus.

(d) Reorganization fissions

The seven macronuclear anlagen continue to increase in size, and reach a diameter of $20\text{--}25\ \mu$. During this later period of growth the fine network-like appearance is lost and the anlagen present a faint homogeneous and granular structure. At this stage the reorganization fissions are initiated. During the first fission the macronuclear fragments (derived from both the conjugants) become somewhat localized at the base of the synconjugant while the macronuclear anlagen lie free in the cytoplasm towards the oral end of the animal. The micronucleus divides by mitosis and the two daughters separate. With the movement and separation of the micronuclei, the macronuclear anlagen also segregate into two groups of three and four (Text-fig. I, fig. *i*). The division of the cytosome also ensures an approximately equal distribution of macronuclear fragments between the two daughter individuals. There is a considerable lapse of time between the first reorganization fission and the second. During this period the macronuclear anlagen increase in size to about $45\text{--}50\ \mu$ and also become progressively deeply stained. The second reorganization fission segregates the macronuclear anlagen among the daughters so that they get 2, 2, 2, and 1 (Text-fig. I, fig. *k*; Pl. IV, fig. 11). There is a considerable time interval between the second and third reorganization fissions. The cell grows in size during this period, as also the macronuclear anlagen, which at this stage show a number of poorly stained furrows. The macronuclear anlagen has reached a size of $120\text{--}150\ \mu$ in diameter by the time the third reorganization fission starts. At the end of the third reorganization fission, each individual has one macronucleus and a micronucleus (Pl. IV, fig. 13). Maximum nucleination of the anlagen is noticed at this period. The macronuclear anlagen retain their more or less spherical shape during reorganization fissions.

An interesting feature in regard to the macronuclear anlagen refers to their rate of nucleination. It was observed that in a number of instances there was no uniformity in this matter in the anlagen derived from the same synkaryon—while in one daughter cell, the nucleination of the anlagen had progressed considerably, and they appeared in Feulgen preparations, brilliantly stained, in the sister individual, nucleination had not advanced to the same extent and the anlagen were relatively faint (Text-fig. I, fig. *l*). It was even noticed that the anlagen in the same organism sometimes differed in their nucleination as judged by their reaction to Feulgen. In an individual with two anlagen, of about the same size, one was decidedly more positive and brilliant than the other. In all such cases where nucleination was poor, the assumption of the final cylindrical form of the macronucleus was delayed until the anlagen had acquired the requisite amount of nucleic acid, the anlagen remaining as polymorphic bodies during the process.

There appears to be an interesting correlation between the rate of nucleination of the macronuclear anlagen and the rate of absorption of the macronuclear fragments. In most cases, with every reorganization fission the macronuclear fragments get distributed between the daughter individuals almost equally, but most of them are absorbed by the second reorganization fission. In a few cases, however, they



TEXT-FIG. 1. (For Explanation see foot of page 179.)

persist till after the second fission and are sometimes seen even in the completely reorganized individuals (Pl. IV, fig. 14). In cases where the fragments are absorbed early, the macronuclear anlagen are conspicuous by their deep Feulgen reaction (Pl. IV, figs. 9, 10 and 12), while in instances where the fragments persist long, the anlagen are faint and only slowly and gradually acquire their final intensity (Pl. IV, figs. 11 and 14). This appears to offer evidence of some type of a relationship between the dissolution of the macronuclear fragments and the nucleination of the anlagen.

DISCUSSION

Nuclear apparatus.

The nuclear apparatus of *Carchesium spectabile* resembles that of other Peritrichous ciliates. The great length and tortuous nature of the macronucleus, however, are very striking. The appearance of Feulgen negative areas in the macronucleus during certain phases of life-history of these ciliates has been recorded in other Peritricha, e.g., *Zoothamnium alternans* (Fauré-Fremiet, 1930), *Vorticella microstoma* (Finley, 1943), *Urceolaria synaptae* (?) (Colwin, 1944) and *Epistylis articulata* (Dass, 1953). Colwin (1944) regards these areas as pits caused by the throwing off of chromatin balls into the cytoplasm and compares the process with the phenomenon of 'hemixis' described by Diller (1936) in *Paramecium aurelia*. I have not observed in *C. spectabile* any chromatin elimination in the vegetative animal. In *E. articulata* (Dass, 1953) also these areas were noticed in the macronucleus and the application of Unna's methyl green-pyronin mixture showed them to be stained deeply with pyronin. A similar condition obtains in *C. spectabile* also and it is possible that these areas represent pockets of ribonucleic acid. It is interesting to see that such areas are present during the height of trophic activity and do not occur during the division phase. In this, as well as in its nucleic acid content, they resemble nucleoli of Metazoa.

Binary fission.

Of the two types of binary fission that have been recorded, it is the second, where the macronucleus becomes a polymorphic body, that is more interesting. A similar type of division was also observed in *E. articulata* (Dass, 1953). The

EXPLANATION of TEXT-FIG. I (see page 178).

- FIGS. a, b, c.—Bi-, tri- and tetramicronucleate individuals. $\times 700$. Feulgen-Light green.
- FIG. d. Microconjugant formation. On one stalk bunch of four microconjugants seen, while on the other they are still in the process of formation. $\times 700$. Feulgen-Light green.
- FIG. e. Conjugation. In the microconjugant first progamic division is over while in the macroconjugant the micronucleus is in prophase. $\times 700$. Feulgen-Light green.
- FIG. f. Conjugation. The second progamic division of the micronucleus of microconjugant and first progamic division of that in macroconjugant are over. $\times 700$. Feulgen-Light green.
- FIG. g. Conjugation. Pronucleus in each conjugant ready. The residual progamic nuclei are seen as small dark bodies. Already a number of them have been absorbed in the cytoplasm. $\times 700$. Feulgen-Light green.
- FIG. h. Synconjugant. The cytosome filled with macronuclear fragments. Macronuclear anlagen differentiated. Faint network-like structure still seen in the anlagen. Micronucleus small and faint. $\times 700$. Feulgen-Light green.
- FIG. i. F_1 individuals. The macronuclear fragments greatly reduced in number. $\times 700$. Feulgen-Light green.
- FIG. j. F_1 individual. All fragments absorbed in the cytoplasm. $\times 700$. Feulgen-Light green.
- FIG. k. F_2 individuals. The macronuclear anlagen have increased in size. All the macronuclear fragments are absorbed. $\times 700$. Feulgen-Light green.
- FIG. l. F_2 individuals. The rate of nucleination of the anlagen is not the same in sister individuals. The macronuclear fragments still persistent, $\times 700$. Feulgen-Light green.

condition seen in *C. spectabile*, however, differs from that in *E. articulata* in that fine filamentar processes given off from the macronucleus in the latter species are not seen. The significance of the process is not clear.

Micronuclear variation.

Generally there is a single micronucleus in *C. spectabile*, but occasionally individuals with two, three or four micronuclei are met with. It would appear, among Peritricha only *Epistylis* shares this feature with *Carchesium*, though in other euciliates it is a common enough phenomenon (*Paramecium bursaria*, Hamburger, 1904; Woodruff, 1931; *P. trichium*, Wenrich, 1926; *P. caudatum*, Wichterman, 1946). Whatever the agency responsible for the introduction of multimicronuclearity in other ciliates, in *C. spectabile* it would seem to be due to a mis-step in binary fission, the cytosome and the macronucleus not following micronuclear division. It was observed that binary fission is initiated by the micronucleus, and only long after the separation of the two daughter micronuclei do the macronucleus and cytosome divide. A failure of the cell to divide after the division of the micronucleus would result in bimicronuclearity, and a repetition of the same phenomenon would lead to a further multiplicity of micronuclei. It was noticed that once this condition was introduced it was perpetuated over a number of generations, until perhaps at conjugation, it was rectified and normalcy restored.

Conjugation.

The phenomenon of conjugation can be broadly divided into four stages: (a) formation of conjugants, (b) fusion of conjugants, (c) formation of nuclear anlagen and (d) reorganization fissions.

(a) *Formation of conjugants*

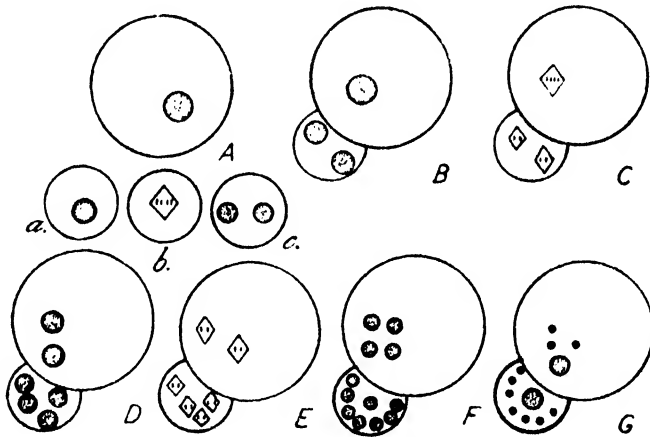
The Peritricha as a rule are characterised by dissimilar conjugants. The macroconjugant is generally a vegetative individual, sometimes with a definite position in the colony as in *Zoothamnium arbuscula* (Furssenko, 1929), *Z. alternans* (Summers, 1938) or placed at random as in *Carchesium polypinum* (Popoff, 1908) and *Ophrydium versatile* (Kaltenbach, 1916) and *E. articulata* (Dass, 1953). It is produced by a special 'sex-differentiating' division of a vegetative individual in *Opercularia coarctata* (Enriques, 1907) and preconjugation division in *Vorticella microstoma* (Finley, 1943) and *Lagenophrys* sp., (Awerinzew, 1912). In *C. spectabile* any vegetative individual of the colony seems capable of being transformed into a macroconjugant. In such individuals the macronucleus shows an incipient skein and the micronucleus, an initiation of the division process.

The microconjugant, on the other hand, is very much smaller. It is produced by at least four different methods in Peritricha: (1) 'Rosette formation', where a vegetative individual of the colony undergoes two or three successive divisions, viz., *Vorticella monilata*, *V. nebulifera* and *V. putrina* (Maupas, 1888), *Carchesium polypinum* (Popoff, 1908), *Zoothamnium (arbuscula) alternans* (Stein, 1867), *Z. geniculatum* (Wesenberg-Lund, 1925), *Epistylis plicatilis* (Claparède and Lachmann, 1858-1861), *E. similans* (Plate, 1888), *E. articulata* (Dass, 1953), *Trichodina* sp., (Padnos, 1939), *Glossatella tintinnabulum* (Penard, 1922), *Opercularia infusionum* (Stein, 1867) and *Ophrydium versatile* (Kaltenbach, 1916); (2) Unequal division of the vegetative individual, smaller of the two products becoming the microconjugant, viz., *Vorticella convallaria* and *V. campanula* (Engelmann, 1876), *V. microstoma* (Finley, 1943), *Vaginicola (Cothurnia) crystallina* (Penard, 1922), *Cothurniopsis* sp., (Penard, 1922), *Lagenophrys labiata* (Awerinzew, 1912; Penard, 1922), *Pyxidium inclinans* and *P. curvicaule* (Penard, 1922), *Opercularia coarctata* (Enriques, 1907), *Opisthonecta henneguyi* (Rosenberg, 1940); (3) Metamorphosis of special cells—the microzooids—

of the colony, viz., *Zoothamnium alternans* (Summers, 1938a); and (4) Sex-differentiating division, producing a macroconjugant and a protoconjugant the latter dividing again once or twice to give rise to microconjugants, viz., *Lagenophrys tattersalli* (Willis, 1948) and *Rhabdostyla vernalis* (Finley, 1952). The microconjugant formation in *C. spectabile* is of the first type, but there is seen a time lag between the first and the succeeding two divisions, thus the microconjugants are found in two bunches of four each borne on different stalks.

(b) Fusion of conjugants

Conjugation involves the meeting of the two conjugants, attendant changes in the nuclear apparatus and the final fusion and merging of the microconjugant into the body of the macroconjugant to produce a synconjugant. The point of interest during conjugation in Peritricha centres round the micronuclear divisions in the two conjugants. Popoff (1908) observed that in *C. polypinum* the micronucleus of the microconjugant undergoes three divisions. He described the first division as 'Preliminary division', which takes a long time to complete while the subsequent two divisions occur in quick succession. Of the eight nuclei so produced one persists and the rest degenerate. This persistent nucleus divides again and two nuclei are produced. One of these degenerates and the other becomes the



TEXT-FIG. II. Diagrammatic representation of the sequence of micronuclear divisions in micro- and macroconjugants. Only the micronucleus and its products are shown.

FIG. A. Macroconjugant ready for conjugation. The micronucleus has entered the prophase of first progamic division.

FIG. a. Free microconjugant just released from the parent stalk. The micronucleus in resting condition.

FIG. b. Free microconjugant. Metaphase of first progamic division in progress.

FIG. c. Free microconjugant. First progamic division is complete.

FIG. B. Conjugation. Microconjugant just come in contact with the macroconjugant. The micronucleus of macroconjugant is still in prophase of first progamic division, while that in microconjugant has completed the first division.

FIG. C. Conjugation. First progamic division in macroconjugant and second progamic division in microconjugant in metaphase.

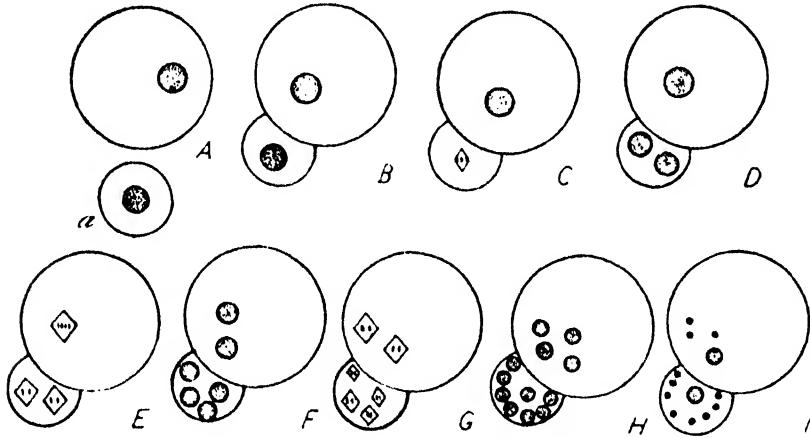
FIG. D. Conjugation. First progamic division of micronucleus in macroconjugant and second progamic division in microconjugant are over.

FIG. E. Conjugation. Second progamic division metaphase in macroconjugant and third progamic division metaphase in microconjugant.

FIG. F. Conjugation. Second progamic division in macroconjugant and third progamic division in microconjugant are over.

FIG. G. Conjugation. The pronucleus in each conjugant is ready. The dark bodies are the residual progamic nuclei.

pronucleus. Thus the pronucleus of the microconjugant, according to Popoff, is a product of the fourth division of the micronucleus. In the macroconjugant also, according to him, a similar process takes place in the production of the pronucleus. However, recent work on other Peritricha (Finley, 1943 and 1952; Dass, 1953) has revealed that the number of divisions of the micronucleus is not the same in both conjugants—the micronucleus of the microconjugant undergoes three divisions, while that of the macroconjugant, two. Generally the first division of the micronucleus of the microconjugant is considered as a 'Preliminary division'. Finley (1952) considers that the first division of the micronucleus of the microconjugant in the members of the order Peritricha 'is a vestigial process reminiscent of a phylogenetically earlier stage when the smaller conjugant was formed by repeated equal divisions'. He has also suggested that 'this extra division has arisen *de novo* in the microconjugant line and has no homologue in the macroconjugant or in the conjugation of other ciliates'. In this context the condition obtaining in *C. spectabile* is illustrative. It may be recalled that in most cases at the time of meeting of the macroconjugant the micronucleus of the microconjugant has undergone the first progamic division, a condition identical with that seen in *Vorticella microstoma* (Finley, 1943) and *Rhabdostyla vernalis* (Finley, 1952). The micronucleus of the macroconjugant



TEXT-FIG. III. Diagrammatic representation of the sequence of micronuclear division in micro- and macro-conjugants when conjugation occurs precociously. Only the micronucleus and its products are shown.

FIG. A. Macroconjugant ready for conjugation. The micronucleus has entered prophase of first progamic division.

FIG. a. Free microconjugant. The micronucleus in resting stage.

FIG. B. Conjugation. The microconjugant just come in contact with macroconjugant. The micronucleus of macroconjugant still in prophase of first progamic division. The micronucleus of microconjugant in resting condition. Compare this with Fig. B of text-fig. II.

FIG. C. Conjugation. The micronucleus of macroconjugant in prophase of first progamic division. The micronucleus of the microconjugant in metaphase of first progamic division.

FIG. D. Conjugation. The micronucleus of macroconjugant in prophase of first progamic division. The micronucleus of the microconjugant has completed the first progamic division. Condition similar to Fig. B of text-fig. II.

FIG. E. Conjugation. First progamic division metaphase in macroconjugant and second progamic division metaphase in microconjugant.

FIG. F. Conjugation. First progamic division in macroconjugant and second progamic division in microconjugant are over.

FIG. G. Conjugation. Second progamic division metaphase in macroconjugant and third progamic division metaphase in microconjugant.

FIG. H. Conjugation. Second progamic division in macroconjugant and third progamic division in microconjugant are over.

FIG. I. Conjugation. The pronucleus in each conjugant is ready. The dark bodies are the residual progamic nuclei.

which has already entered prophase in preparation for conjugation now proceeds further to reach first progamic metaphase. Simultaneously the second progamic metaphase is reached in the microconjugant also. The second progamic division in the macroconjugant and third progamic division in the microconjugant take place synchronously (Text-fig. II, figs. A-G). While this is the normal picture, in some instances, the meeting of the microconjugant and the macroconjugant takes place early, before the first progamic division of the micronucleus of the macroconjugant has taken place. In such instances, though the micronucleus of the macroconjugant has already entered the prophase of first progamic division it stays at the stage till the first progamic division is completed in the microconjugant. It is only after this, the micronucleus of the macroconjugant enters first progamic metaphase and simultaneously the micronucleus in the microconjugant also enters second progamic metaphase. The third division in the microconjugant and second division in the macroconjugant occur simultaneously (Text-fig. III, figs. A-I). The latter condition indicates that the difference in the number of progamic divisions of the micronucleus in the two conjugants may be due to the behaviour of the micronucleus of the macroconjugant. At any rate this seems more plausible than considering the first progamic division in the microconjugant as having arisen *de novo*. The time taken for completion of the first progamic division in the macroconjugant is equivalent to the time taken for the two divisions of the counterpart in the microconjugant. The macroconjugant behaves as a specialized cell which requires a stimulus for the first progamic division to progress and this seems to be provided when the first progamic division is completed in the microconjugant. A similar, but slightly different, condition has been recorded in *Epistylis articulata* (Dass, 1953), where the first division of the micronucleus in both conjugants start simultaneously and proceed up to metaphase. Thereafter, the division process is arrested in the macroconjugant and is resumed only with the second progamic division metaphase in the microconjugant. In this difference in time factor during progamic divisions, as also the size and future behaviour, the macroconjugant of Peritricha resembles the ovum of metazoa.

(c) Formation of nuclear anlagen

Formation of the synkaryon and nuclear anlagen follows the complete fusion of the microconjugant with the macroconjugant. In no instance was a residual microconjugant observed, though Popoff (1908) found it in *Carchesium polypinum*.

Generally, soon after the fusion of the pronuclei the unused progamic nuclei are absorbed in the cytoplasm. In a few cases, viz., *Vorticella microstomu* (Finley, 1943), *Rhabdostyla vernalis* (Finley, 1952), *Zoothamnium arbuscula* (Furssenko, 1929) and *Epistylis articulata* (Dass, 1953) they persist for some time, and can be recognized long after the synkaryon has started its division. In *C. spectabile*, however, all progamic nuclei except one are absorbed in their respective conjugants long before their fusion.

The synkaryon is formed only in the macroconjugant and this is the condition observed in most peritrichous ciliates. But a reciprocal exchange of pronuclei with the formation of a synkaryon in each conjugant has been reported in *Zoothamnium arbuscula* (Furssenko, 1929) and *Urceolaria synaptae* (?) (Colwin, 1944). The synkaryon divides thrice successively to give rise to eight bodies, a feature common to all peritrichous ciliates so far studied. They are all alike and a fine network of thread-like structures is seen in all. Later, however, in one of the eight bodies the network-like structure gives place to a uniform homogeneous appearance. It also undergoes a reduction in size. This is the micronucleus. The other seven are the macronuclear anlagen.

A variation in the number of macronuclear anlagen has been recorded by Colwin (1944) in *Urceolaria synaptae* (?) but Finley (1952) has pointed out that

the author may have confused a macronuclear fragment for a macronuclear anlage. Willis (1948) observed in *Lagenophrys tattersalli* a number of instances where 'the morphologically single macronucleus shows a gross, moniliform character, with two, three, four or seven lobes, i.e., with the number of lobes corresponding to the number of discrete anlagen found in normal distributive stages. This may indicate that in certain cases the anlagen become fused together'. Outside this observation of Willis, in no other Peritricha has such a fusion of macronuclear anlagen been reported. Only in one instance, a departure from the conventional condition has been recorded; in case of *Vorticella convallaria* (Seshachar and Dass, 1951) where instead of seven of the eight bodies becoming transformed into macronuclear anlagen, only six do so and the remaining two become micronuclear anlagen.

(d) Reorganization fissions

Once the macronuclear anlagen are differentiated, the subsequent behaviour is easily followed. The faint network-like structure is soon lost and the anlagen appear homogeneous. This initial differentiation is followed by an increase in size and a progressive nucleination. The first reorganization fission takes place at this stage. The interval between the second and the third reorganization fissions is fairly long and during this period the growth and nucleination of macronuclear anlagen take place. An interesting feature recorded in this form is the differential rate of nucleination of the sister anlagen. Such a condition has not been observed in any other peritrichous ciliate.

The fate of the old macronucleus of the conjugants is interesting. The macronucleus of both conjugants breaks up into a number of fragments which fill the cytosome of the synconjugant. A gradual reduction in their numbers, by absorption, takes place now. Reduction at a more rapid rate takes place later during differentiation of the macro- and micronuclear anlagen. Most fragments are absorbed in the cytoplasm by the third reorganization fission. In some instances, the absorption is so rapid that no fragments are found even in the F_1 individuals. The significance of the rate of absorption of the fragments becomes apparent in instances where there is differential nucleination of the macronuclear anlagen. In some instances the macronuclear fragments are seen to persist up to the end of reorganization fissions and are found even in the fully reorganized individuals. In them, the nucleination of the anlagen is slow and gradual while in cases where the absorption of the fragments takes place early, the nucleination of the anlagen is also early and complete. This confirms the view that the absorption of the macronuclear fragments is perhaps not just 'degeneration' or 'elimination' of the old macronuclear material, but is a reconstitution of the old macronuclear material on a new frame work (Seshachar, 1947).

SUMMARY

The nuclear apparatus of *Carchesium spectabile* consists of an irregularly drawn out cylindrical macronucleus and a small spherical micronucleus.

During trophic activity a number of Feulgen negative spaces appear in the macronucleus.

In addition to unimicronucleate forms, in some colonies, individuals with two, three and four micronuclei are also seen.

Two types of binary fission are observed occurring in members of the colony, the criterion of difference being the behaviour of the macronucleus.

A vegetative individual undergoes a preliminary division and both the daughter cells pass through two further successive divisions to produce four microconjugants each. Hence there are eight microconjugants derived from a vegetative individual.

The macroconjugant is produced by differentiation of a vegetative animal.

The microconjugant is liberated as a free-swimming body and during this free-swimming search period its micronucleus undergoes a division. In those instances where the search period is short, the micronuclear division is not complete at the time of attachment to the macroconjugant.

More than one microconjugant may attach itself to a macroconjugant. All of them undergo nuclear changes.

The micronucleus of microconjugant undergoes three divisions while that of macroconjugant two. One of the progamic nuclei in each conjugant becomes a pronucleus and the rest are absorbed in the cytoplasm. The macronucleus of both conjugants fragment.

The microconjugant merges with the macroconjugant *in toto* to form a synconjugant. Two pronuclei fuse to form a synkaryon. The synkaryon divides thrice successively to form eight metagamic nuclei of which seven become the macronuclear anlagen while the eighth is the micronuclear anlage.

The macronuclear anlagen enlarge and progressively become nucleinated. The nucleination is often not uniform among sister anlagen.

The macronuclear fragments are at first absorbed gradually, but later, during the differentiation and growth of the macronuclear anlagen, the absorption is more rapid. In those instances where the nucleination of macronuclear anlagen takes place slowly, it is noticed that the rate of absorption of the fragments is also slow.

ACKNOWLEDGEMENT

My grateful thanks are due to Dr. B. R. Seshachar for guidance and encouragement. I am deeply thankful to the National Institute of Sciences of India for the award of I.C.I. (India) Research Fellowship which provided me opportunity for this study.

REFERENCES

References marked with asterisks * were not available in the original.

- Awerinzew, S. (1912). Beiträge zur Entwicklungsgeschichte von *Lagenophrys* sp. (Vorläufige Mitteilung). *Biologisches Centralblatt*, 32, 714-718.
- Claparède, E. and Lachmann, J. (1858-1861). Études sur les Infusoires et Rhizopodes. Genève.
- Colwin, L. H. (1944). Binary fission and conjugation in *Urceolaria synaptae* (?) Type II (Protozoa, Ciliata) with special reference to the Nuclear phenomena. *J. Morph.*, 75, 203-249.
- Dass, C. M. S. (1953). Studies on the Nuclear Apparatus of Peritrichous Ciliates. Part I. The Nuclear apparatus of *Epistylis articulata* (From.). *Proc. Nat. Inst. Sci.*, 19, 389-404.
- Diller, W. F. (1928). Binary fission and endomixis in the Trichodina from tadpoles. *Jour. Morph. and Physiol.*, 46, 521-561.
- (1936). Nuclear reorganization process in *Paramecium aurelia*, with description of autogamy and 'hemixis'. *J. Morph.*, 59, 11-67.
- Engelmann, Th. W. (1876). Über Entwicklung und Fortpflanzung der Infusorien. *Morph. Jahrb.*, 1, 573-675.
- Enriques, P. (1907). La conjugazione et il differenziamento sessuale negli Infusori. *Arch. f. Protistenk.*, 9, 195-296.
- (1908). Die conjugation und sexuelle Differenzierung der Infusorien. *Arch. f. Protistenk.*, 12, 213-276.
- Fauré-Fremiet, E. (1930). Growth and differentiation of the colonies of *Zoothamnium alternans* (Clap. and Lachm.). *Biol. Bull.*, 58, 28-51.
- Finley, H. E. (1943). The conjugation of *Vorticella microstoma*. *Trans. Amer. Micro. Soc.*, 52, 97-121.
- (1952). Sexual differentiation in Peritrichous ciliates. *J. Morph.*, 91, 569-605.
- Furssenko, A. (1929). Lebenszyklus und Morphologie von *Zoothamnium arbuscula* Ehrb. *Arch. f. Protistenk.*, 67, 378-500.
- Hamburger, C. (1904). Die Konjugation von *Paramecium bursaria* (Focke). *Arch. f. Protistenk.*, 4, 199-239.
- Kaltenbach, R. (1916). Die Conjugation von *Ophrydium versatile*. *Arch. f. Protistenk.*, 36, 67-71.
- Maupas, E.* (1888). Sur la multiplication des Infusoires cilies. *Arch. de Zool. Expt. et Gen.*, 6, 155-277.
- Padnos, M. (1939). The morphology and life-history of *Trichodina* infecting Puffer. *Anat. Rec.*, 75 (Suppl.), 157.
- and Nigrelli, R. F. (1942). *Trichodina sphaeroidesi* and *T. halli*, spp. nov. Parasite on the gills and skin of marine fishes, with special reference to the life-history of *T. sphaeroidesi*. *Zoologica*, 27, 65-72.
- Penard, E. (1922). Études sur les infusoires d'eau douce. Geneva.
- Plate, L. (1888). Protozoenstudien. *Zool. Jahrb. (Anat. u. Ontog.)*, Bd. 3.
- Popoff, M. (1908). Die Gametenbildung und die Conjugation von *Carchesium polypinum* L. *Zeitschr. f. Wiss. Zool.*, 89, 478-524.

- Pillai, S. C. and Subramanyam, V. (1942). Relation of Protozoa to 'Bulking' of Activated sludge. *Sci. and Cult.*, **8**, 376-378.
- Rosenberg, L. E. (1940). Conjugation in *Ophisthnecta henneguyi*, a free swimming vorticellid. *Amer. Phil. Soc. Proc.*, **82**, 437-448.
- Seshachar, B. R. (1947). Chromatin elimination and the ciliate macronucleus. *Amer. Nat.*, **81**, 316-320.
- and Dass, C. M. S. (1951). Macronucleus of *Vorticella convallaria* Linn. during conjugation. *J. Morph.*, **89**, 187-198.
- Stein, Fr.* (1867). *Der Organismus der Infusientiere*. Bd. 2. Leipzig.
- Summers, F. M. (1938). Normal development in *Zoothamnium alternans*. *Biol. Bull.*, **74**, 117-129.
- Wenrich, D. H. (1926). The structure and division of *Paramecium trichium*. *Anat. Rec.*, **29**, 117.
- Wesenberg-Lund, C.* (1925). Contributions to the Biology of *Zoothamnium geniculatum* Ayroon. *Memoires de l'Acad. Roy des Sciences et des Lettres de Danemark, Copenhagen, Section des Sciences, 8me serie*, **10**, 1-53.
- Willis, A. G. (1948). Studies on *Lagenophrys tattersalli* (Ciliata, Peritricha, Vorticellinae). Part II. Observations on Bionomics, Conjugation, and Apparent Endomixis. *Q.J.M.S.*, **89**, 385-400.
- Wichterman, R. (1946). Unstable micronuclear behaviour in an unusual race of *Paramecium*. *Anat. Rec.*, **94**, 94.
- Woodruff, L. L. (1931). Micronuclear variation in *Paramecium bursaria*. *Q.J.M.S.*, **74**, 537-545.

EXPLANATION OF PHOTOMICROGRAPHS

Key to lettering: M - Macronucleus; m - micronucleus; M.C. - Macroconjugant; m.c. - Microconjugant; M.A. - Macronuclear anlagen; M.f. - Macronuclear fragments.

PLATE IV

- FIG. 1. Vegetative individual showing Feulgen negative spaces in the macronucleus. $\times 720$. Feulgen-Light green.
- FIG. 2. Binary fission Type I. $\times 360$. Feulgen-Light green.
- FIG. 3. Binary fission Type II. $\times 360$. Feulgen-Light green.
- FIG. 4. Bi- and tetra-micronucleate individuals. $\times 360$. Feulgen-Light green.
- FIG. 5. Conjugation. Microconjugant just attached to macroconjugant. $\times 720$. Feulgen-Light green.
- FIG. 6. Conjugation. Macroconjugant with two microconjugants. One of them not in direct contact with the macroconjugant. $\times 720$. Feulgen-Light green.
- FIG. 7. Synconjugant. The cytosome is filled with macronuclear fragments. $\times 720$. Feulgen-Light green.
- FIG. 8. F_1 individuals. The number of macronuclear fragments greatly reduced. $\times 360$. Feulgen-Light green.
- FIGS. 9 and 10. F_1 individuals. All the macronuclear fragments absorbed. The macronuclear anlagen showing maximum nucleation. $\times 720$. Feulgen-Light green.
- FIG. 11. F_2 individuals. In one of the individuals the fragments are still persistent while they are absent in the other. The macronuclear anlagen of sister individuals show different rates of nucleation. $\times 180$. Feulgen-Light green.
- FIG. 12. F_2 individual. Prior to third reorganization fission. No macronuclear fragments in the cytosome. $\times 720$. Feulgen-Light green.
- FIG. 13. F_3 individual. No macronuclear fragments in the cytosome. $\times 720$. Feulgen-Light green.
- FIG. 14. F_3 individual. Macronuclear fragments still persistent. $\times 720$. Feulgen-Light green.

THE BIOLOGY OF THE GREY MULLET, *MUGIL TADE* FORSKÅL, WITH NOTES ON ITS FISHERY IN BENGAL

by T. V. R. PILLAY, *I.C.I. (India) Research Fellow of the National Institute
of Sciences of India **

(From the Laboratories of the Zoological Survey of India, Calcutta)

(Communicated by S. L. Hora, F.N.I.)

(Received 10th June ; read August 7, 1953)

CONTENTS

	<i>Page</i>
Introduction	187
Material and methods	188
Description of the species	189
Distribution	191
Raciation	193
Relationship of body measurements to total length	194
Weight-length relationship	196
Ponderal index	197
Food and feeding habits	200
Sex ratio and fecundity	201
Maturation and spawning	201
Maturation	201
Spawning season	202
Frequency of spawning and the spawning grounds	203
Description of larvae	204
Age and growth	204
Scales as indicative of age and growth	204
Scale characters	204
Annulus formation	205
Age and growth determination	206
Length frequency distribution	209
Migrations	211
Predators and parasites	212
Fishery in Bengal	213
Fishing methods	213
Composition of catches	214
Summary	214
Acknowledgements	215
References	215

INTRODUCTION

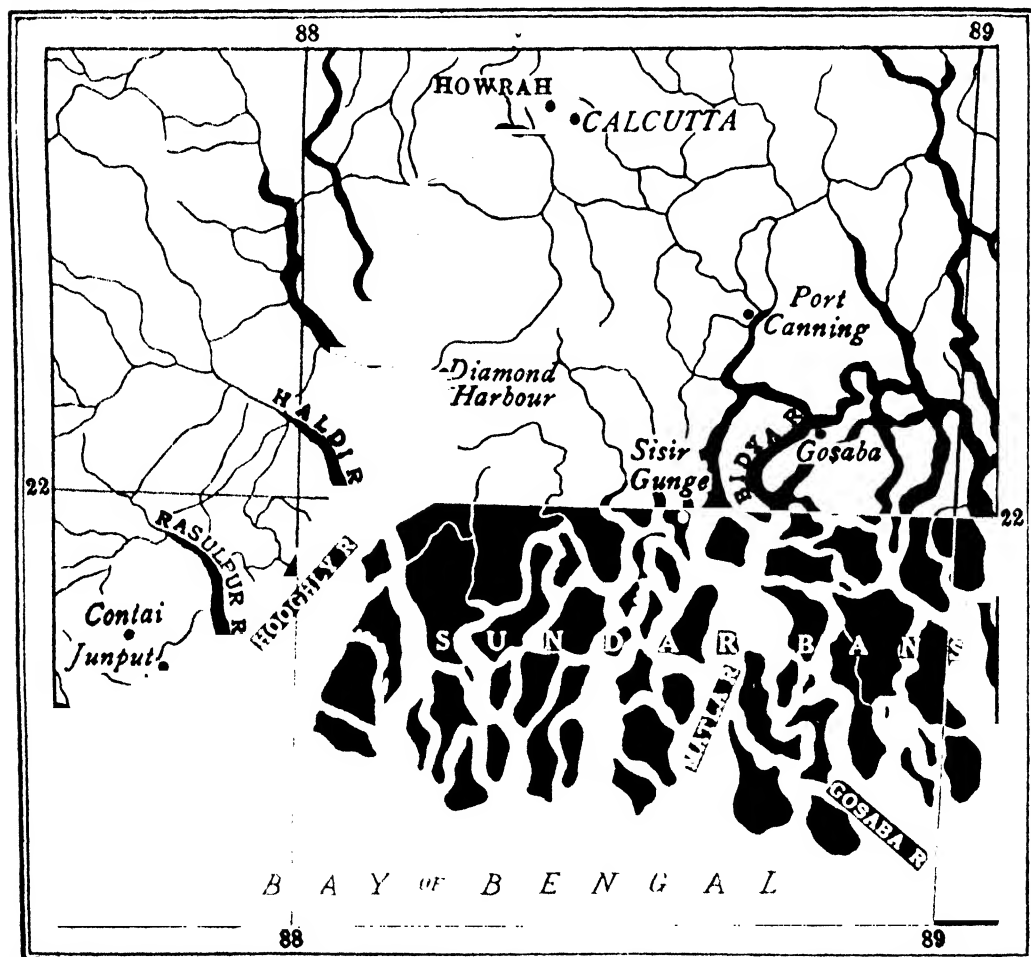
The Grey Mulletts belonging to the family Mugilidae (Order Percosoces) are of major economic importance in the coastal and estuarine fisheries of India. Out of the total of twenty-six species described by Day (1878) from India, only five, viz., *Mugil cephalus* Linn., *M. tade* Forsk., *M. corsula* Ham., *M. parsia* Ham. and *M. speigleri* Blkr. have so far been recorded from Bengal (Pillay, 1951). Very little detailed work has been reported on the biology of these species in Indian waters. This paper is an attempt to contribute to the knowledge of the general biology of

* Present address: Hilsa Fish Enquiry, I.C.M.R., All-India Institute of Hygiene and Public Health, Calcutta.

M. tade, which is one of the common species in Bengal. The report of investigations on its food and feeding habits and culture have been dealt with in detail in two separate papers (Pillay, 1953a and 1953b).

MATERIAL AND METHODS.

Regular collection of material for the purpose of this study was started in the month of January, 1949. Being a species that occurs both in marine and estuarine environments, as also in 'bheris' (embanked brackish water areas), sampling was done from all these representative localities (Text-fig. 1). But the data collected from the sea (Junput on the Contai Coast, Midnapore district) and the estuary (Port Canning on the River Matla, 24-Parganas) only are discussed in this paper. Though most of the mullet fishing and assembly centres in W. Bengal were visited for the collection of material, due to the distance of these localities from the laboratory, lack of proper transport facilities and the total absence of any organization to help in the collection of material, regular sampling work had to be restricted to the nearby centres. The sampling was done once every month at regular intervals. Several difficulties were experienced in obtaining regular representative samples.



TEXT-FIG. 1. Map of lower Bengal showing the centres where observations were made during the investigations.

Both at Junput and at Port Canning, where the catches are landed just in time to be rushed to the market—in the former case to Contai, a distance of six miles by road and in the latter to Calcutta, a distance of twenty-eight miles by rail—the fishermen seldom allow anybody to handle the fish. As mullets are sold only in whole lots mixed with other species, it was not always possible to purchase enough fish for the studies. In the local markets catches from these localities are mixed with fish from other sources, including farms, and so no reliable data could possibly be obtained from there. In spite of these serious handicaps, every effort was made to get fairly representative samples of mullets from the landing places, the actual fishing centres or, as in Port Canning, from the local markets where a small part of the catches are sold in retail. Only samples, the original sources of which could be reliably determined, were collected, and even so the disinclination of the fishermen to sell the fish at the landing places greatly restricted the size of the samples obtained.

All collections were personally made and, in every case, all available field information was gathered. The samples came from catches of the hand seine (*Katti jal*) and the barrier net (*Bher jal*) in Junput, and mostly the bag net (*Behundi jal*) in Port Canning. Short descriptions of these nets are given on pages 27-28. The total length, weight, sex, and condition of gonads of all the specimens in the samples were recorded. During the first year of investigation, the various body measurements referred to on page 7, vertebral count, and scale and fin ray counts, were also made. Scales and stomach contents were examined from all the specimens in the smaller samples or, in the case of larger samples, from smaller sub-samples. The details of techniques employed in the investigation are described in the appropriate sections.

DESCRIPTION OF THE SPECIES.

As observed by Schultz (1946), the family Mugilidae 'is remarkably constant in anatomical structures', and the identification of a species becomes extremely difficult when the descriptions available are inadequate. During the present study it was found that the species had neither been adequately described nor the full range of characters recorded. A fuller description of the species, including the characters of the mouth parts considered useful in the identification of mullets by Schultz (*op. cit.*) and Smith (1948), based on the study of a large series of samples, is given below:

Mugil tade Forskål.

Mugil crenilabris tade: Forskål, *Descr. Anim.*, 1775, p. 74.

Mugil tade: Cuvier and Valenciennes, *Hist. Nat. Poiss.*, 11, 1836, 114.

Klunziger, *Abhandl. Zool. Bot. Ges. Wien.*, 20, 1870, 828.

Sitzungsb. Akad. Wien., 1880, 394.

Fische des rothen Meeres, 1884, 133.

Macleay, *Proc. Linn. Soc., N.S. Wales*, 11, 1884, 40.

Day, *Fauna Brit. India—Fishes*, 2, 1889, 344.

Weber and de Beaufort, *Fish. Indo-Austr. Arch.*, 4, 1922, 236.

Fowler, *Mem. Bernice P. Bishop Mus.*, 10, 1928, 122.

Herre, *Mem. Indian Mus.*, 13, 1941, 348.

Kulkarni, *Journ. Bombay Nat. Hist. Soc.*, 47, 1947, 3.

Devanesan and Chidambaram, *Common Food Fishes Madr. Pres.*, 1948, 30.

Jacob and Krishnamurthy, *Journ. Bombay Nat. Hist. Soc.*, 47, 1948, 663.

John, *Progr. Rep. Fish. Dev. Scheme, Centr. Res. Inst. Trav. Univ.*, 1948, 7.

Devasundaram, *J. Zool. Soc. India*, 3, 1951, 21-22.

Mugil planiceps: Bleeker, *Verb. Bat. Gen.*, 25, 1853, 101.

Günther, *Cat. Brit. Mus.*, 3, 1859-61, 428.

- Kner, *Fische Novara Exp.*, 1865-67, 225.
 Day, *Fishes of India*, 1878, 350.
 Seale, *Occ. Pap.*, Bernice P. Bishop Mus., 1, 3, 1901, 66.
 Evermann and Seale, *Bull. U.S. Bur. Fish.*, 26, 1906, 59.
 Max Weber, *Nova Guinea*, 9, 4, 1913, 569.
 Whitehouse, *Madr. Fish. Bull.*, 15, 1922, 82-84.
Mugil belanak: Bleeker, *Nat. Tijdschr. Ned. Indie*, 13, 1857, 356.
 Günther, *Cat. Brit. Mus.*, 3, 1859-61, 427.
 Day, *Fishes of India*, 1878, 350.
 Day, *Fauna Brit. India—Fishes*, 2, 1889, 345.
 Vinciguerra, *Annal. Mus. Civ. Genova* (2), 9, 1890, 180.
 Fowler, *Proc. Acad. Nat. Sci.*, 57, 1905, 455.
 Max Weber, *Nova Guinea*, 5, 2, 1908, 244.
Mugil bontah: Bleeker, *Verh. Bat. Gen.*, 25, 1853, 48.
 Bleeker, *Nat. Tijdschr. Ned. Ind.*, 13, 1857, 336; 16, 1858-59, 278; 18, 1859, 367.
 Bleeker, *Act. Soc. Sci. Indo-Neerl.*, 8, 1860, 49.
Mugil cephalotus: Cantor (not Cuvier and Valenciennes), *Cat. Malayan Fish, Journ. Asiatic Soc. Bengal*, 18, 2, 1850, 1077.
Mugil kanduensis: Günther, *Fische d. südsee*, 2, 1876-1881, 215.
 D. 4 1/8; P. 17; V. 1/5; A. 3/9; C. 14-15; Ll. 30-35; Ltr. 11; Pyl. Caec. 5; Br. 4.

The rostro-dorsal profile is nearly straight, and from the crown of the head to the snout it is strongly declivous. The height of the body is contained 4 to 6.3 times in the total length, the proportion being 4-4.5 in young specimens below 3 cm. in length. The head is nearly conical in shape and its anterior portion is depressed and pointed. The least height of caudal peduncle is contained 1.4-1.8 times in its own length and 1.5 to 2.4 times in the length of head. The head is contained 4.4 to 4.9 times in the total length in adults, but is relatively larger in juveniles (up to about 5 cm. in length) being only 3.9-4.2 times in the total length. The eyes are provided with gelatinous eyelids in adults. There are adipose thickenings both in front and behind the eyes and there are distinct anterior and posterior eyelids. The anterior lid is narrow and covers only about 1/6 of the eye, whereas the posterior one is broader and covers about $\frac{1}{4}$ of it. The adipose eyelids are absent in young individuals. In 9 cm. long fish, the anterior adipose eyelid is absent, but the posterior one is developed as a narrow flap. Specimens 15 cm. in length show the adult character of the eyelids fully developed. The relative size of the eye varies with the size of the fish. Up to a size of about 5 cm. it is contained 2.2 to 3.5 times in the length of the head and in full grown specimens, 4.7 to 6.7 times. The snout, which is pointed, is nearly equal in length to the diameter of the eye. The preorbital bone is emarginate, strongly curved, and lies over the maxillary reaching far beyond the corner of the mouth posteriorly, in the adults. The posterior end of the preorbital is rounded and the front edge is not notched. The anterior margin of the bone is denticulate. In juveniles, this bone is nearly straight. The end of the maxillary is visible when the mouth is closed and reaches beyond the posterior end of the preorbital. The premaxilla and maxilla are bent downwards. The anterior margin of the premaxilla bordering the mouth is nearly straight. The mouth is slightly inferior in position. The upper lip forms the tip of the snout and is thick, and its breadth is contained 3 to 3.6 times in the orbit. The upper jaw bears numerous minute ciliform teeth with simple undivided truncate tips. The lower lip is thin, the edges of which are sharp and straight. The upper lip overhangs the lower lip. There are no teeth on the lower jaw. The symphyseal knob is single. The uncovered chin space is long and cuneiform anteriorly, but is pointed behind. The interorbital space is distinctly flat and is 1.3-2.5 times the diameter of the eye in adults. In juveniles up to a length of about 5 cm., it is equal

to the diameter of the eye. The two nostrils on either side, are situated close together, the distance between the two being contained 1.1 to 1.2 times in the interorbital space.

Fins: The origin of the first dorsal is slightly nearer to the end of the snout than to the base of the caudal in adults, but in young ones it is nearly in the middle. It is situated opposite 10th-12th scale of the lateral line, separated from the snout by about 19 predorsal scales, and is nearly as high as the second dorsal (1.1-2.0 times in the depth of body). The origin of the second dorsal is opposite 20th-23rd lateral scale, and is about $\frac{1}{3}$ of the length of the base of the anal behind its origin. Both the second dorsal and anal are slightly concave and covered with fine scales on their bases. The anal fin has three spines in adults, but in juveniles there are only two. In 2 cm. long specimens, there are only 2 spines, but the first soft rays have articulations only on the distal ends. This ray gradually becomes thicker as the fish grows and the number of articulations on it decreases. In 47 mm. specimens this ray is developed into a spine. The length of the pelvic fin is contained 1.4-1.7 times in the length of the head. The length of the pectoral fin is contained 1.1-1.6 times in the length of head and it reaches the 8th lateral scale. The caudal is slightly emarginate.

Scales: The scales are ctenoid in adults but are cycloid in juveniles. They become ctenoid when the fish is about 3.4 cm. long. The scales of adults are longer than broad with apicad nuclei, undulate basal margins and basal radii arranged fanwise. The dorsal scales also have only single grooves as the scales on the sides. The axillary scale is small and the enlarged scale at the base of the pelvic is slightly less than half the length of that fin. The bases of all the fins except the spinous dorsal are covered with fine scales which are cycloid.

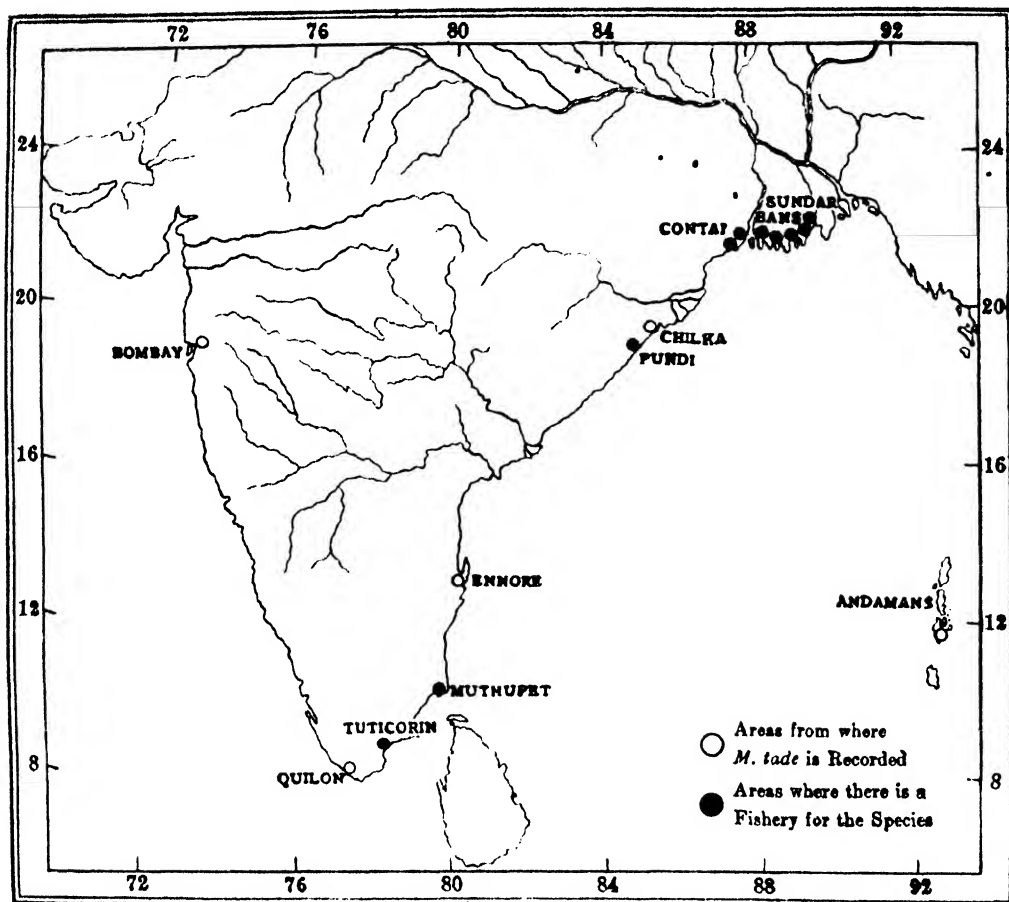
Colour: Specimens from the natural habitats are olivaceous above and silvery below, with 5-7 indistinct dark longitudinal lines on the sides. The edges of the pectoral, soft dorsal and anal are also olivaceous. The caudal is edged with black. Specimens from enclosed brackishwater farms are dark brown above and the dark longitudinal lines on their sides are very prominent. The edges of pectoral, soft dorsal, anal and caudal are also dark brown. The juveniles have the same coloration as adults, but the longitudinal lines appear only when they are about 5 cm. long. Preserved specimens of juveniles show a thick dark line along the middle of the sides. Other parts of the body are covered with scattered pigment spots.

According to Day (1889) *M. tade* grows to at least 18" (45.7 cm.) in length. Specimens measuring up to 67.9 cm. have been collected by the author from the Sundarbans.

DISTRIBUTION

Day (1878) mentioned the 'seas, estuaries and tidal rivers of India to the Malay Archipelago and China' as the habitat of this species. According to Weber and de Beaufort (1922), it occurs in the seas of South East Asia, Red Sea, Sokotra, Bay of Bengal, British India, Ceylon, Andamans, Penang, Malacca, China, Philippines, Marianas, Guam and Australia.

In India, *M. tade* appears to occur all along the coasts, though definite records exist only for certain localities (Text-fig. 2). Kulkarni (1947) recorded it in the Vehar and Borivli streams near Bombay. Dr. S. B. Setna, Director of Fisheries, Bombay, kindly informs me that it is a rare species on the Bombay Coast. John (1948) has included *M. tade* in the list of the ten species of mullets identified from Travancore waters. Mr. K. Gopinath, Marine Biologist, Trivandrum (now Director of Fisheries, Travancore-Cochin), in a private communication has informed me that this species locally known as 'Karincha' is common in Kayamkulam and Quilon backwaters. According to Devanesan and Chidambaram (1948), *M. tade* occurs on the coast of the Madras State, but they do not mention the precise range of its distribution. Mr. K. Chidambaram, Asst. Director of Fisheries (Marine Biology)



TEXT-FIG. 2. Map of India showing the distribution of *Mugil tade*.

West Hill (now Asst. Fisheries Development Adviser to the Government of India), has, however, kindly informed me that the fishery of this species is not important on the West Coast of the Madras State, but on the East Coast they are caught in appreciable numbers in Pundi (Vizagapatam), Mangodu (Tanjore), Muthupet and Arcothurai (Tuticorin). According to Mr. P. I. Chacko, Asst. Director of Fisheries (Freshwater Research), Madras (private communication), this species, locally known as 'Karattukendai', forms only about 5% of the mullet catches. Whitehouse (1922) has described *M. planiceps* (= *tade*) as one of the economically important mullets occurring in the Silavathurai lagoon in Tuticorin (Coromandel Coast). Jacob and Krishnamurthy (1948) have observed the occurrence of *Mugil tade* in the Ennore Creek near Madras. Devasundaram (1951) has recently identified *M. tade* from the Chilka Lake, but it is reported that they are found only in very small quantities there. As will be evident from the above, though the species is widely distributed in India, it does not rank high in production in these localities. Its main commercial fishery is mostly restricted to the estuarine and coastal regions of Bengal. The species has been observed along the coast of Midnapore district to the mouth of the Gangetic system ascending to a distance of about 80 to 90 miles from the sea. In the estuarine area it is being cultured on a large scale in 'bheri' (Hora and Nair, 1944) and on the Contai Coast, in freshwater tanks (Pillay, 1949). They have also been observed to ascend freshwater channels, where they live and grow

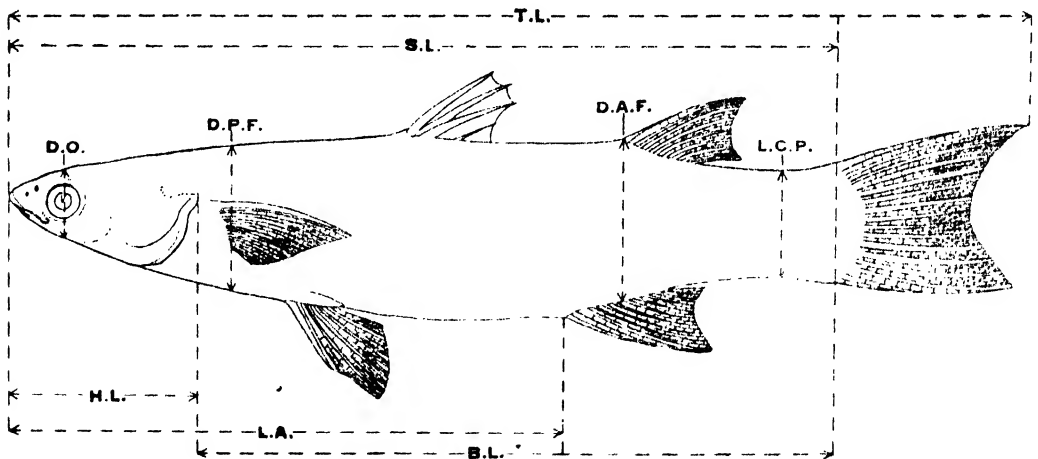
well. In Bengal, the fish is known as 'Bhangon' in Calcutta and nearby places, and 'Dhoka' on the Midnapore Coast.

RACIATION

Distinction is often made between the 'sea mullet' and the 'river mullet'. Even though there were very few easily recognizable differences between them, the possibility of the existence of separate races had to be considered, especially since very little was known definitely about their migrations. Due to the limitations of the present investigation which was confined to Bengal, it was not possible to study specimens of mullets from other parts of India. However, the chief aim of the study was to ascertain whether homogeneous populations were being handled in the present investigation of the biology of the fish. For the purpose of this work, samples were collected from the sea coast at Junput (Contai, Midnapore district) and the estuary at Port Canning (Matlah River, 24-Parganas).

Examination of a large number of specimens showed that the meristic characters were very stable in the species. The range of fin ray and scale counts was the same for samples from both localities. Similarly the number of vertebrae was 24 (11 plus 13) for samples from the two localities. Morphometric data were analysed to determine whether the body proportions showed any significant variations in the specimens from the two localities. Text-fig. 3 shows the measurements concerned in this study. As shown on page 194, there is a straight line relationship between these measurements and the total length, in fish above 5 cm. in size. The measurements of specimens above that size only were utilized for the analysis.

In racial studies, generally, the method of indices (the various proportional measurements expressed as fractions of total length) is made use of. In the present study this method was employed, the indices used being the values of the various measurements, shown in Text-fig. 3* in relation to total length. From the



TEXT-FIG. 3. The measurements of *Mugil tade* used in racial study.

D.O.	..	Depth through orbit.
D.P.F.	..	Depth through pectoral fin base.
D.A.F.	..	Depth through anal fin base.
L.C.P.	..	Least depth of caudal peduncle.
S.L.	..	Standard length.
T.L.	..	Total length.

* The body length was not examined separately as the standard length and head length were being considered.

standard errors of the samples, the standard error of the difference between means of the two sets of samples was estimated using the formula

$$\sigma_d = \sqrt{\frac{N_1}{N_2} \sigma_{M_1}^2 + \frac{N_2}{N_1} \sigma_{M_2}^2}$$

where σ is the standard deviation, σ_{M_1} the standard error of the 1st sample, σ_{M_2} the standard error of the second sample, and N_1 and N_2 , the number of individuals in the first and second samples respectively (Rounsefell and Dahlgren, 1935 and Simpson and Roe, 1939). From this the t value which is an index of the significance of the difference between the samples was calculated by employing the formula

$t = \frac{d}{\sigma_d}$ where d is the difference between the means of the two samples. The data obtained by this analysis are given in the following table:

TABLE I

Index.	N_1	N_2	σ_1	σ_2	SE_1	SE_2	σ_d	t	Significance
Total length/Standard length	200	200	0.173	0.013	0.024	0.002	0.024	0.083	Nil.
Total length/Head length	200	200	0.308	0.162	0.043	0.023	0.049	2.041	"
Total length/Length to anal	200	200	0.060	0.011	0.008	0.002	0.008	2.500	"
Total length/Depth through eye	200	200	1.656	1.453	0.234	0.206	0.224	0.446	"
Total length/Depth through pectoral fin base	200	200	0.384	0.247	0.054	0.035	0.064	0.167	"
Total length/Depth through anal fin base	200	200	0.366	0.242	0.052	0.034	0.062	1.000	"
Total length/Least depth of caudal peduncle	200	200	0.557	0.544	0.079	0.077	0.110	0.239	"

As will be evident from the above table, the morphological differences between *Mugil tade* in the sea off Junput and in the river Matlah are not statistically significant, and the populations in these localities do not constitute separate races. But at present we have no evidence to decide whether the two stocks remain distinct or whether they intermingle.

RELATIONSHIP OF BODY MEASUREMENTS TO TOTAL LENGTH

The relation between the dimensions of the external parts of the fish and its total length was determined from the measurements of over 400 specimens ranging from 5.0 cm. to 45.0 cm. in length. The measurements were (*vide* Text-fig. 3):

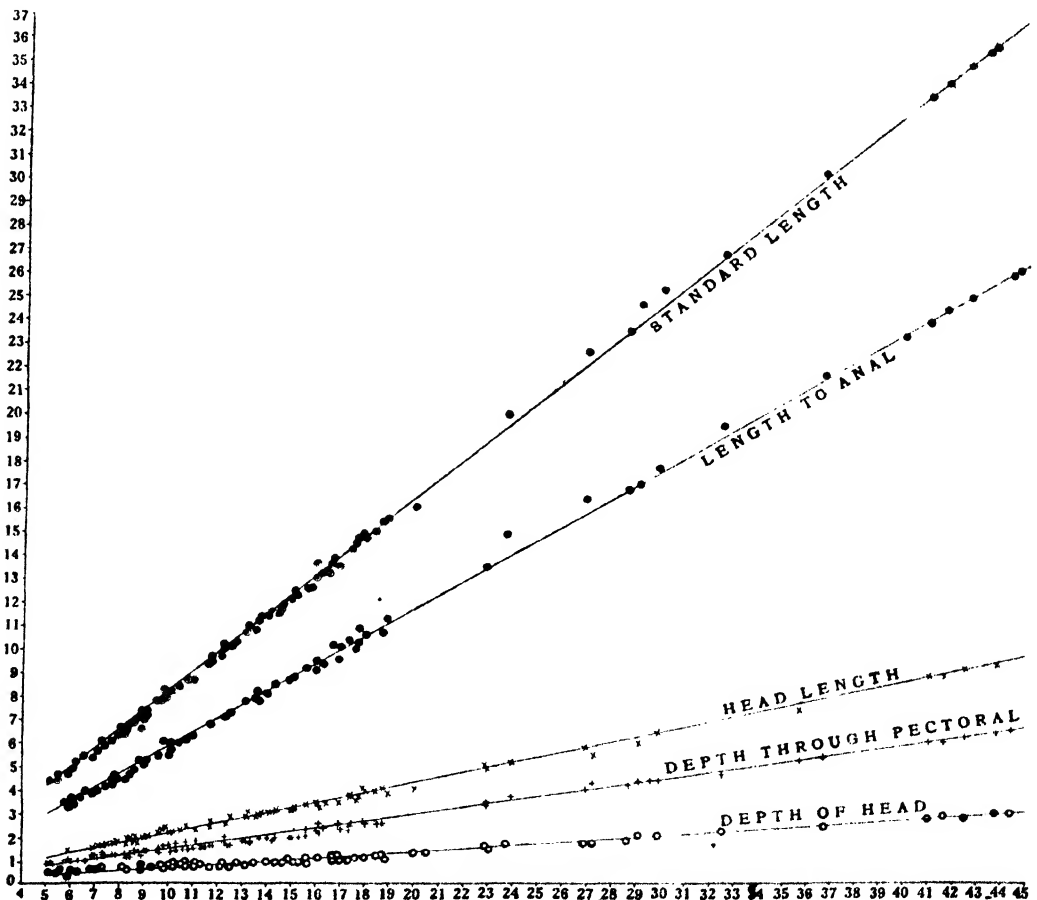
1. Standard length, from tip of snout to the end of hypurals.
2. Head length, from tip of snout to the end of opercle.
3. Body length from the end of opercle to the end of the hypurals.
4. Length to anal, from the tip of snout to the anterior end of anal fin base.
5. Depth of body through the pectoral fin base.
6. Depth of body through the anal fin base.
7. Depth of head at the region of the orbit.
8. Least height of caudal peduncle.

In Text-figs. 4 and 5, the various measurements are plotted against the total length. In each case it is a straight line relationship and suggests that after the 5 cm. stage there is no allometric growth in the species. The rate of growth of the

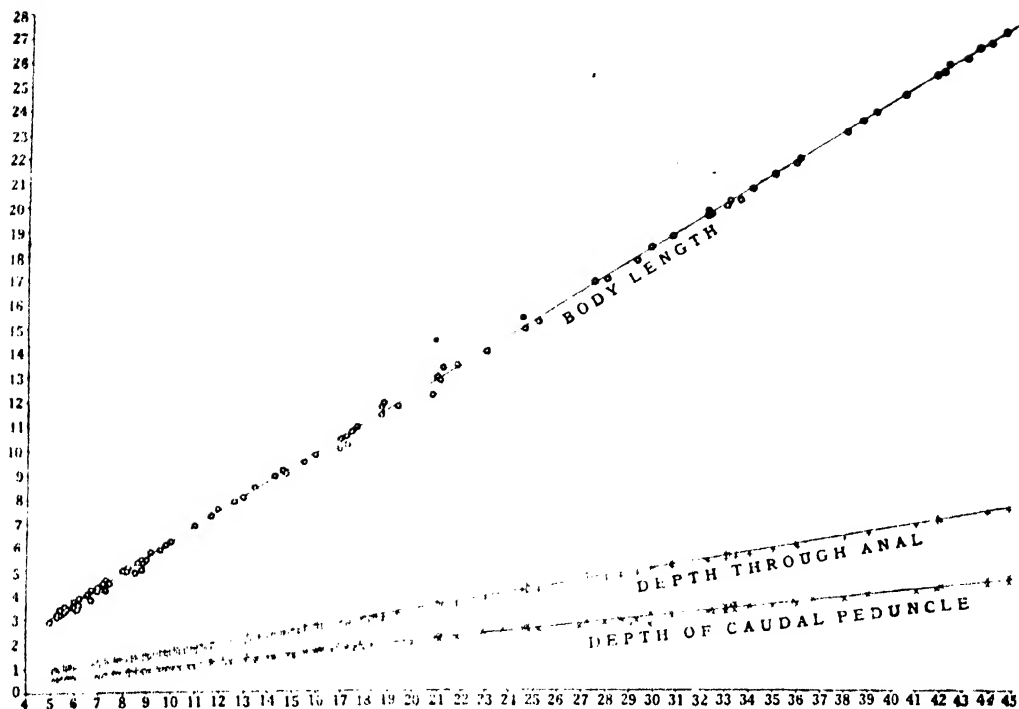
different parts of the body in relation to the increase in total length (not in relation to time) was determined by the tangent method (Crozier and Hecht, 1913). The tangent of each curve was calculated by dividing the vertical distance between two points on each curve, by the horizontal distance. These tangents are as follows:

Standard length	0.815
Body length .:	0.619
Length to anal fin	0.581
Head length	0.212
Depth of body through anal fin base	0.163
Depth of body through pectoral fin base	0.131
Least-depth of caudal peduncle	0.105
Depth of head through orbit	0.068

As is evident from the above, the standard length has the maximum rate of growth. Among the other measurements, the body length from opercle to hypurals has the maximum rate of growth, and the depth through orbit, the minimum. The growth rate of the head is approximately $\frac{1}{3}$ that of the body. The depths of the body at the anterior end of anal fin base and at the pectoral fin base increase nearly at the



TEXT-FIG. 4. Graph showing the relationship of body measurements to total length.



TEXT-FIG. 5. Graph showing the relationship of body measurements to total length.

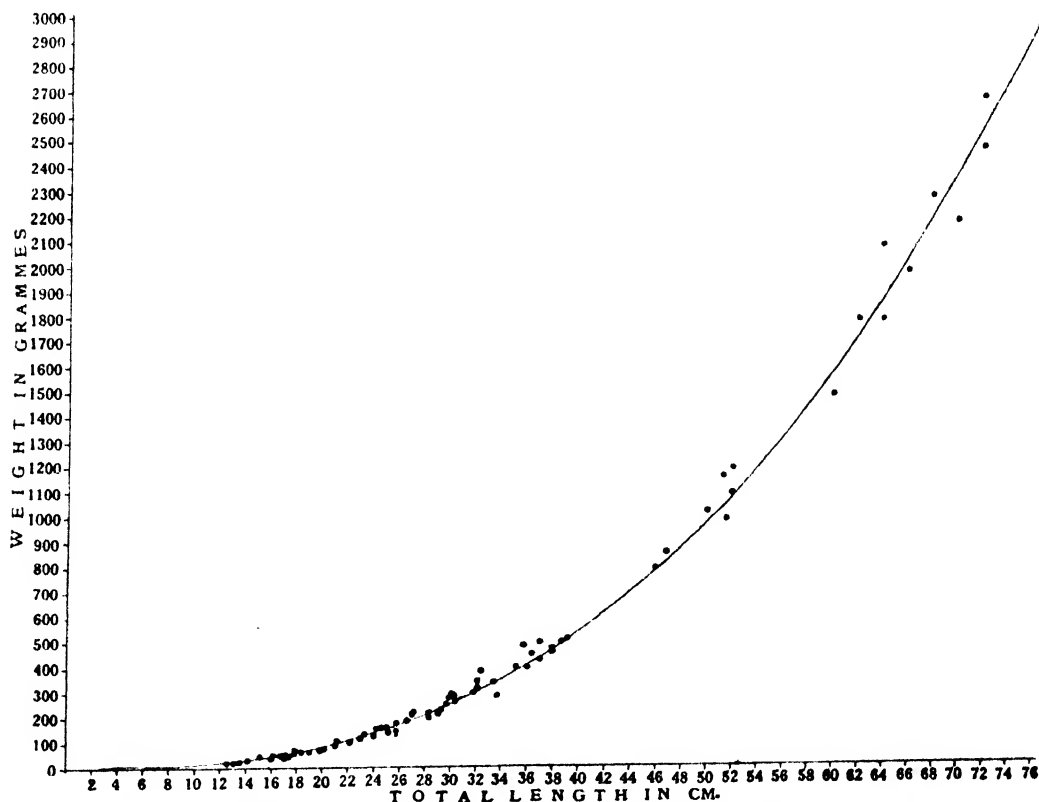
same rate. The rate of increase of the depth through orbit is about half that of the depth through pectoral fin base.

Research workers very often use the standard lengths of fishes in their studies, though total lengths are more readily accepted and understood by the fishermen and the fish traders. Moreover, there is a likelihood of some confusion in measuring standard length, as the base of the caudal fin in mullets is covered by scales and the end of the lateral line series or the tip of the hypurals cannot be located easily. However, to facilitate the comparison of data, the mathematical relationship between the total length and the standard length was determined from a series of 200 measurements. The linear regression line is shown in Text-fig. 4. The coefficient of correlation r , was found to be 0.998. The equation for the regression line, $Y = a + bX$, was used to express the relationship between the two variates, X (= total length) and Y (= standard length). The equation was found to be $Y = 0.81125 X - 0.025$.

WEIGHT-LENGTH RELATIONSHIP

A knowledge of the weight-length relationship of a fish is of great value both to the fishery operatives and the fishery biologist. Besides serving as the basis for the calculation of weights of fishes of known lengths or lengths of fishes of known weights, the coefficients of this relationship have been used as measures of individual or average seasonal and regional differences in the condition or 'degree of well being' of fishes. The average weight-length relationship was determined from measurements of 400 specimens from 4 cm. to 67.9 cm. in total length, collected from the estuarine and coastal waters. The fish were weighed with a spring balance graduated to the nearest gramme. Preliminary analysis of the available data did not show any significant differences in the weight-length relationship of the two sexes and so the average has been calculated for the two sexes combined.

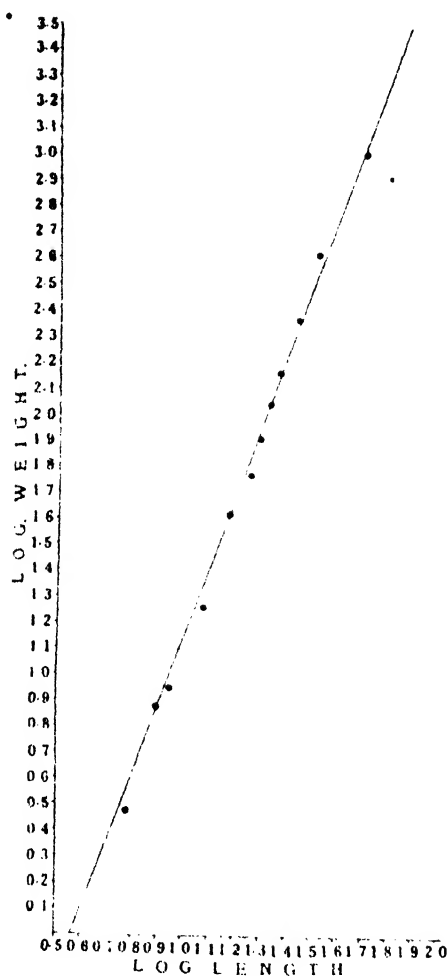
The relationship of the average weight to the length is represented in Text-fig. 6. As can be seen from this figure, the weight of the fish increases as an exponential function of its length. Since the weight-length ratio is a power relationship, the logarithms of the readings were used for calculations. The logarithmic relation of weight and length is illustrated in Text-fig. 7, which clearly shows a straight line relationship. The equation for the weight-length curve was found to be $W = 0.3337 L^{2.6198}$, where the weight is in grammes and the length is in cm. The weight-length data plotted in Text-fig. 6 show that the values are very uniform up to about 36 cm. length, above which there is noticeable variation. Kesteven (1942) and Morrow (1951) have shown that such variations are generally caused by the fluctuations in the weight of the visceral and somatic tissues. When compared with the increase in length, the proportional increase in weight is not marked up to about the 18 cm. stage, whereafter the increase in weight is quite rapid. From the commercial stand-point, it may not, therefore, be economical to catch fish below this size, thus foregoing the advantage of the rapid gain in weight.



TEXT-FIG. 6. Weight-length relationship of *Mugil tade*.

PONDERAL INDEX

Ponderal index or the coefficient of condition has been established to be of help in understanding some important features of the biology of fishes. Hickling (1930), Hart (1946), Menon (1950) and Morrow (1951) have correlated fluctuations in the ponderal index with the attainment of maturity and spawning. In the present study the weight-length data discussed in the previous section were analysed

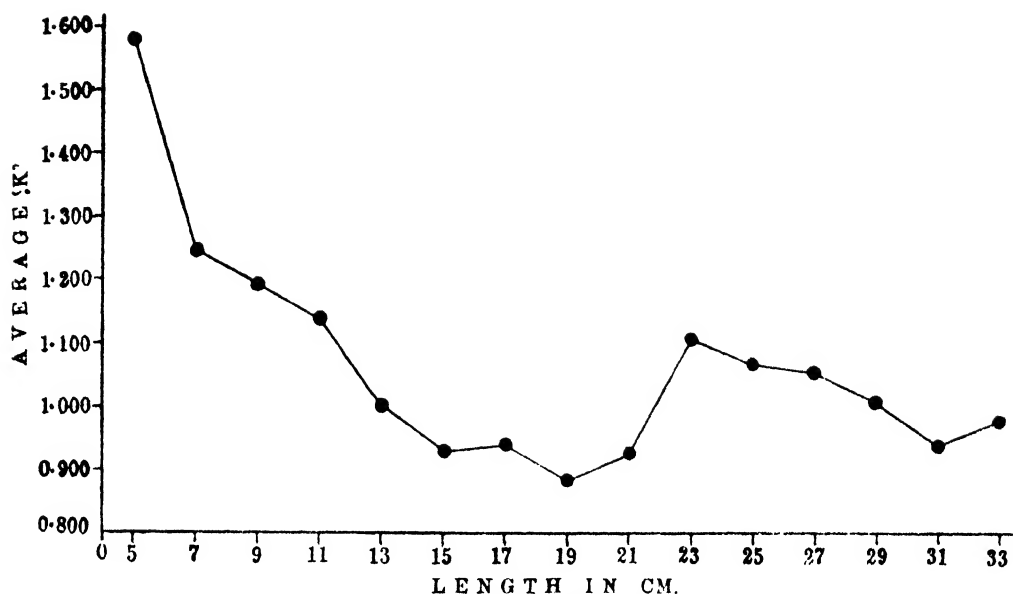


TEXT-FIG. 7. Logarithmic relation of weight and length of *Mugil tade*.

separately for the various size groups and for samples collected during different months. The ponderal index was calculated employing the formula

$$K = \frac{W}{L^3} \times 100$$

where W is the weight of fish in grammes, L is the length of fish in cm. and K is the ponderal index. The average ponderal index for each cm. length group and the average ponderal index for the whole sample in different months have been computed. Lengths up to 34 cm. alone were considered in this study, as the data available for larger fish were very limited for any correct interpretations. Hart (1946) and Menon (1950), have found that besides the seasonal fluctuations in the ponderal index or condition factor, there is a marked lowering of the value, associated with the increased metabolic strain of spawning. Table II gives the average values for K for each cm. length group, and these values are plotted in Text-fig. 8. The curve in this figure shows that the K value progressively decreases with increase in length up to about 21 cm., whereafter it shows a marked rise. If the point of inflection of the curve is indicative of the length at first maturity, it may be said that the fish matures at an average length of 23 cm. Some evidence in



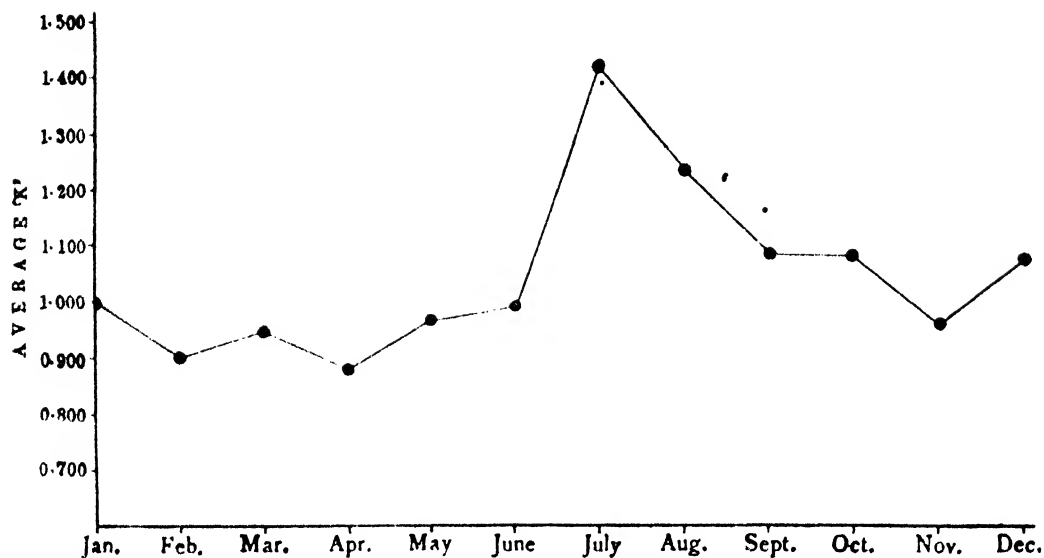
TEXT-FIG. 8. The average K at the different lengths of *Mugilade*.

support of such a conclusion has also been afforded by the fact that the smallest females with maturing eggs in the ovary, examined during this investigation, were also of about this size.

TABLE II

Mean length in cm.	Number of specimens.	K .
5	22	1.581
7	46	1.247
9	76	1.199
11	98	1.092
13	48	1.004
15	52	0.932
17	40	0.941
19	16	0.884
21	6	0.928
23	12	1.103
25	4	1.069
27	10	1.057
29	20	0.989
31	4	0.937
33	4	0.979

The mean K values for the samples in successive months are presented in Table III, and these values are plotted in Text-fig. 9. The samples studied did not contain any spent fish and so a complete picture of the correlation between spawning and the fluctuations of K cannot be read from the data. Morrow (1951) has found that associated with the pre-spawning growth of the gonads in the Longhorn Sculpin, a peak of condition is reached at the beginning of the spawning season. It will be seen from Text-fig. 9 that the condition factor begins to increase steadily from about May and reaches the maximum in July, falling thereafter; but up to about October the values are maintained fairly high.

TEXT-FIG. 9. The monthly fluctuations in the *K* value of *Mugil tade*.

Maturing fish have been observed till about October. Though the actual spawning period cannot be inferred with certainty from these data, it is clear that May-June to September-October is the breeding period of the fish. Evidence in support of this conclusion has been obtained from the ova maturation studies and the seasonal occurrence of larvae and juveniles. The relatively higher values of *K* for December and January are probably to be correlated with the increase in the intensity of feeding noticed (Pillay, 1953a).

TABLE III

Month.	Number.	<i>K</i> .
January	70	1.000
February	60	0.900
March	30	0.950
April	30	0.884
May	30	0.969
June	34	0.994
July	32	1.444
August	30	1.236
September	62	1.087
October	28	1.080
November	45	0.953
December	66	1.071

FOOD AND FEEDING HABITS

The food and feeding habits of *M. tade* in varying environments during different seasons and in different stages of growth have been described in a separate paper (Pillay, 1953a). It is now definitely known that the adult mullet is iliophagous and feeds on algae, diatoms and decayed organic matter occurring in the benthic zones. While diatoms, algae and organic matter are consumed in about equal quantities in marine environments, algae are eaten in larger quantities in the estuarine

habitats. The young ones up to a stage of about 2 cm. length feed on floating or attached algae, mostly Myxophyceae. An increase has been noticed in the feeding activity of the fish during the winter season, when there is a bloom of algal growth in its habitat.

SEX RATIO AND FECUNDITY

A knowledge of the sex ratio in populations is considered essential in the management of a fishery as it will be necessary to devise means of ensuring a proportional fishing of the two sexes. In adult specimens examined during the investigation, in which sex determination was possible 56.3% were females and 43.7% were males. Thus, the number of individuals in the two sexes appears to be more or less equal. Though the possibility of the sex ratio having been influenced by differential fishing exists, there is at present no evidence to show that this is actually the case in *M. tade*. Kesteven (1942) estimated that the gonads of mature *M. dobula* contained from 1,275,000 to 2,781,000 ova. Jacob and Krishnamurthy (1948) have estimated that a mature *M. oeur* (= *cephalus*), 20.6 inches in length, contained 1,32,00,000 eggs in the ovary. In the ovaries of mature *M. tade*, three groups of ova were found. The number of maturing and nearly ripe ova (*vide* the classification on page 203), which gives an indication of the reproductive capacity of the fish during a particular spawning season (see page 203), was estimated from four nearly ripe specimens ranging from 23 cm. to 50 cm. in length, by counting the ova in a small portion of the ovary of known weight and computing the total number of ova based on this count and the total weight of the ovary. The number ranged between 90,416 and 3,22,959. As was only to be expected, the number of ova in smaller individuals was proportionately less, since as a rule the size of ripe eggs is constant for each species.

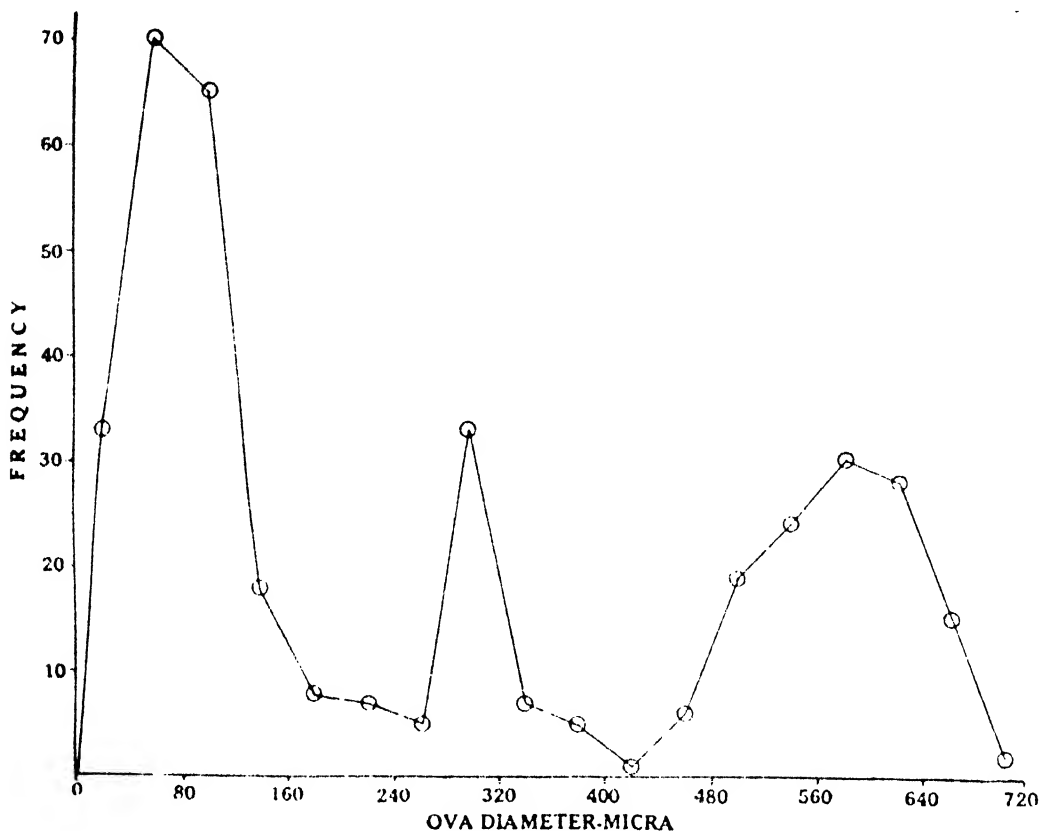
MATURATION AND SPAWNING

Maturation.—The maturation of the female mullet was studied by the measurement of ova diameters.

The measurements of ova were taken from formalin-preserved material. These ova were in many cases somewhat distorted in shape due to preservation. With a view to avoid any possible selection or bias in taking the measurements, a procedure similar to that adopted by Clark (1925) and Arora (1951) was employed as follows. A piece of the ovary was teased out in formalin on a slide and the diameters measured by means of an eye-piece micrometer in a compound microscope. The scale of the micrometer was kept across the field of the microscope from left to right. The diameters of 100 ova, along whichever axes that lay parallel to the micrometer, were taken. This procedure ensured random nature of the readings and unbiased values. Preliminary studies showed that there are no significant differences in the development of the ova in the different regions of the ovary.

Text-fig. 10 represents the curve of the frequency distribution of 380 ova of 8 nearly ripe specimens obtained during the spawning season. From the modes of the curve three distinct stages can be recognized in the maturation of the ova. Stage I consists of eggs measuring up to 180 micra with the mode at about 60 micra. These ova are transparent and are devoid of any yolk accumulations. They have very prominent nuclei filling nearly half of the cell space. These form the immature ova, representing a resting stage between seasons. The next stage (Stage II) consists of an intermediate group of maturing ova with the mode at about 300 micra. The smaller ova of the group (160–280 micra in diameter) are semi-opaque and the larger ones are more heavily laden with yolk. Stage III is composed of nearly mature eggs with the mode at about 580 micra. The eggs of Stage III had their margins transparent but the major part of the ova remained opaque. The smallest female in roe examined during this investigation was 23.1 cm. in total

length. This observation corroborates the inference drawn, from the fluctuation in the ponderal index, that the average size of the fish at first maturity is 23 cm. The samples examined did not contain any fully ripe and oozing fish. Fully ripe ova may probably be slightly larger than the size shown in Text-fig. 10.



TEXT-FIG. 10. Size distribution of ova from mature and maturing females of *Mugil tade*.

Spawning Season.—Just as the related species *M. parsia* Ham., *M. tade* was also generally believed to spawn during winter (Hora and Nair, 1944). As will be seen from the length-frequency distributions of catches from Junput and Port Canning (pages 208-210), the fry of *M. tade* have been obtained during this investigation only during the rainy season. Though the correct period of occurrence of fry is not known to the fishermen and the fish culturists in the Sundarban area, most of the fishermen on the Contai Coast are aware of this, and collect the fry of this fish for stocking tanks during this season (Pillay, 1950). The observation regarding the spawning season was verified by studying the size progression of ova during different months of the year. The data are presented in Text-fig. 11, and show that the immature eggs up to about 160 micra occur in every adult female during all the months of the year. A feeble increase in size of the ova noticed in the month of March becomes conspicuous by April, and as growth is quite rapid thereafter, nearly ripe ova are seen in the gonads by the end of May. Such ova have been found in the ovary from May to September with two peak periods in June and August. It is inferred from this that the spawning season of the fish extends from about May to September with the peak periods in June and August. Actual oozing specimens have not been examined and the nearly ripe ova may take some time to

Maturity	Diameter in micra	Oct.	Nov.	Dec.	Jan.	Feb.	Mar.	Apr.	May	June	July	Aug.	Sept.
Nearly ripe	681-720								○	●	○	●	○
	641-680								●	●	○	●	
	601-640		•	•					●	●	●	●	
	561-600	•							●	●	●	●	
	521-560								●	○	●	●	
	481-520								○	○	○	○	
	441-480								○	○			
Maturing	401-440												
	361-400									●			
	321-360									●			
	281-320									●			
	241-280								○	○			
	201-240							○	●	○	○		
	161-200						○	●	●	○	○		
Immature	121-160						○	●	○	●	○	○	
	20-120	●	●	●	●	●	●	●	●	●	●	●	●

TEXT-FIG. 11. Monthly size progression of ova of maturing *Mugil tade*. (The range in size of ova found in any particular month is represented by the columns of circles. The majority of females had ova of the sizes indicated by the range of solid circles).

become fully transparent and ready for spawning. So the period indicated gives only an approximate picture of the spawning season. Observations during the last three years have shown that the appearance of fry of *M. tade* is dependent on the onset of S.W. monsoons. So the actual beginning of the breeding season appears to fluctuate from year to year.

Frequency of spawning and the spawning grounds.—The ova measurement data discussed above suggest that the fish spawns more than once during each spawning season. The ovaries of nearly ripe females contained immature, maturing and nearly ripe ova at the same time. It appears that by the time the ova of Stage III become fully ripe, those of Stage II advance rapidly in maturity and become nearly ripe, and within a short interval the fish is able to spawn again. The two peak periods of spawning that are indicated in Text-fig. 11, also support such a conclusion. More extensive observations may, however, be necessary to establish this tentative inference.

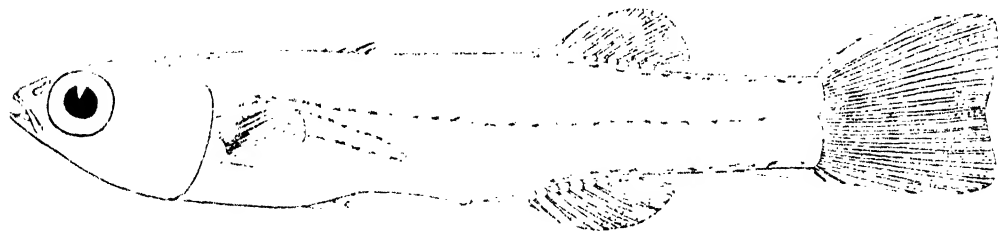
The breeding season of the fish coincides with the off-season for fishing in both the estuarine and coastal waters where the prevailing rough weather prevents fishing with the gear and tackle used by the fishermen. For lack of a suitable sea-going vessel, it has not been possible to make any detailed investigations in these areas during this season. The limited samples examined were those taken by the fishermen in the hand seines from the onshore areas of the Contai Coast and in bag nets from the estuarine regions near Gosaba. The fishermen are of the opinion that the mullet spawns in the sea. The catches of the fishermen on the Contai Coast during this season have been carefully examined, but no fully ripe specimens were ever found among them. Maturing and nearly ripe specimens have been found in the catches from both the lower estuarine areas and the onshore regions of the sea. Several plankton collections were made from the onshore waters at Junput and on

some occasions in the lower reaches of the Sundarbans. Neither eggs nor larvae were seen in the collections, except for a couple of larvae caught in the plankton from off Junput, which, in all probability, were brought in by the high tide. However, juveniles appear in large schools throughout the rainy season in the coastal areas and estuaries. These observations strongly suggest that the fish probably spawns in deeper waters away from the onshore areas. This inference is contrary to the opinions of several workers (*vide* Sarojini, 1951), who believe that the mullets breed in the onshore or inland waters. It is interesting to note that the fish virtually enjoys the benefits of a closed season during its spawning period, since fishing is almost non-existent at this time.

DESCRIPTION OF LARVAE

Two larvae referable to *M. tade*, 8.6 mm. and 9.0 mm. long respectively, were obtained in the plankton collected from Junput on 18th July, 1950. These are the earliest stages obtained during the investigation.

In the 8.6 mm. larva (Text-fig. 12) all the fins are well marked out. There are three spines evident on the first dorsal, and nine rays on the second dorsal. The caudal fin possesses 15 well-developed rays. The anal has two spines and eight rays of which two are in advance of the vertical from the second dorsal. The rays have not been differentiated on the pelvic fins. There are indications of rays on the dorsal aspect of the pectoral fins. The pre-anal fin-fold is present at this stage. There are 11 pre-anal and 13 post-anal vertebrae.



TEXT-FIG. 12. Larva of *Mugil tade*, 8.6 mm. in length $\times 16\tfrac{1}{2}$.

There is a row of chromatophores along the lateral line, one row from the base of the anal fin to the caudal and another row from the base of the second dorsal to the caudal fin, on either side of the body. There are several chromatophores on the dorsal aspect of the head, extending posteriorly up to the nape.

The eye measures about 2.9 times in length of head. The head is about 4.5 times, and the height of body about 6.0 times, in total length. The scales have not yet been formed.

The 9 mm. larva does not show any advance in development beyond what is seen in the one 8.6 mm. long.

AGE AND GROWTH

Scales as indicative of age and growth

Scale characters.—The scale of the adult *M. tade* and its development have been described in detail by the author in a separate paper (Pillay, 1951). The examination of scales from individual fish has shown that while the scale size is variable on different parts of the body, there is a high degree of constancy in size in the scales of the linear series on the sides. Kesteven (1942) has demonstrated that the scales of *M. dobula* on the flanks show very little variation in size, and has

observed a remarkable uniformity in the calculated intermediate lengths and the growth increments, based on many scales from each of a number of fish. He has concluded that there are different coefficients of regression of scale size on fish size, and that these coefficients are real and operative over the whole life of the fish for each scale. The examination of scales of *M. tade* also revealed a similar condition which indicated that any of them from the flank could be utilized for reading. However, it was noted that, as in the case of *M. dobula* (Kesteven, *loc. cit.*, p. 39), there was a minimum of variation in scale size at the region behind the tip of the pectoral fin, and so scales from this region alone were used in the present study of age determination. The assumption that the scale size holds a constant relation to the length of the fish was demonstrated to be correct.

Annulus formation.—Typical growth rings such as are observed on the scales of fishes in temperate regions are not noticeable on the scales of the mullet. Regular markings in the form of 'breaks', are, however, observed in *M. cephalus*, as recorded by Jacot (1920). These breaks generally appear as wide, clear spaces between circuli in the basal sector, formed either by the cutting off of circuli and a difference in their disposition, or by their excessive splitting. Kesteven (1942) and Thomson (1951) have also observed the same type of rings on the scales of *M. dobula*. Kesteven has explained the formation of the rings as follows:

"The appearance of the complete 'break' suggests quite convincingly, that feeding has ceased for a period during which resorption may have occurred; at any rate at this time the circuli were differentially shortened, at the end of the period, with the resumption of feeding, scale accretion was resumed, but in such a manner as to produce complete circuli lying at a different angle to those of the previous annulus. This assumes no more than is normally assumed in interpreting scales, and is sufficient explanation of the origin of 'breaks'."

After a consideration of the probable causes for the formation of such 'breaks' on the scales of *M. dobula*, he inferred that the migrations of the fish in autumn and the consequent cessation of feeding, which are at or near the anniversary of spawning, is the annual event recorded on the scale. He had not sufficient data to say whether the cessation of feeding in the sea alone can give rise to such 'breaks'. Thomson (*op. cit.*) has observed that the annuli are formed on the scales of *M. dobula* in Western Australian waters at the end of September or the beginning of October, when growth re-commences after the winter cessation.

From an examination of the scales of *M. tade* collected during different months of the year it is found that most of the scales obtained during May-July period had recorded wide clear spaces or the excessive cutting off of circuli at the margin. Example of this is shown in Plate V (Fig. 1).

During other parts of the year, the marginal regions did not show any such features, though in a few cases during August and September also such formations have been noticed. The study of the food and feeding habits of the fish (Pillay, 1953a) has not offered any proof to show a specific period of fasting and even mature specimens contained food materials in the gut. From the study of the maturation of ova it has been inferred that the fish attains maturity only when about 23 cm. in length. Smaller specimens of about 16 cm. length had one annulus mark on their scales (Plate V, Fig. 3). So it appears unlikely that the spawning migration is primarily the annual event that is recorded on the scales. Further support for such an inference is afforded by the fact that the scales of fish reared in enclosed farms also had regular formations of 'breaks', just as the fish in the wild. These fish undoubtedly would have had no opportunity of migrating into the sea for spawning. Kesteven (*loc. cit.*, p. 37) has hinted at the possibility of a cessation of feeding in land-locked fish due to an internal rhythm (Dakin, 1939) and the consequent formation of 'breaks'. The study of the gut contents of *M. tade* has afforded some evidence of a real lowering of the feeding intensity during certain periods of the year due to more clearly understood reasons. Though a complete cessation of

feeding is not discernible, Tables I, IV and VII of the paper dealing with the food and feeding habits of the fish (Pillay, 1953a) show that during the rainy season (S.W. monsoon), generally extending from about May-June to August-September, a distinct period of low feeding activity can be noticed. As has already been elucidated, the fish feeds on fresh or decayed bottom flora. During floods consequent upon the heavy rainfall in the area, the benthic flora gets very much disturbed and dislodged due to the strength of the currents, and the normal feeding of the fish is frequently interrupted. A similar condition has been observed by Seshappa and Bhimachar (1951) in the bottom feeding fishes of the West Coast. It therefore appears that the disturbances lowering the intensity of feeding is the prime cause of the formation of 'breaks' on the circuli. This inference also fully explains the formation of more than one 'break' seen quite close together on some of the scales. Whenever there is a serious lack of the abundance of food at the bottom for an appreciably long period due to flood and consequent churning up of the benthic flora, such 'breaks' are likely to be formed on the scales. In the case of mature *M. tade*, this period coincides with the spawning season when they are believed to migrate to the sea. In view of this fact, these 'breaks' can, as will be proved by other methods later, be considered as indicative of a full biological year's growth.

Age and growth determination.—In estimating the age and growth, only regular scales from the region below the tip of the pectoral fin, were utilized. Regenerated scales were often met with (Plate V, Fig. 2); but they lacked most of the earlier markings and so they were always rejected. The scales were washed in a very dilute solution of Potassium hydroxide to remove skin, dirt and adhering pigments and then was cleaned in water. They were mounted dry between two glass slides, the ends of the slides being secured together by means of adhesive paper or in the case of large scales by means of narrow rubber bands. The mounted scales were examined with the aid of a microscope. In the absence of a scale projection apparatus, the smaller scales were measured with the aid of a camera lucida. The larger scales were projected on to a white glossy surface on a photographic enlarger, using the scales as negatives. For the measurement of the scales, paper rulers prepared from mm. graph paper were employed. The zero of the ruler was placed at the nucleus of the projected image and the ruler placed along the most median basal radius. The ruler was then marked at each annulus and the basal margin. For each scale a separate ruler was used. On these were recorded all relevant data regarding date of collection, locality, total length, sex and the magnification of the image. The back calculation of the length of the fish at the end of each year was done employing the formula

$$L_x = \frac{S_x}{S_t} \times L_t$$

where L_x is the total length of the fish at the time annulus X was formed, S_x is the distance from the nucleus of the scale to the particular annulus X ; S_t is the distance from the nucleus to the basal margin of the scale and L_t is the total length of the fish at the time of observation. From the calculated lengths the mean length for each year was estimated. Certain difficulties were experienced in reading the scales especially of the large-sized fish. In some scales more than one 'break' were found close together. This is apparently due to more than one period of low feeding activity. Untimely showers and flooding of rivers is not uncommon in the Gangetic delta and when this happens additional breaks can appear on the scales. However, such additional annuli have generally been observed on the scales of fishes above the size of about 23 cm. when they are known to attain maturity and probably migrate to the sea for spawning. There is therefore some probability that these additional rings are spawning marks; but these rings are usually not very clearly marked out. The converse, *viz.*, the omission of one or two 'breaks' has also

1.

2.

1

1

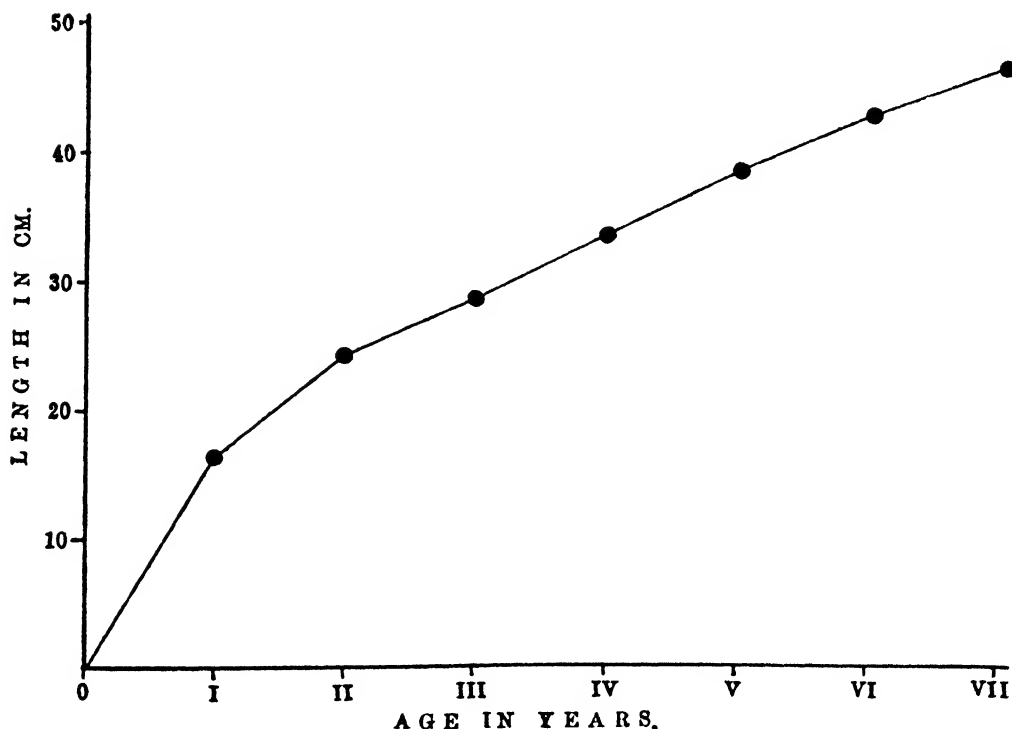
2

3.

4.

been observed, though only rarely. This is probably due to the favourable feeding conditions that existed during the season as a result of the paucity of heavy rains and the consequent absence of floods. Kesteven (*op. cit.*) has also noticed these features on the scales of *M. dobula*. When there are excessive numbers of breaks, he, like Thompson (1928), rejected the intermediate lengths calculated from these, which are not in conformity with the remainder of the sample and the general indication of the length frequency data. When 'breaks' were omitted or had disappeared, they were placed in the appropriate group following the indication of the remainder of the sample and the length frequency data. This procedure was also adopted in the present work.

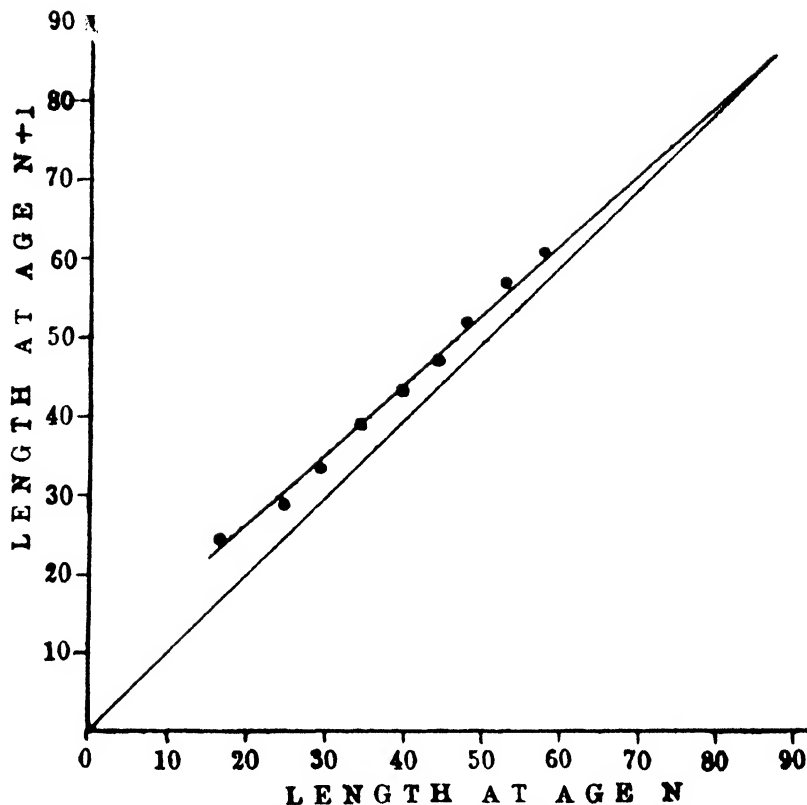
The measurements of 69 scales were taken and the lengths for each year were calculated. The results are given in Table IV. As can be seen from this Table, the numbers of observations of l_8 , l_9 and l_{10} are too meagre, though these may serve to give a rough idea of the growth rate. The data do not show any evidence of Lea's phenomenon of a progressive decrease in the calculated intermediate lengths. The mean growth curve up to the seventh year of life is shown in Text-fig. 13. In Text-fig. 14 this growth curve has been transformed into a straight line, employing Walford's (1946) method. l_8 , l_9 and l_{10} have also been plotted in the figure. The limiting length L has been located graphically as the point where the length at age n equals the length at age n_1 . From the growth characteristics it can be inferred that the fish can attain a size of about 85 cm. The largest fish observed during this investigation was about 70 cm. in length.



TEXT-FIG. 13. Growth curve of *Mugil tade* (lengths calculated from scale measurements).

TABLE IV
Calculated total lengths of Mugil tade at the end of each year of life, as determined from measurements of scales

Age Group.	l ₁		l ₂		l ₃		l ₄		l ₅		l ₆		l ₇		l ₈		l ₉		l ₁₀	
	No.	Mean cm.	No.	Mean cm.	No.	Mean cm.	No.	Mean cm.	No.	Mean cm.	No.	Mean cm.	No.	Mean cm.	No.	Mean cm.	No.	Mean cm.	No.	Mean cm.
I	21	12.7																		
II	24	15.8	20	21.1																
III	6	18.9	6	26.3	5	29.4														
IV	6	18.7	4	25.3	6	29.1	6	32.0												
V	5	16.0	3	24.0	4	30.0	6	33.5	6	38.8	6	44.3	6	47.7						
VII	2	17.0	2	25.8	2	28.5	3	35.0	3	39.4	3	43.4	3	47.8						
VIII	2	16.5	1	24.0	1	28.5	1	35.2	2	39.0	2	43.6	2	46.9	2	52.0	2	59.8	2	61.3
IX	2	16.5	1	25.8	1	28.5	1	34.0	1	39.9	1	43.9	1	47.3	1	52.6	1	55.7	1	61.3
X
All groups	68	16.5	37	24.6	19	29.0	17	34.0	12	39.3	12	43.8	12	47.4	6	52.5	3	57.8	1	61.3



TEXT-FIG. 14. Transformation of the growth curve of *Mugil tade* to show the limiting length.

Length frequency distribution.

Collections suitable for the study of growth trends of *M. tade* from length frequency distributions were available from Junput for a period of twelve months in 1949-50. Samples were available in Port Canning only for a period of six months during the year. The distributions for the two localities are presented in Tables V and VI respectively. The data for each month for Junput are presented graphically in the form of histograms in Text-fig. 15. The average lengths that the fish attains in the first three years of its life, calculated from the scales, are shown as vertical dotted lines. As is evident from the graph, the samples consisted of only the 0 group fish and I group fish with a few of the II group. Selectivity of the fishing gear is thus evident. Distinct modes are noticeable only for the 0 group fish.

Young ones up to 4 cm. in length appear from June to October. These are probably the progeny of fishes that spawned from May to September. The smallest group of the month of June, with its mode at about 2 cm., can be traced to form a distinct mode at about 14 cm. in December, after which it is not quite prominent. This is probably the group 16-20 cm. found in May. The smallest group found in October (those hatched out in about September) can be observed to form a mode at about 6 cm. in January. This group is not clearly seen during other months, but appears in the 12-16 cm. category in May. As can be seen from the range of calculated lengths for the first year's growth, it has a wide range from 12 to 18.9 cm. This is to be expected when the fish has a very extended spawning period as in the present case. The II group fish appears in the graph in December and forms a mode in May when it reaches a size of 24-28 cm. The data available are not sufficient to render possible any inferences on Group III or bigger fish.

TABLE V

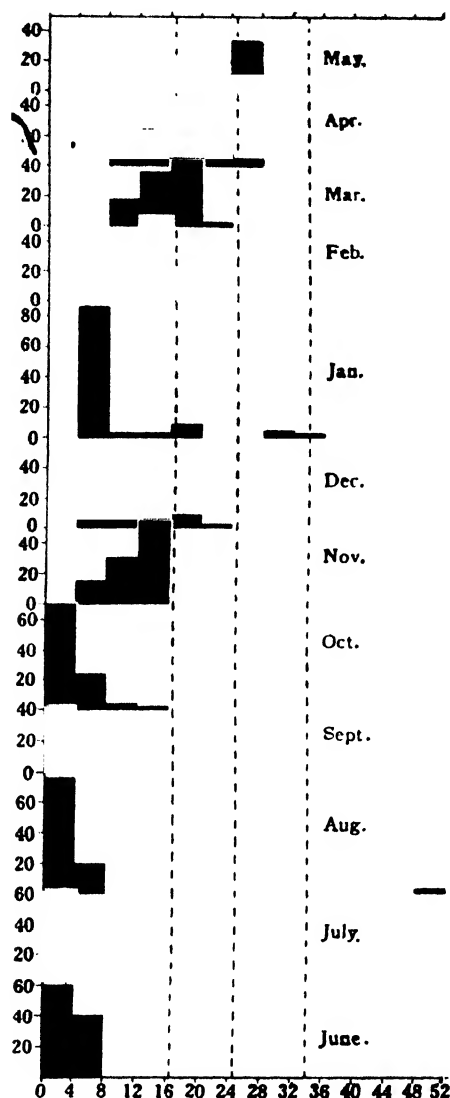
The length frequency distribution (in cm.) of the samples from Junput (expressed as percentages)

Month.	No. in sample.	0.1-4.0	4.1-8.0	8.1-12.0	12.1-16.0	16.1-20.0	20.1-24.0	24.1-28.0	28.1-32.0	32.1-36.0	36.1-40.0	40.1-48.1
(1949) June	68	60.0	40.0	48.1-52.0
July	45	62.0	28.0	10.0
August	58	77.0	20.0
September	45	42.0	36.0	11.0	11.0
October	80	70.0	24.0	4.0	2.0
November	60	..	15.0	30.0	55.0
December	85	..	14.0	18.0	51.0	9.0	2.0
(1950) January	64	..	86.0	3.0	3.0	8.0	4.0	2.0
February	35	22.0	55.0	18.0	5.0
March	15	18.0	36.0	44.0	2.0
April	20	15.0	25.0	45.0	10.0	5.0
May	25	11.0	22.0	22.0	11.0	34.0

TABLE VI.

The length frequency distribution (in cm.) of samples from Port Canning (expressed as percentages)

Month.	No. in sample.	0.1-4.0	4.1-8.0	8.1-12.0	12.1-16.0	16.1-20.0	20.1-24.0	24.1-28.0	28.1-32.0	32.1-36.0	36.1-40.0	40.1-48.1
(1949) June	35	87.0	1.0	5.0	4.0	3.0
July	25
August	140	21.0	100.0	55.0
September	120	11.0	24.0	42.0	25.0
October	40	9.0	22.0	46.0	9.0	9.0
November	75	20.0	60.0	20.0



TEXT-FIG. 15. Length frequency histograms of the samples of *Mugil tade* collected from Junput.

The modes of the distribution for May, which is considered as the beginning of the biological year of the fish, show a fair amount of agreement with the averages of the calculated lengths. The data for Port Canning show that the smallest group that appears in June attains a size of about 4-8 cm. by about November.

MIGRATIONS.

Sarojini (1951) has drawn attention to the contradictory theories held by workers on the migrations of the mullets, especially the spawning migrations. While Panikkar and Nair (1945) and John (1948) observe that mullets ascend rivers

for spawning purposes, Kesteven (1942) and Jacob and Krishna Murthy (1949) believe that they migrate into the inshore waters for spawning. There appear to be no definite records about the migrations of *M. tade*. As has been shown on page 204, the evidence so far available indicates that they migrate into the sea for spawning purposes. This spawning migration appears to start when the fish are about two years old and about 23 cm. in length, when they attain maturity for the first time. There are not sufficient data to prove that the spawned fish immediately return to the estuaries after spawning, but there is some proof to show that the same fish spawns more than once in one spawning season, and that they are likely to remain in the spawning grounds till the second spawning is over. Spent fish have not been obtained during the investigation from catches in any of the localities. However, the fact that fish up to about ten years of age are caught in the estuarine waters indicates that a large part of the stock returns to the estuaries after spawning. The reports of the fishermen are also in favour of this assumption.

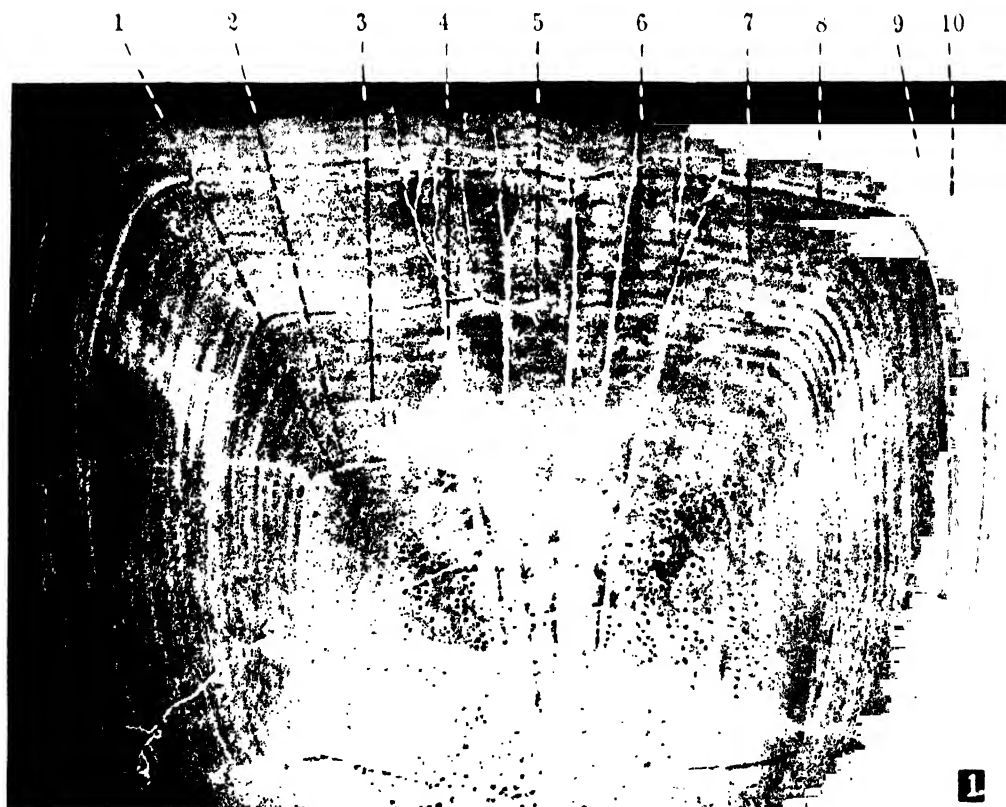
From the early part of June, juveniles and fry begin to appear along the coasts entering the tidal springs and creeks, and migrating in large schools into the estuaries. But the observations made on the Contai Coast and the evidence afforded by the length frequency data show that immature fish are found in the coastal waters throughout the year. It therefore appears probable that a good part of the stock remains in the coastal waters. Evidently the estuaries and the inshore areas of the sea form the natural habitat of the species, which they leave only during the spawning season.

Chacko (1949a and 1949b) states that *M. olivaceus* Day and *M. borneensis* Blkr. ascend the rivers beyond the tidal limit for feeding. *M. tade* have never been observed by the author beyond the tidal limit in the main river. In areas where there are freshwater channels emptying into the estuary or the sea, the fry can be seen to collect together in schools and in several localities they have been observed to enter these channels and establish themselves there. Spurgeon (1947) has observed a similar habit in *M. dussumieri* (C.V.) and *M. oer* (= *cephalus*) (Forsk.).

PREDATORS AND PARASITES

Predators.—The main predators of the mullet in its estuarine habitats in Bengal are believed to be Bhukti (*Lates calcarifer* (Bloch)), Indian Salmon (*Eleutheronema tetradactylum* (Shaw)) and the Bombay duck (*Harpodon nehereus* Ham.). According to Menon (1948) more than 65% of the food of Bhukti consists of fishes, of which mullets have been listed as a predominant group. Though the proportion of *M. tade* consumed is not known, the examination of gut contents of several specimens has shown that *M. tade* forms a common item of food of Bhukti. Usually only fry and fingerlings are eaten. Mr. J. C. Malhotra who has studied the food and feeding habits of *E. tetradactylum*, informs me (private communication) that mullets form only a negligible percentage of the food of this fish, and that its main food consists of prawns. Pillay (1953c) has shown that though occasionally the mullet forms the food of the Bombay duck, the quantities eaten are very small. Kesteven (1942) found sharks to be predators of mullets. Though it has not been possible to collect any data on this aspect, it is most likely that sharks are highly destructive to mullet stocks in the coastal waters.

Parasites.—The material examined during this investigation shows that the mullet is relatively less prone to parasitic attacks. Mortality due to parasitism has not been reported even from farms. The only external parasite observed was *Rosinella latesi* Southwell (1915) found on the fins of a 55.9 cm. long fish collected from Port Canning on 29th July, 1951. They had attached themselves to the soft dorsal, caudal and ventral fins. A 30 cm. long fish obtained from Junput in April 1949 had its palates and pharyngeal cushions covered with parasitic copepods



belonging to a new family.* Other internal parasites collected were all from the intestines and consisted of a new species of Acanthocephala of the genus *Neoechinorhynchus* and a species of nematode.* These forms were very commonly found in adult fish, but were rare in young ones. In no case did the fish show any apparent signs of ill health or loss of weight. The association of a new species of *Zoothamnium* with the fish has been described elsewhere by Khajuria and Pillay (1950).

Five abnormally lean specimens of *Mugil tade* were collected from an enclosed brackishwater farm in Ghutiari Sharif (24-Parganas, W. Bengal, in the month of January, 1950). The relevant measurements of four of these specimens are given below:—

Measurements in cm.

Total length	19.8	17.1	18.4	18.9
Standard length	16.2	13.5	15.4	15.0
Depth of head through orbit	1.9	1.6	1.9	1.5
Depth through pectoral fin base	2.5	2.3	2.5	2.6
Depth through anal fin base	2.8	2.3	2.6	2.5
Width through pectoral fin base	2.3	2.0	2.0	2.3
Width through anal fin base	0.9	0.9	0.9	0.9
Length of caudal peduncle	3.1	2.5	3.0	2.8
Least height of caudal peduncle	1.7	1.4	1.6	1.5

The fin ray, scale and branchiostegal counts, dimensions of fins, etc., were the same as for normal specimens. The main difference was noticed in the relative depth of body and in the height of caudal peduncle. The width of body was also very much less than that of normal specimens.

At first these specimens were suspected to be only starved ones, but it was found on examination that the alimentary canal contained freshly consumed and partly digested food materials. Normal specimens were also obtained from the same locality in the same collections and so it was considered unlikely that the abnormality was due to the influence of hydrological factors. No parasites were found in the viscera, gills, etc., of the specimens. Dr. K. K. Nair informs me that he has noticed specimens of *Cirrhinia mrigala* infested with leeches becoming extremely lean as in the present case. As the specimens of *M. tade* were not examined in fresh condition, it was not possible to detect any marks of attack by leeches. The brackishwater leech *Placobdella emydae* is known to occur in these localities (Sewell, 1934) and it is probable that these fish have become lean due to infestation by leeches.

FISHERY IN BENGAL

Fishing methods

The main gears employed for mullet fishing in Bengal are : (1) Stake nets, (2) Hand Seines, (3) Cast Nets, and (4) Traps.

Stake nets.—The Stake nets generally operated are the *Bher jal*, *Charpatta jal*, *Khalpatta jal* and *Komar jal*. The *Bher jal* or the *Kutti bher jal* as it is known on the Midnapore Coast, is a very long net enclosing considerable portions of the fore-shore areas. It consists of 200–300 rectangular pieces of netting, each measuring 30' × 8' (mesh $\frac{1}{2}$ "–1"), joined end to end and tied in the form of a wall on stakes fixed in the littoral regions, with about a foot of the net tucked in the mud (Plate VI, Fig. 2). Before high tide the net is untied and allowed to lie low on the bottom. At the turn of the tide, the wall of net is raised and fastened to the stakes. When the tide has fully receded, the stranded fish are either removed by hand, or by means of cast nets, if they are stranded in pools. *Charpatta*, a fence made of split bamboo

* Detailed accounts of these parasites will be published elsewhere by Mr. Y. R. Tripathi of the Central Inland Fisheries Research Station, Barrackpore.

is also operated in the same manner as the *Bher jal* in Bagerhat and Bakarganj. *Kalpatta jai* is a smaller rectangular net 40'-50' \times 12' (mesh 1") operated in canals in Sundarban area. The net is tied across the canals by fastening the head rope to strong posts fixed near the banks. It is kept stretched and upright by means of wooden stakes, hooked at the top. The *modus operandi* is the same as for *Bher jal*. Naidu (1939) has described the operation of *Komar jal*. It is operated on the margins of rivers and big canals. Fish are attracted by the decaying twigs and leaves of trees anchored in the area, and the fish arriving with the high tide are enclosed by means of the net. They are then removed towards the shore and the catches hauled up.

Hand seine and drag nets.—A hand seine known as *Katti jal* is operated by the fishermen on the Midnapore Coast. It resembles the *Kattuvalai* (Hornell, 1924) and *Khadi jal* (Chauhan, 1947) and consists of a long shallow bag of netting ($\frac{1}{4}$ "- $\frac{1}{2}$ " mesh) the mouth of which is kept open by means of sticks 8"-9" long. The bag is subdivided into pockets at the bottom. The net is operated both at high and low tides mainly during the rainy season. The net, after being paid out in a direction at right angles to the shoreline, is dragged along the shore for some distance and then hauled up. A large number of prawns, crabs and other small fishes are also caught in the net along with mullets. The catches usually consist of small-sized fish not more than 9"-10" in length. Large drag nets (*Tana jal*) are generally operated in enclosed fisheries. Cast nets (*Khapla jal*) of varying size and mesh are used for fishing mainly in shallow canals, estuaries and enclosed brackishwater farms. *Tras* (Atols) (Hora and Nair, 1944) are designed to capture the fish when it swims against the current and are suitable for operation in farms.

Composition of catches

Unfortunately there are no statistics available regarding the mullet catches in any of the fishing centres of the State. Though *M. tade* grows to a large size, they are relatively less abundant in numbers. This does not, however, prove that they are really less abundant in occurrence as the efficiency of the nets operated has also to be taken into consideration. Though mullets as a group form an important item in the Calcutta fish markets throughout the year, the peak period of supplies is the winter season when the lower reaches of the Sundarbans are exploited by the camping fishermen.

In Port Canning, fishing is done locally throughout the year. Young ones of *M. tade* are abundant during June and July and larger fish are caught from August onwards. In Junput also young ones are caught from June to about October. Larger fish are caught by the fishermen only during the winter season which is the regular fishing season on the coast. The analysis of the size composition (vide Tables V and VI) in both these centres very clearly shows that smaller size groups predominate in the catches. These fish seldom reach the stage of rapid increase in weight (vide page 197) or spawn even once before they are caught. The redeeming feature, however, is that there is a closure of fishing during the spawning season owing to the heavy monsoons prevalent at the time. In coastal areas the fishermen catch mullets by means of hand seines even during this season, but it is very seldom that a fish in roe is caught. This fact must be contributing greatly to the maintenance of population levels.

SUMMARY

Description of the species, distribution, raciation and body measurements.—A detailed description of *M. tade* is presented and the extent of distribution of the species in India is recorded. Statistical analysis of the morphometric data of samples from the sea and the estuary has failed to show any significant differences between them, and it is inferred that the stocks on the Contai Coast and in the estuary of the Matlah River form a homogeneous population. From a study of the growth rate of the different parts of the body, it is inferred that the standard

length, and the body length (from opercle to hypurals) have the maximum rates of growth and depth through orbit, the minimum. The relationship between the total length and the standard length can be expressed by the equation $Y = 0.81125 X - 0.025$, where Y is the standard length.

Weight-length relationship and ponderal index.—The weight of the fish is found to increase as an exponential function of its length and the equation for the curve is $W = 0.0337L^{2.6198}$. From the fluctuations in the ponderal index it has been inferred that the fish attains maturity for the first time when it is about 23.0 cm. in length. The ponderal index of the fish shows seasonal fluctuations and from this it is inferred that the fish spawns during the S.W. Monsoons.

Food and feeding habits.—The juvenile fish feed on unicellular floating or attached algae and the adults feed at the bottom on the benthic flora and decayed organic matter. A marked increase in feeding activity is noticed during the winter season, and a low feeding activity during the rainy season.

Sex ratio, fecundity, maturation and spawning.—The sex ratio of *M. tade* appears to be nearly 1 : 1. The ovaries of nearly ripe specimens contained over ninety thousand to 3 lakhs mature and maturing ova at a time. From the frequency distribution of ova in the gonads of mature females it is seen that there are three distinct groups of ova, viz., immature, maturing and mature. Maturing ova have been observed to appear for the first time in the ovaries of specimens of about 23 cm. length and this is considered to be the size at which first maturity is attained. This inference is also supported by data relating to the fluctuations in the ponderal index. The fish probably spawns more than once during one spawning season, and the spawning season which may start in May-June, depending on the onset of the monsoons, lasts till about September. It appears to breed in the sea away from the inshore regions. The description of larval forms obtained is given.

Age and Growth.—The scales of *M. tade* show annual rings which are most probably the recordings of low feeding activity apparent during the rainy season. From the back-calculated lengths it is inferred that on an average, lengths of 16.5, 24.6, 29.0, 34.0, 39.3, 43.8, 47.4, 52.5, 57.8 and 61.3 cm. are attained by the species in the respective ages attained during the 10 years of its life. The maximum limiting length is estimated to be 85.0 cm.

Length frequency distribution.—The length frequency distributions of *M. tade* collected from Junput and Port Canning for a period of one biological year have been presented and discussed. The trend of the progression of modes is in agreement with the growth rate estimated from scale studies.

Migrations.—The two main migrations of the fish appear to be the seaward migration of the mature fish for spawning and the movements of the fry and fingerlings into estuaries. The presence of large schools of immature fish in the coastal waters throughout the year indicates that all the young ones do not ascend the estuaries and that both the estuary and coastal waters form the natural habitats of the fish.

Predators and parasites.—*Lates calcarifer* forms a major enemy of the fish in estuarine waters. The parasites collected from the fish are listed. It is found that the mullet is relatively free from any large scale infection by parasites. The larger fish are more prone to parasitic attacks. In enclosed fisheries leeches probably infest the mullets.

Fishery.—The fishing methods for the mullet in the estuary and the sea in Bengal are briefly described. Analysis of the catches shows that large quantities of immature fish are caught by the fishermen.

ACKNOWLEDGEMENTS

I am deeply indebted to Dr. S. L. Hora for his guidance and unfailing encouragement. To Dr. G. L. Kesteven my grateful thanks are due for very kindly helping me in planning the work and for valuable advice in the analysis of the data. My thanks are also due to the various fishery workers who readily gave me useful information regarding the occurrence and fishery of *M. tade* in their respective States. I am grateful to the National Institute of Sciences of India for the award of an I.C.I. (India) Research Fellowship which enabled me to take up this work.

REFERENCES

- Arora, H. L. (1951). An investigation of the California Sand dab, *Otharichthys sordidus* (Girard). *Calif. Fish. Game*, San Francisco, 37, 1-42.
 Chacko, P. I. (1949a). Migratory governments of fishes of the Coleroon. *Proc. 36th Indian Sci. Congr.*, Calcutta, Pt. III, 164-165.
 — (1949b). The Krishna River and its fishes. *Proc. 36th Indian Sci. Congr.*, Calcutta, Pt. III, 165-166.

- Chauhan, B. S. (1947). Fishery Survey of Patna State. *Rec. Indian Mus.*, Calcutta, **45**, 267-282.
- Clark, F. N. (1925). The life history of *Leuresthes tenuis*, an atherine fish with tide controlled spawning habits. *Fish. Bull.*, Division of Fish and Game of California, Sacramento, **10**.
- Crozier, W. J., and Hecht, S. (1913). Correlations of weight, length and other body measurements in the weak fish *Cynoscion regalis*. *Bull. U.S. Bur. Fish.*, Washington, **33**, 141-147.
- Dakin, W. J. (1939). The age determination of the tiger flathead *Neofiatycephalus* (*Colefaxia*) *macrodon* (Ogilby) by means of otoliths. *Aust. Mus. Rec.*, **20**, 292-293.
- Day, F. (1878). *Fishes of India*, II, London.
- (1880). *Fauna of British India—Fishes*, II, London.
- Devanesan, D. W., and Chidambaram, K. (1948). *The Common food fishes of the Madras Presidency*, Madras.
- Devasundaram, M. P. (1951). Systematics of Chilka mullets with a key for their identification. *J. Zool. Soc., India*, Calcutta, **3**, 19-25.
- Hart, T. J. (1940). Report on trawling surveys on the Patagonian Continental shelf. *Discovery Rep.*, **23**, 223-403.
- Hickling, C. F. (1930). The natural history of the hake. Parts I and II. *Fish. Inv. Min. Agric. Fish.*, London, Ser. II, 10.
- Hora, S. L., and Nair, K. K. (1944). Suggestions for the development of saltwater bheris or bhasubadha fisheries in Sunderbans. *Bengal Govt. Fish. Dev. Pamphlet*, 1, Calcutta.
- Hornell, J. (1924). The fishing methods of the Madras Presidency, Part I. Coromandel Coast. *Madras Fish. Bull.*, Madras, **18**, 59-110.
- Jacob, P. K., and Krishnamurthy, B. (1948). Breeding and feeding habits of mullets (*Mugil*) in Ennore Creek. *J. Bombay Nat. Hist. Soc.*, Bombay, **47**, 663-668.
- Jacot, A. P. (1920). Age, growth and scale characters of the mullets *M. cephalus* and *M. curema*. *Trans. Amer. Micr. Soc.*, Lancaster Pa, **39**, 199-229.
- John, C. C. (1948). *Progress Report of the Fisheries Development Scheme*, Central Research Institute, Travancore University, Trivandrum, 1.
- Kesteven, G. L. (1942). Studies in the biology of the Australian mullet. I. Account of the fishery and preliminary statement of the biology of *M. dobula* Günther. *Coun. Sci. Ind. Res.*, Melbourne, Bull. No. 157.
- Khajuria, H., and Pillay, T. V. R. (1950). On a new species of *Zoothamnium* Stein (Protozoa—Vorticellidae) from the Grey Mullet *Mugil tade* Forsk. *Rec. Indian Mus.*, Calcutta, **48**, 55-58.
- Kulkarni, C. V. (1947). Notes on freshwater fishes of Bombay and Salsette Islands. *J. Bom. Nat. Hist. Soc.*, Bombay, **47**, 319-326.
- Menon, P. M. G. (1948). On the food of Bekti, *Lates calcarifer* (Bloch) in the cold season. *Curr. Sci.*, Bangalore, **17**, 156-157.
- Menon, M. D. (1950). Bionomics of the poor-cod (*Gadus minutus* L.) in the Plymouth area. *J. Mar. Biol. Ass., U.K.*, Plymouth, **29**, 185-229.
- Morrow Jr., J. E. (1951). Studies on the marine resources of southern New England. VIII. The biology of the longhorn sculpin, *Myrocephalus octodecimspinosus* Mitchell, with a discussion of the Southern New England 'trash' fishery. *Bull. Bingh. Ocean Coll.*, New Haven, Conn., **13**, 2.
- Naidu, M. R. (1939). *Report on a survey of the fisheries of Bengal*. Govt. of Bengal, Dept. of Agriculture and Industries, Calcutta.
- Panikkar, N. K., and Nair, R. V. (1945). *Progress report of the scheme of research on the fish eggs and larvae of the Madras Plankton*, Madras.
- Pillay, T. V. R. (1949). On the culture of grey mullets in association with commercial carps in freshwater tanks in Bengal. *J. Bombay Nat. Hist. Soc.*, Bombay, **48**, 601-604.
- (1951). Structure and development of scales of five species of Grey mullets of Bengal. *Proc. Nat. Inst. Sci. India*, Calcutta, **17**, 413-424.
- (1953a). Studies on the food, feeding habits and alimentary tract of the grey mullet, *Mugil tade* Forskål. *Proc. Nat. Inst. Sci. India*, Calcutta (In Press).
- (1953b). Observations on the ecology of a brackishwater bheri, with special reference to the fish cultural practices and the food relations of the fauna. (Unpublished).
- (1953c). The food and feeding habits of the Bombay-duck *Harporodon nehereus* (Ham.) in the river Matlah. *Proc. Nat. Inst. Sci. India*, Calcutta, **19**, 427-435 (Preliminary note in *Sci. and Cult.*, Calcutta, **17**, 261-262.)
- Rounsefell, G. A., and Dahlgren, E. H. (1935). Races of herring, *Clupea pallasii* in South Eastern Alaska. *U.S. Bur. Fish. Bull.*, Washington, **48**, (17).
- Sarojini, K. K. (1951). The fishery and biology of the Indian grey mullets—A Review. *J. Zool. Soc. India*, Calcutta, **3**, 159-179.
- Schultz, L. P. (1946). A revision of the genera of mullets, fishes of the family Mugilidae, with descriptions of three new genera. *Proc. U.S. Nat. Mus.*, Washington, **96**, 3204, 377-395.
- Seshappa, B., and Bhimachar, B. S. (1951). Age determination studies in fishes by means of scales with special reference to the Malabar Sole. *Curr. Sci.*, Bangalore, **20**, 260-262.
- Sewell, R. B. S. (1934). A study of the fauna of the Salt Lakes, Calcutta. *Rec. Indian Mus.*, Calcutta, **36**, 45-121.

- Simpson, G. G., and Roe, A. (1939). *Quantitative Zoology*, New York and London.
- Smith, J. L. B. (1948). A generic revision of Mugilid fishes of South Africa. *Ann. Mag. Nat. Hist.*, Cape Town, **14**, 833-843.
- Southwell, T. (1915). Notes from the Bengal Fisheries Laboratory, Indian Museum. No. 2. On some Indian parasites of fish, with a note on Carcinoma in trout. *Rec. Indian Mus.*, **11**, 311-330.
- Spurgeon, V. D. (1947). Natural acclimatisation of two species of mullets *M. dussumieri* (C.V.) and *M. ocellatus* (Forsk.) to freshwater conditions on the Nellore Coast. *Curr. Sci.*, Bangalore, **16**, 123-124.
- Thompson, H. (1923). Problems in haddock biology. I. Preliminary report. *Fish. Bd. Scot. Sci. Invest.*, Edinburgh, 1922, **5**, 1-78.
- Thomson, J. M. (1951). Growth and habits of the sea mullet, *Mugil dobula* Günther, in Western Australia. *Austr. J. Mar. Freshw. Res.*, Melbourne, **2**, 193-225.
- Walford, L. A. (1946). A new graphic method of describing the growth of animals. *Biol. Bull.*, **90**, 141-147.
- Weber, M., and de Beaufort, L. F. (1922). *Fishes of the Indo-Australian Archipelago*, Leiden, **IV**, 236-238.
- Whitehouse, G. H. (1922). The grey mullets of Tuticorin. *Madras Fish. Bull.*, Madras, **15**, 71-98.

EXPLANATION OF PLATES.

- PLATE V, FIG. 1. The margin of the scale of a specimen of *Mugil tade* caught in May, 1949.
- „ 2. A regenerated scale.
- „ 3. Scale showing one annulus.
- „ 4. Scale showing two annuli.
- PLATE VI, FIG. 1. Scale of *Mugil tade* showing ten annuli.
- „ 2. A portion of the Barrier net (*Bher jal*) operated on the Contai Coast (Photograph taken at low tide).

Issued March 31, 1954

SOME ASPECTS OF RELATIVE GROWTH IN THE BLUE SWIMMING CRAB *NEPTUNUS PELAGICUS* (LINNAEUS)¹

by R. RAGHU PRASAD and P. R. S. TAMPI, Central Marine Fisheries Research Station, Mandapam Camp

(Communicated by N. K. Panikkar, F.N.I.)

(Received September 5; read October 9, 1953)

CONTENTS

	<i>Page</i>
Introduction	218
Material and Methods	219
Results	
(a) Carapace length	219
(b) Length of the chela	222
(c) Length of the first walking leg	225
(d) Width of the sixth abdominal segment	225
(e) Length of the sixth abdominal segment	230
Discussion	231
Summary	234
Acknowledgements	234
References	234

INTRODUCTION

The Blue Swimming Crab, *Neptunus pelagicus* displays in some of its parts a marked sexual dimorphism (Prasad and Tampi, 1953) and, therefore, the authors felt that a study of the relative growth of such parts might be interesting. Further, as Weymouth and MacKay (1936) pointed out: "This method of analysis makes possible the detection of changes of form which occur at certain physiological epochs, notably that of attaining sexual maturity. In the crab, as in most invertebrates, growth continues although at a decreasing rate throughout life. Accordingly there is no final or definitive size or form as in man. Against this background of constantly changing form it is possible to detect changes in the differential growth-ratios of various parts in response to internal factors such as the maturing of the gonads or their virtual destruction, as shown by G. Smith (1910) in his study of 'parasitic castration'." Information on the size at first maturity is not only of scientific interest but also of practical value in the management of the fisheries.

No analyses on the relative growth have so far been attempted on any Indian crab and in general the study of the relative growth of crustaceans has received little attention here. Alcock (1906) merely pointed out that certain features of sexual dimorphism such as proportionately long rostrum of the female shrimp *Penaeus* represent continued juvenile characters. Tazelaar (1930) made a study of the relative growth of certain parts of *Palaemon carcinus*, a large Indian prawn. The measurements made by Kemp, Henderson and Matthai on *Palaemon malcomsoni*,

¹ Published with the permission of the Chief Research Officer, Central Marine Fisheries Research Station, Mandapam Camp, South India.

P. carcinus and *P. bengalensis* also were analysed by Huxley and others (Huxley, 1927 and 1932).

The present paper deals with the growth of the length of carapace, the chela, the first walking leg and the length and width of the sixth abdominal segment in relation to the width of carapace of *Neptunus pelagicus*. For details regarding the study of relative growth reference may be made to Huxley (1932).

MATERIAL AND METHODS

The material, on which the present findings are based, included 479 specimens ranging from 8 mm. to 158 mm., in carapace width collected from the landings of the local nets *nandu valai* and *konda valai*. In most cases it was not possible to determine the sex of individuals measuring less than about 35 mm., in carapace width from external features and therefore, the specimens were classified into two groups: (1) unsexed, up to 35 mm., and (2) sexed, males and females above 35 mm.

The following measurements, recorded to the nearest quarter of a millimeter by estimation, were made:

- (1) the maximum width of the carapace (distance between the tips of the spines),
- (2) the length of the carapace along the median line,
- (3) the length of the first walking leg when fully stretched out,
- (4) the length of the chela,
- (5) the length and width of the sixth abdominal segment.

In making these measurements no deformed, soft or regenerating parts were included. Similarly, those crabs infested with rhizocephalan parasite as seen from outside were excluded. Appendages on the right side were usually measured but the left ones were substituted when the others were either missing or deformed because normally there is no asymmetry in the appendages.

The method generally employed in the statistical treatment of the relative growth data is that of Huxley (1932). His formula for allometric growth $y = \beta x^\alpha$ is widely used and in almost all such cases, one of the regression lines has been fitted to the logarithms of the data. Recently Kermack and Haldane (1950) pointed out: 'In many cases of organic correlation it is found that the distribution of the variates is heteroscedastic and skewed. Often, however, the distribution of the logarithms is homoscedastic and more nearly normal.... In addition, it may be found that the fitted straight line does not pass through the origin. This may be due to a significant curvature in the trend of the two variates....' So they suggested that 'considerable advantages are obtained in many cases if the reduced major axis of the logarithms is taken.' Following this method

their formula¹ $\alpha = \left[\frac{\log(1+v_y^2)}{\log(1+v_x^2)} \right]^{\frac{1}{2}}$ is used in the present paper for calculating the slope of the reduced major axis.

RESULTS

(a) Carapace length.

The relationship, carapace length on carapace width as found in five groups: (1) young ones up to 35 mm., in which the sexes are indistinguishable, (2) males up to 80 mm., (3) females up to 80 mm., (4) males over 80 mm., and (5) females over 80 mm., is shown in Figs. 1 and 2. Specimens measuring 35 mm., and below

¹ In this formula $v_x = \sigma_x/\bar{x}$ and $v_y = \sigma_y/\bar{y}$. For full details refer Kermack and Haldane (1950).

in which the determination of sex is generally difficult were grouped together and those over 35 mm., were grouped into the respective sexes. A preliminary examina-

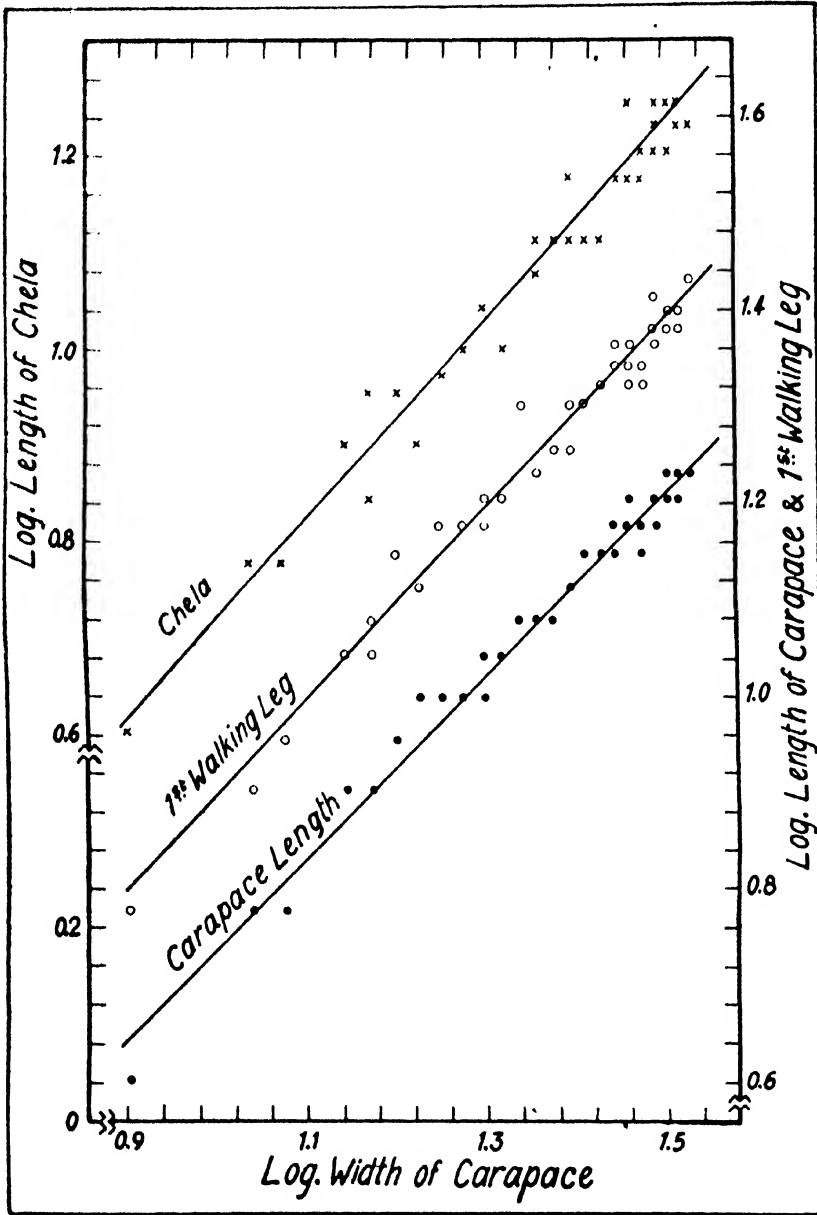


FIG. 1. Logarithmic plot of the length of carapace, first walking leg and the chela on the width of carapace of the unsexed.

tion showed that both males and females exhibit some slight change in relative growth at a carapace width of about 80 mm., and therefore, the growth-coefficients for those from 35-80 mm., and those above 80 mm., were calculated separately. The corresponding values of α are assembled in Table 1. It will be seen from Figs. 1 and 2 that in all the five different groups mentioned above the character

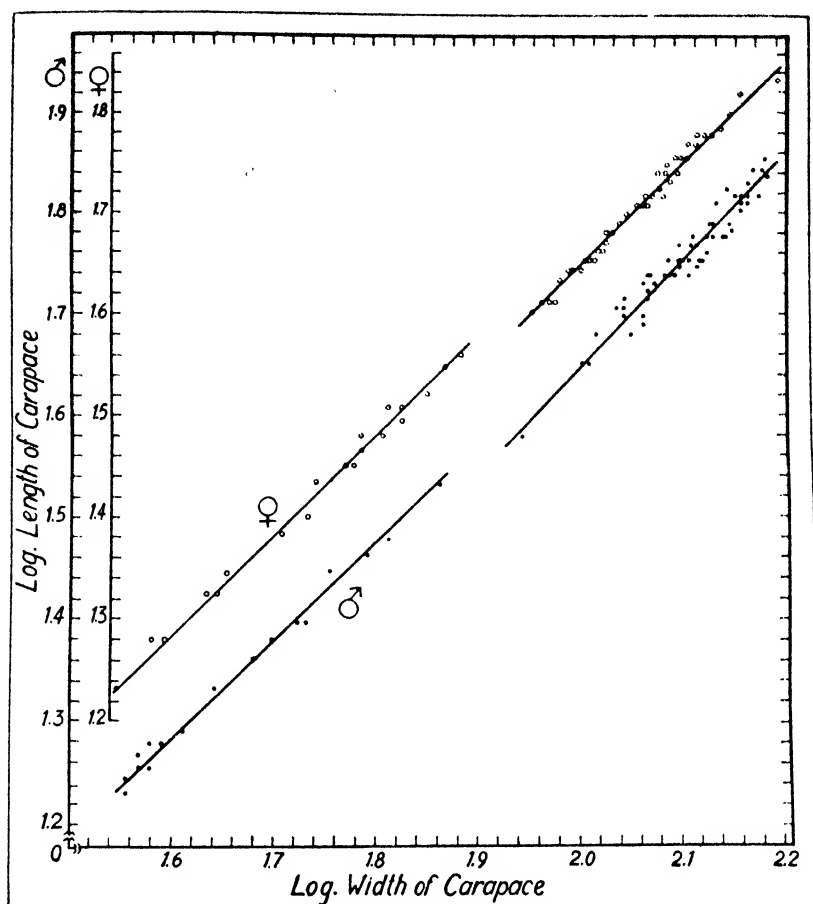


FIG. 2. Logarithmic plot of length of carapace on carapace width in the males and females.

shows simple allometry¹ and the points fall on a straight line on a double logarithmic grid.

TABLE I

Carapace length on carapace width: α values

Size range (mm.)	Sex	σ	σ_{α}
Up to 35	Unsexed ..	0.935	± 0.023
35 to 80	Males ..	0.953	± 0.037
	Females ..	0.951	± 0.027
> 80	Males ..	1.051	± 0.028
	Females ..	1.000	± 0.021

¹ Needham and Lerner (1940) suggested the terms Heterauxesis, with Isauxesis, Bradyauxesis and Trachyauuxesis in place of the earlier terms heterogony, isogony, negative heterogony and positive heterogony respectively. In this paper the terminology suggested by Huxley and Teissier (1936) and Huxley (1950) i.e., allometry with positive allometric growth ($\alpha > 1$), negative allometric growth ($\alpha < 1$) and isometric growth when $\alpha = 1$ will be used.

The relative growth-rate is lowest in the smallest size range. The growth-ratio varies from 0.935 to 1.051 in the different groups, the minimum being that of the unsexed which may be regarded as slightly negatively allometric and the maximum that of males over 80 mm., where it is isometric or even approaching slight positive allometry. Thus, the length of the carapace relative to width shows a slight decrease in the very small crabs, whereas there is a slight but significant increase in the largest individuals. The value of α for the smallest size is significantly lower than those of the males and females of the largest size group studied indicating thereby a gradual acceleration in the relative growth-rate as growth advances but the relative growth-ratio of the unsexed is not significantly different from that of the males and females ranging between 35 and 80 mm., in carapace width. Similarly the values show no significant difference either among the males of the two groups or between the sexes of the same size group. The transformation in the general shape of the carapace from the megalopa to the adult is shown in Fig. 3 which demonstrates clearly how as the individual grows the carapace becomes relatively wider.

Figure 3 further shows that there is no marked variation in the carapace length in relation to sex, a fact already indicated by the growth index. In a closely related species, *Callinectes sapidus*, Newcombe, Sandoz and Rogers-Talbert (1949) found that as the crab grows the length of carapace relative to width shows a slower rate of growth. They further noticed: '... a constant differential growth-ratio in the males throughout the mean range of 17.3 to 185.0 mm., and in the females two separate differential rates. From an empirical standpoint of prediction it is of little moment whether the data are fitted to one or two equations. However, sexual maturity provides a reason for recognising the first displacement at a width of about 95 to 100 mm. The second departure is not explainable at this time. It is noticeable that above a width of 100 mm., the males become somewhat longer in proportion to their width than the females...' The growth in *N. pelagicus* is at first nearly negatively allometric gradually increasing to isometry in the females and to a slight positive allometry (though the α values are not significantly different statistically) in the males above a carapace width of 80 mm. In *Cancer magister*, Weymouth and MacKay (1936) observed a gradual increase in the relative growth-rate of carapace length as in *N. pelagicus* and found no difference between the sexes below a width of approximately 10 cm. They obtained an initial k value¹ of 0.76 at a width of about 0.5 cm., which gradually increased up to 0.94 at a width of 3.5 cm., and although above 10 cm., females become slightly longer for their width the increase in the value of k , they noticed, was not readily calculable. An interesting feature noticed in the carapace length of *N. pelagicus* is that as the log/log, graph (Fig. 2) shows between 80 and 88 mm., carapace width there is an actual decrease in the absolute length in both sexes. After this period of length decrease there is a very slight, non-significant increase in the growth index (Table 1). Shaw (1928) observed a similar phenomenon in all except the third pereopod of the males of *Inachus dorsettensis* but the relative growth-rate in this species following the size decrease does not again reach its previous level.

(b) Length of the chela.

In many crustaceans the growth-coefficient of the chela shows distinct variations in regard to sex, some forms having equal positive allometry in both sexes, others exhibiting positive allometry in both sexes but with a lower growth-coefficient in the females and still others showing allometry in males and isometry in females. The growth-coefficients are likely to change also with age and may show sudden

¹ The values of α given in this paper are not directly comparable to the k values of other authors as the methods employed in calculating these constants are different.

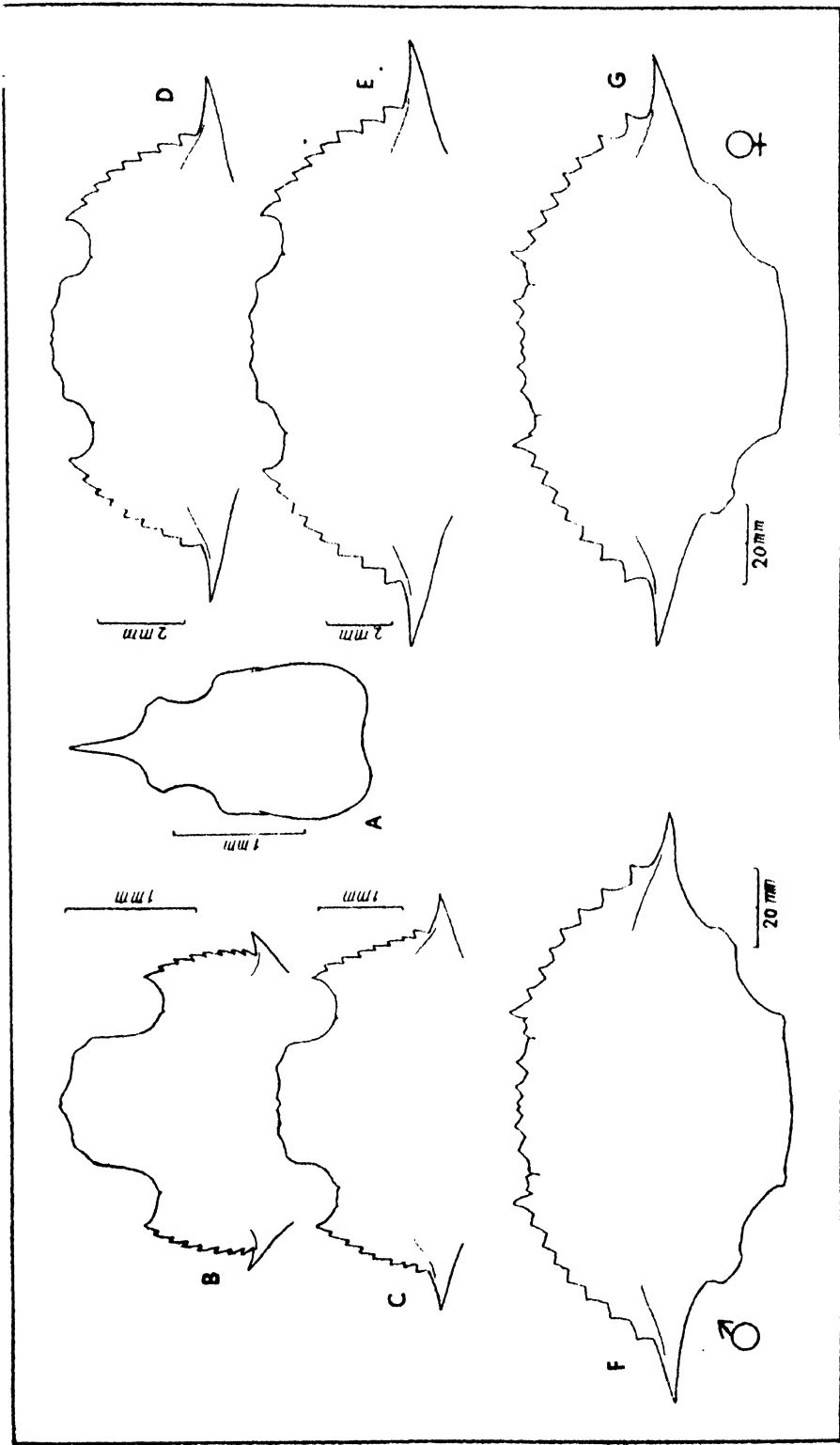


FIG. 3. Changes in the carapaces from the megalopa stage A to the adult male F and female G. B, C, D, and E are carapaces of a first instar and three juvenile crabs measuring 5.0 mm., 12.5 mm., and 19.0 mm., width of carapace respectively.

changes associated with such factors as the onset of maturity. One of the best examples of this is probably the large chela of the male Fiddler Crab. The chelae of the adult *N. pelagicus* show distinct sexual dimorphism, being larger in the males than in the females (Prasad and Tampi, 1953).

In Fig. 1 the log. length of chela of the unsexed is plotted against the log. width of carapace and in Fig. 4 the log./log. data for males and females over 35 mm., are given. The group of unsexed crabs has a differential growth-ratio which is

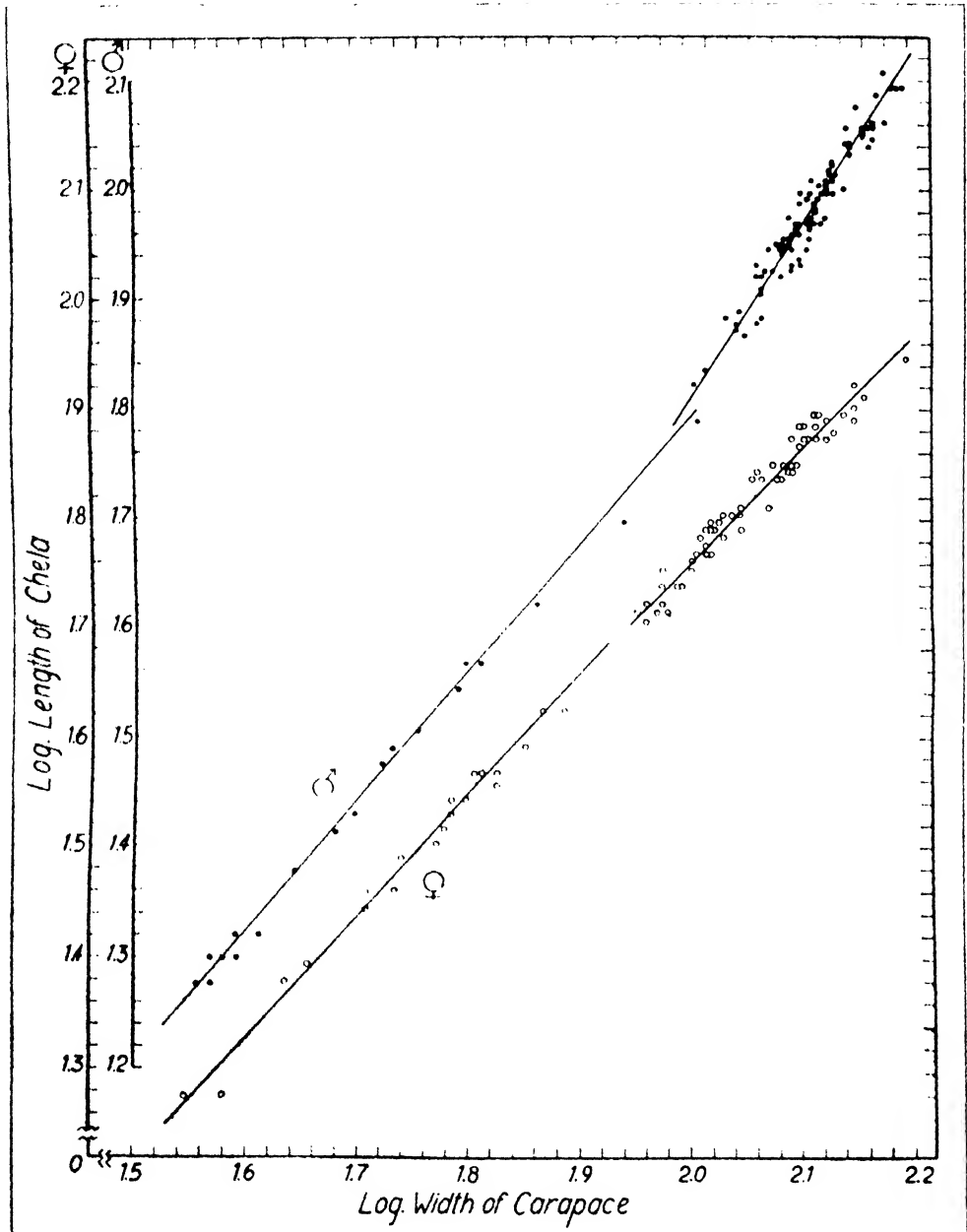


FIG. 4. Logarithmic plot of the length of chela on the width of carapace in the males and females.

only negligibly above unity and therefore, the relative growth may be considered isometric ($\alpha = 1.031 \pm 0.046$). In the case of females over 35 mm., the log. length of chela when plotted against log. width of carapace there is a close approximation to a straight line (Fig. 4) and the value for the size range 35 to 80 mm., is 1.057 ± 0.021 and that for those above 80 mm., is 1.026 ± 0.024 showing a trivial decrease in the relative growth-rate. The growth-ratios of the unsexed and the two groups of females show no significant difference suggesting thereby that the females maintain an almost constant growth-rate. The chela of the males shows somewhat a different condition. The practically isometric growth noticed in the unsexed changes to a slight but non-significant positive allometry in the males up to a carapace width of about 102 mm., when there is a break with an increase in the absolute size followed by a marked change in the growth-coefficient resulting in a distinct positive allometry, the α value increasing from 1.162 ± 0.067 in the smaller ones to 1.593 ± 0.031 in the largest individuals (Fig. 4). It is also found that the rate of relative growth of the chela in the smaller males does not significantly differ from that of the females but the larger males have longer chelae. A similar change in the growth-rate of the chela of the females in the size range studied has not been noticed indicating thereby that in this character the species under consideration shows sexual dimorphism and that the break followed by an increase in the relative growth-rate of chela in the males may be associated with the commencement of sexual maturity. Thus the size at first maturity in the males seems to be about 102 mm., carapace width.

(c) *Length of the first walking leg.*

A log./log. graph representing the relative growth of the first walking leg of the unsexed is shown in Fig. 1. The relative growth characterising this range is almost negative allometry ($\alpha = 0.935 \pm 0.028$) unlike the length of chela. Among the females of 35 mm. and above, the relative growth-rate is nearly isometric but there appears to be a slight change in the relative growth-rate and the line representing the reduced major axis seems to be formed of two segments, the two component lines intersecting at a carapace width of about 108 mm. (Fig. 5). The α for the smaller sized female crabs is 0.988 ± 0.020 and that for the larger ones is 1.063 ± 0.023 . While the smaller females do not show a significant difference in their growth-ratio from those of the unsexed the larger ones have a significantly higher rate of growth than the unsexed. In the males there is a break and a sudden increase in the relative growth at a carapace width of about 102 mm., as with the length of chela, and those above 102 mm., show a distinct positive allometry, α being 1.433 ± 0.031 . The smaller males show a significant difference in the growth-coefficient ($\alpha = 1.033 \pm 0.028$) from that of the unsexed but not from that of the females. According to Huxley (1931) and Sandon (1937) in *Ocypoda aegyptiaca* the walking legs as a whole grow at a slower rate than the carapace showing a negative allometry.

As already mentioned in the case of the chela, the first walking leg too shows definite sexual dimorphism, the larger males having longer walking legs than the females. The sudden increase in the growth-ratio of the first walking leg of the males at a carapace width of about 102 mm., presumably marks the onset of sexual maturity. Huxley (1932) remarked: 'In general, male crustacea appear to have relatively larger pereopods than females'.

(d) *Width of the sixth abdominal segment.*

The abdomen of crabs is another part exhibiting sexual dimorphism and in the female it shows striking allometric growth, for it is always broad in the adult, narrow and of the male type in the juveniles. The gradual transition in the general shape of the abdomen from the megalopa to the adult, both in the males and females,

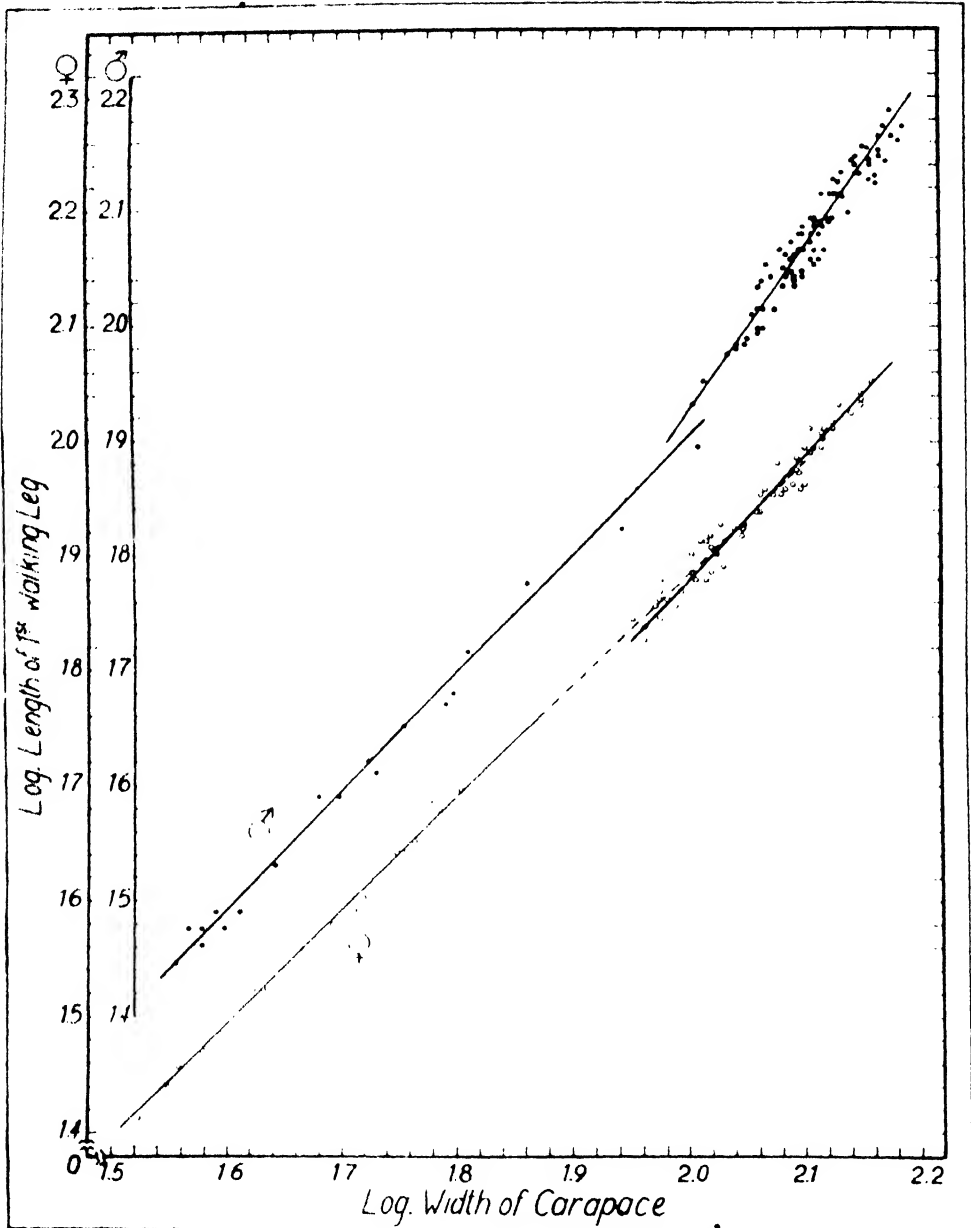


FIG. 5. Relation between the width of carapace and the length of the first walking leg in the males and females. Logarithmic plotting.

is shown in Figure 6. In Figure 7 is plotted the log. width of abdomen of the unsexed against the log. width of carapace. At this stage the growth-coefficient is 1.121 ± 0.055 showing a slight positive allometry. As is to be expected the females show a break in the rate of growth of the width of the sixth abdominal segment in the larger ones (Fig. 8). Up to about 108 mm., the growth-coefficient is 1.209 ± 0.026 , which is not significantly different from that of the unsexed, but following this there is a pronounced acceleration in the growth-ratio, the α value being 1.524 ± 0.057 and this continues up to the maximum size studied. The males, on the other hand,

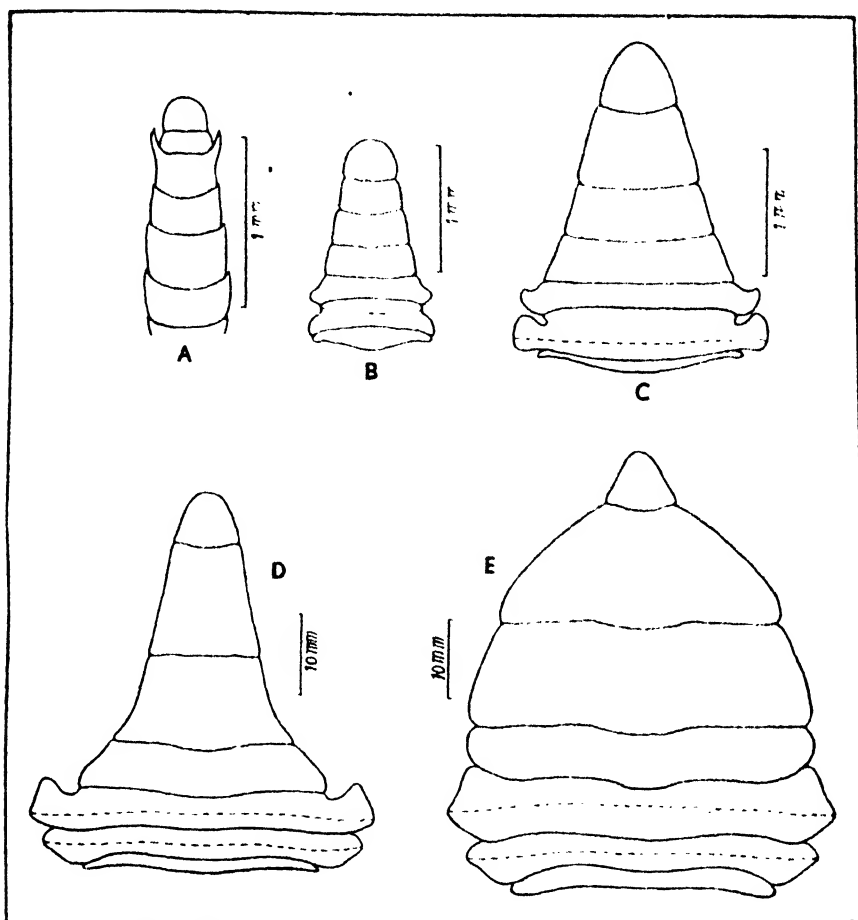


FIG. 6. The abdomen of a megalopa (A), juveniles (B, C, carapace width 2.5 mm. and 7.0 mm., respectively), adult male (D) and adult female (E).

show a constant growth from 35 mm. to the largest size-range included in the present investigation (Fig. 8), but they show a significant difference in the growth-coefficient from those of the unsexed and females of all size ranges (Table 2).

TABLE 2

Width of the sixth abdominal segment: α values.

Size range (mm.)	Sex	α	σ_{α}
Up to 35	Unsexed ..	1.121	± 0.055
> 35	Males ..	0.997	± 0.016
35 to 108	Females ..	1.209	± 0.026
> 108	Females ..	1.524	± 0.057

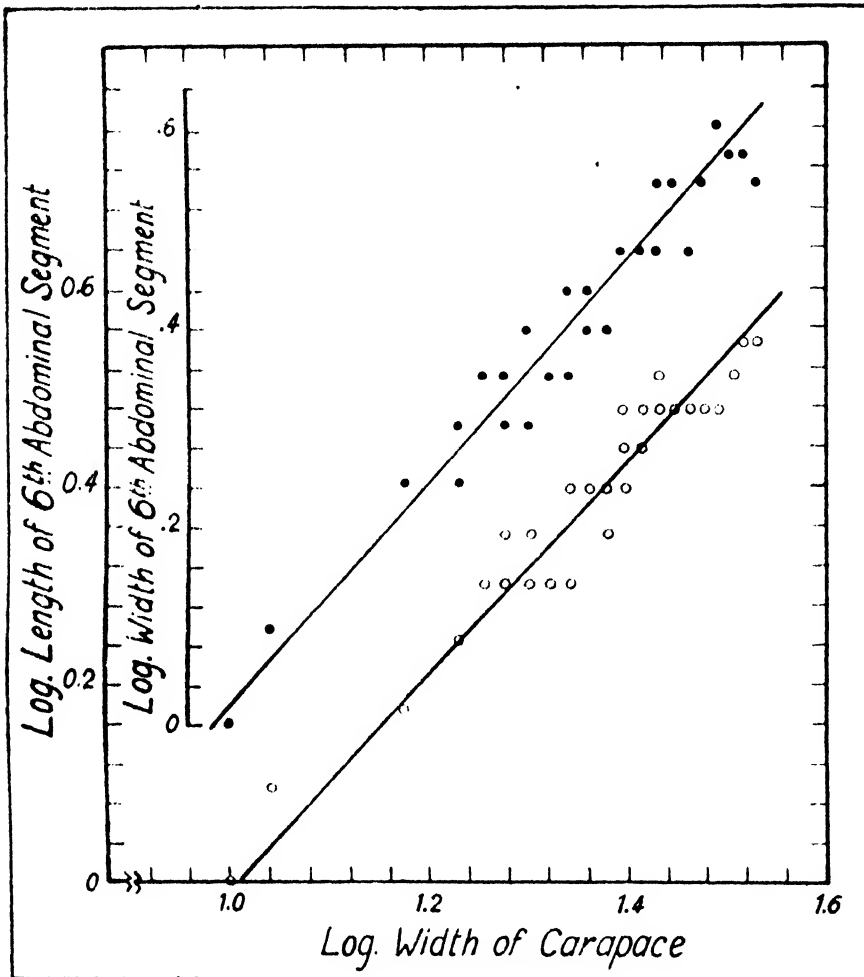


FIG. 7. Logarithmic plot of length and width of the sixth abdominal segment against the width of carapace in the unsexed.

From Table 2 it is further seen that the growth-ratio of the width of the sixth abdominal segment in the males over 35 mm. is nearly isometric and shows a slight but statistically significant decrease from that of the individuals in which sex determination was difficult. The growth index of the females 35 to 108 mm., on the contrary, is not significantly different from that of the unsexed and the change becomes apparent only in the larger females. So it is of interest to note that the rate of growth of the width of the sixth abdominal segment in the smallest *N. pelagicus* is positive allometry, whereas the males all through have a lower relative growth approaching isometry. The females throughout the range of size studied, which includes the largest caught locally, show definite positive allometry in regard to this character. Shaw (1928) noticed in the female *Inachus* 'that the abdomen growth consists of two long periods, one of slight positive heterogony, the other of isogony, separated by a short period of violent heterogony, which presumably begins directly after a moult, since its effects are shown completely by the next moult.' But in the males of the same species the abdomen is isometric in the young crabs becoming slightly negatively allometric in older crabs. Huxley and Richards (1931) observed in *Carcinus maenas* that the abdomen of the female becomes relatively larger with increased absolute size throughout the whole of its life. As in

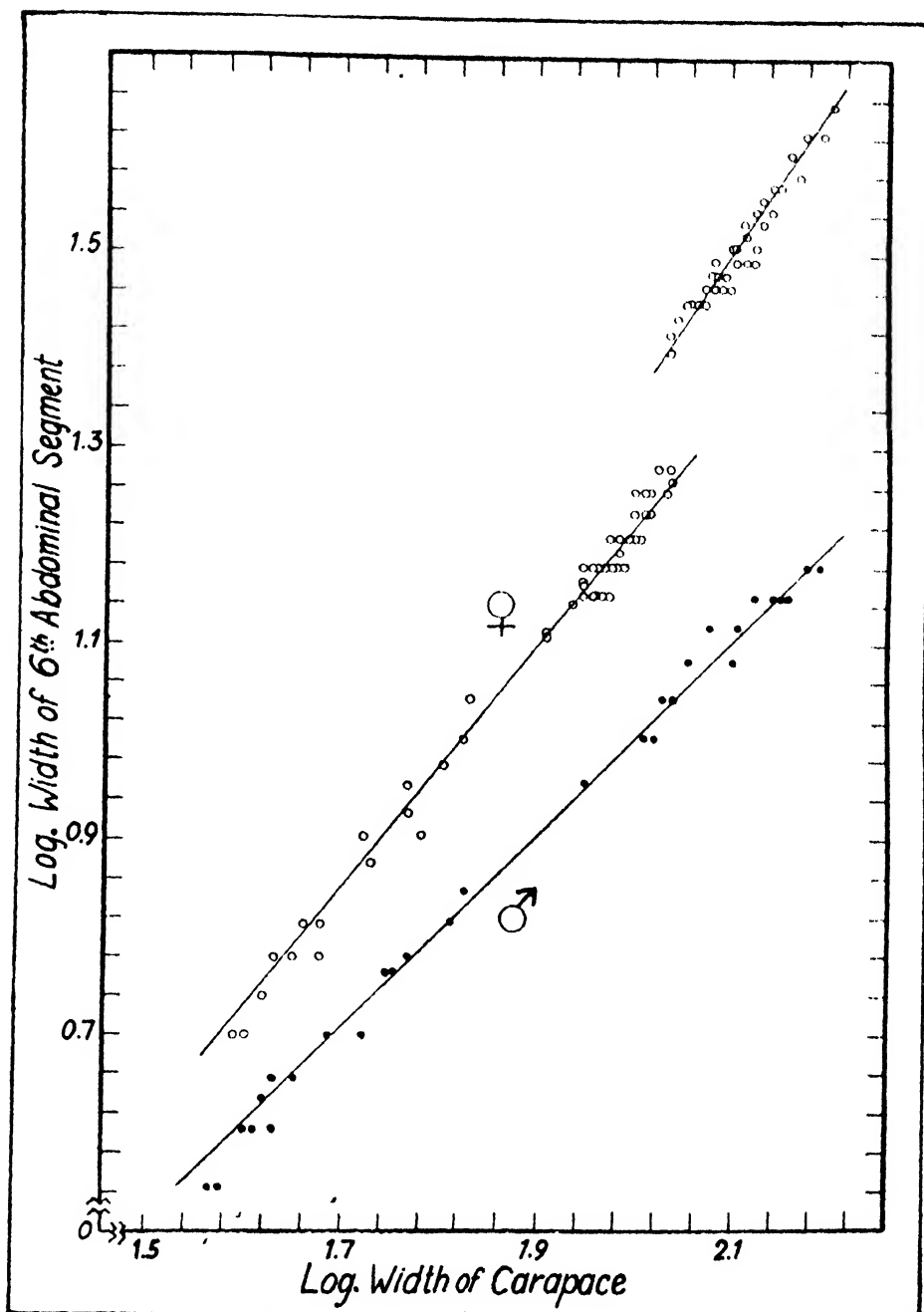


FIG. 8. Logarithmic plot of width of the sixth abdominal segment against the width of carapace in males and females.

C. maenas the abdomen in the female *N. pelagicus* also becomes relatively larger with increase in the absolute size all through its life. The investigations of Williams and Needham (1938) on *Pinnotheres pisum* brought out that the relative growth-rate of all abdominal segments in this particular species is lower at the smallest sizes, almost showing negative allometry, but increases in the larger ones to slight

positive allometry, the value of the growth index varying from 0.98 to 1.13. They have, however, pointed out that they did not have sufficient specimens of the smallest sizes to obtain a definite measure of its growth index.

(c) *Length of the sixth abdominal segment.*

The log. length of the sixth abdominal segment of the unsexed plotted against the log. width of its carapace shows that the slope of the line is almost parallel to that of the log. width of the sixth abdominal segment (Fig. 7). There is a close agreement between the values of the growth index of the length and width of the sixth abdominal segment of the unsexed crabs but these are significantly different in the males and females, the males having a slightly higher relative growth-rate

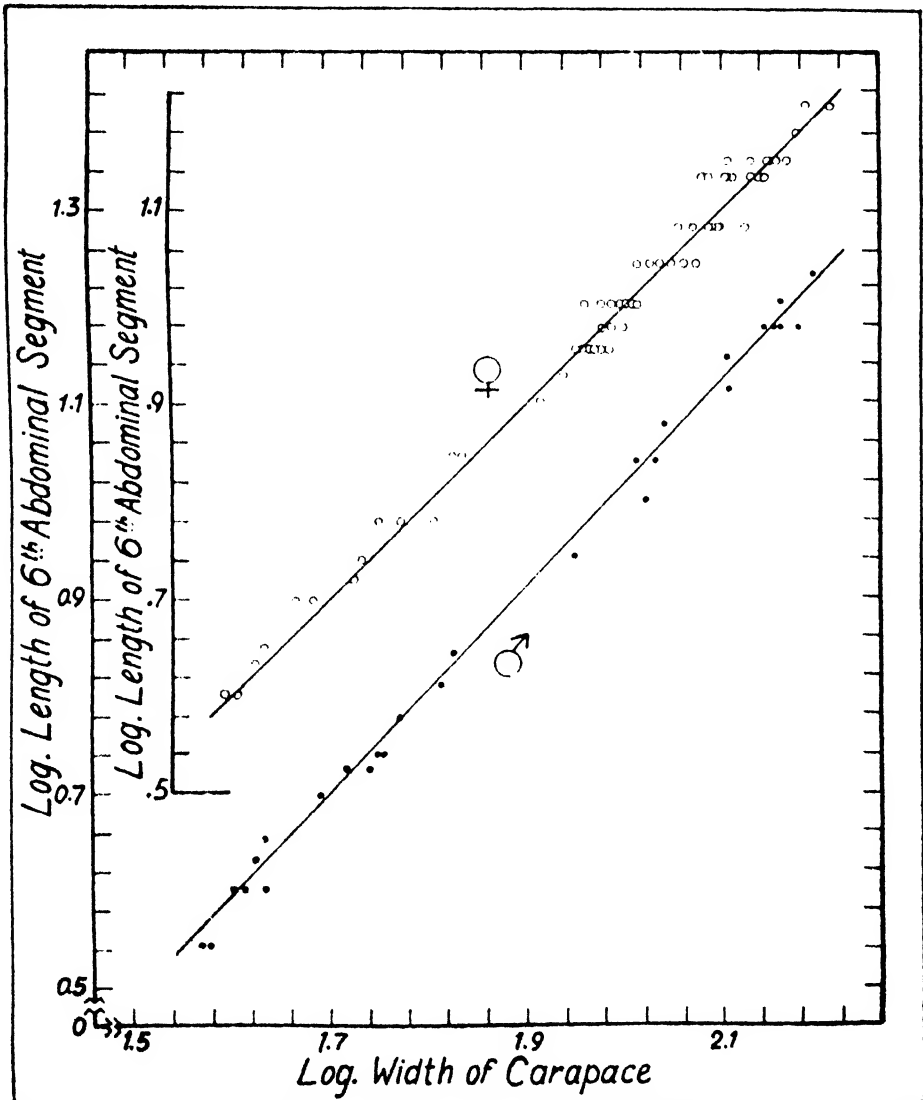


FIG. 9. Logarithmic plot of length of the sixth abdominal segment against the width of carapace in males and females.

in the length while the females show a considerably low α value in relation to the width (Ref. Tables 2 and 3).

TABLE 3
Length of the sixth abdominal segment: α values.

Size range (mm.)	Sex	α	σ_{α}
Up to 35	Unsexed ..	1.091	± 0.054
> 35	Males ..	1.059	± 0.016
	Females ..	0.992	± 0.034

In the males as well as the females over 35 mm., the growth-coefficient is constant throughout and there are no indications of abrupt changes (Fig. 9) and unlike with the width, the growth-ratio of the length of the sixth abdominal segment does not show significant differences between the males and females in the entire size range studied. Although the growth rate in the females falls slightly from that of the unsexed, the difference is not statistically significant. Drach (as cited by Newcombe *et al.*, 1949) studied form changes in the abdomen relative to carapace of *Portunus puber* and found that the data followed three parallel lines. The first discontinuity, according to him, corresponds to the puberty moult and the second due to the moult following the puberty moult. In *Cancer magister* Weymouth and MacKay (*op. cit.*) found that the length of the sixth abdominal segment in the males shows a varying growth-rate, the values of k ranging from 1.00 to 1.06. The growth-coefficient for the females of the same species becomes markedly different at a carapace width of 10 cm., but the smallest available males and females show isometry. In *N. pelagicus* this growth-ratio does not differ markedly even in the largest males and females studied. Throughout the growth may be regarded as isometric in the females and possibly tending towards slight positive allometry in the unsexed and the males.

DISCUSSION

Studies of this nature have usually been undertaken with the main object of mapping out the general pattern of growth intensities and growth centres. Several detailed investigations on many species of crustaceans have established the occurrence of definite growth centres and growth gradients. Evidences have also been given on the effect of the growth-rate of one part on the other, what has been called 'positional effect' where the high positive or negative allometric growth in one appendage influences the rate of growth of the neighbouring appendages. However, in certain species such as *Ocypoda aegyptiaca* Sandon (1937) observed that 'the positive heterogony of the chela has not apparently had any effect on the growth of the legs adjacent to them, nor has the increased growth of the large chela induced an increased growth-rate in the other appendages on the same side of the body.' But Tazelaar (1930) remarked: 'There is undoubtedly a correlation between marked heterogony in an appendage and the growth-rate of neighbouring appendages. The correlation is of the following nature: that the growth of appendages immediately posterior to the heterogonic organ is increased, that of appendages immediately

anterior is decreased, irrespective of whether they are of the same type as the heterogonic organ (e.g., pereopod and chela) or different type (e.g., maxilliped and chela).'

Needham (1950) stated that the 'growth constant' α was not constant, even over restricted periods of growth, but was a continuously variable function of carapace size and therefore, he used Medawar's transformation method, with certain modifications, 'to give a single key relation which, within the scope of the data defines abdomen width completely, spatially and temporally.' But according to Huxley (1950) 'This method, however, although providing much the most comprehensive picture or description of the process of form transformation, sheds little light on the possible biological causes or mechanism underlying the process. On the other hand, analysis in terms of allometry does so, since it strongly suggests a graded distribution of some substance or process concerned with the regulation of relative growth-rate.' The analyses in the present investigation have been carried out in terms of allometry.

The aim of this study, as already pointed out in the introduction, is primarily to ascertain whether the species shows any marked changes in the growth-ratio which may be considered as associated with the attainment of sexual maturity as the species shows distinct sexual dimorphism in regard to the chela and the first walking leg, both being relatively longer in the larger males than in the females of the same size range. Similarly, in the case of females the sudden change in the width of the abdomen from the male type to the female type is also a sure sign of the onset of maturity. As Smith (1906) pointed out for *Inachus scorio*, the deviation from a simple straight line series of points in all probability is due to the phenomenon of 'facultative' high and low dimorphism. Such changes may be displayed by different parts in different ways. Thus, Shaw (1928) observed in *I. dorsettensis* that the normal strong allometry of the male chela is replaced by the female isometric type of growth in the non-breeding season and so also in the pereopods. In *Cancer magister* with the onset of sexual maturity there are significant changes in length-width proportions and in the length and width of the seventh abdominal segment. In the males there is a change in the relative growth of the walking leg (Weymouth and MacKay, 1936).

In *N. pelagicus* certain significant changes in the relative growth-rate of parts which can reasonably be attributed to physiological changes associated with the onset of sexual maturity are observed. The authors, during their investigation on the biology of this species (Ref. Prasad and Tampi, *op. cit.*) found that the smallest crab in berry was 106 mm., in carapace width. An analysis of the relative growth of the width of the sixth abdominal segment has shown that there is an abrupt break, increase in width and further accentuation in the rate of growth, an indication of the onset of sexual maturity, at a carapace width of about 108 mm., which is in very close agreement with the observed size of the smallest crab bearing eggs. This sudden change from the 'intermediate type' of abdomen to the typical female type seems to be completed during a single moult, preceding the attainment of sexual maturity. No such change is, however, noticed in the length of the sixth abdominal segment which maintains an almost isometric growth throughout. The females, even from a very early stage show a significantly higher rate of relative growth than the males in the width of the sixth abdominal segment (Fig. 8) but sex differentiation based on the shape of the abdomen cannot be depended upon until the crabs have grown to a size of about 35 mm., because the 'intermediate' type of abdomen of the juvenile females cannot always be distinguished with certainty from the male type. The increase in the width of the sixth abdominal segment in the males seems to be gradual and constant throughout without any abrupt change as observed in the larger females. In several instances, such as *Pinnotheres pisum* (Williams and Needham, 1938) and *Carcinus* (Day, 1935) a fall in the relative growth-rate at a particular stage has been observed in the female abdomen. The growth

of the female abdomen in *Pinnotheres* is most rapid before maturity, after which growth is practically isometric. A similar phenomenon of a fall in the growth-rate of the sixth abdominal segment of the female has not been noticed in *N. pelagicus* and with the onset of maturity there is an increase in the relative growth-rate which is maintained throughout.

It was also pointed out earlier in this paper that a slight change in the relative growth-rate of the first walking leg in the females is noticed, the lines representing the reduced major axis of the two phases intersecting at a carapace width of approximately 108 mm. This is probably an additional supporting evidence to the conclusion that the females attain maturity when they are about 108 mm., in carapace width.

The problem of ascertaining the sexual maturity in the males is generally more difficult because many species may not show great external changes at the time of sexual maturity. However, *N. pelagicus* shows easily discernible sexual dimorphism at least in one character, the length of chela. A change in the relative growth-rate of the length of chela in the males is observed at a carapace width of about 102 mm. Similarly, a change in the relative growth-rate of the first walking leg was noticed at the same size. Thus it appears that the onset of sexual maturity may be slightly earlier in the males than in the females. Pearson (1908) recorded a similar condition in *Cancer pagurus* and as for the males of *N. pelagicus* in Australian waters Thomson (1951) stated: 'It is true that the crabs mature at a lesser size which is estimated to be about 4 in., when the secondary sexual characteristics become evident.....' The size of 4 inches given by Thomson is in good agreement with that observed locally. In *Callinectes sapidus* Newcombe *et al.* (1949) found 'little difference in this respect between sexes. The changes in the linear ratios suggest that females mature when about 95-100 mm., in width. The moulting data presented here show that sexual maturity in the males is probably attained at about the same size.'

The abrupt nature of changes in the relative growth-rate of the width of the sixth abdominal segment and the length of the first walking leg in the females at a carapace width of 108 mm., and similar changes in the length of chela and the first walking leg of the males at 102 mm., carapace width suggests that in *N. pelagicus* sexual maturity is usually attained by a single moult. A similar phenomenon has been noticed in *Pugettia producta* by Weymouth (personal communication).

The peculiar phenomenon of decrease in the absolute length of carapace in both sexes is hard to interpret. Shaw (1928) who noticed a similar 'back kink' of the curves for all the pereiopods of *Inachus dorsettensis* suggested: 'It may well be that the relative growth-rate of the pereiopods decreases at the same time as that of the chelar propus decrease (i.e., there is a similar slowing down of growth in the non-breeding season) and that after this period when the relative growth-rate of the chela rapidly increases, this acts as a drain on the pereiopods, so that these never again attain to their former relative size.' In *N. pelagicus* the phenomenon takes place long before the attainment of sexual maturity. Therefore, it does not seem to have any correlation with the breeding activity and the explanation will have to be sought elsewhere. The authors (1953) have mentioned in their report on the biology of this species that there is a certain amount of segregation according to size. Analyses of size-frequencies of crabs landed by two different types of nets, one operated in shallow waters and the other in relatively deeper areas, have shown that the latter composed of crabs above 90 mm., and the former 80 mm., and below. This size range coincides with that when there is a decrease in the carapace length. So it is possible that the observed decrease may be caused by a change in the environment during the migration from shallow to deeper waters. Weymouth (personal communication) has suggested that this retardation of growth may be due to a great increase in the gonadial tissue (which sometimes amounts to a third of the bulk of the tissues) at this moult and the crabs then seek deeper water. However, further detailed work is necessary to ascertain the exact cause.

SUMMARY

The paper deals with the relative growth (on the basis of carapace width) of (1) the length of carapace, (2) length of the chela, (3) length of the first walking leg and (4) length and width of the sixth abdominal segment in the unsexed, males and females of *N. pelagicus*.

479 crabs ranging from 8 to 158 mm. are included in this study. Huxley's formula for allometric growth has been employed but instead of fitting the conventional regression line to the logarithms of the data, Kermack and Haldane's method of taking the reduced major axis of the logarithms has been used.

Allometric growth has been found in the majority of the parts studied, the α values ranged from 0.935 to 1.593.

A decrease in the absolute length of the carapace in both males and females has been noticed at a carapace width ranging from 80-88 mm. It is suggested that this is perhaps caused by a change in the environment because there is some evidence of the crabs migrating from shallow to deeper waters at this size.

ACKNOWLEDGEMENTS

The authors wish to thank Prof. J. B. S. Haldane for the interest he took in this work, for suggesting the statistical method employed in the present investigation and arranging to send the relevant literature. The authors likewise express their gratitude to Dr. N. Kesava Panikkar and Dr. Frank W. Weymouth who have critically read the manuscript and have made invaluable suggestions.

REFERENCES

- Alcock, A. (1906). The prawns of the *Penaeus* group. *Catalogue Indian Mus.*, Decapoda Crustacea.—Pt. III, Macrura, 1-55, Calcutta.
- Day, J. H. (1935). Heterogonic growth in the abdomen of *Carcinus maenas*. *Rep. Dove Marine Laboratory* Third Ser., No. 3.
- Huxley, J. S. (1927). Further work on heterogonic growth. *Biol. Zentralb.*, 47, 151-163.
- (1931). Notes on differential growth. *American Naturalist*, 65, 289-315.
- (1932). Problems of relative growth. Methuen & Co., London, 1-276.
- (1950). Relative growth and form transformation (A discussion on the measurement of growth and form under the leadership of S. Zuckerman, F.R.S.). *Proc. Roy. Soc. London*, 137, Ser. B: 465-469.
- Huxley, J. S. and O. W. Richards (1931). Relative growth of the abdomen and the carapace of the Shore-Crab *Carcinus maenas*. *Jour. Mar. Biol. Assoc. U. K.*, 17, 1001-1015.
- Huxley, J. S. and G. Teissier (1936). Terminology of relative growth. *Nature*, 137, 780.
- Kermack, K. A. and J. B. S. Haldane (1950). Organic correlation and allometry. *Biometrika*, 37, 30-41.
- Needham, A. E. (1950). The form-transformation of the abdomen of the female Pea-Crab, *Pinnotheres pisum* Leach. *Proc. Roy. Soc. London*, 137, Ser. B: 113-136.
- Needham, J. and I. M. Lerner (1940). Terminology of relative growth-rates. *Nature*, 146, 618.
- Newcombe, C. L., Mildred D. Sandoz and R. Rogers-Talbert (1949). Differential growth and moulting of the Blue Crab, *Callinectes sapidus* Rathbun. *Jour. Exper. Zool.*, 110, 113-152.
- Pearson, J. (1908). *Cancer*. *Liverpool Mar. Biol. Comm. Mem.*, 16, 1-217.
- Prasad, R. R. and P. R. S. Tampi (1953). A contribution to the biology of the Blue Swimming Crab *Neptunus pelagicus* (Linnaeus) with a note on the zoea of *Thalamita crenata* Latreille. *Jour. Bombay Nat. Hist. Soc.*, 51, 674-689.
- Sandon, H. (1937). Differential growth in the crab *Ocypoda*. *Proc. Zool. Soc. London*, 107, Ser. A: 397-414.
- Shaw, M. E. (1928). A contribution to the study of relative growth of parts in *Inachus dorsalis*. *Brit. Jour. Exp. Biol.*, 6, 145-160.
- Smith, G. W. (1906). Fauna und Flora des Golfes v. Neapel, 29, (*Rhizocephala*), 65-76.
- Tazelaar, M. A. (1930). The relative growth of parts in *Palaemon carcinus*. *Jour. Exp. Biol.*, 7, 165-174.
- Thomson, J. M. (1951). Catch composition of the Sand-Crab fishery in Moreton Bay. *Australian Jour. Mar. and Freshwater Res.*, 2, 237-244.
- Weymouth, F. W. and Donald C. G. MacKay (1936). Analysis of the relative growth of the Pacific edible crab *Cancer magister*. *Proc. Zool. Soc. London*, Pt. 1: 257-280.
- Williams, G. and A. E. Needham (1938). On the relative growth in *Pinnotheres pisum*. *Ibid.*, 108, Ser. A: 539-556.

THE ABSORPTION SPECTRUM OF BiBr

by P. K. SUR and K. MAJUMDAR, *Physics Department, University of Allahabad*

(Communicated by A. C. Banerji, F.N.I.)

(Received January 18, 1952 ; after revision November 9 ; read December 4, 1953)

INTRODUCTION

Howell and Rochester (1934) using a high frequency discharge obtained the emission band spectrum of BiBr molecule, but no vibrational analysis seems to have been done. Morgan (1936) obtained the absorption spectrum by using a long column of vapour formed by heating bismuth metal in a vapour of bromine in an open iron tube to a temperature of 900°C. Besides these no further information is available.

In view of the fact that a system of bands of BiCl molecule was observed by one of the authors (Sur, 1950) in the extreme ultraviolet region ($\lambda\lambda$ 2400–2200) in absorption, it was expected that a molecule of the same group might give a corresponding system in about the same region. With this purpose in view, the present investigation was undertaken.

EXPERIMENTAL

The experimental arrangement was essentially the same as was used by the author in previous investigation on BiCl (1950) and BiS (1951), and other molecules. A chemically pure sample of BiBr₃ salt was obtained from Eimer and Amend, New York, through the kindness of the Head of the Department of Chemistry, University of Cornell. A small quantity of the salt after being dried in an oven was introduced into a vitreosil tube 15 cms. long and 1 cm. internal diameter. This tube was inserted into a closely fitting Acheson graphite tube heated electrically to a temperature ranging from 900°C. to 1020°C. within a water-cooled furnace provided with side windows for making observations. The substance is highly vaporisable and quickly effuses out of the absorbing tube. To prevent this the furnace chamber was kept filled with nitrogen at a pressure of about 30 cms. of mercury. It was not until the vapour had thinned out sufficiently that a spectrogram of measurable intensity was possible, for which a prolonged exposure lasting from two to two and a half, sometimes three hours was found necessary. The band systems, in spite of several try outs under varying conditions, could only be developed feebly. A temperature of about 990°C. was sufficient to bring out the bands to just a measurable intensity. Observations were taken on a E_2 quartz spectrograph on B, 20 Kodak plates. A copper arc was used for comparison spectra, and temperatures were estimated by an optical pyrometer of the vanishing filament type. A water-cooled hydrogen discharge provided with quartz windows was used for the continuum.

RESULTS

Figures I(a) and I(b), Plate VII, are a reproduction of the bands of the ultraviolet system C, and systems D and E respectively. The observed wavenumbers reduced to vacuum, the difference between the observed and calculated wavenumbers, the

estimated intensities on the scale of ten, and the vibrational quantum numbers are recorded in Tables I, II and III for the three systems of bands. Tables IV, V and VI give the Deslander's scheme. These band heads are represented within the experimental error by the following formulae:—

For the system *C*

$$\nu = 34362.9 + 503.8 (v' + \frac{1}{2}) - 40(v' + \frac{1}{2})^2 - 209.3(v'' + \frac{1}{2}) + 40(v'' + \frac{1}{2})^2.$$

For the system *D*

$$\nu = 41633.3 + 652.5(v' + \frac{1}{2}) - 209.2(v'' + \frac{1}{2}) - 25(v' + \frac{1}{2})^2 + 60(v'' + \frac{1}{2})^2$$

and for the system *E*,

$$\nu = 43502.33 + 319(v' + \frac{1}{2}) - 5.5(v' + \frac{1}{2})^2 - 209.2(v'' + \frac{1}{2}) + 60(v'' + \frac{1}{2})^2$$

The last two systems overlap between the wavelengths $\lambda\lambda$ 2350–2336 Å, as the system origins are very close to each other.

TABLE I

λ in Å.	Int.	ν obs. cm. ⁻¹	ν cal. cm. ⁻¹	ν obs. ν cal.	v'	v''
2968.5	0	33677.5	33681	3.5	0	4
2950.3	0	33885.0	33887	2	0	3
2932.0	2	34096.0	34094	2	0	2
2912.7	0	34310.6	34302	8.6	0	1
2893.0	4	34509.0	34510	1	0	0
2872.0	0	34808.0	34805	3	1	1
2856.0	10	35003.7	35013	9.3	1	0
2834.56	..	Atomic line				
2814.7	8	35517.3	35515	2.3	2	0
2794.8	6	35770.2	35778	7.8	5	6
2774.8	2	36028.0	36017	11	3	0
2747.0	4	36393.0	36394	1	5	3
2730.7	0	36609.8	36601	8.8	5	2
2709.9	0	36890.8	36893	2.2	6	3

TABLE II

λ in Å.	Int.	ν obs. cm. ⁻¹	ν cal. cm. ⁻¹	ν obs. ν cal.	v'	v''
2448.6	0	40827	40827	0	0	5
2436.5	2	41030	41030.4	0.4	0	4
2425.5	5	41233	41234.6	1.6	0	3
2412.5	7	41438	41440.2	2.2	0	2
2400.5	7	41645	41647	2	0	1
2388.5	7	41854.5	41855	0.5	0	0
2375.1	9	42090.6	42092	1.4	1	2
2363.5	9	42297	42299	2	1	1
2336.5	7	42786	42782	4	3	5

TABLE III

λ in Å.	Int.	ν obs. cm.^{-1}	ν cal. cm.^{-1}	ν obs. ν cal.	ν'	ν''
2350.6	10	42529	42528	1	0	5
* 2327.8	1	42946	42935.6	10.4	0	3
2317.8	5	43131	43141.2	-10.2	0	2
2306.2	9	43348	43348	0	0	1
* 2295.2	2	43556	43556	0	0	0
2290.0	0	43655	43656	1	1	1
2279.1	2	43864	43864	0	1	0
2264.0	2	44156	44161	5	2	0
* 2246.1	0	44509	44514	5	4	1
* 2232.4	0	44781	44778	3	5	1
* 2222.1	0	44988	44986	2	5	0

Not quite visible under comparator..

TABLE IV

6				36891			
5			36610	36393			35770
4							
3	36028						
2	35517						
1	35004	34808					
0	34509	34310	34096	33885	33677		
ν'/ν''	0	1	2	3	4	5	6

System C

TABLE V

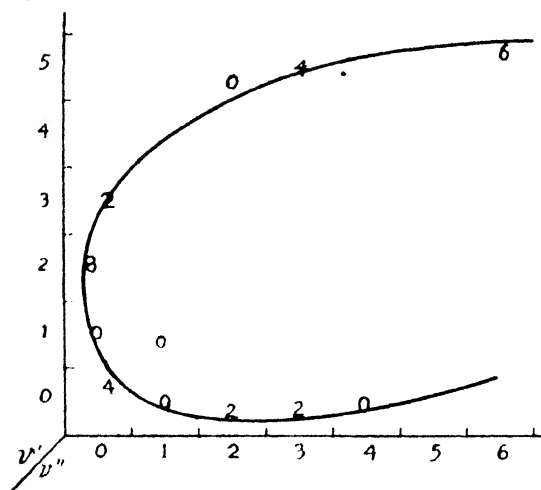
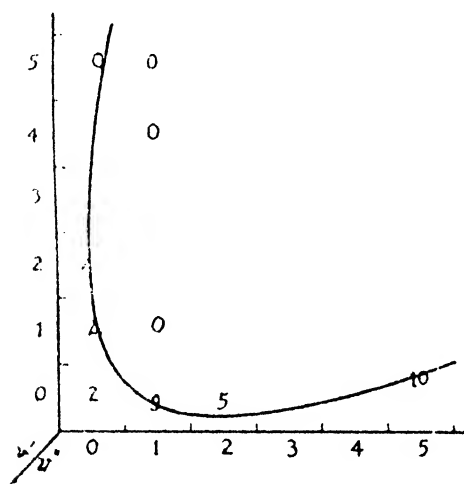
3						42786
2						
1		42297	42091			
0	41855	41645	41438	41233	41030	40827
ν'/ν''	0	1	2	3	4	5

System D

TABLE VI

6						
5	44988	44781				
4		44509				
3						
2	44556					
1	43864	43655				
0	43556	43348	43131	42946		42529
ν'/ν''	0	1	2	3	4	5

System E

FIG. 2. System *C*FIG. 3. System *E*

Figs. 2 and 3 show the Condon parabolas for the systems *C* and *E* respectively.

These parabolas are not well defined on account of few bands in each of the above systems. A parabola could not be drawn for system *D* on account of the same reason. These plots, however, indicate that the intensity plots of the band heads lie on open parabolas as expected from large difference in the values of w_e' and w_e'' in the above systems. The intensity observed for the (0, 5) bands of the system *E* is abnormally high.

DISCUSSION OF RESULTS.

Morgan could observe in absorption band systems due to each of the isotopic molecules BiBr^{79} and BiBr^{81} which have practically the same abundance ratio. He had taken his spectrograms on a 21 ft. grating in the second order, having a dispersion of 48 Å/mm. at 3900 Å. In our case no such isotopic separation in the

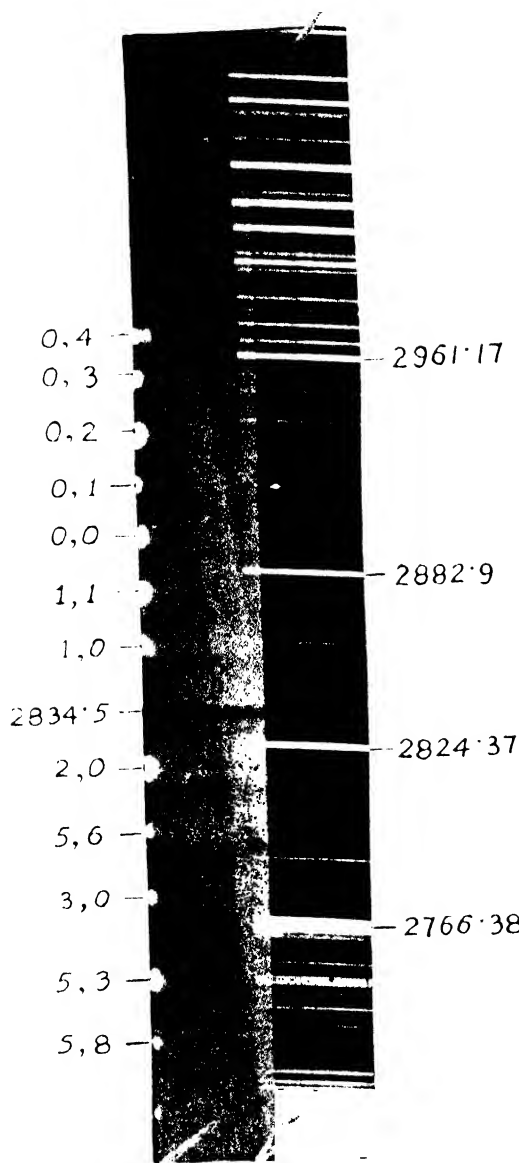


FIG. 1(a)
C System of BiBr

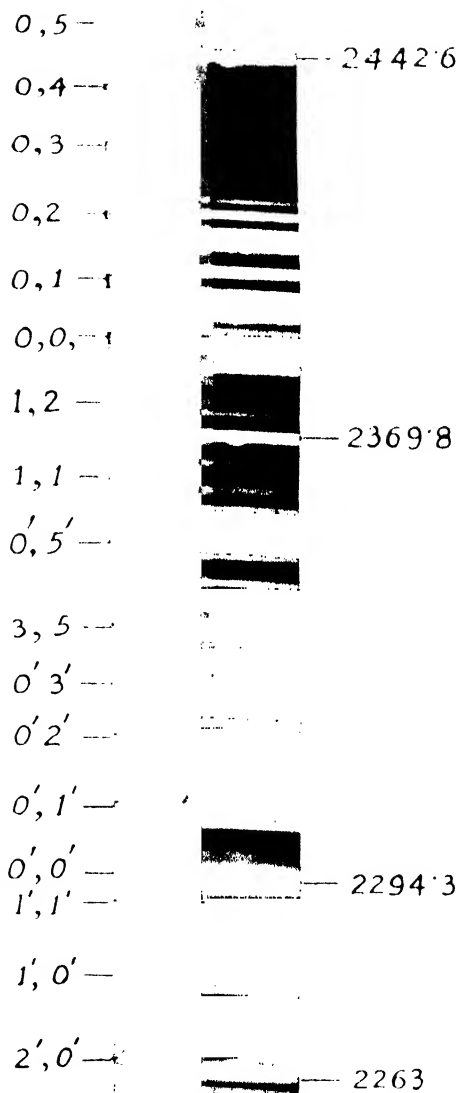


FIG. 1(b)
D and E Systems of BiBr
The bands of the E System are marked with a dash

band heads could be detected, even for the more refrangible systems using a medium quartz spectrograph, having a dispersion of 11 Å/mm. Possibly another reason for its non-appearance may be that a wide slit had to be used for photographing the bands in the extreme ultraviolet region because of the very poor intensity of the continuum in this region from the hydrogen discharge tube. If the slit width was narrowed down below a certain limit, it was observed that no continuum could be recorded on the plates. As a result the band heads were very diffuse, and possibly isotopic heads were lost in the general diffusiveness of the band heads. The increasing diffusiveness of the heads, however, as they move out from the system origin leads one to suspect that there are unresolved bands due to isotopic molecules (BiBr^{79} and BiBr^{81}). An isotopic separation could, however, be observed in the case of BiCl molecule by one of the authors. The three systems observed by the authors as well as the two observed by Morgan in the visible region appear to have the same ground state as can be judged by a comparison of the values of the ground state constants for the different systems observed by the authors, and those determined by Frank Morgan.

For the lower frequency system of BiBr^{79}

Morgan	Authors
	System <i>A</i> (lower frequency)
w_e'' 209.50	w_e'' 209.30
$w_e'' x_e''$ 0.466	$w_e'' x_e''$.40

For the higher frequency system of BiBr^{79}

	Authors
	Systems <i>D</i> and <i>E</i> (higher frequency)
w_e'' 209.17	209.20
$w_e'' x_e''$.469	.60

Besides the agreement of these constants, higher frequency system *B* of Morgan's bands in the visible region were always recorded on the plates, though as a very narrow absorption region (under the small dispersion of a medium quartz spectrograph) with a sharp edge at about λ 4040–45*, which is practically the same as the origin of the system reported by Morgan, thus confirming the assignment of the new systems obtained by the authors to BiBr molecule.

Morgan observed in both the band systems obtained by him in the visible region, a rapid convergence of the band heads. As the number of band heads in each of the systems is sufficiently large, it was possible to obtain the convergence limit at about λ 4520 Å, and to determine the dissociation energy D_0 . In the present case, the number of bands observed is very few, and the heads do not show any convergence at all, even to extrapolate and determine the limit. Thus it is not possible from the existing data to calculate the dissociation energy of the molecule.

Summing up the following schematic diagram Fig. 4 (not drawn to scale) gives an idea of the various electronic levels of the molecule obtained by the authors in relation to those observed by Morgan.

* Actual He d γ at ν 24738.6, i.e. λ 4041 Å. On closer examination of the Morgan's bands as recorded on the plates of the authors, it is easily possible to identify the fairly strong bands of the sequence $\Delta v = 0$, which lie on the shorter wavelength side of λ 4041, (0,0) band.

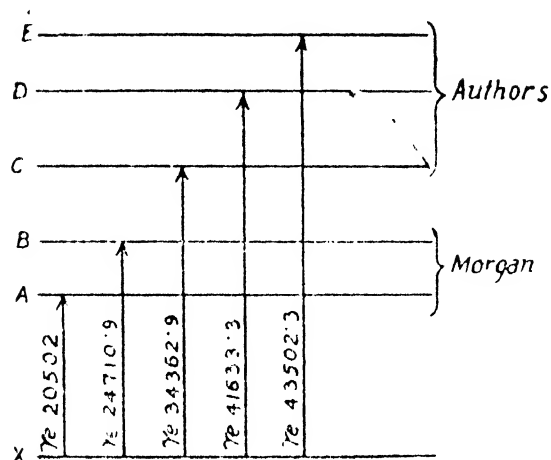


FIG. 4.

SUMMARY

Morgan observed two systems of bands in absorption for BiBr molecule in the visible regions with origins at 4045.7 Å and 4869.1 Å. The lower frequency system degrades to the red, but the direction in which the other system degrades is in doubt. In the present paper are reported three new systems observed in absorption in the ultraviolet regions $\lambda\lambda$ 2968-2709, $\lambda\lambda$ 2450-2336 and $\lambda\lambda$ 2350-2200 respectively. The bands are degraded to the violet in each case, and the band heads fit in the following formulas:

$$\text{System C, } \nu = 34362.9 + 503.8u' - 0.40u'^2 - 209.3u'' + 0.40u''^2$$

$$\text{System D, } \nu = 41633.3 + 652.5u' - 0.25u'^2 - 209.2u'' + 0.60u''^2$$

$$\text{System E, } \nu = 43502.33 + 319u' - 5.5u'^2 - 209.2u'' + 0.60u''^2$$

where $u = v + \frac{1}{2}$

Band heads due to the isotopic molecule BiBr⁸¹ were not recorded.

REFERENCES

- Howell, H. G. and Rochester, G. D. (1934). New Diatomic Band Spectra. *Durham, Phil. Soc. Proc.*, **9**, 196.
 Morgan, F. (1936). Band Spectra of BiBr, BiCl, BiF and BiI in absorption. *Phys. Rev.*, **49**, 41.
 Sur, P. K. (1950). A new band system of BiCl in absorption. *Proc. Nat. Acad. Sci.*, **19**, Part 1, 16.
 Sur, P. K. (1951). The Absorption Spectrum of Bismuth Sulphide. *Ind. Jour. Phys.*, **25**, 65.

Issued 28 April, 1954.

STUDY OF METAL FILM ON GLASS SURFACE

by B. K. BANERJEE, *I.C.I. Research Fellow, N.I.S.I., Indian Association for the Cultivation of Science, Jadarpur, Calcutta 32*

(Communicated by K. Banerjee, F.N.I.)

(Received September 9; read December 31, 1953)

INTRODUCTION

The problem of deposition of metal film at the glass surface has a great technical importance. The electrodeposition of metal on metal is known for a long time and in this case some interesting observations have been made such as lattice distortion, selective orientation, etc., of the deposited metal. Although glass is non-metal, yet numerous methods are known such as metal sputtering process, chemical reduction process, pyrolysis of organometallic compounds, etc., whereby an adherent metal film can be deposited at the glass surface. It is known that the surface structure of glass plays a leading rôle in the process of formation of metal film at the glass surface.

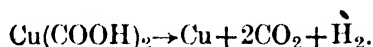
Recently a large amount of work has been done on the structure of glass surface. Weyl (1945, 1948), K. Nakanishi (1933), and a few other workers are responsible for a considerable advancement in that direction. It is quite evident from their works that the structure of glass surface is quite different from that of the bulk. As a matter of fact, by contact with liquids containing metallic cations the glass surface modifies its structure by ion-exchange of the Na ions of the glass surface with the metallic cations of the liquid. H. Devaux and H. Aubel (1927) demonstrated the validity of ion-exchange mechanism on the glass surface with the dilute CaSO_4 solution. Weyl and Williams (1945) made a successful application of ion-exchange process in the preparation of red Cu-glass. In the case of silvering of the glass by the chemical process ion-exchange mechanism is also a potent factor. It is worthwhile to mention here that the ion-exchange mechanism itself produces no colour change at the glass surface; the colour is due to the reduction of the metallic cations to the elemental state by the reducing agent already present in the glass and then the aggregation of metal to the crystal or colloidal size.

In view of the above facts it will be interesting to make an investigation of: (1) the change in the structure of glass undergone by keeping it in contact with the solution of noble metals, (2) the nature of the metal film deposited on the glass surface by the chemical reduction process as well as by the pyrolysis of the organometallic compounds and (3) the effect of temperature on the metal film deposited on the glass surface.

EXPERIMENTAL

Prior to the deposition of the metal film on the glass surface of high alkali content (17% Na_2O), glass specimen was thoroughly cleaned and then heated to about $500\text{--}550^\circ\text{C}$ for half an hour whereby the concentration of Na ions increases at the glass surface. In some cases the glass specimen was treated with a solution of SnCl_2 and due to that operation, some Na ions at the glass surface are exchanged for Sn^{4+} ions. After the above preliminary treatment of the glass specimens, metal films of Au, Cu and Ag were deposited on the surface in the following way.

Cu films were deposited on the glass surface by two distinct processes (1) pyrolysis of organometallic salt of Cu and (2) chemical reduction process. By rapidly heating copper formate in a thin test tube at about 150°–200°C, a bright mirror of Cu is deposited at the inner glass surface of the test tube due to the decomposition of copper formate in the following way:—



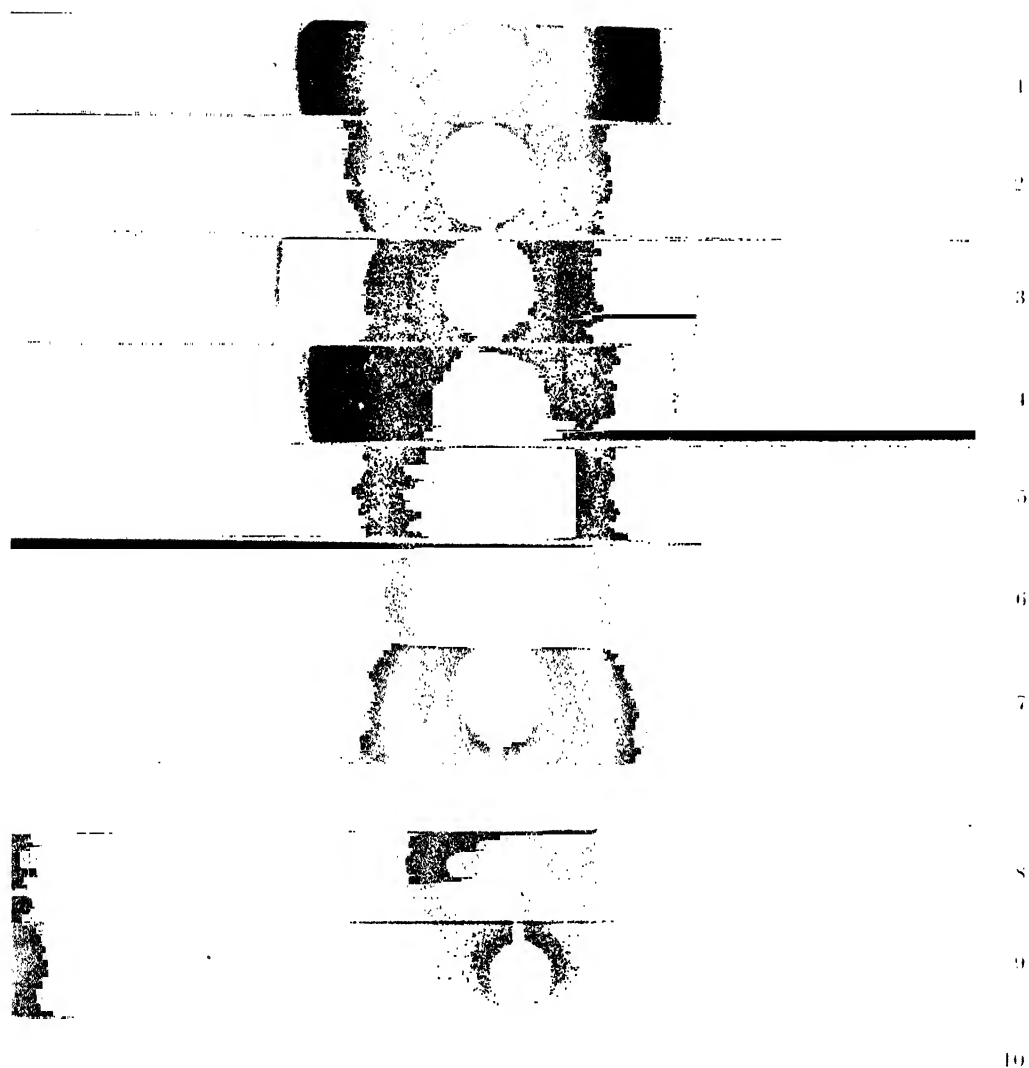
Similarly a film of Cu is also deposited at the glass surface by the reduction of alkaline cupric tartrate solution by formaldehyde solution. Silver is deposited at the glass surface from the ammoniacal silver nitrate solution by formaldehyde reduction process as well as by Brashear's process. Methods adopted for the film deposition of copper and silver are quite well known and the metal is usually supplied in the form of complex ions. In the case of gold, a slight departure was made from the usual process. A thin film of gold was deposited at the glass surface by keeping 7.5 per cent Auric chloride solution in contact with the glass surface for a long time. Similar result was obtained by keeping of 5 per cent AuCl_3 solution and 40 per cent formaldehyde solution in the volume ratio of 1 : 3 for a few days. In the case of gold, the above two processes are very slow. Platinum was deposited on the glass surface by Prof. Bottger's method (vide *The Scientific America Cyclopaedia for Formula*, Vol. I, p. 499).

The thickness of the metal film can be controlled by the manipulation of the experimental condition. Each process has its own limitation and within a certain range the thickness of the metal film can be varied. Generally the thickness of the film is of the order of colloidal dimension. In some cases the film is almost transparent or translucent in transmitted light. Again in some cases the thickness is such that it is almost opaque in transmitted light. But in every case there is a metallic reflexion in the reflected light.

Use has been made of X-ray diffraction method for the determination of the nature of the film as well as for the estimation of the size of the constituents of the metal film. The investigation is confined to the specimens of appreciable thickness, otherwise if the thickness of metal film is very small, no useful result is obtained from the X-ray diffraction study, although in those cases the electron diffraction study is quite helpful. The usual Hadding type of the X-ray apparatus has been used for that purpose and the tube was run at 60 KVP copper anti-cathode with 20 milliamperes tube current. The diffraction photographs of some representative specimens have been shown in Plate VIII. The X-ray pictures of those specimens reveal the presence of both band and lines. Band is due to the glass base and broad lines are due to the metal film. The data of spacing are given in the following table.

TABLE I

Gold			Silver		
Spacing	Intensity	Plane	Spacing	Intensity	Plane
2.35 Å	s	(111)	2.36 Å	s	(111)
2.03 Å	ms	(200)	2.04 Å	ms	(200)
1.439 Å	m	(220)	1.445 Å	m	(220)
1.227 Å	m	(311)	1.232 Å	ms	(311)
1.173 Å	mw	(222)	1.179 Å	mw	(222)
1.019 Å	w	(400)	1.022 Å	w	(400)



1. Silver (Brashear's process).
2. Cu (Alkaline Cupric tartrate process).
3. Cu (Pyrolysis process).
4. Gold (Formaldehyde process).
5. Platinum (Böttger's process).
6. Platinum (After heat-treatment).
7. Cu (After heat-treatment) (Camera radius 3.9 cm.).
8. Silver (Formaldehyde process).
9. Gold (AuCl_3 Solution process).
10. Gold (After heat-treatment) (Camera radius 2.975 cm.).

TABLE I - *contd.*

Copper			Platinum		
Spacing	Intensity	Plane	Spacing	Intensity	Plane
2.08 Å	s	(111)	2.25 Å	s	(111)
1.81 Å	ms	(200)	1.95 Å	ms	(200)
1.277 Å	m	(220)	1.382 Å	ms	(220)
1.089 Å	m	(311)	1.178 Å	m	(311)
1.043 Å	mw	(222)	1.128 Å	w	(222)
0.905 Å	w	(400)			

In each case the composition of the respective metal film consists of metal only with the exception of copper film deposited by the pyrolysis of copper formate where the presence of Cu_2O , denoted by the lines corresponding to the spacing in 3.00 Å (vw), 2.45 Å (mw), 2.12 Å (w), 1.51 Å (w), 1.283 Å (w), are found in the X-ray picture but the amount of Cu(ous) oxide is very very small. It is further observed that by making pyrolysis operation in vacuum, even that trace of Cu(ous) oxide formation can be avoided.

The size of the particle of the film has been determined by the half intensity width method from the following relation of Scherrer :—

$$\beta = \frac{K\lambda}{L \cos \theta} + \mathfrak{S}.$$

where β = the breadth of diffraction interference at points of half maximum intensity in radians.

λ = wavelength of X-rays.

θ = the angle of diffraction

L = the edge-length of the crystal considered as cubic.

\mathfrak{S} = the mutual breadth of the Debye-Scherrer line which is constant depending upon the particular apparatus, size and absorption of the specimen.

K = a constant, the value of which is 0.90. In the present case an apparent particle size has been determined by ignoring the broadening due to the instrumental factor \mathfrak{S} .

TABLE II

Description of the specimen				Apparent Particle size
Metal	Method of Film deposition			
Silver ..	Formaldehyde	35 Å
Silver ..	Brashear's process	44 Å
Gold ..	Formaldehyde and AuCl ₃ solution	40 Å
Gold ..	AuCl ₃ solution only	100 Å
Copper ..	Pyrolysis of Cu-formate	56 Å
Copper ..	Alkaline cupric tartrate formaldehyde reduction Process	120 Å
Platinum	Böttger's process	48 Å

The size of the particle has been given in Table II and the X-ray pictures of some representative specimens have been shown in Plate VIII.

THE EFFECT OF TEMPERATURE ON THE METAL FILM.

It is well known that the same metal film may show a variety of colours if its physical condition is altered. From that point of view it will be interesting to study the effect of heat treatment of those specimens studied in the present paper. Each specimen was kept at 700°C.–800°C. for 8 hours in a large access of air. The silver specimen turns yellow, copper specimen changes to green, platinum specimen turns slightly greyish and gold specimen turns pink. No doubt the metallic reflection of film also disappeared after heat-treatment. This change is evidently due to the diffusion of the metal either in the ionic state or the elemental state as the case may be, into the interior of the specimen. As a matter of fact the specimen which formerly revealed the presence of lines of moderate intensity in the X-ray diffraction picture, only shows very weak lines of the metal in the X-ray picture after heat-treatment. But in the case of Cu-film, after heat-treatment, the lines of α -cristobalite have been identified. The X-ray picture of that specimen has been shown in Plate VIII and the spacings of those lines are:— 4.04 Å, 3.13 Å, 2.85 Å, 2.48 Å, 2.11 Å. That is apparently due to devitrification of glassy matrix.

ABSTRACT

In the present communication, the nature of the adherent film of different metals such as gold, silver and copper deposited by chemical method as well as by the pyrolysis method, has been studied, and in that connection the size of the metal composing the film has been determined. Further the effect of temperature on the nature of the film has also been investigated. It has been found that the size of the particle composing the film is of colloidal dimension and with temperature treatment, the metallic reflection of the film diminishes considerably and ultimately a transparent glass is formed having a distinct colouration different from the original specimen. The vitreous characteristic of the specimen is retained in the case of Au and Ag after heat-treatment whereas in the case of copper, the partial devitrification of the glassy matrix takes place.

ACKNOWLEDGEMENTS

I am thankful to Prof. K. Banerjee for his keen interest and guidance throughout the progress of this work. Thanks are also due to Dr. A. Bose for his keen interest in the work. I am also thankful to the Council of National Institute of Sciences of India for the award of an I.C.I. Research Fellowship to me, and also to the authorities of the Indian Association for the Cultivation of Science for laboratory and other facilities.

REFERENCES

- Devaux, H. and Aubel, H. (1927). The adsorption of ions by glasses. *Compt. Rend.*, **184**, 601.
- Nakanishi, K. (1933). Effect of gases upon the properties of glass. *J. Soc. Chem. Ind. Japan*, **36**, 595 B, 672 B.
- Weyl, W. A. and Marboe, E. C. (1945). Chemical deposition of Copper mirrors on glass. *Glass Ind.*, **26**, 119, 136, 142, 149.
- Weyl, W. A. and Williams, H. S. (1945). Surface dealkalization of finished glassware. *Glass Industry*, **26**, 275, 290, 301, 324, 339, 341 and 344.
- Weyl, W. A. (1948). The effect of polarized heavy metal ions on the surface properties of glass. *J. Soc. Glass Tech.*, **32**, 247.

FORCE CONSTANTS FOR THE BF_3 MOLECULE

by V. SANTHAMMA, *Department of Physics, Andhra University, Waltair*

(Communicated by K. R. Rao, F.N.I.)

(Received September 18; read December 31, 1953)

INTRODUCTION

The method of normal co-ordinates (Wilson, 1939 and 1941) has been applied in the following calculations for the molecule BF_3 . Of the two plausible models—Pyramidal and Plane symmetrical—for BF_3 , the latter has been used in the present calculations as it has been confirmed both by electron diffraction experiments and measurements of dipole moments (Herzberg, 1945). In the plane symmetrical model BF_3 has three in-plane and one out-of-plane vibrations. The simple valence force field is inapplicable to account for the out-of-plane vibration unless a separate angle bending constant is introduced. In this paper, the stretching, bending and interaction force constants are calculated with the observed Raman and infra-red frequencies (Herzberg, 1945) of B^{11}F_3 . The correctness of these values is verified by utilising the set of force constants thus obtained to calculate the corresponding frequencies for the isotopic molecule B^{10}F_3 and comparing these with the observed values.

CALCULATIONS

The Plane symmetrical BF_3 molecule belongs to the point group D_{3h} . From the group characters, it is seen that this molecule has one non-degenerate type A_1' vibration, one non-degenerate type A_1'' vibration and two doubly degenerate type E_1' vibrations. Out of the above six modes, one is non-planar type A_1'' vibration, which is not considered in the present paper.

CONSTRUCTION OF THE SYMMETRY CO-ORDINATES

The internal co-ordinates from the structure of the molecule are $\Delta d_1, \Delta d_2, \Delta d_3$, the changes in the three B-F distances and $\Delta \alpha_1, \Delta \alpha_2, \Delta \alpha_3$, the changes in the inter-bond angles. (Fig. 1.) The symmetry co-ordinates for each species are constructed as linear* combinations of equivalent internal co-ordinates in such a manner that they satisfy orthogonality, normalisation and transformation† properties. In this case $\Delta d_1, \Delta d_2$ and Δd_3 form one set of internal co-ordinates, and $\Delta \alpha_1, \Delta \alpha_2$ and $\Delta \alpha_3$ form another set of internal co-ordinates. The set of symmetry co-ordinates thus formed is given below. For the type A_1' vibration,

$$R_1 = 3^{-\frac{1}{2}} (\Delta d_1 + \Delta d_2 + \Delta d_3) \quad \dots \quad \dots \quad \dots \quad (1)$$

$$R_2 = 3^{-\frac{1}{2}} (\Delta \alpha_1 + \Delta \alpha_2 + \Delta \alpha_3) = 0 \quad (\text{Redundant co-ordinate})$$

* Most general expression for the symmetry co-ordinate is $R_j = \sum_k U_{jk} r_k$ where r_k is the k -th internal co-ordinate and U_{jk} is the coefficient of k -th internal co-ordinate in j -th symmetry co-ordinate, the condition for normalisation and orthogonality being $\sum_k (U_{jk})^2 = 1$ and $\sum_k U_{jk} U_{lk} = 0$ respectively.

† Each symmetry co-ordinate should transform according to the characters of the vibration type concerned under all covering operations of the point group of the molecule.

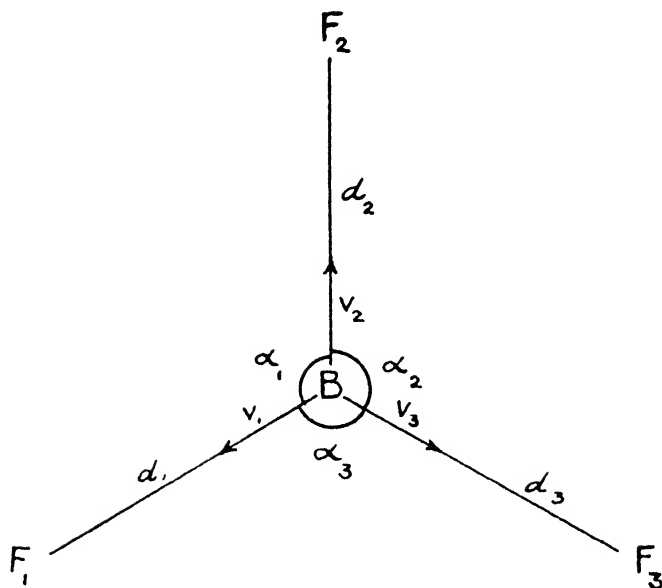


FIG. 1.

F_1 , F_2 , F_3 are the three fluorine atoms.

$\text{B}-\text{F}_1 = d_1$, $\text{B}-\text{F}_2 = d_2$, $\text{B}-\text{F}_3 = d_3$.

For the type E_1' vibration

$$R_{2a} = 6^{-\frac{1}{2}} (2\Delta d_1 - \Delta d_2 - \Delta d_3)$$

$$R_{2b} = 2^{-\frac{1}{2}} (\Delta d_2 - \Delta d_3)$$

$$R_{3a} = 6^{-\frac{1}{2}} (2\Delta \alpha_1 - \Delta \alpha_2 - \Delta \alpha_3)$$

$$R_{3b} = 2^{-\frac{1}{2}} (\Delta \alpha_2 - \Delta \alpha_3)$$

where the suffix a and b denote the degenerate vibrations. Since there are only five vibrational degrees of freedom, only five internal co-ordinates are necessary to define them. But from the structure of the molecule there are six internal co-ordinates. Instead of ignoring one of the internal co-ordinates, one symmetry co-ordinate is constructed in such a manner that it is identically zero. This is justified as this co-ordinate contributes nothing either to P.E. or to K.E. In this case $R_2 = 3^{-\frac{1}{2}} (\Delta \alpha_1 + \Delta \alpha_2 + \Delta \alpha_3)$ is considered to be the redundant co-ordinate, for the sum of the changes of all the angles in a plane around a point is zero.

TRANSFORMATION MATRICES

The transformation matrices which transform the internal co-ordinates of each type of vibrations are then determined. Transformation matrix U for the type A_1' vibration is

$$\begin{array}{c|cccccc} A_1' & \Delta d_1 & \Delta d_2 & \Delta d_3 & \Delta \alpha_1 & \Delta \alpha_2 & \Delta \alpha_3 \\ R_1 & (3^{-\frac{1}{2}} & 3^{-\frac{1}{2}} & 3^{-\frac{1}{2}} & 0 & 0 & 0) \end{array} \quad \dots \quad \dots \quad (2)$$

For the type E_1' vibration it is written in two ways. Considering the coefficients of the internal co-ordinates in R_{2a} and R_{3a} the U matrix is

$$\begin{pmatrix} 2 \times 6^{-\frac{1}{2}} & -6^{-\frac{1}{2}} & -6^{-\frac{1}{2}} & 0 & 0 & 0 \\ 0 & 0 & 0 & 2 \times 6^{-\frac{1}{2}} & -6^{-\frac{1}{2}} & -6^{-\frac{1}{2}} \end{pmatrix} \quad \dots \quad \dots \quad (3)$$

and considering the symmetry co-ordinates R_{2^1} and R_{3h} , the U matrix is

$$\begin{pmatrix} 0 & 2^{-1} & -2^{-1} & 0 & 0 & 0 \\ 0 & 0 & 0 & 0 & 2^{-1} & -2^{-1} \end{pmatrix} \dots \dots \quad (4)$$

The following table explains the transformations of the internal co-ordinates under all the covering operations of the group D_{3h} .

E	σ_h	(C_3^-, S_3^-)	(C_3^+, S_3^+)	(C_2^1, σ_v^1)	(C_2^2, σ_v^2)	(C_2^3, σ_v^3)
$\Delta d_1 \rightarrow \Delta d_1$	Δd_1	Δd_2	Δd_3	Δd_1	Δd_3	Δd_2
$\Delta d_2 \rightarrow \Delta d_2$	Δd_2	Δd_3	Δd_1	Δd_3	Δd_2	Δd_1
$\Delta d_3 \rightarrow \Delta d_3$	Δd_3	Δd_1	Δd_2	Δd_2	Δd_1	Δd_3
$\Delta \alpha_1 \rightarrow \Delta \alpha_1$	$\Delta \alpha_1$	$\Delta \alpha_2$	$\Delta \alpha_3$	$\Delta \alpha_1$	$\Delta \alpha_3$	$\Delta \alpha_2$
$\Delta \alpha_2 \rightarrow \Delta \alpha_2$	$\Delta \alpha_2$	$\Delta \alpha_3$	$\Delta \alpha_1$	$\Delta \alpha_3$	$\Delta \alpha_2$	$\Delta \alpha_1$
$\Delta \alpha_3 \rightarrow \Delta \alpha_3$	$\Delta \alpha_3$	$\Delta \alpha_1$	$\Delta \alpha_2$	$\Delta \alpha_2$	$\Delta \alpha_1$	$\Delta \alpha_3$

With the help of the transformation table and the coefficients of the internal co-ordinates, the transformation property of the symmetry co-ordinate is verified.

F MATRIX ASSOCIATED WITH THE POTENTIAL ENERGY OF THE MOLECULE

The general* quadratic potential energy in terms of valence type co-ordinates is assumed and is given by

$$\left. \begin{aligned} 2V = & f_d (\Delta d_1^2 + \Delta d_2^2 + \Delta d_3^2) + d^2 f_\alpha (\Delta \alpha_1^2 + \Delta \alpha_2^2 + \Delta \alpha_3^2) \\ & 2f_{dd} (\Delta d_1 \Delta d_2 + \Delta d_1 \Delta d_3 + \Delta d_2 \Delta d_3) \\ & 2df_{\alpha d} (\Delta \alpha_1 + \Delta \alpha_3) \Delta d_1 + (\Delta \alpha_1 + \Delta \alpha_2) \Delta d_2 + (\Delta \alpha_2 + \Delta \alpha_3) \Delta d_3 \\ & 2d^2 f_{\alpha\alpha} (\Delta \alpha_1 \Delta \alpha_2 + \Delta \alpha_2 \Delta \alpha_3 + \Delta \alpha_1 \Delta \alpha_3) \end{aligned} \right\} \dots \quad (5)$$

where f_d is the force constant associated with bond stretching, f_α that associated with bending and f_{dd} , $f_{\alpha d}$ and $f_{\alpha\alpha}$ are the constants representing the interactions between stretching and stretching, bending and stretching and bending and bending respectively and 'd' is the equilibrium length of B-F bond. In this P.E. function there are thus five force constants to be determined only by three frequencies. Hence the stretching force constant f_d is calculated from Badger's (Badger, 1935) rule. The remaining four are determined by the three frequencies, f_α and $f_{\alpha\alpha}$ having been obtained only as a difference ($f_\alpha - f_{\alpha\alpha}$).

* In case of valence force field, P.E. is given by $2V = \sum f_{ik} r_i r_k$ (Whittaker) where $f_{ik} = f_{ki}$ is the force constant associated with i and k which extend over all internal co-ordinates. In terms of the symmetry co-ordinates $2V = \sum F_j R_j R_j$, the relation between f and F being $F = U f U'$.

The f matrix associated with the potential energy function is

$$\begin{bmatrix} f_{\parallel} & f_{\parallel d} & f_{\parallel d} & df_{\gamma d} & 0 & df_{\gamma d} \\ f_{\gamma d} & f_{\gamma d} & f_{\gamma d} & df_{\gamma d} & df_{\gamma d} & 0 \\ f_{dd} & f_{dd} & f_{dd} & 0 & df_{\alpha d} & df_{\alpha d} \\ df_{\gamma d} & df_{\gamma d} & 0 & d^2f_{\gamma\gamma} & d^2f_{\gamma\gamma} & d^2f_{\gamma\gamma} \\ 0 & df_{\gamma d} & df_{\gamma d} & d^2f_{\gamma\gamma} & d^2f_{\gamma\gamma} & d^2f_{\gamma\gamma} \\ df_{\gamma d} & 0 & df_{\alpha d} & d^2f_{\gamma\gamma} & d^2f_{\gamma\gamma} & d^2f_{\gamma\gamma} \end{bmatrix} \dots \quad (6)$$

The matrix F for type A_1' vibration consists of only one element and that is given by

$$F_{11} = f_{\parallel} + 2f_{\parallel d} \quad \dots \quad \dots \quad \dots \quad (7)$$

and that of E_1' consists of four elements

$$\begin{bmatrix} F_{22} & F_{23} \\ F_{32} & F_{33} \end{bmatrix} = \begin{bmatrix} (f_{\gamma d} - f_{\parallel d}) & \frac{d}{2}f_{\gamma d} \\ \frac{d}{2}f_{\gamma d} & d^2(f_{\gamma\gamma} - f_{\gamma\gamma}) \end{bmatrix}$$

The elements will be the same whether the expression (3) and its transpose or (4) and its transpose matrices are used. In these calculations the latter matrices are used as they involve more vanishing elements and thus lessen the labour.

G MATRIX ASSOCIATED WITH THE KINETIC ENERGY OF THE MOLECULE

The elements of the kinetic energy matrix for the non-degenerate type A_1' vibration are obtained from the equation (9) and for degenerate type E_1' vibrations the equation (10) is used. It has been shown by Wilson that the K.E. can be expressed as a dot * product of two vectors and finally written in the form of a matrix. As there are three equivalent fluorine atoms it is enough if the vectors are obtained for any one of the atoms. The following is the set of the s_{ki} vectors used. (Cleveland, 1948.) Boron atom

$$\left. \begin{aligned} s_{d_1B} &= -V_1 & s_{x_1B} &= \sqrt{3} (V_1 + V_2)/d \\ s_{d_2B} &= -V_2 & s_{x_2B} &= \sqrt{3} \epsilon (V_2 + V_3) \\ s_{d_3B} &= -V_3 & s_{x_3B} &= \sqrt{3} \epsilon (V_1 + V_3) \end{aligned} \right\} \quad \dots \quad (8)$$

$$G_{ji} = \sum_p \mu_p g_p S_j^i \cdot S_i^j \text{ where } S_j^i = \sum_k U_{jk} s_{ki} \text{ and } \dots \dots \dots (9)$$

$$G_{ji} = 1/x \sum_p \mu_p g_p (S_j^i \cdot S_{ia}^i + S_{jb}^i \cdot S_{ib}^i + \dots) \dots \dots \dots (10)$$

where μ_p is reciprocal mass of the atom in p -th set of equivalent atoms g_p the number of equivalent atoms in p -th set and x is the degree of degeneracy. (Wilson.)

Fluorine atom

$$s_{d_1 F_1} = V_1$$

$$\alpha_{1 F_1} = \epsilon (-V_1/2 + V_3) \sqrt{3}/2, \quad \text{where } \epsilon = 1/d, \text{ } d \text{ is the B-F bond length.}$$

$$s_{\alpha_3 F_1} = \epsilon (-V_1/2 - V_3) \sqrt{3}/2$$

The rest are zero.

V_1 , V_2 and V_3 are the unit vectors directed along the bonds (shown in Fig. 1). In these calculations, $\alpha_1 = \alpha_2 = \alpha_3 = 120^\circ$ as obtained from the electron diffraction experiments. (Pauling, 1939 and 1941.)

From these s_{ki} vectors and the coefficients of the internal co-ordinates of the symmetry co-ordinates, the following S_j^i vectors can be easily obtained.

$$\left. \begin{aligned} S_1^B &= -(V_1 + V_2 + V_3) 3^{-1/2} & S_1^{F_1} &= V_1/\sqrt{3} \\ S_{2a}^B &= 1/\sqrt{6} (-2V_1 + V_2 + V_3) & S_{2a}^{F_1} &= 2V_1/\sqrt{6} \\ S_{2b}^B &= 1/\sqrt{2} (V_3 - V_2) & S_{2b}^{F_1} &= 2\epsilon/\sqrt{18} \left(V_3 - 2V_2 - \frac{V_1}{2} \right) \\ S_{3a}^B &= \epsilon/\sqrt{2} (V_1 + V_2 - 2V_3) & S_{3a}^{F_1} &= 2\epsilon/\sqrt{6} (V_1/2 + V_3) \\ S_{3b}^B &= \sqrt{3}/\sqrt{2} (V_2 - V_1) & & \end{aligned} \right\} \dots \quad (11)$$

The only element of G matrix for type A_1' vibration is

$$G_{11} = \mu_F \quad \dots \quad \dots \quad \dots \quad \dots \quad \dots \quad (12)$$

The four elements of G matrix for type E_1' vibrations are

$$\begin{bmatrix} G_{22} & G_{23} \\ G_{32} & G_{33} \end{bmatrix} = \begin{bmatrix} (3/2 \mu_B + \mu_F) & \frac{-3\sqrt{3}}{4} \mu_B \\ \frac{-3\sqrt{3}}{4} \mu_B & (9\mu_B + \frac{7}{2} \mu_F) \end{bmatrix}$$

where μ_F and μ_B are reciprocal masses of the Fluorine and Boron atoms respectively.

The secular equation for type A_1' vibration is given by

$$\lambda = F_{11} G_{11} \quad \dots \quad \dots \quad \dots \quad \dots \quad (13)$$

where $\lambda = 4\pi^2 \nu_1^2 c^2$, ν_1 being the frequency in cm^{-1} of type A_1' vibration. For the doubly degenerate vibrations the secular equation is

$$\lambda^2 - \lambda (F_{22} G_{22} + 2F_{23} G_{23} + F_{33} G_{33}) + |F| \cdot |G| = 0 \quad \dots \quad \dots \quad (14)$$

The force constants are calculated by solving the two secular equations (13) and (14) making use of the following data:—

$$\left. \begin{aligned} \nu_1 &= 888 \text{ cm}^{-1} \text{ type } A_1' \text{ vibration} \\ \nu_2 &= 1445.9 \text{ cm}^{-1} \\ \nu_3 &= 480.4 \text{ cm}^{-1} \end{aligned} \right\} \text{ type } E_1' \text{ vibrations} \quad \dots \quad \dots \quad (15)$$

$$\mu_B^{11} = 5.469 \times 10^{22} \text{ gm.}^{-1}$$

$$\mu_F = 3.169 \times 10^{22} \text{ gm.}^{-1}$$

$$\text{B-F bond length} = 1.302 \text{ \AA}$$

$$f_d = 7.099 \times 10^5 \text{ dynes/cm. (Badger's rule).}$$

At this stage the numerical values should be substituted.

From (13) $f_d + 2f_{dd} = 8.833 \times 10^5 \text{ dynes/cm.}$

Hence $f_{dd} = 0.867 \times 10^5 \text{ dynes/cm.}$

Substituting the two values for λ as obtained from the two frequencies 480.4 and 1445.9 in the equation (14) simultaneously, we obtain

$$30.156(f_x - f_{\alpha\alpha}) - 7.104 f_{xd} = 11.57 \times 10^5 \quad \dots \quad (16)$$

$$-73.08 f_{xd}'' + 1821.5 \times 10^5 (f_x - f_{\alpha\alpha}) = 608 \times 10^{10} \quad \dots \quad (17)$$

From (16) and (17) it is seen that

$$73.08 f_{xd}'' - 429.1 f_{xd} - 90.8 = 0 \quad \dots \quad (18)$$

Equation (18) leads to two sets of values which are given in the following table:—

	I Set	II Set
f_d	$7.099 \times 10^5 \text{ dynes/cm.}$ (Badger's rule)	
f_{dd}	$0.867 \times 10^5 \text{ dynes/cm.}$	
f_{xd}	-0.2052 „	6.077
$f_\alpha - f_{\alpha\alpha}$	0.3352 „	1.814

CALCULATIONS OF THE FREQUENCIES OF B^{10}F_3

The force constants of the first set are used in calculating the corresponding vibrational frequencies of the isotopic molecule B^{10}F_3 . The same formulae hold good for the isotopic molecule but with different numerical values for the elements of the K.E. matrix since the value of μ_B^{10} is different from that of μ_B^{11} . Further, the element of the K.E. matrix for type A_1' vibration is equal to μ_F and is thus seen to be dependent only on the mass of the Fluorine atom. Hence the corresponding frequency of the totally symmetric vibration of the isotopic molecule B^{10}F_3 is expected to be the same as that of B^{11}F_3 . In these calculations $\mu_{B^{10}} = 6.010 \times 10^{22} \text{ gm.}^{-1}$

The calculated and the observed frequencies are shown below:—

Calculated	Observed
888 cm.^{-1}	888 cm.^{-1}
1499 „	1497 „
497 „	482 „

The agreement is found satisfactory.

VERIFICATION OF THE PRODUCT RULE

Finally the product rule formulated by Redlich and Teller is verified. The rule states that the product of the frequencies of a certain molecule divided by the similar product for the same molecule with isotopic atoms is independent of the P.E. function and depends only on the masses and geometric situation of the case. Wilson expressed this in terms of the K.E. matrix elements and shows that

$$\frac{\Pi_{\lambda} \lambda}{\Pi_{\lambda} \lambda'} = \frac{|G|}{|G'|}$$

Where $\Pi_{\lambda} \lambda$ is the product of all λ 's of the same symmetry class as G .

The primes refer to isotopic molecule. (Glockler, 1943.)

For the type E'_1 vibration

$$\frac{\Pi_{\lambda} \lambda'}{\Pi_{\lambda} \lambda} = \frac{1497^2 \times 482^2}{1445.9^2 \times 480.4^2} = 1.08$$

$$\frac{|G'|}{|G|} = 1.12$$

ABSTRACT

Wilson's F-G matrix method has been applied to determine the force constants for the plane symmetrical molecule BF_3 . The set of the force constants thus obtained are used to determine the vibrational frequencies of the isotopic molecule B^{10}F_3 .

ACKNOWLEDGEMENT

The author wishes to acknowledge her deep indebtedness to Prof. K. R. Rao for his kind interest and guidance during the course of this work. She is indebted to the Government of India for the award of a senior research scholarship.

REFERENCES

- Badger, Richard M. (1935). Relation between the inter-nuclear distances and force constants of molecules and its application to Polyatomic molecules. *J. Chem. Phys.*, **3**, 710-714.
 Cleaveland, F. F. and Murray, M. J. (1948). Interpretation of the Spectra of molecules by use of group theory. *Research Publications of Illinois Institute of Technology*, **6**, 1-9.
 Cleaveland, F. F. Meister, A. G. and Murray, M. J. (1948). Calculation of Vibrational frequencies of polyatomic molecules. *Ibid.*, **6**, 10-24.
 Glockler, G. (1943) The Raman effect. *Review of Modern Physics*, **15**, 111 to 165.
 Herzberg, G. (1945). Infrared and Raman Spectra of polyatomic molecules, p. 299.
 Pauling, L. (1939 and 1941). The Nature of the Chemical Bond. Cornell University Press.
 Whittaker, E. T. (1927). Analytical Dynamics (Cambridge Ed. 2.), p. 178.
 Wilson, Jr., E. B. (1941). Some Mathematical methods for the study of Molecular Vibrations. *J. Chem. Phys.*, **9**, 76 to 84.
 Wilson, Jr., E. B. (1939). A method of obtaining the expanded Secular equation for the vibrational frequencies of a molecule. *Ibid.*, **7**, 1047 to 1052.

Issued May 3, 1954.

ATMOSPHERIC OSCILLATIONS AT HIGH ALTITUDES AND THEIR RELATION TO GEOMAGNETIC FIELD VARIATIONS

by R. PRATAP, *Geophysical Laboratory, Bengal Engineering College, Howrah.*

(Communicated by S. K. Chakrabarty, F.N.I.)

(Received November 30; read December 31, 1953)

The works of Laplace and Lamb have shown that in the atmosphere there exist tides just as in the ocean. Their effects are noticed in the diurnal pressure variations indicated by a barometer. It is known that the solar component of the variations is more pronounced than the lunar, their ratio being about 11 : 5. Lamb has indicated the general method of study of this oscillation taking into consideration its dependence on the temperature distribution. Taylor (1936) pursued the problem further with a model atmosphere and has shown that the atmosphere can have infinite modes of oscillation but the convective equilibrium reduces to a single one of 12 hour duration. Taylor has also shown that the atmosphere has definitely more than one free mode of oscillation and hence more than one free period. Pekeris (1937) has shown that two modes of vibration exist in our atmosphere with periods, one of 10.5 hours and the other of 12 hours. He has also shown that the semi-diurnal vibration has a nodal plane at about 30 kms. At this plane there is no motion of the atmosphere. On either side of this, the air swings in opposite directions and moreover at a height of 100 km, the amplitude is about 100 to 200 times that observed on the ground. These inferences agree well with the conclusions drawn from the Dynamo theory by Chapman (1919). Chapman has shown that for a correct interpretation of the S_q variations on the basis of the Dynamo theory, the semi-diurnal oscillations at the upper layers of the atmosphere must have an amplitude of about 200 times that observed on the ground and that it must be 180° out of phase with the observed barometric oscillations. A different method of obtaining knowledge about the upper atmosphere is based on the Radio data. Appleton and Weekes (1939) have suggested the presence of a lunar oscillation of about 0.93 km. amplitude and approximately in phase with the barometric tide at Greenwich. This result was in conflict with the previous inferences and different explanations have been put forward to account for this. The recent Rocket flights conducted by the United States Naval Research confirm most of the theoretical inferences given above. A lucid exposition of this problem has been given recently by Wilkes (1950). In the present paper an attempt has been made to obtain theoretically the nature of the atmospheric oscillation both in phase as well as in amplitude, at the ionospheric level which is supposed to be the seat of Dynamo current. We shall also discuss how critically the geomagnetic field variations depend on the nature of the atmospheric oscillations.

Recent records of different magnetic observatories distributed widely over the surface of the earth have shown that different anomalies can be explained fairly by the Dynamo theory. The major phenomena of the S_q variations can be explained by the variations resulting from the ring currents produced by the Dynamo effect in the upper atmosphere. The ionised air experiencing an irrotational translatory motion across the earth's magnetic field produces the Dynamo current. This in turn induces a varying magnetic field on the surface of the earth. It has

been shown in an earlier paper (Chakrabarty and Pratap, 1953) that the current function R satisfying the equation

$$a(\rho e)^2 \left[\frac{\partial}{\partial \phi} (v H_z) + \frac{\partial}{\partial \theta} u H_z \sin \theta \right] = (\rho e) \left[\frac{1}{\sin \theta} \frac{\partial^2 R}{\partial \phi^2} + \frac{\partial}{\partial \theta} \sin \theta \frac{\partial R}{\partial \theta} \right] \\ - \left[\frac{1}{\sin \theta} \frac{\partial R}{\partial \phi} \frac{\partial (\rho e)}{\partial \phi} + \sin \theta \frac{\partial R}{\partial \theta} \frac{\partial (\rho e)}{\partial \theta} \right] \quad \dots \quad \dots \quad (1)$$

where u and v are the velocity components of the conducting air, will have the form

$$R = \sum_{\sigma} \sum_{\tau} C K_{\sigma}^{\tau} \sum_n \sum_m p_n^m P_n^m \sin [m t - \alpha_m] \quad \dots \quad \dots \quad (2)$$

If we represent the velocity-potential of the atmospheric oscillation in a series of tesseral harmonics such as

$$\Psi = \sum_{\sigma} \sum_{\tau} K_{\sigma}^{\tau} P_{\sigma}^{\tau} \sin [\tau t - \alpha] \quad \dots \quad \dots \quad (3)$$

where K_{σ}^{τ} is a numerical constant (which has been included in (2) for convenience) and α the phase of the oscillation at the upper layers, then proceeding as in the previous paper (4) we have

$$\frac{1}{2\sigma+1} \sum_{s=-\infty}^{\infty} g_s \left[\sigma(\sigma+2)(\sigma-\tau+1) P_{\sigma+1}^{\tau} + (\sigma^2-1)(\sigma+\tau) P_{\sigma-1}^{\tau} \right] \sin [(\tau+s)t - \alpha] \\ = \sum_{s'=-\infty}^{\infty} \sum_n \sum_m p_n^m R_n^m(s') \sin [(m+s')t - \alpha_m] \quad \dots \quad (4)$$

We also assume for convenience that

$$\alpha \equiv \alpha_m \quad \dots \quad \dots \quad \dots \quad \dots \quad (5)$$

On determining p_n^m we can obtain the current-function (2). The method of solving (4) and obtaining p_n^m has been discussed in detail in (4) together with the residuals as well as the degree of approximation introduced thereby. A reference may be made to the same for the tables of p_n^m as well as the residuals. From the above current-function, the induced magnetic field may be calculated using Maxwell's relation.

$$W = -4\pi \frac{n+1}{2n+1} \left(\frac{a}{r} \right)^n R \quad \dots \quad \dots \quad \dots \quad (6)$$

where W is the total induced magnetic field. We have calculated the different magnetic components using the relations

$$\left. \begin{aligned} X &= -\frac{\partial W}{a \partial \theta} = \frac{4\pi}{a} \frac{n+1}{2n+1} \left(\frac{a}{r} \right)^n \frac{\partial R}{\partial \theta} \quad (\text{southward}) \\ Y &= -\frac{1}{a \sin \theta} \frac{\partial W}{\partial \phi} = \frac{4\pi}{a} \frac{n+1}{2n+1} \left(\frac{a}{r} \right)^n \frac{1}{\sin \theta} \frac{\partial R}{\partial \phi} \quad (\text{eastward}) \\ Z &= \frac{\partial W}{\partial r} = \frac{4\pi}{a} \frac{n(n+1)}{2n+1} \left(\frac{a}{r} \right)^{n+1} R \quad (\text{downward}) \end{aligned} \right\} \quad \dots \quad (7)$$

From X and Y the horizontal components of the variation field may be calculated using the relation

$$\Delta H = \Delta X \cos D + \Delta Y \sin D \quad \dots \quad (8)$$

where D is the declination.

The above results depend on the phase α of the atmospheric oscillation, which occurs in the expression for R . At the ground level the relation between the pressure variation and the velocity-potential is given by the simple relation

$$\frac{1}{V^2} \frac{\partial \psi}{\partial t} = - \frac{\delta p}{p} \quad \dots \quad (9)$$

where δp is the change in pressure and V the velocity of sound. If we extend the same relation to the upper atmosphere then the phase of the atmospheric oscillation has to be taken as 154° which is the phase of the barometric oscillations. Chapman has already suggested that this relation may not be true at greater heights. Recent works on the upper atmosphere also confirm this. We have thus examined a few possible values of α and have compared the results obtained with the results of observation.

The S_q variation in H was calculated for Alibag for different phases, viz. $\alpha = 0^\circ$, 154° , 215° , 275° and the results have been given in Fig. 1. It is observed that the

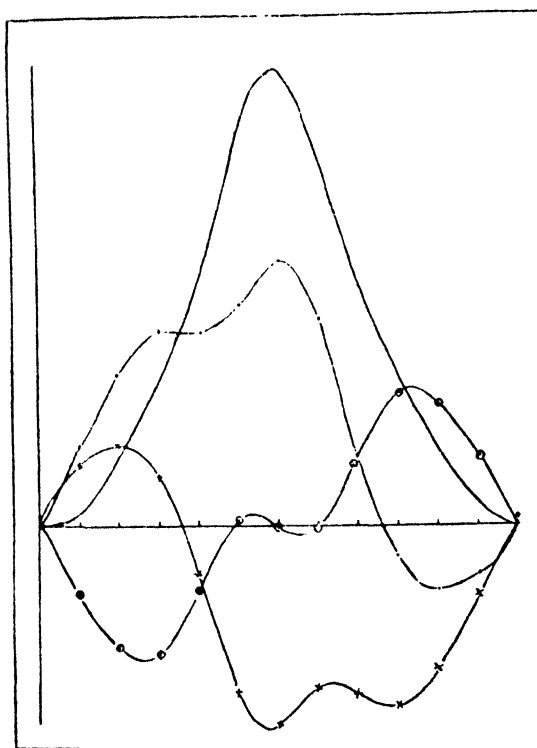


FIG. 1. ΔH variation for Alibag for different phases of the semidiurnal atmospheric oscillation

- phase $\alpha = 0^\circ$.
- ×— „ $\alpha = 154^\circ$.
- „ $\alpha = 215^\circ$.
- — „ $\alpha = 275^\circ$.

calculated curves depend very critically on the phase α . A comparison of these calculated curves with that obtained from the observational data published by Department of Terrestrial Magnetism of Carnegie Institution, Washington, shows that the curve obtained with $\alpha = 275^\circ$ gives the best fit. With this value of α we have also drawn the corresponding curves for some different observatories distributed all over the world. These curves also agree well with the results of observation. The S_q variations for Abhinger ($\phi = 51^\circ.2$, $\lambda = 359^\circ.6$), Alibag ($\phi = 18^\circ.6$, $\lambda = 72^\circ.9$), Huancayo ($\phi = -12^\circ.0$, $\lambda = 284^\circ.7$) and Watheroo ($\phi = -30^\circ.3$, $\lambda = 115^\circ.9$), were calculated with $\alpha = 275^\circ$ and the results are plotted in Fig. 2. The measure of agreement between the observed and the calculated

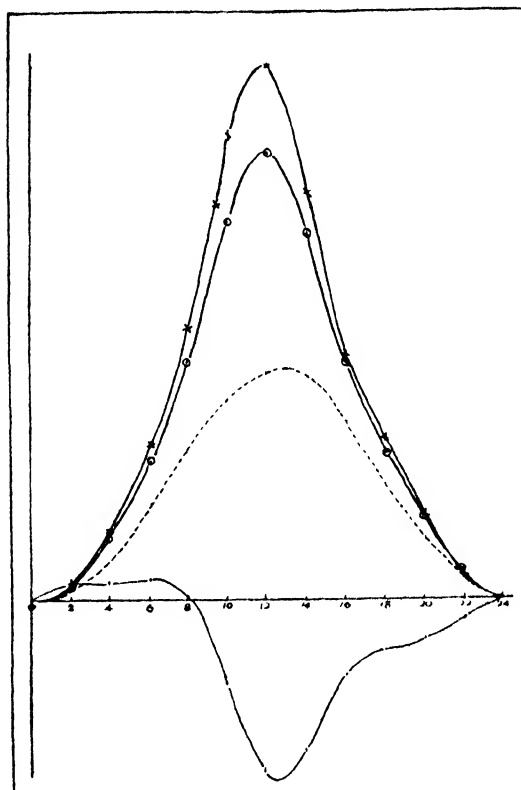


FIG. 2. ΔH variation for different stations with atmospheric oscillations having a phase $\alpha = 275^\circ$.

- • — Abhinger.
- ○ — Alibag.
- × — Huancayo.
- Watheroo.

curves suggests that the value of $\alpha = 275^\circ$ is a *very probable one*. It may be mentioned that the phase of the atmospheric oscillation supposed to be existing at a height of 100 km. as given by Chapman is 296° which agrees well with the phase taken by us in our calculations.

We have also plotted the ring currents in the usual way corresponding to the three different values of α , viz. 0° , 154° , 275° and they are shown in Figs. 3, 4 and 5. It may be observed that in the two former ones we find that besides the two

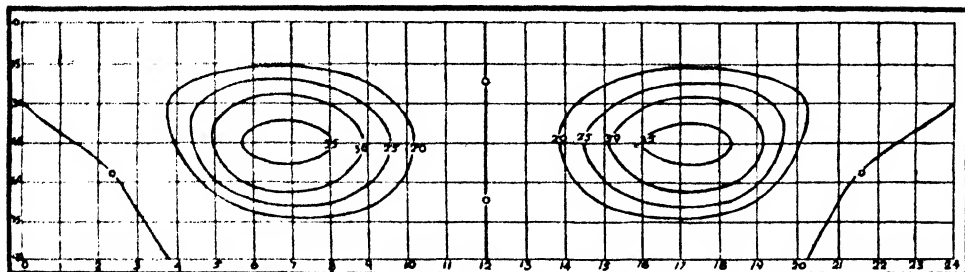


FIG. 3. Ring currents based on the present analysis with the atmospheric oscillation having a phase $\alpha = 0^\circ$ at a height of 100 km.

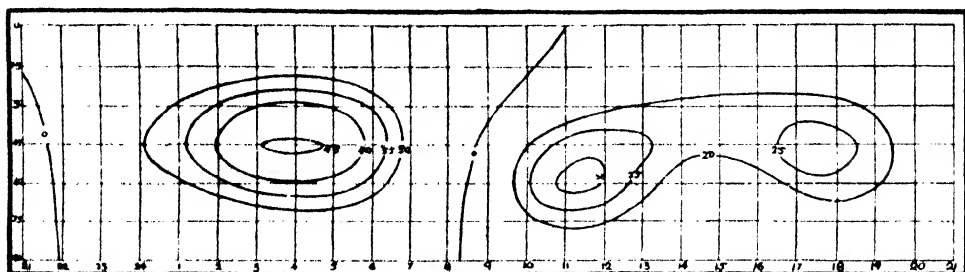


FIG. 4. Ring currents based on the present analysis with the atmospheric oscillation having a phase $\alpha = 154^\circ$ at a height of 100 km.

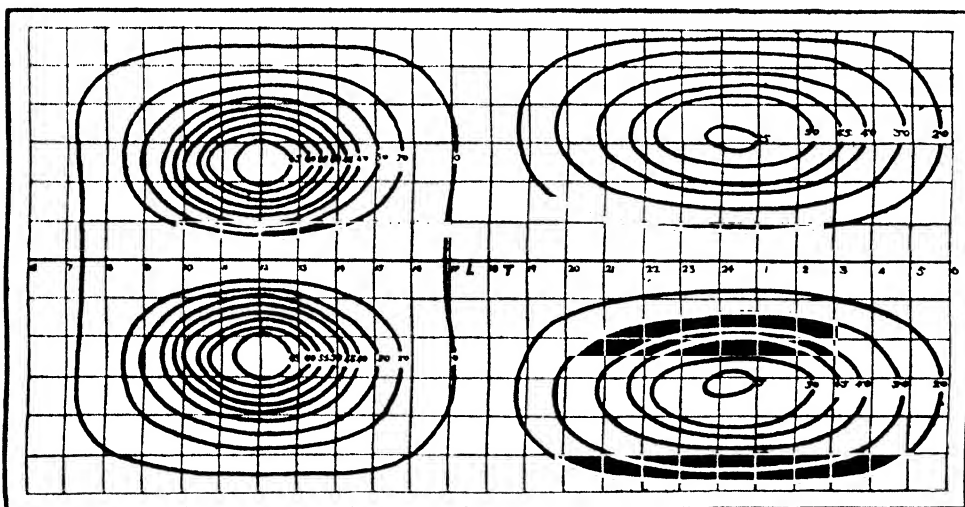


FIG. 5. Isometries showing the ring currents at a height of 100 kms. to account for the S_q variation. The semidiurnal atmospheric oscillation is assumed to have a phase $\alpha = 275^\circ$.

principal circuits there are subsidiary circuits too. But in the ring currents for a phase of 275° , we find only two principal circuits, existing in one hemisphere. It may be pointed out here that since we have assumed symmetry about the equator in our analysis the isometries in the southern hemisphere are just a reflection of the northern ones about the equator and are not given for the phase 0° and 154° . Moreover, there is an overall increase in intensity in the ring-currents when $\alpha = 275^\circ$.

This is evident from the density of lines. For purposes of comparison we have drawn the ring-currents (Fig. 6) based on Chapman's values of p_n'' and with the

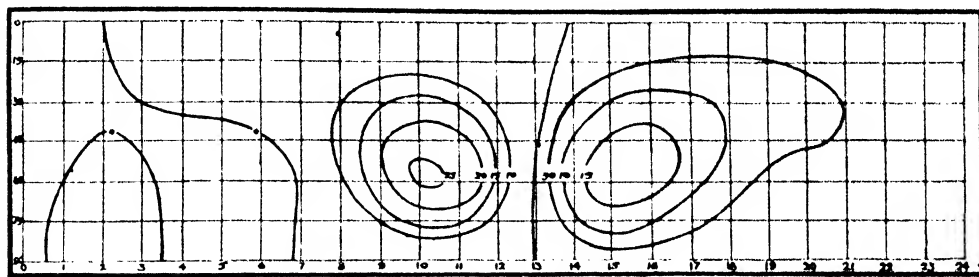


FIG. 6. Ring currents based on Chapman's analysis with the atmospheric oscillation having a phase $\alpha = 154^\circ$ at a height of 100 km.

phase of $\alpha = 154^\circ$. A comparison of these curves with the isometries constructed by Bartels (1928) from the analysis of the data from 21 observatories for the equinox epoch of the sun-spot minimum year 1902 shows a fair agreement between theory and observation. A better agreement is observed with the isometries given by Hasegawa based on his analysis for the sun-spot minimum years 1932-33. A comparison of the Figs. 5 and 6 will show the effect produced by the approximations introduced in the analysis of Chapman to which we have referred in our previous communication.

In the above calculations the undetermined constant $K_2^2 a_0$ may now be considered. Taking the S_q amplitude at Alibag to be 45.12γ (as obtained from D.T.M. publications normalised with the midnight value) a comparison with the calculated amplitude gives $K_2^2 a_0$ to be 1.962×10^3 . Taking the conductivity existing in the E layer (integrated) as 1.44×10^{-5} for the noon value we get the coefficient of the atmospheric oscillation K_2^2 as 7.766×10^8 . It may be remembered that Chapman has taken the value of K_2^2 as $32.4R \times 0.010$ where R is the radius of the earth. On substituting for R we get $K_2^2 = 2.063 \times 10^8$ as assumed by Chapman. In both these values the order agrees whereas the ratio of the numerical factors is about 3.8. It may be mentioned here that the observed H is the combined field due to the external and internal sources of variations. Chapman has given the ratio of the external to the internal contribution as 2.5 based on his analysis referred to above. Taking this into consideration we find that K_2^2 has got a value of 5.546×10^8 which agrees better with that assumed by Chapman. Further, the value of $a_0 K_2^2$, obtained above when multiplied with the isometric intensities gives the correct order of the current flowing in the upper atmosphere to produce the desired S_q variation as inferred by Bartels, Chapman, McNish and others.

SUMMARY

The dynamo equations developed in a previous paper have been used to calculate the S_q variations in H and V . Assuming different 'phases' for the atmospheric oscillations at the ionospheric layer which is possibly the seat of the 'Ring Currents', and comparing them with the observed magnetic field variations at different latitudes, it has been shown that a phase of 275° gives the best possible fit. Theoretical estimates of the S_q variations, based on the present analysis, have been obtained for different observatories, viz. Abhinger, Alibag, Huancayo and Watheroo. 'Ring Currents' have also been calculated with different phases, and that too

show that a phase of 275° for the atmospheric oscillation at a height of about 100 km. is the most probable one.

I am greatly indebted to Prof. S. K. Chakrabarty, for the constant interest he has taken during this work.

REFERENCES

- Appleton and Weekes (1939). On Lunar Tides in Upper Atmosphere. *Proc. Roy. Soc.*, **171**, 171-187.
Bartels, J. (1928). *Handbuch der Exptl. Physic.*, Bd. 25.
Chakrabarty, S. K. and Pratap, R. (1953). *Journal of Geoph. Research.* (In press.) (Referred as A in the text.)
Chapman, S. (1919). The Solar and Lunar diurnal variations of the Earth's magnetism. *Phil. Trans.*, (A) **218**, 1.
Pekeris, C. L. (1937). Atmospheric Oscillations, **158**, 650-671.
Taylor, G. I. (1936). The Oscillations of the Atmosphere. *Proc. Roy. Soc. (A)*, **156**, 318-325.
Wilkes, M. V. (1950). Oscillations of the Earth's Atmosphere. Cambridge Monographs in Physics.

Issued May 3, 1954.

ON THE WORKING OF SOME THEORIES OF VIBRATIONAL TRANSITION PROBABILITIES

by N. R. TAWDE,* *F.N.I.*, and B. B. LAUD,† *Spectroscopic Laboratories, Institute of
Science, Bombay*

(Received November 25 ; read December 31, 1953)

INTRODUCTION

The need for accurate knowledge of vibrational transition probabilities in electronic band spectra of diatomic molecules has been felt by many a worker in the field of Astrophysics and by those engaged in elaborating on fundamental concepts of mechanism causing the intensity of emitted radiation from diatomic oscillators. In view of the earlier findings of some authors that experimental results for the same system differed appreciably from one excitation condition to the other and that different theoretical procedures resulted in giving differing values, the problem of transition probabilities needs close scrutiny from both theoretical and experimental aspects. Under theoretical formulations, the relative efficacy of the methods can be judged only by studying them in comparison with carefully determined experimental data in a system or systems. The present investigation aims at testing the relative merits of a few among them, viz. (a) Hutchisson's method (1930) based upon relatively simpler concepts of harmonic oscillator, and (b) Gaydon and Pearse's method (1939), in order to see how far the latter fulfils the predictions about anharmonicity sought to be introduced by the process of distortion of harmonic wave-functions.

For the purposes of the above problems, Swan bands of C_2 molecule have been chosen for the following reasons: (i) Though the theoretical transition probabilities on this system by Hutchisson's method are available from computations given by some earlier workers, some of the results are found to differ from each other and hence fresh calculations were called for to examine the discrepancies; (ii) further, at the time this investigation was undertaken, the corrections for anharmonicity on this system in transition probability calculations were not available by any of the known methods and hence the use here of the method of numerical integration suggested by Gaydon and Pearse (1939); (iii) there is large accumulation of experimental data on this system which are either inconsistent among themselves or have not been utilised for the purpose of theoretical study. This led the present authors to attempt fresh experimental and theoretical study, which at the same time was directed towards the problems of combustion phenomena in another independent scheme of investigations.

THEORETICAL COMPUTATIONS

(a) *Hutchisson's method.*

The transition probabilities being dependent upon the square of the overlap integral $\int \psi_v \psi_v' dr$, Hutchisson (1930) has, on assumptions of linear oscillations, developed an expression for it in terms of ν_0 , the vibrational frequency; Δr the

* Now Head of the Department of Physics, Karnatak University, Dharwar.

† Now Lecturer in the Department of Physics, University of Poona, Poona 7.

difference in the internuclear distance in the two states and μ the reduced mass of the molecule. With the following constants of vibrational frequencies adopted from latest work of Philips (1948).

$$\nu_0' = 1788.22 \text{ cm.}^{-1}$$

$$\nu_0'' = 1641.35 \text{ cm.}^{-1}$$

and $\Delta r = 0.046$ A.U. close to the value 0.0457 of the same author, the vibrational transition probabilities for some bands of C_2 (Swan) system were calculated by the use of Hutchisson's intensity integral. These values are given below along with the earlier available results. The values of Wurm (1932) are not included as they have been already shown in serious error by McKellar and Buscombe (1948).

TABLE I

Band	Computed transition probabilities from Hutchisson's expression.		
	Tawde and Patel (1950)	McKellar and Buscombe (as corrected) by McKellar and Tawde 1951)	Present Authors
0,0	0.72 ₆	0.71	0.73
0,1	0.24	0.25	0.24
0,2	0.03	0.03	0.03
1,0	0.22 ₅	0.23	0.23
1,1	0.33 ₇	0.31	0.33
1,2	0.36	0.36 ₇	0.36
1,3	0.07 ₆	0.08 ₇	0.08
2,0	0.04 ₅	0.04 ₈	0.04
2,1	0.30	0.30 ₆	0.30
2,2	0.12	0.10	0.12
2,3	0.39	0.39	0.39
2,4	0.13 ₇	0.14 ₇	0.14

It will be seen that all the above computations are close to each other, the disparities being attributable to small differences in constants used.

(b) Method of numerical integration

Owing to many practical difficulties in the evaluation of overlap integral for anharmonic oscillations by analytical methods, involving the use of more complicated mathematical expressions, such as, the one given later by Hutchisson (1931), Gaydon and Pearse (1939) suggested the method of numerical integration in which wave-functions corresponding to the harmonic oscillator are distorted to fit the Morse expression. By this method overlap integrals have been calculated and converted to squares in order to arrive at numbers proportional to transition probabilities. They have been entered in Table 2. As these calculations were completed and incorporated in a thesis, similar independent study of C_2 Swan bands by this method was reported by Pillow (1951). This enabled us to check the correctness of our procedures and at the same time our results appeared to be complementary to that work from the point of view of more comprehensive and consistent

experimental data included in them for comparative aspects of theoretical study, especially of the procedures outlined by Pillow (1951).

EXPERIMENTAL DERIVATIONS

The theoretical results are examined against the background of experimental data available from 4 independent observers: (a) present authors' study of C_2 (Swan) bands in 4 types of ethyl-alcohol flames, (Laud, 1951) forming a part of systematic spectroscopic study of combustion in flames under communication elsewhere; (b) Tawde and Patel's study (1937) in 5 types of oxy-coal gas flames; (c) Patel's (1947) results in 4 different flames and (d) King's (1948) intensity study of Swan bands in furnace. These experimental results are given side by side with all theoretical computations including those of Pillow (1951, 1953) from her original and improved methods in Table 2.

DISCUSSION

It will be seen first of all that our own computed values (column 3 above) from the unmodified distortion process nearly agree with Pillow's values (column 4) except in 3 bands. The few deviations seen are likely to be slips in calculations or may be due to the smaller or larger magnitudes of dr intervals in the numerical integration or both. In general, the two independent calculations by the same integration procedure appear to be quite in keeping with each other and thus the two sets of values can be taken to be quite representative of the method.

The analytical and numerical methods reveal quite a large departure in the resulting values, which cannot be said to be even approximately close. The question therefore is, which of the two sets of theoretical values can be taken as standard for the purposes of experimental verification.

Since the method of numerical integration attempts to take anharmonicity into account by distorting the wave-functions of harmonic oscillator to fit the Morse expression, one should expect fair agreement between the two theories for values of lower quanta. However, this is not the case, and we have therefore to examine the relative efficacy of each of these theories independently by reference to experimental values.

It is rather surprising to note that in spite of the approximate nature of Hutchisson's theory (1930), i.e. its limitations to harmonicity, the weight of agreement is more in favour of it than the method of numerical integration. Further, the general manner of approach of the two theories to experimental results is in contrast with each other, for in a good number of bands, the results of one theory are lower, and of the other, higher than the experimental values.

Whatever has been found as small disagreement with Hutchisson's theory, appears to be systematic, inasmuch as, the experimental values of bands on $r_{\max} \rightarrow r_{\max}$ side, are higher than the theoretical ones and reverse is the case for bands on $r_{\min} \rightarrow r_{\min}$ side. If, therefore, any modification is to be made in Hutchisson's theory to bring it in accord with experimental values, it must be to correct for the above dispersions in the right directions and by right magnitudes. Such corrections are possible to be introduced in the theoretical values by using experimentally justified Morse potential energy function. This is equivalent to introduction of anharmonicity which is not inherent in the basic assumptions of Hutchisson's theory.

The method of numerical integration is supposed to take anharmonicity into account through the process of distortion of Hermitian polynomials to fit the Morse expression. But it appears from the great disparity in results shown by the method that anharmonicity sought to be introduced by it, is not only not effective, but it widens the gulf further between the theory and experiment. There is, no doubt, a tendency in the method to shift the results in the right direction, but the magnitude

TABLE 2

Band	THEORETICAL				EXPERIMENTAL				
	Analytical method of Hutchisson: (authors' computa- tions)	Numerical Integration			Present authors' mean of 4 sets	Tawde and Patel's mean of 5 sets (1937)	Patel's mean of 4 sets (1947)	King's data	
		Authors' computa- tions: (old distortion process)	Pillow's earlier distortion process (1951)	Pillow's improved distortion process (1951)	Pillow's new method (1953)			as calculated by authors.	as calculated by Pillow (1951).
0,0	0.73	0.84	0.83	0.77	0.73	0.69	0.54	0.78	0.67
0,1	0.24	0.13	0.15	0.20	0.22 ₆	0.24	0.32	0.19	0.16
0,2	0.03	0.03	0.02	0.05	0.04	0.07	0.13	0.03	0.03
1,0	0.23	0.39	0.38	0.23	0.23 ₆	0.26	0.35	0.24	0.24
1,1	0.33	0.40	0.40	0.38	0.37 ₆	0.33	0.23	0.35	0.35
1,2	0.36	0.15	0.21	0.28	0.29	0.30	0.26	0.33	0.36 (0.31)
1,3	0.08	0.06	0.04	0.11	0.09 ₇	0.11	0.15	0.08	0.08.
2,0	0.04	0.04	0.07	0.02	0.02 ₇	0.03	0.05	0.03	0.03
2,1	0.30	0.55	0.55	0.38	0.36	0.38	0.35	0.35	0.35
2,2	0.12	0.19	0.23	0.18	0.17 ₆	0.14	0.12	0.17	0.26 (0.17)
2,3	0.39	0.14	0.24	0.25	0.28	0.32	0.23	0.33	0.33
2,4	0.14	0.08	0.08	0.18	0.15	0.13	0.26	0.12	0.13

N.B.—The figures in *italics* in the last column, as now ascertained from Pillow in a private communication, are wrong figures overlooked in proof-checking. The corrected numbers are shown in parenthesis.

of the shift appears to be too much exaggerated, so much so, that it goes beyond the required limit. It is, therefore, thought that the various approximations involved in the distortion process, departure from normalization, etc., are responsible for the large shift, much in excess of what is required to obtain the proper wave-functions, for satisfying anharmonicity.

After the above views were advanced in a thesis by one of the authors (B.B.L.), Pillow's paper (1951) mentioned above appeared, giving a refined process of distortion of harmonic wave-functions, including the corrections for normalization, thus justifying the improvements earlier visualised by (B.B.L.).

Pillow's method of distortion tested by her in the case of C_2 , gives a much closer approach of the theoretical values to experiment and as such it is considered to be a great improvement over the older distortion method. Her values are recorded in column 6 of Table 2.

Pillow tested the performance of the new distortion process by the C_2 (Swan) band computations on it, with one set of experimental results of King (1948) and mean of 5 sets of results of Johnson and Tawde (1932). It may be pointed out that even though the closeness between the results of theory and experiment is good, the major portion of experimental material, i.e., five sets of values of Johnson and Tawde used for comparison by Pillow, have their limitations, because of the diverse conditions of excitation of bands (mild flame excitation to violent spark condition), giving appreciable departures between the different sets. Under these circumstances, the comparison with Johnson and Tawde's mean set of values is not quite justified and if these results are left out of consideration, it cannot be adequate too. On the other hand, the data of experimental observations relied upon for comparative study here, is the mean of 4 sets of reasonably consistent values, resulting from slightly varying conditions of steady flame sources under controlled parameters, which were examined and found in effective temperature equilibrium of vibrational energy. With the authors' results on ethyl-alcohol flames, the data of King (1948) on furnace spectrum, Tawde and Patel's (1937) values on oxy-coal gas flames and Patel's (1947) values on different flames, the performance of Pillow's improved method of distortion, emerges much more satisfactory, than made out earlier by her with the help of experimental material having limitations indicated above.

The way in which the data of King has been used by Pillow to derive the experimental transition probabilities needs some criticism. The values given by King are proportional to transition probabilities and Pillow has explained to us in a private communication that in order to convert these to a scale resulting in her case as 0.67 for the (0, 0) band (column 11), she divided each value by 1.5, which is probably a rough average, according to her, of the sums of v'' -progressions. On this basis, two of the values in her set should have been 0.31 for (1, 2) band and 0.17 for (2, 2) band, instead of 0.36 and 0.26 respectively. These, in fact, as now ascertained from Pillow, are errors overlooked in proof-checking.

Leaving apart the question of small slips mentioned above, the choice of value 1.5 for conversion appears to be arbitrary. (a) It violates the requirement that

$$\sum_{v''} \left[\int \psi_{v'} \psi_{v''} dr \right]^2 = 1,$$

assuming electronic transition moment to be constant; and (b) it ignores the question of distribution of population at various levels. The right procedure should, in our opinion, be to divide each value in a v'' -progression by the sum of the progression. Pillow also seems inclined to favour it as expressed in her latest communication to us. Values thus calculated are given in Table 2. It may be noted that the calculational procedure as adopted by us, brings the experimental transition probabilities of King (column 10) much nearer to Pillow's theoretical

values (column 5), than were her own figures of transition probabilities from King's values (column 11).

Very recently Pillow (1953) has given a fresh set of values of transition probabilities of C_2 (Swan) bands, calculated as per method mentioned by her in the earlier paper (Pillow, 1951). These are included under column 6 of Table 2. It can be seen that they are, in still better agreement, with experimental values, particularly with those of King and of the present authors.

ACKNOWLEDGEMENTS

We have utilized in this paper some results on the problems worked out by us in the scheme 'Mechanism of Explosions' financed by the Council of Scientific and Industrial Research, New Delhi. We are extremely indebted to the Council for according the permission to use them.

ABSTRACT

Attempt has been made to test the relative merits of two theoretical methods of calculating transition probabilities, viz. (i) Hutchisson's method and (ii) Gaydon and Pearse's method of numerical integration. Transition probabilities C_2 (Swan) bands have been calculated by these methods and these have been studied in comparison with the carefully determined experimental data. It has been observed that in spite of the approximate nature of Hutchisson's theory, the weight of agreement is more in favour of it than the method of numerical integration. The disagreement with the latter method is attributable to the various approximations involved in the distortion process, departure from normalization, etc. The new method suggested by Pillow takes these factors into account and values calculated by this method agree with the experimental values of the present authors as well as some earlier observations on flames, thus justifying the improvements previously visualised by the authors.

REFERENCES

- Gaydon, A. G. and Pearse, R. W. B. (1939). The spectrum of rubidium hydride. II. *Proc. Roy. Soc.*, **173**, 37.
- Hutchisson, E. (1930). Band spectra intensities for symmetrical diatomic molecules. I. *Phys. Rev.*, **36**, 410.
- Hutchisson, E. (1931). Band spectra intensities for symmetrical diatomic molecules. II. *Phys. Rev.*, **37**, 45.
- Johnson, R. C. and Tawde, N. R. (1932). Intensity distribution in molecular spectra: The Swan system (C_2). *Proc. Roy. Soc.*, **137A**, 575.
- King, A. S. (1948). Relative transition probabilities of the Swan bands of carbon. *Astr. Phys. Jour.*, **108**, 429.
- Laud, B. B. (1951). Ph.D. Thesis, Bomb. Univ.
- McKellar, A. and Buscombe, W. (1948). Intensities of molecular bands in the spectra of three early R-type stars. *Pub. Dom. Obs. Vict. B.C.*, **7**, No. 24, 361.
- McKellar, A. and Tawde, N. R. (1951). Calculated Transition Probabilities for the C_2 Swan bands. *Astr. Phys. Jour.*, **113**, 440.
- Patel, J. M. (1947). Ph.D. Thesis, Bomb. Univ.
- Philips, J. G. (1948). An extension of the Swan system of the C_2 molecule. *Astr. Phys. Jour.*, **108**, 434.
- Pillow, M. E. (1951). Transition Probabilities in Band-systems of Diatomic molecules: A Modified Distortion Process for the Wave-functions. *Proc. Phys. Soc. A.*, **64**, 772.
- Pillow, M. E. (1953). Application of calculated band intensities to the examination of observed spectra. *Mémoires in-8° de la Société Royale des Sciences de Liège Quatrième Série*, Tome **XIII**, 145.
- Tawde, N. R. and Patel, J. M. (1937). The study of the Oxy-coal gas flame by band spectra. *Bomb. Univ. Jour.*, **VI**, Part II, 29.
- Tawde, N. R. and Patel, J. M. (1950). On the transition probabilities of C_2 Swan bands. *Astr. Phys. Jour.*, **112**, 210.
- Wurm, K. (1932). Intensity of C_2 and CN bands in spectra of R and N-type stars. *Zeits. f. Astro Physik.*, **5**, 280.

IS SALT IN SAMBHAR LAKE WIND-BORNE FROM THE RANN OF CUTCH AND THE ARABIAN SEA ?

by S. K. PRAMANIK, *F.N.I., Deputy Director-General of Observatories*, and
K. P. RAMAKRISHNAN, *Meteorologist, Poona 5*

(Received December 8 ; read December 31, 1953)

The problem of salt in inland lakes has engaged the attention of many workers on the subject. The origin of salt in the lakes of Rajasthan have been attributed to the drying up of an inland sea, salt springs in the crystalline rocks, and to the products of weathering of the rocks and the bringing in of the salts by surface drainage to the lakes with little or no overflow. Holland and Christie (1913) considered these explanations and postulated a new theory about 40 years ago. According to this theory, the salt is brought by strong winds during the hot weather from the evaporation of sea spray from the Arabian Sea coast, and from the dry salt deposits in the Rann of Cutch to Rajasthan in general, and mainly from the Rann of Cutch to Sambhar Lake in particular. The southwesterly winds which blow during the period carry a large amount of sand and salt particles which is dropped when the velocity of winds decreases at night, and once dropped the force of wind is not enough to lift up the particles except near the coast whence they may be picked up again and retransported till the wind drops during the next night. The theory has been more or less generally accepted. In the Symposium on Rajasthan Desert in March 1952, Godbole (1952), however, objected to the theory of Holland and Christie and has since put forward the theory that the salt in Sambhar 'is the result of chemical action among residual solutions during the post-transgressional phase of the great Tethys (sea) at the end of the Tertiary age and the period following it'. During the discussion that followed Godbole's paper in the Symposium, it became clear that a detailed examination of surface and upper winds was necessary with a view to decide whether the salt in Sambhar Lake could have been borne by wind from the Rann of Cutch. Such an examination of wind data has been made in this note.

2. It should be mentioned that we have no information about the strength of the winds and the character of wind circulation more than three-fourths of a century ago, but in this note we are assuming that the wind strength and pattern were more or less the same as they have been during the last 30 years.

3. The mean winds at the surface and at levels of 0.3, 1.0 and 2.0 km. in the morning and evening in the months of April to August, and in the morning only in October and January are given in Figs. 1-12. In these figures, the wind arrow ending at the station shows the direction from which wind blows and each feather (______) represents a mean speed of 10 knots or nearly 11 m.p.h., and each half feather (______) represents a speed of 5 knots or 5.5 m.p.h. When speed is less than 3 knots, only direction is shown by an arrow without any feather. Thus, in the chart for surface in Fig. 1, wind at Karachi is blowing from WSW with a speed of 5 kts.; at Jodhpur, direction is WSW, but the speed is less than 3 knots. In the chart for 0.3 km., wind at Ahmedabad is from NW and has a speed of 15 knots.

4. In these charts, *S* is the position of Sambhar Lake and *C* is the point of the Rann of Cutch nearest to Sambhar. To examine the question of transport of salt by wind, let us start with the wind at surface at *C* (April-morning, Fig. 1), and draw the trajectory of air movement, a line drawn following at each point the wind obtaining there, showing the direction in which salt from *C* would

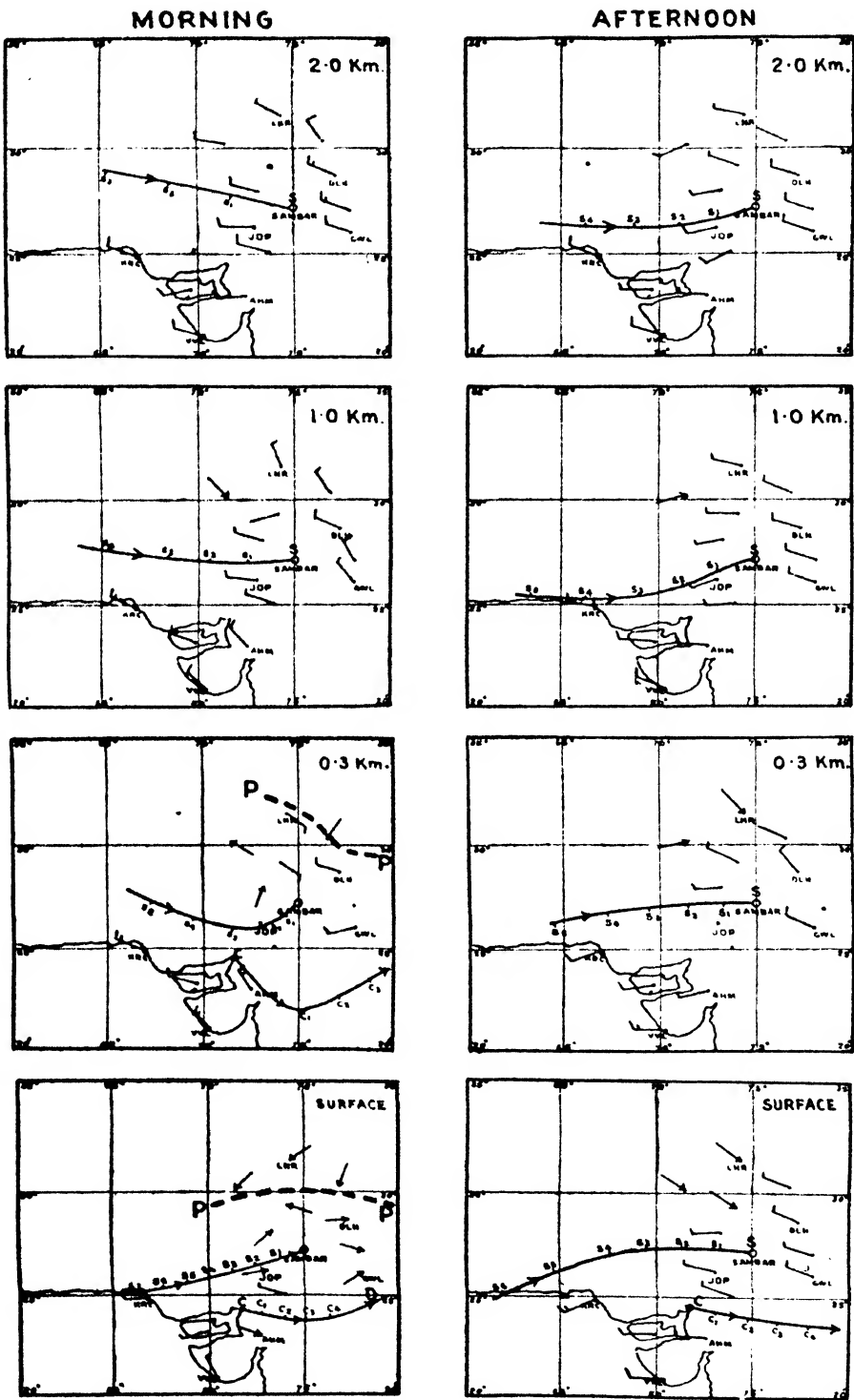


FIG.1.

FIG.2.

MEAN WINDS IN APRIL.

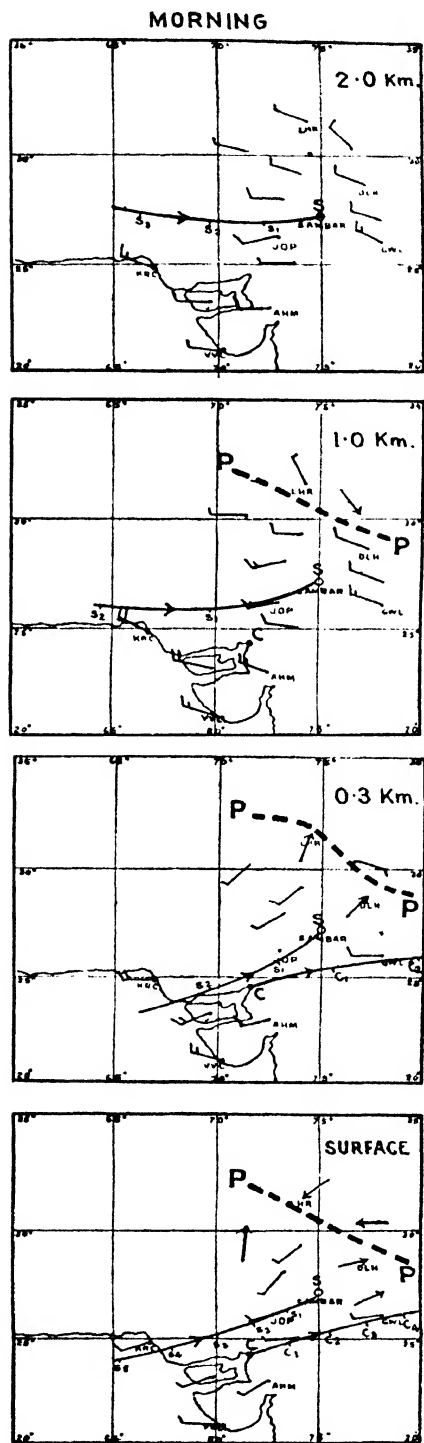


FIG.3.

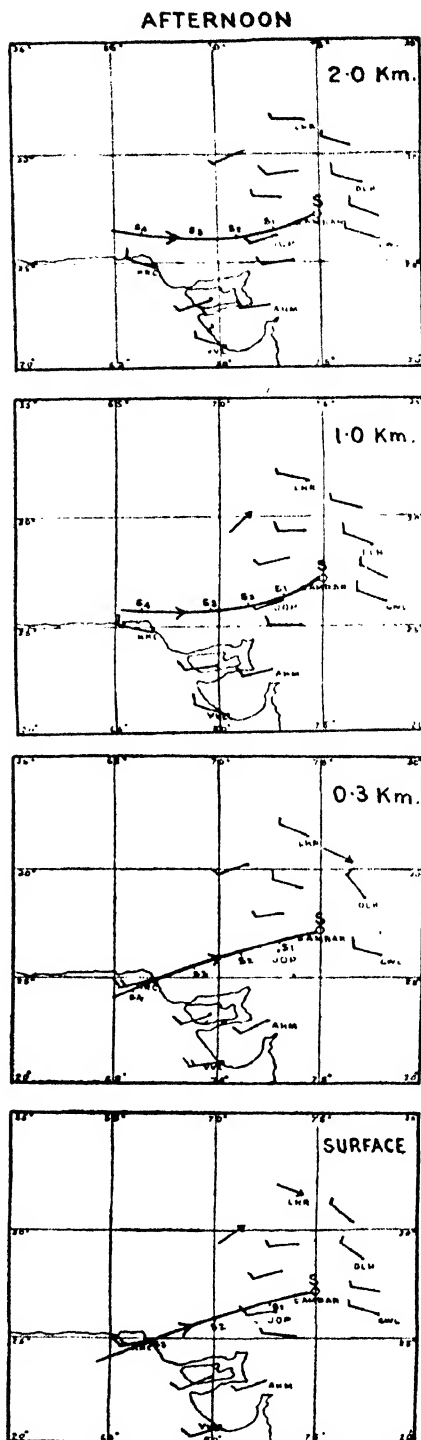
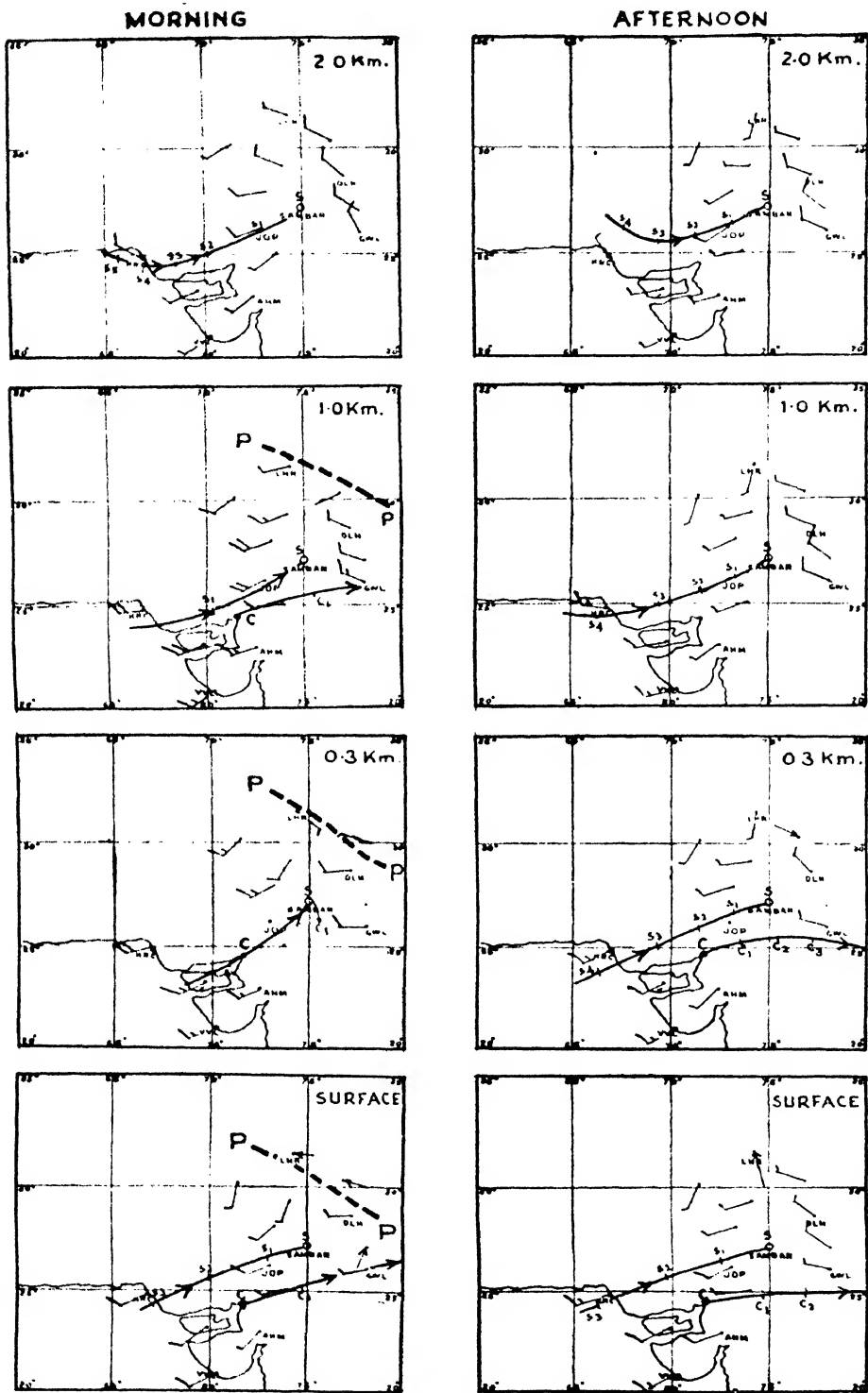
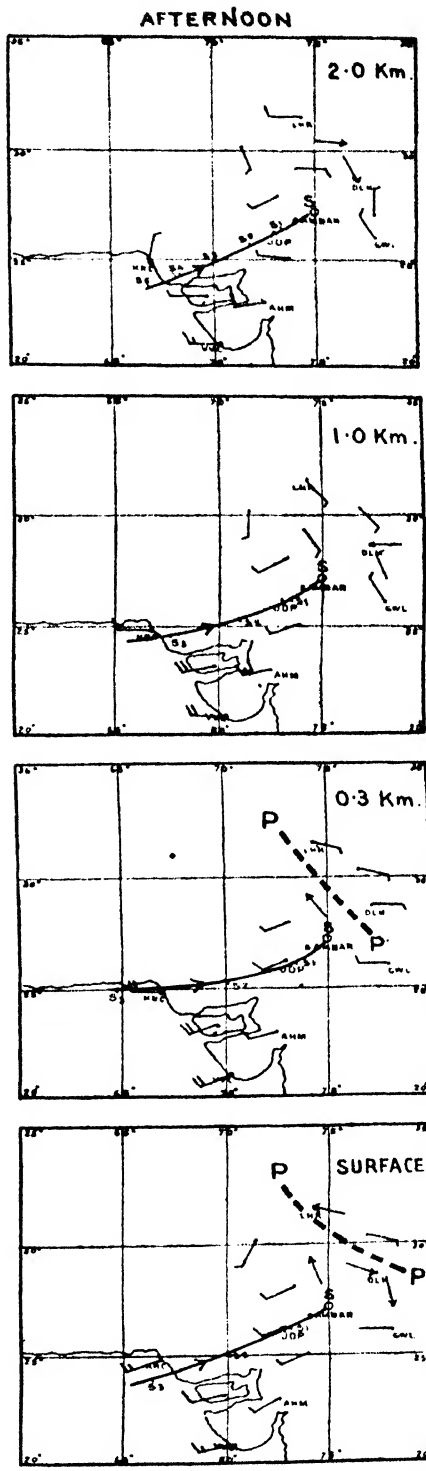
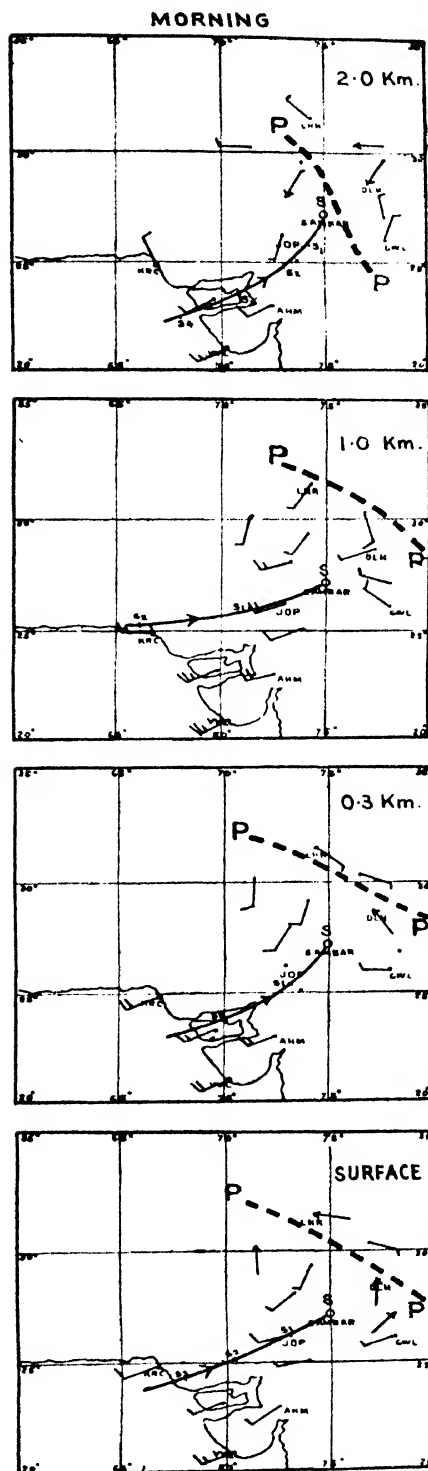


FIG.4.

MEAN WINDS IN MAY.



MEAN WINDS IN JUNE



MEAN WINDS IN JULY.

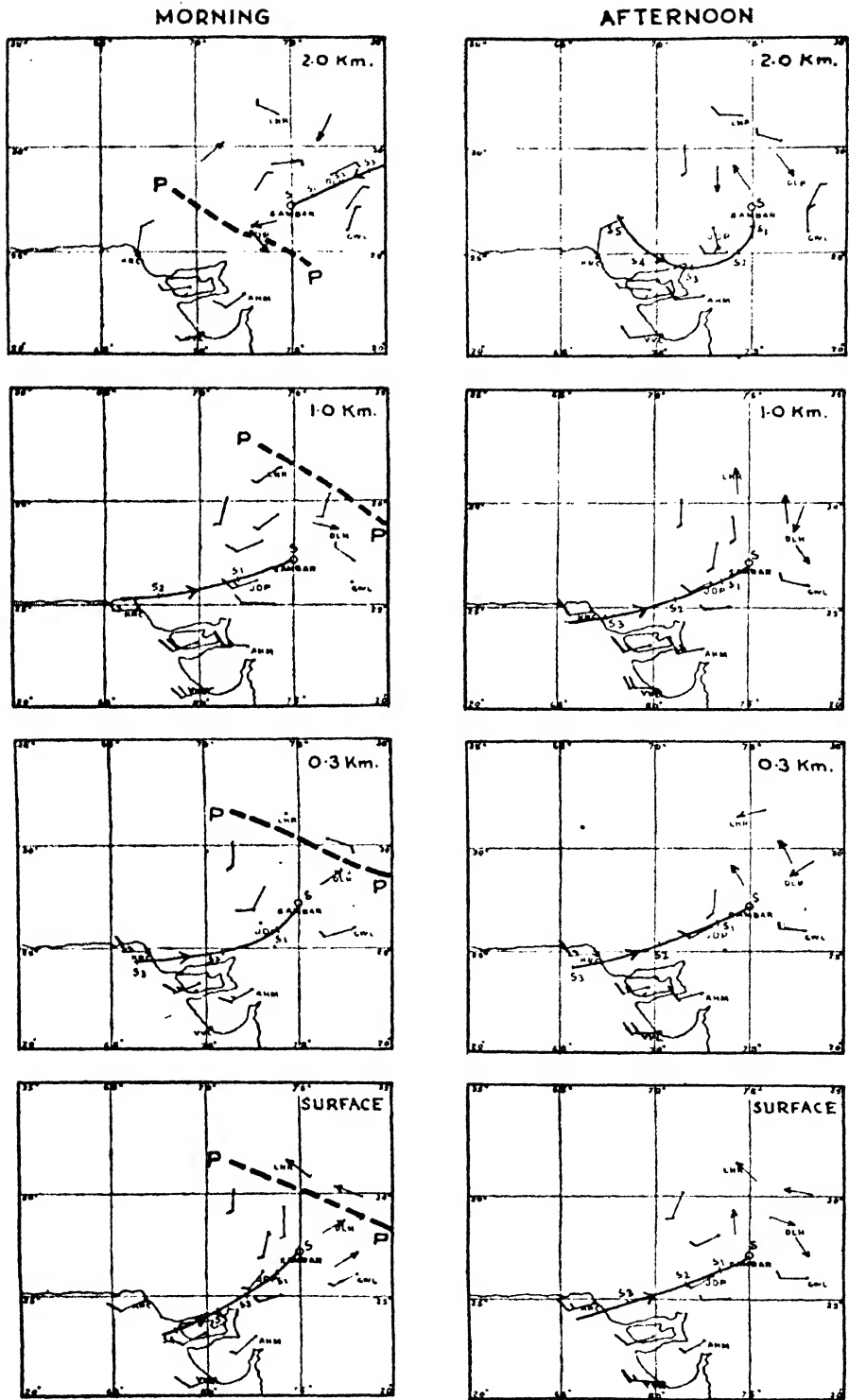


FIG. 9.

FIG.10

MEAN WINDS IN AUGUST

MORNING

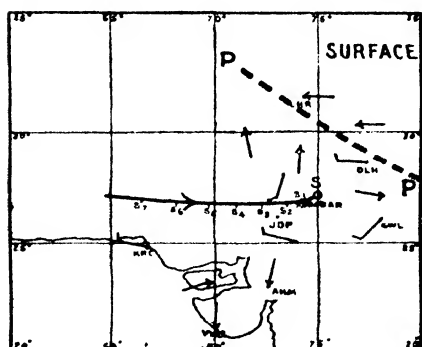
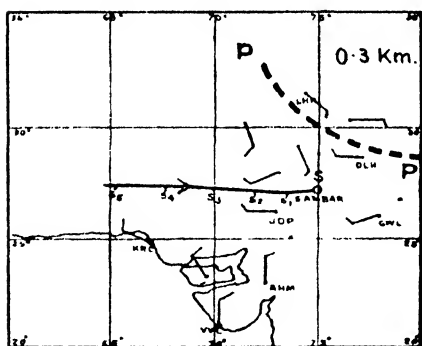
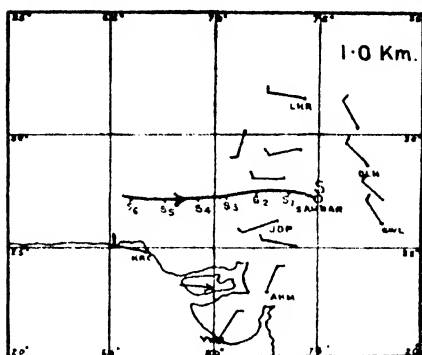
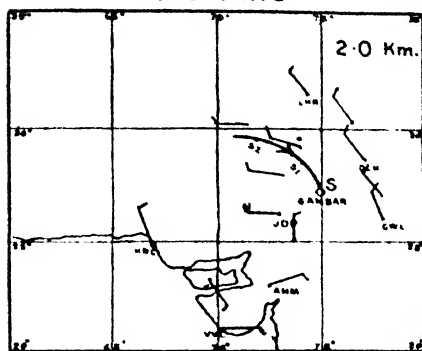


FIG.11.
MEAN WINDS IN OCTOBER.

MORNING

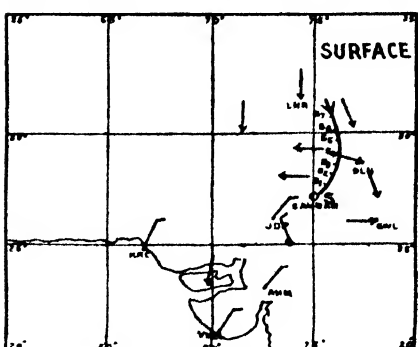
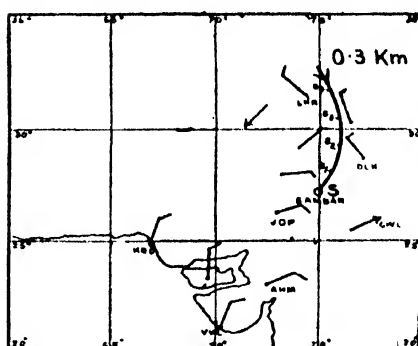
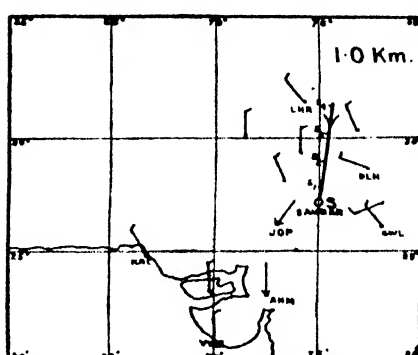
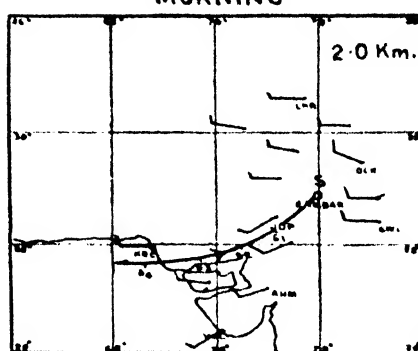


FIG.12.
MEAN WINDS IN JANUARY.

be carried by the wind. The speed in the region traversed is of the order of 3 m.p.h., and so the salt will be carried about 72 miles in a single day. The point the salt will reach at the end of a single day's journey is indicated by C_1 , that it will reach after two days' journey by C_2 , etc., etc. It will be seen that air which starts from C and is carried near the surface will not eventually arrive at the Sambhar region. Other points in the Rann of Cutch are even less favourably situated for transport of salt by winds to the Sambhar region. Conversely, one could start from S and trace the source region wind from which eventually arrives at Sambhar. Such a line has also been drawn in Fig. 1 (Surface) and the points representing one day's journey, two days' journey, etc., indicated by the points S_1, S_2, S_3, S_4 , etc. It will be seen that sea air from near Karachi or the Persian Gulf could reach Sambhar region in about 6 to 7 days in April (see also Fig. 2; afternoon winds). At the height of 0.3 km., wind arriving at Sambhar in April is originally from Baluchistan, according to the morning winds and either from Baluchistan or west Mekran coast, according to the afternoon winds (Figs. 1 and 2). Greater heights are even less favourable.

5. Lines like S, S_1, S_2, S_3 tracing the source of supply of air to Sambhar, . . . and C, C_1, C_2, C_3 indicating the regions where air from the Rann of Cutch goes, have been drawn in the charts for other months wherever it was considered they would be helpful.

6. The two factors regarding wind which have to be considered are direction and force. We will consider direction first. From the figures 1-12 it will be seen that only during May to August (winds for months other than those for which figures are given have also been taken into account) and perhaps during part of April is the wind direction favourable for transport of salt by winds from the Arabian Sea to North-East Rajputana and Sambhar Lake region. If we, however, consider transport of salt from the Rann of Cutch to the Sambhar Lake region, the conditions are favourable only during June to August at a few of the levels during only part of the day. Holland and Christie's supposition that winds are favourable for the transport of salt from the Rann of Cutch to the Sambhar Lake region during the summer months of April, May and June—the ground being wet in July and August after the break of monsoon in June—does not appear to be borne out, except in June during morning and at only 0.3 and 2 km. levels but not at the surface and 1 km. level. We will now consider the force of wind. We will not consider here whether the wind is strong enough to lift up salt and to carry it along. We will take it that the wind near the sea and along the Rann of Cutch is strong enough to lift up salt and carry it along and also that there is enough salt dust available in the Rann of Cutch in the summer months. From the figures it will be seen that in no month is the wind strong enough to carry the salt lifted up in the morning from the Rann of Cutch more than half way to Sambhar Lake by the evening. In the night two things can happen—one is that the salt is carried on during night (when the surface wind drops to about 2.3 the value during daylight hours, but there is no large diminution in winds at 0.3 km. and above) and the other is that the salt is dropped in the evening and picked up again next morning. If the salt is carried on during the night there is no reason as to why it should be dropped in Sambhar Lake region more than elsewhere along the route before and beyond the Sambhar Lake. During certain months at some levels there is an opposing wind current but this is generally to the north of Delhi as shown by thick dotted lines PP in the relevant charts. If we postulate that the salt is dropped during night and picked up again next morning it would imply that the salt is being carried in the layer below the .3 km. level as there is no appreciable decrease in wind strength at .3 km. level and above, and that in this case it is unlikely that the wind-borne salt from the Rann of Cutch would reach the Sambhar region. Again, even if the salt does reach the Sambhar region and is dropped there, it is likely to be picked up again and carried away beyond this region, as there is not much difference in wind strength over the Sambhar and adjoining regions.

7. An examination of the figures indicate that the winds are more favourable for transport of salt from the sea and Rann of Cutch to Jawai and Banas catchments and the lakes near Ajmer and in South-East Rajputana, which all contain fresh water, than to the Sambhar Lake region. We have considered here the mean wind, but the results are not likely to be much different if we take into account winds for individual days for a long period.

8. Again, if the salt in Sambhar region is wind-borne it is likely to be distributed more or less evenly and since there is not much difference in rainfall over the region, one would expect the chloride content in the water of the different rivers in the Sambhar region to be similar, but actually there are very large differences (*vide* Table on p. 159 of Holland and Christie's paper).

9. It will be seen from the preceding paras that it is unlikely that the main origin of salt in Sambhar Lake and also, *a priori* in other lakes in North Rajputana is windborne from the Rann of Cutch or even from the Arabian Sea.

SUMMARY

Many explanations of the origin of salt in Sambhar Lake have been given, the generally accepted one being that of Holland and Christie, advanced about 40 years ago, that the salt is borne by wind from the Rann of Cutch during the summer months. Godbole has recently objected to the theory. In this note the surface and upper winds have been studied with a view to examine whether the salt in Sambhar Lake could have been wind-borne from the Rann of Cutch, and the Arabian Sea. It is found that it is unlikely that the salt in Sambhar Lake and also in other lakes in North Rajputana could have been wind-borne from the Rann of Cutch or even from the Arabian Sea.

REFERENCES

- Godbole, N. W. (1952). The Salinity of Sambhar Lake. *Bull. Nat. Inst. Sci. India*, No. 1, 89-93.
 Holland, T. M. and Christie, W. A. K. (1913). The origin of salt deposits of Rajputana. *Rec. Geol. Surv. Ind.*, 38, pt. 2, 154-186.

Issued June 24, 1954.

TARGET DAMAGES BY EXPLOSIVE CHARGES WITH LINED CONICAL CAVITIES

by SAMPOORAN SINGH, *Defence Science Organization, Ministry of Defence, New Delhi*

(Communicated by R. S. VARMA, F.N.I.)

(Received January 5; read March 5, 1954)

1. INTRODUCTION

High explosive charges with metal-lined cavities (Shaped Charges) were extensively used during the last war by armed forces of the major combatants for destroying concrete fortifications, bridges, pillboxes, tanks and other war machines. The first fairly comprehensive explanation of this phenomena was published by Birkhoff, MacDougall, Pugh and Taylor (1948). They showed that when a detonation wave sweeps from apex to base along a conical liner, it collapses the liner into a small diameter jet (known as 'Munroe' jet) which shoots forward with a tremendous velocity (7 to 12×10^5 cm./sec.). When this high velocity jet impinges upon a target, it produces pressures close to a quarter million atmospheres and the target material flows plastically out of the path of the jet. Recently Pugh, Eichelberger and Rostoker (1952) extended the steady-state hydrodynamic theory and explained the formation of the entire jet (including the 'after jet') and the velocity gradient in the jet.

The aim of the present investigation is to study the damage to massive mild steel targets by explosive charges having (a) copper conical liners of different calibres and (b) copper and mild steel liners of different angles. As the penetration by high velocity 'Munroe' jet is independent of the striking velocity, so the experiments were done by hand placing and statically detonating the shaped charges.

2. COPPER CONICAL LINERS OF DIFFERENT CALIBRES

Let D represent the base diameter of the conical liner and be referred as calibre. The unit of length is assumed to be $1D$ and other parameters, e.g. thickness of conical liner ($0.032D$), charge length ($0.9D$) and stand-off ($1\frac{1}{2}D$) increase *pro rata* to the calibre.

Conical liners of angle 45° , thickness $0.032D$ and of different calibres were machined from rods of copper. The conical liner was soldered at one end of a gas pipe. High explosive, which was a mixture of T.N.T. and tetryl (trinitrophenylmethylnitramine) in the ratio of 70 : 30, was cast. A tetryl pellet was used as a booster. The lay-out of the equipment for firing is shown in Fig. 1 and the relevant information is given in Table 1.

The plot of penetration P against calibre D (Fig. 2) suggests a linear relationship, which is as follows :—

$$P = 3.96D - 0.29 \quad \dots \dots \dots (1)$$

Evans and Ubbelohde (1950) also suggested a linear relationship between penetration and calibre (in the range of 1 to 2 in.). The logarithmic plot of penetration against entry diameter E (Fig. 3) also suggests the following linear relation

$$P = 7.96 E^{0.68} \quad \dots \dots \dots (2)$$

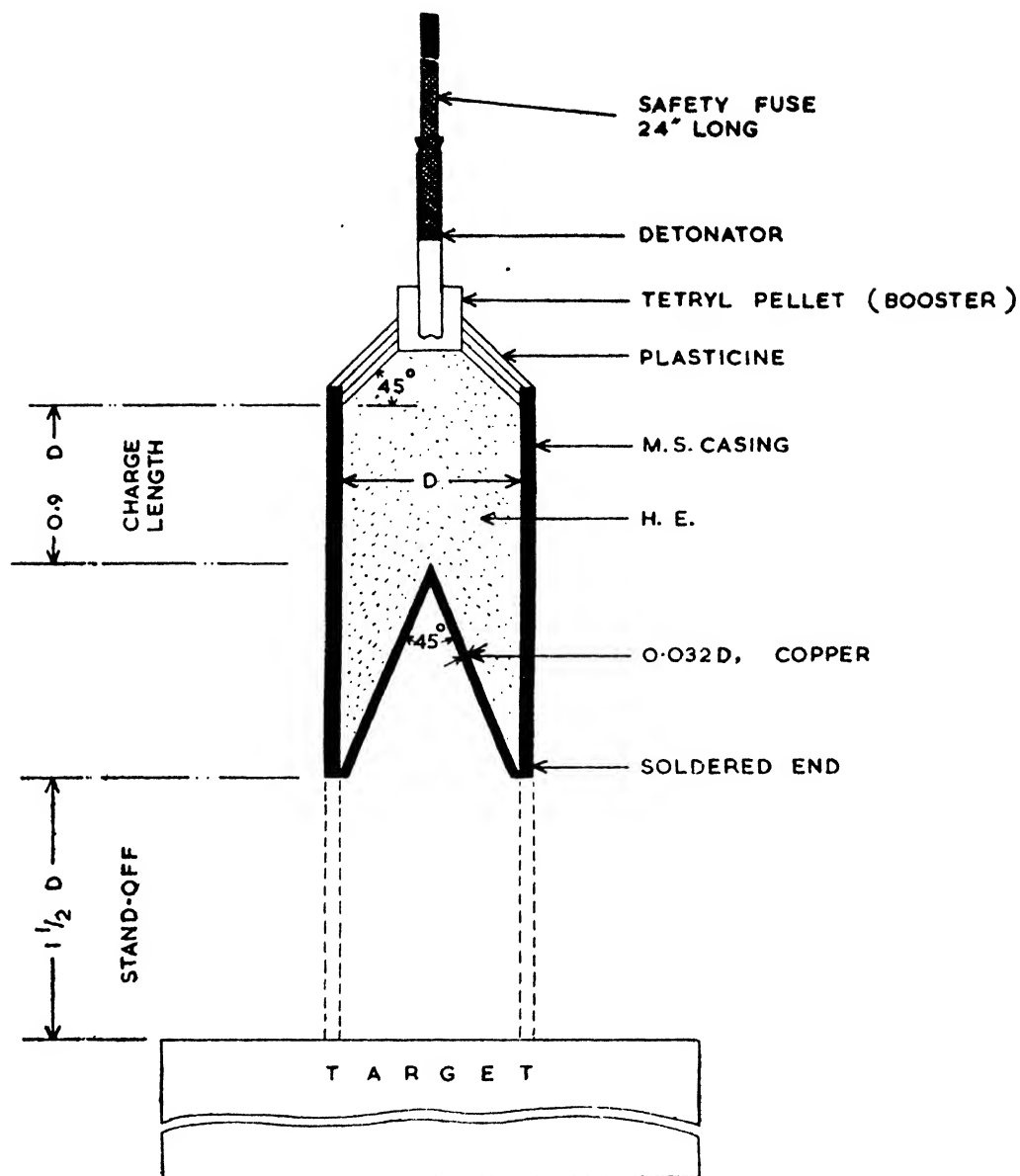


FIG. 1. Lay-out of shaped charge equipment for firing.

TABLE I
Target damages as a function of calibre.

Calibre (inch) D	Wt. of explosives. (lb.) W	Mean parameters of hole.			No. of firings.
		Volume (c.c.) V	Entry dia. (inch) E	Penetration (inch) P	
1.38	0.198	13.7	0.58	5.27	5
1.5	0.258	14.7	0.58	5.67	5
2.0	0.611	46.8	0.85	7.35	5
2.5	1.193	99.1	1.43	9.69	5
3.0	2.061	190.0	1.68	11.63	5

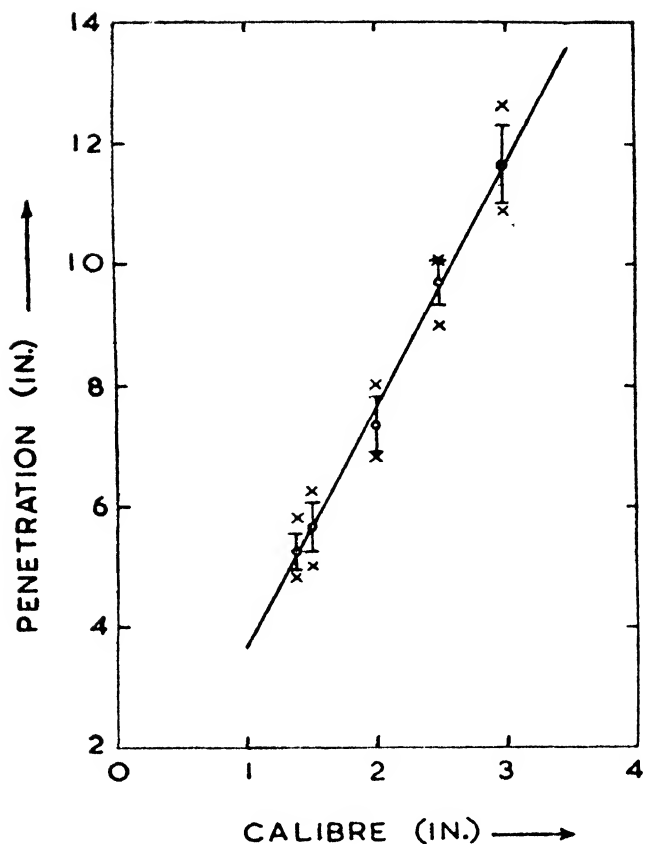


FIG. 2. Penetration in mild steel as a function of calibre. \bar{y} indicates mean penetration with 95% confidence limits. \times indicates maximum and minimum penetration.

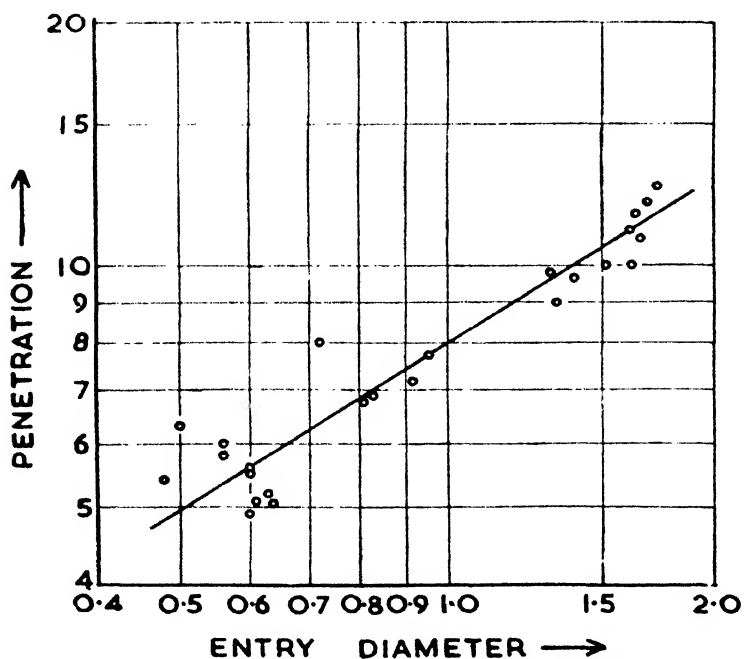


FIG. 3. Variation of the penetration with entry diameter in mild steel.

From the data in Table I, it appears that the relationship $V = KD^3$, where K is some constant, holds approximately. As volume of the hole depends on the kinetic energy of the jet, so kinetic energy of jet is also proportional to the cube of the calibre. Let 2α represent the original angle of the conical liner, D the calibre and ND the charge length. The weight of explosive W in the shaped charge is given by the expression

$$W = \frac{\pi}{12} D^3 \rho_0 [\cot \alpha + 3N] \quad \dots \quad (3)$$

In the experiments discussed above, ND is taken as $0.9D$, ρ_0 is the cast density of the explosive in lbs./cu.in. (0.057 lbs./cu.in.). Eq. (3) reduces to

$$W = kD^3 \quad \dots \quad (4)$$

where $k = 0.076$ lbs. in. $^{\frac{1}{3}}$.

3. COPPER AND MILD STEEL CONICAL LINERS OF DIFFERENT ANGLES

Conical liners of copper and mild steel, calibre $1\frac{1}{8}$ in., thickness 0.044 in. and of different angles— 120° , 100° , 80° , 60° , 50° , 40° , 30° , 20° and 15° —were machined from rods of the metals. The liners were soldered with convenient length of gas pipes $\frac{1}{8}$ in. thickness. High explosive, which was a mixture of T.N.T. and tetryl in the ratio of 70 : 30, was cast. The charge length (3 in.) and stand-off ($2\frac{1}{8}$ in.) were kept constant in all the firings. The lay-out of the equipment for firing is the same as shown in Fig. 1 and the relevant information is given in Table II.

TABLE II

Target damages as a function of angle of conical liner.

Angle of conical liner. (deg.)	Copper conical liner.			Mild steel conical liner.		
	Mean penetration. (inch)	Mean entry dia. (inch)	No. of firings.	Mean penetration. (inch)	Mean entry dia. (inch)	No. of firings.
120	2.91	0.44	6	2.48	0.55	6
100	3.50	0.38	6	3.14	0.49	6
80	3.93	0.42	6	3.65	0.45	6
60	4.16	0.41	6	3.85	0.43	6
50	4.76	0.57	6	4.10	0.61	6
40	5.27	0.54	6	4.58	0.71	6
30	5.51	0.57	6	4.73	0.74	6
20	5.75	0.60	6	5.15	0.66	6
15	5.13	Irregular	5	4.14	Irregular	5

The data in Table II indicate that (a) as the angle of the conical liner decreases, the penetration increases both for copper and mild steel liners. The relation of penetration as a function of the angle is shown in Fig. 4. The firing data of 15° conical liner is wide spread; (b) the penetration by copper liner is about 14% more than that of mild steel liner of the same angle; and (c) the entry diameter by a copper liner is about 16% less than that of mild steel liner of the same angle.

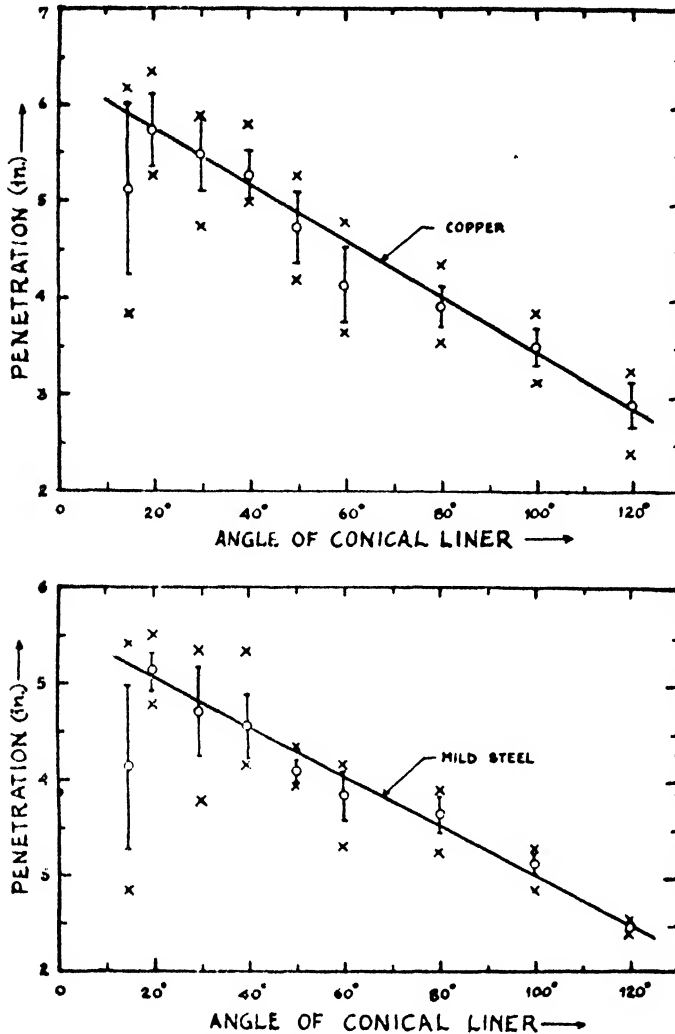


FIG. 4. Penetration versus angle of conical liner.

○ indicates mean penetration with 95% confidence limits.

× indicates maximum and minimum penetration.

ACKNOWLEDGEMENTS

The author is grateful to Dr. D. S. Kothari, Scientific Adviser to the Ministry of Defence, for suggesting this work and for his encouragement and interest. Many thanks are due to the Director-General of Ordnance Factories, Ministry of Defence, and the Director of Technical Development, Army Headquarters, for facilities provided in connection with the above work. Thanks are also due to Mr. M. P. Murgai for help in the experimental work and to Dr. R. S. Varma for advice and help in the preparation of this paper.

ABSTRACT

An investigation has been made of the damage to massive mild steel targets by explosive charges having (a) copper conical liners of different calibres and (b) copper and mild steel liners of different angles. The penetration and the calibre are linearly related. The penetration increases with the decrease of the angle of the copper and the mild steel liners. Copper liner gives more penetration and less entry diameter than that of mild steel liner.

REFERENCES

- Birkhoff, G., MacDougall, D. P., Pugh, E. M. and Taylor, G. (1948). Explosives with Lined Cavities. *J. Appl. Phys.*, **19**, 563-582.
Evans, W. M. and Ubbelohde, A. R. (1950). Some kinematic properties of Munroe Jets. *Research*, **3**, 376-378.
Pugh, E. M., Eichelberger, R. J. and Rostoker, N. (1952). Theory of Jet Formation by Charges with Lined Conical Cavities. *J. Appl. Phys.*, **23**, 532-536.

Issued June 24, 1954.

ON ANGELESCUS POLYNOMIALS

by VIKRAMADITYA SINGH, *Department of Mathematics, University of Delhi.*

(Communicated by R. S. Varma, F.N.I.)

(Received January 3 ; read October 9, 1953)

INTRODUCTION

The Angelescus set of polynomials $[\Pi_n(x)]$ of degree n in x are defined as

$$\Pi_n(x) = e^x \left(\frac{d}{dx} \right)^n \{ e^{-x} A_n(x) \} \quad \dots \quad \dots \quad \dots \quad (1)$$

where

$$A_n(x) = (a_0, a_1, a_2, \dots, a_n, x)^n \quad \dots \quad \dots \quad \dots \quad (2)$$

Shastri (1940) gave some recurrence relations for these polynomials and also their relations with well-known functions. In the present paper a Stieltjes integral representation of these polynomials has been given and it has been shown that the only orthogonal sub-set of this set is the set of confluent hypergeometric polynomials, the most well known among which is the Laguerre polynomial. This problem has also been treated in a more general form, by Meixner (1934) and Sheffer (1939). Meixner has used the generating function relation and Laplace transformation and Sheffer has used a property of zero type polynomials. I have, however, used the integral representation for these polynomials as given in the present paper. With the help of the integral representation some finite and infinite series involving Angelescus polynomials have also been summed.

I. SET OF ANGELESCUS POLYNOMIALS

We begin by proving the *lemma* :

The set of Angelescus polynomials is given by

$$\frac{\Pi_n(x)}{n!} = \int_{-\infty}^{\infty} L_n(x+t) d\beta(t), \quad \dots \quad \dots \quad \dots \quad (3)$$

where $L_n(x)$ is the Laguerre polynomial of degree n in x and $\beta(t)$ is such that for $n = 0, 1, 2, 3, \dots$ the moment constants $[\mu_n]$ given by

$$\mu_n = \int_{-\infty}^{\infty} t^n d\beta(t) \text{ exist and } \mu_0 \neq 0. \quad \dots \quad \dots \quad \dots \quad (4)$$

Proof: From equation (2) it is obvious that

$$\frac{d}{dx} \left\{ \frac{A_n(x)}{n!} \right\} = \frac{A_{n-1}(x)}{(n-1)!},$$

which shows that the set of polynomials

$$\left[\frac{A_n(x)}{n!} \right]$$

belongs to the Appell set. It was proved by Sheffer (1945) that an Appell polynomial $P_n(x)$ can be represented as

$$P_n(x) = \int_0^\infty \frac{(x+t)^n}{n!} d\beta(t)$$

if

$$\mu_n = \int_0^\infty t^n d\beta(t) \quad n = 0, 1, 2, \dots$$

exist and $\mu_0 \neq 0$.

Without any difficulty we can say that under the conditions on $\beta(t)$ as given in the lemma

$$P_n(x) = \int_{-\infty}^\infty \frac{(x+t)^n}{n!} d\beta(t).$$

Hence using (1) we have

$$\begin{aligned} \frac{\Pi_n(x)}{n!} &= e^x \left(\frac{d}{dx} \right)^n \left\{ e^{-x} \int_{-\infty}^\infty \frac{(x+t)^n}{n!} d\beta(t) \right\} \\ &= e^x \int_{-\infty}^\infty \left(\frac{d}{dx} \right)^n \left\{ e^{-x} \frac{(x+t)^n}{n!} \right\} d\beta(t). \end{aligned}$$

There is no difficulty in differentiating under the integral sign, since the differentiated integral is uniformly convergent for all finite values of n and x . We get therefore

$$\begin{aligned} \frac{\Pi_n(x)}{n!} &= e^x \int_{-\infty}^\infty e^t \left[\left\{ \frac{d}{d(x+t)} \right\}^n \left\{ e^{-(x+t)} \frac{(x+t)^n}{n!} \right\} \right] d\beta(t) \\ &= e^x \int_{-\infty}^\infty e^t e^{-(x+t)} L_n(x+t) d\beta(t) \\ &= \int_{-\infty}^\infty L_n(x+t) d\beta(t), \end{aligned}$$

where we have used the well-known Rodrigue's formula for Laguerre polynomials. This establishes our lemma.

II. SOME SERIES INVOLVING ANGELESCUS POLYNOMIALS

RESULT 1. For all finite values of ω

$$\sum_{n=0}^{\infty} \frac{\Pi_n(x)}{n!} \frac{\omega^n}{n!} = e^{\omega} \int_{-\infty}^{\infty} J_0 \{2\sqrt{\omega(x+t)}\} d\beta(t). \quad \dots \quad (5)$$

Multiplying both the sides of (3) by $\frac{\omega^n}{n!}$ and interchanging the order of summation and integration on the right hand side we get

$$\sum_{n=0}^{\infty} \frac{\Pi_n(x)}{n!} \frac{\omega^n}{n!} = \int_{-\infty}^{\infty} \sum_{n=0}^{\infty} L_n(x+t) \frac{\omega^n}{n!} d\beta(t),$$

if the integral on the right exists.

Now, from Szëgo (1939 ; p. 98) we have

$$\sum_{n=0}^{\infty} L_n(x) \frac{\omega^n}{n!} = e^{\omega} J_0(2\sqrt{x\omega}).$$

Hence

$$\sum_{n=0}^{\infty} \frac{\Pi_n(x)}{n!} \frac{\omega^n}{n!} = e^{\omega} \int_{-\infty}^{\infty} J_0 \{2\sqrt{\omega(x+t)}\} d\beta(t).$$

RESULT 2. If $I_0(x)$ is the Bessel function of purely imaginary argument

$$e^{\frac{\omega(x+y)}{1-\omega}} \sum_{n=0}^{\infty} \frac{\Pi_n(x)}{n!} \frac{\Pi_n(y)}{n!} \omega^n = \int_{-\infty}^{\infty} d\beta(t') \int_{-\infty}^{\infty} I_0 \left\{ \frac{2\sqrt{\omega(x+t)(y+t')}}{1-\omega} \right\} e^{-\frac{\omega(t+t')}{1-\omega}} d\beta(t), \quad (6)$$

whenever the integral on the right exists.

Using (3) we get on interchanging the order of summation and integration, whenever it is possible to do so, that

$$\begin{aligned} \sum_{n=0}^{\infty} \frac{\Pi_n(x)}{n!} \frac{\Pi_n(y)}{n!} \omega^n &= \int_{-\infty}^{\infty} d\beta(t') \int_{-\infty}^{\infty} \sum_{n=0}^{\infty} L_n(x+t) L_n(y+t') \omega^n d\beta(t) \\ &= \int_{-\infty}^{\infty} d\beta(t') \int_{-\infty}^{\infty} I_0 \left\{ \frac{2\sqrt{\omega(x+t)(y+t')}}{1-\omega} \right\} e^{-\frac{\omega(x+y+t+t')}{1-\omega}} d\beta(t). \end{aligned}$$

Wherein we have used the Mehler's formula for Laguerre polynomials Szëgo (1939 ; p. 98)

$$\sum_{n=0}^{\infty} L_n(x) L_n(y) \omega^n = \exp \left\{ -(x+y) \frac{\omega}{1-\omega} \right\} I_0 \left\{ \frac{2\sqrt{xy\omega}}{1-\omega} \right\} \frac{1}{1-\omega}.$$

Now multiplying both the sides by $e^{\frac{(x+y)\omega}{1-\omega}}$ we get the result.

RESULT 3.
$$\sum_{\nu=0}^n \frac{\Pi_{\nu}(x)}{\nu!} = - \frac{d}{dx} \frac{\Pi_{n+1}(x)}{(x+1)!} . \quad \dots \quad \dots \quad (7)$$

We get from (3) that

$$\begin{aligned} \sum_{\nu=0}^n \frac{\Pi_{\nu}(x)}{\nu!} &= \int_{-\infty}^x \sum_{\nu=0}^n L_{\nu}(x+t) d\beta(t) \\ &= \int_{-\infty}^x \frac{n+1}{x+t} \left[L_n(x+t) - L_{n+1}(x+t) \right] d\beta(t) \\ &= - \int_{-\infty}^x \frac{d}{dx} L_{n+1}(x+t) d\beta(t) \\ &= - \frac{d}{dx} \frac{\Pi_{n+1}(x)}{(n+1)!} . \end{aligned}$$

Wherein we have used the well-known recurrence relations about Laguerre polynomials.

III. THE ORTHOGONAL SUB-SET

It is a well known result that the necessary and sufficient condition for a polynomial $P_n(x)$ of degree n in x , to be orthogonal is that it should satisfy a difference equation of the form

$$P_n(x) = (-a_n x + b_n) P_{n-1}(x) + C_n P_{n-2}(x) , \quad \dots \quad \dots \quad (8)$$

where a_n, b_n, c_n are constants independent of x and c_n is negative.

From (3) it is clear that a particular sub-set of Angelescus (1938) set of polynomials can be obtained by properly choosing the function $\beta(t)$ and that for different $\beta(t)$ we will get different sets of polynomials all belonging to the Angelescus set. We will now apply the condition (8) to (3) in order to search for what functions $\beta(t)$ do the polynomials $\Pi_n(x)$ satisfy the condition of orthogonality and from there we will get the desired orthogonal sub-set.

Using the expansion of Laguerre polynomials as

$$\left. \begin{aligned} L_n(x+t) &= \sum_{\nu=0}^n (-)^{\nu} \binom{n}{\nu} \frac{(x+t)^{\nu}}{\nu!} \\ &= \sum_{\nu=0}^n (-)^{\nu} \binom{n}{\nu} \sum_{r=0}^{\nu} \binom{\nu}{r} \frac{1}{\nu!} x^r t^{\nu-r} \\ &= \sum_{r=0}^n (-x)^r \binom{n}{r} \sum_{\nu=0}^{n-r} (-t)^{\nu} \binom{n-r}{\nu} \frac{1}{(\nu+r)!} , \end{aligned} \right\} \dots \quad \dots \quad (9)$$

we get

$$\left. \begin{aligned} \frac{\Pi_n(x)}{n!} &= \sum_{r=0}^n (-x)^r \binom{n}{r} \sum_{\nu=0}^{n-r} \binom{n-r}{\nu} (-)^{\nu} \frac{\mu_{\nu}}{(\nu+r)!} \\ &= \mu_0 \frac{(-x)^n}{n!} + (-x)^{n-1} n \left\{ \frac{\mu_0}{(n-1)!} - \frac{\mu_1}{n!} \right\} \\ &\quad + \sum_{r=0}^{n-2} (-x)^r \binom{n}{r} \sum_{\nu=0}^{n-r} (-)^{\nu} \binom{n-r}{\nu} \frac{\mu_{\nu}}{(\nu+r)!}, \end{aligned} \right\} \dots \dots (10)$$

wherein we have separated the terms containing x^n and x^{n-1} from other terms.

In like manner we may write

$$\left. \begin{aligned} (-a_n x + b_n) \frac{\Pi_{n-1}(x)}{(n-1)!} &= \frac{a_n (-x)^n}{(n-1)!} \mu_0 + (-x)^{n-1} \left\{ \frac{b_n \mu_0}{(n-1)!} \right. \\ &\quad \left. + (n-1) a_n \left(\frac{\mu_0}{(n-2)!} - \frac{\mu_1}{(n-1)!} \right) \right\} \\ &\quad + \sum_{r=0}^{n-2} (-x)^r \left\{ \binom{n-1}{r} b_n \sum_{\nu=0}^{n-r-1} (-)^{\nu} \binom{n-r-1}{\nu} \frac{\mu_{\nu}}{(\nu+r)!} \right. \\ &\quad \left. + \binom{n-1}{r-1} a_n \sum_{\nu=0}^{n-r} (-)^{\nu} \binom{n-r}{\nu} \frac{\mu_{\nu}}{(\nu+r)!} \right\}. \end{aligned} \right\} (11)$$

Now, if $\frac{\Pi_n(x)}{n!}$ satisfies (8) we get on equating the coefficients of x^n and x^{n-1} in the right hand side of (10) and (11) that

$$\left. \begin{aligned} a_n &= \frac{1}{n}, \\ \text{and } n \left\{ \frac{\mu_0}{(n-1)!} - \frac{\mu_1}{n!} \right\} &= \left\{ \frac{b_n \mu_0}{(n-1)!} + a_n (n-1) \left(\frac{\mu_0}{(n-2)!} - \frac{\mu_1}{(n-1)!} \right) \right\} \end{aligned} \right\} (12)$$

$$b_n = \frac{2n-1+\alpha}{n}, \quad \dots \dots \dots (13)$$

where

$$\alpha = -\frac{\mu_1}{\mu_0}; \quad \dots \dots \dots (14)$$

and comparing the coefficients of the remaining powers of x on both sides of (8) for $r = 0, 1, 2, \dots, n-2$, we have

$$\begin{aligned}
C_n \binom{n-2}{r} \sum_{\nu=0}^{n-2-r} (-)^{\nu} \binom{n-r-2}{\nu} \frac{\mu_{\nu}}{(\nu+r)!} &= \binom{n}{r} \sum_{\nu=0}^{n-r} (-)^{\nu} \binom{n-r}{r} \frac{\mu_{\nu}}{(\nu+r)!} \\
&\quad - \binom{n-1}{r} b_n \sum_{\nu=0}^{n-r-1} (-)^{\nu} \binom{n-r-1}{\nu} \frac{\mu_{\nu}}{(\nu+r)!} \\
&\quad + \binom{n-1}{r-1} a_n \sum_{\nu=0}^{n-r} (-)^{\nu} \binom{n-r}{\nu} \frac{\mu_{\nu}}{(\nu+r)!}.
\end{aligned}$$

Putting the values of a_n and b_n in this we get after some rearrangement

$$\begin{aligned}
C_n \binom{n-2}{r} \sum_{\nu=0}^{n-2-r} (-)^{\nu} \binom{n-r-2}{\nu} \frac{\mu_{\nu}}{(\nu+r)!} &= \frac{1}{n^2} \binom{n}{r} \sum_{\nu=0}^{n-r} (-)^{\nu} \binom{n-r}{\nu} \\
&\quad \times \frac{\mu_{\nu}}{(\nu+r)!} \left[-\alpha(n-r-\nu) - \{n^2 - n(2r+2\nu+1) + r^2 + r\nu + r + \nu\} \right].
\end{aligned}$$

From the above equation it is quite clear that C_n should be a linear function of α in order that the term containing α in the right hand side may be balanced by a corresponding one on the left hand side. Let us therefore put

$$C_n = \frac{n-1}{n} (\alpha e_n + d_n), \quad \dots \quad \dots \quad \dots \quad (15)$$

e_n and d_n depending only on n .

Transposing we get

$$\begin{aligned}
\sum_{\nu=0}^{n-r} (-)^{\nu} \binom{n-r}{\nu} \frac{\mu_{\nu}}{(\nu+r)!} \left[-\alpha(n-r-\nu) - \{n^2 - n(2r+2\nu+1) + r^2 + r\nu + r + \nu\} \right. \\
\left. - (n-r-\nu)(n-r-\nu-1)(d_n + \alpha e_n) \right] = 0
\end{aligned}$$

$$\begin{aligned}
\text{or,} \quad \sum_{\nu=0}^{n-r} (-)^{\nu} \binom{n-r}{\nu} \frac{\mu_{\nu}}{(\nu+r)!} \left[-\alpha(n-r-\nu) \{1 + e_n(n-r-\nu-1)\} \right. \\
\left. - \{n^2 - n(2r+2\nu+1) + r^2 + r\nu + r + \nu + d_n(n-r-\nu)(n-r-\nu-1)\} \right] = 0 \dots (16)
\end{aligned}$$

It should be noted here that the above equation holds not only for $r = 0, 1, 2, \dots, n-2$ but also for $r = n-1, n$. In the first case it gives the relation (14) and in the second case it shows that $\mu_0 \neq 0$.

The above equations on being solved will give us the values of μ_{ν} . Now, from (4) we see that μ_{ν} is always independent of n and we will utilize this fact to show that

$$d_n = -1 \text{ and } e_n = \frac{a}{n-1}. \quad \dots \quad \dots \quad \dots (17)$$

Putting $r = n-2$ in (16) we get

$$\mu_0(n-1) [-\alpha(1+e_n)-(d_n+1)] - \mu_1\{-\alpha+(n-1)\} + \mu_2 = 0$$

$$\therefore \mu_2 = -\mu_1\alpha - \mu_1e_n(n-1) + \mu_0(n-1)(d_n+1), \dots$$

which shows that in order that μ_2 be independent of n , e and d_n must satisfy (17).

Therefore we can write

$$\mu_2 = -\mu_1\alpha - a\mu_1 = -(\alpha-1)\mu_1 + (a+1)\alpha\mu_0.$$

With these values of e_n and d_n (16) reduces to

$$\sum_{v=0}^{n-r} (-)^v \binom{n-r}{v} \frac{\mu_v}{(\nu+r)!} \left[- \left\{ 1 + \frac{a}{n-1} (n-r-\nu-1) \right\} \alpha(n-r-\nu) + \nu(\nu+r) \right] = 0$$

$$r = 0, 1, 2, \dots, n. \quad \dots \quad (18)$$

We will now show that the system of equations (18) is equivalent to the system

$$\mu_n = -(a-n+1)\mu_{n-1} + \alpha(a+1)(n-1)\mu_{n-2}, \quad \dots \quad (19)$$

for

$$n = 1, 2, 3, \dots$$

if we take

$$\mu_{-1} = 0.$$

Putting

$$n-r = p \text{ (18) reduces to}$$

$$\sum_{v=0}^p (-)^v \binom{p}{v} \frac{\mu_v}{(\nu+n-p)!} \left[- \left\{ \left(1 - \frac{p-r-1}{n-1} \right) + \frac{a+1}{n+1} (p-\nu-1) \right\} \alpha(p-\nu) \right. \\ \left. + \nu(\nu+n-p) \right] = 0$$

$$\text{or,} \quad \sum_{v=0}^p (-)^v \binom{p}{v} \frac{\mu_v}{(\nu+n-p)!} \left[- \{ (n+\nu-p) + (a+1)(p-\nu-1) \} \right. \\ \left. \alpha(p-\nu) + \nu(\nu+n-p) \{ (\nu+n-p-1) - (\nu-p) \} \right] = 0$$

$$\text{or,} \quad \sum_{v=0}^p \frac{(-)^v \binom{p}{v} \mu_v}{(\nu+n-p)!} \left[-\alpha(a+1)(p-\nu)(p-\nu-1) + \nu(\nu+n-p)(\nu+n-p-1) \right. \\ \left. + (\alpha-\nu)(p-\nu)(n+\nu-p) \right] = 0$$

$$\text{or,} \quad \sum_{v=0}^{p-2} \frac{(-)^v p! (a+1)\alpha\mu_v}{(p-\nu-2)! (\nu+1)! (\nu+n-p)!} + \sum_{v=0}^{p-2} \frac{(-)^v \mu_{v+2} p!}{(p-\nu-2)! (\nu+1)! (\nu+n-p)!} - \frac{\mu_1 p}{(n-p-1)!} \\ + \sum_{v=0}^{p-2} \frac{(-)^v \mu_{v+1} p! (\alpha-\nu-1)}{(p-\nu-2)! (\nu+1)! (\nu+n-p)!} - \frac{\mu_0 \alpha p}{(n-p-1)!} = 0$$

$$\sum_{v=0}^{p-2} \frac{(-)^v p!}{(p-\nu-2)! (\nu+1)! (\nu+n-p)!} [\mu_{v+2} - \alpha(\nu+1)(a+1)\mu_v + (\alpha-\nu-1)\mu_{v+1}] = 0$$

$$\dots \quad (20)$$

From (20) it is quite evident that if (19) is satisfied (18) will automatically hold.

To prove the converse we use the method of induction. We have already seen that (19) holds for $n = 2$ and it can easily be verified that it holds for $n = 3$ also. Let us now suppose that it holds for $n = 1, 2, \dots, m$. Then putting $n = m+1$ in (20) we get

$$\sum_{v=0}^{m-1} \frac{(-)^v p! \{ \mu_{v+2} - (v+1)(a+1)\mu_v + (\alpha-v-1)\mu_{v+1} \}}{(p-v-2)! (v+1)! (v+n-p)!} = 0.$$

Whence

$$\mu_{m+1} + (\alpha-m)\mu_m - m(a+1)\mu_{m-1} = 0,$$

because by hypothesis the other terms reduce to zero. But this equation is obtained by putting $n = m+1$ in (19). We thus see that if (19) holds for $n = m$ it also holds for $n = m+1$. Hence it holds for all positive values of n .

IV. THE FUNCTION $\beta(t)$

We have now to determine the function $\beta(t)$ when μ_n satisfies the difference equation (19). It has to be noted that $\beta(t)$ is independent of n . Substituting from (4) in (19) we have for $n = 1, 2, \dots$

$$\begin{aligned} \int_{-\infty}^{\infty} t^n d\beta(t) &= -(\alpha-n+1) \int_{-\infty}^{\infty} t^{n-1} d\beta(t) + \alpha(a+1)(n-1) \int_{-\infty}^{\infty} t^{n-2} d\beta(t) \\ &= -(\alpha+1) \int_{-\infty}^{\infty} t^{n-1} d\beta(t) - \int_{-\infty}^{\infty} t^n d^2\beta(t) - \left[t^n d\beta(t) \right]_{-\infty}^{\infty} \\ &\quad + \alpha(a+1) \left[t^{n-1} d\beta(t) \right]_{-\infty}^{\infty} - \alpha(a+1) \int_{-\infty}^{\infty} t^{n-1} d^2\beta(t). \end{aligned}$$

Where we have assumed $\beta(t)$ to be absolutely continuous. Taking

$$\left[t^{n-1} d\beta(t) \right]_{-\infty}^{\infty} = 0 \quad n = 1, 2, 3, \dots, \quad \dots \quad (21)$$

and we get

$$\{t + (a+1)\alpha\} \frac{d^2\beta(t)}{dt^2} + (t + \alpha + 1) \frac{d\beta(t)}{dt} = T(t) \quad \dots \quad (22)$$

such that

$$\int_{-\infty}^{\infty} x^i T(x) dx = 0. \quad \dots \quad (23)$$

Integrating (22) we get

$$\frac{d\beta(t)}{dt} = e^{-t}(t + \alpha + 1)^{\alpha-1} \left[A + \int_t^{\infty} \frac{T(u)e^u du}{(u + \alpha + 1)^{\alpha}} \right].$$

This implies the existence of the integrals of the form

$$\int \frac{T(u)e^u}{(u+a\alpha+\alpha)^{a\alpha}} du,$$

so that we find from (21) that the limits of integration would be $(-a\alpha-\alpha, \infty)$, $a\alpha < 1$.

Let us now define

$$T_1(t) = \frac{d\beta(t)}{dt} + ce^{-t}(t+a\alpha+\alpha)^{a\alpha-1}, \dots \dots \dots (24)$$

and determine c such that

$$\int_{-a\alpha-\alpha}^{\infty} T_1(t) dt = \int_{-a\alpha-\alpha}^{\infty} \left[\frac{d\beta(t)}{dt} + ce^{-t}(t+a\alpha+\alpha)^{a\alpha-1} \right] dt = 0 \dots \dots (25)$$

Again, we have, when i is an integer ≥ 1

$$\begin{aligned} & \int_{-a\alpha-\alpha}^{\infty} \frac{T_1(x)}{e^{-x}(x+a\alpha+\alpha)^{a\alpha-1}} \frac{d}{dx} \left\{ (x+a\alpha+\alpha)^{a\alpha+i-1} e^{-x} \right\} dx \\ &= \left[(x+a\alpha+\alpha)^i \left\{ \frac{d}{dx} \beta(x) + ce^{-x}(x+a\alpha+\alpha)^{a\alpha-1} \right\} \right]_{-a\alpha-\alpha}^{\infty} \\ & \quad + \int_{-a\alpha-\alpha}^{\infty} (x+a\alpha+\alpha)^{i-1} T(x) dx \\ &= 0 \dots \dots \dots (26) \end{aligned}$$

The integral vanishing by virtue of (23) and the integrating term vanishing by virtue of (21).

But we find that the left hand side of (26) is

$$\int_{-a\alpha-\alpha}^{\infty} T_1(x) \left\{ (a\alpha+i-1)(x+a\alpha+\alpha)^{i-1} - (x+a\alpha+\alpha)^i \right\} dx = 0.$$

Now putting $i = 1$ we find with the help of (25) that

$$\int_{-a\alpha-\alpha}^{\infty} T_1(x)(x+a\alpha+\alpha) dx = 0,$$

i.e.

$$\int_{-a\alpha-\alpha}^{\infty} xT_1(x) dx = 0.$$

Similarly putting $i = 2, 3, 4$, in succession we find that

$$\int_{-a\alpha-\alpha}^{\infty} x^i T_1(x) dx = 0 \dots \dots \dots (27)$$

i.e. $T_1(x)$ is a function whose moments of all order vanish. Hence for all practical purposes we can neglect the function $T_1(t)$ and write

$$\begin{aligned}\frac{d\beta(t)}{dt} &= A e^{-t} (t + a\alpha + \alpha)^{a\alpha-1} & \infty > t > -a\alpha - \alpha \\ &= B e^{-t} t^{a\alpha-1} & \infty > t > 0\end{aligned}$$

With this value of $\frac{d\beta(t)}{dt}$ we will find the generating function for Angelescus Polynomials to be of the form

$$B \frac{\Gamma(a\alpha)}{(1-t)^{-a\alpha}}$$

which is of the same form as that of Laguerre polynomials.

ACKNOWLEDGEMENTS

My thanks are due to Dr. R. S. Varma, Senior Scientist, Defence Science Organization, for suggesting me the problem and for guidance in the preparation of the paper. Thanks are also due to Dr. Ram Behari, Head of the Mathematics Department, Delhi University, for kindly providing me all facilities to carry on research work and for his encouragement.

REFERENCES

- Angelescus, C. R. (1938). *Acad. Sci. Roum.*, **2**, 199-201. (vide also *Zbl. f. Math.*, **1**, 1938, (8), 356.)
 Meixner, J. (1934). *Jour. Lond. Math. Soc.*, **9**, 6-13.
 Shastri, N. A. (1940). Angelescus Polynomial. *Proc. Ind. Acad. Sci.*, **11**, 312-317.
 Sheffer, I. M. (1939). Some properties of polynomial sets of type zero. *Duke. Math. Journ.*, **5**, 590.
 Sheffer, I. M. (1945). Note on Appell Polynomials. *Bull. Amer. Math. Soc.*, **51**, 739-744.
 Singh, V. Appell set of polynomials (in press)
 Szego, G. (1939). *Orthogonal Polynomials*, Ch. V.

Issued June 25, 1954.

ORIGIN OF R.F. OSCILLATIONS IN A.C. 'SILENT' DISCHARGES

by S. R. KHASTGIR, *F.N.I.* and C. M. SRIVASTAVA, *Banaras Hindu University*

(Received December 17, 1953; read May 7, 1954)

1. INTRODUCTION

It was Warburg (1903) who concluded that the discharge current in Siemen's ozonizer had components, the frequencies of which were very high compared to that of the exciting voltage. According to him, the frequency components were within 10^5 – 10^6 cycles/sec. This was supported by Prasad (1949) who in his investigation on Joshi Effect devised a method in which the high frequency components were picked up by an aerial and measured by means of a suitable detecting device. Direct experimental evidence of R.F. oscillations of discrete frequencies set up in some gases and vapour under 'silent' electrical discharge was later given by Khastgir and Setty (1952), using ozonizers and discharge tubes, fitted with external 'sleeve'-electrodes and excited by a suitable high voltage of 50 cycles/sec. The various frequencies appeared to correspond to overtones of an oscillating system. It was observed that for a given distance between the electrodes, the frequency of these oscillations was not dependent on the magnitude of the applied voltage. It was also observed that for a given applied voltage, the frequency was independent of the inter-electrode distance. Further, it was found that for a given discharge tube, the frequency of the R.F. oscillations was independent of both applied voltage and inter-electrode distance. Subsequent experiments of Khastgir and Setty (1953) showed an *increase* in the frequency of the R.F. oscillations in a.c. 'silent' discharges in iodine vapour and hydrogen gas on exposure to visible light. Khastgir and Srivastava (1952) also observed a *decrease* in the frequency of the R.F. oscillations in similar discharges in iodine vapour, hydrogen and chlorine gases on exposure to thermal radiations.

The object of the present paper is to outline a theory as to the origin and nature of the R.F. oscillations set up in a.c. 'silent' discharges and to explain the effects of light and heat on the frequency of such oscillations. As the theory is based on the streamer mechanism of Loeb and Meek (1941), as applied to a.c. 'silent' discharges, we shall first mention very briefly the main features, which we have already developed (Khastgir and Srivastava, 1953), regarding the nature of the 'silent' discharge.

2. EFFECT OF THE INTERVENING GLASS WALL IN A.C. 'SILENT' DISCHARGES

The intervening glass wall in an ozonizer or in a discharge tube fitted with external electrodes introduces certain features which are illustrated in fig. 1(a) and are enumerated below:—

- (i) A negative surface charge is formed on the inner glass surface (AA) opposite to the anode during the half cycle of the applied field.
- (ii) A stationary array of positive ions (GG) is formed very close to the negative surface charge on the glass wall, when the applied field is adequate for Townsend collisions to take place in the enclosed gas or vapour.
- (iii) A gap (GGCC) in the discharge channel is set up between the stationary array (GG) of positive ions and the top surface (CC) of the moving column.

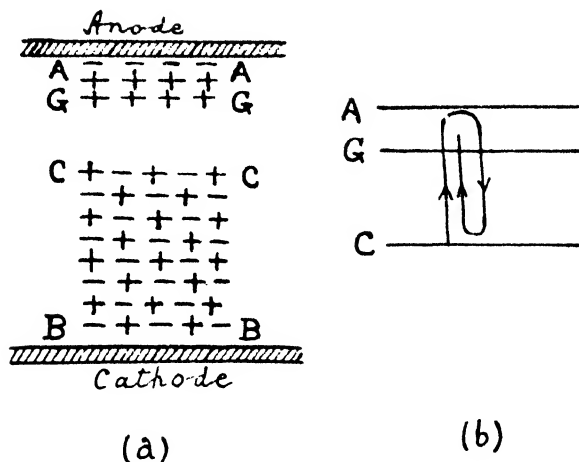


FIG. 1(a). AA—Negative surface charge on glass wall.
 GG—Stationary layer of positive ions.
 GGCC—Gap.
 CCRB—Streamer.
 FIG. 1(b). Electronic oscillation.

- (iv) The streamer formation, as the moving column of positive ions attracts to itself neighbouring electron avalanches and photo-ionized electrons, is possible even at a low pressure in an electric field which has been reduced due to the negative charge on the inner surface of the intervening glass wall.
- (v) The lower boundary (CC) of the gap may be regarded as the *virtual* cathode. The electrons start from the virtual cathode and being in an adequate field move across the gap towards the anode, producing cumulative ionization due to Townsend collisions. The negative charge on the glass wall is built up in this manner during the half-cycle of the applied field.
- (vi) When the density of the negative charge on the glass wall attains a requisite value, the electron avalanches moving towards the anode across the gap are repelled and get mixed up with a large number of positive ions which are already produced due to Townsend collisions during the passage of the electrons through the gap. This makes the gap highly conducting, and the gap gets bridged up.
- (vii) The pulse flashing across, when the gap gets bridged up, has been called by us *Townsend pulse*.

3. ORIGIN OF THE R.F. OSCILLATIONS IN A.C. 'SILENT' DISCHARGES

When the applied field is such that the negative charge on the glass surface is less than the requisite value for the *Townsend pulse* to pass, the electrons start from the virtual cathode and move across the gap under an *accelerating* field towards the stationary array of positive ions. After passing through the array of positive ions, the electrons come under a *retarding* field. In spite of the retarding field, some electrons with large velocities reach the glass surface, while others having relatively small velocities, turn back and move towards the array of positive ions. Some of these returning electrons pass through this array and come to rest somewhere near CC to be attracted once again towards the array of positive ions due to the accelerating field (see fig. 1b). Electronic oscillations of radio frequencies may thus

be set up near the glass surface opposite to the anode in a manner similar to the Barkhausen-Kurz oscillations in a triode. It is evident that these electronic oscillations are maintained till the density of the negative charge on the glass wall attains the requisite value for the Townsend pulse to pass, when, however, these oscillations cease and are immediately followed by a Townsend pulse. According to this view, therefore, the R.F. oscillations observed in a.c. 'silent' discharges are electronic oscillations of the B-K type and are maintained intermittently, each train being followed by a pulse.

4. EXPRESSION FOR THE FREQUENCY (OR WAVELENGTH) OF THE ELECTRONIC OSCILLATIONS IN THE A.C. 'SILENT' DISCHARGE

Consider any point in the discharge channel. The total electric field at that point is given by $X - X_1 + X_2$ where X is the uniform field due to the applied voltage, X_1 the field due to the negative charge on the glass wall and X_2 the field due to the stationary array of positive ions close to the glass wall. It is evident that at the stationary layer of positive ions, $X - X_1 = 0$ and the entire field is due to the positive ionic concentration and is equal to $2\pi\sigma_p$, where σ_p is the density of surface charge in the array of the positive ions. In considering the accelerating field within the gap, let us suppose that the total electric field at any point at a distance r from the virtual cathode is represented by

$$E = Af(r), \quad \dots \dots \dots (1)$$

where A is a constant. Then the potential of the positive ionic concentration with respect to the virtual cathode is given by

$$V_g = A \int_0^l f(r) dr \quad \dots \dots \dots (2)$$

where l is the length of the gap. The average field across the gap can be written as

$$\frac{A}{l} \int_0^l f(r) dr.$$

The average acceleration acting on the electron charge e and mass m moving towards the array of positive ions is then obtained from

$$a_1 = \frac{e}{m} \cdot \frac{A}{l} \int_0^l f(r) dr \quad \dots \dots \dots (3)$$

If v is the velocity of the electron when it reaches the layer of positive ions and t_1 the transit time across the gap then

$$v = a_1 t_1 = \left[\frac{e}{m} \cdot \frac{A}{l} \int_0^l f(r) dr \right] t_1 \quad \dots \dots \dots (4)$$

We shall now find the average *retarding* field across the double layer. Let σ_s be the density of negative charge on the glass wall. Then the field close to it may be taken as $4\pi\sigma_s$, which is very much larger than the applied field. The field close to the layer of positive ions is given by $2\pi\sigma_p$. Assuming here a linear field variation,

the average retarding field is then approximately equal to $\pi(\sigma_p + 2\sigma_s)$. The deceleration acting on the electron in this region of *retarding* field is then obtained from

$$-a_2 = \pi(\sigma_p + 2\sigma_s) \cdot \frac{e}{m} \quad \dots \quad \dots \quad \dots \quad (5)$$

If t_2 is the time when the velocity of the electron is reduced to zero, then the velocity of the electron at the positive ionic concentration is given by

$$v = \pi(\sigma_p + 2\sigma_s) \cdot \frac{e}{m} \cdot t_2 \quad \dots \quad \dots \quad \dots \quad (6)$$

From (4) and (6)

$$t_2 = \frac{\frac{A}{l} \int_0^l f(r) dr}{\pi(\sigma_p + 2\sigma_s)} \cdot t_1.$$

Since the field $4\pi\sigma_s$ due to the charge on the glass wall is very much greater than the average field

$$\frac{A}{l} \int_0^l f(r) dr$$

across the gap, $t_2 \approx 0$, and we can write $t_1 + t_2 \approx t_1$.

The frequency f of the electronic oscillation is then given by

$$f \approx \frac{1}{2t_1} \quad \dots \quad \dots \quad \dots \quad \dots \quad (7)$$

Again, since $l = \frac{1}{2}a_1 t_1^2$, we get

$$t_1 = \sqrt{\frac{2l}{a_1}}$$

Substituting the value of a_1 from (3), we have

$$t_1 = \sqrt{\frac{2l^2 \left(\frac{m}{e}\right)}{A \int_0^l f(r) dr}} = l \sqrt{\frac{2m/e}{V_g}} \quad \dots \quad \dots \quad \dots \quad (8)$$

From (7) and (8)

$$f = \frac{1}{2t_1} = \frac{1}{4l} \sqrt{V_g} \cdot \sqrt{\frac{2e}{m}}.$$

Expressing V_g in volts, the frequency of the electronic oscillation is given by

$$f = \frac{\sqrt{V_g}}{2l} \cdot 3 \times 10^7 \quad \dots \quad \dots \quad \dots \quad (9)$$

The corresponding wavelength in cms. is obtained from

$$\lambda = \frac{3 \times 10^{10}}{f} = 2000 \frac{l}{\sqrt{V_g}} \quad \dots \quad \dots \quad \dots \quad (10)$$

This is the well-known Barkhausen-Kurz formula for electronic oscillations in a triode with plane electrodes, when the anode is connected to the cathode, V_g being the grid voltage and l the distance between the anode and the cathode.

In the present case when electronic oscillations are set up in the a.c. 'silent' discharge, both l and V_g may vary within certain limits. A frequency band is thus expected when these oscillations are being built up. The predominant frequency should, of course, correspond to the instant when these oscillations cease and the Townsend pulse starts. This happens when the electric field attains a definite value E_0 .

5. GAP-LENGTH IN RELATION TO THE POTENTIAL OF THE ARRAY OF POSITIVE IONS

Let v_+ be the velocity of the positive ions moving towards the cathode through the gap; then

$$v_+ \propto \sqrt{V_g}.$$

If now t is the time during which the positive ions in the moving column attract and capture neighbouring electron avalanches and photo-ionized electrons forming thereby the highly conducting streamer, then the limiting length of the gap is given by $(v_+ \cdot t)$. As t depends on the positive ionic concentration and can be taken as some function of the electric field E , the length of the gap may be expressed as

$$l = v_+ \cdot t \propto \sqrt{V_g} \cdot \phi(E)$$

or

$$\phi(E) = K \cdot \frac{l}{\sqrt{V_g}} \quad \dots \quad \dots \quad \dots \quad \dots \quad (11)$$

where K is a constant.

At the time when the gap gets bridged up and the field E attains a certain definite value E_0 , it is evident from (11) that the ratio $\frac{l}{\sqrt{V_g}}$ should be taken as constant.

6. NON-DEPENDENCE OF THE WAVELENGTH OF THE R.F. OSCILLATIONS IN THE A.C. 'SILENT' DISCHARGE ON THE APPLIED VOLTAGE AND THE INTER-ELECTRODE DISTANCE

In finding the predominant wavelength of the R.F. oscillations in the a.c. 'silent' discharge, as given by (10), we have to consider the ratio $\frac{l}{\sqrt{V_g}}$, when the applied electric field has a definite value E_0 . For a given discharge tube, E_0 is constant, so that whatever be the applied voltage and the inter-electrode distance, the values of the gap-length l and the potential, V_g , of the positive ionic concentration must be such that the ratio $\frac{l}{\sqrt{V_g}}$ has always the same value. This explains the constancy of the wavelength of the oscillations observed by us, for a given discharge tube, for any applied voltage and inter-electrode distance.

In considering the particular case, when the magnitude of the applied a.c. voltage is kept fixed and the inter-electrode distance varied, we have to note that

the applied voltage varies sinusoidally and we are concerned with only those instantaneous values of the applied voltage which give the requisite electric field E_0 for the different inter-electrode distances. In considering the wavelength of the electronic oscillations, we have to take the values of the potential V_g of the positive ionic-concentration corresponding to these different instantaneous values of the applied voltage and also the corresponding values of the gap length l . Since

$\frac{l}{\sqrt{V_g}} = \text{const.}$, for $E = \text{const.}$, it follows that the wavelength of the electronic oscillations should be the same for different inter-electrode distances, even when the applied voltage is kept constant. This is what has been actually observed.

In the other particular case, when the inter-electrode distance is kept constant and the applied voltage varied, it can be seen that the wavelength of the electronic oscillations should be independent of the applied voltage. Even though the applied voltage is varied, there is a definite value of the applied voltage for which the electric field attains the requisite value E_0 . For this fixed value of the applied voltage, the potential V_g of the positive ionic concentration must also have a fixed value.

Further, since $\frac{l}{\sqrt{V_g}} = \text{constant}$ for $E = E_0$, the gap length l for the particular inter-electrode distance should also be constant. The wave-length of the oscillations for a given inter-electrode distance should therefore be the same for different applied voltages. This has been substantiated by our experimental results.

7. EFFECT OF LIGHT AND HEAT ON THE FREQUENCY OF THE R.F. OSCILLATIONS

The effect of light and heat on the frequency (or wavelength) of the R.F. oscillations in a.c. 'silent' discharges can be explained in consideration of the formula given by (9) or (10). When the negative charge on the glass surface is exposed to light, there is photo-electric emission and these photo-electrons come near the array of positive ions. Due to closer proximity with the photo-electrons, the attracting field increases resulting in an increase in the positive ionic concentration. This should increase the potential V_g of the array of positive ions, so that according to the formula (9) the frequency of the electronic oscillations is expected to increase on exposure to light. Such photo-increase in the frequency of the R.F. oscillations in a.c. 'silent' discharges has been actually observed.

On exposure to thermal radiations, the temperature of the gas or vapour in the discharge tube is raised. With the rise of temperature the diffusion of the positive ions increases, reducing thereby the concentration of the positive ions. Thus the potential V_g of the stationary array of positive ions is expected to be reduced, causing thereby, according to the formula (9), a decrease in the frequency of the electronic oscillations on exposure to thermal radiations. This has been actually observed in our experiments on the effect of heat on the frequency of the R.F. oscillations. It is interesting to note that at very high temperature when there is thermionic emission from the negative charge on the glass surface, an increase in frequency is expected in the same way as in the case of photo-electric emission. Thus when the temperature of the gas or vapour in the discharge tube is raised sufficiently, the effect of thermionic emission should increase the frequency, whereas greater diffusion of the positive ions due to higher temperature should decrease the frequency of the electronic oscillations. The decrease of frequency due to the latter cause may be counter-balanced to some extent by the increase of frequency due to thermionic emission. This may explain the observed fact that the decrease of frequency of the R.F. oscillations in a.c. 'silent' discharges is not as much as is expected at a comparatively high temperature.

8. MODULATION OF R.F. OSCILLATIONS BY A.F. PULSES IN A.C. 'SILENT' DISCHARGE

Attention will now be drawn to the fact that any current pulse during a discharge does not pass at all points on the surface. With regard to the Townsend pulses which are preceded by the R.F. electronic oscillations in an a.c. 'silent' discharge, it can be said that they pass at a finite number of points on the glass surface. Considering random distribution of these points on the glass surface over a finite interval of time, it is evident that the pulses occurring at a number of points may occur simultaneously with the R.F. oscillations which are set up prior to the pulses, which will occur at other points at some subsequent instant. The R.F. oscillations can, therefore, be modulated by the Townsend pulses. Such modulated R.F. oscillations are actually detected by the galvanometer in the anode circuit of the detector valve of a radio-receiver and also by the loud speaker at the receiver output.

9. CONCLUSIONS

Considering the streamer mechanism of Loeb and Meek, as applied to the a.c. 'silent' discharge, an electronic theory has been developed in the paper. According to this theory, the observed R.F. oscillations in the a.c. 'silent' discharge is regarded as trains of electronic oscillations of the Barkhausen-Kurz type maintained intermittently, each train being followed by what has been called a *Townsend pulse*. The expression for the frequency (or wavelength) of the electronic oscillations which has the same form as the Barkhausen-Kurz formula for electronic oscillations in a triode, has been taken as the basis for explaining the observed non-dependence of frequency (or wavelength) of the R.F. oscillations set up in a.c. 'silent' discharges on the inter-electrode distance and the applied voltage. The observed effects of light and heat on the frequency (or wavelength) of the R.F. oscillations in a.c. 'silent' discharges have also been explained. The statistical consideration of the fact that a current pulse during a discharge passes at a number of points distributed at random on the glass surface can also explain the observed modulation of the R.F. oscillations by the Townsend pulses.

ABSTRACT

An electronic theory of the origin of R.F. oscillations in a.c. 'silent' discharges is given in the paper. According to Loeb and Meek's streamer theory, when the applied field is adequate for Townsend's cumulative ionization, there is a conical distribution of positive ions drifting towards the cathode. In an a.c. 'silent' discharge, the negative charge formed on the intervening glass surface attracts the positive ions of the conical column and forms a stationary array of positive ions close to the glass surface. A gap is also set up between this stationary layer of positive ions and the moving column of positive ions which soon becomes highly conducting by attracting to itself electron avalanches and photo-ionised electrons. The gap is subsequently bridged up when the density of the negative charge on the glass surface attains a requisite value producing what has been called a Townsend pulse. Before this requisite density is attained, the gap exists and electronic oscillations of Barkhausen and Kurz type are set up near the glass surface opposite to the anode. These oscillations are maintained till the gap is bridged up. Accordingly we get electronic oscillations which are maintained intermittently, each train being followed by a Townsend pulse. The expression for the frequency (or wavelength) of the electronic oscillations has been shown to be of the same form as the Barkhausen-Kurz formula for electronic oscillations in a plane triode.

The theory explains the general features of the R.F. oscillations observed in a.c. 'silent' discharges. The effects of light and heat on the frequency of the oscillations recently observed by Khastgir, Setty and Srivastava are also explained.

10. REFERENCES

- *Khastgir, S. R. and Setty, P. S. V. (1952). Radio-frequency Oscillations in a.c. 'Silent' Discharges. *Curr. Sci.*, **21**, 197.
- and — (1953). Effect of light on the frequency of the R.F. Oscillations in a.c. 'Silent' Discharges. *Sci. & Cult.*, **18**, 435.
- and Srivastava, C. M. (1952). Effect of heat on the frequency of the R.F. Oscillations in a.c. 'Silent' discharges. *Curr. Sci.*, **21**, 307.
- and — (1953). Streamer Mechanism in a.c. 'Silent' discharges. *Ind. Journ. Physics*, **27**, 109; *Sci. & Cult.*, **18**, 487.
- Loeb, L. B. and Meek, J. M. (1941). 'Mechanism of Electric Spark'. Stanford University Press.
- Prasad, B. B. (1949). Production of Joshi Effect in the aerial current under electrical discharge in chlorine. *Proc. Ind. Acad. Sc.*, **29**, 322.
- Warburg, (1903). *Verhand. Deutsch. Phys. Ges.*, 382.

Issued June 25, 1954.

ON THE ALGAL GENERA *NEOMERIS* AND *ACICULARIA* FROM THE NINIYUR (DANIAN) BEDS OF THE TRICHINOPOLY AREA (S. INDIA)

by C. P. VARMA, *Birbal Sahni Institute of Palaeobotany, Lucknow*

(Communicated by S. R. N. Rao, F.N.I.)

(Received December 21, 1953; read May 7, 1954)

INTRODUCTION

The Cretaceous system of South India exposed in the Trichinopoly district comprises (in descending order) the following stages:—

Niniyur (Danian),
Ariyalur (Maestrichtian),
Trichinopoly (Turonian-Senonian), and
Utatur (Cenomanian).

Rocks of the Niniyur group comprise fossiliferous limestones and cherts. The presence of fossil algae in these rocks was first recognised by L. R. Rao (1931) and they were described by Pia (1936). The algae described in this paper are from the same horizon and include forms which were either not described previously or were insufficiently described by Pia (Rao and Pia, 1936) in their memoir on the Niniyur algae. The present material was collected by Prof. S. R. N. Rao from the Mattur and Nattakuli localities. As the rock is of a very compact nature the algae had to be studied in thin sections of the rock.

GENERIC CHARACTERS AND THE CLASSIFICATION OF THE GENUS *NEOMERIS*

Diagnostic characters of the genus *Neomeris*, according to Pia (1927, p. 82), 'Die Enden der Äste zweiter Ordnung bilden eine zusammenhängende Rindenschicht. Das Sporangium ist birnförmig, nicht so kugelig, wie bei *Meminella* und *Lemoineella*. Es scheint, dass bei der Gattung *Neomeris* und vielleicht bei der ganzen Untertribus niemals halbrund geschlossene obere Enden der kalkschale auftreten, sondern dass diese stets beiderseits offen ist.'

It is clear from the above diagnosis that the genus is characterised by a pyriform (birnförmig) sporangium, a fact which helps to separate this genus from the allied genera *Meminella* and *Lemoineella* which possess spherical sporangia. Fritsch (1945, p. 391) notes the occurrence of spherical to ovoid gametangia (sporangia) also in the living representatives of this genus.

Fossil *Neomeris* has been treated into two sections *Decaissnella* Mun.-Ch. and *Vaginopora* Defrance by Morellet and Morellet (1913, 1939). *Decaissnella* includes these species of the genus *Neomeris* which are found as detached complete rings or fragments of rings. In *Vaginopora* the rings are found cemented together in the form of a tube. Pia has, however, treated (1927, p. 82-83) the genus *Neomeris* into three sections, viz. *Decaissnella*, *Vaginopora* and *Larvaria*. The genus *Larvaria* Defrance according to him does not possess characters sufficient to deserve a generic status and has, therefore, been included under *Neomeris*.

GEOLOGICAL HISTORY OF *NEOMERIS* AND ITS PREVIOUS RECORDS IN INDIA

Out of the twenty-three species of fossil *Neomeris* 22 belong to the Tertiary formations and only one, viz. *N. cretacea* Steinmann (1899, p. 149) is known from the

Cenomanian stage of the Cretaceous system. The alga described by Raineri (1922) as *N. cretacea undulata* from (Lüneburgian flora) Libya has been revised by Pia (1936, pp. 4-5) to *Dissocladella undulata*, but several other fragments from the same rock have been assigned to *Neomeris* without specific identifications. In India this genus has been recorded from the Inter-trappean (Paleocene) beds of Rajahmundry (J. Pia, S. R. N. Rao and K. S. Rao, 1937) from where the authors have described four forms *a*, *b*, *c* and *d*.

Neomeris (*Decaisnella*) sp. A.

(Pl. IX, figs. 1 and 7)

Description.

Algae from this area have been recognised only in thin rock sections. The genus (Pl. IX, fig. 1) is represented by a broken ring, the section passing somewhat obliquely. Since a section passing through the length of a tube of rings has so far not been obtained and a sporangium with its secondary branches lies in the same plane, the specimen is provisionally referred to the section *Decaisnella*.

In one fragment of ring (Pl. IX, fig. 1) 5 oval sporangia (4 distinctly and one indistinctly) are noticeable with a corresponding number of parts belonging to the calcified primary branches. That each sporangium had two lateral branches is evident from the sporangium on the extreme left. Branches from the adjacent verticil may be noticed owing to the somewhat oblique nature of the section. The sporangia are ovoid (Pl. IX, figs. 1 and 7). In *Neomeris* sp. A. the calcification extends to the primary branches which are, therefore, well preserved (cf. *N. dumetosa*). The most well preserved part of the fragmented ring (Pl. IX, fig. 1) shows the two laterals (secondary branches) arising out of the primary branch, and surround an ovoid sporangium. The sporangia seem to be nearly sessile to sub-sessile.

Measurements.

Length of the sporangium	0.130 mm.
Breadth of the sporangium	0.106 mm.
Length of the secondary branch	0.208 mm.
Breadth of the secondary branch at the base	0.02 mm.
Breadth of the secondary branch at the tip	0.052 mm.

Comparison.

The above description indicates that the specimen belongs to the tribe Neomereae and warrants comparison with the sub-genus *Decaisnella* characterised by 2 sterile secondary branches and a fertile one, borne on a primary branch, all lying in the same plane.

Lemoinema, *Meminella*, *Larvaria* and *Neomeris* are the forms possessing a single sporangium with two sterile secondary laterals on each primary branch arranged in verticils. *Lemoinema* shows a polygonal cross-section of the axial tube bearing a spherical sporangium surrounded by two secondary branches. Although the shape of the cross-section of the axis of our specimen is not revealed, yet it can be distinguished from *Lemoinema* by the ovoid shape of the sporangium. It is also distinguished from *Meminella* in which the sporangium is spherical and lateral, while the two secondary branches lie in the plane of the primary branch extensions. The genus *Larvaria* possesses ovoid sporangia which are placed in a plane different from that of the two laterals.

Montiella is quite different in having only two secondary branches on each primary branch, one (upper) which becomes swollen at the distal end forming an ovoid sporangium which in *Neomeris* terminates in the primary branch. Our specimen cannot be referred to any of the above and its characters indicate that it belongs to *Neomeris*.

N. sp. A. is different from *N. cretacea* Steimann which possesses distinctly stalked and pyriform sporangia.

The species described from Rajahmundry (Pia *et al.*, 1937) do not offer any similarity with this form. Thus the form seems to represent a new species in having a decidedly sessile to sub-sessile ovoid sporangia but a specific name has not been given in view of the incomplete information available at present.

Neomeris (*Vaginopora*) sp. B.

(Pl. IX, figs. 2 and 3)

Description.

This species is represented by many fragments representing parts of rings. In all cases the segments of rings are seen to possess the characteristic pear-shaped sporangia (Pl. IX, figs. 2 and 3). In one of the best fragments (Pl. IX, fig. 2) which is cut obliquely there are seen six sporangia represented entirely or in parts. The first, second and third sporangia counting from the left are well preserved and their pyriform shape indicates that the specimen is a *Neomeris*. Owing to the oblique nature of the section the secondary branches of an adjacent ring are also seen. At the bases of the first and the third sporangia there are definite clues of the two secondary laterals borne by evidently uncalcified branches of the first order. The third sporangium shows a secondary branch which approaches on the left side of the stalk of the sporangium very closely so that its attachment could be reasonably inferred, while on the right side the secondary branch is represented only by a small basal fragment. This form does not seem to have had calcified primary branches.

Measurements.

Length of the sporangium	0.165 mm.
Breadth of the sporangium	0.066-115 mm.
Width of the secondary branches	0.02 mm.

Comparison.

Neomeris sp. B. shows a great similarity with *N. cretacea* Steimann with respect to the size and shape of the sporangia. While describing the sporangia Steinmann (1899, p. 150) states, 'Die birn-oder keulenförmige Ausweitung ist 0.13-0.16 mm. lang und bis zu 0.1 mm. dick; die Länge des Stiel beträgt durchschnittlich 0.1 mm.' But in *N. sp. B.*, as in *N. sp. A.*, we do not know the external and internal diameter of the axial cell and therefore, it is difficult to assign *N. sp. B.* directly to *N. cretacea* with which it resembles so much.

REMARKS ON *ACICULARIA* AND THE ALLIED GENERA OF THE FAMILY ACETABULARIACEAE.

Among the Dasycladaceae, Acetabulariaceae display a highly specialised structure. The various genera included in the tribe exhibit an upright main axis generally bearing alternate verticils of the sterile and fertile whorls extending laterally. A great majority of the forms included in the sections: *Acetabuloides* and *Acetabulum*, produce only a single fertile whorl at the tip. *Acetabularia* (Section: *Acetabuloides*) *crenulata* Lmx. is an exception where the sterile and fertile whorls alternate as in the case of *Halicoryne* Harvey. The most peculiar feature of the sub-family is the form of its reproductive bodies which are much elongated assuming a digitate (as in some fossil forms) to pod-like shape bearing the rounded gametes. Only two of the four living genera, viz. *Acetabularia* and *Acicularia* are represented by their fossil forms. The genera *Chalmasia* Solms and *Halicoryne*



1



2



3



5



6



4



7

Harvey are living forms without a fossil record while (?) *Örioporella* Mun.-Ch., and *Clypeina* Mich. have been recorded only as fossils. It is interesting to note here that the systematic position of the genus *Clypeina* Mich. is still undecided. Pia (1927, p. 68) has put it under the tribe—Dipolporeae and the sub-tribe Macroporellinae while Morellet and Morellet (1913, 1918, 1922, 1939) have included it under Acetabulariaceae.

Acetabularia and *Acicularia* are the only two genera of the family Acetabulariaceae which have both living and fossil forms. *Acicularia* is distinguished from *Acetabularia* in having a deposit of lime even in the cavity of the sporangium which results, on disintegration of the fertile verticils, in dissociating into a number of calcareous spicules pointed at the proximal and broader at the other (distal) end, affording a honey-combed structure due to a peculiar arrangement of the calcified spore cavities.

It is very interesting to note that *Acicularia* was first discovered as a fossil and later found to be represented by a living species also. *Acicularia* was the name given by d'Archiac in 1843 to small longish bodies, pointed at one end, broad and emarginate at the other. D'Archiac did not know the exact nature of these bodies when he named them and referred them to Bryozoa. The opinion was shared by Michelin and Ruess, while Carpenter placed them among the foraminifera. It was as late as in 1877 when Munier-Chalmas recognised the radial partition walls and their radially disposed habit which led him to remove *Acicularia* from the animal kingdom and place them with the Acetabulariaceae. Though a plant nature had been suggested, there was yet no proof to substantiate the proposition till a living species of the genus *Acicularia schenckii* (Möb) Solms (1895–1901) came to light.

DIAGNOSIS AND CLASSIFICATION OF FOSSIL ACICULARIAS.

The diagnostic characters of the genus as noted by Morellet's (1913, p. 31) are as follows:—

'Spicules calcaires (sporangies), élargis à une extrémité, isolés ou associés latéralement, à section circulaire ou aplatie, creusés à la périphérie d'un grand nombre de petites cavités sphériques (spores).'

The genus *Acicularia* is divided into two sections *Acicularia* (sensu-stricto) and *Briardina* Mun.-Ch. *Acicularia* (sensu-stricto) includes spicules in which the rounded cavities are generally distributed peripherally round the spicule. In section *Briardina* are included flattened spicules in which the circular cavities are distributed along the superior and inferior margins only.

GEOLOGICAL HISTORY AND PREVIOUS RECORDS OF ACICULARIA IN INDIA.

Acicularia is represented by a single living form *A. schenckii* Solms and has about 18 fossil species. It makes its first appearance in the Cretaceous. The fossil history of the allied genus *Acetabularia* extends back to Oligocene only.

In India the genus *Acicularia* has so far been recorded from Trichinopoly (Rao and Pia, 1936) Rajahmundry (Pia, Rao and Rao, 1937) and the Punjab Salt Range (Rao and Varma, 1950).

Acicularia indica sp. nov.

(Pl. IX, figs. 4, 5 and 6)

Diagnosis.

Spicules short, stout and club-shaped; about 5 times as long as its maximum breadth. Biconvex to lenticular in cross-section and studded with about eight rows of gamete cavities.

Measurements.

Length of the spicule	1.62 mm.
Maximum breadth of the spicule	0.38 mm.
Breadth at the proximal part	0.18 mm.
Gamete cavity	0.08-0.12
		mostly	0.09 mm.

Description.

Acicularia indica is represented by many sections cutting the spicules crosswise and one section passing in an oblique plane exposing the structure of the spicule lengthwise and the typical arrangement followed by the calcified spore cavities (gamete cavities).

A spicule of *A. indica* is seen containing the gamete cavities all round the margin (Pl. IX, fig. 5). It typically shows a narrow proximal end and rounded, emarginate distal part. The narrow proximal end does not show any trace of a corona like part. Some of the gamete cavities, generally rounded, seem to open on the surface of the spicule. The spicules of this species are short, stout and slightly curved attaining a club-shaped structure but not hooked as in *A. dyumatsenae*. The spicules seem to possess about eight rows of spore cavities studded along the periphery (Pl. XI, fig. 4).

Comparisons.

In assigning this species to *Acicularia* and not to *Terquemella* I have been guided by the following differences between the two genera noted by Pia (1936, p. 25): 'The calcareous substance contained in the compartments of the disc of *Acicularia* has the form of a spicule or a slender club. *Terquemella* is represented by calcareous bodies of a similar general structure (and with similar spore cavities), but of a spherical, discoid or tuberous form.'

For a generic identification we have obviously to consider *Acetabularia*, *Terquemella* and *Acicularia* only. Though *Acetabularia* and *Acicularia* both possess the type of spicules we are dealing with, the former possesses calcified gametangia with uncalcified cysts. Thus *Acetabularia* is ruled out simply by the presence of the rounded gamete cavities inside the gametangium (spicule). Similar spore cavities are present in another genus *Terquemella* with a spherical, discoid or tuberous form. *Terquemella* is segregated because of the presence of club-shaped spicules, a character which directly favours its inclusion among the *Acicularias*. As explained by Pia, Pfender and Termier (1932, p. 14) it is extremely difficult to compare accurately the *Acicularia* in rock sections with those found in loose material. Also one more difficulty arises because the authors of the Tertiary *Acicularias* have in majority of cases, not given the measurements of the gamete cavities.

As already indicated the gamete cavities are arranged all round the periphery and not restricted to the inferior and superior margins only, thereby calling forth only those species for comparison which belong to the section *Acicularia* (sensu stricto). The following Tertiary species *A. michelini*, *A. micropora* and *A. (?) clavata* have been stated to be slightly curved but differ in not having bi-convex or lenticular cross-sections and possess spicules of smaller dimensions as compared to *A. indica*. Moreover, the size of the gamete cavities is not known making a comparison more difficult. Another species with elliptical sections is *A. persica* Morellet and Morellet (1939, p. 31-32) which differs in having spicules of much greater length with marginate, truncated (slightly rounded) distal ends showing no curvature, possessing vaguely distributed gamete cavities measuring 0.1 mm. The maximum breadth of the spicules on average is not mentioned but a calculation from the photograph indicates the maximum breadth to be about 0.5 mm.

Among the Cretaceous species known so far, only two in number, *A. dyumatsenae* Pia and *A. antiqua* Pia are to be considered. Length of the spicules of *A. dyumatsenae* is stated to be about $2\frac{1}{2}$ times its maximum breadth, with hooked spicules and gamete cavities measuring about .05 mm. It is clearly marked out from *A. indica* found in the same rock by the shape and size of the spicules and the dimensions of the gamete cavities. *A. antiqua* known from Tripoli (N. Africa) in the form of oblong discs, unhooked spicules, length not exceeding twice its breadth (breadth 0.33) with gamete cavities .04–.05 mm., is again different from the new form.

Another Indian *Acicularia* sp. Ind. is described from Rajahmundry (Pia *et al.*, 1937, p. 283) as possessing long needle-shaped spicules with their gamete cavities about 0.07 mm. in diameter. This species also does not bear any specific similarity with *A. indica*. I have not been able to collect the data for *A. italica* Clerici, which could not, therefore, be considered.

SUMMARY

From the Cretaceous (Danian) rocks of the Trichinopoly district *Neomeris* sp. A. *Neomeris* sp. B. and *Acicularia indica* sp. nov. have been figured and described.

ACKNOWLEDGEMENT

I am deeply indebted to Prof. S. R. N. Rao for the loan of the material and his helpful suggestions.

REFERENCES

- Fritsch, F. E. (1945). The structure and reproduction of the algae. 1, *Cambridge Univ. Press*.
- Morellet, L. and J. (1913). Les Dasycladacées du Tertiaire Parisien. *Mém. Soc. Géol. France, Paléont.*, 21 (1), *Mém.* 47, 1–42.
- Morellet, L. (1916). Notes sur les Algues Siphonées Vorticillées. In H. Douvillé's 'Le Crétacé et l'Éocène du Tibet Central', *Pal. Ind. N.S.*, 5, *Mem.* 3, 47–49.
- Morellet, L. and J. (1922). Nouvelle contribution à l'étude des Dasycladacées tertiaires., *Mém. Soc. Géol. France, Paléont.*, 25 (2), *Mém.* 58, 1–35.
- Morellet, L. and J. (1926). Les Dasycladacées du Néogène de Kostej (Banat et de Lapugy (Transylvanie)). *Bull. Soc. Géol. France*, 26 (4), 223–228.
- Morellet, L. and J. (1939). Sur une espèce nouvelle d'*Acicularia* du Sarmatien moyen d'Azam, Iran septentrional. *Eclog. Géol. Helvetiae*, 32 (1), 31–32.
- Morellet, L. and J. (1939). Tertiary Siphonous Algae. *Brit. Mus. (Nat. Hist.)*, London.
- Pia, J. (1927). In Hirmer's 'Handbuch der Paläobotanik'. *München*.
- Pia, J. (1936). Calcareous green algae from upper Cretaceous of Tripoli (N. Africa). *Journ. Palaeont.*, 10 (1), 3–14.
- Pia, J., Pfender, J. and Termier, H. (1932). Études géologiques sur les calcaires de Bekrit et de Timhadit (Moyen Atlas). *Mém. Serv. Carte Géol. Maroc.*, No. 20, p. 14.
- Pia, J., Rao, S. R. N. and Rao, K. S. (1937). Dasycladaceen aus Zwischenalgen des Dekkan-trapps bei Rajahmundry in Sudindien. *Akad. Wiss. Wien, Abteil 1*, 146 (5-6), 221–236.
- Rao, L. R. (1931). On the occurrence of *Lithothamnion* in S. Indian Cretaceous. *Nature*, 128, p. 225.
- Rao, L. R. and Pia, J. (1936). Fossil algae from the uppermost Cretaceous beds (the Niniyur group) of the Trichinopoly district, S. India. *Pal. Ind. N.S.*, 21 (4), 1–49.
- Rao, S. R. N. and Varma, C. P. (1950). Tertiary microfossils from the cherts of the Saline Series. *Palaeobotany in India*, 19 (1), p. 28.
- Solms-Laubach, H. (1895). Monograph on the Acetabulariaceae. *Trans. Linn. Soc. London*, ~~2~~ Ser. 2, Bot. 5 (1), 1–41.
- Steinmann, G. (1899). Über fossile Dasycladaceen vom cerro Escamela, Mexico., *Bot. Zeit.*, 57 (8), 137–154.
- Varma, C. P. (1952). *Clypeina* (Dasycladaceae) from the Cretaceous of South India. *Palaeobotanist*, 1, 439–441.

EXPLANATION OF PLATE IX

- FIG. 1. *Neomeris* sp. A. A somewhat oblique section of a fragment of ring showing parts of the calcified primary branches, the four sessile to sub-sessile ovoid sporangia with secondary branches (Type specimen). $\times 72$.
- FIG. 2. *Neomeris* sp. B. An oblique section of a fragment of a ring showing six sporangia with some secondary branches. (Type specimen.) $\times 72$.
- FIG. 3. *Neomeris* sp. B. A nearly vertical section passing through the wall showing the stalked pear shaped sporangia and the secondary branches. $\times 72$.
- FIG. 4. *Acicularia indica* sp. nov. A transverse section of the spicule indicating about eight rows of circular gamete (spore) cavities. $\times 45$.
- FIG. 5. *Acicularia indica* sp. nov. A longitudinal section passing through the entire length of a spicule. (Type specimen). $\times 45$.
- FIG. 6. *Acicularia indica* sp. nov. An obliquely longitudinal section passing through the thickness of a spicule. $\times 45$.
- FIG. 7. *Neomeris* sp. A. An oblique section cutting through three adjoining rings. $\times 72$.

Issued June 26, 1954.

A GENERALIZATION OF CANTOR BENDIXON THEOREM

by K. PADMAVALLY, *Research Fellow, N.I.S.I., Ramanujan Institute of Mathematics, Madras*

(Communicated by T. Vijayaraghavan, F.N.I.)

(Received January 6 ; read May 7, 1954)

Cantor Bendixon theorem gives an upper limit to the stage at which the process of repeated derivation* of a set in Euclidean space stops. The final form of the result given by Cantor (1884) is: For every subset X of a Euclidean space there exists an ordinal γ [$=\gamma(X)$] of the first or second class such that $X^{(\gamma)}$, the γ -th derivative of X , $=X^{(\gamma+1)}$. This note gives a partial extension of this theorem for spaces other than Euclidean spaces. The result is based on the notion of 'intersection character' of a space at a point, which is defined by Alexandroff (1924) as the least cardinal number of a family of neighbourhoods of the point whose intersection is the point. The intersection character of a T_1 -space is evidently defined at every point. Also for a Euclidean space the intersection character at every point is \aleph_0 , so that \aleph_1 is a regular† cardinal number greater than the intersection character of the space at every point. Cantor Bendixon theorem implies that for every subset X of a Euclidean space, $X^{(\omega_1)} = X^{(\omega_1+1)}$ (ω_1 being the initial ordinal corresponding to the cardinal \aleph_1 , i.e., the first ordinal of the class of ordinals each having power \aleph_1). The following result will be seen to be a generalization of this statement.

If R is a regular space (i.e. a T_1 -space in which every neighbourhood of any point contains the closure of another neighbourhood of the point) which is locally bicomact at every point and \aleph_α any regular cardinal number greater than the intersection character of R at every point, then for every set $X \subset R$, $X^{(\omega_\alpha)} = X^{(\omega_\alpha+1)}$.

If possible let p be a point of $X^{(\omega_\alpha)} - X^{(\omega_\alpha+1)}$. Then p is an isolated point of $X^{(\omega_\alpha)}$ and hence has a neighbourhood U such that $U \cap X^{(\omega_\alpha)} = p$. Since R is regular, $U \supset \bar{V}$, the closure of another neighbourhood V of p . Also since R is locally bicomact at p , p has a neighbourhood W such that \bar{W} is bicomact. Let \aleph_p denote the intersection character of R at p . Then p has a set $\{U_\gamma\}_{\gamma < \omega_p}$ of neighbourhoods such that $\cap_{\gamma < \omega_p} U_\gamma = p$. Let $V_\gamma = U_\gamma \cap V \cap W$.

Then $\bar{V}_0 \cap X^{(\omega_\alpha)} = p$ and $\cap_{\gamma < \omega_p} V_\gamma = p$. Hence for each of the sets $\bar{V}_0 - V_\gamma$ (which is closed since V_γ can be taken to be open), $(\bar{V}_0 - V_\gamma) \cap X^{(\omega_\alpha)} = \emptyset$, and $\bar{V}_0 = p \cup \sum_{\gamma < \omega_p} (\bar{V}_0 - V_\gamma)$. Also $X^{(\omega_\alpha)} \cap (\bar{V}_0 - V_\gamma)$ is the inner limiting set of the decreasing series of closed sub-sets $\{(\bar{V}_0 - V_\gamma) \cap X^{(\beta)}\}$, $\beta < \omega_\alpha$, of the bicomact space \bar{W} .

* For any ordinal β the β -th derivative $X^{(\beta)}$ of X is defined by induction as $= \cap_{\gamma < \beta} X^{(\gamma)}$

if β is a limiting ordinal, and $=$ the derivative of $X^{(\gamma)}$ if β is a nonlimiting ordinal $= \gamma + 1$.

† The initial ordinal ω_α of the class of ordinals each having power \aleph_α is said to be regular (Hausdorff, 1908) if every subseries of ω_α cofinal with ω_α is similar to ω_α .

Therefore some member of the series is null. i.e. for each $\gamma < \omega_p$ there exists $\beta [= \beta(\gamma)] < \omega_\alpha$ such that $(\bar{V}_0 - V_\gamma) \cap X^{\beta(\gamma)} = 0$. But since by hypothesis the cardinal number N_p of the set $\{\beta(\gamma)\}_{\gamma < \omega_p}$ is less than N_α , and each $\beta(\gamma) < \omega_\alpha$, and ω_α is a regular initial ordinal, there exists $\beta' < \omega_\alpha$ such that each $\beta(\gamma) \leq \beta'$. Hence each $(\bar{V}_0 - V_\gamma) \cap X^{(\beta')} = 0$, and therefore $X^{(\beta')} \cap \bar{V}_0 = \{p \cup \Sigma_{\gamma < \omega_p} (\bar{V}_0 - V_\gamma)\}$. $\cap X^{(\beta')} \subset p$. Hence p is an isolated point of $X^{(\beta')}$ and therefore p is not $\epsilon X^{(\beta'+1)}$, which contradicts the hypothesis that $p \in X^{(\omega_\alpha)}$, since $\beta'+1 < \omega_\alpha$ (β' being $< \omega_\alpha$ and ω_α being a limiting ordinal).

Since a Euclidean space is regular and locally bicomact at all points, this clearly implies the result stated above. The result corresponding to Cantor Bendixon theorem for a T_1 -space will be: If N_α is a regular cardinal number greater than the intersection character of the space at every point, then for every set X there exists an ordinal $\gamma [= \gamma(X)] < \omega_\alpha$ such that $X^{(\gamma)} = X^{(\gamma+1)}$. The following example shows that this result does not hold in general for all regular bicomact spaces.

Consider the ordered set R consisting of all complexes (x_0, x_1) where x_0, x_1 are any numbers in the interval $0 \leq x < 1$, ordered so that $(x_0^1, x_1^1) < (x_0^2, x_1^2)$ if either $x_0^1 < x_0^2$, or $x_0^1 = x_0^2$ and $x_1^1 < x_1^2$, under its order topology (in which the open sets are all open intervals). The intersection character of every point is clearly N_0 , since every point is easily seen to be the limit of a well ordered sequence similar to ω as well as an inversely well ordered sequence similar to ω^* , the inverse of ω . But the process of derivation of the set X constructed below can be seen to stop only at the ω_1 -th stage.

Since the set of values of x_0 (which is the set of all numbers in $(0, 1)$) has power $2^{N_0} > N_1$, it is possible to find a subset of this set say, Q , having power N_1 , which can therefore be well ordered as an ω_1 series $\{x_0^\beta\}_{\beta < \omega_1}$ (x_0^β being $= x_0^{\beta'}$ if and only if $\beta = \beta'$). For each $\beta < \omega_1$ let I_β denote the interval or R given by (i.e., consisting of all complexes satisfying the equation) $x_0 = x_0^\beta$ ($= \text{constant}$), (x_1 being unrestricted in the open interval $(0, 1)$). Then the I_β 's form a set of disjoint intervals each similar to the open real number interval $(0, 1)$. It has been proved by Cantor that in any interval of the real number space corresponding to any given ordinal γ a set X can be found such that $X^{(\beta)} \neq X^{(\beta+1)}$ for all $\beta < \gamma$. Hence in each interval I_β a set X_β can be found such that $X_\beta^{(\gamma)} \neq X_\beta^{(\gamma+1)}$ for all $\gamma < \beta$. Then if $X = \bigcup_{\beta < \omega_1} X_\beta$, it is clear that since the intervals

I_β are disjoint with each other, for every $\gamma < \omega_1$, $X^{(\gamma)} \cap I_\beta = X_\beta^{(\gamma)}$ and hence for every $\gamma < \omega_1$, $X^{(\gamma)} \neq X^{(\gamma+1)}$.

This paper formed part of a thesis submitted for the M.Sc. Degree of the Madras University. I wish to thank Dr. R. Vaidyanathaswamy, Dr. M. Venkataraman and Dr. V. S. Krishnan for their help and guidance.

SUMMARY

This paper gives a generalization of a well-known result of Cantor and Bendixon to Hausdorff bicomact spaces.

BIBLIOGRAPHY

- Alexandroff (1924). Über die struktur der bikompakten topologischen Räume. *Math. Ann.*, **92**, 267-274.
 Cantor (1884). Ueber unendliche Punktmannichfaltigkeiten, *Ibid.*, **23**, 453-488.
 Hausdorff (1908). Grundzuge einer Theorie der geordneten Mengen, *Ibid.*, **65**, 435-505.

RELATION BETWEEN MAXIMUM PRESSURE AND SHOT-START PRESSURE

by S. P. AGGARWAL, *Defence Science Organization, Ministry of Defence, New Delhi*

(Communicated by R. S. Varma, F.N.I.)

(Received August 1, 1953; read May 7, 1954)

1. INTRODUCTION

The main problem of Internal Ballistics is the calculation of Maximum Pressure and Muzzle Velocity for given loading conditions in a gun.

The equations of Internal Ballistics in their general form are such that it is not possible to integrate them directly but can be treated by numerical integration or by the use of differential analyser. Mr. N. S. Venkatesan (1952) has recently given an explicit expression for the relation between the maximum pressure and shot-start pressure and has solved the equations of Internal Ballistics under the assumptions (Corner, 1950) $\theta = 0$, i.e., the propellant is tubular in shape and (Corner, 1951) $B = 0$, i.e., neglecting the covolume correction for gases.

The object of this paper is to extend the results of Mr. Venkatesan and obtain an explicit expression for the relation between maximum pressure and shot-start pressure for all values of θ . We shall assume that $B = 0$, i.e., the covolume of the gases equals the reciprocal of the density of the solid propellant. This is generally true except at high densities of loading.

2. FUNDAMENTAL EQUATIONS

The four fundamental equations of the Internal Ballistics, in non-dimensional parameters, are shown, in standard books, (Corner, 1950 and 1951), to be

$$z = \zeta (\xi - Bz) + \frac{\gamma - 1}{2M} \eta^2 \quad \dots \quad (1)$$

$$M\zeta = \eta \frac{d\eta}{d\xi} \quad \dots \quad (2)$$

$$\zeta = -\eta \frac{df}{d\xi} \quad \dots \quad (3)$$

$$z = (1-f)(1+\theta f) \quad \dots \quad (4)$$

where

$$\xi = 1 + \frac{x}{l}$$

$$\eta = \frac{AD}{F\beta C} v$$

$$\zeta = \frac{Al}{FC} p$$

$$M = \frac{A^2 D^2}{F\beta^2 C m_1} \text{ (Central Ballistic Constant).}$$

For $\beta = 0$ the above equations reduce to

$$z = \zeta \xi + \frac{\gamma-1}{2M} \eta^2 \quad \dots \quad \dots \quad \dots \quad \dots \quad (I)$$

$$M\zeta = \eta \frac{d\eta}{d\xi} \quad \dots \quad \dots \quad \dots \quad \dots \quad (II)$$

$$\zeta = -\eta \frac{df}{d\xi} \quad \dots \quad \dots \quad \dots \quad \dots \quad (III)$$

$$z = (1-f) (1+\theta f) \quad \dots \quad \dots \quad \dots \quad \dots \quad (IV)$$

The initial conditions at the shot-start are,

$$\xi = 1; \eta = 0; \zeta = \zeta_0 \quad \text{and} \quad z = z_0.$$

From (I) we see that $z_0 = \zeta_0$ so that z_0 itself is a measure of shot-start pressure.

From (II) and (III) we obtain that

$$M = -\frac{d\eta}{df}.$$

Integrating this we get,

$$\eta = M (f_0 - f), \text{ where } f = f_0 \text{ when } \eta = 0. \quad \dots \quad \dots \quad (5)$$

Also from (IV), $z_0 = (1-f_0) (1+\theta f_0)$, so that we can express f_0 in terms of z_0 and f in terms of z , and hence from (5), z can be expressed in terms of η and z_0 .

Equation (IV) can be written as:

$$\theta f^2 - (\theta-1)f + (z-1) = 0$$

$$\therefore f = \frac{(\theta-1) \pm \sqrt{(\theta+1)^2 - 4\theta z}}{2\theta}$$

and hence

$$f_0 = \frac{(\theta-1) \pm \sqrt{(\theta+1)^2 - 4\theta z_0}}{2\theta}$$

Hence equation (5) becomes,

$$\eta = \pm \frac{M}{2\theta} \left[\sqrt{(\theta+1)^2 - 4\theta z_0} - \sqrt{(\theta+1)^2 - 4\theta z} \right] \quad \dots \quad \dots \quad (6)$$

Now $\eta = \frac{AD}{F\beta C} v$; A, D, F, β, C and v are all positive, therefore η is also positive.

As t increases z increases; therefore $z > z_0$ and also the maximum value of z is unity. Since η is always positive, we have to choose the positive sign in (6). Substituting the value of ζ from (II) in equation (I) we have,

$$z = \frac{\eta}{M} \frac{d\eta}{d\xi} \xi + \frac{\gamma-1}{2M} \eta^2$$

or

$$\frac{d\xi}{\xi} = \frac{\eta \frac{d\eta}{d\xi}}{Mz - \frac{\gamma-1}{2} \eta^2} \quad \dots \quad \dots \quad \dots \quad (7)$$

Equation (6) can be written as :

$$\frac{2\theta\eta}{M} = \left[a - \sqrt{(\theta+1)^2 - 4\theta z} \right]$$

where

$$a = \sqrt{(\theta+1)^2 - 4\theta z_0}$$

Squaring and making some simplification, we have,

$$Mz = \frac{1}{M} \left[M^2 z_0 + aM\eta - \theta\eta^2 \right], \text{ for all values of } \theta, \text{ negative or positive.}$$

Substitution of this value of Mz in equation (7) gives,

$$\frac{d\xi}{\xi} = \frac{2M\eta d\eta}{2M^2 z_0 + 2aM\eta - (\gamma-1)M + 2\theta)\eta^2} \quad \dots \quad (8)$$

Hence

$$\frac{d\xi}{\xi} = \frac{2M\eta d\eta}{G + 2F\eta - E\eta^2},$$

where

$$G = 2M^2 z_0, F = aM, E = (\gamma-1)M + 2\theta$$

Integration of this equation gives,

$$\frac{1}{M} \log \xi = -\frac{1}{E} \log (G + 2F\eta - E\eta^2) - \frac{F}{E^2 K} \log \frac{\eta - \frac{F}{E} - K}{\eta - \frac{F}{E} + K} + \text{constant}$$

$$\text{where } K = \sqrt{\left(\frac{G}{E} + \frac{F^2}{E^2} \right)}$$

Initially, when $\xi = 1$, $\eta = 0$, $\xi = \xi_0$ and $z = z_0$ and hence the value of the constant is,

$$\log G^{\frac{1}{E}} \left[\frac{-\frac{F}{E} - K}{-\frac{F}{E} + K} \right]^{\frac{F}{E^2 K}}$$

Therefore

$$\frac{1}{M} \log \xi = -\frac{1}{E} \log (G + 2F\eta - E\eta^2) - \frac{F}{E^2 K} \log \frac{\eta - \frac{F}{E} - K}{\eta - \frac{F}{E} + K} + \log G^{\frac{1}{E}} \left[\frac{-\frac{F}{E} - K}{-\frac{F}{E} + K} \right]^{\frac{F}{E^2 K}}$$

$$\text{or } \xi^{\frac{E}{M}} (G + 2F\eta - E\eta^2) = G \left[\frac{K + \eta - \frac{F}{E}}{K - \eta + \frac{F}{E}} \right]^{\frac{F}{EK}} \left[\frac{K + \frac{F}{E}}{K - \frac{F}{E}} \right]^{\frac{F}{EK}}$$

Substituting the values of G , F and E we have,

$$\xi^{\frac{(\gamma-1)M+2\theta}{M}} [2M^2z_0 + 2aM\eta - (\gamma-1)M+2\theta)\eta^2]$$

$$= 2M^2z_0 \left[\frac{K+\eta - \frac{aM}{\gamma-1M+2\theta}}{K-\eta + \frac{aM}{\gamma-1M+2\theta}} \right]^{\frac{aM}{(\gamma-1M+2\theta)K}} \cdot \left[\frac{K + \frac{aM}{\gamma-1M+2\theta}}{K - \frac{aM}{\gamma-1M+2\theta}} \right]^{\frac{aM}{(\gamma-1M+2\theta)K}} \quad \dots \quad (V)$$

where
$$K = \sqrt{\left\{ \frac{2M^2z_0}{(\gamma-1M+2\theta)} + \frac{a^2M^2}{(\gamma-1M+2\theta)^2} \right\}}$$

3. MAXIMUM PRESSURE

Equation (8) can be written as,

$$\frac{d\eta}{d\xi} = \frac{2M^2z_0 + 2aM\eta - (\gamma-1)M+2\theta)\eta^2}{2M\eta\xi}$$

Using this quantity in (II) we have,

$$\zeta = \frac{[2M^2z_0 + 2aM\eta - (\gamma-1)M+2\theta)\eta^2]}{2M^2\xi} \quad \dots \quad \dots \quad (9)$$

Inserting the value of ξ from (V) here we get,

$$\zeta = \frac{[2M^2z_0 + 2aM\eta - (\gamma-1)M+2\theta)\eta^2]}{2M^2 \left[\frac{2M^2z_0 \left(\frac{1+K_1\eta}{1-K_2\eta} \right)^{\frac{aM}{(\gamma-1M+2\theta)K}}}{\frac{\gamma M+2\theta}{\gamma-1M+2\theta}} \right]^{\frac{aM}{(\gamma-1M+2\theta)K}}} \quad \dots \quad \dots \quad (VI)$$

where

$$\frac{1}{K_1} = K - \frac{aM}{\gamma-1M+2\theta}$$

and

$$\frac{1}{K_2} = K + \frac{aM}{\gamma-1M+2\theta}$$

Now maximum pressure is obtained by eliminating η between (VI) and $\frac{d\zeta}{d\eta} = 0$. Differentiating (9) with respect to η we get,

$$\frac{d\zeta}{d\eta} = \frac{-[2M^2z_0 + 2aM\eta - (\gamma-1)M+2\theta)\eta^2]}{2M^2} \frac{1}{\xi^2} \frac{d\xi}{d\eta} + \frac{[2aM - 2(\gamma-1)M+2\theta)\eta]}{2M^2\xi}$$

Substituting the value of $\frac{d\xi}{d\eta}$ in $\frac{d\zeta}{d\eta} = 0$ and simplifying, we get,

$$\eta = \frac{aM}{(\gamma M+2\theta)} = \eta_1 \text{ (say)}$$

We can tabulate, in double entry table forms, the values of ζ'_1 against z_0 and M , for different values of θ . This is done in the table given below for $\theta = 1$.

TABLE FOR ζ'_1

$\gamma = 1.24$ $\theta = 1$

$Z_0 \backslash M$	1	2	3	4	5
0.00	.5531	.3829	.2929	.2372	.1992
0.01	.5625	.3952	.3063	.2513	.2137
0.02	.5700	.4050	.3165	.2625	.2252
0.03	.5771	.4141	.3271	.2728	.2357
0.04	.5836	.4225	.3364	.2826	.2457
0.05	.5898	.4306	.3454	.2920	.2554

The table shows that maximum pressure increases as the shot-start pressure increases but decreases as M increases.

4. COVOLUME CORRECTION FOR MAXIMUM PRESSURE

We can apply the covolume correction for maximum pressure for different values of M in the following manner:

$$\zeta_1 = \zeta'_1 / [1 - B \{ \zeta'_1 + (1 + \theta)^2 \gamma \lambda_1 / M \}] \quad \dots [\text{Corner, 1951}]$$

where ζ_1 = maximum value of ζ

ζ'_1 = maximum value of ζ for $B = 0$

$$\lambda_1 = \frac{\frac{M}{\theta + \frac{1}{2}(\gamma - 1)M}}{\left[\frac{M}{\theta + \frac{1}{2}(\gamma - 1)M} + 1 \right] \left[\frac{M}{\theta + \frac{1}{2}(\gamma - 1)M} + 2 \right]}$$

and

$$B = \left(b - \frac{1}{\delta} \right) \frac{C}{At}$$

Now we apply this correction to our table for a particular case for which,

Shot-weight $m = 20$ lbs.

Shot travel $x_3 = 36.959$ in.

Chamber capacity $k_0 = 82$ cub. in.

Total capacity $k_3 = 491$ cub. in.

Form coefficient $\theta = 1$.

Ballistic size $D = .016$.

Propellant data are:

$F = 2010$ inch-tons/lb.,

$\beta = 1.08$,

$\gamma = 1.24$,

$\frac{1}{\delta} = 17.3$,

$b = 25.5$ c.in./lb.

For the above data

$$A = \frac{K_3 - K_0}{x_3} = 11.0663$$

We know that B is a function of C , and also M is a function of C in this particular case,

$$M = \frac{A^2 D^2}{F \beta^2 C m_1} \text{ where } m_1 = 1.06m + \frac{1}{3}C$$

For this particular case,

$$M = \frac{k}{C(1.06m + \frac{1}{3}C)}, \text{ where } k = \frac{A^2 D^2}{F \beta^2}$$

or

$$C^2 + 3.18 m C - \frac{3k}{M} = 0$$

This gives,

$$C = \frac{-3.18m + \sqrt{(3.18m)^2 + \frac{12k}{M}}}{2}$$

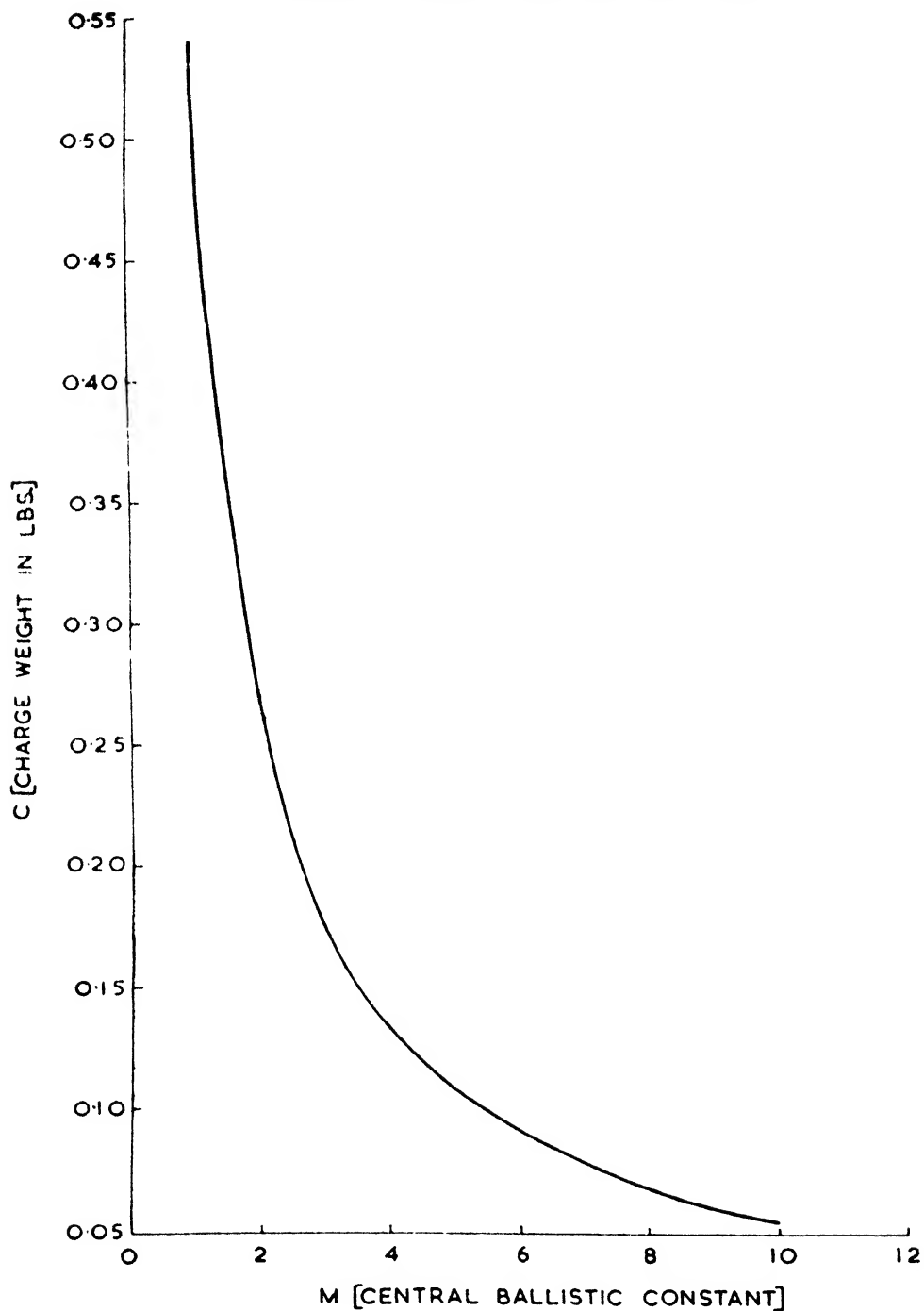
In this present case we get the values of B for different values of M as given below, and graphs have been drawn in this particular case, showing relation between M and C ; and also between B and C . (See graphs 1 and 2.)

M	1	2	3	4	5	6	7	8	9	10
C	.5411	.2717	.1814	.1362	.1090	.0908	.0779	.0682	.0606	.0546
B	.0611	.0288	.0189	.0140	.0112	.0093	.0079	.0069	.0061	.0055

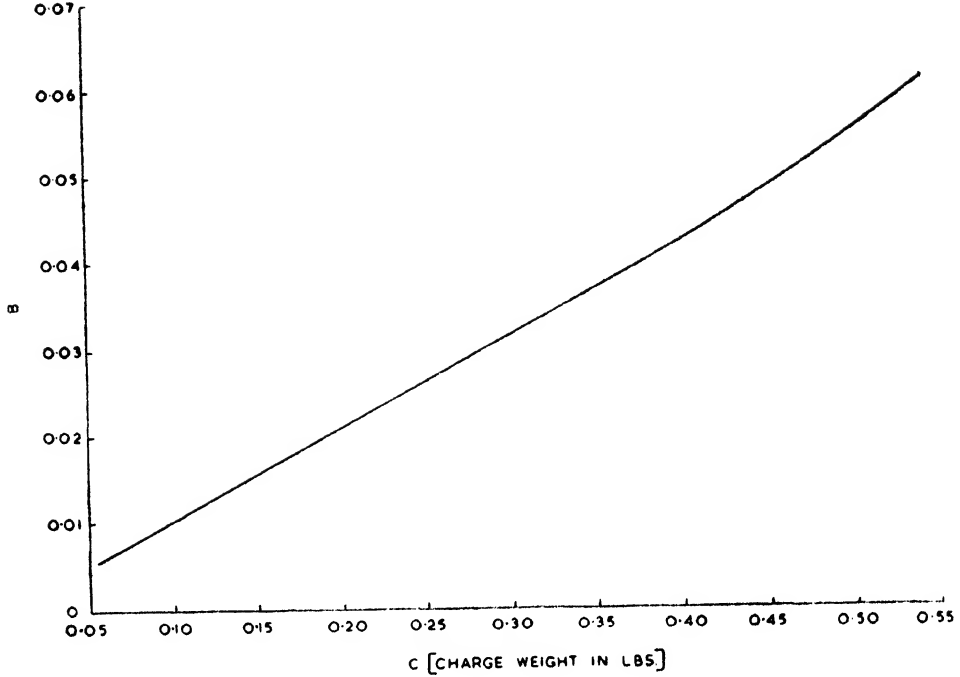
Applying the covolume correction the modified table becomes as follows :

TABLE FOR ζ_1
(Applying covolume correction)

$\gamma = 1.24$		$\theta = 1$				
$Z_0 \backslash M$		1	2	3	4	5
0.00		.5801	.3884	.2949	.2382	.1997
0.01		.5904	.4011	.3085	.2524	.2143
0.02		.5986	.4111	.3188	.2637	.2259
0.03		.6063	.4204	.3296	.2741	.2364
0.04		.6133	.4291	.3390	.2839	.2465
0.05		.6201	.4374	.3482	.2934	.2562



GRAPH 1. RELATION BETWEEN CHARGE WEIGHT
AND CENTRAL BALLISTIC CONSTANT
(IN THE PARTICULAR CASE)



GRAPH 2. RELATION BETWEEN CHARGE WEIGHT AND $B \left[B = (b - \frac{1}{6}) \frac{C}{At} \right]$
(IN THE PARTICULAR CASE)

5. It is to be noted that there is a limitation to the value of M . Equation (6) can be written for the maximum pressure as,

$$\eta_1 = \frac{M}{2\theta} \left[\sqrt{(\theta+1)^2 - 4\theta z_0} - \sqrt{(\theta+1)^2 - 4\theta z_1} \right]$$

From this we get,

$$Mz_1 = \frac{1}{M} \left[M^2 z_0 + a M \eta_1 - \theta \eta_1^2 \right]$$

Since $z_1 \leq 1$ we must have,

$$\frac{1}{M^2} \left[M^2 z_0 + a M \eta_1 - \theta \eta_1^2 \right] \leq 1.$$

$$\text{or} \quad \frac{1}{M^2} \left[M^2 z_0 + \frac{a^2 M^2}{(\gamma M + 2\theta)} - \frac{\theta a^2 M^2}{(\gamma M + 2\theta)^2} \right] \leq 1$$

$$\text{or} \quad (\gamma M + \theta) a^2 \leq (1 - z_0) (\gamma M + 2\theta)^2$$

Substituting the value of a we get,

$$(\gamma M + \theta) \{ (\theta + 1)^2 - 4\theta z_0 \} \leq (1 - z_0) (\gamma M + 2\theta)^2$$

Simplifying we get,

$$\left[\gamma M - \frac{(\theta + 1)^2}{2(1 - z_0)} \right]^2 - \frac{\theta(\theta - 1)^2}{(1 - z_0)} - \frac{(\theta - 1)^4}{4(1 - z_0)^2} > 0$$

$$\therefore M > \left\{ \sqrt{\frac{\theta(\theta - 1)^2}{(1 - z_0)} + \frac{(\theta - 1)^4}{4(1 - z_0)^2}} + \frac{(\theta - 1)^2}{2(1 - z_0)} \right\} / \gamma$$

This gives a lower limit to the value of M . For all values of M less than this value, the maximum pressure occurs at 'all burnt' position.

In particular when $\theta = 0$ the inequality for M is,

$$M > \frac{1}{\gamma(1-z_0)}$$

And when $\theta = 1$, the lower limit for M is given by,

$$M > 0$$

Also in particular when $\theta = 0$ the results (V), (VI) and (VIII) reduce to the following results due to N. S. Venkatesan.

$$\xi^{\gamma-1} [2Mz_0 + 2\eta - (\gamma-1)\eta^2] = 2Mz_0 \left[\frac{K + \frac{1}{\gamma-1}}{K - \frac{1}{\gamma-1}} \right]^{\frac{1}{K(\gamma-1)}} \left[\frac{K + \eta - \frac{1}{\gamma-1}}{K - \eta + \frac{1}{\gamma-1}} \right]^{\frac{1}{K(\gamma-1)}}$$

where

$$K = \sqrt{\left\{ \frac{1}{\gamma-1} \left(2Mz_0 + \frac{1}{\gamma-1} \right) \right\}}$$

$$\xi = \frac{[2Mz_0 + 2\eta - (\gamma-1)\eta^2]^{\frac{\gamma}{\gamma-1}}}{2M \left[2Mz_0 \left(\frac{1+K_1\eta}{1-K_2\eta} \right)^{\frac{1}{K(\gamma-1)}} \right]^{\frac{1}{\gamma-1}}}$$

where

$$\frac{1}{K_1} = K - \frac{1}{\gamma-1}$$

and

$$\frac{1}{K_2} = K + \frac{1}{\gamma-1}$$

Maximum pressure for this case is given by,

$$\zeta_1 = \left[\frac{\gamma+1}{2M\gamma^2 b_0 \gamma} \right]^{\frac{\gamma}{\gamma-1}} \cdot Z_0 [-Mz_0 + \frac{1}{2}M^2 z_0^2 (\gamma-1)]$$

$$\times \left[1+z_0 \left\{ M \log b_0 - \frac{a'_0}{\gamma-1} + \frac{2M\gamma^3}{(\gamma-1)(\gamma+1)} \right\} \right.$$

$$+ \frac{z_0^2}{2} \left\{ M^2 (\log b_0)^2 - 3M^2 (\gamma-1) \log b_0 - \frac{2Ma'_0 \log b_0}{\gamma-1} \right.$$

$$+ 2a'_0 M + \frac{a_0'^2 \gamma}{(\gamma-1)^2} - \frac{2a'_1}{(\gamma-1)} + \left(M \log b_0 - \frac{a'_0}{\gamma-1} \right) \frac{4M\gamma^3}{(\gamma-1)(\gamma+1)}$$

$$\left. + \frac{4M^2 \gamma^5}{(\gamma-1)^2 (\gamma+1)^2} \right\}$$

$$+ \dots \dots \dots]$$

where

$$a_0 = \frac{2(\gamma^2 + 2\gamma - 1)}{(\gamma + 1)^2}, \quad a'_0 = \frac{a_0}{b_0}$$

$$a_1 = -\frac{(\gamma^2 + 6\gamma + 1)(\gamma - 1)^2 M}{2(\gamma + 1)^3}, \quad a'_1 = \frac{a_1}{b_0}$$

$$b_0 = \frac{2}{M(\gamma + 1)}$$

ACKNOWLEDGEMENTS

I am highly grateful to Dr. D. S. Kothari, Scientific Adviser to the Ministry of Defence, for his interest in this work and for according permission to publish this paper. My thanks are due to Dr. R. S. Varma for his advice and help in the preparation of this paper.

SUMMARY

Neglecting the covolume correction and taking any shape of the propellant, i.e., any value of θ , the equations of the internal ballistics of a conventional gun are integrated and an explicit relation between maximum pressure and shot-start pressure is derived. A double entry table is worked out to illustrate the variation of maximum pressure with shot-start pressure and the central ballistic constant; and further this table has been modified by applying the covolume correction for maximum pressure.

REFERENCES

- Corner, J. (1950). *Theory of the Interior Ballistics of Guns*, New York.
 ——— (1951). *Internal Ballistics*, 4, H.M. Stationery Office, London.
 Venkatesan, N. S. (1952). A Note on the Relation Between Maximum Pressure and Shot-Start Pressure. *Proc. Nat. Inst. Sci.*, 18, 265-272.

Issued July 12, 1954.

ABSORPTION SPECTRUM OF 3-CHLORO-THIONAPHTHENE

by K. SREERAMAMURTY, *I.C.I. Research Fellow, N.I.S.I., and P. B. V. HARANATH,*
Department of Physics, Andhra University, Waltair

(Communicated by K. R. Rao, F.N.I.)

(Received January 12; read May 7, 1954)

INTRODUCTION

In recent years there has been a systematic study of the electronic absorption spectra of benzene, naphthalene and their derivatives in the region about λ 3000 to λ 2400. In order to understand and interpret successfully the spectra of these compounds, it is considered beneficial to investigate the electronic spectra of bicyclic compounds containing a five-membered ring and a six-membered ring as these possess configurations intermediate between the benzene and the naphthalene molecules.

On the theoretical side, taking indene as a particular case, the electronic energy levels have been predicted from calculations applying the approximate valence bond or the atomic orbital method and by the antisymmetrized molecular orbital method by Viswanath (1953) and Ramamurty (1953). Viswanath (1952) also made an experimental study of the absorption of some molecules of this type, namely, indene, indole and thionaphthene in the vapour phase. Much information, which will be of help for a complete interpretation of the above spectra, can be obtained if the absorption of some suitable derivatives be studied. The present paper comprises an experimental investigation of the absorption of a chloro-derivative of thionaphthene, 3-chloro-thionaphthene, in the vapour phase. A preliminary report was published in *Current Science* (1953). The absorption of this molecule does not appear to have been studied by any earlier worker.

EXPERIMENTAL

The absorption spectrum of 3-chloro-thionaphthene is photographed on Hilger medium quartz spectrograph using a quartz to pyrex absorption cell of 40 cm. length. A pure specimen of the substance supplied by Light & Co. was redistilled into the absorption tube in vacuum. The amount of vapour of the substance introduced and its pressure was adjusted by varying the temperature of the reservoir containing the liquid. For recording the spectrum the temperature of the container was varied in the range -10°C. to 100°C. While working at higher temperatures the absorption tube was heated to the same temperature or maintained at a slightly higher temperature than that of the container. The windows of the absorption column were kept at a slightly higher temperature than that of the column in order to prevent the condensation of the vapour. A Hilger low voltage hydrogen arc lamp fed by a stabilized power unit supplied by the manufacturers along with the lamp was used as the source of continuous ultraviolet radiation. The spectra were recorded on Ilford special rapid photographic plates (21°Sch.). The exposure time was about 15 to 20 minutes.

DESCRIPTION

The spectrum extended from λ 3000 to λ 2755. About 90 red degraded band heads are measured. The reproduction of the spectrum photographed at 30°C.

is reproduced in Plate X. Most of the bands are sharp. The spectrum resembles closely in general appearance that of thionaphthene. It presents a typical group pattern as in thionaphthene with some overlapping at the violet end. But, whereas an alternation in the intensity of the components of each group was observed in thionaphthene, the bands in each group in the case of 3-chloro-thionaphthene shows a gradual fall in intensity from violet to red. Viewing the spectrum as a whole, there is a rapid fall in intensity of absorption from red to violet unlike the gradual fall observed in the case of thionaphthene. Table 1 records wave number and intensity data of all the bands. The intensities are, following the usual practice, expressed as v st, st, m st indicating very strong, strong, medium strong respectively; similarly vw, w, mw. The fourth column gives the difference from 0, 0 band and the last one the assignment of the bands in terms of the characteristic frequencies.

TABLE 1

Wave number	Intensity	Difference from 0, 0 cm. ⁻¹	Assignment
33319	vvw	414	
33360	vvw	373	0 - 2 × 188
33390	vvw	343	0 - 188 - 4 × 40 ?
33424	vw	309	0 - 188 - 3 × 40
33469	w	264	0 - 188 - 2 × 40
33509	m	224	0 - 188 - 40
33545	m st	188	0 - 188
33572	m st	161	0 - 4 × 40
33614	st	119	0 - 3 × 40
33654	st	78	0 - 2 × 40
33694	v st	39	0 - 40
33728	v st	5	
33733	vv st	0	0, 0
33769	vw	36	
33775	vw	42	
33802	vw	69	
33809	vw	76	
33840	vw	107	
33872	vvw	139	0 + 177 - 40
33877	vw	144	
33910	w	177	0 + 177
33970	w	237	
34008	w	275	
34051	w	318	
34098	w	365	
34148	w	415	0 + 680 - 188 - 2 × 40 ?
34178	vvw	445	
34189	vvw	456	0 + 680 - 188 - 40
34200	vvw	467	
34222	vvw	489	0 + 680 - 188
34256	vvw	523	0 + 680 - 4 × 40
34266	vvw	533	
34294	vvw	561	0 + 680 - 3 × 40
34301	vvw	568	0 + 763 - 188 ?
34331	vw	598	0 + 680 - 2 × 40
34372	w	639	0 + 680 - 40
34413	m st	680	0 + 680
34456	vvw	723	0 + 763 - 40
34463	vw	730	
34496	m	763	0 + 763
34543	vvw	810	
34578	vvw	845	0 + 1025 - 188
34584	vvw	851	0 + 680 + 177
34619	vvw	886	0 + 968 - 2 × 40

TABLE I.—*Contd.*

Wave number	Intensity	Difference from 0, 0 cm. ⁻¹	Assignment
34660	vvw	927	0 + 968 - 40
34682	vvw	949	0 + 763 + 177 ?
34696	vvw	963	
34701	m	968	0 + 968
34726	m bd	993	0 + 1025 - 40 ?
34758	m bd	1025	0 + 1025, 0 + 1213 - 188
34799	w	1066	
34834	w	1101	
34866	vvw	1133	0 + 1213 - 2 × 40
34875	w	1142	
34905	w	1172	0 + 1213 - 40
34912	w	1179	
34946	m	1213	0 + 1213
34965	w	1232	
34982	m	1249	0 + 1321 - 2 × 40 ?
35015	m	1282	0 + 1321 - 40
35047	m	1314	
35054	m st	1321	0 + 1321
35088	w	1355	
35096	w	1363	0 + 2 × 680
35125	w	1392	
35132	w	1399	0 + 763 + 680 - 40 ?
35159	w	1426	
35167	vw	1434	0 + 763 + 680 ?
35205	vw	1472	
35274	vw	1541	
35318	vvw	1585	
35350	vvw	1417	
35414	vvw	1681	
35482	vvw	1769	
35564	vvw	1831	
35615	vvw	1882	
35640	vvw	1907	
35704	vvw	1971	
35778	vvw	2045	0 + 2 × 1025, 0 + 3 × 680
35801	vvw	2068	
35829	vvw	2096	
35904	vvw	2171	0 + 1213 + 968 ?
35955	vvw	2222	
36063	vvw	2330	
36131	vvw	2398	
36165	vvw	2432	0 + 2 × 1213
36234	vvw	2501	
36287	vvw	2554	

ANALYSIS

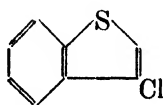
Thionaphthene, of which 3-chloro-thionaphthene is a derivative, is a molecule containing one six and one five-membered rings. It has only two symmetry elements, the plane of the molecule and the identity, characteristic of the molecules belonging to the C₂ group. The spectrum corresponding to the allowed electronic transition A'-A' shows conspicuous group arrangements of the bands. These arrangements are observed to differ from those found in disubstituted benzenes which also belong to the same symmetry class. This may be explained on the basis of the different electronic structures of the two types. However, in general appearance and nature, the spectra resemble each other. The spectrum of thionaphthene extends from λ 3000 to λ 2685. The 0, 0 band is located at ν 34060. The bands in the 0, 0 group

are almost equispaced and exhibit a distinct alternation in intensity. These are analysed assuming a number of difference frequencies. This entire pattern repeats itself with the bands at characteristic upper state frequencies to a greater or a smaller degree depending upon the intensity of the main head. The following prominent frequencies are identified in the upper state :—

672, 736, 936, 1181 and 1331.

Of these 1331 is weak, whereas the rest are of higher intensity. 936 and 1181 are assigned to C—C ring frequencies. 1331 is suggested to probably represent a characteristic vibration of the five-membered ring, since frequencies of this order have not been identified in the ultraviolet spectra of benzene and its derivatives. No frequencies smaller than 672 are reported in this molecule.

3-chloro thionaphthene is a derivative obtained by replacing the hydrogen atom in position three of the five-membered ring by a chlorine atom; and has the structure



In spite of this substitution it retains the two symmetry elements, the minimum possible in the case of plane molecules. However, this substitution results in an effective reduction in the spectroscopic symmetry character of the molecule. The spectrum corresponds to an allowed electronic transition $A'-A'$. Though the spectrum is expected to possess the general appearance of those of the molecules belonging to the same symmetry class, it should show the characteristics of an allowed transition to a much greater degree than thionaphthene. The structure of groups may be different. The number of frequencies that occur in this spectrum are expected to be larger.

The absorption of 3-chloro-thionaphthene presents a distinct group pattern, which is most marked in association with the 0, 0 band, and there is some overlapping at the violet end of the spectrum. The intensity of the groups falls very rapidly from red to violet end of the spectrum. The most intense group is at the red end with the head at ν 33733. This head is taken as the 0, 0 band since in an allowed case the vibrationless electronic transition should be strong. This is accompanied on the red side by a number of almost equispaced bands with a gradual fall in intensity of the individual components, as distinct from the alternation in intensity observed in thionaphthene. This pattern is also prominent at

ν 33910, ν 34413, ν 34496, ν 34701, ν 34758, ν 34946 and ν 35054.

The number of component heads and the intensities of these fall off rapidly towards the violet end. The pattern is partially observed in association with the comparatively weaker frequencies. Only two distinct frequencies 40 and 188 could be suggested from an analysis of the component heads in the different groups. Of these 40 forms long progressions in all the groups. It also occurs as a progression superposed on 188. The gradual reduction in intensity of the components lends support for assuming only one difference frequency of value 40 to explain the group pattern. 188 may be thought of either as a $v-v$ transition or as one of the ground state frequencies. Most probably it is the latter since 177 occurs in the upper state which may correspond to 188. A confirmation has to be obtained from Raman and Infra-red data.

Taking the head of each group as representing a distinct vibration the following upper state frequencies are obtained:

177, 680, 763, 968, 1025, 1213 and 1321.

Of these 680 is most intense next to the 0, 0. It forms a progression as can be seen from the last column of Table 1. Next in order of intensity are the bands 1321 and 1213 and 968; 177 has the smallest intensity, the rest of the frequencies fall in between. In the absence of any data on the ground state frequencies, no assignment of these frequencies could be made, though 680 presents the characteristics of and probably represents a totally symmetric vibration.

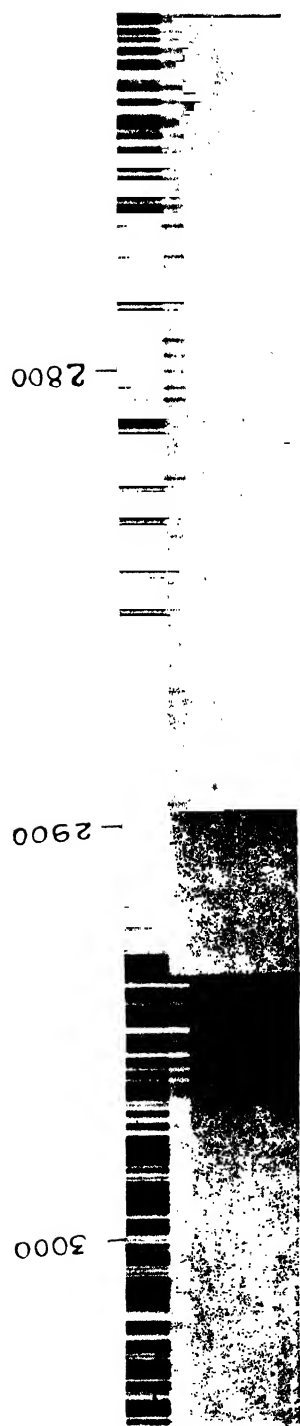
COMPARISON WITH THIONAPHTHENE

3-chloro-thionaphthene is a molecule in which the substitution is in the five-membered ring. Vibrations in this ring should be appreciably affected by this substitution by the chlorine atom while all the frequencies characteristic of vibrations in the six-membered ring may not be influenced. Chlorine is strongly electronegative as a substituent for hydrogen in C-H and can supply migration electrons into the five-membered ring direct, modifying the character and magnitude of the vibrations of the C-H type and those of the ring. A comparison between the vibrational frequencies in both these molecules, should yield interesting information about the nature of the vibrations. They are listed in Table 2. The spectra of the two molecules are presented in juxtaposition in the Plate X. The values given for thionaphthene are those reported by Viswanath. Excepting 1321 and 1331 the rest are slightly and uniformly larger in magnitude and smaller in intensity in the substituted molecule than in thionaphthene. This suggests that these represent frequencies which are not materially affected by the substitution. The indirect effect of the substituent, perhaps manifested itself as a small alteration in magnitude and intensity. These are to be associated with the phenyl ring. On the other hand, 1321 (in 3-Cl-thionaphthene) is stronger than 1331 (in thionaphthene) and is, obviously, influenced by the substitution. The very small change in magnitude suggests that it probably has rather small contribution from the hydrogen atoms. It may either be a C-S vibration (common in both molecules) or a C-C five-membered frequency. The occurrence of a vibration of smaller magnitude than 680, viz., 177 should also be noted. The intensity of the suggested C-C ring frequencies of the phenyl ring, 936 and 1181, is much reduced in the substituted molecule (968, 1213). The 0, 0 band is shifted toward the red by 327 cm^{-1} . The length and the total intensity of the transition has diminished in the substituted molecule. There is a rapid fall in the intensity of the bands from red to violet in this as against the gradual fall in thionaphthene.

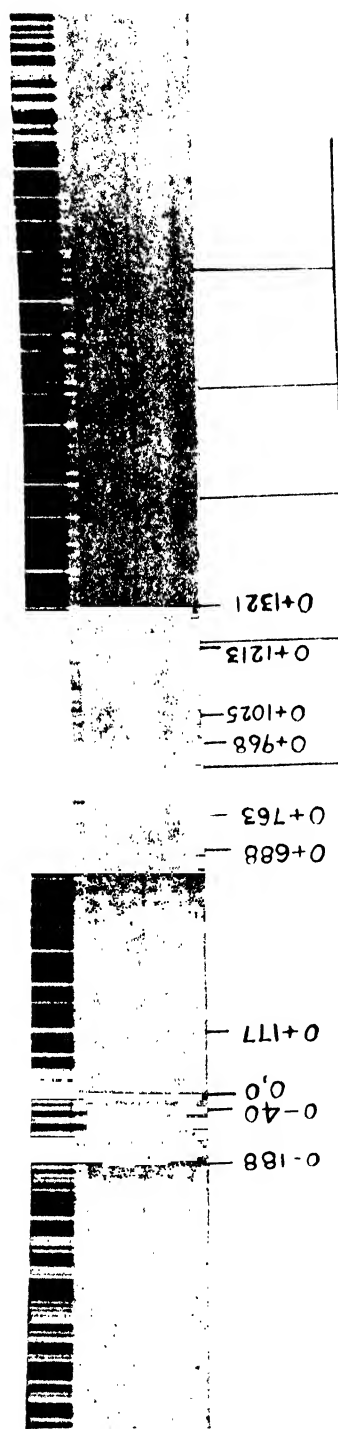
TABLE 2

Thionaphthene (Viswanath)	3-Cl-thionaphthene (Present work)
	177 (w)
672 (m st)	680 (m st)
736 (m st)	763 (m)
936 (st)	968 (m)
	1025 (m bd)
1181 (m st)	1213 (m)
1331 (w)	1321 (m st)

A special feature noteworthy in this case is the occurrence of a sequence of continuous patches superposed at the violet end. Measurements of the wavelengths could not be made because of the low intensity and diffuseness. These are indicated in Plate X. The estimated wavelength data is given in Table 3. They are almost equi-spaced with an average separation of 331 cm^{-1} . The one at $\nu\ 34640$ is most intense and lies at the extreme red end of the sequence. It may be a separate system of weak intensity.



a



b

Diffuse patches

(a) Absorption spectrum of Thiophthalene.
 (b) Absorption spectrum of 3,6-Dithiophthalene.

TABLE 3

Estimated wavelength	Intensity	Wave number	Difference between two consecutive patches in cm.^{-1}
2886	st	34640	339
*2858	m st	34979	321
2832	m	35300	340
2805	w	35640	346
2778	vw	35986	340
2752	vw	36326	

* Overlapped by the discrete absorption bands.

SUMMARY

The absorption of 3-Cl-thionaphthene, a derivative of thionaphthane in the region λ 3000 to λ 2755 is investigated. About 90 red degraded bands are measured. An analysis of these bands is presented using the following upper state frequencies 177, 680, 763, 968, 1025, 1213, 1321. The assignment of certain frequencies have been discussed taking into consideration the possible effect of substitution of the Cl atom on the vibrations. 1321 may be a C-S or C-C five-membered ring frequency. The 0,0 band is shifted towards red by 327 cm.^{-1} from that of thionaphthene. Estimated wavelengths of the sequence of diffuse patches which occur superposed on this system at the violet end are listed.

ACKNOWLEDGEMENT

The authors wish to express their grateful thanks to Prof. K. R. Rao for his interest and many helpful suggestions in the course of these investigations.

REFERENCES

- Ramamurty, S. (1953). Calculation of the Excited levels of Indene. *Ind. Jour. Phy.*, **27**, 504-510.
 Sree Ramamurty, K. and Haranath, P. B. V. (1953). Absorption spectrum of 3-Cl-thionaphthene. *Curr. Sci.*, **22**, 296.
 Viswanath, G. (1952). Absorption spectra of certain bicyclic compounds and disubstituted Benzenes. D.Sc. Thesis of the Andhra University.
 ——— (1953). Electronic spectra of molecules containing six- and five-membered rings. Part I. Calculation of energy levels. *Ind. Jour. Phy.*, **27**, 251-256.

Issued July 12, 1954.

ON POLAR RECIPROCAL CONVEX DOMAINS

ADDENDUM

by R. P. BAMBAH, *Institute for Advanced Study, Princeton, N.J., U.S.A., and Panjab University College, Hoshiarpur.*

(Communicated by H. Gupta, F.N.I.)

(Received March 12, 1954)

1. Let k and K be two plane symmetrical convex domains centred at the origin O , that are polar reciprocal to each other with respect to the unit circle centred at O . In a recent note* [1954] the author proved the best possible inequalities

$$2 \leq \Delta(k) c(K) \leq \frac{9}{4},$$

The object of this addendum is to add the companion inequalities

$$27/4 \leq c(k) c(K) \leq 9, \quad \dots \quad (1)$$

which are also best possible.

Throughout this note we use the notation of PRCD.

2. If H is a symmetrical convex hexagon with vertices $P_1, P_2, P_3, -P_1, -P_2, -P_3$, occurring in that order, then the triangle $P_1P_3-P_2$ has area $a(P_1P_3-P_2) = \frac{1}{2} a(H)$. Also if T is a triangle with area $a(T)$, then the hexagon formed by taking the convex cover of T and $-T$ (the image of T in O) has area at least $2a(T)$. From these observations one easily concludes that in the notation of PRCD

$$c(k) = h_s(k) = 2t(k), \quad c(K) = h_s(K) = 2t(K), \quad \dots \quad (2)$$

where $t(k)$ and $t(K)$ denote the areas of the biggest triangles inscribed in k and K respectively.

We next prove the following lemma, which is a particular case of one due to Mahler, valid in n dimensions:

LEMMA: *If T is a triangle containing O and T' is its polar reciprocal, then*

$$a(T) a(T') \geq 27/4.$$

Let the vertices P, Q, R of T occur in the counter-clockwise order and let their co-ordinates be $(x_1, y_1), (x_2, y_2)$, and (x_3, y_3) respectively. Since O lies inside T , there exist positive numbers ξ, η, ζ such that

$$x_1\xi + x_2\eta + x_3\zeta = 0,$$

$$y_1\xi + y_2\eta + y_3\zeta = 0,$$

so that, for some real number ρ , we have

$$\xi = \rho(x_2y_3 - x_3y_2), \quad \eta = \rho(x_3y_1 - x_1y_3), \quad \text{and} \quad \zeta = \rho(x_1y_2 - x_2y_1).$$

* We refer to this Note as PRCD.

By straight-forward calculations one easily obtains

$$a(T) = \frac{1}{2\rho} (\xi + \eta + \zeta),$$

and

$$a(T') = \frac{1}{2}\rho(\xi + \eta + \zeta)^2/\xi\eta\zeta$$

so that

$$a(T) a(T') = \frac{1}{4}(\xi + \eta + \zeta)^3/\xi\eta\zeta \geq 27/4.$$

Now suppose t is a triangle inscribed in K with area $a(t) = t(K)$. Then, since t is maximal and K is convex it is easy to see that the lines through the vertices of t parallel to opposite sides are tac lines of K , so that K is contained in T , the triangle formed by these lines. Clearly

$$a(T) = 4a(t) = 4t(K).$$

Since K contains O in the interior, so also does T . Consequently if t' denotes the polar reciprocal of T , then

$$a(T) a(t') \geq 27/4.$$

Also t' lies in k . Therefore

$$c(k) = 2t(k) \geq 2a(t'),$$

and

$$c(K) c(k) = 4t(K) t(k) \geq 4a(t) a(t') = a(T) a(t') \geq 27/4. \quad \dots \quad (3)$$

Next suppose H is a hexagon inscribed in K with $a(H) = h_3(K)$. Then H' , its polar reciprocal, contains k , so that

$$c(k) \leq a(k) \leq a(H'),$$

and

$$c(K) c(k) \leq a(H) a(H') \leq 9, \quad \dots \quad (4)$$

the last inequality follows from inequalities A of Mahler [1948]. Inequalities (3) and (4) prove (1).

If k is a regular hexagon inscribed in the unit circle and K its polar reciprocal then

$$c(k) = \frac{3\sqrt{3}}{2}, c(K) = 2\sqrt{3}, \text{ and } c(k) c(K) = 9. \quad \dots \quad (5)$$

On the other hand, if k , and so also K , is the unit circle, then

$$c(k) = \frac{3\sqrt{3}}{2}, c(K) = \frac{3\sqrt{3}}{2}, \text{ and } c(k) c(K) = 27/4,$$

which together with (5) shows that inequalities (1) are best possible.

REFERENCES.

- Bambah, R. P. (1954). On Polar reciprocal Convex Domains. *Proc. Nat. Inst. Sci.*, **20**, 119-120.
 Mahler, K. (1948). *Proc. Kon. Ned. Akad. V. Wet.*, Amsterdam, **51**, 482-485.

INSTABILITY OF NON-RADIAL OSCILLATIONS OF CENTRALLY CONDENSED STARS

by R. C. KHARE, *Research Scholar, Mathematics Department,
University of Allahabad*

(Communicated by A. C. Banerji, F.N.I.)

(Received June 12, 1953; read May 7, 1954)

1. INTRODUCTION

Generally in theoretical discussions of stellar pulsation, non-radial modes of oscillations are left out, with the justification that these modes are likely to be associated with a greater amount of viscous damping than in purely radial oscillations. But it is plausible to argue, that in the lowest modes of non-radial oscillations the viscous damping is not likely to exceed by a great deal the damping in radial oscillations. Also we must take into account the circumstance that, whatever external disturbances may exist, they will always be of a non-radial character. A point of great consequence is, as pointed out by Rosseland, that a limitation to purely radial oscillations fails to reveal the possible instability of the assumed model for a more general type of disturbance. If there is any mode of oscillation for which the assumed model is unstable, then the possibility of the existence of a star built on that model is nil; and therefore the periods of purely radial oscillations of the model can have no application to the actual stars. An investigation of non-radial oscillations should thus lead to an elimination of a large class of oscillating stellar models.

The Eulerian equations which govern the small adiabatic oscillations of non-rotating stars were first derived by Rosseland (1932) in connection with his investigation of the effect of non-adiabatic processes on the stability of stars. The oscillations are found to be governed by an ordinary differential equation of the fourth order, the explicit form of which was eventually obtained by Pekeris (1938). Nothing is known, however, about the solutions of this equation beyond the simplest case of an initially homogeneous sphere, for which an instability with respect to all non-radial oscillations was established by Pekeris.

In order to simplify the problem and gain some insight into the nature of its characteristic frequency spectrum, Emden (1907) conceived the idea of ignoring the effect of the displacement upon the gravitational potential in the outer parts of a centrally condensed configuration—a simplification which reduces the order of the governing differential equation from fourth to second. His work was, however, vitiated by inconsistent approximations made in considering the equation of continuity which he reduced in fact to the form appropriate to a homogeneous incompressible fluid. The correct formulation of a problem so simplified was later given by Cowling (1942). We shall utilise Emden's device in deducing the equations of the problem.

2. EQUATIONS OF MOTION.

Consider the oscillations of a gas sphere under the influence of its own gravity, the oscillations being so small that squares of amplitudes of the displacements and their derivatives can be ignored in comparison with their first powers. In setting

up the equations of motions, we shall neglect viscous forces and assume that the motion of any individual gas particle takes place adiabatically.

Let the pressure P , density ρ , and gravitational potential V at any point be altered by δP , $\delta \rho$ and δV respectively, and let the vector displacement of material from its equilibrium position be \hat{h} . Then written within the scope of our approximations, the Eulerian equations of motion can be written as follows:—

$$\rho \frac{\partial^2 \hat{h}}{\partial t^2} + \text{grad } \delta P + \delta P \text{ grad } V + \rho \text{ grad } \delta V = 0 \quad \dots \quad (1)$$

where t denotes the time, and the equation of continuity becomes

$$\delta \rho + \text{div } (\rho \hat{h}) = 0 \quad \dots \quad (2)$$

Assuming the motion to be simple harmonic we shall seek such solutions of the foregoing system of equations for which

$$\frac{\partial^2 \hat{h}}{\partial t^2} + \sigma^2 \hat{h} = 0 \quad \dots \quad (3)$$

where $\sigma = \frac{2\pi}{\tau}$, τ being the period of the respective oscillation.

Equations (1) and (2) represent a simultaneous system of the fourth order, the solution of which presents, in any case, a problem of great mathematical complexity. In order to simplify it to some extent we follow Emden (1907), Rosseland (1932) and Cowling (1942) and ignore the variation of the gravitational potential on the left side of equation (1). Since in the Roche Model nearly the whole mass is concentrated at its centre, the variation in density accompanying the oscillations will produce but minor variations in the gravitational potential through the interior of the star. The neglect of the variation in gravitational potential will not, therefore, affect in any appreciable manner the characteristic features of our problem. On the other hand, the advantage of such a neglect is the reduction of our mathematical problem to the solution of a single differential equation of the second order.

The fundamental equations are ultimately reducible to the following as in Kopal (1949):—

$$\frac{d\zeta}{dr} - \frac{g}{c^2} \zeta = \left\{ \frac{j(j+1)}{\sigma^2} - \frac{r^2}{c^2} \right\} \cdot \frac{\eta}{\rho} \quad \dots \quad (4)$$

$$\frac{d\eta}{dr} + \frac{g}{c^2} \cdot \eta = \left\{ \sigma^2 + \frac{g}{\rho} \cdot \frac{d\rho}{dr} + \frac{g^2}{c^2} \right\} \cdot \frac{\rho}{r^2} \cdot \zeta \quad \dots \quad (5)$$

where

$$\zeta = r^2 a r$$

$$\eta = \delta P$$

$$g = \text{gravity}$$

$$c^2 = \gamma \frac{P}{\rho} \text{ where } \gamma = \text{ratio of specific heats}$$

$$j = \text{order of surface harmonic}$$

$$\sigma = \text{frequency of oscillation.}$$

The boundary conditions of the problem call for a node (no displacement) at the centre and a loop (no variation in pressure) at the free surface of the oscillating configuration, i.e. they require that $\delta r = 0$ at $r = 0$, while $\delta P = 0$ at a value of r_1 , for which $\rho(r_1) = 0$. These conditions can be satisfied only for particular values of σ .

We first eliminate η between (4) and (5). Put

$$\begin{aligned}\rho &= r^2 dr \\ &= r^2 \xi\end{aligned}$$

where ξ is the amplitude of oscillations and $r = Rx$ where R is the radius of the star.

Elimination of ζ gives

$$x^2 \frac{d^2 \xi}{dx^2} + \left[4x - Rx^2 \frac{A'}{A} \right] \frac{d\xi}{dx} + \left[2 - 2Rx \frac{A'}{A} - Rx^2 A \frac{d}{dx} (g/Ac^2) - \frac{g^2 R^2 x^2}{c^4} - x^2 R^2 AB \right] \xi = 0 \quad \dots (6)$$

where

$$\begin{aligned}A &= \left[\frac{j(j+1)}{\sigma^2} - \frac{R^2 x^2}{c^2} \right] \cdot \frac{1}{\rho} \\ &= \left[k - \frac{R^2 x^2}{c^2} \right] \cdot \frac{1}{\rho} \text{ where } k = \frac{j(j+1)}{\sigma^2} \quad \dots \dots (7)\end{aligned}$$

$$B = \left[\sigma^2 + \frac{g}{\rho} \cdot \frac{d\rho}{dr} + \frac{g^2}{c^2} \right] \frac{\rho}{R^2 x^2} \quad \dots \dots (8)$$

$$A' = \frac{dA}{dr}$$

We now apply equation (6) to the Roche model. Let M denote practically the whole mass of the star which is concentrated at its centre.

Then
$$g = \frac{GM}{R^2 x^2} = \frac{\mu}{R^2 x^2} \quad \dots \dots (9)$$

where G is the gravitational constant.

$$\rho = \rho_0 x^{-2} \quad \dots \dots (10)$$

Therefore

$$\begin{aligned}P &= \int_0^R \rho_0 x^{-2} \frac{GM}{R^2} x^{-2} d(Rx) \\ &= \frac{GM\rho_0}{3Rx^3} (1-x^3) \quad \dots \dots (11)\end{aligned}$$

Hence

$$\begin{aligned}c^2 &= \frac{\gamma P}{\rho} \\ &= \frac{\gamma GM}{3Rx} (1-x^3) = \frac{\alpha(1-x^3)}{Rx} \quad \dots \dots (12)\end{aligned}$$

where

$$\alpha = \frac{\gamma GM}{3}$$

Substitution of these values reduces (6) after simplification to

$$P \frac{d^2 \xi}{dx^2} + Q \frac{d\xi}{dx} + S \cdot \xi = 0 \quad \dots \dots (13)$$

where

$$\left. \begin{aligned} P &= p_5x^5 + p_8x^8 + p_{11}x^{11} + p_{14}x^{14} \\ Q &= q_4x^4 + q_7x^7 + q_{10}x^{10} + q_{13}x^{13} \\ S &= s_0 + s_3x^3 + s_6x^6 + s_9x^9 + s_{12}x^{12} \end{aligned} \right\} \dots \dots \dots (14)$$

where

$$\left. \begin{aligned} p_5 &= R^3k\alpha \\ p_8 &= -3R^3k\alpha - R^6 \\ p_{11} &= 3R^3k\alpha + 2R^6 \\ p_{14} &= -R^3k\alpha - R^6 \\ q_4 &= 2\alpha kR^3 \\ q_7 &= -6\alpha kR^3 + R^6 \\ q_{10} &= 6\alpha kR^3 + R^6 \\ q_{13} &= -2\alpha kR^3 - 2R^6 \\ s_0 &= 2\mu\alpha k^2 - k^2\mu^2 \\ s_3 &= R^3\left(\frac{k\mu^2}{\alpha} - k^2\sigma^2\alpha - \mu k - 2\alpha k\right) \\ &\quad - 6\mu k^2\alpha + 2k^2\mu^2 \\ s_6 &= 6\mu k^3\alpha - k^2\mu^2 + R^3\left(6k\alpha - \mu k + 3k^2\alpha\sigma^2 - \frac{k\mu^2}{\alpha}\right) \\ &\quad + R^6\left(8 - \frac{4\mu}{\alpha} + 2k\sigma^2\right) \\ s_9 &= -2\mu k^2\alpha + R^3(-6k\alpha + 2\mu k - 3k^2\alpha\sigma^2) \\ &\quad + R^6\left(-10 + \frac{4\mu}{\alpha} - 4k\sigma^2\right) + R^9\left(-\frac{\sigma^2}{\alpha}\right) \\ s_{12} &= R^3(2k\alpha + k^2\alpha\sigma^2) + R^6(2 + 2k\sigma^2) + \frac{\sigma^2}{\alpha} \cdot R^9 \end{aligned} \right\} \dots \dots (15)$$

3. SOLUTION OF THE DIFFERENTIAL EQUATION

The equation to be solved is

$$P \frac{d^2\xi}{dx^2} + Q \frac{d\xi}{dx} + S\xi = 0$$

P can be put in the form

$$-R^3x^4(x^3-1)^2(\beta^3x^3-1) \text{ where } \beta^3 = 1 + \frac{R^3}{k\alpha}$$

Q can be put in the form

$$-R^3x^5(x^3-1)[2\alpha k(1-x^3)^2 + R^3x^3(1+2x^3)]$$

S can be put in the form

$$\begin{aligned} &-(x^3-1) \left[\{ 2\mu\alpha k^2 - k^2\mu^2 \} \right. \\ &\quad - x^3 \left\{ 4\mu k^2\alpha - k^2\mu^2 - \frac{R^3k\mu^2}{\alpha} + k^2\sigma^2\alpha R^3 + \mu k R^3 + 2\alpha k R^3 \right\} \\ &\quad + x^6 \left\{ 2\mu k^2\alpha + 4k\alpha R^3 - 2\mu k R^3 + 2k^2\sigma^2\alpha R^3 + 8R^6 - \frac{4\mu}{\alpha} \cdot R^6 + 2k\sigma^2 R^6 \right\} \\ &\quad \left. + x^9 \left\{ -2k\sigma^2 R^6 - 2R^6 - k^2\alpha\sigma^2 R^3 - \frac{\sigma^2}{\alpha} R^9 - 2k\alpha R^3 \right\} \right] \end{aligned}$$

On cancelling throughout $-(x^3-1)$, it is easily seen that there are three singularities

(i) at $x = 0$,

(ii) at $x = 1$,

and (iii) at $x = \frac{1}{\beta}$, i.e. in between the centre and the surface of the star.

Also $x = 0$ is an irregular singularity and therefore a series solution in ascending positive powers is not possible. Further, due to the singularity in between the centre and the surface of the star the problem seems intractable in its present form.

4. SOLUTION OF THE PROBLEM IN THE CASE FOR WHICH $\gamma = 1.5$

We, therefore, consider a restricted problem. We seek a solution for the case in which the constant term in S disappears and therefore the origin becomes a regular singularity.

This condition gives :—

$$2\mu\alpha k^2 - k^2\mu^2 = 0$$

$$\text{or} \quad 2\alpha = \mu$$

$$\text{or} \quad 2\gamma \frac{GM}{3} = GM$$

$$\text{or} \quad \gamma = 1.5$$

With this value of γ , the differential equation reduces to

$$P'\xi'' + Q'\xi' + S'\xi = 0 \quad \dots \quad (16)$$

where

$$\begin{aligned} P' &= R^3x^2(x^3-1)(\beta^3x^3-1) \\ Q' &= R^3x[2\alpha k(1-x^3)^2 + R^3x^3(1+2x^3)] \\ S' &= [-(k^2\sigma^2\alpha R^3 + 4k^2\alpha^2) \\ &\quad + x^3(4k^2\alpha^2 + 2R^3k^2\alpha\sigma^2 + R^62k\sigma^2) \\ &\quad - x^6(2R^3k\alpha + k^2\alpha\sigma^2R^3 + 2R^6 + 2R^6k\sigma^2)] \end{aligned}$$

The regular singularities are $x = 0$, $x = 1$, $x = \frac{1}{\beta}$.

Since $\beta = 1 + \frac{R^3}{k\alpha}$, $\frac{1}{\beta} < 1$, therefore there is a singularity within the star between the centre and the surface.

We first determine the nature of this singularity. If it turns out to be an apparent singularity, we shall try to terminate the series solution after a finite number of terms, so that the question of its becoming divergent at $x = 1$ does not arise.

5. DETERMINATION OF THE NATURE OF THE SINGULARITY, AT $x = \frac{1}{\beta}$

The diff. eqn. (16) can be put in the form

$$\xi'' + \frac{Q'}{P'}\xi' + \frac{S'}{P'}\xi = 0 \text{ where } P', Q', S' \text{ are given in the last section.}$$

Now if the eqn. be of the form

$$w'' + \frac{P_1(z)}{(z-a)} w' + \frac{Q_1(z)}{(z-a)^2} w = 0,$$

where $P_1(z)$, $Q_1(z)$ are holomorphic functions at $z = a$, then the first condition (Forsyth, 1902) (3) for the singularity $z = a$ to be apparent is that $P_1(a)$ must be a negative integer greater than zero numerically.

In our case $P_1(x)$ is given by

$$\frac{2\alpha k(1-x^3) + R^3 x^3(1+2x^3)}{\beta x(x^3-1)(\beta^2 x^2 + \beta x + 1)}$$

$$\text{Therefore } P_1\left(\frac{1}{\beta}\right) = \frac{2\alpha k\left(1 - \frac{1}{\beta^3}\right)^2 + R^3 \frac{1}{\beta^3}\left(1 + \frac{2}{\beta^3}\right)}{3\left(\frac{1}{\beta^3} - 1\right)}$$

Since $\beta^3 = 1 + \frac{R^3}{k\alpha}$, we get after some simplification

$$P_1\left(\frac{1}{\beta}\right) = -k\alpha.$$

The first condition is, therefore, satisfied if $(k\alpha)$ is a positive integer greater than zero. We shall see presently that the assumption of this condition leads to the fulfilment of the next condition.

The second condition (Forsyth, 1902) (3) to be satisfied is that the roots of the indicial eqn. are unequal positive integers.

In our case the indicial eqn. is

$$\rho(\rho-1) + \frac{\left[2\alpha k\left(1 - \frac{1}{\beta^3}\right)^2 + R^3 \frac{1}{\beta^3}\left(1 + \frac{2}{\beta^3}\right)\right]}{3\left(\frac{1}{\beta^3} - 1\right)} \cdot \rho = 0$$

or on simplification

$$\rho(\rho-1) - k\alpha\rho = 0$$

or

$$\rho = 0 \quad \text{or} \quad (1+k\alpha)$$

The roots are unequal positive integers provided $(k\alpha)$ is a positive integer. Hence if the first condition is satisfied, we find that the second condition is also satisfied.

We may assign any convenient value to $(k\alpha)$ only that it should be a positive integer greater than zero. We shall choose it to suit the third and the last condition for the singularity to be apparent.

With the notation in Forsyth (4), we have

$$f_0(\rho) = \rho(\rho-1-k\alpha)$$

so that

$$\rho_0 = (1+k\alpha), \mu = 1, \rho_1 = 0;$$

We thus have to consider $h_\nu(\rho)$ for $\rho = \rho_1 = 0$; $\nu = \rho_0 - \rho_1 = 1+k\alpha$.

But

$$g_{(1+k\alpha)}(\rho) = \frac{h_{(1+k\alpha)}(\rho) - g_0(\rho)}{f_0(\rho+1)f_0(\rho+2) \dots f_0(\rho+1+k\alpha)}$$

Now

$$g_\nu(\rho) = \text{coefficient of } x^{\rho+\nu} \text{ in } \sum_{\nu=0}^{\infty} g_\nu x^{\rho+\nu}$$

which is the solution of the diff. eqn.

Evidently therefore for $\rho = \rho_1 = 0$, $g_{(1+k\alpha)}(\rho_1)$ is either a constant or zero.

Let $g_{(1+k\alpha)}(\rho_1) = A g_0(\rho_1)$ where A is a constant or zero.

Therefore $h_{(1+k\alpha)}(\rho_1) = A f_0(\rho_1+1) \dots f_0(\rho_1+1+k\alpha)$

Now $f_0(\rho+1+k\alpha) = (\rho+1+k\alpha) \cdot \rho$,

therefore $h_{(1+k\alpha)}(\rho_1) = A (\rho_1+1)(\rho_1-k\alpha)(\rho_1+2)(\rho_1+1-k\alpha) \dots \rho_1(\rho_1+1+k\alpha)$

Hence $h_{(1+k\alpha)}(\rho_1) = 0$ for $\rho_1 = 0$

This is the *third* condition which is satisfied if $(k\alpha)$ is a positive integer greater than zero.

We, therefore, conclude that the singularity at $x = \frac{1}{\beta}$ is apparent provided $(k\alpha)$ is a positive integer greater than zero

6. SOLUTION OF THE DIFFERENTIAL EQUATION (16)

We now proceed to construct a series solution of the eqn. (16) about the origin which is a regular singularity, under the assumption that $(k\alpha)$ is a positive integer.

Substitute in the eqn. (16)

$$\xi = \sum_{n=0}^{\infty} a_n x^{\rho+3n}$$

The indicial equation is given by

$$\rho^2 + \rho(2k\alpha - 1) - \left(k^2 \sigma^2 \alpha + \frac{4k^2 \alpha^2}{R^3} \right) = 0 \quad \dots \quad (17)$$

$$\text{Or } \rho = \frac{1}{2} \left[-(2k\alpha - 1) \pm \left\{ (2k\alpha - 1)^2 + 4 \left(k^2 \sigma^2 \alpha + \frac{4k^2 \alpha^2}{R^3} \right) \right\}^{\frac{1}{2}} \right]$$

Now $(k\alpha)$ being a positive integer $(1 - 2k\alpha)$ is negative.

Also the expression under the radical sign is greater than $(2k\alpha - 1)$ as is easily seen. Hence the root with negative sign before the radical is negative which we reject, for we want a series in ascending positive powers of x only.

We therefore take

$$\rho = \frac{1}{2} \left[-(2k\alpha - 1) + \left\{ (2k\alpha - 1)^2 + 4 \left(k^2 \sigma^2 \alpha + \frac{4k^2 \alpha^2}{R^3} \right) \right\}^{\frac{1}{2}} \right] = \rho_0.$$

Hence $\xi = \sum_{n=0}^{\infty} a_n x^{\rho_0+3n}$ is the solution.

7. CONVERGENCE OF THE SERIES.

We next test the convergence of the series

$$\xi = \sum_{n=0}^{\infty} a_n x^{\rho_0+3n}$$

The recurrence formula is found to be

$$\begin{aligned}
 a_n \bigg[& (\rho+3n)(\rho+3n-1)R^3\beta^3 + (\rho+3n)R^3(2k\alpha+2R^3) \\
 & - (2k\alpha R^3 + k^2\alpha\sigma^2 R^3 + 2R^6 + 2R^6 k\sigma^2 + \frac{\sigma^2}{\alpha} R^9) \bigg] \\
 & + a_{n+1} [(\rho+3n+3)(\rho+3n+2)R^3(-1-\beta^3) + (\rho+3n+3)R^3(-4k\alpha+R^3) \\
 & \quad + (4k^2\alpha^2 + 2R^3k^2\alpha\sigma^2 + 2k\sigma^2 R^6)] \\
 & + a_{n+2} [(\rho+3n+6)(\rho+3n+5)R^3 + (\rho+3n+6)R^3 \cdot 2k\alpha - (k^2\sigma^2\alpha R^3 + 4k^2\alpha^2)] \\
 & = 0 \quad \dots \quad \dots \quad (18)
 \end{aligned}$$

Put
$$\frac{a_{n+2}}{a_{n+1}} = N_{n+1}; \quad \frac{a_{n+1}}{a_n} = N_n.$$

Retaining only the highest power of n in (18), we get after dividing by a_{n+1} ,

$$N_{n+1} = 1 + \beta^3 - \frac{\beta^3}{N_n} \quad \dots \quad \dots \quad \dots \quad (19)$$

The difference formula (19) gives

$$N_n = \frac{\left(1 - \frac{1}{N_0}\right)(\beta^{3n} + \beta^{3n-3} + \dots + \beta^3) + 1}{\left(1 - \frac{1}{N_0}\right)(\beta^{3n-3} + \dots + \beta^3) + 1}$$

Therefore

$$\begin{aligned}
 \text{Lt}_{n \rightarrow \infty} N_n &= \beta^3 \\
 &= 1 + \frac{R^3}{k\alpha} > 1
 \end{aligned}$$

Hence the series $\sum_{n=0}^{\infty} a_n x^{\rho_0+3n}$ is divergent on the surface of the star. We therefore

try to terminate the series after a finite number of terms.

Put

$$\begin{aligned}
 k\alpha &= \theta, \\
 R^3 &= d, \\
 k\sigma^2 &= j(j+1) = m \text{ (a positive integer)}.
 \end{aligned}$$

Then

$$\rho^2 + \rho(2\theta-1) - \left(m\theta + \frac{4\theta^2}{d}\right) = 0 \quad \dots \quad \dots \quad \dots \quad (E)$$

is the indicial equation.

In order that the series may terminate, the coefficients of a_n and a_{n+1} in eqn. (18) must vanish for some finite positive integral value of n .

Coefficient of a_n equated to zero gives

$$\begin{aligned}
 & (\rho+3n)(\rho+3n-1)d \left(1 + \frac{d}{\theta}\right) + (\rho+3n)d(2\theta+2d) \\
 & - \left(2\theta d + md\theta + 2d^2 + 2md^2 + \frac{m}{\theta}d^3\right) = 0 \quad \dots \quad \dots \quad \dots \quad (F)
 \end{aligned}$$

Coefficient of a_{n+1} equated to zero gives

$$(\rho+3n+3)(\rho+3n+2)d\left(-2-\frac{d}{\theta}\right)+(\rho+3n+3)d(-4\theta+d)+(4\theta^2+2md\theta+2md^2) \\ = 0 \quad \dots \quad (H)$$

Our object is to evaluate θ with the help of (E), (F) and (H) and to see if these equations are compatible with our assumption that $\theta = k\alpha$ is a positive integer

greater than zero, so that $x = \frac{1}{\beta}$ becomes an apparent singularity.

Simplification with the help of (E) reduces (F) and (H) to the forms

$$md^2-d\{6n\rho+3n(3n-1)+(6n-2)\theta\}-4\theta^2=0 \quad \dots \quad (F_1)$$

$$d^2\left[\left(-\frac{6n}{\theta}-\frac{6}{\theta}+3\right)\rho-\frac{9n^2}{\theta}-\frac{15n}{\theta}+3n-\frac{6}{\theta}+3-m\right] \\ +d[-12\rho-36n-12-20\theta]+4\theta^2=0 \quad \dots \quad (H_1)$$

Equating the coefficient of d^2 and d in these equations, we get

$$\frac{1}{m}\left[\left(-\frac{6n}{\theta}-\frac{6}{\theta}+3\right)\rho-\frac{9n^2}{\theta}-\frac{15n}{\theta}+3n-\frac{6}{\theta}+3-m\right] \\ = \frac{(-12\rho-36n-12-20\theta)}{[-6n\rho-3n(3n-1)-(6n-2)\theta]} \\ = -1$$

From these equations we obtain

$$\left(-\frac{6n}{\theta}-\frac{6}{\theta}+3\right)\rho-\frac{9n^2}{\theta}-\frac{15n}{\theta}+3n-\frac{6}{\theta}+3=0$$

and

$$(-12\rho-36n-12-20\theta)=6n\rho+3n(3n-1)+(6n-2)\theta$$

These reduce to

$$(\theta-2n-2)\rho-(3n^2+5n+2)+3(n+1)\theta=0 \\ (6n+12)\rho+3n(3n+11)+12+(6n+18)\theta=0$$

Elimination of ρ between these two equations gives the following equation in θ alone

$$\theta^2(2n+6)+\theta(5n^2+13n+4)+(2n+4)(3n^2+5n+2)=0$$

Since all the coefficients are positive numbers, there is no positive root of the equation. Hence if (F) and (H) held then θ cannot be a positive integer.

Therefore, if $x = \frac{1}{\beta}$ is an apparent singularity, so that $\theta = k\alpha =$ a positive integer greater than zero, (F) and (H) cannot hold with the consequence that the series cannot be made to terminate after a finite number of terms.

Hence the series diverges on the surface of the star and gives an infinite amplitude of oscillation there.

We therefore, conclude that under the conditions imposed, the non-radial oscillations are unstable and the star in question will throw out expanding gaseous material in case some such oscillations set in.

8. CONCLUSION

Spectroscopic observations have revealed several expanding nebulae. The Crab Nebula is still expanding at the rate of about 800 miles per second. If this expansion is due to the explosion of a super-nova, then that phenomena must have occurred about 900 years ago. Indeed a new star in that position was recorded in 1054 A.D. by Chinese observers. The Filamentary Nebula in the constellation Cygnus shows an expansion with an angular velocity of 0.05 second per year, so that the expansion must have begun about 100,000 yrs. ago. But there was no astronomer then to record the appearance of a new star. The expanding nature of these nebulae is surmised by some astronomers to be the result of nova-explosion in the remote past. But nothing can be said with complete certainty. It has also been suggested that the planetary nebulae are the results of Novae-explosion, but there are good reasons for doubting this theory. The number of Planetary Nebulae is comparatively small, whereas the Nova-explosions are much too frequent.

The investigation carried out in the present paper suggests that if somehow non-radial oscillations are set in in centrally condensed stars consisting of gas, the ratio of whose specific heats is 1.5, the oscillations tend to become unstable.* Consequently the star will throw out columns or shells of expanding gas with considerable velocity.

On the strength of the result of the present investigation and that of Pekeris it is suggested that the expanding nebulae may have their origin in the unstable non-radial oscillations in stars which are either centrally condensed or homogeneous. These oscillations may have originated due to some internal disturbance in the star or due to the disturbance caused by the nearby passage of another star.

My respectful thanks are due to Professor A. C. Banerji, Vice-Chancellor, University of Allahabad and Professor N. R. Sen, Head of the Department of Applied Mathematics, Calcutta University, for their kind help and encouragement during the preparation of this paper.

SUMMARY

The differential equations governing small non-radial adiabatic oscillations of gaseous spheres are derived correctly to the order of accuracy to which changes in the gravitational potential produced by such oscillations can be ignored. They are then applied to the Roche Model in which practically the whole mass is concentrated at the centre and in the surrounding atmosphere density varies as the inverse square of the distance from the centre. It has been shown that for the general value of γ —the ratio of specific heats, the problem seems to be intractable. Next the case for the particular value of $\gamma = 1.5$ is considered and it is shown that with a certain restriction on the form of the frequency function the amplitude of oscillation diverges from zero at the centre of the star to infinity at the surface. The oscillations are thus unstable.

On the basis of this investigation, it has been suggested that the expansion of the Crab Nebula, the Filamentary Nebulae, the Planetary Nebulae and others may have its origin in the instability of non-radial oscillations that might have started in the remote past in centrally condensed stars due to some internal cause or due to the nearby passage of another star.

REFERENCES

- Cowling, T. G. (1942). The Non-Radial Oscillations of Polytropic Stars. *M.N.R. Astro. Soc.*, 101, 367.
 Emden, R. (1907). *Gaskugeln* (Leipzig and Berlin: B. G. Teubner), 448.
 Forsyth, A. R. (1902). *Theory of Differential Equations*, Vol. IV, Part III, § 45.
 — *Ibid.*, § 41.
 Kopal, Z. (1949). Non-Radial Oscillations of the Standard Model. *Astro. Phys. J.*, Vol. 109.
 Pekeris, C. L. (1938). Non-Radial Oscillations of Stars. *Astro. Phys. J.*, Vol. 88.
 Roseeland, S. (1932). *Publ. Oslo. Univ. Obs.*, No. 2.

* Pekeris (1938) has established the instability of Non-radial oscillations in a homogeneous star, for all modes.

A NOTE ON THE KARMAN'S SPECTRUM FUNCTION OF ISOTROPIC TURBULENCE

by K. M. GHOSH, *Department of Applied Mathematics, University College of Science and Technology, Calcutta*

(Communicated by S. K. CHAKRABARTY, F.N.I.)

(Received November 30, 1953; read May 7, 1954)

INTRODUCTION

If $F(k, t)$ be the spectrum function of isotropic turbulence, the decay of turbulence, according to the theory proposed by Heisenberg (1949), takes place according to the equation

$$-\frac{\partial}{\partial t} \int_0^k F(k', t) dk' = 2(\nu + \eta_k) \int_0^k F(k', t) k'^2 dk', \quad \dots \quad (1)$$

where ν is the kinematic viscosity, and η_k turbulent viscosity, for which Heisenberg (1949) assumed the form

$$\eta_k = K \int_k^\infty \sqrt{\frac{F(k', t)}{k'^3}} dk' \quad \dots \quad (2)$$

A self-preserving solution of this equation in the form

$$F(k, t) \sim \frac{1}{\sqrt{t}} f(k\sqrt{t}) \quad \dots \quad (3)$$

was given by Heisenberg, which has the property that $f(x) \sim x$, for small x and $f(x) \sim x^{-\frac{5}{3}}$ for large x . They correspond to the linear and Kolmogoroff parts of the spectrum respectively. The above solution was investigated more completely by Chandrasekhar (1949) who has given numerical tables for $f(x)$. While solution (3) gives a complete similarity throughout the spectrum, it gives neither Loitsiansky's result (1939), nor the ultimate law of dissipation with time as $(t-t_0)^{-\frac{5}{3}}$, observationally verified by Batchelor and Townsend (1948).

N. R. Sen (1951) has recently shown that at the initial stages when the low frequency eddies are predominant (ν small compared to η_k) equations (1) and (2) admit a more general type of solution of the form

$$F(k, t) \sim \frac{1}{K^2} \cdot \frac{1}{k_0^3 t_0^2} \left(\frac{t_0}{t}\right)^{2-3c} f((k/k_0)(t/t_0)^c) \quad \dots \quad (4)$$

where c is an arbitrary constant. Limiting c to $< \frac{2}{3}$, it can be used as a parameter determining a family of early period solutions. It was shown by Sen that this solution has the following characteristics:

$$f(x) \approx \text{const. } x^{(2-3c)/c}, \text{ as } x \rightarrow 0;$$

and

$$f(x) \approx \text{const. } x^{-5/3}, \text{ as } x \rightarrow \infty$$

whatever c may be.

While $c = \frac{1}{2}$ gives Heisenberg's results, the above solution (4) is remarkable in the respect that for $c = \frac{2}{3}$, it gives on the one hand Loitsiansky's result, viz.,

(i) $F \sim \text{const. } k^4$ as $k \rightarrow 0$, and on the other hand the decay-law and characteristic length * namely $u^2 \sim \text{const. } t^{-10/7}$, and $\lambda^2 \sim 7\nu t$ respectively, which were first pointed out by Kolmogoroff (1941) to be true when Loitsiansky's result is assumed. Sen's solution (4) shows that all the above three conclusions follow from this self-preserving solution (4) of Heisenberg's equations (1), (2), without any ad hoc assumption of Loitsiansky's result. The initial lack of isotropy at $k \rightarrow 0$ is, of course, outside the scope of the present solution in which similarity has been assumed. It has been suggested that the parameter c may be connected with the mode of excitation of turbulence.

The object of this note is to point out that the form of the spectrum (4) given by Sen is also associated with a more general decay equation suggested by Karman in 1948.

2. SELF-PRESERVING SOLUTION OF DECAY EQUATION WITH KARMAN'S SPECTRUM FUNCTION

Assuming the existence of a transition function for energy between the intervals dk and dk' (which depends on the energy density and wave numbers k and k'), Karman (1948) obtained by dimensional reasoning the following equation for the decay of the spectrum function

$$-\frac{\partial F}{\partial t} = C \left[\{F(k)\}^\alpha k^\beta \int_0^k \{F(k')\}^{\frac{3}{2}-\alpha} k'^{\frac{1}{2}-\beta} dk' - \{F(k)\}^{\frac{3}{2}-\alpha} k^{\frac{1}{2}-\beta} \int_k^\infty \{F(k')\}^\alpha k'^\beta dk' \right] - 2\nu k^2 F \quad \dots \quad (5)$$

where ν is the molecular viscosity, α , β , as yet unspecified constants, and C an absolute constant. When the first term on the right of (5) is entirely negligible the form would include Heisenberg's equation (1), (2) for $\alpha = \frac{1}{2}$, $\beta = -\frac{3}{2}$.

For steady state under negligible molecular viscosity, (5) has been shown to give the Kolmogoroff spectrum by Karman.

When the turbulent viscosity is dominant the above equation will have the form

$$-\frac{\partial F}{\partial t} = C \left[F^\alpha k^\beta \int_0^k F^{\frac{3}{2}-\alpha} k'^{\frac{1}{2}-\beta} dk' - F^{\frac{3}{2}-\alpha} k^{\frac{1}{2}-\beta} \int_k^\infty F^\alpha k'^\beta dk' \right] \quad \dots \quad (5a)$$

Let us seek a self-preserving solution of this equation in the form

$$F = \frac{1}{C^2} \cdot \frac{\{u(\lambda)\}^q \cdot \{s(\tau)\}^p}{k_0^3 t_0^2 \cdot \tau^r} \cdot f(\lambda \cdot s(\tau)) \quad \dots \quad (6)$$

where p , q , r are constants, $\lambda = k/k_0$, $\tau = t/t_0$, $u(\lambda)$ a function of λ and $s(\tau)$, a function of τ . On substitution of (6) in (5a) and simplification one obtains the relation

$$\begin{aligned} & \int_0^x u^q(\lambda) \left[r - \frac{p \cdot \tau \cdot s_\tau}{s} \right] f(x) dx - \int_0^x u^q(\lambda) \cdot \tau \cdot s_\tau \cdot \frac{x}{s} \cdot \frac{df}{dx} dx \\ &= \int_0^\infty u^{q\alpha}(\lambda) \cdot x^\beta \cdot f^\alpha(x) dx \times \int_0^x u^{(\frac{3}{2}-\alpha)q} \cdot \frac{s^{\frac{p-3}{2}}}{\tau^{\frac{r-2}{2}}} \cdot x^{\frac{1}{2}-\beta} f^{\frac{3}{2}-\alpha}(x) dx \quad \dots \quad (7) \end{aligned}$$

* This last result was pointed out to me by Prof. Sen.

where $x = s \cdot \lambda$, and s_τ denotes $\frac{ds}{d\tau}$. The condition of similarity will be satisfied if

$$\left. \begin{aligned} q &= 0 \\ s &= \alpha' \tau^c \\ r &= (p-3)c+2 \end{aligned} \right\} \dots \dots \dots (8)$$

where α' is the constant of integration of

$$\tau \cdot \frac{s_\tau}{s} = c,$$

c being another constant. The interesting point here is that equations (8) do not involve α and β . The argument of the function f in (6) does not depend on α and β , but its *form* does. On substitution of (8), (7) will have the form

$$\begin{aligned} & (2-3c) \int_0^x f(x) dx - c \int_0^x x \frac{df(x)}{dx} dx \\ &= \int_x^c x^\beta f^\alpha(x) dx \times \int_0^x x^{\frac{1}{2}-\beta} f^{\frac{1}{2}-\alpha}(x) dx \dots \dots \dots (9) \end{aligned}$$

Again substituting the values of q, s, r from (8) in (6), one finds that the *form* of the self-preserving solution $F(k, t)$ of Karman's equation (5a) is the same as (4) given by Sen. The constituent function $f(x)$ of self-preservation is now given by a different equation, namely (9), which involves α and β .

It may be easily shown that equation (9) admits of similar solutions of the form $h^3 f(hx)$, $f(x)$ being any solution of the same equation, and h any constant (which is unconnected with α and β). This similarity property is known also to belong to the solution of Heisenberg's equation.

When the inertia terms in the equation of decay (1) are comparable to the viscous term, i.e., the viscosity part can no longer be neglected, the equation of decay of turbulent energy will have the general form (5). If we assume a solution of the form (8) for the complete equation (5), the similarity condition will be satisfied for $s = \alpha' \tau^c$, only if $c = \frac{1}{2}$. This again means that Heisenberg's form of solution (3) is the only similar solution which is valid for the entire general Karman spectrum of turbulence.

We shall now examine the behaviour of $f(x)$ satisfying equation (9) as $x \rightarrow 0$, and also as $x \rightarrow \infty$.

(a) *Asymptotic behaviour of $f(x)$ at $x \rightarrow 0$.*

If

$$f(x) \sim Ax^n \quad (x \rightarrow 0) \dots \dots \dots (10)$$

then proceeding in the usual way we find the following equation for n ,

$$n^2 \left(\frac{c}{2} - \alpha c \right) + n \{ (2\alpha - 1) + c(2 - \beta - 3\alpha) \} + (2 - 3c)(\beta - \frac{1}{2}) = 0 \dots (11)$$

This quadratic equation in n has two solutions, viz.,

$$n_1 = \frac{2-3c}{c} \dots \dots \dots (12.1)$$

and,

$$n_2 = \frac{2\beta-1}{1-2\alpha} \dots \dots \dots (12.2)$$

N. R. Sen (1951) obtained the asymptotic solution (12.1) (which is free from α , β) for the Heisenberg spectrum. It is to be noted that in the case $\alpha = \frac{1}{2}$, $\beta = -\frac{1}{2}$ (Heisenberg spectrum) the above equation (11) becomes linear, which gives the root

$$n_1 = \frac{2-3c}{c}$$

agreeing with Sen's result; for $c = \frac{2}{3}$, n_1 is equal to 4. We take this value of c in our subsequent argument. In any other case different from that of Heisenberg, (12.1) is a root, which we take as equal to 4 ($c = \frac{2}{3}$). There is a second root $n_2 = \frac{2\beta-1}{1-2\alpha}$. In order that n_2 may be positive, we should have any one of the two alternatives:—

$$(i) \alpha > \frac{1}{2}; \beta < \frac{1}{2} \text{ or } (ii) \alpha < \frac{1}{2}; \beta > \frac{1}{2}.$$

(i) when $\alpha > \frac{1}{2}$; $\beta < \frac{1}{2}$, the expansion of $f(x)$, for $x \rightarrow 0$ will begin with x^4 , if $4\alpha + \beta < \frac{5}{2}$; but if $4\alpha + \beta > \frac{5}{2}$, the expansion of $f(x)$, as $x \rightarrow 0$ begins with x^{n_2} , n_2 being < 4 . These are really the conditions given by Karman.

(ii) But when $\alpha < \frac{1}{2}$; $\beta > \frac{1}{2}$, the above statements are reversed. Karman's conditions have validity for the first alternative only.

(b) *Asymptotic behaviour of $f(x)$ for $x \rightarrow \infty$.*

Putting $f(x') = e^{-\omega(x')}$ and following Heisenberg's method of approximation the behaviour of $f(x)$, for $x \rightarrow \infty$, will be given by the behaviour at large x of f , when it is governed by the following equation:—

$$\frac{d}{dx} \left\{ (2-3c)x^{-\beta} f^{1-\alpha} - cx^{1-\beta} f^{-\alpha} f' + \frac{x^{1-\beta} f^{1-\alpha}}{(\beta+1) + \alpha x \frac{f'}{f}} \right\} + x^{\frac{1}{2}-\beta} f^{1-\alpha} = 0 \quad (13)$$

$$\text{provided we assume that} \quad \alpha\omega' - \beta - 1 > 0 \quad \dots \dots \dots (14)$$

(ω' meaning differentiation with respect to $\log x$). If we seek a solution such as

$$f(x) \sim Ax^{-n} \quad (x \rightarrow \infty), \quad A \neq 0 \quad \dots \dots \dots (15)$$

where n is positive, (13) gives the following equation (where only the highest order terms are retained)

$$\begin{aligned} & x^{[\beta - \frac{1}{2} + n(\frac{1}{2} - \alpha)]} A^{\frac{1}{2}-\alpha} \left[\frac{\frac{3}{2}-\beta}{(\beta+1)-\alpha n} - (\frac{3}{2}-\alpha) \frac{n}{(\beta+1)-\alpha n} + 1 \right] \\ & + x^{[n(1-\alpha) + \beta + 1]} A^{1-\alpha} [n^2(\alpha c - c) + n\{(3c-2)(1-\alpha) - \beta c\} + (3c-2)\beta] \\ & + \dots = 0 \quad \dots \dots \dots (16) \end{aligned}$$

If the first term be the significant one (i.e. algebraically be with higher power of x)

$$\beta - \frac{1}{2} + n(\frac{1}{2} - \alpha) < n(1-\alpha) + \beta + 1$$

$$\text{or} \quad n < 3;$$

then the solution will be given by equating the coefficient of

$$x^{[\beta - \frac{1}{2} + n(\frac{1}{2} - \alpha)]}$$

to zero, which gives $n = \frac{5}{3}$.

If we assume the second term to be dominant, then $n > 3$, and vanishing of the coefficient in the second term would give two values

$$n = \beta/(\alpha-1), \text{ or } (3c-2)/c.$$

The second of these two values is now a violation of the condition $n > 3$, as c is restricted to have a value less than $\frac{1}{2}$.

We note that for the assumption (15), the inequality (14) reduces to

$$n\alpha - \beta - 1 > 0 \quad \dots \dots \dots (14a)$$

This is not violated in any of the above arguments, but is a restriction on α and β .

Under this restriction we have asymptotic expansion of $f(x)$ for $x \rightarrow \infty$ as, either

$$(1) f(x) \approx Ax^{-\frac{1}{2}}$$

or

$$(2) f(x) \approx Ax^{-\beta/(\alpha-1)} \quad (\beta/(\alpha-1) > 3).$$

The first is the well-known Kolmogoroff spectrum but the second is also a mathematical possibility for equation (5a). If we, however, closely analyze (5a), and (16), we note that the first term in the latter equation is contributed by the two terms on the right hand side of equation (5a), and the second term of (16) by the term on the left side of (5a). Hence in case (1) above when the solution approaches the Kolmogoroff spectrum, each of the two terms on the right of (5a) makes finite contribution but their difference is a small term of an order which is neglected. The steady condition in the spectrum is reached by any spectral band receiving from outside and also transmitting to the outside finite and equal amounts of energies. The entire spectrum is far from the decaying stage. But when condition (2) is satisfied each of these two amounts of energies is at least a small quantity of the first order. The spectrum then is very near its state of complete decay.

SUMMARY

The general self-preserving form of the spectrum function governed by Heisenberg's equation for decay of turbulence at the stage when the effect of molecular viscosity is negligible, recently given by N. R. Sen, is found to be valid under the same condition for the more general decay equation proposed by Karman. The form of the constituent function f of self-preservation depends on the arbitrary constants α and β introduced by Karman. The asymptotic behaviour of the self preserving solution of Heisenberg's equation as $k \rightarrow 0$ still remains valid under certain inequality condition satisfied by α and β in the general case of Karman; but under the opposite condition a second behaviour of the asymptotic solution at $k \rightarrow 0$ is possible. For $k \rightarrow \infty$ the Kolmogoroff spectrum is obtained as a (transient) steady state condition with finite transfer of equal amounts of energies between a spectrum band and its outside, but for Karman's spectrum function when $\beta/(\alpha-1) > 3$, a second steady state behaviour becomes mathematically possible at near the complete decay end of the spectrum.

REFERENCES

- Batchelor, G. K. and Townsend, A. A. (1948). Decay of isotropic turbulence in the initial period. *Proc. Roy. Soc. A*, **193**, 539.
- Chandrasekhar, S. (1949). On Heisenberg's elementary theory of turbulence. *Ibid.*, **A**, **200**, 20.
- Heisenberg, W. (1948). Zur Statistischen Theorie der Turbulenz. *Z. Phys.*, **124**, 628.
- (1949). On the theory of Statistical and isotropic turbulence. *Proc. Roy. Soc. A*, **195**, 402.
- Karman, T. V. (1948). Progress in the Statistical theory of turbulence. *Proc. Nat. Acad. Sci., Wash.*, **34**, 530.
- Kolmogoroff, A. N. (1941). On degeneration of isotropic turbulence in an incompressible viscous liquid. *C.R. Acad. Sci., U.R.S.S.*, **31**, 538.
- Loitsiansky, L. G. (1939). Some basic laws of isotropic turbulent flow. Rep. Cent. Aero Hydrodyn. Inst. (Moscow) No. 440. (Translated as *Tech. Memor., Nat. Adv. Comm. Aero., Wash.*, No. 1079.)
- Sen, N. R. (1951). On Heisenberg's spectrum of turbulence. *Bull. Cal. Math. Soc.*, **43**, 1.

APPELL SET OF POLYNOMIALS

by VIKRAMADITYA SINGH, *Department of Mathematics, University of Delhi*

(Communicated by R. S. VARMA, F.N.I.)

(Received November 13, 1952 ; read May 7, 1954)

1. INTRODUCTION

A set of polynomials $\{P_n(x)\}$, where $P_n(x)$ is of degree n in x , is said to be an Appell set, if it satisfies the relation

$$P'_n(x) = P_{n-1}(x). \quad \dots \quad (1)$$

An equivalent definition is the existence of a power series

$$A(t) = \sum_{n=0}^{\infty} a_n t^n \quad a_0 \neq 0 \quad \dots \quad (2)$$

such that

$$A(t) e^{tx} = \sum_{n=0}^{\infty} t^n P_n(x) \quad \dots \quad (3)$$

and $A(t)$ is called the generating function of the set of polynomials $P_n(x)$.

Varma [4] has recently given a generalization of Sheffers [1] representation of Appell polynomials. His result may be stated as follows :

If

$$I_{n,r} = \int_0^x \delta_n(t) t^r d\beta(t) \quad \dots \quad (4)$$

$$n, r = 0, 1, 2, \dots$$

exists such that $I_{0,0} \neq 0$, then the Appell set is given by

$$P_n(x) = \int_0^x K_n(x, t) d\beta(t) \quad \dots \quad (5)$$

where

$$K_n(x, t) = \sum_{r=0}^n \delta_{n-r}(t) \frac{(x+t)^r}{r!}. \quad \dots \quad (6)$$

In particular

$$P_n(x) = \frac{x^n}{n!} \int_0^x {}_3F_2 \left\{ \begin{matrix} -n, a, b \\ c, d \end{matrix} ; -\frac{t}{x} \right\} d\beta(t)$$

and the generating function then is

$$A(t) = \int_0^x {}_2F_2 \left\{ \begin{matrix} a, b \\ c, d \end{matrix} ; ut \right\} d\beta(u)$$

In the present paper we give an extension of Varma's result to

$$P_n(x) = \frac{x^n}{n!} \int_0^x {}_{r+1}F_r \left\{ \begin{matrix} -n, a_1, a_2, \dots, a_r \\ b_1, b_2, \dots, b_r \end{matrix}; -\frac{t}{x} \right\} d\beta(t)$$

and

$$A(t) = \int_0^\infty {}_rF_r \left\{ \begin{matrix} a_1, a_2, \dots, a_r \\ b_1, b_2, \dots, b_r \end{matrix}; ut \right\} d\beta(u)$$

and also give, by means of operational calculus, some expressions for $P_n(x)$ in terms of confluent hypergeometric functions.

2. A NEW INTEGRAL REPRESENTATION

We begin by establishing the following lemma:

$$\begin{aligned} \sum_{n=0}^{\infty} \frac{(xu)^n}{n!} {}_{r+1}F_r \left\{ \begin{matrix} -n, a_1, a_2, \dots, a_r \\ b_1, b_2, \dots, b_r \end{matrix}; -\frac{t}{x} \right\} \\ = e^{xu} {}_rF_r \left\{ \begin{matrix} a_1, a_2, \dots, a_r \\ b_1, b_2, \dots, b_r \end{matrix}; ut \right\}. \end{aligned} \quad (7)$$

Proof: with the usual notation

$$(a_p, r) = a_p(a_p+1) \dots (a_p+r-1)$$

we can write the left hand side of (7) as

$$\sum_{n=0}^{\infty} \frac{(xu)^n}{n!} \sum_{p=0}^n (-n, p) \frac{(a_1, p) \dots (a_r, p)}{(b_1, p) \dots (b_r, p)} \frac{1}{p!} \left(-\frac{t}{x}\right)^p.$$

Now

$$\begin{aligned} (-n, p) &= (-1)^p n(n-1) \dots (n-p+1) \\ &= (-1)^p n! / (n-p)!, \end{aligned}$$

therefore the left hand side

$$\begin{aligned} &= \sum_{n=0}^{\infty} \frac{(xu)^n}{n!} \sum_{p=0}^n \frac{(a_1, p) \dots (a_r, p)}{(b_1, p) \dots (b_r, p)} \frac{n!}{p! (n-p)!} \left(\frac{t}{x}\right)^p \\ &= \sum_{p=0}^{\infty} \frac{(ut)^p}{p!} \frac{(a_1, p) \dots (a_r, p)}{(b_1, p) \dots (b_r, p)} \sum_{n=p}^{\infty} \frac{(xu)^{n-p}}{(n-p)!} \\ &= e^{xu} {}_rF_r \left\{ \begin{matrix} a_1, a_2, a_3, \dots, a_r \\ b_1, b_2, b_3, \dots, b_r \end{matrix}; ut \right\}, \end{aligned}$$

by an inversion of the order of summation.

Rice's result [3]

$$\sum_{n=0}^{\infty} \frac{(xu)^n}{n!} {}_3F_2 \left\{ \begin{matrix} -n, a_1, a_2 \\ b_1, b_2 \end{matrix}; -\frac{t}{x} \right\} = e^{xu} {}_2F_2 \left\{ \begin{matrix} a_1, a_2 \\ b_1, b_2 \end{matrix}; ut \right\}$$

follows at once from our lemma by taking $r = 2$.

On interchanging the order of integration and summation and using our lemma we get

$$\begin{aligned} A(u) e^{ux} &= \sum_{n=0}^{\infty} P_n(x) u^n \\ &= e^{xu} \int_0^{\infty} {}_rF_r \left\{ \begin{matrix} a_1, a_2, \dots, a_r \\ b_1, b_2, \dots, b_r \end{matrix}; ut \right\} d\beta(t). \end{aligned}$$

Therefore

$$A(u) = \int_0^{\infty} {}_rF_r \left\{ \begin{matrix} a_1, a_2, \dots, a_r \\ b_1, b_2, \dots, b_r \end{matrix}; ut \right\} d\beta(t). \quad \dots \quad (11)$$

It is easy to see that

$${}_rF_r \left\{ \begin{matrix} a_1, a_2, \dots, a_r \\ b_1, b_2, \dots, b_r \end{matrix}; ut \right\}$$

can be written as

$${}_rF_r \left\{ \begin{matrix} a_1, a_2, \dots, a_r \\ b_1, b_2, \dots, b_r \end{matrix}; ut \right\} = \prod_{p=1}^r \frac{\Gamma(b_p)}{\Gamma(a_p)\Gamma(b_p-a_p)} \int_0^1 x_p^{a_p-1} (1-x_p)^{b_p-a_p-1} e^{ut - \prod_{p=1}^r x_p} dx_p. \quad \dots \quad (12)$$

$$R(a_p) > 0, \quad R(b_p - a_p) > 0.$$

If we denote the generating function in (11) by $A_r(u)$ and use (12) we get

$$\begin{aligned} A_r(u) &= \prod_{p=1}^r \frac{1}{B(a_p, b_p - a_p)} \int_0^1 x_p^{a_p-1} (1-x_p)^{b_p-a_p-1} dx_p \int_0^{\infty} e^{ut - \prod_{p=1}^r x_p} d\beta(t) \\ &= \prod_{p=r-q+1}^r \frac{1}{B(a_p, b_p - a_p)} \int_0^1 x_p^{a_p-1} (1-x_p)^{b_p-a_p-1} A_{r-q} \left(u \prod_{p=r-q+1}^r x_p \right) dx_p, \end{aligned} \quad (13)$$

which gives us a relation between the generating functions obtained by the different choice of the order of the hypergeometric functions.

4. RELATION BETWEEN APPELL POLYNOMIALS AND SOME KNOWN FUNCTIONS

If x and y be two independent variables it is easy to see by Taylor's theorem and property of Appell polynomials that

$$P_n(x+y) = \sum_{p=0}^n \frac{y^p}{p!} P_{n-p}(x), \quad \dots \quad (14)$$

and in particular

$$P_n(x) = \sum_{r=0}^n \frac{x^r}{r!} P_{n-r}(0) \dots \dots \dots (15)$$

If we multiply both sides of (15) by e^{-px} and integrate from 0 to ∞ , we get

$$p \int_0^{\infty} e^{-px} P_n(x) dx = \sum_{r=0}^n P_{n-r}(0) \frac{1}{p^r} \dots \dots \dots (16)$$

In the notation of operational calculus we can write (16) as

$$P_n(x) \doteq \sum_{r=0}^n P_{n-r}(0) p^{-r}. \quad \dots \quad \dots \quad \dots \quad (17)$$

4.1. By means of an important theorem in operational calculus we have from (17)

$$e^{-x} P_n(x) \doteq \sum_{r=0}^n P_{n-r}(0) p/(p+1)^{r+1}. \quad \dots \quad \dots \quad \dots \quad (18)$$

But we know that [Humbert and McLachlan 6]

$$x^{-\nu-\frac{1}{2}} e^{-x} W_{\mu, \nu}(x) \doteq (-)^{\mu+\nu+\frac{1}{2}} \Gamma(\mu-\nu+\frac{1}{2}) \frac{p^{\mu+\nu-\frac{1}{2}}}{(1+p)^{\mu-\nu+\frac{1}{2}}}.$$

Hence taking

$$\mu = \frac{r+2}{2} \text{ and } \nu = -\frac{r-1}{2},$$

we get

$$x^{\frac{r-2}{2}} e^{-x/2} W_{\frac{r+2}{2}, -\frac{r-1}{2}}(x) \doteq \Gamma(r+1) p/(p+1)^{r+1}.$$

Now from (18) and using Lerch's theorem we get

$$e^{-x} P_n(x) = \sum_{r=0}^n \frac{P_{n-r}(0)}{r!} x^{\frac{r-2}{2}} e^{-x/2} W_{\frac{r+2}{2}, -\frac{r-1}{2}}(x),$$

and finally

$$P_n(x) = \sum_{r=0}^n \frac{P_{n-r}(0)}{r!} x^{\frac{r-2}{2}} e^{x/2} W_{\frac{r+2}{2}, -\frac{r-1}{2}}(x). \quad \dots \quad \dots \quad (19)$$

4.2. From (17) as before we have

$$e^{-x/2} P_n(x) \doteq \sum_{r=0}^n P_{n-r}(0) p/(p+\frac{1}{2})^{r+1}. \quad \dots \quad \dots \quad (20)$$

But we know that [6]

$$M_{\mu, \nu}(t) \doteq \Gamma(\nu+3/2) \frac{p}{(p+\frac{1}{2})^{\nu+3/2}} {}_2F_1 \left\{ \nu+3/2, -\mu+\nu+\frac{1}{2}; \frac{1}{p+\frac{1}{2}} \right\},$$

$$R(\nu) > -3/2.$$

Putting $\nu = r-\frac{1}{2}$ and $\mu = r$ we get

$$M_{r, r-\frac{1}{2}}(t) \doteq \Gamma(r+1) p/(p+\frac{1}{2})^{r+1},$$

and hence as before

$$P_n(x) = \sum_{r=0}^n \frac{P_{n-r}(0)}{r!} M_{r, r-\frac{1}{2}}(x) e^{x/2}. \quad \dots \quad \dots \quad (21)$$

4.3. It is well known from operational calculus that if $f(t) \doteq \phi(p)$ then

$$\frac{1}{\sqrt{\pi t}} \int_0^\infty e^{-x^2/4t} f(x) dx \doteq \phi(\sqrt{p}).$$

Therefore from (17) we have

$$\frac{1}{\sqrt{\pi x}} \int_0^x \exp \left[-s - \frac{s^2}{4x} \right] P_n(s) ds = \sum_{r=0}^n P_{n-r}(0) \frac{\sqrt{p}}{(1+\sqrt{p})^{r+1}} \quad \dots \quad (22)$$

But we know that [6]

$$\sqrt{\frac{2}{\pi}} (2x)^{1/2(n-1)} e^{x/2} D_{-n}(\sqrt{2}x) = \frac{\sqrt{p}}{(1+\sqrt{p})^n},$$

where $D_n(x)$ is Weber's parabolic cylindrical function. Therefore as before

$$\frac{1}{\sqrt{\pi x}} \int_0^x \exp \left[-s - \frac{s^2}{4x} \right] P_n(s) ds = \sqrt{\frac{2}{\pi}} \sum P_{n-r}(0) (2x)^{r/2} e^{x/2} D_{-(r+1)}(\sqrt{2}x),$$

and finally

$$\int_0^\infty e^{-s-s^2/4x} P_n(s) ds = \sum P_{n-r}(0) (2x)^{\frac{r+1}{2}} e^{x/2} D_{-(r+1)}(\sqrt{2}x) \quad \dots \quad (23)$$

4.4. The set of polynomials $\{ \Pi_n(x) \}$, where $\Pi_n(x)$ is a polynomial of degree n in x defined by the relation

$$\Pi_n(x) = e^x \left(\frac{d}{dx} \right)^n \{ e^{-x} A_n(x) \}, \quad \dots \quad \dots \quad (24)$$

where

$$A_n(x) = (a_0, a_1, \dots, a_n, x)^n,$$

is called Angelescus' set.

It is quite apparent that $\frac{A_n(x)}{n!}$ behaves like an Appell polynomial, and so from (24) we get

$$\frac{\Pi_n(x)}{n!} = e^x \left(\frac{d}{dx} \right)^n \left\{ e^{-x} P_n(x) \right\}. \quad \dots \quad \dots \quad (25)$$

Taking the integral representation for $P_n(x)$ from (10) we get

$$\begin{aligned} \frac{\Pi_n(x)}{n!} &= e^x \sum_{p=0}^n \frac{1}{p!} \frac{(a_1, p) \dots (a_r, p)}{(b_1, p) \dots (b_r, p)} \left(\frac{d}{dx} \right)^n \left(\frac{e^{-x} x^{n-p}}{(n-p)!} \right) \mu_p \\ &= \sum_{p=0}^n \frac{1}{p!} \mu_p \frac{(a_1, p) \dots (a_r, p)}{(b_1, p) \dots (b_r, p)} L_{n-p}^{(p)}(x), \quad \dots \quad \dots \quad (26) \end{aligned}$$

where $L_{n-p}^{(p)}(x)$ is the generalized Laguerre polynomial.

The generating function for Angelescus' polynomials was given by Sastri [5] and satisfies the relation

$$\frac{1}{1-t} \exp \left(\frac{-xt}{1-t} \right) \phi \left(\frac{-t}{1-t} \right) = \sum_{n=0}^{\infty} \frac{\Pi_n(x)}{n!} t^n. \quad \dots \quad \dots \quad (27)$$

It is now clear that the generating function for Angelescus' polynomials is obtained from that of Appell polynomials by replacing t by $\frac{-t}{1-t}$ and then dividing by $(1-t)$. Therefore we have

$$\frac{1}{1-t} \phi\left(\frac{-t}{1-t}\right) = \frac{1}{1-t} \int_0^\infty r^r \left\{ \begin{matrix} a_1, a_2, \dots, a_r \\ b_1, b_2, \dots, b_r \end{matrix}; -\frac{ut}{1-t} \right\} d\beta(t). \quad \dots (28)$$

Putting $y = -t/(1-t)$ in (27) we have

$$\begin{aligned} \exp(yx) \phi(y) &= \sum_{n=0}^{\infty} \frac{\Pi_n(x)}{n!} (-)^n y^n (1-y)^{n+1} \\ &= \sum_{r=0}^{\infty} y^r \sum_{n=0}^r \frac{\Pi_n(x)}{n!} \frac{r! (-)^n}{(r-n)! n!}, \end{aligned}$$

Comparing this with (3) we get

$$\frac{P_r(x)}{r!} = \sum_{p=0}^r (-)^p \frac{\Pi_p(x)}{p!} \frac{1}{p! (r-p)!},$$

or

$$P_r(x) = \sum_{p=0}^r (-)^p \frac{\Pi_p(x)}{p!} \binom{r}{p}. \quad \dots \dots \dots (29)$$

The corresponding inverse relation can be obtained from (25) by applying Leibnitz theorem and we readily get

$$\frac{\Pi_n(x)}{n!} = \sum_{r=0}^n (-)^r \binom{n}{r} P_r(x). \quad \dots \dots \dots (30)$$

ACKNOWLEDGEMENT

My thanks are due to Dr. R. S. Varma, Senior Scientist, Defence Science Organization, for suggesting me the problem and for guidance in the preparation of the paper. Thanks are also due to Dr. Ram Behari, Head of the Mathematics Department, University of Delhi, for kindly providing me all facilities to carry on research work and for his general encouragement.

REFERENCE

Singh, Vikramaditya (1954). On Angelescus Polynomials. *Proc. Nat. Inst. Sc.*, **20**, 280-289.

Issued July 22, 1954.

PRODUCTS OF SUMMABILITY METHODS

by T. PATI, *Department of Mathematics, Allahabad University*

(Communicated by B. N. Prasad, F.N.I.)

(Received September 15, 1953; read May 7, 1954)

1. In a recent paper Szász (1952) raised the following question.

Let A and B denote any two regular methods of summability for sequences $\{s_n\}$, and let AB denote the iteration-product which associates with a given sequence the A -transform of its B -transform; then does A -summability imply AB -summability?

In the same paper Szász demonstrated that the answer to this question is in the affirmative when A is Abel and B is (C, α) , $\alpha > 0$. *

In the present paper we generalize this result of Szász by replacing (C, α) by the wider class of regular Hausdorff transformations (H, μ) , of which Cesàro, Hölder and Euler transformations are well known special cases.

I should like to express my indebtedness to Dr. B. N. Prasad for his kind guidance and encouragement.

2. Definitions.

We write

$$f(x) = (1-x) \sum s_n x^n = \sum a_n x^n \quad (0 \leq x < 1).$$

If the limit

$$\lim_{x \rightarrow 1-0} f(x) = s$$

exists, then the sequence $\{s_n\}$, or the series $\sum a_n$, is said to be summable (A) .

The general Hausdorff transformation (H, μ) is defined by

$$t_m = \sum_n \lambda_{m,n} s_n,$$

where

$$\lambda_{m,n} \begin{cases} = \binom{m}{n} \Delta^{m-n} \mu_n & (n \leq m), \\ = 0 & (n > m). \end{cases}$$

* For the case $\alpha = 1$ see Zygmund (1926), p. 189. Incidentally it may be mentioned that the analysis in section 2 of Szász's paper has been vitiated by an obvious oversight in the step just preceding identity (2.4). Indeed (2.4) should read:

$$\frac{1}{y+1} \sum_0^x \sigma_n^x \left(1 - \frac{1}{y+1}\right)^n = \frac{x}{y} \int_0^y \left(1 - \frac{u}{y}\right)^{x-1} \phi(u) du,$$

where

$$\phi(u) = f(1 - (u+1)^{-1}),$$

and, following the notations of Szász's paper, we should finally have

$$A(C, \alpha) \{s_n\} = (\bar{C}, \alpha) \{\phi(u)\}.$$

We shall write

$$\mu_{n,p} = \Delta^p \mu_n,$$

so that

$$\lambda_{m,n} = \binom{m}{n} \mu_{n,m-n} \quad (0 < n < m).$$

If

$$\mu_n = \int_0^1 t^n d\chi(t), *$$

where $\chi(t)$ is a real function of bounded variation in $0 < t < 1$, then μ_n is called the *moment constant*, of rank n , of $\chi(t)$. We may suppose without loss of generality that

$$\chi(0) = 0.$$

If, further,

$$\chi(1) = 1,$$

and

$$\chi(+0) = \chi(0) = 0,$$

so that $\chi(t)$ is continuous at $t = 0$, then μ_n is said to be a *regular moment constant*.

We have, in general,

$$\mu_{n,p} = \Delta^p \mu_n = \int_0^1 t^n (1-t)^p d\chi(t).$$

We assume throughout that (H, μ) is a regular Hausdorff transformation.

3. We prove the following theorem.

THEOREM. *If A and B denote two regular methods of summability for sequences $\{s_n\}$, and AB denote their iteration product which associates with a given sequence the A -transform of its B -transform, then A -summability implies AB -summability where A is Abel and B a regular Hausdorff method.*

We require the following lemmas for the proof of our theorem.

LEMMA 1. † *In order that the (H, μ) -transform should be regular it is necessary and sufficient that μ_n should be a regular moment constant.*

LEMMA 2. ‡ *In order that the transformation*

$$G(y) = \int_0^1 g(ty) d\chi(t)$$

should be regular, i.e. that ' $g(y) \rightarrow s$, as $y \rightarrow \infty$ ' should imply ' $G(y) \rightarrow s$, as $y \rightarrow \infty$ ', it is necessary and sufficient that $\chi(1) = 1$ and $\chi(+0) = \chi(0) = 0$.

* The function t^0 is defined at $t = 0$ so as to be continuous. Thus

$$\mu_0 = \int_0^1 d\chi(t).$$

† Hardy (1949), Theorem 208 (i), p. 260.

‡ Hardy (1949), Theorem 217, p. 276.

Proof of the THEOREM.

Let t_m denote the regular (H, μ) -transform of the sequence $\{s_n\}$. Then our object is to show that if

$$f(x) = (1-x) \sum_n s_n x^n \rightarrow s,$$

as $x \rightarrow 1-0$, then

$$F(x) = (1-x) \sum_m t_m x^m \rightarrow s,$$

as $x \rightarrow 1-0$.

We have

$$\begin{aligned} t_m &= \sum_{n=0}^m \binom{m}{n} \Delta^{m-n} \mu_n s_n \\ &= \sum_{n=0}^m \binom{m}{n} \mu_{n, m-n} s_n \\ &= \sum_{n=0}^m \binom{m}{n} \left(\int_0^1 t^n (1-t)^{m-n} d\chi(t) \right) s_n \\ &= \int_0^1 \left(\sum_{n=0}^m \binom{m}{n} t^n (1-t)^{m-n} s_n \right) d\chi(t). \end{aligned}$$

Hence

$$\sum_{m=0}^{\infty} t_m x^m = \int_0^1 \left(\sum_{m=0}^{\infty} x^m \sum_{n=0}^m \binom{m}{n} t^n (1-t)^{m-n} s_n \right) d\chi(t).$$

Now, putting

$$I \equiv \sum_{m=0}^{\infty} x^m \sum_{n=0}^m \binom{m}{n} t^n (1-t)^{m-n} s_n,$$

we have

$$\begin{aligned} I &= \sum_{n=0}^{\infty} x^n t^n s_n \sum_{m \geq n} x^{m-n} (1-t)^{m-n} \binom{m}{n} \\ &= \sum_{n=0}^{\infty} x^n t^n s_n (1-x(1-t))^{-n-1} \\ &= (1-x(1-t))^{-1} \left(\sum_{n=0}^{\infty} x^n t^n (1-x(1-t))^{-n} s_n \right). \end{aligned}$$

Thus

$$\begin{aligned} F(x) &= (1-x) \int_0^1 I d\chi(t) \\ &= \int_0^1 \frac{1-x}{1-x(1-t)} \left(\sum_{n=0}^{\infty} \left(\frac{xt}{1-x(1-t)} \right)^n s_n \right) d\chi(t), \end{aligned}$$

and, therefore, putting

$$x = 1 - \frac{1}{y+1} = \frac{y}{y+1},$$

we have

$$\begin{aligned} F\left(\frac{y}{y+1}\right) &= \int_0^1 \left(1 - \frac{yt}{1+yt}\right) \left(\sum_{n=0}^{\infty} \left(\frac{yt}{1+yt}\right)^n s_n\right) d\chi(t) \\ &= \int_0^1 f\left(\frac{yt}{1+yt}\right) d\chi(t). \end{aligned}$$

Hence, setting

$$f\left(\frac{y}{1+y}\right) \equiv g(y)$$

and

$$F\left(\frac{y}{1+y}\right) \equiv G(y),$$

we have finally

$$G(y) = \int_0^1 g(yt) d\chi(t).$$

Now, as

$$x \rightarrow 1-0, \quad y \rightarrow \infty,$$

and

$$\lim_{y \rightarrow \infty} g(y) = \lim_{x \rightarrow 1-0} f(x) = s,$$

by hypothesis.

Therefore, by Lemmas 1 and 2,

$$G(y) = F\left(\frac{y}{1+y}\right) \rightarrow s, \text{ as } y \rightarrow \infty,$$

that is,

$$F(x) \rightarrow s, \text{ as } x \rightarrow 1-0.$$

This completes the proof of the theorem.

REFERENCES

- Hardy, G. H. (1949). *Divergent Series*, Oxford.
 Szász, O. (1952). On products of summability methods. *Proc. American Math. Soc.*, **3**, 257-263.
 Zygmund, A. (1926). Remarque sur la sommabilité des séries de fonctions orthogonales. *Bulletin international de l'Académie Polonaise des Sciences et des Lettres, Classe des Sciences. Math. et Nat., Série A*, 185-191.

Issued July 22, 1954.

FERTILIZATION AND THE DEVELOPMENT OF EMBRYO AND SEED IN *EUPHORBIA HIRTA* LINN.

by L. B. KAJALE, *Maharashtra Association for the Cultivation of Science,
Law College Buildings, Poona 4*

(Communicated by S. P. Agharkar, F.N.I.)

(Received August 28, 1952 ; after revision March 1 ; read May 7, 1954)

In an earlier publication the author in collaboration with Rao (Kajale and Rao, 1943) described the development of the embryo sac and pollen in *Euphorbia hirta* and *Jatropha gossypifolia* with some observations on the organization of the obturator in two more species of the genus *Euphorbia*. In this paper it is proposed to deal with fertilization and the development of the embryo, endosperm and seed coat in *Euphorbia hirta*.

The earlier embryological literature dealing with the Euphorbiaceae is not summarized here since it has already been reviewed by Johri and Kapil (1953), Banerji (1951), Johansen (1950), and Gopinath and Gopalkrishnan (1949).

The material was collected locally and fixed in Navaschin's fluid. It was dehydrated and embedded in paraffin according to the customary methods. Sections were cut 8 to 14 μ thick, stained in Heidenhain's haematoxylin and destained in a saturated solution of picric acid.

FERTILIZATION

Fertilization is porogamous. After entering the embryo sac the pollen tube passes along one of the synergids, in between the latter and the wall of the embryo sac. It travels up to the base of the egg, its tip enlarges and bursts open discharging the two male gametes inside the embryo sac. During its passage, the pollen tube generally destroys one and sometimes both the synergids (Figs. 2 and 3). Inside the embryo sac the pollen tube may persist till the proembryo becomes two- to four-celled and several endosperm nuclei are formed, but ultimately it collapses and disappears (Fig. 6).

The male gametes at this stage present a spherical shape and take a deep stain. One of them fuses with the egg and the other with the two polar nuclei (Figs. 1 and 2).

During triple fusion the two polar nuclei increase in size and lie, closely pressed together, near the egg apparatus. The male gamete comes in contact with these two nuclei (Figs. 1 and 2). By this time the male gamete in the egg is already in process of fusion to accomplish syngamy (Fig. 2). Further details could not be observed and it could not be ascertained whether there is a formation of the secondary nucleus prior to triple fusion or all the three nuclei fuse simultaneously to form the primary endosperm nucleus. It appears probable, however, that syngamy precedes triple fusion in *E. hirta* unlike in *E. oreophila* and *Homonium retusa* (Gopinath and Gopalkrishnan, 1949) in which syngamy and secondary fertilization are reported to be simultaneous. Johri and Kapil (1953) have recently reported that syngamy precedes fertilization of the fusion nucleus in *Acalypha indica*.

EMBRYO

The fertilized egg becomes somewhat uniformly vacuolate (Fig. 4) and before it divides, four to eight endosperm nuclei are present in the embryo sac (Fig. 5).

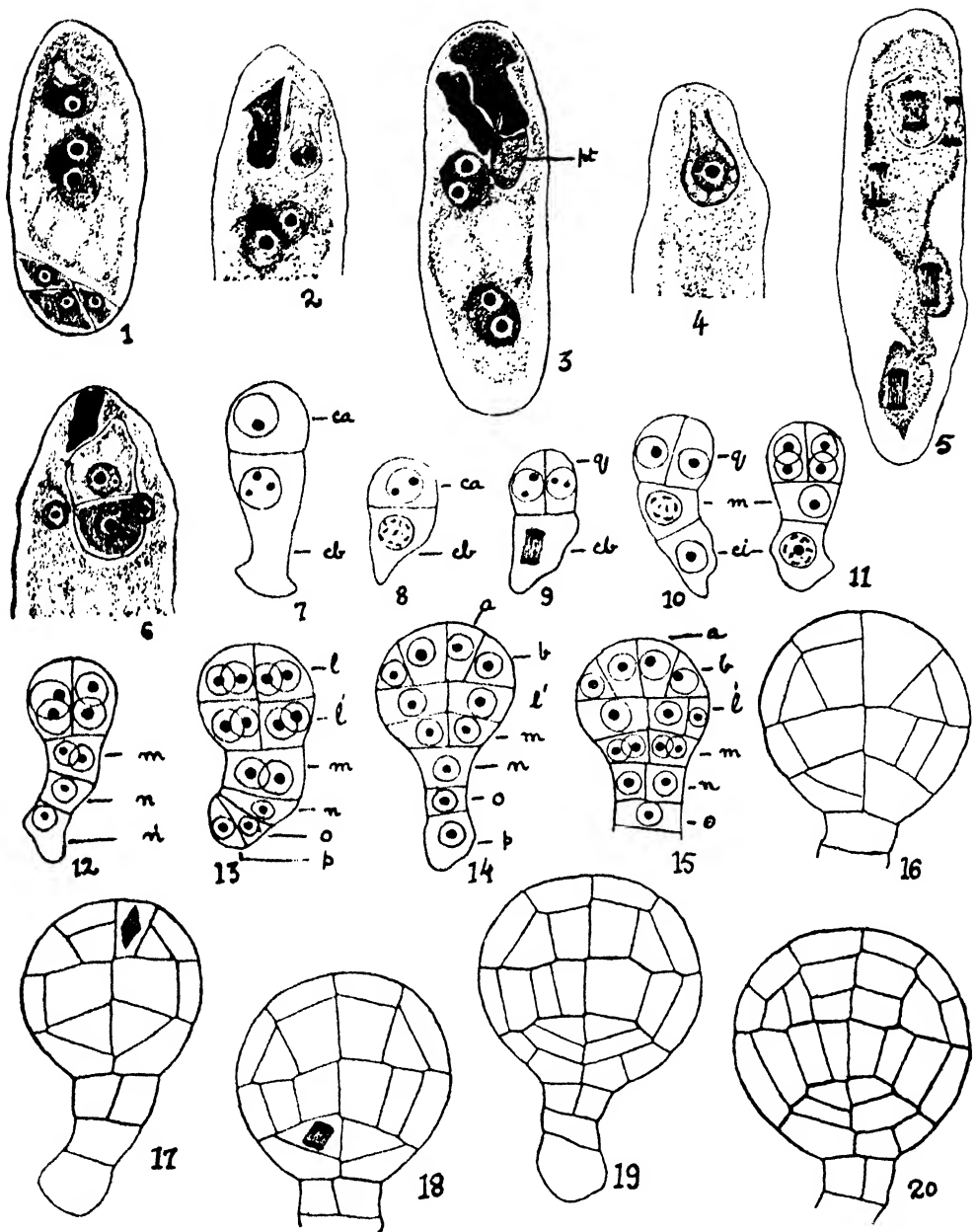
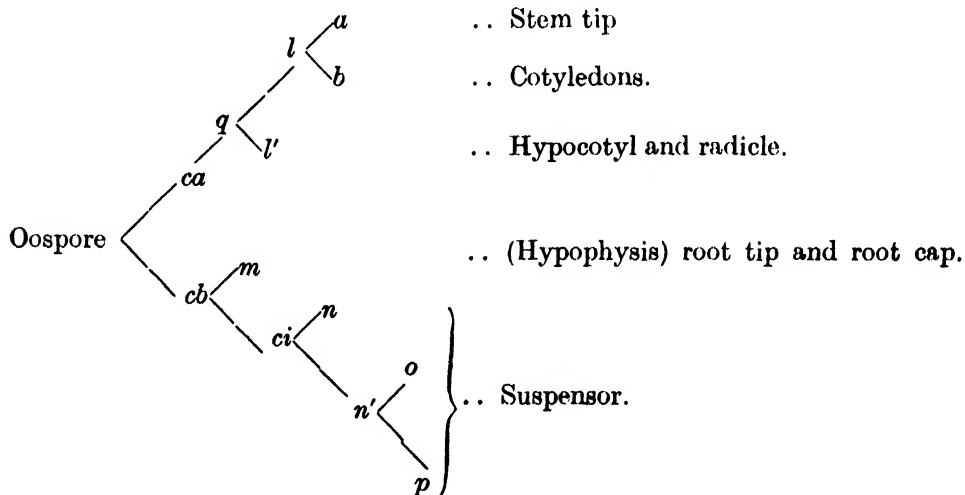
TEXT-FIGS. 1-20. *Euphorbia hirta*.

Fig. 1. Embryo sac showing double fertilization. Note the presence of antipodals. Fig. 2. The same as fig. 1 with one degenerating synergid. Figs. 3 and 4. Successive sections of the same embryo sac; fig. 3 shows two degenerating synergids, the tip of the pollen tube (*pt*) and two endosperm nuclei, while fig. 4 shows the micropylar part of embryo sac with the fertilized egg. Fig. 5. Embryo sac showing division of the oospore and endosperm nuclei. Fig. 6. Micropylar part of the embryo sac with two-celled proembryo and degenerating pollen tube. Figs. 7 to 20. Various stages in the development of the embryo. $\times 600$.

The first division of the oospore is transverse and results in the formation of two cells, the terminal cell and the basal cell (Figs. 5, 7 and 8). These cells are designated by the letters *ca* and *cb* respectively. Generally the first division of the oospore in the Euphorbiaceae is transverse but it is claimed to be longitudinal in *E. preslii* (Weniger, 1917) and *E. rothiana* (Shrivastava, 1952).

The basal cell *cb* varies in shape and size. Generally it is larger and more vacuolate than the terminal cell *ca*. Sometimes it is elongated (Fig. 7). The basal cell *cb* divides transversely either before or after the terminal cell *ca* has divided longitudinally and gives rise to the upper cell *m* and the lower cell *ci*. At this stage the proembryo is T-shaped and consists of three or four cells (Figs. 9 and 10). The cell *ci* divides further and forms the cells *n* and *n'* (Fig. 12). Normally the division of the cell *ci* is in a transverse plane but occasionally it may be oblique or nearly vertical. The cell *n'* by a further transverse division gives rise to two cells, *o* and *p* (Figs. 13 and 14). Thus *m*, *n*, *o* and *p* are all derived from the basal cell of the two-celled proembryo.

The terminal cell *ca* divides longitudinally to form two juxtaposed cells designated together as *q* (Fig. 10). Both these cells divide again by a longitudinal wall at right angles to the first and a quadrant is formed (Figs. 11 and 12). Shortly thereafter each cell of the quadrant divides transversely into two tiers *l* and *l'* and the octant stage is reached (Fig. 13). The upper four cells of the octant eventually give rise to the stem tip and the two cotyledons, and the lower four cells to the hypocotyl. The cell *m* derived from the basal cell (*cb*) functions as a hypophysis which completes the root cap and the root tip. The remaining cells *n*, *o*, *p* and their derivatives develop into the suspensor. The origin of the various parts of the embryo from the cells of the proembryo is as follows:—



Thus the embryogeny of *E. hirta* in all essential features resembles that of *E. exigua* described by Souèges (1925) and conforms to the *Euphorbia* variation of the Onagrad Type (Johansen, 1950) or to the Crucifer Type of Maheshwari (1950). Similarly, according to Johansen (1950), the development of the embryo in *E. procera* (Modilewski, 1909), *E. splendens* (Weniger, 1917), *E. esula* (Souèges, 1924) and *Acalypha australis* * (Tateishi, 1927) also conforms to the *Euphorbia* variation. Two other variations have also been reported from this family. In *E. preslii* (Weniger, 1917) and *E. rothiana* (Shrivastava, 1952) the embryo development

* According to Johri and Kapil (1953) the embryo development in this species is like that of *A. indica*.

conforms to the *Scabiosa* variation of the Piperad type (Johansen, 1950) while in *Acalypha indica* (Johri and Kapil, 1953) and *A. lanceolata* * (Thathachar, 1952) it conforms to the *Lotus* variation under the Onagrad Type (Johansen, 1950).

Details of the development of the various parts of the mature embryo are discussed in the following paragraphs.

At about the time when the octants are formed, the embryo consists of six tiers: the two terminal tiers *l* and *l'* of four cells each, the next one *m* of two cells, and the lower three tiers, i.e., *n*, *o* and *p* consist of one cell each (Fig. 13). Each cell of the terminal tier *l* divides obliquely and gives rise to two cells, *a* and *b* (Fig. 14). The inner cells *a* by transverse and longitudinal divisions give rise to the plumule, while the outer cells *b*, two on each side, form the initials of the cotyledons (Figs. 20 to 22). Simultaneously with this development the cells of the tier *l'* divide periclinally to cut off the dermatogen (Fig. 15). Shortly afterwards the dermatogen is completed in the other two tiers *l* and *m* also (Figs. 16 and 17). The differentiation of the dermatogen in the tier *l* does not follow any regular sequence and it may be completed first either in the inner cells *a* or the outer cells *b* (Figs. 16 and 17).

The cells of the tier *l'* at first divide longitudinally and then undergo a series of longitudinal and transverse divisions so as to form the region of the hypocotyl and radicle (Figs. 18 to 21). As the development proceeds the periblem and the plerome become gradually differentiated. At about the stage represented by Fig. 22 the plerome consists of five to six layers and the periblem of three to four layers as seen in longitudinal sections.

It has already been stated that the cell *m* derived from the basal cell (*cb*) of the two-celled proembryo functions as an hypophysis. Before the octant is organized, it divides by a vertical wall and gives rise to two cells which in turn also divide vertically to form a group of four cells (Figs. 12 to 15). All these cells divide periclinally to produce four outer cells and four inner cells (Fig. 16). The former complete the dermatogen and represent the primordium of the root cap. The inner cells once more divide obliquely and the resulting eight cells are placed in two tiers of four cells each (Figs. 18 to 20). These two tiers function as the initials of the root cortex and form the root tip. The upper four cells contribute to the plerome while the lower four form the periblem (Fig. 22).

SUSPENSOR

Except the cell *m*, the remaining cells *n*, *o* and *p* derived from the basal cell (*cb*) give rise to the suspensor. It consists of a few cells and becomes multiseriate especially towards the embryo side (Fig. 21), and persists even in the mature seed. Its cells become packed with starch grains during later stages of development. The absence of the suspensor in this family has been previously reported by Weniger (1917) in *E. preslii* and Shrivastava (1952) in *E. rothiana*.

MATURE EMBRYO

The mature embryo is straight and dicotyledonous (Fig. 23). The three histogenic layers become prominent at about the stage shown by Fig. 22. The cells of the periblem are broader than long. In the region of the plerome they are more elongated. The cells of the mature embryo become packed with food material mostly starch grains. Their distribution, however, in the different histogenic layers is not uniform. More grains are deposited in the periblem than in the plerome. In the periblem, they are also bigger in size than those in the plerome. An interesting point about the structure of the embryo is the development of the

* See discussion by Johri and Kapil (1953).

long, elongated and narrow laticiferous cells which are densely cytoplasmic. They are present in the hypocotyl and the cotyledons.

ENDOSPERM

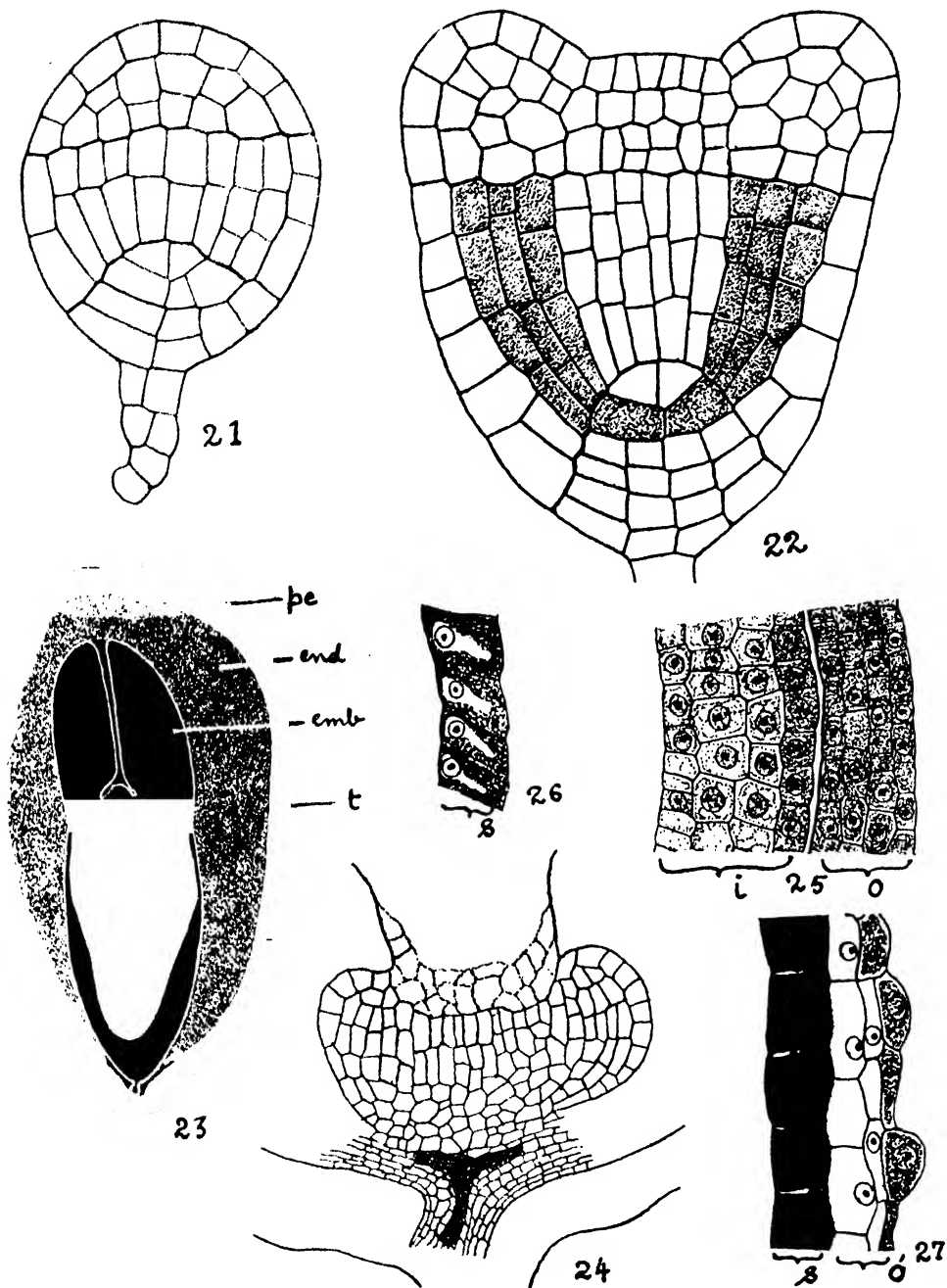
The primary endosperm nucleus divides earlier than the oospore and forms two free nuclei. One of them moves towards the chalazal end and soon both of them divide to form four to eight nuclei before the oospore segments transversely (Figs. 3 and 5). In *E. splendens* (Weniger, 1917) as many as 32 to 64 endosperm nuclei are formed before the division of the oospore. The free nuclear division in the endosperm continues until many nuclei are formed in the peripheral layer of the cytoplasm. They are somewhat evenly distributed except at the two poles of the embryo sac where they are more crowded. During earlier stages of development, the divisions of the endosperm nuclei are synchronous but later on the nuclei are in different stages of division. The endosperm nuclei are further characterized by the presence of a varying number of nucleoli as reported by Modilewski (1909, 1911) in *E. procera* and *E. palustris*. In *E. hirta* the nucleoli vary from one to four in number. The free nuclear endosperm later becomes cellular. Wall formation starts all round at the periphery and extends towards the centre. The process of wall formation begins before the embryo becomes cordate-shaped and after the differentiation of the dermatogen in the octant.

In the beginning the cells of the endosperm are highly vacuolate but soon they become filled with cytoplasm and appear more compact and conspicuous. Such a change occurs first in the cells at the two poles of the embryo sac. In the mature seed the cells of the endosperm are loaded with starch grains. The latter are bigger in size than those in the embryo. A part of the endosperm is consumed by the growing embryo but a considerable part of it persists in the mature seed surrounding the embryo except at the tip of the root cap (Fig. 23). A part of the nucellus, described later, also persists in the mature seed at the chalazal end along with the endosperm (Fig. 23).

DEVELOPMENT OF THE HYPOSTASE

Some other interesting changes also occur during post-fertilization stages which deserve consideration. At the chalazal end the embryo sac elongates and destroys some of the cells of the nucellus. The remaining cells, however, become rich in cytoplasm, take a deeper stain and appear more regularly placed. They multiply and become conspicuously differentiated to form a thick saucer-shaped pad of tissue below the chalazal end of the embryo sac, the further growth of which is arrested as soon as it reaches this pad (Fig. 24). Afterwards, however, the embryo sac extends laterally above the pad and eventually destroys all the adjoining cells of the nucellus. The formation of such a pad is analogous to the hypostase and its occurrence is also reported by Gopinath and Gopalkrishnan (1949) in *E. oreophila* and by Landes (1946) in *Acalypha rhomboidea* and some other species of the genus *Euphorbia* investigated by her. The vascular supply of the ovule ends below the hypostase, which persists in the mature seed as perisperm. Like the endosperm it functions as an organ of storage and its cells become packed with starch grains as the seed matures (Fig. 23). The function of this tissue is a matter of dispute. Either it is considered to be of nutritional nature or it is supposed to arrest the downward growth of the embryo sac. Whatever be its earlier function, in later stages at least it is definitely an organ of storage in *E. hirta*.

An interesting change occurs in the structure of the nucellus during the formation of the hypostase. As reported by Landes (1946) for other species of *Euphorbia*, the cells of the inner integument at the chalazal end become enlarged at the expense of the nucellus and divide the latter into a bigger micropylar portion and a smaller chalazal portion. The former consists of a few layers of large and vacuolate cells

TEXT-FIGS. 21-27. *Euphorbia hirta*.

Figs. 21 and 22. Stages in development of embryo. $\times 600$. Fig. 23. L.S. of mature seed showing embryo, endosperm, persisting hypostase and seed coat. Note the absence of endosperm at the tip of the root cap. $\times 60$. *emb* = embryo, *end* = endosperm, *pe* = perisperm, *t* = testa. Fig. 24. Chalazal part of the ovule showing the hypostase. Note constriction above the hypostase caused by the inner integument. Cells shown by dotted lines represent the degenerating cells of the nucellus. $\times 260$. Figs. 25 to 27. Stages in the development of testa. Fig. 26 shows a few cells of the stony layer only. $\times 600$. *i* = inner integument, *o* = outer integument, *o'* = part of the testa derived from the outer integument, *s* = stony layer.

while the latter consists of compact, regular and densely cytoplasmic cells which later develop into the hypostase. The division of the nucellus into two such portions thus appears to be a characteristic feature of the genus *Euphorbia*.

SEED COAT

There are two integuments in *E. hirta*, the outer consisting of four layers and the inner of four to five layers of cells over the greater part of their length. But at the tip the outer integument is thicker while the inner one is thinner. The latter sometimes consists of six to seven layers of cells towards the chalazal end. In general the cells of the outer integument are richer in cytoplasm than those of the inner integument except the outer epidermal layer of the latter, the cells of which are densely cytoplasmic as those of the outer integument (Fig. 25). As the embryo develops the integuments close over the nucellus and the nucellar beak disintegrates.

Both the integuments take part in the formation of the testa. In the mature seed it consists generally of four and occasionally of three layers of cells. Out of these four layers, the innermost layer of the testa represents the outer epidermis of the inner integument while the remaining two or three layers belong to the outer integument. The outer epidermal layer of the inner integument finally becomes most conspicuous and forms the brittle stony layer of the seed coat as reported by Netolitzky (1926) and Landes (1946) for many other members of the Euphorbiaceae.

The remaining part of both the integuments comprising the inner layers of the inner integument and the inner layer of the outer integument disappears during the differentiation of the testa. Before they disappear their cells increase in size and become vacuolate and those of the inner integument may also multiply to increase the number of layers temporarily.

During maturation of the seed the cell walls of the brittle stony layer become thickened due to the deposition of a chemical substance which looks yellow or yellowish brown when stained with haematoxylin. The thickening matter is first deposited on the radial and the outer tangential walls (Fig. 26). It later extends to the inner tangential walls of the cells. During this time the nucleus shifts to the inner tangential wall and the cytoplasm is gradually reduced. By the time the cytoplasm is completely used up the thickening has progressed centripetally to meet in the middle along an irregular line to form fully thickened stony cells (Fig. 27). The nucleus in these cells is seen to persist for a considerable time but later on it is completely enclosed by the thickening matter and is therefore not visible. The thickening of the cell walls starts at the micropylar end and extends towards the chalaza.

Majority of the cells of the epidermal layer of the testa increase in size and become dome-shaped as a result of which the testa presents a finely warty appearance (Fig. 27). The epidermal cells contain in them the granular deposit of the same substance present in the cell walls of the brittle stony layer (Fig. 27). The nucleus persists in these cells also.

The cells of the middle two layers are without any granular deposits. Out of these two layers, the cells of the outer one are narrow and elongated while those of the inner one are somewhat oblong and bigger than those in the outer layer. The cells in both the layers are vacuolate and show the presence of nuclei in them (Fig. 27).

SUMMARY

Fertilization is porogamous. The pollen tube passes in between the wall of the embryo sac and one of the synergids. Generally one and sometimes both the synergids are destroyed. The polar nuclei increase in size prior to triple fusion. Probably syngamy precedes triple fusion.

The proembryo consists of three to four cells and is T-shaped. Embryo development conforms to the *Euphorbia* variation of the Onagrad Type. The small suspensor is multiseriate

towards the embryo side and persists in the mature seed. The structure of the mature embryo and the distribution of starch are described.

The primary endosperm nucleus divides earlier than the oospore. The free nuclear endosperm later becomes cellular. Wall formation starts at the periphery and extends towards the centre. One to four nucleoli are present in the nuclei of the endosperm cells. The endosperm surrounds the embryo except at the tip of the root cap.

The hypostase persists in the mature seed as perisperm and serves as an organ of storage.

The testa consists of four layers of cells. The innermost layer representing the outer epidermis of the inner integument becomes brittle and stony. Next come three more layers derived from the outer integument. Granular deposits are present in the epidermal cells of the testa which have a finely warty appearance. There is a difference in the size and shape of the cells of the different layers.

ACKNOWLEDGEMENTS

I wish to express my sincere thanks to Prof. S. P. Agharkar and Prof. A. C. Joshi for their interest in my work.

LITERATURE CITED

- Banerji, I. (1951). Pollen and embryo sac of two Euphorbiaceae. *Proc. Ind. Acad. Sci. B.*, **34**, 172-181.
- Gopinath, D. M. and Gopalkrishnan, K. S. (1949). The ovule and the development of the female gametophyte in *Homonia retusa* Muell. and *Euphorbia oreophila* Miquel. *Amer. Midl. Nat.*, **41**, 759-764.
- Johansen, D. A. (1950). Plant Embryology, Waltham, Mass., U.S.A.
- Johri, B. M. and Kapil, R. N. (1953). Contribution to the morphology and life history of *Acalypha indica* L. *Phytomorphology*, **3**, 137-151.
- Kajale, I. B. and Rao, G. V. (1943). Pollen and embryo sac of two Euphorbiaceae. *Jour. Ind. Bot. Soc.*, **22**, 229-235.
- Landes, M. (1946). Seed development in *Acalypha rhomboidea* and some other Euphorbiaceae. *Amer. Jour. Bot.*, **33**, 562-568.
- Mahoshwari, P. (1950). An Introduction to the Embryology of Angiosperms. New York.
- Modilowski, J. (1909). Zur Embryobildung von *Euphorbia procera*. *Ber. deutsch. Bot. Ges.*, **27**, 21-26.
- (1911). Über die abnormale Embryosackentwicklung bei *Euphorbia palustris* L. und anderen Euphorbiaceen. *Ibid.*, **29**, 430-436.
- Netolitzky, F. (1926). Handbuch der Pflanzenanatomie. 2 Abt. 2 Teil. Anatomie der Angiospermen-Samen. Berlin.
- Shrivastava, R. K. (1952). Contribution to the embryology of Indian Euphorbiaceae: 1, *Euphorbia rathiana* Spreng. *Ann. Bot.*, **16**, 505-511.
- Soudges, R. (1924). Embryogénie des Euphorbiacées. Développement de l'embryon chez l'*Euphorbia esula* L. *C. R. Acad. Sci.*, Paris, **179**, 989-991.
- (1925). Développement de l'embryon chez l'*Euphorbia exigua* L. *Bull. Soc. Bot. France*, **72**, 1018-1031.
- Tateishi, S. (1927). On the development of the embryo sac and fertilization of *Acalypha australis* L. *Bot. Mag.*, Tokyo, **41**, 477-485 (quoted by Johansen, 1950).
- Thathachar, T. (1952). Morphological studies in the Euphorbiaceae: 1. *Acalypha lanceolata* Willd. *Phytomorphology*, **2**, 197-201.
- Weniger, W. (1917). Development of embryo sac and embryo in *Euphorbia preslii* and *E. splendens*. *Bot. Gaz.*, **63**, 266-281.

THE EGG-WALL OF THE AFRICAN MIGRATORY LOCUST, *LOCUSTA MIGRATORIA MIGRATORIOIDES* REICH. AND FRM. (ORTHOPTERA, ACRIDIDAE)

by M. L. ROONWAL, F.N.I., Forest Entomologist, Forest Research Institute, Dehra Dun

(With 1 Table, 2 Text-figures and 2 Plates)

(Received October 26, 1953; read May 7, 1954)

CONTENTS

	Page
I. Introduction	361
II. Composition of Egg-wall	
(a) Description of egg-wall	361
(b) Discussion	365
III. Summary	368
IV. References	368
V. Explanation of Plates	369

I. INTRODUCTION

The composition of the egg-wall of the European Migratory Locust, *Locusta migratoria migratoria* Linn., was briefly described by Plotnikov (1926, pp. 271-272) and that of the African Migratory Locust, *L. migratoria migratorioides* Reich. and Frm., by me (Roonwal, 1936a). However, in the light of later findings, particularly those of Slifer (1937-1950) on the American grasshopper, *Melanoplus differentialis* Thomas¹, and of Matheé (1951) on the Brown Locust of South Africa, *Locustana pardalina* (Walker), a re-investigation of the egg-wall of the African Migratory Locust, *Locusta migratoria migratorioides* Reich. and Frm. (Orthoptera, family Acrididae), was carried out and the results are presented here. At 33° C. and in moist soil the total period of incubation from the moment of oviposition to that of hatching is about 12½-13 days, and blastokinesis or turning of the embryo occurs at the 5½ to 6-day stage. The developmental stages (e.g., the 40-hour stage, 5-day stage, etc.) mentioned in the present paper refer to the above-mentioned temperature of incubation. For fixing, section-cutting and staining of eggs, the techniques mentioned in my earlier account (Roonwal, 1936b, pp. 392-393) were employed.

II. COMPOSITION OF EGG-WALL

(a) Description of egg-wall

The egg-wall of the fully formed egg, whether lying in the egg-calyx shortly prior to oviposition or freshly-laid, consists of the outer layer or chorion (composed of a thinner external layer or exochorion and a thicker internal layer or endochorion) and inside it a very fine vitelline membrane. As the embryo develops, the vitelline membrane disappears, and one of the two embryonic membranes, viz., the serosa, successively secretes three membranes, one behind the other, in the following

¹ Slifer (1937, p. 494) stated that she examined certain stages of the eggs of *Locusta migratoria migratorioides* R. and F. also; she, however, did not give either a description or illustrations of that species.

chronological order: a thin 'yellow cuticle', a thick 'white cuticle' and a thin 'embryonic cuticle'. Of these, the last named persists until hatching when it is cast off by the freshly-hatched hopper as an 'intermediate moult'. The fate of the remaining two layers could be followed only up to 5 days before hatching, but it is presumably similar to that in *Melanoplus differentialis* (Slifer, 1937) in which the 'yellow cuticle' persists until hatching, while the 'white cuticle' is digested by a 'hatching enzyme' (secreted, according to Slifer, by the pleuropodia) sometime before hatching. The details of the composition of the egg-wall of *L. migratoria migratorioides* in various developmental stages may now be described.

The wall of the fully developed eggs (Pl. XI, Fig. 2; and Text-fig. 2c) which have descended from the ovarioles into the egg-calyx, ready for oviposition, has essentially the same composition as that of the freshly-laid egg described below, with this difference that in the former case the exochorion is more smooth and well-defined and the knob-like tubercles (*t.*) of the endochorion are more 'amorphous' and less compact. In the freshly-laid egg, on the other hand, the exochorion is more ragged, but the knob-like tubercles of the endochorion are more compact and better defined in sections of eggs.

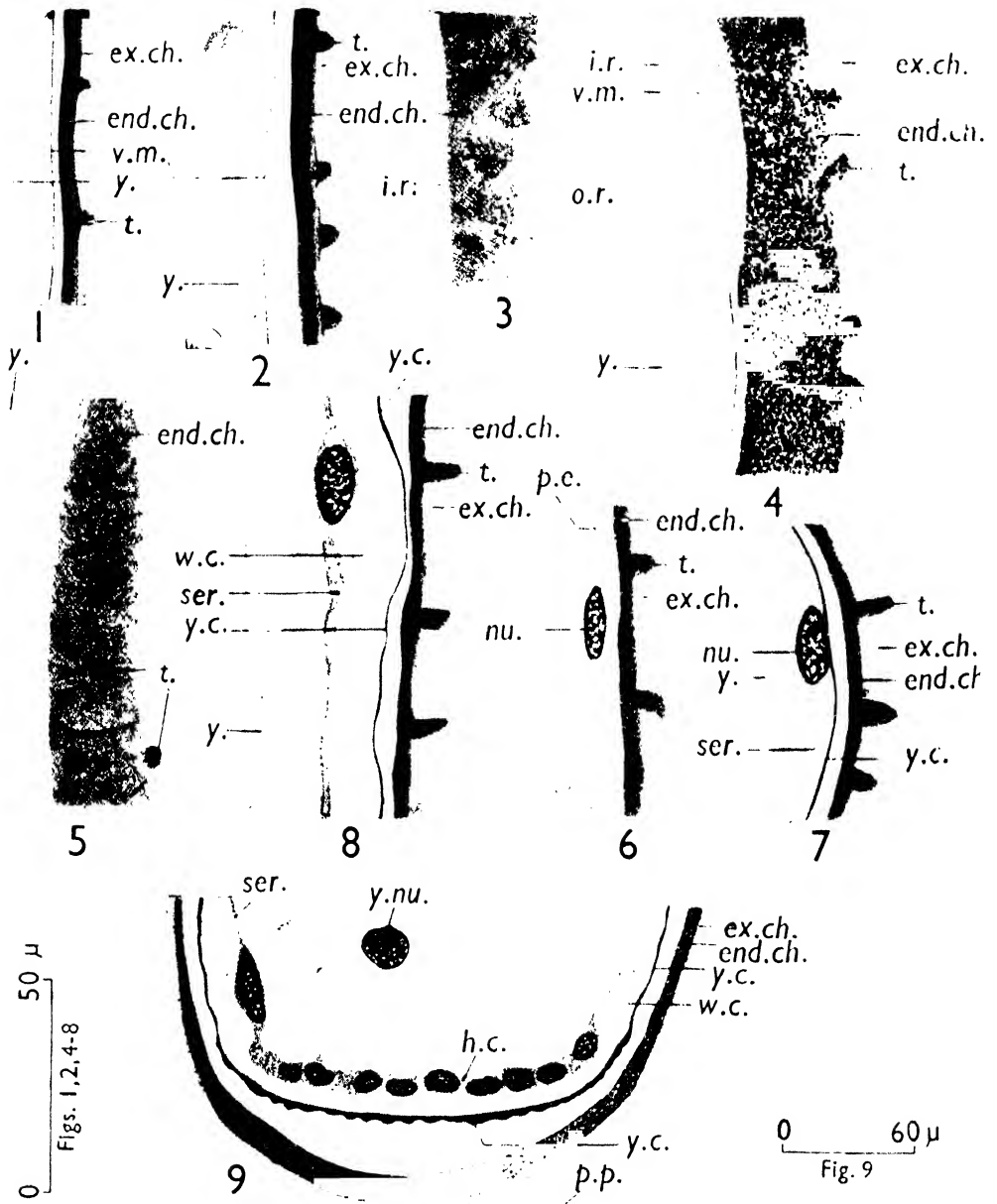
In the freshly-laid egg (Pl. XI, Fig. 2) the egg-wall consists of three layers in the following order from the outside: (i) the outer refractile layer or exochorion ('temporary coat' of Slifer, 1937); (ii) inside it, and contiguous¹ with it, the thick endochorion ('chorion' of Slifer); and, finally, (iii) the vitelline membrane (*vide* Table 1). Both the two outer layers, *viz.*, the exochorion and the endochorion, are much thicker at the poles (especially at the posterior pole of the egg, Pl. XI, Fig. 4) than elsewhere. The exochorion (*ex.ch.*) is comparatively thin (*ca.* 6 μ at the posterior pole and *ca.* 2–3 μ elsewhere), refractile and rather amorphous-looking, and does not stain with haematoxylin or with eosin. The endochorion (*end.ch.*) is *ca.* 28–30 μ thick at the posterior pole and *ca.* 5–6 μ elsewhere. It stains deeply dark-violet with haematoxylin and shows a semi-granular, felt-like structure of 'tangled hairs' except on the extreme outer and inner surfaces which are smooth and refractile (Pl. XI, Fig. 3). The felt-like structure is especially noticeable in a tangential section (Pl. XI, Fig. 5). On its outer face the endochorion is produced into a series of subcylindrical or rounded protuberances (*t.*) which, in surface view of the egg-wall, are visible (Pl. XI, Fig. 5; and Text-fig. 2a) as a pattern of closely lying, rather irregularly arranged tubercles (*t.*). Each tubercle is discrete and distinct and is not connected with its neighbours by means of hexagonal ridges (Text-fig. 2b) as obtains, for instance, in the Desert Locust, *Schistocerca gregaria* (Roonwal, 1954). In tangential sections (Pl. XI, Fig. 5) the tubercles often appear to lie in the 'body' of the chorion.

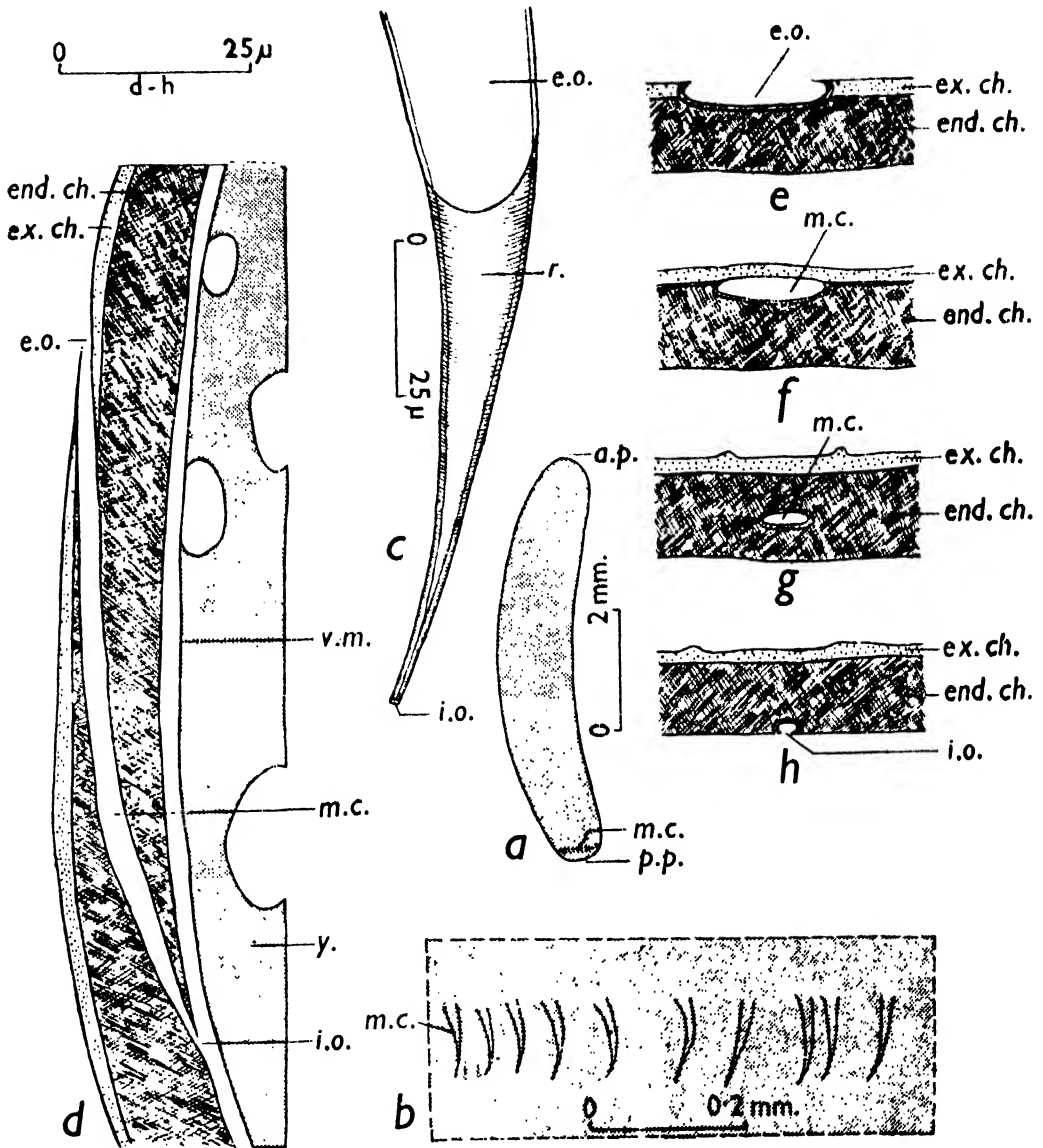
Next to the endochorion is the extremely thin (less than 1 μ) and structureless vitelline membrane (*v.m.*). In sections, at places where the yolk-mass (*y*) is separated from the egg-wall, the vitelline membrane adheres to the yolk-mass rather than to the chorion.

The micropylar apparatus (Text-fig. 1a–h), as seen in a freshly-laid egg, consists of a ring of about 35–43 elongated (60–120 μ long), funicular canals—the micropylar canals (*m.c.*)—near the posterior pole of the egg. From its shallow and oblique external opening (*e.o.*), which is about 8.5–28 μ in width, each canal runs obliquely downward (posteriorward) and inward along the longitudinal axis of the egg-wall, traversing the entire chorion and opening, at the inner surface of the endochorion, into the interior of the egg by means of an extremely fine, rounded aperture or internal opening (*i.o.*). The canals do not appear to penetrate the vitelline membrane.

In the 40½-hour old egg (Pl. XI, Fig. 6), the egg-wall is substantially as in the freshly-laid egg, except that the exochorion is less well-defined and has evidently

¹ See further (under Discussion) for two types of egg-walls in the Acrididae.





TEXT-FIG. 1 (a-h). Micropylar apparatus of the freshly-laid egg of *Locusta migratoria migratorioides* R. and F.

- (a) Egg in side view, showing the ring of micropylar canals near the posterior pole.
 (b) Surface view of a portion of the egg-wall near the posterior pole of an egg, showing a few micropylar canals.
 (c) A micropylar canal, from Fig. b, in surface view. Greatly enlarged.
 (d) Longitudinal-vertical section of the egg-wall, showing the micropylar canal.
 (e)-(h) Transverse sections of the egg-wall, showing a micropylar canal cut at various levels, from the outer surface (e) to the inner end (h). Only the exochorion and the endochorion are shown; the vitelline membrane and the yolk are not shown.
 a.p., anterior pole of egg; end. ch., endochorion; e.o., external opening of micropylar canal; ex. ch., exochorion; i.o., internal opening of micropylar canal; m.c., micropylar canal; p.p., posterior pole of egg; r., roof of micropylar canal; v.m., vitelline membrane; y., yolk.

begun to disintegrate, and the vitelline membrane is seen no longer. Between the yolk and the endochorion lies the thin primary epithelium¹ (*p.e.*) (membranous portion between the nuclei *ca.* $1\ \mu$ thick), a membrane whose extra-embryonic portion shortly afterwards, with the differentiation of the amnion, is termed the serosa and, as such, practically surrounds the entire yolk mass. According to Roonwal (1936b, p. 412), the serosa first makes its appearance as a fold at the cephalic end of the germ band in the 42-hour stage; by the 46-hour stage, the caudal and the lateral folds also make their appearance. The primary epithelium is thus converted into the serosa, and, by the 50-hour stage, completely envelops the yolk mass.

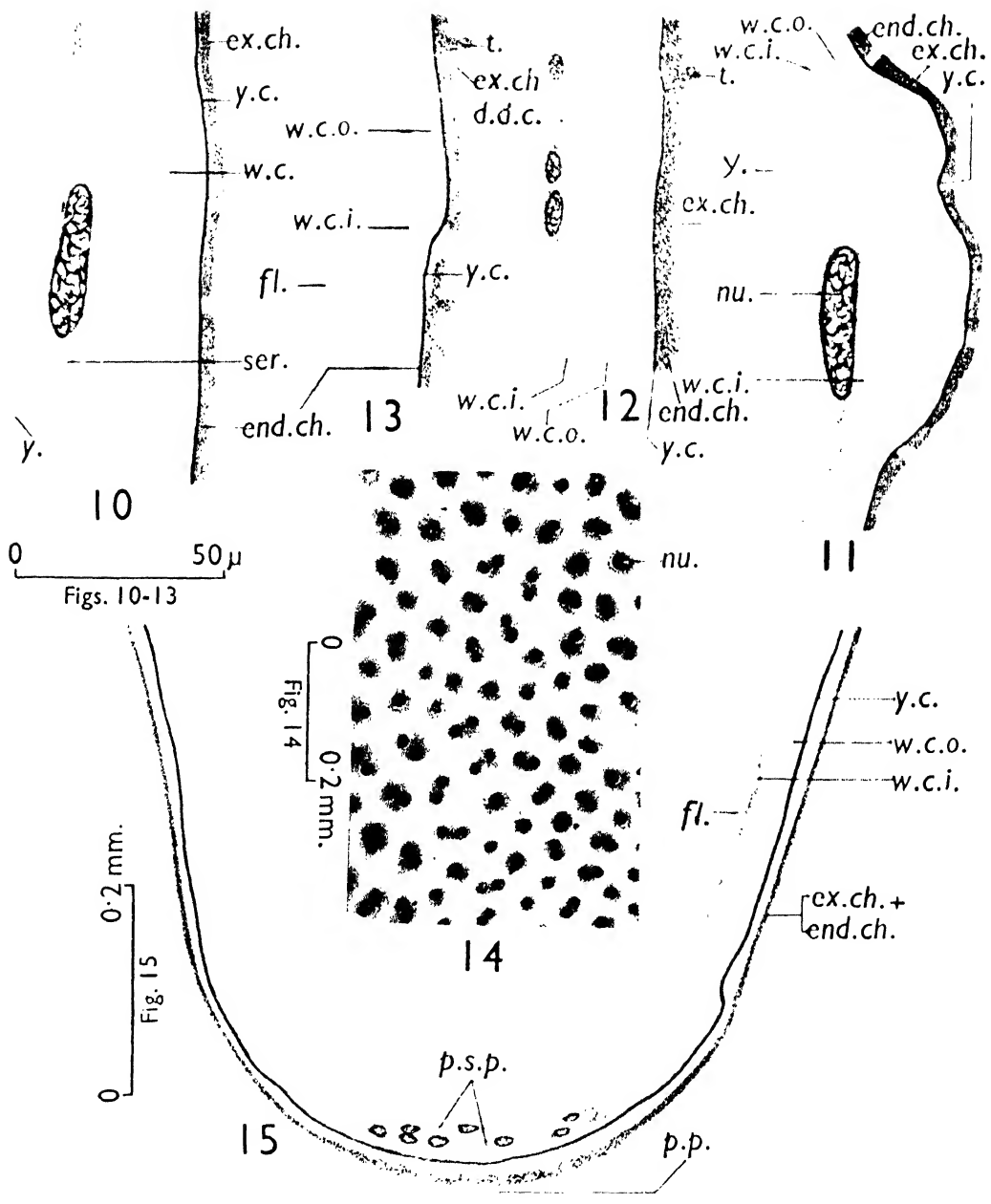
By the time the egg is 66 hours old (Pl. XI, Fig. 7), the serosa has become thickened, the membranous portion in between the neighbouring nuclei measuring about $3\text{--}4\ \mu$ thick. It has assumed secretory activity and has secreted on its outer surface (*i.e.*, between the serosa and the endochorion) a thin (*ca.* $1\ \mu$ thick) yellowish, refractile membrane which does not take either the haematoxylin or the eosin stain; this is the 'yellow cuticle' of Jahn (1935-1936) and of Slifer (1937). It is smooth throughout, and neither now nor later does it show in *Locusta* a spiny outer surface as was reported by Slifer (1937) in *Melanoplus differentialis* and by Matheé (1951) in *Locustana pardalina*.

About the 75-hour stage the serosa secretes, between its outer surface and the yellow cuticle, a second membrane which is thick (*ca.* $8\text{--}10\ \mu$), whitish and granular in sections; this is the 'white cuticle' (Pl. XI, Fig. 8, *w.c.*) of Jahn and of Slifer. Like the yellow cuticle, it does not stain either with haematoxylin or with eosin. The serosa itself now appears to be somewhat thinner than in the 66-hour stage, evidently as a result of the secretory material largely having been released in the shape of the white cuticle.

The posterior pole in this stage presents interesting features (Pl. XI, Fig. 9). The yellow cuticle here is about double its normal thickness elsewhere and is crenulated on the outside. On the other hand, the white cuticle at the posterior pole is much thinner (*ca.* $2\text{--}3\ \mu$) than elsewhere (*ca.* $5\text{--}6\ \mu$). Beneath this small, circular polar patch of thickened yellow cuticle and thinned white cuticle the serosa cells are grouped together in a patch of large cells with numerous rounded nuclei lying close together; these are the 'hydropyle cells' of Slifer. This entire patch evidently corresponds to the 'water-absorbing' area or 'hydropyle' described by Slifer (1938, 1950) in *Melanoplus differentialis*. (Also see below, 7-day old stage.)

In an egg about 117 hours (*ca.* $4\frac{1}{2}$ days) old (Pl. XII, Fig. 10), it is seen that the inner margin (*ca.* $2\ \mu$ wide) of the thick white cuticle (which in this stage is about $22\text{--}25\ \mu$ thick) is glassy, refractile and structureless and stains deeply with eosin, in contrast to the rest of the white cuticle which shows a pattern of fine, parallel laminations (in transverse sections of the egg) and stains lightly with eosin. This 'inner layer' almost presents the appearance of a new layer secreted by the serosa, but, as subsequent development shows, it is only a modified portion of the white cuticle. In this and subsequent stages, the chorion is seen to be longitudinally cracked in several places, a phenomenon recorded by me earlier (Roonwal, 1936a, pp. 10-11 and Fig. 3b). In the 125-hour or about $5\frac{1}{2}$ -day stage (Pl. XII, Fig. 11), *i.e.*, shortly before blastokinesis or turning of embryo (which begins at the $5\frac{1}{2}$ to 6-day stage), this inner layer (*w.c.i.*) of the white cuticle remains unchanged in appearance, but its width and discreteness from the outer layer (*w.c.o.*) of the white cuticle is even more marked than before, and it is seen, in sections of eggs, that at several places the inner layer is completely separated or torn away from the outer layer. The latter is now also appreciably thinner (*ca.* $8\text{--}15\ \mu$). During blastokinesis (*ca.* $5\frac{1}{2}$ -day stage) (Pl. XII, Fig. 12), the inner layer is less glassy in appearance than before and becomes partly laminated like the outer layer; and the latter is now

¹ For a definition, see Roonwal (1936b, p. 411; and 1939, p. 25).



evidently thicker (ca. $16\ \mu$). The serosa has ruptured and has turned over (Roonwal, 1937).

Soon after blastokinesis (ca. $6\frac{1}{2}$ -day stage) (Pl. XII, Fig. 13), the inner layer of the white cuticle has lost its glassy and structureless appearance and is fully laminated like the outer layer, but it is still clearly discernible from the latter by taking a deeper eosin or orange G stain. The outer layer of the white cuticle is again considerably thinner, being only about $8\text{--}10\ \mu$ thick. (Also *vide infra*, under Discussion.) In a 7-day old egg (i.e., 1 day after blastokinesis) the position remains substantially unaltered except in the following respects:—(i) The posterior remnants of the serosa form a circular area, termed the 'posterior serosal patch' by Roonwal (1937, p. 195). The patch corresponds to the 'hydropyle cells' described above in the 75-hour stage. (ii) The embryonic body-wall secretes a thin 'embryonic cuticle'. In an egg 8 days old (2 days after blastokinesis), no substantial change is noticeable, but the 'hydropyle area' is now well-defined and is characterised by the presence of the thinned white cuticle (Pl. XII, Fig. 15). The inner layer of the white cuticle is still distinguishable from the outer layer but less clearly than before.

The further fate of the layers of the egg-wall was not followed owing to want of material of the older stages. But, if the fate is similar to the one shown by Slifer (1937, 1938) for *Melanoplus differentialis*, it may be presumed that the white cuticle is digested by the 'hatching enzyme' secreted, according to Slifer, by the pleuropodia, while the yellow cuticle and the chorion persist. As for the embryonic cuticle it has already been shown by me (Roonwal, 1937, pp. 234-235) that it acquires a pattern of spine-like papillae which aid in the hatching operation; the cuticle is cast off during the intermediate moult immediately after hatching.

(b) Discussion

The chemical and physical properties of some of the egg-coverings of the grasshopper, *Melanoplus differentialis*, have been investigated by Campbell (1929) and Jahn (1935a, b; 1936), while Slifer (1937-1950) has studied in detail the morphological structure of the egg-coverings in the same species. The chorion (especially the endochorion) is semi-opaque and non-chitinous and, according to Slifer (1945), can be rapidly (within about 2 minutes) and completely dissolved in a 2 per cent solution of sodium hypochlorite with no apparent effect on the development of the embryo. Slifer (1948) has further shown that the chorion is covered, on both the outer and inner surfaces, by a thin layer of hard, white, waxy material at least a portion of which seems to be deposited on the inner surface of the chorion before the egg is laid; a secondary wax layer is probably deposited at the hydropyle near the posterior pole of the egg when diapause begins.

Regarding the physico-chemical nature of the membranes of *Melanoplus* eggs, Jahn (1935a, p. 38) concluded as follows: '... it seems as if the exochorion and either one or both layers of the cuticle (the "yellow cuticle"¹ and the "white cuticle") are impermeable to $K_4Fe(CN)_6$ or $FeCl_3$. Similar results were obtained with methylene blue and acid fuchsin. Since these layers are apparently freely permeable to water, CO_2 and O_2 , we must classify them as semi-permeable membranes.' The endochorion of *Melanoplus* freely took the Prussian blue [$K_4Fe(CN)_6$ and $FeCl_3$] stain. In *Locusta*, as stated above, the endochorion stains deeply with iron-haematoxylin, but the other layers, viz., the exochorion, the yellow cuticle and the white cuticle, do not take that stain.

The yellow cuticle in *Melanoplus*, according to Jahn (1935-1936), is non-chitinous, possesses a high degree of ionic impermeability and may be related to the 'cuticulin' of the insect exoskeleton. The thick and fibrous 'white cuticle' consists, according to the same author, of chitin or a compound closely related to

¹ The yellow cuticle is highly impermeable (see further).

chitin. Slifer (1937, p. 498) has pointed out that 'the yellow layer confers a high degree of impermeability¹; while the white layer is responsible for a greatly increased toughness and resistance to mechanical injury.'

It is interesting to note that in *Locusta* the 'thinning' of the white cuticle begins even before blastokinesis. In *Melanoplus*, Slifer (1937) reported that the digestion of the white cuticle, resulting in its ultimate complete dissolution, begins about 7 to 8 days before hatching (at 25° C., when development is much slower), i.e., long after blastokinesis, from a 'hatching enzyme' secreted by the embryonic pleuropodia. It may be mentioned that in the 75-hour stage (i.e., a considerable time before blastokinesis which begins about the 5½-day stage) in *Locusta*, either the embryo or the serosa or both start secreting a clear fluid which first accumulates in the posterior part of egg. During blastokinesis this fluid fills almost the entire posterior half of the egg and also extends between the serosa and the white cuticle. I (Roonwal, 1936a, p. 11) called attention to the presence of this fluid and had assumed that the absorption of this fluid by the 'vitelline membrane' ('white cuticle' of the present account) 'not only causes it to swell but is also responsible for the change into a laminated structure.' This fluid has probably little to do with the 'hatching enzyme' of Slifer (1937) which is secreted by the pleuropodia in *Melanoplus* and is responsible for the digestion of the white cuticle. In *Locusta* also, as mentioned above, a certain degree of thinning of the white cuticle is observable before and soon after blastokinesis, but its cause is problematic.

For facility of comparison, the various interpretations and the nomenclature of the layers of the egg-wall of the Acrididae are given in Table I.

TABLE I

Interpretation and nomenclature of the layers of the egg-wall of the Acrididae by various authors.

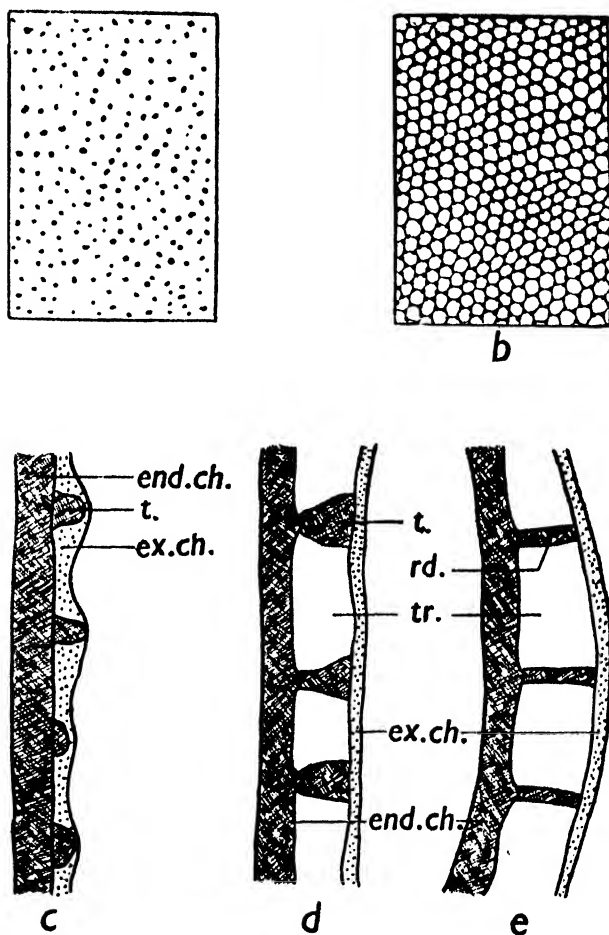
<i>Schistocerca gregaria</i> (Forsk.) (Husain and Roonwal, 1933); <i>Locusta migratoria</i> <i>migratorioides</i> R. and F. (Roonwal, 1936a, 1937)	<i>Melanoplus differentialis</i> (Th.) (Slifer, 1937, 1938)	<i>Locusta migratoria</i> <i>migratorioides</i> , R. and F. (Roonwal, present paper)
1. Exochorion	1. Temporary coating ..	1. Exochorion
2. Endochorion	} 2. Chorion	} 2. Endochorion
3. Vitelline membrane ..		
	3. Vitelline membrane ..	3. Vitelline membrane
	4. Yellow cuticle	4. Yellow cuticle
	5. White cuticle	5. White cuticle (a) Outer layer (b) Inner layer
4. Embryonic cuticle ..	6. Embryonic cuticle ..	6. Embryonic cuticle

Two types of egg-wall in the Acrididae.—As regards the chorion, the eggs of the Acrididae appear to fall into two principal types (Text-fig. 2) thus:

Type I, in which the exochorion throughout lies contiguously with the endochorion and is not separated from the latter by means of large, discrete trabeculae or air spaces. (Example: *Locusta migratoria migratorioides* R. and F., Text-fig. 2, a, c)

¹ Except in the hydropyle area at the posterior pole where it is freely permeable to water.

Type II, in which the exochorion does not lie contiguously with the endochorion (except in certain narrow areas, *e.g.*, the micropylar area), but is largely separated from the latter by means of large, well-defined trabeculae or air spaces. (Example: *Schistocerca gregaria*, Text-fig. 2, *b, d, e*; see Roonwal, 1954, for fuller details.) The physiological function of the air spaces is problematic.



TEXT-FIG. 2 (*a-e*). Diagrammatic representations of surface views of longitudinal-vertical sections of the egg-chorion of Acrididae eggs, showing the two principal types of arrangements.

(*a*) Surface view of chorion of *Locusta migratoria migratorioides* R. and F.

(*b*) Same, of *Schistocerca gregaria* (Forsk.).

(*c*) Longitudinal-vertical section of egg-wall of *Locusta migratoria migratorioides* in middle of egg-length.

(*d*) Same, of *Schistocerca gregaria* in middle of egg-length.

(*e*) Same, *S. gregaria*, at posterior pole of egg.

Type I. (Figs. *a* and *c*). With no trabeculae or air spaces between the exochorion and endochorion, the two layers being contiguous. (Example: *Locusta migratoria migratorioides* R. and F.)

Type II (Figs. *b, d*, and *e*). With trabeculae or air spaces present between the exochorion and endochorion. (Example: *Schistocerca gregaria* Forsk.)

end. ch., endochorion; *ex. ch.*, exochorion; *rd.*, ridge of endochorion; *t.*, tubercle of endochorion; *tr.*, trabeculae or air spaces between exochorion and endochorion.

III. SUMMARY

1. In the fully developed egg which lies in the egg-calyx and in the freshly-laid egg, the egg-wall is composed of three layers, which, starting from the outside, are as follows:—A thin exochorion; a thicker endochorion with outer tubercles; and an extremely thin vitelline membrane.

2. The micropylar apparatus, as seen in the freshly-laid egg, consists of a ring of about 35–43 small, funicular canals—the micropylar canals—near the posterior pole of the egg. Each canal obliquely traverses the entire width of the exochorion and the endochorion and opens into the egg at the inner end by means of an extremely fine aperture.

3. By the 40-hour stage (incubation in all cases at 33° C. and in moist sand), the vitelline membrane is no longer seen.

4. By the 66-hour stage, one of the embryonic membranes, viz., the serosa (which was formed earlier), has secreted on its outer side (i.e., between itself and the inner face of the endochorion) a thin 'yellow cuticle'.

5. About the 75-hour stage, the serosa secretes a second layer, viz., the thick, laminated 'white cuticle'. Later on (117-hour stage), the white cuticle is seen to be divisible into two sharply defined layers, viz., an outer laminated layer which is much thicker and an inner and much thinner, glassy, non-laminated layer. The distinction between the two layers gradually disappears after blastokinesis.

6. Copious amounts of fluid accumulate in the posterior half of the egg from the 75-hour stage onward. This fluid may be responsible for the initial swelling and lamination of the white cuticle.

7. From the 75-hour stage onward is discernible, at the posterior pole of the egg, a small, circular area which is composed of a thickened and crenulated yellow cuticle, a greatly thinned white cuticle and a close accumulation of heavily nucleated serosal cells. This area constitutes the water-absorbing area or hydropyle.

8. Shortly before and after blastokinesis, the white cuticle is comparatively shrunk in thickness apparently through chemical digestion by means of some secretions of the embryo. The precise cause of this shrinkage is not known.

9. In the 7-day stage (about one day after blastokinesis), the embryonic body-wall secretes a thin 'embryonic cuticle' which covers the embryo until hatching and is then cast off as the 'intermediate moult'.

10. The final fate of the egg-membranes, during the last 4 days of development, was not followed.

11. As regards the chorion, there are two types of egg-wall in the Acrididae, thus; Type I, in which the exochorion and the endochorion are throughout contiguous with each other (as in *Locusta migratoria migratorioides*); and Type II, in which the exochorion and the endochorion do not usually run contiguously but are separated by means of large trabeculae or air spaces (as in *Schistocerca gregaria*).

IV. REFERENCES

- Campbell, F. L. (1929). 'The detection and estimation of insect chitin; and the irrelation of 'chitinization' to hardness and pigmentation of the cuticula of the American Cockroach, *Periplaneta americana* L. *Ann. Ent. Soc. Amer.*, Columbus (Ohio), 22, 401–426.
- Husain, M. A. and Roonwal, M. L. (1933). Studies on *Schistocerca gregaria* Forsk. I. The micropyle in *Schistocerca gregaria* Forsk. and some other Acrididae. *Indian J. Agric. Sci.*, Delhi, 3(4), 639–645, 1 pl.
- Jahn, T. L. (1935a). The nature and permeability of the grasshopper egg membranes. I. The E.M.F. across membranes during early diapause. *J. Cell. Comp. Physiol.*, Philadelphia, 7(1), 23–46.
- Jahn, T. L. (1935b). The nature and permeability of the grasshopper egg membranes. II. Chemical composition of membranes. *Proc. Soc. Exp. Biol. Med.*, New York, 33, 159–163.
- Jahn, T. L. (1936). The nature and permeability of the grasshopper egg membranes. III. Changes in electric properties of the membranes during development. *J. Cell. Comp. Physiol.*, Philadelphia, 8(2), 289–300.
- Matthee, J. J. (1951). The structure and physiology of the egg of *Locustana pardalina* (Walk). *Sci. Bull. Dept. Agric. S. Afr.*, Pretoria, No. 316. (Locust Res. Ser., No. 13, 1–83.)
- Plotnikov, V. J. (1926). *Insects Injurious to Cultivated Plants in Central Asia*. (In Russian.) 1–292.—Tashkent (Uzbekistan Exper. Sta. Plant Prot.).
- Roonwal, M. L. (1936a). The growth-changes and structure of the egg of the African Migratory Locust, *Locusta migratoria migratorioides* R. and F. (Orthoptera, Acrididae.) *Bull. Ent. Res.*, London, 27(1), 1–14.
- Roonwal, M. L. (1936b). Studies on the embryology of the African Migratory Locust, *Locusta migratoria migratorioides* R. and F. I. The early development, with a new theory of multiphased gastrulation among insects. *Philos. Trans. R. Soc. Lond.* (B), London, 226, 391–421, 3 pls.

- Boonwal, M. L. (1937). Studies on the embryology of the African Migratory Locust, *Locusta migratoria migratorioides* Reich. and Frm. II. Organogeny. *Philos. Trans. R. Soc. Lond. (B)*, London, 227, 175-244, 7 pls.
- Boonwal, M. L. (1939). Some recent advances in insect embryology, with a complete bibliography of the subject. *J. R. Asiatic Soc. Bengal (Sci.) (N.S.)*, Calcutta, 4(2) [1938], 17-105.
- Boonwal, M. L. (1954). Size, sculpturing, weight and moisture content of the developing eggs of the Desert Locust, *Schistocerca gregaria* (Forskål) (Orthoptera, Acrididae). *Proc. Nation. Inst. Sci. India*, Calcutta, 20.
- Slifer, E. H. (1937). The origin and fate of the membranes surrounding the grasshopper egg; together with some experiments on the source of the hatching enzyme. *Quart. J. Micr. Sci.*, London, 79(3), 493-506, 3 pls.
- Slifer, E. H. (1938). The formation and structure of a special water-absorbing area in the membranes covering the grasshopper egg. *Quart. J. Micr. Sci.*, London, 80(3), 437-457, 1 pl.
- Slifer, E. H. (1945). Removing the shell from living grasshopper eggs. *Science*, New York, 102, 282.
- Slifer, E. H. (1948). Isolation of wax-like substance from the shell of the grasshopper egg. *Discussion of Faraday Society*. (Interaction of water and porous materials), 182-187.
- Slifer, E. H. (1950). A microscopical study of the hydropyle cells in the developing egg of the grasshopper, *Melanoplus differentialis*. *J. Morph.*, Philadelphia, 87(2), 239-274 (10 pls.).

V. EXPLANATION OF PLATES

LETTERING

- | | |
|--|---|
| <i>a.p.</i> , anterior pole of egg. | <i>p.p.</i> , posterior pole of egg. |
| <i>d.d.c.</i> , 'definitive dorsal closure' of embryo. | <i>p.s.p.</i> , posterior serosal patch (hydropyle cells). |
| <i>end.ch.</i> , endochorion. | <i>r.</i> , roof of micropylar canal. |
| <i>e.o.</i> , external opening of micropylar canal. | <i>rd.</i> , ridges of endochorion. |
| <i>ex.ch.</i> , exochorion. | <i>ser.</i> , serosa. |
| <i>f.</i> , fluid. | <i>t.</i> , tubercle or protuberance of endochorion. |
| <i>h.c.</i> , 'hydropyle cells' of serosa. | <i>tr.</i> , trabeculae or air spaces between exochorion and endochorion. |
| <i>hx.</i> , pattern of hexagonal ridges on endochorion. | <i>v.m.</i> , vitelline membrane. |
| <i>i.o.</i> , internal opening of micropylar canal. | <i>w.c.</i> , white cuticle. |
| <i>i.r.</i> , inner refractile portion of endochorion. | <i>w.c.i.</i> , inner layer of white cuticle. |
| <i>m.c.</i> , micropylar canal. | <i>w.c.o.</i> , outer layer of white cuticle. |
| <i>nu.</i> , nucleus. | <i>y.</i> , yolk. |
| <i>o.r.</i> , outer refractile portion of endochorion. | <i>y.c.</i> , yellow cuticle. |
| <i>p.e.</i> , primary epithelium ('blastoderm' of some authors). | <i>y.nu.</i> , nucleus of secondary yolk cells. |

PLATE XI

Sections of eggs of *Locusta migratoria migratorioides* R. and F., to show the structure of the egg-wall. (Eggs incubated at 33° C. and in moist soil).

FIG. 1. Portion of longitudinal-vertical section in middle of egg-length of fully developed egg in egg-calyx shortly before oviposition.

FIG. 2. Ditto of freshly-oviposited egg.

FIG. 3. Ditto. Portion of endochorion greatly enlarged, to show the refractile margins and the granular, felted core.

FIG. 4. Ditto. Portion of egg-wall at the posterior pole of freshly-laid egg. Note the thick endochorion.

FIG. 5. Portion of tangential section of freshly-laid egg in middle of egg-length, to show the felted structure of the endochorion.

FIG. 6. Portion of longitudinal-vertical section in middle of egg-length of 40½-hour old egg. Note the absence of the vitelline membrane and the presence of the extra-embryonic portion of the primary epithelium (the future serosa).

FIG. 7. Portion of transverse section of 66-hour old egg near posterior one-third of egg-length. Note the yellow cuticle.

FIG. 8. Portion of longitudinal-vertical section near middle of egg-length of 75½-hour old egg.

FIG. 9. Ditto of posterior pole of 75½-hour old egg. Note the 'hydropyle cells' and the related structures.

PLATE XII

Sections, etc. of eggs of *Locusta migratoria migratorioides* R. and F., to show the structure of the egg-wall. (Eggs incubated at 33° C. and in moist soil).

FIG. 10. Portion of transverse section near middle of egg-length of 117½-hour old egg. Note the thick, laminated white cuticle and the chorion (*ex.ch.*; *end.ch.*) which is cracked in several places.

FIG. 11. Portion of transverse section near middle of egg-length of egg about 125 hours (*ca.* 5½ days) old, *i.e.*, shortly before blastokinesis. Note the inner (*w.c.i.*) and outer (*w.c.o.*) layers of white cuticle.

FIG. 12. Portion of longitudinal-vertical section near middle of egg-length of egg during blastokinesis (*ca.* 5½-day stage).

FIG. 13. Portion of transverse section near middle of egg-length of egg soon after blastokinesis (*ca.* 6½ to 7-day stage). Note the fluid (*fl.*) next to the white cuticle.

FIG. 14. Photomicrograph of a flat mount of serosa from middle portion of egg soon after blastokinesis (*ca.* 6½ to 7-day stage). Serosa stained with borax carmine. Note that several serosal cells have two nuclei.

FIG. 15. Longitudinal-vertical section of posterior end of 8-day old egg (2 days after blastokinesis), to show the egg-wall and the serosal remnants. Note the 'posterior serosal patch' in the hydropyle area. The yolk-mass inside the egg is not shown.

Issued August 13, 1954.

STUDIES ON THE PHYSIOLOGY OF RICE

VII. EFFECT OF VARYING WATER LEVELS ON GROWTH OF RICE IN RELATION TO NITROGEN ABSORPTION

by B. N. GHOSH,* *Department of Botany, Calcutta University*

(Communicated by I. Banerji, F.N.I.)

(Received February 16; after revision September 10; read December 4, 1953)

INTRODUCTION

It has been found in America by Briggs and Shantz (1914) and in Bengal at the Dacca Agricultural Farm (1925-26) that water requirement of rice is not much different from cereals like rye which are grown in dry field conditions. But rice is well known for its characteristic adaptation to wet condition. In practice rice is grown under a variety of field conditions. At one end, fields are situated at high levels without standing water and at the other, there are fields which are several feet under water during the growing period of the plant, and there are many intermediate conditions between these extremes. In low lands it is practically the only cereal crop grown. So the relation of water to operations like puddling the soil and transplanting the seedlings and also the maintenance of proper conditions in the fields is very important. The success of the crop depends on an adequate supply of water. Excessive supply by irrigation not only consumes water that might advantageously be used elsewhere, it has also an injurious effect on the soil, causing deterioration of its physical condition, accumulation of soluble salts and the formation of toxic products. Further it is expensive to irrigate the fields while rainfall is uncertain. These present difficult problems in rice cultivation. It therefore seems essential to investigate the optimum water relations of the plant as well as to study the resistance of varieties to comparative drought and flood water.

In order to elucidate the water relations of the rice plant under different conditions and to determine its optimum water requirements and the critical stages of watering, investigations have been taken up in this laboratory. The present paper deals with a study of the effect of watering on growth and nitrogen content of three varieties of rice, *Kataktara*, *Bhutmuri* and *Bhasamanik*, which are widely cultivated in West Bengal.

EXPERIMENTAL PROCEDURE

The effects of water supply were studied in plants grown in pots in the cemented tanks situated in the fields of the Department of Botany, Calcutta University. There were four levels of watering: (A) no water in the tank, pots watered to maintain a certain condition of soil moisture; (B) water in the tank up to the soil level of the pots; (C) and (D) 3" and 6" water level above the soil surface. The experimental tanks are shown in Fig. 1; these are 10' x 7' in size and 2' deep, one foot below the ground level and one foot above. The tanks were provided with stoppered outlets at different levels so that they could either be completely drained

* Present address, State Agricultural Research Station, Chinsurah, District Hooghly.

out or the desired level of water could be maintained in them. Four such tanks were used for the four watering treatments.

Seeds of pureline varieties of early ripening *aus*, *Kataktara* and *Bhutmuri* and a late ripening *aman*, *Bhasamanik*, were graded for uniformity of size and colour, sterilized in 0.2% formalin for four hours, dried and sown in replicated seedbeds on June 4, 1934. After six weeks of sowing, the seedlings were transplanted in 10"×10" earthenware pots which were filled with an equal quantity of soil previously well mixed with one-eighth part by volume of cowdung manure.

The seedlings were carefully uprooted from the seedbeds, and their roots washed. They were selected for uniformity of size and any seedling showing a tiller was rejected. They were transplanted singly. At the time of transplantation the pots were immersed in water and a level of water approximately an inch above the soil in pots was maintained in all the four tanks for five days after transplantation to enable the seedlings to settle in their new habitat. Ten seedlings of each variety were taken for each treatment. The pots were placed in the middle of the tank in five rows of six pots each, leaving about one and a half to two feet space between these and the walls to avoid shading of the plants.

Watering treatment was started from the sixth day after transplantation. Tank 'A' was completely drained. Water level in tank 'B' was lowered up to the soil level in the pots. In tanks 'C' and 'D' there were three and six inches of water standing on the soil in pots. When ear emergence was complete in these varieties the plants were gradually brought to condition 'A' with a view to bring them under drier condition during the period of ripening.

Tiller count and measurement of growth in height of the plants were made every week during their growing period. Ear emergence note was taken in *Kataktara* and *Bhutmuri*, during the 7th, 8th and 9th week after transplantation; ears in *Bhasamanik* were counted only at harvest.

Five out of ten plants of each variety under all the watering treatments were sampled during the 7th week after transplantation. To make the sampling uniform, equal number of plants of the different varieties under the different treatments were taken every day. In all, sixty pots were sampled at this time, twenty-four pots a day on the first two days and twelve pots on the third day. The leaves were removed at their base, weighed and kept in a beaker dipping their cut ends in the water. Their area was subsequently determined. At this stage one or two leaves on the plant were dead; these were separated from the green leaves and their dry weight only was determined. The plants were separated from the roots at the base. The crown was cleared by removing the soil attached to it. The stems were then weighed. The roots in the pot were thoroughly washed in a stream of water in a sieve. To obtain the dry weights, the different parts were dried to constant weight in an electric oven at 100°C. The replicates were subsequently mixed, ground and then stored in sealed bottles for nitrogen determinations.

The remaining pots were sampled at harvest. *Kataktara* and *Bhutmuri* were harvested on October 10 and 11 and *Bhasamanik* on November 19, 1934.

The final height of the plant was determined by measuring the length of the longest shoot of the plant. The ears were separated from the shoots at the node and their length measured. The dry weight of the straw, the ears and the roots were determined. The grains were subsequently separated from the ears and their dry weights determined. The grains of the replicated plants were mixed and the dry weight of a single grain was determined at the average of 750 grains taken from these at random.

EXPERIMENTAL RESULTS

The results are presented without statistical analysis as the individual data are not now available. The differences between the treatments are so marked that valid conclusions can be drawn without statistical evidence.

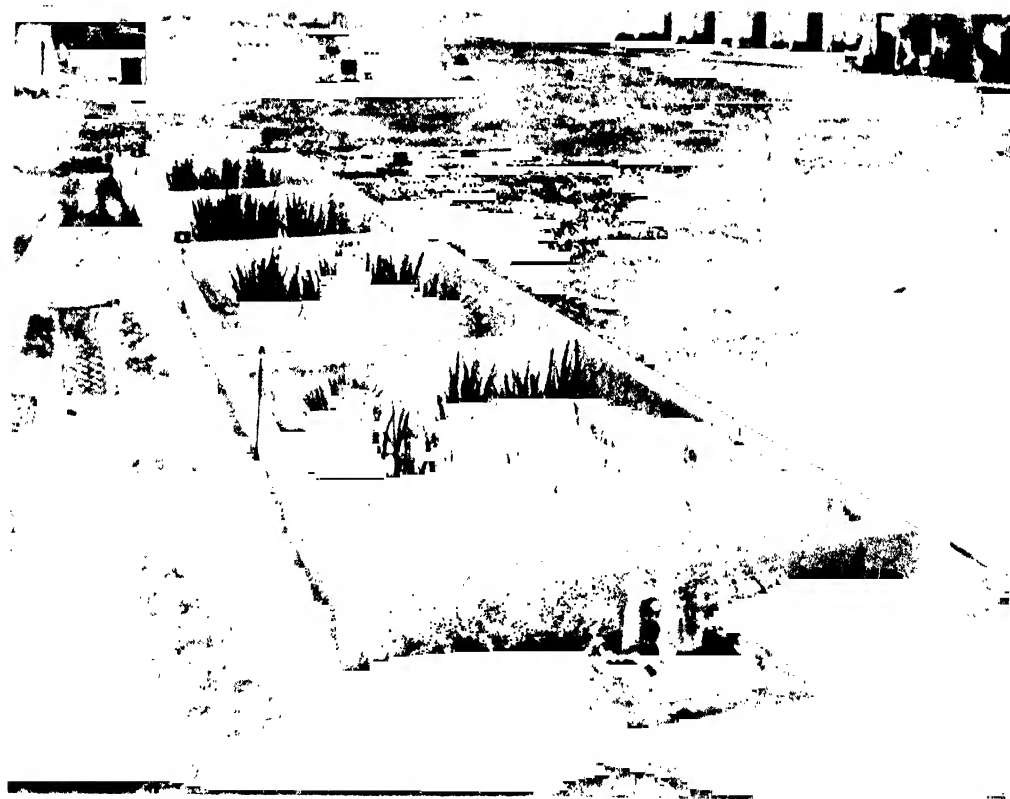


FIG. 1. Showing the general view of the experimental tanks.

Tillering.—The tillers were counted every week from the 2nd week after transplantation to the 9th week in *Kataktara* and *Bhutmuri*, and 10th week in *Bhasamanik*; the final count was made at harvest. The figures obtained for tiller numbers include the main shoot. The data are given in Table I, and graphically represented in Fig. 2. The curves show that the number of tillers steadily rises and reaches a maximum within seven or eight weeks after transplantation. This is followed by a fall to a constant number which is maintained at harvest.

TABLE I
Mean number of tillers per plant

Watering	Weeks after Transplantation										Harvest	
	2	3	4	5	6	7	8	9	10	Ripe	Unripe	
<i>Kataktara</i>												
A	..	2.0	3.8	5.0	6.7	7.1	7.3	7.2	7.2	..	7.2	7.2
B	..	1.3	4.7	7.2	11.0	11.0	11.7	12.2	12.2	..	12.2	7.8
C	..	1.0	2.3	4.8	9.7	10.3	10.7	10.8	10.8	..	10.8	5.6
D	..	1.0	2.0	3.5	7.7	8.1	8.2	7.8	7.8	..	7.8	5.2
<i>Bhutmuri</i>												
A	..	3.0	6.4	9.3	12.9	14.7	15.0	15.0	15.2	..	14.6	9.0
B	..	2.9	9.4	15.2	19.1	19.2	19.7	19.2	19.2	..	17.8	8.8
C	..	1.7	6.4	11.3	19.8	19.9	20.3	20.6	20.2	..	18.4	6.6
D	..	1.4	4.8	9.3	17.0	17.0	17.5	16.4	16.4	..	16.4	3.8
<i>Bhasamanik</i>												
A	..	3.1	6.2	9.3	14.4	18.3	18.0	17.8	17.2	17.2	17.2	0.4
B	..	2.2	5.8	12.2	20.1	20.0	20.8	19.2	18.6	18.0	15.8	1.0
C	..	1.4	4.2	8.9	16.2	16.1	17.7	17.0	16.8	16.0	15.2	0.8
D	..	1.3	3.2	7.4	14.1	14.2	14.0	12.8	12.8	12.2	11.8	0.2

In *Kataktara* tillering was maximum under 'B'; with further increase in water under 'C' and 'D', it was reduced. Tillering was minimum under 'A'. In *Bhutmuri* tillering was most rapid under 'B' up to the fourth week after which it was largest in 'C'. The maximum number of tillers in this variety was produced in 'C', but under 'D' it was reduced. Tillering was minimum in 'A'. In *Bhasamanik* tillering was maximum under 'B', * under 'C' and 'D' it was progressively reduced. Tillering under 'A' lies between 'B' and 'C'.

The nature of the effect of watering on tiller growth in all the varieties used appears to be the same. *Bhutmuri* indicates a greater affinity for water than the other two varieties, *Kataktara* and *Bhasamanik*. Singh *et al.* (1935) have observed varietal differences in the water requirement of rice.

The level of the curves shows that water standing above the soil suppresses tillering. This result corroborates the findings of Agricultural Department of

* In another paper on 'Physiological studies on the effect of varying water levels on growth of rice in relation to carbohydrate metabolism of the leaves', tillering was maximum under 'A' and not under 'B' as observed in the present paper. This difference may be due to the difference in watering under 'A' in the two experiments. The exact moisture content of the soil was not measured.

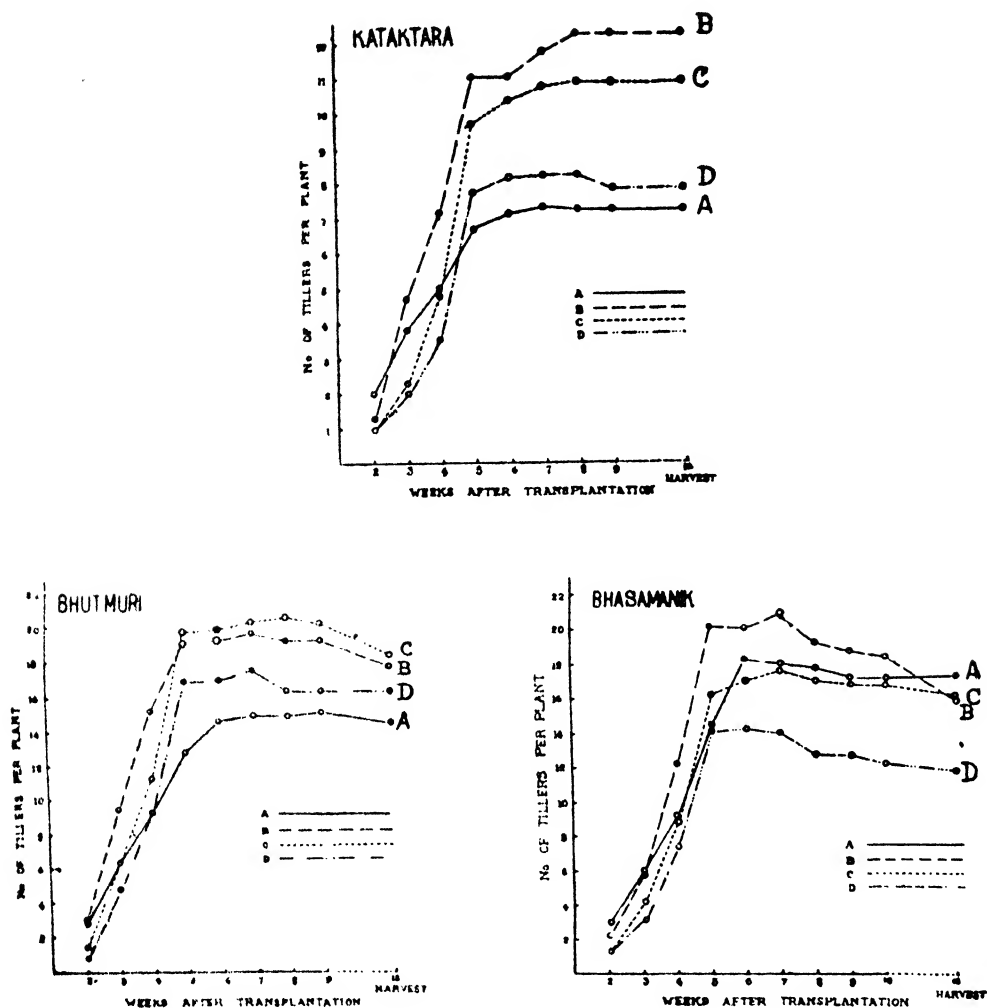


FIG. 2. Showing the effect of varying water levels on tillering in *Katakara*, *Bhutmuri* and *Bhasamanik*.

Bengal (Report, 1925-26) that water standing in the field during early period of growth after transplantation suppresses tillering in rice.

In the early ripening varieties, *Katakara* and *Bhutmuri*, tillering was minimum probably because water was limiting their rapid growth. In *Bhasamanik* which grows more slowly over a longer period, condition 'A' does not show a limiting effect to an equal extent.

With the maturation of the shoots there was a second crop of tillers from the base of the plants. In *Katakara* and *Bhutmuri* the number of these new tillers was considerable. Immature tillers at harvest in *Bhasamanik* were very small. Watering treatments had important effects on these new tillers. The number of these new tillers was maximum under 'A', and progressively reduced under conditions of increased water supply.

Height.—Two measurements were taken; one from the surface of the soil up to the base of the uppermost leaf on the biggest shoot of the plant, and another up to the highest leaf tip. The first measurement indicated the development of

the stem, while the second was the measure of the height of the plant. The data are given in Table II.

TABLE II
Plant height and stem length in centimetre

Watering	Weeks after Transplantation									Harvest
	2	3	4	5	6	7	8	9	10	
<i>Kataktara</i>										
A ..	14.8	19.9	22.9	27.4	50.2	76.4	89.5	90.4	..	90.8
	62.6	66.6	74.9	82.8	91.6	109.9	120.4	110.5	..	115.7
B ..	15.4	21.0	24.1	27.7	39.9	65.5	92.3	95.7	..	94.4
	60.9	65.2	73.2	84.4	91.5	100.6	119.4	121.0	..	124.2
C ..	14.6	19.4	23.6	26.5	33.4	52.4	78.2	95.2	..	97.3
	60.7	66.0	72.1	78.8	88.1	97.9	110.7	122.0	..	124.4
D ..	14.2	20.6	24.5	28.2	34.3	51.7	73.3	94.7	..	100.5
	61.7	63.8	70.0	79.2	91.8	102.0	111.3	123.9	..	125.1
<i>Bhutnuri</i>										
A ..	18.6	24.0	25.9	28.5	40.3	64.9	82.5	84.2	..	89.0
	67.3	70.2	72.4	79.4	87.0	102.0	116.4	115.8	..	108.1
B ..	13.0	23.8	27.2	28.9	36.7	61.6	83.9	95.0	..	96.3
	68.8	69.9	73.8	81.2	84.3	96.3	112.1	119.9	..	118.5
C ..	18.4	22.9	26.5	27.9	33.5	53.6	80.1	96.9	..	99.5
	69.4	69.8	72.3	77.2	83.3	93.0	108.6	120.0	..	122.4
D ..	18.1	24.2	28.2	28.9	33.8	53.7	80.1	96.6	..	101.7
	64.8	65.2	73.9	78.6	84.7	93.7	108.7	120.8	..	122.6
<i>Bhasamanik</i>										
A ..	14.9	19.3	22.1	24.2	25.7	28.0	29.5	32.3	38.8	95.4
	58.5	64.2	68.6	72.9	77.9	84.8	88.7	93.9	102.3	120.3
B ..	13.9	20.2	23.2	23.9	25.9	28.9	32.7	35.1	43.2	106.6
	57.2	61.4	68.9	71.3	73.7	81.7	89.5	96.1	103.9	131.7
C ..	14.1	20.1	22.8	23.7	26.3	29.4	32.2	35.9	43.4	110.0
	58.9	62.1	70.7	73.8	77.3	85.0	93.9	100.1	105.9	135.7
D ..	15.3	21.9	24.6	25.5	27.5	30.1	32.8	35.8	43.1	113.0
	58.2	63.1	70.2	75.1	78.8	85.9	93.9	99.7	107.1	138.8

During the first six weeks after transplantation the stem grew very slowly in *Kataktara* and *Bhutnuri*, after this it elongated very rapidly up to a point after which the rate of elongation fell again. In *Bhasamanik* the slow rate of growth is prolonged corresponding to its longer growing period. During the early period when growth rate of the stem was very slow, showing very little effect of watering on the plants. But in the other varieties stem elongation started first under 'A' and it was delayed with increasing water. Finally, however, the stem length increased with increasing water level. In *Bhasamanik* the growth rate of the

stem was more or less uniform up to the 10th week after which there was only one measurement at harvest. The effect of water increasing the height of the plant in this case was evident comparatively earlier.

From the data it is seen that there is no sudden rise in the case of the actual height of the plant like that in the stem. The rise is uniform. This is due to the fact that the earlier leaves are longer and the later leaves are gradually smaller. The effect of the watering treatments on the height of the plant is determined by the height of the stem. The final plant height and stem length determined at harvest are shown in Fig. 3. The effects of water level on the increase in the height of the plant and stem length are very marked. These have also been confirmed by Sen (1937) in field culture.

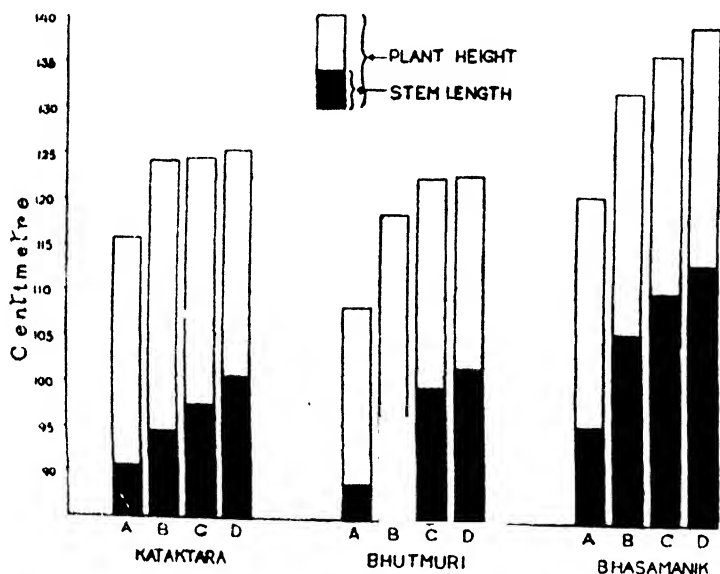


FIG. 3. Effect of varying water levels on plant height and stem length in three varieties of rice. Note increase in plant height and stem length with rise in water level.

Ear emergence.—Ears began to emerge in *Katakara* and *Bhutmuri* seven weeks after transplantation. The data for ear emergence were taken thrice, and a final count was made at harvest. In *Bhasamanik* ears were counted only at harvest.

Flowering was most rapid under 'A' and it was increasingly delayed with increasing water level (Table III), while in the field experiment (Sen, 1937) cracked condition delayed flowering in the *aus* varieties and the process was hastened under increasing moisture conditions of the soil.

These contradictory results are due to the amount of soil moisture. In the pot culture experiment water under 'A' was limiting, thus inducing rapid flowering, while under increasing water levels the vegetative growth was prolonged. In the field soil moisture even under cracked condition was not limiting, but the comparative moisture deficiency of the soil reduced the rate of growth.

The total number of ears per plant was primarily determined by the number of shoots in a plant. In *Bhasamanik* largest number of ears was produced under 'A'. The percentage of ears produced in a plant (Table III) shows an inverse relationship to tillering in their response to watering. In *Katakara* and *Bhasamanik* this value is minimum under 'B' where tillering is maximum.

The data for length of ears per plant are given in Table III. The length of ear was reduced under 'A' irrespective of varieties. In *Katakara* it rose to a

TABLE III
Number and length (in cm.) of ears per plant

Watering		Weeks after Transplantation					Length of Ears
		7	8	9	Harvest	Ears as p.c. of maximum tillers	
<i>Kataktara</i>							
A	..	3.6	6.8	6.8	6.8	93	24.9
B	..	0.17	6.4	10.6	10.6	87	29.8
C	..	0.0	2.4	10.0	10.0	93	27.1
D	..	0.0	1.2	7.8	7.8	95	24.6
<i>Bhutmuri</i>							
A	..	1.0	8.8	13.2	13.2	87	19.1
B	..	0.0	7.8	15.2	15.2	77	22.2
C	..	0.0	4.8	16.2	16.2	70	22.8
D	..	0.0	4.0	15.0	15.0	86	20.9
<i>Bhasamanik</i>							
A	17.2	94	24.9
B	14.6	73	25.1
C	14.4	81	25.7
D	11.6	82	25.8

maximum under 'B', under 'C' and 'D' it was reduced. In *Bhutmuri* length of ears under 'B' and 'C' was almost similar but maximum under 'C'; under 'D' it was reduced. In *Bhasamanik* the length of ears under 'C' and 'D' was greater than that under 'B'.

Leaf Area.—The area of the total leaf surface of the plants was determined at the time of 1st sampling, made six weeks after transplantation. The leaves were removed at their base. The length and maximum breadth of each leaf was measured directly with a metre scale. At the same time an estimation of the area of all the leaves from the three largest tillers of three of the five plants sampled was made with a planimeter. The length and breadth of each individual leaf when multiplied gave a 'leaf product' which was an estimate of the leaf area. Dividing the actual area of every planimetered leaf by the leaf product 'a factor' was obtained. The average of this factor for the plants under each treatment was employed to convert the leaf product to real leaf area. The data are presented in Table IV.

From the data it is clear that the total leaf area of the plant is determined by the number of tillers. The effect of the watering treatments on tillering is reflected on the total area of leaf surface.

The low value for leaf area in *Bhutmuri* under 'C' in spite of high figures for tiller number may be explained by the fact that under this condition tillering was lower than under 'B' up to the fourth week after transplantation; it was only after the fifth week that tillering was maximum under 'C' (Table I). A considerable number of tillers at this stage, therefore, must be very young which had produced only a few leaves.

The average area of a single leaf is also given in Table IV. In all the varieties of rice used, area of a single leaf increased with increasing water level. The effect was most clearly shown in *Bhasamanik*.

TABLE IV
Leaf area in sq. cm.

Watering	<i>Kataktara</i>		<i>Bhutmuri</i>		<i>Bhasamanik</i>	
	Average leaf area per plant	Average area of a single leaf	Average leaf area per plant	Average area of a single leaf	Average leaf area per plant	Average area of a single leaf
A ..	831.7	30.5	1,188.7	18.1	1,281.5	14.9
B ..	1,291.3	31.2	1,635.3	18.8	1,254.5	15.1
C ..	1,105.6	31.4	1,340.7	18.8	1,102.0	16.4
D ..	1,001.7	31.1	1,299.9	19.2	1,179.1	17.2

Water content.—Water content of the stem and leaf of the plant was determined at the time of 1st sampling, i.e., after six weeks of transplantation. The data are presented in Table V as percentage of dry matter. Percentage of water content in both stem and leaf increased with rise of water level.

The increase of water content of leaf from 'C' to 'D' was little, but in stem percentage of water considerably increased from 'C' to 'D'.

TABLE V
Water content of stem and leaf as percentage of dry weight

Watering	<i>Kataktara</i>		<i>Bhutmuri</i>		<i>Bhasamanik</i>	
	Stem	Leaf	Stem	Leaf	Stem	Leaf
A ..	532	236	440	253	625	269
B ..	553	289	507	264	624	298
C ..	590	322	567	272	709	305
D ..	703	320	618	286	751	306

Dry weight data.—The data for total dry weight per plant and its distribution in root, stem and leaf after six weeks of transplantation are given in Table VI and graphically represented in Fig. 5.

In all the varieties used, the total dry weight of the plant and its distribution in root, stem and leaf increases in 'B', and then falls with further rise of water level. Plants of different varieties at this stage are shown in Fig. 4. In Table VII are given the dry weight data of the plant at harvest. The total dry weight of the plant at this stage shows the same relationship as before. Dry weight of root, straw and ears also show a similar effect in *Kataktara* and *Bhutmuri*. In *Bhasamanik* the dry weight of ears under 'A' is very much reduced, as a result the dry weight of straw in this variety of rice is maximum under 'A'.

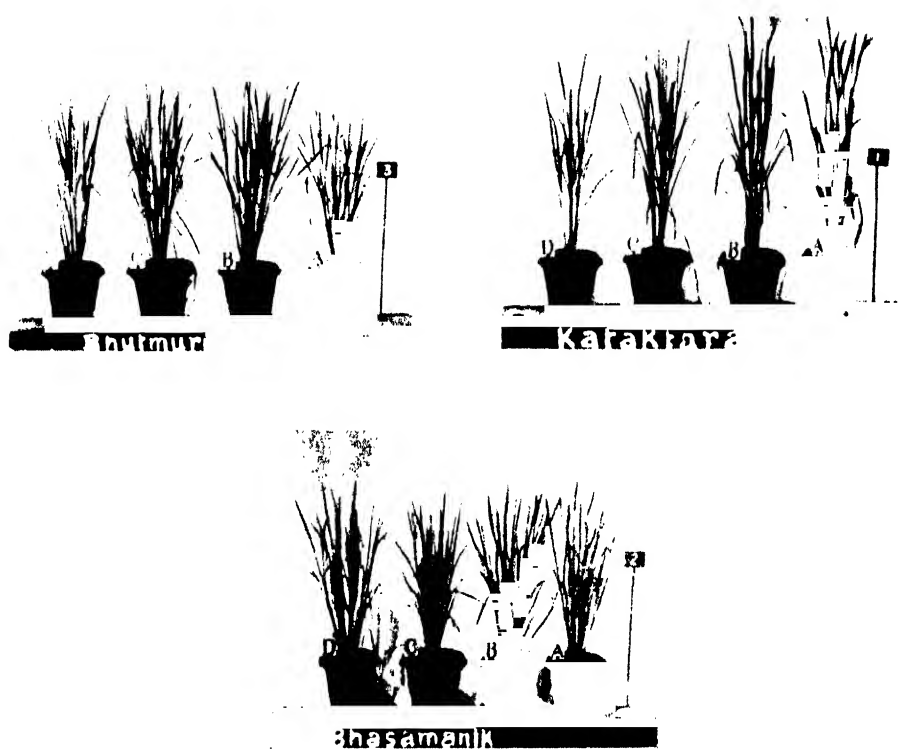


FIG. 4. Showing plants of *Bhutnuri*, *Katakura* and *Bhasamanik* after six weeks of transplantation under different levels of watering.

TABLE VI
Dry weight in gm. per plant after six weeks of transplantation

Water- ing	Kataktara				Bhutmuri				Bhasamanik			
	Root	Stem	Leaf	Whole plant*	Root	Stem	Leaf	Whole Plant*	Root	Stem	Leaf	Whole Plant*
A ..	2.85	10.50	4.44	18.20	3.35	12.24	5.85	22.37	4.30	7.17	5.64	17.5
B ..	3.38	12.50	6.13	22.40	4.12	15.79	7.07	28.30	5.47	8.03	5.96	20.6
C ..	2.52	8.27	5.50	16.90	3.52	11.67	6.41	22.50	3.75	6.46	5.46	16.8
D ..	2.22	6.96	4.98	14.90	3.31	10.65	5.14	20.50	3.31	5.90	4.78	14.9

* The dead parts of the shoot are included in the dry weight of the whole plant.

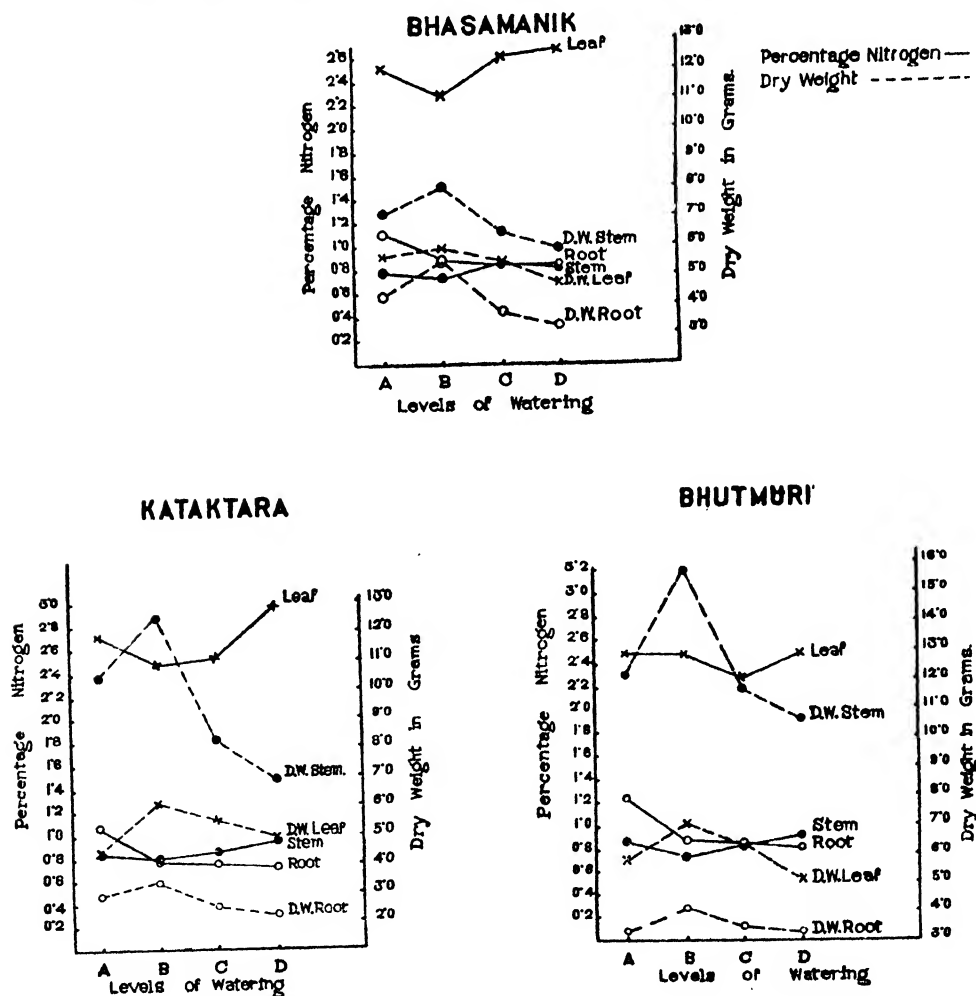


FIG. 5. Showing the effect of varying water levels on the dry weight and nitrogen content of root, stem and leaf of *Bhasamanik*, *Kataktara*, and *Bhutmuri* after six weeks of transplantation.

TABLE VII

Dry weight in gm. per plant at harvest

Water- ing	<i>Kataktara</i>				<i>Bhutmuri</i>				<i>Bhasamanik</i>			
	Root	Straw	Ears	Whole plant	Root	Straw	Ears	Whole plant	Root	Straw	Ears	Whole plant
A ..	1.65	18.3	21.6	41.5	1.66	23.5	24.6	48.1	8.59	66.1	29.4	104.1
B ..	3.80	27.1	28.4	59.3	2.87	30.3	29.4	62.6	10.60	62.2	40.9	113.7
C ..	2.48	22.6	24.3	49.4	2.76	27.4	27.6	57.8	9.42	58.2	39.0	106.6
D ..	1.90	18.2	21.5	41.6	2.09	25.7	26.0	53.8	7.17	50.2	35.4	92.8

The total dry weight of grains per plant and the dry weight of a single grain are presented in Table VIII. Yield of grains per plant increased in 'B', with further increase in the water level it was reduced. Single grain weight was similarly affected in *Kataktara* and *Bhutmuri*, but in *Bhasamanik* single grain weight is found to have increased with rise in water level.

Grain yield was calculated on the basis of 100 gms. dry weight of the whole plant in order to study its relation with the dry matter produced per plant under different conditions of water supply, and the data are presented in Table VIII. The effect was very little in the two varieties, *Kataktara* and *Bhutmuri*, but in the late ripening *aman* variety, *Bhasamanik*, the percentage of grain yield increased with increased soil moisture. This difference in the varieties of *aus* and *aman* paddy is possibly due to the differences in the time of their flowering. The early ripening *aus* varieties started flowering about seven weeks after transplantation, i.e., in early September when the rains were not yet over. For this reason the soil moisture under 'A' was not limiting. But in late October during the period of floral development in *Bhasamanik* rainwater was scarce, consequently soil moisture under 'A' was deficient for the development of flowers.

TABLE VIII

Grain yield of three varieties of rice

Water- ing	<i>Kataktara</i>			<i>Bhutmuri</i>			<i>Bhasamanik</i>		
	Grain per plant (gm.)	Single grain (mg.)	% grain to whole plant	Grain per plant (gm.)	Single grain (mg.)	% grain to whole plant	Grain per plant (gm.)	Single grain (mg.)	% grain to whole plant
A ..	20.1	16.9	48.4	22.6	18.8	46.9	19.8	14.7	19.0
B ..	26.9	17.9	45.3	27.3	20.3	43.6	34.5	17.0	30.3
C ..	23.2	17.1	46.9	25.9	18.9	44.8	32.3	17.4	30.3
D ..	20.6	16.7	49.5	24.8	19.1	46.1	30.3	17.8	32.7

In this work watering was not controlled by determining the soil moisture at regular intervals. The treatments were designed mainly for the first seven weeks after transplantation. An investigation controlling watering during the flowering period should elucidate the water relations of the plant with its floral development.

Chakladar (1946), in an investigation on the influence of soil moisture on the yield of paddy, has reported that none of the plants under 33% saturation formed seeds though some of them had flowered, while the plants under 75 and 50% saturation formed seeds showing that water is essentially necessary during the flowering stage for seed formation.

Dry weight of root in the *aus* varieties did not show any increase at harvest than that after six weeks of transplantation, on the other hand, it was very much reduced (Tables VI and VII). In the *aman* variety root increased in dry matter showing that at the time of the first sampling the plant was at an early stage of growth.

The reduction of dry matter in root was greatest under 'A' when the largest number of second crop of tillers produced. The roots translocate all their reserve materials for the development of the new shoots thus decreasing in their weight.

In 1935 the effect of varying conditions of water on growth and nitrogen content was repeated with *Bhasamanik*. Two more tanks 'E' and 'F' had been added, which had 9" and 12" of water respectively above the soil level in the pots. In this case four samples were taken. The first sample was taken three weeks after transplantation, the second after six, the third after nine and the fourth at harvest. To obtain the dry weights of the different parts of the plant, roots, stems, leaves, straw and grains, were dried to constant weight in a gas oven at $100 \pm 1^\circ\text{C}$. The replicates were subsequently mixed, ground, and then stored in sealed bottles with proper labelling for nitrogen determinations.

The data for total dry weight per plant and its distribution in root, stem, leaf, straw and grain of *Bhasamanik* of four samples are given in Tables IX and X, and graphically represented in Fig. 6.

TABLE IX

Dry weight in gm. of root, stem and leaf of Bhasamanik after three, six and nine weeks of transplantation (1935).

Water- ing.	Root			Stem			Leaf		
	Weeks after Transplantation								
	3	6	9	3	6	9	3	6	9
A ..	0.43	1.50	3.91	0.74	3.96	11.14	0.61	3.14	6.16
B ..	0.53	3.68	5.48	0.95	6.45	12.91	0.83	3.89	5.33
C ..	0.40	2.69	5.25	0.82	4.64	9.95	0.74	2.98	4.18
D ..	0.46	2.45	3.76	0.84	4.13	8.17	0.66	2.74	3.60
E ..	0.33	2.08	3.70	0.89	3.73	7.52	0.67	2.49	3.26
F ..	0.24	1.47	2.83	0.66	2.93	6.78	0.45	2.22	2.68

TABLE X

Dry weight in gm. per plant of Bhasamanik at harvest (1935).

Watering	Root	Straw	Ears	Grain	Single grain (mg.)
A ..	4.13	29.00	14.99	11.48	11.75
B ..	4.86	24.84	16.18	13.65	14.60
C ..	4.10	21.17	15.29	13.19	14.79
D ..	3.49	18.76	14.53	12.40	15.21
E ..	2.80	15.12	13.14	11.78	15.34
F ..	2.10	14.45	9.74	8.66	15.10

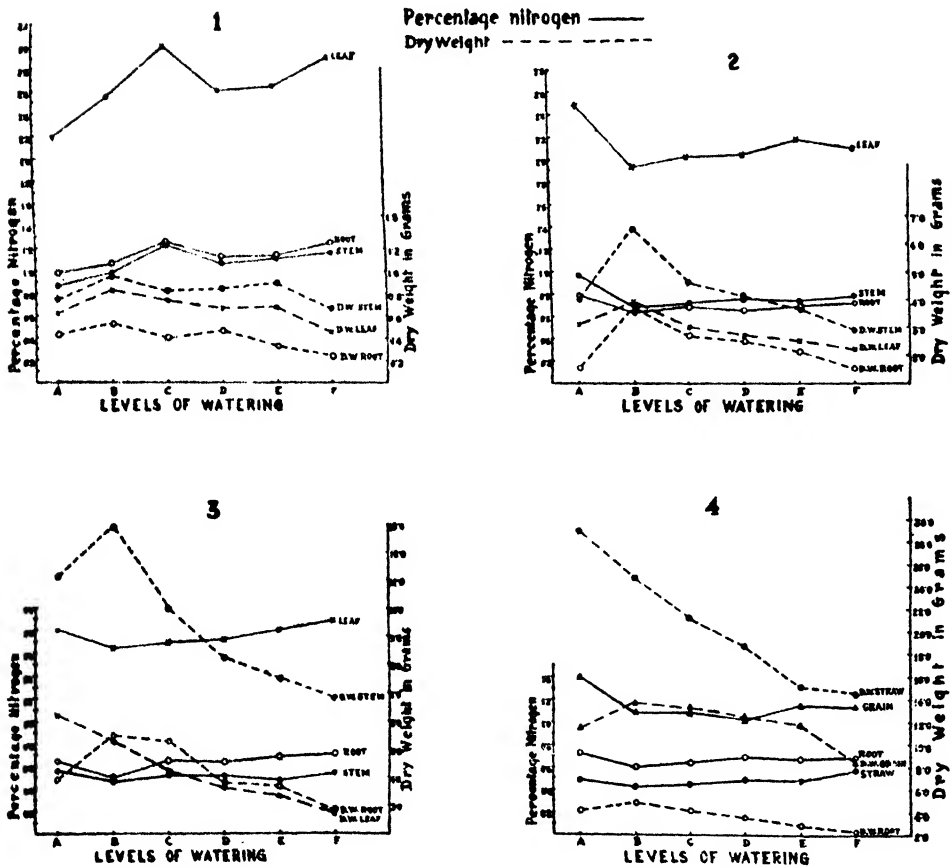


FIG. 6. Showing the effect of varying water levels on the dry weight and nitrogen content of root, stem, leaf, straw and grain of *Bhasamanik*. 1—three weeks after transplantation; 2—six weeks after transplantation; 3—nine weeks after transplantation; and 4—at harvest.

The total dry weight of the plant of first three samples and its distribution in root, stem and leaf increases in 'B', but it is falling with further rise of water level. At harvest, however, the dry weight of the straw has its maximum value in 'A', decreasing steadily with increasing the water level. The dry weight of root, ears and grains per plant has a maximum value in 'B', and then falling with increase of water level. Dry weight of a single grain increases with increase of water up to 'E' and then falling in 'F'.

NITROGEN CONTENT

In 1934 the percentage of total nitrogen in root, stem and leaf of *Kataktara*, *Bhutmuri* and *Bhasamanik* was determined after six weeks of transplantation by the usual Kjeldahl method. The previously powdered and dried material was first finely ground in a mortar, and then three samples each about 2 gms. were weighed. Two of these were taken for nitrogen estimation as replicates and the third dried to constant weight at 100°C. for finding the dry matter.

All the results were calculated on the dry weight basis and corrected for a small blank for the reagents. The agreement between replicates was very good. The nitrogen content data are presented in Table XI and graphically represented in Fig. 5.

TABLE XI

Total Nitrogen as percentage of dry weight after six weeks of transplantation (1934).

Water- ing	<i>Kataktara</i>			<i>Bhutmuri</i>			<i>Bhasamanik</i>		
	Root	Stem	Leaf	Root	Stem	Leaf	Root	Stem	Leaf
A ..	1.06	0.85	2.72	1.23	0.88	2.49	1.11	0.70	2.52
B ..	0.77	0.79	2.48	0.89	0.74	2.48	0.89	0.74	2.29
C ..	0.76	0.86	2.52	0.86	0.84	2.27	0.84	0.85	2.62
D ..	0.72	0.94	2.96	0.82	0.92	2.49	0.84	0.83	2.67

Percentage of nitrogen in roots of *Kataktara*, *Bhutmuri* and *Bhasamanik* is maximum in 'A', and then steadily decreases with increase in water level; while the maximum dry weight of root in these varieties is found in 'B' and then falling with increasing water levels under 'C' and 'D'. Both nitrogen content and dry weight of root are minimum in 'D', irrespective of varieties. This shows that the nitrogen content of root decreases with increase in water level.

In stem and leaf of *Kataktara*, *Bhutmuri* and *Bhasamanik* nitrogen content is maximum in 'D' and minimum in 'B', while the number of tillers, total leaf area per plant and the dry weight of stem and leaf is maximum under 'B' and gradually decreases with increase in water level. This shows an inverse relationship between tillering, total leaf area and dry weight on the one hand and nitrogen content on the other.

Again in 1935 the percentage of total nitrogen in root, stem, leaf, straw and grain of four samples of *Bhasamanik* which were taken three, six and nine weeks after transplantation and the fourth one at harvest, was estimated as before. The data are given in Tables XII and XIII and graphically represented in Fig. 6.

TABLE XII

Nitrogen content of root, stem and leaf of Bhasamanik after three, six and nine weeks of transplantation (1935).

Water- ing.	Root			Stem			Leaf		
	Weeks after Transplantation								
	3	6	9	3	6	9	3	6	9
A ..	0.99	0.79	0.65	0.86	0.96	0.56	2.19	2.49	1.80
B ..	1.06	0.63	0.50	0.99	0.67	0.47	2.55	1.93	1.64
C ..	1.26	0.69	0.65	1.24	0.71	0.52	3.01	2.02	1.69
D ..	1.13	0.65	0.64	1.06	0.75	0.51	2.61	2.04	1.71
E ..	1.14	0.69	0.69	1.11	0.74	0.48	2.65	2.18	1.80
F ..	1.25	0.71	0.71	1.16	0.78	0.54	2.92	2.10	1.89

TABLE XIII

Nitrogen content of Bhasamanik at harvest (1935).

Watering	Root	Straw	Grain
A ..	0.73	0.49	1.40
B ..	0.60	0.42	1.09
C ..	0.64	0.45	1.09
D ..	0.69	0.49	1.02
E ..	0.67	0.48	1.15
F ..	0.69	0.57	1.14

Percentage of nitrogen in root, stem and leaf of the first sampling which was taken three weeks after transplantation, increases generally with increase of water level. Nitrogen content of root, stem and leaf is found maximum under 'C' and minimum under 'A'. In early stages nitrogen content of root, stem and leaf seems to be accumulated under water-logged condition due to very restricted growth of the plant.

Percentage of nitrogen in roots, stems and leaves of second and third sampling which were taken after six and nine weeks of transplantation respectively, is minimum under 'B', and then gradually increases with the increase of water. The dry weight of roots, stems and leaves of second and third sampling is maximum under 'B' and then gradually decreases with increase of water level, minimum being under 'F'. Thus the percentage of nitrogen shows an inverse relation to the dry weight. The results of stem and leaf of second and third sampling confirm the previous years data (Table XI).

With advancing age of the plant there is a gradual tendency of falling of nitrogen content in root, stem and leaf in all the treatments, except in 'A' and 'B' where percentage of nitrogen in root somewhat rises again at harvest. This corresponds with the decrease of nitrogen in the stem and leaf—the soluble nitrogen being translocated into the root with the death of the upper part of the plant. This downward translocation of nitrogen is possibly related with the growth of the new tillers. The number of these new tillers was maximum under 'A', and increasingly reduced with increased water levels, as is found in Table I. Under relatively deeper water treatments no such rise of nitrogen is noticed. Percentage of nitrogen in the straw seems to be very little affected by the treatments, except under 'F' where a higher nitrogen content is found. On the other hand, the highest percentage of nitrogen in the grains is obtained under 'A'.

In root, stem and leaf, percentage of nitrogen is highest in the early stages of growth of the plant. Sen (1946) also found higher percentage of nitrogen in the earlier leaves than in the later leaves.

DISCUSSION

The results presented in this paper show that water standing above the soil level suppresses tillering and consequently the total yield is much reduced (Tables I and VIII). Height of the plant increases as the water level rises (Table II). The mechanism of the increase cannot be precisely explained since in this study the measurement of the length of the internodes with the rise of water level has not been taken. However, it may be stated that the increase in plant height dependent on the expansion phase of the growth of the internodal cells is related to the water content of the stem. This is clearly indicated in the treatments where rise of water level has increased the water content of stem (Table V) along with plant height. In 'A' and 'B' water content is less than under 'C' and 'D'; water supply in these cases may not be available to the same extent for the elongation of the internodal cells as under standing water levels 'C' and 'D'. This would possibly explain why the individual internodes remain shorter than those where rise of water level accelerates the extension growth of the stem length. Crowther (1934) has reported increased plant height and internodal length of cotton with increased water supply. In leaves also similar relation between water content and leaf area is noted (Tables IV and V). Thoday (1910) working with *Helianthus* showed that the leaves expand with increase of water. In the leaves of barley similar relation has been recorded by Richards (1932).

From the nitrogen content in different parts of the paddy varieties, it is evident that there exists a close relationship between tillering, total leaf area per plant and dry weight on the one hand and nitrogen content on the other. Percentage of nitrogen in roots of *Kataktara*, *Bhutmuri* and *Bhasamanik* is maximum in 'A', and then gradually decreases with increase in water level (Table XI), while the maximum dry weight of root in these varieties is found in 'B' and then falling with increasing water levels 'C' and 'D' (Table VI). Both nitrogen content and dry weight of root are minimum in 'D' irrespective of varieties. This shows that the nitrogen content of root decreases with increase in water level. From the results, it appears that water-logged condition associated with reduced soil aeration has checked both root growth and the uptake of nitrogen, while in comparatively dry condition under 'A', in spite of maximum nitrogen content in the roots of the three varieties, the root growth decreases due to insufficient water-supply.

In stem and leaf nitrogen content is maximum in 'D' and minimum in 'B', while the number of tillers, total leaf area per plant and the dry weight of stem and leaf is maximum under 'B' and gradually decreases with increase in water level, indicating an inverse relation between tillering, total leaf area and dry weight on the one hand and nitrogen content on the other. Although percentage of nitrogen

increased in stem and leaf under water-logged conditions ('C' and 'D'), plant growth as indicated by tillering is not correspondingly increased under these conditions; it is restricted by the influence of increasing water levels and therefore nitrogen not being utilized accumulates in stem and leaf. On the other hand, maximum tillering, total leaf area and dry weight of stem and leaf are found in 'B' where percentage nitrogen content is minimum, irrespective of varieties. This corresponds with the fact that the demand for nitrogen for growth and yield is greatest in 'B', consequently nitrogen content is in minimum percentage of the dry weight of the plant. In 'B' maximum plant growth and yield of the varieties may be due to better utilization of nitrogen and moisture status of the soil. Here both nitrogen and moisture content of the soil influence tillering, total leaf area and ultimately its total dry weight and grain yield, while under relatively deeper water treatments ('C' and 'D') standing water reduces meristematic activity; here factor or factors other than nitrogen are limiting the growth and yield of the plant. Under partial drought in 'A' plant growth has suffered due to insufficient water-supply rather than nitrogen as nitrogen content is not much reduced. The author (1949), in his work on the effect of varying water levels on growth of rice in relation to carbohydrate metabolism, has reported that the synthesis of sugar is not limiting the production of tillers in treatments with standing water, since sugar is in excess in the leaves under water-logged condition. Other reasons that might account for this difference in growth due to variation in water level are: (1) insufficient aeration to the submerged parts, and (2) pressure of water column acting upon the region where meristems for tillers are laid down.

Asana (1950) on growth analysis of the sugarcane crop has reported that the tillering phase was not so much affected by hot weather (high temperature and low relative humidity) as by the nitrogen supply, while in low-lying water-logged areas growth was checked due to depression in the rate of uptake of nitrogen and leaf growth. Vlamis and Davis (1944) have suggested that oxygen can be transported from the shoots to the roots by anatomical adaptation, improving thereby the growth of rice under submerged condition particularly with respect to the root system. The increased growth as they have measured by the fresh weight of roots and shoots may be due to the increased water content. In the present experiment it is seen that the water content of different parts of the rice plant increases as the water level rises (Table V), while the dry weight decreases increasingly with the rise of water level (Tables VI, VII and IX). From the results it appears that the plant growth as measured by tillering, total leaf area per plant and dry weight has suffered a lot under water-logged condition. Woodford and Gregory (1948) have studied the growth of barley plant under anaerobic conditions of the roots and concluded that the growth under anaerobic conditions can be maintained at a level as high as that with full aeration by merely increasing the nutrient concentration, for it appears that the poor growth in badly aerated soils may to a large extent be due to a starvation of the primary nutrients consequent upon a slower uptake for a given concentration of soil nutrients.

SUMMARY

The effects of varying water levels on growth, yield and nitrogen content of three varieties of paddy are reported in this study.

Number of tillers, total leaf area, total dry matter and grain yield increase in the treatments with water up to the soil level in pots, but gradually decrease with the rise of water level. Varietal difference in the optimum water requirement is established.

Plant height and individual leaf area are found to increase with the rise of water level. Water content of stem and leaf is similarly affected, the increase being greater in the stem. The cause of the variation in plant height and individual leaf area under different water levels has been discussed.

Both nitrogen content and dry weight of root decrease with increasing water level. In stem and leaf nitrogen content, on the other hand, is high under water-logged condition, nitrogen

not being utilized accumulates. Under partial drought plant growth has suffered due to insufficient water supply rather than nitrogen as nitrogen content of stem and leaf is not much reduced. Stem and leaf nitrogen is low where water is maintained up to the soil level (puddling condition) because of its utilization for optimum growth.

The results of this experiment indicate the necessity of maintaining different water levels at different stages of growth and development. 2-3 inches of water in the field for two weeks after transplantation followed by drainage and maintenance of the soil in the puddling condition for another 5-6 weeks for *aus* and 7-8 weeks for *aman* would give optimum tillering. Standing water, however, has some beneficial effect at the time of ear emergence and grain formation.

The author expresses his grateful thanks to Dr. P. K. Sen for suggesting the problem, to Dr. S. P. Agharkar for granting facilities to conduct this work and to Dr. S. M. Sircar for many helpful criticisms and suggestions in the preparation of this paper.

REFERENCES

- Asana, R. D. (1950). Growth analysis of the sugarcane crop in North Bihar (India). I. Seasonal variation in growth and yield in unmanured plots. *Ann. Bot., N.S.*, **14**, 465-486.
- Bengal, Department of Agriculture (1925-26). Annual Report, 1925, 26, 11.
- Briggs, L. J. and Shantz, H. L. (1914). Relative water requirement of plants. *Jour. Agri. Res.*, **3**, 1-63.
- Chakladar, M. N. (1946). Influence of soil moisture on the yield of paddy. *Ind. Jour. Agri. Sci.*, **16**, 152-157.
- Crowther, F. (1934). Studies in growth analysis of the cotton plant under irrigation in the Sudan. I. The effects of different combinations of nitrogen applications and water supply. *Ann. Bot.*, **48**, 877-913.
- Ghosh, B. N. (1949). Physiological studies on the effect of varying water levels on growth of rice in relation to carbohydrate metabolism of the leaves. *Bull. Bot. Soc., Bengal*, **3**, 1-8.
- Richards, F. J. (1932). Physiological studies in plant nutrition. III. Further studies of the effect of potash deficiency on the rate of respiration in leaves of barley. *Ann. Bot.*, **46**, 367-388.
- Sen, P. K. (1937). Studies in the water relations of rice. I. Effect of watering on the rate of growth and yield of four varieties of rice. *Ind. Jour. Agri. Sci.*, **7**, 89-117.
- Sen, N. K. (1946). Nitrogen metabolism in rice leaves. *Jour. Ind. Bot. Soc.*, **25**, 71-75.
- Singh, B. N., Singh, R. B. and Singh, K. (1935). Investigations into the water requirement of crop plants. *Proc. Ind. Acad. Sci.*, **1**, 471-495.
- Thoday, D. (1910). Experimental researches on vegetable assimilation and respiration. V. A. critical examination of Sach's method for using increase of dry weight as a measure of carbon dioxide assimilation in leaves. *Proc. Roy. Soc., London*, **82**, B1.
- Vlams, J. and Davis, A. R. (1944). Effects of oxygen tension on certain physiological responses of rice, barley and tomato. *Plant Physiology*, **19**, 33-51.
- Woodford, E. K. and Gregory, F. G. (1948). Preliminary results obtained with an apparatus for the study of salt uptake and root respiration of whole plant. *Ann. Bot., N.S.*, **12**, 335-370.

Issued September 10, 1954.

SIZE, SCULPTURING, WEIGHT AND MOISTURE CONTENT OF THE DEVELOPING EGGS OF THE DESERT LOCUST, *SCHISTOCERCA* *GREGARIA* (FORSKÅL) (ORTHOPTERA, ACRIDIDAE)

by M. L. ROONWAL, *F.N.I., Forest Entomologist, Forest Research Institute,
Dehra Dun*

With 4 Tables, 3 Text-figures and 2 Plates

(Received October 26, 1953; read May 7, 1954)

CONTENTS

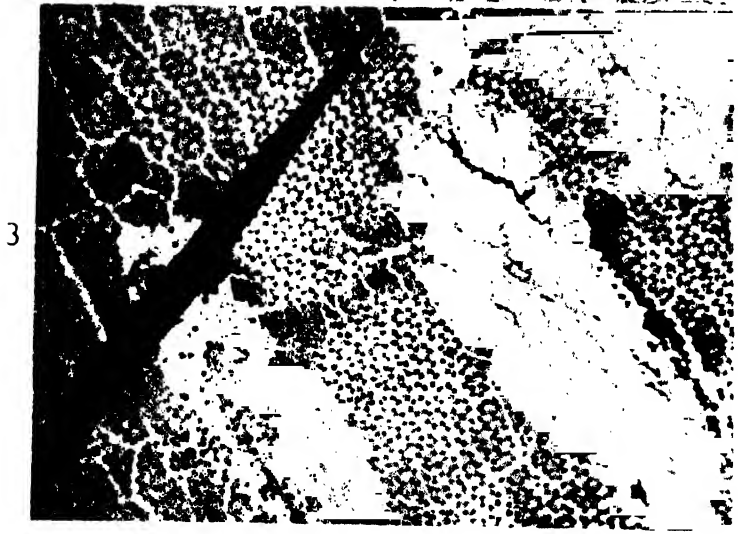
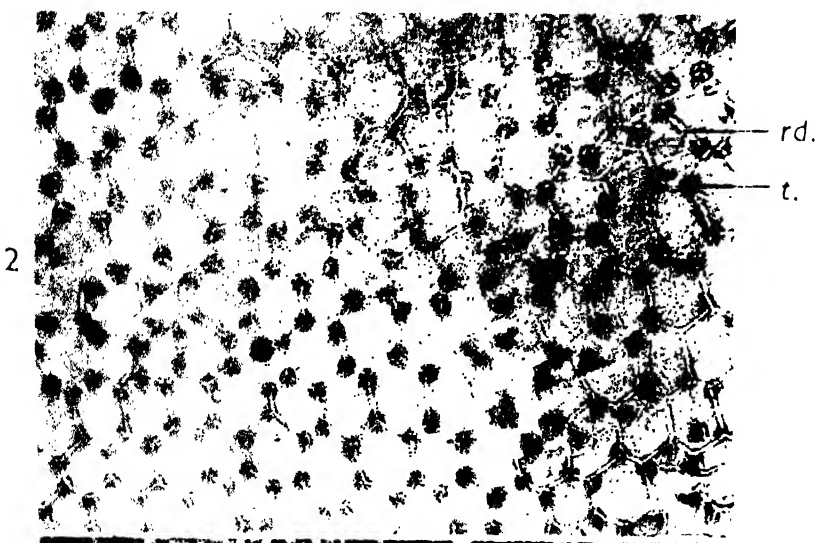
	<i>Page</i>
I. Introduction	388
II. Egg-sculpturing, etc.	389
III. Size of eggs	389
IV. Weight and moisture content of eggs	
(a) Increase of weight and moisture content during development	391
(b) Resorption of water from atmosphere by dehydrated eggs	392
(c) Rate of loss of water in young eggs in still, dry air at constant temperature (33.3° C.)	395
V. Summary	397
VI. References	397
VII. Explanation of Plates	398

I. INTRODUCTION

Little is known of the egg-sculpturing and water-balance of the eggs of the Desert Locust, *Schistocerca gregaria* (Forskål). Husain and Roonwal (1933) described the structure of the micropylar canals. Mathur (1944) demonstrated that water is absorbed by the developing eggs from the surrounding moist soil (in which the eggs are laid) only through a specialized region at the posterior pole of egg. The specialized region exists even in the freshly laid eggs and corresponds to the area demonstrated earlier in *Melanoplus differentialis* (Th.) by Slifer (1938) and termed 'hydropile' by her. Shulov (1952) studied the intake of water by the eggs of *S. gregaria*, but he did not refer to the earlier work of Mathur (1944). Shulov stated that egg-development is interrupted if contact water is lacking and is resumed when the egg is moistened; this occurs during late anatrapsis (a stage in the process of blastokinesis or 'turning round' of the embryo), which is the stage in which the embryos of some other species of locusts and grasshoppers undergo diapause or temporary cessation of development.

Absorption of external water by eggs during development after they have been laid has been shown to occur in several species of locusts, grasshoppers, other insects and indeed many other Arthropods. (For a summary, see Roonwal, 1936a, 1942, 1944.) The sculpturing of the outer cuticle of the egg-wall has been studied by Roonwal (1936a, 1954) in the African Migratory Locust, *Locusta migratoria migratorioides* R. & F. The sculpturing presents interesting features which help in distinguishing eggs of different species of Acrididae, and a study of this feature is, therefore, of practical interest.

In the present account I have described first, the egg-sculpturing of *Schistocerca gregaria*. Secondly, I have presented the results of my observations on the swelling of eggs during development, on the increase of weight and of water-content of eggs as they develop, and finally, on the rate of loss of water in young eggs in a still dry atmosphere at a constant temperature, and on certain other related features.



II. EGG-SCULPTURING, ETC.

(Pls. XV and XVI; and Text-figs. 1 and 2)

If the chorion of a freshly laid egg is cleaned, mounted on a slide and examined under the microscope, it presents a mosaic pattern of hexagonal (at places pentagonal) 'cell-walls', with a thick, circular dot or tubercle at each of the angles (Pl. XV, Figs. 2, 3 and Pl. XVI, Figs. 4, 5). In sections of the egg-wall (Pl. XV, Fig. 1 and Pl. XVI, Figs. 6-8) it is seen that the chorion is composed of two layers as follows: (i) A thin outer layer or exochorion which is about $6-8\ \mu$ thick near the poles and about $3-5\ \mu$ elsewhere. It is refractile, slightly granular and does not stain with haematoxylin. (ii) A thicker (ca. $9-10\ \mu$ at the poles and $6-8\ \mu$ elsewhere) inner layer or endochorion which stains deeply with haematoxylin and shows a semigranular, felt-like structure, similar to the one described by me (Roonwal, 1954) in *Locusta migratoria migratorioides* R. & F. Except in the micropylar region (Pl. XVI, Fig. 6) the exochorion and endochorion are not contiguous with each other but are widely separated by trabeculae or air spaces which are about $18-20\ \mu$ wide all over the egg except at the two poles where they are somewhat wider.

The trabeculae are divided into hexagonal or pentagonal cells, as the case may be, by means of endochorionic ridges which meet the exochorion and are the cause of the hexagonal (or pentagonal) chorionic pattern mentioned above. At the angles, the ridges are thickened so as to form a strut or pillar which is broad externally, i.e., towards the exochorion, and narrows towards the endochorion (Pl. XV, Fig. 1 and Pl. XVI, Fig. 7); the struts appear in surface view as the 'dots' or tubercles mentioned above. The tubercles (*t.*) are wanting at the poles (Pl. XVI, Fig. 8) where only the ridges (*rd.*) are present. Inside the endochorion is the extremely thin (less than $1\ \mu$ thick), structureless vitelline membrane which, in sections of eggs, tends to adhere to the surface of the yolk-mass.

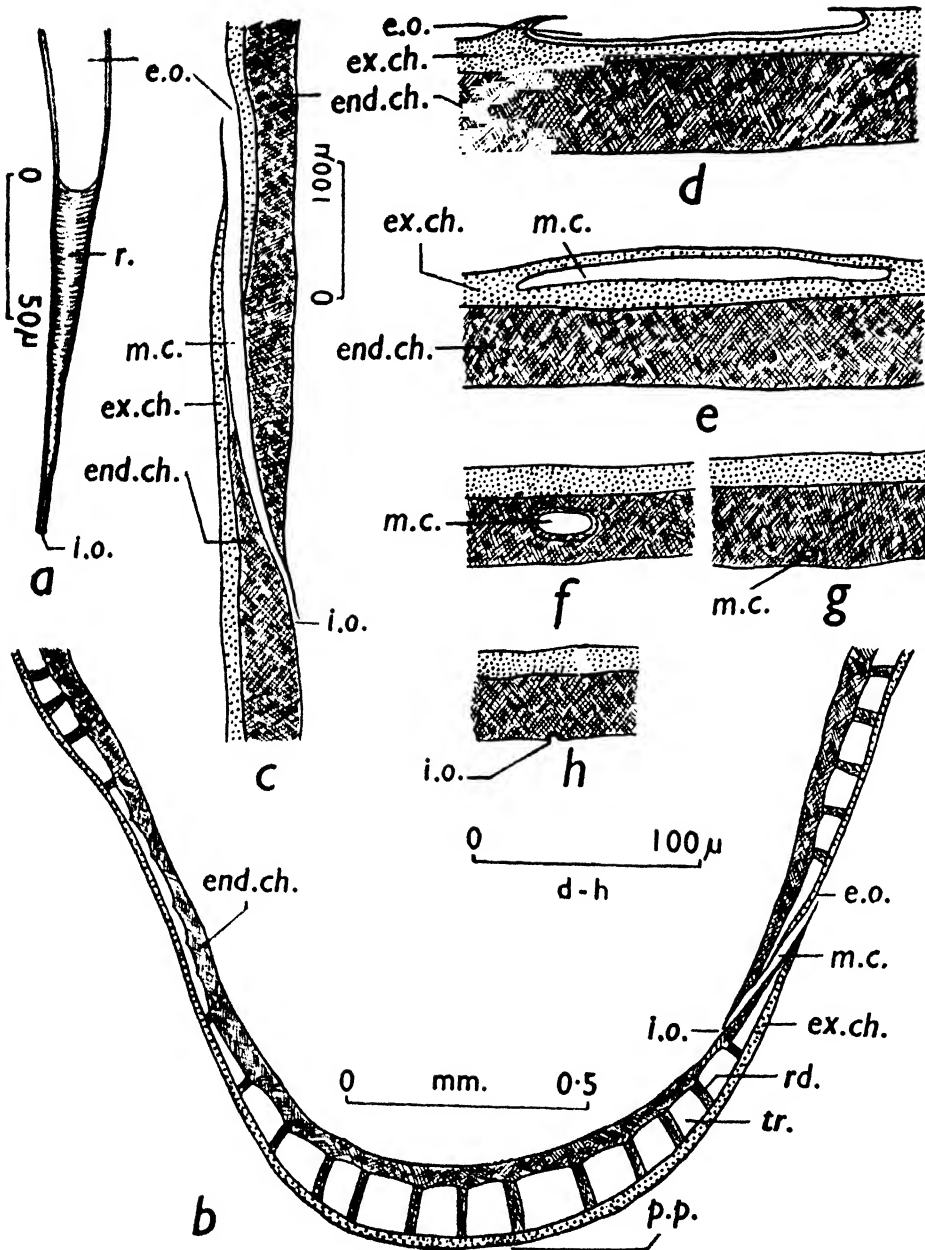
As shown by me recently (Roonwal, 1954), there appear to be two principal types of egg-walls in the Acrididae as regards the chorion, viz., one in which the exochorion is throughout contiguous with the endochorion and is not separated from the latter by means of trabeculae of air spaces (example: *Locusta migratoria migratorioides*), and another which is characterized by the presence of the trabeculae or air spaces mentioned above (example: *Schistocerca gregaria*).

The micropylar apparatus (Pl. XVI, Fig. 4; and Text-figs. 1 and 2).—Around a slight constriction near the posterior pole of the egg of *Schistocerca gregaria* there runs, at a distance of about $0.4-0.5\ \text{mm.}$ from the posterior pole, a ring of about $44-65$ funicular canals (*m.c.*). Each canal runs obliquely throughout the width of the exochorion and the endochorion; its wide external opening (ca. $7-11\ \mu$ wide) lies anteriorly on the egg-surface, and the extremely fine inner opening lies posteriorly. These canals, which measure about $123-151\ \mu$ in length, are the micropylar canals (*vide* also Husain and Roonwal, 1933).

III. SIZE OF EGGS

(Text-fig. 2)

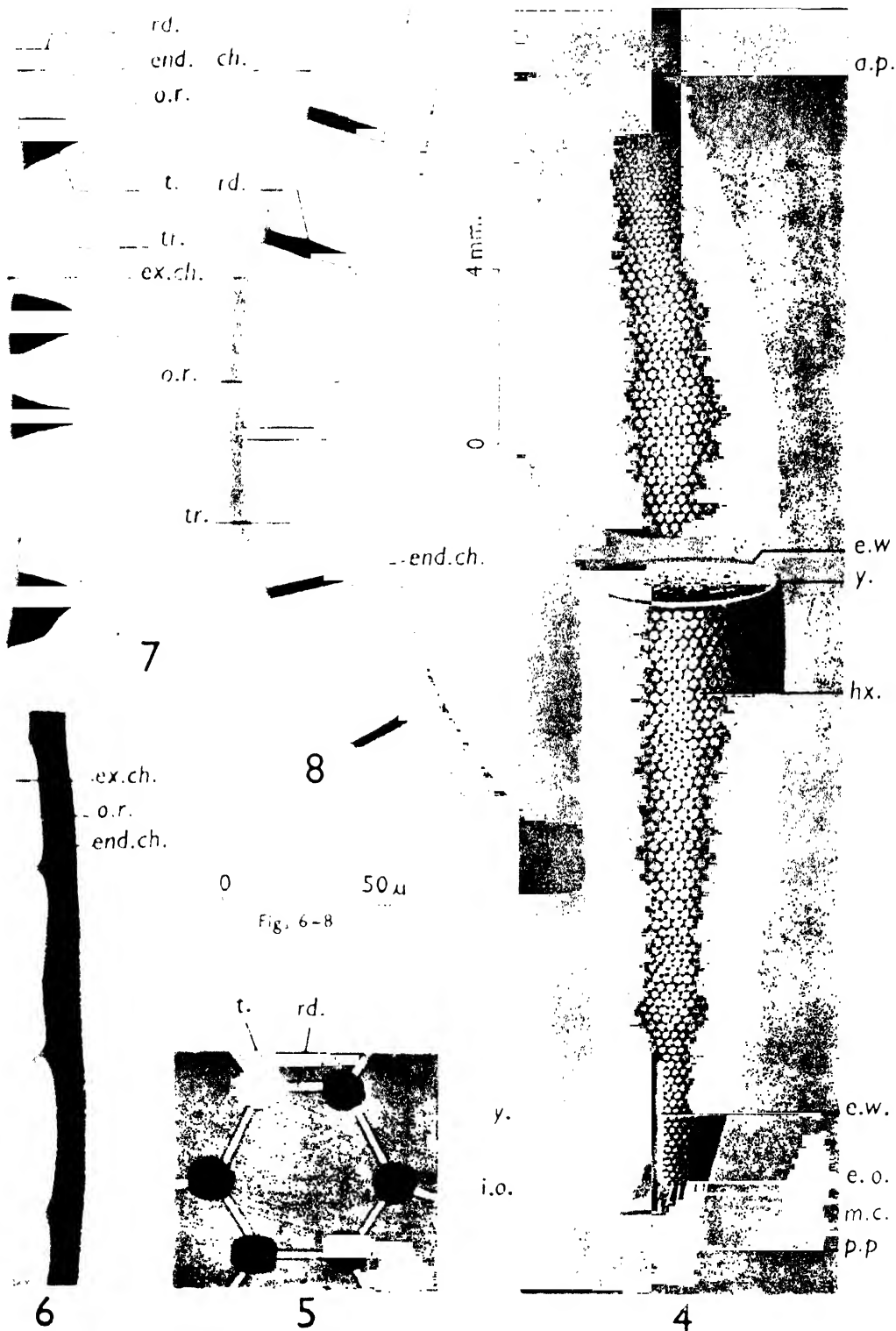
The egg of *Schistocerca gregaria* (Text-fig. 2) is slightly curved, more or less cylindrical and tapers towards both ends which are rounded. The size of eggs after oviposition (as measured by means of a vernier callipre reading up to $0.1\ \text{mm.}$ and under a stereo-binocular-microscope) increases during development as follows:—The maximum length, measured as a straight line from pole to pole, increases from about $5.1-8.0\ \text{mm.}$ (mean 6.93) in freshly laid eggs to about $8.1-9.6\ \text{mm.}$ (mean 8.92) in eggs about to hatch, i.e., there is a mean increase of about 29 per cent. Similarly, the maximum width or diameter (which occurs about the middle of the egg-length) increases from about $0.9-1.6\ \text{mm.}$ (mean 1.25) in freshly laid eggs to about $1.5-2.9\ \text{mm.}$



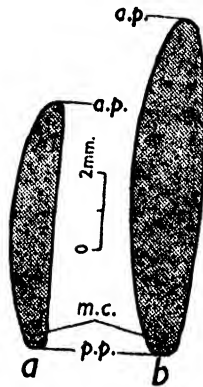
TEXT-FIG. 1(a-h).—The micropylar apparatus of *Schistocerca gregaria* (Forsk.).

(a) One of the micropylar canals in surface view from the outside. (b) Longitudinal-vertical section of the egg-wall at the posterior end of egg, to show the micropylar canal (*m.c.*) and the trabeculae or air spaces (*tr.*) between the exochorion and the endochorion. Semidiagrammatic. (c) A longitudinal-vertical section of the micropylar canal. Greatly enlarged. (d)–(h) Portions of transverse sections of the egg-wall in the micropylar region, showing the course of a micropylar canal through the exochorion and the endochorion beginning from the outside (Fig. d) and ending (Fig. h) at the inner opening of the canal.

end.ch., endochorion; *e.o.*, external opening of micropylar canal; *ex.ch.*, exochorion; *i.o.*, internal opening of micropylar canal; *m.c.*, micropylar canal; *p.p.*, posterior pole of egg; *r.*, roof of micropylar canal; *rd.*, ridge of endochorion connecting the latter with the exochorion; *tr.*, trabeculae or air spaces between exochorion and endochorion.



(mean 2.27) in eggs about to hatch, i.e., there is a mean increase of about 70 per cent. Fully developed eggs obtained from the egg-calyx of females in the process of egg-laying are usually smaller than freshly laid eggs, and measure about 4.1–5.0 mm. in length and 0.4–0.5 mm. in width. This feature is probably explicable by two reasons: (i) That in the egg-calyx the eggs are crowded and are not able to swell up to their full dimensions; and (ii) that the egg-shell is still soft and pale yellow, whereas soon after egg-laying it becomes harder and darkens in colour by coming in contact with air. The post-oviposition eggs, therefore, which are now free from mutual pressure, swell up to their full dimensions and, because of the comparative hardening of the egg-shell, stay swollen.



TEXT-FIG. 2.—Eggs of *Schistocerca gregaria* (Forsk.), to show the increase in size during development after oviposition.

(a) Freshly laid egg, side view. (b) Same, about to hatch.

a.p., anterior pole of egg; m.c., ring of micropylar canals; p.p., posterior pole of egg.

As shown by Roonwal (1936a) for the African Migratory Locust, *Locusta migratoria migratorioides*, the swelling of eggs is due to the absorption of water from the outside. This phenomenon occurs in a large number of insects, other Arthropods of even other groups of animals. (For a review, see Roonwal, 1936a, 1942, 1944.)

IV. WEIGHT AND MOISTURE CONTENT OF EGGS

(Tables 1–4 and Text-figs. 2 and 3)

(a) *Increase of weight and moisture content during development* (Table 1).

For the determination of moisture content, normally developing eggs (laid in moist soil) of various stages were washed quickly in distilled water and cleaned with a fine sable brush to remove sand particles and other foreign matter adhering to them. The eggs were then quickly dried by rolling them on a filter paper, transferred to a previously dried glass tube and weighed in an analytical balance. Weighments were usually made in lots of 10–35 eggs, each lot being taken from a single egg-pod. Subsequent drying was done over concentrated sulphuric acid in a dessicator until the weight was constant. The developmental stages of eggs studied were as follows: (i) just-laid; (ii) about 6–12 hours after oviposition (at 33.3° C.); (iii) about two-thirds developed; and (iv) about to hatch (these being taken from eggs-pods from which hatching had already started). Eggs were incubated at 33.3° C. (in one case at 32° C.) in moist sandy-loam but without ‘apparently free’ water. The results are discussed below.

TABLE 1

Schistocerca gregaria. Weight and moisture content (determined by drying over concentrated sulphuric acid) of eggs after oviposition. (Except where otherwise stated, eggs were weighed in lots of 10-35 in an analytical balance.)

G., from parents cage-bred under crowded conditions; Sw., from parents captured from swarms.

Serial No.	Develop-mental stage of eggs after oviposition	Source of eggs	Number of eggs weighed in sample	Weight (mg.) of eggs in sample			Calculated average weight (mg.) of one egg			Per-centage of water in terms of wet wt. of eggs	Remarks
				Wet wt.	Dry wt.	Loss in wt.	Wet wt.	Dry wt.	Loss in wt.		
1	2	3	4	5	6	7	8	9	10	11	12
1	Just laid	G.	20	171	93	78	8.6	4.65	3.95	45.6
2	"	G.	35	330	175	155	9.4	5.0	4.4	47.0
3	"	Sw.	10	90	48	42	9.0	4.8	4.2	46.7
AVERAGE (just laid) ..											
4	Ca. 6-12 hours old at 33.3° C.	G.	1	9.3	4.5	4.8	9.3	4.5	4.8	51.6%	Weighed in torsion balance.
5	24 hours old at 33.3° C.	G.	10	64	27	37	6.4	2.7	3.7	57.5
6	"	G.	10	87	37	50	8.7	3.7	5.0	57.5
AVERAGE (24 hours old) ..											
							7.6	3.2	4.4	57.5%

7	Ca. 2/3rds developed *	G.	10	118	52	66	11.8	5.2	6.6	55.9%	* Ca. 8 days old at 32° C. (when total incubation period is about 12 days).
8	Just before hatching	G.	1	17.6	3.6	14.0	17.6	3.6	14.0	79.6	Weighed in torsion balance.
9	"	G.	1	15.2	4.6	10.6	15.2	4.6	10.6	69.7	"
10	"	Sw.	10	192	51	141	19.2	5.1	14.1	73.4	"
11	"	Sw.	(9-10)	177	44	115.3	17.7	4.9	12.1	72.4	Out of 10 eggs, one hatched the day after the start of expt., and 9 eggs were, therefore, weighed. For comparison, the average calculated wet wt. of eggs was taken as 159.3 mg.
AVERAGE (just before hatching) ..											
				(10 eggs. Calculated for 9 eggs as 159.3)	(9 eggs)	(9 eggs)	(Average of 10 eggs)	(Average of 9 eggs)	(Average of 9 eggs)		
							17.4	4.6	12.7	73.8%

Wet weight.—The wet weight of a single egg increases from about 8.6–9.4 mg. (average 9.0 mg.) when freshly laid to about 11.8 mg. (31.1 per cent increase) when two-thirds developed and, finally, to about 15.2–19.2 mg. (average 17.4 mg.) (93.3 per cent increase over freshly laid eggs) when about to hatch¹. The weight of the egg is thus nearly doubled during development.

Shulov (1952), from eggs of *Schistocerca gregaria* obtained in the Jordan Valley, Jerusalem, recorded the average increase as from 10.5 when freshly laid to about 24.6 mg. at the beginning of hatching (incubation at 27° C.), an increase of about 134 per cent. These values, especially the last two, are much higher than those obtained by me. At first sight it seems difficult to reconcile the differences, but a consideration of the remarks made by Shulov may perhaps help in doing so. Shulov wrote (p. 474): 'The maximum weight of an egg that develops normally is about 27 mg., but some eggs weighing only 16 mg. may also hatch under conditions of contact moisture. These weights represent increase of 170 per cent and 60 per cent respectively of the original weight. Experimentally, it is possible to obtain fully developed embryos, and even for some of them to hatch, from eggs weighing as little as 11 mg.' The great diversity recorded by Shulov may be due to the greatly differing conditions of moisture availability in the soil or other media in which Shulov incubated his eggs—he did not mention precisely the nature of the medium which he used and the state of its wetness. In my experiments, it may be stated, the eggs were uniformly incubated in moist sandy-loam but without any apparently free water.

Dry weight.—The dry weight of an egg apparently decreases during development—from about 4.8 mg. in the freshly laid egg to 4.6 mg. when about to hatch, a decrease of nearly 4 per cent. It would be desirable to obtain more extensive data in this respect for *Schistocerca gregaria*. It has been demonstrated (Roonwal, 1936a) from extensive data that in the African Migratory Locust, *Locusta migratoria migratorioides*, there is a decrease of about 20 per cent in dry weight, the greater part of the decrease occurring in the second half of the developmental period. Roonwal explained it as 'due to the energy expended upon the normal activities of the developing embryo' (p. 7).

Moisture content.—The amount of water in eggs, in terms of the wet weight of eggs, increases during development by about 27.4 per cent, as follows (*vide* also Table 1):—

Stage	Water content
Just laid ..	46.4% of wet weight of egg
6–12 hrs. old ..	51.6% " "
24 hrs. old ..	57.5% " "
3/4rds developed ..	55.9% " "
About to hatch ..	73.8% " "

The absolute amount of water present in an egg increases from about 4.18 mg. in freshly laid eggs to about 12.7 mg. in eggs about to hatch, an increase of nearly 3 times. A similar order of increase (3.3 times) was found in *Locusta migratoria migratorioides* by Roonwal (1936a, p. 5).

(b) *Resorption of water from atmosphere by dehydrated eggs* (Table 2)

When freshly laid eggs are dehydrated and then exposed to moist atmosphere at a fairly high temperature, they re-absorb a small quantity of water from the

¹ The decline of average weight in 24 hours old eggs to 7.6 mg. (*vide* Table 1) is difficult to explain. It may be fortuitous, due possibly to the special smallness of the size of eggs in the different eggs-pods taken for these experiments. In another experiment, where 10 freshly laid eggs from a pod were weighed together, allowed to develop normally, and then re-weighed after 24 hours the weight increased during the first 24 hours from 6.7 mg. per egg (calculated) to 8.7 mg., an increase of 2 mg. or nearly 30 per cent.

atmosphere. This was demonstrated in two experiments in which freshly laid eggs, which were experimentally dehydrated for determining their moisture content, were exposed to an atmosphere of 80 per cent relative humidity at 33° C. This moderately high temperature was employed in order to preclude the possibility of condensation of atmospheric water on the eggs which would have occurred at low temperatures. The number of eggs employed was 35 in one experiment and 17 in another; the former lot re-absorbed 0.43 mg. of water per egg, the latter lot 0.47 mg. It took about 24 hours for the maximum resorption, after which there was no further increase of weight.

TABLE 2

Schistocerca gregaria. Resorption of water from the atmosphere (80% R.H.; 30° C.) by freshly laid dehydrated eggs

Expt. No.	Total No. of eggs in expt.	Final weight of dehydrated eggs (mg.)	Weight of eggs after full resorption of water (mg.)	Amount of water resorbed (mg.)	Calculated amount of water resorbed by one egg (mg.)
1	35	175	190	15	0.43
2	17	165	173	8	0.47

(c) *Rate of loss of water in young eggs in still, dry air at constant temperature (33.3° C.)*
(Tables 3-4; and Text-fig. 3)

The rate of loss of water was studied for just-laid and for 24-hour-old eggs. After the usual cleaning, eggs were weighed and kept in dry glass tube in dry air in a desiccator over sulphuric acid. The desiccator was kept in an electric incubator at a constant temperature of 33.3° C., and weighments were made periodically in a chemical balance.

Just-laid eggs (Table 3; and Text-fig. 3).—In the first 1½ hours, the total loss of water is 4.68 per cent of the initial wet weight of egg or at the average rate of 3.74

TABLE 3

Schistocerca gregaria. Rate of loss of water from 20 fresh-laid eggs in still, dry air at a constant temperature of 33.3° C.

Sl. No. of weighing	Age of eggs from moment of oviposition (hours)	Interval from previous weighing (hours)	Actual wet weight of 20 eggs (mg.)	Loss in weight of 20 eggs (mg.) by drying	Calculated weight of one egg (mg.)	Loss in weight of one egg by drying	Percentage loss of water	
							Total loss	Loss per hour
1	0	0	171	0	8.55	0
2	1½	1½	163	8	8.15	0.4	4.68	3.74
3	3¼	2	155	8	7.75	0.4	4.68	2.34
4	22½	19	103	52	5.15	2.6	30.41	1.6
5	45½	23½	93	10	4.65	0.5	5.84	0.25
6	69¼	24	93	0	4.65	0	0	..
Total loss in weight:				78	..	3.9	45.61%	..

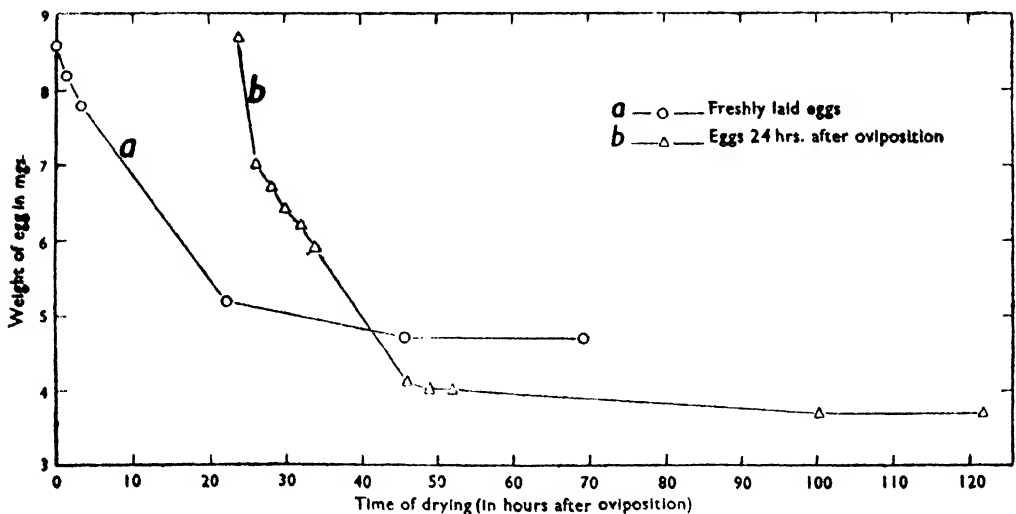
per cent per hour. In the next 2 hours the average rate of loss declines to 2.34 per cent per hour, in the next 19 hours to 1.6 per cent, and in the next 23½ hours to 0.25 per cent. It will thus be seen that the rate of loss of water is the fastest in the

TABLE 4

Schistocerca gregaria. Rate of loss of water from 10 young eggs (24 hours after oviposition) in still, dry air at a constant temperature of 33.3° C.

Sl. No. of weighing	Age of eggs from moment of oviposition (hours)	Interval from previous weighing (hours)	Actual wet weight of 10 eggs (mg.)	Loss in weight of 10 eggs (mg.) by drying	Calculated wet weight of one egg (mg.)	Loss in weight of one egg (mg.) by drying	Percentage loss of water	
							Total loss	Loss per hour
1	0	0	(67)	(—)	(6.7)	(—)
2	24	24	87	*(Increase 20 mg.)	8.7	*(Increase 2 mg.)
3	26	2	70	17	7.0	1.7	19.54	9.77
4	28	2	67	3	6.7	0.3	3.45	1.73
5	30	2	64	3	6.4	0.3	3.45	1.73
6	32	2	62	2	6.2	0.2	2.30	1.15
7	34	2	59	3	5.9	0.3	3.45	1.73
8	46	12	41	18	4.1	1.8	20.69	1.72
9	49	3	40	1	4.0	0.1	1.14	0.38
10	52	3	40	0	4.0	0	0	0
11	100	48	37	3	3.7	0.3	3.45	0.006
12	121½	21½	37	0	3.7	0	0	0
Total loss in weight:				50	..	5.0	57.47%	..

* Eggs not dried but kept in moist sand.



TEXT-FIG. 3.—*Schistocerca gregaria* (Forsk.). Graph to show the rate of loss of water from young eggs in still, dry air at a constant temperature of 33.3° C. (a) Freshly laid egg. (b) Egg 24 hours old.

first few hours, and then gradually slows down until about 22 hours by which time the bulk of the water loss has occurred. The loss continues very slowly until about 45 hours, after which there is no further loss. The total loss is about 45.5 per cent of the wet weight of egg.

24-hour old eggs (Table 4; and Text fig. 3).—The general trend here is similar to that in the just-laid eggs, viz., that the rate of loss of water is the fastest in the first few hours and gradually declines; the bulk of the water is lost by about 22 hours (Table 4, Serial No. 8), after which the loss is negligible. Some differences in detail are, however, noticeable. Thus, the average rate of loss in the first 2 hours is about 9.77 per cent per hour as compared to about 3.7 per cent or less in the just-laid eggs. Subsequently, that is, between about 2–22 hours (Table 4, Serial Nos. 4–8), the average rate of loss is nearly constant, being about 1.15–1.73 per cent; this is similar to the rate in the just-laid eggs (1.6 per cent) during a nearly similar period.

V. SUMMARY

1. The egg-wall of the freshly laid egg consists of 3 layers, viz., a thin outer layer, the exochorion, next to it a thicker endochorion and, finally, an extremely fine and structureless vitelline membrane.

2. The endochorion presents a mosaic pattern of hexagonal (occasionally pentagonal) ridges and tubercles and is separated from the exochorion by means of large trabeculae or air spaces.

3. The micropylar apparatus consists of a ring of small, funicular canals which obliquely traverse the exochorion and the endochorion and open on the inside by means of an extremely fine aperture on the inner surface of the endochorion.

4. The eggs increase in size during development from mean dimensions of about 6.93×1.25 mm. when freshly laid to about 8.92×2.27 mm. when about to hatch.

5. The mean wet weight of an egg increases from 9.0 mg. when freshly laid to 11.8 mg. (31.1% increase) when two-thirds developed and 17.4 mg. (93.3% increase over freshly laid egg) when about to hatch.

6. The dry weight of an egg decreases from about 4.8 mg. when freshly laid to about 4.6 mg. (a decrease of about 4%) when about to hatch.

7. The moisture content of an egg increases from about 46.4% (of the wet weight of egg) when freshly laid to about 73.8% when about to hatch. The absolute amount of water increases from about 4.18 mg. in the freshly laid egg to about 12.7 mg. when about to hatch.

8. Dehydrated eggs, when exposed to moist air, re-absorb a very small quantity of moisture.

9. The rate of loss of water from young eggs in still, dry air at a constant temperature (33.3° C.) was studied. The rate of loss, which progressively declines, is very rapid in the first few hours. The bulk of the water is lost by 22 hours; the loss continues slowly until about 45 hours after which there is no further loss.

VI. REFERENCES

- Husain, M. A. and Roonwal, M. L. (1933). Studies on *Schistocerca gregaria* Forsk. I. The micropyle in *Schistocerca gregaria* Forsk. and some other Acridiidae. *Indian J. Agric. Sci.*, Delhi, 3(4), 639–645, 1 pl.
- Jhingran, V. G. (1949). Early embryology of the Desert Locust, *Schistocerca gregaria* (Forsk.) (Orthoptera, Acrididae). *Rec. Indian Mus.*, Calcutta, 45(2 and 3) (1947), 181–200, 4 pls.
- Mathur, C. B. (1944). The site of the absorption of water by the egg of the Desert Locust (*Schistocerca gregaria* Forsk.). *Indian J. Ent.*, New Delhi, 5(1-2) (1943), 35–40.
- Mattheé, J. J. (1951). The structure and physiology of the egg of *Locustana pardalina* (Walk.). *Sci. Bull. Dept. Agric. S. Afr.*, Pretoria, No. 316. (Locust Res. Ser., No. 13), 1–83.
- Roonwal, M. L. (1936a). The growth-changes and structure of the egg of the African Migratory Locust, *Locusta migratoria migratorioides* R. & F. (Orthoptera, Acrididae). *Bull. Ent. Res.*, London, 27(1), 1–14.
- (1936b). Studies on the embryology of the African Migratory Locust, *Locusta migratoria migratorioides* R. & F.—I. The early development, with a new theory of multi-phased gastrulation among insects. *Philos. Trans. R. Soc. Lond.* (B), London, 226, 391–421, 3 pls.
- (1937). Studies on the embryology of the African Migratory Locust, *Locusta migratoria migratorioides* Reiche and Frm.—II. Organogeny. *Philos. Trans. R. Soc. Lond.* (B), London, 227, 175–244, 7 pls.

- Roonwal, M. L. (1942). Earliest observations on the swelling of insect eggs after oviposition, A historical note. *Indian J. Ent.*, New Delhi, 4(2), 145-151.
- (1944). Some observations on the breeding biology, and on the swelling, weight, water-content and embryonic movements in the developing eggs of the Moluccan King Crab, *Tachypleus gigas* (Müller) (Arthropoda, Xiphosura). *Proc. Indian Acad. Sci. (B)*, Bangalore, 20(4), 115-129, 1 pl.
- (1954). The egg-wall of the African Migratory Locust, *Locusta migratoria migratorioides* Reich. and Frm. (Orthoptera, Acrididae). *Proc. Nat. Inst. Sci. India*, Calcutta, 20. (In press.)
- Salt, R. W. (1949). Water uptake in eggs of *Melanoplus bivittatus* (Say). *Canad. J. Res. (D)*, Ottawa, 27, 236-242.
- Shulov, A. (1952). The development of eggs of *Schistocerca gregaria* (Forskål) in relation to water. *Bull. ent. Res.*, London, 43(3), 469-476.
- Slifer, E. H. (1937). The origin and fate of the membranes surrounding the grasshopper egg; together with some experiments on the source of the hatching enzyme. *Quart. J. Micr. Sci.*, London, 79(3), 493-506, 3 pls.
- (1938). The formation and structure of a special water-absorbing area in the membranes covering the grasshopper egg. *Quart. J. Micr. Sci.*, London, 80(3), 437-457, 1 pl.

VII. EXPLANATION OF PLATES

Lettering

<i>a.p.</i> , anterior pole of egg.	<i>i.r.</i> , inner refractile portion of endochorion.
<i>end. ch.</i> , endochorion.	<i>m.c.</i> , micropylar canal.
<i>e.o.</i> , external opening of micropylar canal.	<i>p.p.</i> , posterior pole of egg.
<i>e.w.</i> , egg-wall.	<i>rd.</i> , ridges of endochorion.
<i>ex.ch.</i> , exochorion.	<i>t.</i> , tubercle or protuberance of endochorion.
<i>hz.</i> , pattern of hexagonal ridges on endochorion.	<i>tr.</i> , trabeculae or air spaces between exochorion and endochorion.
<i>i.o.</i> , internal opening of micropylar canal.	<i>y.</i> , yolk.

PLATE XV

Egg-wall of *Schistocerca gregaria* (Forsk.)

FIG. 1.—Longitudinal section of the egg-wall of a freshly laid egg, showing the exochorion, endochorion, tubercles and trabeculae or air spaces. Greatly enlarged.

FIG. 2.—Surface view of the chorion of an egg 6 hours after oviposition, showing the hexagonal (occasionally pentagonal) pattern formed by ridges, with the 'round' tubercles at the angles. Greatly enlarged.

FIG. 3.—Surface view of the chorion of an egg about to hatch. Note the hexagonal (occasionally pentagonal) pattern and tubercles as in Fig. 2; also note the cracks in the chorion. Low magnification.

PLATE XVI

Egg and egg-wall of *Schistocerca gregaria* (Forsk.)

FIG. 4.—Egg, to show the sculpturing and the micropylar canals. The egg is cut transversely in the centre; also, a portion of the egg-wall near the posterior pole is removed to show the disposition of the micropylar canals.

FIG. 5.—Surface view of the egg-wall, to show one of the hexagons formed by the ridges of the endochorion of egg-wall, enlarged to show the position of the tubercles. (Cf. Pl. I, Figs. 2 and 3.)

FIG. 6.—Portion of longitudinal-vertical section of egg-wall in the posterior region of the egg near the micropyle, but not passing through a micropylar canal. Note the absence of tubercles. The vitelline membrane is not shown.

FIG. 7.—Ditto, near middle of egg. Note the endochorionic tubercles and the trabeculae or air-spaces.

FIG. 8.—Ditto, at the posterior pole of egg. Note that the endochorionic tubercles are long and thin rather than stout and broadened externally (cf. Fig. 7).

THE ECOLOGY OF A BRACKISHWATER *BHERI*, WITH SPECIAL REFERENCE TO THE FISH-CULTURAL PRACTICES AND THE BIOTIC INTERACTION

by T. V. R. PILLAY, *National Institute of Sciences of India Research Fellow **

(*From the Laboratories of the Zoological Survey of India, Calcutta*)

(Communicated by S. L. Hora, F.N.I.)

(Received December 2, 1953; read May 7, 1954)

CONTENTS

	<i>Page</i>
Introduction	399
Topographical and hydrological features	400
Biota	405
Fish cultural practices	407
Ecological classification of the fauna	409
Dominant animals	
(1) Mulletts	410
(2) Cock-up	414
(3) Prawns	414
Sources of food supplies	414
Biotic interaction	
(1) Methods	415
(2) Food of dominants	415
(3) Food of influents	416
(4) Food of sub-influents	419
(5) Inter-relations of the food of the fauna	421
Discussion and recommendations	
(1) Water supply	423
(2) Selective stocking	424
(3) Predator control	424
(4) Production of food for fish	425
(5) Extension of rearing period	425
(6) Development of subsidiary industries	425
Summary	425
Acknowledgements	426
References	426

INTRODUCTION

Brackishwater fish-farming is considered to hold out great potentialities in easing the protein food shortage in underdeveloped tropical countries. Among the countries in South-East Asia, Java, Formosa and the Philippines have extensive brackishwater farms where the Milk fish, *Chanos chanos* (Forskål), is cultivated on a commercial scale. In India, a specialised type of brackishwater fish culture exists in Lower Bengal, in what are known as *bheris*. In these so-called *bhasabadha* fisheries or *bheris* mullets are cultured along with Cock-up (*Lates calcarifer*) and prawns. As in Hawaii and Formosa, mullets are cultured in brackishwaters of India on a commercial scale.

* Present Address: Hilsa Fish Enquiry, All-India Institute of Hygiene and Public Health, Calcutta.

Calcutta fish markets receive considerable quantities of fish raised in *bheris* situated in the Salt Lake area and the Sundarbans. These *bheris* not only support several fishermen but also contribute greatly to the fish supplies of the city. Hora and Nair (1944) have given a description of a *bheri* in the Sundarbans. Except for some general remarks contained in Gupta's report (1908) and the references in Chatterjee's article (1933), there are no detailed records of the fishes or the cultural practices in the *bheris* of the Salt Lake area. There are general surveys of the flora (Biswas, 1927), but the ecological features and the economic aspects of the fisheries have not been investigated.* As a part of an investigation of the biology of the Grey Mullet, *Mugil tade* Forskål, the author had opportunities of making some observations on the ecology of a *bheri* in Ghutiari Sharif, situated about 20 miles south of Calcutta on the Port Canning line of Eastern Railway. As the main object of the observations was to assess the conditions of existence of mullets in the *bheri*, particular attention was paid to the fish culture practices and the food relations of the mullets and their associates. An account of these observations is given below.

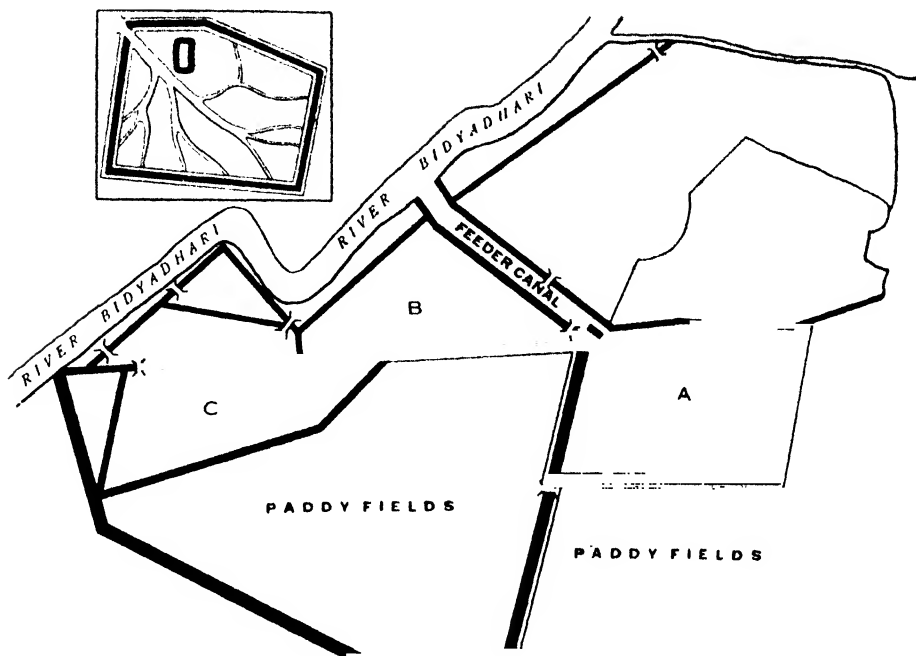
TOPOGRAPHICAL AND HYDROLOGICAL FEATURES

The *bheri* selected for observations is located on the bank of the tidal river, Bidyadhari. It has been constructed by embanking the extensive spill area of the river and is divided by subsidiary embankments into eight ponds ranging from about 200 to 800 bighas† (Text-fig. 1). The ownership of the *bheri* is rather complicated, and the proprietary right of a sizeable portion of it is still unsettled. Most of the studies have been made in the two ponds marked *A* and *B* in Text-fig. 1, which are approximately 400 and 300 bighas in extent respectively. These ponds were under the control of one Mr. Mohamed Hanif during the time of investigations, which extended from 1949 to 1951.

The main embankments of the ponds are 6-8 ft. high, 10-12 ft. wide at the base and 6-7 ft. at the crest. Grass (*Graminae*) and *Suaeda maritima* (Family Chenopodiaceae—N. Order: Centrospermae) growing on the embankments serve to bind the soil and thus check erosion. All round the ponds within the embankments, is a deep canal system formed by the excavation of earth for bunding. These canals are about 4-5 ft. below the pond level. Connected to this canal system is another branching canal system spread over the general pond bottom. The remaining portion of the pond bottom is of level ground except for a deeper portion in pond *B*. Besides these, each of the ponds has a subsidiary pond about 4-5 ft. deep with separate embankment all round which is about 2 ft. high. The canals, the subsidiary ponds and the deep areas of the pond always hold a certain height of water, but the other portions generally remain dry during the dry months (Plate I, Fig. 1). The depth of water in the canals varies from 2-4 ft. except during the rainy season when it may be as much as 6-8 ft. As during the spring tides in February, March and April large quantities of tide water are taken into the *bheri*, the water level is usually much higher in this season. The average depths of water in the canals during the dry seasons before and after the tide water is taken in, are 2 to 2½ ft. and 3 ft. respectively. In the shallow portions of the pond, the average depth of water is 6"-9" in the rainy season and about 1'-2' when a good supply of tide water is obtained. The rapid silting and the consequent deterioration of the

* An abstract of a paper 'On the biological productivity of a typical brackishwater Tarn (Bheri) of Lower Bengal' by H. K. Mookerjee, D. N. Ganguly and R. S. Mookerjee has been published in *Proc. 38th Indian Sci. Congr.*, Pt. III, 1952. The full paper has not been published, but in the abstract, it is mentioned that the phyto- and zooplankton of the Tarn were studied and the adult fish populations described. The authors have expressed the view that both lentic and mixed environments are exhibited in the tarn.

† 3 bighas = one acre.



TEXT-FIG. 1. A diagrammatic sketch of the *bheri*. Inset—Diagrammatic representation of the layout of canals and subsidiary pond in a section of the *bheri*.

Bidyadhari river feeding the *bheri* referred to by O'Malley (1914) and Banerjee (1931), have gone on so much further since then that irrigation engineers consider it almost a defunct river. The maximum tidal range, in the month of August, is about 5 ft. and the minimum, in the month of March or April about 1 ft. These changes have naturally affected the water supply of the *bheris* considerably. Formerly when the tidal range was high, it was possible to take water daily into the farm at high tides, but now owing to the weak tidal impulse, it is possible to do so only for about 4 days during the highest spring tides. The tidal water from the river is led into the ponds through a long canal (Text-fig. 1 and Plate XVII, Fig. 2) and taken in through sluice gates (Plate XVII, Figs. 3 and 4). During spring tides the sluice gates are opened and water is let in. At the turn of the tide the gates are closed so as to prevent the water from flowing out. Due to the absence of any big trees or even growth of bushes, the area is fully exposed to the action of wind, which is very severely felt during squally weather?

The pond bottom consists of ooze-like mud deposited by the silt-laden water as it flows through. The soil is of recent formation and its mineralogical components are listed below in the order of their abundance:

Chlorite
Quartz
Biotite mica
Opaque minerals
Muscovite mica and sericite
Felspar
Calcite.

There is a good deal of variation in the size of individual mineral grains ranging from specks to grains nearly 0.3 mm. (= 0.12 inches) across. Calcite, felspar and

muscovite mica are of smaller size than the rest. Chloritic material and biotite are by far the most abundant. The soil contains about 3% of humus and the moisture content is about 31%. The top layer is composed of fine sticky mud with sizeable quantities of organic matter, consisting mainly of decayed plant and animal matter. Chemical analysis of the soil samples showed the presence of the following radicals:

Chlorides—0.137%.
 Silica and other insoluble matter—79.47%.
 Iron and aluminium as oxides—8.88%.
 Sulphate as SO_3 —0.05%.
 Calcium as CaO —3.34%.
 Magnesium as MgO —1.12%.
 Total nitrogen—0.42%.
 Nitrate nitrogen—0.004%.
 Phosphates as P_2O_5 —1.53%.

Meteorological data could not be collected at Ghutiari Sharif, but the monthly normal rainfall figures * in Canning Town which is only about 8 miles from there, and the atmospheric temperature at Alipore † which is nearly 20 miles from this place are available for the period, February, 1949 to January, 1950. These data presented in Table I will serve to give an approximate picture of the climatic conditions of the locality.

TABLE I
Rainfall and temperature data

Month.	Normal rainfall at Canning Town in inches.	Mean atmospheric temperature at Alipore.	
		Maximum (°C.).	Minimum (°C.).
February (1949) ..	0.88	29.7	15.9
March ..	1.45	34.6	22.0
April	1.90	33.2	24.3
May	6.12	33.4	25.3
June	12.07	34.3	26.3
July	14.19	32.2	26.4
August ..	14.61	32.1	26.4
September ..	9.77	32.3	26.1
October ..	4.60	32.8	24.7
November ..	1.14	28.9	16.8
December ..	0.08	26.5	12.2
January (1950) ..	0.45	27.7	14.1

Table II gives the hydrological data for the same period collected during monthly visits. The range of pH values was rather limited (7.5–8.3) and the water

* From the data published by the Director of Agriculture, West Bengal.

† Obtained from the Meteorological Office, Alipore.

always remained alkaline in reaction. Table II clearly shows the wide range of salinity obtaining in the ponds. While the salinity may be high during the dry months, the water becomes almost fresh during the rainy season. The rise in salinity is chiefly due to rapid evaporation during the inter-spring-tide periods. If the salinity of the pond water goes high, dilution with the almost fresh tide water at high tides in this season may slightly lower it. While the salinity does not generally go above 35 ‰ in canals and deeper areas of the ponds even during the driest months, the concentration of salt increases rapidly in the shallow regions, and with the complete drying up of these areas (Plate XVIII, Fig. 4) a layer of salt deposit may be seen on the bottom. Except for the extremes in hydrological conditions during the height of the rainy and summer seasons, the interval between two spring tides is the regular period of greatest fluctuations in the quality of the pond water. Table III illustrates the variations in the depth and salinity of the pond water during an inter-spring tide period in the month of May, 1951. The water level and salinity data are represented in graphic form in Text-fig. 2. They bring out the remarkable fact of a rapid lowering of water level during the inter-spring-tide period. Associated with this, is the salinity increase as seen in Text-fig. 2, reaching a high level of 35 ‰ by the next spring tide period. These wide fluctuations in the hydrological conditions exercise a very strong influence on the faunal elements of the *bheri*, the strongly euryhaline of which are able to sustain themselves under the conditions prevailing.

TABLE II

The water temperature, pH and salinity of the bheri water during the period of observation ().*

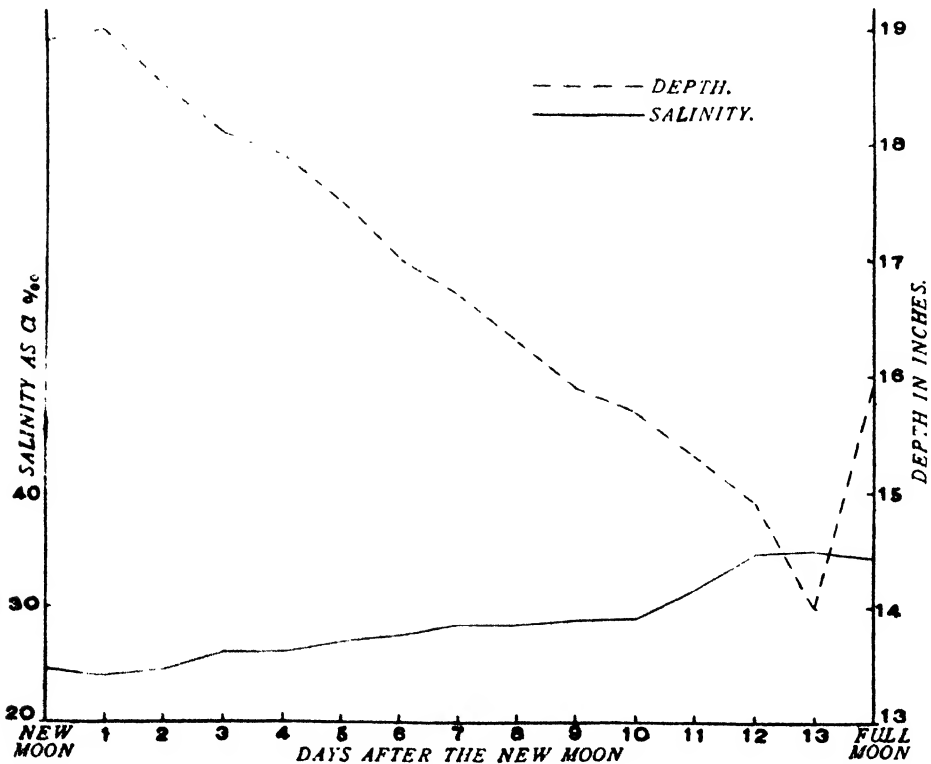
Date.	Water temp. (°C.).	pH.	Chlorinity (‰).
22- 2-49 ..	30.0	7.5	9.90
24- 3-49 ..	28.9	8.0	1.60
23- 4-49 ..	30.0	8.3	9.80
24- 5-49 ..	28.3	8.1	10.89
24- 6-49 ..	29.4	8.0	11.10
24- 7-49 ..	27.5	8.3	1.80
23- 8-49 ..	29.4	7.8	1.57
24- 9-49 ..	35.0	7.9	2.20
24-10-49 ..	26.5	8.0	6.05
23-11-49 ..	25.4	8.2	7.80
23-12-49 ..	24.5	8.3	9.60
24- 1-50 ..	14.4	8.2	9.70

(*) All observations were made at about 8 a.m. in the morning.

TABLE III

The hydrological changes in the bheri water during an inter-spring-tide period in May, 1951.

Day.	Depth of water in inches.	Atm. temp. (°C).	Water temp. (Surface, °C.).	pH.	Salinity (‰).
New moon	18.9	30.59	30.50	8.3	24.5
1st day after new moon ..	19.0	30.50	30.60	8.3	24.0
2nd	18.5	30.60	30.50	8.3	24.5
3rd	18.1	30.60	30.60	8.3	26.0
4th	17.9	30.60	30.60	8.5	26.0
5th	17.5	30.66	30.60	8.5	27.0
6th	17.0	30.60	30.60	8.4	27.7
7th	16.7	30.50	30.50	8.4	28.4
8th	16.3	30.25	30.60	8.3	28.5
9th	15.9	30.00	30.60	8.3	28.6
10th	15.7	30.60	30.60	8.5	29.0
11th	15.3	30.60	30.50	8.4	31.4
12th	14.9	30.50	30.55	8.4	34.6
13th	14.0	30.25	30.10	8.3	35.0
Fullmoon	15.9	30.00	30.00	8.3	34.2



TEXT-FIG. 2. The depth and salinity of the pond water during an inter-tidal period.

BIOTA

FLORA.—A very striking feature of the *bheri* is the complete absence of submerged phanerogamic vegetation. Even on the embankments and exposed regions, there are few larger plants. Neither the mangrove formation of the type described by Biswas (1927) in the Salt Lake area, nor the dense jungle seen in the *bheris* of lower Sundarbans, is present in this region. The exposed parts of the pond bottom are covered with grass (Family Graminae). The plankton of the ponds is rich in floral elements during a good part of the year. Among the phytoplankters, diatoms form a predominant group. The most common forms are of the genera, *Navicula*, *Pleurosigma* and *Gyrosigma*. Among these, *Gyrosigma scalproides* is very common, especially during the colder months. Other common forms identified from the ponds are *Cymbella*, *Coscinodiscus*, *Cyclotella*, *Fragilaria* and *Amphipleura*. Biswas (*op. cit.*) has given a detailed list of the surface and benthic algae other than diatoms, occurring in brackishwater *bheris* of the Salt Lake area. The Myxophyceean genera found in the surface plankton were, *Oscillatoria*, *Lyngbya*, *Spirulina*, *Anabaena*, *Nodularia*, and *Rivularia* and the Chlorophyceean genera *Protococcus*, *Pediastrum*, *Hydrodictyon* and *Ankistrodesmus*. The only desmid was *Cosmarium*. There were considerable quantities of algal spores in the plankton almost throughout the year.

A notable feature is the thick growth of benthic flora on the pond bottom. Associated with this algal matrix are many microscopic animalcules, more particularly during the cold months when thick mats of this growth are dislodged from the bottom to float on the surface near the pond margins or to be stranded on the haulms of emergent grass. Schuster (1951) has described this type of phenomenon in great detail. Different species of *Oscillatoria* are the most predominant. *Gloeocapsa*, *Symploca*, *Protococcus*, *Enteromorpha*, *Chaetomorpha* and *Polysiphonia* are also common, besides *Lyngbya*, *Anabaena* and *Microcoleus* of the surface plankton. The presence of many of the benthic algae in the surface plankton is due to the constant stirring of the waters by wave and wind action. Diatoms, especially, *Gyrosigma scalproides* are found growing on filamentous algae in the benthic zones. The cold season between December and March appears to be the peak period of floral growth in the ponds, while in the rainy season the quantity of flora decreases considerably. However, *Oscillatoria* and allied forms are comparatively abundant during the rainy season. *Spirogyra* spp. occur in the littorophic layer during this season.

FAUNA.—Sewell (1934) has listed the animals that occur in the Gangetic delta and in the Salt Lake area, giving an account of the zooplankton of the area with special reference to copepods. A remarkable feature of the fauna in this *bheri* also, as observed by Chopra (Sewell, *op. cit.*), is the great abundance of individuals of different species of animals. Copepods (*Diaptomus*, *Pseudodiaptomus*, *Acartia*, *Cyclopina*, *Cyclopsis*) and Cladocerans form the most predominant items of the zooplankton in the ponds. Zoea and megalopa larvae, mysids and the young of prawns and shrimps were also generally found in the plankton. Ciliates and Flagellates, Helminths and Rotifers are found only in small quantities, during the rainy months and up to the beginning of winter. The quantity of zooplankton in the ponds, which is fairly high in the rainy season, is gradually reduced as winter approaches.

The dominant elements of macro-fauna, other than the few polychaete worms and the Gastropod molluscs, *Stenothrya* and *Melanoides*, are the Crustaceans and fishes. The common crustaceans are the following:—

Penaeus semisulcatus De Maan, *Penaeus indicus* M. Edw., *Metapenaeus monoceros* Fab., *Leander styliferus* M. Edw., *Palaemon rudis* Heller, *Scylla serrata* (Forsk.), *Varuna litterata* (Fab.), *Metaplex dentipes* (Heller). During the rainy season swarms of megalopa larvae of the common crab *Varuna litterata* abound in the pond waters. The crabs *Scylla serrata* and *Varuna litterata* make holes in the

embankments of the ponds weakening them and ultimately leading to the complete collapse of *bheris* in certain areas.

The following fishes have been identified from the ponds:

Sub-Class Actinopterygii

Family Clupeidae

Pellona elongata (Bennett)

Family Engraulidae

Setipinna phasa (Ham.)

Thriassocles hamiltonii (Gray)

Family Cyprinidae

Barbus (Puntius) stigma (Ham.)

Family Bagridae

Mystus gulio (Ham.)

Family Anguillidae

Anguilla bengalensis (Gray & Hardeo)

Family Ophichthyidae

Pisodonophis boro (Ham.)

Family Belontiidae

Xenentodon cancila (Ham.)

Family Hemirhamphidae

Hemirhamphus limbatus Cuv. & Val.

Family Cyprinodontidae

Aplocheilichthys panchax (Ham.)

Oryzias melastigma (McClelland)

Family Mugilidae

Mugil corsula Ham.

Mugil parsia Ham.

Mugil tade Forsk.

Family Polynemidae

Eleutheronema tetradactylum (Shaw)

Family Centropomidae

Ambassis baculis (Ham.)

Lates calcarifer (Bl.)

Family Theraponidae

Therapon jarbua Forsk.

Family Lobotidae

Lobotes surinamensis (Bloch)

Family Leiognathidae

Gerres setifer (Ham.)

Gerres abbreviatus Blkr.

Leiognathus insidiator (Cuv. & Val.)

Family Scatophagidae

Scatophagus argus (Bloch)

Family Eleotridae

Eleotris butis (Ham.)

Family Gobiidae

Apocryptes lanceolatus (Bl. Schn.)*Brachygobius nusus* (Ham.)*Glossogobius giuris* (Ham.)*Gobiopertus chuno* (Ham.)*Periophthalmus schlosseri* (Pallas)*Scartelaos viridis* (Ham.)*Stigmatogobius sadanandio* (Ham.)

Family Cynoglossidae

Cynoglossus cynoglossus (Ham.)

It will be seen from the above list that a large majority of the common estuarine fishes of the area is found in the *bheri*. However, the conspicuous absence of two species found in large numbers in the River Matlah is noteworthy. The grey mullet, *Mugil speigleri* Blkr. and the Bombay duck, *Harpodon nehereus* (Ham.), are common in Port Canning and the neighbouring areas during a major part of the year. These fishes have not been found in the Ghutiari Sharif *bheri* at any time of the year, nor in the *bheris* of the lower Sundarbans.

The common frogs *Rana cyanophlyctis* and *Rana tigrina* are occasionally found in the ponds. The little Cormorant (*Phalacrocorax niger* (Vieillot) and the Darter (*Anhinga melanogaster* Pennant), the Common King Fisher (*Alcedo atthis* Linn.), the Common Sandpiper (*Actitis hypoleucos* Linn.), the Brahminy Kite (*Haliastur indus* (Boddaert), the Cattle Egret (*Bubulcus ibis* Linn.), the King Crow (*Dicrurus macrocercus* Vieillot), the Pied King Fisher (*Ceryle rudis* (Linn.)), and the Yellow Wattle Lapwing (*Lobipluvya malabarica* Boddaert) are often seen either on the embankments or in the shallow regions of the ponds. The common crow is closely associated with the homesteads of the fishermen on the embankments.

FISH CULTURAL PRACTICES

The methods of fish culture in the Ghutiari Sharif *bheri* are very much like those described by Hora and Nair (1944). The cultural operations commence about January-February when the ponds are stocked with fish fry. The ponds, which contain only little water at that time as a result of dewatering for fishing in September-December, are filled with water to the maximum extent possible. Generally, each pond has only one main sluice gate, but during this period emergency inlets are also made so that the intake of water could be enhanced. As stated above it is only during the spring tides that the tidal water reaches the sluice gates. The main sluices are provided with shutters (Plate XVII, Figs. 3 and 4) to regulate the water level. At high tide these doors are opened and the tidal water is allowed to flow in. At the turn of the tide the gates are closed and the water is prevented from flowing out. In front of each main sluice gate is a V- or W-shaped screen of bamboo-gratings (Plate XVII, Fig. 5) with gaps at the apex of the V or apices of the W. In these gaps are placed *atols* (Hora and Nair, *op. cit.*) (Plate XVII, Fig. 6). These *atols* do not serve the purpose of collecting fry for stocking. In fixing them, the open side with the valve-like arrangement of bamboo spindles, is kept facing the pond. Some of the fishes in the ponds such as the mullets have the habit of swimming against currents, and in doing so are caught in these *atols*. The bamboo gratings are kept in front of the sluice gates to prevent the fishes in the ponds from escaping when the gates are open. When emergency gaps are made in the embankments to let in additional quantities of water, the fishermen have an ingenious

device for preventing the escape of fishes from the ponds (Plate XVIII, Fig. 1). The floor of the gap made in the embankment is usually about 4"-8" above the level of the water. The floor which slants away from the pond is paved with a *putta* of bamboo grating, the end of which projects into the pond. Over this bamboo work is smeared a thick layer of clay. The tidal water that flows over the floor of the gap falls into the pond at a steep angle. Those fishes which approach the inflow of water find it impossible to negotiate the current and are unable to escape from the pond. The fishermen believe that fry of almost all the fishes in the ponds are obtained during this period. But the author's observations in this *bheri* as well as in other areas (Pillay, 1949 and 1954) show that from among the important fishes, only the young of *Mugil parsia* and *Mystus gulio* and the prawns are available during this period. Along with these, fingerlings of other fishes also enter the ponds. From this period onwards, until dewatering takes place, tidal water is let into the ponds at spring tides. But no special effort is made to capture the fry at this time as the water that flows in through the main sluice gates, contains the fry of various fishes. Fry of *Mugil tade* and *M. corsula* have been noticed only during the rainy season, while small fry of the cock-up (*Lates calcarifer*) (1" to 2" long) have been found only in July-August.

After the comparatively intensive stocking of ponds from February to April, no attention is paid by the fishermen to improving the growth of the fish crop, apart from letting in water into the ponds, attending to the occasional repairs of the embankments, etc., and keeping watch over the stock. The fishes feed on the autochthonous food material of the ponds as well as those brought in by the tidal water. During the dry months, when the water level falls, several twigs are stuck into the bottom of the canals, to prevent easy fishing by poachers (Plate XVIII, Fig. 3). From about May-June the ponds are fished on a small scale mainly to meet the fishermen's needs. Whenever tidal water is taken in, some fish, prawns, and crabs are caught in the *atols*. 'Tengra' (*Mystus gulio*) are caught by the fishermen by a very ingenious method. These fish also, like the mullets, have a tendency to swim against currents. But they are generally unable to negotiate streams with a strong current. So, on the side of the main sluice gate and the canal leading from it, they dig a shallow canal. The mouth of this shallow channel is guarded by a low fence of bamboo grating and some distance away from it is another similar fencing with a gap in the middle. Tide water from the main feeder channel leading from the river is allowed to flow into the pond through this channel. The fish ascend the channel and gather below the bamboo fencing. At the turn of the tide or when a sufficient number of fish has gathered in the channel it is closed at the mouth either by means of shutters or by putting an earthen bund. The gap in the lower bamboo fencing is also closed. After the water in the channel drains off, the fish that have been trapped in the channel are removed by hand. Cast nets are operated (Plate XVIII, Fig. 6) for the capture of all fishes from the ponds during all seasons.

Large-scale fishing operations are carried out between September and November. As no tidal water is required in the ponds during this period as much water as possible in them is let out. The fishes move into the canals and deeper areas of the ponds where these are fished by means of drag nets (Plate XVIII, Fig. 5), generally during the evening or at night so that the catches could be sold early in the morning. The catches are sometimes kept in live wells (Plate XIX, Fig. 2) or live cages known as *Hapar* (Plate XIX, Fig. 1).

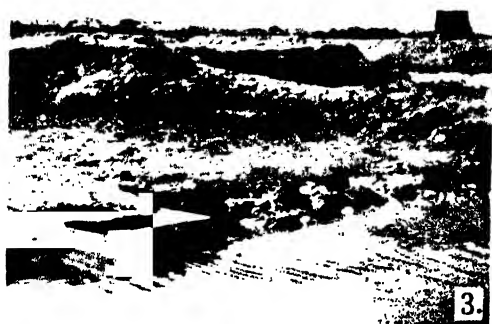
Special deep Crab cages known as *khonga* (Plate XIX, Fig. 3) are also used for keeping fish alive in water but more commonly for emptying the catches from the *atols*. From the *khonga*, the catches are transferred to *hapars*. In the morning the catches are brought in baskets to the Ghutiari Sharif Railway Station, a mile and a half away from the *bheri* (Plate XIX, Fig. 4), and sold wholesale to fish merchants on the station platform, who in turn take them to Calcutta by the first morning train at 4-30 a.m. reaching Calcutta at about 6 a.m.



1.



2.



3.



4.

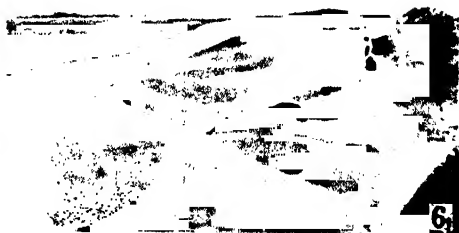
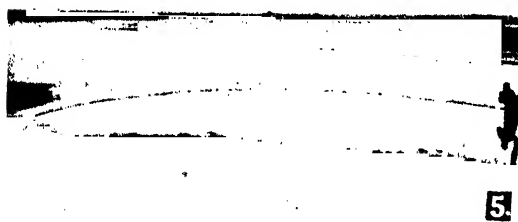


5.



6.

FIG. 1. A general view of a portion of the *bheri*.
 .. 2. The feeder canal through which tide water flows into the ponds.
 .. 3. The sluice box through which water is let in.
 .. 4. A sluice gate for controlling water supply.
 .. 5. Bamboo gratings arranged in the form of a 'W' in front of the sluice gate.
 .. 6. An 'Atol' fixed in the gap between two bamboo gratings, erected in the form of a V.



- FIG. 1. An emergency gap in the embankment showing the device for preventing the escape of fish.
- .. 2. A subsidiary pond for keeping immature fishes.
- .. 3. Twigs stuck into the bottom in a canal in the *bheri*, during summer, to prevent poaching.
- .. 4. A dried up portion of the pond bed.
- .. 5. Fishing in the *bheri* with a drag net.
- .. 6. Cast net fishing in the *bheri*.

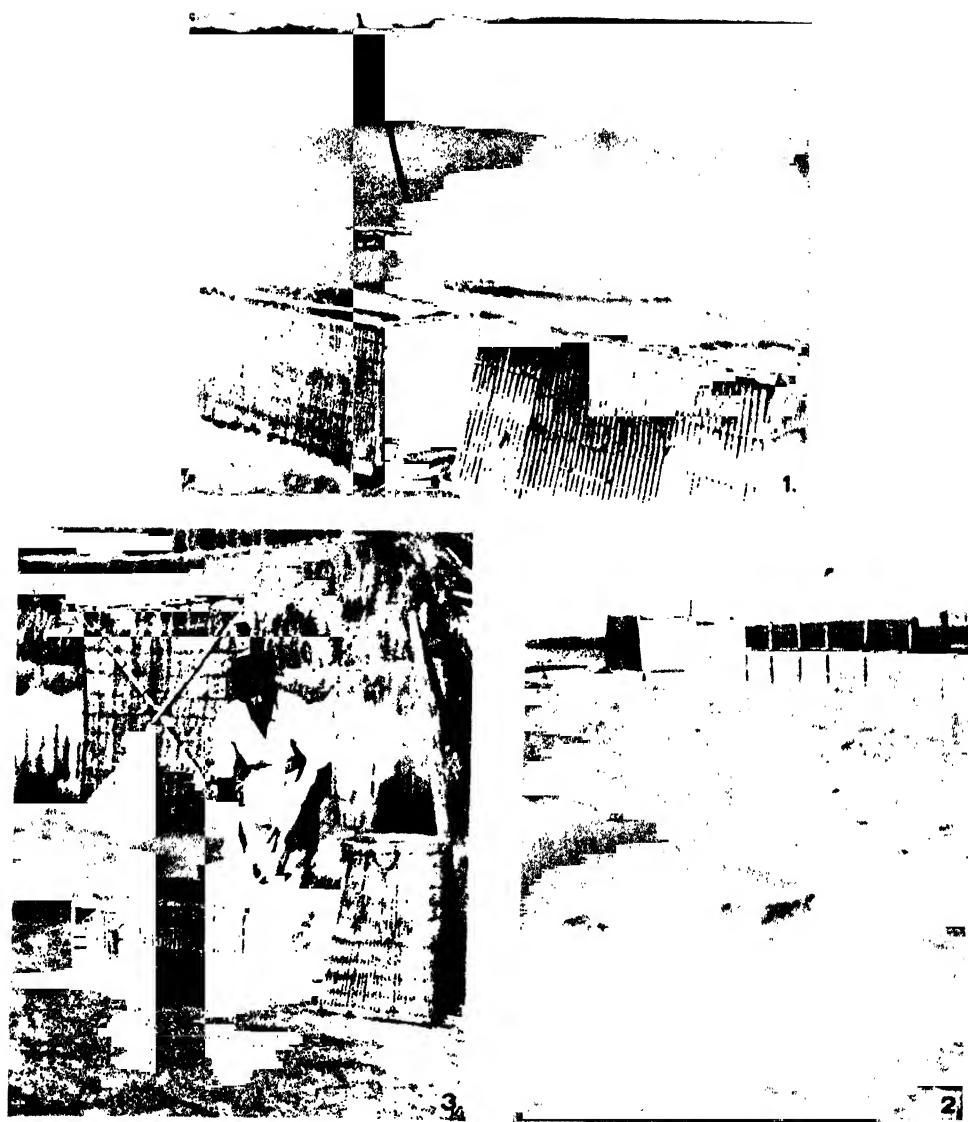


FIG. 1. Live cages known as *Hapar*, used for keeping catches alive till marketed.
 .. 2. Live wells dug near the *bheri* for keeping fish alive till marketed.
 , 3. Crab cages known as *Khonga*.

During the usual annual intensive fishing, large numbers of immature fish are also caught and sold. Formerly, it was the general practice to stock them in the subsidiary ponds (Plate XVIII, Fig. 2), where they were allowed to grow till the main pond was again filled with water, and could gain access to the canal system and the pond proper, a practice which is now seldom followed. Another wholesome practice now obsolete, is the annual ploughing of the pond bottom after dewatering, the discontinuance of which is bound to have an adverse effect on the productivity of the *bheri*.

The ponds which were formerly operated by the owners, are now leased out for a period of one or two years on an annual rental of Rs.40 to Rs.50 per acre. As the period of lease is short the lessees are naturally interested in marketing all sizes of fish from the ponds that would fetch a price and not in increasing the productivity of ponds. Due to the complicated nature of the ownership and of the practice of leasing, it has been difficult to collect any reliable statistics of production. It is noteworthy that the canals and the deeper portions of the ponds, which occupy 30% to 40% of their area, are the most productive ones. The present output from such productive areas ranges between 100 and 150 lbs. of fish and prawns per acre. The average prevailing prices of fish in the local market at the time of the investigation were as follows:—

			Rs.	a.	p.	
Small mullets	1	0	0	per lb.
Large mullets, specially <i>Mugil tade</i>	1	8	0	„
Cock-up	1	8	0	„
Tengra (<i>Mystus gulio</i>)	0	12	0	„
Large prawns	1	4	0	„
Crabs	0	8	0	„
Small crabs	0	2	0	„
Miscellaneous fish and small prawns	0	8	0	„

ECOLOGICAL CLASSIFICATION OF THE FAUNA

Based on their ecological significance, the more important elements of the fauna of fish ponds have been classified as dominants, influents and sub-influents (Hiatt, 1944). Dominants are 'animals of outstanding abundance of conspicuous influence in the community', and influents are 'common animals which are usually effective in modifying the well-being or numbers of the dominant group or of other influents without changing the essential structure of the community, their rôles are generally shown in ponds as benefactors, competitors, or predators'. Those animals that 'affect the life of the community, but to a lesser extent than do the influents' are termed sub-influents. Following the classification adopted by Hiatt the faunal elements in the *bheri* have been classified as shown below. With the restricted facilities available to the author, it was not possible to try any of the quantitative methods which provide a more accurate classification. Hence the adoption of the standards employed by Hiatt (*op. cit.*). In addition to the species shown below some rare ones not taken into account in this classification are found, which do not affect the biotal conditions in the ponds in any noticeable manner.

DOMINANTS.

Mugil parsia
Mugil tade
Lates calcarifer
Penaeus semisulcatus

INFLUENTS.

Myxus gulio
Apocryptes lanceolatus
Periophthalmus schlosseri
Leander styliiferus
Metapenaeus monoceros
Scylla serrata

SUB-INFLUENTS.

Aplocheilichthys panchax
Oryzias melastigma
Eleutheronema tetradactylum
Scatophagus argus
Eleotris butis
Gobioplecterus chuno
Stigmatogobius sadanandio
Varuna litterata

DOMINANT ANIMALS

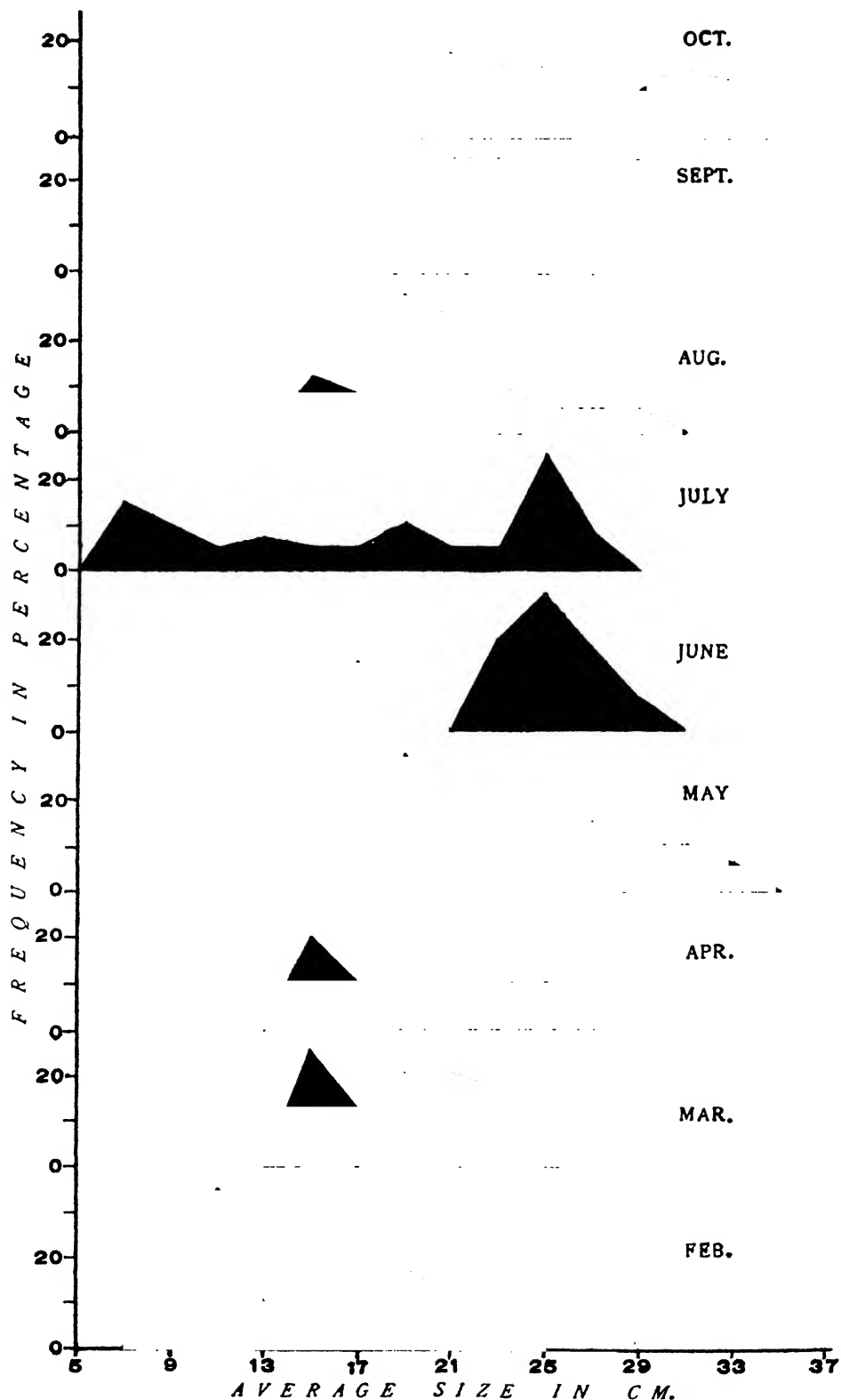
(1) *Mulletts*

Grey Mulletts.—The Grey Mulletts, *Mugil parsia* locally known as 'Parse' and *M. tade* known as 'Bhangon' together form the most dominant group in the ponds. As intensive stocking operations are conducted in late winter when the estuaries teem with their fry, the ponds have always a predominant population of *M. parsia*. From February to April, fry 1"-2" long are taken into the farm. By the end of the season, that is in about 8 months' time, they attain a size of 4" to 6" in the ponds. Though mature females in the fourth and fifth stages of maturity and ripe males with milt oozing out on the application of slight pressure have been seen in the catches, no evidence of their breeding in the ponds has so far been noticed.*

Young of *Mugil tade* $\frac{3}{4}$ " to $1\frac{1}{2}$ " in length enter the ponds along with the tide water during the rainy season and grow up to $1\frac{1}{2}$ "-2" when the ponds are ready for dewatering. A small percentage of them which survives the fishing activities thus obtains a further lease of life up to the end of the next season when they grow up to $9\frac{1}{2}$ " to 10" in length. A still smaller percentage surviving up to the end of the third season reaches a length of $13\frac{1}{2}$ " to $14\frac{1}{2}$ ". Text-fig. 3 represents the length frequency distribution of the samples obtained from the *bheri* in 1949, and shows that the large majority of the catches consists of O group and I group fishes (*vide* classification given by Pillay, 1954). The available data indicate that the rate of growth of the fish in the ponds is faster than in the natural habitats (Pillay, 1954), though not as fast as that observed in several freshwater fishes cultured in ponds.

Distinction is often made by the fishermen and the fish traders between river mullets, sea mullets and *bheri* mullets. The author (Pillay, 1954) has shown that there are no significant differences between the fish stocks of the estuaries in Port Canning and the sea coast at Junput. A statistical comparison of the morphometry of samples of *M. tade* from the farm and of samples from the sea was made. The values obtained for each of the indices employed for the comparison are given in Table IV. These values indicate statistically significant differences in the six characters examined. In a recent paper the author (Pillay, 1953) has shown that the alimentary canal of *bheri* mullets is significantly longer than that of the river

* A detailed study of the bionomics of this species has been made by Miss K. K. Sarojini, Asst. Research Officer, Central Inland Fisheries Research Station, Barrackpore.



TEXT-FIG. 3. The length frequencies of the samples of the Grey Mullet, *Mugil tade*, examined from the *bheri*.

TABLE IV.
The biometrical data for samples from Junput and from the bheri.

	N ₁	N ₂	Size range for sample 1 in cm.	Size range for sample 2 in cm.	σ_1	σ_2	SE ₁	SE ₂	SEd	t
TL/SL	..	200	1.1 - 1.3	1.17 - 1.31	0.173	0.0519	0.024	0.007	0.025	4.000
TL/L.D.C.P.	..	200	8.95-11.25	9.5 - 12.10	0.544	0.808	0.077	0.114	0.138	3.115
TL/D.E.	..	200	9.89-17.18	10.8 - 15.9	1.453	1.201	0.206	0.170	0.289	3.890
TL/HD	..	200	3.1 - 4.9	4.3 - 4.9	0.308	0.153	0.043	0.022	0.048	4.375
TL/A.L.	..	200	1.6 - 1.8	1.60 - 1.80	0.060	0.057	0.008	0.008	0.011	4.000
TL/D.A.F.B.	..	200	5.2 - 6.85	5.7 - 7.6	0.366	0.390	0.052	0.071	0.089	4.150

TL = Total length.
 SL = Standard length.
 L.D.C.P. = Least depth of caudal peduncle.
 D.E. = Depth through eye.
 HD = Head length.
 AL = Length of body from snout to beginning of anal fin.
 D.A.F.B. = Depth through anal fin base.

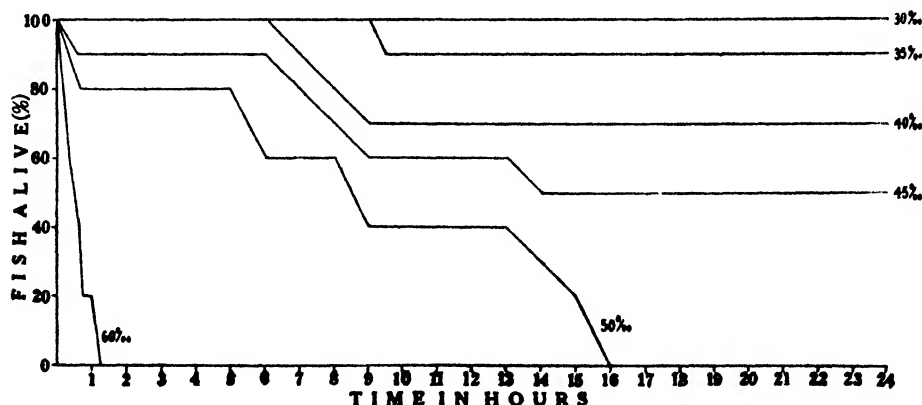
Number 1 denotes samples from the sea (Junput) and Number 2 denotes samples from the bheri.

and sea mullets. Sunier (1922) has described similar changes in the external morphology of the Milk fish (*Chanos chanos*) raised in Indonesian *Tambaks* (brackish water ponds). Despite such marked differences, the *bheri* stocks cannot justifiably be considered as belonging to a separate race, as they are raised from those occurring in the estuaries. The changes in the morphometry of the fish are therefore likely to have been brought about by a land-locked environment, as the ecological conditions in the *bheri* are in many ways different from those of the estuaries.

The extreme variations in the salinity of the *bheri* have already been referred to. The mullets belong to a strongly euryhaline group, capable of adapting themselves to lowered salinities as evidenced by the direct acclimatisation practices in some parts of Bengal (Pillay, 1949). But very little is known about their adaptability to the high range of salinities which may prevail in summer in shallow waters as happen in isolated pools of the *bheris*.^{*} To ascertain the lethal limits of higher salinities on *Mugil tade*, a series of experiments were conducted, in the field, with simple equipment consisting of large wide-mouthed jars of about 3½ litre capacity. In the absence of equipment such as used by Sunier (1922) in Indonesia, waters of different concentrations were obtained by dissolving the calculated quantities of unrefined solar salt in fresh pond water.

Fry $\frac{3}{4}$ "–1½" long were used in the experiment which was repeated thrice with a control in each case, to estimate the mortality due to rise in salinity. The results discussed below constitute the mean of the three separate observations.

Twenty fry $\frac{3}{4}$ " to 1½" long caught from the creeks were directly transferred to different jars containing water of salinity 30‰, 35‰, 40‰, 45‰, 50‰, 60‰, respectively. The survival data (Table V) under the different salinity levels are delineated in Text-fig. 4. Even though it was not possible to study the effect of different pH concentrations and also repeat the experiments with larger fish, the results obtained indicate that a salinity higher than 30–35‰ is not conducive to the well-being of mullets, at least of the young ones ($\frac{3}{4}$ "–1½" in length), in the ponds. This observation is of special importance to the *bheri* owners of the Calcutta Salt Lakes, as owing to the diminishing water supply from the Bidyadhari and evaporation and seepage in the ponds, the salinity of the water may increase considerably.



TEXT-FIG. 4. The survival of *Mugil tade* fry under different salinity levels.

^{*} Pillai in a recent paper (Pillai, V. K.—Some factors controlling algal production in Salt-water lagoons. Proc. 5th meeting, I.P.F.C./C. 54/Sym. 3) mentions about his observation that the blue-green alga *Phormidium tenue* can withstand salinities up to 100 parts per thousand. Such observations on Indian fishes do not appear to have been made.

(2) *Cock-up*

Lates calcarifer.—This fish, locally known as *Bhekkti*, is an important and highly-priced species. Very little precise information is available on its bionomics. Naidu (1942) observed *bhekkti* breeding in the Sunderbans in the winter season, where large numbers of young ones were seen in the pools and ditches on the sides of the estuaries in April. According to Yingthavorn (1951), the spawning season of the fish is in the rainy season (May-September) in Thailand waters. In the present observations also, fry of *Bhekkti* 1" to 2" long have been found to enter the ponds in the rainy months only. They attain a size of about 5" by October-November, when they are fished. Their average growth in the second year is up to 10" in length. Hora and Nair (1944) reported that in the *bheris* of the lower Sunderbans, the Cock-up was raised in separate canals, so that mullets and other important fishes may not be eaten up by this predaceous species. But in this *bheri* no such segregation is permitted. However there are no intensive stocking operations during the rainy season when their fry are found in considerable numbers, and so the population of *bhekkti* in the ponds is not as high as in the larger *bheris* of lower Sunderbans. The species is capable of acclimatisation to very low salinities and can be seen in adjacent freshwater areas into which they ascend from the river through the brackishwater canals. They have never been observed in the highly saline isolated pools during periods of drought.

(3) *Prawns*.

Penaeus semisulcatus is a dominant prawn of very great value in the markets, on the culture of which the fishermen bestow great attention. The *bagda chingri*, as it is locally called, does not breed in the confined waters of the *bheri*. The larvae and young are brought in with the tide during the winter months. They bury themselves in the muddy bottom of the ponds and grow very rapidly, feeding on the food resources of the iliotrophic layer. A length of 3"-5" is attained by the end of the season when most of them are caught and marketed.

SOURCES OF FOOD SUPPLIES

The main sources of food supplies for fish in the *bheri* are the tidal waters and the autochthonous biotal complex. As during the spring tides the river and the *bheri* are connected, the incoming tides bring with them considerable quantities of plankton and suspended detritus. Within a short time after the tidal water is taken in, the suspended matter settles down to the bottom of the *bheri*. This detritus is rich in decaying organic matter which is an efficient fertilizer. During the rainy season, the *bheri* receives some amount of rainwater that flows into it from the embankments. This water also contains some nutrient salts that are washed down from the soil. The scanty decaying macroflora on the embankments also contribute in a small way to the fertility of the ponds. The exposed areas of the *bheri*, as already mentioned, are generally overgrown with grass and *Suaeda maritima*. When inundated for a sufficiently long period with the tide water, these plants decay and add to the fertility of the ponds. Besides these chiefly external sources of fertility, there is the inherent richness of the soil, which mainly contributes to the growth of organisms which serve as food. The thick layers of benthic vegetation on the pond bottom play an important rôle in the sustenance of fish life. In shallow waters, however, the distinction between the benthic flora and the surface flora is not marked. The very considerable zooplankters in the *bheri* water do not, however, seem to be of any great importance as a source of food for the fish.

BIOTIC INTERACTION

(1) *Methods*

The biotic interaction in the *bheri* was studied by the examination of stomach contents of samples of ecologically important fauna, viz. fishes and crustaceans, collected at different times of the year. The main aim of this study was to obtain a general picture of the food habits and to understand the inter-relationship of the fauna with regard to their food and feeding habits. So the seasonal or other variations in the food elements were not examined in detail. The items of food of dominants, influents and sub-influents alone are presented here, although the gut contents of the rarer species which exercise no significant biotic interaction in the ponds were also studied. For the purpose of this study smaller fishes were fixed and preserved in 5% formaldehyde. The alimentary tracts of larger fish were removed by dissection and fixed and preserved in 5% formaldehyde. Generally, only the contents of the stomach were examined, but when the stomach was empty the foregut was also examined. The contents of the rectum were studied regularly to ascertain the presence of undigested food. The stomach contents were analysed volumetrically by the displacement method in the case of carnivorous species where they were easily separable and were found in measurable quantities. In other cases, the volumes were determined by eye estimation. The prevalence of each item was also estimated and expressed as a percentage of the total number of stomachs examined.

(2) *Food of Dominants*

MULLETS.—The author has in a recent paper (1953) described the food and feeding habits of *Mugil tade* in this *bheri*. It was found that it feeds mainly on algae and decayed organic matter in these surroundings. Diatoms and miscellaneous items such as copepods, cladocerans, polychaete remains and foraminiferan shells were also found to have been consumed in small quantities. The food of *M. parsia* in the *bheri* has been independently studied by Miss K. K. Sarojini of the Central Inland Fisheries Research Station. She has found (Private communication) that the food of this species is more or less similar to that of *M. tade*. Both the species feed on the benthic vegetation and organic deposits on the margins and bottom of the ponds.

COCK-UP (*Lates calcarifer*).—The Cock-up or the *bhekki* is a well known predaceous species. Day (1878) found that *Boleophthalmus koelreuteri* was the favourite food of this fish, while Wallinger (1907) observed the mullet and the goby (*Boleophthalmus boddarti*) to be its main food on the Konkan Coast. Mookerjee, Ganguly and Mazumdar (1946) have stated, however, that 60% of its food consists of crustacea and only about 22% of fish, the rest of the food consisting of algae (10%) and miscellaneous matter (Sponge spicules) (5%). Job and Chacko (1947), Devanesan and Chidambaram (1949) and Chacko (1949) have also stated that the main food of *bhekki* consists of fish and prawns. Chacko (1949a) found that the young stages were also piscivorous, consuming *Oryzias*, *Aplocheilus* and *Spratelloides* in large numbers. Hora (1947) did not consider its culture a paying proposition. Menon (1948) found that Teleosts formed the major portion (65.34%) of its food, the other items of food being Decapod crustacea, Anomura (23.71%), Brachyura (2.23%), and minor crustacea (2.95%).

During this investigation 75 specimens of *Bhekki* ranging from 3.0 cm. to 24.4 cm. collected from the *bheri* during different seasons of the year have been examined. Table V summarises the food items consumed by the fish.

TABLE V

Gut contents analysis of Lates calcarifer in the Bheri

Food items.	% composition by volume.	% of occurrence.
Fish (<i>Mugil parsia</i> , <i>Mugil tade</i> , <i>Mystus gulio</i> , <i>Pseudapocryptes</i>).	74.1	89.0
Crustacea (<i>Penaeus semisulcatus</i> , <i>Metapenaeus monoceros</i> , <i>Leander styliferus</i> , <i>Varuna litterata</i> , Crustacean appendages).	25.8	45.0
Plant matter (Dried grass).	0.1	2.5

The above table shows that the economic species of fish and prawns in the *bheri* form part of the regular dietary of *bhekti*.

PRAWN (*Penaeus semisulcatus*).—There appear to be no published records of the food of the common *Bagda chingri* of Bengal (*Penaeus semisulcatus*). Sadasivan (1950) has observed that the young of the allied species *Penaeus indicus* feed on 'fine particulate matter at the bottom, Harpacticid copepods, other small crustaceans and algal matter'. Table VI presents the summary of the gut contents analysis of 104 specimens, 8 cm.–18 cm. in length, examined during this study.

TABLE VI

Gut contents analysis of Penaeus semisulcatus

Food items.	% composition by volume.	% of occurrence.
Crustaceans (copepods)	49.1	88.2
Algal matter (Macro-vegetation and algae: <i>Chlorella</i> , <i>Microcoleus</i> , <i>Polysiphonia</i> , <i>Symploca</i> , <i>Cladophora</i>).	42.4	70.6
Insect larvae	4.4	5.9
Detritus	2.6	23.5
Fish remains (<i>Oryzias</i>)	1.3	23.5
Miscellaneous matter (Foraminiferan shells).	0.2	11.8

The above table indicates that crustaceans and algae are the two most important items of food of the species. A good quantity of benthic vegetation forms a regular item of food of the prawn. The adult prawns feed at the bottom of the ponds while the young ones often bury themselves in the mud at the pond bottom.

(3) Food of Influents

TENGRA (*Mystus gulio*)

Tengra has been considered as a larvivorous fish. Pearse (1932) found a snail in the stomach of one fish he examined. Chacko (1947) found diatoms,

copepods, prawns, small fish (*Barbus*, *Oryzias*) fish eggs, fish scales and sand in their guts. The gut contents of 44 specimens, 2" to 7.9" in length, are presented in Table VII.

TABLE VII
Gut contents of Mystus gulio

Food items.	% composition by volume.	% of occurrence.
Detritus	36.7	66.7
Copepods	17.5	50.0
Plant matter (Filamentous algae).	14.6	16.7
Decapod crustacea (Adults and larvae).	12.5	33.3
Prawns and their larvae	10.0	50.0
Fish (<i>Oryzias</i>)	8.7	16.7

The above results indicate that the fish is omnivorous, detritus being the major item of food. Mature specimens obtained in July-August had empty stomachs.

Goby (*Pseudapocryptes lanceolatus*)

Pearse (1932) observed filamentous algae, plant remains and mud to constitute the major part of its dietary. Hora (1936) found young ones up to the 20 mm. stage feeding mainly on planktonic copepods, and adults entirely on mud. Mookerjee, Ganguly and Mazumdar (1946) recorded algae as the major food (85%); and Protozoans (5%), insects (3%), and sand and mud (7%) as minor items. The summary of the gut contents analysis of 180 specimens of the fish ranging from 2.6" to 6.9" in length is presented in Table VIII.

TABLE VIII
The gut contents of Pseudapocryptes lanceolatus

Food items.	% composition by volume.	% of occurrence.
Algae and algal spores (<i>Cosmarium</i> , <i>Desmidium</i> , <i>Spirogyra</i> , <i>Microcoleus</i> , <i>Anabaena</i> , <i>Enteromorpha</i> , <i>Poly-siphonia</i> , <i>Oscillatoria</i> , <i>Chaetomorpha</i>).	78.1	100
Decayed organic matter	10.0	57.1
Diatoms (<i>Cyclotella</i> , <i>Gyrosigma</i> , <i>Navicula</i>)	7.6	71.4
Sand grains	4.3	57.1

It is seen that this fish is strongly herbivorous in habits and takes benthic vegetation as its main food.

WALKING GOBY (*Periophthalmus schlosseri*)

According to Hora (1936) this fish has a varied menu including almost everything found on the mud flats, and can jump up in the air to a height of few inches

to catch flying insects. The gut contents analysis of 80 specimens, 1.2" to 2.5" in length is given in Table IX.

TABLE IX
The gut contents of Periophthalmus schlosseri

Food items.	% composition by volume.	% of occurrence.
Detritus	67.3	100.0
Insects (water beetles) and young spiders ..	18.5	70.0
Microbenthic algae and diatoms ..	9.0	25.0
(<i>Microcoleus</i> , <i>Oscillatoria</i> , <i>Anabaena</i> , <i>Navicula</i>).		
Copepods	5.2	45.0

The table shows that this species of fish has a clear bias to detritus with insects and microbenthic vegetation playing a minor part in its dietary.

SHRIMP (*Leander styliferus*)

The author is not aware of any records of the food of this shrimp in Indian waters. Hiatt (1944) found *Leander debilis* and *Leander pacificus* in Hawaiian fish ponds feeding on microbenthos and detritus. The results of gut contents analysis of 300 specimens, 0.5"-1.75" long in this investigation are summarised in Table X.

TABLE X
Gut contents of Leander styliferus

Food items.	% composition by volume.	% of occurrence.
Detritus (with decayed and dried up plant matter and sand grains)	53.3	100.0
Filamentous algae (<i>Polysiphonia</i> , <i>Enteromorpha</i> , <i>Oscillatoria</i>).	43.3	90.0
Diatoms (<i>Coscinodiscus</i> , <i>Navicula</i> , <i>Gyrosigma</i>).	3.1	66.7
Miscellaneous matter (Crustacean append- ages, Polychaete remains)	0.3	5.0

This table shows that the food of *L. styliferus* is very much like that of its congeners in the Hawaiian fish ponds, consisting mainly of microbenthic vegetation and organic detritus found on the bottom of the ponds.

PRAWN (*Metapenaeus monoceros*)

The gut contents analysis of sixty-six specimens of *Metapenaeus monoceros* ranging from 2.3" to 4" in length is given below in Table XI.

TABLE XI

Gut contents of Metapenaeus monoceros

Food items.	% composition by volume.	% of occurrence.
Detritus (consisting of decayed plant matter, animal remains, sand grains, etc.).	79.1	100.0
Copepods and copepod appendages ..	18.6	63.6
Filamentous algae (<i>Oscillatoria</i> , <i>Polysiphonia</i> , <i>Cladophora</i>).	1.8	27.5
Diatoms (<i>Coscinodiscus</i> , <i>Navicula</i>).	0.5	2.5

The main food of this prawn in these ponds appears to be detritus. The copepods consumed may have been dead or live ones associated with the benthic vegetation.

CRAB (*Scylla serrata*)

Hiatt (1944) found this crab feeding on shrimps. The gut contents analysis of 88 crabs from the *bheri*, 0.8" to 4.5" across the carapace, is presented in Table XII.

TABLE XII

Gut contents of Scylla serrata

Food items.	% composition by volume.	% of occurrence.
Prawns and shrimps (<i>Leander styliiferus</i> , <i>Metapenaeus</i> spp.).	65.8	83.3
Fish (gobeids, mullet fry)	13.2	41.6
Detritus and sand	11.1	41.6
Algae and higher plant fragments (<i>Chaetomorpha</i> , <i>Microcoleus</i> , <i>Polysiphonia</i>)	8.5	41.6
Molluscan shells	1.4	8.3

The main food of the crab consists of prawns and shrimps. Hiatt (*op. cit.*) found no evidence of piscivorous habits in this species in Hawaiian ponds, but the present study indicates that small fishes also form a minor item of its diet.

(4) Food of Sub-influents

INDIAN KILLIFISH (*Aplocheilichthys panchax*)

The Indian Killifish (*Aplocheilichthys panchax*) has been considered a highly efficient larvivorous fish by numerous workers (for an account of previous work *see* Job, 1941). Hora (1938) observed this fish feeding normally on ants and other insects and on mosquito larvae only when introduced into special areas under favourable conditions. Job (*op. cit.*) corroborated this with his observations in natural environments where the percentage of mosquito larvae consumed by this fish was as low as 4%, the main items of food being ants, water beetles, lower crustaceans, young stages of crabs and shrimps. These organisms together with traces of

minute Gastropods, other molluscs and some miscellaneous animals made up 98½% of the total foods, the rest (1½%) being made up of diatoms, algal filaments, plant remains with sand and inorganic fragments. The gut contents analysis of 20 specimens of the fish from 1.3" to 2" in length from the *bheri* given in Table XIII shows that under the ecological conditions prevailing in these ponds, water beetles, insects and insect larvae constitute the main items of food. No mosquito larvae were identified from the guts.

TABLE XIII

Gut contents of Aplocheilus panchax

Food items.	% composition by volume.	% of occurrence.
Water beetles	65.0	75.0
Insects and insect larvae	27.5	50.0
Plant matter (Filamentous algae)	6.25	75.0
Daphnids	1.25	25.0

KILLIFISH (*Oryzias melastigma*)

Oryzias melastigma, like *Aplocheilus panchax*, is regarded as an efficient larvivore by several workers, though no detailed work appears to have been done on the food and feeding habits of this species. Guts of forty specimens 0.7" to 1.2" in length were examined and the analysis of the contents is shown in Table XIV.

TABLE XIV

Gut contents analysis of Oryzias melastigma

Food items.	% composition by volume.	% of occurrence.
Algae (Filamentous and unicellular)	87.1	100.0
Diatoms	8.8	53.8
Sand grains	4.1	46.1

It is noteworthy that no animal matter of any kind was found in the guts of the specimens which were collected mostly from small pools on the margins of ponds where benthic vegetation is obviously the main source of its nutriment.

INDIAN SALMON (*Eleutheronema tetradactylum*)

The Indian Salmon is a well known predaceous fish of the estuaries, feeding on prawns and crabs, small fishes, and bivalves (Gadsen, 1898; Job and Chacko, 1947; Chacko, 1949). Macdonald (1948) observed the young grey mullet to be a 'dainty morsel' of these fish. In twenty specimens ranging from 2.7" to 11.2" in length examined by the author prawns and shrimps were found to be the most dominant item of food. The percentage of fish in the gut contents is not high enough to class it as a major enemy of the dominants in the ponds though young mullets are also found in the guts occasionally. The majority of specimens had fed on shrimps (*Leander styliferus*) and Mysids. During the rainy season megalopa larvae of *Varuna litterata* have figured as an important item of food.

LEOPARD POMFRET (*Scatophagus argus*)

Day (1887) found this fish to be a foul feeder, while Mookerjee, Ganguly and Mazumdar (1946) found 72% of its gut contents composed of plant matter (unicellular, multi-cellular and higher plants), and the rest consisting of protozoa, worms, crustaceans, fish scales and sponge spicules. The same authors (1949) found the young stages feeding mainly on diatoms, and fry above 0.8" long, on animal food. The piscivorous tendency begins to manifest itself from the 1.4" stage, but the adults are omnivorous. Chacko (1949) reported algae (*Oedogonium*, *Cladophora*, *Spirogyra*, *Oscillatoria* and *Lyngbya*) as the main food of the species. Fourteen specimens of the fish 0.8" to 3.3" in length examined by the author had fed on filamentous algae (*Polysiphonia*, *Chaetomorpha* and *Enteromorpha*).

SLEEPER (*Eleotris butis*)

Hora (1936) found in its intestines fragments of shrimps, etc., and classed it as a voracious indiscriminate feeder. In the ten fish examined by the author, only *Leander styliferus* and mysids were found in the guts.

TRANSPARENT GOBY (*Gobiophterus chuno*)

The food habits of this species have been described in a separate paper (Pillay and Sarojini, 1950). The fish from the *bheri* seemed to live mainly on copepods, and occasionally on nauplius and zoea larvae.

GOBY (*Stigmatogobius sadanandio*)

Hora (1936) found remains of amphipods in the guts of this fish. Fifteen examples 1.2" to 1.7" in length, from the *bheri* had 67.5% of the gut-contents in the form of detritus, 22.5% of filamentous algae (*Polysiphonia*, *Chaetomorpha*) and 10% animal matter, mainly insect remains. The nature of the gut contents strongly suggests it to be an iliophage, feeding at the bottom of the ponds.

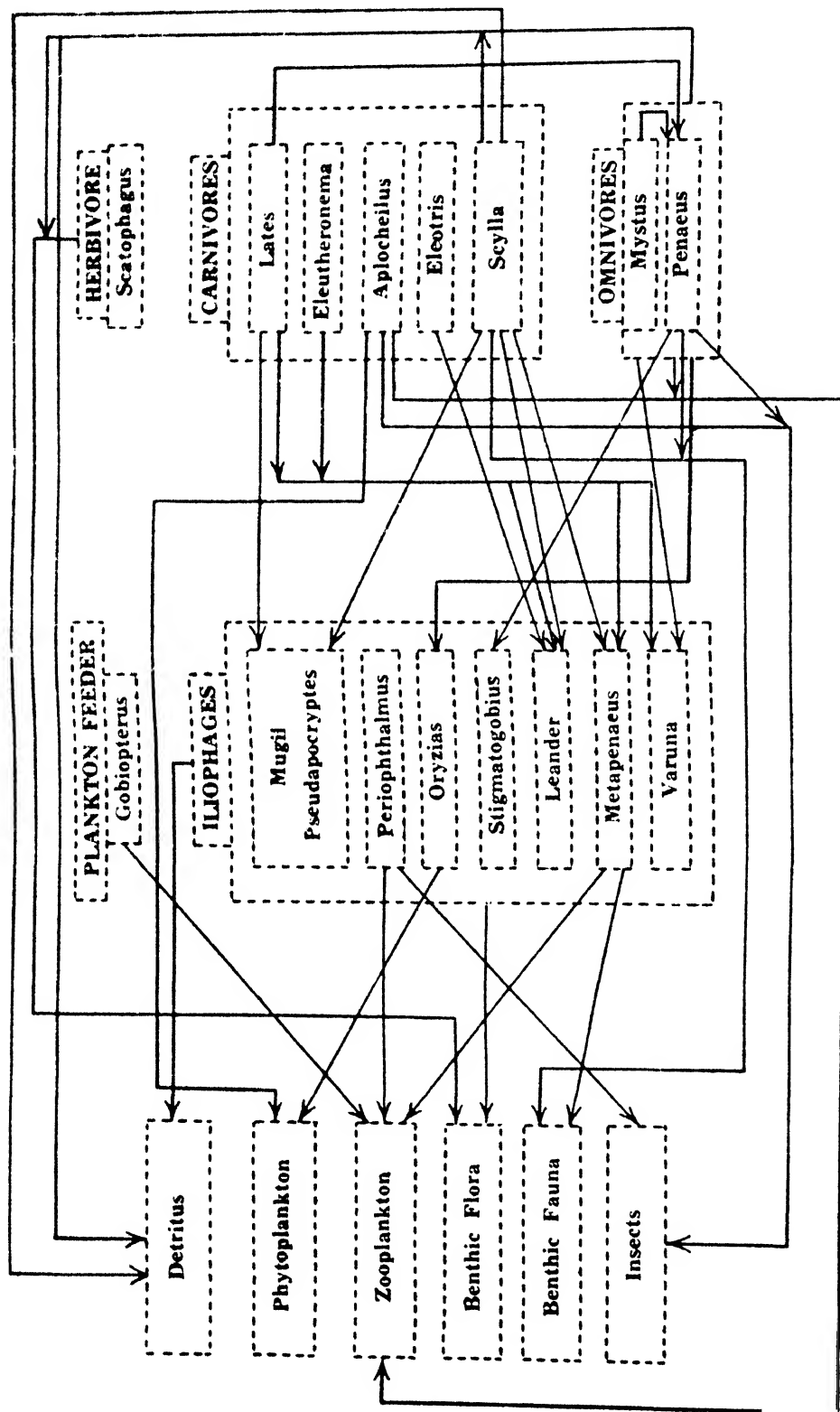
CRAB (*Varuna litterata*)

There does not appear to be any record of the food of this species in Indian waters. Twenty-one specimens of this crab, 0.9" to 1.2" across the carapace, had their guts almost full (92.3%) of benthic vegetation (*Polysiphonia*, *Enteromorpha* and *Cladophora*), diatoms (*Cyclotella*, *Surirella* and *Spirulina*). Detritus containing large quantities of decayed and decaying plant matter formed about 7.3% and miscellaneous matter constituted 0.2% of the gut contents. As *Megalopa* larvae of this crab feed on fish larvae, they might prove detrimental to the fish larvae entering the ponds.

(5) Inter-relations of the food of the fauna

The food relations of the ecologically important animals in the *bheri* are represented in Text-fig. 5. One outstanding feature of this relationship is the predominance of iliophagous animals. The benthic flora and detritus form major items of food of the mullets, prawns and shrimps. While the mullets (*Mugil parsia* and *M. tade*), the prawns (*Penaeus semisulcatus*), and the Crabs (*Scylla serrata*) are of economic importance, the gobies (*Apocryptes lanceolatus*, *Periophthalmus schlosseri*, *Stigmatogobius sadanandio*) and the Killifish (*Oryzias melastigma*), are not of any market value. They compete with the dominants in the ponds for food, and should therefore be eradicated as far as possible.

An examination of the tables of analysis of gut contents shows that the surface phyto- and zoo-plankton are not consumed in any appreciable quantities by the



TEXT-FIG. 5. Diagrammatic representation of the biotic interaction of the ecologically important fauna of the bheri. The arrows point from the animal to its main food items.

majority of the ecologically important fauna. Tengra (*Mystus gulio*), the Bagda chingri (*Penaeus semisulcatus*), the Killifish (*Aplocheilichthys panchax*), and the Transparent and Walking gobies do feed on them; but it is only the Bagda chingri that consumes any appreciable quantities of plankton.

The bhekti (*Lates calcarifer*), the Indian Salmon (*Eleutheronema tetradactylum*), the Sleeper (*Eleotris butis*) and the Crab (*Samudra kenkra*) (*Scylla serrata*) are the main carnivorous species in the ponds. Of these, the bhekti is definitely a major predator of the dominant animals. As the number of Indian salmon and the sleeper (*Eleotris butis*) in the ponds is not very high, the harm done by them is not very conspicuous. But the crab, *Scylla serrata*, is found in such large numbers that they take a heavy toll of prawns and shrimps, especially their young stages.

The picture of biotic interaction in the ponds indicates a high demand on the benthic vegetation and detritus and a negligible one on surface plankton.

DISCUSSION AND RECOMMENDATIONS

The present status of fish culture in the bheri is not very satisfactory owing to the conspicuous lack of concerted effort to improve production. As in many other bheris, the fishery consists more of capture operations than fish culture. Since such operations ultimately help in reclaiming these areas for paddy cultivation, many of the bheri owners attach only a secondary importance to this industry, resulting in this old and beneficial fish cultural practice being given up. Rao (1949) has referred to the great contribution that fish culture in brackishwaters, can make towards fish production in India. An all round intensification of culture operations is essential to increase the productivity of the embanked brackishwaters (bheris) in Bengal.

(1) *Water supply*.—An important reason for the deterioration of the bheri under observation, like many others in the area, is the unsatisfactory water supply, due to the greatly diminished tidal range in the river in recent years. Although the improvement of water supply by excavation of the river bed is the only obvious solution under the circumstances, it is generally held that the enormous quantities of silt carried down by the river will soon silt up the excavated river bed, reverting to the original conditions in a short period. It has, however, been found that at Taldi only about four miles down the river, a tidal range of 8 to 12 ft. now obtains, giving rise to bheris with a perennial water supply in that area. This tidal range is not appreciably different from that obtaining in the river Matlah at Port Canning.* As the distance from Taldi to Ghutiari Sharif is very short, it should not be difficult to improve the river conditions, here by the removal of the accumulated silt. Engineers consider this suggestion feasible, and it merits a trial as this will improve the condition of many other bheris in the locality.

In the pond system itself, the canals and the main feeder channel can be deepened by proper excavation, resulting in larger quantities of water flowing into the ponds.

The fishes, prawns and crabs in the ponds can withstand wide variations in salinity, and can therefore acclimatise themselves to life in freshwater. It would appear, therefore, that the place of tidal water can be taken by freshwater from the canals outside the bheri in which a more or less constant depth of water is maintained throughout the year, even after considerable quantities of freshwater have been drained off during the rainy season. These canals can also be employed for the storage of freshwater, thus converting a portion of the bheri into a reservoir for the purpose. The possibility of pumping in river water or providing tube-wells worked with the cheap aid of windmills to feed the ponds; is also worth investigation.

* Information obtained from Mr. A. N. Banerjee, Outfall Engineer, Calcutta.

(2) *Selective stocking*.—One of the main reasons for low production in the ponds is inadequate stocking. As stated above (page 408) intensive stocking is done during the winter season when the fry of only a few important fishes are available, and the supply of tidal water for stocking purposes has diminished as a result of the silting up of the river. As fry of mullets and young prawns are available in thousands in the shallow pools and swampy areas near the river and the *bheri*, they can be collected with nets made of mosquito-netting during the monsoon season when the fry of *Mugil tade* are also available. A circular type of dip net such as is used by the fishermen for crab fishing (Hora, 1935) in this area and for mullet fry on the Contai coast (Pillay, 1949) can be employed with the aid of a string attached to the circular frame to facilitate dragging in pools. The fry can be transported in earthen handies in the manner adopted by the fishermen of the Contai Coast. The adoption of the stocking method suggested above will not only allow selectivity of fry but also prevent the entry of a large number of undesirable species. A sufficient number of fry of *M. tade* can also be stocked in the ponds.

(3) *Predator control*.—The dominant and palatable *Bhekṭi*, is a voracious feeder and a confirmed enemy of the economically important fishes including mullets, and the methods of its culture deserve therefore special consideration. Hiatt (*op. cit.*) has expressed the opinion that the rearing of carnivores for market purposes takes the income of the operators into the realm of diminishing returns. According to MacGinitie (1935) the plant weight at the beginning of the food chain is greater than any weight following, due to the dissipation of weight along the food chain. It has been considered (*vide* Pearse, 1939) that bottom feeding fish consume a total of about ten times their own weight each year. He estimated that 10,000 pounds of algae make 1,000 pounds of tiny crustaceans, which make 100 pounds of small fish, and in turn 100 pounds of small fish make 10 pounds of large fish or one pound of man. As in the Hawaiian fish ponds these proportions are very much altered in this brackishwater *bheri* also, since the small and large fish consume algae and detritus directly. The weight ratios estimated by Hiatt (*op. cit.*) viz., 10,000 lbs. of algae and detritus for 1,000 lbs. of herbivorous fish, 1,000 lbs. of herbivorous fish for about 100 pounds of carnivorous fish, might be more indicative of the conversion processes in this *bheri*. About 100 lbs. of small carnivorous fishes may be necessary to make up 10 lbs. of large carnivorous fish. These facts are certainly suggestive of the uneconomic nature of the culture of predaceous fish. However, the fishing industry like any other industry, has to run on the principles of demand and supply. As the Cock-up is a well-relished fish and commands a good market, it would not be advisable to stop their culture. It may be economical, however, to culture them in separate ponds and thus prevent the destruction of the other economic varieties of fish and prawns. The gobies form an uneconomic group of predominant fauna in the ponds. But in the ponds the Cock-ups do not seem to feed on them in large numbers, probably because they are too agile and capable of taking shelter on the exposed mud flats. However, if the fish culturists can capture these numerous small gobies and artificially feed the Cock-up with their flesh, it may serve to fatten them and accelerate their rate of growth. *Eleutheronema tetradactylum* is not a predominant species in the ponds and if selective stocking is resorted to, it should not be difficult to control their population. The crab, *Scylla serrata*, is harmful in more than one way. It is predatory as stated above (page 419) and is responsible, along with *Varuna litterata*, for burrowing and thus weakening the embankments. However, its main food consists of the shrimp (*Leander styliferus*) which is only of secondary importance in the pond-economy. The only means of controlling it appears to be intensive fishing for adults and preventing the entry of young ones through sluice gates by means of suitable wire-net fencing. If selective stocking is adopted, the sluice gates can be covered with such protective devices to prevent the entry of undesirable species.

(4) *Production of food for fish.*—At present the fish culturists do not attempt the augmentation of food resources for the fish in the *bheri*, as is done in the culture of freshwater fishes in ponds. The author (Pillay, 1953) has referred to the best means of increasing fish food resources in the brackishwater farms in India through the culture of algae as practised in Indonesian and Philippine waters, where periodic draining and fertilization contribute to rich growths of algae in ponds. In East Java, ponds are drained as many as four times a year, and sometimes every few days to stimulate growth of Myxophyceae in them (Schuster, 1951). The same phenomenon may be observed in the *bheri*, if it is drained and exposed to the sun for a couple of days. The high organic contents of the soil in these ponds allow of such drainings without much detriment to the basic fertility of the soil, but as pointed out already, the lack of an adequate water supply makes this method impracticable. This circumstance makes it essential that all available water should be conserved for the proper operation of the ponds. So, the most practicable means of increasing the growth of myxophyceae in these ponds seems to be the application of manures to the soil and not to the water which will help to grow only phytoplankton. Schuster (1951) has recommended for Java the use of green manure, about 1,500 lbs. of grass or mangrove leaves per acre, to produce good results. In view of the fact that the fishery owner usually cultivates paddy also in the nearby fields, he may be in a position to use sufficient quantities of green manure to fertilize the ponds, if not superior types of organic manure, as there are considerable swamps overgrown with grass and other vegetation near the *bheri*. These could be collected and deposited in the ponds in suitable localities to decay slowly and supply the necessary nutrient material for the growth of algae.

The provision of 'collectors' for the attachment of algal spores was also suggested by the author in a recent paper (Pillay, 1953). As these will help the young fry only, and not fish larger than about 2" in length, it will not be economical to adopt this suggestion, unless separate nursery ponds are maintained for the purpose.

(5) *Extension of rearing period.*—As stated above (p. 408) the majority of the dominant fishes are caught at the end of about three to nine months. The former practice of transferring these immature fish into the subsidiary ponds at the time of draining and final cropping should be revived so that a better yield could be obtained. At the end of the second year they would have attained a marketable size fetching a better price. As *Mugil tade* and *Lates calcarifer* rapidly increase in weight after the first one or two years of their life, they should be reared for periods longer than two years.

(6) *Development of subsidiary industries.*—*Suaeda maritima*, the characteristic vegetation of the embankments of the *bheri*, is often collected by people for consumption as a vegetable. The fishermen do not evince any interest in the cultivation, utilization and sale of this plant from which they could derive a good subsidiary income. The embankments of the *bheri* are devoid of any large shrubs or trees. Under similar conditions Schuster (1951) has recommended the planting of Tamarind trees (*Tamarindus indicus* L.) on the embankments of *tambaks* in Indonesia. Besides providing good shade, the tamarind fruits command a good market. A full grown tamarind tree produces above 50 lbs. of fruit annually if planted at distances of about 50 ft.

The coconut palm has very strong halophytic tendencies (Ferguson, 1937) and can thrive well on brackish soils. The soil of the embankments of the *bheri*, which is also rich in humus, may prove quite suitable for the cultivation of coconuts.

SUMMARY

A detailed description of the topography of a brackishwater *bheri* at Ghutiar sharif is presented. The salinity of the water was found to fluctuate considerably during different

seasons. The depth of water in the ponds varied with the seasons and the spring and neap tides. The main features of the flora are the scarcity of macrovegetation and the richness of microbenthic growths of algae. Copepods occur in large numbers in the surface plankton. Prawns, shrimps and fishes form the main macrofauna of the ponds. The young of these are allowed into the ponds for purposes of culture. A classified list of the fishes occurring in the ponds is given.

The fish culture practices are described. Young fish and prawns are admitted into the ponds at spring tides, mainly from January-April. A sufficient level of water is maintained in the ponds by letting in water through sluice gates during spring tides. By about October-November, the ponds are dewatered and the fishes and prawns are removed for sale. Mulletts, Prawns and Cock-up are the dominant animals cultured. The catfish (*Myxus gulosus*) and the shrimp (*Leander styliferus*) also grow in the ponds in large numbers. The estimated production from the ponds is about 100-150 lbs. per acre of inundated area per year.

The ecologically important fauna of the ponds is divisible into three categories, viz., dominants, influents and sub-influents. Their food relations were studied by the examination of the gut contents of specimens caught from the ponds. A predominance of Iliophages has been observed. It was found that the surface plankton is consumed only by very few animals. The Cock-up and the Crab (*Scylla serrata*) are the main predatory species.

Possible means of increasing production from the *bheri* are considered. An intensification of operations is essential for better yields. The water supply has to be improved either by facilitating tidal flow or supply of fresh water at suitable periods.

Selective stocking will enable a better control of the pond fauna. The main predator, the Cock up, can be cultured in isolated canals or ponds, so that it will not feed on the economically important fishes and prawns.

Regular draining of ponds for increasing algal growths as in Java and the Philippines may not be possible in this *bheri* due to the restricted water supply. However, the production of algae can be increased by the application of suitable organic manures on the pond bottom.

An extension of the rearing period of the fishes like *Mugil tade* and *Lates calcarifer* to two or three years will be desirable from the point of view of economics.

The planting of coconut palms and tamarind trees on the embankments may, besides providing good shade in this open area, help in enhancing the income of the fish culturists.

ACKNOWLEDGEMENTS

In this work the author had to call upon the help of many specialists. The Chemist of the Central Inland Fisheries Research Station, Barrackpore, helped in the chemical analysis of water samples, the Petrologist of the Geological Survey of India and the Chemist of the Hilsa Fish Enquiry, Indian Council of Medical Research, helped in analysing the soil samples and the Carcinologist, Zoological Survey of India, in the identification of prawns, shrimps and crabs. Mr. A. N. Banerjee, the Outfall Engineer gladly gave useful information regarding the hydraulics of the River Bidyadhari and the authorities of the Meteorological Office at Alipore made available some meteorological data. Mr. Mohamed Hanif provided facilities for observations on the *bheri*. Grateful thanks are due to them all for their kind co-operation. I am indebted to Dr. S. L. Hora, for his guidance, to Dr. H. S. Rao and Mr. W. H. Schuster for going through the manuscript, and to the National Institute of Sciences of India for the award of a Research Fellowship to conduct this work.

REFERENCES

- Banerjee, A. N. (1931). *History and hydraulics of the river system near Calcutta*, Calcutta.
 Biswas, K. P. (1927). Flora of the Salt-lakes. *J. Dep. Sci. Cal. Univ.*, 8, 1-48.
 Chacko, P. I. (1947). Extraction of visceral oil from inland water fishes in the Collair Lake area, Madras. *Curr. Sci.*, 16, 288-289.
 — (1949). Food and feeding habits of fishes of the Gulf of Mannar. *Proc. Indian Acad. Sci.*, 29, 83-97.
 — (1949a). Nutrition of the young stages of estuarine fishes of Madras. *Sci. and Cult.*, 15, 32-33.
 Chatterjee, G. C. (1933). Relation of fisheries to the malaria problem of Bengal. *Sonar Bangla*, 9.
 Day, F. (1878). *Fishes of India*, London.
 — (1889). *Fauna of British India—Fishes*, 2 Vols., London.
 Devanean, D. W., and Chidambaram, K. (1949). *The common food-fishes of the Madras Presidency*. Dept. of Industries and Commerce, Madras.

- Ferguson, J. (1907). *Coconut Planter's manual or all about the 'Coconut palm'*. (4th Edition). Colombo and London.
- Gadsen, F. O. (1898). Fishing in Indian Waters. The Bahmin. *J. Bombay Nat. Hist. Soc.*, **12**, 194-201.
- Gupta, K. G. (1908). *Results of enquiry into fisheries of Bengal and into fishery matters in Europe and America*, Calcutta.
- Horre, A. W. and Mendoza, J. (1929). Bangos culture in the Philippine Islands. *Philipp. J. Sci.*, **38**, 451-509.
- Hiatt, R. W. (1944). Food chains and food cycle in Hawaiian fish ponds II. Biotic interaction. *Trans. Amer. Fish. Soc.*, **74**, 262-280.
- Hora, S. L. (1935). Crab-fishing at Uttarbhag, Lower Bengal. *Curr. Sci.*, **3**, 543-546.
- (1936). Ecology and bionomics of the gobioid fishes of the Gangetic Delta. *Compt. Rend. Congr. Int. Zool.*, **12**(5), 841-863.
- (1938). Larvicidal Fish. *Bayer Records*, May-June, 1938.
- (1947). Food and game fishes of Bengal. *Introducing India* (Part I) (Royal Asiatic Society of Bengal, Calcutta).
- Hora, S. L., and Nair, K. K. (1944). Suggestions for the development of saltwater bheris or bhasabadha fisheries in Sunderbans. *Fish. Dev. Pamphlet*, Govt. of Bengal, Calcutta 1.
- Job, T. J. (1941). Efficiency of the Killifish, *Aplocheilichthys panchax* (Ham.) in the control of mosquitoes. *Proc. Nat. Inst. Sci.*, **8**, 317-350.
- Job, T. J., and Chacko, P. I. (1947). Rearing of saltwater fish in freshwaters of Madras. *Ind. Ecol.*, **2**, 1-9.
- Macdonald, St. J. (1948). *Circumventing the mahseer and other sporting fish in India and Burma*, Bombay.
- MacGinitie, G. E. (1935). Ecological aspects of a California marine estuary. *Amer. Midl. Nat.*, **16**, 629-765.
- Menon, P. M. G. (1948). On the food of the 'Bekti' *Lates calcarifer* (Bloch) in the cold season. *Curr. Sci.*, **17**, 156-157.
- Mookerjee, H. K., Ganguly, D. N., and Mazumdar, T. C. (1946). On the food of the estuarine fish of Bengal. *Sci. and Cult.*, **11**, 564-565.
- (1949). On the food and feeding habits of the Leopard Pomphret, *Scatophagus argus* (Pallas) and the possibility of its culture, near estuaries of Bengal. *Sci. and Cult.*, **15**, 76-77.
- Naidu, M. R. (1942). *Report on a survey of the Fisheries of Bengal*, Calcutta. (Revised Edition.)
- O'Malley, L. S. S. (1914). *Bengal District Gazetteer—24 Parganas*, Calcutta.
- Pearse, A. S. (1932). Observations on the ecology of certain fishes and crustaceans along the bank of the Matlah River at Port Canning. *Rec. Indian Mus.*, **34**, 289-298.
- (1939). *Animal Ecology*, New York.
- Pillay, T. V. R. (1949). On the culture of grey mullets in association with commercial carps in freshwater tanks of Bengal. *J. Bombay Nat. Hist. Soc.*, **48**, 601-603.
- (1953). Studies on the food, feeding habits and alimentary tract of the grey mullet, *Mugil tade* Forsk. *Proc. Nat. Inst. Sci. India*, **19**, 777-828.
- (1954). The Biology of the grey mullet, *Mugil tade* Forsk. with observations on its fishery in Bengal. *Proc. Nat. Inst. Sci. India*, **20**, 187-217.
- Pillay, T. V. R., and Sarojini, K. K. (1950). On the larval development of the Indian Transparent Goby, *Gobiopsis chuno* (Hamilton) with observations on its bionomics. *Proc. Nat. Inst. Sci. India*, **16**, 181-187.
- Rao, H. S. (1949). Research in fishery conservation (Techniques used in studying fisheries; and the integration of hydrological, biological and other studies in a well-rounded marine fisheries research programme in India). *U.N. Scientific Conference on the Conservation and Utilization of Resources*, Vol. III. (Wild life and fish resources), Lake Success.
- Sadasivan, S. (1951). Preliminary observations on the rate of growth of the common marine prawn of the Madras Coast, *Penaeus indicus* Milne Edwards. *Proc. 39th Indian Sci. Congr.*, Pt. III (Abstracts), 318-319.
- Schuster, W. H. (1951). *Fish Culture in Saltwater ponds in Java* (Mimeograph edition) Indo-Pacific Fisheries Council, Bangkok.
- Sewell, R. B. (1934). A study of the fauna of the salt lakes, Calcutta. *Rec. Indian Mus.*, **36**, 45-121.
- Sunier, A. L. J. (1922). Contribution to the knowledge of the natural history of the marine fish ponds of Batavia. *Treubia*, **2**, 156-400.
- Wallinger, W. A. (1907). Estuary fishing, some remarks on its decadence, as an industry in the Konkan, Western India. *J. Bombay Nat. Hist. Soc.*, **17**, 620-634.
- Yingthavern, P. (1951). Notes on Pla-Kapong (*Lates calcarifer* Bloch) culturing in Thailand. *Proc. Indo-Pac. Fish. Coun.*, 3rd Meeting, IPFC/C51/Tech-20 (Mimeo).

STUDIES ON CYTOCHEMISTRY OF HORMONE ACTION

PART XV. THE EFFECT OF ADRENOCORTICOTROPHIC HORMONE (ACTH) ON ALKALINE PHOSPHATASE ACTIVITY IN THE PARS INTERMEDIA OF THE CAT'S HYPOPHYSIS

by J. N. KARKUN and AMIYA B. KAR, *Central Drug Research Institute, Lucknow*

(Communicated by B. Mukerji, F.N.I.)

(Received February 24; read May 7, 1954)

INTRODUCTION

Karkun *et al.* (1954) reported a marked hypertrophy of the basophile cells of the pars intermedia of cats treated with ACTH. They also observed cytological changes in these elements which clearly resembled the hyaline changes of Crooke (1935). On the basis of these findings they suggested that the basophiles were probably stimulated by ACTH to secrete excess amounts of melanophore hormone. The data presented hereunder subscribe additional evidence in support of this concept.

The presence of alkaline phosphatase has been demonstrated in the pars distalis of the guinea-pig (Abolins, 1948) and the cat (Romieu *et al.*, 1951). But no attention appears to have been paid to the localization of the enzyme in the pars intermedia. We, therefore, take this opportunity of reporting the distribution of alkaline phosphatase in the pars intermedia of the cat's hypophysis.

EXPERIMENTAL PROCEDURE

Eight female kittens, weighing 896 ± 8.5 gms., were used in this study of which 4 were injected with ACTH ('Corticotrophin', Wilson Lab., Chicago, U.S.A.) at the rate of 2 mg. (in 0.5 c.c. of sterile distilled water) twice daily. The injections were given at intervals of 12 hours. This dosage was continued for 5 days and from the 6th day it was increased to 3 injections of 2 mg. daily spaced at intervals of 8 hours. This rate was maintained for 7 days after which the animals were sacrificed. In all, the period of treatment lasted 12 days during which a total of 62 mg. of the hormone was administered to each of the experimental animals. The control animals were injected with 0.5 c.c. of sterile distilled water in a similar manner.

Autopsy followed 24 hours after the final injections. The pituitaries were carefully dissected out and fixed immediately in chilled 80 per cent ethyl alcohol. The serial paraffin sections of the gland were processed according to the technique of Gomori (1941) for the demonstration of alkaline phosphatase. The sites of phosphatase activity in the tissue sections were marked by the deposition of cobalt sulphide in the fine black granules. In order to allow critical observation of these granular deposits no counterstain was used. The sections were dehydrated and mounted in the usual manner.

RESULTS

Controls: The cellular architecture of the pars intermedia of this species has already been described in detail (Karkun *et al.*, 1954). In brief, the basophile cells constitute 95 per cent, chromophobes only 0.5 per cent and the macrophages 4.5 per cent of the total cellular elements of this pituitary component.



The nucleus of the basophile cells shows positive reactions for the enzyme but the cytoplasm stains rather faintly (Fig. 1). A similar pattern is noticeable in the chromophobes but the macrophages exhibit an intense phosphatase activity both in the nucleus as well as in the cytoplasm. The endothelium of the vascular sinusoids also react in a strong positive manner (Table I).

TABLE I.

The distribution of alkaline phosphatase in the pars intermedia of normal and ACTH treated cats.

			Normal	ACTH treated
Basophiles—				
Nucleus	+	++
Cytoplasm	+(F)	++
Chromophobes—				
Nucleus	+	++
Cytoplasm	+(F)	+(F)
Macrophages—				
Nucleus	++	++
Cytoplasm	++	++
Vascular sinusoids—				
Endothelium	++	++

Evaluation:—

+ = Positive reaction.
 +(F) = Positive reaction but faint.
 ++ = Strong positive reaction.

ACTH treated: ACTH treatment evokes considerable hypertrophy of the basophile cells. Their cytoplasmic granules become much coarser and aggregate in a peri-nuclear manner leaving the rest of the cytoplasm as a dense hyaline matter (Karkun *et al.*, 1954). The nucleus of these cells stains more intensely for the enzyme than in the controls. The basophilic granules of the cytoplasm also react in a strong positive manner (Fig. 2). It may be recalled that in the control animals only negligible amounts of phosphatase are visible in the cytoplasm of these cells. The macrophages and the chromophobes do not show any change in size or morphology after ACTH treatment. However, their nuclei stain slightly deeper than in the controls. The endothelium of the vascular sinusoids continues to give a strong positive reaction for the enzyme (Table I).

DISCUSSION

The interesting fact which emerges from the present study is the pronounced increase in alkaline phosphatase activity in the cytoplasm of the basophile cells after ACTH treatment. In contrast to this, the cytoplasmic phosphatase of other cellular elements does not show any response to the hormone though a slight increase in enzyme activity is noticeable in the nuclei of all the cell types. Now, according to recent views protein synthesis proceeds at par with the activity of the phosphatases (Roche, 1950). In view of these, it may be reasonable to assume that the enhanced phosphatase activity in the basophile cells signifies an increased formation of some

protein material, probably melanophore hormone. Interestingly, pars intermedia is regarded as the only source of this hormone in the species under study (Turner, 1948) and the basophiles are the cellular elements concerned with its elaboration (Karkun *et al.*, 1954).

SUMMARY

Intramuscular injections of ACTH into kittens cause a pronounced increase in alkaline phosphatase activity in the cytoplasm and the nucleus of the basophile cells of the pars intermedia. In contrast to this, the chromophobes and the macrophages show only a slight augmentation of enzyme activity only in the nucleus after the hormone treatment. The increase in phosphatase activity in the basophile cells, however, is extremely significant and probably signifies an enhanced synthesis of melanophore hormone.

ACKNOWLEDGEMENTS

The authors wish to express their indebtedness to Dr. B. Mukerji for the keen interest he has taken in this study. Thanks are due to Sri S. Banerjee for the photomicrographs which illustrate this paper.

REFERENCES

- Abölin, L. (1948). Alkaline phosphatase in various cell types of anterior pituitary of guinea-pig. *Nature*, **161**, 556-557.
- Crooke, A. C. (1937). A change in the basophil cells of the pituitary gland common to conditions which exhibit the syndrome attributed to basophil adenoma. *J. Path. and Bact.*, **41**, 309-349.
- Gomori, G. (1941). The distribution of alkaline phosphatase in various cells and tissues. *J. Cell and Comp. Physiol.*, **17**, 71-83.
- Karkun, J. N., Kar, A. B. and Mukerji, B. (1954). Responses of the pars intermedia of the cat's hypophysis to adrenocorticotrophic hormone. *J. Endocrinol.*, **10**, 124-128.
- Roche, J. (1950). *The enzymes*. Academic Press, New York, 1(1).
- Romieu, M., Stahl, A. and Seite, R. (1951). Les phosphatases alcalines dans l'hypophyse du chat. *C. R. Soc. Biol.*, (Paris), **145**, 415-416.
- Turner, C. D. (1948). *General Endocrinology*. W. B. Saunders Co., London and Philadelphia.

EXPLANATION OF FIGURES, PLATE XX

(All figures are photomicrographs and are magnified $\times 350$)

- FIG. 1. Section through the hypophysis of a control cat showing the distribution of alkaline phosphatase in the pars intermedia. Only the basophile cells are shown in the field. *p.i.*, pars intermedia; *p.n.*, pars nervosa.
- FIG. 2. Section through the hypophysis of an ACTH treated cat. Note the Crooke's change in the basophile cells and the increase in phosphatase activity (indicated by arrow). Lettering as in Fig. 1.

Issued September 13, 1954.

POLLINATION MECHANISM IN *PASSIFLORA FOETIDA* LINN.

by M. V. S. RAJU, *Department of Botany, Central College, Bangalore*

(Communicated by P. Maheshwari, F.N.I.)

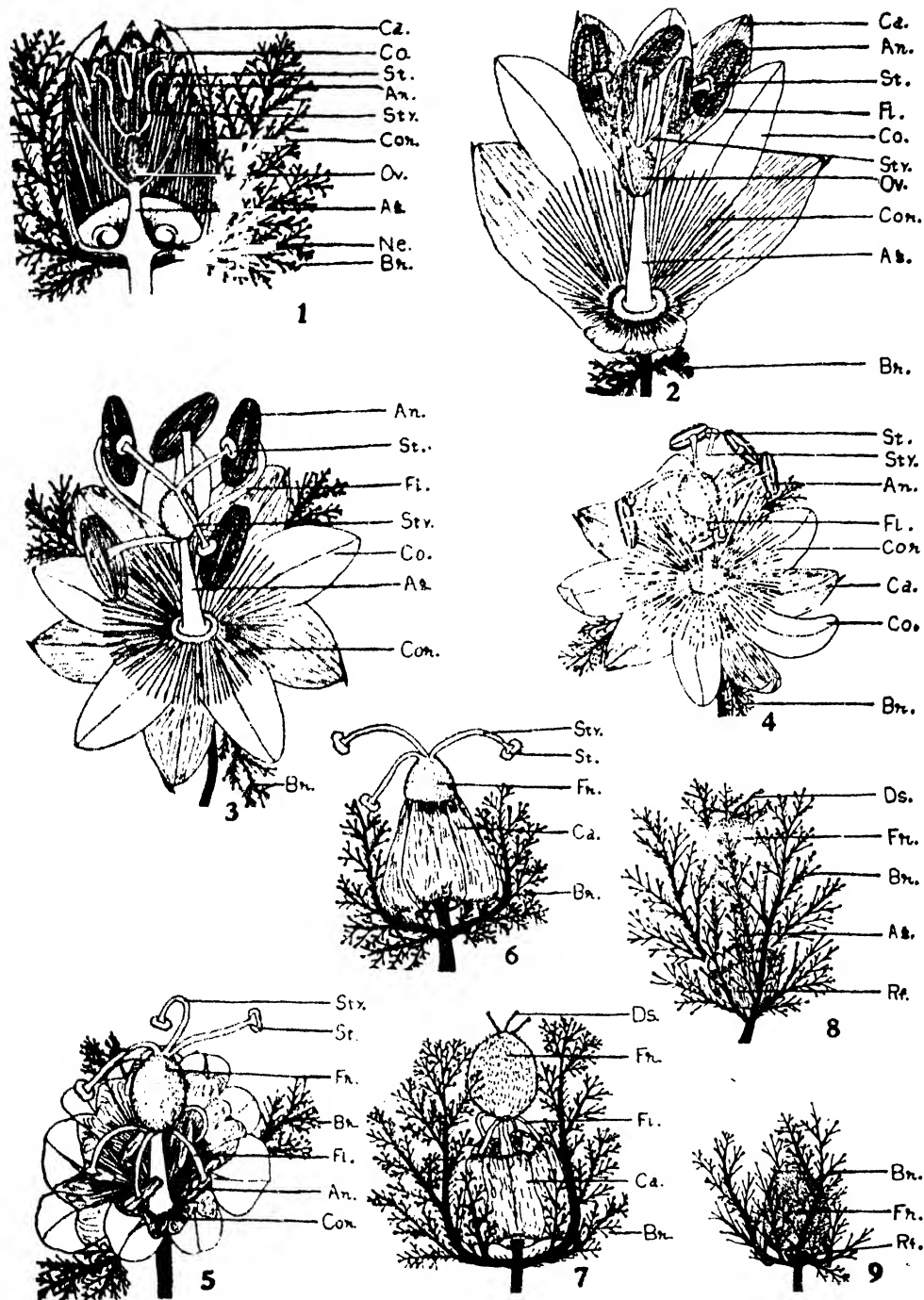
(Received April 21 ; read August 6, 1954)

A detailed account of the various types of pollination mechanism has been given by Kerner (1891) in his monumental work entitled 'Natural History of Plants'. Information concerning the mode of pollination in members of the Passifloraceae is also available from the work of Knuth (1908). The information presented by these authors does not, however, appear to be quite precise in every case. In the course of an embryological study of some members of the Passifloraceae I was able to observe certain interesting details concerning the pollination mechanism of *Passiflora foetida* grown in the Central College Botanical Gardens.

The solitary hermaphrodite flower has three highly dissected bracteoles at the base. The five calyx lobes enclose five white membranous petals. In the centre of the flower is an androgynophore around the base of which is a shallow cup with nectar bounded by one to many rows of filiform white or slightly violet coloured segments forming the corona. The androgynophore bears at its top the tricarpellary ovary with its three styles and stigmas. The stigmatic surface has a number of multicellular papillate outgrowths. At the base of the ovary five stamens emerge from the androgynophore. The anthers are oblong and introrse. The filament is stiff and flat and to this is attached the anther by a hinge-like arrangement. The filament shows two pegs which act as a pivot so as to allow the anther to rotate slightly with a jerky movement in any direction on the filament.

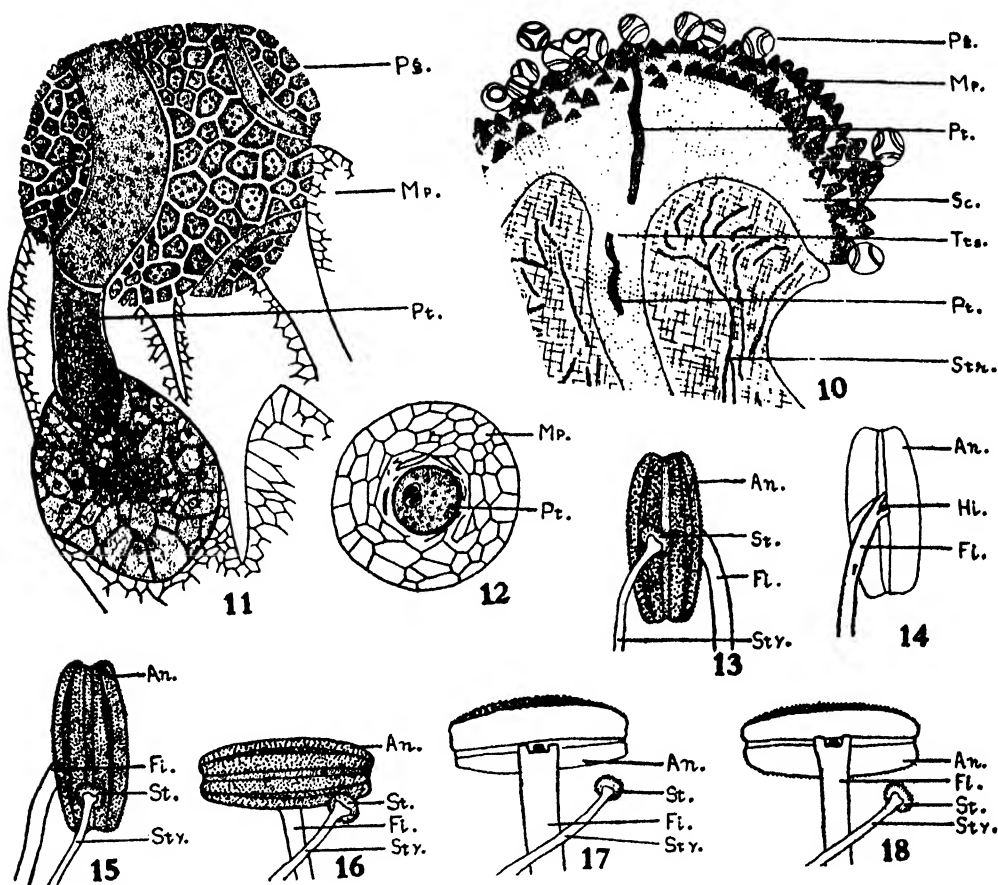
OBSERVATIONS

Figure 1 shows the arrangement of the floral parts as seen in a median longitudinal section of the flower bud prior to anthesis. The anthers are in close contact with the stigmatic lobes and the other floral members are erect in position (Fig. 1). The bracteoles are highly dissected, the branches forming ramifications and terminating in glands which secrete a highly sticky substance in later stages. Anthesis takes place during nights and lasts from a few minutes to a few hours. The first indication of anthesis is the horizontal spreading of the bracteoles and the subsequent opening of the calyx and corolla (Figs. 2-4). By about this time the anthers dehisce and their dehiscent faces are pressed against the stigmatic lobes by a downward movement of the latter (Figs. 2-4). At first the anther lobes are in a line with the filament (Figs. 2 and 13). One of the stigmatic lobes comes in contact with the dehiscent surface of the anther at its middle (Figs. 2, 3 and 13). Subsequently, the stigmatic lobe becomes closely pressed against the dehiscent surface of the anther and a kind of mechanical tension is brought about by mutual pressure. The stigmatic lobe is now brushed against the pollen carrying surface of the anther, but finally slips out due to the slow jerking movement of the latter (Figs. 15-17). As a result, the tension originally created between the anther and the stigma is released and the anther begins to tilt suddenly on the filament (Figs. 15-18). Thus the dehiscent surface of the anther now becomes directed downwards (Figs. 4, 5, 17 and 18).



FIGS. 1-9. Fig. 1. L.S. young flower bud just before anthesis showing the arrangement of flower parts. Fig. 2. L.S. view of a flower just after anthesis with dehiscence surfaces of anthers in contact with the stigmatic lobes. A few calyx and corolla lobes removed. Fig. 3. Still later stage after anthesis showing the horizontal spreading of bracteoles, calyx, corolla and corona; and bending of the styles over their respective anther lobes. Fig. 4. Pollinated flower showing the incurving of the margins of sepals and petals. Fig. 5. A view of the flower with inrolling petals and sepals gradually enveloping downwardly

bent stamens. Fig. 6. Side view of flower with erect bracteoles and the margins of petals and sepals lying at the base of the ovary also enveloping the stamens completely. Fig. 7. Flower showing downward shrinking of sepals with the enclosed petals, corona and stamens. Fig. 8. Fruit with fading styles and drying floral parts at the base of the androgynophore. Fig. 9. Same at later stage showing the fruit enveloped by the sticky bracteoles. (*Ag*, androgynophore; *An*, anther; *Br*, bracteoles; *Ca*, calyx; *Co*, corolla; *Cor*, corona; *Ds*, fading style; *Fi*, filament; *Fr*, fruit; *Nc*, nectary; *Ov*, ovary; *Rf*, remnants of floral parts; *St*, stigma; *Sty*, style.) All figures diagrammatic.



Figs. 10-18. Fig. 10. Longitudinal free-hand section of the stigmatic lobe showing multi-cellular outgrowths bearing pollen grains; note the penetration of pollen tube through the outgrowth and into the transmitting tissue, $\times 50$. Fig. 11. A portion of the stigmatic crest showing the germination of a pollen grain and the entry of the pollen tube in the multi-cellular outgrowth, $\times 485$. Fig. 12. T.S. of the multi-cellular outgrowth and the pollen tube, $\times 485$. Fig. 13. Stigma in contact with the dehiscent surface of the anther. Fig. 14. Back-view of the same showing the hinge attachment. Figs. 15-18. Stages showing the movement of anther with respect to the stigmatic lobe. (*An*, anther; *Fi*, filament; *Hi*, hinge; *Mp*, multi-cellular papillate outgrowth; *Pg*, pollen grain; *Pt*, pollen tube; *Sc*, stigmatic crest; *St*, stigma; *Str*, stylar tracheids; *Sty*, style; *Tts*, transmitting tissue.) (Figs. 13-18. All diagrammatic.)

The movement of the anther takes place in both the vertical and horizontal planes (Figs. 13 and 15-18). In the final stage when the dehiscent surface becomes downwardly directed, the anther comes to lie at right angles to its filament (Figs. 17 and 18). The movement itself seems to be due largely to the peculiar hinge-like mechanism which aids in drawing down the anther and also in helping it to become laterally tilted (Figs. 14, 17 and 18). The anthers of a flower which are not in contact with any of the stigmatic surfaces also perform these movements. The dehiscent anthers may also touch the stigmatic lobes and deposit their pollen subsequently.

Early in the day, after pollination is over and as the temperature begins to rise, the bracteoles, sepals and petals gradually move towards the centre of the flower (Figs. 4 and 5). Concurrently, the stamens also begin to droop down (Figs. 5 and 7). The inrolling sepals, petals and coronary filaments thus begin to enclose the stamens and touch the base of the developing fruit (Fig. 6). Later, the petals and sepals begin to dry up and move towards the base of the androgynophore (Fig. 7). The developing fruit is now well protected against ants and other insects by the latticed bracteoles which secrete a sticky fluid. Frequently ants were found to be caught in the meshes of the bracteoles. At the base of the androgynophore, inside the bracteoles, the shrivelled sepals, petals and coronary filaments as well as the dried up anthers can be seen (Figs. 8 and 9). The bracteoles themselves dry up finally and wither away only when the fruits are fairly old.

The stigmatic lobe is slightly reniform in shape and possesses multi-cellular papillate outgrowths on its surface (Fig. 10). The pollen grains with their reticulate exine are easily caught by these outgrowths on account of their rubbing against their anther surfaces. Beneath the papillate outgrowths is the expanded stigmatic crest through which the pollen grains send their pollen tubes which grow ultimately through the transmitting tissue of the style and reach the ovary (Figs. 10-12).

DISCUSSION AND CONCLUSIONS

The above observations confirm those of Warnstorf, especially regarding the movement of the anthers and the styles (*see* Knuth, 1908). Warnstorf has pointed out that anthesis lasts for a whole day. From my observations, however, made on a large number of flowers, I find that anthesis occurs only for a brief time during the early hours of the morning when the atmosphere is relatively cool.

The large size of the flower, the occurrence of the complicated brightly coloured coronary filaments, the hidden nectary and the elevated position of the essential organs all suggest that cross-pollination occurs and that it is aided by some special insect visitors. Knuth (1908) says: 'In the first stage of anthesis a large insect (such as a humble-bee) when sucking nectar, receives pollen on its back from the downwardly dehiscent anthers. In the second stage the styles have curved downwards to such an extent that the now receptive stigmas are lower than the empty anthers. It follows that the older flowers are fertilized by pollen from younger ones.' According to my observations, however, the second stage described by Knuth occurs only subsequent to pollination, when the styles move up and the stamens move down so that once again a contact may be established between dehiscent surfaces of anthers and the stigmatic crests. Warnstorf explains the upward deflection of purple-flecked styles from the anthers as suggesting that autogamy would be excluded under such circumstances, but that the stigmas and anthers may be brought into contact when the flower closes at the end of single day's anthesis (*see* Knuth, 1908). The above observations of Warnstorf make one feel doubtful about the statement that 'the older flowers are fertilized by pollen of younger ones'.

In *Passiflora foetida* the flower undoubtedly closes gradually after pollination. This makes the dehiscent anthers which have moved down after pollination to

become enclosed by the corona, corolla and the calyx and no contact can, therefore, be brought about between the stigma and such anthers at this stage. Thus Warnstorff's suggestion probably owes itself to his having found the styles spread out and the anthers with their dehiscent surfaces directed downwards. The mechanism involved in the downward and later upward movement of the styles or the movement of the anthers themselves on their filaments with reference to the apposed stigmatic surfaces seem to have been overlooked by him. Basing his observations on plants grown in a green house, his interpretation of the chasmogamic flower being adapted to autogamy appears to be exaggerated. Perhaps, some of the post-pollination features like the downward movement of the styles and stamens and displacement of anthers were presumed by Warnstorff to be stages preceding actual pollination.

Delpino's (see Knuth, 1908) suggestions of humming birds as pollinating agents and a subsequent corroboration of the same by Müller in some of the Brazilian *Passifloras* probably deserve further study and confirmation. In *Passiflora foetida*, occasionally, insects were found to be moving about on the floral parts during post-pollination stages. The insects were very small, however, and it is improbable that they can be considered as pollinating agents. Very rarely, especially in the mornings when there is bright sunshine, a small honey bee would seem to alight on the corona in a flower completely spread out. By this time, however, pollination is completed and pollen tubes were actually observed to have reached the transmitting tissue. Doubtless, the honey bee collects some pollen grains on its back and legs, but this takes place only subsequent to pollination. The suggestion made by earlier workers that the honey bee alone brought about cross-pollination, is therefore erroneous.

'It is true that cross-pollination appears to be the primary object aimed at, but it is not true that autogamy is avoided. If cross-pollination takes place there is naturally no necessity for subsequent autogamy, but if cross-pollination fails autogamy assumes an importance of its own, and the contrivances which have been observed to bring about autogamy are no less numerous than those which favour cross-pollination. That flowers should be adapted at different times to two such diverse purposes as cross- and self-pollination is one of marvels of floral construction' (Kerner, 1891). One of these marvels of floral construction adapted to autogamy is seen in *Passiflora foetida*. The structure and behaviour of different entities and their unified action have made autogamy a successful mode of pollination in this plant. A good example of an intermediate case between cleistogamy and chasmogamy seems to be demonstrated in *Passiflora foetida*.

The pollen grains have such characteristic thickenings that they are easily caught by the stigmatic crest. The pollen tubes emerging out from the furrows of the pollen grains penetrate directly into the multicellular outgrowths and not in between them. The highly dissected bracteoles form a lattice work enveloping and protecting the fruits in later stages. The glandular tips of their ramifications secrete a juicy fluid which, probably, attracts the neighbouring ants or small insects. The remnants of those ants are later seen on the bracteoles.

SUMMARY

Pollination mechanism in the flowers of *Passiflora foetida* grown in Central College Botanical Gardens has been studied. Anthesis of flowers occurs during nights and lasts for a brief time. The unified action of the different entities of the flower helps in self-pollination. The stigmatic crests with their multicellular papillate outgrowths easily catch the pollen grains which have reticulate exine thickenings. The pollen tube emerging out from one of the furrows of the pollen grain penetrates directly into the multicellular outgrowth. During post-pollination stages the latticed bracteoles protect the developing fruits. Autogamy is successfully ensured in the flowers of *Passiflora foetida* and it can be taken as a good example of an intermediate case between cleistogamy and chasmogamy.

ACKNOWLEDGEMENTS

I am extremely grateful to Prof. P. Maheshwari, University of Delhi, and Prof. L. N. Rao and Dr. S. B. Kausik, Central College, Bangalore, for their kind interest and helpful suggestions.

REFERENCES

- Kerner, A. (1891). The Natural History of Plants. (English translation), Vol. II. London.
Knuth, P. (1908). Handbook of Flower Pollination. (English translation), Vol. II. Oxford, England.

Issued September 17, 1954.

THE RÔLE OF CULTURE MEDIUM AND ITS CONSTITUENTS ON THE GROWTH AND VIABILITY OF *ENTAMOEBA HISTOLYTICA*

by A. K. MUKHERJEA, *Research Fellow, N.I.S.I., Department of Protozoology, Indian Institute for Medical Research, Calcutta*

• (Communicated by J. C. Ray, M.D., F.N.I.)

(Received April 1, 1953; after revision April 7; read August 6, 1954)

INTRODUCTION

Attempts have been made in the past by several workers to prepare a medium which would encourage the growth of *Entamoeba histolytica* free from bacteria, so that a pure line strain of this protozoon may conveniently be used for several purposes, particularly for screening antiamoebic drugs, and for preparing specific antigens for the diagnosis of amoebiasis. The progress of our work in this direction and the results obtained have already been reported (Mukherjea, 1951: 9, 35 and 47).

The present work which is a continuation of the past investigation already referred to, has been undertaken to determine the rôle of the culture medium and its constituents on the growth and viability of this protozoal parasite. This has been described under the following headings: (1) Isolation of *E. histolytica*, (2) Isolation of bacteria; (3) Growth of *E. histolytica* under conditions of changed composition of the medium; (4) The slant in relation to the growth of *E. histolytica*; (5) The activation of bacteria and its effect on the constituents of the medium; (6) The constituents of a medium and reduction of the substrates.

MATERIALS AND METHODS

1. Isolation of *E. Histolytica*

All the following experiments were carried out with strains of *E. histolytica* isolated from stools of persons suffering from amoebiasis. For isolation of the amoeba normal saline emulsion of fresh stool, after separation of the coarse faecal particles by standing, was used for inoculating the culture medium. It was incubated at 37°C. and examined microscopically after 48 hours and thereafter.

E. histolytica strains no. 4, 5 and 6: In case of 4 and 6 Dobell and Laidlaw's medium (hereafter referred to as D.L. medium) was used. After 48 hours' incubation the growth in the primary cultures was scanty and did not live longer than 48 hours. There was no growth on subculture. In isolating the amoeba from strain no. 5, two separate cultures were made, one in pure D.L. medium and the other in the same medium to which acriflavine in 1:40,000 had been added. Growth occurred in both the culture tubes. It persisted for 48 hours in the tube without acriflavine whereas for 72 hours in the tube with acriflavine. Subcultures from these tubes produced no growth.

E. histolytica strain no. 8: Cultures were made in several E_3 media whose composition is given later. A fair growth was noticed. The amoebae, however, disappeared after 72 hours. This strain perished after the second subculture.

E. histolytica strain no. 7*: This strain was isolated from the stool of a patient suffering from amoebiasis together with ariboflavinosis. As usual the primary

* With a view to determining the pathogenicity of the amoebae, intrarectal inoculation in two kittens, led to the appearance of motile trophozoites in the stool. The kittens died within 72 to 96 hours. No signs of ulceration were, however, detected in the large intestine.

culture was made in D.L. medium. After 48 hours, growth occurred in the primary culture; it persisted up to 72 hours. Serial subcultures in D.L. medium at 48 hours' intervals were positive although the growth was always feeble.

2. Isolation of Bacteria

Bacteria accompanying E. histolytica strain no. 7: These were isolated by culturing a loopful of fluid from an amoebic culture tube on a McConkey's plate. After 48 hours' incubation at 37°C. two types of lactose-fermenting colonies were seen, viz. (i) deep pink and (ii) of a lighter colour. Two colonies from (i) were grown separately on nutrient agar, and labelled as *A* and *B*. Two light pink colonies from (ii) were similarly grown on nutrient agar, and labelled as *C* and *D*. The morphology, growth and biochemical reactions of these four cultures were studied and the results are given below:

(1) On nutrient agar:

- (a) *A and B:* Small, circular and convex colonies; Gram-negative bacilli with well developed capsules; no spores.
- (b) *C and D:* Large, circular, convex and mucoid colonies; Gram-negative bacilli with well developed capsules; non-sporing.

(2) In nutrient broth:

- (a) *A and B:* Uniform turbidity with deposits at the bottom. No pellicle on the surface. Non-motile.
- (b) *C and D:* Uniform turbidity with deposits at the bottom. Surface-pellicle observed. Non-motile.

(3) In litmus milk medium:

- (a) *A and B:* Acid but no clotting.
- (b) *C and D:* No acid and no clotting, but after 48 hours, acid and clotting were observed.

(4) In Koser's and uric acid media:

- (a) *A and B:* No growth in either medium.
- (b) *C and D:* Growth in both the media.

(5) Sugar fermentation:

A, B also C and D were inoculated separately into four sets of sugar tubes each containing eleven different sugars. Fermentation reactions, as noticed after 24 hours' incubation at 37°C., are tabulated in Table I.

(6) Voges-Proskauer reaction (V.P.):

A and B, also *C* were V.P. negative, but *D* was V.P. positive.

(7) Methyl-red reaction (M.R.):

A and B gave positive, but *C and D* negative reactions.

The important features which emerged from the several tests, stated above, are tabulated in Table II.

TABLE I

Sugar fermentation reactions with bacteria from cultures in A, B and C and D tubes

Culture in tube.	Glucose.	Lactose.	Mannite.	Saccharose.	Arabinose.	Xylose.	Rhamnose.	Inositol.	Raffinose.	Dulcite.	Maltose.	Remarks.
A	A.G.	A.G.	A.G.	Nil	A.G.	A.G.	A.G.	Nil	Nil	Nil	A.G.	{ Uniform reactions in both the tubes A and B.
B	A.G.	A.G.	A.G.	Nil	A.G.	A.G.	A.G.	Nil	Nil	Nil	A.G.	
C	A.G.	A.G.	A.G.	A.G.	A.G.	A.G.	A.G.	A.G.	A.G.	A.G.	A.G.	{ Uniform reactions in both the tubes C and D.
D	A.G.	A.G.	A.G.	A.G.	A.G.	A.G.	A.G.	A.G.	A.G.	A.G.	A.G.	

A.G. = Acid and gas.

TABLE II

Showing the characteristic reactions of the bacteria in cultures A, B and C and D

Culture in tube.	Motility.	Capsule.	Saccharose.	Dulcite.	M.R.	V.P.	Growth in Koser's and uric acid media.	Litmus milk.	Remarks.
A	—	+	—	—	+	—	—	Acid only.	{ Uniform reactions in both the tubes A and B.
B	—	+	—	—	+	—	—	Acid only.	
C	—	+	A.G.	A.G.	—	—	+	No acid and no clotting in 24 hours.	{ Reactions slightly differ in the two tubes C and D.
D	—	+	A.G.	A.G.	—	+	+	No acid and no clotting in 24 hours.	

From the morphology, growth in Koser's and uric acid media, sugar and other biochemical reactions (*vide* Table above), it is clear that A and B were one and the same organism, whereas C and D included two different types. A and B were, therefore, combined and labelled as bacterial strain no. 2, C as bacterial strain no. 1 and D as strain no. 3. Strains no. 1 and 3, as Table II shows, belonged to the saprophytic type of *B. coli*, whereas no. 2 was of intestinal origin. As very little difference was noticed in bacteria in strains no. 1 and 3 and since both appeared as saprophytic they will henceforth be referred to as strain no. (1+3).

Bacteria growing with E. histolytica strains no. 4, 5, 6 and 8 (see page 437). All these were noticed to be pathogenic strains of intestinal *B. coli*.

3. *Growth of E. histolytica under conditions of changed composition of the medium*

(4)* As has been mentioned previously the growth of *E. histolytica* (strain no. 7) was always feeble in D.L. medium and continuous subcultures in the same medium further deteriorated the growth and viability. Attempts were, therefore, made to improve the growth by changing the composition of the medium. With this object in view and also for the purpose of studying which constituents (e.g. serum, peptone, meat extract, etc.) when added to the 'basal medium' (see combination A in Table III) were responsible for stimulating the growth, the following investigations were carried out.

In the beginning, a simple type of slant and the fluid overlay were prepared as follows. The solid slant was made of 2½% agar in 0.5% saline solution. The overlay fluid was made by dissolving egg albumin in sterile salt solution having the composition: sodium chloride—0.85 gm.; potassium chloride—0.02 gm.; calcium chloride—0.02 gm.; distilled water—100 c.c. The white portion of two hen's eggs was mixed with 250 c.c. of this salt solution which had been previously autoclaved. Starting with such a plain agar slant, its composition was progressively altered by adding other substances such as peptone, meat extract, etc. as is shown below. Likewise, the composition of the fluid portion was changed.

Slant:

- (a) Plain agar slant.
- (b) Plain agar+1% peptone+meat extract (50 gm. ox-heart extracted in 100 c.c. water) = nutrient agar slant.
- (c) Nutrient agar+horse serum (10%) = serum agar slant.
- (d) Serum agar+haemoglobin (5% rabbit's blood) = blood agar slant.
- (e) Blood agar: heated to 80°C. for 10 minutes = altered blood agar slant.
- (f) Horse serum: this was inspissated into a slant = Dobell and Laidlaw's slant.

Fluid overlay:

- (a) Egg albumin in salt solution.
- (b) Egg albumin in salt solution+horse serum (9 : 1).
- (c) Egg albumin in salt solution+serum+acriflavine (1 : 40,000).
- (d) Egg albumin in salt solution+1% peptone water (3 : 1).
- (e) Egg albumin in salt solution+meat extract (3 : 1).
- (f) Egg albumin in salt solution+nutrient broth (3 : 1).
- (g) Serum in normal saline solution (1 : 9).
- (h) Serum in normal saline solution+haemoglobin solution† (2 : 5).

The peptone used in these experiments was prepared by digesting meat with pancreas. In making nutrient agar or broth this impure peptone was employed. Apart from peptones, the pancreatic meat digest also contained polypeptides, amino acids, reducing substances, etc. as impurities.

To understand in what ways the different components of the slant and also of the fluid influenced the growth and viability of the amoebae, the slants and the fluid overlays were differently combined. Before inoculating the trophozoites, starch was added in every tube. The results have been shown in Table III.

* For (B), see page 443.

† In preparing haemoglobin solution 10 c.c. of rabbit's blood was at first laked in 90 c.c. of sterile distilled water which was then made isotonic by mixing with sterile 1.2% sodium chloride solution in the proportion of 2 : 4.

TABLE III

Showing the growth and viability of the amoebae in various combinations of slants and fluid overlays

Group.	Combinations of slants + fluids.	Growth after 48 hours.	Viability.
A	*1. Slant (a) + Fluid (a)	+	48 hours.
	2. Slant (a) + Fluid (d)	+++	72 hours.
	3. Slant (a) + Fluid (e)	+++	72 hours.
	4. Slant (a) + Fluid (f)	+++	72 hours.
	5. Slant (b) + Fluid (a)	+++	72 hours.
B	1. Slant (a) + Fluid (b)	+++	96 hours.
	2. Slant (f) + Fluid (a)	+	72 hours.
C	1. Slant (c) + Fluid (a)	++	96 hours.
	2. Slant (d) + Fluid (a)	+++	96 hours.
	3. Slant (e) + Fluid (a)	+++	96 hours.
D	1. Slant (c) + Fluid (b)	+++	96 hours.
	2. Slant (d) + Fluid (b)	++++	96 hours.
	3. Slant (e) + Fluid (b)	++++	96 hours.
E	1. Slant (c) + Fluid (c)	++++	120 hours.
	2. Slant (d) + Fluid (c)	+++++	144 hours.
	3. Slant (e) + Fluid (c)	+++++	144 hours.
	4. Slant (f) + Fluid (c)	++++	144 hours.
F	1. Nil + Fluid (g)	+	48 hours.
	2. Nil + Fluid (g) + Hb.	+++	120 hours.
	3. Slant + Fluid (g) + Hb.	++++	96 hours.
G	1. Slant (a) + Fluid (a) + acriflavine ..	+	48 hours.

From the above table the following conclusions are made:—

1. The basal medium was very feeble as regards its power to support the growth of the amoebae.

2. Peptone and meat extract used either separately (A_2 , A_3), or in combination (A_4) activated the growth of the amoebae in the basal medium. No difference could be discovered when they were added to the fluid (A_2 , A_3 , A_4) or incorporated in the slant (A_5).

3. The addition of serum to either the fluid overlay (B_1) or the slant (C_1) had a marked effect on the growth and viability of the amoebae which, however, did not improve on the addition of serum to both the fluid and the slant (D_1).

4. Acriflavine † when mixed with the basal medium did not lead to any improvement of the growth of the amoebae (G_1), but when added to an enriched medium containing serum, peptone or meat extract, it caused a very marked stimulation of the growth and an increase in the viability of the organisms (E_1 , E_2 , E_3 and E_4).

5. Though serum solution itself (F_1) failed to stimulate the growth of the amoebae, addition of haemoglobin (F_2) always encouraged the growth which further improved when serum solution containing haemoglobin was put as overlay (F_3). There was no appreciable increase in the growth of the amoebae when haemoglobin was included in the slant of an enriched medium.

6. The growth and viability of the trophozoites were diminished when the serum was inspissated (B_2).

7. Heating the haemoglobin made no difference in the growth of the amoebae.

* The combination in A_1 constitutes the 'basal medium'.

† Details of the action of dyes and other bacteriostatic substances will be reported in a later communication.

From the above it will be seen that the combinations as stated in E_1 , E_2 and E_3 were most conducive to the growth and viability of the amoebae. Due to this the combinations in E_1 , E_2 and E_3 were chosen as the 'preserving media'.

It may be noted that when serum was added to the basal medium, there was an appreciable improvement of the growth and viability of the amoebae. Such improvements were also noticed when stock peptone, meat extract and nutrient broth were used. These observations, therefore, led us to undertake studies to explain in what different ways serum, stock peptone, meat extract and nutrient broth influenced the growth of *E. histolytica* (strain no. 7).

Improved growth of the amoebae on addition of serum to the basal medium may be regarded to have been effected by some of its constituents such as, albumin, globulins, urea, uric acid, creatine, creatinine, other undetermined nitrogen, amino acids, fatty acids, cholesterol, inorganic salts, glucose, vitamins, etc. or by some unknown factors. In order to determine the rôle of these substances on the growth of the amoebae, the different constituents of the serum have been placed in three groups:

- (a) Urea, uric acid, etc. and amino acids—as 'alternate sources of nitrogen'.
- (b) Sterols, e.g. cholesterol—as food for the amoebae.
- (c) Vitamins, especially B-complex group—as accessory growth substances.

It has been observed that the behaviour of the amoebae in solution of albumin and globulins of serum is the same as when they are grown in that of pure egg albumin. The growth of amoebae in presence of serum may thus be directly due to the introduction of either of the following substances: (1) alternate sources of nitrogen, (2) sterols and (3) accessory growth substances. Tests in proving these points were therefore undertaken.

Stock preparations of the above substances were made as follows:

(1) *Alternate sources of nitrogen*: Urea and uric acid were used in the same proportions as they are present in the serum. Ammonium chloride was used in trace as substitute for creatine, creatinine and other undetermined nitrogen of serum. The composition thus stands as: urea—0.20 gm.; uric acid—0.12 gm.; ammonium chloride—0.24 gm.; salt solution (stock)—1,000 c.c. After sterilisation the white portion of two hen's eggs was mixed with 250 c.c. of the solution. The composition of this fluid is now identical with that of the fluid portion of the basal medium after the addition of urea, etc. in the same proportions as they exist in the serum.

(2) *Cholesterol*: Sterile cholesterol powder+sterile starch (1:5). One loop of this mixture was used for each culture tube.

(3) *Amino acid solution*: 50 mgm. each of glycine, alanine, cystine, leucine, tryptophane and aspartic acid were mixed in 10 c.c. of normal saline and sterilised. 0.2 c.c. of this solution was used for each culture tube.

(4) *Vitamin B-complex solution*: This was prepared by dissolving the contents of one 'Betalin compound' capsule (Lilly) in 50 c.c. normal saline. After sterilisation, 8 to 10 drops were used for each culture tube.

The effect of the different constituents of the serum on the growth of *E. histolytica* (strain no. 7) is shown in Table IV.

An analysis of the effects of different constituents of the serum indicates that vitamin B-complex with the addition of cholesterol and amino acids influenced the nutrition of the amoeba. However, a closer study led us to believe that amongst the substances tested vitamin B-complex was essentially the most important factor which brought about an increase in growth of the amoeba together with augmentation of its viability.

While vitamin B-complex when added to the basal medium no doubt stimulated the growth of the amoebae, though feebly, it exercised profound influence on

TABLE IV

Showing the effects of the different constituents of serum on the growth of E. histolytica

Substances added to the basal medium.	Growth after 48 hours.	Viability.
Alternate sources of nitrogen	+	48 hours.
Alternate sources of nitrogen + cholesterol	+	48 hours.
Alternate sources of nitrogen + cholesterol + amino acids	+	48 hours.
Alternate sources of nitrogen + cholesterol + amino acids + vitamin B-complex	+	72 hours.
Cholesterol	+	48 hours.
Vitamin B-complex	+ to ++	72 hours.
Amino acids	+	48 hours.
Cholesterol + amino acids + vitamin B-complex	+ to ++	72 hours.

their growth when mixed with an enriched medium containing serum, peptone and meat extract (e.g. E_3 medium). This is manifest in the results given in Table V.

TABLE V

Showing the effects of vitamin B-complex on the growth of amoebae when mixed with enriched medium

Medium.	Growth after			Remarks.
	48 hrs.	72 hrs.	96 hrs.	
E_3 ..	++	+	—	} The growth and also the viability are distinctly feeble in all the tubes.
E_3 ..	+	+	—	
E_3 ..	++	+	—	
E_3 + vitamin B-complex ..	++++	+++	+	} The growth is profuse and the viability prolonged.
E_3 + vitamin B-complex ..	++++	+	—	
E_3 + vitamin B-complex ..	++++	++	+ / 2	

+ / 2 indicates five or less than five trophozoites per field as observed under low power.

(B) The physical and chemical changes which directly lead to increased multiplication of *E. histolytica*, and whether they are due to putrefactive reaction or to reaction of fermentation, have been discussed in a previous paper (Mukherjea, 1951: 9). Indeed, such changes are due to the presence of different types of bacteria which are found in association with the amoebae.

While the bacteria are responsible for the type of reaction that is taking place in the culture medium, the constituents of the medium themselves, on the other hand, can modify the intensity of the reaction. The latter has now been observed by culturing *E. histolytica* (strain no. 7) in B_2 , D_1 , D_2 and D_3 and also in E_1 , E_2 , E_3 and E_4 media. After 48 hours' incubation, observations were made for signs of reactions such as smell and changes of pH. The details of these observations are given in Table VI.

TABLE VI

Showing the relation between composition of the medium, reactions taking place as a result of bacterial growth and growth of the amoebae

Medium.				Smell (foetid).	pH.	Growth after 48 hours.
B_2 (basal medium)	Nil	4.8 to 5.0	+
D_1 (B_2 + peptone + meat extract + serum)	+	5.4 to 5.6	++
D_2 (D_1 + blood)	+	5.8 to 6.0	++
D_3 (D_1 + heated blood)	+	5.6 to 5.8	++
E_1 (B_2 + peptone + meat extract + serum + acriflavine)	+++	6.6 to 6.8	++++
E_2 (E_1 + blood in the slant)	+++	6.4 to 6.8	++++
E_3 (E_1 + heated blood in the slant)	+++	6.4 to 6.8	++++
E_4 (D.L. medium + serum and acriflavine)	++	5.6 to 6.4	+++

The table shows that:

(1) The sign of putrefaction such as foetid smell, was absent in B_2 . The pH was below 5.0 and the growth of the amoebae was feeble (+).

(2) Putrefaction was apparent in D_1 , D_2 and D_3 . The pH remained above 5.4 and the growth of the amoebae was from fair to moderate (++).

(3) The putrefying reactions were intense in E_1 , E_2 and E_3 . The pH remained close to 6.8. The growth of the amoebae was profuse (++++).

The following conclusions are thus made from the above observations:—

- (i) Substances such as peptone, meat extract and serum are responsible for stimulating the putrefaction (D_1 , D_2 and D_3).
- (ii) Acriflavine further increases putrefaction (E_1 , E_2 and E_3).
- (iii) With increase in the intensity of putrefaction the growth and viability of the amoebae also increase.
- (iv) Inspissation of serum leads to the depression of the growth-promoting properties of the serum slant.

4. The slant in relation to the growth of *E. histolytica*

It has already been reported in this paper that a slant containing agar and salt (i.e. the 'inert' slant) does not provide any nourishment to the amoebae. On the other hand, slants in A_5 , C_1 , C_2 and C_3 media (*vide* Table III) contain substances which directly go to nourish them. In order to study in what other ways a slant may directly encourage the growth of the amoebae, an 'inert' slant was overlaid by solution of egg albumin and horse serum. In actual experiments, the height of the fluid in all the tubes, whether with the slant or without it, was the same. The results are noted in Table VII.

As has previously been mentioned, a slant of agar and salt in presence of an 'inert' fluid consisting of egg albumin in normal saline acts in an inert manner as it does not stimulate the amoebae to grow. On the other hand, when the slant is overlaid by the same fluid enriched by the addition of horse serum there is an abundant growth (*vide* tubes no. 1, 2 and 3 in Table VII). In absence of the 'inert' slant (agar+salt), the fluid itself is unable to encourage the multiplication of the amoebae (*vide* tubes no. 4 and 5 in Table VII). This indicates that in some unaccountable ways the 'inert' slant under certain conditions can activate the growth of the amoebae.

TABLE VII

Showing the effects of 'inert' slant on the growth of E. histolytica

Tube No.	Medium.	Growth after				Remarks.
		48 hrs.	72 hrs.	96 hrs.	120 hrs.	
1.	Egg albumin and serum solution + inert slant ..	+ + +	+	—		} The growth and the viability are increased.
2.	Egg albumin and serum solution + inert slant ..	++	+++	+	—	
3.	Egg albumin and serum solution + inert slant ..	+++	+++	++	—	
4.	Egg albumin and serum solution ..	+	—	—	—	} The growth is uniformly feeble in all the tubes.
5.	Egg albumin and serum solution ..	++	1/2	—	—	

+ / 2 indicates five or less than five trophozoites per field as observed under low power.

It was further observed that while combination of the 'inert' slant and the fluid containing egg albumin and horse serum was more effective than the fluid itself, the growth of the amoebae was noticed to be definitely feeble when the same fluid, but without the slant, was mixed with agar to make it viscous. In actual experiments this semisolid medium was prepared by mixing 5 c.c. of a 3% agar solution with 28 c.c. of the fluid. It may be stated that the slant is made mainly of agar. When the slant is withdrawn and agar is incorporated in the albuminous fluid enriched by the addition of horse serum, this semisolid or viscous material behaves in a remarkably different manner than when the agar in the form of slant is used.

5. *The activation of bacteria and its effect on the constituents of the medium*

In stimulating the growth and viability of the amoebae the associated bacteria and the individual constituents of the medium are equally important. The conditions leading to the growth of the amoebae develop as a result of their mutual actions. This is explained by stating that while some constituents of the medium, *e.g.* peptone, help the growth and rapid multiplication of the bacteria, others, such as egg albumin, are unable to perform the same function. After bacteria have been activated by growing in a medium containing peptone, they are able to attack the albumin and break it into simpler constituents. Without peptone, as has been stated, the same bacteria cannot hydrolyse albumin or any other proteins. These observations were the results of the experiments described below.

Bacteria, strains no. 2 and (1+3), were cultivated in several liquid media, *e.g.* (a) egg albumin solution; (b) egg albumin solution + peptone; (c) egg albumin solution + horse serum; (d) nutrient broth; and (e) glucose broth. At the end of 24 and 48 hours' incubation the growth of the bacteria and the pH of the culture fluid were noted. At the end of 48 hours, tests were made for proteoses and peptones in culture fluids (a) and (c). The results have been incorporated in Table VIII.

It will thus be seen that:

1. (a) In all the above experiments in the case of strain no. 2, irrespective of the growth of the bacteria, starch was not affected in any way.

TABLE VIII

Showing the action of bacterial strains no. 2 and (1+3) when grown in different fluid media

Serial no.	Medium.	Bacterial strain no. 2.	Bacterial strain no. (1+3).
(a)	Egg albumin soln. + starch (pH 6.8).	pH after 24 hrs. : 6.8 pH after 48 hrs. : 6.8 Growth after 24 hrs. Nil Growth after 48 hrs. + Proteoses + peptones: Nil	pH after 24 hrs. : 6.8 pH after 48 hrs. : 6.8 Growth after 24 hrs. + Growth after 48 hrs. ++ Proteoses + peptones: +
(b)	Egg albumin soln. + peptone + starch (pH 6.8).	pH after 24 hrs. : 6.4 to 6.6 Growth after 24 hrs. + + + +	pH after 24 hrs. : 6.8 Growth after 24 hrs. + + + +
(c)	Egg albumin soln. + horse serum + starch (pH 6.8).	pH after 24 hrs. : 6.8 Growth after 24 hrs. + + + + Proteoses + peptones: + + +	pH after 24 hrs. : 6.8 Growth after 24 hrs. + + + + Proteoses + peptones + + + +
(d)	Nutrient broth + starch (pH 6.8).	pH after 24 hrs. : 6.4 to 6.6 Growth after 24 hrs. + + + +	pH after 24 hrs. : 6.8 Growth after 24 hrs. + + + +
(e)	Glucose broth (pH 6.8).	pH after 24 hrs. : 4.4 to 4.6 Growth after 24 hrs. + + + +	pH after 24 hrs. : 5.4 to 5.8 pH after 48 hrs. : 6.2 to 6.6 Growth after 24 hrs. + + + +

(b) Although there was no growth of the bacteria in egg albumin solution up to 24 hours, a feeble growth was noticed after 48 hours. There was no hydrolysis of egg albumin (*vide* no. (a) in Table VIII).

(c) The same strain of bacteria showed a profuse growth in a medium containing a small quantity of peptone or horse serum in addition to egg albumin. This was accompanied by hydrolysis of egg albumin (*vide* nos. (b) and (c)).

(d) In nutrient broth (peptone+meat extract), and glucose broth (glucose+nutrient broth) growth was profuse but acid was produced in the latter medium only (*vide* nos. (d) and (e)).

2. (a) In the case of strain no. (1+3), as with strain no. 2, starch was not affected.

(b) There was feeble growth in egg albumin up to 24 hours, thereafter the growth increased. There was slight hydrolysis of egg albumin (*vide* no. (a)).

(c) The growth of the bacteria was profuse in a medium containing a small quantity of peptone or horse serum in addition to egg albumin; there was also hydrolysis of egg albumin (*vide* nos. (b) and (c)).

(d) In nutrient broth and glucose broth, growth was likewise profuse. In case of glucose broth there was slight acidity at first which became neutral after 48 hours (*vide* nos. (d) and (e)).

6. The constituents of a medium and reduction of the substrates

As amoebae are obligatory anaerobes, for anaerobic respiration they require a medium which has already undergone reduction. In absence of chemical substances such as cysteine, glutathione, etc., which when mixed with the culture fluid

are themselves able to reduce the medium, the lowering of the oxidation-reduction potential of the medium is accomplished by the bacteria. Some common constituents of the medium such as peptone, meat extract, etc., also contribute to some extent in bringing about reduction for the purpose of respiration of the amoebae. The constituents, however, do not act independently in the same way as the

TABLE IX

Showing how the different constituents of the medium such as serum, egg albumin, etc. react with Bacterial Strain no. (1+3) causing reduction of methylene blue

Substrates.		Decolouration of methylene blue after an interval of						Remarks.		
		10 mts.		10 mts.		20 mts.			18 hours.	
Serum solution	Emulsion of bacteria from strain no. (1+3) —0.3 c.c. put into the tubes.	Methylene blue solution—2 drops put into the tubes.	40%	2 more drops of methylene blue solution added.	10%	Further addition of 2 drops of methylene blue solution.	Nil	Additional 10 drops of methylene blue solution.	80%	Reactions are delayed, weak and unstable in both the tubes.
Egg albumin solution.			40%		10%		Nil		60%	
Peptone water			100%		100%		80%		100%	Reactions are quick, strong and stable in all the tubes.
Meat extract			100%		100%		100%		100%	
Nutrient broth			100% in 3 mts.		100% in 3 mts.		100% in 5 mts.		100%	

TABLE X

Showing how the different constituents of the medium such as serum, egg albumin, etc. react with Bacterial Strain no. 2 causing reduction of methylene blue

Substrates.	Decolouration of methylene blue after an interval of						Remarks.	
	10 mts.		10 mts.		20 mts.			18 hours.
Serum solution	Emulsion of bacteria from strain no. 2—0·3 c.c. put into the tubes. Methylene blue solution—2 drops put into the tubes.	10%	2 more drops of methylene blue solution added.	Nil	Further addition of 2 drops of methylene blue solution.	Nil	50%	Reactions are extremely feeble and also unstable in both the tubes.
Egg albumin solution.		10%		Nil		Nil	20%	
Peptone water		50%		20%		20%	100%	Reactions are delayed, weak and unstable in all the tubes.
Meat extract		10%		10%		Nil	100%	
Nutrient broth		60%		40%		20%	100%	

chemical reducing agents but act conjointly with the bacteria. This was proved by taking several test tubes each containing 4 c.c. of the fluid. The different substrates used were horse serum, egg albumin, peptone, meat extract and nutrient broth. 0.3 c.c. of bacterial emulsion from strain no. (1+3) and a few drops of a buffered methylene blue solution (pH 7.2) were added gradually in all the tubes as shown in Table IX. The degree of reduction was judged by the extent of decolouration of the dye. At every step care was taken to prevent bacterial contamination. Similar experiments were carried out with bacterial strain no. 2 in place of strain no. (1+3). The results are noted in Table X.

It will thus be seen from Tables IX and X that the reactions induced by the bacteria varied not only with the constituents but also with the type of bacteria employed.

DISCUSSION

In order to keep *E. histolytica* alive and for its growth and reproduction certain requirements must be fulfilled. These are:

(1) The proper type of the culture medium. Though different types of media are recommended for its cultivation, the results are never satisfactory in all cases. It is likely that the necessary conditions and substances favouring their growth are not present in the same manner in all these different media.

(2) Suitable types of bacteria growing with the amoebae; and

(3) Optimum temperatures for the growth and its viability.

The preparation of a medium containing proportionate amounts of nutrient materials for the amoebae is, therefore, of fundamental importance. The culture medium in addition to containing all the elements necessary for the growth and viability of the amoebae should also be properly constructed. How the construction of a medium influences the growth of the amoebae can be demonstrated by culturing them in the following media:

(a) in a fluid medium but without a slant. The growth is markedly feeble (Table VII).

(b) in the same medium with an 'inert' agar slant. Growth profuse (Table VII).

(c) in the same fluid when mixed with agar making it viscous. Growth feeble.

It follows that besides the constituents of a medium its construction is also important. It also appears that though the fluid itself can sustain the amoebae, the presence of a slant leads to a remarkable increase in their growth. In order to study in what ways a slant may encourage the growth of the protozoa, investigations were undertaken using slants having different compositions. While slants in A_5 , C_1 , C_2 and C_3 combinations (Table III) caused a distinct stimulation of the growth by providing the necessary nutritive factors, the 'inert' agar slant, on the other hand, which as a rule does not contain any growth-promoting or nutritive substances, also produced a noticeable effect on the growth of the amoebae (Table VII). In what way the 'inert' agar slant itself influences the physiological activities of the amoebae is difficult to explain.

Composition of the medium: To determine how the composition of the medium influences the growth of the amoebae, the various constituents which have been used in our work, are divided into three groups, namely:

(1) *basic substances*, e.g. starch, egg albumin, serum proteins, meat extract and peptone.

(2) *accessory growth substances*, e.g. haemoglobin and vitamin B-complex.

(3) *salts*, including the buffers, e.g. NaCl, KCl, $CaCl_2$, Na_2HPO_4 , KH_2PO_4 .

Basic substances: The basic substances, enumerated above, are essential for the growth of the amoebae. They encourage the growth and also prolong the viability of the parasites by the following ways:

(i) Serving as food materials, *e.g.* starch, coagulated egg and serum albumins.

(ii) *Promoting bacterial growth and metabolism:* It is known that *E. histolytica* cannot thrive in the absence of bacteria. In what way bacteria encourage growth of the amoebae will be mentioned in a subsequent paper; it may, however, be stated now that they do so by decomposing proteins. It is interesting to note that while the growth of the amoebae is stimulated by the products resulting from the action of the bacteria on egg albumin and serum proteins, the latter substances alone are unable to support the growth of the bacteria. To accomplish the growth of the bacteria in egg albumin or serum protein solution, addition of small quantities of peptone, meat extract, nutrient broth or even serum will be needed (*vide* Table VIII). This indicates that peptone, meat extract and serum contain some substance or substances which are essential not only for stimulating the metabolic activities of the bacteria, but also for inducing the bacteria to hydrolyse complex proteins such as egg albumin and serum proteins. The increase of foetid smell and the growth of the amoebae, noticed on the addition of peptone, meat extract and serum to the basal medium (*vide* Table VI), strongly suggest that these are due to stimulation of the putrefying reactions of the bacteria.

(iii) *Lowering the E_h of the medium:* *E. histolytica* being an obligatory anaerobe, requires a strongly reduced medium for respiration. In reducing the medium, apart from the bacteria growing in it, some of its basic constituents also contribute to a great extent. This will be evident from the results noted in Tables IX and X. The tables show that while in the case of peptone, meat extract and nutrient broth the reduction was quick and strong, on the other hand, it was slow and feeble in the case of egg albumin and serum. The tables also show that the extent of reduction and the time required for this to develop varied not only with the constituents but also with the type of the bacteria employed. When the reduction is quick, strong and stable, trophozoites after inoculation in such a medium are able to thrive and multiply. In the case of egg albumin, as has been reported, the reaction is delayed, weak and unstable and as a result of this many of the trophozoites tend to succumb.

When the growth and viability of the amoebae were noticed to increase following addition of serum to the basal medium containing egg albumin as the only protein constituent, it was surmised that the growth and viability were directly the result of the action of urea, uric acid, creatinine, etc. present in the serum. It may be stated in this connexion that egg albumin alone is unable to stimulate the growth of the amoebae. As observed by Bainbridge (1911) and confirmed by us and reported in this paper (*vide* Table VIII), the proteolytic bacteria always require an 'alternate sources of nitrogen' for hydrolysing egg albumin. The urea, uric acid, etc. of the serum may perhaps serve the same purpose, *i.e.* they function as the 'alternate sources of nitrogen' and thus encourage the growth of the amoebae. This is done by stimulating the bacteria enabling them to hydrolyse egg albumin. However, in actual experiments it became manifest that urea, uric acid, etc. in the proportions as these exist in the serum are incapable of serving as the 'alternate sources of nitrogen'. This was proved by adding urea, uric acid and ammonium chloride to the basal medium.

The other explanation which may be put forward to account for the growth-promoting properties of the serum itself is by its power to reduce the substrate. Tables IX and X show that unlike peptone, meat extract, etc. serum is not a powerful agent capable of reducing the substrate. Therefore, the idea that the serum itself improves the growth of the amoebae by supplying the reducing substances, cannot be entertained.

It is difficult to explain why amino acids and cholesterol either separately or in combination with other constituents of the serum, *e.g.* urea, uric acid, etc. fail to stimulate the growth of the amoebae. It may be mentioned that it has not been possible to study the rôle of the fatty acids on the growth of the amoebae and hence whether their growth is due to the fatty acids or some unknown substances present in the serum is also difficult to say.

Accessory growth substances: It has been demonstrated that the addition either of vitamin B-complex or haemoglobin (*vide* Tables V and III) leads to a remarkable increase in the growth of the amoebae in an enriched medium.

It is known that vitamins, especially the B-complex, are synthesised by bacteria. Continuous cultivation of the amoebae in any medium in course of time affects their growth and viability. Addition of a few drops of vitamin B-complex solution at this stage always profoundly increases the growth and viability (*vide* Table V). This leads us to conclude that the growing amoebae are in need of vitamin B-complex and that the bacteria being devitalised due to prolonged subcultures fail to produce this essential requirement.

It is not possible to advance the correct explanation on the mode of action of haemoglobin in stimulating the growth of the amoebae, but it seems probable that it does so by supplying the amoebae with respiratory enzymes.

Salts and buffers: The inorganic salts are mainly responsible for the maintenance of the osmotic pressure of the culture fluid. A change in the proportion of sodium chloride from 0.9% to 0.5% does not seem to appreciably affect the growth of the amoebae. This has been reported by Mukherjea (1951 : 9) while cultivating *E. histolytica* (strain no. 1). The present observations suggest that the amoebae are normally provided with the required amounts of CaCl_2 and KCl in the culture medium, these being met from such substances as serum, meat extract and peptone. Addition of any further quantity of these salts to the medium does not serve any additional advantage.

To counteract the fall in pH, buffers are used. This is not necessary in case where the proper type of bacteria is present. When grown in E_3 medium with or without the addition of a buffer, the amoebae (strain no. 7) showed no change in their growth and viability. However, the incorporation of buffer salts would be a safeguard against changes in reaction in the event of an unfavourable type of bacteria growing with the amoebae.

SUMMARY

The important features that have emerged from the present investigations are:

- (1) Two types of *B. coli*, one saprophytic, the other intestinal, were seen growing with *E. histolytica* strain no. 7 in the culture media.
- (2) In stimulating the growth of the amoeba the constituents of a medium and its construction are equally important.
- (3) Changes in the composition of the slant and also of the fluid have profound influences on the growth and viability of the amoeba.
- (4) Some of the constituents of serum such as urea, uric acid, cholesterol, etc., fail to stimulate the growth of the amoeba.
- (5) The basic constituents of a medium such as egg albumin, peptone, meat extract, serum, etc., supply the nutritional requirements of the amoeba. They also stimulate the growth and metabolism of the bacteria and supply the reducing substances necessary for the growth of the amoeba.
- (6) Accessory growth substances such as haemoglobin, vitamin B-complex, etc., serve merely as stimulants for activating the basic constituents of the medium.
- (7) External buffers are not required if the bacteria are of the putrefactive type.
- (8) Addition of such substances as impure peptone, meat extract and serum, helps the growth and viability of the amoeba by stimulating the putrefactive process by the bacteria.
- (9) The slant of a medium serves the function of providing nutrition to the amoeba and probably increases the E_A of the medium.

ACKNOWLEDGEMENT

Grateful thanks are due to Dr. J. C. Ray, M.D., F.N.I., Director, Indian Institute for Medical Research, Calcutta, for placing all laboratory facilities at my disposal. I am indebted to the Bengal Chemical and Pharmaceutical Works, Ltd., for the supply of horse serum and to the National Institute of Sciences of India for awarding a research fellowship. Miss Kamala Chakraborty, Technical Assistant, has helped me in the most efficient manner in carrying out this work.

REFERENCES

- Bainbridge, F. A. (1911). The action of certain bacteria on proteins. *J. Hyg., Camb.*, **11**, 341.
- Mukherjee, A. K. (1951). Rôle of bacteria on the growth of *Entamoeba histolytica*. A preliminary note on studies in relation to an unusual strain of *Entamoeba histolytica*. Part I. The growth characteristics of *E. histolytica*. *Ann. Biochem. Exptl. Med.*, **11**, 9.
- (1951). Rôle of bacteria on the growth of *Entamoeba histolytica*. A preliminary note on studies in relation to an unusual strain of *Entamoeba histolytica*. Part II. The effects on the growth and viability of *E. histolytica* on inhibition of the original bacteria and on addition of new bacteria. *Ibid.*, **11**, 35.
- (1951). Rôle of bacteria on the growth of *Entamoeba histolytica*. A preliminary note on studies in relation to an unusual strain of *Entamoeba histolytica*. Part III. Detection of enzymes in the culture media. *Ibid.*, **11**, 47.

Issued September 22, 1954.

STUDIES ON THE PHYSIOLOGY OF RICE

VIII. THE EFFECTS OF LOW AND HIGH TEMPERATURE GERMINATION WITH OR WITHOUT SHORT DAYS ON SUMMER AND WINTER VARIETIES

by S. M. SIRCAR, *F.N.I.* and B. N. GHOSH,* *Department of Botany,
Calcutta University*

(Received February 12 ; read May 7, 1954)

INTRODUCTION

The effects of different temperatures and photoperiods on the flowering of summer and winter varieties of rice grown in the tropics have been reviewed elsewhere (Sircar, 1948). The results indicate marked differences in their behaviour towards the temperature of germination and day length. Thus by short day treatment of a winter variety, *Rupsail*, Sircar and Parija (1948) showed an acceleration of flowering from 133 to 47 days, a period known to be the shortest for winter rice to flower. This effect noticed only in the primary axis and the first and second tillers showing varying degree of earliness, appeared to be of varietal difference and localised in the shoot apices of the treated seedlings. Both low and high temperatures are without any vernalising effect in this variety. On the other hand, acceleration of flowering by high temperature and low temperature retardation led Ghosh (1949) to suggest that high temperature is an essential feature for the initiation of the reproductive phase in summer varieties. The short day effect in them is, however, to retard flowering or even to annul the effect of high temperature. In view of these contrasting behaviours the present investigation was undertaken to examine more critically the effects of low and high temperatures with or without short days on growth, flowering and yield of the two main crops of rice. In this paper the effects of such treatments are also discussed in the light of recent views on the physiology of flowering.

MATERIALS AND METHODS

Summer Rice.—The effects of high temperature alone and in combination with short days were studied in 1946 with two summer varieties, *Charnock* and *Panbira*. Seeds graded and sterilised, were imbibed in water to 30 per cent of fresh weight in order to sprout the embryos without radicles and plumules emerging out of the seed coat (Sircar and Ghosh, 1947). The sprouted unsplit seeds were then vernalised at 35°C. for 10 and 20 days, and sown along with the respective control in earthenware seedbed pans on April 6 and 16. One week old seedlings of three seedbeds were then exposed to 8 hours photoperiod from 8 a.m. to 4 p.m. for 4 weeks and the remaining ones allowed to grow under natural day length. After photoperiodic treatment was over the seedlings were transplanted all on the same day in pots with 15 replicates for each treatment.

In 1948 the effects of short days for 6 weeks were studied with two other varieties, *Kataktara* and *Dhairal*. Seeds were sown on April 19, and the same method of short day treatment was used in this experiment.

* At present Assistant Botanist, State Agricultural Research Station, Chinsurah, West Bengal.

The earthenware pots were filled with an equal quantity of soil dressed with one-eighth part of cowdung manure. Four seedlings were transplanted at first in each pot, after a week thinned down to two uniform plants. The data for tillering, plant height, stem length at the flowering stage, leaf number, ear emergence and grain yield were collected from randomised blocks. More important of these data were analysed statistically.

Winter Rice.—In 1947 the effects of high and low temperatures with or without short days were investigated with one winter variety, *Rupsail*.

Seeds treated as before were vernalised at 35°C. for 10 and 20 days and at low temperature, 10°C. for 5 days, and sown along with the controls between July 3 and 17. Subsequent experimental procedure was similar to that of the previous experiments.

EXPERIMENTAL RESULTS

The effects of different treatments on vegetative growth as indicated by the tillering, plant height, stem length and leaf number of both summer and winter varieties of paddy are presented in Tables I to III.

Tillering.—The influence of short day exposure, high temperature and high temperature followed by short days on tillering of four varieties of summer paddy, *Charnock*, *Panbira*, *Dhairal* and *Kataktara*, do not show any appreciable difference as compared with the control (Tables I and II). This is in conformity with the observation noted previously that there is no significant difference between high temperature treated and control plants of two summer varieties, *Dhairal* and *Thoranga*; on the other hand, pre-sowing low temperature treatment caused greater production of tillers (Ghosh, 1949). Sircar and Parija (1949) reported that pre-sowing low temperature (3°C.) treatment induced all the tillers to bear ears in the summer variety, *Jhanji*, but in *Bhutmuri* a marked depressing effect was noticed.

A tendency to increase in tillering by short days with or without pre-sowing temperature treatment is apparent in winter varieties. In *Bhasamanik* a temperature lower than the present one in combination with short days increased the tiller number considerably (Sircar and Parija) and in *Rupsail* the short day effect of increasing tillering is very marked (Sircar and Sen, 1953).

Height.—Two measurements were taken at the flowering stage; one from the surface of the soil up to the topmost leaf tip on the main shoot and another up to the base of this leaf. The first one is the plant height and the second one, the stem length. In summer varieties, *Charnock*, *Panbira*, *Dhairal* and *Kataktara*, short day treatment caused reduction of both height and stem length, while high temperature for 10 or 20 days increased both in *Panbira* and *Charnock* (Tables I and II). In two other varieties, *Thoranga* and *Dhairal*, maximum plant height at an initial stage of vegetative growth was obtained by temperature 35°C. for 25 days, while the effect of low temperature was reduction (Ghosh, 1949). It appears that the effect of short days on plant height is similar to low temperature.

Height and stem length at the flowering stage of the winter variety, *Rupsail*, show a reduction in treatments with low or high temperatures plus short days, whereas low or high temperatures alone are without any effect.

Leaf number.—It is interesting to note that in summer paddy short day treatment causes an increase in leaf number with retardation of flowering while high temperature acceleration has no effect on the leaf number (Tables I and IV). In winter paddy, *Rupsail*, short day exposure is associated with reduced leaf number and acceleration of flowering. High or low temperatures alone have no significant differences. From the results it appears that there exists a very high and significant correlation between leaf number and the time of flowering. Analyses of covariances of the data are presented in Tables V to VII. Regression and correlation coefficients to each item in the analyses are given, logarithms being used only on series 1 of *Rupsail*. Regression coefficients are, therefore, independent of the units

in which the two variables are expressed, and tend to unity as correlation increases. It is seen that the correlations are in all cases positive and significant.

TABLE I. (1946)

Tiller, height and leaf number (average of 30 plants)

Varieties.	Treatment.	Tiller No. at the flowering stage.	Height and stem length in cm. at the flowering stage.	Leaf No. on the main shoot.
CHARNOCK	<i>Series I</i>			
	Control (A)	3.0	90.8	14.4
	8 hrs. for 4 weeks (B) ..	2.9	58.9	15.5
	35°C. for 10 days (C) ..	3.2	80.3	49.8
	35°C. for 10 days + 8 hrs. for 4 weeks (D). ..	3.1	90.7	14.3
			58.9	15.8
			81.2	
			44.5	

Treatment means for the variate leaf number significant at 1% level.

D.B. > C.A.

Series II

35°C. for 20 days (E) ..	3.1	90.1	15.1
35°C. for 20 days + 8 hrs. for 4 weeks (F). ..	3.1	60.9	16.0
Control (G)	3.1	73.4	25.6
		83.6	15.2
		56.3	

Treatment means for the variate leaf number significant at 5% level.

F > G.E.

PANBIRA	<i>Series I</i>			
	Control (A)	2.4	114.9	14.5
	8 hrs. for 4 weeks (B) ..	2.9	71.6	15.8
	35°C. for 10 days (C). ..	2.9	106.7	63.2
	35°C. for 10 days + 8 hrs. for 4 weeks (D). ..	2.8	117.9	14.8
			72.8	15.7
			103.5	
			59.9	

Treatment means for the variate leaf number significant at 1% level.

R.D. > C.A.

Series II

35°C. for 20 days (E) ..	2.6	120.0	14.8
35°C. for 20 days + 8 hrs. for 4 weeks (F). ..	1.9	81.9	15.4
Control (G)	2.9	109.3	67.2
		120.5	15.1
		81.0	

Treatment means for the variate leaf number not significant.

TABLE II. (1948)
Tiller and height (average of 20 plants)

Varieties.	Treatments.	Tiller No. at the flowering stage.	Height and stem length in cm. at the flowering stage.
DHAIRAL	Control	4.8	118.3 72.8
	8 hrs. for 6 weeks	5.4	103.1 53.5
KATAKTARA	Control	4.7	119.1 76.2
	8 hrs. for 6 weeks	4.6	117.9 65.1

TABLE III. (1947)
Tiller, height and leaf number (average of 20 plants)

Varieties.	Treatments.	Tiller No. at the flowering stage.	Height and stem length in cm. at the flowering stage.	Leaf No. on the main shoot.
RUPSAIL	<i>Series I</i>			
	Control (A)	4.4	71.7 51.8	15.3
	10°C. for 5 days (B) ..	4.4	72.0 54.6	15.5
	10°C. for 5 days + 8 hrs. for 6 weeks (C) ..	4.6	49.0 29.9	8.3
	8 hrs. for 6 weeks (D) ..	5.0	48.3 22.2	8.4
Treatment means for the variate leaf number significant at 1% level. <u>A.B.</u> > <u>C.D.</u>				
	<i>Series II</i>			
	Control (E)	3.3	76.7 53.7	15.1
	35°C. for 10 days (F) ..	4.4	72.5 53.9	15.1
	35°C. for 10 days + 8 hrs. for 6 weeks (G) ..	4.6	45.9 26.1	8.2
Treatment means for the variate leaf number significant at 1% level. <u>E.F.</u> > <u>G.</u>				
	<i>Series III</i>			
	Control (H)	4.0	73.4 56.5	13.8
	35°C. for 20 days (I) ..	4.8	73.4 53.8	13.4
	35°C. for 20 days + 8 hrs. for 6 weeks (J) ..	All died.

TABLE IV

Leaf number on the main shoot (1948)

Varieties.	Treatments.	No. of leaves.	Calculated value of 't'.	't' values.	
				$p = .05$	$p = .01$
DHAIKAL	Control	13.7	7.53	2.110	2.898
	8 hrs. for 6 weeks ..	15.5			
KATAKTARA	Control	13.2	13.35	2.101	2.878
	8 hrs. for 6 weeks ..	16.0			

Ear Emergence.—The data for ear emergence of the primary axis and tillers of summer and winter varieties are recorded in Tables VIII to X.

In *Charnock* high temperature of 35°C. for 10 and 20 days induce slight acceleration of flowering in the primary axis, but the effect is not statistically significant, while in *Panbira* a significant earliness by high temperature for 20 days is observed. In all the varieties flowering is retarded significantly with increased number of leaves by short days. This retarding effect does persist even after high temperature treatment indicating that the acceleration of flowering by high temperature is completely annulled. Flowering in the tillers was similarly effected.

Regarding winter paddy, *Rupsail*, low temperature followed by short days has an accelerating effect on the flowering of the primary axis as well as the tillers, while short days alone induce early flowering in the primary axis only. The results are highly significant at 1% level.

TABLE V

*Analysis of covariance (variety 'Panbira')**Covariance of number of leaves per plant (L) and the number of days required for flowering (D)**Series I*

Sources of covariance.			D.F.	Correlation coefficient.	Regression of \bar{D} on \bar{L} .
Total	23	0.6996	5.6686
Blocks	5	0.3409	2.8248
Treatments	3	0.9081	7.5831
Remainder	15	0.3894	2.9351

Series II

Total	26	0.3827	3.9722
Blocks	8	0.4175	2.5354
Treatments	2	0.9986	26.1580
Remainder	16	-0.0277	-0.2136

TABLE VI

*Analysis of covariance (variety 'Charnock')**Series I*

Sources of covariance.			D.F.	Correlation coefficient.	Regression of <i>D</i> on <i>L</i> .
Total	59	0.6497	6.0959
Blocks	14	0.2271	2.0428
Treatments	3	0.9689	7.4892
Remainder	42	0.3231	3.0297

Series II

Total	23	0.5191	4.3679
Blocks	7	0.3180	1.9013
Treatments	2	0.9986	19.3505
Remainder	14	0.4611	1.0169

TABLE VII

*Analysis of covariance (variety 'Rupsail')**Series I*

Sources of covariance.			D.F.	Correlation coefficient.	Regression of <i>D</i> on <i>L</i> .
Total	31	0.9866	1.2900
Blocks	7	0.8740	1.2605
Treatments	3	0.9952	1.3000
Remainder	21	0.7884	1.0313

Series I

Total	31	0.9898	9.7456
Blocks	7	0.8792	10.4061
Treatments	3	0.9978	9.8470
Remainder	21	0.7594	6.6986

Series II

Total	29	0.9927	7.8619
Blocks	9	0.4501	3.4999
Treatments	2	0.9999	7.9598
Remainder	18	0.7417	3.9047

TABLE VIII. (1946)

Showing number of days for ear emergence and length of ears (average of 30 plants)

Varieties.	Treatments.	No of days from sowing to flowering.			Average length of ears (in cm.).		
		Main shoot.	1st tiller.	Second tiller.	Main shoot.	1st tiller.	Second tiller.
CHARNOCK	<i>Series I</i>						
	Control (A)	113.8	115.1	120.0	23.6	23.3	19.2
	8 hrs. for 4 weeks (B)	120.6	122.7	125.0	24.1	23.5	22.6
	35°C. for 10 days (C)	109.8	112.4	117.8	23.5	22.2	21.4
	35°C. for 10 days + 8 hrs. for 4 weeks (D)	122.1	122.3	125.3	21.9	18.1	13.6

Treatment means for the variate number of days for ear emergence of the main shoot significant at 1% level. D.B. > A.C.

<i>Series II</i>							
	35°C. for 20 days (E) ..	110.4	114.7	119.0	22.7	15.1	18.9
	35°C. for 20 days + 8 hrs. for 4 weeks (F)	126.2	125.8	128.0	21.5	22.2	..
	Control (G) ..	113.0	114.9	114.5	19.9	18.4	16.3

Treatment means for the variate number of days for ear emergence of the main shoot significant at 1% level. F. > G.E.

<i>Series I</i>							
PANBIRA	Control (A) ..	110.9	118.6	120.4	20.0	18.8	18.5
	8 hrs. for 4 weeks (B) ..	122.0	123.4	127.8	20.9	16.0	17.3
	35°C. for 10 days (C) ..	109.6	112.5	115.0	23.7	20.1	18.8
	35°C. for 10 days + 8 hrs. for 4 weeks (D)	122.7	125.8	..	23.6

Treatment means for the variate number of days for ear emergence of the main shoot significant at 1% level. D.B. > A.C.

<i>Series II</i>							
	35°C. for 20 days (E) ..	99.8	98.1	98.7	23.8	24.3	23.8
	35°C. for 20 days + 8 hrs. for 4 weeks (F)	113.4	110.0	..	22.5	23.0	..
	Control (G) ..	107.9	109.8	115.3	22.2	22.5	21.8

Treatment means for the variate number of days for ear emergence of the main shoot significant at 1% level. F. > G. > E.

TABLE IX. (1948)

Showing number of days for ear emergence and length of ears (average of 20 plants)

Varieties.	Treatments.	No of days from sowing to flowering.			Average length of ears in cm.		
		Main shoot.	1st tiller.	2nd tiller.	Main shoot.	1st tiller.	2nd tiller.
DHAIRAL	Control	108.9	108.2	111.5	23.0	22.3	22.8
	8 hrs. for 6 weeks ..	126.6	119.7	123.1	20.6	18.1	20.5

Treatments, shoots, interaction (treatment \times shoot) for the variate number of days for ear emergence significant at 1% level. $B. > F. D. > E. A. C.$

Treatment means for the variate length of ears significant at 1% level.

$A. E. C. B. F. D.$

KATAKTARA	Control	106.8	106.9	109.7	25.8	25.2	25.4
	8 hrs. for 6 weeks ..	127.8	121.7	125.7	27.1	25.9	25.7

Treatments, shoots, interaction (treatment \times shoot) for the variate number of days for ear emergence significant at 1% level. $B. F. > D. > E. C. A.$

Treatment means for the variate length of ears not significant.

A—Main shoot of control.

C—1st tiller of control.

E—2nd tiller of control.

B—Main shoot of treated plant.

D—1st tiller of treated plant.

F—2nd tiller of treated plant.

Grain Yield.—The effects of different treatments on the yield were determined by measuring the ear length, number of grains set per ear and finally the weight of the grains. The data are given in Tables XI and XII.

With retardation of flowering grain yield and the number of grains per ear has been adversely affected in *Dhairal* at 1% level, while in *Kataktara* no significant difference was noticed. The differences in the length of the ears, however, did not show marked variation from those of the respective control indicating that the treatments have little effect on ear length. A highly significant increase at 1% level in the number of empty spikelets was noticed in both the varieties indicating that to some extent short day treatment leads to the failure of grain setting. The length of ears, the number of grains and the yield were all adversely affected by short days and temperature treatments in *Rupsail* (Tables X and XI).

From the results obtained in the rice varieties an overall effect of the different treatments on grain yield may be visualised. Short days appear to reduce the yield of the summer varieties because of the failure of a large number of spikelets to form grains (Table XII). While high temperature treatment causes an increased yield together with increased number of fertile spikelets (Ghosh, 1949). Reduction of grain yield in the winter variety by short days is, however, due to the reduction in ear length and the number of total spikelets (Table XI).

TABLE X. (1947)

Showing number of days for ear emergence and length of ears (average of 20 plants)

Varieties.	Treatments.	No of days from sowing to flowering.			Average length of ears in cm.		
		Main shoot.	1st tiller.	2nd tiller.	Main shoot.	1st tiller.	2nd tiller.
RUPSAIL	<i>Series I</i>						
	Control (A) ..	126.7	127.8	128.6	19.0	18.39	16.72
	10°C. for 5 days (B) ..	125.3	127.2	128.7	17.2	17.55	16.37
	10°C. for 5 days + 8 hrs. for 6 weeks (C) ..	54.3	98.3	103.4	14.3	13.02	14.14
	8 hrs. for 6 weeks (D) ..	61.8	127.3	126.3	11.5	15.99	15.40

Treatment means for the variate number of days for ear emergence of the main shoot significant at 1% level. A. B. > D. > C.

Treatment means for the variate number of days for ear emergence of the 1st and 2nd tillers significant at 1% level. A. B. D. > C.

<i>Series II</i>						
Control (E) ..	119.8	122.1	123.0	19.3	18.19	15.97
35°C. for 10 days (F) ..	119.8	121.0	121.9	17.2	..	17.78
35°C. for 10 days + 8 hrs. for 6 weeks (G) ..	65.3	136.6	143.0	13.0	16.99	15.88

Treatment means for the variate number of days for ear emergence of the main shoot significant at 1% level. E. F. > G.

Treatment means for the variate number of days for ear emergence of the 1st and 2nd tillers significant at 1% level. G. > E. F.

<i>Series III</i>						
Control (H) ..	112.9	113.2	114.3	18.0	17.96	17.17
35°C. for 20 days (I) ..	114.3	116.8	116.8	18.5	18.48	17.93
35°C. for 20 days + 8 hrs. for 6 weeks (J) ..	All died.					

DISCUSSION

From the results presented in this paper two outstanding differences in the effects of temperature and day-length on flowering of rice varieties are noteworthy. In summer varieties pre-sowing high temperature accelerates flowering and short days delay it and even annul the acceleration by high temperature. Other workers (cf. Sircar, 1948) have also reported acceleration by high temperature in summer varieties adapted to different tropical climates. These varieties grow in different States of India under conditions of longer day-length and further increase in the day-length appears to have no effect on the flowering (Misra, 1950, 1951). They appear to be intermediate (Allard, 1938) in their day-length requirement as day-length below 10 hours retards flowering and above 13 hours is without any accelerating effect.

TABLE XI. (1947)

Grain yield and number of fertile and empty spikelets per ear

Varieties	Treatments.	Grain yield in gms.			No. of fertile spikelets.			No. of empty spikelets.		
		Main shoot.	1st tiller.	2nd tiller.	Main shoot.	1st tiller.	2nd tiller.	Main shoot.	1st tiller.	2nd tiller.
RUPSAIL	<i>Series I</i>									
	Control ..	0.710	0.486	0.370	56.6	45.4	31.3	53.4	49.5	46.9
	10°C. for 5 days	0.596	0.490	0.581	43.9	40.1	34.5	43.7	39.1	45.2
	10°C. for 5 days + 8 hrs. for 6 weeks	0.226	0.144	0.107	14.6	10.9	8.3	28.6	24.9	37.1
	8 hrs. for 6 weeks	0.139	0.280	0.196	11.6	19.1	12.6	18.8	57.3	43.9
	<i>Series II</i>									
	Control ..	0.845	0.505	0.406	62.3	41.1	31.0	71.2	67.8	50.1
	35°C. for 10 days	0.714	..	0.257	55.4	..	20.2	40.7	..	53.8
	35°C. for 10 days + 8 hrs. for 6 weeks ..	0.160	0.146	0.109	12.5	12.3	9.4	10.3	66.6	60.8
	<i>Series III</i>									
	Control ..	0.414	0.306	0.290	32.5	21.4	20.3	82.2	75.0	62.5
	35°C. for 20 days	0.597	0.531	0.328	46.8	39.2	26.7	69.2	61.1	68.8
	35°C. for 20 days + 8 hrs. for 6 weeks ..	All died.								

In winter varieties the effect of short photoperiod is different; it induces early flowering irrespective of temperature treatment which is not an obligatory factor for flowering. The short day acceleration of flowering is remarkable; in some varieties it is more than two months ahead of the natural ones. Long day combinations of even 13 hours or above are detrimental to flowering (Saran, 1945; Mukherjee, 1946), as it has been shown by Mukherjee that plants raised in February did not flower till the natural day-length decreased in October or a period of artificial short day applied.

It is interesting to note that the short day effect is diluted—it induces early flowering in the primary axis and a varying degree of earliness in the first two tillers, while later formed tillers are without any photoperiodic response. This variation in the flowering times of the primary axis and tillers has been explained by Sircar and Parija on the assumption of difference in the distribution and concentration of flower-forming substance in the stem apices formed at the time of the photoperiodic exposure. In the present work it has further been noticed that when short day is preceded by low temperature there is an acceleration of flowering in the primary shoot as well as the tillers (Table XI). The cause of this variation in flowering by short photoperiods and in combination with low temperature may be explained that low temperature stimulates early formation of tillers in the seedbeds (Sircar and Parija) and when this is followed by short photoperiods flower-forming substance synthesised in the leaves travels to the apices of the primary shoot as well as the tillers already formed before the photoperiodic exposure resulting in the

TABLE XII. (1948)

(Grain yield, and number of fertile and empty spikelets per ear)

Varieties.	Treatments.	Grain wt. in gms.			No. of fertile spikelets.			No. of empty spikelets.		
		Main shoot.	1st tiller.	2nd tiller.	Main shoot.	1st tiller.	2nd tiller.	Main shoot.	1st tiller.	2nd tiller.
DHAIRAL	Control ..	2.406	1.928	2.108	95.7	70.8	81.0	20.6	24.4	21.8
	8 hrs. for 6 weeks ..	0.903	0.895	0.882	39.3	35.3	39.6	46.1	31.1	37.8

Treatment means for the variate grain weight and number of fertile spikelets significant at 1% level. A. E. C. > B. D. F.

Treatment means for the variate number of empty spikelets significant at 1% level. B. F. D. C. E. A.

KATAKTARA	Control ..	2.693	2.398	2.340	133.8	119.3	117.7	22.9	26.0	30.7
	8 hrs. for 6 weeks ..	2.606	2.469	2.160	128.6	129.0	107.4	76.9	59.0	74.7

Treatment means for the variates grain weight and number of fertile spikelets not significant.

Treatment means for the variate number of empty spikelets significant at 1% level. B. F. D. > E. C. A.

A—Main shoot of control.
C—1st tiller of control.
E—2nd tiller of control.

B—Main shoot of treated plant.
D—1st tiller of treated plant.
F—2nd tiller of treated plant.

initiation of floral primordia, while in absence of tillering in the seedbed of short day treated plants flower-forming substance synthesised during the treatment accumulates at the growing apex of the primary shoot and accelerates its flowering. It thus appears that the short day effect on rice is different from other short day plants. In winter rye the tillers show the same behaviour as the primary shoot indicating that the whole plant is affected by the treatment (Purvis and Gregory, 1937) and in *Xanthium* (Hamner and Bonner, 1938) the photoperiodic stimulus is not only transmitted to non-induced parts of the plant, but these parts continue to produce flowers indefinitely even if the induced plant part is removed. This led Lang (1952) to consider the possibility that the photoperiodic effects are self-perpetuating. Since the tillers in rice formed after the exposure failed to show the response, and they flower only after a second dose of short day treatment (Mukherjee, 1946), it follows that the effect is localised and related to the concentration of the substance formed during the effective photoperiod, and there is no indication of the stimulus transmitted to the later formed tillers of the same plant. Taking this fact into consideration it is difficult to conceive that the photoperiodic effect in rice is self-perpetuating.

With acceleration of flowering by short days alone and in combination with the low temperature, a significant decrease in leaf number on the primary axis of

Rupsail is noticed. Between high and low temperature no significant difference is observed, while in summer paddy short photoperiods alone and in combination with high temperature increase the leaf number with retardation of flowering. From the results it appears that there exists a very high and significant correlation between leaf number and the time of flower formation (Tables V to VIII). Similar relation between leaf number and the time of flower formation has been reported by McKinney and Sando (1935) in wheat and Purvis and Gregory (1937) in Petkus winter rye. Similar to the effects of short days alone and in combination with low or high temperatures on leaf number, plant height and stem length are also appreciably reduced together with grain yield where marked acceleration of flowering is noticed. While the tillering is not reduced, on the contrary, increase in the number by short days has been reported by Sircar and Sen (1953). The decrease in grain yield is however due to the reduction in ear-length and the number of spikelets (Tables XI and XII). Leopold (1949) reported increase in tillering in winter barley with decrease in stem length. It thus appears that with the reduction of leaf number and stem length by short days, the materials for the growth of extra leaves and stem length become available for the production of more tillers.

In summer varieties, the effects of day length and temperature are different; short photoperiods alone and in combination with high temperature reduce plant height, stem length and grain yield, but the total number of leaves on the main shoot is increased and the flowering retarded. On the other hand, high temperature induces early flowering with increased grain yield. In these varieties the short day effect in addition to delay in flowering leads to the reduction in the number of spikelets and a large percentage of failure of grain formation (Table XII). It is not possible without further work to say precisely how short days cause a large number of spikelets empty. Since the ear emergence has taken place and a large number of spikelets found empty, it follows that flower initiation and floral organisation have taken place, possibly the floral maturation consisting of the differentiation of sporogenous tissues or pollen or embryo-sac development has been adversely affected by short days.

In recent years considerable attention has been paid to study the physiology of flowering. Based on the general features of vernalisation and photoperiodism several possibilities have been suggested by workers in this field to explain the changes from vegetative to flowering state. Two recent reviews by Sen (1951) and Lang (1952) have presented the problem in greater detail. The points at issue are how far these hypotheses can explain the peculiarities noticed in rice plant.

Cajlachjan's hypothesis (1937) on the formation of a transmissible stimulus-florigen has been further elaborated by Lang (1952) with several arguments. One important consideration in this is that the substance is self-perpetuating. But the substance is not in rice has been argued before. It has been suggested by a group of workers (Lang, 1952) that the effect of day length consists not in the formation of flower-promoting substance under inductive condition but in the formation of flowering-inhibiting substances under non-inductive conditions. These inhibiting substances are identified with auxins, and photoinduction involves the production of anti-auxins. But Leopold and Thimann (1948, 1949) have shown that the auxins may not be acting simply in opposition to flowering but number of flowers increased by low concentration of auxin and in pineapple flowering is induced by auxin (Clark and Kerns, 1942). Certain considerations from the behaviour of rice plant are contrary to this assumption. On the basis of the formation of growth inhibiting substances during non-inductive condition it would be difficult to explain the fact that only the main shoot of rice plant flowers under short day exposure but when the tillers after short day exposure kept in long day for more than one month did not flower; flowering was, however, noticed in these tillers after four days short day exposure (Mukherjee, 1946). If the flower-inhibiting substance is formed in the non-inductive condition, the long day exposure would lead to large

accumulation of this substance in the tillers. It is very unlikely that short day exposure of the tillers for 4 days would neutralise all the accumulated inhibiting effect and flowering initiated. In earlier papers from this laboratory attempts have been made to explain the behaviour of the tillers on the assumption that some substance is formed under inductive condition and the subsequent behaviour of the tillers is related to the concentration of this substance. Whether this is a flowering hormone or something else is not possible to say with the data at hand. To elucidate this further work is in progress in this laboratory.

SUMMARY

The effects of high and low temperature during germination with or without subsequent short day exposure of seedlings on tillering, height, leaf number, ear emergence, number of fertile and empty spikelets in summer (*Aus*) and winter (*Aman*) varieties of rice have been investigated.

In summer varieties low temperature treatments are without any acceleration of flowering. High temperature accelerates flowering but short days delay it and annul the high temperature acceleration. On the other hand, short day induces early flowering of the winter variety, acceleration being noticed in the primary axis only, but when short day exposure is preceded by low temperature flowering is accelerated in the primary shoot as well as the tillers. Low and high temperatures alone do not seem to have any influence on the flowering of the winter variety.

Associated with the acceleration of flowering there occurs a reduction in leaf number, while in summer varieties short days increase the number. Height and stem length are reduced both in summer and winter varieties by short days with or without low temperature treatment. High temperature, on the other hand, has increased the height and stem length. The effects on tillering are different; the number is not reduced, on the contrary, an increase by short day or low temperature treatment has been reported.

Short days appear to reduce the grain yield both in summer and winter varieties; the reduction in summer varieties is due to the failure of a large number of spikelets to set grains, while in winter variety reduction is associated with decrease in ear length.

The results with rice plant have been discussed in the light of recent views on the physiology of flowering.

The cost of this investigation was met from a grant-in-aid from the Indian Council of Agricultural Research, New Delhi, for which we express our sincere thanks to the Council.

REFERENCES

- Allard, H. A. (1938). Complete or partial inhibition of flowering in certain plants when days are too short or too long. *Jour. Agri. Res.*, **57**, 775-789.
- Cajlachjan, M. H. (1937). On the Hormonal theory of plant development (Russian). *Cf. Bot. Gaz.*, **100**, 1938-39, 245.
- Clark, H. E. and Kerns, K. R. (1942). Control of flowering with phytohormones. *Science*, **95**, 536-537.
- Ghosh, B. N. (1949). A study on vernalization of rice by temperature treatments. *Jour. Ind. Bot. Soc.*, **28**, 124-133.
- Hamner, K. C. and Bonner, J. (1938). Photoperiodism in relation to hormones as factors in floral initiation and development. *Bot. Gaz.*, **100**, 388-431.
- Lang, A. (1952). Physiology of flowering. *Annual Review of Plant Physiology*, **3**, 265-306.
- Leopold, A. C. and Thimann, K. V. (1948). Auxin and flower initiation. *Science*, **108**, 664.
- (1949). The effect of auxin on flower initiation. *Amer. Jour. Bot.*, **36**, 342-347.
- Leopold, A. C. (1949). The controlling of tillering in grasses by auxins. *Amer. Jour. Bot.*, **36**, 437.
- McKinney, H. H. and Sando, W. J. (1935). Earliness of sexual reproduction in wheat as influenced by temperature and light in relation to growth phases. *Jour. Agri. Res.*, **51**, 621-641.
- Misra, G. D. (1950). Effect of photoperiod on the flowering time of two late varieties of paddy. *Cur. Sci.*, **19**, 126-127.
- (1951). Photoperiodic response in some early varieties of paddy. *Ibid.*, **20**, 209-210.
- Mukherjee, S. K. (1946). Effects of the time of sowing and the application of photoperiods on different sowings. M.Sc. thesis, Calcutta University.
- Purvis, O. N. and Gregory, F. G. (1937). Studies in vernalization of cereals. I. A comparative study of vernalization of winter rye by low temperature and by short days. *Ann. Bot.*, **N.S.**, **1**, 569-591.
- Saran, A. B. (1945). Studies on the effect of short and long day treatment on the growth period and the flowering dates of different paddy varieties. *Jour. Ind. Bot. Soc.*, **31**, 153-161.

- Sen, S. P. (1951). The biochemical aspects of flowering. *Bull. Bot. Soc., Bengal*, **5**, 87-113.
- Sircar, S. M. (1946). Studies in the physiology of rice. III. Vernalization by short days (A preliminary report). *Proc. Nat. Inst. Sci.*, **12**, 191-198.
- Sircar, S. M. and Ghosh, B. N. (1947). Effects of high temperature and short days on vernalization response of summer varieties of rice. *Nature*, **159**, 605.
- Sircar, S. M. (1948). Vernalization and photoperiodism in the tropics. (In Vernalization and Photoperiodism. Lotsya, Vol. 1. *Chronica Botanica*, Co., Waltham, Mass., U.S.A.)
- Sircar, S. M. and Parija, B. (1949). Studies in the physiology of rice. V. Vernalization and Photoperiodic response in five varieties. *Proc. Nat. Inst. Sci.*, **15**, 93-107.
- Sircar, S. M. and Sen, S. P. (1953). Studies on the Physiology of rice. VI. Effect of Photo-periods on the development of the shoot apex. *Bot. Gaz.*, **114**, 436-448.

Issued September 27, 1954.

FISH GEOGRAPHY OF THE HIMALAYAS *

by A. G. K. MENON, Assistant Zoologist, Zoological Survey of India, Calcutta

(Communicated by S. L. Hora, F.N.I.)

(Received April 15 ; read August 6, 1954)

CONTENTS

	Page
Introduction	467
Physical features and description of localities surveyed	
1. Structural features	468
2. Himalayan rivers and localities surveyed	469
(a) The Brahmaputra and its tributaries	470
(b) The Ganges and its tributaries	470
(c) The Indus and its tributaries	478
Evolution and distribution of torrential fishes of the Himalayas	478
Factors governing the dispersal of torrential fishes	479
Palaeogeography of the Himalayas as evidenced by the distribution of fishes	480
Probable sequence of migration along the Himalayas	490
Summary	491
Acknowledgements	492
References	492

INTRODUCTION

In 1937, Hora in two papers dealt with certain aspects of the zoogeography of the Himalayas and broadly discussed the distribution of torrential fishes on such data as were then available. It seems to be a well recognised fact concerning the distribution of all groups of animals that the fauna along the Himalayas becomes poorer and poorer as we go towards the west and the large assemblage of the so-called Malayan forms found in the Brahmaputra watershed and the Assam Hills reappears again in the hills of Peninsular India, but not to any appreciable extent to the west of the Brahmaputra drainage. As a result of extensive field surveys along the Vindhya (Hora, 1949), the Satpuras (Hora and Nair, 1941), the Peninsular India (Hora, 1944) and the Orissa Hills and the Eastern Ghats (Menon, 1951) it has now been established that the route of migration of the Malayan elements in the freshwater fish fauna of India lay along the Assam Hills and the Vindhya-Satpura trend of mountains across the Garo-Rajmahal Gap during periods of Pleistocene glaciation when the sea-level fell by several hundred feet (Hora, 1951). The systematic studies of the Peninsular isolates *vis-à-vis* the Malayan forms have shown that this migration has been accomplished through four waves during the Pleistocene epoch (Silas, 1952). In this paper, an attempt has been made to analyse in detail the composition of the Himalayan fish fauna in order to demarcate the extent of penetration of the Malayan fauna † along the Himalayas, the barriers that obstructed its westward migration and the approximate age of such events.

* Published with the kind permission of the Director, Zoological Survey of India, Calcutta.

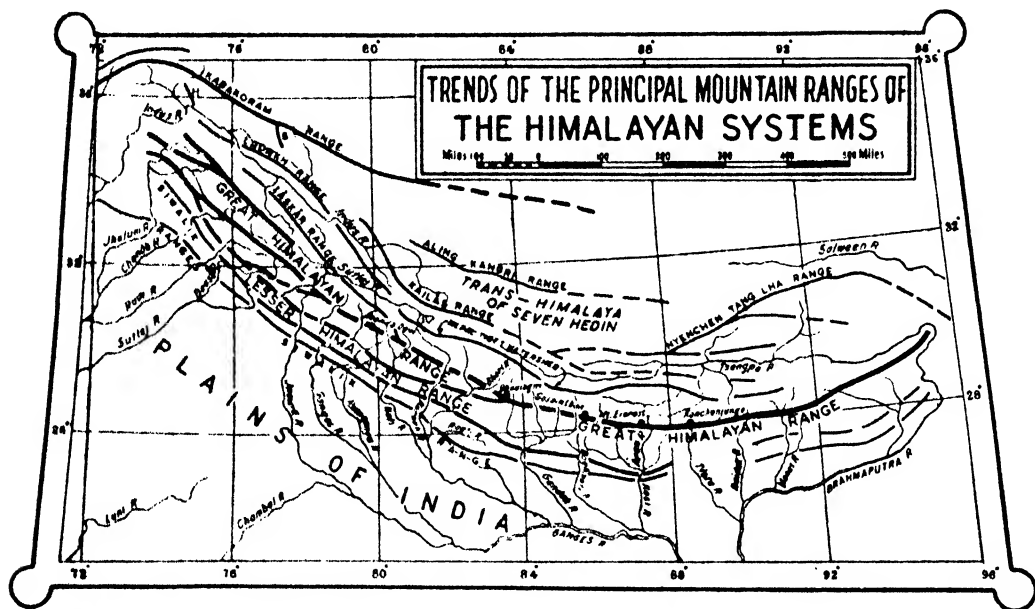
† As for palaeogeographical and zoogeographical studies, widely distributed species cannot be of any very great help, only fishes normally living in fast currents of rocky streams have been taken into consideration.

PHYSICAL FEATURES AND DESCRIPTION OF THE AREAS SURVEYED

(1) *Structural features*.—The Himalayas extend between latitudes 28° N. and 36° N. and longitudes 72° E. and 96° E. This segment is a complete mountain rampart, convex towards the south, the orientation of its western extremity being generally N.W.-S.E. and that of eastern extremity being W.S.W.-E.N.E. The great chain of Himalayas is 1,600 miles long and the total width varies between 90 miles and 250 miles. Geologists believe that greater part of this vast tract was under the waters which was the eastern extension of the Mediterranean sea—the Tethys—from the end of the Carboniferous period to the end of the Eocene*.

The Himalaya is the 'Youngest, largest and highest chain of mountains in the world, a chain that is probably still growing in altitude'. On the Himalayan region, 'overfolding, faulting, thrusting, contortion and recumbency'—all the accompaniments and causes of mountain building—are to be observed and date mostly from Tertiary or later times.

Himalayas comprise a series of parallel mountain ranges—the Himalaya proper and the Zaskar, Ladakh and Kailas ranges. The Aling Kangri and the Karakoram ranges lie further north.



TEXT-FIG. 1. Trends of the Principal mountain ranges of the Himalayan systems. (After Burrard and Hayden, 1933.)

The Himalayan region may be divided into four zones on the basis of its geology and geography (Pascoe, *loc. cit.*, p. 14). These are longitudinal zones parallel to their length—from north to south: (1) the Tibetan Himalaya, (2) the Great Himalaya, (3) the Lesser Himalaya and (4) the Sub-Himalaya†. The outer

* Writing about the age of the Himalayas, Oldham observed that 'the occurrence of marine nummulitic beds at a height of many thousand feet on the northern face of the main snowy range in Hundes, and at a height of 20,000 feet in Zaskar, shows that the elevation of this part of Himalayas must have taken place entirely within the tertiary period'. Dr. Blanford also arrived at the same conclusion basing his arguments on geological and faunistic evidences (Pascoe, 1950).

† The three-fold division of the Himalayan system is also correct in which the Tibetan Himalaya is excluded. On this zone, i.e., the Tibetan Himalaya, only the influence of the Himalayan movements can be detected (*vide* Krishnan, 1943, p. 142). Stratigraphically and

belt of the foot-hills, known by different names in different sections, as the Duars and the Siwaliks, is occupied by Tertiary sandstones and clays. The Great Himalayan zone is a complex of crystalline rocks—igneous rocks, granite and pegmatites. The foot-hill zone is about 25 to 30 miles wide with an average height of about 3,000 feet. The Lesser Himalayan zone, lying north of the foot-hill zone, has an average altitude of 10,000 feet and a width of 40 to 50 miles. The Great Himalayan zone consists of a great line of snow-clad peaks and the average height is about 20,000 ft.

From the geographer's point of view, both altitude and longitude (west to east) are significant as differences in both altitude and longitude can be correlated with differences in geographical landscapes. Altitudinally, 'temperate, but still ever-green forests' with oak as the prevailing tree are to be found above 5,000 feet, this succeeding the tropical forest below 5,000 ft.; coniferous forest dominates above 9,000 ft. while near about 12,000 feet lie the alpine meadows. Longitudinally, the Himalayan zone can be divided into the drier west and the humid east. This west-east division is based on the differences in length and intensity of rainy season and natural vegetation. On the east are to be found dense jungles and humid forests with sal (*Shorea robusta*) while the west is characterised by 'dry monsoon type of forest—xerophytic—with the dhak replacing the sal. The zone between 78° and 82° longitudes is the transitional zone between the west and the east, but no detailed study of this zone has yet been carried out to draw the exact boundary between the two zones.

Biologically the limits of the Himalayas are governed by climatological considerations. Rainfall, temperature, humidity, etc. are important factors governing the distribution of plant life, and the dispersal of animal life is dependent on that of the flora. Thus the hills of Assam, though geologically much older as representing a part of Peninsular India, are climatically very similar to the Eastern Himalayas and would thus faunistically be included as parts of the Himalayas for the purpose of this paper.

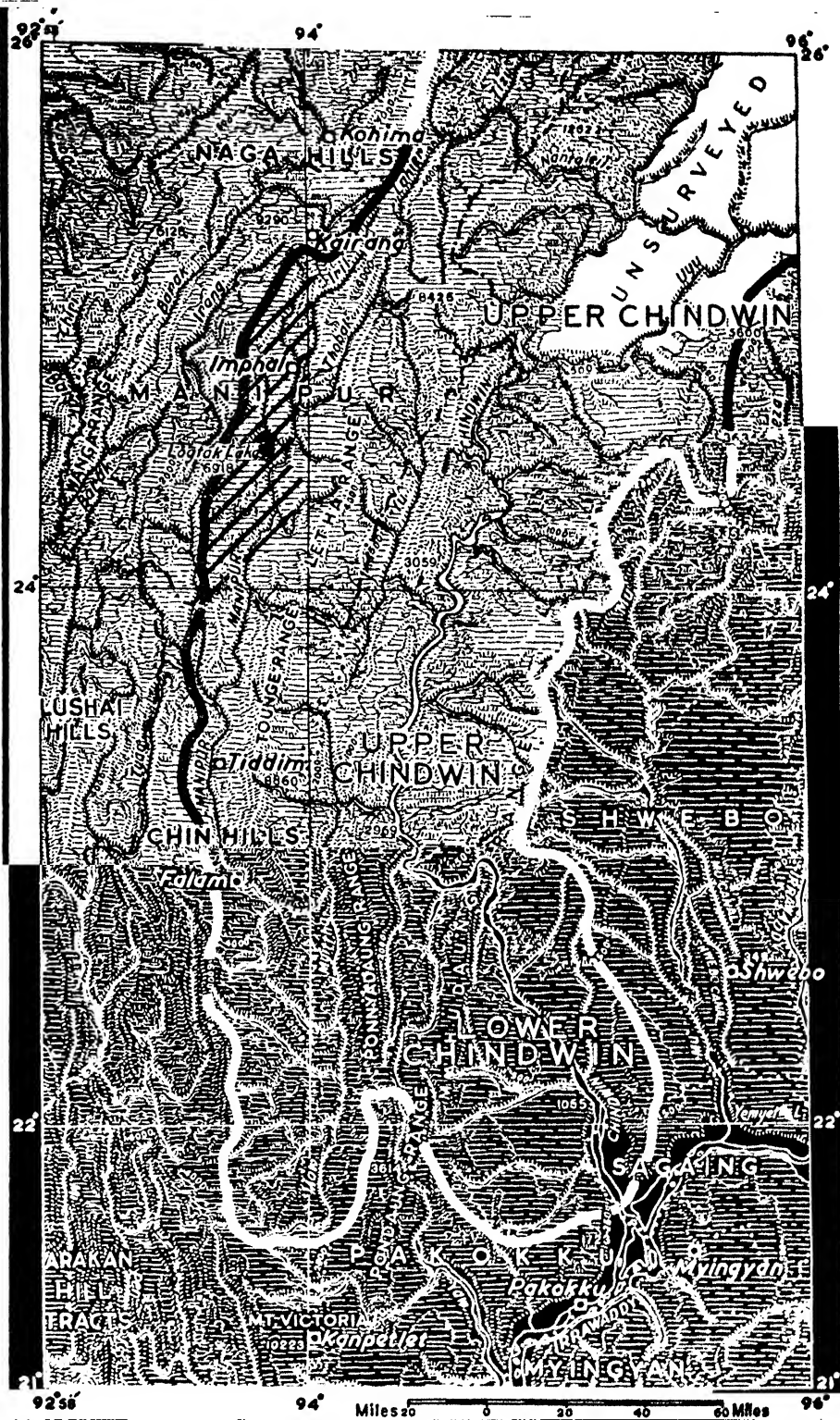
In dealing with the distribution of fishes along the Himalayas some knowledge of the present-day watersheds is necessary as dispersal of torrential fishes can only take place if connections between watersheds take place at some period or another.

(2) *The Himalayan rivers and localities surveyed.*—The Himalayan region is drained by two principal river systems: the Indus and the Ganges. The Ganges is connected with the Brahmaputra and the Meghna; hence the Ganges system may be taken to include the rivers of Assam also.

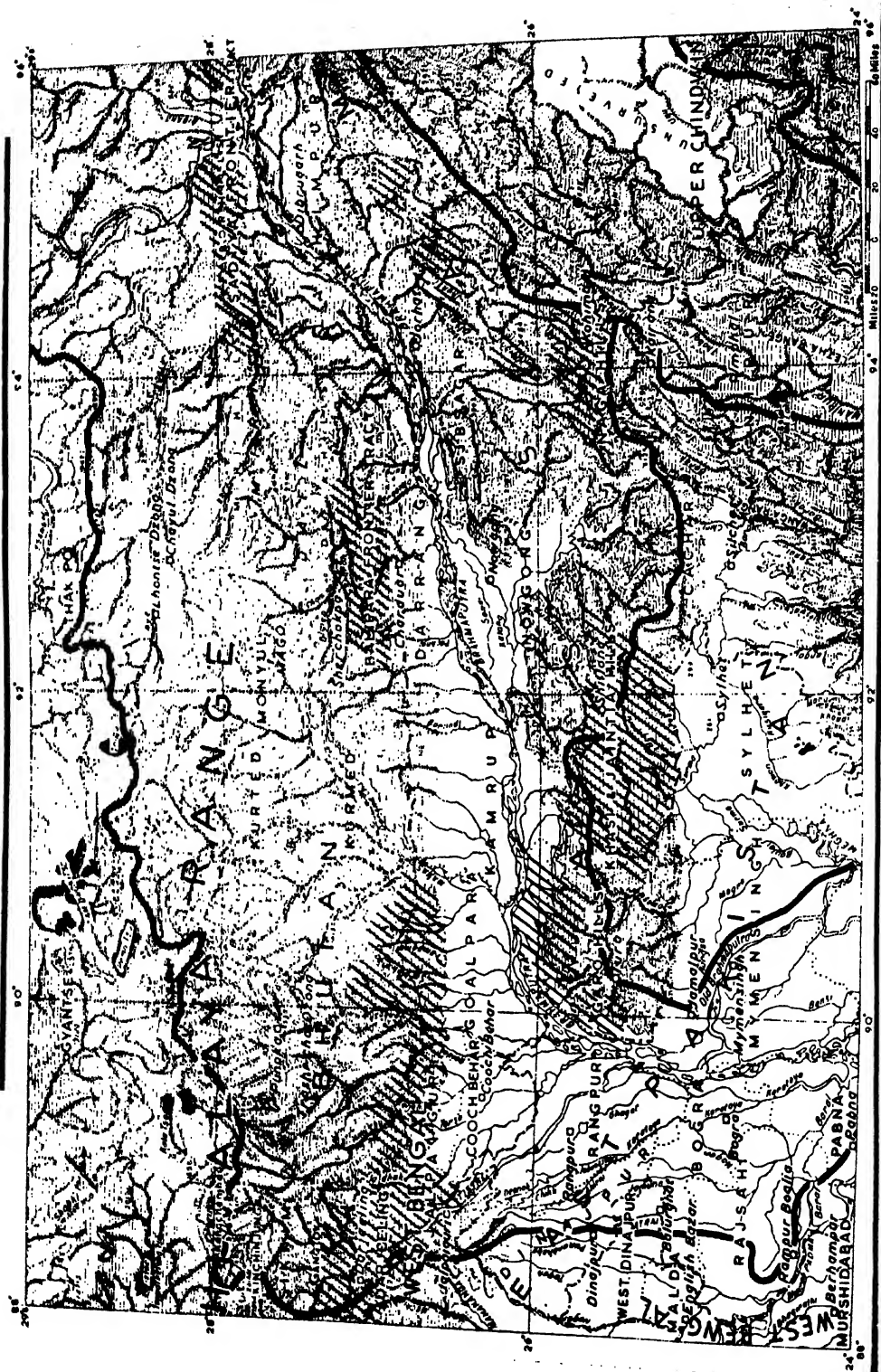
For descriptive purposes the Himalayan rivers can be divided into four groups. Burrard *et al.* (1933) have selected for the dividing lines of the Himalayan range the Tista, the Kali and the Sutlej. The rivers of the eastern section between Brahmaputra and Tista are grouped as the rivers of the Assam Himalayas, the next group between the Tista and the Kali, the Nepal Himalayas, the third between the Kali and Sutlej, the Kumaon and the last, west of the Sutlej, the Punjab Himalayan rivers.

In this classification the Tista has been considered as one of the Assam rivers although it does not drain the Assam Himalayan region. The Brahmaputra is the greatest river of Assam and since the Tista flows into it, as do all the other Assam rivers, it has been included among the rivers of the Assam Himalayas. Zoogeographically also the inclusion of Tista along with the Assam Himalayan rivers is sound as most of the Assam Himalayan forms, especially of the fish fauna, are found in the Tista drainage system. In the above classification, the Kali has been included with the rivers of the Kumaon Himalayas and the Sutlej with the Punjab.

orographically the Tibetan Himalaya may be included in the Himalayan group, but not geographically, i.e., on the basis of climate, vegetation, altitude and human responses to environment.



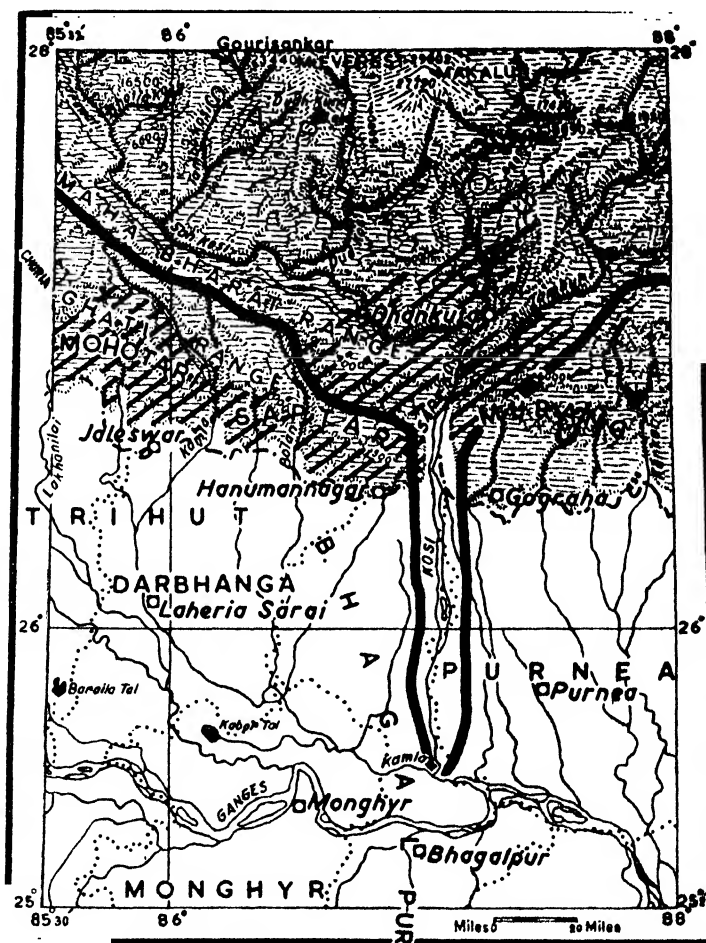
TEXT-FIG. 3. Map of the hill-ranges of Assam showing the localities in which the fishes were collected. The stripes represent the area surveyed. The area drained by the Chindwin is marked by thick black line.



TEXT-FIG. 4. Map of the Himalayan area drained by the Brahmaputra (indicated by thick black line) showing localities in which fishes were collected. The stripes represent the areas surveyed.

Zoological Survey of India in November, 1947, January-February, 1948 and April, 1948 (Menon, 1949).

The Kosi provides a typical example of the westward drift of the Himalayan rivers referred to earlier. It may be mentioned that in the early part of the 18th century, the Kosi flowed below the town of Purnea but it has gradually worked westwards across 75 miles of the country as is evidenced by its deserted channels (Chibber, 1949, pp. 4-5). The large commercial town of Nathpur, from where Hamilton collected several species of fish from the Kosi river, was several miles to the west of the river even up to 1850 but it has not only been washed away but the site of its ruins now lies many miles to the east of the river.

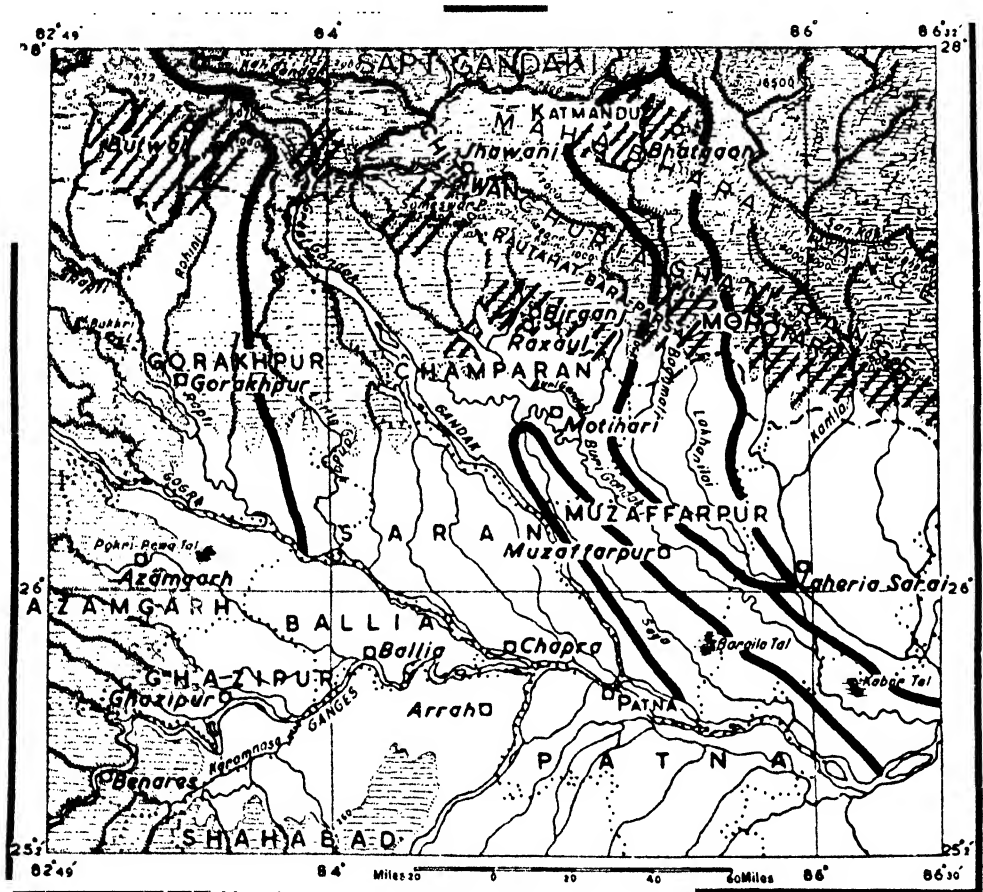


TEXT-FIG. 5. Map of the Himalayan area drained by the Kosi (indicated by thick black line) showing localities in which the fishes were collected. The stripes represent the areas surveyed.

This westward movement of the Kosi is also very strongly marked in its fish fauna as it shows a very close affinity to that of the Tista river, Eastern Himalayas and the Assam hills (Menon, *op. cit.*). This is suggestive of the fact that some of its earlier tributaries must have drained the region of the Darjeeling Himalayas and are now probably the feeder systems of the Tista river.

To the west of Kosi, the next important Himalayan river is the Gandak which drains the area between longitudes 83° 28' and 85° 32' E. It rises from the central

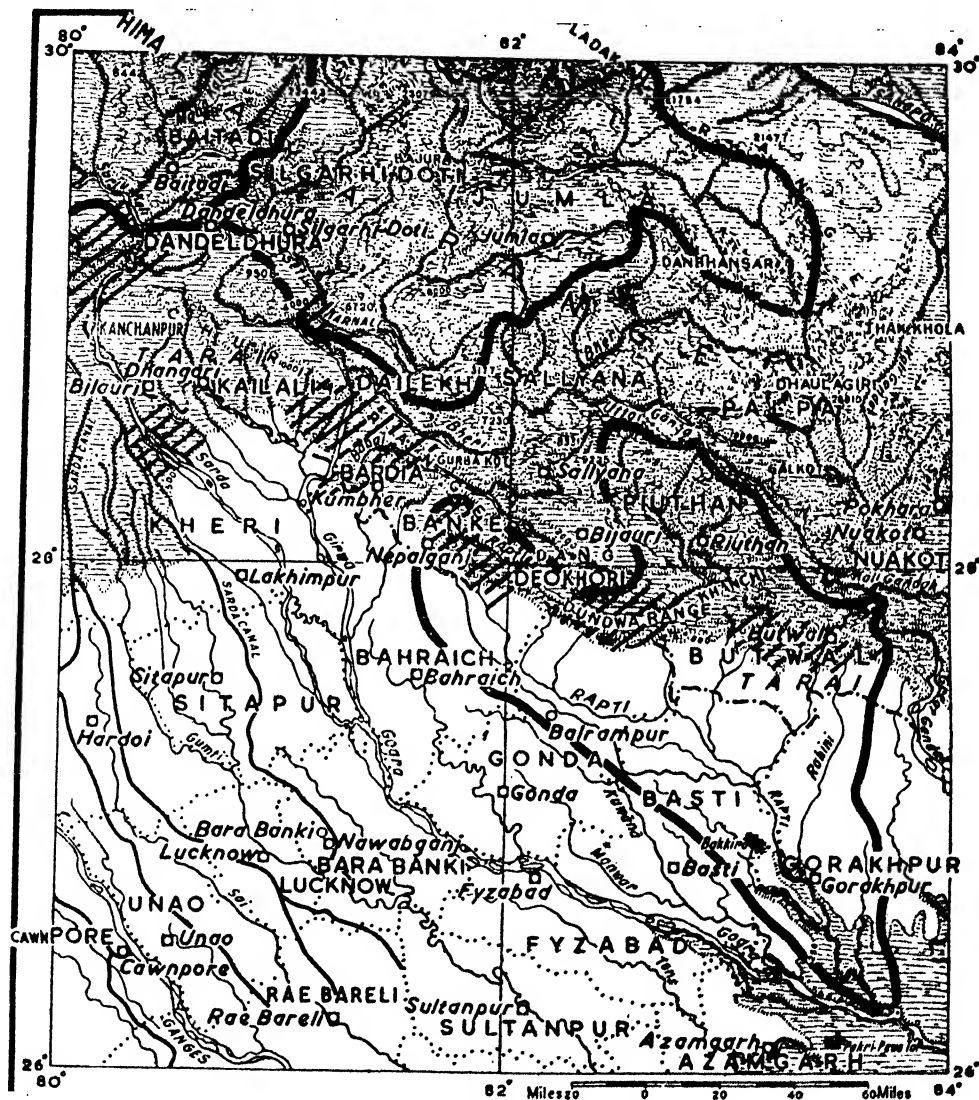
mountain basin of Nepal and flows southwards in a series of rapids, and finally leaves the mountain ranges at Tribeni, near Someswar hills, where it is joined by two of its major tributaries. On entering the plains, it flows for a short distance over a rocky bed between high banks covered with thick forests. The places from where fish collections were made by a party of officers of the Zoological Survey of India in January, 1948, by the author in February-March, 1949, and also places surveyed and recorded in literature (Hora, 1937a) are shown in Text-fig. 6. The fish fauna of the Gandak also shows a strong affinity to that of the Assam Himalayas thereby indicating that at some time or other there must have been some sort of intermingling of the drainage systems of the Gandak and that of the rivers to the east of it.



TEXT-FIG. 6. Map of the Himalayan area drained by the Baghmata and the Gandak (indicated by the thick black line) showing localities in which the fishes were collected. The stripes represent the areas surveyed.

The Rapti, the Karnali and the Kali (Text-fig. 7) are the next three important tributaries of the Ganges, west of the Gandak. They drain the Himalayan area between longitudes 80° and 83° 40' E. The Rapti takes its origin in the lower ranges of the Himalayas in the Nepal territory and after flowing through Nepal for about a hundred miles enters the Bahraich district in U.P. It then flows in a sinuous course through the districts of Bahraich, Gonda, Basti and Gorakhpur, and finally joins the Gogra near the village Barhaj Bazar in Gorakhpur district. It

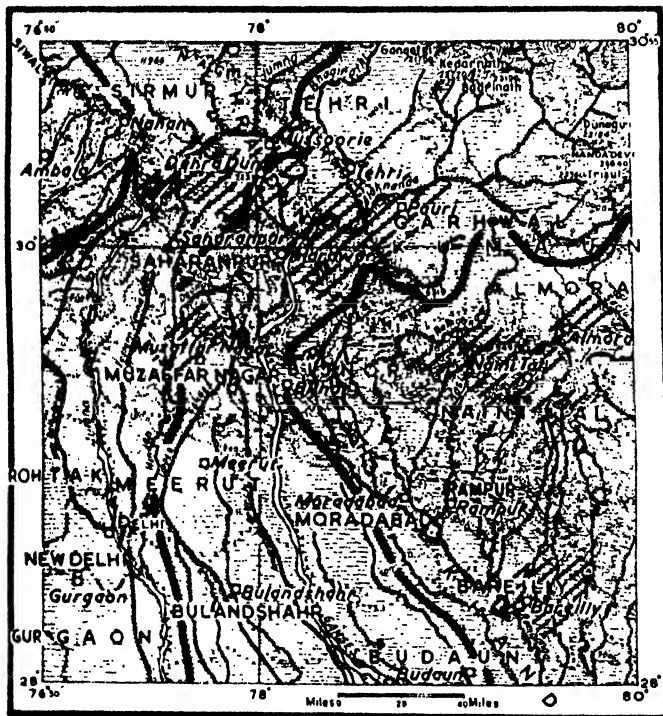
flows for the most part in a deep channel. Fish collections were made by the author at various places in February, 1949, camping at Gorakhpur in U.P. and Butwal and Nepalganj in the Nepal territory. The places of collection are marked in Text-fig. 7.



TEXT-FIG. 7. Map of the Himalayan area drained by the Rapti, Karnali and Kali (indicated by thick line) showing the localities in which fishes were collected. The stripes represent the areas surveyed.

The Karnali has a trans-Himalayan source and drains the trans-Himalayan trough of about 200 miles in length, between Gurla Mandhata and Diji pass, by two affluents, one flowing E.S.E. and the other W.N.W. The main river after receiving waters from all its tributaries runs due south and branches into the Kauriala and the Girwa in the plains. Both these branches are rapid flowing violent rivers with beds strewn with big boulders. After a course of about 30 miles, these rivers reunite near village Birthapur in Bahraich district in U.P. to form the Gogra. Collections were made in the Girwa as well as the Kauriala at various localities by the author in March, 1949.

The Kali is formed by two main streams called the Mahakali and the Sarju Kali. The Mahakali originates in the high ridge that separates Almora and Nepal from Tibet, the Sarju rises on the eastern side of the Nandakot peak and flows south-eastwards through Almora to the Mahakali at Rameshwar (Nevilli, 1905). The joint stream which is generally known as Kali flows southwards and finally leaves the mountain ranges near Tanakpur under the name of Sarda. Like the Kauriala and the Girwa, the Sarda also is a very rapid flowing, violent river with its beds strewn with big boulders brought down from higher reaches in the Himalayas. The fish collections from the Kali river were made by the author at Tanakpur at a place where the river leaves the hills and enters the plains. At the time of the visit by the author there were a large number of rocky pools in the beds of the river from where good collections of fish could be easily made after treating the water with bleaching-powder. The fish fauna of the Rapti, Karnali and Kali also indicates a close relationship of these drainage systems to that of the rivers in the Eastern Himalayas and further east.

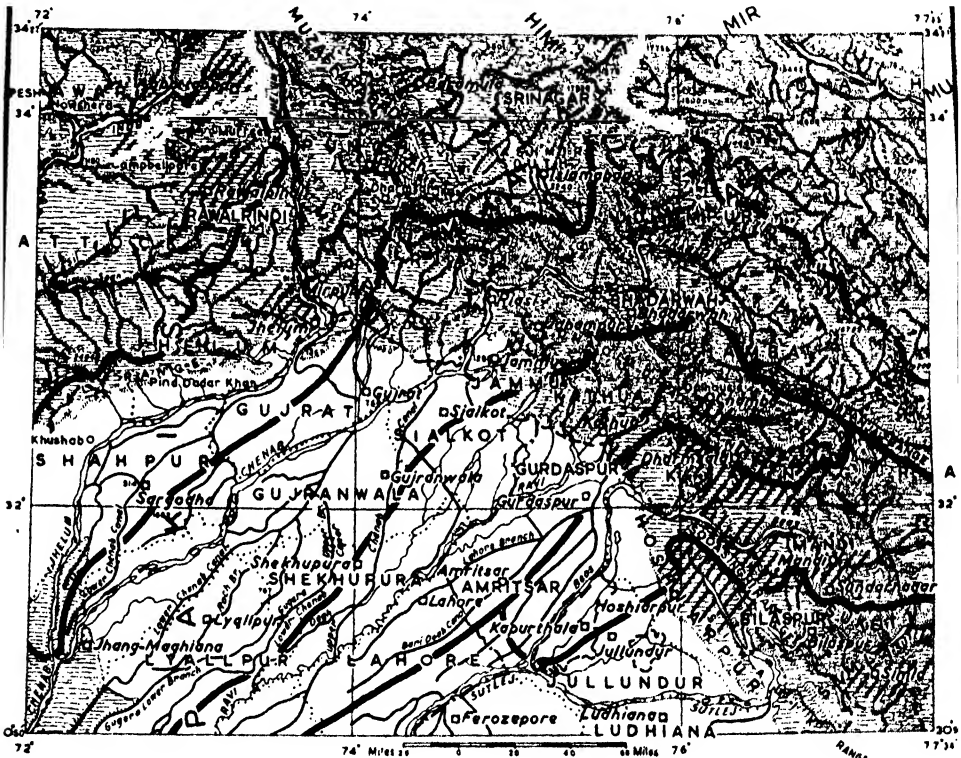


TEXT-FIG. 8. Map of the Himalayan area drained by Ramganga, Ganges and Jumna (indicated by thick line) showing the localities in which fish were collected. The stripes represent the areas surveyed.

The Ramganga, the Ganges and the Jumna (Text-fig. 8), the principal rivers of the Kumaon and Garhwal Himalayas, drain the Himalayan area between longitudes $78^{\circ} 35'$ and 80° E. The Ramganga is the smallest of these rivers draining the outer Himalayan range of Kumaon; its base is triangular in shape because the rivers on either side of it, the Ganges and the Kali have converged in all their branches in order to pierce the outer ranges and thus leaving only a small intermediate area undrained. The principal affluents of the river are the Kosi, Nandhapur and Kalaunia. These tributaries of the Ramganga drain the whole of the Nainital and Almora districts in U.P. from where extensive collections were made by

Messrs. E. O. Shebbeare and M. P. Bhola (Hora, 1937b, pp. 338-48) and by the author in May-June, 1948 (Menon, 1949a).

The name Ganges, regarded as a Himalayan river, is applied to the particular affluent that issues from the mountains at Hardwar. The two important Himalayan branches of the Ganges are the Alaknanda and the Bhagirathi. They drain the area lying between longitudes 78° and 80° E. The Alaknanda rises to the north of Badrinath and flows south-west to Nandaprayag and thence turns west as far as Rudraprayag where it receives one of its affluent, the Mandagiri. From the confluence of Mandagiri it turns south and flowing past Srinagar is joined by Bhagirathi at Deo-prayag to form the Ganges.



TEXT-FIG. 9. Map of the Himalayan area drained by the Indus (areas drained by the various tributaries, the Sutlej, the Beas, the Ravi, the Chenab and the Jhelum being marked by thick lines) showing the localities in which fish were collected. The stripes represent the areas surveyed.

The Alaknanda has an average breadth of about 35 to 40 yds., but at one place before its confluence with the Mandagiri it narrows down very much and rushes through a cut in the rocks which rise high up perpendicularly on either side (Walton, 1910). Here the river flows with very great force over a bed of big boulders. From this point the river again broadens out and flows over a succession of long reaches between it and Deo-prayag with intervening short rapids. At Deo-prayag the river again narrows down to almost half its proper breadth before it is joined by Bhagirathi. A representative collection of fish from the headwaters of the Ganges, especially from the narrowed down portion of the Alaknanda above Srinagar, was made by Babu Gonur Singh, Collection Tender of the Zoological Survey of India. The localities from where fish collections were either examined by the author or referred to earlier in literature are marked in Text-fig. 8.

The Jumna takes its origin in the south-western slopes of Bandarpunch which is the main watershed between Ganges and Jumna. Behind the Mussoorie hills, the Jumna is joined by its tributary, the Tons, which drains the area between Bandarpunch and Chor peak. It then pierces the Mussoorie range and a little further down is joined by the Giri river which drains the area between Simla and the Chor peak. The Jumna drains the Himalayan area between longitudes $77^{\circ} 35'$ and $78^{\circ} 35'$ E. from where extensive collections of fish were made by Hora and Mukerji in 1935 (Hora and Mukerji, 1936).

The Jumna is said to have flowed westwards from Karnal straight to sea in former days. In course of time, it took a more and more easterly course and ultimately merged into the Ganges at Prayag (Krishnan, *loc. cit.*, p. 25).

(c) *The Indus and its tributaries.*—The Indus and its tributaries drain the westernmost part of the Himalayas between longitudes 72° and $77^{\circ} 35'$ E. The Jhelum, Chenab, Ravi, Beas and Sutlej are the five great tributaries of the Indus; they take their origin in the Himalayas and after traversing the Punjab unite to form the Panjnad and falls into the Indus. Extensive collections of fish from the Punjab Himalayas were made at different times by the members of the Zoological Survey of India and the localities from where they were made are shown in Text-fig. 9.

The east-west movement of the Himalayan rivers referred to earlier is evident in the Punjab rivers also. There is evidence to show that during historic times, the Sutlej flowed through Rajputana into the sea independently of the Indus. In fact it was only during the 11th century that the Sutlej became confluent with the Beas and flowed the latter's channel deserting its own (Wadia, 1938, p. 391). All the other rivers also have repeatedly shifted their channels. The Chenab and the Jhelum joined the Indus at Uch in the 16th century; now the confluence is at Mithankot, 60 miles down-stream. Multan was then situated on the Ravi, but now it is 36 miles to the east of its combined waters with the Chenab. Likewise, there is also evidence to show that the Indus flowed more than 80 miles to the east of its present course into the Rann of Cutch which was then the gulf of the Arabian Sea (Wadia, *op. cit.*).

EVOLUTION AND DISTRIBUTION OF TORRENTIAL FISHES OF THE HIMALAYAS

With the exception of the remains of a Schizothoracine fish, *Schizothorax oreinus*, described by Hora (1937c) from the Karewas of Kashmir, no other torrential fish is known in a fossil state from the Himalayas, though forms like *Silurus* and *Bagarius*, which live in somewhat deeper, clearer and cold waters at the bases of hills are known from the Upper Siwalik rocks (Hora and Menon, 1953). The Karewas of Kashmir are believed to be the Second Interglacial period, which lasted from approximately 440,000 to 250,000 years ago. It would thus appear that the typical torrential fauna of the Himalayas is not older than the Pleistocene. In this connection it is interesting to point out that one of the major upheavals of the Himalayas took place at the end of Pliocene or at the beginning of the Pleistocene (Krishnan, 1952, p. 46). This and the subsequent orogenic movements would seem to have been responsible for the evolution of the typical Himalayan fauna during the various stages according to the location and intensity of these movements.

Hora (1954) has explained that the evolution of the Schizothoracinae probably occurred during the First Interglacial period when, with the melting of the snow, turbulent streams must have been formed in Central Asia necessitating the reduction of scales characteristic of the Schizothoracinae. Since primitive forms of the sub-family occur today in South China (Hora, *op. cit.*), it is presumed that they originated there probably during the First Interglacial period. During the favourable ecological conditions of the Second Glacial period and east-west drainage they migrated westwards as far as Kashmir or even Seistan. The great proliferation of genera

and species of the Schizothoracinae probably occurred during the Second and subsequent Interglacial periods. Today the Schizothoracine fishes are mainly Central Asiatic in distribution though a few species are also known along the southern face of the Himalayas. One genus *Lepidopygopsis* Raj has even gone as far afield as Peninsular India over the Assam Hills and Satpura trend of mountains (Silas, *loc. cit.*, p. 445). Since several Himalayan rivers have Trans-Himalayan sources, it is reasonable to presume that along these channels the Schizothoracine fishes may have come down to the Himalayan rivers and have now become distributed along the southern face (Hora, *loc. cit.*, p. 244).

From the earlier accounts (*op. cit.*) and also from my own extensive field-work along the foot of the Himalayas, I have been able to make out the following table (Table I) showing the distribution of torrential fishes in the various drainage systems of the Himalayas.

The most important and striking fact that is evident from the table (Table I) is the occurrence of a great variety of forms towards the east as compared with the west. In the Brahmaputra drainage system, for instance, forms like *Aborichthys*, *Acanthopthalmus*, *Batasio*, *Chaca*, *Conta*, *Erethistoides*, *Exostoma* and *Olyra* are present, whereas none of these genera extend along the Himalayas beyond the limits of the Brahmaputra System. *Lissocheilus* and *Pseudecheneis* extend up to the Kosi drainage, while *Balitora*, *Euchiloglanis*, *Myersglanis*, *Semiplotus* and *Somileptes* extend further as far as the Gandak system of drainage. *Laguvia* extends still further west to the Kali river, while the range of *Psilorhynchus* is up to the Jumna. Of the remaining twelve genera, eleven, namely *Amblyceps*, *Bagarius*, *Botia*, *Gagata*, *Garra*, *Glyptothorax*, *Nemachilus*, *Oreinus*, *Schizothorax*, *Sisor* and *Tor*, are distributed along the entire length of the Himalayas and in the case of *Garra*, *Glyptothorax*, *Nemachilus*, *Oreinus*, *Schizothorax*, *Tor* and *Silurus* even beyond the Himalayas. While several forms of the Brahmaputra drainage and the Assam Hills do not occur in the western Himalayas, these very same genera or some closely allied forms are found in Burma, Southern China, Siam, the Malay Peninsula, the Archipelago and Indo-China on the one hand and the hills of Peninsular India on the other. It is very remarkable that the specialised forms of the Assam Hills and the Brahmaputra drainage, instead of spreading along the present-day ecologically and geomorphologically continuous Himalayan range towards the west, became deflected towards the south-west. The following chart of distribution (Table II) showing the relationships of the fish-fauna of the Himalayas with the neighbouring countries and the rest of the subcontinent of India will be helpful in bringing out this interesting zoogeographical point.

Of the 29 genera, *Garra*, *Nemachilus* and *Tor* are common to the countries towards the east as well as Africa in the west. *Aborichthys*, *Conta*, *Myersglanis* and *Somileptes* are endemic to the Eastern Himalayas. The remaining 22 genera are common to the Himalayas and the countries towards east and south-east. It has already been indicated that this fauna is again represented in the Western Ghats and the Satpura trend of mountains. Thus, the close relationship of the Himalayan fish-fauna to the South-East Asian and the Malay Archipelago can be clearly seen. Taking the endemic forms, the genera to which they belong are only those closely allied to South-East Asian forms (Hora, *op. cit.*). These facts prove that the Himalayas had undoubtedly derived its fish-fauna from the east, most probably from the Yunnan area (Hora, 1948, p. 306) and had spread to the west as far as Africa as and when the ecological conditions favoured their dispersal.

FACTORS GOVERNING DISPERSAL OF TORRENTIAL FISHES

The torrential fishes enumerated in Table II can be divided into six groups according to their habitats and consequently the degree of development of their adaptive characters for torrential environment.

TABLE I

List of Torrential fishes known from the southern face of the Himalayas

[illegible]

[illegible]

TABLE I.—Contd.

List of Torrential fishes known from the southern face of the Himalayas.

	Chindwin.	Brahmaputra. 88° 90' E.	Kosi. 85° 32'–88° E.	80°–83° 28' E.					Kangra. 78° 35'–80° E.	(Ganges. 78°–80° E.	Jumna. 77° 35'–78° 35' E.	72°–77° 35' E.					Sutlej.	Bos.	Ravi.	Chenab.	Jhelum.	Indus.																																																																																																																																																																																																																																																																																																																																																																																																																																																																																																																																																																																																																																																																																																																																																																																																																																																																																																																																																																																																																																																																																																																																																																																																																																																																																																																											
				Bagmati. 83° 28'–85° 32'	Gandak.	Rapti.	Karnali.	Kali.																																																																																																																																																																																																																																																																																																																																																																																																																																																																																																																																																																																																																																																																																																																																																																																																																																																																																																																																																																																																																																																																																																																																																																																																																																																																																																																																									
39. <i>Nemachilus carletoni</i> Fowler																																																																																																																																																																																																																																																																																																																																																																																																																																																																																																																																																																																																																																																																																																																																																																																																																																																																																																																																																																																																																																																																																																																																																																																																																																																																																																																																																	

[illegible]

List of Torrential fishes known from the southern face of the Himalayas.

[illegible]

[illegible]

List of genera of Himalayan fishes to show the relations with those of the adjacent countries.

[illegible]

Family SILURIDAE

14. *Silurus*

Family BAGRIDAE

15. *Batasio*

Family AMBLYCEPIDAE

16. *Amblyceps*

Family SISORIDAE

17. Bagarius

18. Conta

19. *Erethistoides*

20. Euchiloglanis

21. Exostoma ..

22. Gagata

23. Glyphothorax

24. *Laguvia* ..

25. *Myersglanis*

26. *Pseudecheneis*

27. Sisor ..

Family CHACIDÆ

28. Chaca

Family OLYRIDAE

29. *Olyra* ..

It may, however, be understood that though according to similarities of habitat certain genera of fishes are put under a particular group, it need not necessarily mean that they all have a uniform distribution along the Himalayas. The distribution is governed both by their habitat conditions as well as their period of evolution. For instance, *Silurus* and *Bagarius*, though placed under the same group, have different evolutionary history and hence their range of distribution today along the Himalayas differs very much. *Silurus* is a very old fish with fossil representatives in the Eocene beds of Europe. It is distributed in Europe, northern Asia, the northern portion of South-East Asia, Burma, Thailand and Malaya. *Bagarius*, on the other hand, is restricted in its distribution to South-East Asia and its fossils are known from the Siwalik beds of India and the Tertiary beds of the highlands of Pedong in Sumatra. Along the Himalayas *Silurus* is today known only from the Brahmaputra drainage, whereas *Bagarius* is seen all along the base of it.

It would appear from the distribution in time and space of *Silurus* that it had originated in Europe during the Eocene epoch and spread south and south-east and during the Pliocene colonised the Siwalik fore-deep of the Himalayas where it perished subsequently. On the other hand, *Bagarius* had originated somewhere in South-East Asia during the Tertiary period and began spreading along the Himalayas during the Pliocene epoch (*vide infra*, p. 489). Though its fossils are known from the Siwalik rocks of the Himalayas, the present-day distribution of *Bagarius* does not, however, indicate that the genus had entirely perished along the Himalayas then.

Again, the highly specialised genera of torrential fishes placed under Group VI below are distributed only along the Eastern Himalayas and do not extend westwards. This pattern of distribution can be attributed to the fact that their spread along the Himalayas was made possible only at a very late period and sufficient time had not probably lapsed for their colonisation of the whole of the Himalayan region (*vide infra*, p. 490).

Group I

This group consists of fishes which live in somewhat shallow, clear and cold waters at the base of hills and have, therefore, scarcely any striking adaptive characters. The genera coming under this group are: (1) *Silurus*, (2) *Bagarius*, (3) *Batasio*, (4) *Gagata* and (5) *Chaca*.

Group II

The following group consists of fishes living at the bottom of deep swift waters. The members of this group are cylindrical in form and possess a powerful muscular body. They are: (1) *Oreinus*, (2) *Schizothorax*, (3) *Tor*, (4) *Lissocheilus* and (5) *Semiplotus*.

Group III

Group III consists of fishes which are modified for a burrowing habit. They bury themselves in sand among pebbles and stones and thereby escape from the force of rushing water. They are: *Psilorhynchus* and *Sisor*.

Group IV

Fishes which live among pebbles and shingles at the bottom of shallow waters are grouped here; these fishes have to contend with a considerably less force of rushing water and, therefore, do not have any specially modified apparatus for adhesion, but are elongated and loach-like in form. They are: (1) *Amblyceps*, (2) *Nemachilus*, (3) *Somileptes*, (4) *Aborichthys*, (5) *Acanthophthalmus*, (6) *Olyra*, (7) *Conta* and (8) *Botia*.

Group V

This group consists of fishes which cling to exposed surface of bare rocks in comparatively slower waters. Since they have to bear a greater force of rushing water than the fishes in the preceding group, they have developed discs formed by the modification of the skin on the ventral surface by means of which they adhere to rocks. The fishes grouped here are: (1) *Glyptothorax*, (2) *Laguvia* and (3) *Garra*.

Group VI

Group VI consists of fishes which cling to exposed surface of bare rocks in swift waters. They have to bear the greatest force of rushing water than the fishes of the preceding group and hence they are very highly modified; in some the whole body is modified into a limpet-shape which helps the fish to adhere to stones in the rushing torrents, while others have developed adhesive discs (Hora, 1930, pp. 231-33). In these forms the mouth parts, the gills and the fins have all been modified in correlation with their habitat (Hora, 1947, p. 4). The genera coming under this group are: (1) *Balitora*, (2) *Erethistoides*, (3) *Pseudecheneis*, (4) *Euchiloglanis*, (5) *Myersglanis* and (6) *Exostoma*.

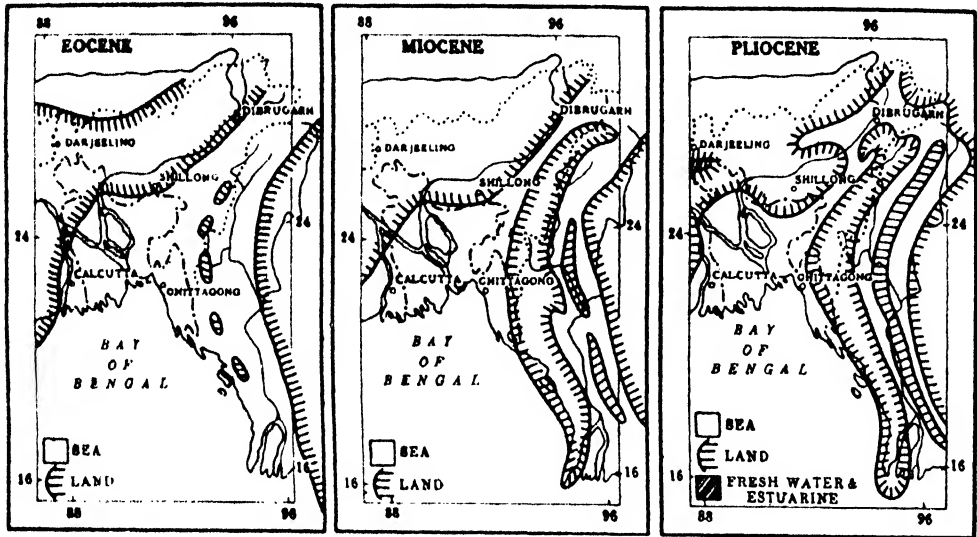
It will thus be seen from the above grouping of the Himalayan fishes that their migration would depend not only on the presence of continuous water courses, but also on the presence of their characteristic habitat conditions. It will now be possible to explain the distribution of torrential fishes along the Himalayas on certain palaeogeographical considerations.

PALAEOGEOGRAPHY OF THE HIMALAYAS AS EVIDENCED BY THE DISTRIBUTION OF FISHES

From stratigraphical and palaeontological evidences we know that from the Middle Eocene period an arm of the sea transgressed the Assam-Eastern Himalayan region and thus separated India from Burma (Hora, 1953; Menon, 1953). This condition seems to have lasted probably till the late Miocene period. The upheaval of the Himalayas during the Middle or Upper Miocene periods which is thought to have been the most violent of the movements (Krishnan, 1952, p. 45), probably made this arm of the sea recede southwards leaving at its head marshy conditions that allowed the invasion of the newly formed northern lands by those Chinese fishes capable of tolerating slightly brackish waters. The fossil records of *Clarias* and *Heterobranchus* from the early Pliocene deposits of the Siwalik support this view. Gradually with the rise of the Himalayas the marshy gap seems to have been replaced by low east-westward hills enabling such forms which normally live in somewhat deeper, clearer and colder waters at the base of hills to migrate from the east along the young Himalayas. Palaeontological records support this view, for fishes like *Bagarius* and *Silurus* are known from the later Siwalik beds of the Himalayas. Between the migration of the marsh-loving fauna during the early Pliocene and the hill-stream fauna during the late Pliocene, we have fossil records from the Siwalik beds of *Rita* and *Chrysichthys* which are pond-dwelling fishes capable of withstanding certain amount of salinity and foulness of water.

The Pleistocene orogenic movements of the Himalayas are stated by Geologists to have been of very great intensity and, as pointed out earlier, these intensive orogenic movements appear to have caused the evolution of the highly specialised torrential fishes in South-East Asia. But from the present-day distribution of torrential fishes along the Himalayas, it is evident that they did not spread westwards along the Himalayas till very recent times. It can be very reasonably inferred from this that the establishment of torrential ecological conditions in the region of the gap referred to earlier probably took place only recently, geologically

speaking. Till then most of the monsoon winds probably crossed over to the Central Asian region through this gap. According to Dr. S. K. Banerji, Retired Director-General of Meteorology of the Government of India, the 'south-west monsoon in its present form apparently commenced to be established at the close of the würm glaciation, that is about 20,000 years ago' (Hora, *loc. cit.*, p. 96). This means that the major upheaval of the Himalayas during the Pleistocene of Sub-Recent period (Krishnan, *op. cit.*) probably raised the low hills in the gap region high enough to obstruct the south-westerly winds and to produce torrential ecological conditions there. Consequently, the highly specialised torrential fishes would have been enabled to spread over gap portion of the Himalayas only during the Sub-Recent periods, probably roundabout 20,000 years ago.



TEXT-FIG. 10. Distribution of land and sea in the Bengal, Assam and Burma regions during the Eocene, Miocene and Pliocene periods (modified from Dr. M. S. Krishnan, *Bull. Nat. Inst. Sci. India*, 1, pp. 26-28, 1952).

PROBABLE SEQUENCE OF MIGRATION ALONG THE HIMALAYAS

I have already pointed out that *Oreinus*, *Schizothorax*, *Bagarius* and *Silurus* had spread along the Himalayas earlier than the final upheaval of the Himalayas during the late Pleistocene times. *Nemachilus*, *Garra*, *Tor* and *Glyptothorax* also appear to have migrated along the Himalayas at a much earlier period than the other more specialised torrential fishes. It has been pointed out earlier that *Garra* and *Glyptothorax* generally live on exposed surface of bare rocks, *Nemachilus* among pebbles and shingle at the bottom of shallow waters and *Tor* at the bottom of swift, deeper waters. None of these show the highly specialised torrential adaptations characteristic of forms like *Balitora* and *Pseudecheneis*. From the ecological and distributional points of view, therefore, it can be safely concluded that these forms would have spread along the Himalayas, earlier than the upheaval of the Himalayas during the late Pleistocene when probably only low hills may have stretched in the region of the gap referred to earlier. This is further strengthened by the fact that *Balitora* and other Homalopterid fishes have migrated to Peninsular India and not to the Western Himalayas. This means that torrential ecological conditions existed over the Garo-Rajmahal gap area during the Pleistocene pluvial periods enabling the highly specialised torrential fishes to cross over to the Peninsula. It would further

appear from this that the monsoon-bearing winds at first struck the Garo-Rajmahal region during the pluvial periods of the Pleistocene when the sea-level fell by a few hundreds of feet and created torrential conditions there. From there as the winds rose up it would have probably passed through the gap to the Central Asian region, the mountain ranges in the gap area being too low to obstruct the monsoonic winds then and to make the Eastern Himalayas the recipient of heavy rainfall as at the present day.

Further, *Garra*, *Nemachilus* and *Tor* have great habitat tolerance having been found to live in mountainous lakes (Hora, 1921b, 1936a). It is, therefore, likely that *Garra*, *Tor* and *Nemachilus* had spread along the Himalayas and even further westwards as far as Africa during the early Pleistocene. During the pluvial periods of the Pleistocene when there was an uninterrupted greater flow of water in the streams at the base of the Himalayas these forms probably got dispersed. *Glyptothorax* had also probably spread likewise along the Himalayas during the early Pleistocene period for its present-day range extends as far as Syria. It could not extend its range as far as Africa owing to the fact that it is more specialised for torrential waters and has not so far been recorded from lakes, pools or other sluggish waters in the hills.

Silas (*op. cit.*) has shown that forms like *Botia*, *Gagata* and *Batasio* may have migrated south-westwards during the Second Glacial period of the Pleistocene. From a consideration of their habitat and range of distribution along the Himalayas, it would appear that the migration of these forms along the Himalayas may also have taken place during the Second Glacial period of the Pleistocene. Silas has also shown that *Balitora* may have spread south-westwards during the early 'Post-Tilt' period, *i.e.* probably during the Third Glacial period. Taking into consideration the ecological requirements of *Balitora* and its present-day range along the Himalayas, it can be concluded that the spread of *Balitora* along the Himalayas may have commenced only subsequent to the Sub-Recent upheaval of the Himalayas. *Amblyceps*, *Laguvia*, *Erethistoides*, *Psilorhynchus* and *Sisor* may have spread south-westwards during the last Glacial period of the Pleistocene (Silas, *op. cit.*). Along the Himalayas, however, they seem to have spread only during the Holocene Glacial period by which time the Himalayas would have sprung up to over 10,000 feet in the region of the gap referred to earlier and the south-west monsoon, as we know them in India today, had become established. All the other forms that are today found along the Himalayas should be considered to have either evolved in the Eastern Himalayas, or spread over there from the east during the last 10,000 years by which time the Holocene Glaciation ended and the Garo-Rajmahal gap became a barrier against their spread south-westwards.

SUMMARY

A brief sketch of the physical features of the Himalayas, particularly the river system with special emphasis on the general drift of the rivers towards the west is given and the areas from where fish collections were either made by the author, or referred to in literature are indicated. Evolution and distribution of torrential fishes of the Himalayas are then discussed. With the exception of the remains of a Schizothoracine fish from the Kerwas of Kashmir (2nd interglacial period of the Pleistocene), no other torrential fish is known in a fossil state from the Himalayas indicating that the typical torrential fauna of the Himalayas is not older than the Pleistocene. The major upheaval of the Himalayas during the early Pleistocene period and the subsequent orogenic movements seem to have been responsible for the evolution of the typical Himalayan fauna during the various stages according to the location and intensity of the movements. Ninety-two species of torrential fishes found in the Himalayan rivers are tabulated according to their occurrence, or otherwise in the various drainage systems and the zoogeographical significance of the distribution of the various genera is then fully analysed. From such a critical analysis of the distribution of the torrential fishes it has been concluded that the Himalayas had derived its fauna from the east and that this fauna had moved westwards as far as Africa as and when ecological conditions favoured their dispersal.

The ecological factors governing the distribution of torrential fishes are then discussed. The torrential fish fauna of the Himalayas is divided into six groups according to their habitats and it has been pointed out that the range of distribution along the Himalayas of a fish is

dependent not only on its habitat, but also on the time of its evolution. Finally, the distribution of torrential fishes along the Himalayas is explained on certain palaeogeographical considerations.

During the Eocene-Miocene period an arm of the sea transgressed the Assam-Eastern Himalayan region and this separated India from Burma. The upper Miocene upheaval of the Himalayas made the arm of the sea recede southwards which enabled the marsh-loving forms to spread along the Himalayas. With the gradual rise of the Himalayas during the Pliocene this gap seems to have been replaced by low east-westward hills enabling the clear water forms to spread along the Himalayas. Thus during the Pliocene period forms like *Bagarius* and *Silurus* migrated along the Himalayas. Even fishes like *Nemachilus*, *Tor*, *Garra* and *Glyptothorax* appear to have migrated along the Himalayas during the early Pleistocene period. But the typical torrential fishes like *Balitora* and *Pseudecheneis* did not spread along the Himalayas till the major upheaval of the Himalayas during the Pleistocene of Sub-Recent period. This upheaval seems to have raised the low hills in the gap high enough to obstruct the monsoon winds and to produce torrential ecological conditions there. The spread of the torrential fishes along the Himalayas is, therefore, dated as subsequent to the late Pleistocene or Sub-Recent period.

The probable sequence of migration of torrential fishes along the Himalayas is also dealt with in the last section.

ACKNOWLEDGEMENTS

I am deeply indebted to Dr. S. L. Hora, Director, Zoological Survey of India, for his valuable suggestions, kind guidance and supervision in the preparation of this paper. I am also grateful to Dr. K. Jacob, Palaeontologist, Geological Survey of India, and through him to the Director, Geological Survey of India, for affording me facilities to examine the fossil fish collections of the Survey.

REFERENCES

- Burrard, S. C. and Haydon, H. H. (1933). *A sketch of the Geography and Geology of the Himalayan mountains and Tibet*. Revised by Burrard and Heron (Delhi).
- Chaudhuri, B. L. (1912). Zoological results of the Abor expedition. XVIII. Fish. *Rec. Ind. Mus.*, 8, 243-57.
- Chhibber, H. L. (1949). Westward drift of the rivers in North India. *Bull. Nat. Geogr. Soc. India*, 12, pp. 1-15.
- Hora, S. L. (1921). Fish and Fisheries of Manipur with some observations on those of the Naga Hills. *Ibid.*, 22, 166-214.
- (1921a). On some new or rare species of fish from the Eastern Himalayas. *Ibid.*, 22, 731-744.
- (1921b). Indian Cyprinoid fishes belonging to the genus *Garra*, with notes on related species from other countries. *Ibid.*, 22, 633-687.
- (1924). Fish of the Siju cave, Garo Hills, Assam. *Ibid.*, 27, 27-31.
- (1930). Ecology, Bionomics and Evolution of the Torrential fauna with special reference to the organs of attachment. *Phil. Trans. Roy. Soc.*, London, 218, 171-282.
- (1934). The fishes of Chitral. *Rec. Ind. Mus.*, 36, 279-319.
- Hora, S. L. and Mukerji, D. D. (1935). Fishes of the Naga Hills, Assam. *Ibid.*, 37, 381-404.
- Hora, S. L. (1936). On a further collection of fish from the Naga Hills. *Ibid.*, 38, 317-331.
- (1936a). Report on fishes. Part I. Cobitidae. *Mem. Conn. Acad. Arts. Sci.*, 10, 299-321.
- Hora, S. L. and Mukerji, D. D. (1936). Fishes of the Eastern Doons. *Rec. Ind. Mus.*, 38, 133-146.
- Hora, S. L. (1937). Comparison of the Fish faunas of the Northern and the Southern faces of the Great Himalayan Range. *Ibid.*, 39, 241-250.
- (1937a). Distribution of Himalayan fishes and its bearing on certain Palaeogeographical problems. *Ibid.*, 39, 251-259.
- (1937b). Notes on Fishes in the Indian Museum. XXIX. On a collection of Fish from Nepal. *Ibid.*, 39, 43-46.
- (1937c). Notes on Fishes in the Indian Museum. XXXIII. On a collection of Fish from the Kumaon Himalayas. *Ibid.*, 39, 338-348.
- (1937d). On Fossil Fish remains from the Karewas of Kashmir. *Rec. Geo. Surv. India*, 72, 178-187.
- Hora, S. L. and Nair, K. K. (1941). Fishes of the Satpura Range, Hoshangabad district, Central Province. *Rec. Ind. Mus.*, 43, 361-373.
- Hora, S. L. (1944). On the Malayan affinities of the Freshwater Fish-fauna of Peninsular India and its bearing on the problem age of the Garo-Rajmahal gap. *Proc. Nat. Inst. Sci. India*, 10, 432-39.

- Hora, S. L. (1947). Torrential fishes and the significance of their distribution in zoogeographical studies. *Bull. Nat. Geogr. Soc. India*, **7**, 1-10.
- (1948). The distribution of Crocodiles and Chelonians in Ceylon, India, Burma and further East. *Proc. Nat. Sci. India*, **15**, 285-310.
- (1949). The Fish-fauna of the Rihand river and its zoogeographical significance. *Journ. Zool. Soc. India*, **1**, 1-7.
- Hora, S. L. (1951). Some observations on the palaeogeography of the Garo-Rajmahal gap as evidenced by the distribution of Malayan fauna and flora to Peninsular India. *Proc. Nat. Inst. Sci. India*, **17**(6), 437-444.
- (1953). Fish distribution and Central Asian Orography. *Curr. Sci.*, **22**, 93-97.
- Hora, S. L. and Menon, A. G. K. (1953). Distribution of the fishes of the past and their bearing on the geography of India. 2. The extinct freshwater Teleostean fishes of India. *Everyday Science*, **2**, 105-113.
- Hora, S. L. (1954). The evolution of the Indian torrential environment and its fishes. *Bull. Nat. Inst. Sci. India* (in Press).
- Krishnan, M. S. (1943). *Geology of India and Burma*.
- (1952). The Ganges, its geography and development. *Himalaya*, **1**(1), 35-49.
- Menon, A. G. K. (1949). Fishes of the Kosi Himalayas, Nepal. *Rec. Ind. Mus.*, **47**, 1.
- (1949a). Fishes of the Kumaon Himalayas. *Journ. Bomb. Nat. Hist. Soc.*, **48**, 535-542.
- (1951). Rôle of the Eastern Ghats in the distribution of the Malayan flora and fauna to Peninsular India. *Proc. Nat. Inst. Sci. India*, **17**, 475-497.
- (1953). Age of the transgression of the Bay of Bengal and its significance in the evolution of the freshwater fish fauna of India. *Bull. Nat. Inst. Soc. India* (in Press).
- Nevilli, H. R. (1905). District Gazetteers of the U.P. **31**, 9-12.
- Pæcoe, E. H. (1950). *A Manual of the Geology of India and Burma*. (3rd Ed.)
- Shaw, G. E. and Shebbeare, E. O. (1937). The Fishes of Northern Bengal. *Journ. Roy. As. Soc. Bengal, (Science)*, **3**, 1-137.
- Silas, E. G. (1952). Taxonomic assessment and levels of evolutionary divergence of fishes with the so-called Malayan affinities in Peninsular India. *Proc. Nat. Inst. Sci. India*, **18**(5), 423-447.
- Wadia, D. N. (1938). The Post-tertiary hydrography of Northern India and the changes in the courses of its rivers during the last glacial epoch. *Ibid.*, **4**, 387-394.
- Walton, H. C. (1910). District Gazetteers of the U.P., **36**, 140-41.

Issued September 28, 1954.

EMBRYOLOGICAL STUDIES IN MENISPERMACEAE

I. *TILIACORA RACEMOSA* COLEB.

by R. L. N. SASTRI, *Department of Botany, Andhra University, Waltair*

(Communicated by P. Maheshwari, F.N.I.)

(Received March 26 ; after revision May 12 ; read August 6, 1954)

INTRODUCTION

Menispermaceae, a large family comprising 65 genera and 350 species (Willis, 1948), distributed throughout the warmer parts of the world, is one of the embryologically little-investigated families of Ranales. Hooker (1897) divided the family into four tribes: Tinosporeae, Cocculeae, Cissampelideae and Pachygoneae. Our knowledge of the embryology of the family is limited to an account of the development of the pollen and embryo sac in *Cocculus villosus* DC and *Tinospora cordifolia* Miers. (Joshi and Rao, 1935; Joshi, 1937, 1939) belonging to the tribes Cocculeae and Tinosporeae respectively. The anther tapetum in these plants is of secretory type and of sporogenous origin according to Joshi and Rao (1935). The ovule in *Cocculus* is bitegmie but in *Tinospora* it is unitegmie and Joshi (1939) considers that it represents two integuments. A nucellar cap is developed at the micropylar end owing to periclinal divisions of the nucellar epidermis. The embryo sac conforms to the Polygonum type. There is practically no information on fertilization, endosperm, embryo and seed development in any member of the family.

The present paper deals with the embryology of *Tiliacora racemosa* Coleb., a woody climbing shrub with glabrous leaves, small yellow flowers and reddish fruits, belonging to the tribe Cocculeae. The plant occurs throughout tropical India.

MATERIAL AND METHODS

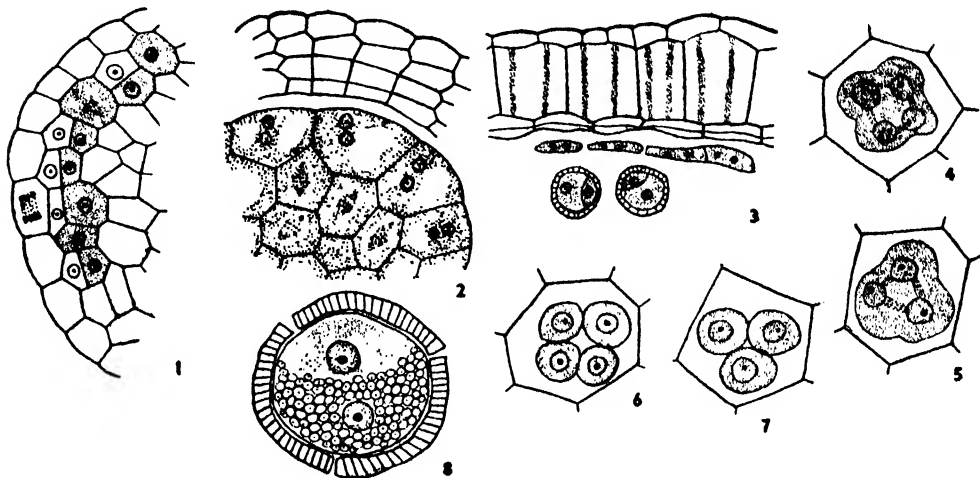
The material was collected at Yanam and Waltair and fixed in formalin-acetic-alcohol. Customary methods of dehydration and embedding were employed. Sections were cut from 6–10 μ in thickness and stained in Delafield's haematoxylin and safranin and fast green.

MICROSPOROGENESIS

The anthers are tetralocular. The primary archesporium consists of a row of hypodermal cells. A periclinal division gives rise to an outer layer of primary parietal cells and an inner layer of primary sporogenous cells (Fig. 1). The wall of the fully developed anther is five-layered, including the epidermis. The innermost layer is the tapetum which is of the secretory type. Each cell of the tapetum is two nucleate (Fig. 2). The tapetum is biseriate at certain places. The subepidermal wall layer develops into the fibrous endothecium which is organized only after the pollen grains are fully formed (Fig. 3). The middle layers become crushed and gradually degenerate in the mature anther. The tapetum is also absorbed as the pollen grains mature.

The primary sporogenous cells undergo mitotic divisions and form a small mass of spore mother cells. All the spore mother cells undergo meiotic divisions and give rise to microspore tetrads. No degeneration of spore mother cells such as

recorded by Joshi and Rao (1935) in *Cocculus* and *Tinospora* has been observed. Divisions of the pollen mother cells are of the simultaneous type and cytokinesis takes place by furrowing (Figs. 4 and 5), as in *Cocculus* and *Tinospora*. During the division of the spore mother cells the cytoplasm shrinks from the walls resulting in the formation of a space in the peripheral region of the mother cell (Figs. 4 and 5). The tetrads are tetrahedral or isobilateral (Figs. 6 and 7). The pollen grains are shed at the two-celled stage (Fig. 8). The mature pollen grains are filled with starch grains. The exine shows three germ pores and bar-like thickenings which give a reticulate appearance in the surface view of the pollen grain. The mature pollen grains are small in size and measure about $10\ \mu$ in diameter.



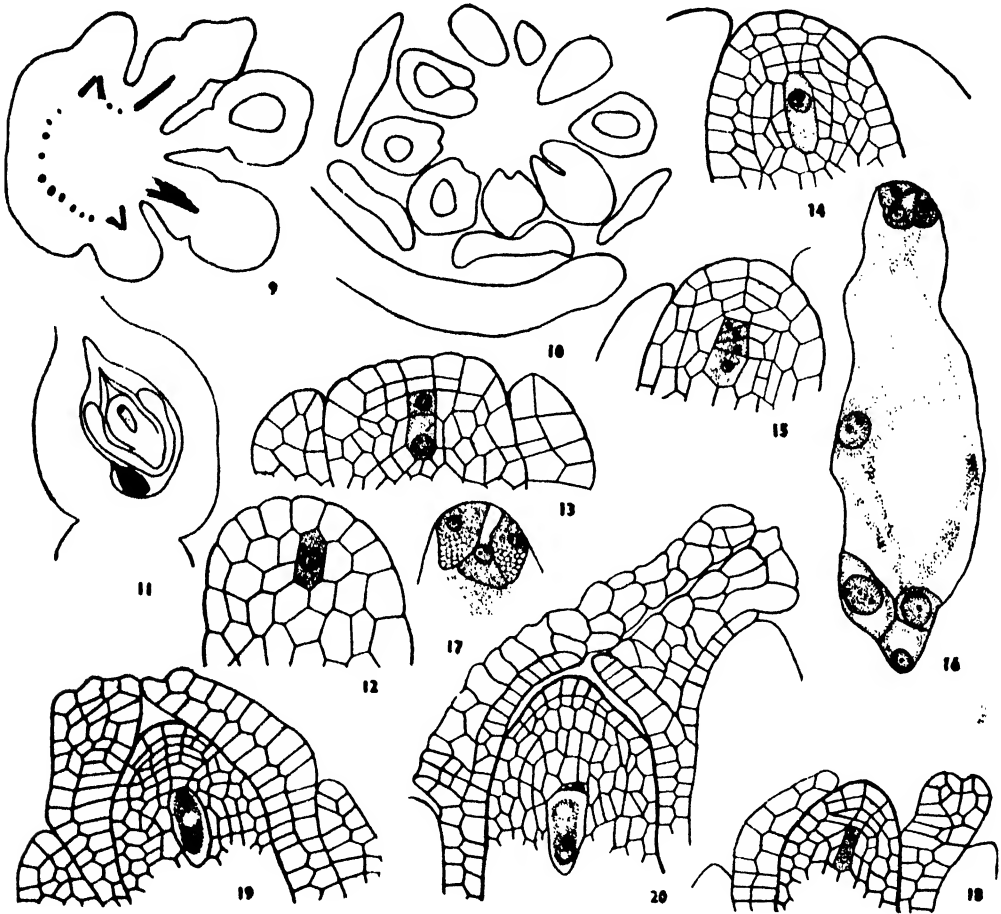
TEXT-FIG. 1

Figs. 1-8: Fig. 1. L.s. portion of anther lobe showing primary archesporium. Most of the cells have divided periclinally, cutting off the parietal cells ($\times 582$). Fig. 2. T.s. portion of anther lobe showing divisions in the spore mother cells ($\times 872$). Fig. 3. T.s. mature anther wall showing fibrous endothecium and remnants of the middle layers and tapetum ($\times 582$). Figs. 4 and 5. Division in the pollen mother cells showing furrowing ($\times 872$). Figs. 6 and 7. Microspore tetrads ($\times 872$). Fig. 8. Mature two-celled pollen grain ($\times 1424$).

THE OVULE

The gynaecium usually consists of nine free carpels arranged spirally on the receptacle. The spiral arrangement is brought out in serial microtome sections of a flower (Figs. 9 and 10) in which the different carpels are seen to arise at different levels from the receptacle. Each carpel has two ovules borne on a marginal placenta. In *Cocculus* there are only four carpels of which one degenerates early. In *Tinospora* there may rarely be up to six carpels of which one degenerates early. Joshi (1937) is of the opinion that the gynaecium of Menispermaceae might have arisen from an ancestral condition with numerous spirally arranged carpels. On the basis of this view the gynaecium of *Tiliacora* seems to be less evolved than that of *Cocculus* and *Tinospora*. In *Tiliacora*, as in *Cocculus* and *Tinospora* (Joshi, 1937 and 1939), only the upper ovule reaches maturity while the lower one degenerates early (Fig. 11). Usually this happens at the megaspore mother cell stage but very rarely development may proceed to the eight nucleate embryo sac stage. In the degenerating ovule the integuments develop rather feebly although the nucellus may become massive. In the course of development, the upper ovule becomes curved upwards and the lower downwards (Fig. 11), as in *Cocculus* (Joshi, 1937). The two ovules continue to grow straight in the early stages till they touch the carpel walls. Joshi

expressed the view that due to the pressure exerted by the opposing carpel walls at this stage the ovules change the direction of their growth and the upper becomes bent upwards and the lower downwards. The fact that the ovules become flattened at this stage furnishes a proof for this view. A similar condition is also seen in *Tiliacora* as suggested by the flattening of the ovule. The ovule is bitegmic and crassinucellate. It is curved but the curvature does not affect the embryo sac till the eight nucleate embryo sac stage. After fertilization, however, the curvature extends also to the embryo sac. Thus according to Maheshwari's (1950) definition, the ovule is campylotropous in the early stages and becomes amphitropous after



TEXT-FIG. II

Figs. 9-20: Figs. 9 and 10. T.s. flower showing serial microtome sections of gynaecium to illustrate the spiral arrangement of carpels ($\times 25$). Figs. 11. L.s. carpel showing upper functional ovule and lower degenerated ovule ($\times 35$). Fig. 12. L.s. ovule primordium showing single celled archesporium ($\times 485$). Fig. 13. L.s. ovule showing parietal cell cut off by the archesporial cell and periclinally divided nucellar epidermis ($\times 339$). Fig. 14. L.s. nucellus showing megaspore mother cell ($\times 291$). Fig. 15. L.s. nucellus showing linear tetrad of megaspores ($\times 339$). Fig. 16. A fully developed embryo sac; one of the antipodal nuclei has 3 nucleoli ($\times 291$). Fig. 17. Egg-apparatus showing synergids devoid of hooks ($\times 485$). Fig. 18. L.s. ovule showing growth of the inner integument in the micropylar region and first division of the megaspore mother cell ($\times 215$). Fig. 19. L.s. ovule showing growth of the inner integument in the micropylar region and two nucleate embryo sac ($\times 215$). Fig. 20. L.s. ovule showing advanced stage in the outgrowth of the inner integument and functional megaspore ($\times 50$).

fertilization. The micropyle is straight. The inner integument is two cells thick to start with and the outer several cells thick. A little later in the development of the ovule the inner integument becomes many cells thick at the micropylar region (Figs. 18, 19, 20 and 21), as will be described later. There is a small air space between the inner integument and the nucellus in the micropylar region (Figs. 19, 20 and 21). In the early stages the integuments are closely pressed against each other and also against the nucellus. In *Cocculus* both the integuments are two to three cells thick and in the mature ovule the inner becomes many layered in the micropylar region. There is an air space between the inner integument and the nucellus in the micropylar region. In *Tinospora* the single integument is as thick as both the integuments of *Cocculus* put together. The closely appressed condition of the integuments of *Tiliacora* lends support to Joshi's (1939) view that the single integument of *Tinospora* might have arisen from a two-integument condition.

MEGASPOROGENESIS AND EMBRYO SAC

The single hypodermal archesporial cell makes its appearance before the integuments are differentiated in the young ovule (Fig. 12). It undergoes a periclinal division to form an outer primary parietal cell and an inner megaspore mother cell (Fig. 13). The primary parietal cell, by a series of anticlinal and periclinal divisions, gives rise to 3-4 layers of parietal tissue. The nucellar epidermis undergoes a periclinal division and becomes two-layered in the apical region (Fig. 13). In *Cocculus* the nucellus has an epidermal cap of 2-4 layers thickness (Joshi, 1937). In *Tiliacora* the megaspore mother cell becomes elongated and its nucleus lies towards the micropylar end (Fig. 14). It then undergoes two meiotic divisions and gives rise to a linear tetrad (Fig. 15). The chalazal megaspore functions, and forms an embryo sac of the Polygonum type (Fig. 16), while the rest of the three megaspores degenerate (Fig. 20). The egg apparatus is small relative to the size of the embryo sac. The antipodals are ephemeral and some show two to three nucleoli (Fig. 16). In *Cocculus* and *Tinospora* the antipodals are persistent and the synergids have small hooks; in *Tinospora* the synergids may sometimes show an egg-like appearance. In *Tiliacora* the nuclei in the synergids are towards the micropylar end and numerous small vacuoles are found at the lower end; hooks are absent (Fig. 17). In the egg the nucleus lies towards the lower end while there is a large vacuole at the micropylar end. The two polar nuclei fuse near the middle of the embryo sac. In the full grown ovule the parietal tissue is composed of five to six layers of which the outer two are epidermal derivatives.

FERTILIZATION

The short style is solid and is provided with transmitting tissue consisting of two layers of richly protoplasmic cells formed by the inner epidermis of the adjoining carpellary margins. The pollen grains germinate on the stigmatic surface which is situated on one side of the style. The pollen tube makes its way through the transmitting tissue in an intercellular manner. Fertilization is porogamous.

As mentioned before the inner integument is at first only two-layered. Some of its cells in the micropylar region begin to divide in various planes by the time the megaspore mother cell undergoes the first division (Fig. 18). The divisions continue to take place (Figs. 19 and 20), until about the time of fertilization, and result in the formation of a filamentous structure which projects towards the base of the style (Fig. 21). The divisions of the integumentary cells do not take place at the same rate in all the ovules. In one ovule the protrusion of the integument was already far advanced at the uninucleate embryo sac stage (Fig. 20) while in another ovule it was still in the initial stages even at the two nucleate embryo sac

stage (Fig. 19). Its cells are flared up, irregular in shape and filled with rich protoplasmic contents. It is suggested that this protrusion of the inner integument serves as an obturator although the passage of the pollen tube through this structure has not been observed.

Several kinds of obturators differing in their morphology have been described in plants belonging to diverse families. They include outgrowths from the placenta, from the base of the stylar canal or even from the integument (Maheshwari, 1950). Fagerlind (1944) described in *Myriocarpa* and *Leukosyke* the development of an obturator from the inner integument. The structure described in *Tiliacora* resembles the integumentary obturator of *Myriocarpa* although it is not so extensive. To the writer's knowledge the presence of such a structure has not so far been reported in any member of the Ranales.

Triple fusion takes place much earlier than syngamy. The secondary endosperm nucleus is large in size with a big nucleolus.

ENDOSPERM

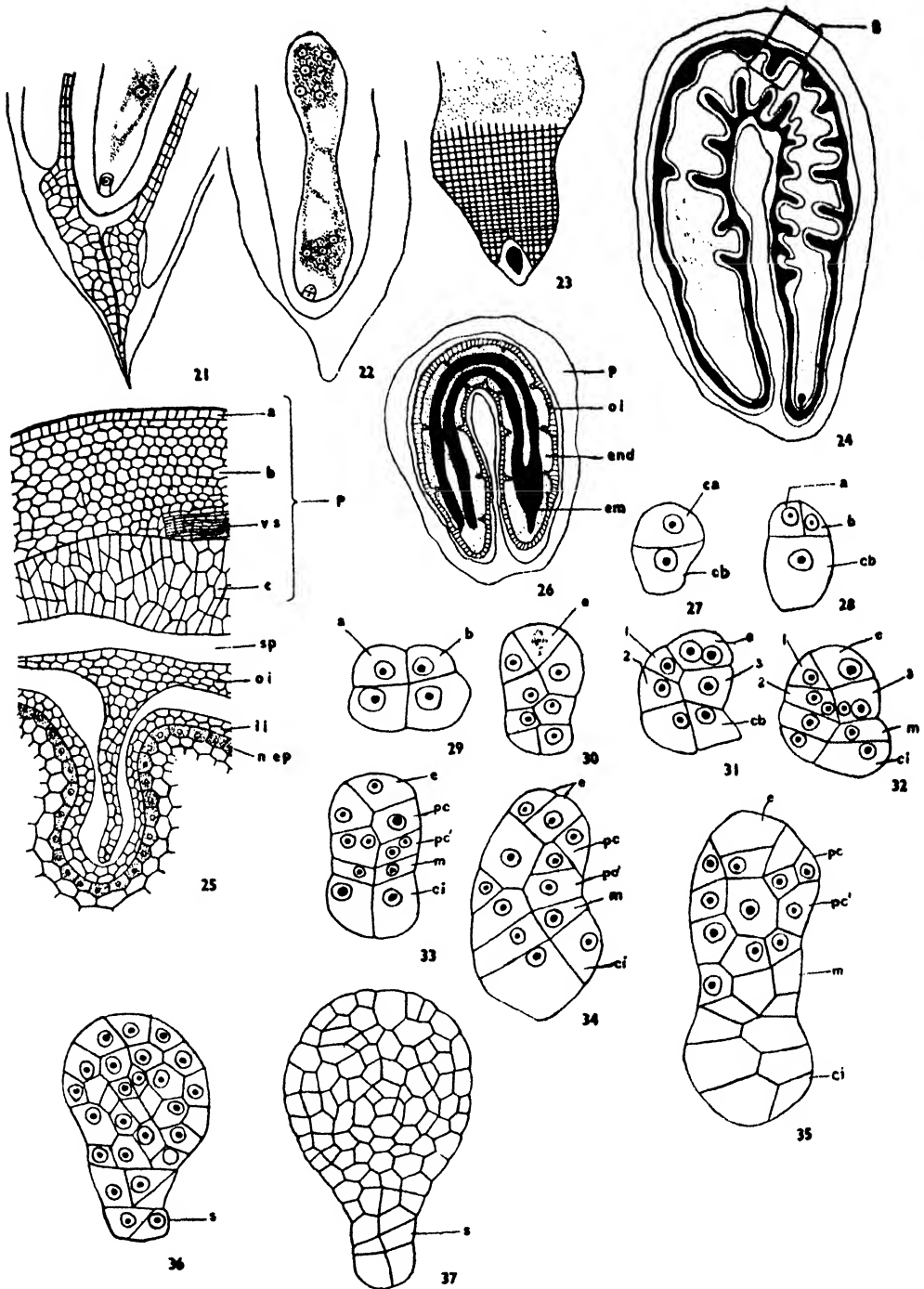
The endosperm primordium divides earlier than the fertilized egg. By the time the zygote undergoes the first division there are already 10–12 endosperm nuclei in the embryo sac (Fig. 22). The endosperm remains nuclear till a late stage. Some of the endosperm nuclei show 2-3 nucleoli. At first the endosperm nuclei lie along the periphery of the embryo sac leaving a central vacuole but as they increase in number they occupy the entire space of the embryo sac. Wall formation commences at the micropylar end at about the time the embryo becomes globular (Fig. 23). In certain members of the related families like Magnoliaceae and Anonaceae (Earle, 1938; Corner, 1949) the endosperm grows enormously and becomes cellular even by the time the fertilized egg completes the first division. In *Tiliacora* the endosperm gradually grows at the expense of the nucellus and ultimately consumes it. Prior to the absorption of the nucellus and during the period of growth of the endosperm the cells of the nucellar epidermis become glandular. In the Anonaceae Corner (1949) observed that the cells of this layer are filled with oil globules. These are not observed in *Tiliacora*.

At about the time the proembryo is 3 or 4 celled the outer integument begins to give out small protuberances towards the inside. The protuberances gradually elongate and extend from the periphery towards the middle of the nucellus. The inner integument is seen as a thin membrane surrounding the nucellus. The infoldings of the outer integument are plate like in form and are arranged in a transverse manner, more or less parallel to one another. They become deeper and deeper (Fig. 24) and render the nucellus ruminant. As the infoldings of the outer integument elongate the inner integument is pushed to the inside and stretched up. It then gradually degenerates and its remnants can be seen till a late stage. In the later stages the nucellus is replaced by the expanding endosperm. In the different genera of Anonaceae the ruminations are variously formed. In some both the integuments may take part or in others only the outer or the inner (Corner, 1949). In *Degeneria*, a member of Degeneriaceae, ruminations which are not so well developed, are formed by the outer integument (Swamy, 1949) while in Myristicaceae (Mauritzon, 1939) it is the inner integument which gives rise to the ruminations.

It will thus be seen that in *Tiliacora* as in members of Anonaceae (Corner, 1949), the ruminations are initially a feature of the nucellus and it is only later that the endosperm grows into the nucellus and gradually replaces it.

EMBRYO

The interval between fertilization and the first division of the zygote is very short as compared with the enormous postponement of embryo development in



TEXT-FIG. III

Figs. 21-37: Fig. 21. L.s. micropylar region of the ovule showing fully formed outgrowth of the inner integument, fertilized egg and endosperm primordium ($\times 104$). Fig. 22. L.s. ovule showing a few endosperm nuclei and two-celled proembryo ($\times 30$). Fig. 23. Cell wall formation in the endosperm and globular embryo ($\times 24$). Fig. 24. L.s. fruit showing ruminated nucellus and endosperm ($\times 18$). Fig. 25. Sector marked 'B' in Fig. 24 showing:

other families of Ranales like Anonaceae and Magnoliaceae. The first division of the zygote takes place six weeks after pollination in *Magnolia grandiflora* (Earle, 1938). In several of the Anonaceae, the zygote divides several weeks after fertilization and by that time the seed is full grown (Corner, 1949). In *Tiliacora*, however, the first division of the zygote takes place soon after fertilization.

The first division of the fertilized egg is transverse resulting in the formation of the apical cell *ca* and the basal cell *cb* (Fig. 27). The apical cell divides by a vertical wall into two daughter cells of unequal size, *a* and *b* (Fig. 28). This is followed by an oblique-vertical division of the basal cell resulting in two juxtaposed cells (Fig. 29). The four-celled proembryo thus consists of two superposed tiers of two cells each.

The bigger of the daughter cells, *a*, divides by an oblique wall and gives rise to a triangular cell *e* which functions as the epiphyseal initial (Figs. 30, 31 and 32) and another daughter cell numbered 3 in Figs. 31 and 32. The second daughter cell functions as a subepiphyseal cell. The smaller daughter cell *b* derived from *ca* divides by an obliquely vertical wall and gives rise to two daughter cells numbered 1 and 2 in Figs. 31 and 32. These two also function as subepiphyseal cells. Thus as a result of 3 divisions in *ca*, there are formed 4 daughter cells of which one functions as the epiphyseal initial and the rest as subepiphyseal cells. The epiphyseal initial divides transversely (Figs. 30 and 35) giving rise to two superposed cells the derivatives of which form the stem apex.

The subepiphyseal cells divide transversely (Figs. 32 and 33) and form two superposed tiers, *pc* and *pc'*. Further divisions in these tiers are irregular (Figs. 34 and 35). Tier *pc* contributes to the central cylinder of the stem and the cotyledons, while *pc'* gives rise to the hypocotyledonary region.

The two daughter cells of the basal cell undergo transverse division resulting in the formation of two superposed tiers of cells, the upper *m* and the lower *ci* (Figs. 30, 32 and 33). Further divisions in the tier *m* are rather irregular (Figs. 34, 35 and 36) and contribute to the formation of the hypophyseal region. The lower tier *ci* gives rise to the suspensor. The suspensor is usually short consisting of two tiers of two cells each (Fig. 37). Occasionally the cells of the suspensor may enlarge in size to give rise to a foot-like structure (Fig. 35).

The mature embryo is dicotyledonous and curved and is imbedded in the massive endosperm (Fig. 26). The ratio between the size of the embryo and that of the seed is far greater in *Tiliacora* than in most members of Ranalian families like Anonaceae and Magnoliaceae (Corner, 1949; Earle, 1938). The cotyledons are very much elongated.

The derivatives of the apical cell of the two-celled proembryo take a major part in the formation of the embryo proper while *ci* gives rise to the suspensor and the hypophyseal region is formed by *m*. So the embryo development conforms to the Onagrad Type of Johansen (1950) and keys out to the Trifolium Variation which is characterized by the formation of an epiphysis.

It was formerly regarded that the development of the embryo in many of the Ranales is irregular and that it resembles the condition in monocotyledons (Earle, 1938). However, it has recently been shown by Johansen (1950) on the basis of published figures and descriptions that the embryo development in some members of Ranalian families like Ranunculaceae, Magnoliaceae and Berberidaceae conforms to the Myosurus Variation, Onagrad Type. Recently Swamy (1949) described the

p—pericarp, *a*—epidermis, *b*—outer zone of parenchymatous cells, *vs*—vascular strand, *o*—inner zone of elongated cells, *sp*—space between pericarp and outer integument, *oi*—outer integument, *ii*—inner integument, *nep*—nucellar epidermis ($\times 60$). Fig. 26. L.s. mature fruit showing mature dicotyledonous embryo imbedded in the ruminant endosperm. *p*—pericarp, *oi*—outer integument, *end*—endosperm, *em*—embryo ($\times 5$). Figs. 27–37. Various stages in the development of the embryo. 1, 2, 3 in Figs. 31 and 32 represent subepiphyseal cells (Figs. 27–35: $\times 582$; Fig. 36: $\times 406$; Fig. 37: $\times 290$).

development of the embryo in *Degeneria*. He found that, although there is an apparent irregularity in the development, the method of tissue differentiation in the undifferentiated mass of cells is regular. However, he did not assign it to any type. As the derivatives of the apical cell alone seem to form the embryo proper, the development of the embryo in *Degeneria* probably conforms to the Onagrad Type. The Trifolium Variation has not so far been reported in any other Ranales.

FRUIT AND SEED DEVELOPMENT

After fertilization the ovule increases in size. The funicle elongates enormously as a result of which the ovule becomes greatly curved. In this it resembles *Cocculus* and differs from *Tinospora* in which the elongation of the funicle is not so well marked and the ovule undergoes only a slight curvature.

The nucellar cells begin to divide and the nucellus occupies the entire space of the ovule except for a small region at the micropyle, a condition found in many Anonaceae (Corner, 1949). Finally in the mature seed the nucellus is completely replaced by the endosperm.

The fruit is a drupe. In the early stages the carpel wall is made up of a number of layers of parenchymatous cells traversed by vascular strands. As the fruit enlarges in size, during the development of embryo and endosperm, the ovary wall becomes differentiated into an epidermis of radially elongated cells (a), an outer zone consisting of 6 or 7 layers of polygonal parenchymatous cells (b) and an inner zone of elongated cells (Fig. 25). In the mature fruit the outer layer becomes fleshy.

The outer integument which is made up of 4-5 layers of cells forms the outer seed coat. It shows infoldings protruding into the nucellus and later into the endosperm (Fig. 25). The inner integument, which remains two cells thick and thin walled, becomes gradually disorganized, and only its remnants are found in the mature seed.

DISCUSSION

So far only three genera of the Menispermaceae, namely, *Cocculus*, *Tinospora* and *Tiliacora* (the last forming the subject of the present study) have been investigated embryologically. Secretory type of tapetum, triplicate pollen grains, degeneration of one of the ovules, crassinucellate ovule, formation of a nucellar cap and Polygonum type of embryo sac are features common to all three. Out of these *Tiliacora* and *Cocculus*, both of which belong to the tribe Cocculeae, show the following features in common: the nature and number of integuments and their spatial relations, the formation of the micropyle by the inner integument alone, the elongation of the funicle after fertilization and the straight nature of the micropyle.

The presence of an obturator-like outgrowth of the inner integument, ephemeral nature of the antipodals and the hookless synergids are features in which *Tiliacora* differs from both *Cocculus* and *Tinospora*.

Details about fertilization, embryo, endosperm and seed coat development are available only in *Tiliacora racemosa* (present report) and comparison of these phases of life history in the various genera of the family must await further studies in the family.

SUMMARY

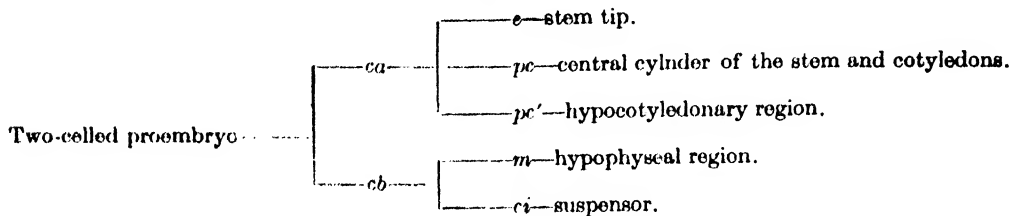
The anther wall is five-layered. The tapetum is of secretory type. Endothecium is fibrous. Cytokinesis is by furrowing. Pollen tetrads are tetrahedral or isobilateral. Pollen grains are triplicate and two-celled at the time of shedding.

The ovule is bitegmic, amphitropous-campylotropous and crassinucellate and shows a nucellar cap. The micropyle is formed by the inner integument alone, which at the time of fertilization gives rise to an obturator like outgrowth. The megaspore mother cell forms a

linear tetrad of which the chalazal megaspore functions. The embryo sac is of the Polygonum type. The antipodals are ephemeral and synergids are devoid of hooks. Polar nuclei fuse before fertilization. Fertilization is porogamous.

The endosperm is free nuclear. Wall formation starts from the micropylar end at the globular stage of the embryo. First the nucellus and later the endosperm become ruminant on account of infoldings of the outer integument in post-fertilization stages.

Embryo development conforms to the Onagrad type and keys out to the *Trifolium* Variation of Johansen (1950). The following scheme summarises the derivation of the various organs of the mature embryo from the proembryonic cells:



The fruit wall is made up of an epidermis, an outer fleshy zone of 6 or 7 layers of parenchymatous cells and an inner zone of elongated cells.

ACKNOWLEDGEMENTS

I am greatly indebted to Prof. J. Venkateswarlu for suggesting the problem and for his valuable guidance. I am grateful to Prof. P. Maheshwari for his helpful criticism of the manuscript. My thanks are due to Dr. C. Venkata Rao for some suggestions and to Mr. L. L. Narayana for fixing a part of the material used in this investigation.

REFERENCES

- Cornor, E. J. H. (1949). The Annonaceous seed and its four integuments. *New Phyt.*, **48**, 332-364.
- Earle, T. T. (1938). Embryology of certain Ranales. *Bot. Gaz.*, **100**, 257-278.
- Fagorlind, F. (1944). Die Samenbildung und die Zytologie bei agamospermischen und sexuellen Arten von *Elatostema* und einigen nahestehenden Gattungen nebst Beleuchtung einiger damit zusammenhängender Probleme. K. Svenska Vet.—Akad. Handl. III, **21**(4), 1-130.
- Hooker, J. D. (1897). *Flora of British India*. Vol. I. London.
- Johansen, D. A. (1950). *Plant Embryology*, Waltham, Mass.
- Joshi, A. C. (1937). Contributions to the embryology of Menispermaceae. I. *Cocculus villosus* DC. *Proc. Indian Acad. Sci., Ser. B.*, **5**, 57-63.
- (1939). Morphology of *Tinospora cordifolia* with some observations on the origin of the single integument, nature of synergidae and affinities of Menispermaceae. *Amer. Jour. Bot.*, **26**, 433-439.
- Joshi, A. C. and Rao, B. V. R. (1935). A study of microsporogenesis in two Menispermaceae. *La Cellule*, **44**, 221-234.
- Maheshwari, P. (1950). *An introduction to the embryology of Angiosperms*, New York.
- Mauritzon, J. (1939). Contributions to the embryology of the orders Rosales and Myrtales. *Lunds. Univ. Årsskr. N.F. Afd. II*, **35**, 1-120.
- Swamy, B. G. L. (1949). Further contributions to the morphology of the Dogeneriaceae. *Jour. Arnold Arboretum*, **30**, 10-38.
- Willis, J. C. (1948). *A dictionary of flowering plants and ferns*. Cambridge.

ALKALINE PHOSPHATASE AND PERIODIC ACID-SCHIFF REACTIONS IN THE THYMUS OF *CALOTES VERSICOLOR* (DAUD.)

by M. APPASWAMY RAO, *Department of Zoology, Central College, Bangalore*

(Communicated by B. R. Seshachar, F.N.I.)

(Received April 15; after revision July 3; read August 6, 1954)

CONTENTS

	<i>Page</i>
Introduction	503
Material and Methods	503
Observations:	
(a) Alkaline phosphatase activity	504
(b) Periodic acid-Schiff reaction	504
Discussion	505
Summary	506
Acknowledgement	506
References	506
Explanation of photomicrographs	507

INTRODUCTION

Histological and histochemical studies on the thymus of mammals (Dearth, 1928; Kingsbury, 1928 and 1941; Smith and Parkhurst, 1949) have shown that the multicellular Hassall's corpuscles resemble to a large extent the keratinizing cells of the stratified squamous epithelium. The application of Gomori's (1939) technique for alkaline phosphatase and the periodic acid-Schiff reaction of Hotchkiss (1948) has led to the conclusion that in two widely different cell elements such as these, the same essential processes of the production and deposition of keratin are taking place. It is well known that in reptiles (Jordan and Looper, 1928) these complex type of concentric corpuscles of Hassall, so characteristic of mammalian thymus, are wanting, but instead, there are unicellular Hassall's corpuscles and a group of interesting cell elements known as multinucleated plasmodial masses. From histogenetic point of view the origin of multicellular Hassall's corpuscles of mammals is not clear. It is also not clear which cell elements in the mammalian thymus represent the unicellular Hassall's corpuscles or multinucleated plasmodial masses, though the plasmodial masses resemble to some extent the thymic canals of the mammalian thymus.

It was felt that application of histochemical techniques to the thymus of a reptile would perhaps yield information useful in establishment of a histogenetic relationship of these diverse cell elements in the thymus. The lizard, *Calotes versicolor*, served as the animal of choice in this study.

MATERIAL AND METHODS

The thymus of *Calotes versicolor* was dissected out and fixed in chilled 80% ethyl alcohol for alkaline phosphatase and ice-cold Rossman's fluid for periodic acid-Schiff reaction. Paraffin sections of 6 μ thickness were cut and the technique of Gomori (1939) for demonstration of alkaline phosphatase was employed. No counter-stain was used and control sections were not incubated in the substrate. A few slides were

also stained in Heidenhain's haematoxylin and Mallory's triple stains. Deparaffinized sections of material fixed in Rossman's fluid were stained by the periodic acid-Schiff method according to the procedure of Hotchkiss (1948). For histological studies the material was fixed in Zenker's formol-acetic and Bouin's fluids. Sections 10 μ thick were cut and stained in Heidenhain's haematoxylin, Mallory's triple and Shorr's differential stains.

OBSERVATIONS

(a) Alkaline phosphatase activity.

In the thymus of *Calotes versicolor* the multinucleated plasmodial masses arise as fusion products of reticular cells. Dissolution of their cytoplasm takes place at the periphery and extends inwards forming lacunae lined by flattened reticulum with central degenerating masses (Figs. 1, 4 and 5). In these degenerating masses granules of irregular shape appear, stained dark in Heidenhain's haematoxylin, dark blue in Mallory's triple and deep green with Shorr's differential stains. It is hard to determine the cells in which these granules appear, as cell boundaries are indistinct. Many a time the central portion of plasmodial mass is compact and appears as a solid homogeneous mass stained heavily in all stains (Figs. 4 and 5).

An examination of sections prepared according to Gomori's (1939) method for alkaline phosphatase shows that the capsular wall, trabeculae, endothelia and plasmodial masses are positive to this reaction. In the plasmodial masses, where degeneration has not yet set in, the reaction is almost negative. As soon as degeneration starts, dark granules appear indicating the sites of alkaline phosphatase activity (Fig. 6). Gradually, as degeneration progresses, black patches of cobalt sulphide appear, indicating increased amounts of this enzyme. It is interesting to note that the wall of lacunae containing these degenerating plasmodial masses does not indicate any phosphatase activity (Figs. 2 and 6).

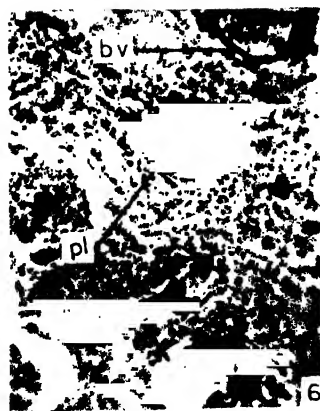
This enzyme is absent in unicellular Hassall's corpuscles and basophilic granulocytes. The thymocytes, however, offer a different picture. Those that are in the proximity of blood vessels and plasmodial masses are positive, whereas those that are away from them show faint or negative reactions. It is difficult to provide an adequate explanation for this fact where morphologically the same type of cell, the thymocyte, gives two different reactions depending on its location with reference to other cells showing a positive reaction. It leads me to the conclusion that perhaps a diffusion from blood vessels and plasmodial masses which show a high concentration of this enzyme, takes place, and that the thymocytes in close proximity to them give a positive reaction. Doyle (1950) has found a similar phenomenon in the lymphocytes of the appendix of irradiated rats.

(b) Periodic acid-Schiff reaction (PAS).

The capsular wall, trabeculae, endothelia, basophilic granulocytes and plasmodial masses are positive to this reaction. The plasmodial masses, however, show a particularly intense one. Here too, as in alkaline phosphatase, the reaction varies with the progressive degeneration of cell masses. Newly formed plasmodial masses present a pale reaction, while in those where degeneration has advanced considerably the reaction is deep red (Figs. 3 and 7). The walls of the lacunae of the plasmodial masses always present a negative reaction, while the endothelium of the blood vessel is positive.

The basophilic granulocytes are generally in groups and many are multinucleated (Figs. 8 and 9). They are filled with refringent granules. In preparations stained with Mallory's triple, they are coloured pale blue and appear light green when stained with Shorr's method. These cells show a strong positive reaction to the PAS technique (Fig. 9) and appear to have coarse red granules in their cytoplasm.

The unicellular Hassall's corpuscles and thymocytes are negative to this reaction.



DISCUSSION

The mammalian thymus differs from that of reptiles in the presence of the complex type of Hassall's corpuscles. These are large cell groups which lie in the medulla and which display a concentric arrangement of fusiform cells (Jordan and Horsley, 1927; Dearth, 1928; Kingsbury, 1928; Smith and Parkhurst, 1949). Such corpuscles are absent in the thymus of amphibians and reptiles, but in their place occur unicellular Hassall's corpuscles, much smaller in size and consisting of a single cell element. In addition to the unicellular Hassall's corpuscles there are in the thymus of these vertebrates, groups of cells fused to form plasmodial masses which are derived from reticular cells (Jordan and Looper, 1928; James, 1939; Fabrizio and Charipper, 1941).

The relationship between these different cell elements is a subject of much interest and an understanding of the homology becomes clear on the employment of specific histochemical techniques. The work of Smith and Parkhurst (1949) has shown that the concentric corpuscles of the mammalian thymus are positive for alkaline phosphatase and PAS reactions. It has been interpreted that during degeneration of these corpuscles there is production and deposition of keratin. Many investigators (Dempsey and Wislocki, 1945; Bradfield, 1950; Doyle, 1951; Ring, 1952) are of the opinion that alkaline phosphatase is probably related to the elaboration of keratin. Comparative studies on the Hassall's corpuscles of the thymus and skin of guinea-pig have shown that in both cases the production and deposition of keratin are closely associated with alkaline phosphatase activity and PAS reaction (Smith and Parkhurst, 1949).

The present studies reveal some interesting differences between the Hassall's corpuscles of the mammalian thymus and those of reptiles. The multicellular Hassall's corpuscle of the mammalian thymus is strongly positive to alkaline phosphatase (Smith and Parkhurst, 1949), whereas the unicellular Hassall's corpuscle of the thymus of *Calotes versicolor* is completely negative for this enzyme. Thus these two cell elements—the concentric corpuscles of Hassall of the mammalian thymus and unicellular Hassall's corpuscles of the reptile—though resembling externally in the concentric system of striations (Jordan and Looper, 1928), are widely different in their reactions to alkaline phosphatase. The absence of this enzyme from the unicellular Hassall's corpuscles of reptiles shows that there is probably no deposition of keratin in these cells.

The above conclusion is supported by the results of PAS reaction. Recent work of Moog and Wenger (1952) has shown that PAS reactive substance and alkaline phosphatase are physiologically related and that wherever the latter is present the PAS reaction is positive. It is known from the studies of Smith and Parkhurst (1949) that the concentric corpuscles of mammalian thymus are positive to PAS reaction, just as they are positive for alkaline phosphatase. On the other hand, the unicellular Hassall's corpuscles in the thymus of *Calotes versicolor* are negative to both PAS and alkaline phosphatase reactions. This indicates that these thymic cell elements in the two vertebrate classes are different in function.

The plasmodial masses in the thymus of *Calotes versicolor*, however, react differently. In contrast to the unicellular Hassall's corpuscles, these masses show intense alkaline phosphatase and PAS reactions (Figs. 2, 3, 6 and 7). The significance of the positive alkaline phosphatase and PAS reactions in the plasmodial masses and negative reactions in the unicellular Hassall's corpuscles is interesting. Jordan and Looper (1928) have tried to establish a genetic relationship between the unicellular Hassall's corpuscle of the thymus of the box turtle (*Terrapene carolina*) and the mammalian Hassall's corpuscle, because of the superficial resemblance in these two cell elements. They consider the multinucleated plasmodial masses, which do not show any characteristic concentric arrangement of cells, as the progenitors of thymic canals of mammals. The alkaline phosphatase and PAS reactions in the thymus of

Calotes versicolor indicate that the multinucleated plasmodial masses resemble the complex type of Hassall's corpuscles of mammals as both show intense positive reactions, whereas the unicellular Hassall's corpuscles are negative and hence cannot be compared as far as these reactions are concerned. It is suggested that the multicellular Hassall's corpuscles of the mammalian thymus have probably been derived from the reptilian thymic plasmodial masses.

It was observed that another group of cell elements in the thymus of *Calotes versicolor* behaved in an interesting manner to these two reactions. The basophilic granulocytes are positive to PAS but are negative to alkaline phosphatase. It is well known that in tissues where the PAS reaction is positive, the interpretation is that large amounts of lipids and polysaccharides are being produced (Hotchkiss, 1948; Moog and Wenger, 1952). The fact that these granulocytes are strongly positive to PAS but negative to alkaline phosphatase indicates the presence of compounds in their cytoplasm which can be oxidized to aldehydes, probably of a lipid nature. That is also the conclusion of Loewenthal and Smith (1952) in the foamy cells of the thymus of mouse.

SUMMARY

1. The unicellular Hassall's corpuscles of the thymus of *Calotes versicolor* are negative to alkaline phosphatase and periodic acid-Schiff reactions and are not comparable with the multicellular Hassall's corpuscles of the thymus of mammals, which are positive to these two reactions.

2. The plasmodial masses of the thymus of *Calotes versicolor* resemble to a very great extent the concentric corpuscles of Hassall of the mammalian thymus, because of the striking resemblance of these two cell elements in their reactions to Gomori's treatment and PAS technique. The intensity of alkaline phosphatase and PAS reactions in these multinucleated plasmodial masses of the thymus of *Calotes versicolor* probably depends upon the degree of degeneration and keratin formation.

3. The basophilic granulocytes are generally in groups. They are large, multinucleated and contain refringent granules. An intense reaction of these cells to PAS treatment is probably due to elaboration of lipids. Generally they are negative to alkaline phosphatase.

ACKNOWLEDGEMENT

I am greatly indebted to Prof. B. R. Seshachar for guidance and encouragement. I am thankful to the University of Mysore for the award of Research Fellowship which provided me the opportunity for this study. My thanks are due to Mr. M. M. Veerabhadraiah for helping me in the preparation of photomicrographs.

REFERENCES

- Bradfield, J. R. G. (1950). The localization of enzymes in cells. *Biol. Reviews*, **25**, 113-157.
- Dearth, O. A. (1928). Late development of the thymus in the cat; nature and significance of the corpuscles of Hassall and cystic formations. *Am. J. Anat.*, **41**, 321-351.
- Dempsey, E. W. and G. B. Wislocki (1945). Histochemical reactions associated with basophilia and acidophilia in the placenta and the pituitary gland. *Am. J. Anat.*, **76**, 277-301.
- Doyle, W. L. (1950). The distribution of the alkaline phosphatase in the rabbit appendix after X-irradiation. *Am. J. Anat.*, **87**, 79-117.
- (1951). Quantitative aspects of the histochemistry of phosphatases. *Symposium on cytology*, Michigan State College Press. 1-20.
- Fabrizio, M. and H. A. Charipper (1941). The morphogenesis of the thymus of *Rana sylvatica* as correlated with certain stages of metamorphosis. *J. Morph.*, **68**, 179-195.
- Gomori, G. (1939). Microtechnical demonstration of phosphatases in tissue sections. *Proc. Soc. Exp. Biol. and Med.*, **42**, 23-26.
- Hotchkiss, R. D. (1948). A microchemical reaction resulting in the staining of polysaccharide structures in fixed tissue preparations. *Arch. Biochem.*, **16**, 131-141.
- James, E. S. (1939). The morphology of the thymus and its changes with age in the neotenus amphibian (*Necturus maculosus*). *J. Morph.*, **64**, 455-481.
- Jordan, H. E. and G. W. Horsley (1927). The significance of the thymic corpuscles (Hassall). *Anat. Rec.*, **38**, 141-160.

- Jordan, H. E. and J. B. Looper (1928). The histology of the thymus gland of the box turtle, *Terrapene carolina*, with special reference to the concentric corpuscles of Hassall and the eosinophilic granulocytes. *Anat. Rec.*, **40**, 309-337.
- Kingsbury, B. F. (1928). On the nature and significance of the thymic corpuscles. *Anat. Rec.*, **38**, 141-159.
- (1941). The interpretation of thymic bodies. *Endocrin.*, **29**, 155-160.
- Loewenthal, L. A. and C. Smith (1952). Studies on the thymus of the mammal. IV. Lipid laden foamy cells in the involuting thymus of the mouse. *Anat. Rec.*, **112**, 1-16.
- Moog, F. and E. L. Wenger (1952). The occurrence of a neutral mucopolysaccharide at sites of high alkaline phosphatase activity. *Am. J. Anat.*, **90**, 339-378.
- Ring, J. R. (1952). Alkaline phosphatase activity of healing wounds in the rat. *J. Dent. Res.*, **31**, 329-334.
- Smith, C. and H. T. Parkhurst (1949). Studies on the thymus of the mammal. II. A comparison of the staining properties of Hassall's corpuscles and of the thick skin of the guinea-pig. *Anat. Rec.*, **103**, 649-674.

EXPLANATION OF PHOTOMICROGRAPHS

KEY TO LETTERING

- bg.—Basophilic granulocytes.
 bv.—Blood vessel.
 pl.—Plasmodial mass.

PLATE XXI

- FIG. 1. Sagittal section of thymus of *Calotes versicolor* showing degenerating plasmodial masses in the medulla. Bouin: Heidenhain's haematoxylin. $\times 40$.
- FIG. 2. The thymus showing the distribution of alkaline phosphatase. Gomori's technique. $\times 30$.
- FIG. 3. The thymus showing the regions positive to PAS reaction. $\times 33$.
- FIG. 4. Enlarged view of sagittal section of thymus showing degenerating plasmodial masses. Bouin: Heidenhain's haematoxylin. $\times 210$.
- FIG. 5. A portion of the thymus enlarged to show the progressive degeneration of multinucleated plasmodial masses. Zenker's formol-acetic: Mallory's triple. $\times 360$.
- FIG. 6. Enlarged view of sagittal section of thymus. Degenerating plasmodial masses and endothelia of blood vessels show high concentration of alkaline phosphatase. Thymocytes near regions of high concentration are also heavily stained. Gomori's technique. $\times 216$.
- FIG. 7. A portion of the thymus enlarged. Only the degenerating portion of the plasmodial masses and basophilic granulocytes are positive to PAS reaction. $\times 225$.
- FIG. 8. A portion of thymus enlarged to show the grouping of the basophilic granulocytes. Bouin: Shorr's differential stain. $\times 570$.
- FIG. 9. Enlarged view of a portion of thymus to show the positive reaction of the basophilic granulocytes to PAS technique. $\times 570$.

Issued September 29, 1954.

THE IRREDUCIBLE REPRESENTATIONS OF THE LIE-ALGEBRA OF THE ORTHOGONAL GROUP WITH SPIN $\frac{1}{2}$

by K. VENKATACHALIENGAR, *Professor of Mathematics, University of Mysore, Mysore*, and K. N. SRINIVASA RAO, *N.I.S. Junior Research Fellow, University of Mysore, Mysore*

(Communicated by B. S. Madhava Rao, F.N.I.)

(Received May 13, 1953; read May 7, 1954)

1. INTRODUCTION

In recent years, the Lie-algebras of the orthogonal group, considered as associative algebras generated by a number of symbols satisfying a set of relations have been found to be of importance in the theory of elementary particles in Quantum Mechanics. The Clifford-Dirac algebra of 4 symbols which is the Lie-algebra of the orthogonal group in 5 dimensions was employed by Dirac in his theory of the electron whose spin is $\frac{1}{2}$. Explicit matrices of the representation of the Clifford-Dirac algebra with any number of symbols were given by Brauer and Weyl (1935). The Lie-algebra associated with an elementary particle of spin 1 was investigated by Kemmer (1939) and the matrices of the representations were obtained in an explicit form by D. E. Littlewood (1947).

The investigation of the Lie-algebras for higher spins is more complicated. It was, however, proved by Madhava Rao, Thiruvengkatachar and Venkatachaliengar (1946) that the algebra for the case of half-odd-integral spins is the direct product of the corresponding Clifford-Dirac algebra and another algebra called the ξ -algebra generated by the symbols $\xi_1, \xi_2, \dots, \xi_n$ satisfying the commutation rules

$$(i) \{ \xi_r, \{ \xi_r, \xi_s \} \} = \xi_s,$$

$$(ii) [\xi_r, \{ \xi_s, \xi_t \}] = 0; r \neq s \neq t,$$

where $\{a, b\}$ is the anticommutator $ab+ba$ and $[a, b]$ is the commutator $ab-ba$

This direct product resolution simplifies the problem of determining the irreducible representations of the Lie-algebra considerably. The matrices of the irreducible representations of the Lie-algebra are then the Kronecker products of the matrices of the irreducible representations of the ξ -algebra and those of the corresponding Clifford-Dirac algebra. In the case of spin $\frac{3}{2}$, the symbols generating the original Lie-algebra satisfy a quartic and the corresponding symbols ξ_r satisfy the quadratic

$$\xi^2 = \frac{3}{4} - \xi.$$

In this paper, we take up the investigation of the ξ -algebra A_n generated by the n symbols $\xi_1, \xi_2, \dots, \xi_n$ with spin $\frac{3}{2}$. We show that the centre of the algebra is generated by a single element θ and obtain the minimal equation it satisfies. We set $\xi_{r-1} = \omega_{1r}$; $\{\omega_{1r}, \omega_{1s}\} = \omega_{rs}$ and show that the irreducible representations of the algebra A_n are given by

I (a) when n is even ;

$$D_{nr}(\omega_{n,n+1}) = \frac{1}{2} E_{f_1} + \left| \begin{array}{cc} \frac{(2r-n-6)}{2(n-2r+4)} & 1 \\ \frac{(n-2r+4)^2-1}{(n-2r+4)^2} & \frac{(2r-n-2)}{2(n-2r+4)} \end{array} \right| \times E_{f_2} + \frac{1}{2} E_{f_3}$$

$$1 \leq r \leq \frac{n}{2} + 1$$

(b) when n is odd, we have the same expression for $D_{nr}(\omega_{n,n+1})$ as I(a) with $1 \leq r \leq \frac{n+1}{2}$ and an additional representation.

$$D_{n, \frac{n+3}{2}}(\omega_{n,n+1}) = \frac{1}{2} E_{f_4} + -\frac{3}{2} E_{f_5}$$

where E_k is the unit matrix of order k .

$$\text{II. } D_{nr}(\omega_{p,p+1}) = D_{n-1,r-1}(\omega_{p,p+1}) + D_{n-1,r}(\omega_{p,p+1})$$

$$p = 1, 2, 3, \dots, (n-1).$$

By taking the anticommutators of the $\omega_{p,p+1}$ repeatedly, we obtain the matrices for ξ_r .

We prove also that the dimension of the algebra A_n is given by the simple expression $\frac{2}{n+2} \binom{2n+1}{n}$. It follows, therefore that the dimension of the corresponding Lie-algebra of the orthogonal group is given by

$$\frac{2^{n+1}}{n+2} \binom{2n+1}{n}.$$

2. THE ξ -ALGEBRA

Let A_n be the ξ -algebra generated by the n symbols $\xi_1, \xi_2, \dots, \xi_n$, which satisfy the following relations :—

$$(1) (a). \quad \xi^2 = \mathbb{I} - \xi^*$$

$$(1) (b). \quad \{\xi_r, \{\xi_r, \xi_s\}\} = \xi_s; \quad \{\xi_r, \xi_s\} = \xi_r \xi_s + \xi_s \xi_r.$$

$$(1) (c). \quad [\xi_r, \{\xi_s, \xi_t\}] = 0 \quad [\xi_r, \xi_s] = \xi_r \xi_s - \xi_s \xi_r$$

$$r \neq s \neq t.$$

We set

$$\xi_{r-1} = \omega_{1r} = \omega_{r1}; [r = 2, 3, \dots, (n+1)]$$

and

$$\{\xi_{r-1}, \xi_{s-1}\} = \{\omega_{1r}, \omega_{1s}\} = \omega_{rs}.$$

It follows easily that $\{\xi_r, \xi_s\}^2 = \mathbb{I} - \{\xi_r, \xi_s\}$.

* In the paper by Madhava Rao and collaborators referred to, ξ is taken to satisfy $\xi^2 = \xi + \mathbb{I}$. We have here replaced ξ by $-\xi$ for the slight simplification of some of the formulae.

Hence the ω 's satisfy the relations :

$$(1') (a). \quad \omega_{pq}^2 = \frac{3}{4} - \omega_{pq} \quad (p \neq q).$$

$$(1') (b). \quad \{\omega_{1r}, \omega_{rs}\} = \omega_{1s}.$$

$$(1') (c). \quad [\omega_{1r}, \omega_{st}] = 0; \quad \omega_{fr} = \omega_{qr}.$$

$$r \neq s \neq t.$$

From 1' (a), it follows that in any representation ω_{pq} has the eigen-values $\frac{1}{2}$ or $-\frac{1}{2}$. Consider a representation in which ω_{1r} is diagonal, say $|\lambda_r|$ and let $\omega_{1s} = |a_{pq}|$.

We have
$$\{\omega_{1r}, \omega_{1s}\} = |(\lambda_p + \lambda_q) a_{pq}|.$$

Since
$$\{\omega_{1r}, \omega_{rs}\} = \omega_{1s}$$

$$(\lambda_p + \lambda_q)^2 a_{pq} = a_{pq}$$

$$\therefore 4\lambda_p^2 a_{pp} = a_{pp},$$

i.e. either
$$\lambda_p = \frac{1}{2} \text{ or } a_{pp} = 0.$$

Now
$$\text{spur } \omega_{1s} = \sum a_{pp}$$

and

$$\text{spur } \{\omega_{1r}, \omega_{1s}\} = \sum 2\lambda_p a_{pp} = \sum a_{pp} = \text{spur } \omega_{1s}.$$

Similarly, taking ω_{1s} diagonal, we obtain

$$\text{spur } \omega_{1r} = \text{spur } \{\omega_{1s}, \omega_{1r}\}.$$

We therefore have

$$(2) \quad \text{spur } \omega_{1r} = \text{spur } \omega_{1s} = \text{spur } \omega_{rs}.$$

It is clear that (2) is true for any spin.

We now proceed to obtain explicit matrices for the irreducible representations of the algebra A_n . From the theory of the orthogonal group (cf. F. D. Murnaghan : The theory of group representations) it follows that the dimension formula for the irreducible representations of the Lie-algebra (generated by n symbols) is

$$(3) (a) \quad D_{\lambda_1 \lambda_2 \dots \lambda_k} = \frac{2^k l'_1 l'_2 \dots l'_k}{1 \cdot 3 \dots (2k-1)} \prod_{p < q}^k (l_p^2 - l_q^2); \quad n = 2k$$

and

$$(3) (b) \quad D_{\lambda_1 \lambda_2 \dots \lambda_k} = \frac{2^{k-1}}{2 \cdot 4 \dots (2k-2)} \prod_{p < q}^k (l_p^2 - l_q^2); \quad n = 2k-1,$$

where $\lambda_1, \lambda_2, \dots, \lambda_k$ are half-odd integers such that $\lambda_1 \geq \lambda_2 \geq \dots \geq \lambda_k$; $l_p = \lambda_p + (k-p)$; $l'_p = l_p + \frac{1}{2}$; and λ_1 is the spin. Denoting by $f_{\lambda_1 \lambda_2 \dots \lambda_k}$, the dimension of the corresponding irreducible representation of the ξ -algebra, we have, since 2^k (or 2^{k-1}) is the dimension of the irreducible representation of the Clifford-Dirac algebra according as $n = 2k$ (or $2k-1$),

$$(3') (a) \quad f_{\lambda_1 \lambda_2 \dots \lambda_k} = \frac{D_{\lambda_1 \lambda_2 \dots \lambda_k}}{2^k}; \quad n = 2k,$$

$$(3') (b) \quad f_{\lambda_1 \lambda_2 \dots \lambda_k} = \frac{D_{\lambda_1 \lambda_2 \dots \lambda_k}}{2^{k-1}}; \quad n = 2k-1.$$

If spin $= \frac{3}{2}$, the λ 's are all either $\frac{3}{2}$ or $\frac{1}{2}$.

Let $f_{nr} \equiv f_{\frac{1}{2}, \dots, \frac{1}{2}, \frac{1}{2}, \dots, \frac{1}{2}}$ with $(r-1) \rightarrow \frac{3}{2}$'s and $(k-r+1) \rightarrow \frac{1}{2}$'s, r taking the values $1, 2, \dots, (k+1)$ where $n = 2k$ or $2k-1$; there will be $(k+1)$ irreducible representations of the algebra A_n .

We obtain after some simplification that the formulae 3'(a) and 3'(b) both reduce to

$$(4) \quad f_{nr} \equiv f_{\frac{1}{2}, \dots, \frac{1}{2}, \frac{1}{2}, \dots, \frac{1}{2}} = \frac{n-2r+4}{n+2} \binom{n+2}{r-1}$$

we define $f_{nr} = 0$ for $r > \frac{n+4}{2}$, since $f_{nr} = 0$ for $n = 2r-4$ and negative for $n < 2r-4$. i.e. r takes the values

$$1, 2, 3, \dots, \frac{n}{2}+1 \text{ if } n \text{ is even}$$

and

$$1, 2, 3, \dots, \frac{n+1}{2}, \frac{n+3}{2} \text{ if } n \text{ is odd.}$$

We denote by D_{nr} the irreducible representation (of the algebra A_n) whose dimension is f_{nr} and by $D_{nr}(\omega_{pq})$ the matrix of representation for ω_{pq} in the representation D_{nr} .

It follows from the theory of the orthogonal group that the algebra A_n branches over the algebra A_{n-1} according to the law

$$(5) \quad D_{nr}(\omega_{pq}) = D_{n-1, r-1}(\omega_{pq}) + D_{n-1, r}(\omega_{pq})$$

[It is verified easily that $f_{nr} = f_{n-1, r-1} + f_{n-1, r}$].

We next show that if S_{nr} is the spur of any ω_{pq} in the irreducible representation D_{nr} , then

$$(6) \quad \begin{aligned} S_{nr} &= f_{nr} \frac{n^2 + (5-4r)n + 4(r-1)(r-3)}{2n(n+1)} \\ &= (n-2r+4) \frac{(n-1)(n-2) \dots (n-r+4)}{2 \cdot \underline{r-1}} \times \\ &\quad \times \{n^2 + (5-4r)n + 4(r-1)(r-3)\} \end{aligned}$$

Proof:

We assume the result to be true for the algebra A_{n-1} and prove it for A_n . From (5) it follows that

$$S_{nr} = S_{n-1, r-1} + S_{n-1, r}.$$

Now $S_{n-1, r-1} + S_{n-1, r} =$

$$\begin{aligned} &= \frac{(n-2r+5)}{2 \cdot \underline{r-2}} (n-2)(n-3) \dots (n-r+4) \{n^2 + (7-4r)n + 4(r-2)(r-3)\} \\ &\quad + \frac{(n-2r+3)}{2 \cdot \underline{r-1}} (n-2)(n-3) \dots (n-r+3) \{n^2 + (3-4r)n + 4(r-1)(r-2)\} \\ &= \frac{(n-2) \dots (n-r+4)}{2 \cdot \underline{r-1}} \left[\frac{(n-2r+5)(r-1)}{(n-2r+3)(n-r+3)} \{n^2 + (7-4r)n + 4(r-2)(r-3)\} + \right. \\ &\quad \left. \{n^2 + (3-4r)n + 4(r-1)(r-2)\} \right] \end{aligned}$$

i.e. $S_{n-1, r-1} + S_{n-1, r} =$

$$= \frac{(n-2) \dots (n-r+4)}{2 \lfloor r-1 \rfloor} \left[(n-2r+4)(n-1) \{ n^2 + (5-4r)n + 4(r-1)(r-3) \} \right]$$

on simplification.

$$= S_{nr}.$$

Now $D_{n1}(\omega_{pq}) = \frac{1}{2}$ for all n so that $S_{n1} = \frac{1}{2}$ and for the algebra A_2 , one can see easily that

$$D_{22}(\omega_{12}) = \begin{vmatrix} \frac{1}{2} & 0 \\ 0 & -\frac{3}{2} \end{vmatrix} \text{ or } S_{22} = -1.$$

That is, the formula is true for S_{n1} and S_{22} and hence by induction it is universally true.

3. THE IRREDUCIBLE REPRESENTATIONS OF A_n

We consider the algebra A_n as generated by the n symmetric symbols $\omega_{12}, \omega_{23}, \dots, \omega_{p, p+1}, \dots, \omega_{n, n+1}$ and define

$$\omega_{rs} = \{ \omega_{1r}, \omega_{1s} \}; r \neq s \text{ with the relations (I')}.$$

From (I') (c) it follows that

$$[\omega_{pq}, \omega_{st}] = 0; \quad p, q \neq s, t.$$

Therefore, $\omega_{n, n+1}$ commutes with $\omega_{12}, \omega_{23}, \dots, \omega_{n-2, n-1}$, i.e. with the algebra A_{n-2} . We also have the branching law

$$D_{nr}(\omega_{p, p+1}) = D_{n-1, r-1}(\omega_{p, p+1}) + D_{n-1, r}(\omega_{p, p+1}); \quad p = 1, 2, 3, \dots, (n-1).$$

We now show that—

(7) (a). When n is even

$$D_{nr}(\omega_{n, n+1}) = \frac{1}{2} E_{f_1} + \begin{vmatrix} \frac{2r-n-6}{2(n-2r+4)} & 1 \\ \frac{(n-2r+4)^2-1}{(n-2r+4)^2} & \frac{(2r-n-2)}{2(n-2r+4)} \end{vmatrix} \times E_{f_2} + \frac{1}{2} E_{f_3}$$

$$1 \leq r \leq \frac{n}{2} + 1.$$

(7) (b). When n is odd, we have the same expression for $D_m(\omega_{n, n+1})$ as (7) (a) with

$1 \leq r \leq \frac{n+1}{2}$ and an additional representation

$$(8) \quad D_{n, \frac{n+3}{2}}(\omega_{n, n+1}) = \frac{1}{2} E_{f_4} + -\frac{3}{2} E_{f_5},$$

where $E_f, E_{f_2}, E_{f_3}, E_{f_4}, E_{f_5}$ are unit matrices of orders

$$f_1 = f_{n-2, r-2}$$

$$f_2 = f_{n-2, r-1}$$

$$f_3 = f_{n-2, r}$$

$$f_4 = f_{n-2, \frac{n-1}{2}}$$

$$f_5 = f_{n-2, \frac{n+1}{2}} \text{ respectively}$$

with $E_k = 0$ for $k < 0$ and $E_1 = 1$.

Proof:

We first of all determine $D_{n, \frac{n+3}{2}}(\omega_{n, n+1})$ when n is odd. We have, by the branching law, that $D_{n, \frac{n+3}{2}}$ is the same as $D_{n-1, \frac{n+1}{2}}$ over the algebra A_{n-1} . Taking the branching again over A_{n-2} , we have

$$D_{n, \frac{n+3}{2}}(\omega_{p, p+1}) = D_{n-2, \frac{n-1}{2}}(\omega_{p, p+1}) + D_{n-2, \frac{n+1}{2}}(\omega_{p, p+1}) \text{ over } A_{n-2};$$

$$(1 \leq p \leq n-2).$$

Since $\omega_{n, n+1}$ commutes with the algebra A_{n-2} , we have by the Schur lemma,

$$D_{n, \frac{n+3}{2}}(\omega_{n, n+1}) = \lambda_1 E_{f_4} + \lambda_2 E_{f_5}.$$

Writing $n = 2m+1$, we have

$$f_4 = f_{2m-1, m} = \frac{3(m+3)(m+4) \dots (2m)}{[m-1]}$$

$$f_5 = f_{2m-1, m+1} = \frac{(m+2)(m+3) \dots (2m)}{[m]}.$$

Hence taking the spur of $\omega_{n, n+1}$, we have

$$(9) \quad \lambda_1 f_4 + \lambda_2 f_5 = S_{n, \frac{n+3}{2}} = S_{2m+1, m+2}$$

$$= \frac{-3(m+3)(m+4) \dots (2m)}{[m]},$$

i.e.

$$\lambda_1 3m + \lambda_2 (m+2) = -3$$

or

$$\lambda_1 = \frac{1}{2} \text{ and } \lambda_2 = -\frac{3}{2}.$$

Thus, we have

$$(8) \quad D_{n, \frac{n+3}{2}}(\omega_{n, n+1}) = \frac{1}{2} E_{f_4} - \frac{3}{2} E_{f_5}.$$

To prove (7), we observe, first of all by the branching law, that

$$D_n(\omega_{p, p+1}) = D_{n-1, r-1}(\omega_{p, p+1}) + D_{n-1, r}(\omega_{p, p+1}) \text{ over } A_{n-1}$$

$$= D_{n-2, r-2}(\omega_{p, p+1}) + D_{n-2, r-1}(\omega_{p, p+1})$$

$$+ D_{n-2, r-1}(\omega_{p, p+1}) + D_{n-2, r}(\omega_{p, p+1}) \text{ over } A_{n-2}$$

$$= D_{n-2, r-2}(\omega_{p, p+1}) + E_2 \times D_{n-2, r-1}(\omega_{p, p+1})$$

$$+ D_{n-2, r}(\omega_{p, p+1}) \text{ over } A_{n-2}.$$

Since $\omega_{n, n+1}$ commutes with the algebra A_{n-2} , we have by the Schur lemma,

$$D_{nr}(\omega_{n, n+1}) = a_{11} E_{f_1} + \begin{vmatrix} a_{22} & a_{23} \\ a_{32} & a_{33} \end{vmatrix} \times E_{f_2} + a_{44} E_{f_3},$$

where

$$f_1 = f_{n-2, r-2}; \quad f_2 = f_{n-2, r-1}; \quad f_3 = f_{n-2, r}.$$

Since

$$\omega_{n, n+1}^2 = \frac{3}{4} - \omega_{n, n+1},$$

$$a_{11}, a_{44} = \frac{1}{2} \text{ or } -\frac{3}{2}; \quad a_{22} + a_{33} = -1$$

and

$$a_{22}^2 + a_{23} a_{32} = \frac{3}{4} - a_{22}.$$

Taking the spur of $\omega_{n, n+1}$, we have

$$a_{11} f_1 + (a_{22} + a_{33}) f_2 + a_{44} f_3 = S_{nr},$$

i.e.

$$\begin{aligned} (10) \quad & \frac{(n-r+4)(n-r+5) \dots (n-1)}{r-3} \left\{ a_{11} (n-2r+6) - \frac{(n-2r+4)(n-r+3)}{r-2} \right. \\ & \left. + a_{44} \frac{(n-2r+2)(n-r+2)(n-r+3)}{(r-1)(r-2)} \right\} \\ & = (n-2r+4) \frac{(n-r+4)(n-r+5) \dots (n-1)}{2(r-1)} \times \\ & \quad \times \{ n^2 + (5-4r)n + 4(r-1)(r-3) \}. \end{aligned}$$

It is easily seen that (10) will be consistent for the value $\frac{1}{2}$ only for a_{11} and a_{44} .

We now assume the result (7) for $n = m$ and prove it for $(m+1)$.

We have just proved that

$$D_{m+1, r}(\omega_{m+1, m+2}) = \frac{1}{2} E_{f'_1} + \begin{vmatrix} a_{22} & a_{23} \\ a_{32} & a_{33} \end{vmatrix} \times E_{f'_2} + \frac{1}{2} E_{f'_3},$$

where

$$f'_1 = f_{m-1, r-2}; \quad f'_2 = f_{m-1, r-1}; \quad f'_3 = f_{m-1, r} \text{ and } a_{22} + a_{33} = -1.$$

Hence

$$\text{spur}(\omega_{m+1, m+2}) = \frac{1}{2} f'_1 - f'_2 + \frac{1}{2} f'_3 = S_{m+1, r}.$$

Now

$D_{m+1, r}(\omega_{m, m+1}) = D_{m, r-1}(\omega_{m, m+1}) + D_{m, r}(\omega_{m, m+1})$ by the branching law

$$\begin{aligned} & = \frac{1}{2} E_{f''_1} + \begin{vmatrix} \frac{(2r-m-8)}{2(m-2r+6)} & 1 \\ \frac{(m-2r+6)^2-1}{(m-2r+1)^2} & \frac{(2r-m-4)}{2(m-2r-6)} \end{vmatrix} \times E_{f''_2} + \frac{1}{2} E_{f''_3} \\ & + \frac{1}{2} E_{f'_1} + \begin{vmatrix} \frac{(2r-m-6)}{2(m-2r+4)} & 1 \\ \frac{(m-2r+4)^2-1}{(m-2r+4)^2} & \frac{(2r-m-2)}{2(m-2r+4)} \end{vmatrix} \times E_{f'_2} + \frac{1}{2} E_{f'_3}. \end{aligned}$$

where

$$\begin{aligned} f_1' &= f_{m-2, r-3}; \quad f_2' = f_{m-2, r-2}; \quad f_3' = f_{m-2, r-1} \\ f_1 &= f_{m-2, r-2}; \quad f_2 = f_{m-2, r-1}; \quad f_3 = f_{m-2, r}. \end{aligned}$$

It follows easily from (1')(b) and (1')(c) that $\{\omega_{rs}, \omega_{st}\} = \omega_{rt}$ and hence $\text{spur } \{\omega_{m, m+1}, \omega_{m+1, m+2}\}$ is also $S_{m+1, r}$; we thus have

$$\begin{aligned} (11) \quad & \frac{1}{2} f_1' - \frac{(m-2r+8)}{2(m-2r+6)} f_2' - \frac{(m-2r+4)}{(m-2r+6)} a_{22} f_2' \\ & + a_{22} f_3' + a_{33} f_1 - \frac{(m-2r+6)}{(m-2r+4)} a_{33} f_2 \\ & - \frac{(m-2r+2)}{2(m-2r+4)} f_2 + \frac{1}{2} f_3 = S_{m+1, r} \end{aligned}$$

[Observe that $f_1' - f_1' = f_2'$; $f_2' - f_2' = f_3'$; $f_2' - f_1 = f_2$; $f_3' - f_2 = f_3$].

We also have

$$(12) \quad a_{22} + a_{33} = -1.$$

On solving for a_{22} and a_{33} from (11) and (12), we obtain,

$$\begin{aligned} a_{22} &= \frac{2r-m-7}{2(m-2r+5)} \\ a_{33} &= \frac{2r-m-3}{2(m-2r+5)} \end{aligned}$$

from $a_{22}^2 + a_{32} a_{23} = \frac{3}{4} - a_{22}$, we have

$$a_{32} a_{23} = \frac{(m-2r+5)^2 - 1}{(m-2r+5)^2}.$$

If $a_{22} = \frac{1}{2}$ or $-\frac{3}{2}$, $r = \frac{m+6}{2}$ or $\frac{m+4}{2}$ respectively and this is clearly not possible.

Hence $a_{22} \neq \frac{1}{2}$ or $-\frac{3}{2}$ or $a_{32} a_{23} \neq 0$.

We now effect a similarity transformation of the matrices $D_{m+1, r}(\omega_{m+1, m+2})$ and $D_{m+1, r}(\omega_{m, m+1})$ by the matrix $\frac{1}{a_{23}} E_{f_{m, r-1}} + E_{f_{m, r}}$. This leaves $D_{m+1, r}(\omega_{m, m+1})$ unaltered while in $D_{m+1, r}(\omega_{m+1, m+2})$ it changes a_{23} to 1 and a_{32} to $a_{32} a_{23}$. We have thus proved the result for $n = m+1$ if it is true for $n = m$. Before completing the proof by induction, we observe that the foregoing does not cover the case $r = \frac{n}{2} + 1$ when n is even; for then

$$\begin{aligned} D_{n, \frac{n+2}{2}}(\omega_{n-1, n}) &= D_{n-1, \frac{n}{2}}(\omega_{n-1, n}) + D_{n-1, \frac{n+2}{2}}(\omega_{n-1, n}) \\ &= D_{n-1, \frac{n}{2}}(\omega_{n-1, n}) + \frac{1}{2} E_{f_{n-3, \frac{n-2}{2}}} + -\frac{3}{2} E_{f_{n-3, \frac{n}{2}}} \end{aligned}$$

We therefore treat this case separately: i.e. writing $n = 2p$, we show that

$$D_{2p, p+1}(\omega_{2p, 2p+1}) = \frac{1}{2} E_{f_{2p-2, p-1}} + \begin{vmatrix} -1 & 1 \\ \frac{3}{2} & 0 \end{vmatrix} \times E_{f_{2p-2, p}}.$$

We assume the result for $n = 2p$ and prove it for $2p+2$. The preceding result shows that (7) is true for $n = 2p+1$.

Now

$$\begin{aligned} D_{2p+2, p+2}(\omega_k, k+1) &= D_{2p+1, p+1}(\omega_k, k+1) + D_{2p+1, p+2}(\omega_k, k+1) \text{ over } A_{n-1} \\ &= D_{2p, p}(\omega_k, k+1) + D_{2p, p+1}(\omega_k, k+1) + D_{2p, p+1}(\omega_k, k+1) \text{ over } A_{n-2}. \end{aligned}$$

Hence from the Schur lemma,

$$D_{2p+2, p+2}(\omega_{2p+2, 2p+3}) = a_{11} E_{f_{2p, p}} + \begin{vmatrix} a_{22} & 1 \\ a_{32} & a_{33} \end{vmatrix} \times E_{f_{2p, p+1}}$$

where a_{23} is taken to be 1 as before.

From $\omega_{2p+2, 2p+3}^2 = \frac{3}{4} - \omega_{2p+2, 2p+3}$, we have again $a_{11} = \frac{1}{2}$ or $-\frac{3}{2}$ and $a_{22} + a_{33} = -1$.

Taking the spur of $\omega_{2p+2, 2p+3}$, we have

$$\begin{aligned} a_{11} \frac{4(p+4)(p+5) \dots (2p+1)}{p-1} - \frac{2(p+3)(p+4) \dots (2p+1)}{p} &= S_{2p+2, p+2} \\ &= -6 \frac{(p+1)(p+4)(p+5) \dots (2p+1)}{p+1} \end{aligned}$$

from which $a_{11} = \frac{1}{2}$ only. Therefore,

$$D_{2p+2, p+2}(\omega_{2p+2, 2p+3}) = \frac{1}{2} E_{f_{2p, p}} + \begin{vmatrix} a_{22} & 1 \\ a_{32} & a_{23} \end{vmatrix} \times E_{f_{2p, p+1}}$$

and

$$D_{2p+2, p+2}(\omega_{2p+1, 2p+2}) = D_{2p+1, p+1}(\omega_{2p+1, 2p+2}) + D_{2p+1, p+2}(\omega_{2p+1, 2p+2}),$$

i.e.

$$\begin{aligned} D_{2p+2, p+2}(\omega_{2p+1, 2p+2}) &= \\ \frac{1}{2} E_{f_{2p-1, p-1}} + \begin{vmatrix} -\frac{5}{6} & 1 \\ \frac{4}{9} & -\frac{1}{6} \end{vmatrix} \times E_{f_{2p-1, p}} + \frac{1}{2} E_{f_{2p-1, p+1}} \\ &\quad + \frac{1}{2} E_{f_{2p-1, p}} + -\frac{3}{2} E_{f_{2p-1, p+1}}. \end{aligned}$$

Since spur of $\{\omega_{2p+1, 2p+2}, \omega_{2p+2, 2p+3}\}$ is also $S_{2p+2, p+2}$ we have

$$\begin{aligned} \frac{1}{2} f_{2p-1, p-1} - \frac{5}{6} f_{2p-1, p} - \frac{1}{6} f_{2p-1, p} a_{22} + f_{2p-1, p+1} a_{22} + f_{2p-1, p} a_{33} - 3 f_{2p-1, p+1} \\ = S_{2p+2, p+2} = \frac{1}{2} f_{2p, p} - f_{2p, p+1} \end{aligned}$$

and we also have $a_{22} + a_{33} = -1$. On solving for a_{22}, a_{33} , we obtain

$$a_{22} = -1, a_{33} = 0; a_{32} = \frac{3}{4}.$$

We have thus shown that in all cases (7) is true for $n = m+1$ if it is true for $n = m$. Now for the algebra A_2 , one can show easily that

$$D_{22}(\omega_{12}) = \begin{vmatrix} \frac{1}{2} & 0 \\ 0 & -\frac{3}{2} \end{vmatrix}; D_{22}(\omega_{23}) = \begin{vmatrix} -1 & 1 \\ \frac{3}{4} & 0 \end{vmatrix}$$

and $D_{n1}(\omega_{p,p+1}) = \frac{1}{2}$ for all n . This proves that the irreducible representations of A_n are given by (7) and in case n is odd, we have an additional representation given by (8)

We observe that the representation matrices are chosen in such a way that their elements are rational numbers. If, however, we want them to be symmetric matrices as is generally required in Quantum Mechanics we can take

$$a_{23} = a_{32} = \sqrt{\frac{(n-2r+4)^2-1}{(n-2r+4)^2}}.$$

As an illustration, we give below the matrices of the irreducible representations for $\omega_{12}, \omega_{23}, \dots, \omega_{56}$ of the algebra A_5 . By taking the anti-commutators of these $\omega_{p,p+1}$ repeatedly we can compute the matrices for $\xi_{r-1} = \omega_{1r}$.

The algebra A_5 has 4 irreducible representations $D_{51}, D_{52}, D_{53}, D_{54}$ of orders 1, 5, 9, 5 respectively.

(i) $D_{51} : -$

$$\omega_{r,r+1} = \frac{1}{2}; \quad r = 1, 2, 3, 4, 5.$$

(ii) $D_{52} : -$

$$\begin{aligned}\omega_{12} &= \frac{1}{2} E_4 + \frac{3}{2} E_1 \\ \omega_{23} &= \frac{1}{2} E_3 + \begin{vmatrix} -1 & 1 \\ 3 & 0 \end{vmatrix} \\ \omega_{34} &= \frac{1}{2} E_2 + \begin{vmatrix} -\frac{5}{6} & 1 \\ 5 & -\frac{1}{6} \end{vmatrix} + \frac{1}{2} E_1 \\ \omega_{45} &= \frac{1}{2} E_1 + \begin{vmatrix} -\frac{3}{4} & 1 \\ \frac{1}{6} & -1 \end{vmatrix} + \frac{1}{2} E_2 \\ \omega_{56} &= \begin{vmatrix} -\frac{7}{6} & 1 \\ \frac{3}{2} & -\frac{1}{6} \end{vmatrix} + \frac{1}{2} E_3\end{aligned}$$

(iii) $D_{53} : -$

$$\begin{aligned}\omega_{12} &= \frac{1}{2} E_3 + \frac{3}{2} E_1 + \frac{1}{2} E_2 + \frac{3}{2} E_1 + \frac{1}{2} E_1 + \frac{3}{2} E_1 \\ \omega_{23} &= \frac{1}{2} E_2 + \begin{vmatrix} -1 & 1 \\ 3 & 0 \end{vmatrix} + \frac{1}{2} E_1 + \begin{vmatrix} -1 & 1 \\ 3 & 0 \end{vmatrix} \times E_2 \\ \omega_{34} &= \frac{1}{2} E_1 + \begin{vmatrix} -\frac{5}{6} & 1 \\ 5 & -\frac{1}{6} \end{vmatrix} + \frac{1}{2} E_1 + \begin{vmatrix} -\frac{5}{6} & 1 \\ 5 & -\frac{1}{6} \end{vmatrix} + \frac{1}{2} E_2 + \frac{3}{2} E_1 \\ \omega_{45} &= \begin{vmatrix} -\frac{3}{4} & 1 \\ \frac{1}{6} & -1 \end{vmatrix} + \frac{1}{2} E_3 + \begin{vmatrix} -1 & 1 \\ 3 & 0 \end{vmatrix} \times E_2 \\ \omega_{56} &= \frac{1}{2} E_1 + \begin{vmatrix} -\frac{5}{6} & 1 \\ 5 & -\frac{1}{6} \end{vmatrix} \times E_3 + \frac{1}{2} E_2\end{aligned}$$

(iv) D_{54} :—

$$\omega_{12} = \frac{1}{2} E_2 + -\frac{3}{2} E_1 + \frac{1}{2} E_1 + -\frac{3}{2} E_1$$

$$\omega_{23} = \frac{1}{2} E_1 + E_2 \times \begin{vmatrix} -1 & 1 \\ 3 & 0 \end{vmatrix}$$

$$\omega_{34} = \begin{vmatrix} -5 & 1 \\ 8 & -1 \end{vmatrix} + \frac{1}{2} E_2 + -\frac{3}{2} E_1$$

$$\omega_{45} = \frac{1}{2} E_1 + \begin{vmatrix} -1 & 1 \\ 3 & 0 \end{vmatrix} \times E_2$$

$$\omega_{56} = \frac{1}{2} E_3 + -\frac{3}{2} E_2.$$

4. THE DIMENSION OF THE ALGEBRA A_n

We now prove that the dimension of the algebra A_n is given by the simple

expression $\frac{2}{n+2} \binom{2n+1}{n}$; i.e. we show that

$$\sum_{r=1}^{m+1} f_{nr}^2 = \sum_{r=1}^{m+1} \left(\frac{n-2r+1}{n+2} \right)^2 \binom{n+2}{r-1}^2 = \frac{2}{n+2} \binom{2n+1}{n}$$

for $n = 2m$ or $2m-1$

(i) Let $n = 2m$; to show that

$$\sum_0^m (m-p+1)^2 \binom{2m+2}{p}^2 = (m+1) \binom{4m+1}{2m}$$

Proof :— $(1+x)^{2m+2} = \sum_0^{2m+2} \binom{2m+2}{2m+2-p} x^{2m+2-p}.$

$$\therefore x^{-m-1} (1+x)^{2m+2} = \sum_0^{2m+2} \binom{2m+2}{2m+2-p} x^{m-p+1}$$

$$\therefore \frac{d}{dx} \{ x^{-m-1} (1+x)^{2m+2} \} = \sum_0^{2m+2} (m-p+1) \binom{2m+2}{2m+2-p} x^{m-p}$$

Also $(1+x)^{2m+2} = \sum_0^{2m+2} \binom{2m+2}{p} x^p.$

$$\therefore \frac{d}{dx} \{ x^{-m-1} (1+x)^{2m+2} \} = - \sum_0^{2m+2} (m-p+1) \binom{2m+2}{p} x^{p-m-2}$$

Hence, in

$$-\left\{ \sum_0^{2m+2} (m-p+1) \binom{2m+2}{2m+2-p} x^{m-p} \right\} \left\{ \sum_0^{2m+2} (m-p+1) \binom{2m+2}{p} x^{m-p-2} \right\}$$

the coefficient of $\frac{1}{x^2} = - \sum_0^{2m+2} (m-p+1)^2 \binom{2m+2}{p}^2$

$$= -2 \sum_0^m (m-p+1)^2 \binom{2m+2}{p}^2.$$

This must therefore be equal to the coefficient of $\frac{1}{x^2}$ in

$$\left[\frac{d}{dx} \{ x^{-m-1} (1+x)^{2m+2} \} \right]^2,$$

i.e. to the coefficient of $\frac{1}{x^2}$ in

$$\begin{aligned} & \{ (2m+2) (1+x)^{2m+1} x^{-m-1} - (m+1) (1+x)^{2m+2} x^{-m-2} \}^2 \\ &= \frac{(m+1)^2 (1+x)^{4m+2} (1-x)^2}{x^{2m+1}}. \end{aligned}$$

Coefficient of $\frac{1}{x^2} = (m+1)^2 \left\{ \binom{4m+2}{2m+2} - 2 \binom{4m+2}{2m+1} + \binom{4m+2}{2m} \right\}$

$$= -2(m+1) \binom{4m+1}{2m} \text{ on simplification.}$$

Hence

$$\sum_0^m (m-p+1)^2 \binom{2m+2}{p}^2 = (m+1) \binom{4m+1}{2m}.$$

When $n = 2m-1$, one can similarly prove the result by considering the expansion for $(1+x^2)^{2m+1}$. We thus obtain that the dimension of the Lie-algebra of the orthogonal group with spin $\frac{n}{2}$ is

$$\frac{2^{n+1}}{n+2} \binom{2n+1}{n}.$$

5. THE CENTRE OF THE ALGEBRA A_n

Let $P_r = \sum \xi_{p_1 p_2 \dots p_r}$, where $\xi_{p_1 p_2 \dots p_r} = \xi_{p_1} \xi_{p_2} \dots \xi_{p_r}$, and the summation extends over $n P_r$ permutations.

Thus $\xi_1 P_{2m+1} = \sum \xi_1 \xi_{q_1 q_2 \dots q_{2m+1}} + \sum \xi_1 \xi_{1 q_2 \dots q_{2m+1}} + \sum \xi_1 \xi_{q_2 1 q_3 \dots q_{2m+1}}$

$$+ \dots + \dots + \sum \xi_1 \xi_{q_2 \dots q_{2m+1}, 1}$$

where the q_r are to be summed up over all indices excepting 1.

Since $[\xi_1, \{\xi_{q_1}, \xi_{q_2}\}] = 0$, we obtain

$$\xi_1 P_{2m+1} = \xi_{1q_1 \dots q_{2m+1}} + (m+1) \xi_{11q_2 \dots q_{2m+1}} + m \xi_{1q_2 1q_3 \dots q_{2m+1}},$$

the q_r being summed up over all indices excepting 1.

Now

$$\begin{aligned} 2\xi_{1q_1} + \xi_{q_1 1} &= \xi_q - \xi_{11q} \\ \therefore \xi_1 P_{2m+1} &= \xi_{1q_1 q_2 \dots q_{2m+1}} + \frac{m}{2} \xi_{q_2 q_3 \dots q_{2m+1}} \\ &\quad - \frac{m}{2} \xi_{q_2 11q_3 \dots q_{2m+1}} + \left(\frac{m}{2} + 1\right) \xi_{11q_2 \dots q_{2m+1}}. \end{aligned}$$

From $\xi_{11} = \frac{1}{2} - \xi_1$ we obtain

$$\begin{aligned} \xi_1 P_{2m+1} &= \xi_{1q_1 \dots q_{2m+1}} + \frac{2m+3}{4} \xi_{q_2 \dots q_{2m+1}} \\ &\quad - \frac{m+2}{2} \xi_{1q_2 \dots q_{2m+1}} + \frac{m}{2} \xi_{q_2 1q_3 \dots q_{2m+1}} \end{aligned}$$

we have similarly

$$\begin{aligned} P_{2m+1} \xi_1 &= \xi_{q_1 q_2 \dots q_{2m+1}, 1} + (m+1) \xi_{11q_2 q_3 \dots q_{2m+1}} \\ &\quad + m \xi_{1q_2 1q_3 \dots q_{2m+1}} \text{ and hence} \\ [\xi_1, P_{2m+1}] &= [\xi_1, \xi_{q_1 q_2 \dots q_{2m+1}}]. \end{aligned}$$

Forming in the same way $\xi_2 P_{2m+1}, \dots, \xi_n P_{2m+1}, P_{2m+1} \xi_2, \dots, P_{2m+1} \xi_n$, we obtain.

$$(13) \quad P_1 P_{2m+1} = P_{2m+2} - P_{2m+1} + \frac{(n-2m)(2m+3)}{4} P_{2m} = P_{2m+1} P_1.$$

It can be seen similarly that

$$\xi_1 P_{2m} = \xi_{1q_1 q_2 \dots q_{2m}} + \frac{m}{2} \xi_{q_2 \dots q_{2m}} - \frac{m}{2} \xi_{1q_2 \dots q_{2m}} + \frac{m}{2} \xi_{q_2 1q_3 \dots q_{2m}},$$

and

$$P_{2m} \xi_1 = \xi_{1q_1 q_2 \dots q_{2m}} + \frac{m}{2} \xi_{q_2 \dots q_{2m}} + \frac{m}{2} \xi_{1q_2 \dots q_{2m}} - \frac{m}{2} \xi_{q_2 1q_3 \dots q_{2m}}$$

from which we have

$$[\xi_1, P_{2m}] = m(\xi_{q_2 1q_3 \dots q_{2m}} - \xi_{1q_2 \dots q_{2m}}) = -m[\xi_1, \xi_{q_2 \dots q_{2m}}],$$

i.e. $P_{2m} + m P_{2m-1}$ is an element of the centre.

[We take $P_0 = 1$ and $P_r = 0$ for $r > n$ and $r < 0$; we notice that there will be $(k+1)$ elements of this form for $n = 2k$ or $2k-1$.]

We also obtain

$$(14) \quad P_1 P_{2m} = P_{2m+1} + \frac{m(n-2m+1)}{2} P_{2m-1} = P_{2m} P_1.$$

From (13) we have $P_1^2 = P_2 - P_1 + \frac{3n}{4}$

$$\therefore P_1 + P_2 = P_1^2 + 2P_1 - \frac{3n}{4}.$$

$$\begin{aligned} \therefore (P_1 + P_2) P_{2m} &= P_1 P_{2m+1} + \frac{m(n-2m+1)}{2} P_1 P_{2m-1} \\ &\quad + 2P_1 P_{2m} - \frac{3n}{4} P_{2m}. \end{aligned}$$

$$\begin{aligned} (P_1 + P_2) P_{2m-1} &= P_1 P_{2m} + P_1 P_{2m-1} \\ &\quad + \frac{(n-2m+2)(2m+1)}{4} P_1 P_{2m-2} - \frac{3n}{4} P_{2m-1}. \end{aligned}$$

We thus obtain

$$\begin{aligned} (P_1 + P_2)(P_{2m} + mP_{2m-1}) + \frac{3n}{4}(P_{2m} + mP_{2m-1}) &= \\ P_1 P_{2m+1} + (m+2) P_1 P_{2m} + \frac{m(n-2m+3)}{2} P_1 P_{2m-1} \\ + \frac{m(n-2m+2)(2m+1)}{4} P_1 P_{2m-2} \\ = P_{2m+2} - P_{2m+1} + \frac{(n-2m)(2m+3)}{4} P_{2m} \\ + \frac{m(n-2m+3)}{2} P_{2m} + (m+2) P_{2m+1} \\ + \frac{m(m+2)(n-2m+1)}{2} P_{2m-1} - \frac{m(n-2m+3)}{2} P_{2m-1} \\ + \frac{m(n-2m+3)(n-2m+2)(2m+1)}{8} P_{2m-2} \\ + \frac{m(n-2m+2)(2m+1)}{4} P_{2m-1} \\ + \frac{m(m-1)(2m+1)(n-2m+2)(n-2m+3)}{3} P_{2m-3} \end{aligned}$$

or we obtain the recurrent relation

$$\begin{aligned} (15) \quad (P_1 + P_2)(P_{2m} + mP_{2m-1}) &= (P_{2m+2} + \overline{m+1} P_{2m+1}) + m(n-2m)(P_{2m} + mP_{2m-1}) \\ &\quad + \frac{m(2m+1)(n-2m+3)(n-2m+2)}{8} (P_{2m-2} + \overline{m-1} P_{2m-3}). \end{aligned}$$

It is evident that on utilising (15) in succession, we can express a central element

$$P_{2m} + m P_{2m-1} \text{ as a polynomial in } \mathfrak{g} = P_1 + P_2 = \sum_{r=1}^n \xi_r + \sum_{r,s=1}^n \{ \xi_r, \xi_s \}; \quad r \neq s.$$

We obtain the minimal equation that $\theta = P_1 + P_2$ satisfies indirectly as follows :

Since $\text{spur } \xi_r = \text{spur } \xi_s = \text{spur } \{ \xi_r, \xi_s \},$

$\text{spur of } \theta = \frac{n(n+1)}{2} S_{nr}$ in the irreducible representation $D_{nr},$

i.e. $\text{spur } \theta = \frac{n(n+1)}{2} f_{nr} \frac{n^2 + (5-4r)n + 4(r-1)(r-3)}{2n(n+1)}.$

Hence the roots of θ are $\frac{n^2 + (5-4r)n + 4(r-1)(r-3)}{4}$

$r = 1, 2, 3, \dots (k+1)$ where $n = 2k$ or $2k-1$

or the minimal equation that θ satisfies is

$$(16) \quad \prod_{r=1}^{k+1} \left\{ \theta - \frac{n^2 + (5-4r)n + 4(r-1)(r-3)}{4} \right\} = 0.$$

We wish to thank Prof. B. S. Madhava Rao for his interest in the work and kind encouragement.

SUMMARY

In this paper we determine explicitly the matrices of all the finite-dimensional representations of the Lie-algebra of the orthogonal group with any number of symbols with spin $\frac{3}{2}$. For this purpose we use the direct product resolution of such an algebra into that of a Dirac algebra and a ξ -algebra due to Madhava Rao and others. We find first of all the matrices for the representations of the ξ -algebra; since those of the Dirac-algebra are known one can work out the same for the Lie-algebra. We determine finally the centre of the ξ -algebra.

REFERENCES

- Brauer and Weyl (1935). Spinors in n -dimensions. *Jour. Amer. Math. Soc.*, **57**, 425.
 Kemmer (1939). The particle aspect of Meson theory. *Proc. Roy. Soc. A.*, **173**, 91-116.
 Littlewood, D. E. (1947). An equation of Quantum Mechanics. *Camb. Phil. Soc.*, **43**, 406-413.
 Madhava Rao, Thiruvengkatachar and Venkatachaliengar (1946). Algebra related to elementary particles of spin $= \frac{3}{2}$. *Proc. Roy. Soc., A*, **187**, 385-397.

Issued October 15, 1954.

RADIATION DAMPING IN COMPTON SCATTERING

by T. C. ROY, *Research Fellow, N.I.S.I., Department of Applied Mathematics,
University College of Science and Technology, Calcutta*

(Communicated by N. R. Sen, F.N.I.)

(Received February 3 ; read August 6, 1954)

The influence of radiation damping in the Compton scattering phenomenon has already been investigated by Wilson (1941) and Power (1945) from the quantum mechanical point of view. One has to tackle Heitler's integral equation in such a case which is extremely difficult to solve exactly. Wilson therefore attempted to solve it after averaging the kernel of the integral equation over the scattering angles. The result that he got by this process showed that the effect of damping is small and can be neglected for all practical purposes in those cases in which the incident photon energy is not unnaturally high. The averaging procedure of Wilson being a very rough approximation, the same problem was again tackled by Power by making a different type of approximation. Her idea is that if the effect of damping be really small then a solution of the above-mentioned integral equation in a series of ascending powers of the fine structure constant may be assumed. By this procedure she calculated the first extra term (1st order approximation term) of the series, the zeroth order term being the usual Klein Nishina term. This extra term she actually demonstrated to be small, compared to the other one and concluded that the effect of damping confirms Wilson's result.

Recent experience about expansion in powers of the fine structure constant shows that in no way can one assure or ascertain by simple means the convergency of such a procedure. In fact one has to consider the radiative corrections to the Compton scattering which has been considered and discussed in some detail by Feynman (1949). Due to this obvious reason it seems desirable to reconsider the problem yet from another point of view which in our case will be the semivariational procedure of Hsueh and Ma (1945). The reason for doing this is that though approximate this method does not necessitate any further justification on the procedure (as the convergency of the series in the previous case). It therefore seems to be of interest to calculate the scattering cross-section by this procedure and to see to what extent the damping is effective in such a case. The result of our calculation shows that the effect of damping is really small in conformity with the results obtained by Wilson and Power. However, there is a bit of difference. The previous calculations fail to show that the effect of damping is small when the incident photon energy is sufficiently high, owing to the appearance of the factor $\log\left(\frac{k}{\mu}\right)$

in the solution (Wilson, 1941). Though, however, the term does not make its appearance in Power's first order calculation it has not been shown that the same feature will occur in the higher order calculations also. In this respect our calculation shows that the damping effect remains small with any high value of the incident photon energy and even when it is made theoretically infinite. Thus the Klein Nishina formula remains valid even at high energies.

We start with the Heitler's following integral equation and sketch in short the semi-variational procedure of Hsueh and Ma for its solution.

$$U_{\mathbf{k}\mathbf{k}_0} = H_{\mathbf{k}\mathbf{k}_0} + i\pi \sum \int H_{\mathbf{k}\mathbf{k}'} U_{\mathbf{k}'\mathbf{k}_0} \rho_{\mathbf{k}'} d\Omega_{\mathbf{k}'} \quad \dots \quad (1)$$

where \mathbf{k}_0 corresponds to the initial state, \mathbf{k} the final state, \mathbf{k}' an intermediate state $\rho_{\mathbf{k}'}$ is the number of states per unit energy interval per unit solid angle. The summations integration means really the integration over the whole solid angle and summation over all directions of polarization. Equation (1) can be written in the variational form as follows :—

$$\sum_{k_0 k} \int \delta U_{\mathbf{k}_0 \mathbf{k}}^* \left[U_{\mathbf{k} \mathbf{k}_0} - H_{\mathbf{k} \mathbf{k}_0} + i\pi \sum_{\mathbf{k}'} \int H_{\mathbf{k} \mathbf{k}'} U_{\mathbf{k}' \mathbf{k}_0} \rho_{\mathbf{k}'} d\Omega_{\mathbf{k}'} \right] \rho_{\mathbf{k}} d\Omega_{\mathbf{k}} = 0. \quad \dots (2)$$

Now to obtain an approximate solution of equation (1) we get,

$$U_{\mathbf{k} \mathbf{k}_0} = x H_{\mathbf{k} \mathbf{k}_0}$$

where x is a parameter ; equation (2) then becomes,

$$\delta x^* \sum_{\mathbf{k}} \int H_{\mathbf{k} \mathbf{k}_0} \left[H_{\mathbf{k}_0 \mathbf{k}} (x-1) + i\pi x \sum_{\mathbf{k}'} \int H_{\mathbf{k} \mathbf{k}'} H_{\mathbf{k}' \mathbf{k}_0} \rho_{\mathbf{k}'} d\Omega_{\mathbf{k}'} \right] \rho_{\mathbf{k}} d\Omega_{\mathbf{k}} = 0 \quad \dots (3)$$

which gives

$$x = \frac{\gamma}{\gamma + i\delta}$$

where

$$\gamma = \sum_{k k_0} \int H_{\mathbf{k}_0 \mathbf{k}} H_{\mathbf{k} \mathbf{k}_0} \rho_{\mathbf{k}} d\Omega_{\mathbf{k}} \quad \dots \quad \dots \quad \dots (4)$$

and

$$\delta = \pi \sum_{k k_0 k'} \int H_{\mathbf{k}_0 \mathbf{k}} H_{\mathbf{k} \mathbf{k}'} H_{\mathbf{k}' \mathbf{k}_0} \rho_{\mathbf{k}'} \rho_{\mathbf{k}} d\Omega_{\mathbf{k}'} d\Omega_{\mathbf{k}}. \quad \dots \quad \dots (5)$$

One then easily gets the cross-section of scattering as

$$dQ = dQ_0 \left(1 + \frac{\delta^2}{\gamma^2} \right)^{-1} \quad \dots \quad \dots \quad \dots (6)$$

where dQ is the scattering cross-section without damping. Our discussion is therefore mainly focussed on the relative magnitudes of the quantities γ and δ .

To facilitate our calculation we take a Lorentz system in which the total momentum is zero so that the photon momenta \mathbf{k} and \mathbf{k}_0 are the same in magnitude but only differ in directions. Also the matrix element $H_{\mathbf{k} \mathbf{k}_0}$ in this high energy region is given by Heitler, 1944

$$H_{\mathbf{k} \mathbf{k}_0} = \frac{\pi e^2}{k^2} A_{\mathbf{k} \mathbf{k}_0} \quad \dots \quad \dots \quad \dots (7)$$

where

$$A_{\mathbf{k} \mathbf{k}_0} = U_0^* \alpha_0 \alpha u + k_0 \frac{u_0^* \alpha [(\alpha \mathbf{k}_0) + (\alpha \cdot \mathbf{k})] \alpha_0 u}{k_0 E_0 + \mathbf{k}_0 \cdot \mathbf{k}}$$

with

$$\alpha_0 = (\alpha \cdot \mathbf{e}_0), \quad \text{and} \quad \alpha = (\alpha \cdot \mathbf{e})$$

\mathbf{e}_0 and \mathbf{e} being the unit polarization vectors in the \mathbf{k}_0 and \mathbf{k} states respectively. The reason for writing E_0 in the denominator is given in Heitler, 1944. U 's are as usual normalised Dirac wave functions. One also notes that

$$\rho_{\mathbf{k}} = \frac{1}{2} \frac{k^2 d\Omega}{(2\pi)^3}, \quad \dots \quad \dots \quad \dots (8)$$

we have all through used $\hbar = c = 1$.

CALCULATION OF γ

To obtain γ from equation (4) one has got to sum over the spin states first. The usual procedure is then to calculate the spur of,

$$\left\{ \alpha_0 \alpha(E + \beta\mu - \alpha \cdot \mathbf{k}) + \frac{k_0 \alpha[(\alpha \cdot \mathbf{k}_0) + (\alpha \cdot \mathbf{k})] \alpha_0(E + \beta\mu - \alpha \cdot \mathbf{k})}{K_0 E_0 + \mathbf{k}_0 \cdot \mathbf{k}} \right\} \times \\ \left\{ \alpha \alpha_0(E_0 + \beta\mu - \alpha \cdot \mathbf{k}_0) + \frac{k_0 \alpha_0[(\alpha \cdot \mathbf{k}) + (\alpha \cdot \mathbf{k}_0)] \alpha(E_0 + \beta\mu - \alpha \cdot \mathbf{k}_0)}{K_0 E + \mathbf{k}_0 \cdot \mathbf{k}} \right\} \\ = \text{sp. } \alpha_0 \alpha(E + \beta\mu - \alpha \mathbf{k}) \alpha \alpha_0(E_0 + \beta\mu - \alpha \mathbf{k}_0) \\ + \lambda^2 \text{ sp. } \alpha[\alpha \mathbf{k}_0 + \alpha \cdot \mathbf{k}] \alpha_0(E + \beta\mu - \alpha \cdot \mathbf{k}) \alpha_0[(\alpha \cdot \mathbf{k}) + (\alpha \cdot \mathbf{k}_0)] \alpha(E_0 + \beta\mu - \alpha \cdot \mathbf{k}_0) \\ + \lambda \text{ sp. } \alpha_0 \alpha(E + \beta\mu - \alpha \mathbf{k}) \alpha_0[\alpha \mathbf{k} + \alpha \cdot \mathbf{k}_0] \alpha(E_0 + \beta\mu - \alpha \cdot \mathbf{k}_0) \\ + \lambda \text{ sp. } \alpha[\alpha \mathbf{k} + \alpha \mathbf{k}_0] \alpha_0(E + \beta\mu - \alpha \cdot \mathbf{k}) \alpha \alpha_0(E_0 + \beta\mu - \alpha \mathbf{k}_0) \quad \dots \quad (9)$$

where

$$\lambda = \frac{k_0}{k_0 E_0 + \mathbf{k}_0 \cdot \mathbf{k}} \quad \dots \quad \dots \quad \dots \quad (10)$$

On evaluation of the spurs and writing

$$\cos \theta = \frac{(\mathbf{k}_0 \mathbf{k})}{k_0^2} \quad \dots \quad \dots \quad \dots \quad (11)$$

(9) reduces to

$$4k_0^2(1 + \cos \theta) + 16\lambda k_0 \left[-k_0^2 \cos \theta - 1(\mathbf{e}_0 \mathbf{e})(\mathbf{e} \mathbf{k}_0)(\mathbf{e}_0 \mathbf{k}) + 2(\mathbf{e} \cdot \mathbf{k}_0)^2(\mathbf{e}_0 \cdot \mathbf{k})^2 \right. \\ \left. + 2(\mathbf{e} \cdot \mathbf{e}_0)^2 k_0^2(1 + \cos \theta) \right] \quad \dots \quad \dots \quad \dots \quad (12)$$

In the above, and also in the following calculations we have cancelled $(1 + \cos \theta)$ with $\frac{1}{k_0 \lambda}$, the justification for which is given in the appendix.

Since now we are to sum over all directions of polarization and to integrate over $d\Omega$, we here adopt the following artifice. Let us first take,

$$\mathbf{e}' = \frac{[\mathbf{e}_0 \times \mathbf{k}]}{|[\mathbf{e}_0 \times \mathbf{k}]|} \quad \dots \quad \dots \quad \dots \quad (13)$$

and integrate (12) over $d\Omega$; and secondly take,

$$\mathbf{e}'' = \frac{|[\mathbf{e}_0 \times \mathbf{k}] \times \mathbf{k}|}{|[\mathbf{e}_0 \times \mathbf{k}] \times \mathbf{k}|} \quad \dots \quad \dots \quad \dots \quad (14)$$

and integrate equation (12) over $d\Omega$, the required result is then the sum of these two integrals. Performing these integrations we get,

$$\gamma = \frac{e^4}{8k_0^2} \left[4 \log \left(\frac{E_0 + k_0}{E_0 - k_0} \right) - \frac{2}{3} \right] \quad \dots \quad \dots \quad \dots \quad (15)$$

CALCULATION OF δ

To obtain δ from equation (5) one has again to sum over the spin states. A part of the calculation has already been done by Power which is stated below,

$$\sum_{\mathbf{k}'} \int H_{\mathbf{k}\mathbf{k}'} H_{\mathbf{k}'\mathbf{k}_0} \rho_{\mathbf{k}'} d\Omega_{\mathbf{k}'} = -\frac{e^4}{4k_0^2} B_{\mathbf{k}\mathbf{k}_0} \quad \dots \quad \dots \quad \dots \quad (16)$$

where

$$B_{\mathbf{k}\mathbf{k}_0} = a u_0^* \alpha_0 \alpha u + \frac{b}{k_0} \left[(\mathbf{e} \cdot \mathbf{k}_0) u_0^* \alpha_0 u + (\mathbf{e}_0 \cdot \mathbf{k}) u_0^* \alpha u \right] \\ + c (\mathbf{e}_0 \cdot \mathbf{e}) u_0^* u + \frac{d}{k_0^2} (\mathbf{e}_0 \cdot \mathbf{k}) (\mathbf{e} \cdot \mathbf{k}_0) u_0^* u \quad \dots \quad \dots \quad \dots \quad (17)$$

and

$$a = (1 + \cos \theta)L - 3, \\ b = \frac{2}{1 + \cos \theta} \left\{ \cos \theta \cdot L + \frac{1 + 3 \cos \theta}{1 - \cos \theta} \right\}, \\ c = \frac{2}{1 + \cos \theta} \left\{ (1 - \cos \theta)L + 2 \right\} \\ d = \frac{2}{(1 + \cos \theta)^2} \left\{ (3 \cos \theta - 1)L + \frac{8 \cos \theta}{1 - \cos \theta} \right\} \quad \dots \quad \dots \quad (18)$$

where

$$L = \frac{2}{1 + \cos \theta} \log \frac{1 - \cos \theta}{2} \quad \dots \quad \dots \quad \dots \quad (19)$$

Hence in order to calculate δ from equation (5), one uses equations (7) and (16) and calculates the sum over the spin states of,

$$A_{\mathbf{k}\mathbf{k}_0} B_{\mathbf{k}_0\mathbf{k}}$$

which is of the form,

$$\frac{1}{8E_0 E} (Aa + Bb + Cc + Dd) \quad \dots \quad \dots \quad \dots \quad (20)$$

where A , B , C , D are to be evaluated, they being,

$$A = \text{sp.} \left\{ \alpha_0 \alpha (E + \beta \mu - \alpha \cdot \mathbf{k}) \alpha \alpha_0 (E_0 + \beta \mu - \alpha \cdot \mathbf{k}_0) + \lambda \alpha_0 \alpha (E + \beta \mu - \alpha \cdot \mathbf{k}) \times \right. \\ \left. \alpha_0 (\alpha \mathbf{k} + \alpha \mathbf{k}_0) \alpha (E_0 + \beta \mu - \alpha \cdot \mathbf{k}_0) \right\} \quad \dots \quad \dots \quad \dots \quad (21)$$

$$B = \frac{(e k_0)}{k_0} \text{sp.} \left\{ \alpha_0 (E + \beta \mu - \alpha \mathbf{k}) \alpha \alpha_0 (E_0 + \beta \mu - \alpha \mathbf{k}_0) + \lambda \alpha_0 (E + \beta \mu - \alpha \mathbf{k}) \right. \\ \left. \times \alpha_0 (\alpha \mathbf{k} + \alpha \mathbf{k}_0) \alpha (E_0 + \beta \mu - \alpha \mathbf{k}_0) \right\} + \frac{(\mathbf{e}_0 \mathbf{k})}{k_0} \text{sp} \left\{ \alpha (E + \beta \mu - \alpha \cdot \mathbf{k}) \alpha \alpha_0 (E_0 + \beta \mu - \alpha \mathbf{k}_0) \right. \\ \left. + \lambda \alpha (E + \beta \mu - \alpha \mathbf{k}) \alpha_0 (\alpha \mathbf{k} + \alpha \mathbf{k}_0) \alpha (E_0 + \beta \mu - \alpha \mathbf{k}_0) \right\} \quad \dots \quad \dots \quad (22)$$

$$\frac{C}{(\mathbf{e}_0 \cdot \mathbf{e})} = \frac{D}{\frac{(\mathbf{e}_0 \mathbf{k})(\mathbf{e} \mathbf{k}_0)}{k_0^2}} = \text{sp} \left\{ (E + \beta \mu - \alpha \mathbf{k}) \alpha \alpha_0 (E_0 + \beta \mu - \alpha \mathbf{k}_0) + \lambda (E + \beta \mu - \alpha \mathbf{k}) \right. \\ \left. \times \alpha_0 (\alpha \mathbf{k} + \alpha \mathbf{k}_0) \alpha (E_0 + \beta \mu - \alpha \mathbf{k}_0) \right\} \quad (23)$$

Calculating the spurs we get,

$$4A = E_0^2 + \mu^2 + (\mathbf{k} \mathbf{k}_0) - \lambda E_0 \left\{ 2(\mathbf{k} \mathbf{k}_0) + 2k_0^2 - 4(\mathbf{e} \mathbf{e}_0)^2 (\mathbf{k} \mathbf{k}_0) \right. \\ \left. + 4(\mathbf{e} \mathbf{e}_0)(\mathbf{e}_0 \mathbf{k})(\mathbf{e} \mathbf{k}_0) - 4k_0^2 (\mathbf{e} \mathbf{e}_0)^2 - 2(\mathbf{e} \mathbf{k}_0)^2 - 2(\mathbf{e}_0 \mathbf{k})^2 \right\} \quad \dots \quad \dots \quad (24)$$

$$\frac{16B}{k_0} = \frac{E_0}{4} \left\{ (e\mathbf{k}_0)^2 + (e_0\mathbf{k})^2 \right\} + \lambda(e_0\mathbf{k})^2(e\mathbf{k}_0)^2 - \frac{\lambda}{2}(\mathbf{k}\mathbf{k}_0) \left\{ (e\mathbf{k}_0)^2 + (e_0\mathbf{k})^2 \right\} \\ - \lambda k_0^2(ee_0)(e_0\mathbf{k})(e\mathbf{k}_0) - \lambda(ee_0)(\mathbf{k}\mathbf{k}_0)(e_0\mathbf{k})(e\mathbf{k}_0) \quad \dots \quad (25)$$

$$\frac{4C'}{(e \cdot e_0)} = \frac{4D}{(e_0\mathbf{k})(e\mathbf{k}_0)} = (e \cdot e_0)(E_0^2 + \mu^2) + (e \cdot e_0)(\mathbf{k} \cdot \mathbf{k}_0) - (e_0\mathbf{k})(e\mathbf{k}_0) \\ + 2\lambda E_0[(ee_0)(\mathbf{k}\mathbf{k}_0) + (ee_0)k_0^2 - (e\mathbf{k}_0)(e_0\mathbf{k})] \quad \dots \quad (26)$$

Equation (20) is now therefore completely known. We now proceed to integrate over the solid angle $d\Omega$ and sum over all directions of polarization which we do just in the same way as in the case of evaluation of γ . We therefore integrate using once,

$$\mathbf{e}' = \frac{[\mathbf{e}_0 \times \mathbf{k}]}{|\mathbf{e}_0 \times \mathbf{k}|}$$

and then

$$\mathbf{e}'' = \frac{[(\mathbf{e}_0 \times \mathbf{k}) \times \mathbf{k}]}{|(\mathbf{e}_0 \times \mathbf{k}) \times \mathbf{k}|}$$

and sum the two results. Performing these integrations we finally get,

$$\delta = \frac{e^6}{32k_0^2} \left[\frac{7\pi^2}{12} + \frac{296}{9} - 5 \log \left(\frac{E_0 + k_0}{E_0 - k_0} \right) \right] \quad \dots \quad (27)$$

From equation (6) we see that the quantity $\frac{\delta^2}{\gamma^2}$ measures the effect of damping.

We are now in a position to evaluate this quantity with the help of equations (15) and (27) for different values of the incident photon energy. The behaviour of this quantity is shown in the following table for all large values of k_0 for which the approximation is valid and in which case the effect of damping is not at all important.

TABLE

k_0/μ	137	137^2	137^3	∞
δ^2/γ^2	$1.4 \cdot 10^{-6}$	$2.6 \cdot 10^{-7}$	$1.2 \cdot 10^{-6}$	$5.2 \cdot 10^{-6}$

We therefore see that for all values of the incident photon energies the effect of radiation damping is entirely negligible.

CONCLUSION

The power series treatment in the fine structure constant of the Heitler's integral equation does not allow one to conclude that the effect of radiation damping is really small at all energies owing to the appearance of the factors $\log \left(\frac{k}{\mu} \right)$ in the terms which not only increase with k but may make the series expansion divergent, and it is not even possible to find an upper bound of k for which the series remains convergent. Though the situation was thought to be understandable

from the 1st order term, calculated by Power which fortunately did not contain any such $\log\left(\frac{k}{\mu}\right)$ factor, the calculation does not enable one to understand the nature of the higher order terms. In fact the convergency of the series cannot be tested for any value of k , unless one gets an idea of its general term. The semi-variational treatment of the integral equation, however, states that even for any arbitrarily large values of k the effect of damping is really small.

The author wishes to thank Prof. S. C. Kar, Prof. N. R. Sen and Prof. S. N. Bose for their helpful criticisms.

APPENDIX

Let us consider an expression of the form

$$\frac{(1 + \cos \theta)}{1 + \cos \theta + \frac{\mu^2}{2k_0^2}}$$

we can write it as

$$1 - \frac{\mu^2/2k_0^2}{1 + \cos \theta + \mu^2/2k_0^2}$$

now (from the very start) we have neglected quantities of the order of μ^2/k_0^2 in the numerator (Heitler) and hence we write,

$$\frac{1 + \cos \theta}{1 + \cos \theta + \mu^2/2k_0^2} \simeq 1$$

However, we can show that even when the part neglected above be taken into account its integral will again go to zero as μ^2/k_0^2 is made zero as it should be. This is as follows :—

$$\int_{-1}^1 \left\{ \frac{\mu^2}{2k_0^2} \right\} \left(1 + \cos \theta + \mu^2/2k_0^2 \right) d(\cos \theta) = \frac{\mu^2}{2k_0^2} \left[\log \left(\frac{2 + \mu^2/2k_0^2}{\mu^2/2k_0^2} \right) \right]$$

and this $\rightarrow 0$ as $\frac{\mu^2}{2k_0^2} \rightarrow 0$.

REFERENCES

- Feynman (1949). Space-time approach to quantum Electrodynamics. *Phys. Rev.*, **76**, 767-789.
 Heitler (1944). Quantum Theory of Radiation, Chap. V, § 25.
 Hsueh and Ma (1945). Approximate solutions of the integral equations in scattering problems. *Phys. Rev.*, **67**, 303-306.
 Power (1945). Radiation damping on Compton scattering. *Proc. Roy. Irish Acad.*, Vol. **50**, Sec. A, 139-143.
 Wilson (1941). The Quantum Theory of Radiation damping. *Proc. Cam. Phil. Soc.*, **37**, 301-316.

ON THE PROBLEM OF SOFTENING OF RADIATION BY MULTIPLE COMPTON SCATTERING IN STELLAR ATMOSPHERES CONTAINING FREE ELECTRONS

by K. K. SEN, *Chandernagore College*

(Communicated by N. R. Sen, F.N.I.)

(Received February 9; read May 7, 1954)

Chandrasekhar (1948) in his treatment of the transfer of radiation in a plane parallel, electron scattering atmosphere worked out the modification of radiation of a particular wavelength caused by multiple Compton scattering to the first order, by his new method of approximation. The coefficient of scattering was assumed to be independent of the wavelength as in Thomson scattering and the Compton change in wavelength given by

$$\delta\lambda = \gamma(1 - \cos \theta), \text{ where } \gamma = \frac{h}{mc},$$

was taken into account. The scattered intensity was expanded in a Taylor's series in powers of γ (eqn. (5)) and only the term proportional to γ in the expansion was taken for subsequent calculation in an isotropic conservative case. The external boundary condition was simply the absence of incident radiation, while the internal boundary in the form of an infinite plane surface was supposed to radiate with a known spectral distribution. The intensity distribution in a spectral line when plotted against the wavelength shift showed a displacement of the maximum in the right direction, but a finite part of the distribution of intensity corresponded to negative values of the wavelength shift. This error was suspected to be due to the approximation involved in using the first term in the Taylor's series.

It was thought worth while to consider the contribution of the second term of the Taylor's series, proportional to γ^2 . This has been carried through in the present paper. The method of solving the boundary value problem followed here is, however, different and is dependent on expansion in trigonometrical series. It is found that the use of trigonometrical series in the problem of this kind is quite handy and appropriate, and yields rapidly convergent series for calculation.

The results of the second order calculation considerably reduces the error mentioned above. The correction term is negative all throughout, so that the effect of the second order term is to lower the intensity curve. The shift, however, is of the right type and the shift of maximum is slightly increased. The contribution of the second order term cannot thus be called negligible. It appears quite plausible that a calculation up to third order will again slightly raise the curve, and may give non-negligible contribution.

§ 2. The equation of transfer appropriate to the problem is given by (p. 509, *Proc. Roy. Soc., London*, Vol. 192, 1948)

$$\mu \frac{\partial I(\tau, \mu, \lambda)}{\partial \tau} = I(\tau, \mu, \lambda) - \frac{1}{4\pi} \int_{-1}^{+1} \int_0^{2\pi} I(\tau, \mu', \lambda - \gamma(1 - \cos \theta)) d\mu' d\phi' \dots \quad (1)$$

where γ , the Compton wavelength is given by

$$\gamma = \frac{h}{mc} = 0.24 \text{ \AA}, \quad \dots \quad (2)$$

$\mu = \cos \vartheta$ and τ , the optical thickness is given by

$$\tau = \int_z^x \rho \sigma dz, \quad \dots \quad (3)$$

where ρ is the density and σ the scattering coefficient. $I(\tau, \mu, \lambda)$ is the specific intensity of the radiation of wavelength λ at the optical depth τ and in a direction ϑ to the outward drawn normal. θ is the angle of scattering and

$$\cos \theta = \mu \mu' + (1 - \mu^2)^{\frac{1}{2}} (1 - \mu'^2)^{\frac{1}{2}} \cos \phi' \quad \dots \quad (4)$$

The source function represented by the second term of the right-hand side of eqn. (1) means that a radiation of wavelength $\lambda - \gamma(1 - \cos \theta)$ in the direction (μ', ϕ') , when scattered in the direction $(\mu, 0)$, will have the wavelength λ .

We shall now suppose that $I(\tau, \mu', \lambda - \gamma(1 - \cos \theta))$ can be expanded in Taylor's series, so that

$$\begin{aligned} I(\tau, \mu', \lambda - \gamma(1 - \cos \theta)) &= I(\tau, \mu', \lambda) - \gamma(1 - \cos \theta) \frac{\partial I(\tau, \mu', \lambda)}{\partial \lambda} \\ &\quad + \frac{\gamma^2}{2} (1 - \cos \theta)^2 \frac{\partial^2 I(\tau, \mu', \lambda)}{\partial \lambda^2} - \dots \quad \dots \quad (5) \end{aligned}$$

The equation of transfer on substitution of this becomes

$$\begin{aligned} \mu \frac{\partial I(\tau, \mu, \lambda)}{\partial \tau} &= I(\tau, \mu, \lambda) - \frac{1}{2} \int_{-1}^{+1} \left[I(\tau, \mu, \lambda) - \gamma(1 - \mu \mu') \frac{\partial I(\tau, \mu', \lambda)}{\partial \lambda} \right. \\ &\quad \left. + \gamma^2 \left(\frac{3}{4} - \mu \mu' + \frac{3}{4} \mu^2 \mu'^2 - \frac{1}{4} \mu^2 - \frac{1}{4} \mu'^2 \right) \frac{\partial^2 I(\tau, \mu', \lambda)}{\partial \lambda^2} \right] d\mu' \quad \dots \quad (6) \end{aligned}$$

when second order terms of Taylor's expansion are retained.

In solving this equation, Chandrasekhar's method of replacing the integrals by sums given by Gauss's formula for numerical quadratures, has been used. Thus in the n -th approximation,

$$\begin{aligned} \mu_i \frac{\partial I_i(\tau, \lambda)}{\partial \tau} &= I_i(\tau, \lambda) - \frac{1}{2} \left[\sum_j a_j I_j - \gamma \sum_j a_j (1 - \mu_i \mu_j) \frac{\partial I_j(\tau, \lambda)}{\partial \lambda} + \gamma^2 \left\{ \sum_j a_j \left(\frac{3}{4} - \mu_i \mu_j \right. \right. \right. \\ &\quad \left. \left. \left. + \frac{3}{4} \mu_i^2 \mu_j^2 - \frac{1}{4} \mu_i^2 - \frac{1}{4} \mu_j^2 \right) \frac{\partial^2 I_j}{\partial \lambda^2} \right\} \right] \end{aligned}$$

where $i = (\pm 1, \pm 2, \dots, \pm n)$, $j = (\pm 1, \pm 2, \dots, \pm n)$ \therefore \dots (7)

where μ_i 's are the zeros of the Legendre polynomial $P_{2n}(\mu)$ and the a_j 's are the appropriate Gaussian weights.

$$a_j = a_{-j} \text{ and } j = \pm 1, \pm 2, \dots, \pm n. \quad \dots \quad (8)$$

Now restricting ourselves to the case of first approximation only, we put

$$a_{+1} = a_{-1} = 1 \text{ and } \mu_{+1} = -\mu_{-1} = \frac{1}{\sqrt{3}}. \quad \dots \quad (9)$$

Eqn. (7) gives the following two equations:—

$$\frac{1}{\sqrt{3}} \frac{\partial I_{+1}}{\partial \tau} - \frac{\gamma}{3} \frac{\partial I_{+1}}{\partial \lambda} - \frac{2\gamma}{3} \frac{\partial I_{-1}}{\partial \lambda} + \frac{\gamma^2}{6} \frac{\partial^2 I_{+1}}{\partial \lambda^2} + \frac{\gamma^2}{2} \frac{\partial^2 I_{-1}}{\partial \lambda^2} = \frac{1}{2} (I_{+1} - I_{-1}) \quad \dots \quad (10)$$

and

$$\frac{1}{\sqrt{3}} \frac{\partial I_{-1}}{\partial \tau} + \frac{2\gamma}{3} \frac{\partial I_{+1}}{\partial \lambda} + \frac{\gamma}{3} \frac{\partial I_{-1}}{\partial \lambda} - \frac{\gamma^2}{2} \frac{\partial^2 I_{+1}}{\partial \lambda^2} - \frac{\gamma^2}{6} \frac{\partial^2 I_{-1}}{\partial \lambda^2} = \frac{1}{2} (I_{+1} - I_{-1}) \quad \dots \quad (11)$$

Now introducing the variables

$$x = \frac{3}{2} \tau \text{ and } y = \frac{3}{2\gamma} (\lambda - \lambda_0) \quad \dots \quad \dots \quad \dots \quad (12)$$

where λ_0 is some suitably chosen wavelength of constant value, equations (10) and (11) can be written in the following forms:—

$$\frac{\sqrt{3}}{2} \frac{\partial I_{+1}}{\partial x} - \frac{1}{2} \frac{\partial I_{+1}}{\partial y} - \frac{\partial I_{-1}}{\partial y} + \frac{3}{8} \frac{\partial^2 I_{+1}}{\partial y^2} + \frac{9}{8} \frac{\partial^2 I_{-1}}{\partial y^2} = \frac{1}{2} (I_{+1} - I_{-1}) \quad \dots \quad (13)$$

$$\frac{\sqrt{3}}{2} \frac{\partial I_{-1}}{\partial x} + \frac{\partial I_{+1}}{\partial y} + \frac{1}{2} \frac{\partial I_{-1}}{\partial y} - \frac{9}{8} \frac{\partial^2 I_{+1}}{\partial y^2} - \frac{3}{8} \frac{\partial^2 I_{-1}}{\partial y^2} = \frac{1}{2} (I_{+1} - I_{-1}) \quad \dots \quad (14)$$

Adding (13) and (14) and writing

$$K(x, y) = I_{+1}(x, y) + I_{-1}(x, y) \text{ and } H(x, y) = I_{+1}(x, y) - I_{-1}(x, y) \quad \dots \quad (15)$$

we get

$$\frac{\sqrt{3}}{2} \frac{\partial K}{\partial x} + \frac{1}{2} \frac{\partial H}{\partial y} - \frac{3}{4} \frac{\partial^2 H}{\partial y^2} = H \quad \dots \quad \dots \quad (16)$$

• and also subtracting (14) from (13)

$$\frac{\partial H}{\partial x} - \sqrt{3} \frac{\partial K}{\partial x} + \sqrt{3} \frac{\partial^2 K}{\partial x^2} = 0 \quad \dots \quad \dots \quad (17)$$

To satisfy (17), we write

$$K = \frac{\partial F(x, y)}{\partial x}, \quad H = \sqrt{3} \left(\frac{\partial F(x, y)}{\partial y} - \frac{\partial^2 F(x, y)}{\partial y^2} \right) \quad \dots \quad (18)$$

Substituting these in eqn. (16), we get

$$\frac{\partial^2 F}{\partial x^2} + \frac{3}{2} \frac{\partial^4 F}{\partial y^4} - \frac{5}{2} \frac{\partial^3 F}{\partial y^3} + 3 \frac{\partial^2 F}{\partial y^2} - 2 \frac{\partial F}{\partial y} = 0 \quad \dots \quad (19)$$

From equation (18) we obtain

$$I_{+1}(x, y) = K + H = \frac{1}{2} \left[\frac{\partial F}{\partial x} + \sqrt{3} \left(\frac{\partial F}{\partial y} - \frac{\partial^2 F}{\partial y^2} \right) \right] \quad \dots \quad (20)$$

and

$$I_{-1}(x, y) = K - H = \frac{1}{2} \left[\frac{\partial F}{\partial x} - \sqrt{3} \left(\frac{\partial F}{\partial y} - \frac{\partial^2 F}{\partial y^2} \right) \right] \quad \dots \quad (21)$$

The boundary conditions are—

- (i) existence of a known spectral distribution at the lower boundary denoted by $\tau = \tau_1$ or $x = x_1$; and

(ii) absence of inward radiation at the upper boundary denoted by $\tau = 0$ or $x = 0$. These boundary conditions are equivalent to

$$\frac{1}{2} \left[\frac{\partial F}{\partial x} + \sqrt{3} \left(\frac{\partial F}{\partial y} - \frac{\partial^2 F}{\partial y^2} \right) \right]_{x=x_1} = a \text{ known function of } y = \psi(y) \quad \dots \quad (22)$$

$$\text{and} \quad \left[\frac{\partial F}{\partial x} - \sqrt{3} \left(\frac{\partial F}{\partial y} - \frac{\partial^2 F}{\partial y^2} \right) \right]_{x=0} = 0. \quad \dots \quad (23)$$

The problem before us is to solve eqn. (19) under the boundary conditions (22) and (23).

§ 3. The boundary value problem formulated in § 2 can be solved by the method of expansion in trigonometrical series.

Let us take as trial solution of (19) *

$$F(x, y) = A_0(x^2 + y) + B_0x + Ae^{mx+iny}. \quad \dots \quad (24)$$

Substituting in (19) we obtain

$$\begin{aligned} m^2 &= 3n^2(1 - \tfrac{1}{2}n^2) + in(2 - \tfrac{5}{2}n^2) \\ &= (\alpha_n + i\beta_n)^2 \quad (\text{say}). \end{aligned}$$

$$\text{Hence} \quad m = \pm (\alpha_n + i\beta_n) \quad \dots \quad (25)$$

$$\text{where} \quad \alpha_n^2 - \beta_n^2 = 3n^2(1 - \tfrac{1}{2}n^2) \quad \dots \quad (26)$$

$$\text{and} \quad 2\alpha_n\beta_n = n(2 - \tfrac{5}{2}n^2) \quad \dots \quad (27)$$

From (27) it is clear that when n is a positive integer, α_n and β_n will be of opposite signs and when n is a negative integer α_n and β_n are of the same sign. It should also be noted that as n approaches zero, α_n and β_n will be of the same sign.

Now from (26) and (27) we have

$$\alpha_n^2 + \beta_n^2 = \sqrt{\frac{9}{4}n^8 - \frac{11}{4}n^6 - n^4 + 4n^2} \quad \dots \quad (28)$$

and from (26) and (28)

$$\alpha_n = \sqrt{\frac{3}{2}n^2 \left(1 - \frac{1}{2}n^2\right) + \frac{1}{2}\sqrt{\frac{9}{4}n^8 - \frac{11}{4}n^6 - n^4 + 4n^2}} \quad \dots \quad (29)$$

$$\beta_n = -\sqrt{\frac{1}{2}\sqrt{\frac{9}{4}n^8 - \frac{11}{4}n^6 - n^4 + 4n^2} - \frac{3}{2}n^2 \left(1 - \frac{1}{2}n^2\right)} \quad \dots \quad (30)$$

when n is a positive integer.

We see that the solution of (19) can be expanded as the sum of the following series

$$\begin{aligned} F(x, y) &= A_0(x^2 + y) + B_0x + a_0 + \sum_{n=1}^{\infty} \left\{ A_n e^{(\alpha_n + i\beta_n)x + iny} + B_n e^{(\alpha_n - i\beta_n)x - iny} \right. \\ &\quad \left. + C_n e^{-(\alpha_n + i\beta_n)x + iny} + D_n e^{-(\alpha_n - i\beta_n)x - iny} \right\} \quad \dots \quad (31) \end{aligned}$$

* The first two terms in eqn. (24) have been introduced to adjust the boundary conditions of our problem. This will be shown in § 4 and § 7.

and n having only integral values. Writing the solution in the real form

$$F(x, y) = A_0(x^2 + y) + B_0x + a_0 + \sum_{n=1}^{\infty} \left[e^{x_n x} \{ a_n \cos(\beta_n x + ny) + b_n \sin(\beta_n x + ny) \} \right. \\ \left. + e^{-x_n x} \{ c_n \cos(\beta_n x - ny) + d_n \sin(\beta_n x - ny) \} \right] \quad \dots \quad (32)$$

§ 4. Now substituting in the boundary condition (23), the values of $\frac{\partial F}{\partial x}$, $\frac{\partial F}{\partial y}$ and $\frac{\partial^2 F}{\partial y^2}$ derived from (32), we get

$$B_0 - \sqrt{3}A_0 + \sum_{n=1}^{\infty} \left[\{ a_n(\alpha_n - \sqrt{3}n^2) + b_n(\beta_n - \sqrt{3}n) - c_n(\alpha_n + \sqrt{3}n^2) \right. \\ \left. + d_n(\beta_n + \sqrt{3}n) \} \cos ny \right. \\ \left. + \{ b_n(\alpha_n - \sqrt{3}n^2) - a_n(\beta_n - \sqrt{3}n) + c_n(\beta_n + \sqrt{3}n) + d_n(\alpha_n + \sqrt{3}n^2) \} \sin ny \right] = 0 \quad \dots \quad (33)$$

From this it is clear that the individual coefficients of $\cos ny$ and $\sin ny$ are zeros.

$$\therefore B_0 = \sqrt{3}A_0 \quad \dots \quad (34)$$

and

$$a_n = \frac{(\alpha_n^2 + \beta_n^2 - 3n^2 - 3n^4)c_n + 2\sqrt{3}n(n\beta_n - \alpha_n)d_n}{(\beta_n - \sqrt{3}n)^2 + (\alpha_n - \sqrt{3}n^2)^2} \\ b_n = \frac{2\sqrt{3}n(n\beta_n - \alpha_n)c_n - (\alpha_n^2 + \beta_n^2 - 3n^2 - 3n^4)d_n}{(\beta_n - \sqrt{3}n)^2 + (\alpha_n - \sqrt{3}n^2)^2} \quad \dots \quad (35)$$

Now substituting in the boundary condition at the lower bound of the atmosphere given by equation (22) the values of $\frac{\partial F}{\partial x}$, $\frac{\partial F}{\partial y}$ and $\frac{\partial^2 F}{\partial y^2}$ derived from equation (32) and simplifying, we find that

$$\frac{1}{2} \{ B_0 + 2A_0x_1 + \sqrt{3}A_0 \} + \sum_{n=1}^{\infty} \left[\frac{1}{2} e^{x_n x_1} \{ (a_n(\alpha_n + \sqrt{3}n^2) + b_n(\beta_n + \sqrt{3}n)) \cos \beta_n x_1 \right. \\ \left. + (b_n(\alpha_n + \sqrt{3}n^2) - a_n(\beta_n + \sqrt{3}n)) \sin \beta_n x_1 \} \right. \\ \left. + \frac{1}{2} e^{-x_n x_1} \{ (d_n(\beta_n - \sqrt{3}n) - c_n(\alpha_n - \sqrt{3}n^2)) \cos \beta_n x_1 \right. \\ \left. - (d_n(\alpha_n - \sqrt{3}n^2) + c_n(\beta_n - \sqrt{3}n)) \sin \beta_n x_1 \} \right] \cos ny \\ + \sum_{n=1}^{\infty} \left[\frac{1}{2} e^{x_n x_1} \{ (b_n(\alpha_n + \sqrt{3}n^2) - a_n(\beta_n + \sqrt{3}n)) \cos \beta_n x_1 \right. \\ \left. - (a_n(\alpha_n + \sqrt{3}n^2) + b_n(\beta_n + \sqrt{3}n)) \sin \beta_n x_1 \} \right. \\ \left. + \frac{1}{2} e^{-x_n x_1} \{ (d_n(\alpha_n - \sqrt{3}n^2) + c_n(\beta_n - \sqrt{3}n)) \cos \beta_n x_1 \right. \\ \left. + (d_n(\beta_n - \sqrt{3}n) - c_n(\alpha_n - \sqrt{3}n^2)) \sin \beta_n x_1 \} \right] \sin ny \\ = \psi(y) \quad \dots \quad (36)$$

We now assume that the distribution at the base of the atmosphere is capable of Fourier's expansion in the form,

$$\psi(y) = A'_0 + \sum_{n=1}^{\infty} A'_n \cos ny + \sum_{n=1}^{\infty} B'_n \sin ny \quad \dots \quad (37)$$

Thus comparing the coefficients of $\cos ny$ and $\sin ny$ in (36) and (37), and replacing in them values of B_0 , a_n and b_n by (34) and (35) it can be shown that

$$A'_n = M_n c_n + N_n d_n \quad \dots \quad (38)$$

$$B'_n = N_n c_n - M_n d_n \quad \dots \quad (39)$$

$$A'_0 = A_0(x_1 + \sqrt{3}) \quad \dots \quad (40)$$

where

$$\begin{aligned} M_n = \frac{1}{2} e^{\alpha_n x_1} & \left\{ \frac{(\alpha_n^2 + \beta_n^2 - 3n^2 - 3n^4)(\alpha_n + \sqrt{3}n^2) + 2\sqrt{3}n(n\beta_n - \alpha_n)(\beta_n + \sqrt{3}n)}{(\alpha_n - \sqrt{3}n^2)^2 + (\beta_n - \sqrt{3}n)^2} \cos \beta_n x_1 \right. \\ & \left. - \frac{(\alpha_n^2 + \beta_n^2 - 3n^2 - 3n^4)(\beta_n + \sqrt{3}n) - 2\sqrt{3}n(n\beta_n - \alpha_n)(\alpha_n + \sqrt{3}n^2)}{(\alpha_n - \sqrt{3}n^2)^2 + (\beta_n - \sqrt{3}n)^2} \sin \beta_n x_1 \right\} \\ & - \frac{1}{2} e^{-\alpha_n x_1} \{ (\alpha_n - \sqrt{3}n^2) \cos \beta_n x_1 + (\beta_n - \sqrt{3}n) \sin \beta_n x_1 \} \quad \dots \quad (41) \end{aligned}$$

and

$$\begin{aligned} N_n = \frac{1}{2} e^{\alpha_n x_1} & \left\{ \frac{2\sqrt{3}n(n\beta_n - \alpha_n)(\alpha_n + \sqrt{3}n^2) - (\alpha_n^2 + \beta_n^2 - 3n^2 - 3n^4)(\beta_n + \sqrt{3}n)}{(\alpha_n - \sqrt{3}n^2)^2 + (\beta_n - \sqrt{3}n)^2} \cos \beta_n x_1 \right. \\ & \left. - \frac{(\alpha_n^2 + \beta_n^2 - 3n^2 - 3n^4)(\alpha_n + \sqrt{3}n^2) + 2\sqrt{3}n(n\beta_n - \alpha_n)(\beta_n + \sqrt{3}n)}{(\alpha_n - \sqrt{3}n^2)^2 + (\beta_n - \sqrt{3}n)^2} \sin \beta_n x_1 \right\} \\ & + \frac{1}{2} e^{-\alpha_n x_1} \{ (\beta_n - \sqrt{3}n) \cos \beta_n x_1 - (\alpha_n - \sqrt{3}n^2) \sin \beta_n x_1 \}. \quad \dots \quad (42) \end{aligned}$$

From (38), (39) and (40), it can be shown that

$$A_0 = \frac{A'_0}{x_1 + \sqrt{3}} \quad \dots \quad (43)$$

and

$$\left. \begin{aligned} c_n &= \frac{M_n A'_n + N_n B'_n}{M_n^2 + N_n^2} \\ d_n &= \frac{N_n A'_n - M_n B'_n}{M_n^2 + N_n^2} \end{aligned} \right\} \quad \dots \quad (44)$$

From (43) and (44) it is clear that A_0 , c_n and d_n can be evaluated when the values of the Fourier coefficients are known. (M_n and N_n can be calculated from (41) and (42) for different values of n). And from (35), we can calculate the values of a_n and b_n once the values of c_n and d_n are known.

§ 5. Thus completing the determination of constants a_n , b_n , c_n and d_n as in § 4, it is easy to find out the values of $K(x, y)$ and $H(x, y)$ at any level of the atmosphere (equation (18)). But we are mainly concerned with the distribution of the

emergent radiation at the outer boundary of the atmosphere. This from equation (32), and equations (18), (21) and (20) is given by

$$I_{+1}(0, y) = \sqrt{3}A_0 + \sum_{n=1}^{\infty} \left[\{ (a_n - c_n)\alpha_n + (b_n + d_n)\beta_n \} \cos ny + \{ (b_n + d_n)\alpha_n - (a_n - c_n)\beta_n \} \sin ny \right] \quad \dots \quad (45)$$

where a_n , b_n , c_n and d_n are given by the method described in § 4.

§ 6. It has been supposed that an infinite plane surface is radiating outwards uniformly with a known spectral distribution. Above such a radiating surface there exists an atmosphere of free electrons which modifies the distribution at the base. The expression for the modified emergent radiation at the upper boundary of the atmosphere has been given in § 5.

Let us suppose now that the spectral distribution at the lower bound of the atmosphere is given by

$$\psi(y) = \frac{2}{\sqrt{\pi}} e^{-y^2} \quad \dots \quad (46)$$

We expand this in a Fourier series of cosines between $-\pi$ and $+\pi$ as follows

$$\psi(y) = \frac{1}{\pi} + \frac{2}{\pi} \sum_{n=1}^{\infty} e^{-n^2/4} \cos ny \quad \dots \quad (47)$$

This range $(-\pi, \pi)$ practically covers the significant part of the function $\psi(y)$.

Then in equation (37)

$$A_n' = \frac{2}{\pi} e^{-n^2/4}, \quad A_0' = \frac{1}{\pi} \text{ and } B_n' = 0. \quad \dots \quad (48)$$

From (43)

$$A_0 = \frac{1}{\pi(x_1 + \sqrt{3})} \quad \dots \quad (49)$$

and from (44),

$$\left. \begin{aligned} c_n &= \frac{2}{\pi} \frac{M_n}{M_n^2 + N_n^2} e^{-n^2/4} \\ \text{and } d_n &= \frac{2}{\pi} \frac{N_n}{M_n^2 + N_n^2} e^{-n^2/4} \end{aligned} \right\} \quad \dots \quad (50)$$

and a_n and b_n are given by (35).

For a particular value x_1 or τ_1 (the optical thickness of the atmosphere) the value of M_n and N_n are obtained from (41) and (42) for different values of n . These values are used for determining the constants a_n , b_n , c_n and d_n . Substituting these in equation (45), we can find out the value of $I_{+1}(0, y, \psi)$, the emergent radiation from the outer surface of the atmosphere, when the distribution at the base is given by (46). The values of $I_{+1}(0, y, \psi)$ obtained for $x_1 = 1$ or $\tau_1 = \frac{2}{3}$ are shown in the third column of Table 1.

§ 7. To compare the effect of retaining the second order term of Taylor's series in the representation of $I(\tau, \mu', \lambda - \gamma(1 - \cos \theta))$ it was thought worth while to repeat the calculations by the present method of expansion in trigonometrical

series for the case obtained by retaining only the first order term of Taylor's series and compare the results with those obtained by the use of Green's function by Chandrasekhar. In this case of first order calculation the equation corresponding to equation (19) will be (cf. Eq. (23), (20), (21), p. 511, *Proc. Roy. Soc. London*, Vol. 192, 1948)

$$\frac{\partial^2 s(x, y)}{\partial x^2} + \frac{\partial^2 s(x, y)}{\partial y^2} = 2 \frac{\partial s}{\partial y} \dots \dots \dots (51)$$

where

$$I_{+1}(x, y) - I_{-1}(x, y) = \sqrt{3} \frac{\partial s(x, y)}{\partial y} \dots \dots \dots (52)$$

$$I_{+1}(x, y) + I_{-1}(x, y) = \frac{\partial s(x, y)}{\partial x} \dots \dots \dots (53)$$

The boundary conditions are representable in the present case as

$$\frac{1}{2} \left[\frac{\partial s}{\partial x} + \sqrt{3} \frac{\partial s}{\partial y} \right]_{x=x_1} = \psi(y) = \text{a known distribution in } y \dots (54)$$

and

$$\left[\frac{\partial s}{\partial x} - \sqrt{3} \frac{\partial s}{\partial y} \right]_{x=0} = 0. \dots \dots \dots (55)$$

Taking a trial solution of the type

$$s(x, y) = A_0(x^2 + y) + B_0x + Ae^{mx+iny}$$

as before, the general solution can be written in the form by a similar type of arguments as

$$s(x, y) = A_0(x^2 + y) + B_0x + a_0 + \sum_{n=1}^{\infty} \left[e^{\alpha_n' x} \{ a_n' \cos(\beta_n' x + ny) + b_n' \sin(\beta_n' x + ny) \} \right. \\ \left. + e^{-\alpha_n' x} \{ c_n' \cos(\beta_n' x - ny) + d_n' \sin(\beta_n' x - ny) \} \right] \dots \dots (56)$$

where

$$\alpha_n' = \sqrt{\frac{1}{2}(n^2 + \sqrt{n^4 + 4n^2})} \dots \dots \dots (57)$$

$$\beta_n' = \sqrt{\frac{1}{2}(\sqrt{n^4 + 4n^2} - n^2)}. \dots \dots \dots (58)$$

Relations corresponding to equations (26) and (27) are now found to be

$$\alpha_n'^2 - \beta_n'^2 = n^2 \dots \dots \dots (59)$$

$$2\alpha_n'\beta_n' = 2n \dots \dots \dots (60)$$

for n positive, α_n' and β_n' will be of the same sign, and for n negative, α_n' and β_n' will be of opposite signs.

Now applying the boundary condition (55), and putting the coefficients of $\cos ny$ and $\sin ny$ individually equal to zero, we get two relations between the constants of the type,

$$B_0 = \sqrt{3}A_0 \dots \dots \dots (61)$$

$$\left. \begin{aligned} a'_n &= \frac{(\alpha_n'^2 + \beta_n'^2 - 3n^2)c_n' - 2\sqrt{3n}\alpha_n'd_n'}{\alpha_n'^2 + (\beta_n' - \sqrt{3n})^2} \\ b'_n &= -\frac{2\sqrt{3n}\alpha_n'c_n' + (\alpha_n'^2 + \beta_n'^2 - 3n^2)d_n'}{\alpha_n'^2 + (\beta_n' - \sqrt{3n})^2} \end{aligned} \right\} \quad \dots \quad (62)$$

Now from the boundary condition (54), we get

$$\begin{aligned} & \frac{1}{2} \{ B_0 + 2A_0x_1 + \sqrt{3}A_0 \} + \sum_{n=1}^{\infty} \left[\frac{1}{2} e^{\alpha_n' x_1} \left\{ (a_n'\alpha_n' + b_n'(\beta_n' + \sqrt{3n})) \cos \beta_n' x_1 \right. \right. \\ & \quad \left. \left. + (b_n'\alpha_n' - a_n'(\beta_n' + \sqrt{3n})) \sin \beta_n' x_1 \right\} \right. \\ & \quad \left. + \frac{1}{2} e^{-\alpha_n' x_1} \left\{ (d_n'(\beta_n' - \sqrt{3n}) - c_n'\alpha_n') \cos \beta_n' x_1 \right. \right. \\ & \quad \left. \left. - (d_n'\alpha_n' + c_n'(\beta_n' - \sqrt{3n})) \sin \beta_n' x_1 \right\} \right] \cos ny \\ & + \sum_{n=1}^{\infty} \left[\frac{1}{2} e^{\alpha_n' x_1} \left\{ (b_n'\alpha_n' - a_n'(\beta_n' + \sqrt{3n})) \cos \beta_n' x_1 \right. \right. \\ & \quad \left. \left. - (a_n'\alpha_n' + b_n'(\beta_n' + \sqrt{3n})) \sin \beta_n' x_1 \right\} \right. \\ & \quad \left. + \frac{1}{2} e^{-\alpha_n' x_1} \left\{ (d_n'(\beta_n' - \sqrt{3n}) - c_n'\alpha_n') \sin \beta_n' x_1 \right. \right. \\ & \quad \left. \left. + (d_n'\alpha_n' + c_n'(\beta_n' - \sqrt{3n})) \cos \beta_n' x_1 \right\} \right] \sin ny \\ & = \psi(y) \quad \dots \quad (63) \end{aligned}$$

As before, the distribution at the base is supposed to be capable of Fourier expansion

$$\psi(y) = A_0' + \sum_{n=1}^{\infty} A_n' \cos ny + \sum_{n=1}^{\infty} B_n' \sin ny \quad \dots \quad (64)$$

Comparing the coefficients, we find that

$$A_n' = M_n'c_n' + N_n'd_n' \quad \dots \quad (65)$$

$$B_n' = N_n'c_n' - M_n'd_n' \quad \dots \quad (66)$$

$$A_0' = A_0(x_1 + \sqrt{3}) \quad \dots \quad (67)$$

where

$$\begin{aligned} M_n' &= \frac{1}{2} e^{\alpha_n' x_1} \left\{ -\frac{2\sqrt{3n}\alpha_n'^2 + (\alpha_n'^2 + \beta_n'^2 - 3n^2)(\beta_n' + \sqrt{3n})}{\alpha_n'^2 + (\beta_n' - \sqrt{3n})^2} \sin \beta_n' x_1 \right. \\ & \quad \left. + \frac{(\alpha_n'^2 + \beta_n'^2 - 3n^2)\alpha_n' - 2\sqrt{3n}\alpha_n'(\beta_n' + \sqrt{3n})}{\alpha_n'^2 + (\beta_n' - \sqrt{3n})^2} \cos \beta_n' x_1 \right\} \\ & - \frac{1}{2} e^{-\alpha_n' x_1} \{ \alpha_n' \cos \beta_n' x_1 + (\beta_n' - \sqrt{3n}) \sin \beta_n' x_1 \} \quad \dots \quad (68) \end{aligned}$$

and

$$\begin{aligned} N_n' &= \frac{1}{2} e^{\alpha_n' x_1} \left\{ -\frac{(\alpha_n'^2 + \beta_n'^2 - 3n^2)\alpha_n' - 2\sqrt{3n}\alpha_n'(\beta_n' + \sqrt{3n})}{\alpha_n'^2 + (\beta_n' - \sqrt{3n})^2} \sin \beta_n' x_1 \right. \\ & \quad \left. - \frac{2\sqrt{3n}\alpha_n'^2 + (\alpha_n'^2 + \beta_n'^2 - 3n^2)(\beta_n' + \sqrt{3n})}{\alpha_n'^2 + (\beta_n' - \sqrt{3n})^2} \cos \beta_n' x_1 \right\} \\ & + \frac{1}{2} e^{-\alpha_n' x_1} \{ (\beta_n' - \sqrt{3n}) \cos \beta_n' x_1 - \alpha_n' \sin \beta_n' x_1 \}. \quad \dots \quad (69) \end{aligned}$$

From (65) and (66) it is seen that

$$c_n' = \frac{M_n' A_n' + N_n' B_n'}{M_n'^2 + N_n'^2} \quad \dots \quad \dots \quad \dots \quad (70)$$

and

$$d_n' = \frac{N_n' A_n' - M_n' B_n'}{M_n'^2 + N_n'^2} \quad \dots \quad \dots \quad \dots \quad (71)$$

It is clear from (70) and (71) that c_n' and d_n' can be determined, when the values of A_n' and B_n' are known. We can calculate the values of a_n' and b_n' from (62).

It is now easy to find out the values of $I_{+1}(x, y)$ and $I_{-1}(x, y)$ at any depth (equations (52) and (53)). But we are mainly concerned with the intensity distribution at the outer surface of the stellar atmosphere and this from (52), (53), (56), is given by

$$I_{+1}(0, y) = \sqrt{3}A_0 + \sum_{n=1}^{\infty} \left[\left\{ (a_n' - c_n')\alpha_n' + (b_n' + d_n')\beta_n' \right\} \cos ny + \left\{ (b_n' + d_n')\alpha_n' - (a_n' - c_n')\beta_n' \right\} \sin ny \right] \dots \dots \dots (72)$$

Again supposing that $\psi(y) = \frac{2}{\sqrt{\pi}} e^{-y^2}$, and expanding in a Fourier series in cosines as before and comparing the coefficients we get from equations (67), (70) and (71)

$$A_0' = \frac{1}{\pi}, \text{ and hence } A_0 = \frac{1}{\pi(x_1 + \sqrt{3})} \quad \dots \quad \dots \quad \dots \quad (73)$$

and

$$\left. \begin{aligned} c_n' &= \frac{2}{\pi} \frac{M_n' e^{-n^2/4}}{M_n'^2 + N_n'^2} \\ d_n' &= \frac{2}{\pi} \frac{N_n' e^{-n^2/4}}{M_n'^2 + N_n'^2} \end{aligned} \right\} \quad \dots \quad \dots \quad \dots \quad (74)$$

The constants a_n' and b_n' are given by (62).

For a given value of x_1 the values of M_n' and N_n' have been calculated, and these values are used to determine a_n' , b_n' , c_n' , d_n' . From (72), we obtain the values of emergent intensity at the outer boundary of the stellar atmosphere, when the

intensity distribution at the base is given by $\psi(y) = \frac{2}{\sqrt{\pi}} e^{-y^2}$. The results for $x_1 = 1$ or $\tau_1 = \frac{2}{3}$ are shown in the first column of Table 1.

§ 8. The second column of Table 1 contains the values of the intensity obtained by the method of Chandrasekhar (1948) in the case discussed in § 7. Chandrasekhar calculated the values of $I_{+1}(0, y, \delta)$ for different values of y (Radiative Transfer, p. 332) supposing the distribution at the lower boundary to be $\delta(y)$. It was also mentioned that the solution for any other distribution $\psi(y)$ at the lower bound of the atmosphere could be obtained by

$$I_{+1}(0, y, \psi) = \int_{-\infty}^{\infty} I_{+1}(0, y - \eta, \delta) \psi(\eta) d\eta \quad \dots \quad \dots \quad (75)$$

In the present paper we take

$$\psi(\eta) = \frac{2}{\sqrt{\pi}} e^{-\eta^2}$$

$$\text{and} \quad I_{+1}(0, y, \delta) = \frac{\sqrt{3}}{\pi} e^y \int_0^\infty \frac{(p \cos \beta y + \beta q \sin \beta y) \sqrt{1 + \beta^2}}{(p^2 + \beta^2 q^2)} d\beta \quad (76)$$

(cf. eqn. (104), p. 333, Radiative Transfer.)

The values of $I_{+1}(0, y, \psi)$ have been calculated for values of y ranging from $y = 1$, to $y = 3$, using the values of $I_{+1}(0, y - \eta, \delta)$ from Chandrasekhar's Table 1, (*Proc. Roy. Soc. (London)*, Vol. 192, p. 516). The values of $I_{+1}(0, y, \psi)$ for y 's beyond this range are not calculated, as these cannot be obtained from the data of the Table 1 mentioned above. It is found that within the range allowed by the table, the values obtained by the method of trigonometrical series followed here, agree completely with those obtained by Chandrasekhar's method.

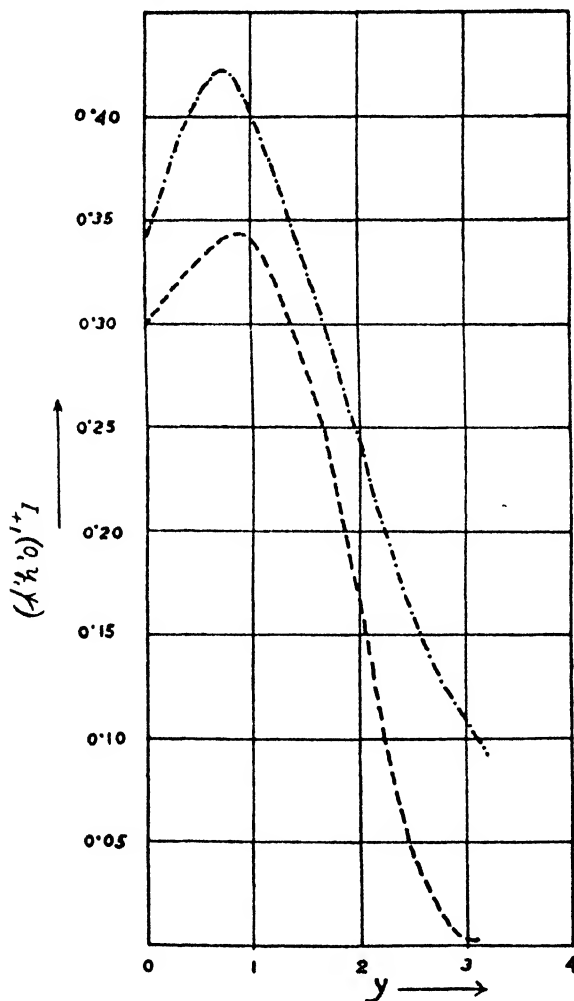


Fig. 1.

The abscissae y denote wavelength shifts in units of $\frac{1}{2}$ Compton wavelength and the ordinates $I_{+1}(0, y, \psi)$, the emergent intensities from the outer boundary of the atmosphere.

TABLE I

		$I_{+1}(0, y, \psi)$ First approx. (with first order term in Taylor's series).	$I_{+1}(0, y, \psi)$ First approx. (by Chandra- sekhar's method).	$I_{+1}(0, y, \psi)$ Second approx. (with 2nd order term in Taylor's series).
0	..	0.34	0.30
0.5	..	0.41	0.33
1.0	..	0.40	0.40	0.34
1.5	..	0.33	0.33	0.28
2.0	..	0.24	0.24	0.17
2.5	..	0.16	0.16	0.05
3.0	..	0.11	0.11	0.003
3.142	..	0.09	0.003

§ 9. The comparative results of the first and second order calculations are illustrated in Fig. 1. It should be remembered that y means wavelength shift in units of $\frac{1}{2}$ Compton wavelength. It is clear from Fig. 1 that in passing from the first to the second approximation the shift and intensity distribution are affected to a marked degree. The second approximation curve is drawn in dashes and the first approximation results are traced as dots and dashes. The additional term of Taylor's series which we have included for the second approximation makes negative contribution to the intensity. Thus the reduction of intensity for different values of y is evident, and this overall lowering of intensity reduces the error of the first order calculation noticed by Chandrasekhar. There is possibility of the intensity curve being again raised a little, if we include the third order term Taylor's series in our consideration.

It is clear from the above treatment that the trigonometrical series gives us a very effective method of treating problems of this type. The agreement between the results obtained by the present method and that of Green's function used by Chandrasekhar, show that the accuracies obtained by the two methods are practically the same. The series representing $I_{+1}(0, y, \psi)$ is highly convergent and hence easy to calculate numerically.

The problem of transfer, allowing for the partial polarisation of the scattered radiation is also being considered by the same method. The results will be published shortly.

In conclusion, I have much pleasure to acknowledge my indebtedness to Prof. N. R. Sen for many helpful discussions and encouragement during the preparation of this work.

ABSTRACT

The problem of softening of radiation by multiple Compton scattering in stellar atmospheres containing free electrons, has been solved in the first approximation (in Chandrasekhar's method of solution by Gaussian approximation) by the method of trigonometrical series. The intensity distribution at the outer surface has been calculated by retaining the first and the second order terms of Taylor's expansion of scattered intensity. The first order calculation by the method of trigonometrical series gives result which is identical with that found by Chandrasekhar's method with the aid of Green's function. The second order calculation considerably reduces the error which was noticed by Chandrasekhar in the first order calculation.

REFERENCES

- Chandrasekhar, S. (1948). The softening radiation by multiple Compton scattering. *Proc. Roy. Soc.*, **192**, 508-518.
 Chandrasekhar, S. (1950) Radiative Transfer, Clarendon Press, Oxford, p. 328-334.

A MATRIX TREATMENT OF FOUR-DIMENSIONAL ROTATION IN HYPERSPACE *

by N. N. GHOSH, *Department of Physics, Calcutta University*

(Communicated by S. N. Bose, F.N.I.)

(Received February 9; read August 6, 1954)

A vector in n -space rotating about a point can undergo all types of $2r$ -dimensional rotations, where r admits of all integral values such that $2 \leq 2r \leq n$. It was shown in a previous paper (Ghosh, 1948) that the general rotation of a vector X about the origin with co-ordinates (x_1, x_2, \dots, x_n) referred to a rectangular system of axes in a Euclidian n -space can be represented in symbolic form by means of the orthogonal transformation $X \rightarrow X'$, where

$$X' = e^{\Omega} X = X + \Omega X + \frac{\Omega^2}{2!} X + \dots \quad (1.1)$$

Ω being the skew-symmetric matrix of rotation (ω_{ij}) of rank $2r$ and ΩX denoting the vector Y with components $y_i = \sum_{j=1}^n \omega_{ij} x_j$. In the case of a four-dimensional rotation Ω is of rank 4 satisfying the characteristic equation †

$$\Omega^5 + p_1^2 \Omega^3 + p_2^4 \Omega = 0, \quad \dots \quad (1.2)$$

where

$$p_1^2 = \sum_{i,j} \omega_{ij}^2 \quad \dots \quad (1.3)$$

$$p_2^4 = \sum_{i,j,k,l} (\omega_{ij}\omega_{kl} - \omega_{ik}\omega_{jl} + \omega_{il}\omega_{jk})^2 \quad \dots \quad (1.4)$$

On reducing the exponents of Ω in (1.1) below 5 by means of the relation (1.2), we obtain

$$X' = X + f_1(p_1, p_2)\Omega X + f_2(p_1, p_2)\Omega^2 X + f_3(p_1, p_2)\Omega^3 X + f_4(p_1, p_2)\Omega^4 X, \quad \dots \quad (1.5)$$

where

$$\left. \begin{aligned} f_1(p_1, p_2) &= 1 - \frac{p_2^4}{5!} + \frac{p_1^2 p_2^4}{7!} - \frac{p_1^4 p_2^4 - p_2^8}{9!} + \dots \\ f_2(p_1, p_2) &= \frac{1}{2!} - \frac{p_2^4}{6!} + \frac{p_1^2 p_2^4}{8!} - \frac{p_1^4 p_2^4 - p_2^8}{10!} + \dots \\ f_3(p_1, p_2) &= \frac{1}{3!} - \frac{p_1^2}{5!} + \frac{p_1^4 - p_2^4}{7!} - \frac{p_1^6 - 2p_1^2 p_2^4}{9!} + \dots \\ f_4(p_1, p_2) &= \frac{1}{4!} - \frac{p_1^2}{6!} + \frac{p_1^4 - p_2^4}{8!} - \frac{p_1^6 - 2p_1^2 p_2^4}{10!} + \dots \end{aligned} \right\} \quad (1.6)$$

* Read at the 41st Session of the Indian Science Congress, 1954.

† If ω_{ij} is of the form $\alpha_i \delta_j - \alpha_j \delta_i + \gamma_i \delta_j - \gamma_j \delta_i$, where α 's, β 's, γ 's, δ 's, are the components of four arbitrary vectors A, B, C, D , the matrix Ω is of rank 4 and the rotation takes place in the four-space spanned by A, B, C, D .

The object of the present paper is generally to deal with a four-dimensional rotation in n -space, showing that it can always be performed by two suitable plane rotations, and to study some of the properties of the four functions f of two arguments p_1, p_2 involved in (1.5).

2. By a straight-forward calculation it is easy to obtain successive terms in (1.6). We notice that corresponding terms in f_1 and f_2 have the same numerator, as also those in f_3 and f_4 . Denoting the numerator of the $(k+1)$ th term in either f_1 or f_2 by a_k and that corresponding to either f_3 or f_4 by c_k , it can be verified that they satisfy the following recurrence relations :

$$\left. \begin{aligned} a_k &= -a_{k-1} p_1^2 - a_{k-2} p_2^4 & (k = 3, 4, 5, \dots), \\ c_k &= -c_{k-1} p_1^2 - c_{k-2} p_2^4 & (k = 2, 3, 4, \dots), \\ a_k &= -c_{k-1} p_2^4 & (k = 1, 2, 3, \dots) \end{aligned} \right\} \dots \dots (2.1)$$

with

$$a_0 = c_0 = 1, \quad c_1 = -p_1^2.$$

We make now some further observations on the transformation (1.5) :

(i) If the vector X remains invariant, that is, if $X' = X$, then X must satisfy the linear equation

$$\Omega X = 0 \quad \dots \dots \dots (2.2)$$

and since Ω is of rank 4, all these invariant vectors lie on a $(n-4)$ -flat.

(ii) If $p_2^4 = 0$, the matrix Ω is of rank 2 and satisfies the characteristic equation *

$$\Omega^3 + p_1^2 \Omega = 0. \quad \dots \dots \dots (2.3)$$

The reduced expression for X' in (1.5) then becomes (Schwerdtfeger, 1945)

$$X' = X + \frac{\sin p_1}{p_1} \Omega X + \frac{1 - \cos p_1}{p_1^2} \Omega^2 X, \quad \dots \dots \dots (2.4)$$

which corresponds to a plane rotation.

3. To examine more fully the structure of the functions f let us start with the roots of the algebraic equation

$$x^5 + p_1^2 x^3 + p_2^4 x = 0 \quad \dots \dots \dots (3.1)$$

which we denote by

$$0, \quad \pm i\beta_2, \quad \pm i\beta_4 \quad (i = \sqrt{-1}),$$

so that

$$\beta_2^2 + \beta_4^2 = p_1^2, \quad \beta_2^2 \beta_4^2 = p_2^4. \quad \dots \dots \dots (3.2)$$

Since now the relation

$$e^x = 1 + x f_1(p_1, p_2) + x^2 f_2(p_1, p_2) + x^3 f_3(p_1, p_2) + x^4 f_4(p_1, p_2) \quad \dots (3.3)$$

holds good only when x satisfies the equation (3.1), we get the following set of identities

$$e^{\pm i\beta_2} = (1 - \beta_2^2 f_2 + \beta_2^4 f_4) \pm i(\beta_2 f_1 - \beta_2^3 f_3), \quad \dots \dots (3.4)$$

$$e^{\pm i\beta_4} = (1 - \beta_4^2 f_2 + \beta_4^4 f_4) \pm i(\beta_4 f_1 - \beta_4^3 f_3), \quad \dots \dots (3.5)$$

* If ω_{ij} is of the form $\alpha_i \beta_j - \alpha_j \beta_i$, where α 's and β 's are the components of two arbitrary vectors A and B , the rank of the matrix Ω is 2 and the corresponding rotation takes place in the plane of A, B .

whence

$$\left. \begin{aligned} \sin \beta_2 &= \beta_2 f_1 - \beta_2^3 f_3, & \cos \beta_2 &= 1 - \beta_2^2 f_2 + \beta_2^4 f_4, \\ \sin \beta_4 &= \beta_4 f_1 - \beta_4^3 f_3, & \cos \beta_4 &= 1 - \beta_4^2 f_2 + \beta_4^4 f_4. \end{aligned} \right\} \quad \dots \quad (3.6)$$

Solving these equations, we get

$$\left. \begin{aligned} f_1(p_1, p_2) &= \frac{\beta_4^3 \sin \beta_2 - \beta_2^3 \sin \beta_4}{\beta_2 \beta_4 (\beta_4^2 - \beta_2^2)}, \\ f_2(p_1, p_2) &= \frac{\beta_4^4 (1 - \cos \beta_2) - \beta_2^4 (1 - \cos \beta_4)}{\beta_2^2 \beta_4^2 (\beta_4^2 - \beta_2^2)}, \\ f_3(p_1, p_2) &= \frac{\beta_4 \sin \beta_2 - \beta_2 \sin \beta_4}{\beta_2 \beta_4 (\beta_4^2 - \beta_2^2)}, \\ f_4(p_1, p_2) &= \frac{\beta_4^2 (1 - \cos \beta_2) - \beta_2^2 (1 - \cos \beta_4)}{\beta_2^2 \beta_4^2 (\beta_4^2 - \beta_2^2)}. \end{aligned} \right\} \quad \dots \quad (3.7)$$

The equations (3.6) and (3.7) show the connection of f -functions with the circular functions. It should be noticed that the exponents of β_2 or β_4 greater than 4 are reducible by means of the relations

$$\left. \begin{aligned} \beta^{2k+3} &= (-1)^k (c_k \beta^3 - a_k \beta) \\ \beta^{2k+4} &= (-1)^k (c_k \beta^4 - a_k \beta^2) \end{aligned} \right\} \quad (k = 1, 2, 3 \dots) \quad \dots \quad (3.8)$$

where β stands for either β_2 or β_4 . An explicit expression for the coefficient c_k is given by

$$(-1)^k c_k = \frac{\beta_4^{2k+2} - \beta_2^{2k+2}}{\beta_4^2 - \beta_2^2}. \quad \dots \quad (3.9)$$

4. The four functions f satisfy among themselves two identical relations which may be derived as follows:

Squaring (3.6) and adding, we have

$$\sin^2 \beta_2 + \cos^2 \beta_2 = 1 = (\beta_2 f_1 - \beta_2^3 f_3)^2 + (1 - \beta_2^2 f_2 + \beta_2^4 f_4)^2, \quad \dots \quad (4.1)$$

$$\sin^2 \beta_4 + \cos^2 \beta_4 = 1 = (\beta_4 f_1 - \beta_4^3 f_3)^2 + (1 - \beta_4^2 f_2 + \beta_4^4 f_4)^2. \quad \dots \quad (4.2)$$

Simplifying (4.1) and making use of (3.8) to reduce the exponents of β_2 below 5, we get finally

$$0 = \{f_1^2 - 2f_2 + a_1(f_3^2 - 2f_2 f_4) - a_2 f_4^2\} + \beta_2^2 \{f_2^2 + 2f_4 - 2f_1 f_3 - c_1(f_3^2 - 2f_2 f_4) + c_2 f_4^2\}.$$

Similarly, from (4.2), we get the same equation with β_2^2 replaced by β_4^2 . Hence, the required identities are

$$\left. \begin{aligned} f_1^2 - 2f_2 + a_1(f_3^2 - 2f_2 f_4) - a_2 f_4^2 &= 0, \\ f_2^2 + 2f_4 - 2f_1 f_3 - c_1(f_3^2 - 2f_2 f_4) + c_2 f_4^2 &= 0. \end{aligned} \right\} \quad \dots \quad (4.3)$$

5. We now proceed to show how the general four-dimensional rotation is obtained by two suitable plane rotations, the rotation in either plane being independent of the rotation in the other.

From (1.5) we see that the four-dimensional rotation operator Δ is of the form

$$\Delta = E + f_1 \Omega + f_2 \Omega^2 + f_3 \Omega^3 + f_4 \Omega^4 \quad \dots \quad (5.1)$$

where E denotes the unit matrix. Utilizing the explicit expressions (3.7) for the functions f , the operator Δ takes the form

$$\Delta = E + \frac{\sin \beta_2}{\beta_2} \left\{ \frac{\beta_4^2 \Omega + \Omega^3}{\beta_4^2 - \beta_2^2} \right\} + \frac{1 - \cos \beta_2}{\beta_2^2} \left\{ \frac{\beta_4^2 \Omega^2 + \Omega^4}{\beta_4^2 - \beta_2^2} \right\} \\ - \frac{\sin \beta_4}{\beta_4} \left\{ \frac{\beta_2^2 \Omega + \Omega^3}{\beta_4^2 - \beta_2^2} \right\} - \frac{1 - \cos \beta_4}{\beta_4^2} \left\{ \frac{\beta_2^2 \Omega^2 + \Omega^4}{\beta_4^2 - \beta_2^2} \right\}. \quad \dots \quad (5.2)$$

Let Γ_2 and Γ_4 denote the matrices $(\beta_4^2 \Omega + \Omega^3)/(\beta_4^2 - \beta_2^2)$ and $(\beta_2^2 \Omega + \Omega^3)/(\beta_2^2 - \beta_4^2)$ respectively; then $\Gamma_2 + \Gamma_4 = \Omega$,

$$\Gamma_2 \cdot \Gamma_4 = - \frac{\Omega^5 + (\beta_2^2 + \beta_4^2) \Omega^4 + \beta_2^2 \beta_4^2 \Omega^2}{(\beta_2^2 - \beta_4^2)^2} = \Gamma_4 \cdot \Gamma_2 = 0. \quad \dots \quad (5.3)$$

Consequently,

$$\Gamma_2^2 = \Omega \Gamma_2, \quad \Gamma_4^2 = \Omega \Gamma_4, \quad \Gamma_2^2 + \Gamma_4^2 = \Omega^2.$$

Written in terms of Γ_2 and Γ_4 the operator (5.2) therefore becomes

$$\Delta = E + \frac{\sin \beta_2}{\beta_2} \Gamma_2 + \frac{1 - \cos \beta_2}{\beta_2^2} \Gamma_2^2 + \frac{\sin \beta_4}{\beta_4} \Gamma_4 + \frac{1 - \cos \beta_4}{\beta_4^2} \Gamma_4^2. \quad \dots \quad (5.4)$$

Since $\Gamma_2 \cdot \Gamma_4 = 0$, the above admits of being written in the product form

$$\Delta = \left(E + \frac{\sin \beta_4}{\beta_4} \Gamma_4 + \frac{1 - \cos \beta_4}{\beta_4^2} \Gamma_4^2 \right) \left(E + \frac{\sin \beta_2}{\beta_2} \Gamma_2 + \frac{1 - \cos \beta_2}{\beta_2^2} \Gamma_2^2 \right) \quad \dots \quad (5.5)$$

where the order of rotations due to Γ_2 and Γ_4 is immaterial. It may be seen that Γ_2 and Γ_4 are of rank 2, satisfying the characteristic equations

$$\Gamma_2^3 + \beta_2^2 \Gamma_2 = 0, \quad \Gamma_4^3 + \beta_4^2 \Gamma_4 = 0 \quad \text{respectively.} \quad \dots \quad (5.6)$$

Let us represent the rotation of X due to Γ_2 by X_2' and that due to Γ_4 by X_4' as in (2.4). Then $X_2' - X$ will represent all vectors lying in the plane of rotation of Γ_2 , while $X_4' - X$ will represent those corresponding to Γ_4 . Now from (2.4)

$$X_2' - X = \frac{\sin \beta_2}{\beta_2} \Gamma_2 X + \frac{1 - \cos \beta_2}{\beta_2^2} \Gamma_2^2 X. \quad \dots \quad (5.7)$$

Therefore

$$\Gamma_4(X_2' - X) = 0.$$

Thus all vectors lying in the plane of rotation of Γ_2 belong to the invariant $(n-2)$ -flat of Γ_4 . Similarly we prove that all vectors lying in the plane of rotation of Γ_4 belong to the invariant $(n-2)$ -flat of Γ_2 . It must be noted the $(n-4)$ -flat defined in (2.2) remains invariant for both Γ_2 and Γ_4 .

Let $\bar{\Delta}$ denote the transposed of Δ , then from (5.4) we have

$$\frac{\Delta - \bar{\Delta}}{2} = \frac{\sin \beta_2}{\beta_2} \Gamma_2 + \frac{\sin \beta_4}{\beta_4} \Gamma_4, \quad \dots \quad (5.8)$$

$$\frac{\Delta + \bar{\Delta}}{2} = E + \frac{1 - \cos \beta_2}{\beta_2^2} \Gamma_2^2 + \frac{1 - \cos \beta_4}{\beta_4^2} \Gamma_4^2. \quad \dots \quad (5.9)$$

Representing $(\Delta - \bar{\Delta}) \frac{1}{2}$ by ϕ , it may be proved that ϕ satisfies the characteristic equation

$$\phi^5 + q_1^2 \phi^3 + q_2^4 \phi = 0 \quad \dots \quad (5.10)$$

where

$$q_1^2 = \sin^2 \beta_2 + \sin^2 \beta_4, \quad q_2^4 = \sin^2 \beta_2 \sin^2 \beta_4.$$

Thus corresponding to a pair of characteristic roots $\pm i \sin \beta_{2k}$ of ϕ there is a pair $\pm i \beta_{2k}$ of Ω . To express Ω in terms of ϕ we may, however, use the determinantal equation

$$\begin{vmatrix} \Omega & \beta_2 & \beta_4 \\ \phi & \sin \beta_2 & \sin \beta_4 \\ -\phi^3 & \sin^3 \beta_2 & \sin^3 \beta_4 \end{vmatrix} = 0. \quad \dots \dots \dots (5.11)$$

The symmetric operators ϕ^2, ϕ^4, \dots are all expressible in terms of Γ_2^2 and Γ_4^2 . We observe that in (5.9) the operator $\frac{\Delta + \bar{\Delta}}{2} - E$, which we denote by ψ , is symmetric and involves Γ_2^2 and Γ_4^2 . To express ψ in terms of ϕ^2 and ϕ^4 , we make use of the following determinantal equation

$$\begin{vmatrix} \psi & 1 & 1 \\ \phi^2 & 1 + \cos \beta_2 & 1 + \cos \beta_4 \\ -\phi^4 & \sin^2 \beta_2 (1 + \cos \beta_2) & \sin^2 \beta_4 (1 + \cos \beta_4) \end{vmatrix} = 0. \quad \dots (5.12)$$

The above yields a notable property of the orthogonal matrix Δ of order n and rank 4.

6. Let us next consider the case of a four-dimensional rotation in 4-space. Ω is now a matrix of order 4 and rank 4. The structure of the functions f remaining unchanged, the values of the arguments are given by

$$p_1^2 = \omega_{12}^2 + \omega_{13}^2 + \omega_{14}^2 + \omega_{23}^2 + \omega_{24}^2 + \omega_{34}^2, \quad \dots \dots (6.1)$$

$$p_2^4 = (\omega_{12}\omega_{34} - \omega_{13}\omega_{24} + \omega_{14}\omega_{23})^2. \quad \dots \dots (6.2)$$

Introducing the conjugate matrix Ω^* , we have the following well-known relations

$$\left. \begin{aligned} \Omega\Omega^* &= -p_2^2 E, \\ \Omega^2 + \Omega^{*2} &= -p_1^2 E, \\ \Omega^3 &= -p_1^2 \Omega + p_2^2 \Omega^*, \\ \Omega^{*3} &= -p_1^2 \Omega^* + p_2^2 \Omega. \end{aligned} \right\} \dots \dots (6.3)$$

The four-dimensional rotation operator (5.1) now reduces to the form

$$(1 - p_2^2 f_4)E + (f_1 - p_1^2 f_3)\Omega + p_2^2 f_3 \Omega^* + (f_2 - p_1^2 f_4)\Omega^2, \quad \dots (6.4)$$

which, on substitution from (3.7) becomes $1/(\beta_4^2 - \beta_2^2)$ times

$$\begin{aligned} &\{(\beta_4^2 \cos \beta_2 - \beta_2^2 \cos \beta_4)E + (\beta_4 \sin \beta_4 - \beta_2 \sin \beta_2)\Omega \\ &\quad + (\beta_4 \sin \beta_2 - \beta_2 \sin \beta_4)\Omega^* + (\cos \beta_2 - \cos \beta_4)\Omega^2\}. \end{aligned} \quad \dots (6.5)$$

The matrices Γ_2 and Γ_4 are now expressible as

$$\Gamma_2 = \frac{\beta_2}{\beta_4^2 - \beta_2^2} (\beta_4 \Omega^* - \beta_2 \Omega), \quad \dots \dots (6.6)$$

$$\Gamma_4 = \frac{\beta_4}{\beta_2^2 - \beta_4^2} (\beta_2 \Omega^* - \beta_4 \Omega), \quad \dots \dots (6.7)$$

and being of rank 2, they determine the component plane rotations (Cole, 1890) as in (5.5).

7. We conclude this paper by proving that f -functions with multiple arguments (mp_1, mp_2) are in general expressible in terms of f -functions with arguments (p_1, p_2) .

Consider the equation

$$x^5 + (mp_1)^2 x^3 + (mp_2)^4 x = 0, \quad \dots \quad (7.1)$$

where m is a positive integer. The roots of this equation are related to those of (3.1) and are $0, \pm im\beta_2, \pm im\beta_4$. Reducing e^* by means of (7.1) it follows that the relation

$$e^* = 1 + \sum_{s=1}^4 x^s f_s(mp_1, mp_2) \quad \dots \quad (7.2)$$

holds good if x satisfies the equation (7.1). Substituting a root $im\beta_2$ for x in the above and referring to the relation (3.4), the left-hand side of (7.2) can be written in the form

$$\{(1 - \beta_2^2 f_2 + \beta_2^4 f_4) + i(\beta_2 f_1 - \beta_2^3 f_3)\}^m \dots \quad (7.3)$$

Reducing the above to the form which does not involve powers of β_2 greater than 4, by means of the relations (3.8) and computing similar coefficients together in (7.2), we obtain the required formulae.

Thus, for $m = 2$, we have

$$\left. \begin{aligned} 2f_1(2p_1, 2p_2) &= 2f_1 + 2a_1(f_1 f_4 + f_2 f_3) + 2a_2 f_3 f_4, \\ 2^2 f_2(2p_1, 2p_2) &= 2f_2 + f_1^2 + a_1(f_3^2 + 2f_2 f_4) + a_2 f_4^2, \\ 2^3 f_3(2p_1, 2p_2) &= 2f_3 + 2f_1 f_2 + 2c_1(f_1 f_4 + f_2 f_3) + 2c_2 f_3 f_4, \\ 2^4 f_4(2p_1, 2p_2) &= 2f_4 + f_2^2 + 2f_1 f_3 + c_1(f_3^2 + 2f_2 f_4) + c_2 f_4^2. \end{aligned} \right\} \dots \quad (7.4)$$

REFERENCES

- Cole, F. N. (1890). On rotations in space of four dimensions. *Amer. Jour. of Math.*, **12**, 208.
 Ghosh, N. N. (1948). Rigid Rotations in Hyperspace. *Bull. Cal. Math. Soc.*, **40**, 119.
 Schwerdtfeger, H. (1945). On the representation of rigid rotations. *Jour. of Appl. Phys.*, **16**, 573.

Issued October 23, 1954.

AN EQUATION OF STATE FOR THE DETONATION OF CONDENSED EXPLOSIVES

by M. P. MURGAI, *Defence Science Organization, Ministry of Defence,
New Delhi*

(Communicated by D. S. Kothari, F.N.I.)

(Received April 15; read May 7, 1954)

1. INTRODUCTION

Hirschfelder and Roseveare (1939) proposed a state equation, for high temperature and pressure, in the virial form, with expansion in terms of v , in which the second virial coefficient is, as usually determined in the theory of slightly imperfect gases, and higher coefficients third and fourth are retained in terms of the second, as found out by Boltzmann (1939). Happel (1906) and others, for non-attracting rigid spheres. The fifth virial coefficient is assigned a value, chosen so that for small values of the volume, the equation may approximate the behaviour of closely packed spheres. Paterson (1948) applied this equation of state to the detonation of condensed explosives. Recently there have been some attempts by De Boer and Michels (1941) and Montroll and Mayer (1941), to evaluate the cluster integral, relating to the third virial coefficient, directly in terms of the Lennard-Jones spherical potential.

Corner (1946) making use of these results calculated the high temperature coefficients for various gases, and applied the state equation thus obtained to the investigation of the properties of propellants. The present is an attempt to extend the validity of this state equation, to higher pressure regions, and to apply the results to the investigation of detonation parameters of condensed explosives. This necessitates the evaluation of another virial coefficient. Due to the inherent difficulty of calculating this in terms of the Lennard-Jones potential, it was chosen to find out its value, from the experimental data on explosives, by the application of the hydrodynamic theory of detonation, by an inverse approach. The oxygen balanced explosive PETN, admits of such a possibility, for its products are mainly determined, by the water gas equilibrium, and there is no change in the number of gm. moles of the products, with pressure or temperature.

2. FUNDAMENTAL EQUATIONS

Let the state equation for the mixture of products of detonation be expressed in the form

$$\frac{pv}{nRT} = (h + \psi) \quad \dots \quad \dots \quad \dots \quad \dots \quad (1)$$

where h is the factor known from Corner's results, and ψ is to be determined.

$$h = 1 + \frac{nb}{v} + \frac{n^2c}{v^2}$$

b and c being the coefficients for the mixture and $nb = \sum n_i B_i$, $nc = \sum n_i c_i$, B_i and C_i being those for the individual gases. Determining the composition from water gas equilibrium, at 4000°K ., and making use of Corner's tables,

$$nb = 3.4603 \times 10^2$$

$$n^2c = 2.6986 \times 10^4$$

by the linear law of combination.

From (1)

$$\psi = \frac{pv}{nRT} - h.$$

Differentiating this w.r.t. v we have

$$\frac{d\psi}{dv} = \frac{1}{nRT} \left[v \left(\frac{dp}{dv} \right)_H + p \right] - \frac{pv}{nRT^2} \left(\frac{dT}{dv} \right)_H + \frac{g}{v}$$

where

$$g = \frac{nb}{v} + \frac{2n^2c}{v^2} \quad \dots \quad \dots \quad \dots \quad \dots \quad \dots \quad \dots \quad (2)$$

The well known Rankine Hugoniot equation in detonation is,

$$E - H = \frac{1}{2}p(v_0 - v) \quad \dots \quad \dots \quad \dots \quad \dots \quad (3)$$

where E is the energy of the product gases, w.r.t. their value at room temperature, per gm. mole of the explosive, H the heat of the reaction, v_0 and v the original and the final volume (per gm. mole). For oxygen positive explosive PETN ($E - H$) is linear over a wide range of temperature, and may be expressed as

$$E - H = \alpha T - \beta$$

$$\alpha = 1151 \text{ kil. cal./degree/gm. mole of PETN}$$

$$\beta = 528.05 \text{ kil. cal./gm. mole of PETN} \quad \dots \quad \dots \quad \dots \quad (4)$$

α , β being constants having dimensions of sp. heat and energy respectively. With the introduction of (4), (3) becomes

$$2(\alpha T - \beta) = p(v_0 - v)$$

or

$$T = \frac{p}{2\alpha} (v_0 - v) + \beta/\alpha \quad \dots \quad \dots \quad \dots \quad \dots \quad (5)$$

Differentiating (5) we have,

$$\left(\frac{dT}{dv} \right)_H = \frac{1}{2\alpha} (v_0 - v) \left(\frac{dp}{dv} \right)_H - \frac{p}{2\alpha} \quad \dots \quad \dots \quad \dots \quad (6)$$

Substituting from (6) and (1), (2) is given by,

$$\frac{d\psi}{dv} = \frac{2\alpha \left[v \left(\frac{dp}{dv} \right)_H + p \right]}{nR[p(v_0 - v) + 2\beta]} - \frac{(h + \psi) \left[(v_0 - v) \left(\frac{dp}{dv} \right)_H - p \right]}{p(v_0 - v) + 2\beta} + g/v \quad \dots \quad (7)$$

The Chapman Jouguet condition, fixing unique value of the detonation velocity, is expressed by the relation

$$\left(\frac{dp}{dv}\right)_H = -\frac{p}{v_0 - v} \quad \dots \quad (8)$$

This enables $\left(\frac{dp}{dv}\right)_H$ from (7) to be eliminated leading to the equation,

$$\frac{d\psi}{dv} = \frac{2\alpha \left[-\frac{pv}{v_0 - v} + p \right]}{nR[p(v_0 - v) + 2\beta]} + \frac{2p(h + \psi)}{p(v_0 - v) + 2\beta} + g/v. \quad \dots \quad (9)$$

The experimentally determined quantity is the detonation velocity. Before the equation expressing $\frac{d\psi}{dv}$ can be usefully employed, the pressure p has to be eliminated. The relation between pressure and the detonation velocity is expressed by

$$D^2 = \frac{p}{(v_0 - v)m} v_0^2 \quad \dots \quad (10)$$

m being the molecular weight of the explosive. Putting the value of p from (10) and defining the following dimensionless variables, namely

$$\xi = \frac{v}{v_0}; \quad \eta = \frac{\beta}{mD^2}; \quad \phi = \frac{nR}{\alpha}$$

(9) reduces to

$$v_0 \frac{d\psi}{dv} = \frac{2(1 - 2\xi)}{\phi[(1 - \xi)^2 + 2\eta]} + \frac{2(h + \psi)(1 - \xi)}{[(1 - \xi)^2 + 2\eta]} + g/\xi = \Theta(\xi\eta\phi \dots). \quad \dots \quad (11)$$

Now

$$\begin{aligned} \frac{d\psi}{d\xi} &= \frac{d\psi}{dv} \cdot \frac{dv}{d\xi} \\ \frac{dv}{d\xi} &= v_0 + \xi \frac{dv_0}{d\xi}. \end{aligned}$$

With this (11) becomes

$$\frac{d\psi}{d\xi} = \Theta \left[1 + \frac{\xi}{v_0} \frac{dv_0}{d\xi} \right]. \quad \dots \quad (12)$$

Elimination of T and p between (1), (5) and (10) provides another relation in terms of the dimensionless variables, namely

$$\phi(h + \psi)[(1 - \xi)^2 + 2\eta] + 2\xi(\xi - 1) = 0. \quad \dots \quad (13)$$

The equations (12) and (13) are the two equations giving two relations between ψ and ξ from which v_0 can be eliminated and $\psi(v)$ found out. There is, however, no a priori information available on $v_0(\xi)$ relation to enable (12) to be integrated. In order to proceed towards solution, we put

$$\psi = \frac{n^3 d}{v^3} \quad (n \text{ being } = 11.0) \quad \dots \quad (14)$$

as a first approximation. This changes the differential equation (11) into an ordinary algebraic equation given by

$$2\xi\phi(h + \psi)(\xi - 1) - \phi(g + 3\psi)[(1 - \xi)^2 + 2\eta] + 2\xi(2\xi - 1) = 0. \quad \dots \quad (15)$$

This combined with (13) while giving a ψ vs. v solution, also provides $\eta(\xi)$ and $v_0(\xi)$ relations. This solution is tabulated in Table 1.

TABLE 1

Loading density ρ_0 gms./c.c.	Volume v_0	Volume v	ξ	η	$d \times 10^{-6}$
.25	1264.8	840.1	.6642	.6649	.968
.50	632.4	441.6	.6983	.4589	.204
.75	421.6	308.3	.7313	.3133	.134
1.00	316.2	238.5	.7543	.2266	.096
1.50	210.8	167.2	.7932	.1209	.075
1.72	183.8	147.3	.8014	.1013	.059

The difference between the experimental value of the detonation velocity and that calculated for a constant value of the fourth virial coefficient is reflected in the variation of the value of d thus obtained. The value of this coefficient calculated for non-attracting rigid spheres is equal to $.0893 \times 10^6$ so that it corresponds to about the middle of the above table.

Logarithmic plot of v_0 and ξ as shown in Fig. 1 gives a straight line which gives the following relation between v_0 and ξ .

$$v_0 = 16.38 \xi^{-10.417} \quad \dots \dots \dots (16)$$

Making use of this approximation (12) reduces to

$$\frac{d\psi}{d\xi} = -9.417 \left[\frac{2(1-2\xi)}{\phi[(1-\xi)^2 + 2\eta]} + \frac{2(h+\psi)(1-\xi)}{[(1-\xi)^2 + 2\eta]} + g/\xi \right] \quad \dots \dots (17)$$

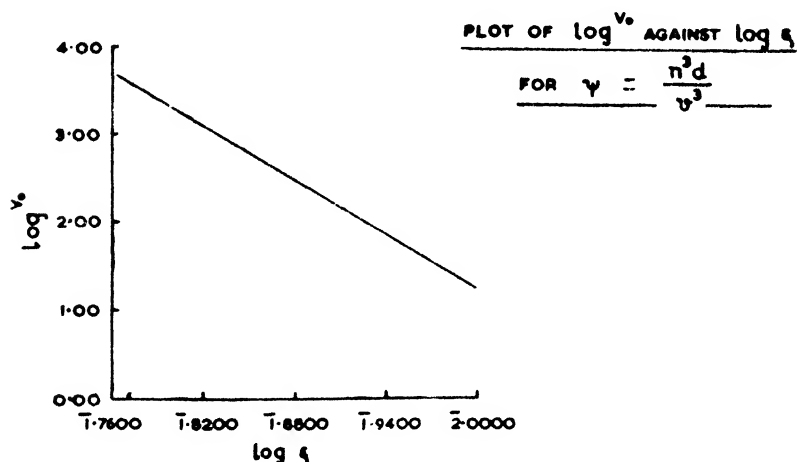


FIG. 1

Figure (2) below gives the relation between η and ξ extrapolated to low densities. Numerical integration of (17) with the help of (16) and Fig. 2 leads to a $\psi(\xi)$

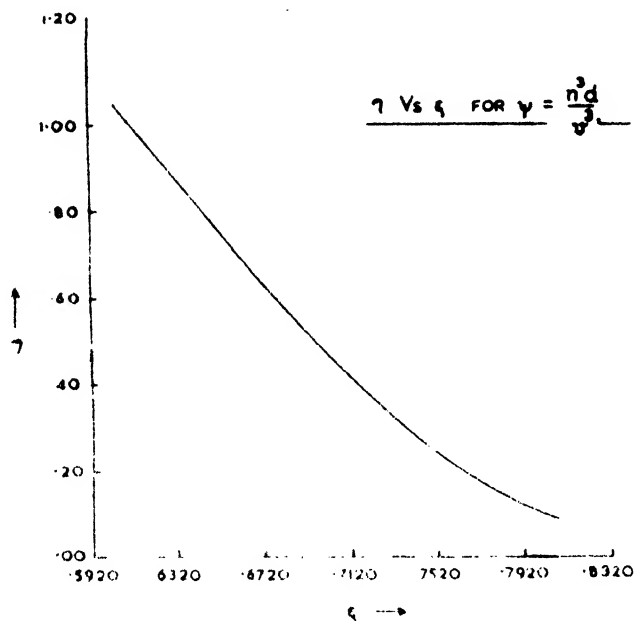


FIG. 2

relation of a better approximation. The initial conditions chosen were $\psi = 0$ for $\rho_0 = 1$ gm./c.c. Combining it with (13) the final $\psi(v)$ relation can be mapped out. It is graphed in Fig. 3. The other parameters pressure and temperature

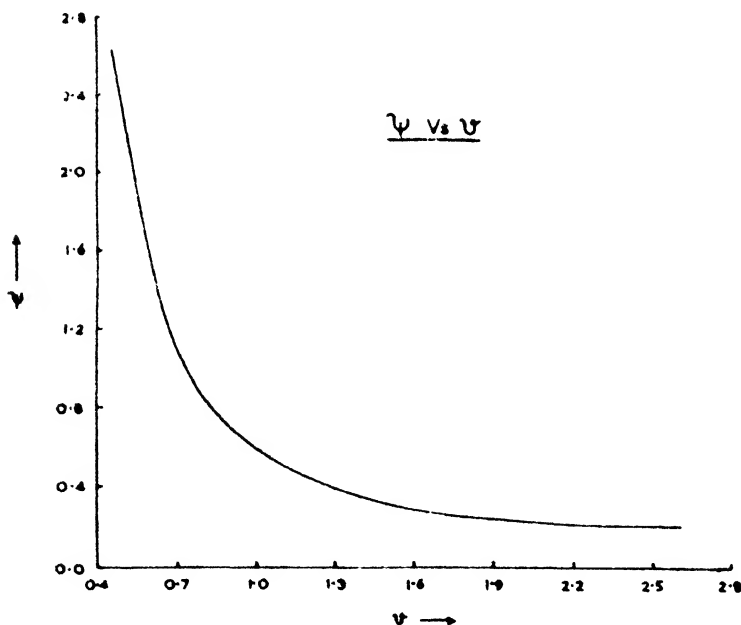


FIG. 3.

for PETN can now be easily found out by virtue of the relations (1) and (10). The results are given in Table 2.

TABLE 2

Loading density ρ_0 gms./c.c.	Volume c.c./gm.	ψ	Pressure $p \times 10^{-10}$ dynes/cm. ²	Temperature $T^\circ\text{K.}$
.25	2.616	.2144	.908	4917
.50	1.341	.3388	2.504	5045
.75	.934	.6564	5.001	5155
1.00	.724	1.012	8.514	5277
1.50	.514	2.278	19.85	5491
1.72	.453	2.603	26.22	5599

Leaving aside the value for $\rho_0 = .25$ gms./c.c., ψ can be represented by

$$\psi = \frac{5.74 \times 10^4}{v^2} \quad \dots \dots \dots (18)$$

Before this result can be applied to other explosives, n the number of gm. moles of the gaseous products has to be separated out. The volume per gm. mole is a property through which the value of ψ thus found can be switched over to other explosives. This will entail the assumption that ψ remains the same function of $\frac{v}{n}$ from one explosive to another. So we have

$$\psi = 475.5 \left(\frac{n}{v} \right)^2 \quad \dots \dots \dots (19)$$

Thus the correction so found can be absorbed in the coefficient of v^{-2} , leading to the following state equation, suitable for the investigation of other explosives

$$\frac{pv}{nRT} = 1 + 31.46 \left(\frac{n}{v} \right) + 698.5 \left(\frac{n}{v} \right)^2 \quad \dots \dots \dots (20)$$

It is interesting to note that ψ can be thus absorbed, in spite of the fact that, as a first approximation, it was put as a function of v^{-3} . An examination of the Table 1 would reveal that the variation in d is about the same as the variation in v (except for the value for $\rho_0 = .25$ gms./c.c.) so that even at that stage it could have been put as a function of v^{-2} in which case d would be sensibly constant in the specified volume range.

3. APPLICATION TO OTHER EXPLOSIVES

Having constructed the equation of state it can now be applied to the investigation of other explosives.

For oxygen positive or oxygen balanced explosives the value of the detonation velocity can be found out just by the application of equations (3), (8) and (10) mentioned above along with the equation (20). For the former type of explosives the composition of the products can be fairly accurately put, straight from the constitution of the explosives without any resort to chemical equilibria. For the later type it is mainly determined by the water gas equilibrium. In view of the assumptions embodied in the state equation (that of the same field of force for all species in the mixture of products) the correction for the equilibrium constant K reduces to unity, and the products therefore can be determined by the value of K for ideal gas condition. On the other hand, the products of oxygen negative explosives do not get determined unless some equilibria in addition to the water gas are considered. That needs a correction to the equilibrium constant for which the fugacity p_i^\bullet given by the integral

$$RT \ln p_i^\bullet = \int_v^\infty \left[\left(\frac{\delta p}{\delta n_i} \right)_{v, T, n_j} - \frac{RT}{v} \right] dv - RT \ln \frac{v}{n_i RT} \quad \dots \quad (21)$$

has to be calculated. Solving this with the help of equation (20) we have

$$p_i^\bullet = \frac{n_i RT}{v} \exp \left[62.92 \left(\frac{n}{v} \right) + 1048 \left(\frac{n}{v} \right)^2 \right] \quad \dots \quad (22)$$

The equilibrium constant for a reaction like

$$a_i + a_j = a_{ij}$$

is given by

$$K \times \frac{\left(\frac{p_i^\bullet}{p_i} \right) \times \left(\frac{p_j^\bullet}{p_j} \right)}{\left(\frac{p_{ij}^\bullet}{p_{ij}} \right)} \frac{p}{n} = \frac{n_{ij}}{n_i n_j}.$$

We have

$$\frac{p_i^\bullet}{p_i} = \frac{p_j^\bullet}{p_j} = \frac{p_{ij}^\bullet}{p_{ij}} = \frac{p^\bullet}{p}$$

(same field of force for all gases), therefore

$$\frac{n_{ij}}{n_i n_j} = K \frac{n}{p^\bullet}.$$

In a previous publication the author (1953) has explained the procedure needed for the solution of the problem of oxygen negative explosives, once p^\bullet has been found out. Due to the wide variation in composition, number of gm. moles, etc., with pressure and temperature, the same value of b and c cannot hold good for the entire range of loading density in this case. Solution with the above state equation, however, provides a data for the next approximation to be carried out with improved values of b and c , which can be found out from the tables. In doing so the value of the third virial coefficient for methane, however, is not available. Adjusting the value of c arbitrarily, for one loading density, a value of 436 (c.c./mole)² for

methane was found to give good fit. With this value the results for the other loading density were calculated. The results are given in Table 3.

TABLE 3

Explosive	Loading density ρ_0 gms./c.c.	Pressure $p \times 10^{-10}$ dynes/cm. ²	Temperature $T^\circ\text{K.}$	$D_{\text{cal.}}$ met./sec.	$D_{\text{obs.}}$ met./sec.
Nitroglycerine ..	1.62	19.10	5200	7360	7500 \pm 500
TNT50	1.67	3200	3425	3200
	1.55	14.6	4280	6667	6800

4. DISCUSSION

The approach adopted here is in principle similar to that of Cooks (1947), who starting with the Abel's equation of state, determined the covolume from the data on various explosives regarding it as a function of the loading density. The pressure and temperature obtained therefore agree very closely with his results for corresponding loading densities. The calculations in this attempt, however, reveal, as shown by Table 3, that the agreement of the detonation velocity with the experimentally observed value is better for the oxygen balanced explosives nitroglycerine than for TNT. Another feature of the result is that for higher pressure regions the calculated value is less than the experimental one while for low pressures it is the reverse. The procedure followed in the present case has been of finding ψ as a function of $\frac{v}{n}$ from oxygen balanced explosive and regarding

it the same function $\frac{v}{n}$ for other explosives. This quantity is connected with

$$\left(\frac{\partial \mu}{\partial p}\right)_{T, n_j, \dots}$$

μ being the chemical potential of the mixture. The method consisting in finding ψ from explosive data carries with it the assumption as mentioned earlier of a common value of the chemical potential μ for the mixture. There is a reason to believe that this value of μ and hence of $\frac{v}{n}$ may not be the same for O_2 -balanced and O_2 -negative explosive, for they do not form exactly similar mixtures, and ψ may be a different function $\frac{v}{n}$ in the later case. The agreement obtained may therefore be considered satisfactory.

The value of the third coefficient for methane can only be regarded an approximate one, giving only a correct order of magnitude, for it has been determined on the basis of the composition found with a common value of p^* in the first instance.

The author is grateful to Prof. D. S. Kothari, Scientific Adviser, Ministry of Defence, Government of India, for his interest during the course of this work. Useful discussions with some of the members of the ballistic group are thankfully acknowledged.

ABSTRACT

The range of validity of Corner's equation of state, hitherto applied by him to the investigation of the properties of propellants, has been extended to higher pressure regions by the application of the hydrodynamic theory of detonation and the results applied to the determination of the detonation parameters of O_2 -balanced and O_2 -negative explosives. An estimate of the third virial coefficient of the methane gas has been made.

REFERENCES

- Boltzmann, L. and Jager, G. (1939). Statistical Thermodynamics by Fowler, R. H. and Guggenheim, E. A., Cambridge University Press, p. 289.
- Cook, M. A. (1947). An Equation of State for Gases at Extremely High Pressure and Temperatures from the Hydrodynamic Theory of Detonation. *J. Chem. Phys.*, **15**, 518.
- Corner, J. (1946). The Thermodynamic Properties of the Products of High Pressure Combustion. *Proc. Phys. Soc. Lond.*, **58**, 737.
- De Boer, J. and Michels, A. (1938, 1939). Contribution to the Quantum Mechanical Theory of the Equation of State and the Law of Corresponding States. *Physica*, **5**, 945; **6**, 409.
- Happel, H. *Loc. cit. ref.*, Boltzman.
- Hirschfelder, J. O. and Roseveuro, W. E. (1939). Intermolecular Forces and the Properties of Gases. *J. Phys. Chem.*, **43**, 15.
- Montroll, E. W. and Mayer, J. E. (1941). Statistical Mechanics of Imperfect Gases. *J. Chem. Phys.*, **9**, 626.
- Murgai, M. P. (1953). On the Explosion of O_2 -Negative Explosives. *Proc. Nat. Inst. Sci.*, **19**, 541.
- Peterson, S. (1948). The Hydrodynamic Theory of Detonation. *Research*, **1**, 221.

Issued October 23, 1954.

EFFECT OF E.M. RADIATION ON THE SELF-ENERGY OF FREE-ELECTRONS. I.

by **INDERJIT SINGH**, *University of Delhi*

(Communicated by F. C. Auluck, F.N.I.)

(*Received May 1; read August 6, 1954*)

I. A unique feature of quantum electrodynamics is the zero-point fluctuations of the electro-magnetic field. An electron, in vacuum, is in constant interaction with these oscillations of infinite energy, and the result is, an increase in the self-energy of the electron. This interaction energy is usually called the Transverse Self-Energy of the Electron. What happens may be visualised thus:

The fluctuations induce a current in the vacuum, as does the virtual photon emission. But, as the current due to virtual photon emission interacts with the emitted virtual field, so the current due to the zero-point amplitude interacts with the amplitude itself (Sawada, 1949). The transverse interaction energy has been calculated by many authors (Weisskopf, 1939) and comes out infinite both on Dirac's one-electron theory, and on 'hole' theory, though in reality (so we suppose) it is a small effect. This assumption is very necessary, in that one cannot restore to the renormalisation procedure, without it, which in turn, has proved of immense use, in interpreting the Lamb Shift (Bethe, 1947) and the anomalous magnetic moment of the electron (Schwinger, 1948). The apparent divergence is ascribed to improper handling of the electro-magnetic mass by present theories which seem to suffer from some deep-seated limitation. In fact, the objectionable features of quantum electrodynamics are much too obvious in all processes which involve virtual transitions in the ultraviolet.

However, there arise additional contributions to the electronic self-energy, if the electron happens to be situated in a transverse radiation field (Auluck and Kothari, 1953, I. Singh, 1953) or is surrounded by other electrons (Salam, 1953). Here we will confine ourselves to the case of a free-electron in an atmosphere of 'free photons'. Due to interaction with the transverse radiation field, the electron is perturbed to undergo transitions involving real photons, which on Dirac's one-electron theory are induced in two ways: the electron in state, $|n\rangle$, in interaction with an assembly of $N(k)$ quanta, of momentum \vec{k} and of energy $|\vec{k}|$ (the velocity of light is taken as unity) may jump to the intermediate state, $|i\rangle$, by either the emission of a photon of momentum \vec{k} or by the absorption of a surrounding photon. In the first case, there will be two more photons per oscillator of the radiation field than there will be in the second case. The interaction energy, arising due to such transitions, is given by the second order matrix element,

$$W = \sum_i \frac{(n|H'|i)(i|H'|n)}{E_n - E_i} \quad \dots \quad \dots \quad \dots \quad (1)$$

where the summation is over all intermediate states. H' , is the contribution, due to interaction between the two subsystems, to the total Hamiltonian of the system consisting of the electron and the radiation field, and is given by—

$$H' = -\sum e (\vec{\alpha} \cdot \vec{A}) \quad \dots \quad \dots \quad \dots \quad (2)$$

where, e is the unit electronic charge, α is the Dirac vector matrix ($\alpha_x, \alpha_y, \alpha_z$) and \vec{A} is the vector potential of the external transverse field, given by

$$A = \sum_{\lambda} \vec{e}_{\lambda} (A_{\lambda}/\sqrt{2}) (c_{\lambda} \exp(i k_{\lambda} x) + c_{\lambda}^* \exp(-i k_{\lambda} \cdot x))$$

with $A_{\lambda} = (4\pi/k_{\lambda} \cdot V)^{\frac{1}{2}}$. $\dots \dots \dots$ (3)
 V , is the normalisation volume, and $c_{\lambda}^*, c_{\lambda}$ are respectively the creation and destruction operators of a photon, in a state with momentum \vec{k}_{λ} and polarisation vector, \vec{e}_{λ} such that,

$$\left. \begin{aligned} \alpha_{\lambda} &\equiv \vec{e}_{\lambda} \cdot \vec{\alpha} \\ \text{and } c_{\lambda} c_{\lambda'}^* - c_{\lambda'}^* c_{\lambda} &= \delta_{\lambda\lambda'}, \text{ etc.} \end{aligned} \right\} \dots \dots \dots (4)$$

since both emission and absorption processes are possible, we have, instead of (1),

$$W = 2\pi e^2 h^2 \sum_i \left\{ \frac{N(k)+1}{k} \frac{(n|\alpha|i_1)(i_1|\alpha|n)}{E_n - E_{i1}} + \frac{N(k)}{k} \frac{(n|\alpha|i_2)(i_2|\alpha|n)}{E_n - E_{i2}} \right\} \dots (5)$$

where the sum is also over the two directions of polarisation of the quanta.

Summing over spin directions of the initial and final state of the electron, and over the two possible kinds of energy in the intermediate state, we have for a free electron at rest, in an atmosphere of free photons,

$$W = 2\pi e^2 h^2 \sum \left\{ \frac{N(k)+1}{k} \cdot \frac{1}{2} \cdot \text{sp} \frac{(\mu-k)(H+E) + \alpha H' \alpha (H+E)}{-4\mu E} \right. \\ \left. + \frac{N(k)}{k} \cdot \frac{1}{2} \cdot \text{sp} \frac{(\mu+k)(H+E) + \alpha H'' \alpha (H+E)}{4\mu E} \right\} \dots (6)$$

$$\left. \begin{aligned} \text{where, } H+E &\equiv \mu(1+\beta) \\ H' &\equiv \beta\mu + (\vec{\alpha} \vec{p}') \\ H'' &\equiv \beta\mu + (\vec{\alpha} \vec{p}'') \\ \text{with, } \vec{p}' &= -\vec{k} \\ \text{and } \vec{p}'' &= +\vec{k} \end{aligned} \right\} \dots \dots \dots (7)$$

Here β is another Dirac matrix such that

$$\alpha_i \beta + \beta \alpha_i = 0, \quad (i = x, y, z),$$

and μ is the mechanical mass of the electron. Assuming the photons to obey black-body distribution,

$$N(k) = \frac{1}{\exp(k/RT) - 1} \dots \dots \dots (8)$$

where R is the Boltzmann gas constant, and T is the temperature of the photon gas.

A summation over all quanta in expression (6) leads to an infinite result. But, this divergence is due to the presence of the usual transverse (vacuum) self-energy term, in the said expression. This term will arise even when there is a complete absence of photons. Subtracting therefore, from eq. (6), this term, we get for the self-energy due to photons,

$$W = \frac{2\alpha}{\pi\mu} (RT)^2 \cdot \xi(1, 1) \quad \dots \quad \dots \quad \dots \quad (9)$$

where

$$\xi(s, a) = \frac{1}{\Gamma(s)} \int_0^\infty \frac{x^{s-1} \exp(-ax)}{1 - \exp(-x)} dx \quad \dots \quad \dots \quad \dots \quad (10)$$

is the well-known Rieman Zeta function. When one substitutes in expression (9), the value for the first Zeta function, $\xi(1, 1)$, one gets,

$$W' = \frac{\pi}{3} \cdot \alpha \cdot \frac{RT'}{\mu} \cdot RT \quad \dots \quad \dots \quad \dots \quad (11)$$

for the additional interaction energy due to the presence of a transverse field, obeying Planck's distribution. Here, α is the Sommerfeld fine-structure constant.

II. The above calculations have been made on Dirac's One-electron theory, wherein the electron can find itself even in the physically unacceptable states of negative mass. On the positron theory, however, such states in general, are all supposed to be occupied by electrons, thus preventing the positive states from the otherwise inevitable decay. Transitions to these occupied negative states are forbidden by Pauli Exclusion Principle.

Because of its special (charged) structure, the vacuum, on hole theory, has important physical properties, which have a decisive bearing on the self-energy problem of electrons. The vacuum is characterised by an infinite charge density, and behaves in many respects, like an intense electro-magnetic field. An electron placed in the vacuum, will obviously deform the latent electron distribution. A hole is created at the position of the electron, and the electron-charge is effectively spread, in that it can be located up to distances comparable to the Compton Wavelength, h/μ . At a distance, ξ , the charge-density is governed by the Weiskoff relation (with a quadratic singularity at $\xi = 0$)

$$G(\xi) = \frac{ie^2}{2\pi} \cdot \frac{\mu}{h} \cdot \frac{1}{\xi} \frac{\partial}{\partial \xi} H_0^{(1)}(i\mu\xi/h), \quad \dots \quad \dots \quad \dots \quad (12)$$

where $H_0^{(1)}(x)$ is a Hankel function of the first kind. The vacuum polarisation increases the effective charge of the electron by a small amount. The interaction between the electron and the oscillations of the field is also modified by the presence of the latent electron pairs in the vacuum, and the perturbation is greater for the higher (compared to the minimum frequency of pair-creation, $2\mu/h$) frequencies of the field. The expression for the transverse (vacuum) self-energy is made more convergent, in that the infinity changes from a quadratic to one, which is of a logarithmic order, only.

The self-energy of an electron in a state $|n\rangle$ on positron theory is the 'self-energy of one electron in state $|n\rangle$ plus the vacuum electrons', minus the 'self-energy of the vacuum electrons alone', or

$$W = W_{vac+1} - W_{vac} \quad \dots \quad \dots \quad \dots \quad (13)$$

In considering the influence of electro-magnetic radiation on the transverse self-energy of a free electron at rest, on Dirac's One-electron theory, we had to deal with four intermediate states, two of them being of negative energy. On the 'hole' theory, this number will be maintained, but instead of the two negative-energy intermediate states in which the electron has momentum, $\pm \vec{k}$, we have now, two new states in which the latent electrons take part. The vacuum electron of momentum, $\vec{p}-\vec{k}$, absorbs a photon from the radiation field and goes over to the state, \vec{p} of the original electron, which on the other hand jumps into the hole so created, emitting a photon, in the process. Thus in the intermediate state we have an electron-positron pair, and in the annihilation process, it is not this electron which takes part, but the electron with which we started. The positive state decays and is recreated by an electron supplied from the vacuum. The second intermediate state arises by the emission of a photon, \vec{k} , by a vacuum electron of momentum $\vec{p}+\vec{k}$ which goes over to \vec{p} , while the original electron fills the hole, by absorbing a photon \vec{k} . Thus, we have, using eq. (13),

$$W = 2\pi e^2 \hbar^2 \sum_{r,v} \left[\frac{N(k)+1}{k} \left\{ \frac{(n|\alpha|r)(r|\alpha|n)}{E_n-k-E_r} + \frac{(n|\alpha|v)(v|\alpha|n)}{E_n+k+E_v} \right\} + \frac{N(k)}{k} \left\{ \frac{(n|\alpha|r)(r|\alpha|n)}{E_n+k+E_r} + \frac{(n|\alpha|v)(v|\alpha|n)}{E_n-k-E_v} \right\} \right] \dots \dots (14)$$

There is no need to consider processes involving vacuum electrons explicitly. They are automatically taken account of, if one makes use of the familiar relation

$$(n_1|O|n_1)+(n_2|O|n_2)-(n_3|O|n_3)-(n_4|O|n_4) = \frac{1}{E} \text{sp } O.H \dots (15)$$

where $|n_1\rangle$ and $|n_2\rangle$ are the Eigen-functions of the Dirac equation, corresponding to the positive energy states and $|n_3\rangle$ and $|n_4\rangle$, to the remaining two states of negative energy. Proceeding in this way, we get,

$$W = 2\pi e^2 \hbar^2 \sum \left\{ \frac{N(k)+1}{k^2} \cdot \frac{1}{2} \cdot \text{sp} \frac{\alpha(H'+E')\alpha(E'+k+H)H}{-4EE'(k+E')} + \frac{N(k)}{k^2} \cdot \frac{1}{2} \text{sp} \frac{\alpha(H''+E'')\alpha(E''-k+H)H}{4EE''(k-E'')} \right\} \dots (16)$$

Again, separating out the transverse (vacuum) self-energy term and using expression (8), we have—

$$W' = \frac{\pi}{3} \cdot \alpha \cdot \frac{RT}{\mu} \cdot RT$$

as before. Thus, the calculations on Dirac's One-electron theory and on 'hole' theory lead to the same result. This result could be anticipated, because the process is symmetric, in that we have both emission and absorption transitions of the original electron, and also because the wave-functions are antisymmetric in the co-ordinates of the initial and the final electrons, on 'hole' theory.

It is interesting, that while the usual transverse self-energy of an electron (absence of all quanta) comes out different on Dirac's One-electron theory and on 'hole' theory, this is not the case for the additional effects arising due to the presence of an external transverse radiation field, which are, so to say, independent of the approach employed.

III. So far, we have tacitly assumed, that the electron under consideration has no momentum. The more general case is to associate a momentum p with the electron so that

$$E^2 = p^2 + \mu^2. \quad \dots \dots \dots (17)$$

After making this change in expression (5), we have to carry out the summations exactly as before. Therefore, we shall not enter into the details of this straightforward calculation, but shall only quote the final expression for the self-energy of the electron of energy E due to the presence of external radiation. This is

$$W' = \frac{\pi}{3} \cdot \alpha \cdot \frac{RT}{E} \cdot RT \quad \dots \dots \dots (18)$$

which is identical with eq. (11) for $p = 0$. In both absorption and emission, we get a term,

$$\left(\frac{\mu^2}{2p} \log \frac{(E+p)}{(E-p)} - E \right) \int N(k) dk \quad \dots \dots \dots (19)$$

which, obviously suffers from an infra-red catastrophe. However, the two processes lead to terms which are opposite in sign, and so the divergent elements disappear from the final expression (18) which, therefore, is finite.

In investigating the effect of radiation on the self-energy problem, we have so far assumed that the photon distribution obeys Planck's law. We can treat however, a very general case, by assuming that the intensity of the radiation of frequency $|\vec{k}|$ is some unspecified function of $|\vec{k}|$ and the radiation is enclosed in a volume G which also contains the electron under consideration. Then

$$N(k) = G \cdot \frac{I(k)}{k} \quad \dots \dots \dots (20)$$

and (18) is given by

$$W' = \frac{2\alpha \cdot G}{\pi E} \int I(k) dk. \quad \dots \dots \dots (21)$$

The limits of integration are determined by the particular range of quanta in loose interaction with the electron. Expression (21) shows, that the transverse self-energy is the same for two different frequencies of the photons, so long as their respective intensities are equal in the radiation bath.

The problem of a bound electron will be treated in a subsequent paper.

IV. In conclusion, it is indeed, a pleasure to thank Dr. F. C. Auluck for valuable guidance, and Professor D. S. Kothari for his kind interest and stimulating discussions. Last, but not the least, my thanks are due to the Atomic Energy Commission, Government of India, for the award of a Fellowship.

SUMMARY

The change in self-energy of an electron due to the presence of an electro-magnetic field is investigated. It is shown that this contribution is finite and comes out the same on Dirac's One-electron theory (all negative energy states empty) and on 'hole' theory (all negative states occupied).

REFERENCES

- Auluck, F. C. and Kothari, D. S. (1952). Effect of E.M. Radiation on the Lamb Shift. *Proc. Roy. Soc., A.*, **214**, 137.
- Bethe, H. A. (1947). The E.M. Shift of Energy Levels. *Phys. Rev.*, **72**, 339.
- Salam, Abdus (1953). Modified propagation Functions in Perturbation Theory. *Pros. Camb. Phil. Soc.*, **49**, 638.
- Sawada, Katurō (1949). Note on the Finite Extension of Electron. *Prog. Theor. Phys.*, **4**, 275.
- Schwinger, Julian (1948). On Quantum-Electrodynamics and the Magnetic Moment of the Electron. *Phys. Rev.*, **73**, 416.
- Singh, Inderjit (1953). Effect of E.M. Radiation on Lamb Shift. *Prog. Theor. Phys.*, **10**, 476.
- Weisskopf, V. F. (1939). On the self-energy and the E.M. Field of the Electron. *Phys. Rev.*, **56**, 72.

Issued October 27, 1954.

VARIATION OF PRESSURE WITH TIME IN ROCKET CHAMBER

by S. K. GUPTA and A. K. MEHTA, *Defence Science Laboratory, New Delhi*

(Communicated by R. S. Varma, F.N.I.)

(Received April 12 ; read August 6, 1954)

INTRODUCTION

The pressure in a rocket is the result of the balance between two main factors—the burning of the propellant which tends to increase the pressure and the escape of the gases through the nozzle tending to reduce the pressure. During burning in a rocket, the mass rate of burning is equal to the mass rate of discharge plus the mass rate of accumulation in the chamber ; that is (Kershner, 1944)

$$S\rho r = C_D A_t P + \frac{d}{dt}(V\rho_g) \quad \dots \quad \dots \quad \dots \quad (1)$$

where S is the area of the constant burning surface of the propellant,
 ρ is the density of the propellant which is about 0.057–0.059 lb./in.³ for most of the propellants,
 r is the rate of surface regression in in./sec.,
 C_D is the discharge coefficient which is about 0.007 sec.⁻¹ for most rockets using smokeless powder as propellant,
 A_t is the area of the throat,
 P is the chamber pressure,
 ρ_g is the density of the gas in the chamber,
 and V is the volume of the chamber available to the gas.

Putting $\frac{dV}{dt} = Sr$ and $\frac{d}{dt}(\rho_g) = 0$ for a steady state and assuming a linear law of burning, $r = a + bP$, we get the steady state solution of equation (1) as

$$P_{eq} = \frac{K\rho'a}{C_D - K\rho'b} \quad \dots \quad \dots \quad \dots \quad (2)$$

where P_{eq} is the equilibrium pressure,

$$K = S/A_t$$

and $\rho' = \rho - \rho_g$; in ρ' , the term ρ_g is numerically only about two or three per cent of ρ' for most cases of ρ so that it is not too inaccurate to consider ρ' as constant.

Equation (1) can be expressed as

$$S\rho'r = C_D A_t P + V \frac{d}{dt}(\rho_g) \quad \dots \quad \dots \quad \dots \quad (3)$$

Kershner (1944) has solved this equation by assuming the volume V as constant which is not a fact.

As a matter of fact, the volume at any instant is given by

$$V = V_0 + \int_0^t rS dt \quad \dots \quad \dots \quad \dots \quad (4)$$

where V_0 is the initial volume in the chamber available to the gas.

We have solved equation (3) when the volume is given by equation (4) and have compared our results for a specific case with those obtained from Kershner's results.

PRESSURE RISE IN ROCKETS

We may assume $\rho_\kappa = BP$ (B a constant), i.e., a constant chamber temperature as has been done by Kershner (1944). Hence from equation (3) we get

$$VB \frac{dP}{dt} = rS\rho' - C_D A_t P. \quad \dots \quad \dots \quad \dots \quad (5)$$

Substituting (4) in (5),

$$\begin{aligned} \left\{ V_0 + \int_0^t (a+bP) S dt \right\} B \frac{dP}{dt} &= (a+bP) S \rho' - C_D A_t P \\ &= aS\rho' + P(bS\rho' - C_D A_t). \end{aligned} \quad \dots \quad (6)$$

Differentiation with respect to t gives

$$B \left\{ V_0 + \int_0^t (a+bP) S dt \right\} \frac{d^2 P}{dt^2} + (a+bP) BS \frac{dP}{dt} = \frac{dP}{dt} (bS\rho' - C_D A_t)$$

which becomes using (2) and (6)

$$a\rho'(1-P/P_{eq}) \frac{d^2 P}{dt^2} + \left(\frac{dP}{dt} \right)^2 \left(\frac{a\rho'}{P_{eq}} + aB + bBP \right) = 0.$$

Putting $\frac{dP}{dt} = q$ so that $\frac{d^2 P}{dt^2} = q \frac{dq}{dP}$, we get

$$\frac{dq}{q} + \frac{\left(\frac{a\rho'}{P_{eq}} + aB + bBP \right)}{(1-P/P_{eq})a\rho'} dP = 0$$

which after integration gives

$$\log q - \frac{bBP_{eq}}{a\rho'} P - \left(1 + \frac{B}{\rho'} P_{eq} + \frac{bB}{a\rho'} P_{eq}^2 \right) \log (1-P/P_{eq}) = \log \frac{aS\rho'}{BV_0}$$

the boundary conditions being

$$q = \frac{aS\rho'}{BV_0} \text{ when } P = 0,$$

or

$$qe^{-MP}(1-P/P_{eq})^{-L} = \frac{aS\rho'}{BV_0},$$

where

$$L = 1 + \frac{BP_{eq}}{\rho'} + \frac{bB}{a\rho'} P_{eq}^2$$

and

$$M = \frac{bB}{a\rho'} P_{eq}$$

or

$$\frac{aS\rho'}{BV_0} t = \int_0^P (1-P/P_{eq})^{-L} e^{-MP} dP. \quad \dots \quad (7)$$

In most of the cases $MP \sim 0.01$ we may take $e^{-MP} = 1 - MP + \frac{1}{2}M^2P^2$ without any appreciable error.

Thus

$$\begin{aligned} \frac{aS\rho'}{BV_0} t &= \int_0^P (1-P/P_{eq})^{-L} (1 - MP + \frac{1}{2}M^2P^2) dP \\ &= \frac{1 - MP_{eq} + \frac{1}{2}M^2P_{eq}^2}{1-L} P_{eq} \left\{ 1 - (1-P/P_{eq})^{1-L} \right\} + \\ &\quad \frac{M(1 - MP_{eq})}{2-L} P_{eq}^2 \left\{ 1 - (1-P/P_{eq})^{2-L} \right\} + \frac{M^2P_{eq}^3}{2(3-L)} \left\{ 1 - (1-P/P_{eq})^{3-L} \right\}. \quad \dots \quad (8) \end{aligned}$$

Kershner obtains

$$\frac{aS\rho'}{BV_0} t = P_{eq} \log_e \frac{P_{eq}}{P_{eq} - P} \dots \dots \dots (9)$$

We may compare equations (8) and (9) by computing values of the time t for various values of pressure P according to both the equations in the case of 4.5" rocket which has the following specifications:—

$$\begin{aligned} S &= 555 \text{ in.}^2 \\ \rho' &= 0.058 \text{ lb./in.}^3 \\ a &= 0.28 \text{ in./sec.} \\ b &= 0.00037 \text{ in.}^3/\text{lb. sec.} \\ B &= 2.64 \times 10^{-7} \\ P_{eq} &= 1442 \text{ lb./in.}^2 \\ V_0 &= 120 \text{ in.}^3 \\ L &= 1.019071 \\ M &= 0.86733 \times 10^{-5} \\ MP_{eq} &= 0.012507. \end{aligned}$$

Table I gives the variation of pressure with time for 4.5" rocket according to equations (8) and (9).

TABLE I

Variation of pressure with time

S. No.	Pressure P in lbs./in. ²	Time t in milli seconds	
		Kershner	Authors
1.	500	2.16	2.17
2.	750	3.72	3.74
3.	1000	6.00	6.08
4.	1250	10.22	10.56
5.	1350	13.95	14.24
6.	1428	23.49	24.21

Table I shows an important fact that taking into account the variation of the volume available to the gases in the chamber does not appreciably alter the pressure-time relation. The time required to attain 99 per cent of the equilibrium pressure in the two cases differs by 3 per cent.

ACKNOWLEDGEMENTS

The authors thank Dr. D. S. Kothari, Dr. R. S. Varma, Shri M. S. Sodha and Shri A. Bhattacharjee for their kind interest in the investigation and are also grateful to the Scientific Adviser to the Ministry of Defence for according permission to publish this paper.

SUMMARY

Kershner (1944) has discussed the phenomenon of pressure rise in rockets on the assumption that the volume available to the propellant gases in the rocket chamber is constant which is not a fact.

Taking this variation into account, the authors have developed a relation between pressure and time in a rocket chamber. Comparison of the results of Kershner with authors for 4.5" rocket shows that the pressure-time relationship is not appreciably altered by taking this volume variation into account.

REFERENCE

- Kershner, R. B. (1944). *Rocket Fundamentals*. Edited by B. L. Crawford, Jr., George Washington University, N.D.R.C. Division 3, Section H. OSRD No. 3711, June 12 (unclassified). Chapter 3.

Issued October 27, 1954.

TRANSIENTS OF MAGNETOGRAPHS AND INSTANTANEOUS VALUES FROM RECORDINGS

by S. L. MALURKAR, Colaba Observatory, Bombay-5

(Communicated by D. S. Kothari, F.N.I.)

(Received May 8; read August 6, 1954)

In a previous note (Malurkar, 1953), the transients that are recorded in a magnetograph were briefly referred to. It is, however, necessary to work out the pattern in a few cases which would be of interest. Among them is, for example, that of an impulse in a sudden commencement storm or sometimes even without a storm. These impulses can be isolated from the disturbance and may be amenable for theoretical study much easier than the complete disturbance. It is worth recalling a few of the stages from the last communication.

The value of the 'impulse is derived by measuring the sudden displacement in terms of the scale value. The scale value is determined by superposing a known magnetic variation near the magnetographs' (by placing subsidiary magnets) 'allowing the magnets' of the photographic instruments 'to become steady and measuring the resultant displacements. The magnification is a *static* determination.'

The need for the investigation arose due to the fact that from Jan. 1949, the Watson Magnetographs at Alibag were on some selected occasions used with an open time scale (nearly 12 times the ordinary one). With a small time scale, many of the doubts remain in the background. 'While tabulating the equivalent magnetic variations, a doubt arose whether the displacements as instantaneously recorded represented genuine variations in the magnetic field... Would one be justified in using the static values when the magnetographs were moving rapidly?'

Changing the magnetic field by electric currents was unsatisfactory as the transients due to electric currents would complicate the problem. The changes in the magnetic field were brought about by suddenly changing the position of the permanent subsidiary magnets, referred to above, from a horizontal position to a vertical one and vice versa. By this method the magnetic field changes unidirectionally from one value to another.

During the above period the recorders were put on quick-run to clearly observe the transients.

The traces for V and H are reproduced in Fig. (see Malurkar, 1953).

When the field changed, no lag in recording was noticed. The initial displacement was greater than that expected from the scale value. The trace is a damped harmonic one, and it ultimately settles down to a constant value.

The equation for the deflection angle θ can be written as:

$$\ddot{\theta} + 2k\dot{\theta} + (k^2 + n^2)\theta = A(k^2 + n^2)F$$

where k is the damping factor,

$2\pi/n = T$ —period of oscillation of the inst.,

A —a constant,

F —change in the magnetic field and

$\dot{\theta}$ and $\ddot{\theta}$ are the time differentials of θ .

The general form of the solution is

$$\theta = \frac{\sin nt}{n} \epsilon^{-kt} \int A(k^2 + n^2) F \epsilon^{kt} \cos nt \, dt - \frac{\cos nt}{n} \epsilon^{-kt} \int A(k^2 + n^2) F \epsilon^{kt} \sin nt \, dt.$$

In particular cases, the solutions can be got by other methods (e.g. Heaviside operators).

(1) Change from one constant magnetic field to another constant one. The change in magnetic field at time $t = 0$ takes place suddenly and F is a constant. Taking p as the usual Heaviside operator θ can be expressed as

$$\frac{1}{p^2 + 2kp + k^2 + n^2} \cdot A(k^2 + n^2) F = AF \left\{ 1 - \epsilon^{-kt} \left(\cos nt + \frac{k}{n} \sin nt \right) \right\}$$

$\theta = 0$ if $\sin nt = 0$, i.e. $nt = \pi$; $t = \pi/n = T/2$ for the first deflection. Hence the ratio of the first deflection to the static value is $(1 + \epsilon^{-kT/2}) : 1$

In most instruments, this ratio is appreciably greater than 1. By increasing the value of the damping factor, the defect may be diminished. The optimum value of the factors would be when the damping is so adjusted that it is *critical*. In the above notation then $n = 0$.

(2) Critical damping. $n = 0$.

$$\text{The solution is } \theta = \frac{1}{p^2 + 2kp + k^2} \cdot Ak^2 F$$

$$\text{i.e.} = AF \{ 1 - \epsilon^{-kt}(1 + kt) \} ;$$

$$\theta/\theta' = 1 - (1 + kt)\epsilon^{-kt}$$

where θ' is the limiting or terminal value.

It may also be put in a different way. If δ is a small fraction, the time required by the magnetograph speck to reach a value just a fraction δ short of the true value is given by

$$\delta = (1 + kt)\epsilon^{-kt}; \quad \theta/\theta' = 1 - \delta$$

or

$$t = \frac{1}{k} \log_e \frac{1}{\delta} + \frac{1}{k} \log_e (1 + kt).$$

In a critically damped magnetograph (with quick run), the values registered would remain short of the true value.

(3) The next case when $F = \alpha t$, the magnetogram has a sharp bend. Then

$$\theta = A\alpha \left\{ t - \frac{2k}{k^2 + n^2} (1 - \epsilon^{-kt} \cos nt) + \frac{1}{n} \epsilon^{-kt} \sin nt \right\}$$

which shows a superposition of some extraneous terms. The damped harmonic terms have the free periods of the recording instrument.

So long as the time co-ordinate or scale is small, the period of vibration of the instrument occupies a very small length. Hence vibrations of that order of period can hardly be noticed. But when an open time scale is used and attempts are made to estimate points to an accuracy of a few seconds, i.e. the same order as the periods of vibration of the recording instruments, it would not be possible to neglect the superposed effects. As it appears, the accuracy of timing any particular effect is subject to an error of an order comparable to the period of vibration of the instrument.

The effect of resonance of a periodic magnetic field whose period is near about that of the recording instrument has been discussed by Vestine *et al.* (1947). When more than one recording instrument is used at a place, and the free periods of the recording instruments are different, those micropulsations which have common periods in all the instrumental records are likely to be genuine, i.e. when the free periods of the horizontal and vertical component magnetographs have different free periods, those pulsations which have been recorded in both the instruments with the same interval of time as period are genuine.

In large magnetic disturbances, the records at many stations consist of rapidly changing traces and sometimes consist of only disjointed specks at the extremities which will need to be connected up. Even if quick-run be used, it is quite likely that rapid variations will be found in many instances. Then the application of the static magnification value would need modification. This would particularly be true if one wished to find the equivalent currents by using magnetic displacements as recorded at various observatories with different types of instruments. The constants of the individual magnetometers would be needed. Similarly if detailed correlation of individual peaks in the magnetograms are to be made with ionospheric records, where the free period of the recording system is extremely small or negligible, it will be necessary to bear in mind the transients recorded in the magnetograms.

Leaving off the finer details, the general character of a magnetic storm disturbance has till now been tabulated at intervals of time large compared with the free periods of the instrument. In fact most of the analysis has been from the slow-run records where it is almost impossible to tabulate at intervals of time of the order of the free period of the instruments. The broad feature of the superposed magnetic field has no period as considered comparable to those of the instruments. Hence in these instances it is possible to ignore the time differentials of the deflection and the static magnification is the result. The general character of the disturbance curves as calculated by Moos (1910), Chapman (1936), Chapman and Bartels (1940) will be essentially maintained.

I thank Prof. Sydney Chapman for helpful discussion on the subject.

REFERENCES

- Chapman, S. (1936). The Earth's Magnetism. Methuen's Monographs, p. 74, *et seq.*
Chapman, S. and Bartels, J. (1940). Geomagnetism. Oxford University Press, Chap. 9.
Malurkar, S. L. (1953). *Ind. Jr. Met. Geophys.*, 4, 190.
Vestine, E. H., Laporte, Lucile, Lange, Isabelle, and Scott, W. E. (1947). The Geomagnetic Field, its description and analysis. Carnegie Inst., Washington (U.S.A.). Chap. IX.

Issued October 27, 1954.

THE EFFECT OF VORTICITY ON THE SPECIFIC HEAT RATIO OF A NON-RELATIVISTIC FERMI-DIRAC GAS

by M. S. VARDYA, *Delhi University, Delhi*

(Communicated by F. C. Auluck, F.N.I.)

(Received May 1 ; read August 6, 1954)

Beeton (1950) has recently investigated the effect of vorticity on the pressure-volume index at different adiabatic compression and expansion ratios in a classical gas. In an actual fluid there will be generally a number of vortices interacting with each other and therefore the general problem is difficult to formulate. To avoid this difficulty Beeton has considered the case of only one cylindrical vortex present in the fluid. He assumes that initially total energy (enthalpy and kinetic energy) is constant throughout the vortex. He has neglected the effect of viscosity. He has shown that the pressure-volume index increases with vorticity. We have generalised the above result in the case of non-relativistic Fermi-Dirac gas taking degeneracy into account.

Consider an assembly of N free electrons occupying a volume V at temperature T . The energy E , pressure P and entropy S are given for a non-relativistic Fermi-Dirac gas by the following relations (Kothari and Singh, 1942) :

$$E = \frac{2\pi g N}{h^3 n} (2mkT)^{\frac{5}{2}} kT F_{\frac{5}{2}}(A), \quad \dots \dots \dots (1)$$

$$P = \frac{2\pi g}{3h^3} (2mkT)^{\frac{5}{2}} kT F_{\frac{5}{2}}(A), \quad \dots \dots \dots (2)$$

$$\text{and} \quad S = \frac{4\pi g N}{h^3 n} (2mkT)^{\frac{5}{2}} k \left\{ \frac{5}{2} F_{\frac{5}{2}}(A) + \frac{3}{2} \ln A \cdot F_{\frac{3}{2}}(A) \right\}. \quad \dots \dots (3)$$

Here,

m = rest mass of the electron,

k = Boltzmann constant,

g = Weight factor,

n = concentration = N/V ,

A = degeneracy parameter = $nh^3/g(2\pi mkT)^{\frac{3}{2}}$,

h = Planck's constant,

$F_{\beta}(A)$ = Fermi-Dirac function corresponding to index β

$$= \int_0^{\infty} \frac{x^{\beta}}{\frac{1}{A} e^x + 1} dx = \text{a function of } A$$

where $x = \epsilon/kT$ and ϵ = kinetic energy of a particle.

We can put the entropy in the form

$$S = \frac{4Ngk}{\sqrt{\pi}A} \left\{ \frac{5}{2} F_{\frac{5}{2}}(A) + \frac{3}{2} \ln A \cdot F_{\frac{3}{2}}(A) \right\} \quad \dots \dots (4)$$

An adiabatic change is an isentropic process. Hence, from equation (3) or (4), it is evident that $T^{\frac{1}{2}}/n$ or A remains constant for an adiabatic process. The relations (1) and (2) then reduce to

$$E = \frac{3}{2} CNkT, \quad \dots \dots \dots (5)$$

and

$$P = C\rho NkT \dots \dots \dots (6)$$

where ρ is the density. Here $C = 4F_{\frac{1}{2}}(A)/3\pi^{\frac{1}{2}}A$, A being a constant quantity.

The above relations (5) and (6) differ from those given for a classical gas by the constant C .

Following Beeton, we assume initially that total energy for every element remains constant throughout the vortex. Then using suffix (0) for initial conditions, we have, for an element of the vortex moving with the velocity v_0 ,

$$\frac{v_0^2}{2} + E_0 + P_0 V_0 = (\text{constant})_0,$$

or

$$v_0^2 = 5 CNk(T_{t_0} - T_0) \dots \dots \dots (7)$$

where $\frac{5}{2} CNkT_{t_0} = (\text{constant})_0$. Here we will call T_{t_0} the initial total temperature.

Further we define the total pressure P_t in this case as

$$\left(\frac{T_{t_0}}{T_0}\right) = \left(\frac{P_{t_0}}{P_0}\right)^{\frac{2}{3}} \dots \dots \dots (8)$$

For an element of gas moving with a velocity v at a radius r of the cylindrical vortex, we have for equilibrium,

$$\frac{v^2}{r} \rho dr = dP \dots \dots \dots (9)$$

or for initial conditions,

$$\frac{v_0^2}{r_0} \rho_0 dr_0 = dP_0 \dots \dots \dots (10)$$

Eliminating v_0^2 from equations (7) and (10) and using equation (8), we get,

$$5 \frac{dr_0}{r_0} = \frac{dP_0}{P_0 \left\{ \left(\frac{P_{t_0}}{P_0}\right)^{\frac{2}{3}} - 1 \right\}} \dots \dots \dots (11)$$

If $r_0 = r_0'$ and $P_0 = P_0'$ at the outer periphery of the vortex, then for the initial state the integral gives,

$$\left(\frac{r_0}{r_0'}\right)^2 = \frac{1 - \left(\frac{P_0'}{P_{t_0}}\right)^{\frac{2}{3}}}{1 - \left(\frac{P_0}{P_{t_0}}\right)^{\frac{2}{3}}} \dots \dots \dots (11)$$

As r decreases towards the centre of the vortex, the pressure also decreases. At some radius \bar{r} the pressure has become zero, therefore,

$$\left(\frac{\bar{r}_0}{r_0'}\right)^2 = 1 - \left(\frac{P_0'}{P_{t_0}}\right)^{\frac{2}{3}} = 1 - \frac{T_0'}{T_{t_0}}, \quad \dots \dots \dots (12)$$

and hence

$$\left(\frac{\bar{r}_0}{r_0}\right)^2 = 1 - \left(\frac{P_0}{P_{t_0}}\right)^{\frac{2}{\gamma}} = 1 - \frac{T_0}{T_{t_0}}. \quad \dots \quad (13)$$

We have also from equation (7)

$$\frac{v_0^2}{5CNk} = T_{t_0} \left(\frac{\bar{r}_0}{r_0}\right)^2. \quad \dots \quad (14)$$

Hence the angular momentum is everywhere the same. For the sake of simplicity, we assume that there are no viscous forces. Hence the angular momentum of every element remains constant no matter what happens to the vortex as a whole in the way of expansion or compression. Therefore the condition that the product (vr) is constant throughout the vortex, which has been shown above to hold initially, will remain true during subsequent changes. Therefore, we have,

$$v^2 r^2 = 5CNk T_{t_0} \bar{r}_0^2. \quad \dots \quad (15)$$

Assuming the change in a particular element of the vortex to be reversible, we have,

$$\frac{T}{T_0} = \left(\frac{P_0}{P}\right)^{\frac{\gamma}{\gamma-1}}.$$

But by the definition of total temperature and pressure,

$$\frac{T_0}{T_{t_0}} = \left(\frac{P_0}{P_{t_0}}\right)^{\frac{\gamma}{\gamma-1}}.$$

Hence

$$\frac{T}{T_{t_0}} = \left(\frac{P}{P_{t_0}}\right)^{\frac{\gamma}{\gamma-1}}$$

i.e. the temperature and pressure at all points of the vortex and at any instant are related by,

$$\frac{T}{P^{\frac{\gamma}{\gamma-1}}} = \text{constant}. \quad \dots \quad (16)$$

At any instant, therefore, we have,

$$\frac{dT}{dP} = \frac{2}{5} \frac{T}{P}. \quad \dots \quad (17)$$

Now we will show that our earlier assumption that initially the total energy and hence the total temperature are the same for all points holds good for all subsequent states after expansion or compression by external forces.

We get, from equations (6), (9) and (15),

$$\frac{dP}{dr} = 5T_{t_0} \bar{r}_0 \frac{P}{r^3 T}. \quad \dots \quad (18)$$

Now with equations (17) and (18),

$$\frac{dT}{dr} = \frac{dT}{dP} \cdot \frac{dP}{dr} = 2T_{t_0} \bar{r}_0 \frac{1}{r^3}. \quad \dots \quad (19)$$

Integrating the above equation, and taking $T = T'$ for $r = r'$, we get,

$$T = T' - T_{t_0} \bar{r}_0^2 \left(\frac{1}{r^2} - \frac{1}{r'^2} \right) \dots \dots \dots (20)$$

Equation (20) thus gives temperature as a function of radius.

Putting $r = r'$ for $T = 0$, we get,

$$T' = T_{t_0} \bar{r}_0^2 \left(\frac{1}{\bar{r}^2} - \frac{1}{r'^2} \right) \dots \dots \dots (21)$$

Hence,

$$\left(\frac{T}{T'} \right) = \left(\frac{\frac{1}{\bar{r}^2} - \frac{1}{r^2}}{\frac{1}{\bar{r}^2} - \frac{1}{r'^2}} \right) \dots \dots \dots (22)$$

Therefore

$$\begin{aligned} T_t &= T + \frac{v^2}{5NCk} \\ &= T_{t_0} \frac{\bar{r}_0^2}{\bar{r}^2} = \text{constant for all elements of the vortex.} \dots \dots (23) \end{aligned}$$

The mass of an element of the vortex is given by

$$\begin{aligned} \delta m &= \rho (2\pi r dr) \\ &= 2\pi \rho' \left(\frac{\frac{1}{\bar{r}^2} - \frac{1}{r^2}}{\frac{1}{\bar{r}^2} - \frac{1}{r'^2}} \right)^{\frac{3}{2}} r \delta r, \end{aligned}$$

as $\rho \propto T^{\frac{3}{2}}$ for a non-relativistic Fermi-Dirac gas.

Therefore,

$$\frac{m}{2\pi\rho'} = \int_{\frac{r}{\bar{r}}}^{r'} \left(\frac{\frac{1}{\bar{r}^2} - \frac{1}{r^2}}{\frac{1}{\bar{r}^2} - \frac{1}{r'^2}} \right)^{\frac{3}{2}} r dr. \dots \dots \dots (24)$$

Putting

$$\left(\frac{1}{\bar{r}^2} - \frac{1}{r^2} \right) = Z \left(\frac{1}{\bar{r}^2} - \frac{1}{r'^2} \right),$$

and $t = \text{vorticity parameter} = \frac{r'^2}{r'^2 - \bar{r}^2} = \frac{T_t}{T'}$,

equation (24) reduces to the simple form,

$$\begin{aligned} \frac{m}{2\pi\rho'} &= \frac{r'^2}{2t} \left(1 - \frac{1}{t} \right) \int_0^1 Z^{\frac{3}{2}} \left\{ 1 - \frac{Z}{t} \right\}^{-2} dZ, \\ &= r'^2 f(t), \dots \dots \dots (25) \end{aligned}$$

where

$$\begin{aligned} f(t) &= \frac{1}{2t} \left(1 - \frac{1}{t}\right) \int_0^1 Z^{\frac{1}{2}} \left\{1 - \frac{Z}{t}\right\}^{-2} dZ, \\ &= \frac{3}{2} t - 1 - \frac{3}{4} \sqrt{t} (t-1) \ln \frac{\sqrt{t}+1}{\sqrt{t}-1}. \end{aligned} \quad \dots \quad (26)$$

Since $\rho \propto P^{\frac{1}{2}}$ for a Fermi-Dirac gas, we have by the conservation of mass,

$$\left(\frac{P'}{P_0}\right)^{\frac{1}{2}} \left(\frac{r'^2}{r_0'^2}\right) \left(\frac{f(t)}{f(t_0)}\right) = 1. \quad \dots \quad (27)$$

Further

$$\begin{aligned} t &= \frac{T_t}{T'} = 1 + \frac{T_{t_0} \bar{r}_0'^2}{T' r'^2}, \\ t_0 &= 1 + \frac{T_{t_0} \bar{r}_0'^2}{T_0' r_0'^2}. \end{aligned}$$

Therefore,

$$\frac{t-1}{t_0-1} = \frac{T_0' r_0'^2}{T' r'^2}.$$

Hence

$$\left(\frac{t-1}{t_0-1}\right) \left(\frac{P'}{P_0}\right)^{\frac{1}{2}} \left(\frac{r'^2}{r_0'^2}\right) = 1. \quad \dots \quad (28)$$

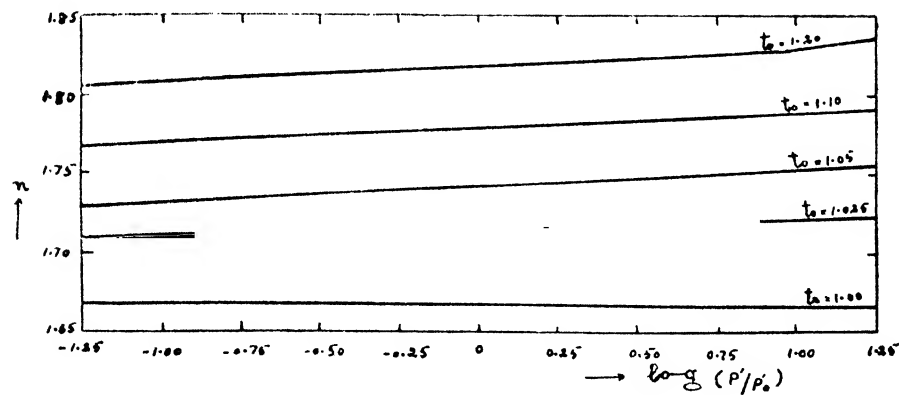
Therefore, equations (27) and (28) together give,

$$\left(\frac{P'}{P_0}\right)^{\frac{1}{2}} \left(\frac{f(t)}{f(t_0)}\right) = \frac{t-1}{t_0-1}. \quad \dots \quad (29)$$

Since $f(t)$ is a known function, equations (28) and (29) are enough to determine the variation of volume ratio $\left(\frac{r'^2}{r_0'^2}\right)$ with the applied pressure ratio $\left(\frac{P'}{P_0}\right)$ if the initial vorticity parameter t_0 be known.

It is convenient to express the results by comparison with a homogeneous gas expanding according to a pressure volume index n , i.e.,

$$\left(\frac{P'}{P_0}\right) = \left(\frac{r_0'^2}{r'^2}\right)^n.$$



Pressure-Volume Characteristic for a Fermi-Dirac Gas.

Hence,

$$n = -\ln \left(\frac{P'}{P_0'} \right) / \ln \left(\frac{r'^2}{r_0'^2} \right). \quad \dots \quad (30)$$

Substituting values in term of t and $f(t)$, we get

$$n = -\frac{5}{3} \frac{\ln \frac{t-1}{t_0-1} - \ln \frac{f(t)}{f(t_0)}}{\ln \frac{t-1}{t_0-1} - \frac{2}{3} \ln \frac{f(t)}{f(t_0)}}. \quad \dots \quad (31)$$

Now
$$n < \frac{5}{3} \quad \text{if} \quad \frac{d}{dt} f(t) \quad \text{is positive}$$

and
$$n > \frac{5}{3} \quad \text{if} \quad \frac{d}{dt} f(t) \quad \text{is negative.}$$

But

$$\begin{aligned} \frac{d}{dt} f(t) &= \frac{9}{4} - \frac{3}{4} \left(\frac{3}{2} \sqrt{t} - \frac{1}{2\sqrt{t}} \right) \ln \frac{1 + \frac{1}{\sqrt{t}}}{1 - \frac{1}{\sqrt{t}}}, \\ &= -\frac{9}{4} \left(\frac{1}{3t} + \frac{1}{5t^2} + \frac{1}{7t^3} + \dots \right) \\ &\quad + \frac{3}{8} \left(\frac{1}{t} + \frac{1}{3t^2} + \frac{1}{5t^3} + \dots \right) \\ &< 0. \end{aligned}$$

Hence,

$$n > \frac{5}{3}.$$

Thus we see that the presence of vorticity in a non-relativistic Fermi-Dirac gas effectively increases the value of n .

The value of n has been calculated for initial vorticity parameters t_0 equal to 1.025, 1.05, 1.10 and 1.20 and is plotted in the figure. It will be observed that the amount of increase in n is chiefly dependent on the initial degree of vorticity.

I take this opportunity to thank Professor D. S. Kothari for his constant help and encouragement during the work and Dr. F. C. Auluck for his valuable guidance.

SUMMARY

We have investigated in this note the effect of vorticity on the specific heat ratio of a non-relativistic Fermi-Dirac gas. We find that the ratio increases with vorticity.

REFERENCES

- Beeton, A. B. P. (1950.) Technical Note No. Aero. 2060, Royal Aircraft Establishment, Farnborough.
Kothari, D. S. and Singh, B. N. (1942.) *Proc. Roy. Soc., Ser. A*, **180**, 414.

FORCE CONSTANTS FOR 1, 3, 5 TRIMETHYL BENZENE

by V. SANTHAMMA, *Department of Physics, Andhra University, Waltair*

(Communicated by K. Rangadhama Rao, F.N.I.)

(Received April 5; read May 7, 1954)

INTRODUCTION

This paper presents the calculation of the valence force constants for the non-planar vibrations of the 1, 3, 5 trimethyl benzene molecule, namely, H , the methyl diagonal bending constant, h_m , the interaction constant between the methyl bendings, \bar{a}_m , the interaction constant between a methyl bending and an adjacent ortho hydrogen bending and lastly, \bar{a}_p , the interaction between a methyl bending and a para hydrogen bending. The values of the vibrational frequencies for the molecule are then deduced and compared with the assignments made by previous investigators from other considerations. For the purpose of this calculation, the results of the normal co-ordinate analysis of the non-planar vibrations of Benzene and its Deuterium derivatives (Miller and Crawford, 1946) have been utilised. The method of calculation is that given by the author (1953) in an earlier paper on the Force constants for the BF_3 molecule.

1, 3, 5 Trimethyl Benzene (commonly known as Mesitylene) belongs to the point group D_{3h} , if, as a first approximation, the CH_3 substituent is considered as a single atom, ignoring thereby the interactions within the methyl group, which affect the skeletal bending. The nine non-planar vibrations of 1, 3, 5 trimethyl benzene are divided into the two symmetry species as $3A_2'' + 3E''$, the latter being doubly degenerate. The vibrations of species A_2'' are infrared active and those of E'' are Raman active. One of the A_2'' fundamentals has not been recorded in infrared but only tentatively assigned (Pitzer and Scott, 1943) from Raman effect observations. Two weak Raman lines 145 cm.^{-1} and 182 cm.^{-1} are stated by Pitzer and Scott to have been observed by two different investigators. Of these, 182 cm.^{-1} has been assigned by Pitzer and Scott as one of the A_2'' fundamentals on the basis of the product rule analogous to that of Tellar and Redlich. The present calculations of the force constants of this molecule have led to the confirmation of this tentative assignment.

Pitzer and Scott have also suggested the frequency 439 cm.^{-1} as one of the E'' fundamentals of Mesitylene. In assigning the degenerate modes, it may be noted that certain frequencies should be either exactly or approximately the same as in Meta-Xylene (3, 5 dimethyl benzene). The three fundamentals 10, 16 and 17 (in Wilson's notation) of E'' species in 1, 3, 5 trimethyl benzene will be split up into 10a, 16a and 17a of A_2 species and 10b, 16b and 17b of B_2 species in case of (3, 5) *m*-Xylene. Here the degeneracy is removed, one component changing and the other remaining almost equal, i.e. 10a, 16a and 17a in *m*-Xylene will be exactly same as 10, 16 and 17 of mesitylene. Pitzer and Scotts' assignment is based on this consideration. No line appears in the Mesitylene spectrum where No. 16 in Pitzer and Scotts' notation is expected. A very weak line is observed at 439 cm.^{-1} in the Raman spectrum of *m*-Xylene (assigned as 16a). This is regarded by Pitzer and Scott (1943) as the corresponding frequency No. 16 in mesitylene. It is possible to compare this assignment with the value derived in these calculations from the force constants, but the author finds the agreement unsatisfactory.

A preliminary report of the results have been published in *Current Science* (Vol. 23, 115, 1954).

CALCULATIONS

Three types of non-planar valence force co-ordinates are used to construct the symmetry co-ordinates for the two species and they are schematically represented in Fig. 1.

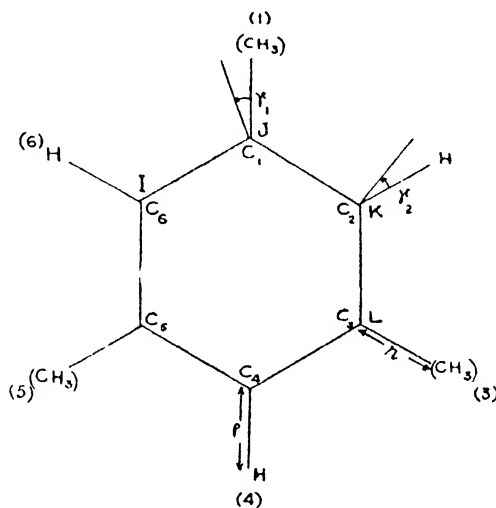


FIG. 1.

(1) The perpendicular displacement of the i -th CH_3 group defined by the two adjacent $\text{C}-\text{C}$ bonds is termed as $r\gamma_i$, where γ_i is the angle between $\text{C}-\text{CH}_3$ bond and the plane formed by C_1C_6 and C_1C_2 bonds of the molecule and r is the equilibrium distance of $\text{C}_{\text{arom}}-\text{C}_{\text{aliph}}$. (2) The corresponding perpendicular displacement of the i -th hydrogen atom is termed as $\rho\gamma_i$, where ρ is the equilibrium distance of $\text{C}-\text{H}$ bond length. (3) The non-planar ring bending deformations are regarded as torsions around $\text{C}-\text{C}$ bonds. The angle between the plane containing 6, 1, 2 carbon atoms and that containing 1, 2, 3 carbon atoms is termed as δ_1 . The corresponding internal co-ordinate is $R\delta_1$ where R is the equilibrium value of $\text{C}-\text{C}$ bond distance. The complete set of internal co-ordinates is $r\gamma_1, \rho\gamma_2, r\gamma_3, \rho\gamma_4, r\gamma_5, \rho\gamma_6, R\delta_1, R\delta_2, R\delta_3, R\delta_4, R\delta_5$ and $R\delta_6$. The symmetry co-ordinates are constructed with the above internal co-ordinates and are found to be just the same as those used in the case of 1, 3, 5 trifluoro benzene recently worked out by Ferguson (1953) and are given in Table I.

TABLE I

Species	Symmetry Co-ordinates
	$R_1 = 6^{-\frac{1}{2}} (r\gamma_1 + \rho\gamma_2 + r\gamma_3 + \rho\gamma_4 + r\gamma_5 + \rho\gamma_6)$
A_2''	$R_2 = 6^{-\frac{1}{2}} (r\gamma_1 - \rho\gamma_2 + r\gamma_3 - \rho\gamma_4 + r\gamma_5 - \rho\gamma_6)$
	$R_3 = R \times 6^{-\frac{1}{2}} (\delta_1 - \delta_2 + \delta_3 - \delta_4 + \delta_5 - \delta_6)$
	$R_{1a} = \frac{1}{2} (r\gamma_3 - \rho\gamma_2 - r\gamma_5 + \rho\gamma_6)$
	$R_{1b} = 12^{-\frac{1}{2}} (-2r\gamma_1 + \rho\gamma_2 + r\gamma_3 - 2\rho\gamma_4 + r\gamma_5 + \rho\gamma_6)$
E''	$R_{2a} = \frac{1}{2} (\rho\gamma_2 + r\gamma_3 - r\gamma_5 - \rho\gamma_6)$
	$R_{2b} = 12^{-\frac{1}{2}} (-2r\gamma_1 - \rho\gamma_2 + r\gamma_3 + 2\rho\gamma_4 + r\gamma_5 - \rho\gamma_6)$
	$R_{3a} = R \times 12^{-\frac{1}{2}} (-\delta_1 + 2\delta_2 - \delta_3 - \delta_4 + 2\delta_5 - \delta_6)$
	$R_{3b} = \frac{R}{2} (\delta_1 - \delta_3 + \delta_4 - \delta_6)$

P.E. Matrix

Table II gives the f matrix in terms of the valence force co-ordinates. In writing down this matrix, the notation of Miller and Crawford (1946) is retained for the ring deformation and the applicable hydrogen bending constants; o , m and p refer to ortho, meta and para relationship between the internal co-ordinates. The elements of the F matrix for the species A_2'' and E'' are given in Tables III and IV respectively.

TABLE II

	$r\gamma_1$	$r\gamma_3$	$r\gamma_5$	$\rho\gamma_2$	$\rho\gamma_4$	$\rho\gamma_6$	$R\delta_1$	$R\delta_2$	$R\delta_3$	$R\delta_4$	$R\delta_5$	$R\delta_6$
$r\gamma_1$	H	h_m	h_o	\bar{a}_o	\bar{a}_p	\bar{a}_o	\bar{e}_o	\bar{e}_m	$-\bar{e}_p$	$+\bar{e}_p$	$+\bar{e}_m$	$+\bar{e}_o$
$r\gamma_3$		H	h_m	\bar{a}_o	\bar{a}_o	\bar{a}_p	$+\bar{e}_m$	$+\bar{e}_o$	$-\bar{e}_o$	$-\bar{e}_m$	$-\bar{e}_p$	$+\bar{e}_p$
$r\gamma_5$			H	\bar{a}_p	\bar{a}_o	\bar{a}_o	$-\bar{e}_p$	$+\bar{e}_p$	$+\bar{e}_m$	$+\bar{e}_o$	$-\bar{e}_o$	$-\bar{e}_m$
$\rho\gamma_2$				A	a_m	a_m	$+\bar{c}_o$	$-\bar{c}_o$	$-\bar{c}_m$	$-\bar{c}_p$	$+\bar{c}_p$	$+\bar{c}_m$
$\rho\gamma_4$					A	a_m	$+\bar{c}_p$	$+\bar{c}_m$	$+\bar{c}_o$	$-\bar{c}_o$	$-\bar{c}_m$	$-\bar{c}_p$
$\rho\gamma_6$						A	$-\bar{c}_m$	$-\bar{c}_p$	$+\bar{c}_p$	$+\bar{c}_m$	$+\bar{c}_o$	$-\bar{c}_o$
$R\delta_1$							B	b_o	b_m	b_p	b_m	b_o
$R\delta_2$								B	b_o	b_m	b_p	b_m
$R\delta_3$									B	b_o	b_m	b_p
$R\delta_4$										B	b_o	b_m
$R\delta_5$											B	b_o
$R\delta_6$												B

The table is symmetrical about the principal diagonal.

TABLE III

$$\begin{aligned}
 F_{11} &= \frac{1}{2} A + a_m + \frac{1}{2} H + h_m + 2\bar{a}_o + \bar{a}_p \\
 F_{12} &= \frac{1}{2} H + h_m - \frac{1}{2} A - a_m \\
 F_{13} &= (c_o + c_p - c_m) (\bar{e}_o + \bar{e}_p - \bar{e}_m) \\
 F_{22} &= \frac{1}{2} A + a_m + \frac{1}{2} H + h_m - 2\bar{a}_o - \bar{a}_p \\
 F_{23} &= (c_o + c_p - c_m) (\bar{e}_o - \bar{e}_p - \bar{e}_m) \\
 F_{33} &= B + 2b_m - 2b_o - b_p
 \end{aligned}$$

TABLE IV

$$\begin{aligned}
 F_{11} &= \frac{1}{2} (A - a_m + H - h_m - 2\bar{a}_o + 2\bar{a}_p) \\
 F_{12} &= \frac{1}{2} (H - h_m - A + a_m) \\
 F_{13} &= \frac{1}{2} \times 3^{\frac{1}{2}} (\bar{e}_o + c_o - \bar{e}_p + c_p) \\
 F_{22} &= \frac{1}{2} (A - a_m + H - h_m + 2\bar{a}_o - 2\bar{a}_p) \\
 F_{23} &= \frac{1}{2} \times 3^{\frac{1}{2}} (\bar{e}_o - c_o - \bar{e}_p + c_p) \\
 F_{33} &= B - b_o - b_m + b_p
 \end{aligned}$$

The following assumptions are made in order to simplify the above matrix elements:—

(1) The forces involved in the distortion of the benzene ring are essentially the same in mesitylene as in benzene. Thus F_{33} of species A_2'' equals to Miller and Crawfords' β and that of E'' to their θ . (2) The interaction between a CH_3 motion out of the plane and a non-planar ring deformation is equal to the interaction between a hydrogen motion out of the plane and a non-planar ring deformation, or in other words $\bar{c}_o = c_o$, $\bar{c}_m = c_m$, and $\bar{c}_p = c_p$. With the latter assumption F_{23} of species A_2'' and F_{13} of species E'' are equal to Miller and Crawfords' (1946) η and ω respectively. F_{13} of species A_2'' and F_{23} of E'' are zero. These assumptions were also made by Ferguson to determine the force constants for 1, 3, 5 trifluoro benzene. Thus the constants A , a_m , η , β , θ and ω are carried over to this problem from benzene.

K.E. Matrix

The elements of the K.E. matrices are calculated by the method adopted by Wilson (1939). The vector expressions are obtained considering a unit vector perpendicular to the equilibrium plane of the molecule. These expressions are given in Table V.

TABLE V

$$\begin{aligned} s_{K\delta_1}^I &= \frac{2V}{3}, & s_{K\delta_1}^J &= -\frac{4V}{3}, & s_{K\delta_1}^K &= \frac{4V}{3}, & s_{K\delta_1}^L &= -\frac{2V}{3} \\ s_{r\gamma_{1,3,5}}^H &= V, & s_{r\gamma_{2,4,6}}^{\text{CH}_3} &= V, & s_{r\gamma_1}^{C_1} &= -V(1+2\rho_{\text{CH}_3}), & s_{r\gamma_1}^{C_2} &= s_{r\gamma_1}^{C_6} = \rho_H V \end{aligned}$$

Where V is unit vector perpendicular to the equilibrium plane of I , J , K (Fig. 1). The remaining expressions can be similarly written down.

With the help of these expressions, the matrix elements are derived. Tables VI and VII represent the G matrix elements for the species A_2'' and E'' respectively.

TABLE VI

$$\begin{aligned} G_{11} &= \frac{1}{2}(\mu_{\text{CH}_3} + \mu_H) + (\mu_C)[1 + 4(\rho_H - \rho_{\text{CH}_3})^2] \\ G_{12} &= \frac{1}{2}(\mu_{\text{CH}_3} - \mu_H) + 2\mu_C(\rho_{\text{CH}_3} - \rho_H)[1 + 2(\rho_H + \rho_{\text{CH}_3})] \\ G_{13} &= 8 \times 3^{\frac{1}{2}} \mu_C(\rho_H - \rho_{\text{CH}_3}) \\ G_{22} &= \frac{1}{2}(\mu_{\text{CH}_3} + \mu_H) + \mu_C(1 + 2\rho_{\text{CH}_3} + 2\rho_H)^2 \\ G_{23} &= -4 \times 3^{\frac{1}{2}} \mu_C(2\rho_{\text{CH}_3} + 2\rho_H + 1) \\ G_{33} &= 48\mu_C \end{aligned}$$

TABLE VII

$$\begin{aligned} G_{11} &= \frac{1}{2}[\mu_H + \mu_{\text{CH}_3} + \mu_C \{ (2\rho_{\text{CH}_3} + \rho_H + 1)^2 + (2\rho_H + \rho_{\text{CH}_3} + 1)^2 \}] \\ G_{12} &= \frac{1}{2}[\mu_{\text{CH}_3} - \mu_H + \mu_C(5\rho_{\text{CH}_3}^2 + 4\rho_{\text{CH}_3} - 5\rho_H^2 - 4\rho_H)] \\ G_{13} &= 2\mu_C(3\rho_{\text{CH}_3} + 3\rho_H + 2) \\ G_{22} &= \frac{1}{2}[\mu_{\text{CH}_3} + \mu_H + \mu_C \{ (1 + 2\rho_{\text{CH}_3} - \rho_H)^2 + (1 + 2\rho_H - \rho_{\text{CH}_3})^2 \}] \\ G_{23} &= 6\mu_C(\rho_{\text{CH}_3} - \rho_H) \\ G_{33} &= 16\mu_C \end{aligned}$$

where μ 's are reciprocal atomic masses in atomic weight units.

$$\rho_H = \text{C—H/C—C} \text{ and } \rho_{\text{CH}_3} = \text{C}_{\text{arom}}\text{—C}_{\text{aliph.}}/\text{C—C}.$$

DETERMINATION OF THE FORCE CONSTANTS

With the help of the above assumptions the F matrix of species A_2'' will involve only two unknown combinations of valence force constants, $\frac{1}{2}H+h_m$ and $2\bar{a}_o+\bar{a}_p$ and that of E'' will involve another two combinations $H-h_m$ and $2\bar{a}_o-2\bar{a}_p$. To determine these four combinations, only four frequencies, two of species A_2'' and two of E'' are required. The remaining fundamental for each species is then calculated. From the four combinations, the individual values of H , h_m , \bar{a}_o and \bar{a}_p are obtained.

Vibrations of species A_2''

Two of the fundamentals 690 cm.^{-1} and 840 cm.^{-1} are very definitely assigned, but the lowest infra-red active fundamental 182 cm.^{-1} is assigned by Pitzer and Scott on the basis of the product rule. Miller and Crawford's first set of constants for β and η of benzene led to imaginary force constants. The second set gave two sets of values for $\frac{1}{2}H+h_m$ and $2\bar{a}_o+\bar{a}_p$ because of the quadratic nature of the secular equation and they are given below.

	$\frac{1}{2}H+h_m$	$2\bar{a}_o+\bar{a}_p$
Set 1	0.340918	0.850213
Set 2	0.297849	0.03602

The calculations are repeated with both the sets to obtain the value of the third fundamental. With the first set a value so high as 1286 cm.^{-1} and with the second set, 179 cm.^{-1} which is in very close agreement with 182 cm.^{-1} is obtained. The first set of the constants is discarded, confirming the assignment of 182 cm.^{-1} as the third A_2'' fundamental, made by Pitzer and Scott.

Vibrations of species E''

Two of the fundamentals of species E'' , namely, 275 cm.^{-1} and 847 cm.^{-1} with Miller and Crawford's first set of constants for θ and ω have once again led to the imaginary values for the combinations $H-h_m$ and $2\bar{a}_o-2\bar{a}_p$. The second set of constants result in two sets of values as shown in the following table.

	$H-h_m$	$2\bar{a}_o-2\bar{a}_p$
Set 1	0.32016	-0.460656
Set 2	0.275677	-0.190547

With the first set of the above force constants a value 771 cm.^{-1} and with the second set a value 561 cm.^{-1} are obtained as the third fundamental of the E'' species. Neither of the values agrees with the value 439 cm.^{-1} suggested by Pitzer and Scott. A reinvestigation of the infra-red and Raman spectra of this molecule is desirable to establish this fundamental. From a comparison with the frequencies of 1, 3, 5 Trifluoro Benzene, it may be seen that 179 cm.^{-1} of A_2'' and 561 cm.^{-1} of E'' (mesitylene) calculated by the author compare well with the corresponding frequencies 214 cm.^{-1} of A_2'' and 595 cm.^{-1} of E'' (1, 3, 5 trifluoro benzene) observed by Nielsen (1950) and confirmed recently by Ferguson (1953).

In arriving at the individual values of the force constants the combinations which led to the fundamentals 179 cm.^{-1} of A_2'' and 561 cm.^{-1} of E'' are considered. These are given below.

$$\begin{array}{ll}
 \frac{1}{2}H+h_m = 0.297849 & H = 0.382 \\
 H-h_m = 0.275677 & h_m = 0.107 \\
 2\bar{a}_o+\bar{a}_p = 0.03602 & \bar{a}_o = -0.02 \\
 2\bar{a}_o-2\bar{a}_p = -0.190547 & \bar{a}_p = 0.076
 \end{array}$$

The numerical values of the above force constants are to be finally multiplied by 10^5 and expressed in dynes/cm.

DISCUSSION OF THE RESULTS

The diagonal methyl wagging constant H is found to be 0.382 which is slightly greater than that of the corresponding Hydrogen constant $A = 0.378$ in benzene. This may imply that it is energetically more difficult to displace CH_3 group out of the plane than to displace a Hydrogen atom out of the plane of the benzene ring. F_{11} of species A_2'' refers to the dish-like symmetry co-ordinate representing bending of all the H and CH_3 atoms above and below the plane of the ring whereas F_{22} refers to puckered co-ordinate corresponding to a motion where CH_3 's and H's are displaced in the opposite sides of the ring. In case of benzene the energy required for the dish-like distortion must be less than that for the puckered displacement. But in this $F_{11} > F_{22}$. This may be attributed to the repulsive forces being predominant between hydrogen atoms and the CH_3 groups.

The following numerical values are used in the present calculations. $\text{C—C} = 1.39 \text{ \AA}$, $\text{C—H} = 1.08 \text{ \AA}$, $\text{C}_{\text{arom}}\text{—C}_{\text{aliph}} = 1.54 \text{ \AA}$, $\mu_{\text{H}} = 0.99206$, $\mu_{\text{C}} = 0.08326$, $\mu_{\text{CH}_3} = 0.066516$, $\rho_{\text{H}} = 0.7770$, $\rho_{\text{CH}_3} = 1.10791$.

ACKNOWLEDGEMENTS

The author wishes to acknowledge her deep indebtedness to Prof. K. R. Rao for his kind interest and valuable guidance during the course of this work. The author takes this opportunity to express her grateful thanks to Mr. D. Premaswarup for his kind help in the calculation of the vector expressions and to the Government of India for awarding a Senior Research Fellowship.

SUMMARY

Wilson's F - G matrix method has been applied to the non-polar vibrations of 1, 3, 5 trimethyl benzene to determine the out-of-plane valence force constants. The value 182 cm.^{-1} assigned by Pitzer and Scott as the lowest A_2'' fundamental is confirmed from the present calculations. The assignment of 439 cm.^{-1} as one of the E'' fundamental appears doubtful, the calculated value being 561 cm.^{-1} .

REFERENCES

- Ferguson, Eldon (1953). Normal co-ordinate analysis for the non-planar vibrations of 1, 3, 5 trifluoro benzene. *J. Chem. Phys.*, **21**, 886
 Miller, F. A. and Crawford (Jr.) B. L. (1946). The non-planar vibrations of Benzene. *Ibid.*, **14**, 282.
 Nielsen, J. Rud. (1950). Ching-Yu Liang and Smith, D. Infra-red and Raman spectra of 1, 3, 5 Trifluoro Benzene. *Disc. of Faraday Soc.*, **9**, 177.
 Pitzer, Kenneth S. and Scott, W. (1943). The thermodynamics and molecular structure of benzene and its methyl derivatives. *J. Amer. Chem. Soc.*, **65**, 803.
 Santhamma, V. (1954). Force constants for the BF_3 molecule. *Proc. Nat. Inst. Sci. Ind.*, **20**, 245-51.
 Wilson, Bright (Jr.) (1939). A method of obtaining the expanded secular equation for the vibrational frequencies of a molecule. *J. Chem. Phys.*, **7**, 1047.

ON A GENERATING FUNCTION IN PARTITION THEORY

by HANSRAJ GUPTA, *F.N.I., Panjab University College, Hoshiarpur*

(Received June 7; read August 6, 1954)

1. In this note, we shall be concerned with the partial fractions of

$$f(x, r) = r! / (1-x)(1-x^2)(1-x^3) \dots (1-x^r); \quad |x| < 1.$$

This function is of importance in the Theory of Partitions. In fact, it is well known that

$$\frac{1}{r!} f(x, r) = \sum_{n=0}^{\infty} p(n, r) x^n, \quad \dots \dots \dots (1)$$

where $p(n, r)$ denotes for $n > 0$, the number of partitions of n into at the most r summands and $p(0, r) = 1$.

2. Let

$$f(x, r) = \sum_{j=0}^r A_j(r) \cdot (1-x)^{j-r};$$

so that

$$y^r f(1-y, r) = \sum_{j=0}^r A_j(r) y^j, \quad 0 < y < 2. \quad \dots \dots \dots (2)$$

Then, since

$$f(x, r) = \frac{r}{1-x} f(x, r-1),$$

we must have

$$\{1 - (1-y)^r\} f(1-y, r) = r f(1-y, r-1);$$

or

$$\frac{1}{r} \left\{ \sum_{i=1}^r (-1)^{i-1} \binom{r}{i} y^{i-1} \right\} \cdot \sum_{j=0}^r A_j(r) \cdot y^j = \sum_{j=0}^r A_j(r-1) \cdot y^j. \quad \dots \dots \dots (3)$$

Comparing the coefficients of the powers of y on the two sides of (3), we readily obtain

$$\binom{r}{1} A_j(r) - \binom{r}{2} A_{j-1}(r) + \binom{r}{3} A_{j-2}(r) - \dots + (-1)^j \binom{r}{j+1} A_0(r) = r A_j(r-1). \quad (4)$$

Hence

$$A_j(r) = \sum_{k=2}^r \frac{1}{k} \left\{ \binom{k}{2} A_{j-1}(k) - \binom{k}{3} A_{j-2}(k) + \dots + (-1)^{j+1} \binom{k}{j+1} A_0(k) \right\}, \quad (5)$$

with $A_0(r) = 1$.

Eliminating $q_{i-1}(j), q_{i-2}(j), \dots, q_0(j)$ from these relations, we get

$$q_i(j) = t_{i+2}(j) - \binom{i+1}{1} t_{i+1}(j) + \binom{i+1}{2} t_i(j) - \dots + (-1)^i \binom{i+1}{i} t_2(j). \quad \dots \quad (8)$$

Also comparing the coefficients of k^{2j-1} on the two sides of (7), we get

$$\begin{aligned} q_{2j-2}(j) &= \frac{2j-1}{2} q_{2j-4}(j-1) = \frac{(2j-1)(2j-3) \dots (1)}{2^j} \\ &= \frac{(2j)!}{4^j j!}, \quad \dots \quad \dots \quad \dots \quad \dots \quad \dots \quad \dots \quad \dots \quad (9) \end{aligned}$$

since $q_0(1) = \frac{1}{2}.$

3. The following tables give $A_j(r)$ for values of $j \leq 5$. These give also values of $A_j(r)$ for $2 \leq r \leq 12$.

TABLE I

j	$A_j(r)$
0	1.
1	$\frac{1}{2} \binom{r}{2}.$
2	$\frac{3}{4} \binom{r}{4} + \frac{2}{3} \binom{r}{3} + \frac{1}{4} \binom{r}{2}.$
3	$\frac{15}{8} \binom{r}{6} + \frac{10}{3} \binom{r}{5} + \frac{9}{4} \binom{r}{4} + \frac{2}{3} \binom{r}{3} + \frac{1}{8} \binom{r}{2}.$
4	$\frac{105}{16} \binom{r}{8} + \frac{35}{2} \binom{r}{7} + \frac{2665}{144} \binom{r}{6} + \frac{49}{5} \binom{r}{5} + \frac{45}{16} \binom{r}{4} + \frac{4}{9} \binom{r}{3} + \frac{1}{16} \binom{r}{2}.$
5	$\frac{945}{32} \binom{r}{10} + 105 \binom{r}{9} + \frac{11095}{72} \binom{r}{8} + \frac{602}{5} \binom{r}{7} + \frac{7805}{144} \binom{r}{6} + \frac{1289}{90} \binom{r}{5}$ $+ \frac{9}{4} \binom{r}{4} + \frac{2}{9} \binom{r}{3} + \frac{1}{32} \binom{r}{2}.$

TABLE II

$\begin{matrix} j \rightarrow \\ r \downarrow \end{matrix}$	0	1	2	3	4	5
2	1	1/2	1/4	1/8	1/16	1/32
3	1	3/2	17/12	25/24	91/144	91/288
4	1	3	59/12	17/3	715/144	479/144
5	1	5	155/12	45/2	20831/720	20237/720
6	1	15/2	85/3	425/6	31037/240	85823/480
7	1	21/2	329/6	1127/6	112357/240	85225/96
8	1	14	581/6	875/2	344897/240	18039/5
9	1	18	319/2	1843/2	929377/240	149845/12
10	1	45/2	995/4	14335/8	1127777/120	9108953/240
11	1	55/2	1485/4	26125/8	1256431/60	24887203/240
12	1	33	6413/12	33847/6	3911809/90	9333863/36

4. Some asymptotic Results.

From (9) it readily follows that for any fixed j and a sufficiently large r ,

$$A_j(r) \sim \frac{r^{(2j)}}{4^j \cdot j!}, \text{ where } r^{(k)} = r(r-1)(r-2) \dots (r-k+1). \quad \dots \quad (10)$$

Expanding (2) by the binomial theorem, we have for any fixed r and a sufficiently large n ,

$$r! p(n, r) \sim \sum_{j=0}^{r-1} A_j(r) \binom{n+r-j-1}{r-j-1}. \quad \dots \quad (11)$$

Writing C_{r-j-1} for $\binom{n+r-j-1}{r-j-1}$,

and $\widehat{\exp} \left(\frac{r^2}{4x} \right)$ for $1 + \frac{r^{(2)}}{4 \cdot 1! x} + \frac{r^{(4)}}{4^2 \cdot 2! x^2} + \frac{r^{(6)}}{4^3 \cdot 3! x^3} + \dots$

where the symbol $\widehat{\exp}$ indicates that the indices of the powers of r in the expansion of $\exp \left(\frac{r^2}{4x} \right)$ are to be enclosed within brackets, we can say that $r! p(n, r)$ is asymptotically equal to the term independent of x in

$$\{ C_{r-1} + C_{r-2}x + C_{r-3}x^2 + \dots \} \widehat{\exp} \left(\frac{r^2}{4x} \right) \quad \dots \quad (12)$$

These results compare favourably with those given by me earlier.

REFERENCES

- H. Gupta (1942). On an Asymptotic Formula in Partitions. *Proc. Indian Acad. Sci.*, **16**, 101-102.
 --- (1943). On the Maximum values of $p_k(n)$ and $\pi_k(n)$. *Jour. Indian Math. Soc.*, **7**, 72-75.
 --- (1946). An Asymptotic Formula in Partitions. *Jour. Indian Math. Soc.*, **10**, 73-76.
 --- (1942). An Inequality in Partitions. *Jour. Bombay Univ.*, **11**/3, 16-18.

Issued November 17, 1954.

THERMAL CONDUCTIVITY OF ARGON-NEON MIXTURE

by B. N. SRIVASTAVA,* *F.N.I.*, and M. P. MADAN, *Department of Physics,
University of Lucknow*

(Received April 10; read May 7, 1954)

I. INTRODUCTION

Gas analysis based on the thermal conductivity of gases was suggested by Daynes and Shakespear (1920), Daynes (1933) and suitable katharometers were constructed by them and by Ibbs and Hirst (1929), Trenner (1937), Archer (1938), Grew (1941) and others but the apparatus has so far been used more or less in an empirical way and calibration curves have been given in terms of galvanometer deflections against concentration. The disadvantages of this procedure are obvious. Ibbs and Hirst have tried to determine the conductivity of any gas or mixture of gases by reference to such an empirical curve and utilizing the experimentally determined values of thermal conductivity of any known gaseous mixture. The assumptions made by them that the apparatus will give the same reading for all gases or mixtures having the same thermal conductivity is not however sufficiently exact on account of the different accommodation coefficients and the unequal wall effects for different gases. As the katharometer is a very useful and inexpensive instrument for gas analysis, we attempt here to develop in the following pages a suitable design of the instrument from which accurate values of thermal conductivity can be readily obtained for any gas or mixture of gases.

A comprehensive account of the methods which have been employed in the past for the measurement of thermal conductivity of gases has been given by Gregory and Archer (1926), Trautz and Zundel (1931), and Bosworth (1952), and a short account of modern methods has been given by Keyes (1949). Nearly all precise thermal conductivity measurements on gases have been made with some form of the hot wire method. In this a metal wire which is heated by an electric current is mounted axially in a vertical glass or metal tube, immersed in a constant temperature bath. The wire remains at a uniform temperature along a central portion which will be relatively greater the longer the wire and the smaller its diameter. The lateral heat transfer through the gas is radial only for a limited central portion of the tube and the principal correction to be applied is for the heat conducted longitudinally by the wire. This difficulty has been met by applying three different types of procedure. In the first due to Schleiermacher, Weber (1917), Taylor and Johnston (1946) and others, a long thin wire is used and the resistance of the central portion of the wire which is at a uniform temperature is measured by attaching two very fine potential leads to the wire. In this potential lead method the end conduction is thus reduced to a very small correction of the order of 1%, but a very small and not accurately calculable lead wire correction is introduced. In the second method given by Goldschmidt, Gregory and Archer (1926), Dickins (1934) and others two tubes are employed, one long and the other short, usually called compensating cells. The differential measurements then refer to the central portion of the longer tube, where radial flow conditions hold. In this the end conduction cancels out but the difficulty of having exactly identical and inconveniently long columns is a great drawback. In the third type usually

* Present address:—Indian Association for the Cultivation of Science, Jadavpur, Calcutta.

called the thick wire cell method developed by Kannuliik and Martin (1933), Kannuliik and Carman (1952), the end effect is very large but is corrected almost exactly by a rigorous application of the theory with the help of relatively simple boundary conditions.

In the present series of investigations we have adopted the third method with the modification that a much thinner wire is used so that the end conduction is minimized. The detailed theory as developed by Kannuliik and Martin (1934) will still give the various corrections exactly and in particular the end correction and the correction for the curvature of lines of flow at the ends of the wire. Thus a simple apparatus has been developed to give relative conductivities of gases and gas mixtures readily, using an improved form of balance bridge method as adopted by Grew (1941).

2. METHOD AND THEORY

The general theory of the distribution of temperature along the axially mounted wire was given by Kannuliik and Martin (1933, 1934) which as applied to our case may be briefly stated as follows:

Let us assume that the ends of the wire are held at the same steady temperature as the walls of the tube and this temperature is taken as an arbitrary zero. Neglecting convection and radiation for the present, the differential equation for the steady flow of heat is

$$\pi r_1^2 \lambda \frac{d^2 \theta}{dz^2} + 2\pi r_1 K_u \left(\frac{d\theta}{dr} \right)_{r=r_1} + \frac{I^2 \rho_0 (1 + \alpha \theta)}{J} = 0, \quad \dots \quad (1)$$

where λ and K_u are respectively the thermal conductivities of the wire and the gas in calories/cm. sec. deg., ρ_0 the resistance per unit length of the wire at 0°C ., α the mean temperature coefficient of resistance of the wire between 0°C . and θ° and r_1 the radius of the wire. The radial flow of heat is

$$2\pi r_1 K_u \left(\frac{d\theta}{dr} \right)_{r=r_1} = - \frac{2\pi K_u \theta}{\log_e r_2/r_1} = -2\pi r_1 h \theta \text{ (say)}, \quad \dots \quad (2)$$

where r_2 is the internal radius of the tube. Equation (1) then becomes

$$\pi r_1^2 \lambda \frac{d^2 \theta}{dz^2} - 2\pi r_1 h \theta + I^2 \rho_0 (1 + \alpha \theta)/J = 0. \quad \dots \quad (3)$$

For the case when the cell is highly evacuated the second term in eq. (3) is to represent the loss by radiation from the wire, h denoting the loss of heat per unit area per unit difference of temperature.

Writing eq. (3) in the form

$$d^2 \theta / dz^2 = P^2 \theta - Q,$$

where

$$\left. \begin{aligned} P^2 &= 2h/r_1 \lambda - I^2 \rho_0 \alpha / \pi r_1^2 \lambda J, \\ \text{and} \quad Q &= I^2 \rho_0 / \pi r_1^2 \lambda J, \end{aligned} \right\} \quad \dots \quad (4)$$

assuming P to be positive, we get as solution

$$\theta = Q/P^2 + A \sinh z + B \cosh z. \quad \dots \quad (5)$$

The constants A and B are determined from the boundary conditions $\theta = 0$ at $x = \pm l$, $2l$ being the length of the wire. Eq. (5) then yields

$$\theta = \frac{Q}{P^2} \left[1 - \frac{\cosh Pz}{\cosh Pl} \right]. \quad \dots \quad (6)$$

The resistance R of the wire under present conditions of heating is given by

$$R = \int_{-l}^{+l} (1 + \alpha\theta) dz. \quad \dots \dots \dots (7)$$

Substituting the value of θ from (6) and integrating for z from $-l$ to $+l$ we obtain

$$\frac{R - R_0}{R_0} = \frac{Q\alpha}{P} \left[1 - \frac{\tanh Pl}{Pl} \right], \quad \dots \dots \dots (8)$$

where

$$R_0 = 2\rho_0 l.$$

This equation can be written in the form

$$\left(\frac{1}{Pl} \right)^2 \left(1 - \frac{\tanh Pl}{Pl} \right) = \frac{2\pi r_1^2 \lambda J (R - R_0)}{R_0^2 I^2 \alpha l}. \quad \dots \dots \dots (9)$$

Substituting the experimentally determined values of R , R_0 , α and λ , the value of the L.H. side of eq. (9) is known and hence the conductivity K_* of the gas found from eqs. (4) and (2).

To determine λ the experiment is performed in perfect vacuum. The solution is again given by (9). Calculation shows that for the small current and thin wire used in the experiments P^2 is positive and therefore eq. (9) cannot be further simplified as done by Kannuliuk. Hence eq. (9) was used to determine λ .

Eq. (9) has been obtained above on the assumption that the flow of heat through the gas is strictly radial. Actually, however, the lines of heat flow show some curvature at the ends of the tube. Under these conditions the exact solution of eq. (1) has been given by Kannuliuk and Martin (1934), who show that the error due to this correction is less than 1%. Convection is eliminated by working at sufficiently low pressures when the observed conductivity becomes independent of the pressure.

3. DESCRIPTION OF THE APPARATUS

The apparatus consists of (i) the conductivity cell, (ii) the electrical bridge, (iii) the thermostatic bath, (iv) the gas mixing apparatus and (v) the pressure regulation unit.

The conductivity cell forms part of the thermal conductivity analyser, originally intended for measurements of gaseous separation in the thermal diffusion experiments and is based on an analyser described by Grew (1941), and depicted in Fig. 1. A very thin metallic wire was welded to short platinum wires which were then sealed in a uniform capillary tubing. A 4-mm. side tube led to the bulb L of about 14 c.c. capacity and the mercury reservoir R , the pressure being measured by the mercury manometer M . The assembly was suitably mounted on a wooden stand and immersed in thermostat containing paraffin oil and fitted with a glass side to enable readings to be taken from outside. Efficient stirring and mercury toluene regulator enable the bath temperature to be kept constant, which was recorded on a Hartmann-Braun NiCr-Ni thermocouple.

The cell wire forms one arm of a Wheatstone bridge and a thicker wire (compensating resistance) made of the same material forms the second arm, the remaining two arms consisted of two equal eureka resistances, all being immersed in the bath. The temperature and therefore resistance of the cell wire depends on the conductivity of the gas surrounding it and on the current flowing through it. Its resistance was measured at the bath temperature and the compensating resistance so adjusted that when the bridge is balanced, the cell wire is about 20°C. above the bath

temperature. As the compensating resistance was made of the same material as the cell wire, but relatively many times thicker so that its resistance may be practically independent of the bridge current, the fluctuations in the temperature of the bath do not affect the bridge balance. To ensure this the compensating coil was mounted as near the conductivity cell as possible.

In operation the conductivity apparatus is completely evacuated by an oil diffusion pump and a small amount of the desired gas or gas mixture of known composition prepared with the aid of a gas mixing system, is introduced by turning slowly the stopcock *S* (Fig. 1). The gas so introduced into the system is then com-

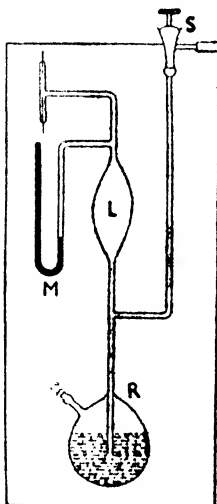


Fig. 1

pressed to the desired pressure below 20 cm. with the help of a pressure regulation unit attached to the reservoir *R*, which consisted of a manometer, an air-chamber and a mechanical pump capable of creating a rough vacuum. The current is then adjusted approximately to balance the bridge and sufficient time allowed for the temperature of the cell wire and surrounding bath liquid to attain steady state. The current is then exactly adjusted for the balance and is measured across a standard 1 ohm.

4. EXPERIMENTAL PROCEDURE AND CORRECTIONS

The geometrical constants of the apparatus, namely the length and the diameter of the wire and the internal and external radii of the tube, were first accurately determined. Then the tube was highly evacuated and different currents passed through it and *R* measured for each current by the potentiometer method, and extrapolated to zero current.

The temperature coefficient of resistance was determined by placing the cell in a constant temperature bath, filling it with hydrogen at low pressures and sending a very small heating current through the wire and then measuring the resistance by the potentiometer method. This resistance was measured for various very small heating currents and graphically extrapolated for zero current. In this way *R* is determined at different temperatures giving α . This value of α was substituted in (9) and the observations already obtained for the evacuated cell giving *R* for different *I*'s, were utilized to determine λ . h was calculated by assuming 0.032 as

the emissivity of aged tungsten at the experimental temperature. By substituting the value of h in (4) and utilizing (9), six values of λ were calculated for the different currents and the mean taken.

Next the experimental gas, single or mixed in known proportions was introduced into the cell, and confined at a suitable pressure below 20 cm. of mercury and the bridge balanced by sending the proper current. For this balance the resistance of the cell will be equal to the resistance of the compensating coil at the temperature of the bath, which is known from the previous calibration. This value of R , along with the value of R_0 , α and λ is substituted in eq. (9) to give P from which h and K_u are calculated with the help of eq. (4). This value of K_u has to be corrected for radiation. For a single heating current observations are taken at various gas pressures.

This value of K_u requires to be further corrected for the temperature gradient across the wall, for the accommodation coefficient (or the temperature jump effect) at the surfaces of the wire and the tube, and for the curvature of the lines of heat flow near the ends.

The wall effect is corrected for by treating the present case as a conduction through composite cylinders of gas and glass. We have for the heat transmission

$$\frac{2\pi K_u'(\theta_1 - \theta_w)}{\log_e r_2/r_1} = \frac{2\pi K_g \theta_w}{\log_e r_3/r_2}, \quad \dots \quad (10)$$

where θ_1 is the excess temperature of the wire over that of the bath, θ_w the difference in temperature between inner and outer walls of the tube, r_3 is the external radius of the tube and K_g the conductivity of the glass tube.

$$\therefore \theta_w = (K_u'/K_g) [(\log_e r_3/r_2)/(\log_e r_2/r_1)] (\theta_1 - \theta_w) \quad \dots \quad (11)$$

and in place of the second term in eq. (1), we have

$$\frac{2\pi K_u'}{\log_e(r_2/r_1)} (\theta - \theta_w) = \frac{2\pi K_u'}{\log_e r_2/r_1} \theta \left(1 - \frac{K_u'}{K_g} \frac{\log_e r_3/r_2}{\log_e r_2/r_1} \right), \quad \dots \quad (12)$$

and hence on taking the wall correction, h in eq. (3) must be replaced by h' where

$$h' = \frac{K_u'}{r_1 \log_e r_2/r_1} \left(1 - \frac{K_u'}{K_g} \frac{\log_e r_3/r_2}{\log_e r_2/r_1} \right). \quad \dots \quad (13)$$

Thus knowing K_g , K_u' (corrected for wall effect) can be determined.

The correction for the temperature jump at the wire and the tube surfaces has been fully discussed by Gregory and Archer (1926) and Taylor and Johnston (1946). It has been shown by them that

$$\frac{1}{K_a} = \frac{1}{K} + \frac{1}{p \log_e r_2/r_1} \left[\frac{g_1}{K_1 r_1} + \frac{g_2}{K_2 r_2} \right], \quad \dots \quad (14)$$

where K_a is the apparent conductivity, K the conductivity corrected for temperature jump effect, K_1 , K_2 the gas conductivities at the temperatures of the wire and the tube surface; and g_1 , g_2 depend upon the accommodation coefficient at the surface of the wire and of the tube. Thus by plotting $1/K_a$ against $1/p$, the true conductivity can be determined from the intercept.

Kannuliuk and Martin (1934) have discussed the effect of slight displacement δ of the wire from the axis of the tube and have shown that

$$K = K_u \left[1 - \frac{\delta^2/(r_2^2 - r_1^2)}{\log_e r_2/r_1} \right] = K_u(1 - C), \quad \dots \quad (15)$$

where K_u is the uncorrected conductivity, and C is independent of the gas. By working with a gas whose conductivity is known, the constant C for the cell is determined once for all and the apparatus can then be used for finding the conductivity of any gas or gaseous mixture.

5. EXPERIMENTAL RESULTS

The experimental procedure has already been explained in detail in § 4. The constants of the cell are given in Table I.

TABLE I

Constants of the Cell

Length of the cell wire	=	8.343 cm.
Radius of the cell wire	=	0.001867 cm.
External radius of the tube	=	0.313 cm.
Internal radius of the tube	=	0.088 cm.
		α	=	20.92×10^{-4}
Mean	..	λ	=	0.094 cal./cm. sec. deg.
Resistance of the wire at the temperature of the bath (35°C.)	=	7.510 ohms.

The resistance of the compensating arm and the combined resistance of the equal arms, when measured at the temperature of the bath, were found to be 7.788 ohm and 21.32 ohm. From the value of α and the resistance of the compensating arm, it was calculated that the bridge would be balanced at a temperature difference of 17.7°C., half of which when added to the bath temperature may be taken as the temperature to which conductivity measurements refer, i.e. 43.8°C.

The argon and neon gases used for the conductivity measurements were supplied by the British Oxygen Co. both being spectroscopically pure. The thermal conductivity calculated with the help of eqs. (4) and (9), together with the values after applying various corrections, are given in Tables II and III.

TABLE II

Pressure cm.	Current through wire (amps.)	Uncorrected $K_u \times 10^5$ (cal./cm. sec. deg.)	Pressure cm.	Current through wire (amps.)	Uncorrected $K_u \times 10^5$ (cal./cm. sec. deg.)
% A = 0			% A = 24.06		
13.4	0.1349	13.88	8.5	0.12133	11.19
12.1	0.1351	13.92	10.2	0.12145	11.20
12.3	0.1352	13.93	13.2	0.12168	11.25
			12.8	0.12140	11.19
% A = 57.4			% A = 79		
6.8	0.10205	7.893	10.4	0.09143	6.325
7.3	0.10210	7.902	13.1	0.09137	6.323
12.8	0.10220	7.918	8.0	0.09131	6.301
8.5	0.10215	7.905			
% A = 100					
7.5	0.08588	5.568			
11.2	0.08606	5.588			
12.3	0.08600	5.576			

Experiments were performed in the pressure range from 2 cm. to 14 cm. and calculation showed that the temperature jump effect vanishes at the higher pressures and convection losses were negligible. Hence only readings at higher pressures are recorded in Table II. The values of the conductivities were reduced to 0°C. by applying the temperature coefficient of conductivity whose value as given by Kannuliik and Martin (1934) for inert gases is 0.003, and are recorded in Table III.

TABLE III
Mean Values

% A	Mean $K_a \times 10^5$	Corrected for wall effect $K_a' \times 10^5$	$K_0 \times 10^5$
0.0	13.910	14.300	12.630
24.06	11.210	11.470	10.130
57.40	7.904	8.026	7.089
79.00	6.316	6.395	5.648
100.00	5.577	5.637	4.979

As already emphasized, the aim of our experiments has been to devise a quick method of obtaining relative values of conductivity of mixtures of different concentrations and not their absolute values. Eq. (15) shows that the absolute value may be less than the observed value on account of the asymmetries in the cell. For this reason the absolute value of neon as determined by Weber was used to determine C and thereby calibrate the cell.

Weber's value was chosen because it agrees well with the theoretically calculated value of conductivity from the 12 : 6 model using the force constants from thermal diffusion and viscosity, as shown in the next section. This value of C was used to correct the observed values at various concentrations and the corrected values are given in Table V. The theoretically calculated values for the conductivity of argon does not agree so well with Weber's value and so argon was not used for calibrating the cell.

6. COMPARISON OF THEORY WITH EXPERIMENT

For the case of a monatomic gas the first approximation to the coefficient of conductivity can be written for the case of inverse power model in the form (Chapman and Cowling, 1939)

$$[K]_1 = \frac{5}{2} [\mu]_1 C_v, \quad \dots \quad (16)$$

where $[\mu]_1$ is the first approximation to the coefficient of viscosity and C_v is the specific heat of the gas at constant volume.

For the case of Lennard-Jones 12 : 6 model, eq. (16) takes the form (Hirschfelder *et al.*, 1954)

$$[K]_1 \times 10^7 = 1989.1 \frac{(T/M)^{\frac{1}{2}}}{r_0^2 W_2^{(2)}}, \quad \dots \quad (17)$$

where K is the thermal conductivity in cal./cm. sec. deg., T the temperature in °K, M the molecular weight, r_0 the collision diameter in Å and $W_2^{(2)}$ the collision integral depending on kT/ϵ .

For the case of binary mixture of two monatomic gases the coefficient of conductivity can be written in the form (Chapman and Cowling, 1939)

$$[K_{\text{mix}}]_1 = \frac{R_1[K_1]_1(x_1/x_2) + R_2[K_2]_1(x_2/x_1) + R'_{12}}{R_1(x_1/x_2) + R_2(x_2/x_1) + R_{12}}, \quad \dots \quad (18)$$

where

$$\begin{aligned} R_{12} &= 3 \left(\frac{M_1 - M_2}{M_1 + M_2} \right)^2 (5 - 4B) + \frac{4M_1 M_2}{(M_1 + M_2)^2} A (11 - 4B) + \frac{2F^2}{[K_1]_1 [K_2]_1} \\ R'_{12} &= 2F \{ F/[K_1]_1 + F/[K_2]_1 + (11 - 4B - 8A) M_1 M_2 / (M_1 + M_2)^2 \} \\ R_1 &= F [6 \{ M_2 / (M_1 + M_2) \}^2 + \{ M_1 / (M_1 + M_2) \}^2 (5 - 4B) \\ &\quad + 8M_1 M_2 A / (M_1 + M_2)^2] / [K_1]_1 \end{aligned}$$

and a similar expression for R_2 .

F is connected with the coefficient of diffusion by the relation

$$F = \frac{5}{2} p [D_{12}]_1 / T. \quad \dots \quad (19)$$

The constants A and B depend upon the law of molecular interaction and have been tabulated by Hirschfelder *et al.* (1948) for the 12 : 6 model. For the purpose of calculation eq. (18) has been written in a more convenient form by Hirschfelder *et al.* (1954).

It is convenient to define a quantity by the relation

$$[K_{12}]_1 \times 10^7 = 1989 \cdot 1 \frac{[T(M_1 + M_2)/2M_1 M_2]^{1/2}}{r_{12}^2 (\text{\AA}) W^{(2)}(2; kT/\epsilon_{12})}; \quad \dots \quad (20)$$

then in terms of this quantity and the thermal conductivities of the pure components, the thermal conductivity of a mixture of monatomic gases may be written as

$$\frac{1}{[K_{\text{mix}}]_1} = \frac{X_\lambda + Y_\lambda}{1 + Z_\lambda}, \quad \dots \quad (21)$$

where

$$\begin{aligned} X_\lambda &= x_1^2/[K_1]_1 + 2x_1 x_2/[K_{12}]_1 + x_2^2/[K_2]_2 \\ Y_\lambda &= x_1^2 U^{(1)}/[K_1]_1 + 2x_1 x_2 U^{(Y)}/[K_{12}]_1 + x_2^2 U^{(2)}/[K_2]_1 \\ Z_\lambda &= x_1^2 U^{(1)} + 2x_1 x_2 U^{(Z)} + x_2^2 U^{(2)} \\ U^{(1)} &= \frac{4}{15} A_{12}^* - \frac{1}{12} \left(\frac{12}{5} B_{12}^* + 1 \right) \frac{M_1}{M_2} + \frac{1}{2} \frac{(M_1 - M_2)^2}{M_1 M_2} \\ U^{(2)} &= \frac{4}{15} A_{12}^* - \frac{1}{12} \left(\frac{12}{5} B_{12}^* + 1 \right) \frac{M_2}{M_1} + \frac{1}{2} \frac{(M_2 - M_1)^2}{M_1 M_2} \\ U^{(Y)} &= \frac{4}{15} A_{12}^* \left[\frac{(M_1 + M_2)^2}{4M_1 M_2} \right] \frac{[K_{12}]_1^2}{[K_1]_1 [K_2]_1} - \frac{1}{12} \left(\frac{12}{5} B_{12}^* + 1 \right) \\ &\quad - \frac{5}{32 A_{12}^*} \left(\frac{12}{5} B_{12}^* - 5 \right) \frac{(M_1 - M_2)^2}{M_1 M_2} \\ U^{(Z)} &= \frac{4}{15} A_{12}^* \left[\frac{(M_1 + M_2)^2}{4M_1 M_2} \left(\frac{[K_{12}]_1}{[K_1]_1} + \frac{[K_{12}]_1}{[K_2]_1} \right) - 1 \right] \\ &\quad - \frac{1}{12} \left(\frac{12}{5} B_{12}^* + 1 \right) \end{aligned}$$

and M_1 , M_2 are the molecular weights of species 1 and 2, x_1 , x_2 the mole fractions of species 1 and 2 and $A^* = A/0.4$ and $B^* = B/0.6$, the constants A and B being the same as those in eq. (18).

Using eqs. (17), (18) and (21) we have calculated the values of the coefficient of conductivity of neon-argon mixture at various concentrations. These are given in Table V. The force constants ϵ_{12} , r_{12} , ϵ_{ii} , r_{ii} used in these calculations were those already determined by us at 0°C. from the thermal diffusion data (Srivastava and Madan, 1953 *a* and *b*) of argon and neon-argon mixture. The force constants ϵ and r for pure neon were obtained in a similar way by using the experimental data of Stier (1942). These force constants are listed in Table IV, while the values of the conductivities are given in Table V.

TABLE IV

Argon	Neon	Ne-A.
$\epsilon_1/k = 139^\circ\text{K}$ $r_1 = 3.358\text{\AA}$	$\epsilon_2/k = 44.79^\circ\text{K}$ $r_2 = 2.733\text{\AA}$	$\epsilon_{12}/k = 56.92^\circ\text{K}$ $r_{12} = 3.17\text{\AA}$

TABLE V

K_0 (Weber: listed by Chapman and Cowling, 1939) = 1087×10^{-7} cal./cm. sec. deg.

% A	$K_0 \times 10^7$ in cal. cm. ⁻¹ sec. ⁻¹ deg. ⁻¹			K_0/K_0 (exp.)		
	Present exp.	12 : 6 model	Inverse power model	Present exp.	12 : 6 model	Inverse power model
0.0	1087	1092	1087	1	1.005	1
24.06	871.6	881	780.2	0.8017	0.8106	0.7194
57.4	610.3	640.4	502	0.5614	0.5892	0.4618
79.0	486.3	507.5	432	0.4473	0.4669	0.3975
100	428.7	389.8	392.2	0.3944	0.3587	0.3608

The values of the coefficient of conductivity for the inverse power model are given in column 4 of Table V. They were calculated by using eq. (18). The value of r_{12} , the force index for unlike molecules was taken from thermal diffusion data (Chapman and Cowling, 1939) as 7.9 for neon-argon mixture. As experimental measurements on inter-diffusion are not available, the value of the factor F was determined by using the calculated value of D_{12} for this mixture as 0.265 at 0°C. (Madan, 1953).

As already explained, the neon values of Weber were taken to be correct and ratios to this were found for the conductivity of other mixtures calculated theoretically or obtained experimentally. The ratios thus obtained are also given in Table V and plotted in figure 2. It is seen from the figure that the agreement is very good indeed, the deviation being less than 3% for the different concentration ratios. The experimental errors in these ratios due mainly to error in the determination of α and in measuring the change in resistances will be about $\pm 2\%$. The experimentally determined ratio for pure argon differs by about 10% and is probably due to some experimental error, which however could not be checked due to some accident to the apparatus.

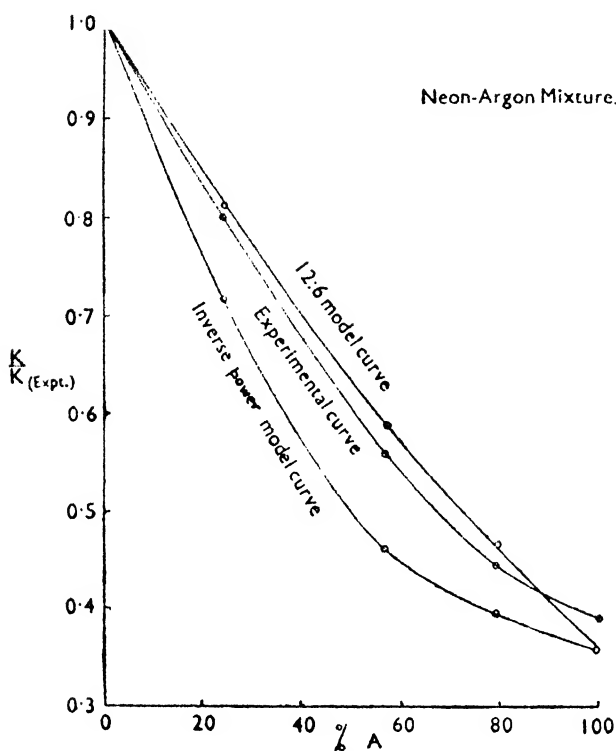


FIG. 2

Table V and figure 2, show that the 12 : 6 model is more in accord with the experimental values than the inverse power model. This has also been shown by Hirschfelder for He-A mixture. Improvements in the design of the cell are being undertaken after which a whole programme of determining conductivity of different mixtures will be taken up.

We are indebted to Prof. J. O. Hirschfelder for his kindness in communicating to us certain portions of his book 'Molecular Theory of Gases and Liquids' in advance of publication. We express our gratitude to Prof. M. R. Nayar of the Chemistry Department for many helpful suggestions and to Prof. P. N. Sharma for affording the laboratory facilities. Thanks are also due to Mr. F. Kiss, Chief Glass Technologist, National Physical Laboratory of India, for the construction of the glass apparatus used in these investigations. We also record our thanks to the Government of Uttar Pradesh for the award of a research grant.

SUMMARY

A gas analysis apparatus based on the thermal conductivity of gas mixtures has been constructed using a hot-wire cell. A rigorous mathematical theory has been applied to calculate the various corrections and yield the value of the thermal conductivity in terms of the conveniently observed quantities. The measurements have been made for argon-neon mixtures of various concentrations and the experimentally determined thermal conductivities for each concentration tabulated. The results are compared with the theory of the thermal conductivity of binary mixtures using the Lennard-Jones 12 : 6 model and the inverse power model, utilizing the known force constants. The results show a satisfactory agreement with the 12 : 6 model but not with the inverse power model.

REFERENCES

- Archer, C. T. (1938). Thermal Conduction in hydrogen-deuterium mixture. *Proc. Roy. Soc.*, A 165, 474.
- Bosworth, R. C. L. (1952). Heat Transfer Phenomena. John Wiley & Sons, INC., New York.
- Chapman, S. and Cowling, T. G. (1939). The Mathematical theory of Non-uniform gases, Cambridge University Press.
- Daynes, H. A. and Shakespear, G. A. (1920). The Theory of Katharometer. *Proc. Roy. Soc.*, A 97, 273.
- Daynes, H. A. (1933). Gas Analysis by measurement of Thermal Conductance, Cambridge University Press.
- Dickins, B. G. (1934). The effect of accommodation on heat conduction through gases. *Proc. Roy. Soc.*, A 143, 517.
- Grew, K. E. (1941). Thermal diffusion in Hydrogen-Deuterium mixtures. *Ibid.*, A 178, 390.
- Gregory, H. S. and Archer, C. T. (1926). Experimental Determination of the Thermal Conductivities of gases. *Ibid.*, A 110, 91.
- Hirschfelder, J. O., Bird, R. and Spotz, E. L. (1948). The Transport Properties for nonpolar gases. *J. Chem. Phys.*, 16, 968.
- Hirschfelder, J. O., Curtiss, C. F., and Bird, R. B. (1954). Molecular Theory of Gases and Liquids.
- Ibbs, T. L. and Hirst, A. A. (1929). Thermal Conductivity of gas mixtures. *Proc. Roy. Soc.*, A 123, 134.
- Kannuluik, W. G. and Martin, L. H. (1933). Conductivity of heat in Powders. *Proc. Roy. Soc.*, A 141, 144.
- (1934). Thermal Conductivity of some gases at 0°C. *Ibid.*, A 144, 496.
- Kannuluik, W. G. and Carman, E. H. (1952). The Thermal Conductivity of rare gases. *Proc. Phys. Soc. (Lond.)*, 65, 701.
- Keyes, F. G. (1949). Measurement of heat conductivity of Nitrogen-carbon dioxide mixtures. *Trans. Amer. Soc. Mech. Engrs.*, 71, 966-7.
- Madan, M. P. (1953). Transport properties of some gas mixtures. *Proc. Nat. Inst. Sci. India*, 19, 713.
- Srivastava, B. N. and Madan, M. P. (1953a). Intermolecular force constants from Thermal diffusion and other properties of gases. *J. Chem. Phys.*, 21, 807.
- (1953b). Thermal diffusion of gas mixtures and force between unlike molecules. *Proc. Phys. Soc. (Lond.)*, A 66, 278.
- Stier, L. (1942). The Coefficients of Thermal diffusion of Neon and their variation with temperature. *Phys. Rev.*, 62, 548.
- Taylor, W. J. and Johnston, H. L. (1946). An improved hot-wire cell for Thermal Conductivity measurements. *J. Chem. Phys.*, 14, 219.
- Trautz, M. and Zundel, A. (1931). *Zeits. f. tech. Physik*, 12, 273.
- Trenner, Nelson R. (1937). A Thermal Conductivity Method for the determination of Isotopic exchanges in simpler gaseous molecules. *J. Chem. Phys.*, 5, 382.
- Weber, S. (1917). The heat conductivity of gas mixtures. *Ann. d. physik*, 54, 325.

Issued November 19, 1954.

LIGHT SCATTERING FROM GEL-FORMING SYSTEMS DURING AND AFTER SETTING

PART I. ALUMINIUM MOLYBDATE AND THORIUM ARSENATE GELS: INTENSITY MEASUREMENTS

by R. L. DESAI and V. SUNDARAM, *The Institute of Science, Bombay*

(Communicated by K. R. Dixit, F.N.I.)

(Received February 2 ; read May 7, 1954)

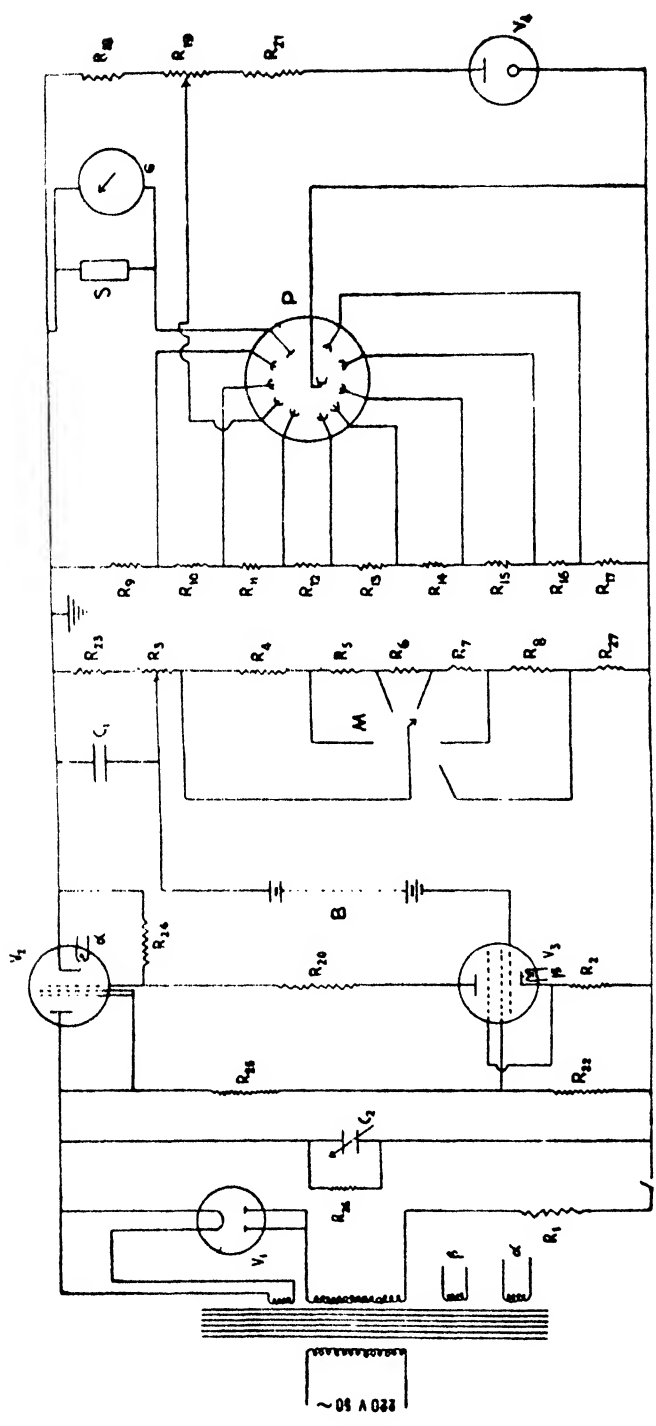
The study of the distribution of intensity of light scattered at different angles gives an idea of the size and shape of particles in solution or in suspension. The theoretical calculations of Mie (1908), Shoulejkin (1924), Blumer (1925, 1926), and Krishnan (1934) have shown that the ratio of the intensity of light scattered at an angle in the forward direction to that scattered at an angle in the backward direction situated symmetrically about the transverse direction is unity for small particles and that this ratio increases with an increase in the size of the particles. Recently, Doty and Steiner (1950) have given a Table showing the variation in the values of the ratio $I_{45^\circ}/I_{135^\circ}$ with particle size when the shape of the particles is similar to that of either rods or spheres or coils. So far the intensity of light scattered in the transverse direction only has been studied during the setting of several gel-forming systems (cf. Mardles, 1923; Krishnamurti, 1929, 1930; Ramaiah, 1937; Prasad and Guruswamy, 1944; Prasad and Doss, 1949; Desai and Sundaram, 1953; Desai, 1953). The total intensity of light scattered by 1 cm. layer of several gel-forming systems has been measured by Katti (1948, 1949, 1953). However, no work has been reported on the measurement of the angular variation of the intensity of light scattered from gel-forming systems. The present investigation deals with the measurement of the intensity of light scattered at 45° (forward), 90° (transverse) and 135° (backward) to the direction of the incident light from gel-forming systems of aluminium molybdate and thorium arsenate during their setting. The depolarization factors of the transversely scattered light have also been determined for one concentration of each of these gels in order to study the density and anisotropy scattering during their gelation.

EXPERIMENTAL

A. Preparation of the gel-forming systems:—

(i) *Aluminium molybdate gels.*—These gels were prepared by the method used by Desai (1952). Varying amounts of 20% solution of aluminium nitrate (A_1) and 10% solution of potassium molybdate (B_1) were mixed and the total volume (T.V.) was made to 50 c.c. in all cases by the addition of the requisite amount of distilled water. The turbid gel-forming mixture obtained immediately on mixing the two solutions was shaken till it became clear and the test-tube containing the clear liquid was transferred immediately to the observation bath for scattering measurements.

(ii) *Thorium arsenate gels.*—These were prepared by the method of Prakash and Dhar (1929). Varying amounts of 6% solution of thorium nitrate (A_2) and 10% solution of potassium arsenate (B_2) were mixed and the total volume (T.V.)



Circuit diagram of apparatus used for intensity measurements

- | | | |
|--------------------------------|---|---------------------------------|
| B — 90 V dry battery pack | R_3-R_8 — 10,000 ohms wire wound | R_{21} — 30,000 ohms, 5 watts |
| C_1 — 0.01 μF | R_9-R_{17} — 10,000 ohms | R_{22} — 50,000 ohms |
| C_2 — 2.0 μF | R_{18} — 20,000 ohms, 2 watts | R_{23} — 140,000 ohms |
| G — 'spot' galvanometer | R_{19} — 20,000 ohms, 2 watts, variable | R_{24} — 250,000 ohms |
| P — photomultiplier RCA 931A | R_1 — 1,500 ohms | R_{25} — 500,000 ohms |
| M — manual control | R_2 — 6,000 ohms wire wound | R_{26} — 1 megohm |
| S — shunt | R_{20} — 25,000 ohms | R_{27} — 1 megohm wire wound |

was made to 48 c.c in all cases by adding the necessary amount of distilled water. The clear mixture was taken in a test-tube which was immediately placed in the observation bath for scattering measurements.

B. Measurement of the depolarization factors:—

The depolarization factors of the transversely scattered light were measured by Cornu's method taking all the necessary precautions.

C. Measurement of intensity of light scattering:—

The intensity of scattered light was measured by a photoelectric method using a photomultiplier. The apparatus consists of two parts, viz. (i) the power supply unit and (ii) the photomultiplier unit.

The power supply unit was built up using the circuit suggested by Zimm (1948). A detailed description of the circuit has been given by Zimm and only the circuit diagram is given here (cf. Plate XXII) for reference. The unit was adjusted to supply a steady current of two milliamperes at 600 volts.

The photomultiplier unit was based on the circuit given by Muller, Garmon and Droz in their book 'Experimental Electronics' (p. 76), and the circuit diagram is given in Plate XXII. The photomultiplier unit was built up on a small metal chassis which was properly earthed. The photomultiplier tube RCA 931A was placed in a metal cover mounted on the chassis. The metal cover had an extended side tube of metal through which the scattered light could enter and fall perpendicularly on the sensitive vane of the photomultiplier.

The test-tube containing the gel-forming mixture was placed in the centre of a beaker containing water at 30°C. which was used as the observation bath. The beaker was painted black on the outside and a black paper was wrapped round it. There were two slits on the paper diametrically opposite each other, which served as the entrance and the exit of the incident light. On one side of the beaker, slits were made corresponding to the angles of scattering studied. Care was taken to see that there was no black paint on the beaker at the places corresponding to these slits. All the slits were 6 mm. \times 6 mm. A slit of the same size was attached to the side tube of the metal cover of the photomultiplier tube.

A parallel beam of light, obtained by placing a lens at a suitable distance from a 400 watts mercury vapour lamp, was passed through the test-tube containing the gel-forming mixture. The photomultiplier unit was placed in front of a slit on the beaker in such a way that only the light scattered at a particular angle fell perpendicularly on the sensitive vane of the photomultiplier tube. The current generated was measured by a 'Spot galvanometer' manufactured by the Cambridge Instrument Company Ltd. The sensitivity of the galvanometer was 110 divisions per microampere, each division on the galvanometer being equivalent to 1.6 mm. Since the intensities of light scattered at different angles by different gels were not the same, suitable shunt resistances were used in each case.

Care was taken to see that the track of incident light was exactly horizontal. It was ascertained that the deflections on the galvanometer were due entirely to the scattered light falling on the photomultiplier and all stray light was eliminated by using suitable screens. The distance between the photomultiplier and the centre of the test-tube was kept the same and constant at all the angles of scattering. The solutions used for preparing the gel-forming mixtures were made dust-free by repeated filtration through sintered glass filters.

RESULTS

Since different shunt resistances were used in each case, from the readings obtained have been calculated the deflections which would have been observed if

no shunt resistances were used with the galvanometer. The deflections thus calculated have been plotted against the time (in minutes) elapsed from the moment the test-tube containing the gel-forming system was placed in the observation bath and the graphs obtained are shown in Figs. 1 to 6. From these graphs the values of intensity at definite intervals of time have been interpolated and the values are given in Tables I to VI, in which t represents the time interval in minutes, I_{45° , I_{90° and I_{135° represent the intensity of the light scattered at 45° , 90° and 135° , respectively, and T denotes the time of setting of the gel as determined by Fleming's method, that is, the time interval at which the gel-forming mixture just ceases to flow even when the test-tube is inverted. The other notations used, namely, A_1 , A_2 , B_1 , B_2 and T.V. have already been mentioned in the experimental section.

TABLE I

Intensity measurements

Aluminium molybdate gels $A_1 = 21.0$ c.c. $B_1 = 20.0$ c.c.T.V. = 50.0 c.c. $T = 58' 50''$

t in minutes	I_{45°	I_{90°	I_{135°	$I_{45^\circ}/I_{135^\circ}$
5	2.0	2.0	2.0	1.00
10	3.0	3.0	3.0	1.00
15	5.0	4.0	4.5	1.11
20	8.0	6.0	6.0	1.33
25	15.0	11.5	11.0	1.36
30	26.5	19.5	18.0	1.47
40	86.0	44.5	44.0	1.95
50	143.0	76.0	73.5	1.95
60	186.5	95.0	88.5	2.11
70	205.0	103.5	95.5	2.15
80	220.0	108.5	99.0	2.22

TABLE II

Intensity measurements

Aluminium molybdate gels $A_1 = 25.0$ c.c. $B_1 = 20.0$ c.c.T.V. = 50.0 c.c. $T = 66' 45''$

t in minutes	I_{45°	I_{90°	I_{135°	$I_{45^\circ}/I_{135^\circ}$
5	1.0	1.0	1.0	1.00
10	2.0	2.0	2.0	1.00
15	3.0	3.0	3.0	1.00
20	5.0	4.0	4.0	1.25
25	8.5	6.0	6.5	1.31
30	16.0	9.5	11.0	1.45
40	50.0	26.5	28.5	1.75
50	104.5	57.0	57.0	1.83
60	153.0	81.5	78.0	1.96
70	183.0	93.0	87.5	2.09
80	202.0	97.0	91.0	2.22

TABLE III

Intensity measurements

Aluminium molybdate gels $A_1 = 25.0$ c.c. $B_1 = 24.0$ c.c.T.V. = 50.0 c.c. $T_1 = 51' 40''$

t in minutes	I_{45°	I_{90°	I_{135°	$I_{45^\circ}/I_{135^\circ}$
5	4.0	4.0	4.0	1.00
10	4.5	4.5	4.5	1.00
15	8.0	7.0	6.0	1.33
20	12.5	10.5	10.0	1.25
25	25.0	19.5	19.5	1.28
30	50.0	34.0	33.5	1.49
40	135.0	69.5	68.0	1.99
50	183.5	95.0	90.0	2.04
60	204.0	109.0	98.5	2.07
70	219.0	116.0	102.0	2.15
80	230.0	120.0	104.0	2.21

TABLE IV

Intensity measurements

Thorium arsenate gels $A_2 = 36.8$ c.c. $B_2 = 4.8$ c.c.T.V. = 48.0 c.c. $T = 70' 50''$

t in minutes	I_{45°	I_{90°	I_{135°	$I_{45^\circ}/I_{135^\circ}$
5	2.0	0.8	1.0	2.00
10	4.0	1.8	2.0	2.00
15	9.0	4.5	4.0	2.25
20	18.0	8.3	7.3	2.47
25	32.0	12.3	10.8	2.96
30	50.5	16.0	13.8	3.66
40	76.5	20.8	18.0	4.25
50	90.0	23.3	21.0	4.29
60	98.5	25.0	22.0	4.48
70	104.5	26.5	22.5	4.64

TABLE V

Intensity measurements

Thorium arsenate gels $A_2 = 40.0$ c.c. $B_2 = 4.8$ c.c.T.V. = 48.0 c.c. $T = 55' 30''$

t in minutes	I_{45°	I_{90°	I_{135°	$I_{45^\circ}/I_{135^\circ}$
5	1.0	0.8	0.8	1.25
10	1.5	1.0	1.3	1.15
15	3.0	2.3	2.3	1.30
20	9.0	4.5	5.0	1.80
25	20.5	7.8	7.5	2.73
30	30.0	10.5	10.0	3.00
40	45.0	12.8	12.8	3.52
50	55.0	14.8	13.8	3.99
60	62.0	16.3	14.8	4.19
70	66.5	17.5	15.5	4.29

TABLE VI

Intensity measurements

Thorium arsenate gels $A_2 = 40.0$ c.c. $B_2 = 6.4$ c.c.T.V. = 48.0 c.c. $T = 45' 15''$

t in minutes	I_{45°	I_{90°	I_{135°	$I_{45^\circ}/I_{135^\circ}$
5	14.5	11.3	11.0	1.32
10	30.5	18.8	17.5	1.74
15	54.0	25.0	23.0	2.35
20	83.0	30.5	28.0	2.96
25	112.0	35.3	32.3	3.47
30	141.5	39.5	36.0	3.93
40	189.0	45.5	41.8	4.52
50	217.5	49.3	45.8	4.75
60	237.0	51.8	48.5	4.89
70	250.5	53.5	50.3	4.98

The results obtained on the measurement of the depolarization factors of the light transversely scattered are given in Tables VII and VIII, in which ρ_u , ρ_v and ρ_h represent the depolarization factors of the transversely scattered light when the incident light is unpolarized, vertically polarized and horizontally polarized, respectively.

TABLE VII

Depolarization measurements

Aluminium molybdate gels $A_1 = 21.0$ c.c. $B_1 = 20.0$ c.c.T.V. = 50.0 c.c. $T = 58' 50''$

t in minutes	ρ_u (%)	ρ_v (%)	ρ_h (%)
1	0.4	..	88.5
3	..	0.2	86.9
5	0.6	0.2	..
7	..	0.3	85.3
10	1.3	0.5	81.1
15	2.0
20	2.6	1.0	63.3
25	3.1	1.1	..
30	3.8	1.2	..
40	..	1.3	61.0
50	5.8	1.8	59.9
60	6.5	2.5	..
70	7.2	2.5	..
80	7.2	2.5	59.9

TABLE VIII

Depolarization measurements

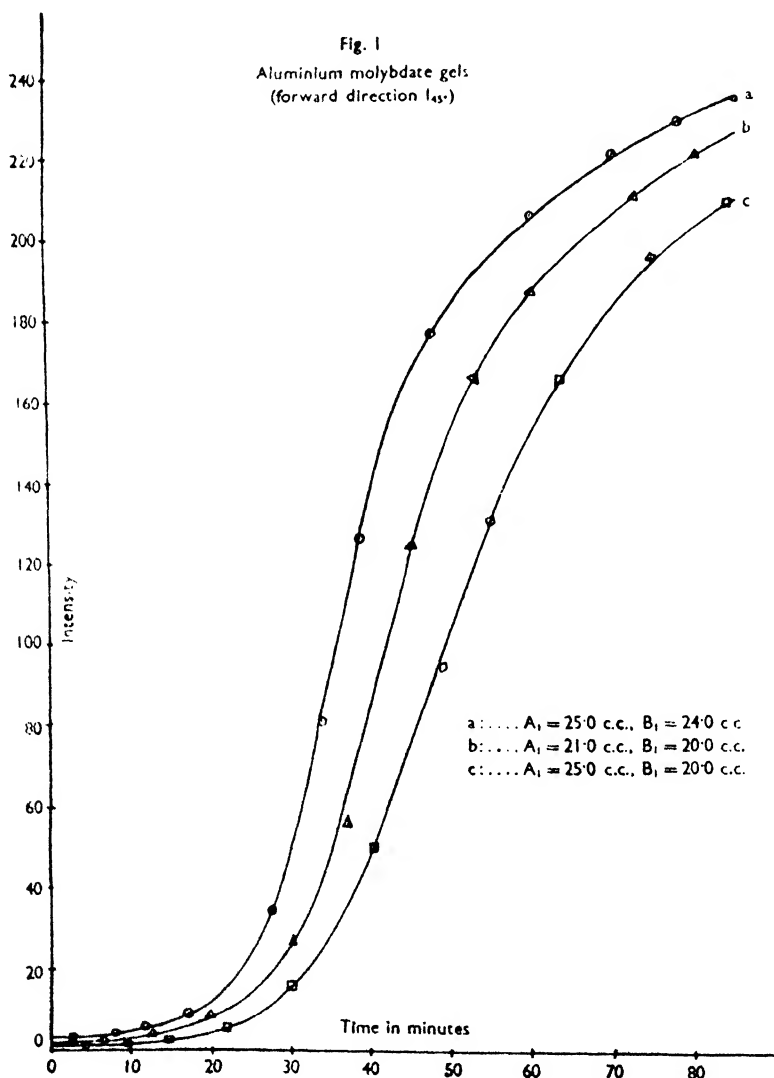
Thorium arsenate gels $A_2 = 40.0$ c.c. $B_2 = 6.4$ c.c.T.V. = 48.0 c.c. $T = 45' 15''$

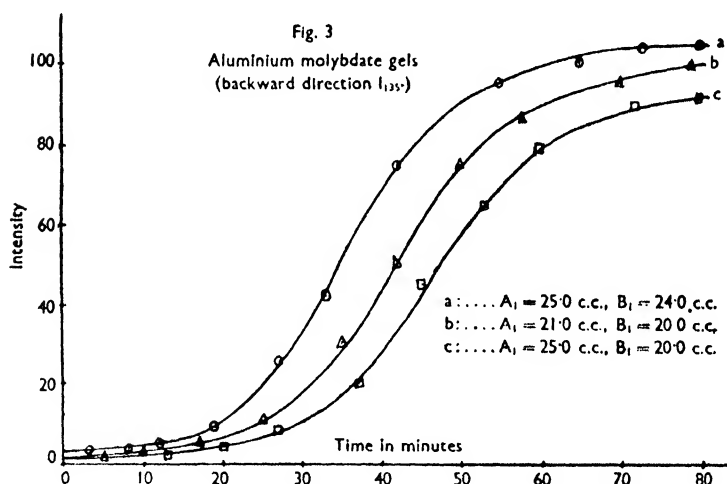
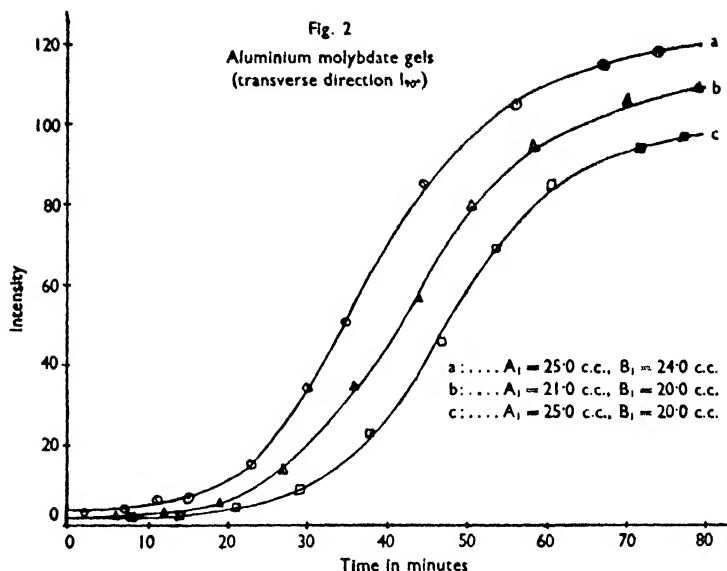
t in minutes	ρ_u (%)	ρ_v (%)	ρ_h (%)
1	4.1	..	91.6
3	4.3	2.1	..
5	4.0	2.2	..
10	5.1	2.2	89.0
15	..	2.5	82.5
20	6.7	2.7	78.3
25	7.2	..	70.4
30	7.7	3.0	..
40	..	3.1	65.6
50	8.2	3.3	62.1
60	8.8	3.4	..
70	8.8	3.4	59.8

DISCUSSION OF RESULTS

It is seen from Tables I to VI and Figs. 1 to 6 that, in both aluminium molybdate and thorium arsenate gels, the intensity of light scattered at any angle is initially small and that the intensity increases at first slowly and then rapidly and finally attains an almost constant value. From this it can be inferred that the particles increase in size and/or number during gelation. The results also show that the increase in intensity, that is, the increase in the size and/or number of the particles, continues even after the systems have ceased to flow (i.e. the time of setting of the gel).

The intensity of the transversely scattered light, I_{90° , can be split up into I_D , the density scattering resulting from the local inhomogeneities produced due to the thermal agitation of the particles in the medium, and I_A , the anisotropy scattering

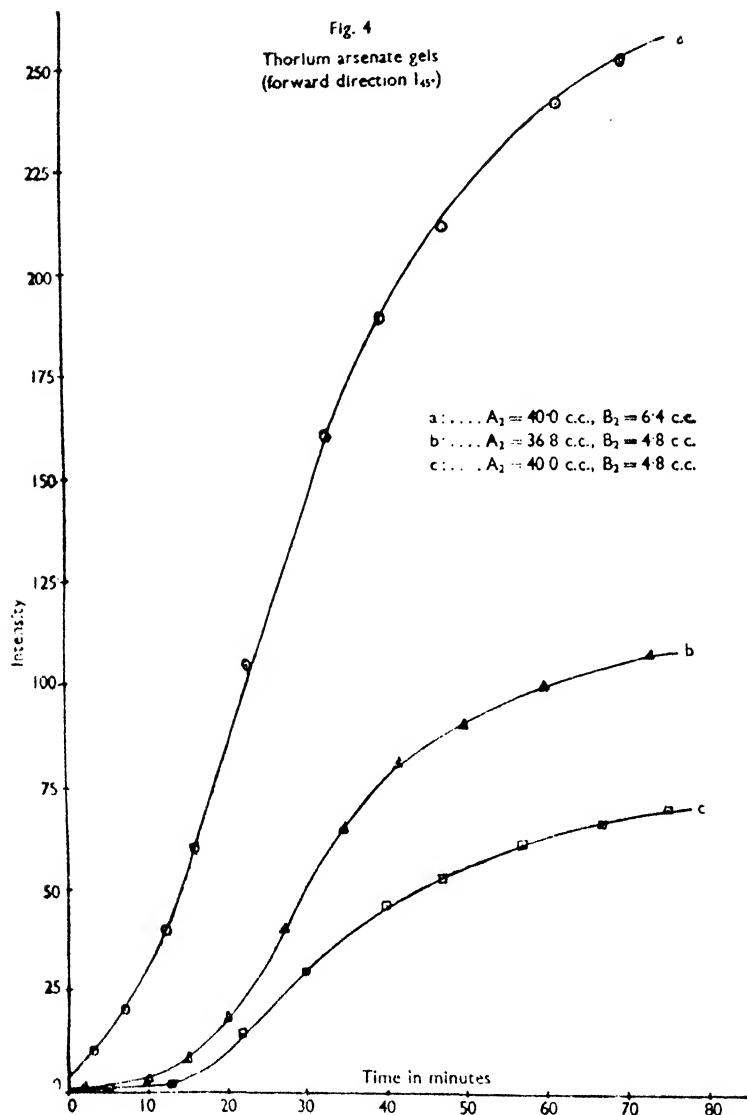




arising from the fact that the moment induced by an electric vector is not, in general, parallel to the direction of the incident electric vector, using the relations (cf. Ramanathan, 1923; Zimm, Stein and Doty, 1945),

$$I_D = I_{90^\circ} \times \frac{6-7\rho_u}{6+6\rho_u}; \quad I_A = I_{90^\circ} - I_D.$$

Recently, Zimm, Stein and Doty (1945) have pointed out that the above relations are valid only when the particle size is small and the value of ρ_u is due to the anisotropy of the particles only, and that, whenever the value of ρ_u is partly due to the appreciable size of the particles, the value of ρ_u in the above relations should be substituted by that of the factor $\frac{2\rho_v}{1+\rho_v}$ which represents, to a first approximation,



the part of ρ_u value due to the anisotropy of the particles. In the present case, the low values of ρ_h (cf. Tables VII and VIII) indicate that in both gels the particle size becomes appreciable in the later stages of gelation and hence the values of I_D and I_A have been calculated using the factor $\frac{2\rho_v}{1+\rho_v}$ instead of the value of ρ_u in the

above relations. The values of I_D and I_A thus separated are given in columns 6 and 7, respectively, of Tables IX and X. It can be seen from these tables that the values of both I_D and I_A increase during gelation indicating that the particles increase in size and anisotropy as gelation proceeds. It is also seen that the density scattering predominates over anisotropy scattering throughout the process of gelation.

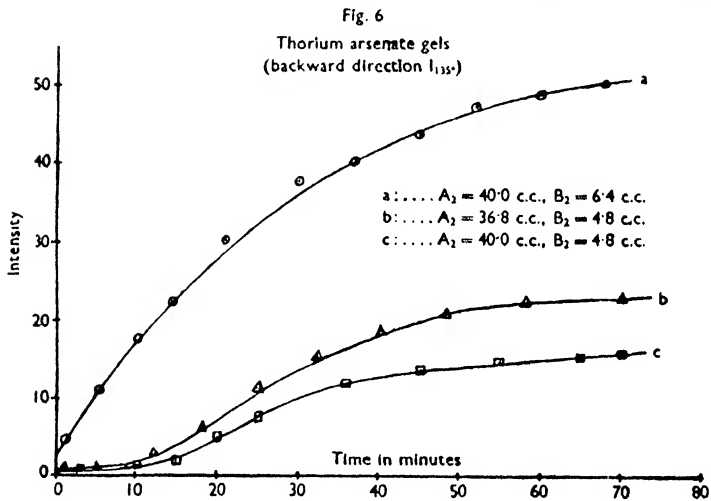
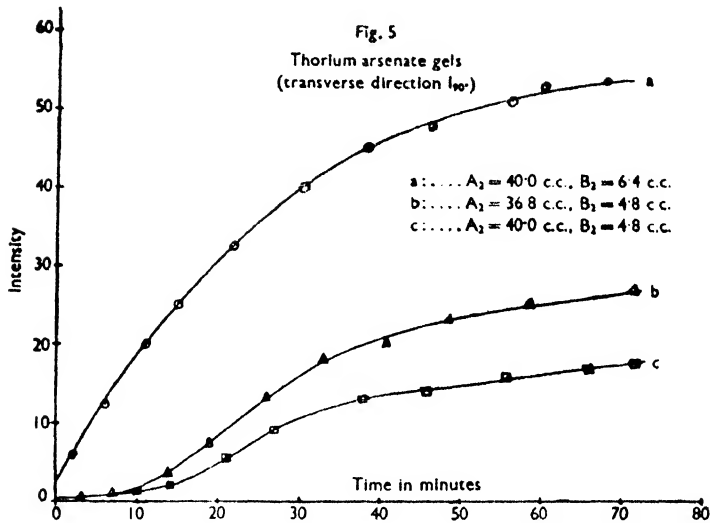


TABLE IX

Values of I_D and I_A of the light transversely scattered during the setting of aluminium molybdate gels

$A_1 = 21.0$ c.c.; $B_1 = 20.0$ c.c. (cf. Tables I and VII)

t in minutes	ρ_v (%)	$\rho = \frac{2\rho_v}{1+\rho_v}$	$\frac{6-7\rho}{6+6\rho}$	I_{90°	$I_D = I_{90^\circ} \times \frac{6-7\rho}{6+6\rho}$	I_A
5	0.2	0.004	0.99	2.0	1.98	0.02
10	0.5	0.010	0.98	3.0	2.94	0.06
20	1.0	0.020	0.96	6.0	5.76	0.24
30	1.2	0.024	0.95	19.5	18.52	0.98
40	1.3	0.026	0.94	44.5	41.83	2.67
50	1.8	0.035	0.93	76.0	70.68	5.32
60	2.5	0.049	0.90	95.0	85.50	9.50
70	2.5	0.049	0.90	103.5	93.15	10.35
80	2.5	0.049	0.90	108.5	97.65	10.85

TABLE X

Values of I_D and I_A of the light transversely scattered during the setting of thorium arsenate gels

$A_2 = 40.0$ c.c.; $B_2 = 6.4$ c.c. (cf. Tables VI and VIII)

t in minutes	ρ_v (%)	ρ $\frac{2\rho_v}{1+\rho_v}$	$\frac{6}{6+6\rho}$ $\frac{7\rho}{6+6\rho}$	I_{90°	$I_D = I_{90^\circ} \times \frac{6-7\rho}{6+6\rho}$	I_A
5	2.2	0.043	0.91	11.3	10.3	1.0
10	2.2	0.043	0.91	18.8	17.1	1.7
15	2.5	0.049	0.90	25.0	22.5	2.5
20	2.7	0.053	0.89	30.5	27.1	3.4
30	3.0	0.058	0.88	39.5	34.8	4.7
40	3.1	0.060	0.88	45.5	40.0	5.5
50	3.3	0.064	0.87	49.3	42.9	6.4
60	3.4	0.066	0.86	51.8	44.5	7.3
70	3.4	0.066	0.86	53.5	46.0	7.5

The results given in Tables I to VI also show that initially the intensity of the light scattered in the forward direction (45°) is the same as that in the backward direction (135°); however, during gelation, the increase in intensity of light scattered in the forward direction is far greater than that in the backward direction. This statement is clearly brought out by the values of the ratio $I_{45^\circ}/I_{135^\circ}$ given in the last columns of Tables I to VI. The continuous increase in the values of this ratio definitely indicates that the particles increase in size during gelation.

It has been pointed out by Oster (1950) that, in a system containing large independent particles, with increase in particle size the values of the ratio $I_{45^\circ}/I_{135^\circ}$ approach the limiting values of 2.44 in the case of rod-shaped particles and 5.98 in the case of disc-shaped particles, whereas in the case of spherical particles the value of the ratio increases very rapidly with increase in particle size and the limiting value is very high. In both aluminium molybdate and thorium arsenate gels the particle size is fairly large as can be inferred from the low values of ρ_h (cf. Tables VII and VIII). Although in gel systems the particles cannot be considered to be strictly independent of each other, the fact that the final value of the ratio $I_{45^\circ}/I_{135^\circ}$ is about 2.2 in aluminium molybdate and about 4.6 in thorium arsenate gels indicates that the particles in aluminium molybdate gels are probably rod-shaped while those in thorium arsenate gels are probably disc-shaped.

A comparison of Tables II and V with III and VI, respectively, shows that, in both aluminium molybdate and thorium arsenate gels, an increase in the amount of potassium molybdate or potassium arsenate in the corresponding gel-forming mixture increases the intensity of the light scattered and in the case of thorium arsenate gels the final value of the ratio $I_{45^\circ}/I_{135^\circ}$ is also increased with the increase in the amount of potassium arsenate. On the other hand, a comparison of Tables I and IV with II and V, respectively, shows that an increase in the amount of thorium nitrate or aluminium nitrate in the corresponding gel-forming mixture causes a decrease in the intensity of the light scattered in both thorium arsenate and aluminium molybdate gels and a decrease in the final value of the ratio $I_{45^\circ}/I_{135^\circ}$ in the case of thorium arsenate gels. Since the amount of aluminium nitrate or thorium nitrate, as the case may be, in the gel-forming mixture is always in excess of that required to combine with potassium molybdate or potassium arsenate, it is possible that with an increase in the amount of potassium molybdate or potassium arsenate a larger amount of the gel-forming substance (aluminium molybdate or thorium arsenate) is formed; this increase in the amount of the gel-forming

substance may be resulting in the increase in the number and in the size of the gel-forming particles, as revealed by the increase in the values of the intensity of the light scattered and of the ratio $I_{45^\circ}/I_{135^\circ}$. The reverse effect observed on increasing the amount of aluminium nitrate or thorium nitrate is evidently due to the peptizing action of aluminium or thorium ions.

SUMMARY

The measurement of the intensity of light scattered in different directions during the setting of gel-forming systems of aluminium molybdate and thorium arsenate shows that the size and anisotropy of the particles increase continuously during gelation. The ratio $I_{45^\circ}/I_{135^\circ}$ is found to increase continuously during the process of gelation and it has been inferred from the final values of these ratios that the particles in aluminium molybdate gels are probably rod-shaped while those in thorium arsenate are probably disc-shaped. The ultimate size and number of the particles is found to increase with an increase in the amount of potassium molybdate or potassium arsenate in the corresponding gel-forming mixture while the reverse is observed when the amount of aluminium nitrate or thorium nitrate, as the case may be, is increased.

ACKNOWLEDGEMENTS

The authors desire to express their sincere thanks to Dr. Mata Prasad, D.Sc., F.R.I.C., F.N.I., for valuable suggestions and advice and to Dr. K. R. Dixit, Ph.D., F.N.I., for his keen interest in the work. One of the authors (V. S.) is indebted to the Council of the National Institute of Sciences of India for the award of a Junior Research Fellowship and the other (R. L. D.) to the authorities of the University of Bombay for the award of a Research Studentship.

REFERENCES

- Blumer, H. (1925). Radiation diagrams of small dielectric spheres. *Z. Physik*, **32**, 119-134.
 ——— (1926). Radiation diagram of smaller dielectric globes. *Z. Physik*, **38**, 304-328.
 Desai, R. L. (1952). A note on the preparation of aluminium molybdate gels. *J. Univ. Bombay*, **20**, Pt. 5, 24.
 ——— (1953). Studies on the optical properties of gels. Part IV. Aluminium molybdate gels. *J. Univ. Bombay*, **22**, Pt. 3, 8-14.
 Desai, R. L. and Sundaram, V. (1953). Studies on the optical properties of gels. Part I. Ceric arsenate gels. *J. Univ. Bombay*, **22**, Pt. 3, 24-28.
 Doty, P. and Steiner, R. F. (1950). Light scattering and spectrophotometry of colloidal solutions. *J. Chem. Phys.*, **18**, 1211-1220.
 Katti, P. K. (1948). Studies in colloid optics. Part I. The sol-gel transformation in agar-agar gels. *Proc. Indian Acad. Sci.*, **28A**, 216-235.
 ——— (1949). Studies in colloid optics. Part II. The sol-gel transformation of gelatin gels. *Proc. Indian Acad. Sci.*, **30A**, 35-48.
 ——— (1953). Studies in colloid optics. Part III. Sol-gel transition of some lyophobic gels. *Proc. Indian Acad. Sci.*, **38A**, 148-160.
 Krishnamurti, K. (1929). The scattering of light in colloidal solutions and gels. I. Agar sol and gel. *Proc. Roy. Soc.*, **A122**, 76-103.
 ——— (1930). Scattering of light in protein solutions. I. Gelatin solutions and gels. *Proc. Roy. Soc.*, **A129**, 490-508.
 Krishnan, R. S. (1934). Scattering of light by particles suspended in a medium of higher refractive index. *Proc. Indian Acad. Sci.*, **1A**, 147-155.
 Mardles, E. W. J. (1923). The scattering of light by organosols and gels of cellulose acetate. *Trans. Faraday Soc.*, **18**, 318-326.
 Mie, G. (1908). Optics of turbid media. *Ann. Physik*, **25**, 377-445.
 Oster, G. (1950). Chapter on 'Scattering of visible light and X-rays by solutions of proteins' (pp. 73-84) in Vol. I of 'Progress in Biophysics and Biophysical Chemistry' (Butterworth-Springer Ltd., London), p. 80.
 Prakash, S. and Dhar, N. R. (1929). Preparation of jellies of some inorganic substances. *J. Indian Chem. Soc.*, **6**, 587-598.
 Prasad, M. and Doss, K. D. V. (1949). Scattering of light during the process of gel-formation. *J. Colloid Sci.*, **4**, 349-365.

- Prasad, M. and Guruswamy, S. (1944). Study of the optical properties of gels. Part I. Thorium molybdate gels. Part II. Thorium arsenate gels. Part III. Silicic acid gels. *Proc. Indian Acad. Sci.*, **19A**, 47-65, 66-76, 77-87.
- Ramaiah, K. S. (1937). Colloid optics. II. Scattering of light by silicic acid sols and gels. *Proc. Indian Acad. Sci.*, **5A**, 138-147.
- Ramanathan, K. R. (1923). Electromagnetic theory of the scattering of light in fluids. *Proc. Indian Assoc. Cultivation Sci.*, **8**, 1-22, 181-198.
- Shoulejkin, W. (1924). Scattering of light by very big colloidal particles. *Phil. Mag.*, **48**, 307-320.
- Zimm, B. H. (1948). Apparatus and methods for measurement of the angular variation of light scattering; preliminary results on polystyrene solutions. *J. Chem. Phys.*, **16**, 1099-1116.
- Zimm, B. H., Stein, R. S. and Doty, P. M. (1945). Classical theory of light scattering from solutions. *Polymer Bull.*, **1**, 90-119.

Issued November 20, 1954.

LIGHT SCATTERING FROM GEL-FORMING SYSTEMS DURING AND AFTER SETTING

PART II. SODIUM STEARATE IN OCTYL ALCOHOL AND SODIUM STEARATE IN DECYL ALCOHOL : DEPOLARIZATION MEASUREMENTS

by K. P. BUCH and V. SUNDARAM, *The Institute of Science, Bombay*

(Communicated by K. R. Dixit, F.N.I.)

(Received February 6; read May 7, 1954)

In two recent communications, Sundaram (1953*a*, 1953*b*) has measured the depolarization factors of the light scattered in different directions from gel-forming systems of sodium oleate in xylene and has observed that the particles in a gel-forming system of sodium oleate in a non-polar solvent like xylene increase in size during gelation, thereby confirming the inferences drawn by previous investigators on the cooling curves (Prasad and Hattiangdi, 1945; Adarkar and Hattiangdi, 1945), viscosity (Prasad, Hattiangdi and Vishvanath, 1945; Hattiangdi and Adarkar, 1946) and syneresis (Prasad, Hattiangdi and Mathur, 1945; Prasad and Sundaram, 1951) of these systems. In the present investigation, a systematic study has been made of the depolarization factors of the light scattered in different directions during the cooling of gel-forming systems of sodium stearate in octyl and in decyl alcohols.

EXPERIMENTAL

A. Preparation of the gel-forming systems:---

Gel-forming solutions containing 0.6%, 1.0% and 1.5% of sodium stearate in octyl and in decyl alcohols were prepared in Pyrex glass test-tubes of internal diameter 1.5", adopting the method described by Sundaram (1953*a*). When the temperature of the solution reached 130°C., the test-tube was removed from the oil-bath and transferred to the observation bath for the depolarization measurements.

B. Experimental arrangement and procedure:---

The experimental arrangement and procedure adopted for the depolarization measurements were exactly the same as the one used by Sundaram (1953*b*). All necessary precautions were taken to minimise errors, and the depolarization factors of the light scattered at 45° (forward), 67°, 90°, 112° and 135° to the direction of the incident beam were measured.

C. Measurement of the gelation temperatures:—

The gelation temperature of these gel-forming systems were measured in the usual manner (Sundaram, 1953*a*), using Fleming's method for noting the gelation point.

RESULTS

The values of the depolarization factors of the light scattered in different directions are given in Tables I to VI in which T represents the temperature at which measurements were made, t_g represents the temperature of gelation, C represents the percentage concentration of soap in the system, and ρ_u , ρ_v and ρ_h have their usual significance.

TABLE I
Sodium Stearate in Octyl Alcohol
 $C = 0.6\%$ $t_2 = 40^\circ\text{C}.$

T $^\circ\text{C}.$	Angle of scattering 45°			Angle of scattering 67°			Angle of scattering 90°			Angle of scattering 112°			Angle of scattering 135°		
	ρ_h	ρ_v	ρ_u	ρ_h	ρ_v	ρ_u	ρ_h	ρ_v	ρ_u	ρ_h	ρ_v	ρ_u	ρ_h	ρ_v	ρ_u
120	13.2	10.9	70.4	24.9	13.2	61.0	39.0	11.8	37.5	37.5	14.7	49.0	18.0	..	70.4
110	13.2	10.9	70.4	24.9	13.2	61.0	39.0	11.8	37.5	37.5	14.7	49.0	18.0	11.2	70.4
100	13.2	10.9	70.4	24.9	13.2	61.0	39.0	11.8	37.5	37.5	14.7	49.0	18.0	11.2	70.4
90	13.2	..	70.4	24.9	..	61.0	39.0	11.8	37.5	37.5	14.7	49.0	18.0	11.2	70.4
80	13.2	10.9	70.4	24.9	13.2	61.0	39.0	11.8	37.5	37.5	14.7	49.0	18.0	11.2	70.4
70	13.2	10.9	70.4	..	13.2	61.0	39.0	11.8	37.5	37.5	14.7	49.0	18.0	11.2	70.4
65	24.9	13.2	61.0	39.0	11.8	..	37.5	37.5	14.7	18.0	11.2	70.4
60	13.2	10.9	70.4	24.9	13.2	61.0	..	11.8	37.5	47.2	18.0	7.2	58.9
55	11.8	7.7	63.3	20.8	10.6	50.8	33.3	42.2	..	6.7	..
50	11.8	..	63.3	..	6.7	39.0	39.0	11.8	37.5	16.3	30.7	10.6	9.9	5.8	52.8
45	9.9	..	58.9	17.2	6.7	..	49.0	11.2	32.3	12.2	24.9	6.7	9.9	..	52.8
40	9.9	6.2	58.9	17.2	..	39.0	52.8	9.9	27.3	9.2	24.9	6.7	9.9	..	52.8
35	9.9	6.2	58.9	17.2	6.7	39.0	52.8	9.9	27.3	9.2	24.9	6.7	9.9	5.8	52.8

TABLE II
Sodium Stearate in Octyl Alcohol

$C = 1.0\%$ $t_g = 40^\circ\text{C.}$

T $^\circ\text{C.}$	Angle of scattering 45°			Angle of scattering 67°			Angle of scattering 90°			Angle of scattering 112°			Angle of scattering 135°		
	ρ_h	ρ_v	ρ_u	ρ_h	ρ_v	ρ_u	ρ_h	ρ_v	ρ_u	ρ_h	ρ_v	ρ_u	ρ_h	ρ_v	ρ_u
120	..	14.0	75.6	27.3	15.5	65.6	40.6	12.5	36.1	13.6	28.3	13.2	18.9	13.2	75.6
110	19.8	14.0	75.6	27.3	..	65.6	40.6	12.5	36.1	13.6	28.3	13.2	18.9	13.2	75.6
100	19.8	14.0	75.6	27.3	15.5	65.6	40.6	12.5	36.1	13.6	28.3	..	18.9	13.2	75.6
90	19.8	14.0	75.6	27.3	15.5	65.6	36.1	13.2	18.9	13.2	75.6
80	19.8	14.0	75.6	27.3	15.5	65.6	40.6	12.5	36.1	13.6	28.3	13.2	18.9	13.2	75.6
70	16.3	9.9	67.9	..	15.5	65.6	40.6	12.5	..	13.6	28.3	13.2	18.9	13.2	75.6
65	14.0	..	63.3	13.6	28.3	..	10.6	7.2	72.1
60	14.0	8.2	63.3	17.2	7.2	42.2	40.6	12.5	36.1	13.2	..	7.2	..
55	15.5	45.5	11.8	34.7	13.5	23.8	8.2	9.9	6.2	68.0
50	14.0	8.2	63.3	15.5	5.3	33.3	49.0	9.3	27.3	10.2	21.7	7.2	..	6.2	68.0
45	15.5	5.3	33.3	..	7.7	20.8	6.7
40	14.0	8.2	63.3	..	5.3	33.3	56.8	7.7	20.8	6.7	21.7	6.2	68.0
35	14.0	8.2	63.3	15.5	5.3	33.3	56.8	7.7	20.8	6.7	21.7	7.2	9.9	6.2	68.0

TABLE III

Sodium Stearate in Octyl Alcohol $C = 1.5\%$ $t_g = 63.5^\circ\text{C.}$

T $^\circ\text{C.}$	Angle of scattering 45°				Angle of scattering 67°				Angle of scattering 90°				Angle of scattering 112°				Angle of scattering 135°			
	ρ_h	ρ_l	ρ_u	ρ_v	ρ_h	ρ_l	ρ_u	ρ_v	ρ_h	ρ_l	ρ_u	ρ_v	ρ_h	ρ_l	ρ_u	ρ_v	ρ_h	ρ_l	ρ_u	ρ_v
120	11.8	7.2	65.6	11.2	21.7	49.0	43.8	13.2	37.5	14.1	27.3	13.2	54.8	18.0	14.0	81.0	14.0	14.0	81.0	14.0
110	11.8	7.2	65.6	11.2	21.7	49.0	43.8	13.2	37.5	14.1	27.3	13.2	54.8	18.0	14.0	81.0	14.0	14.0	81.0	14.0
100	11.8	7.2	65.6	11.2	21.7	49.0	43.8	13.2	37.5	14.1	27.3	13.2	54.8	18.0	14.0	81.0	14.0	14.0	81.0	14.0
90	11.8	7.2	65.6	11.2	21.7	49.0	43.8	13.2	37.5	14.1	27.3	13.2	54.8	18.0	14.0	81.0	14.0	14.0	81.0	14.0
80	11.8	7.2	65.6	11.2	21.7	49.0	45.5	11.8	32.3	11.1	27.3	13.2	54.8	18.0	14.0	81.0	14.0	14.0	81.0	14.0
75	11.8	7.2	..	8.8	18.9	45.5	21.7	8.2	39.0	15.5	11.2	72.9	14.0	14.0
70	..	4.5	..	4.9	14.0	34.7	50.9	7.2	23.8	7.7	20.8	7.2	36.1	15.5	11.2	72.9	11.2	11.2	72.9	11.2
65	7.7	4.5	58.9	34.7	54.8	30.7	15.5	11.2	66.5	6.2	6.2	66.5	6.2
60	7.2	3.8	52.8	4.1	..	29.5	23.8	11.2	11.2	63.3	6.2	6.2	63.3	6.2
55	7.2	3.8	52.8	4.1	13.2	29.5	58.9	6.2	15.5	3.8	17.2	4.9	30.7	11.2	11.2	63.3	6.2	6.2	63.3	6.2
50	58.9	6.2	15.5	3.8	17.2	4.9	30.7	11.2	11.2	..	6.2	6.2
40	7.2	3.8	52.8	4.1	13.2	29.5	58.9	6.2	15.5	3.8	17.2	4.9	30.7	11.2	11.2	63.3	6.2	6.2	63.3	6.2
35	7.2	3.8	52.8	4.1	13.2	29.5	58.9	6.2	15.5	3.8	17.2	4.9	30.7	11.2	11.2	63.3	6.2	6.2	63.3	6.2

TABLE IV
Sodium Stearate in Decyl Alcohol
 $C = 0.6\%$ $t_g = 53.0^\circ\text{C}.$

T $^\circ\text{C}.$	Angle of scattering 45°			Angle of scattering 67°			Angle of scattering 90°			Angle of scattering 112°			Angle of scattering 135°		
	ρ_h	ρ_v	ρ_u	ρ_h	ρ_v	ρ_u	ρ_h	ρ_v	$\Delta\rho_u$	ρ_h	ρ_v	ρ_u	ρ_h	ρ_v	ρ_u
120	11.2	6.7	58.9	20.8	9.3	50.9	47.2	11.8	32.3	11.1	22.7	52.8	22.7	..	52.8
110	11.2	6.7	58.9	20.8	9.3	50.9	47.2	11.8	32.3	11.1	22.7	52.8	22.7	10.6	52.8
100	11.2	6.7	58.9	20.8	9.3	50.9	47.2	11.8	32.3	11.1	22.7	52.8	22.7	10.6	52.8
90	11.2	6.7	58.9	20.8	9.3	50.9	47.2	11.8	32.3	11.1	22.7	52.8	22.7	10.6	52.8
80	11.2	6.7	58.9	20.8	9.3	50.9	47.2	11.8	32.3	11.1	..	52.8	..	10.6	52.8
70	11.2	6.7	58.9	20.8	9.3	50.9	47.2	10.6	..	11.1	22.7	..	22.7	10.6	..
65	11.2	6.7	58.9	10.6	28.3	9.1
60	..	4.9	..	16.3	6.2	42.2	47.2	..	28.3	..	18.0	39.0	18.0	6.2	39.0
55	8.2	4.1	50.9	15.5	4.5	32.3	58.9	8.8	24.9	8.7	..	39.0	..	6.2	39.0
50	6.2	3.1	49.0	15.5	4.5	32.3	61.0	6.2	19.8	8.1	15.5	32.3	15.5	4.9	32.3
45	6.2	3.1	49.0	65.6	4.9	17.2	7.8	15.5	32.3	15.5	4.9	32.3
40	15.5	4.5	32.3	65.6	4.9	17.2	7.8	15.5	32.3	15.5	4.9	32.3
35	6.2	3.1	49.0	15.5	4.5	32.3	65.6	4.9	17.2	7.8	..	32.3	..	4.9	32.3

TABLE V
Sodium Stearate in Decyl Alcohol
 $C = 1.0\%$ $t_g = 60^\circ\text{C.}$

T $^\circ\text{C.}$	Angle of scattering 45°			Angle of scattering 67°			Angle of scattering 90°			Angle of scattering 112°			Angle of scattering 135°		
	ρ_h	ρ_v	ρ_u	ρ_h	ρ_v	ρ_u	ρ_h	ρ_v	$\Delta\rho_u$	ρ_h	ρ_v	ρ_u	ρ_h	ρ_v	ρ_u
120	13.2	10.6	78.3	29.5	8.8	36.1	34.7	12.5	34.7	12.2	13.2	58.9	15.5	..	78.3
110	13.2	..	78.3	29.5	8.8	36.1	34.7	12.5	34.7	12.2	13.2	58.9	..	11.2	78.3
100	..	10.6	..	29.5	8.8	36.1	34.7	12.5	34.7	12.2	13.2	58.9	15.5	11.2	..
90	13.2	10.6	78.3	29.5	8.8	36.1	34.7	12.5	34.7	12.2	13.2	58.9	15.5	11.2	78.3
80	13.2	10.6	78.3	27.3	7.2	30.7	34.7	12.5	34.7	12.2	13.2	58.9	78.3
75	78.3	34.7	12.5	34.7	12.2	20.8	..	15.5	11.2	78.3
70	..	10.6	78.3	18.9	3.8	21.7	34.7	12.5	34.7	12.2	20.8	6.7	..	11.2	78.3
65	13.2	10.6	78.3	..	2.8	19.8	34.7	..	34.7	..	14.7	4.5	15.5	11.2	..
60	9.9	6.2	58.9	15.5	2.8	19.8	36.1	7.7	26.0	11.7	14.7	4.5	11.8	8.2	72.9
55	9.9	19.8	39.0	7.7	22.7	10.2	8.2	..	67.9
50	8.8	4.5	49.0	42.2	6.2	20.8	9.0	14.7	4.5	8.2	5.3	..
45	15.5	2.8	19.8	45.5	5.8	18.0	7.1	14.7
35	8.8	4.5	49.0	15.5	2.8	19.8	45.5	5.8	18.0	7.1	14.7	4.5	8.2	5.3	67.9

TABLE VI

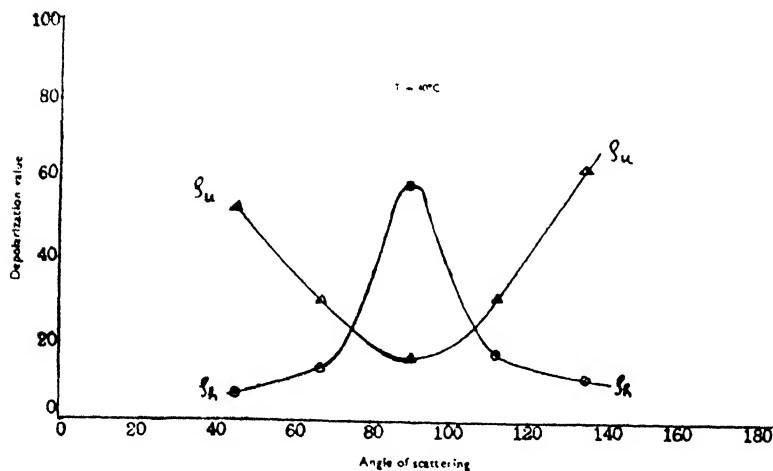
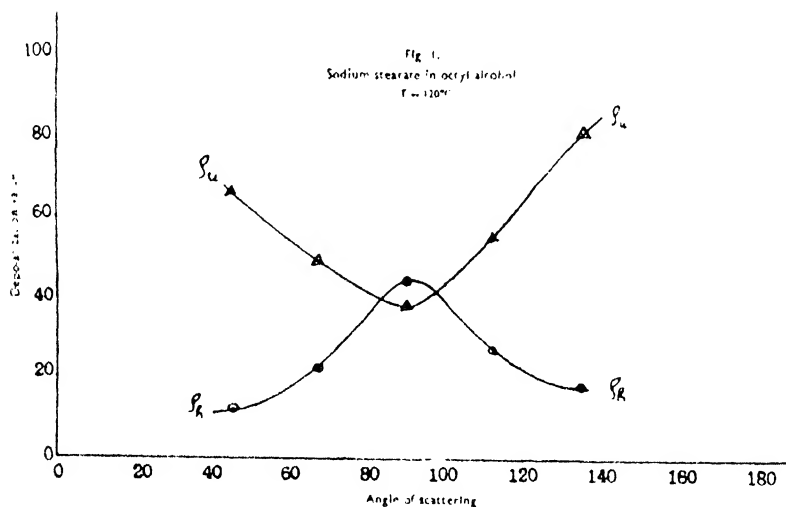
Sodium Stearate in Decyl Alcohol $C = 1.5\% \quad t_g = 75^\circ\text{C.}$

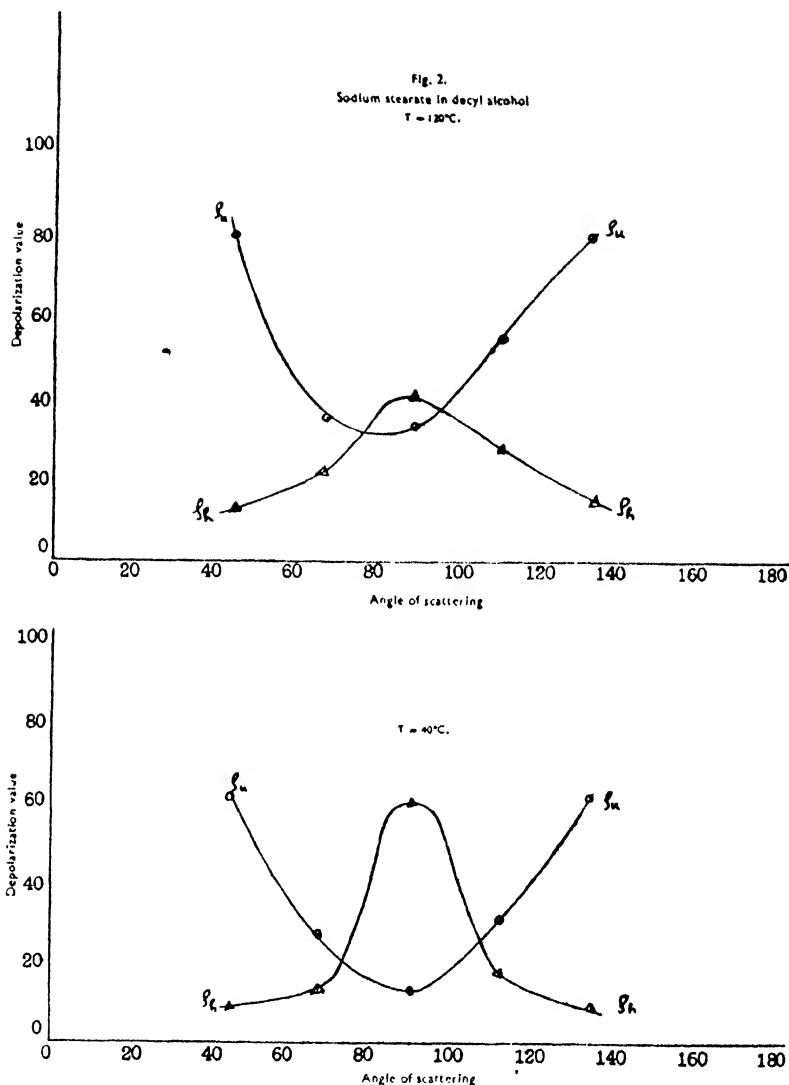
T $^\circ\text{C.}$	Angle of scattering 45°			Angle of scattering 67°			Angle of scattering 90°			Angle of scattering 112°			Angle of scattering 135°		
	ρ_h	ρ_v	ρ_u	ρ_h	ρ_v	ρ_u	ρ_h	ρ_v	ρ_u	ρ_h	ρ_v	ρ_u	ρ_h	ρ_v	ρ_u
120	13.2	9.9	81.0	21.7	7.2	34.7	40.6	13.2	33.3	10.0	27.3	13.2	14.7	10.6	81.0
110	13.2	9.9	..	21.7	7.2	34.7	40.6	13.2	33.3	10.0	..	13.2	14.7	10.6	81.0
100	13.2	9.9	81.0	21.7	7.2	34.7	40.6	13.2	33.3	10.0	27.3	13.2	14.7	10.6	81.0
90	13.2	9.9	81.0	14.7	7.2	..	47.2	9.9	26.0	8.6	27.3	13.2	..	10.6	81.0
80	10.6	7.2	67.9	13.2	3.8	32.3	52.8	8.2	21.7	6.6	27.3	9.9	14.7	10.6	..
75	9.9	7.2	3.1	27.3	54.8	7.2	19.8	6.4	21.7	8.2	11.8	7.2	67.9
70	9.3	5.8	61.0	13.2	3.1	27.3	58.9	5.8	14.7	3.7	20.8	7.2	..	5.8	..
60	9.3	..	61.0	13.2	..	27.3	60.3	4.9	12.5	3.2	..	4.9	9.3	5.8	61.0
50	..	5.8	61.0	..	3.1	4.9	17.2	5.8	..
40	9.3	5.8	..	13.2	..	27.3	60.3	..	12.5	..	17.2	4.9	9.3	5.8	..
35	9.3	5.8	61.0	13.2	3.1	27.3	60.3	4.9	12.5	3.2	17.2	4.9	9.3	5.8	61.0

DISCUSSION OF RESULTS

It is seen from Tables I to VI that the values of ρ_u , ρ_v and ρ_h at any two angles of scattering situated symmetrically about the transverse direction (90°) are not the same, that is to say, the polarization of scattering is unsymmetrical with respect to the transverse direction.

The relations put forward by Ganesan (1924) and by Guinand and Tonnelat (1947) connecting the depolarization value with the angle of scattering are not found to hold good in the present investigation. The values of ρ_u and ρ_h have been plotted against the angle of scattering at two temperatures for one concentration of each system and the graphs obtained, shown in Figs. 1 and 2, clearly bring out the unsymmetrical nature of the polarization of scattering. It is seen that the graphs combine the features exhibited in the theoretical graphs of Krishnan (1938) for small anisotropic particles and for large spherical particles. This indicates that the particles in these systems are anisotropic and of appreciable size. Since the unsymmetrical nature of the graphs is more prominent at a higher temperature than at a lower one, it seems probable that the particles decrease in size during the cooling and gelation of these systems.





It is also seen from Tables I to VI that the values of ρ_h of the transversely scattered light are initially (at 130°C.) low and remain constant on cooling the systems up to a temperature a few degrees higher than the gelation temperature; on further cooling, however, the values increase over a short range of temperature and again become constant. The values of ρ_v of the transversely scattered light are initially low and remain constant till the systems are cooled to about the gelation temperature while the values of ρ_u are initially high and remain constant during this initial stage of cooling. On further cooling both the values of ρ_u and of ρ_v decrease for a while and again become constant. The increase in the value of ρ_h and the decrease in the value of ρ_v indicate that the particles decrease in size and in anisotropy during the cooling and gelation of these systems. The changes in the values of ρ_u are due to the changes in the values of ρ_v and ρ_h since the three de-

polarization factors are connected by the relation, $\rho_u = \frac{1 + 1/\rho_h}{1 + 1/\rho_v}$ (cf. Krishnan,

1935a, 1935b, 1938). The value of ρ_u can be split up into two parts, one due to the anisotropy of the particles and the other due to their size. The anisotropic part of ρ_u value is given, to a first approximation, by the factor, $\frac{2\rho_v}{1+\rho_v}$ and that due to size

is given by $\Delta\rho_u$, where $\Delta\rho_u = \rho_u - \frac{2\rho_v}{1+\rho_v}$ (cf. Sivarajan, 1951). The values of $\Delta\rho_u$ have been calculated in the present case and are given in column 11 of Tables I to VI. The values of $\Delta\rho_u$ decrease during the cooling of the systems indicating that the size of the particles decreases during gelation. This supports the inference made on the basis of the changes in the values of ρ_h .

The observed results may be explained on the following considerations. It has been observed that in soap-water systems the soap does not go into molecular solution but forms clusters which are colloidal in nature (colloidal micelles). A similar phenomenon may be taking place in the polar solvents used in the present investigation and the soap may be forming colloidal clusters when dispersed in the polar solvents at the higher temperature. During the cooling of the soap-solvent systems, the forces holding the soap molecules in the form of clusters may be weakening and thereby causing the breakdown of the clusters. This will cause a reduction in the size of the particles. The broken-up particles may be getting solvated at the same time and, due to the decrease in the thermal energy of the system, the system sets to a gel.

The study of X-ray diffraction of soap solutions in polar solvents has shown that the soap particles are oriented with the hydrocarbon chains end to end and the polar group turned towards the solvent molecules. On cooling, the decrease in the thermal energy of the system probably causes an alteration in the orientation of the particles in such a manner that the 'effective size' of the particles decreases. This decrease in 'effective size' continues till the particles take up the solvent and the system sets to a gel. Once the systems have set to gels at their gelation temperatures, very little changes can take place in the orientation of the particles and hence the values of the depolarization factors attain constancy on further cooling.

A comparison of the Tables I to VI shows that the trend of the changes in the values of the depolarization factors is the same in systems of different concentrations. Further, in the case of transverse scattering, the values of $\Delta\rho_u$ at lower temperatures are distinctly higher in systems containing lower amount of soap, indicating that the 'effective size' of the particles is bigger in systems of lower concentrations than in those of higher ones. This may be due to the fact that the particles in systems of lower concentrations may be undergoing lesser changes in orientation than those in systems of higher concentrations. This view is supported by the fact that the final particles in systems of lower concentration show a higher value for ρ_v , that is, are more anisotropic, than the final particles in systems of higher concentration.

ACKNOWLEDGEMENTS

The authors are grateful to Dr. Mata Prasad, D.Sc., F.R.I.C., F.N.I., for his valuable suggestions and advice and to Dr. K. R. Dixit, Ph.D., F.N.I., for his keen interest in the work. One of the authors (V. S.) is indebted to the Council of the National Institute of Sciences of India for the award of an I.C.I. Research Fellowship.

SUMMARY

The measurement of the depolarization factors, ρ_u , ρ_v and ρ_h , of the light scattered at different directions from gel-forming systems of sodium stearate in octyl and in decyl alcohols has shown that the particles in these systems are anisotropic and of appreciable size. The

changes taking place in the values of the depolarization factors of the transversely scattered light during the cooling of these systems have shown that the particles decrease in size and in anisotropy during gelation. The size of the final particles seems to be bigger in gels of lower concentrations than in those of higher ones. An attempt has been made to explain the observed results on the consideration of the behaviour of soap in polar solvents.

REFERENCES

- Adarkar, S. P., and Hattiangdi, G. S. (1945). Cooling Curves of gel-forming systems of some soaps in pinene. *J. Univ. Bombay*, 14, Pt. 3, 23-26.
- Ganesan, A. S. (1924). Oblique scattering of light in gases and liquids. *Phys. Rev.*, 23, 63-68.
- Guinand, S., and Tonnelat, J. (1947). The intensity and polarization of light diffused by colloidal suspensions of silver. *Compt. rend.*, 225, 1029-1031.
- Hattiangdi, G. S., and Adarkar, S. P. (1946). Inorgano-organic gels in pinene. Part VI. Viscosity changes with time and shear during the gelation of some soap systems in pinene. *Proc. Indian Acad. Sci.*, 24A, 295-303.
- Krishnan, R. S. (1935a). On the depolarization of Tyndall scattering in colloids. *Proc. Indian Acad. Sci.*, 1A, 717-722.
- (1935b). The reciprocity theorem in colloid optics. *Proc. Indian Acad. Sci.*, 1A, 782-788.
- (1938). The reciprocity theorem in colloid optics and its generalization. *Proc. Indian Acad. Sci.*, 7A, 21-34.
- Prasad, M., and Hattiangdi, G. S. (1945). Inorgano-organic gels in pinene. Part I. Gels of some sodium soaps in pinene and their cooling and heating curves. *Proc. Indian Acad. Sci.*, 21A, 1-7.
- Prasad, M., Hattiangdi, G. S., and Mathur, K. N. (1945). Inorgano-organic gels in pinene. Part IV. The kinetics of syneresis of sodium oleate gels in pinene. *Proc. Indian Acad. Sci.*, 21A, 105-113.
- Prasad, M., Hattiangdi, G. S., and Vishvanath, C. V. (1945). Inorgano-organic gels in pinene. Part III. Viscosity measurements of gel-forming solutions of sodium oleate and sodium stearate in pinene. *Proc. Indian Acad. Sci.*, 21A, 90-102.
- Prasad, M., and Sundaram, V. (1951). Syneresis of sodium oleate gels in organic solvents.. Part II. Effect of time on the syneresis of sodium oleate gels in pinene and xylene. Part III. Effect of temperature on the syneresis of sodium oleate gels in pinene. *Proc. Indian Acad. Sci.*, 33A, 305-308, 333-338.
- Sivarajan, S. R. (1951). Scattering of light in colloidal dye solutions. *Current Sci.*, 20, 202-203.
- Sundaram, V. (1953a). Light scattering in soap-solvent systems. Part I. Depolarization factors of the light transversely scattered from sodium oleate-xylene systems during and after gel-formation. Accepted for publication in *Proc. Indian Acad. Sci.*
- (1953b). Light scattering from sodium oleate-xylene systems: Variation of the depolarization factors with the angle of scattering. Communicated for publication in the *J. Univ. Bombay*.

Issued November 20, 1954

ON THE EXISTENCE OF HYDROGEN ATMOSPHERES IN RED GIANT STARS

by U. R. BURMAN, *Department of Applied Mathematics, University of Calcutta*

(Communicated by N. R. Sen, F.N.I.)

(Received March 13; read August 6, 1954)

1. INTRODUCTION

The study of the problem of the internal constitution of the red giant stars has received considerable attention in recent years. These stars, found to be scattered rather irregularly in a belt which branches towards the right off the upper region of the main sequence in the Hertzsprung-Russell diagram, are characterised by high luminosities in spite of their comparatively low surface temperatures. Since low surface temperature implies a rather small intensity of light emitted per unit surface, the high luminosities can be understood only on the hypothesis of extremely large dimensions. It was pointed out by Öpik that an increase in the radius of a normal star might be obtained by assuming that the star has a central convective core with a higher value of the molecular weight than the surrounding radiative envelope. Hoyle and Lyttleton (1942), however, suggest that a large extension in the radius is possible only if this non-uniformity in the composition of the stellar material takes place somewhere in the radiative region of the star. These authors also remark that the desired non-uniformity in the atmospheric composition may be brought about by the accretion of hydrogen from interstellar space to the surface of the star. It is convenient for purposes of analysis to represent this non-uniformity in the composition by a sharp discontinuity of the molecular weight μ , though in an actual case there will probably be a small transition zone of continuously varying μ . If however the accretion of hydrogen is solely responsible for the non-uniformity in composition, as is contemplated here, the discontinuity in μ is indeed strictly sharp.

Hoyle and Lyttleton (1949), as well as Li Hen and Schwarzschild (1949) constructed a number of stellar models under the assumption that the model consists of *three* parts: a central convective core, an intermediate radiative region with the same chemical composition as that of the core, and an outer radiative envelope composed purely of hydrogen and hence differing in composition from the rest of the star. The inhomogeneity in chemical composition thus takes place at the interface between the intermediate zone and the hydrogen envelope. Some of these models also yield quite large extensions of radii, as demanded by the observations on red giants. None of these models, however, have been tested by reference to an actual red giant whose mass (M), radius (R) and luminosity (L) are known from observations; in other words, the models have not been used to determine the composition, the central density and temperature of the star from a knowledge of its L , M and R . Unless a model conforms to this requirement, it must be regarded as a tentative one. There is also another point in the construction of these models which deserves some careful consideration. The opacity of the stellar material has been assumed to be given by Kramers' formula duly corrected for the guillotine factor, in both the intermediate zone and the hydrogen envelope. This assumption is not, however, free from objection in view of the fact that the opacity of a pure hydrogen atmosphere is not given by Kramers' law in the usual form.

The purpose of the present paper is to examine whether a three phase stellar configuration of the type discussed above can be built up with an opacity in the outer region appropriate to highly ionised hydrogen, Kramers' formula for opacity being, however, retained to govern the structure of the intermediate radiative zone, the central core as usual being in convective equilibrium. The model should also be able to furnish complete information regarding the internal constitution of the star from a knowledge of its three observable parameters, L , M and R . Further, the possibility of constructing a two-phase configuration, namely, a configuration with a central convective core surrounded by an envelope of pure hydrogen in radiative equilibrium, has also been considered. It is found that a configuration consistent with all the conditions of thermodynamic and mechanical equilibrium, and with an energy output* of the prescribed amount, does not exist under the assumptions involved. This conclusion leads one to believe that the outer layers of a giant star are probably not composed of hydrogen alone. An admixture in suitable proportions of other elements, with hydrogen in the outer layers of the star, may be regarded as an alternative hypothesis.

2. THE BASIC ASSUMPTIONS AND THE STRUCTURE OF THE INTERMEDIATE ZONE

As outlined above, the stellar model has been assumed to consist of three zones as follows:—

- (i) a central convective core within which almost the entire energy generation takes place,
- (ii) an intermediate zone in radiative equilibrium having the same chemical composition as that of the core, and
- (iii) an outer envelope of pure hydrogen also in radiative equilibrium.

The model would thus have a single discontinuity of composition occurring somewhere in the radiative region. In accordance with the usual convention, we shall regard the perfect gas law as valid throughout the configuration and shall ignore the influence of radiation pressure. Kramers' law for photoelectric opacity as modified by Li Hen and Schwarzschild (1949) to account for the variation of the guillotine factor, will be adopted for the intermediate radiative zone, while an appropriate opacity law for highly ionised hydrogen will govern the structure of the outer envelope.

The equilibrium equations in the intermediate zone embodying the above assumptions can be written down in the usual notations as

$$\frac{dP}{dr} = -G \frac{M(r)}{r^2} \rho, \quad \dots \dots \dots (1)$$

$$\frac{dM(r)}{dr} = 4\pi r^2 \rho, \quad \dots \dots \dots (2)$$

$$\frac{d}{dr} \left(\frac{1}{3} a T^4 \right) = - \frac{\kappa \rho}{c} \frac{L}{4\pi r^2}. \quad \dots \dots \dots (3)$$

The opacity coefficient, according to Li Hen and Schwarzschild (1949), is given by

$$\kappa = \kappa_0 \rho^{0.75} T^{-3.5}, \text{ with } \kappa_0 = 10^{25} (1+X)(1-X-Y), \quad \dots \dots (4)$$

where X , Y denote respectively the hydrogen and helium contents in the material.

* The carbon-nitrogen cycle and the proton-proton reaction have both been considered as energy generating mechanisms in this connection.

In terms of the dimensionless variables p, t, q, x (Schwarzschild, 1946) defined by

$$P = p \frac{GM^2}{4\pi R^4}, \quad T = t \frac{\mu H}{k} \frac{GM}{R}, \quad M(r) = qM, \quad r = xR, \quad \dots \quad (5)$$

the equations (1)–(3) become

$$\frac{dp}{dx} = -\frac{p}{t} \frac{q}{x^2}, \quad \dots \quad (6)$$

$$\frac{dq}{dx} = \frac{p}{t} x^2, \quad \dots \quad (7)$$

$$\frac{dt}{dx} = -\frac{C}{x^2} \frac{p^{1.75}}{t^{8.25}}, \quad \dots \quad (8)$$

where

$$C = \frac{3\kappa_0}{4ac} \left(\frac{k}{\mu H G} \right)^{7.5} \left(\frac{1}{4\pi} \right)^{2.75} \frac{LR^{1.25}}{M^{5.75}} \cdot \dots \quad (9)$$

Introducing the following substitutions in equations (4)–(6),

$$\lambda = \log \frac{p}{p_0}, \quad \psi = \log \frac{q}{q_0}, \quad \tau = \log \frac{t}{t_0}, \quad y = \log \frac{x}{x_0}, \quad \dots \quad (10)$$

and assuming that the *four* constants with zero suffix can be chosen so as to satisfy the three conditions

$$\frac{q_0}{t_0 x_0} = 1, \quad \frac{p_0 x_0^2}{t_0 q_0} = 1, \quad \frac{C p_0^{1.75}}{t_0^{8.25} x_0} = 1, \quad \dots \quad (11)$$

Li Hen and Schwarzschild (1949) re-write the equations in the forms

$$\log \left(-\frac{d\lambda}{dy} \right) = \psi - \tau - y, \quad \dots \quad (12)$$

$$\log \left(\frac{d\psi}{dy} \right) = \lambda - \tau - \psi + 3y, \quad \dots \quad (13)$$

$$\log \left(-\frac{d\tau}{dy} \right) = 1.75 \lambda - 9.25 \tau - y. \quad \dots \quad (14)$$

These equations are to be integrated outwards with starting values of the variables appropriate to the conditions of fit obtaining at the interface between the radiative zone and the convective core which is an Emden polytrope of index $n = 1.5$. Since there is no discontinuity of composition across this interface, the homology invariants

$$U = \frac{d \log M(r)}{d \log r}, \quad V = -\frac{d \log P}{d \log r}, \quad n+1 = \frac{d \log P}{d \log T} \quad \dots \quad (15)$$

must be continuous across it. Using these conditions Li Hen and Schwarzschild (1949) have integrated the equations (12)–(14) and given the solutions in tabular forms. These solutions which depend on one parameter ξ_1 (ξ is the independent Emden variable, i.e., the radial distance for the polytrope $n = 1.5$) defining the radius of the central convective core and chosen arbitrarily, determine uniquely the structure of the intermediate zone.

3. THE STRUCTURE OF THE HYDROGEN ENVELOPE

The structure of the hydrogen envelope is governed by equations (1), (2) and (3), except that in equation (3) the opacity coefficient κ has the value appropriate to highly ionised hydrogen, viz.

$$\kappa = BP T^{-\frac{11}{2}} e^{-\frac{\chi_1}{kT}}, \quad \dots \quad (16)$$

where B is a numerical constant and χ_1 the ionisation potential of hydrogen. This formula for the hydrogen opacity has been obtained by Wasiutinsky (1946) and has been used by him to find an approximate * pressure-temperature relation in the hydrogen envelope in the form

$$P = \frac{2}{\sqrt{19\alpha}} T^{\frac{19}{4}} e^{-\frac{21}{38} \frac{\chi_1}{kT}}, \quad \dots \quad (17)$$

where

$$\alpha = \frac{3BL}{16\pi acGM}. \quad \dots \quad (18)$$

We shall now use equation (17) to calculate the temperature distribution in this region.

Inserting the value of κ from equation (16) in the radiative equilibrium equation (3), and using the perfect gas law

$$P = \frac{k}{\mu H} \rho T,$$

one obtains

$$\frac{dT}{dr} = - \frac{3BL}{16\pi ac} \frac{\mu H}{k} T^{-\frac{19}{2}} e^{-\frac{\chi_1}{kT}} \frac{P^2}{r^2},$$

which with the help of equations (17) and (18) can be written as

$$\frac{dT}{dr} = - \frac{4}{19} GM \frac{\mu H}{k} e^{-\frac{2}{19} \frac{\chi_1}{kT}} \cdot \frac{1}{r^2}.$$

An integration of this equation, taking $\mu = \frac{1}{2}$ leads to

$$\begin{aligned} \frac{2}{19} GM \frac{H}{k} \left(\frac{1}{r} - \frac{1}{R} \right) &= \int_{T_s}^T e^{\frac{2}{19} \frac{\chi_1}{kT}} dT \\ &= \left[T e^{\frac{2}{19} \frac{\chi_1}{kT}} - \frac{2}{19} \frac{\chi_1}{k} \left\{ \log \left(\frac{2}{19} \frac{\chi_1}{kT} \right) + \frac{2}{19} \frac{\chi_1}{kT} \frac{1}{1!} \right. \right. \\ &\quad \left. \left. + \left(\frac{2}{19} \frac{\chi_1}{kT} \right)^2 \frac{1}{2 \cdot 2!} + \left(\frac{2}{19} \frac{\chi_1}{kT} \right)^3 \frac{1}{3 \cdot 3!} + \dots \right\} \right]_{T_s}^T \quad (19) \end{aligned}$$

where T_s refers to the surface temperature of the star assumed to be non-zero to avoid the divergence in the integral.

* The variation of mass in the region under consideration has been ignored in this derivation.

The mass distribution inside the hydrogen region can now be obtained as

$$\begin{aligned} M(r) &= M + \int_R^r 4\pi r^2 \rho \, dr \\ &= M + \frac{4\pi}{\sqrt{19\alpha}} \frac{H}{k} \int_R^r T^{\frac{15}{4}} e^{-\frac{21}{38} \frac{x_1}{kT}} r^2 \, dr. \quad \dots (20) \end{aligned}$$

The integral in equation (20) is to be evaluated numerically by using the T - r table that may be constructed from equation (19).

4. THE EQUATIONS OF FIT

At the interface (where the discontinuity in composition occurs) between the intermediate radiative zone and the hydrogen envelope, the usual conditions for the continuity of r , $M(r)$, P and T expressed in terms of the dimensionless variables in equation (10) lead to the following relations,

$$y_2 = \log \frac{r_2}{R x_0}, \quad \dots \dots \dots (21)$$

$$\psi_2 = \log \frac{M(r_2)}{q_0 M}, \quad \dots \dots \dots (22)$$

$$\lambda_2 = \log \left\{ P_2 \left/ \left(p_0 \frac{GM^2}{4\pi R^4} \right) \right. \right\} = \log \frac{p_2}{p_0}, \quad \dots \dots \dots (23)$$

$$\tau_2 = \log \left\{ T_2 \left/ \left(t_0 \frac{GM}{R} \frac{\mu H}{k} \right) \right. \right\}, \quad \dots \dots \dots (24)$$

where the suffix 2 refers to the interface under consideration and μ denotes the constant molecular weight in the entire region interior to this interface. The four constants x_0 , q_0 , p_0 , t_0 are connected by equations (11). There is the further condition of the continuity of $L(r)$ across the interface, which may be obtained thus—

The equations of hydrostatic and radiative equilibrium in the hydrogen envelope give

$$\frac{d(\frac{1}{3}aT^4)}{dP} = \frac{\kappa L(r)}{4\pi cGM(r)},$$

which with the help of equation (17) may be written in the form

$$\begin{aligned} \frac{L(r)}{M(r)} &= \frac{1}{n+1} \frac{16\pi acG}{3B} \frac{T^{\frac{19}{2}}}{P^2} e^{-\frac{x_1}{kT}} \\ &= \frac{16\pi acG}{3B} \frac{T^{\frac{19}{2}}}{P^2} e^{-\frac{x_1}{kT}} \left(\frac{19}{4} + \frac{21}{38} \frac{x_1}{kT} \right)^{-1} \dots \dots \dots (25) \end{aligned}$$

In the intermediate radiative zone, one similarly obtains

$$\begin{aligned} n+1 &= \left(\frac{d \log P}{d \log T} \right)_{\text{rad}} = \frac{16\pi acG}{3\kappa_0} \frac{T^{7.5}}{P \rho^{0.75}} \frac{M(r)}{L(r)} \\ &= \frac{16\pi acG}{3\kappa_0} \frac{T^{7.5}}{\bar{P}} \left(\frac{k}{\mu H} \right)^{0.75} \left(\frac{T}{\bar{P}} \right)^{0.75} \frac{M(r)}{L(r)}. \quad \dots \dots (26) \end{aligned}$$

Equality of $\frac{L(r)}{M(r)}$ from equations (25) and (26) therefore gives the desired condition at the interface as

$$\left(\frac{k}{H}\right)^{0.75} \frac{1}{\mu^{0.75} \kappa_0 (n_i + 1)} = e^{-\frac{\chi_1}{kT_2}} \left\{ R \left(\frac{19}{4} + \frac{21}{38} \frac{\chi_1}{kT_2} \right) \right\}^{-1} \frac{T_2^{1.25}}{P_2^{0.25}}, \quad \dots \quad (27)$$

where the suffix i denotes the value on the inner side of the interface.

5. CONSTRUCTION OF THE MODEL

We have seen how with an assumed set of values for L , M and R , the structure of the hydrogen envelope can be completely determined. The compilation of the complete model may then be proceeded with with the help of the homology invariants U and V . Starting with the definitions of U , V and using equations (1) and (2), one easily obtains

$$\frac{U}{V} = \frac{4\pi}{G} \frac{r^4 P}{\{M(r)\}^2}, \quad \dots \quad \dots \quad \dots \quad (28)$$

which shows that the ratio $\frac{U}{V}$ is continuous across the interface between the hydrogen envelope and the intermediate radiative zone, i.e. across the surface of discontinuity of μ . Since the quantities occurring on the right of equation (28) can all be calculated at any point inside the hydrogen region, the ratio $\frac{U}{V}$ will therefore be known at every point of it. Further, this ratio can also be calculated at any point of the intermediate zone, corresponding to each of the tabulated solutions provided by Li Hen and Schwarzschild (1949). Starting therefore from the surface of the star, we follow the hydrogen envelope solution, terminate it at an arbitrary point r_2 , and pass on to any chosen solution (from the tables of Li Hen and Schwarzschild) of the intermediate zone characterised by its parameter ξ_1 and satisfying the continuity condition for $\frac{U}{V}$ at the point r_2 where we break off the envelope solution.

Along any solution of the intermediate zone, the ratio $\frac{U}{V}$ decreases steadily outwards.

These solutions have the further property, as will be evident from the integrations of Li Hen and Schwarzschild (1949), that some of them ($\xi_1 < 1.12009$) show a steadily increasing n outwards and ultimately behave like isothermals ($n \rightarrow \infty$), while for others ($\xi_1 > 1.12009$) n increases steadily at first, attains a maximum and then gradually diminishes. These latter solutions will cease to be applicable for a fit with the hydrogen envelope after n drops below 1.5. It appears therefore quite possible that within the range of applicability of these solutions, they may not be fitted on, as far as the continuity of the ratio $\frac{U}{V}$ is concerned, to the envelope solution at an arbitrary point. When, however, the fit is possible, at the junction of the two solutions, the variables y_2 , ψ_2 , λ_2 , τ_2 for the intermediate zone will all be known and equations (21)–(24) will then fix up the values of the quantities x_0 , q_0 , p_0 and μt_0 appropriate to the fit. It should, however, be observed that the quantities x_0 , q_0 , p_0 thus determined must conform to the restriction

$$q_0^2 = p_0 x_0^4, \quad \dots \quad \dots \quad \dots \quad \dots \quad (29)$$

imposed on them by the first two of equations (11). A suitable choice of the position of the surface of discontinuity of μ will enable one to secure this adjustment without much difficulty. The condition

$$\frac{q_0}{t_0 x_0} = 1$$

in equation (11) then determines the value of t_0 which in conjunction with the already known value of μt_0 would fix up the value of μ , the molecular weight of the material in the region interior to the hydrogen envelope. The composition parameters (viz. the hydrogen and helium contents) as well as the central density and temperature are now to be found for the complete model. This is done as follows:—

The condition (Equation (11))

$$\frac{C p_0^{1.75}}{t_0^{0.25} x_0} = 1$$

determines C . Writing

$$\mu = \frac{2}{1+3X+0.5Y} = f_1(X, Y), \quad \dots \dots \dots (30)$$

where X, Y denote respectively the hydrogen and helium contents, equation (9) may be put in the form

$$C = f_2(X, Y, T_c, \rho_c, \xi_1), \quad \dots \dots \dots (31)$$

The energy-output equation will furnish another relation of the type

$$L = f_3(X, Y, T_c, \rho_c, \xi_1), \quad \dots \dots \dots (32)$$

T_c, ρ_c being the central temperature and density of the model sought. Finally we have equation (27) which we rewrite in the equivalent form

$$0 = f_4(X, Y, \xi_1, r_2), \quad \dots \dots \dots (33)$$

The four equations (30)–(33) therefore fix the values of the four quantities X, Y, T_c, ρ_c and a set of physically admissible values, for these would complete the construction of the desired model.

It will be observed that the procedure adopted here involves two arbitrary choices, viz. the position (r_2) of the surface of discontinuity of composition and the size (ξ_1) of the central convective core.

6. THE ENERGY GENERATION LAW

While it may be generally admitted that the carbon-nitrogen cycle of Bethe is capable of explaining the energy production in the main sequence stars, the corresponding question for the red giants appears to need further investigation. We shall here examine the rôles of both the C—N cycle and the Proton-Proton reaction as mechanisms of energy liberation in the red giants. The luminosities according to the two processes are given by (Epstein (1950))

$$L_c = \frac{2.84 \times 10^7}{0.0585} \cdot \frac{1}{\mu^{\frac{1}{2}}} X \alpha_{14} \rho_c^{\frac{1}{2}} T_c^{\frac{43}{2}} \int_0^{\xi_1} \theta^{23} \xi^2 d\xi \quad \dots \dots (34)$$

and

$$L_P = \frac{6.23 \times 10^{25}}{0.3396} \cdot \frac{1}{\mu^{\frac{1}{2}}} X^2 \rho_c^{\frac{1}{2}} T_c^{\frac{11}{2}} \int_0^{\xi_1} \theta^7 \xi^2 d\xi, \quad \dots \quad (35)$$

where α_{14} is the relative abundance of N^{14} having the value 0.01, θ the dependent variable in the Emden polytrope of index 1.5, and T_c is expressed in millions of degrees. The integrals in equations (34), (35) are to be evaluated numerically and should become sensibly constant within the convective core. The integral in equation (34) does indeed attain a nearly constant value at about $\xi = 1.20$, while that in equation (35) does not become constant till almost the boundary of the polytrope is reached. In other words the energy generating core in the P-P reaction will be unusually large and this will have the effect of violating the equations of fit which must necessarily hold at the junction of the intermediate radiative zone and the hydrogen envelope. In fact we shall see that no model of the desired type can exist with the core radius (ξ_1) exceeding 1.20. It therefore follows that the P-P reaction alone is incapable of accounting for the energy generation in a model of the type considered here. Under the present assumptions therefore the C—N cycle must be looked upon as the probable mechanism for the energy production in the red giants.

7. NUMERICAL RESULTS

It is now necessary to carry out numerical calculations according to the scheme outlined in the previous sections in respect of some observed red giants. But, unfortunately the observational data regarding masses of these stars appear to be somewhat uncertain and of a very limited extent. However the best available data seem to be provided by the red components of the two binaries, Capella and Zeta Auriga. The direct observational value of four solar masses for the red component of Capella has recently been called into question by Struve (1951), who ascribes to it a mass value of about 2.7 in solar units. This new value also in its turn is not free from uncertainty.

For the red component of Zeta Auriga, a mass value around 15 solar masses is furnished by observational data. This observational result is based on the determination of the mass function and the mass ratio, which latter appears to be quite unreliable on account of a very limited range of observation. In view of these uncertainties, we have adopted the earlier observed values for the mass, radius and luminosity of the red component of Capella for the purpose of calculations in the present paper. Calculations for the red component of Zeta Auriga have not been undertaken on the same ground of uncertainty.

The observed values (in solar units) for the red component of Capella are

$$\log L = 2.08, \quad \log M = 0.64, \quad \log R = 1.02.$$

With these values the surface temperature T_s calculated from the formula

$$\frac{L}{4\pi R^2} = \frac{1}{4} acT_s^4,$$

comes out to be $T_s = 4.79 \times 10^{-3}$ expressed in millions of degrees. The temperature distribution inside the hydrogen envelope is now given by equation (19) and is shown in Table I.

With the temperature distribution in Table I, the integral in equation (20) is evaluated numerically, and the mass distribution obtained as in Table II. The values

TABLE I

Temperature distribution inside the hydrogen envelope

$\frac{x_1}{k} = 1.571 \times 10^6$

$T. 10^{-6}$	$\frac{r}{R}$	$\frac{r}{R}$	$T. 10^{-6}$
4.79×10^{-3}	1.0	1.00	4.79×10^{-3}
1.0×10^{-2}	0.912	0.90	1.25×10^{-2}
0.1	0.755	0.80	6.25×10^{-2}
0.2	0.667	0.75	10.25×10^{-2}
0.3	0.600	0.70	14.76×10^{-2}
0.4	0.546	0.65	21.24×10^{-2}
0.5	0.502	0.60	0.30
0.6	0.464	0.55	0.40
0.7	0.432	0.50	0.50
0.8	0.404	0.47	0.56
0.9	0.380	0.44	0.65
1.0	0.358	0.41	0.75
1.2	0.322	0.38	0.90
1.6	0.267	0.35	1.05
2.0	0.229	0.32	1.20
		0.30	1.34
		0.28	1.49
		0.26	1.67
		0.24	1.87
		0.22	2.11
		0.20	2.40

of μ and T_c are then computed in some sample cases corresponding to arbitrary choices inside the model of the position at which the composition changes, and the size of the central convective core. These values are listed in Table III.

TABLE II

Distribution of mass inside the hydrogen envelope

$\frac{r}{R}$	$\frac{M(r)}{M}$
1.00	1.00
0.70	1.00
0.50	0.9694
0.44	0.9254
0.41	0.8906
0.38	0.8206
0.35	0.7096
0.32	0.5587
0.30	0.3580
0.28	0.2330
0.26	0.0346

TABLE III

The values of μ and T_c in some sample cases corresponding to arbitrary choices of r_2 and ξ_1

ξ_1	$\frac{r_2}{R}$	$\frac{U}{V}$	$\frac{r_1}{R} = x_0$ (radius of convective core)	μ	$T_c \cdot 10^{-6}$
1.1189	0.32	0.7865	0.2043	0.288	1.90
	0.35	0.3663	0.1694	0.339	2.09
	0.38	0.1804	0.1445	0.356	2.23
	0.41	0.0857	0.1142	0.296	2.08
	0.44
1.1204	0.32	0.7865	0.2043	0.290	1.90
	0.35	0.3663	0.1695	0.344	2.11
	0.38	0.1804	0.1461	0.375	2.36
	0.41	0.0857
1.1213	0.32	0.7865	0.2044	0.292	1.91
	0.35	0.3663	0.1696	0.354	2.17
	0.38	0.1804	0.1495	0.396	2.46
	0.41	0.0857
1.1250	0.32	0.7865	0.2046	0.294	1.92
	0.35	0.3663	0.1714	0.360	2.21
	0.38	0.1804
1.1400	0.32	0.7865	0.2075	0.302	1.97
	0.35	0.3663
1.2000	0.32	0.7865

8. DISCUSSION OF THE RESULTS

The missing figures in Table III imply that the equations of fit admit of no solution in the corresponding cases, because along the relevant intermediate zone solution defined by ξ_1 , the ratio $\frac{U}{V}$ does not attain the requisite value before n drops below 1.5. This feature will be common to all intermediate zone solutions defined by $\xi_1 > 1.12009$, while for solutions with $\xi_1 < 1.12009$, the fit with an hydrogen envelope as far as the continuity of $\frac{U}{V}$ is concerned, can be obtained at any place inside the model. It is also easy to see that for any intermediate solution of the former class ($\xi_1 > 1.12009$), if the continuity condition for $\frac{U}{V}$ becomes invalidated at a particular point r_2 of the hydrogen atmosphere, it will become so at all points further outwards. For this family of intermediate solutions therefore it has not been possible to extend the calculations beyond (outwards) $\frac{r_2}{R} = 0.38$ roughly. For the latter class of intermediate solutions ($\xi_1 < 1.12009$), however, the fit equations can be solved even beyond

$\frac{r_2}{R} = 0.38$, but the computed values of μ and T_c will gradually diminish and render the fitted solutions physically inadmissible. It has also been verified that for both families of the intermediate solutions considered here, the initial value of the ratio $\frac{U}{\bar{V}}$, viz., the value on the surface of the convective core, is less than the value of the corresponding quantity at any point given by $\frac{r_2}{R} < 0.32$ (approximately) inside the hydrogen envelope. This remark will not, however, be applicable to intermediate solutions characterised by ξ_1 sufficiently smaller than 1.1189, but such small values of ξ_1 will not be compatible with the hypothesis that there shall be no appreciable energy generation outside the convective core. This shows that a fit of the hydrogen envelope with the intermediate region cannot be obtained at a distance smaller than 32 per cent of the star's radius. A solution of the fit equations, if any, should thus be sought for in the range $0.32 < \frac{r_2}{R} \leq 0.38$. It is here necessary to emphasise that the different solutions of the equations of fit constitute a two-parametric family, as will be evident from Table III which shows that corresponding to a given position of the surface of discontinuity of composition, there are more than one values for the radius of the central convective core.

9. IMPOSSIBILITY OF THE THREE-PHASE CONFIGURATION

The results in Table III have been presented graphically in Fig. 1, where μ has

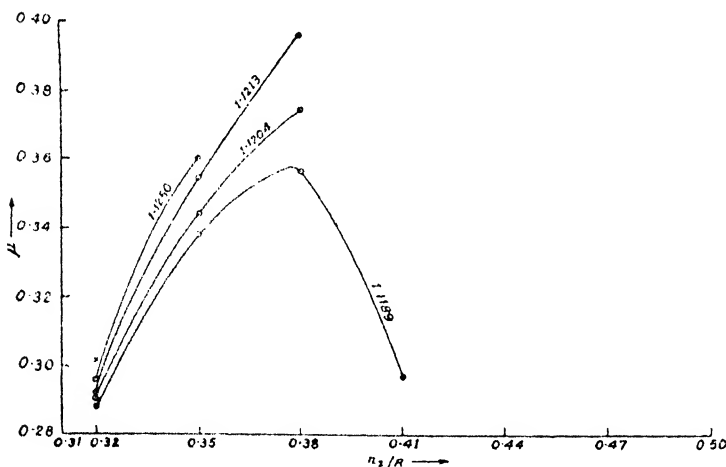


FIG. 1. The numbers alongside the curves refer to values of the radii of the convective cores (ξ_1) corresponding to the computed models. The point marked (x) refers to $\xi_1 = 1.1400$.

been plotted against $\frac{r_2}{R}$. It will be observed that the computed values of μ cor-

responding to either a constant value of ξ_1 or a constant value of $\frac{r_2}{R}$ are all less than 0.5. These values of μ are clearly physically inadmissible because for any medium different from pure hydrogen the average molecular weight cannot drop below 0.5. Any solution of the stellar equations that envisages a model of this type must therefore be discarded as being contrary to physical reality. Moreover,

the central temperatures of these models are found to be so low (2-3 million degrees) that thermonuclear reactions involving energy releases can hardly occur under such conditions. Even if it is admitted that the proton cycle of energy generation is operative at these low temperatures, it will not be possible to account for the high luminosity of the star unless a value of the central density in the neighbourhood of 10^{12} gm./cm.³* is permitted for the model. Such high values of the central density would inevitably imply a breakdown of the perfect gas equation of state which is the very basis of the present investigation.

There is no doubt that particular values for L , M and R appropriate to an actual red giant star have been used in these calculations, but it has been verified that the calculations are not quite sensitive to these L , M , R values. Furthermore, the results do not also depend on the form of the energy generation law, viz. the C-N cycle or the P-P reaction. In fact the opacity law for pure hydrogen which prevents a rapid rise of temperature inwards from the surface of the star is responsible for these extraordinarily low central temperatures for the computed models. A three-phase configuration with an outer atmosphere of pure hydrogen cannot therefore be regarded as a possible model for the red giant stars.

10. THE TWO-PHASE CONFIGURATION

It is now necessary to examine whether a two-phase configuration consisting of a central convective core (a $3/2$ -polytrope) surrounded by a hydrogen envelope in radiative equilibrium can serve as a possible model for a red giant. The discontinuity in composition occurs on the surface of the convective core and the conditions to be satisfied here are

$$\left(\frac{U}{V}\right)_e = \left(\frac{U}{V}\right)_i \quad \dots \quad \dots \quad \dots \quad \dots \quad \dots \quad (36)$$

$$T_e = T_c \theta_i \quad \dots \quad \dots \quad \dots \quad \dots \quad \dots \quad (37)$$

$$r_e = \left(\frac{5k}{8\pi\mu GH} \frac{T_c}{\rho_c}\right)^{\frac{1}{2}} \xi_i \quad \dots \quad \dots \quad \dots \quad \dots \quad (38)$$

$$M(r_e) = 4\pi\rho_c \left(\frac{5k}{8\pi\mu GH} \frac{T_c}{\rho_c}\right)^{\frac{3}{2}} \left(-\xi^2 \frac{d\theta}{d\xi}\right)_i, \quad \dots \quad \dots \quad (39)$$

where the indices e and i refer respectively to the envelope and core side values on the common boundary.

The energy output equation will furnish a relation of the form

$$f(X, Y, T_c, \rho_c, \xi_i) = 0 \quad \dots \quad \dots \quad \dots \quad (40)$$

and also there will be another relation analogous to equation (33) and of the form

$$F(X, Y, \xi_i) = 0. \quad \dots \quad \dots \quad \dots \quad (41)$$

Equations (36)–(40) would enable one to determine the five quantities ξ_i , X , Y , T_c and ρ_c and equation (41) would serve as a check to test the correctness of the fit.

Calculations on exactly similar lines as in the three-phase configuration have been made for the red component of Capella using the P-P reaction as the energy generating mechanism and the results given in Table IV.

* An actual application of formula (35) under assumed conditions $T_c \sim 4$ millions. $X \sim 1$, $\mu \sim 0.5$ leads to this result.

TABLE IV

Approximate values of the central temperatures and densities for the two-phase configurations

$\frac{r_c}{R}$	ξ_c (convective core radius in Emden variable)	$T_c \cdot 10^{-6}$	ρ_c (gm./cm. ³)
0.70	3.60	13.0	1.5×10^7
0.60	3.50	6.8	2.5×10^{10}
0.50	3.20	5.0	8.0×10^{11}
0.40	2.90	4.0	9.1×10^{12}
0.30	1.11	1.6	1.5×10^{17}

It will appear from Table II that the mass of the hydrogen envelope up to a depth of about 30 per cent of the star's radius may be regarded as negligibly small, and under this circumstance a two-phase configuration with a convective core extending beyond 70 per cent of the star's radius would hardly have any physical significance. Calculations in Table IV have not therefore been extended beyond this range. The orders of the computed central densities and temperatures definitely indicate a breakdown of the perfect gas law, so that a two-phase configuration in conformity with our basic assumptions cannot also serve as a red giant model. The problem, however, of the existence of a red giant model (with no convective core) in radiative equilibrium at the centre and having a hydrogen atmosphere also in radiative equilibrium has not been attempted here for want of a lack of more detailed knowledge regarding the integration of the radiative equations from the centre outwards.

Lastly there remains the question whether it is possible to construct a red giant model with pure hydrogen in radiative equilibrium throughout. The decisive answer to this question requires numerical integration of the stellar equations for the appropriate hydrogen opacity which is not available at the present moment, but from the temperature distribution inside the hydrogen envelope we have considered, one may reasonably conjecture that the central temperatures of the integrated models would be too low to account for the high luminosities of the red giants. Moreover, there is also the difficulty of thermonuclear energy generation in a pure hydrogen star.

Therefore the conclusion may be drawn that red giant stars cannot possess atmospheres of pure hydrogen.

SUMMARY

This paper attempts to answer the question whether a three-phase configuration consisting of a central convective core, an intermediate radiative zone (having the same chemical composition as that of the core) and an outer envelope of *pure* hydrogen also in radiative equilibrium, can serve as a suitable model for a red giant star, whose mass, radius and luminosity are known from observations. An opacity formula appropriate to highly ionised hydrogen has been used for the outer envelope, while the usual Kramers' law of opacity has been assumed for the intermediate region. The central temperatures for the computed models satisfying all these conditions are found to be extremely low (about 2.3 million degrees), so as to be totally inadequate to account for the high luminosities of these stars by any of the known mechanisms of thermonuclear reactions. A two-phase configuration consisting of a central convective core surrounded by a radiative hydrogen envelope has also been considered in this connection. It is found that here also the equations furnish no physically admissible solutions.

It is, however, known that three-phase configurations can be built up with central temperatures appropriate for thermonuclear energy generation, when Kramers' law of opacity is assumed to hold throughout the model outside the central convective core. The different

behaviour obtained in the present case is clearly to be attributed to the opacity governing the structure of the hydrogen envelope.

It is thus reasonable to conclude that under the conditions envisaged here an atmosphere of pure hydrogen is not compatible with the structure of a red giant star.

REFERENCES

- Epstein, I. (1950). A note on energy generation. *Ap. J.*, **112**, 207.
Hen, Li, and Schwarzschild, M. (1949). Red giant models with chemical inhomogeneities. *M.N.*, **109**, 631.
Hoyle, F. and Lyttleton, R. A. (1942). On the nature of red giant stars. *M.N.*, **102**, 218.
Hoyle, F. and Lyttleton, R. A. (1949). The structure of stars of non-uniform composition. *M.N.*, **109**, 614.
Schwarzschild, M. (1946). On the helium content of the sun. *Ap. J.*, **104**, 203.
Struve, O. (1951). The spectrum of Capella. *Proc. Nat. Acad. Sci.*, **37**, 327.
Wasiutinsky, J. (1946). The structure of the hydrogen envelope in radiative equilibrium. *Astrophysica Norvegica*, **4**, 443.

Issued November 22, 1954.

DEPENDENCE OF EROSION RATIO AND RATE OF BURNING ON POSITION AND TIME IN A ROCKET MOTOR

by SHIV KUMAR GUPTA and MAHENDRA SINGH SODHA, *Defence Science Laboratory, New Delhi*

(Communicated by R. S. Varma, F.N.I.)

(Received April 12; read August 6, 1954)

INTRODUCTION

Kershner (1944) has discussed the variation of pressure along the length of a rocket motor, having tubular or multi-tubular propellant, for a given value of A_t/A_p . We have extended his treatment and derived an explicit expression for pressure which gives its variation along the length of the motor as well as with time. We have also expressed C_D'/C_D as a function of time.

The temperature, gas velocity, u^2/bT , reduced mass velocity, erosion ratio and rate of burning have also been expressed as explicit functions of time t after ignition and distance x from the head end.

VARIATION OF PRESSURE

Kershner (1944) has stated that an analysis of the equation of motion of the propellant gases shows that the distribution of pressure along the length of the rocket motor is approximately parabolic for rockets, using tubular or multitubular propellants. He expresses the pressure P_L at the nozzle end of the propellant grain and the space average pressure for a given small value of A_t/A_p as:—

$$P_L = P_0 \left\{ 1 - 2\phi \left(\frac{A_t}{A_p} \right)^2 \right\} \quad \dots \quad \dots \quad \dots \quad (1)$$

$$P_{(v)} = P_0 \left\{ 1 - \frac{2\phi}{3} \left(\frac{A_t}{A_p} \right)^2 \right\} \quad \dots \quad \dots \quad \dots \quad (2)$$

where P_0 is the pressure at the head of the chamber,

A_t is the area of the throat,

A_p is the port area at any instant,

and

$$\phi = \frac{\gamma}{2} \left(\frac{2}{\gamma+1} \right)^{\frac{\gamma+1}{\gamma-1}}$$

From Eqns. (1) and (2) it is evident that the pressure at any point distant x from the head end along the length of the motor is given by:

$$P/P_0 = 1 - 2\phi \left(\frac{A_t}{A_p} \right)^2 (x/L)^2 \quad \dots \quad \dots \quad \dots \quad (3)$$

where L is the length of the propellant grain.

Substituting for A_p from Appendix I we obtain P/P_0 as a function of distance x from head end and time t after ignition:—

$$P/P_0 = 1 - 2\phi(x/L)^2 A_t^2 / (b + ct)^2 \quad \dots \quad (4)$$

The space average of P/P_0 at any instant is given by:—

$$\overline{P/P_0} = \frac{\int_0^L (P/P_0) dx}{\int_0^L dx} = 1 - \frac{2\phi}{3} \cdot \frac{A_t^2}{(b + ct)^2} \quad \dots \quad (5)$$

The time average of P/P_0 at any point is given by:—

$$\overline{P/P_0} = \frac{\int_0^{t_B} (P/P_0) dt}{\int_0^{t_B} dt} = 1 - \frac{2\phi(x/L)^2 A_t^2}{A(A - 4\pi N r R_0 t_B)} \quad \dots \quad (6)$$

The space time average is

$$\overline{P/P_0} = \frac{\int_0^{t_B} \int_0^L (P/P_0) dx dt}{\int_0^{t_B} \int_0^L dx dt} = 1 - \frac{2\phi}{3A} \frac{A_t^2}{(A - 4\pi N r R_0 t_B)} \quad \dots \quad (7)$$

Kershner has illustrated the variation of P/P_0 with x/L for a given value of A_t/A_p , i.e., at a particular instant. Fig. 1 illustrates the variation of P/P_0 with time for $x/L)^2 = 0.95$ for 2.25" rocket motor (Appendix II).

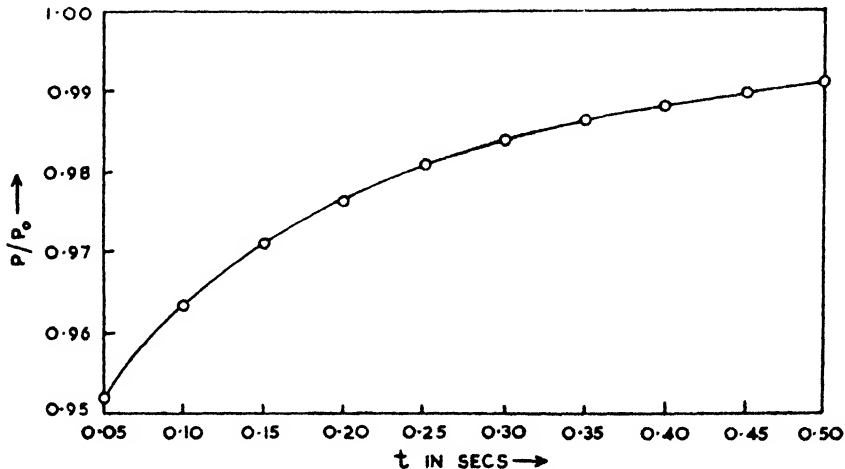


FIG. 1. Variation of P/P_0 with t in 2.25" rocket motor at $(x/L)^2 = 0.95$.

VARIATION OF C'_D/C_D

For low values of (A_t/A_p) Kershner gives:—

$$\left(\frac{C'_D}{C_D}\right) = 1 - \phi(A_t/A_p)^2 \quad \dots \quad (8)$$

This may be expressed as a function of time by substituting for A_p from the appendix:—

$$\left(\frac{C'_D}{C_D}\right) = 1 - \phi \frac{A_t^2}{(b+ct)^2} \quad \dots \quad (9)$$

The time average is given by:—

$$\left(\frac{C'_D}{C_D}\right) = 1 - \frac{\phi}{A} \frac{A_t^2}{(A - 4\pi N r R_0 t_B)} \quad \dots \quad (10)$$

The variation of $\left(\frac{C'_D}{C_D}\right)$ with time for 2.25" rocket motor is illustrated in Table I and Figure 2.

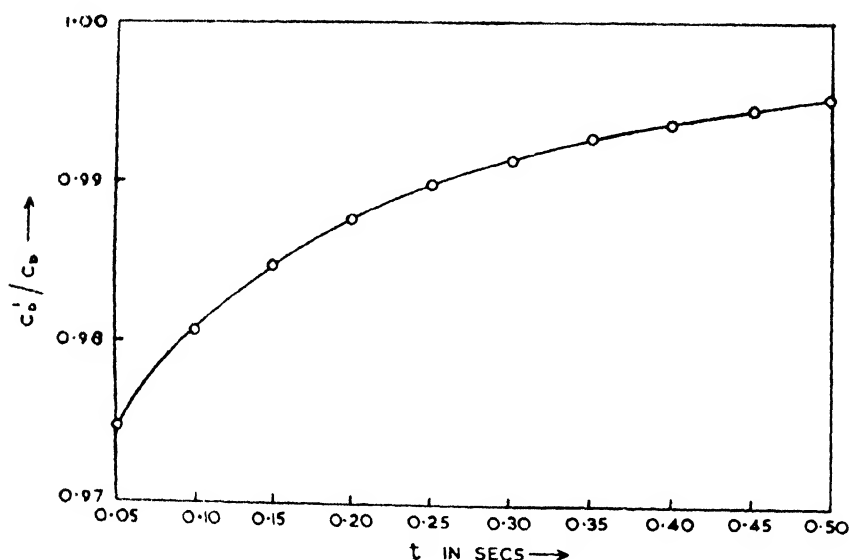


FIG. 2. Variation of C'_D/C_D with time in 2.25" rocket motor.

TABLE I

Variation of (C'_D/C_D) with time for 2.25" Rocket Motor

t in secs.	0.05	0.1	0.15	0.20	0.25	0.3	0.35	0.4	0.45	0.5
$\left(\frac{C'_D}{C_D}\right)$.9746	.9806	.9847	.9876	.9898	.9914	.9927	.9937	.9945	.9952

VARIATION OF u^2/bT

The function u^2/bT where u is the gas velocity and T the temperature of gases is of much use in internal ballistics of rockets. Wimpers (1950) gives the following relation between u^2/bT and P/P_0

$$(u^2/bT) = (P_0 - P)/P = (1 - P/P_0)/(P/P_0)$$

If we now use the relation (3) given above and the relation (1A) given in the Appendix I to this paper, we get that

$$\begin{aligned} u^2/bT &= \frac{2\phi(x/L)^2}{\left(\frac{A_p}{A_t}\right)^2 - 2\phi(x/L)^2} \\ &= \frac{2\phi(x/L)^2}{\left(\frac{b+ct}{A_t}\right)^2 - 2\phi(x/L)^2} \quad \dots \quad \dots \quad \dots \quad (11) \end{aligned}$$

This relation is not valid at $x = L$ because there the relation between u^2/bT and P/P_0 given by Wimpres (1950) is no longer true (Kershner, 1944).

VARIATION OF TEMPERATURE OF PROPELLANT GASES

Similarly the temperature of propellant gases related to u^2/bT by the well-known relation

$$T/T_0 = \left\{ 1 + \frac{\gamma-1}{2\gamma} \frac{u^2}{bT} \right\}^{-1} \quad \dots \quad \dots \quad \dots \quad (12)$$

can be put in the form

$$T/T_0 = \left\{ 1 + \frac{\gamma-1}{2\gamma} \frac{2\phi(x/L)^2}{\left\{ (b+ct)/A_t \right\}^2 - 2\phi(x/L)^2} \right\}^{-1} \quad \dots \quad \dots \quad (13)$$

VARIATION OF GAS VELOCITY

We have

$$u = (u^2)^{\frac{1}{2}} = \left[\frac{u^2}{bT} \cdot \frac{T}{T_0} bT_0 \right]^{\frac{1}{2}}$$

Hence

$$(u/\sqrt{bT_0}) = \frac{\left[\frac{2\phi(x/L)^2}{\left\{ (b+ct)/A_t \right\}^2 - 2\phi(x/L)^2} \right]^{\frac{1}{2}}}{\left[1 + \frac{\gamma-1}{2\gamma} \frac{2\phi(x/L)^2}{\left\{ (b+ct)/A_t \right\}^2 - 2\phi(x/L)^2} \right]^{\frac{1}{2}}} \quad \dots \quad \dots \quad (14)$$

Figure 3 and Figure 4 illustrate the variation of $u/\sqrt{bT_0}$ with x/L and t for $t = 0.1$ secs. and $(x/L)^2 = 0.95$ for 2.25" rocket motor (Appendix II).

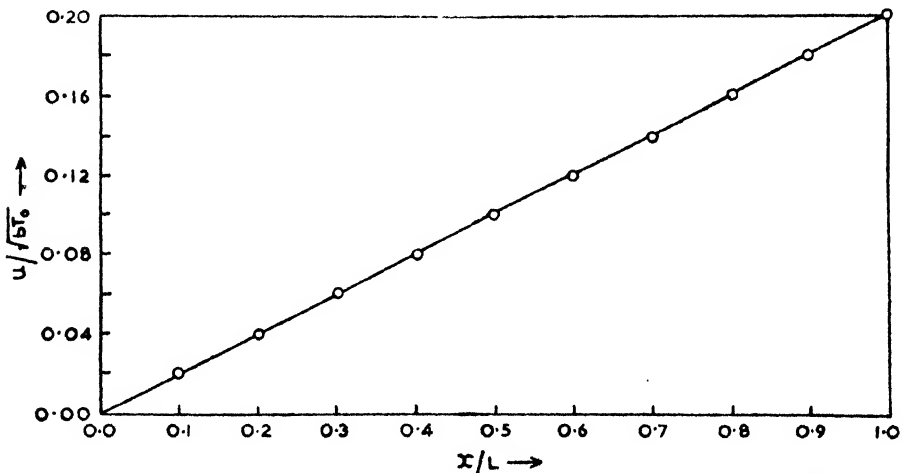


FIG. 3. Variation of $u/\sqrt{bT_0}$ with x/L for 2.25" rocket motor at $t = 0.1$ sec.

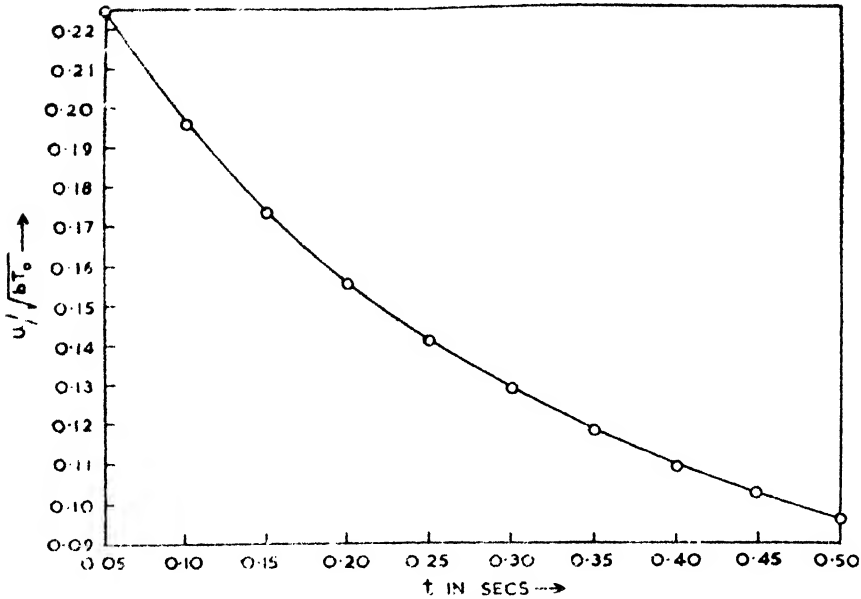


FIG. 4. Variation of $u/\sqrt{bT_0}$ with t for 2.25" rocket motor at $(x/L)^2 = 0.95$.

VARIATION OF REDUCED MASS VELOCITY

The mass velocity G and the critical mass velocity G^* to produce unit Mach number are given (Green, 1954) by

$$\frac{P}{P_0} = \frac{1}{(\gamma+1)} + \frac{\gamma}{(\gamma+1)} \left[1 - 2 \left(\frac{\gamma+1}{\gamma} \right) \frac{bT_0}{P_0^2} G^2 \right]^{\frac{1}{2}} \quad \dots \quad (15)$$

and

$$G^* = \left[\frac{\gamma}{\gamma+1} \cdot \frac{P_0^2}{2bT_0} \right]^{\frac{1}{2}} \quad \dots \quad (16)$$

Combining (15) and (16) we get

$$\frac{G}{G^*} = \left[1 - \left\{ \frac{\gamma+1}{\gamma} \left(\frac{P}{P_0} - \frac{1}{\gamma+1} \right) \right\}^2 \right]^{\frac{1}{2}} \quad \dots \quad (17)$$

Using eqn. (4) we get

$$\begin{aligned} \frac{G}{G^*} &= \left[1 - \left\{ \frac{\gamma+1}{\gamma} \left(\frac{\gamma}{\gamma+1} - 2\phi \cdot \frac{At^2(x/L)^2}{(b+ct)^2} \right) \right\}^2 \right]^{\frac{1}{2}} \\ &= \left[1 - \left\{ 1 - \frac{\theta At^2(x/L)^2}{(b+ct)^2} \right\}^2 \right]^{\frac{1}{2}} \quad \dots \quad (18) \end{aligned}$$

where $\theta = \left(\frac{2}{\gamma+1} \right)^{2(\gamma-1)}$

VARIATION OF EROSION RATIO

Several expressions for the dependence of erosion ratio ϵ on the gas velocity have been proposed. The expression first proposed on the basis of British

experiments with double base propellants relates the erosion ratio ϵ to the linear gas velocity

$$\epsilon = 1 + k_u u \quad \dots \quad (19)$$

Another commonly used expression is

$$\epsilon = 1 + k_1 \frac{u}{a_0} \quad \dots \quad (20)$$

where a_0 is the sound velocity.

Some experiments have suggested the existence of a threshold velocity u_0 for erosion, i.e.

$$\epsilon = 1 \text{ for } u \leq u_0 \quad \dots \quad (21A)$$

$$\epsilon = 1 + k_0(u - u_0) \text{ for } u > u_0 \quad \dots \quad (21B)$$

Aerojet Report No. 445 (1950) suggests

$$\epsilon = 1 + k_G G \quad \dots \quad (22)$$

On the basis of careful experiments and analysis Green (1954) finds best agreement with experiment when the erosion ratio is correlated to the reduced mass-velocity by the relations

$$\epsilon = 1 \text{ for } \frac{G}{G^*} \leq \left(\frac{G}{G^*} \right)_0 \quad \dots \quad (23A)$$

$$\epsilon = 1 + k \left\{ \frac{G}{G^*} - \left(\frac{G}{G^*} \right)_0 \right\} \text{ for } \frac{G}{G^*} > \left(\frac{G}{G^*} \right)_0 \quad \dots \quad (23B)$$

where $\left(\frac{G}{G^*} \right)_0$ is the threshold reduced mass velocity for erosion. The average values of k and $(G/G^*)_0$ for a number of propellants are 0.8 and 0.15 ± 0.05 respectively.

The space-time variation of erosion ratio is given by

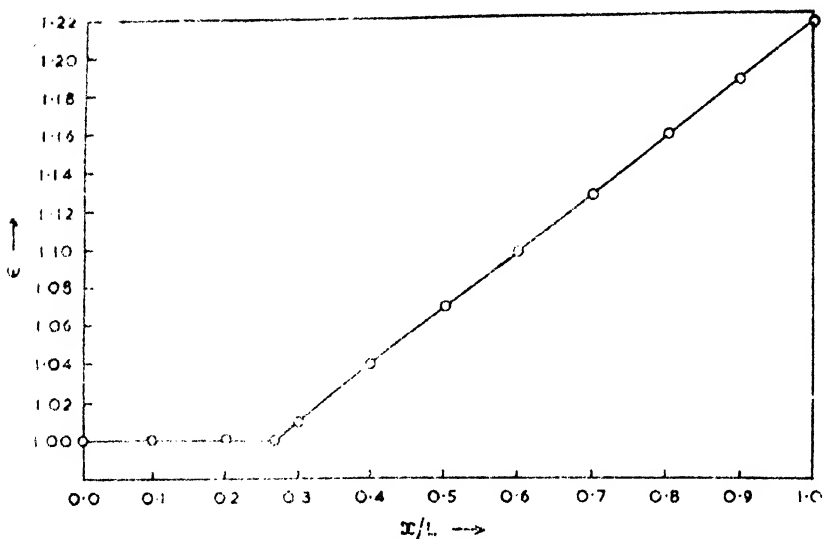
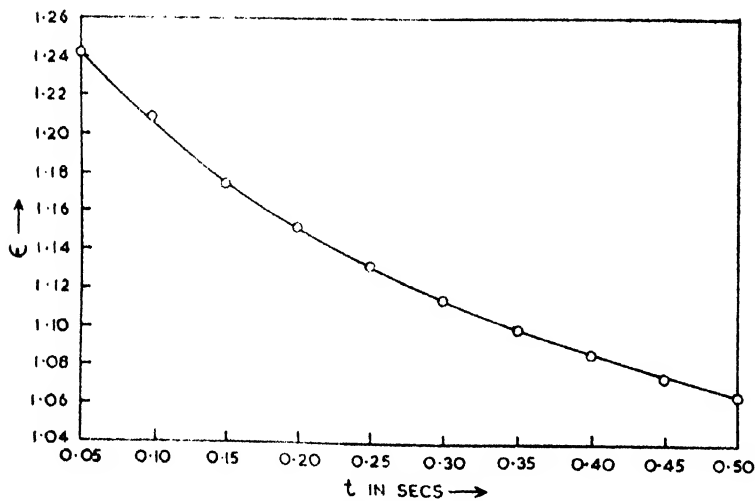
$$\epsilon = 1 \text{ for } \frac{G}{G^*} \leq \left(\frac{G}{G^*} \right)_0 \quad \dots \quad (24A)$$

$$\epsilon = 1 + k \left[1 - \left\{ 1 - \frac{\theta A_t^2 (x/L)^2}{(b+ct)^2} \right\}^{\frac{1}{2}} - k \left(\frac{G}{G^*} \right)_0 \right]$$

for

$$\frac{G}{G^*} > \left(\frac{G}{G^*} \right)_0 \quad \dots \quad (24B)$$

Figs. 5 and 6 illustrate the variation of ϵ with (x/L) and t for $t = 0.1$ secs. and $(x/L)^2 = 0.95$ in the case of 2.25" rocket motor, taking $(G/G^*)_0 = 0.1$ and $k = 0.8$.

FIG. 5. Variation of ϵ with x/L for 2.25" rocket motor at $t = 0.1$ sec.FIG. 6. Variation of ϵ with t for 2.25" rocket motor at $(x/L)^2 = 0.95$.

VARIATION OF RATE OF BURNING

The rate of burning (Wimpress, 1950) is given by

$$\frac{r}{r_0} = \epsilon \left(\frac{p}{p_0} \right)^n \quad \dots \quad (25)$$

Hence

$$\frac{r}{r_0} = \left\{ 1 - \frac{2\phi A_t^2 (x/L)^2}{(b+ct)^2} \right\}^n \quad \text{for} \quad \left(\frac{G}{G^*} \right) < \left(\frac{G}{G^*} \right)_0 \quad \dots \quad (26A)$$

and

$$\frac{r}{r_0} = \left\{ 1 - \frac{2\phi A_t^2 (x/L)^2}{(b+ct)^2} \right\}^n \times \left[1 + k \left\{ 1 - \left(1 - \frac{\theta A_t^2 (x/L)^2}{(b+ct)^2} \right)^2 \right\}^{\frac{1}{2}} - k \left(\frac{G}{G^*} \right)_0 \right]$$

for

$$\frac{G}{G^*} > \left(\frac{G}{G^*} \right)_0 \quad \dots \quad \dots \quad \dots \quad \dots \quad (26B)$$

Figs. 7 and 8 illustrate the variation of $\frac{r}{r_0}$ with x/L and t for $t = 0.1$ secs. and $(x/L)^2 = 0.95$ in the case of 2.25" rocket motor (Appendix II).

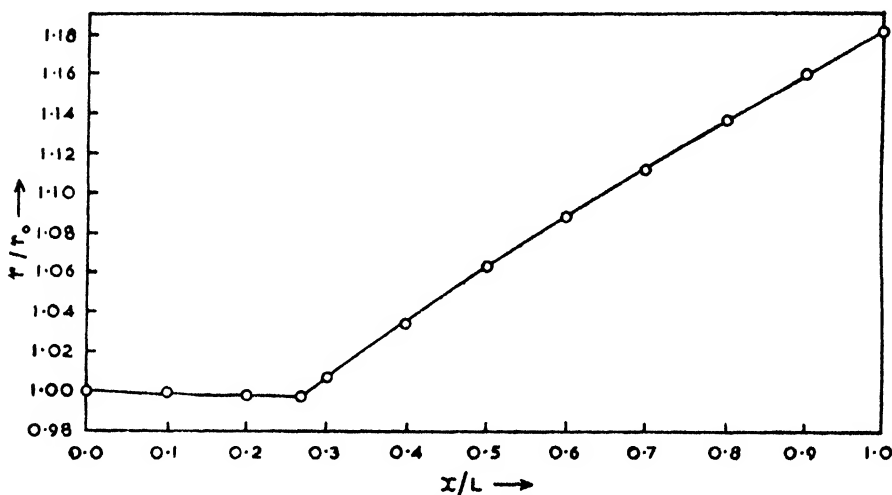


FIG. 7. Variation of r/r_0 with x/L for 2.25" rocket motor at $t = 0.1$ sec.

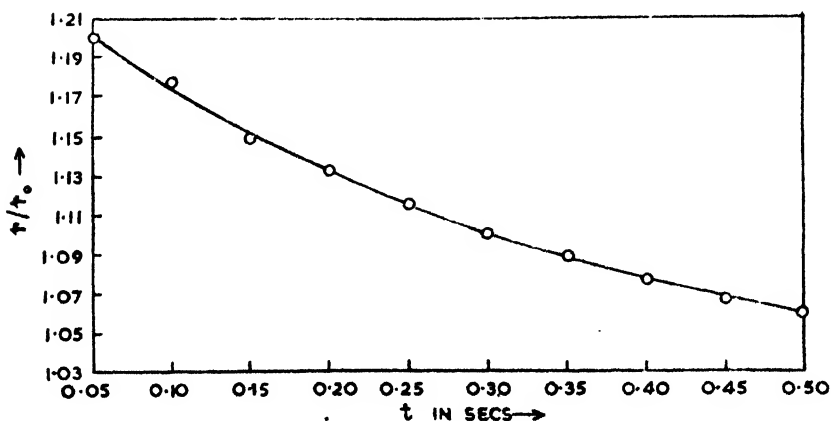


FIG. 8. Variation of r/r_0 with t in 2.25" rocket motor at $(x/L)^2 = 0.95$.

ACKNOWLEDGEMENTS

The authors are extremely grateful to Dr. D. S. Kothari and Dr. R. S. Varma for their kind interest in the investigation. They are also thankful to Shri Askaran Mehta and Shri K. C. Chaturvedi for helpful discussion.

SUMMARY

The authors have derived and discussed expressions for the pressure, temperature, gas-velocity, mass-velocity, erosion ratio and rate of burning as functions of distance x , from the head-end along the length and time t after ignition in a rocket motor chamber, using tubular or multitubular propellants.

REFERENCES

- Aerojet Report No. 445 (1950). Aerojet General Corporation, Azusa, California, June 23.
 Crawford, B. L. Jr. (1944). Rocket Fundamentals (N.D.R.C. Division 3, Section II. OSRD No. 3711, June 12, (Kershner, Chapter 3)).
 Green, Leon Jr. (1954). Jet Propulsion, 24, 9.
 Wimpers, R. N. (1950). Internal Ballistics of Solid Fuel Rockets, McGraw Hill Book Co., New York.

APPENDIX I

PORT AREA AT ANY INSTANT

Consider a rocket motor of internal area A , having N tubular propellants of burning thickness d . If the rate of burning is r , the thickness after time t is $d - 2rt$. Hence, the port area A_p at any instant is given by

$$A_p = A - 2\pi NR_0(d - 2rt) \quad \dots \quad (1)$$

where R_0 is the mean radius which remains constant throughout burning. Eqn. (1) may be expressed as

$$A_p = b + ct \quad \dots \quad (1A)$$

where $b = A - 2\pi NR_0d$ and $c = 4\pi NrR_0$. If t_B is the time of burning $d = 2rt_B$ and hence $b + ct_B = A$.

APPENDIX II

2.25" ROCKET MOTOR MARK 9

Wimpers (1950) gives the following specifications for 2.25" Rocket Motor Mark 9 -

Inside Diameter	= 2.01"
Nozzle Throat Area	= 0.479 in. ²
Length of Propellant Grain	= 11.5"
External Diameter of Propellant Grain	= 1.7"
Internal Diameter of Propellant Grain	= 0.6"

If the propellant used is J.P.N. ballistite, calculations show $\bar{r} \approx .55$ " / sec. and $t_B \approx 0.5$ secs. at an ambient temperature of 70°F. Further

$$b = 1.18 \text{ in.}^2$$

$$c = 3.98 \text{ in.}^2/\text{sec.}$$

For J.P.N. ballistite $\gamma = 1.20$, hence

$$\phi = 0.2103$$

$$\theta = 0.3855$$

Tables II and III illustrate the variation of P/P_0 , u^2/bT , T/T_0 , $u/\sqrt{bT_0}$, G/G^* , ϵ and r/r_0 with (x/L) and t for $t = 0.1$ secs. and $(x/L)^2 = 0.95$ for $2.25''$ rocket.

TABLE II

Variation of P/P_0 , u^2/bT , T/T_0 , $u/\sqrt{bT_0}$, G/G^ , ϵ and r/r_0 with x/L for $2.25''$ rocket motor at $t = 0.1$ sec.*

x/L	P/P_0	u^2/bT	T/T_0	$u/\sqrt{bT_0}$	G/G^*	ϵ	r/r_0
0.0	1.00000	0.00000	0.00000	0.00000	0.0000	1.0000	1.0000
0.1	0.99961	0.00039	0.99997	0.01975	0.0407	1.0000	0.9997
0.2	0.99844	0.001563	0.99987	0.03953	0.0755	1.0000	0.9989
0.266	0.99723	0.1000	1.0000	0.9981
0.3	0.99650	0.003512	0.99971	0.05925	0.11225	1.00980	1.0073
0.4	0.99380	0.00624	0.99948	0.07899	0.1500	1.0400	1.0355
0.5	0.99020	0.0099	0.99917	0.09945	0.1884	1.07072	1.0635
0.6	0.98605	0.01415	0.99882	0.11874	0.2241	1.09928	1.0886
0.7	0.98101	0.01936	0.99839	0.13893	0.2615	1.1292	1.1143
0.8	0.97520	0.02543	0.99788	0.15937	0.2978	1.1582	1.1383
0.9	0.96861	0.03241	0.99730	0.17972	0.3342	1.1874	1.1615
1.0	0.96125	0.04031	0.99644	0.20050	0.3699	1.2160	1.1833

TABLE III

Variation of P/P_0 , u^2/bT , T/T_0 , $u/\sqrt{bT_0}$, G/G^ , ϵ and r/r_0 with time in case of $2.25''$ rocket motor for $(x/L)^2 = 0.95$*

t in secs.	P/P_0	u^2/bT	T/T_0	$u/\sqrt{bT_0}$	G/G^*	ϵ	r/r_0
0.05	0.95180	0.0506	0.9958	0.2254	0.4021	1.2417	1.2001
0.10	0.96319	0.0382	0.9968	0.1957	0.3610	1.2088	1.1780
0.15	0.97100	0.0299	0.9975	0.1732	0.3110	1.1733	1.1497
0.20	0.9765	0.0241	0.9980	0.1552	0.2891	1.1513	1.1325
0.25	0.9806	0.0198	0.9983	0.1407	0.2640	1.1312	1.1159
0.30	0.9837	0.0166	0.9986	0.1288	0.2423	1.1138	1.1012
0.35	0.9862	0.0140	0.9988	0.1183	0.2232	1.0986	1.0881
0.40	0.9881	0.0120	0.9990	0.1095	0.2076	1.0861	1.0771
0.45	0.9896	0.0105	0.9991	0.1025	0.1939	1.0751	1.0674
0.50	0.9909	0.0092	0.9992	0.0959	0.1814	1.0651	1.0584

OBSERVATIONS ON THE ATRIOVENTRICULAR CONDUCTING (CONNECTING) SYSTEM OF THE HEART OF HUMAN TWINS OBTAINED FROM AN ABORTED FOETUS *

by RAVI PRAKASH, *Department of Zoology, Government College, Ajmer* †

(Communicated by K. N. Bagchi, F.N.I.)

(Received March 11; read May 7, 1954)

INTRODUCTION

Kent (1893) believed that in the heart of cold blooded animals (fish, amphibia and reptiles) a perfect muscular continuity exists between atria and the ventricles. On this assumption he maintained that in the mammalian heart also there is no break or interval in the atrioventricular connexions and that the fibres sweep uninterruptedly through from atria to ventricles. According to Kent (1893) the number of such fibres between atria and ventricles is much larger in foetal hearts than in the hearts of adult mammals. Subsequent investigators, however, failed to confirm Kent. Keith and Flack (1906) stated, 'In short, all the evidence we have been able to collect from human and comparative anatomy, from embryology, physiology and pathology, substantiates the theory that the muscular bundle which perforates the central fibrous body of the heart and connects together its atrial and ventricular parts, is the sole path by which the atrial wave of contraction passes to, and is distributed within the ventricles.' Kistin (1949) also reported the absence of multiple connexions of Kent in the normal human hearts. He observed an atrioventricular bundle (bundle of His) at the cephalic end of the atrioventricular septum for conducting the cardiac stimulus to contraction from atria to ventricles. Prakash (1953, 1954a, b, c) on the basis of his studies on the heart of vertebrates derives the following conclusions: (1) The 'break' denied by Kent in the atrioventricular muscular continuity of lower vertebrates and mammals exists in both, (2) an atrioventricular plug in fishes and tadpoles of frog and an atrioventricular bundle in mammals and birds are present at the atrioventricular junction of the heart and that these structures only afford the necessary pathway through which cardiac impulse will pass from atria to ventricles, (3) the occurrence of multiple connexions of Kent in mammalian heart will cause anomalous atrioventricular excitations (Wolff-Parkinson-White syndrome). These conclusions (specially the last one) require serious consideration. Moreover, Keith and Flack (1906), Kistin (1949) and Prakash (1954b) all have contradicted Kent (1893) as far as the hearts of newly born and adult mammals are concerned but to verify Kent's findings further, a study of foetal hearts is also desirable.

In the present investigation the atrioventricular conducting (connecting) system of the heart of human twins has been studied and described. The twins were obtained from an aborted foetus after about five months of pregnancy.

MATERIAL AND METHODS

The hearts after being removed from the twins of the aborted foetus were fixed in Bouin's picroformol. Blocks were prepared according to paraffin embedding

* Contribution No. 10 from the Department of Zoology, Government College, Ajmer.

† Now Head of Department of Zoology, Government Hamidia College, Bhopal,

method and serially sectioned at 8μ . The sections were stained with acid fuchsin. Although a complete serial of sections was obtained of the heart of one of these twins, from the heart of the other only scattered sections could be mounted. The serial of the first heart included all the sections through the atrioventricular junction and as such the anatomy of the atrioventricular node, the atrioventricular bundle and of the limbs of the bundle, was easily studied. However, these observations were confirmed by having a look over the scattered sections of the second heart. As far as the author could ascertain the structure and disposition of the atrioventricular conducting tissue resembled in the hearts of the twins.

OBSERVATIONS

Atrioventricular node (Node of Tawara): It lies as a well-marked and distinct structure on the right lateral border of the interventricular septum at a little distance from its cephalic end (Fig. 1). It can be located in the tissue lying between the right atrium and the ventricular septum. The node is easily distinguishable in cross-sections because of its circumscribed character. The atrial fibres penetrate freely at the dorsal and cephalic portions of the node. The atrioventricular node at its caudal side receives fibres from the interventricular septum. Ventrally the fibres from the node extend into the body of the atrioventricular bundle (bundle of His) which is situated just beneath the node on the interventricular septum.

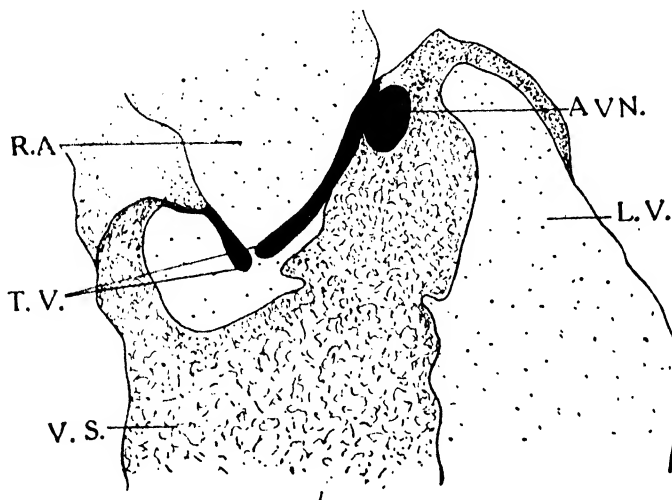


FIG. 1. Diagram of the longitudinal section of the heart passing through the atrioventricular node (Node of Tawara). Approx. $\times 22$.

The fibres constituting the node are comparatively large but are very fine and narrower than those present in the atria or on the ventricular septum. These fibres of the node are crossing each other so as to look like cells in longitudinal sections. A number of nuclei are also present in the node. The fibres and the nuclei of the node resemble, in their general histological character, those described in the atrioventricular nodes of the rat (Prakash, 1954b) and the fowl (Prakash, unpublished). Almost similar histological peculiarities have been mentioned for Purkinje fibres by various authors (Purkinje, 1845; Davies, 1930 and Kistin, 1949).

Atrioventricular bundle (Bundle of His): In serial sections it appears as if the bundle of His is arising from the mid-ventral region of the atrioventricular node. After taking its origin from the node, the bundle proceeds upwards towards the

cephalic portion of the interventricular septum. The free cranial portion of this ventricular septum is membranous and is also curved so as to assume rather a sickle-shaped appearance (Gray, 1949). Because of its curved nature, this part of the septum intervenes not only between the right and the left portions of the ventricle but also between the right atrium and the left ventricle. The bundle of His which is present in close association with this portion of the septum thus occupies an important intermediate position between the right atrium and the left ventricle on the one hand and between the right and left ventricles on the other. Due to this the cardiac stimulus to contraction which is being transmitted from the right atrium will have no other probable pathway except that through the bundle of His to reach either of the ventricles.

Immediately before the interventricular septum is curved cranially, it is continuous at its right lateral surface with the caudal portion of the interatrial septum. As the bundle of His extends across this area (Fig. 2) it is sure to pick up the impulses from the interatrial septum also before they are conducted to the ventricles.

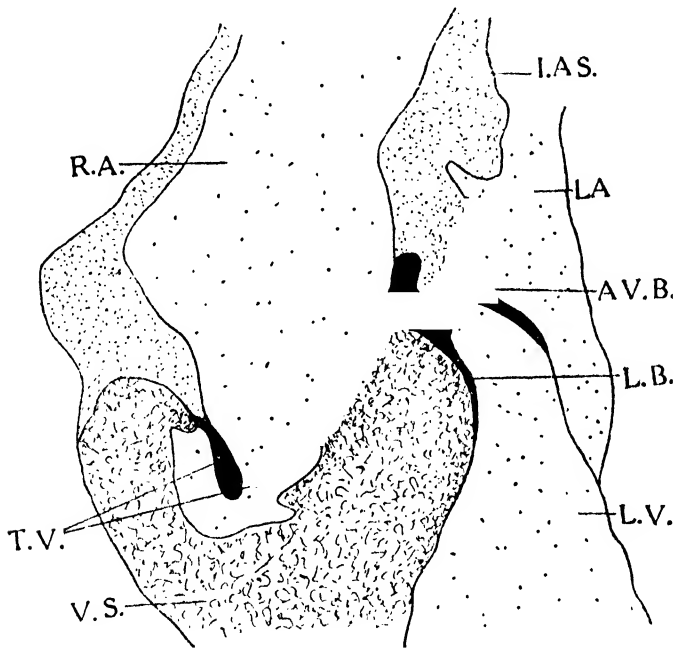


FIG. 2. Diagram of the longitudinal section of the heart to show the atrioventricular bundle (bundle of His) and its left branch. Approx. $\times 22$.

The fibres of the bundle are rather thicker and are more compactly interlaced than the fibres of the atrioventricular node. The cells which are formed by the intercrossing of the fibres appear to be thick-walled and show prominent nuclei. The whole structure takes a deep stain with acid fuchsin showing its special histological nature.

A considerable amount of connective tissue is present between the atria and the ventricles particularly in the region of the free membranous portion of the interventricular septum. The bundle of His extends over this connective tissue and proceeds forwards to reach the cephalic end of the ventricular septum. At this point the bundle of His bifurcates to form a right and a left limb. These limbs immediately descend on to the respective sides of the ventricular septum. The right limb which is a continuation of the bundle itself at its caudal end proceeds downwards to reach the base of the tricuspid valve. It appears as if the fibres of

the limb are extending into the component of the medial cusp of the tricuspid valve. Davies and Francis (1946) believe that due to functional requirement it is only in the avian heart that the right muscular valve receives a special early branch from the right limb of the bundle. According to these authors in mammals where the corresponding valve (tricuspid) is fibrous such a continuity between the fibres of the limb of the bundle and the valve is not necessary. To verify the validity of such an assertion further investigation is desirable.

The left limb of the bundle travels downwards a relatively long distance along the left side of the interventricular septum. Afterwards its fibres become indistinguishable from those of the septum. A thick band of Purkinje fibres arises from beneath the cranial portion of the atrioventricular bundle and proceeds across the left ventricular cavity to become continuous with the fibres of the ventricular wall (Fig. 2).

In none of the sections a direct continuity between the atrial and ventricular fibres of the heart was observed. The disposition of the bundle of His as revealed by the present study is such that the atrial wave of contraction is sure to be picked up by the bundle before it is distributed within the ventricles. The atrioventricular gap is bridged over by the bundle of His and the atrioventricular node.

DISCUSSION

The object of this research had been to find out if in the heart of human embryos the atria are connected to the ventricles directly or through an atrioventricular bundle only. The present investigation confirms the absence of multiple atrioventricular connexions of Kent (1893) and points out that in the foetal hearts also as in the hearts of newly born and adult mammals (Kistin, 1949; Prakash, 1954b) there exists a constant muscular atrioventricular bundle at the atrioventricular junction of the heart. The bundle of His is the only connecting tissue between the atria and the ventricles, and as such plays an important rôle in transmitting the cardiac stimulus to contraction from the former chamber to the latter. The clinical importance of the bundle becomes all the more greater because now it is apparent that if it is cut or damaged the atria will have no connexion with the ventricles and the atrial stimulus to contraction will fail to reach the ventricles. There will be no co-ordination in atrial and ventricular contractions and disturbances of rhythm may arise leading to partial or complete heart block. Keith and Flack (1906) also emphasised this and further maintained that the bundle passes along the upper margin of the interventricular septum because it is the least disturbed part during systolic changes of the heart.

The absence or otherwise of the multiple muscular connexions between atria and ventricles rather assumes special significance in the light of the observations of Davies (1930) who found in birds the bundle of His as well as the multiple connexions of Kent. He correlated this with functional requirements of the avian heart and remarked that due to the rapid rate of heartbeat in birds, a rapid diffusion of the impulse through different cardiac chambers is necessary and hence the presence of both the bundle of His and the multiple connexions of Kent to act as transmitting apparatus. This means that multiple connexions are desirable in birds where they serve as accessory pathways in addition to the bundle of His, for conveying the cardiac stimulus of contraction from atria to ventricles. In mammals as the rate of heartbeat is comparatively slow a quick transmission of the impulse from atria to ventricles is to be prevented but if multiple atrioventricular connexions are present the atrial wave of contraction is bound to reach the ventricle much earlier than has hitherto been noted in normal hearts without such connexions. In those hearts where the bundle of His is the sole transmitting apparatus for the cardiac stimulus between atria and ventricles, because of the peculiar structure of the bundle (Prakash, 1954b) sufficient time elapses between the atrial and ventricular

contractions. This 'pause' or delay in the passage of the impulse allows the ventricle to be filled completely with blood before it in turn begins to contract (Prakash, 1954b) and thus checks premature excitation of the ventricle. The absence of any other connexion other than through the bundle of His in foetal hearts also thus confirms the view that anomalous atrioventricular excitation (Wolff-Parkinson-White syndrome) may be due to accessory pathways at the atrioventricular bridge.

The right atrioventricular valve in mammals is membranous while the corresponding valve in birds is muscular. Davies and Francis while referring to the avian heart (1946) stated 'To prevent regurgitation of blood into the right atrium, it is necessary that this muscular valve should contract at the *outset* of ventricular systole, and it is noteworthy that a special early branch from the right limb of the A.V. bundle (the branch erroneously homologised by Drennan (1927) with the mammalian right limb) passes directly into the valve and becomes continuous with its musculature'. The present investigation reveals that in the heart of mammals also the right limb of the bundle proceeds towards the base of the tricuspid valve to enter into the component of its medial cusp. However, further study specially of the adult human heart is desirable to decide whether Drennan was right or wrong to homologise this branch of the atrioventricular bundle of the bird's heart with the right limb of the mammalian bundle of His.

Kistin (1949) for the first time drew attention to the two different interpretations of the term 'Purkinje fibres'. One view is that only those fibres of the heart should be designated as Purkinje fibres which resemble in their microscopical characteristics the fibres first described by Purkinje (1845) in sheep and other mammals. While some authors (Tawara, 1906) believe that the fibre component of the atrioventricular connecting tissue may be regarded to be of Purkinje type irrespective of its histological nature. Tawara (1906) also stated that the fibres described by Purkinje (1845) and the bundle demonstrated by His (1893) are parts of a single atrioventricular conducting system which is involved in the conduction of the cardiac stimulus from atria to ventricles. Kistin (1953) in a private communication to the author informed that Purkinje's paper does not assign any conduction function to the fibres now known as Purkinje fibres.

It has been observed by the author in the hearts of rats (Prakash, 1954b) and fowls (Prakash—unpublished) that continuous tracts of 'Purkinje fibres' (fibres resembled those described by Purkinje) exist at the junctional sites of the various cardiac chambers. Specially a thick band of Purkinje fibres was seen to connect the caudal ends of the atrial septum and the atrioventricular node which suggested that the impulse travels from the septum along this band to reach the node. Moreover, it has been seen that as in the hearts of the fowl and the rat so also in the heart of human embryos, the node of Tawara and the bundle of His are composed of Purkinje fibres. And as it has now been established that the node and the bundle are the only structures to convey the cardiac stimulus from atria to ventricles and that they consist of 'Purkinje fibres', there seems to be sufficient basis to believe that 'Purkinje fibres' are impulse-conducting fibres.

SUMMARY

1. The anatomy of the atrioventricular conducting (connecting) tissue resembles in the heart of twins.
2. Multiple muscular atrioventricular connexions of Kent are absent in the heart of human embryos also. It is argued that these accessory connexions, if present in the heart of mammals, may be responsible for anomalous atrioventricular excitations (Wolff-Parkinson-White syndrome).
3. Views regarding the atrioventricular bundle to be the only connexion between atria and ventricles for the propagation of the cardiac stimulus to contraction in mammalian heart have been confirmed and expanded.
4. Evidence has been produced to show that 'Purkinje fibres' form an integral part of the impulse conducting tissue.

ACKNOWLEDGEMENT

I am specially indebted to Dr. P. N. Mathur, Professor of Zoology, Government College, Ajmer, for giving me an opportunity to study this material and for guidance. I wish to express my gratitude to Mr. V. V. John, Principal, Government College, Ajmer, for providing me with facilities in connexion with this investigation.

REFERENCES

- Davies, F. (1930). The conducting system of the bird's heart. *J. Anat. Lond.*, **64**, 129.
 Davies, F. and Francis, E. T. B. (1946). The conducting system of the vertebrate heart. *Biol. Rev. Cambridge*, **21**, 173, 182.
 Drennan, M. R. (1927). The auriculo-ventricular bundle in the bird's heart. *Brit. Med. J.*, **1**, 321.
 Gray's Anatomy (1949). Thirtieth edition edited by T. B. Johnston and J. Whillis, p. 155.
 His, W. Jr. (1893). *Arbeit. Anat. med-klinik zu Leipzig*, p. 14.
 Keith, A. and Flack, M. W. (1906). The auriculoventricular bundle of the human heart. *Lancet*, **2**, 35.
 Kent, A. F. S. (1893). Researches on the structure and function of the mammalian heart. *J. Physiol.*, **14**, 233.
 Kistin, A. D. (1949). Observations on the anatomy of the atrioventricular bundle (bundle of His) and the question of other muscular atrioventricular connexions in normal human hearts. *Am. Heart. J.*, **37**(6), 849.
 Kistin, A. D. (1953). Private communication.
 Prakash, R. (1953). The heart of the common Indian catfish, *Heteropneustis fossilis* (Bloch). *Proc. Zool. Soc. Bengal*, **6**(2), 113.
 ——— (1954a). The heart and its conducting system in the tadpoles of the frog, *Rana tigrina* Daud. *Proc. Zool. Soc. Bengal*, **7**(1) (in press).
 ——— (1954b). The heart of the rat (*Rattus rattus rufescens* Gray) with special reference to the conducting system. *Am. Heart. J.*, **47**(2), 241.
 ——— (1954c). Evolution in the conducting system of the vertebrate heart. *Ind. Med. J.*, July, 1954, 164.
 ——— (unpublished). The heart and its conducting system in the common Indian fowl, *Gallus domesticus*.
 Purkinje, J. E. (1815). Mikroskopisch neurologische Beobachtungen. *Arch. f. Anat. Physiol. u. wissenschaft. Med.*, 281.
 Tawara, S. (1906). Das Reitzleitungssystem des Säugetierherzens, *Jena*, 1906, Gustav Fischer.

ABBREVIATIONS

- A.V.B. — Atrioventricular bundle.
 A.V.N. — Atrioventricular node.
 I.A.S. — Interatrial septum.
 L.A. — Left atrium.
 L.B. — Left branch of the bundle of His.
 L.V. — Left ventricular cavity.
 R.A. — Right atrium.
 T.V. — Tricuspid valve.
 V.S. — Interventricular septum.

Issued December 7, 1954.

BACTERIOLOGY OF INSHORE SEA WATER AND OF MACKERELS OFF TELLICHERRY (MALABAR) *

by R. VENKATARAMAN and A. SREENIVASAN, *Fisheries Technological Station,
Kozhikode, Madras State*

(Communicated by B. S. Bhimachar, F.N.I.)

(Received April 26 ; read August 6, 1954)

INTRODUCTION

The bacterial flora of marine fish and of sea water has been studied all the world over with a view to explain the spoilage of fish and to control or prevent spoilage by the application of suitable techniques of preservation. The importance of various groups of bacteria can be assessed chiefly on the basis of their biochemical activities such as liquefaction of gelatin, peptonization of milk and production of indole, hydrogen sulphide, etc. (Snow and Beard, 1939; Shewan, 1949; Castell and Mapplebeck, 1952).

Most of the work on fish spoilage has been carried out on marine fish. The existence of specific 'marine' bacteria has been postulated by ZoBell and co-workers (ZoBell, 1946; ZoBell and Conn, 1940; ZoBell and Upham, 1944) and quite recently Canadian workers also support this hypothesis (McLeod *et al.*, 1953). It has been pointed out that gram negative types predominate in marine water in contrast to gram positive soil types. Wood (1950a) on the other hand considers the existence of specific 'marine' bacteria to be doubtful but believes in a gradation from soil forms through estuarine to gram negative marine flora. His further work (1950b) has shown that the flora (of shark) may be regarded as a modified marine flora in which the gram positive elements have been enriched and the gram negative ones are of little importance. Burke (1934) is of the view that there is an interchange of bacteria between the sea and fresh water. The question of occurrence or not of coliform bacteria in sea water and in guts of fish has been reviewed by Griffiths (1937). Coliforms are not normally inhabitants of the digestive tracts of marine fish from unpolluted areas (Gibbons, 1934 cited by Griffiths, *loc. cit.*).

MATERIAL AND METHODS

The samples were collected off Tellicherry in Malabar. The surface inshore water samples were collected 1½ miles away from the shore, in sterile glass stoppered bottles. Fresh mackerels were taken from the same area, direct from gill nets. Methods of collection and plating were the same as described earlier (Venkataraman and Sreenivasan, 1952). Ability of the organisms to grow in fresh water media was also tested. The procedure for their identification was that as described in the 'Manual of methods for pure culture study of bacteria' (1952), with the modifications needed for specific marine bacteria (ZoBell and Upham, *loc. cit.*). The organisms were classified according to Bergey's Manual (1948). *Corynebacteria* were identified by the angular arrangement of their cells and 'snapping division' (Jensen, 1952) in addition to the characteristics described in Bergey's Manual.

* Published with the kind permission of the Director of Industries and Commerce, Madras.

RESULTS

Twenty-two bacteria isolated from inshore sea water and one hundred from mackerels were studied. Many of the colonies on the original plates were phosphorescent but on sub-culturing ceased to be so. Contrary to the notion (Burke, 1934) that 'spreader' type of colonies do not occur in sea water media, we observed invariably two-types of spreaders—one, a thin effuse subsurface colony and the other, a rhizoid spreader, especially in low dilution plates. Other marine materials like sea prawns and green mussels also yielded such spreader colonies.

Coliforms: They were absent in the inshore sea water as well as in guts and flesh of mackerels, when tested by enrichment in standard lactose broth and by direct plating on 'V.R.B.' (Violet red bile) agar. In the plate isolates, however, there was a single strain of *Aerobacter aerogenes*, which is not of any significance, since it does not indicate faecal contamination. Three of the isolates were slow lactose fermenting bacteria belonging to the sub-genus *Paracolobactrum*, and one of them was a strictly 'marine' form failing to grow in fresh water media, even after subculturing for months (Venkataraman and Sreenivasan, 1953a).

Bacterial flora: Bacteria belonging to the following genera were noted among the 122 cultures studied—*Micrococcus*, *Bacillus*, *Achromobacter*, *Sarcina*, *Flavobacterium*, *Paracolobactrum*, *Pseudomonas*, *Corynebacterium*, *Bacterium*, *Aerobacter*, and *Alcaligenes*. Some of the commonly occurring species are, *Achromobacter superficiale*, *A. thalassius*, *A. aquamarinus*, *A. stenohalis*, *Micrococcus citreus*, *M. flavus*, *M. epidermidis*, *M. varians*, *M. conglomeratus*, *M. caseolyticus*, *Sarcina flava*, *S. lutea*, *Flavobacterium dormitator*, *Fl. halohydrium*, *Fl. diffusum*, *Fl. invisible*, *Fl. maris*, and *Pseudomonas sessilis* (ZoBell and Upham, 1944). Some of the aerobic sporeforming *Bacillus* having rose-red to pink colour resemble *Bacillus subtilis* morphotype *globigii*.

From Table I it is seen that the flora of slime and gills (external parts) are to some extent identical with regard to the genera and even the ratio of these. *Achromobacter*, *Bacillus* and *Paracolobactrum* are present in nearly the same percentage in both. The gut flora differs from these, in that the *Micrococcaceae* account for 60% of the strains, while *Bacillus* is the next important group with 17.5%. Other genera are poorly represented in guts and *Alcaligenes* was present. A red *Bacterium* was present in the gills.

TABLE I

Showing the numerical distribution of bacteria according to genus in various parts of fish and in inshore water

Genus	Inshore sea water	Gills	Guts	Slime	Flesh	Total
<i>Achromobacter</i> ..	3	6	1	15	3	28
<i>Flavobacterium</i> ..	4	..	1	3	4	12
<i>Bacillus</i> ..	2	3	3	6	16	30
<i>Micrococcus</i> ..	11	1	6	1	11	30
<i>Sarcina</i> ..	1	..	4	..	7	12
Miscellaneous ..	1	3	2	2	2	10
	(Aero-bacter)	(Pseudo-monas 2 Paracolo-bact-rum 1)	(Bact-erium 1 Alkali-genes 1)	(Para-colo-bact-rum)	(Coryne-bact-erium)	
	22	13	17	27	43	122

'*Marine*' species: As regards their ability to develop on fresh water media, the results are quite interesting. In the inshore water flora only three *Flavobacter* failed to grow in fresh water media, and can therefore be regarded as 'marine' forms. Similarly from the gill flora, five *Achromobacter*, two *Pseudomonas*, and one *Paracolobactrum* were of marine species, while from the slime cultures only eight *Achromobacter* belonged to this category. Among the gut flora, one *Achromobacter* and one *Flavobacterium* and from the flesh, three *Achromobacter* were of marine species.

Active motility, a characteristic of marine bacteria (ZoBell, 1946) was noted in 69 (57%) of the 122 cultures, including one micrococcus. Fermentative powers were very poor, only about 50% of the cultures produced just a faint acidity from at least one sugar. Only four cultures were aerogenic in sugars. The thermal sensitivity (ZoBell and Conn, 1940) was not evident as most of the cultures grew luxuriantly at 37°C. and at slightly higher temperatures. Growth at room temperature was a little less than at 37°C. There was no growth at 4°C. for 12 weeks.

DISCUSSION

Bacteria belonging to *Micrococcaceae* form the largest group, accounting for nearly a third of the isolates. Wood (1940) in Australia, and Dyer (1947) in Canada also obtained large numbers of micrococci in fish. Shewan (1949) recorded that 30 to 35% of fresh slime flora were micrococci. *Bacillus*, the aerobic sporeformer formed between 18 to 24% of the flora of slime, guts and gills of mackerels and to a lesser extent in sea water. Next in numerical importance were the *Achromobacter* and *Flavobacterium* respectively. Fluorescent rods and *Proteus* were conspicuous by their absence, though both formed a large percentage of the flora of green mussels in the sea, examined by us (unpublished results).

The fact that some of the bacteria fail to grow in fresh water media, even after repeated subculturing confirms ZoBell's views regarding the existence of specific 'marine' bacteria. Seventeen *Achromobacter*, four *Flavobacter*, two *Pseudomonas* and one *Paracolobactrum* did not grow in fresh water media and may therefore be regarded as 'marine' forms. All these are gram negative, non-sporing rods and are actively motile. Very few of them are fermentative and only one produced gas from lactose after 9 days. In contrast, all the cocci, *Bacillus* and *Bacterium* grew equally well in fresh water and sea water media. Most of these are gram positive and thus resemble the soil flora. Wood (1950a, b) who has recorded a large number of gram positive bacteria in sharks, is also of the view that these are soil types. Further, from his latest work (Wood, 1953), it will be seen that cocci, *Bacillus* and *Corynebacterium*, the gram positive types, account for 55% of the total isolates from marine environments. In view of the above findings it is possible to reconcile the views of ZoBell and Wood. There may be a specific 'marine' bacterial flora in the same sense as there are specific milk, soil and sewage forms and this may quite often be modified by environment. It seems reasonable to believe that many fresh water bacteria carried into the sea can maintain themselves and carry on their activities as in fresh water (Burke and Baird, 1931). However, the prospect of survival of the 'marine' bacteria in fresh water seems very remote.

Among the *Bacillus* a large number were chromogenic, being rose-red to pink. A few were pale yellow, cream coloured or brown. Since these rose-red *Bacillus* were frequently isolated from marine environments, it is quite possible that they are autochthonous to the sea. They tolerate high concentrations of salt (Venkataraman and Sreenivasan, 1954) although growing profusely in salt free media. The presence of chromogenic *Bacilli* in marine environment have not been so far reported except by Wood (1953). The probable explanation for the frequent occurrence of *Bacillus* is the high temperatures of surface waters. Wood (1953) has correlated

the high surface temperatures with thermotolerance of bacteria of Australian waters. He further emphasised that the differences observed in bacterial flora by various workers 'largely reflect the differences in different parts of the world, and in different seasons'. Thjotta and Somme (1943) and Gee (1930) also suggested the possibility of geographical and seasonal variations in the bacterial flora.

The absence of coliform group, especially *E. coli*, in sea water and guts of mackerels confirms ZoBell's (1946) findings. The occurrence of *Paracolobactrum*, however, is interesting, since, apart from a report of their occurrence in fresh water fish (Venkataraman and Sreenivasan, 1953b), there is no reference in the literature about their presence in marine fish (Venkataraman and Sreenivasan, 1953a).

A comparison of the present work with that of Bhat and Albuquerque (1953) on Bombay-duck will be useful. These authors noted only the presence of *Micrococci*, *Sarcina* and *Bacillus* in the stomach, which is similar to what we found in the guts. Similarly, their flora of 'skin, gills and flesh' were also recorded by us in slime, gills and flesh, with very slight variations. While they have mentioned the presence of *Escherichia*, we did not find any. Since they state that their cultures did not ferment lactose but fermented only glucose and other sugars with 'gas' it is to be considered that they were dealing with the paracolon bacteria. If this is true, it agrees with our results on the occurrence of *Paracolobactrum* in fish. However, the fact that they isolated *Sarcina littoralis* from the alimentary tract in large numbers is surprising inasmuch as these are obligate halophiles, requiring a minimum of 16% NaCl for growth. On the whole, the flora of Bombay-duck and those of our mackerels are not much different.

The significance of the bacterial flora associated with fish lies in the fact, that it must explain the pattern and probable extent of its spoilage. The occurrence of a high percentage of proteolytic types points to the high spoilage potential. As shown in Table II about 75% of the isolates were gelatinolytic, while 37% peptonized casein. The presence of indole producers and hydrogen sulphide producers indicates the possible putrefactive types of spoilage. The occurrence of a large number of *Achromobacter*, which include all the indole producers listed in Table II, and a few which produced hydrogen sulphide, points to the same conclusion. The *Flavobacter*, however, exhibited poor proteolytic and saccharolytic tendencies, and as pointed out by Castell and Mapplebeck (1952), their rôle in spoilage is not of much importance. *Bacillus*, also exhibited proteolytic properties on gelatin and casein. This and its curviline nature point to its capacity in playing an adverse rôle in fish spoilage, in fresh as well as in salted condition.

TABLE II

Showing the Biochemical types in various parts of fish and inshore water

Type	Inshore water	Gills	Guts	Slime	Flesh	Total 122
Gelatin liquefiers ..	14	10	14	15	36	89
Milk peptonizers ..	13	3	6	6	17	45
Indole producers	5	..	1	..	6
Nitrate reducers ..	11	11	8	15	28	73
H ₂ S producers	5	..	5
Saccharolytic ..	13	10	7	12	22	64
	(1 aero-genic)	(1 aero-genic)		(2 aero-genic)		
Chromogenic ..	11	2	11	9	23	56

SUMMARY

Bacteria belonging to the genera, *Micrococcus*, *Bacillus*, *Achromobacter*, *Flavobacterium*, *Sarcina*, *Paracolobactrum*, *Pseudomonas*, *Corynebacterium*, *Bacterium* and *Alcaligenes* are associated with mackerels and sea water off Tellicherry. *E. coli* was not detected in sea water or in guts of mackerels but a few slow lactose fermenting paracolons were isolated. The existence of 'marine' bacteria incapable of growing under hypotonic conditions is confirmed, and these were all gram negative, actively motile rods with faint fermentative properties. Many of the isolates were proteolytic on gelatin and casein and a few produced indole and hydrogen sulphide. Nitrate reduction was very common. Apart from chromogenic cocci and flavobacter, spore-forming *Bacillus* also were seen to possess chromogens quite often. The rôle of bacterial flora in fish spoilage is discussed.

REFERENCES

- Bergey's manual of Determinative Bacteriology, 6th Ed. (1948). The Williams and Wilkins Co., Baltimore.
- Bhat, J. V. and Albuquerque, M. J. (1953). 'Micro-organisms associated with the Bombay duck or *bombil* (*Horopodon nehereus* Buch)'. *Proc. Ind. Acad. Sci.*, 3813, 101-108.
- Burke, V. (1934). Interchange of Bacteria between fresh water and the sea. *J. Bact.*, 27, 201-205.
- Burke, V. and Baird, L. (1931). Fate of fresh water bacteria in the sea. *Ibid.*, 21, 287.
- Castell, C. H. and Mapplebeck, E. G. (1952). The importance of flavo-bacterium in fish spoilage. *Jour. Fish. Res. Bd. (Can.)*, 9, 148-156.
- Dyer, F. E. (1947). The micro-organisms of the Atlantic Cod. *Ibid.*, 7, 128-136.
- Gee, A. H. (1930). Bacteria concerned in the spoilage of haddock. III. Further observations on the flora of live fish. *Contr. Canad. Biol. Fish. N.S.*, 5, 433.
- Griffiths, F. P. (1937). A review of the bacteriology of fresh marine fishery products. *Food Res.*, 2, 121-134.
- Jensen, H. L. (1952). The coryneform bacteria. *Ann. Rev. Microbiol.*, 6, 79.
- Manual of methods for the pure culture study of Bacteria (1952). Biotech. Publications, Geneva, New York.
- MacLeod, R. A., Onofrey, E. and Norris, M. E. (1953). Studies on the nutrition and metabolism of marine bacteria. I. Isolation and identification of the micro-organisms and a preliminary study of their nutritional requirements. *Fish Res. Bd. (Can.)*, *Progr. Rep. Pacific Coast Stas.*, 96, 11-14.
- Shewan, J. M. (1949). Some bacteriological aspects of handling, processing and distributing of fish. *J. Roy. Sanit. Inst.*, 69, 394-421.
- Snow, J. E. and Board, P. J. (1939). Studies on the flora of North Pacific Salmon. *Food Res.*, 4, 563-586.
- Thjottta, Th., and Somme, O. (1942 and 1943). The bacterial flora of normal fish. *Skrifter utgitt av det Norske Videnskaps-Akademi I. Oslo I. Mat-Naturv Klasse, Nr. 4*, 1-86.
- Venkataraman, R. and Sreenivasan, A. (1952). A Preliminary investigation of the bacterial flora of the mackerels of the West Coast. *Ind. Jour. Med. Res.*, 40, 529-533.
- (1953a). A marine species of slow lactose fermenting bacterium. *Curr. Sci.*, 22, 120-121.
- (1953b). The Bacteriology of fresh water fish. *Ind. Jour. Med. Res.*, 41, (4) 385-392.
- (1954). Salt tolerance of Marine Bacteria. *Food Res.*, 19 (3). 311-313.
- Wood, E. J. F. (1940). Studies on the marketing of fresh fish in eastern Australia. Part II. The bacteriology of spoilage of marine fish. *Pamphlet Coun. Sci. Ind. Res. Austr.*, 100, 1-92.
- (1950a). Bacteria in marine environments. *Indo-Pacific Fisheries Council. 2nd Meeting, Cronulla, N.S.W. Australia. Tech. Paper No. 3*.
- (1950b). The bacteriology of shark spoilage. *Austr. J. Marine Freshw. Res.*, 1, 129-138.
- (1953). Heterotrophic bacteria in marine environments of E. Australia. *Austr. J. Mar. Freshw. Res.*, 4 (1), 160-200.
- ZoBell, C. E. (1946). *Marine Microbiology*. Chronica Botanica Co., Waltham, Mass., 1-240.
- ZoBell, C. E. and Conn, J. E. (1940). Studies on the thermal sensitivity of marine bacteria. *J. Bact.*, 40, 223.
- ZoBell, C. E. and Upham, H. C. (1944). A list of marine bacteria, including descriptions of sixty new species. *Bull. Scripps Inst. Oceanogr.*, 5, 239-292.

PHOTOMETRIC STUDY OF DESOXYRIBONUCLEIC ACID (DNA) SYNTHESIS IN REGENERATING MACRONUCLEUS OF *EPISTYLIS ARTICULATA* FROM.

by B. R. SESHACHAR, F.N.I., and C. M. S. DASS, Department of Zoology,
University of Mysore, Central College, Bangalore

(Received July 24 ; read October 20, 1954)

INTRODUCTION

It was reported (Seshachar and Dass, 1953) that in *Epistylis articulata* the vegetative micronucleus could, in some cases, regenerate a macronucleus. This method of regeneration of the macronucleus in a vegetative animal is very different from that after conjugation. In the latter case, it has been noticed (Dass, 1953), that the synkaryon divides thrice in the synconjugant, producing eight metagametic nuclei; of them, one remains as micronucleus while the other seven nuclei form the macronuclear anlagen. The future behaviour of these anlagen is one of continuous enlargement and acquisition of desoxyribonucleic acid (DNA). A photometric study of this process has revealed a close correlation between the increase in volume of the macronuclear anlagen and the rate of synthesis of DNA (Seshachar and Dass, 1954). It was felt that a study of the process of macronuclear regeneration, with particular reference to the rate of synthesis of DNA would also be interesting.

MATERIAL AND METHODS

Colonies of *E. articulata* fixed in hot Carnoy's fluid and stained with Feulgen were used for photometric measurements. Pollister (1952), and more recently Swift (1953), have described the methods of measurement and discussed their application to the determination of the amounts of DNA in cell nuclei. The methods adopted in the present investigation were essentially similar.

The apparatus consisted of a light source, microscope mounted on a photomicrographic stand with a special back accommodating a photo-electric cell connected with a galvanometer. The light source was a 6V Tungsten ribbon filament lamp, the power to which was supplied from the mains through a voltage stabilizer to ensure constant illumination. A Farrand interference filter with peak transmission at 558 m μ (half-band width 14 m μ and transmission 29%) was used to isolate green light for measuring Feulgen reaction in the nuclei. A Leitz research microscope with a centering substage condenser was used. It was mounted on a photomicrographic stand with a special back possessing an iris diaphragm, and accommodating a scanner and a photo-cell. The scanner consisted of a Leitz $\times 6$ eyepiece with micro-meter and centering graticule. The photo-tube was an RCA photo-multiplier, 931A type. The galvanometer (Farrand Optical Co. Inc.) was highly sensitive and readable to 1/500 micro-ampere.

The methods of making measurements were as follows:—(a) The nuclear anlage to be measured was moved into the optical axis of the system and centered to the iris diaphragm of the camera back by means of the scanner; (b) The aperture of the iris diaphragm was reduced until it just enclosed the nucleus; (c) The photo-tube was then moved into place and the deflection of the galvanometer was recorded (T_1); (d) The nucleus was moved out of the field, a clear area of the cytoplasm was brought into position, and maintaining the same aperture, the galvanometer reading

was recorded (T_2). T_1 divided by T_2 gives the transmission of the nucleus (T). The extinction was then calculated ($E = \log_{10} \frac{1}{T}$). The extinction (E) is the value which varies directly with concentration and thickness of the absorbing material, according to Beer-Lambert law. Given the extinction for a spherical nucleus the relative amount per nucleus in arbitrary units is given by the expression $E\pi r^2$ and relative concentration by $E/\frac{1}{3}r$. The large majority of nuclear anlagen measured were spherical. A few were slightly elliptical and in such cases the mean diameter was taken into consideration for the calculations.

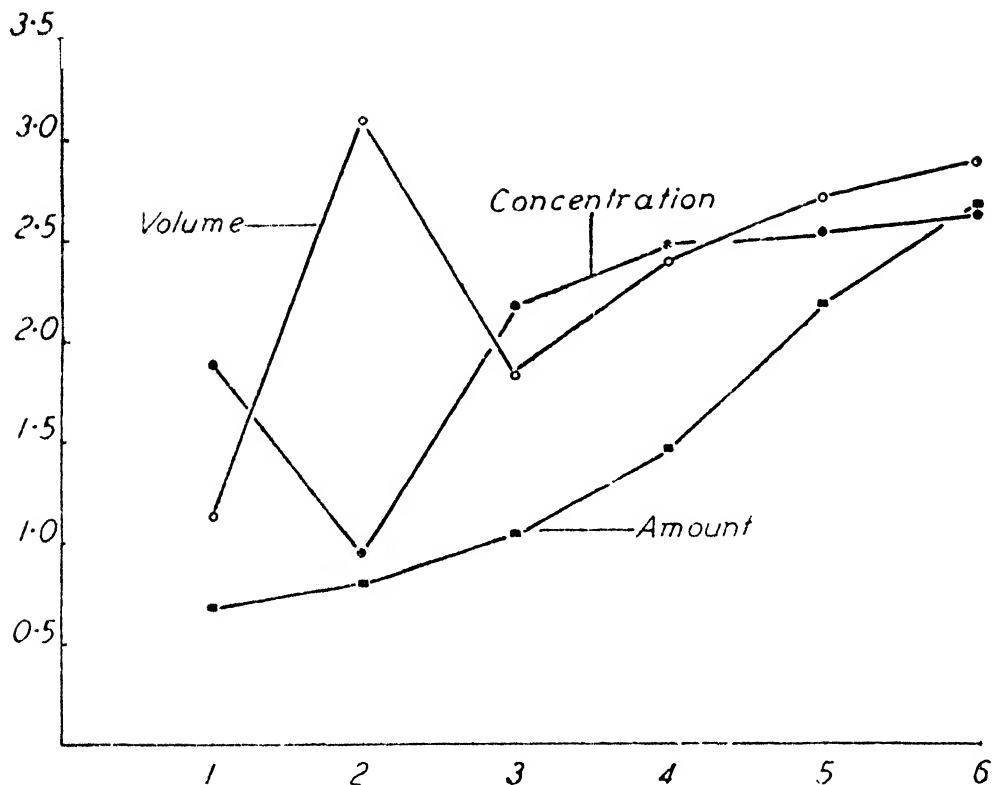
OBSERVATIONS

Amacronucleate individuals of *E. articulata* occur among the normal members of the colony scattered at random and without any specific distribution. They arise as a result of an upset of the process of binary fission, where the macronucleus fails to orientate across the division plane. As a result two individuals, one with both macronucleus and micronucleus, and the other with only the micronucleus, are produced. The micronucleus of the latter individual sooner or later divides and one of the daughters develops into the macronucleus. At first both the bodies are similar and have a volume of $6.28 \mu^3$, DNA content of 0.3255 and concentration 0.0736. Soon one of them starts increasing in size. When its volume has reached $13.43 \mu^3$, it is seen that the amount of DNA is 4.86 and concentration, 0.7574 (see table and graph). The enlargement of the anlage progresses until it occupies almost the entire cytosome. At this stage the volume of the anlage is $1192.5 \mu^3$ and DNA content is 6.95. The concentration of DNA, however, is so low, i.e., 0.093, that the anlage appears very faint. This represents the maximum enlargement of the anlage, and soon after, the anlage starts diminishing in size. At a stage when the volume has shrunk to $69.3 \mu^3$ the DNA content is seen to be 11.9 and concentration 1.334. From this point DNA synthesis takes place rapidly. Thus when the anlage has a volume of about $211.2 \mu^3$ the DNA content is 28.9 and concentration, 2.531. When the anlage is about $328.0 \mu^3$ in volume the DNA content is 154.6 and concentration, 3.257 and when it has a volume of $703.6 \mu^3$ the DNA content reaches 238.0 and concentration 4.077. This was the last stage that could be measured, as in the later stages, the macronucleus became drawn out into a bent cylinder and accurate measurements could not be made. But from the appearance of the nucleus and its reaction to Feulgen, it could be seen that the synthesis of DNA kept pace with further increase in volume.

TABLE 1

Desoxyribonucleic acid determination of regenerating macronuclear anlagen of E. articulata.
Extinction at 558 m μ of the Feulgen reaction of whole anlagen.

Stage.	Volume μ^3	Extinction 558 m μ	DNA content in arbitrary units. $E\pi r^2$	Relative concentration. $E/\frac{1}{3}r$
1	13.4	0.310	4.8	0.757
2	1192.5	0.056	6.9	0.093
3	69.3	0.409	11.9	1.334
4	211.2	0.420	28.9	2.531
5	328.0	0.699	154.6	3.257
6	703.6	0.854	238.0	4.077



Graph showing the relationship between the volume of regenerating macronucleus of *E. articulata* and the amount and concentration of DNA. In constructing the graph the different stages of macronuclear regeneration were marked on the abscissa and the logarithmic values of nuclear volume and DNA amount plotted along the ordinate. The relative concentration values were multiplied by 100 and logarithmic values plotted along the ordinate.

DISCUSSION

The history of the development of the macronucleus of *E. articulata* during vegetative reorganization shows that both in regard to volume changes as well as nucleination, it offers points of interest. Soon after division of the micronucleus, the two anlagen,—micronuclear as well as macronuclear,—are similar in size. They each have a volume of $6.28 \mu^3$. One of them, the macronuclear anlage, soon enlarges until it attains a volume nearly 200 times that of the original ($1192.5 \mu^3$). But photometric analysis shows that the synthesis of DNA has not kept pace with the great increase in volume; hence the anlage looks pale and faintly staining. It then shrinks in size while undergoing a consolidation. During this latter period also DNA is being synthesised; this, along with a decrease in volume, contributes to a deeper Feulgen reaction of the macronuclear anlage during this period. The nucleination of the anlage progresses steadily until the macronucleus attains the adult form and size.

An observation of this kind has not been reported before; actually macronuclear regeneration in a vegetative animal was unknown until Seshachar and Dass (1953) reported it for the first time in *E. articulata*. But it is interesting to see how in another ciliate, *Chilodonella uncinatus*, a strikingly similar situation obtains, but after conjugation (Seshachar, 1950). Here too, the synkaryon products which are two in number, are similar in size but the macronuclear anlage increases enormously

until it literally fills the cytosome. After this maximum enlargement, when it looks pale and faintly staining, the anlage shrinks and attains the definitive size and form of the macronucleus of the adult. While recognizing that the macronuclear changes described above are taking place in two entirely different situations, i.e., in *E. articulata* in vegetative reorganization, in *C. uncinatus* in the exconjugant, the similarity of the two processes is striking and involves a preliminary increase in volume without a corresponding increase in DNA synthesis, followed by a shrinkage in volume. During both periods DNA synthesis is proceeding steadily, perhaps slowly at first, but more rapidly later.

It is particularly interesting to note that such an increase in volume and later shrinkage do not occur in *E. articulata* after conjugation. Here, the DNA synthesis keeps pace with volume increase.

SUMMARY

The development and nucleination of the macronuclear anlage during vegetative reorganization have been studied by photometric methods. The anlage, which starts in amacronucleate animals as a product of division of the micronucleus, enlarges greatly in size and later shrinks. The synthesis of desoxyribonucleic acid is continuous throughout, but is slightly more rapid in the later stages than in the earlier ones.

ACKNOWLEDGEMENT

Thanks are due to the National Institute of Sciences of India for the award of an I.C.I. (India) Research Fellowship to one of us (C.M.S.D.).

REFERENCES

- Dass, C. M. S. (1953). Studies on the nuclear apparatus of Peritrichous ciliates. Part I. The nuclear apparatus of *Epistylis articulata* (From.). *Proc. Nat. Inst. Sci.*, **19**, 389-404.
- Pollister, A. W. (1952). Microspectrophotometry of fixed cells by visible light. *Lab. Invest.*, **1**, 231-49.
- Seshachar, B. R. (1950). The nucleus and nucleic acids of *Chilodonella uncinatus* Ehrbg. *J. Expt. Zool.*, **114**, 517-44.
- Seshachar, B. R. and Dass, C. M. S. (1953). Macronuclear regeneration in *Epistylis articulata*. *Q.J.M.S.*, **94**, 185-192.
- (1954). The macronucleus of *Epistylis articulata* From. during conjugation—A photometric study. *Physiol. Zool.*, **27**, 280-286.
- Swift, H. H. (1950). Desoxyribonucleic acid content of animal nuclei. *Physiol. Zool.*, **23**, 169-200.
- (1953). International Review of Cytology, II. Chapter 1, pp. 1-76. Acad. Press, New York, N.Y.

THE RÔLE OF BACTERIA ON THE GROWTH AND VIABILITY OF *ENTAMOEBIA HISTOLYTICA*

by A. K. MUKHERJEA, *Research Fellow, N.I.S.I., Department of Protozoology,
Indian Institute for Medical Research, Calcutta*

(Communicated by J. C. Ray, F.N.I.)

(Received April 1, 1953; after revision April 7; read August 6, 1954)

INTRODUCTION

Out of the three essential requirements for the growth and viability of *Entamoeba histolytica*, namely, (1) the culture medium, (2) bacteria, and (3) temperature, the first one has already been studied (Mukherjea, 1954). In this paper the other two factors which also exercise a marked influence over the physiological activities of the amoebae, have been included. In all the investigations now reported *E. histolytica* (strain No. 7) has been employed.

MATERIALS AND METHODS

growth and viability of *E. histolytica* (strain No. 7) on account of continuous subcultures became feeble. Several methods were, therefore, adopted to counteract this condition and to stimulate their growth. The methods included the following: (a) Addition of bacteria to the culture medium, (b) addition of acriflavine, (c) combination of bacteria and acriflavine, and (d) addition of aureomycin hydrochloride.

(a) *Addition of bacteria*: 5 to 10 drops of a thick normal saline emulsion of young cultures of *B. coli* type of bacteria from strains no. 1, 2 and 3, grown on nutrient agar, were added to the culture medium prior to or during inoculation of the trophozoites. Their effects on the growth and viability of the amoebae are shown in Table I.

(b) *Addition of acriflavine*: On addition of acriflavine in 1 : 40,000 strength to the fluid overlay of D₁ medium (Mukherjea, 1954), there occurred marked alteration in the growth and viability of the amoebae as will be seen in Table I.

(c) *Combination of bacteria and acriflavine*: When the two, i.e., bacterial emulsion from strains no. 1, 2 and 3 and acriflavine (1 : 40,000) were combined, the growth and viability of the amoebae were still further increased as will be noticed from Table I.

(d) *Addition of aureomycin hydrochloride*: That aureomycin, in exceedingly small doses, has a profound effect on the growth of the amoebae will be noticed in Table I. Two sets of experiments were put up. In the first set 1 to 2 drops of a 1 : 4,000 solution of aureomycin hydrochloride and in the second set 10 drops of a 1 : 1,000 strength were added to the fluid overlay of D₁ media.

From the results given in Table I, it becomes manifest that both bacteria and acriflavine when used separately, are able to stimulate the growth and increase the viability of the amoebae which, however, are still further augmented when the two are combined together. Though aureomycin can stimulate the growth, this depends on the dosage. While 1 to 2 drops of 1 : 4,000 solution will enhance the growth, 10 drops of 1 : 1,000 solution will definitely inhibit it.

TABLE I
Showing the effects of (a) bacteria, (b) acriflavine, (c) combination of bacteria and acriflavine, and (d) aureomycin on the growth and viability of E. histolytica.

Medium	Bacterial emulsion	Aureomycin	Growth after					Remarks
			48 hrs.	72 hrs.	96 hrs.	120 hrs.	144 hrs.	168 hrs.
B ₂	—	—	+	—	—	—	—	—
B ₂	5 drops	—	+	+	—	—	—	—
B ₂	10 drops	—	+	+	—	—	—	—
B ₂	—	—	+	+	—	—	—	—
D ₁	—	—	+	+	—	—	—	—
D ₁	—	—	+	+	—	—	—	—
D ₁ +acriflavine	—	—	+	+	+	—	—	—
D ₁ +acriflavine	—	—	+	+	+	—	—	—
D ₁ +acriflavine	5 drops	—	+	+	+	—	—	—
D ₁ +acriflavine	10 drops	—	+	+	+	—	—	—
D ₁	—	1 drop of 1:4,000	+	+	+	+	+	+
D ₁	—	2 drops of 1:4,000	+	+	+	+	+	+
D ₁	—	10 drops of 1:1,000	+	+	+	+	+	+
D ₁	—	—	—	—	—	—	—	—

+ /2 indicates five or less than five trophozoites per field as observed under low power.

Other methods that were employed for the study of the rôle of bacteria on the growth and viability of *E. histolytica* were the following:

A. Replacement of stale culture fluid

After $\frac{1}{2}$ to $\frac{3}{4}$ ths of the fluid after cultivation of the amoebae was removed, the same quantity of fresh fluid was added at intervals of 24 hours or longer. There were distinct changes in the growth and viability of the amoebae, which have been shown in Table II. In control tubes the fluid was not replaced.

TABLE II

Showing the effects of replacement of stale fluid by stock (fresh) fluid of the culture medium on the growth and viability of E. histolytica.

Medium	Growth after						Remarks
	48 hrs.	72 hrs.	96 hrs.	120 hrs.	144 hrs.	168 hrs.	
E ₃	+++	+++	+	-	-	-	Control.
E ₃	+++	+++	++	-	-	-	"
E ₃ *	+++ + §	+++	++ §	+++ §	++	+	Experimental.
E ₃ *	+++ + §	+++	++ §	++	+	+	"
B ₂	++	++	-	-	-	-	Control.
B ₂ *	++ §	+++ §	+++	+++ §	++	-	Experimental.

* indicates the tube in which the stale fluid was partially replaced by fresh fluid.

§ indicates the time when replacement of the fluid was effected; where this sign is absent, the culture fluid was not changed.

Thus frequent changing of the stale fluid by fresh fluid has a definite tendency towards prolonging the viability of the amoebae.

B. Washing the sediment

The sediment in a culture medium in addition to starch, bacteria, trophozoites, etc., contains a number of other substances. It also contains metabolites which are the products of the activities of the bacteria and amoebae. The metabolites are also present in the fluid itself. After discarding the supernatant fluid, the sediment is centrifuged and repeatedly washed in normal salt solution to remove the metabolic products. The effects of the removal of these products on the growth of the amoebae were next studied. The procedure followed is given below:

Before washing the sediment, the starch and the fluid from several culture tubes containing large numbers of trophozoites were pooled together and centrifuged at a low speed. After decanting off the fluid the sediment was resuspended in sterile normal saline and washed at least four times. After the final washing a portion was inoculated into fresh E₂ media and the rest incubated at 37°C., after suspension in sterile normal saline. At intervals samples were used for seeding the same type of media as stated in Table III. In control tubes the inoculation was effected by the direct method, i.e., from one tube to the other without the sediments having been washed.

The results showed that: (i) the growth of amoebae was feeble for the first 48 hours after which it became profuse; (ii) their viability was increased; (iii) on inoculation of washed trophozoites after 1 to 4 hours' suspension in normal saline, the viability increased still further.

TABLE III

Showing the effects of inoculation of washed sediment on the growth and viability of E. histolytica.

Tube No.	Inoculated from	How inoculated	Growth after					Remarks
			24 hrs.	48 hrs.	72 hrs.	120 hrs.	144 hrs.	
1	Tube no. 282 ..	Directly from tube-to-tube.	+++	+++	+	-	-	{ Growth is early and profuse. Viability is short.
2	Tube no. 284 ..	" "	+++	+++	++	-	-	
3	Sediment from tubes 282+284.	Immediately after washing.	+	++	+++	-	-	
4	" "	" "	+	+	+	+	+	{ Growth is feeble and delayed. After 48 hours it is increased. Viability is long.
5	Sediment ..	After 1 hour's suspension in normal saline.	-	+	+	+	+	
6	Sediment ..	After 1½ hours' suspension.	-	+	+	+	+	
7	Sediment ..	After 2 hours' suspension.	-	-	+	+	+	{ Viability prolonged still further.
8	Sediment ..	After 4 hours' suspension.	-	+	+	+	+	

TABLE IV
Showing the effects of temperatures on the growth and viability of L. histolytica.

Series of experiments	Temperatures to which the tubes were exposed	Growth after						Remarks
		48 hrs.	72 hrs.	96 hrs.	120 hrs.	144 hrs.	168 hrs.	
*1	A constant temperature of 37°C. . .	+	+	+	+	+	+	The growth is early and profuse; viability short. Growth is inhibited. Viability prolonged.
2	A constant temperature of 22°C. . .	—	—	—	—	—	—	
3	At first at 37°C. for 48 hrs., } (a) thereafter at room temperature varying from 21.6°C. to 36.1°C. } (b)†	+	+	+	+	+	+	
4	Room temperature varying from 21.6°C. to 36.1°C.	+	+	+	+	+	+	Viability prolonged. Growth is feeble all along. Viability prolonged.
5	At first at room temperature varying from 21.6°C. to 36.1°C. for 72 hrs. then kept at 37°C.	+	+	+	+	+	+	Viability greatly prolonged. The growth is feeble at first but increased after 72 hours.

* This may be regarded as the controlled condition for comparison with the rest.
† At the end of 96 hours this tube was transferred from laboratory bench to an incubator at 22°C.

C. *Effects of different temperatures on the growth and viability of E. histolytica*

In order to find out how temperature influences the growth and viability of *E. histolytica*, the culture tubes after inoculation in the usual way were exposed to different temperature conditions such as the following: (1) the tubes were exposed to a constant temperature of 37°C.; (2) in the second series of experiments the tubes after inoculation were left in an incubator at a constant temperature of 22°C.; (3) in the third set of experiments, the tubes were kept at 37°C. for 48 hours, thereafter they were left on the laboratory bench at temperatures varying from 21.6°C. to 36.1°C.; at the end of 96 hours some of these tubes were placed in an incubator at 22°C.; (4) the tubes were kept constantly on the laboratory bench at temperatures varying between 21.6°C. and 36.1°C.; (5) in the fifth series of experiments the tubes after inoculation in the usual way were kept on the laboratory bench at temperatures varying from 21.6°C. to 36.1°C. for 72 hours; at the end of this period they were incubated at 37°C. The results obtained have been shown in Table IV.

The results indicate that: (a) A temperature of 37°C. stimulates the growth and multiplication of the amoebae whereas 22°C. inhibits both. (b) When the amoebae are grown at 37°C., their subsequent transfer to fluctuating room temperatures prolongs the viability; on the other hand, if they are first kept at 37°C. and thereafter exposed to 22°C., the multiplication is inhibited, though many of them may be still alive and actively motile.

D. *Relation between pH and E_h of the medium*

When the bacteria grow in a culture medium there takes place a lowering of the oxidation-reduction potential. If the bacteria growing with the amoebae are not of the 'right type', there is also a tendency for the culture medium to become acid. In order to determine the relationship between these two factors, i.e., lowering of oxidation-reduction potential and fall of pH, and how they jointly influence the growth of the amoebae, several tubes containing glucose broth were taken. Bacterial emulsions from strains no. 2 and (1+3) were added separately to these tubes. The pH and E_h at intervals of 12, 24 and 48 hours were noted, the former by capillator, and the latter by methylene blue. The results are given in Table V.

TABLE V

Showing the relation between the pH and the E_h of a medium.

	Glucose broth tube no. 1	Glucose broth tube no. 2	Glucose broth tube no. 3
Row 1	Results after 12 hours	Results after 24 hours	Results after 48 hours
Inoculated with bacterial strain no. 2	(i) pH .. 4.6 (ii) Quantity of M.B. decolourised +	(i) pH .. 4.6 (ii) Quantity of M.B. decolourised +	(i) pH .. 4.4 (ii) Quantity of M.B. decolourised ±
Row 2			
Inoculated with bacterial strain no. (1+3)	(i) pH .. 5.8 (ii) Quantity of M.B. decolourised +++	(i) pH .. 5.2 (ii) Quantity of M.B. decolourised ++	(i) pH .. 6.8 (ii) Quantity of M.B. decolourised ++++

M.B. stands for methylene blue.

The reduction of the culture fluid has been expressed in terms of the quantity of methylene blue decolourised (i.e. reduced); thus:

- ++++ indicates strong reduction.
- +++ indicates moderate reduction
- ++ indicates fair reduction.
- +
- indicates feeble reduction.
- ± indicates doubtful reduction.

It is true that the reduction of a medium expressed in terms of the quantity of methylene blue reduced is inversely proportional to the E_h as estimated by potentiometer. Thus a medium which decolourises a large amount of methylene blue such as that indicated by + + + +, will have the inverse effect on E_h (— — — —). It is apparent, therefore, that as the pH of a medium falls, there is a proportionate rise of E_h or in other words the pH varies inversely as the E_h .

E. Nature of end products of protein decomposition

(a) It has already been noticed that as a result of bacterial action complex proteins undergo hydrolysis into proteoses and peptones. The object of carrying on further studies in this direction is to find out the end products of protein breakdown brought about by the action of the associated bacteria. The end products are the results of decarboxylation and other changes. For this purpose the fluid portion of a D_1 medium culturing *E. histolytica* (strain no. 7) with the associated bacteria was used after it was passed through cotton wool filter. The different tests and the results obtained are given in Table VI.

TABLE VI
Demonstration of the formation of acids and amines in D_1 medium culturing *E. histolytica* (strain no. 7) with the associated bacteria.

Experiments	Observation	Inference
1. 0.5 c.c. of fluid* + 0.5 c.c. of Ehrlich's <i>p</i> -dimethyl-aminobenzaldehyde reagent + 0.5 c.c. HCl (concentrated).	(i) No red colour. (ii) No blue colour.	(i) Indole absent. (ii) Skatole absent.
2. Fluid + 2 drops of nitric acid + 2 drops of KNO_3 solution.	(i) Red colour absent. (ii) White turbidity developed.	This suggests : (i) absence of Indole. (ii) presence of Skatole.
3. 1 c.c. fluid + a few drops of Millon's reagent.	White precipitate turns reddish on heating.	Compounds containing hydroxy-phenyl group present in traces.
4. 1 c.c. fluid + a few drops of bromine water.	Copious white precipitate.	Cresols, phenol or hydroxy aromatic acids present.
5. 5 c.c. of 1.1% Na_2CO_3 solution + 2 c.c. freshly prepared <i>p</i> -diazobenzene-sulfonic acid reagent. After 1 minute 1 c.c. of fluid added.	(a) Yellowish red colour formed immediately. (b) The pink colour was not conspicuous. No bluish red colour.	(a) This suggests that the yellow colour was due to phenol or <i>o</i> - and <i>m</i> -cresol and the red colour was due to <i>p</i> -cresol, <i>p</i> -oxyphenylpropionic acid, <i>p</i> -oxyphenylacetic acid or <i>p</i> -oxyphenyllactic acid. (b) Histidine, histamine and other iminazoles absent (?). Tyrosine and tyramine absent (?).
6. The above made strongly alkaline with NaOH + a crystal of hydroxylamine hydrochloride; shaken.		

* The pH of this fluid was 6.8.

Whether the end products are due to the action of bacteria alone or both bacteria and amoebae on the proteins, it is difficult to say. However, in order to find out the rôle of bacteria and amoebae acting independently on the proteins, similar experiments were carried out with the fluid from a D₁ medium culturing only bacteria (strains no. 1, 2 and 3). Identical reactions, as stated in Table VI, were obtained. There was, however, the exception that while the compounds containing hydroxyphenyl group were found in presence of amoebae growing with bacteria, these compounds were absent where bacteria alone were cultivated. The results suggest that at least some of the end products are due to the direct action of the amoebae on proteins.

(b) *Demonstration of hydroxy acids in culture fluid*: When amino acids deaminate before losing CO₂ from the carboxyl radicle, ammonia and ketonic acids such as pyruvic acid, make their appearance as intermediate products. The ketonic acids being reducible substances are likely to be reduced to the corresponding hydroxy acids, such as lactic acid, provided the necessary conditions to bring about this change are present. Acting on the supposition that the hydroxy acids have some influence on the growth of *E. histolytica*, attempts were first made to demonstrate the presence of these acids in the stale culture fluid and thereafter to determine the rôle of these products on the growth of the amoebae. The fluid from the culture tube growing *E. histolytica* (strain no. 7) with the associated bacteria was filtered through cotton wool. 5 c.c. of this fluid and 20 c.c. of ether were taken in a separatory funnel and shaken thoroughly. After the separation of the ether the entire fluid with the exception of the top 5 c.c. of ether was allowed to run out. The latter was next mixed with 20 c.c. of distilled water to which 2 drops of a 10% ferric chloride solution were added. The appearance of straw-yellow colour of moderate intensity indicated the presence of lactic acid in the culture fluid. Control tubes containing 20 c.c. of distilled water and 5 c.c. of pure ether did not yield the same reaction with ferric chloride.

DISCUSSION

I. *The rôle of bacteria on the growth of E. histolytica*

At the time of cultivation of *E. histolytica* by using suspension of washed and disinfected cysts, two things were noticed. First, excystation of cysts was checked and secondly, there was no breaking down of the medium as was known from absence of any opacity of the culture fluid, formation of gas and smell, and alteration of the pH of the medium. When a few drops of an emulsion of bacteria such as from strains no. 1, 2 and 3 were added to the fluid portion of the same medium, it was followed by excystation leading to growth and multiplication of the trophozoites. It was also noticed that excystation was always preceded by profuse growth of the bacteria as well as by the break-down of the protein constituents of the medium. Therefore, the explanation as to how the presence of bacteria in the culture medium is responsible for the excystation of the amoebae lies in the bacteria themselves primarily acting on the protein decomposing it into simpler forms. Thus the products of decomposition brought about by the bacteria provide the necessary stimulus for excystation as well as growth and multiplication of the amoebae. It may be pointed out in this connection that starch which constitutes the only carbohydrate element in the culture medium, generally remains unaltered except where the particular bacteria growing with the amoebae possess starch-splitting properties also (Mukherjee, 1954). Even when there is no hydrolysis of starch, the amoebae still grow profusely which suggests that the products of hydrolysis of starch are in no way helpful to the growth of the amoebae.

During cultivation of *E. histolytica* strains no. 1 and 7 it was noticed that the growth of the amoebae was profuse, viability increased and the amoebae survived on repeated subcultures. In case of *E. histolytica* strains no. 3, 4, 5 and 6 the results

were the opposite. Such differences in the nature of growth of the two types of *E. histolytica* strains were attributed to the different types of bacteria growing with them. This was supported when it was observed that the bacteria growing with *E. histolytica* strains no. 1 and 7 were putrefactive in type, but those growing with strains no. 3, 4, 5 and 6 were identified as fermentative types of intestinal *B. coli* (Mukherjea, 1951: 9 and 1954). This suggests that while the putrefactive type of bacteria provides the necessary stimulus for the growth of the amoebae, the other type does not.

The reactions which are responsible for the putrefaction of the proteins of the culture medium occur in successive orders of hydrolysis and decarboxylation. *Hydrolysis* of proteins is the first to occur and this leads to the formation of the simpler proteins such as proteoses and peptones. Signs of digestion of the inspissated serum slant, such as gradual reduction of its thickness noticed while cultivating *E. histolytica* strain no. 1 in D.L. medium (Mukherjea, 1951: 9), were evidently due to hydrolysis of the protein. Another evidence of bacterial hydrolysis of complex proteins has been based on finding proteoses and peptones in a solution of egg albumin containing horse serum in which bacterial strains no. 1, 2 and 3 were allowed to grow for 48 hours. The egg albumin solution containing horse serum (19:1) normally does not contain proteoses or peptones, unless the egg albumin and serum proteins have been hydrolysed. For detection of proteoses and peptones, the culture fluid was first slightly acidified with dilute acetic acid and then heated to boiling. The filtrate obtained after separation of the coagulum, was half-saturated with $(\text{NH}_4)_2\text{SO}_4$. This led to the precipitation of primary proteoses which were removed. The secondary proteoses were next separated by fully saturating the filtrate with $(\text{NH}_4)_2\text{SO}_4$ by heating. The filtrate was then tested for peptones by the biuret test. Proteoses and peptones resulting from the cleavage of complex proteins are themselves next hydrolysed into several amino acids.

The subsequent changes are due to *decarboxylation*. This depends on the nature of the bacteria growing in the culture fluid. If the bacteria are of the putrefactive type, they will break down the amino acids still further, giving rise to several amines such as histamine, tyramine, putrescine, cadaverine, etc., and/or to aromatic acids such as phenylacetic acid, phenylpropionic acid, etc. The presence of these acids (vide Table VI) and putrid smell in culture tubes growing the amoebae, strongly indicates that decarboxylation of the amino acids has taken place. Although the amines such as histamine and tyramine could not be demonstrated in the stale culture fluid (vide Table VI), yet the faetid smell indicated that it was due to the presence of other amines such as putrescine and cadaverine.

Decarboxylation may also take place in a somewhat different manner. Here the amino acids instead of losing CO_2 from the carboxyl radicle, at first deaminate (oxidative deamination) into ketonic acids, *e.g.*, pyruvic acid and then decarboxylate (oxidative decarboxylation) into fatty acids such as acetic acid. Being reducible the ketonic acids may also undergo reduction side by side with decarboxylation. This will lead to the formation of the corresponding hydroxy acids, *e.g.*, lactic acid. The presence of lactic acid in the culture fluid growing *E. histolytica* (strain no. 7) with the associated bacteria has been demonstrated.

From the chemical nature it appears that some of the end products such as the hydroxy acids serve as hydrogen donors, while others perform altogether different functions.

II. Growth-stimulating and growth-inhibiting factors

In a previous communication (Mukherjea, 1951: 9) mention was made of the two factors, the growth-stimulating and growth-inhibiting, influencing the life of the amoebae. At that time no direct proof of the occurrence of these factors was

given. With *E. histolytica* (strain no. 7) it has now been possible not only to demonstrate the existence of these two factors but also to study their nature.

In actual experiments profuse and early growth (within 24 hours) of the amoebae was noticed when *E. histolytica* (strain no. 7) was subcultured in E_3 media by direct tube-to-tube inoculation; on the other hand, delayed and feeble growth of the parasites was the result when washed trophozoites were used for inoculation of the same type of media (vide Table III). In direct subcultures the culture fluid which is used as the inoculum contains starch, trophozoites, bacteria and a number of other substances including the metabolites of bacteria and amoebae. But instead of this fluid when the sediment is used after washing, it contains starch, trophozoites and bacteria only. Therefore the explanation why in case of direct subcultures there was early and profuse growth of the amoebae and delayed and scanty in the case of washed sediment, lies in the production of some growth-stimulating substances which appear during the growth of the bacteria and amoebae. As a result of washing the growth-stimulating substances which are essential requirements for the growth of the amoebae, are removed. As a result of this, the inoculated trophozoites suffer from the absence of these essential substances resulting in feeble and delayed growth.

The existence in the culture fluid of some growth-inhibiting substances after it has supported the growth of bacteria and amoebae was also evident from the observations noted in Table II and in tubes no. 3 and 4 in Table III. In these observations there was an increase of viability, this being brought about by the partial replacement of the stale fluid by fresh fluid (vide Table II) and inoculation of washed trophozoites (vide tubes no. 3 and 4 in Table III). Replacement of the stale fluid evidently remove a large amount of the growth-inhibiting substances that have accumulated in the old culture fluid. The prolongation of viability observed after inoculation of washed sediment is probably due to the same cause.

Having discovered the existence of the growth-stimulating and growth-inhibiting factors, attempts were next made to study their nature. The results are discussed below.

NATURE OF THE VARIOUS FACTORS RESPONSIBLE FOR THE STIMULATION OF THE GROWTH OF THE AMOEBAE

The stimulation of the growth and viability of the amoebae in presence of the putrefactive types of bacteria is due to:

(a) *Lowering of the E_h of the medium*: It is already known that a strongly reduced medium is essential for the growth and multiplication of the amoebae. There are strong grounds to hold, from what has been stated before, that the bacteria growing in association with the amoebae are alone responsible for lowering the oxidation-reduction potential of the culture fluid. These bacteria can exist with the help of dual enzyme systems aerobically as well as anaerobically. Following inoculation into a culture medium they at first grow aerobically though for a short time and completely use up the oxygen from the culture fluid. After the oxygen has been absorbed by the bacteria, the latter grow anaerobically after lowering the oxidation-reduction potential of the medium. The above is evident from the decolourisation (reduction) of methylene blue taking place in a freshly prepared emulsion of bacteria (strain no. 1+3) in nutrient broth containing excess of dissolved oxygen as a result of shaking in air. Methylene blue is reduced in an anaerobic medium alone.

(b) *Supply of dehydrogenase system*: Most of the oxidations in living organisms including the amoebae take place by anaerobic dehydrogenation. It has been noticed that although the amoebae are obligatory anaerobes their behaviour in the culture medium is not the same as that of anaerobic bacteria such as *Cl. welchii*. The anaerobic bacteria are unable to lower the E_h of the culture fluid themselves,

but can maintain the reduction when the medium has already been reduced by such means as displacement of oxygen, addition of reducing substances, etc. *E. histolytica*, on the other hand, can neither produce nor maintain the reduction of the culture fluid. This suggests that the dehydrogenase system of the amoeba is probably incomplete and that the bacteria support the life of the parasite by supplying it with the missing portion of its dehydrogenase system.

(c) *Formation of buffers*: The putrefactive types of bacteria produce some alkaline substances in the culture medium at the time the organic acids are formed. These alkaline substances counteract the injurious effects of the acids. The fact that alkaline substances are actually formed during putrefaction of complex proteins has been proved by experimental observations. The maintenance of the pH of the culture fluid at the neutral point even when large numbers of acids have accumulated in the same fluid (vide Table VI) and the rise of pH after its initial fall in glucose broth culturing bacterial strain no. (1+3) (Mukherjea, 1954) strongly support the view of the formation of certain alkaline substances.

It is difficult at this moment to say anything definitely about the nature of these alkaline substances. However, it may be suggested that ammonia or amines formed during the decomposition of the amino acids are probably those substances. Discussions on this point are reserved for the present.

(d) *Production of accessory growth substances*: The most important of the accessory growth-substances are serum, whole blood, etc., which have also other functions. The bacteria provide the accessory growth factors of the nature of vitamin B-complex and experimental proofs have been adduced in its support (Mukherjea, 1954).

NATURE OF THE VARIOUS FACTORS INHIBITING THE GROWTH OF THE AMOEBAE

The stimulation of the growth and viability of the amoebae in presence of the putrefactive types of bacteria is intimately related with the decomposition of the complex proteins of the culture medium. During decomposition the bacteria cause formation of some metabolic substances also, such as organic acids (vide Table VI). The amoebae themselves are also responsible for the production of metabolites which interfere with their own growth. The products of metabolism of the bacteria and amoebae and the associated conditions of fall of pH, rise of E_h etc., which result from the presence of acid metabolites in the culture medium, constitute the growth-inhibiting factors.

The acid metabolites accumulate in the culture fluid and tend to inhibit the growth of the amoebae. This is effected by various ways such as: (i) In absence of buffers the pH of the medium is lowered and thus its E_h is raised (vide Table V). (ii) The amoebae suffer from prolonged contact with the acids. This is deduced from the results noted in Table III. The enhanced vitality of the amoebae which is observed when the trophozoites are washed and then suspended in normal saline for some time is explained as due to revival of the trophozoites from the toxic effects of the acids. Such revival may be effected by exosmosis of the acids accumulating in the protoplasm of the trophozoites. The degree of damage which the amoebae have sustained in the stale fluid will bear a direct relation to the concentration of the acids in the fluid and also to the length of contact between the acids and the trophozoites. The revival of the trophozoites from the injurious effects will, therefore, depend on the two factors stated above. (iii) The acids are likely to inhibit the growth of the amoebae by inactivating the enzymes.

III. *Velocity of enzyme action*

The reactions which are responsible for changing the composition of complex proteins such as, hydrolysis and decarboxylation, are effected by bacterial enzymes

acting on the medium. The rate at which the enzyme disintegrates the substance has been termed as the velocity of enzyme action. The velocity of enzyme action depends, among others, on factors such as, (i) biochemical activities primarily of the bacteria; (ii) temperature; (iii) toxic metabolites of bacteria and amoebae, and (iv) bacteriostatic substances, e.g., antibiotics, dyes, etc., when added to the culture medium.

(i) *Biochemical activities of bacteria*: The biochemical activities of bacteria depend on such factors as composition of the medium, duration of subcultures of the bacteria in culture medium and the manner in which they are cultivated such as, aerobically or anaerobically. The facultative anaerobic bacteria which are generally concerned in the growth and excystation of the amoebae, grow luxuriantly in presence of oxygen. The growth and multiplication, however, diminish greatly if, on the other hand, they are grown anaerobically (Topley and Wilson, 1938). It is a known fact that prolonged subcultures on artificial media affect the pigment-producing properties of many bacteria, such as *B. pyocyaneus*. These observations clearly point out that continuous subcultures of the bacteria, particularly in anaerobic conditions, interfere with their essential biological properties.

When the growth and viability of *E. histolytica* (strain no. 7) were found to diminish on account of repeated subcultures, addition at this stage of a few drops of an emulsion of fresh culture of bacteria from strains no. 1, 2 and 3 grown aerobically on nutrient agar caused a marked increase of the growth and prolonged the viability also (vide Table I). Stimulation of the growth and viability under such conditions, indicates that this was due to the bacteria being now biologically healthier due to their growth in presence of oxygen. Such bacteria induce stronger chemical reactions than the weak ones.

(ii) *Temperature*: The velocity of enzyme action is also influenced by temperature. With cultures of *B. coli* it has been demonstrated that with each rise of 1°C. between 20°C. and 40°C., there is an increase of 1.072 times the rate of growth of the bacteria (Chick, 1912). From this it has been concluded that temperature through stimulation of bacterial growth and metabolism also regulates the velocity of enzyme action. According to the above findings the velocity in the present case should be at its maximum at 37°C., depressed at room temperature which is a little lower than 37°C. and inhibited at 22°C. At 22°C. the bacteria remain more or less static, and it is least likely that strong chemical reaction influencing the growth of the amoebae may occur. While the growth of the amoebae is at its highest at 37°C., its viability on the other hand, as has been mentioned previously, increases at a slightly lower temperature (vide Table IV). The explanation which may be offered for this interesting phenomenon is that temperatures slightly lower than 37°C. lessen the output of the growth-inhibiting factors by depressing the velocity of enzyme action and as such the viability of the amoebae is enhanced.

Apart from such indirect effects of temperature on the growth and viability of amoebae, the former also affects the growth and viability directly. It has been observed with *E. histolytica* (strain no. 7) that when the amoebae after growth at 37°C., are transferred to 22°C. they remain alive for at least 48 hours (vide Table IV). This indicates that these amoebae under certain conditions can resist temperatures much lower than 37°C.

(iii and iv) *Metabolites of bacteria and amoebae and bacteriostatic substances*: Since there is no mechanism whereby the acids formed during the metabolism of bacteria and amoebae are eliminated, these necessarily accumulate in the culture fluid. Unless some arrangements are there for removing the acids or counteracting the acid-producing activities of the bacteria and amoebae, these products are likely to endanger the amoebae. However, on the strength of experimental observations it may be stated that addition of bacteriostatic substances, such as, acriflavine or aureomycin, when used in exceedingly small doses, readily suppresses such forma-

tion of acids. The rise of pH, augmentation of putrefying reactions in the culture fluid and stimulation of the growth and viability of the amoebae all these following the addition of acriflavine (1 : 40,000) to the culture medium, indicate that acriflavine encourages the growth of the amoebae indirectly in the manner just stated (Mukherjea, 1954 and also vide Table I).

SUMMARY

The important features that have emerged from the present studies are :

(a) The existence of the various growth-stimulating factors in culture fluids supporting the growth of amoeba, such as, dehydrogenase systems, buffers, accessory growth substances, low E_h , has been demonstrated. The character of the various growth-inhibiting factors such as a strong acid reaction of the medium, rise of its E_h , etc., has also been studied.

(b) The bacteria growing with the amoeba are primarily responsible for production of both the growth-stimulating and the growth-inhibiting factors.

(c) While the optimum temperature for stimulating the growth of the amoeba is about 37°C., slightly lower temperatures prolong the viability. Under certain conditions the amoeba is able to resist temperatures much lower than 37°C. for a long time.

(d) Temperature, toxic metabolites and bacteriostatic substances modify the growth and viability of the amoeba probably by altering the velocity of enzyme action.

ACKNOWLEDGEMENT

This work was conducted at the Indian Institute for Medical Research, Calcutta, and I must express my thanks to Dr. J. C. Ray, M.D., F.N.I., Director, Indian Institute for Medical Research, Calcutta, for placing all laboratory facilities at my disposal. I am indebted to the Bengal Chemical and Pharmaceutical Works, Ltd., for supply of horse serum and to the National Institute of Sciences of India for awarding a research fellowship. Miss Kamala Chakraborty, Technical Assistant, has helped me in the most efficient manner in carrying out this work.

REFERENCES

- Chick, H. (1912). The bactericidal properties of blood serum. The reaction-velocity of the germicidal action of normal rabbit-serum on *B. coli commune* and the influence of temperature thereon. *J. Hyg., Camb.*, **12**, 414.
- Mukherjea, A. K. (1951). Rôle of bacteria on the growth of *Entamoeba histolytica*. A preliminary note on studies in relation to an unusual strain of *Entamoeba histolytica*. Part I. The growth characteristics of *E. histolytica*. *Ann. Biochem. Exptl. Med.*, **11**, 9.
- (1951). Rôle of bacteria on the growth of *Entamoeba histolytica*. A preliminary note on studies in relation to an unusual strain of *Entamoeba histolytica*. Part III. Detection of the enzymes in the culture media. *Ibid.*, **11**, 47.
- (1954). The rôle of culture medium and its constituents on the growth and viability of *Entamoeba histolytica*. *Proc. Nat. Inst. Sci. India.*, **20**, 437.
- Topley, W. W. C., and Wilson, G. S. (1938). The Principles of Bacteriology and Immunity. 2nd ed., Edward Arnold & Co., London, 81.

Issued January 22, 1955.

STUDIES ON THE PHYSIOLOGY OF RICE

IX. AUXIN CONTENT OF THE VERNALISED SEED

by S. M. SIRCAR, *F.N.I.*, and T. M. DAS, *Department of Botany,
Calcutta University*

(Received August 8, 1954)

INTRODUCTION

There has appeared difference of opinion regarding auxin production and its relation to vernalisation and photoperiodism. Cholodny (1936, 1939) put forward the hypothesis that the embryo is stimulated to activity by the pretreatment method, it absorbs from the endosperm auxins that are present in it in great quantity. Thus there occurs an increase in the concentration of auxin in the cells of the embryo and this increase causes an acceleration in the progress of the meristematic cells of the young plant through the earlier phase of development with the result that the phases of later stages connected with reproduction are shortened. Gregory and Purvis (1936, 1938) and Hatcher (1945) have concluded from a number of experiments that vernalisation of embryo is possible without the endosperm taking any part. According to them auxin of endosperm far from being accumulated in the embryo undergoing vernalisation as suggested by Cholodny is not concerned in the process. Cholodny has further concluded that the manufacture of a flower forming substance in the leaf is possibly related with chemical transformation of auxin.

The relation of auxin to the initiation of flowering has been stressed by a number of workers. Cholodny (1939) and Galston (1943) formulated the hypothesis that high auxin levels in the plant may be unfavourable to flowering. This was later supported by other observation that flower formation of shortday plants can be suppressed by treating the plants with auxin or synthetic growth regulating substances and can be induced under non-inductive conditions by treatment with auxin antagonists or the agents which destroy the auxin (Bonner and Bandurski, 1952). On the other hand, Leopold and Thimann (1949) have reported that continuous application of indole acetic acid may actually increase the number of floral primordia. These observations led Thimann (1948) to conclude that low concentration of auxin may increase flowering while higher doses inhibit flowering. Leopold (1949) has further shown that increased tiller production is an indication of reduced auxin level. In the rice plant several important peculiarities pertinent to the auxin relation of the plant have been noted. The main features are that the influence of low temperature stimulation does not lead to the acceleration of flowering but results in increased vegetative growth (Sircar, 1948; Sircar and Parija, 1949) while short days accelerate flowering and increase tillering (Sircar and Sen, 1953). In order to elucidate the response of the rice plant towards the temperature of germination and photoperiodic induction it was felt that a systematic study of auxin production in the rice plant during its life cycle will be of considerable importance. The present paper gives an account of the method of extraction of auxin which has been standardised for the plant and its variation in the seed during the process of vernalisation.

EXPERIMENTAL METHOD

The estimation of auxin was made by the *Avena* test; Skoog's deseeded method (Skoog, 1937) was applied. In order to carry out all operations for *avena* test a

chamber for phytohormone researches in the tropics devised by the authors was used in this investigation. This chamber having a regulated temperature of $25^{\circ}\text{C} \pm 2$ and 88 to 90 % humidity was successfully employed for germination of oat seeds under red light, decapitation, blocking, and taking the shadow graphs of the curvatures without removing them to other atmosphere. The details of the apparatus and arrangements for the culture of test plants were described elsewhere (Sircar and Das, 1950 and 1951). Seeds of a pure strain of *Avena Sterilis* Var. *Culta* obtained from the Indian Agricultural Research Institute, New Delhi, were employed for *avena* curvatures.

The procedure of Skoog's deseeded method partly modified by the authors is as follows:—Grains of oat were soaked in water for 2 to 3 hours, water is drained off and the grains with grooved side downwards and $\frac{1}{2}$ " apart were set in $\frac{3}{4}$ " apart rows in petri dishes. The dishes were subsequently kept in the operating compartment of the test chamber and exposed under red light in order to inhibit the growth of the first internode. The seeds were allowed to germinate undisturbed for two days. In the early morning of the third day seeds with sprouting embryos were fixed at the bent mouth of the glass holder (cf. fig. 3K of Sircar and Das, 1950) with the radicle immersed in water and set in position approximately at a 60° angle, so that the coleoptile would grow upward and straight. These sets were then transferred to the middle humid compartment of the chamber and allowed to grow under complete darkness.

In the evening between 8 and 9 p.m. coleoptilers of 1.2 cm. in length were selected and their endosperms carefully broken off with finger. A small tuft of absorbent cotton was wound round the region of the removed endosperm. The seedling was then carefully pulled into the ring of the holder (cf. fig. 3L). The process of deseeding was done in the operating compartment; after deseeding the test sets were removed in the darkness of the humid compartment. In the evening (5 to 6 p.m.) of the fourth day perfectly straight coleoptiles of uniform length were selected, decapitated only once and immediately the agar blocks of hormone extract were placed unilaterally on the tips. Shadow graphs were taken after the agar blocks were in contact with the decapitated coleoptile for 5 hours.

Dilution of plant extracts.—The extract from the plant tissue was first diluted to a definite volume with 50 c.c. of water. 1 c.c. of this aqueous extract was then mixed with 1 c.c. of 3% agar. This was the same as diluting the original residue in 100 c.c. of $1\frac{1}{2}$ % agar. The agar was previously washed and allowed to soak in several changes of distilled water for 4 to 5 days, then dried and made up to the required percentage. 1 c.c. of this 100 c.c. dilution was then mixed with 1 c.c. of the $1\frac{1}{2}$ % agar, the equivalent of making up the original extract to 200 c.c. of $1\frac{1}{2}$ % agar. Thus several dilutions were prepared to make certain that the test was within the proportionality range.

Casting of agar plates.—The molds for the agar plates were prepared by cutting rectangular openings out of plastic sheet of thickness of 1.5 mm. The agar plate was then cut into twelve blocks, each of size $2.67 \times 2.67 \times 1.5$ mm. and of volume 10 c.mm. This size of agar block was specially chosen as the results were expressed in T.D.C. units.

Computation of results.—Results were expressed in terms of T.D.C./gm. This has been used in preference to the indole acetic acid equivalent (Avery *et al.*, 1941). T.D.C. units can also be easily converted to units of other methods as 100,000 T.D.C. are equivalent to 1.0 gamma of β -indole acetic acid. T.D.C. = total degree curvature was calculated from the expression

$$\frac{C \cdot 100 \cdot V}{W}$$

where C = average degree of curvature produced by one 10 c.mm. block, $100 =$

number of such blocks. V = total volume in c.c. of agar extract, W = weight in gms. of the tissue extracted.

The minimum number of *avena* test plants used for any single determination was 12, although in many cases 24 to 36 plants were used. For a single determination two different dilutions were used separately in order to ascertain that the curvatures were within the proportionality range. Curvatures of the shadow graphs were measured with the help of a special type of transparent plastic protector fitted with a revolving arm (Went, 1937).

EXPERIMENTAL RESULTS

Comparison of different extraction methods. (Fig. 1.)

The main object was to devise a suitable method for the extraction of auxin from rice grains. Although several test methods have been developed by workers in the field, but it has been shown by Avery *et al.* and Hatcher that a good deal of variation in the auxin content is due to the extraction method and the type of solvent used. After using alcohol they have recommended water to be superior as a solvent for the extraction of auxin from maize and rye. Avery *et al.* further emphasised the need for standardising the extraction method for each species before any reliable observation on the behaviour of auxin in the developmental process of a plant can be made. Accordingly a number of extraction methods were tried to find out a suitable one for rice.

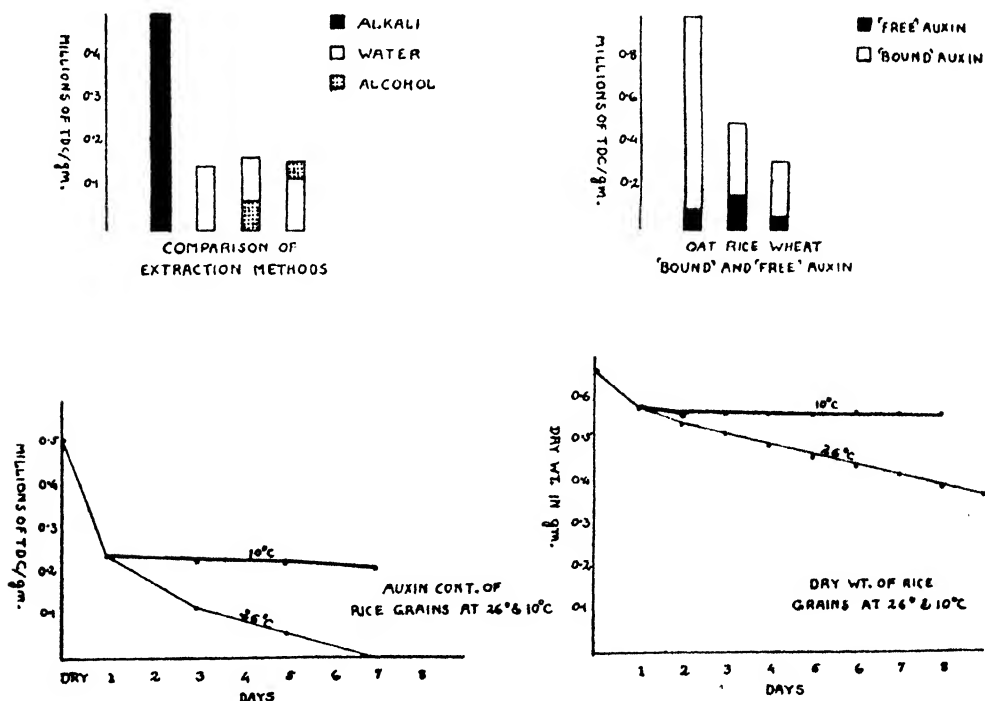


FIG. 1.

Water extraction:

The original method of Van Overbeek (1938) was partly modified by the authors to get the best results in this investigation. The procedure is as follows:—50 air

dry endosperms of rice with carefully removed embryo portions weighing approximately 0.75 gms. were ground finely with 5 c.c. of water for 3 min. in a glass mortar with an equal quantity of specially cleaned sand (washed in steam, alkali, acid and water and then dried). The thoroughly ground material was carefully transferred to a 25 c.c. heavy walled pyrex glass centrifuge tube, the residue remaining with the mortar and pestle being washed into the tube by another 10 c.c. of water (cleared up by 3 washes of 3 c.c. in each time). The material was subsequently centrifuged with an electric centrifuge for 15 min. At the end of the operation the clear supernatant liquid was transferred to a measuring flask and diluted to a definite volume and assayed for auxin activity by *avena* test.

This method has been found comparatively easier than other methods. As there is no organic solvent present, it is unnecessary to heat the extract to dryness; hence comparatively much shorter time is needed for extraction. From the data presented in the Table I it will be found that the yields of the auxin by water extraction is not at all insufficient in comparison with that of multisolvent method. For the extraction of 'free auxin' present in the endosperm of rice water extraction has been proved to be the best one; accordingly this method has been adopted in this investigation.

TABLE I

*Auxin yield from rice endosperm as determined by the different extraction methods. Determinations were made from batches of 50 dormant endosperms with excised embryos. All *avena* curvatures were within the proportionality range.*

Extraction methods	Fresh weight of 50 endosperms in gms.	Total vol. in c.c. of agar extract mixture	Millions of T.D.C./gm.
Water	0.78	50	0.15
Multisolvent extraction			
First 20 washes of alcohol	0.75	50	0.07
Second 20 washes of water		50	0.11
First 20 washes of water	0.77	50	0.12
Second 20 washes of alcohol		25	0.04
Alkali hydrolysis			
N/100 NaOH at 100°C. over water bath for 2 mins.	0.74	200	0.49
N/100 NaOH at room temperature (26°C.) for 48 hours	0.78	200	0.50

Multisolvent extraction:

Avery *et al.* (1941) have shown that neither alcohol nor chloroform can extract all auxins from maize endosperm. Their results indicate that the auxin yields after multisolvent extraction are slightly higher than those obtained with water. Accordingly successive extraction with water and alcohol in different sequences were tried in rice endosperm. Weighed endosperm was finely ground with 5 c.c. of alcohol and equal weight of washed sand in a glass mortar and pestle for 3 min. The ground material was poured on the filter paper and suction applied. The first twenty washes, each with 5 c.c. of the solvent were collected in one flask; each wash lasted one min. only. The filtrate was then evaporated to dryness under reduced pressure at 60°C. in order to remove all the organic solvents present in the mixture. The dry residue thus obtained was again diluted with water to a definite volume and assayed for auxin activity. After the extraction with one solvent the tissue remaining on the filter paper was dried for 15 min. at 45°C. The second

solvent water was then used in a similar manner for further extraction of auxin from the original tissue. From the data presented in the Table I it will be seen that the total yield of auxin extracted by the sequence of alcohol and water was 0.175 million of T.D.C. per gm. of endosperm tissue; of this first twenty washes of alcohol removed 0.07 million units of auxin and the last 20 washes of water 0.105 million units. Thus of the total amount of auxin about 40% removed by alcohol and 60% by water. On the other hand, the total yield of auxin extracted by the sequence of water and alcohol was 0.16 million of T.D.C.; of this the first 20 washes of water removed 75% and the last 20 washes of alcohol 25%.

Alkali hydrolysis :

The sample of rice endosperm was finely ground with equal weight of washed sand in a known volume of alkali at pH 9.5 for 3 to 10 mins. The pH 9.2 to 9.6 of the extract was maintained by using alkaline soda borax buffer. The ground material was transferred to a 25 c.c. heavy walled Pyrex glass centrifuge tube and either boiled over water bath for 2 mins. or kept for 48 hours at room temperature under direct exposure to light. The clear supernatant liquid after centrifuging in an electric centrifuge was neutralised with acid and appropriately diluted for assay by the avena test. From the table it will be seen that after hydrolysis at pH 9.5 the yield of auxin is 0.5 million T.D.C. per gm. of endosperm tissue which is about 3 times greater than the best yield obtained by water or multisolvent extraction. The amount of auxin liberated at 100°C. for 2 min. is approximately equal to the amount obtained by the prolonged hydrolysis for 48 hours at room temperature (26°C.). From a comparison of these methods it will appear that water alone is a fairly effective solvent for the removal of free auxin from rice endosperm. In multisolvent method, however, yields obtained in most instances are only a little higher than those with water alone. The higher yield was noted if a greater number of washes are made with water, which according to Avery *et al.*, 1941, is due to slow hydrolysis. The striking effect of alkali-hydrolysis is the liberation of bound auxin from its precursor in rice endosperm. Of the several methods for liberating bound auxin from rice endosperm alkali hydrolysis gave about 70% of total content while 30% exist as free auxin extractable with water alone.

A comparison of the auxin content of several grains was made in this connection. From the data presented in the Table II and fig. 1 it will be seen that maize grain contains the highest amount of free auxin as well as bound auxin. Of the two varieties of rice, *Rupsail* and *Bhasamanik*, each of them contains a fairly high amount of free and bound auxin.

TABLE II

'Free' and 'bound' auxin from different cereals of local varieties. Determinations were made from 5 batches of 50 dormant endosperms with excised embryos and the auxin content expressed in millions of T.D.C./gm. units

Cereals	Free auxin	Bound auxin
Rice—		
var. <i>Rupsail</i> ..	0.15	0.35
„ <i>Bhasamanik</i> ..	0.14	0.37
Oat ..	0.09	0.91
Wheat ..	0.07	0.25
Maize ..	0.53	0.97

Auxin content of the vernalised grain :

The purpose of the experiment was to study the effect of vernalisation on the consumption of auxin by the germinating embryo during growth. Rice grains were first soaked in water for 4 hours and further 20 hours on moist filter paper in petri dishes. After soaking some of the petri dishes were transferred to the refrigerator (10°C.) and others to a dark chamber at room temperature 25° to 27°C. As the germination proceeded from day to day the total auxin content of the endosperm after hydrolytic extraction were assayed by Skoog's deseeded test. A few minutes before extraction the embryos and the pericarps were carefully removed from the endosperm. A group of 50 endosperms from uniform sized seedlings were always used for extraction.

Along with the determination of auxin content the fresh and dry weights of the endosperm and the growth of the seedlings were recorded and presented graphically in fig. 1 and in Tables III, IV and V. The data in Table III show that as the

TABLE III

Auxin yield from 50 endosperms of rice variety Rupsail cultured at room and vernalisation temperatures

Materials	Room temperature 26°-27°C.			Vernalisation temperature 10°C.		
	Fresh wt. of 50 endosperms in gms.	Total vol. in c.c. of agar extract	Million of T.D.C./gms.	Fresh wt. of 50 endosperms in gms.	Total vol. in c.c. of agar extract	Million of T.D.C./gms.
Dormant ..	0.75	140	0.51
1 day ..	1.21	140	0.24
3 days ..	1.11	140	0.12	1.2	140	0.23
5 days ..	1.0	75	0.06	1.3	140	0.23
7 days	1.2	180	0.21
15 days	1.2	160	0.18

TABLE IV

Fresh and dry weights in gms. of 50 endosperms of rice var. Rupsail cultured at room and vernalisation temperatures

Days of germination	Room Temperature (26° to 27.5°C.)		Vernalisation Temperature (10°C.)	
	Fresh weight	Dry weight	Fresh weight	Dry weight
Dormant ..	0.784	0.665
12 hours ..	1.263	0.625
1 day ..	1.212	0.580
2 days ..	1.110	0.545	1.205	0.565
3 ..	1.112	0.520	1.202	0.565
4 ..	1.050	0.490	1.201	0.565
5 ..	1.020	0.460	1.201	0.564
6 ..	0.975	0.445	1.200	0.564
7 ..	0.915	0.420	1.200	0.562
8 ..	0.855	0.390	1.200	0.562
9 ..	0.802	0.370	1.200	0.562
10 ..	0.750	0.330	1.198	0.560

TABLE V

Growth of rice seedlings germinating at the room and vernalisation temperatures. The data are the average of 10 individuals

Days of germination	Room temp. (26°-27.5°C.)			Vernalisation temp. (10°C.)		
	Length of root in mm.	Length of shoot in mm.	No. of leaves unfolded	Length of root in mm.	Length of shoot in mm.	No. of leaves unfolded
1	2.4	1.5	..	2.5	1.5	Nil
2	13.0	5.0	..	2.6	2.5	"
3	37.0	14.0	1	3.0	2.6	"
4	56.0	31.0	1	3.0	2.6	"
5	62.0	42.0	2	3.0	2.6	"
6	67.0	52.0	2	3.0	2.6	"
7	71.0	64.0	2	3.0	2.6	"
8	75.0	75.0	3	3.0	2.6	"
9	78.0	88.0	3	3.0	2.6	"
10	81.0	92.0	3	3.0	2.6	"

germination at room temperature proceeded the total yield of auxin per gm. of endosperm tissue rapidly decreased with corresponding decrease of fresh and dry weights of the material. More than 88% of the total auxin present in the dormant endosperm was consumed during 5 days of germination at the room temperature; the corresponding loss in dry weight was about 30% and the seedlings have two unfolded leaves with 6.2 cm. root and 4.2 cm. shoot length. After 7 days of germination no extractable hormone was detected in the endosperm. While the auxin consumption during vernalisation treatment at 10°C. was very small, even after 15 days the auxin level was as much as 0.18 million T.D.C. During this period there was also little change in fresh and dry weights nor any increment in the size of the seedlings. A remarkable effect of temperature on the consumption of auxin is thus very apparent. After 24 hours of soaking the total consumption of auxin per gm. of endosperm tissue was 0.27 million of T.D.C. units. But when these sprouting grains were transferred to the refrigerator at 10°C. the rate of consumption was promptly inhibited which was evident from the fact that during the next 48 hours the total consumption was only 0.012 million T.D.C.

CAUSE OF THE GRADUAL DISAPPEARANCE OF AUXIN FROM THE GERMINATING ENDOSPERM

From the foregoing experiment it is apparent that the growth hormone is gradually disappearing from the endosperm at high temperature. But the question arises whether during germination it is consumed by embryo or destroyed or masked by the inhibitor substances formed in the embryo. In order to elucidate this the following experiment was carried out. In the first set rice grains were allowed to germinate at room temperature under proper conditions described before. After 24 hours of germination sprouting embryos with the epithelial layer were completely removed from the endosperm. The excised endosperm was then cultured for further 24 hours and subsequently assayed for the hormone content. In another set, germination of grains proceeded as before and the auxin content of the endosperm was assayed after 24 and 48 hours (the embryo was excised just before the extraction of auxin). From the results presented in Table VI it is interesting to note that excised endosperm 48 hours old contains as much hormone as the intact

one 24 hours old, in other words, after excision there is little or no appreciable change of the auxin level in the endosperm. A much reduced yield of auxin has, however, been recorded from intact endosperm 48 hours old indicating the fact that constant reduction of auxin from the endosperm can only take place in the presence of embryo. It is, therefore, evident that the gradual disappearance of auxin from the germinating rice grain is solely due to the activity of the growing embryo.

TABLE VI

Auxin content of rice endosperm with embryo intact and excised

Experiments	Fresh wt. of 50 endosperms in gms.	Total vol. in c.c. of agar extract	Millions of T.D.C./gm.
Endosperm after 48 hrs.—24 hrs. with embryo and 24 hrs. without embryo	1.20	130	0.255
Endosperm after 24 hrs. with intact embryo ..	1.25	130	0.262
Endosperm after 48 hrs. with intact embryo ..	1.18	100	0.155

EFFECT OF LOW TEMPERATURE ON THE HYDROLYSIS OF AUXIN PRECURSOR

The previous experiment indicates that at low temperature the consumption of auxin is markedly inhibited. In order to ascertain whether this inhibition is caused by the interruption of the hydrolytic reaction yielding auxin from its precursor a series of experiments were carried out in which hydrolytic reaction of the auxin extract was maintained at different temperatures. The alkali hydrolysis extraction method was followed. The endosperm material after grinding was kept in the centrifuge tube for 48 hours at different temperatures, 5°, 10°, 22° and 27°C. and subsequently centrifuged and auxin content assayed by the avena test. It shows (Table VII) that by lowering the temperature, the hydrolysis of auxin precursor is markedly interrupted.

TABLE VII

Effect of low temperature on the hydrolysis of auxin precursor in rice. 50 endosperms weighing approximately 0.75 gms. were extracted in mixture of 150 c.c. of agar extract

Temperature of hydrolysis	Millions of T.D.C./gm.
27°C.	0.51
22°C.	0.44
10°C.	0.32
5°C.	0.18

DISCUSSION

Different methods of extraction of auxin from rice endosperm have been tried. In water extraction an appreciable quantity of hormone has been detected. Hatcher (1945) has also noted that repeated water extraction gives about the same auxin in winter rye as multisolvent extract.

The amount of free auxin in rice is as high as that of oat and wheat. Oat, however, contains much higher quantity of bound auxin than that present in rice

and wheat. In the endosperm of maize Yamaki and Nakamura (1952) have noted a very low content of indole acetic acid. They have suggested that auxins are produced by the embryo itself and for this purpose tryptophan as one of the precursor is transferred from the endosperm. While Das (1953) has shown that the isolated embryos are capable of synthesising auxin without the intervention of the auxin precursor derived from the endosperm. The production of auxin in the isolated embryo is related to the carbohydrate and oxygen supply. Sucrose is considered to be the substrate for the synthesis of auxin.

A marked inhibition of the consumption of auxin from the endosperm tissue has been recorded at 10°C. together with the inhibition of seedling growth and loss of dry weight of the tissue. Thus during 144 hours of low temperature period the total consumption of auxin from germinating endosperm is nearly 0.027 millions of T.D.C./gm. and there is little or no increase in the size of the embryo detected. But during the same interval of time over 0.45 millions of T.D.C./gm. of auxin has disappeared from the endosperm tissue cultured at 26°C. and the seedlings attained the size of 119 mm. length with 2 unfolded leaves. It appears that the disappearance of auxin is due to the activity of the growing embryo as the auxin content is very little changed after the excision of the embryo. The gradual disappearance of auxin from the germinating grain is of considerable significance. Following the variation of auxin content during development of spring and winter rye Hatcher noted a peak value during development, followed by disappearance at maturity. He suggested that this is due to the desiccation of the grain during ripening and not to translocation from the grain nor any growth activity. He further noted a large hormone concentration in the rye endosperm but it was not known what happens to this stored auxin during germination. In rice it has, however, been shown that hormone gradually disappears during germination as it is needed by the growing embryo. Since no separate estimation of auxin content from rice embryo was made it may be possible that the hormone released from the endosperm accumulates in the embryo proper. But it has been shown by Das that little auxin disappears from the endosperm when the embryo growth is checked by low temperature treatment or the embryo excised from the endosperm. This apparently suggests that disappearance from the endosperm is due to the growth activity of the embryo and not a case of its accumulation in the embryo.

Auxin content of the rice seeds vernalised at low temperature (Table III) is higher, but there is no acceleration of flowering (Sircar and Parija, 1949). This shows that high auxin level in the seeds is not related with the acceleration of flowering which Cholodny has claimed. On the other hand, low temperature vernalisation induced increased vegetative growth (Sircar and Parija, 1949). As auxin disappears with the growth of the seedling, it appears that high auxin level of the vernalised seeds is related to increased vegetative growth.

SUMMARY

Different methods of extraction of auxin from rice endosperm have been tried. By *avena* test a comparison of the auxin content of different grains was made.

Auxin content of the endosperm of rice during vernalisation at low temperature remains fairly high while at the normal temperature of germination it disappears gradually. The disappearance of auxin from the endosperm is due to the activity of the growing embryo as the auxin content is very little changed in the endosperm after the excision of the embryo. The effect of low temperature on the interruption of the hydrolysis of auxin precursor is indicated.

REFERENCES

- Avery, G. S. Jr. and Shalucha, B. (1941). Extraction of hormone yields in relation to different *Avena* Test methods. *Amer. Journ. Bot.*, 28, 498-506.
 Avery, G. S. Jr., Berger, J. and Shalucha, B. (1941). The total extraction of free auxin and auxin precursor from plant tissue. *Ibid.*, 28, 596-607.

- Bonner, J. and Bandurski, R. S. (1952). Studies on the physiology, pharmacology and biochemistry of the Auxins. *Ann. Rev. Plant Physiol.*, **3**, 59-86.
- Cholodny, N. G. (1936). *Comptes Rendus Acad. Sci.*, 391-4. U.R.S.S. III. Cited from R. G. Whyte, Crop Production and Environment. Faber and Faber, London.
- (1939). *Herb. Rev.* VII. *Ibid.*
- Das, T. M. (1953). Ph.D. Thesis, University of London.
- Gregory, F. G. and Purvis, O. N. (1936). Vernalisation of winter rye during ripening. *Nature*, **138**, 973.
- (1938). Studies in Vernalisation of cereals. II. The Vernalisation of excised mature embryos and of developing ears. *Ann. Bot. N.S.*, **2**, 237-251.
- Hatcher, E. S. J. (1945). Studies in the Vernalisation of Cereals. IX. Auxin production during development and ripening of the anther and carpel of spring and winter rye. *Ibid.*, **9**, 235-266.
- Leopold, A. C. and Thimann, K. V. (1948). Auxin and Flower initiation. *Science*, **108**, 664.
- (1949). The effect of auxin on flower initiation. *Amer. Journ. Bot.*, **36**, 342-347.
- (1949). The control of tillering in grasses by auxin. *Ibid.*, **36**, 437-439.
- Sircar, S. M. (1948). Vernalisation and Photoperiodism in the tropics. Vernalisation and photoperiodism, a symposium. *Lotsya*, Vol. I, Chronica Botanica Co., U.S.A.
- Sircar, S. M. and Parija, B. (1949). Studies in the physiology of rice. V. Vernalisation and photoperiodic response in five varieties. *Proc. Nat. Inst. Sci. Ind.*, **15**, 93-107.
- Sircar, S. M. and Das, T. M. (1950). A chamber for phytohormone researches in the tropics. *Sci. and Cult.*, **15**, 282-84.
- (1951). Growth hormones of rice grains germinated at different temperatures. *Nature*, **168**, 382.
- Sircar, S. M. and Sen, S. P. (1953). Studies on the physiology of rice. VI. Effect of photoperiod on the development of the shoot apex. *Bot. Gaz.*, **114**, 436-448.
- Skoog, F. (1937). A deseeded *Avena* test method for small amounts of auxin and auxin precursor. *Jour. Gen. Physiol.*, **20**, 311-34.
- Van Overbeek, J. (1938). A simplified method for auxin extraction. *Proc. Nat. Acad. Sci.*, **24**, 42-46.
- Went, F. W. and Thimann, K. V. (1937). *Phytohormone*. The Macmillan & Co., New York, pp. 294.
- Yamaki, T. and Nakamura, K. (1952). Formation of indole acetic acid in maize embryo. *Sc. pap. of Coll. Gen. Edn. Univ. of Tokyo*, **2**, 81-98.

Issued January 24, 1955.

STUDIES ON THE REPRODUCTIVE TRACT OF *ARIOPHANTA* *MADERASPATANA* (GRAY) (MOLLUSCA: PULMONATA)

PART I. HISTOCHEMISTRY OF THE AMMATORIAL ORGAN

by V. K. SUNDARARAJA IYENGAR, *Department of Zoology, Central College,
Bangalore*

(Communicated by B. R. Seshachar, F.N.I.)

(Received June 15; read October 20, 1954)

INTRODUCTION

The reproductive system of pulmonate gastropods is highly complicated and consists of a number of distinct regions. A recent paper on the reproductive tract of *Ariophanta ligulata* (Dasen, 1933) details the possible rôle which some of these different regions fill, but much remains to be done in regard to the others. Among them is a characteristic structure called the ammatatorial organ which is an invariable component of the reproductive apparatus of *Ariophanta*. It is believed by Dasen that this structure, situated near the external genital aperture and given off as an outpushing of the vagina, is in the nature of an organ intended to excite the partner during copulation. It is believed to elaborate secretions, whose function, however, is not known. It was felt that an application of modern methods of histochemistry and cytochemistry would help reveal the true nature of the substances formed in the ammatatorial organ. Besides, it was felt that an application of these methods would also throw some light on the functional importance of this complicated organ.

MATERIAL AND METHODS

For histological and cytological studies the material was fixed in chilled 80% ethyl alcohol, Bouin's fluid and Carnoy's fluid. Sections 10 micra thick were cut by the paraffin method. While the material fixed in Carnoy's fluid was stained with Feulgen's reagent after a preliminary hydrolysis at 60° C. for five minutes, that fixed in Bouin's fluid and in 80% alcohol, was stained either in Heidenhain's iron haematoxylin or in Mallory's triple stain.

For detection of alkaline phosphatase, Gomori's technique was employed on sections of material fixed in chilled 80% ethyl alcohol. After fixation, the material was dehydrated in alcohols in the refrigerator (as suggested by Bradfield, 1951), cleared in benzene, and infiltrated *in vacuo*, at 56° C. Precautions suggested by Danielli (1946) were taken during the course of treatment. Sections were then incubated in a substrate medium, consisting of glycono-phosphate at pH 9.4 and were later treated with cobalt chloride and ammonium sulphide. Upon hydrolysis of the ester by the tissue enzyme, a black deposit of cobalt sulphide was observed at sites of enzymatic activity. Controls were run as a matter of routine and these showed no signs of reaction. No counterstain was used.

For demonstration of glycogen and other carbohydrate protein complexes, sections of material fixed in 80% alcohol and Carnoy's fluid were subjected to the periodic acid Schiff (PAS) reaction of Hotchkiss (1948) and McManus (1946, 1948). Results thus obtained were supplemented by the use of the Bauer-Feulgen and Best's carmine techniques for glycogen and mucin. In all these cases controls

were run by incubating the slides in human saliva for one hour at a temperature of 37° C. prior to routine treatment, in order to distinguish polysaccharides such as glycogen from other reactive carbohydrates. While using the PAS routine, controls with the omission of periodic acid were also run, and these slides were made to stand in distilled water at the same temperature and for the same length of time as the test slides stood in periodic acid. Some of these preparations were counter-stained either with toluidine blue, or with light green.

To distinguish the acidophilic part of the secretory material from the basophilic part, a few sections were also treated, either with the methylene blue-eosin method employed by Wimsatt (1951) or by Nocht's azure-eosin method employed by Lillie (1948).

OBSERVATIONS

The ammatorial organ of *Ariophanta maderaspatana* resembles in histological structure that of *A. ligulata* described by Dasen (1933). In a transverse section it is made up of four layers: (1) an outermost layer of glandular cells covered externally by thin connective tissue, (2) thick musculature beneath, (3) a layer of connective tissue lying next to it, internally, (4) the lining of the central canal which is thrown adradially into a number of pouches (Text-fig. 1 A, C).

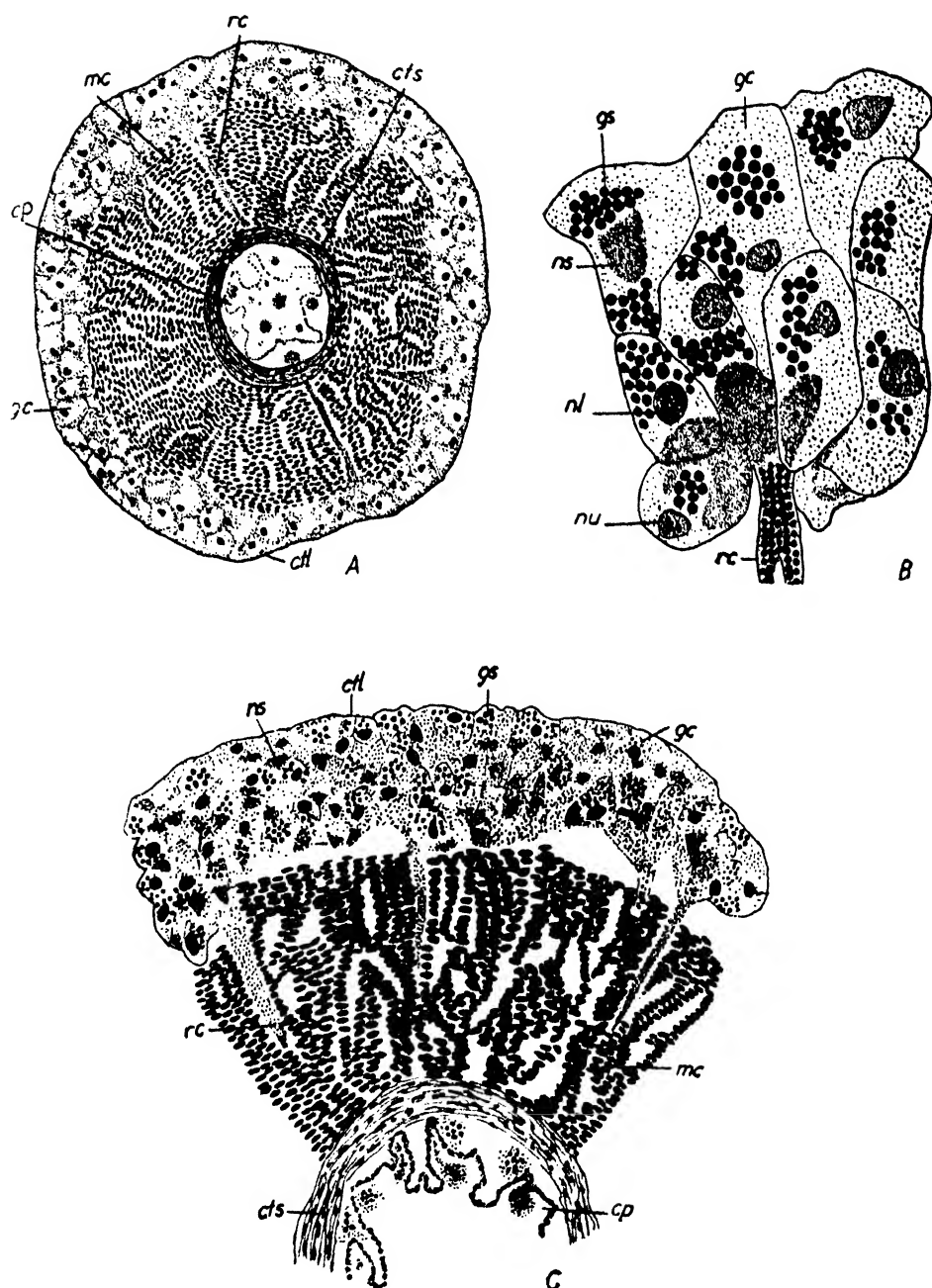
The glandular part of the ammatorial organ is made up of four layers of cells. Each cell is large, more or less polygonal in shape, with a conspicuous polymorphic nucleus. The cytoplasm is filled with granular as well as non-granular secretions which are conveyed to the central pouches by a number of radial canals traversing the musculature (Text-fig. 1 B).

The application of techniques mentioned above seems to indicate the elaboration, by the glandular cells, of two very different and independent substances. In haematoxylin preparations granules fill the cytoplasm of the gland cells (Text-fig. 1 B, C; Plate XXIII, fig. 1; Plate XXIV, fig. 12). These granules are Feulgen negative (Plate XXIII, fig. 4; Plate XXIV, fig. 14) but stain blue in Mallory's triple preparations (Plate XXIII, fig. 2; Plate XXIV, fig. 13) and are eosinophilic in methylene blue-eosin and azure-eosin preparations (Plate XXIII, fig. 3 and Plate XXIV, fig. 15). The most interesting reaction, however, is found in the PAS treated material where the cytoplasmic granules in the gland cells show up deep pink (Plate XXIII, fig. 5). Incubation in human saliva does not dissolve them. These granules also stain green in Bauer-light green preparations. These facts make it clear that the granular secretion of the glandular cells is made up of glycoprotein, acidophilic in nature, and resistant to human saliva, perhaps a neutral mucopolysaccharide.

In addition to the granular secretion, the gland cells appear to elaborate a non-granular material. This substance shows up particularly clearly in haematoxylin preparations (Text-fig. 1 B, C; Plate XXIII, fig. 1; Plate XXIV, fig. 12). It is also stained pink in Bauer-light green and Best's carmine techniques for glycogen and mucin (Plate XXIII, figs. 7 and 10) and is resistant to the action of human saliva (Plate XXIII, figs. 8 and 11). It is negative to Mallory's triple stain and does not show up either in methylene blue-eosin or in Nocht's azure II-eosin preparations. Its distinctness from the granular secretion is clear. It is a glycoprotein, resistant to human saliva and is perhaps mucin.

The two kinds of secretory material, granular as well as non-granular, were also found in the radial canals as well as in the central pouches of the ammatorial organ.

The application of Gomori's technique to the glandular cells reveals that they display a particularly intense positive reaction. All parts of the cell show up dark,—cytoplasm, nucleus and nucleolus. The cytoplasmic reaction takes the form of fine dark granules, specially abundant in the granular secretion (Plate XXIII, fig. 9 and Plate XXIV, fig. 17). It seems to indicate a granular localization of alkaline phosphatase in the cytoplasm of these cells.



TEXT-FIGURE I

- (A) Transverse section through the ammatatorial organ. $\times 61$.
 (B) A group of gland cells and a part of the radial canal magnified to show the granular and non-granular secretions. $\times 610$.
 (C) A portion of figure A magnified. $\times 122$.

chl.—connective tissue layer; *gc.*—gland cell; *mc.*—muscular cylinder; *cts.*—connective tissue sheath; *cp.*—central pouches; *rc.*—radial canals; *gs.*—granular secretion; *ns.*—non-granular secretion; *nu.*—nucleus; *nl.*—nucleolus.

The muscular layer of the ammatorial organ presents cytochemical evidences of a rather interesting nature. In PAS preparations the musculature gives a deep positive reaction (Plate XXIII, fig. 5) while it is less intense in Bauer-Feulgen and Best's carmine material (Plate XXIII, figs. 7 and 10). The significance of these reactions becomes clear on application of human saliva for one hour, when the reaction becomes totally negative (Plate XXIII, figs. 6, 8 and 11; Plate XXIV, fig. 16). This clearly indicated a heavy accumulation of glycogen in the musculature of the ammatorial organ. The musculature was totally negative to Gomori's technique and to methylene blue-eosin (Plate XXIII, figs. 3 and 9).

The connective tissue of the ammatorial organ also gives a positive reaction with the PAS, Bauer-Feulgen and Best's carmine techniques (Plate XXIII, figs. 5, 7 and 10). The reaction is not abolished on incubation in human saliva (Plate XXIII, figs. 6, 8 and 11).

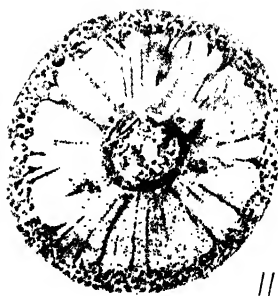
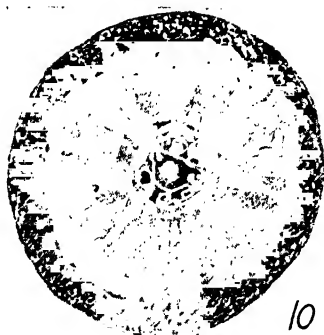
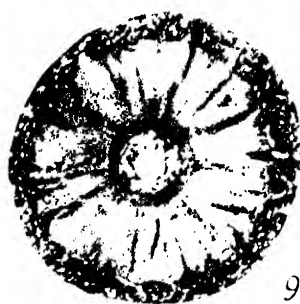
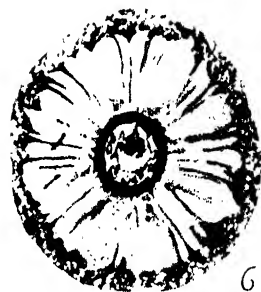
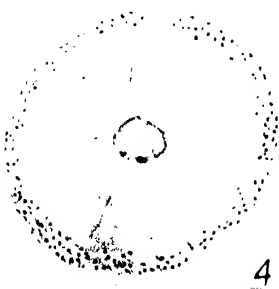
TABLE

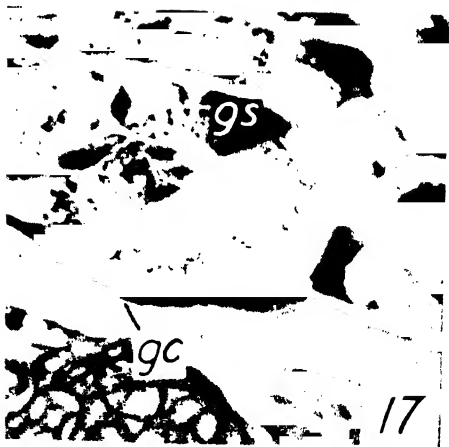
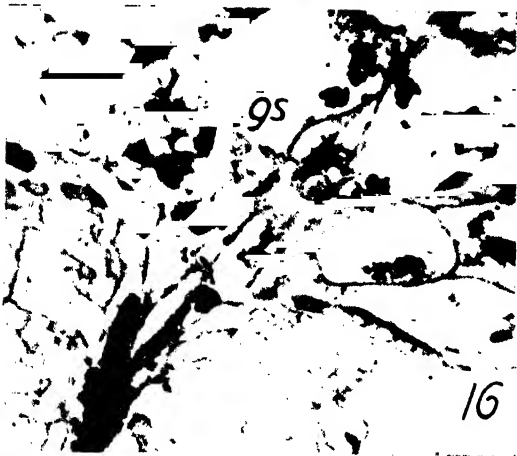
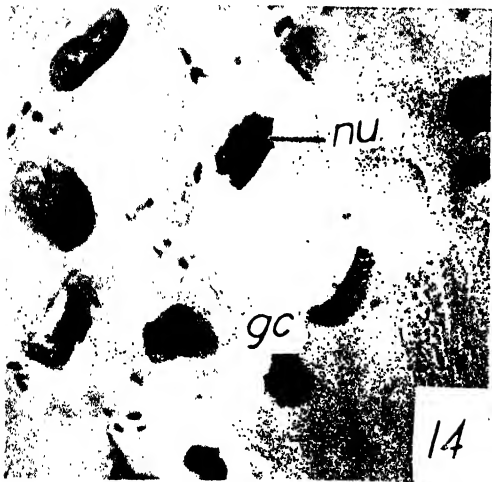
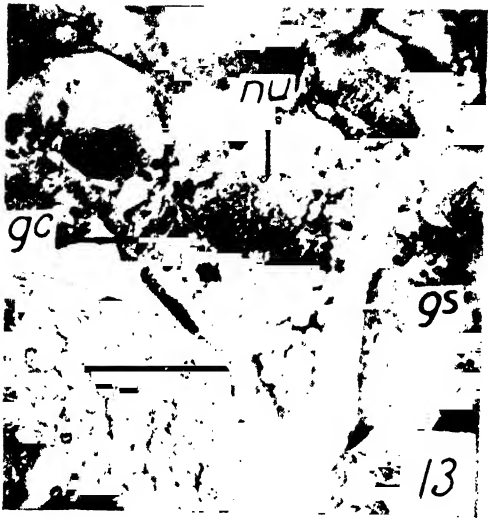
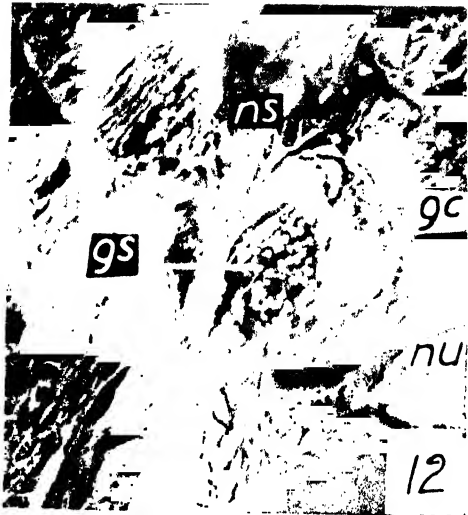
Table indicating the histochemical reactions of different regions of the ammatorial organ.

	Gland Cells				Muscle	Con- nective tissue
	Nuclei	Nucleoli	Secretion			
			Granular	Non- granular		
Haematoxylin ..	† (dark blue)	† (blue)	† (blue)	† (blue)	† (blue)	† (blue)
Mallory's triple stain ..	† (purple)	..	† (blue)	..	† (purple)	† (blue)
Feulgen reagent ..	† (purple)
Methylene blue-eosin ..	† (violet)	..	† (purple)	† (purple)
PAS (normal)	† (pink)	..	† (pink)	† (pink)
PAS (control, incubated in saliva)	† (purple)	† (purple)
Bauer-Feulgen (normal)	† (pink)	† (pink)	† (pink)
Bauer-Feulgen-light green (normal)	† (green)	† (green)	† (green)	† (pink)	† (pink)	† (pink)
Best's Carmine (normal)	† (pink)	† (pink)	† (pink)
Best's Carmine (control, incubated in saliva)	† (pink)	..	† (pink)
Alkaline Phosphatase ..	† (black)	† (black)	† (black)
Nocht's azure II-eosin ..	† (blue)	† (blue rim and pink centre)	† (pink)	† (pink)

DISCUSSION

Investigations with the use of histochemical techniques on the localization and distribution of alkaline phosphatase in a variety of animal tissues have proved that the enzyme plays an important rôle in a large number of metabolic processes. It is suggested by Danielli (1953), that if we assume alkaline phosphatase to represent the enzymic centre of a contractile protein the rôle of alkaline phosphatase in a wide variety of tissues can be easily explained, the fundamental significance of enzyme





activity being the ability to make the chemical energy of a high energy phosphate bond available for the contraction of protein. In a number of widely different animal tissues, the presence of alkaline phosphatase seems related to protein synthesis (Bradfield, 1951). It is also well known that the nucleolus is an important site of protein synthesis (Caspersson, 1950; Ludford, 1925; Gresson, 1929 and 1932; and Raven, 1948). In the light of these observations, the occurrence of a positive reaction in the nucleolus of the glandular cells of the ammatorial organ of *Ariophanta* for alkaline phosphatase, seems to indicate that here, too, the nucleolus is participating in the elaboration of protein secretions.

It has been observed that in the gland cells of the ammatorial organ the nuclei also give a positive reaction to Gomori's technique. It would be interesting to speculate on the possible rôle of the nuclear phosphatase in the gland cells of the ammatorial organ. Among the major functions of alkaline phosphatase in animal nuclei are two which are related to the immediate functioning of the cell: (a) synthesis of nucleic acids and nucleoproteins required for mitosis, (b) secretion and elaboration of formed substances and their transference into the cytoplasm (Chivremont and Firket, 1953). The nuclei of gland cells are in a state of almost permanent interphase. No mitotic figures have ever been found in them and we can rule out nucleic acid synthesis from the purview of the possible rôle of alkaline phosphatase. It seems to me that in the present material the occurrence of nuclear phosphatase is related to the second of these functions. Instances of association of alkaline monoesterase with intracellular secretion are not uncommon among animals. Recent studies on the spermatogenesis of the crustacean *Asellus aquaticus* have led Montalenti *et al.* (1950) to conclude that there is a close correlation between alkaline phosphatase and intracellular secretion. While recognizing the fact that secretory phenomena in animals must involve a number of highly complicated biochemical processes, the occurrence of large amounts of alkaline phosphatase in the conspicuous polymorphic nuclei of the outer glandular cells of the ammatorial organ leads me to conclude that here is yet another instance of the participation of the enzyme in cellular secretory activity.

The occurrence, on the other hand, of large amounts of PAS positive material in the cytoplasm of these cells would seem to indicate that the nucleus is in some manner contributing to its production. As to the exact manner of this formation, we have no precise idea. Leuchtenberger and Schrader (1952) working on the salivary gland cells of *Helix pomatia* and also the ovary of the hemipterous insect *Acanthocephala* (Schrader and Leuchtenberger, 1952) have developed the view that the elaboration of cell substances and glandular secretions is to be related to the degradation products of the nucleic acids particularly desoxyribonucleic acid (DNA). I am inclined to support the view of Leuchtenberger and Schrader. The occurrence of large amounts of alkaline phosphatase associated with DNA of the nucleus as well as the accumulation of cytoplasmic polysaccharides in these cells, seem to indicate a possible relation between the DNA of the nuclei and the polysaccharides in the cytoplasm.

It was observed that this PAS positive material is granular in appearance, and is resistant to incubation in human saliva. On the other hand, the acidophilic properties exhibited by this material as revealed by its affinity for eosin (in eosin-methylene blue and azure-eosin preparations) suggest that the polysaccharide might be neutral in character (Wislocki and Padykula, 1953). The associated occurrence of alkaline phosphatase and PAS positive material (probably neutral) suggests an intimate relationship between the two (Kroon, 1952). Recent work by Moog and Wenger (1952) has emphasized the fact that in a variety of animal tissues there is an intimate association of alkaline phosphatase and neutral polysaccharides and the concept is developed, that the phosphatase-associated mucopolysaccharide constitutes part of a dynamic cytoskeletal mechanism and provides suitable chemical conditions for its activity. Confirmation of these views

has been provided by the work of Leshner (1952) on the salivary glands of *Drosophila robusta*, and Ruyter, Kroon and Neumann (1952) on the kidney of the male albino rat.

On the other hand, the pattern of distribution of alkaline phosphatase and the polysaccharides in the secretory material of the ammatorial organ suggests that alkaline phosphatase is of the nature of a secretory phosphatase, i.e., phosphatase elaborated as a part of the secretion. It is interesting to recall here, that very similar secretory phosphatases have been reported, elsewhere, as in the sex accessories of male mammals (Bern, 1949).

The possible rôle of alkaline phosphatase in the cytoplasm which, as we have just noticed, is associated with PAS positive material, now remains to be examined. It has already been observed that in addition to the granular secretion in the cytoplasm of the gland cells of the ammatorial organ, there is also another secretion which is non-granular. This has been identified by its reactions as mucin. I am of the opinion that this mucin (glycoprotein) is probably derived from the polysaccharide of the granular secretion by some type of a phosphorylation-dephosphorylation mechanism involving the alkaline phosphatases. It may be interesting to mention here that in other animal tissues where secretory phosphatases are reported, as in the sex accessories of male mammals (Bern, 1949), a function of dephosphorylating an ester present in the secretory material is attributed to the alkaline enzyme, in much the same manner as acid phosphatase of the prostate splits acetylcholine of the human semen, as reported by Lundquist (1947). It however seems interesting to find in an organ which is considered as an essential part of the female reproductive apparatus, material parallel with that reported for the male parts of the reproductive system of vertebrates.

I am unable to develop any conclusive views in regard to the function of the two secretory materials in the gland cells, granular and non-granular, but recent work by Anderson (1950) on the nature of secretions of the accessory reproductive glands of the Japanese Beetle, *Popilla japonica* seems to indicate certain possibilities. In this animal, an accessory reproductive gland produces material which consists of mucus and mucopolysaccharides (along with lipids and ribonucleoproteins) which is believed to have a function of lubrication. I am aware that an intimate comparison between the substances secreted by the ammatorial gland cells of *Ariophanta* and the accessory reproductive gland of *Popilla* can hardly be made, and is perhaps even unwarranted, but I am unable to resist the temptation of hazarding that among the possible functions of the secretions in *Ariophanta*, is also one of lubrication. The occurrence and localization of glycogen in the musculature of the ammatorial organ seem to point to the possible rôle of this polysaccharide in this organ. Glycogen in muscle is intimately related with contraction; in fact the whole secret of muscular contraction lies in an anaerobic breakdown of glycogen, and the energy made available during glycolysis is made use of in contractile phenomena. It seems logical to conclude that glycogen present in the ammatorial organ is meant to furnish energy for the contractility of its musculature.

Histochemical reactions show that the connective tissue material of the ammatorial organ lying next to the musculature is perhaps made of both water soluble and water insoluble glycoproteins. These must form the ground substance of the connective tissue. The work of Gersh and Catchpole (1949) has shown that in a variety of tissues of the rat, the nature of glycoproteins is related to the state of their polymerization and also to their properties, and they cite instances where in both normal as well as pathological tissues a continual change in the state of polymerization indicative of change in properties is taking place. The simultaneous occurrence, in the connective tissue of the ammatorial organ, of both types of glycoproteins is a highly interesting phenomenon but I am unable at the moment to present any views in regard to their function.

SUMMARY

Histologically the ammatorial organ of the snail *Ariophanta maderaspatana* presents in transverse section, an outermost layer of glandular cells, a layer of musculature lying next to it internally, a thick layer of connective tissue and an innermost lining of the central canal which is thrown adradially into a number of pouches. The secretion of the glandular cells is conveyed to the central pouches through radial canals traversing the musculature.

The secretory material consists of two essentially separate substances; (a) a neutral mucopolysaccharide, granular in appearance, and (b) mucin, which is non-granular.

Localization of alkaline phosphatase in nucleoli of the glandular cells is perhaps related to its rôle in protein synthesis, while its presence in the rest of the nucleus suggests a part in the degradation of desoxyribonucleic acid and in intracellular secretion of polysaccharides.

The simultaneous occurrence in the secretory material of the ammatorial organ of a neutral mucopolysaccharide and an alkaline enzyme suggests an intimate relationship between the two. It seems possible that the polysaccharide-associated phosphatase plays a rôle in the synthesis of certain glycoproteins of the nature of mucin and other carbohydrate protein complexes.

It seems possible that the secretory material of the gland cells consisting of alkaline phosphatase, mucus and mucopolysaccharides has lubrication as one of its functions.

Heavy mobilization of glycogen in the musculature of the ammatorial organ indicates a means of furnishing energy by glycolysis for contractile phenomena.

Localization of glycoproteins in the connective tissue would mean that they form its ground substance.

The occurrence of both mucopolysaccharides and mucin in the connective tissue is probably indicative of the state of their polymerization.

ACKNOWLEDGEMENT

I wish to express my thanks to Professor B. R. Seshachar for his guidance and kind suggestions. My thanks are also due to Mr. M. M. Veerabhadraiah for his help in photomicrography, and to the Ministry of Education, Government of India, for the award of a Senior Research Fellowship which enabled me to carry out the present investigation.

REFERENCES

- Anderson, J. M. (1950). A cytological and cytochemical study of the male accessory reproductive glands in the Japanese beetle, *Popilla japonica* Newman. *Biol. Bull.*, **99**, 49.
- Bern, H. A. (1949). The distribution of alkaline phosphatase in the genital tract of male mammals. *Anat. Rec.*, **104**, 361.
- Bradfield, J. R. G. (1951). Phosphatases and nucleic acids. Cytochemical aspects of fibrillar protein secretion. *Quart. J. Micros. Sci.*, **92**, 87.
- Caspersson, T. (1950). Cell growth and Cell function. Norton, New York.
- Chivremont and Firket (1953). In International review of cytology. Vol. 2. Academic Press, New York.
- Danielli, J. F. (1946). A critical study of the techniques for the localization of alkaline phosphatase. *J. Exp. Biol.*, **22**, 110.
- (1953). Cytochemistry. A critical approach. Wiley, New York.
- Dasen, D. D. (1953). Structure and function of the reproductive system in *Ariophanta ligulata*. *Proc. Zool. Soc., London*, **97**, 118.
- Gersch, I., and Catchpole, H. R. (1949). The organisation of the ground substance and basement membrane, and its significance in tissue injury, disease, and growth. *Am. J. Anat.*, **85**, 457.
- Gresson, R. A. R. (1929). Nucleolar phenomena during oogenesis in certain Tenthredinidae. *Quart. J. Micros. Sci.*, **73**, 177.
- (1932). Studies on the gametogenesis of *Stenophylus stellatus* Curt. (Trichoptera). Oogenesis. *Proc. Roy. Soc., Edin.*, **13**, 322.
- Hotchkiss, R. D. (1948). A microchemical reaction resulting in the staining of polysaccharide structures, in fixed tissue preparations. *Arch. Biochem.*, **16**, 131.
- Kroon, D. B. (1952). Phosphatase and formation of protein carbohydrate complexes. *Acta Anatomica*, **15**, 317.
- Leshner, S. W. (1952). Studies on the larval salivary gland of *Drosophila*. III. The Histochemical localization and possible significance of ribonucleic acid, alkaline phosphatase and polysaccharides. *Anat. Rec.*, **114**, 633.
- Leuchtenberger, C., and Schrader, F. (1952). Variation in the amount of Desoxyribonucleic acid (DNA) in the cells of the same tissue and its correlation with secretory function. *Proc. Nat. Acad. Sci.*, **38**, 99.
- Lille, R. D. (1948). Histopathological technique. The Blackiston Co., Philadelphia.
- Ludford, R. J. (1925). Nuclear activity in tissue cultures. *Proc. Roy. Soc., B*, **98**, 4.

- Lundquist, F. (1947). Studies on the biochemistry of human semen. I. The natural substrate of prostatic phosphatase. *Acta. Physiol., Scandinav.*, **13**, 322.
- McMannus, J. F. A. (1946). Histological demonstration of mucin after periodic acid. *Nature*, **158**, 202.
- Montalenti, G. (1948). Histological and histochemical uses of periodic acid. *Stain. Tech.*, **23**, 99.
- Montalenti, G., Vitagliano, G., and Nicola, M. (1950). The supply of ribonucleic acid to the male germ cells during meiosis in *Asellus aquaticus*. *Heredity*, **4**, 75.
- Moog, F., and Wenger, F. L. (1952). The occurrence of neutral mucopolysaccharides at sites of high alkaline phosphatase activity. *Am. J. Anat.*, **90**, 339.
- Raven, C. P. (1948). The chemical and experimental embryology of Limnaea. *Biol. Rev.*, **23**, 333.
- Ruyter, J. H. C., Kroon, D. B., and Neumann, H. (1952). Effect of bilateral adrenalectomy on alkaline phosphatase in the rat in relation to regressive changes in the nephron. *Acta Anatomica*, **14**, 42.
- Schrader, F., and Leuchtenberger, C. (1952). The origin of certain nutritive substances in the eggs of Hemiptera. *Exp. Cell Res.*, **3**, 136.
- Wimsatt, W. A. (1951). Observations on the morphogenesis, cytochemistry and significance of the binucleate giant cells of the placenta of ruminants. *Amer. J. Anat.*, **89**, 233.
- Wislocki, G. B., and Padykula, H. A. (1953). Reichert's membrane and yolk sac of the rat investigated by histochemical means. *Amer. J. Anat.*, **92**, 117.

EXPLANATION OF PLATES

PLATE XXIII

- Fig. 1. Transverse section of the ammatorial organ stained with Heidenhain's iron haematoxylin, after fixation in Bouin's fluid. $\times 22$.
- .. 2. Transverse section of the ammatorial organ stained with Mallory's triple, after fixation in chilled 80% alcohol. $\times 22$.
- .. 3. Transverse section of the ammatorial organ stained with methylene blue-eosin, after fixation in chilled 80% alcohol. $\times 22$.
- .. 4. Transverse section of the ammatorial organ stained with Feulgen's reagent, after fixation in Carnoy's fluid. $\times 22$.
- .. 5. Transverse section of the ammatorial organ stained with PAS technique, after fixation in chilled 80% alcohol. $\times 22$.
- .. 6. Control preparation of the same, incubated in human saliva for one hour at 37° C. prior to treatment with the PAS technique. Note the abolition of the reaction in the musculature, the saliva resistant granular secretion and the connective tissue sheath. $\times 22$.
- .. 7. Transverse section of the ammatorial organ stained with Bauer-Feulgen technique, after fixation in Carnoy's fluid. $\times 22$.
- .. 8. Control preparation of the same incubated in human saliva for one hour at 37° C. prior to treatment. Bauer-Feulgen technique. Note the abolition of reaction in the musculature, and saliva resistant nature of the connective tissue sheath and secretory materials. $\times 22$.
- .. 9. Transverse section of the ammatorial organ incubated in sodium glycerophosphate at pH 9.4 for 5 hrs. 45 mins., after fixation in chilled 80% alcohol. Note the deposition of cobalt sulphide in the gland cells, radial canals and in the central pouches, indicating sites of localization of alkaline phosphatase. $\times 22$.
- .. 10. Transverse section of the ammatorial organ stained with Best's carmine stain, after fixation in chilled 80% alcohol. $\times 22$.
- .. 11. Control preparation of the same incubated in human saliva for one hour at 37° C. prior to staining in Best's carmine. Note the abolition of staining in the musculature. $\times 22$.

PLATE XXIV

- Fig. 12. A portion of fig. 1 magnified, showing the granular as well as non-granular secretions. $\times 250$.
- .. 13. A portion of fig. 2 magnified, showing the granular secretion. The non-granular secretion is unstained. $\times 250$.
- .. 14. A portion of fig. 4 magnified to show the nuclei of the gland cells. The nucleoli are Feulgen negative. $\times 250$.
- .. 15. A portion of fig. 3 magnified to show the eosinophilia of the granular secretion. The non-granular secretion is unstained. $\times 250$.
- .. 16. A portion of fig. 5 magnified. The secretory granules are PAS positive and saliva resistant. $\times 250$.
- .. 17. A portion of fig. 9 magnified to show localization of alkaline phosphatase in nucleus, nucleolus and granular secretion. $\times 250$.

ORE MICROSCOPIC STUDIES OF THE VANADIUM-BEARING TITANIFEROUS IRON ORES OF MAYURBHANJ WITH A DETAILED NOTE ON THEIR TEXTURE

by SUPRIYA ROY, *Council of Scientific and Industrial Research,
Calcutta University*

(Communicated by D. N. Wadia, F.N.I.)

(Received May 29; read October 20, 1954)

INTRODUCTION

This paper aims at a more or less elaborate discussion on the vanadium-bearing titaniferous magnetite deposits related to the Mayurbhanj Gabbro-Anorthosite suite, on the evidences collected by the study of polished sections under the reflecting microscope. The area lies to the south of Gorumahisani in Mayurbhanj and the specimens for study had been collected from lodes *in situ* traced to the west of Kumhardubi village ($22^{\circ} 17' N.$ and $86^{\circ} 19' E.$) and further south to the north-east of Betjharan ($22^{\circ} 16' N.$ and $86^{\circ} 23' 30'' E.$). Near Kumhardubi the lodes occur as veins in Gabbros and Epidiorites striking roughly NNE-SSW. The veins are variable in width (at places 20 feet or more) and form an irregular and impersistent pattern. The hill slope is covered with float ore. The Gabbros, Epidiorites and Anorthosites occurring in near proximity are charged with magnetite and as a result of this the specific gravity of these rocks tend to be very high. Here the Gabbro is pegmatitic and sometimes grey feldspar bearing. Near Betjharan the ore bodies occur in gabbros as pockets and minor intrusives. Here too, the float ores cover the hill slopes. It is to be emphasised at the outset that the petrological aspects of this suite of rocks will not be taken up in this paper and only the microscopic criteria of the ore minerals will be dealt with. The texture will first be described and then interpreted to throw some light on the mineral paragenesis.

This particular deposit of vanadium bearing titaniferous iron ores was first described by Dunn and Dey in the *Transactions of the Mining, Geological and Metallurgical Institute of India* in 1937. Dunn also submitted the results of his work in the *Memoir of the Geological Survey of India* in the same year. Another paper on the same area by S. C. Chatterjee (1945) dealt with the petrology of the different rock types, but he did not work with the ore minerals themselves. Dunn and Dey (1937) identified a number of minerals along with the magnetites and the ilmenites and described some of the textures exhibited by them. They, however, did not mention the occurrence of some of the minerals like Ulvöspinel, Limonite, Pyrite and Martite, of which the first is being described for the first time from an Indian deposit. Their observations regarding the textural relation of the minerals do not present a complete picture and little attempt has been made to interpret the textures. The present author, therefore, has attempted to describe fully all the textures noted and to put forward a well knit interpretation of such textures amply supported by evidences. The derivation of the magnetite-ilmenite exsolution texture from the original metastable mineral Titano-magnetite has been proved experimentally by the author by heating the specimens in vacuum at high temperatures for 24 hours and chilling them immediately with water. This particular procedure has been followed by other eminent workers like Ramdohr (1926), Kamiyama (1929) and Edwards (1938).

Similar deposits have been reported from other parts of the world and the interesting point is that almost all the descriptions of these varied and faraway deposits tally to a great extent. As early as in 1913 Singewald described the micro-structure of the titaniferous magnetites. Schwellmus and Willamse (1943) reported and investigated such occurrences of the Bushveld complex. Vaasjoki (1947) submitted an excellent paper on the titaniferous magnetite ores of Otanmaki. F. F. Osborne (1928) discussed certain magmatic titaniferous iron ores and their origin. Among other important contributors on the subject, references may be made to Ramdohr (1926 and 1953), Kamiyama (1929), Ishimura (1931), Warren (1918), etc. The results of the investigations carried out by the present author with reference to the characters of the ore minerals and their textural relationship, are given in the following pages.

MICROSCOPIC CHARACTERS OF THE ORE MINERALS

The following minerals have been identified under the ore microscope on optical criteria, reflectance and etch reactions with different reagents. They are Magnetite, Ilmenite, Hematite, Rutile, Limonite, Martite, Goethite, Lepidocrosite, Pyrite and Ulvöspinel. Coulsonite, the new vanadium-bearing mineral identified by Dunn and Dey (1937), could not be confirmed beyond doubt as according to the present author only a slight variation of optical characters without accurate determination of structure, chemical composition, etc., is not enough to name a new mineral. The problem is being studied by the present author from different angles and the results will be published later on. The author has also submitted in this paper the values of power of reflection for the different minerals based on his determination with the aid of Berek's slit microphotometer. He used the green light for this purpose. In the paper by Dunn and Dey (1937) the power of reflection for each of the minerals has been given without giving any reference to the apparatus or colour of light used for the purpose. As the results obtained by the determination of reflectance by photometer ocular vary within a fairly long range from those obtained by photo-electric cell, it is not safe to refer to the results given in the above-mentioned paper. In course of his investigation the present author has always tried to note all the characters of the ore minerals in every detail and has attempted to give a complete picture in the following pages. He has described some of the minerals which Dunn and Dey (1937) have missed, e.g. Ulvöspinel, Limonite, Pyrite and Martite, and he has also put forward in detail the etch reactions given by each of them. The mode of distribution of the different minerals in the polished section has also been carefully described by the present author.

Magnetite

The mineral takes a fairly good polish. The reflecting power, as in other cases, was determined by Berek's microphotometer in green light and it came to about 20.05% in air. The colour of the magnetite varies from greyish white to rose brown, though in the former cases the magnetite is mostly changed into hematite. The rose brown colour of the hematite-free magnetites has been imparted by its titanium content, and in some cases when it was examined in high magnification, it was found to contain very fine lamellae of ilmenite arranged in it. The triangular cleavage pits, typically present in other minerals of the same system (e.g. in galena), are visible (Pl. XXV, Fig. 1) and inter-growths of other minerals, viz. ilmenite, ulvöspinel, etc., with it, in consistent orientation, bring out the cleavage lines. The cleavage lines otherwise not visible, are brought out by slight etching in some cases (Pl. XXV, Fig. 2). The typical character of magnetite yielding to pressure, may be examined by drawing a needle on it. The powder is strongly magnetic. It exhibits no reflecting pleochroism and is isotropic in crossed nicols. The magnetite usually

forms the general body of the specimens and it is associated with the ilmenites where the exsolution lamellae of the latter are oriented in the octahedral direction of the former. Many other minerals are also associated with the magnetites. Martitisation of the magnetite is commonly noted along the border.

Etch Reactions.—Etching was done with different reagents and the time fixed was one minute. The results obtained are as follows:—

Positive: HCl .. Mineral darkens and the fumes around the drop tarnish.
Solution turns yellow.

.....HF .. Turns the mineral sooty black. Shows effects of corrosion.

Negative: HNO₃, KCN, KOH, FeCl₃, HgCl₂.

Ilmenite

The mineral takes a very good polish after careful and prolonged treatment but usually some pits occur. The reflecting power in air, as determined by Berek's slit microphotometer, came to 18.50%. This value is lower than that of the magnetite. Colour pink to pinkish brown showing slight reflecting pleochroism. Strong anisotropism and lamellar twinning are noticed in some of the specimens. Closely related to the magnetite.

Etch Reactions.—Negative to all standard reagents excepting HF which after about two minutes darkens the specimen and feebly corrodes it. The ilmenite occurs in the following ways:—

- (i) Individual and separate grains.
- (ii) In graphic intergrowth with the magnetites.
- (iii) As exsolution lamellae.
- (iv) In the form of veins and crack fillings.

(i) Individual and separate grains.

Individual grains vary very widely in size—from very minute dots they vary in range up to 2.3 mm. in diameter. These show also excellent birefractance in shades of grey. They are slightly pitted in almost all the cases and they have a high relief against the magnetites. They are replaced by hematites and limonites and also contain inclusions of hematite, magnetite and goethite.

(ii) In graphic intergrowth with the magnetite.

The ilmenite is found to occur in graphic intergrowth with the magnetites. The characteristic texture (Pl. XXVIII, Fig. 16, and Pl. XXIX, Fig. 17) and its implications will be taken up in detail later in this paper. The ilmenite is very fine grained wherever found to take part in the intergrowth.

(iii) As exsolution lamellae.

The ilmenites are found to be oriented in the crystallographic directions of the magnetites with which they exhibit exsolution texture. In sections they generally show as lines and are oriented in the octahedral plane of the magnetites. Hence in a single magnetite crystal they are oriented in three possible directions. The typical texture is very well shown in Fig. 5 (Pl. XXVI). The details of this texture will be given later in this paper.

(iv) In the form of veins and crack fillings.

Irregular veins of ilmenite, cutting through the Widmanstätten intergrowth of magnetite and ilmenite, have been noticed. The veins are, in most cases, very narrow. The earlier developed cracks in the magnetite in the magnetite-ilmenite intergrowth are also filled up by later ilmenite which does not project tongues in the former.

Hematite, Limonite and Martite

These minerals are grouped together because martite and hematite are almost identical, the only difference being that the former retains the form of magnetite. The limonite is again only a hydrated product of hematite. Dunn and Dey (1937) have not mentioned the occurrence of limonite and no adequate reference has been made in their paper about the martitisation of the magnetites or the specific identifying characters of the martites.

These minerals are very difficult to polish. Power of reflection for the hematite in air and in green light varies between 23 to 27% (when mixed with magnetites it is 23%). This is the highest among all the minerals present, but for the few minute specks of pyrite scattered over the magnetites. Colour white to bluish grey for the hematites, and the typical brick red internal reflection is visible in some cases. These hematites commonly replace the magnetites in the octahedral plane as also following an irregular pattern. They show conspicuous anisotropism. Microscopic twinning has also been detected in the hematites.

Martitisation of the magnetites is fairly a common phenomenon noticed in these specimens. It follows in general the octahedral plane and the grain boundaries of the magnetites. The martites were identified on the basis that they retain the form of the magnetites but exhibit anisotropism. They are not etched by HCl and are slightly corroded by HF after long treatment.

There has been noticed another variety of mineral with fairly low reflectance, brownish black colour and it shows at places the brick red internal reflection of hematite. This mineral, in spite of consistent efforts, did not take a good polish and appears dull in association with magnetites and ilmenites; but it has been proved beyond doubt to be some opaque mineral and not a gangue. On careful observation these minerals are found to contain some amount of goethite and a fair proportion of hematite and the author has identified the mineral to be limonite.

Etch Reactions.—The bluish grey hematite is negative to all standard reagents excepting HF to which it responds very feebly after long treatment. In association with the magnetites the latter are etched considerably by concentrated HCl while the former stands out in contrast. The martites give the same etch reactions as the hematites.

Rutile

This mineral, found in patches, is comparatively rare. It takes a good polish. Reflecting power 21% in green light of Berek's microphotometer. Colour pale bluish grey. Strongly anisotropic in shades of grey. Replaces ilmenites and thus exhibits intergrowth texture with magnetite (Pl. XXVIII, Fig. 15). From the nature of replacement and from the patchy occurrence at some places, it may be concluded as a secondary mineral. It may be the ferriferous variety of Rutile, 'Nigrine', though it could not be conclusively proved.

Goethite

It takes a fairly good polish except in the earthy variety. Reflecting power is low—in green light and in air it comes to about 16%. Colour grey, reflecting pleochroism distinct, anisotropism strong in shades of grey. Occurs in more weathered specimens as spherulitic grains with hematite, limonite, lepidocrosite. Replaces ilmenite at places.

Etch Reactions.—Dunn and Dey (1937) have declared the mineral to be negative to all standard reagents. The present author has, however, found the following results:

Positive : SnCl_2 (Sat.) + HCl (0.2N) .. Stains yellowish brown.
 HCl .. Fumes tarnish.
 Negative : HNO_3 , H_2O_2 , HF, H_2SO_4 , etc.

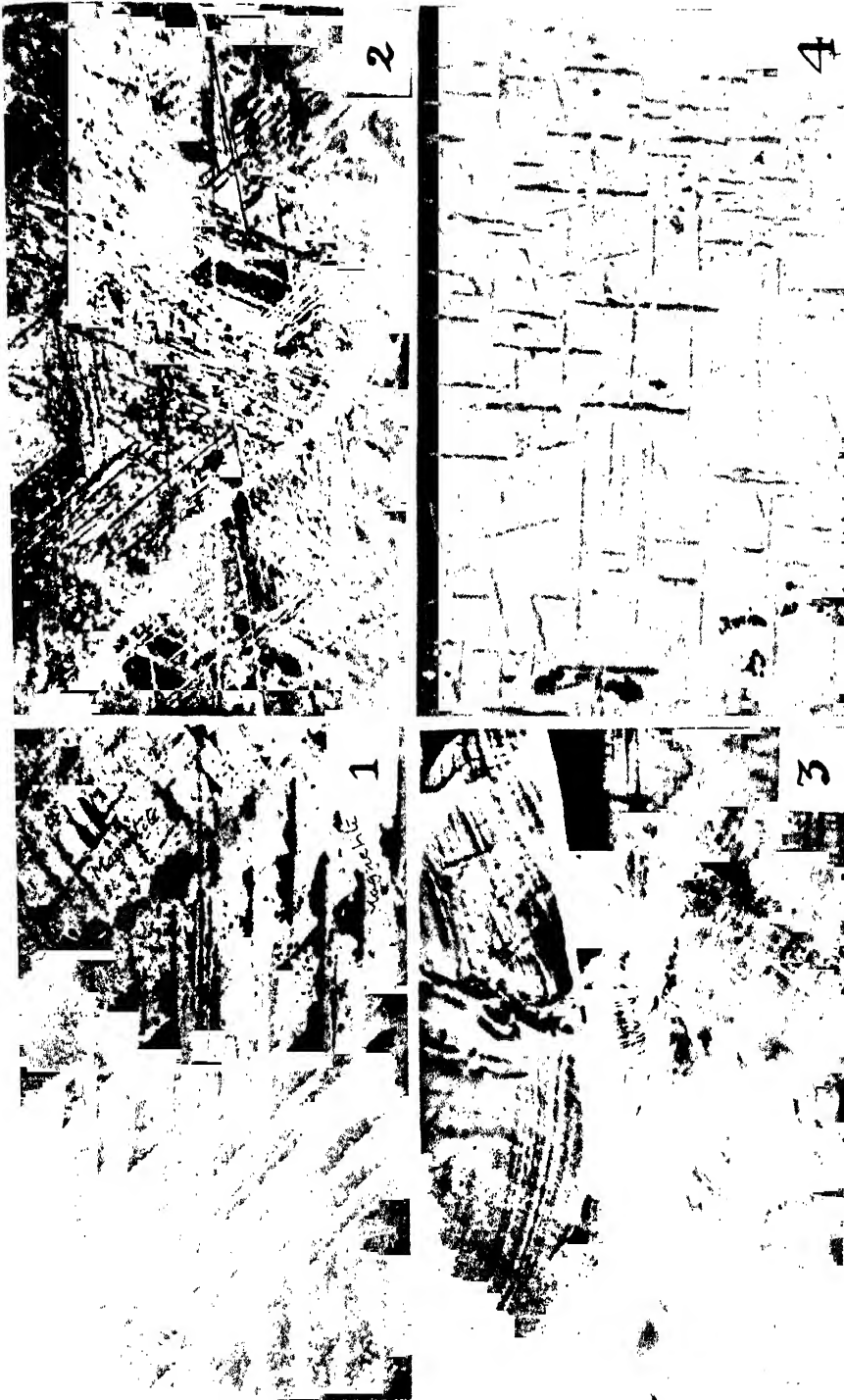


FIG. 1. Typical triangular cleavage pits in magnetite as in general. Inset: 1000x magnification showing in some places 200x.
 FIG. 2. Magnetite etched by HCl, exhibiting the cleavage pattern. Inset: 1000x magnification showing in some places 200x.
 FIG. 3. Graphite slibbing the collar rim and banded texture. Inset: 1000x magnification showing in some places 200x.
 FIG. 4. Thin needle-like lamellae of a xospinel mineral arranged in the 100 plane. Inset: 1000x magnification showing in some places 200x.



FIG. 5. Exsolution lamellae of ilmenite arranged in the octahedral direction of the magnetite (Widmanstätten intergrowth). Oil immersion. $\times 800$.
 FIG. 6. Two crystals of ilmenite cut, but there is no elongation of the point of contact, indicating growth on origin. $\times 80$.
 FIG. 7. Mottled intergrowth of ilmenite (dark grey) and magnetite (pale grey). Note the regular orientation of ilmenite in magnetite. Oil immersion. $\times 500$.
 FIG. 8. Ilmenite (dark grey) and hematite (white) replacing ilmenite (dark grey). (See p. 149, fig. 2, p. 150, fig. 3).

Lepidocrosite

It occurs very rarely as a few bands within the goethite. Reflectance definitely higher than that of the goethite. Colour greyish white. Anisotropic in shades of grey. Negative to all standard reagents.

Coulsonite

This controversial 'species' has been traced associated with the magnetites, replacing them along the octahedral plane and also forming an irregular and spongy pattern. In places it replaces the magnetites retaining wholly intact the cleavage lines of the host mineral, exhibiting pseudomorphism (Pl. XXVII, Fig. 12). The colour of the mineral is bluish grey and it is isotropic between crossed nicols. The reflectance is higher than that of magnetite (about 22% in green light in air. There are, however, some magnetites associated intimately with them and therefore the reflectance recorded may be somewhat lower than the actual value). HCl and Aqua Regia etch the magnetite but this bluish grey variety remains unetched. The ilmenite laths proceed through the coulsonite unperturbed (Pl. XXVII, Fig. 11). Its difference with the hematite is a difference in the colour tone as well as in the fact that hematite is anisotropic. It resembles maghemite very much, but it gives positive test for vanadium on which criterion Dunn and Dey (1937) created a new name for it. According to Dunn and Dey the 'possibility of its being a vanadium rich maghemite made the introduction of a distinct name advisable to avoid confusion'. The author is not in a position to comment on the validity of this new name at present, because he has only the ore microscopic, etch reaction, and the reflectance data in hand at the present moment. X-ray powder analysis and magnetic studies are, however, being carried out at present with the isolated (by means of a dentist's drill) grains of the doubtful mineral which may add some more information to the present state of knowledge of the problem.

Pyrite

This mineral, missed by Dunn and Dey, has been spotted by the author as minute grains often retaining the cubic shape, scattered over the magnetite. It has got a distinct yellow colour and a very high reflectance. These are isotropic between crossed nicols.

Ulvöspinell

This mineral is being described for the first time from India. Fine lamellae of this mineral have been identified, occurring as needles in the section of magnetite parallel to the (100) face. The lamellae are oriented in the cubic direction of the magnetite making an angle of 90° among themselves (Pl. XXV, Fig. 4). They are isotropic, resistant to all reagents and with these criteria can easily be distinguished from the ilmenites, the only other mineral exhibiting similar texture in these specimens. The reflecting power of this mineral could not be determined as the minerals are very minute even at very high magnification in oil immersion. This variety has recently been described fully by Ramdohr (1953) in his paper in the *Economic Geology*.

DESCRIPTION OF TEXTURES

In describing the textures noted during the observation of the specimens, the author intends to proceed in a systematic way by classifying them into different types. Dunn and Dey (1937) in their descriptions of the textures exhibited by these minerals did not attempt any elaborate study and only some of the textures (viz. Widmanstätten and Graphic intergrowth) were touched. They have not either mentioned or have given inadequate consideration to the mottled intergrowth

texture and the replacement textures exhibited by hematite-ilmenite, limonite-ilmenite, goethite-ilmenite, etc. The investigations by the present author reveal the following types of textures:—

(i) Crystallographic intergrowths, (ii) Graphic intergrowths, (iii) Mottled intergrowths, (iv) Replacement textures.

(i) *Crystallographic intergrowth.*

This is the typical intergrowth texture noticed in all the specimens and almost all the ilmenite grains, apart from those forming the individual and separate big grains and veinlets, take part in the formation of such intergrowths with the magnetites. The ilmenite lamellae are oriented in the octahedral plane of the magnetite and a maximum of three different directions of orientation has been noticed. The angle made by the lamellae among themselves varies within short limits and is more or less 60° in average (Pl. XXVI, Fig. 5). In some cases the lamellae are all equally thin or equally coarse, whereas in other places they are different in different directions. Where two different veinlets or lamellae meet there is no enlargement at the point of contact, rather a sort of contraction and pinching out phenomenon is observed (Pl. XXVI, Fig. 6). The oriented needles of ilmenite may best be observed by etching the magnetites by HCl when the ilmenites are not affected and stand out prominently. Almost nowhere have the ilmenite lamellae bitten into the magnetite proving that no replacement by the former has taken place.

Similar crystallographic intergrowth texture has been presented by magnetite and ulvöspinel on the (100) face of the magnetite (Pl. XXV, Fig. 4). The ulvöspinels are not attacked by HF which distinguishes them from the ilmenites. They are also isotropic. The ulvöspinels do not bite into the magnetite and show no evidence of replacement.

(ii) *Graphic intergrowth.*

This type of intergrowth between the curved lamellae of ilmenite and magnetite (almost changed to hematite subsequently) has been noted by the author at several places (Pl. XXVIII, Fig. 16 and Pl. XXIX, Fig. 17). The grains involved in such intergrowth are very minute and can only be seen in very high magnification. The intergrowth is guided by no crystallographic plane and the texture has no continuity at all. This type of intergrowth occurs in a very scattered way in the specimens.

(iii) *Mottled intergrowth.*

Microscopic inclusions of ilmenite into magnetite has been recorded in many specimens. These inclusions are rounded as well as extremely irregular and vary from very fine specks to coarser variety. They are arranged sometimes in the crystallographic direction of the magnetite (Pl. XXVI, Fig. 7), though commonly they are irregularly scattered.

(iv) *Replacement textures.*

Undoubted replacement textures have been found in a number of cases and the following minerals are involved:—

(a) Hematite replaces magnetite; (b) Hematite replaces ilmenite; (c) Limonite replaces ilmenite; (d) Goethite replaces ilmenite, and (e) Coulsonite (?) replaces magnetite.

These will be taken up one by one.



9



10



11.



12.

FIG. 9. *Homalium* (white) in flowering stage (the root system is shown in the foreground).
FIG. 10. *Homalium* (white) in flowering stage (the root system is shown in the foreground).
FIG. 11. *Homalium* (white) in flowering stage (the root system is shown in the foreground).
FIG. 12. *Homalium* (white) in flowering stage (the root system is shown in the foreground).
FIG. 13. *Homalium* (white) in flowering stage (the root system is shown in the foreground).



FIG. 13. Ilmenite lamellae (darker grey) oriented in the magnetite matrix (paler grey) in a north-south direction and with the change of orientation of the magnetite grains the development of the ilmenite lamellae (20X). Oil immersion. 500.

FIG. 14. Remnant white replacing magnetite (20X). Oil immersion. 200.

FIG. 15. Rutile arranged in the coralloidal form of the magnetite (paler grey). This in the less previously reported ilmenite-magnetite sand (oil immersion. 800).

Copyright © 1972 by the Indian Academy of Sciences. Printed in India.

(a) Hematite replaces magnetite.

The hematite has replaced magnetite mainly along the grain boundaries and the octahedral cleavage planes. Wherever the magnetite has been changed to hematite there may be noticed an intermediate product which, though retaining the form of the magnetite, is anisotropic and has been identified to be martite. In almost all the specimens, and particularly in the case of more or less titanium-free magnetites, the change from magnetite to hematite is nearest to completion. Only patches of unreplaced magnetite remain to prove the original mineral present.

(b) Hematite replaces ilmenite.

This is a very clear case exhibited in the specimens. The ilmenites have been replaced along the borders in most cases and it may also be noticed that larger grains of ilmenite almost invariably have a rim of hematite (Pl. XXVI, Fig. 8).

(c) Limonite replaces ilmenite.

The dull looking mineral containing hematite and goethite and identified to be limonite, has replaced ilmenite both along the boundary penetrating into the grains and also in the cleavage directions. Figure 8 (Pl. II) will show the actual mode of replacement.

(d) Goethite replaces ilmenite.

Goethite has been found to replace ilmenite in the grain borders and in some cases the replacement proceeded in the vertical plane (plane vertical to the plane of the polished surface) so that the goethite has been enclosed by the ilmenite (Pl. XXVII, Fig. 10).

(e) Coulsonite replaces magnetite.

Coulsonite (?) which shows crystallographic continuity with the magnetite, replaces the latter without affecting the ilmenite exsolution lamellae in the least (Pl. XXVII, Fig. 11). The colour gradation due to variable vanadium content masks the sharp boundary between the minerals but as the accompanying Figure 12 will indicate, coulsonite replaces the magnetite wholly with the cleavage planes of the latter retained intact. The replacement texture can only be clearly visible when the specimen is etched with HCl so that magnetite responds whereas coulsonite is negative.

INTERPRETATION OF TEXTURES AND MINERAL PARAGENESIS.

In the preceding section a mere description of the textures exhibited by different minerals has been given. The possible origin of such textures will now be taken up and a paragenesis of the minerals will be drawn up based on the interpretation of the varied types of textures in which all the minerals present have taken part. The author has used in this section the term 'exsolution' synonymously with 'unmixing' as advocated by Schwartz (1931) in connection with the interpretation of textures of ore minerals.

(i) *Crystallographic intergrowth.*

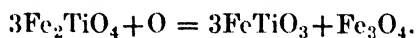
Most systems break down along a curve of decreasing solubility. A gradual precipitation is thus effected resulting in an unmixing texture which in most cases may be referred to the crystallographic orientation of the major component. The Widmanstätten texture exhibited by magnetite and ilmenite probably resulted in this way. In these crystallographic intergrowths, as already observed, both the coarse and fine lamellae have taken part, the former being, according to Dunn and Dey (1937), contemporaneous with the vein ilmenites in age. The author has also noted coarse ilmenite lamellae merging into veinlets of the same mineral. The finer lamellae of ilmenite, however, do not exhibit any such character and are definitely different in age, originating by the process of unmixing. In this texture

the ilmenites are oriented in the octahedral plane of the magnetite making an angle of approximately 60° among themselves. In these the minor component is ilmenite which is arranged in the crystallographic direction of the magnetite (much altered to hematite) which in this case is the major component. The absence of any ilmenite biting into the magnetite testifies that the ilmenite is not replacing the magnetite taking advantage of the particular weak zones. The ilmenite laths are oriented in different directions on the polished surface according to the varied orientation of the magnetite grains (Pl. XXVIII, Fig. 13). In case of replacement such consistency in the textural relations between magnetite and ilmenite cannot be expected. All these suggest an unmixing origin of the magnetites and at least the fine ilmenite lamellae.

According to Dunn and Dey (1937) the coarse lamellae of ilmenite originated by internal segregation after crystallization of the 'titanomagnetites' while the finer lamellae were formed when the latter became unstable at about the same time. They also stated that compared to the distortion of the feldspar lattice of the soda rich areas described by Spencer and others, a gradual concentration of titanium ions along certain planes during the cooling of the original 'titanomagnetite' crystals, without disturbance of the cubic lattice may be pictured, until a certain limiting value of concentration is reached and the cubic framework in these areas then contracts and rotates to give the framework of rhombohedral ilmenite.

Whether Dunn and Dey's theory of segregation is the process or G. M. Schwartz's suggestion of exsolution is the cause for such a texture is a debatable question which cannot be easily solved with microscopic study of the specimens only, for the resulting texture in both may be more or less the same. The titanomagnetite described by Dunn and Dey (1937) as 'primary homogeneous Fe-Ti oxide of cubic symmetry' has nowhere been conclusively identified, rather in all suspected cases the 'mineral' was found in high power to be intergrowth of very fine lamellae of magnetite and ilmenite. The author, however, tried to verify the theoretical deduction of the derivation of magnetite-ilmenite crystallographic intergrowths from 'titanomagnetite' a metastable mineral. Therefore following the procedure of Ramdohr (1926), Edwards (1938) and Kamiyama (1929), he studied the polished sections of these ore minerals first and recorded his observations. Then the same polished specimen was heated in vacuum in an electric furnace for 24 hours at temperatures ranging from 500°C . to 1300°C . at intervals of 100°C . After 24 hours the specimen was chilled in water to arrest the mineralogical and textural changes due to that particular temperature. The crystallographic intergrowths between magnetite and ilmenite began to be affected at 800°C . when the ilmenite lamellae gradually began to widen and this widening with the intermixture of the two minerals continued at high temperatures till at 1200°C . all the intergrowths were gone, the two minerals mingled into one another to form a mixed mineral. The resulting mixed mineral is 'titanomagnetite' which exhibits slight anisotropism, rose brown colour and has the reflecting power round about 19.5%, which is intermediate between the values of the original minerals. The reflectance was measured with photometer ocular in green light. Thus tracing back to the original mother mineral experimentally, the derivation of the ilmenite-magnetite exsolution texture can easily be established.

The presence of ulvöspinel with the intergrowths of magnetite and ilmenite may complicate the theory of the origin of the ilmenites, as the ulvöspinel (Fe_2TiO_4) is liable to destruction by oxidation by giving out ilmenite and magnetite as may be seen below:—



The extinction direction of the ilmenite was therefore determined and it was found to exhibit parallel extinction in almost all the cases. No parquet of sublamellae of ilmenite was present in spite of vigorous search and as such, following Ramdohr

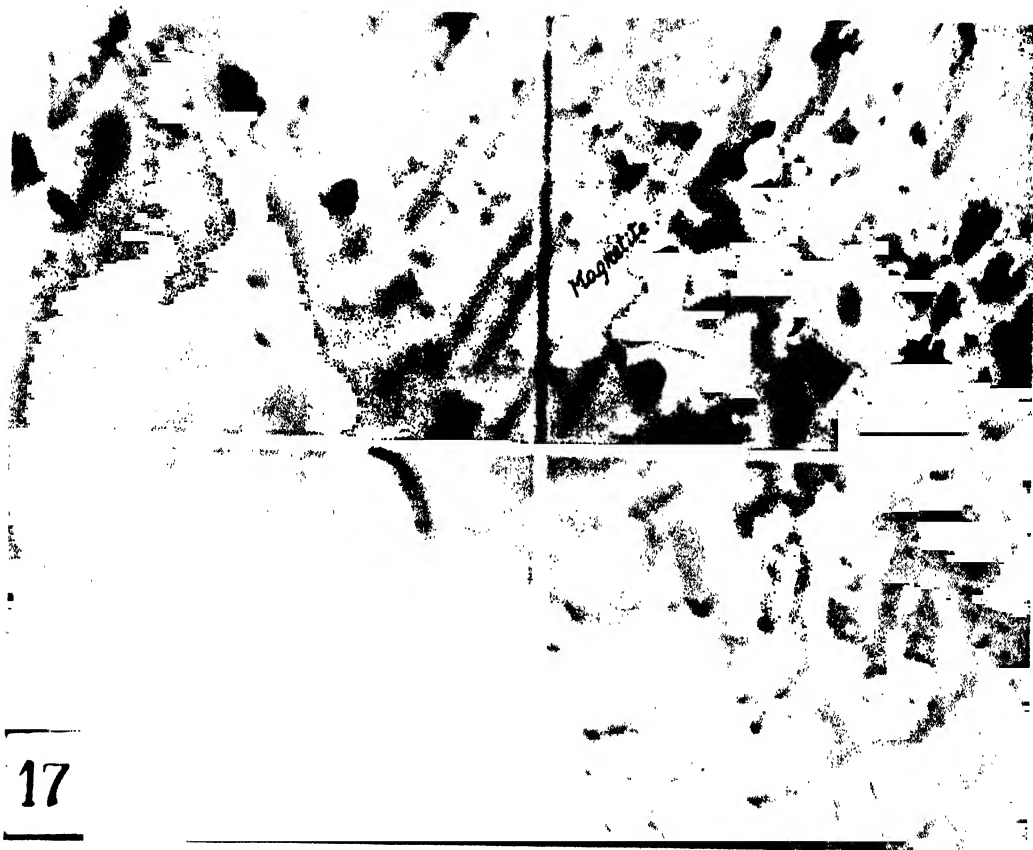
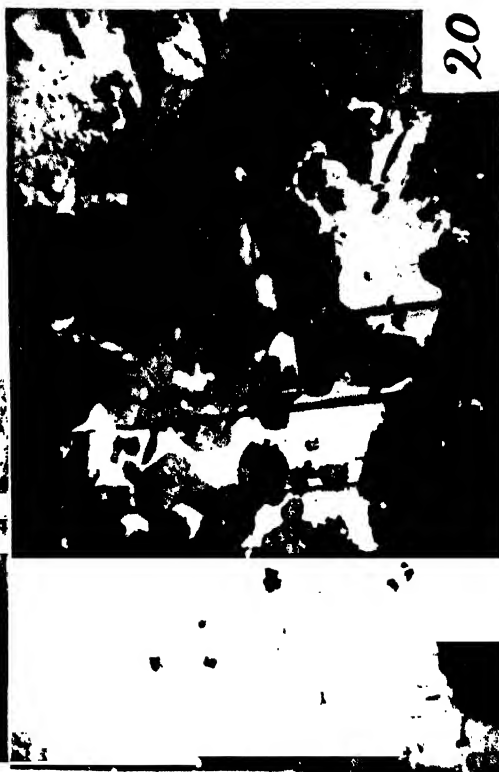


FIG. 17. Graphic intergrowth of ilmenite (grey) and magnetite (altered to hematite—white) with fine exsolution lamellae of ilmenite arranged in it. Oil immersion, $\times 1500$.



18



20

- FIG. 18. Coulsonite (white and unetched), replacing illmenite (etched, sooty black by HCl) and maintaining smooth boundary with illmenite (unetched grey). Oil immersion. $\times 520$.
- FIG. 19. Coulsonite (white) replacing illmenite in the octahedral plane. The ilmenite laths are arranged in the octahedral direction of the illmenite exhibiting exsolution relation. Oil immersion. $\times 520$.
- FIG. 20. Rutile replacing illmenite with the host pressure as well as the guest. Oil immersion. $\times 200$.

(1953), the author discards the possibility of the origin of the ilmenites by oxidation of the ulvöspinel.

(ii) *Graphic intergrowth.*

The intergrowth of typically curved lamellae of ilmenite and magnetite (Pl. XXVIII, Fig. 16 and Pl. XXIX, Fig. 17) is fairly common in specimens studied under high magnification. As to the origin of these graphic intergrowths there is much controversy. Some like Whitehead, Rogers, Lindgren, Schwartz, etc., account replacement for the origin of this texture whereas others conclude that the minerals have originated contemporaneously. The evidences against replacement in this particular case are as follows:—

- (i) The boundaries are not serrate under high magnification and no tongue from the 'guest' projects into the 'host'.
- (ii) No veinlet of the 'guest' traverses the 'host'.
- (iii) There is no transition from the intergrowths of 'guest' and 'host' into unquestionable peripheral replacement of 'host' by 'guest', rather such textures merge into the crystallographic intergrowths of the same minerals.
- (iv) No caries of 'guest' in 'host' at the boundary of the intergrowth.
- (v) Lindgren's (1930) comments on the pseudotectic textures do not hold good in this case because he considered the soft minerals only.
- (vi) The intergrowth is very closely associated with the rod-like exsolution lamellae of ilmenite which are definitely of the same age as its corresponding member taking part in the intergrowth.

From the above considerations the replacement origin of the graphic intergrowths of ilmenite and magnetite may be discarded. This also finds support in the fact that the deposits are of magmatic origin and that a micrometric analysis of the minerals reveals that the proportion of the magnetites and ilmenites in the intergrowths is fairly constant (ilmenite approximately 40% and magnetite approximately on the average 60%). It therefore seems to the author more probable that the excess of ilmenite after the mineral had completed the Widmanstätten texture, could not fit in the octahedral plane of the magnetite and these formed the graphic intergrowths.

(iii) *Mottled intergrowth.*

The texture is characterised by ilmenite blebs, plates and rods included in the magnetites arranged more or less in some definite direction parallel to one another. The ilmenite grains are very minute and can only be observed under very high magnification. The absence of 'caries' and the presence of a very constant arrangement, all suggest a process of unmixing, though by this texture a definite conclusion can never be made. Their mode of origin can be ascertained from the nature of origin of the associated grains, contemporaneous in age and having substantial proofs as regards their mode of origin. The association in this case with the Widmanstätten texture, the members in both the cases being of the same age, suggests that the mottled intergrowth might have resulted by unmixing or furthermost by segregation.

(iv) *Replacement texture.*

Undoubted replacement textures have been encountered with, in which hematite, magnetite, ilmenite, limonite, goethite, rutile and coulsonite have taken part. The hematite has replaced magnetite and ilmenite whereas limonite, goethite and rutile have replaced ilmenite only. Coulsonite exhibits replacement texture with

magnetite only but not with ilmenite. Not a single example of ilmenite replacing other minerals has been sighted.

The hematite has replaced the magnetite mostly in the octahedral direction (Pl. XXVII, Fig. 9), although patchy alterations have been noticed quite often (Pl. XXVIII, Fig. 14). The gradual progress of martitisation is quite vivid. The origin of hematite here is attributed to weathering and these are secondary products. Again the accumulation of hematite around coarse laths of ilmenite and magnetite suggests that the hematite has accumulated side by side with the separation of the coarse laths of ilmenite. The hematite has replaced the larger grains of ilmenite in the form of veins traversing through the latter as well as along the boundary (Pl. XXVI, Fig. 8). The limonite, with some hematite and goethite, also replaces the ilmenite along the border (Pl. XXVI, Fig. 8), as well as along the cleavage lines of the latter. Goethite exhibits replacement texture with ilmenite and its tongues are projected into the latter (Pl. XXVII, Fig. 10). All these replacing minerals are secondary in origin. Rutile replaces ilmenite along the grain boundary and sometimes replaces the latter while arranged along the octahedral plane of the magnetite (Pl. XXVIII, Fig. 15). The much debated 'species' coulsonite shows replacement relations with the magnetites though the ilmenites are not affected at all. It replaces the latter pseudomorphically when all the cleavage faces of the magnetite are retained (Pl. XXVII, Fig. 12). In Fig. 18 (Pl. XXX) the contact of coulsonite and ilmenite is shown to be a sharp line while the magnetite is etched sooty black. In Fig. 19 (Pl. XXX) the coulsonite may be seen to replace magnetite (etched sooty black by concentrated HCl) cutting inside from the octahedral face. From the texture it seems that the vanadium ions have segregated in the magnetite to form coulsonite.

MINERAL PARAGENESIS

It seems from all available data that the Widmanstätten intergrowths of fine lamellae of ilmenite and magnetite were first to be formed by unmixing. The coarse lamellae of ilmenite were formed after them, probably by accumulation through segregation, and these are contemporaneous in age with the vein ilmenites which often cut through the magnetite-ilmenite intergrowth. Patches of magnetites free from ilmenite lamellae have been encountered with but no vein of this magnetite has been spotted. It seems probable that after the crystallisation of the original magnetite-ilmenite intergrowth the ilmenite and titanium-free magnetite remained in solution and crystallised later, the ilmenite probably crystallising slightly earlier. The later titanium-free magnetite is thoroughly altered by hematite and it has been suggested that this variety had excess of oxygen which facilitated the alteration to hematite. The hematite which replaced the ilmenite and some magnetite in the intergrowths, is secondary, formed due to weathering. Goethite is another secondary product and is much later than the coarse grained ilmenites which it replaces. Rutile is also later than the ilmenites (fine and coarse grained). No relation between hematite, goethite and rutile could be established and therefore they may be grouped together as much later minerals any of which might be formed earlier than the other. Coulsonite, which replaces the magnetite in the intergrowth with the ilmenite is much later but its relation with the coarse grains of the ilmenite cannot be established as nowhere has the ilmenite or coulsonite exhibited any replacement relation between themselves. But according to Dunn and Dey (1937) hematite (secondary) replaces coulsonite which, if correct, testifies that the latter mineral was formed earlier than the secondary minerals.

CONCLUSION

In the preceding pages the results of the mineragraphic study of the vanadium-bearing titaniferous iron ores of Mayurbhanj, India, have been tabulated. In this

connection polished sections of the ore minerals were examined under the ore microscope, subjected to etch reaction with various reagents and the reflecting power of each of the minerals was determined by Berek's Slit Microphotometer in green light. The textural features exhibited by the minerals were all described and interpreted so that their mode of origin was understood. To determine the origin of the crystallographic intergrowth between magnetite and ilmenite, the specimens were subjected to heat treatment at very high temperatures and then they were examined under the microscope. Such a procedure confirmed the intermixing of the ilmenite and the magnetite at high temperature to one metastable mineral titanomagnetite, which was thus proved to be the parent mineral for those taking part in the crystallographic intergrowths. The mineral paragenesis was drawn up on the basis of textural interpretation.

This paper deals with the results of only one line of attack to the problem--the X-ray powder analysis, magnetic studies, etc., are, however, not included here. Even the results of the heating experiments with the ore minerals have not been given in detail, only the relevant portion with respect to the mode of formation of the crystallographic intergrowths has been enumerated. It is expected that more facts will come to light when other methods of study are successfully applied and the various problems (viz., problem of coulsonite) will then be solved.

ACKNOWLEDGEMENT

The author acknowledges with heartfelt gratitude the help rendered to him by various individuals and institutions in many ways. These investigations were and are being carried out in connection with a research scheme kindly sanctioned by the Council of Scientific and Industrial Research, Government of India, which rendered all the financial help required for the work. Prof. N. N. Chatterjee, Head of the Department of Geology, Calcutta University, guided the work and offered many valuable suggestions. The author is equally grateful to Dr. S. Deb and Prof. B. C. Mukherjee, College of Engineering and Technology, Bengal, for their ungrudging help in the ore microscopic work and in the determination of reflectivity of ore minerals by Berek's Slit Microphotometer. The authorities of the College of Engineering and Technology, Bengal, very kindly allowed the author to use their well equipped laboratory. The author is also grateful to the Director, Central Glass and Ceramic Research Institute, who very kindly permitted him to carry out experiments on heat treatment of the ore minerals in the well equipped laboratory of the Institute. In this respect the author also wishes to acknowledge the help rendered by Messrs. K. D. Sharma, B. M. Bishui and J. C. Banerjee.

SUMMARY

In this paper the ore microscopic characters of the vanadiferous and titaniferous iron ores related to the Mayurbhanj Gabbro-Anorthosite suite have been discussed. It is an attempt to put forward in every detail the characters of the ore minerals, their mode of distribution in the polished sections and the textural features exhibited by them. The optical characters, etch reaction results, reflectance and spot test data, all were taken into account and the minerals conclusively identified were Magnetite, Ilmenite, Hematite, Limonite, Goethite, Martite, Lepidocrosite, Rutile, Pyrite and Ulvöspinel. Among these, Limonite, Pyrite, Martite and Ulvöspinel were not noted by Dunn and Dey, the previous workers in this area. The Ulvöspinel is being described for the first time from India and this mineral is so intimately mixed up with the exsolution lamellae of the ilmenite exhibiting identical arrangement that it can easily be confused with the latter. Coulsonite, the new 'species' described originally by Dunn and Dey (1937), could be easily spotted but that it is a distinctly new species different from the magnetites in which it occurs, could not be confirmed beyond doubt. The typical characters of this 'mineral' have, however, been noted together with its relations with the other minerals. The important portion of this paper has been devoted to the description and interpretation of the textures exhibited by the ore minerals. The present author has, in this case, examined in much greater detail the textural features and has given a more complete account than that recorded by Dunn and Dey (1937), who only touched the crystallographic and graphic intergrowth textures of the

magnetites and ilmenites. The mode of replacement of the different minerals has not been described by Dunn and Dey. In this paper the author has attempted to describe all such textures fully and has also given a well knit interpretation based on evidences, which again formed the basis of the mineral paragenesis. The crystallographic and graphic intergrowths were all investigated in much greater detail than what has been reported by Dunn and Dey and all possible evidences were furnished regarding the possible mode of origin of these textures. In this connection the author subjected the specimens with such intergrowths to heat treatment at high temperature and confirmed that the intergrowths of these two minerals were derived from original titanomagnetite.

REFERENCES

- Dunn, J. A. and Dey, A. K. (1937). Vanadium bearing titaniferous iron ores in Singhbhum and Mayurbhanj, India. *Trans. Min. Geol. Inst. Ind.*, **31**, Pt. 3, 130-161.
- Dunn, J. A. (1937). Mineral deposits of Eastern Singhbhum and surrounding areas. *Mem. G.S.I.*, **69**, Pt. 1.
- Edwards, A. B. (1938). Some ilmenite microstructures and their interpretation. *Aust. Inst. Min. Meta. Proc.*, **110**, 39-58.
- Ishimura, T. (1931). Notes on the titaniferous magnetite deposits of Shaepe-to Chosen. *Tai-hoku Imp. Univ. Faculty of Science, Mem.*, **3**(3), 249-265.
- Kamiyama, M. (1929). Report of a heating experiment on the titaniferous magnetite from Korea. *Journ. Geol. Soc. Tokyo*, **36**, 12-29.
- Osborne, F. F. (1928). Technique of investigation of iron ores. *Econ. Geol.*, **23**, 442-450.
- (1928). Certain magnetic titaniferous iron ores and their origin. *Econ. Geol.*, **23**, 895-922.
- Ramdohr, P. (1926). Beobachtungen an Magnetit, Ilmenit, Eisenglanz und Ueberlegungen über das system FeO Fe_2O_3 TiO_2 . *Neues Jahrb. Min. Geol. Pal.*, **54**, Beil. Bd. Abt. A, 320-379.
- (1953). Ulvöspinel and its significance in the titaniferous iron ores. *Econ. Geol.*, **48**.
- Schwartz, G. M. (1931). Textures due to unmixing of solid solutions. *Econ. Geol.*, **26**, 736-763.
- Schwellnus and Willmsee (1943). Titanium and vanadium in the magnetic iron ores of Bushveld complex. *Trans. Geol. Soc. S. Africa*, **46**.
- Singewald, J. T. (1913). The microstructure of titaniferous magnetites. *Econ. Geol.*, **8**, 207-214.
- Warren, C. H. (1918). On microstructure of certain titaniferous iron ores. *Econ. Geol.*, **13**, 419-446.

Issued January 27, 1955.

STUDIES ON THE NUCLEAR APPARATUS OF PERITRICHOUS CILIATES

PART III. THE NUCLEAR APPARATUS OF *Epistylis* SP.

by C. M. S. DASS, *I.C.I. Research Fellow, N.I.S.I., Department of Zoology, Central College, Bangalore*

(Communicated by B. R. Seshachar, F.N.I.)

(Received July 2 ; read October 20, 1951)

CONTENTS

	<i>Page</i>
Introduction	703
Material and Methods	703
Observations:—	
The vegetative individual	705
Binary fission	705
Conjugation—	
(a) Formation and fusion of conjugants	705
(b) Micronuclear divisions	707
(c) Macronucleus	707
(d) Formation of nuclear anlagen	709
(e) Reorganization fissions	709
(f) Macronuclear fragments	710
Discussion:—	
Nuclear apparatus	710
Binary fission	711
Conjugation	711
Acknowledgement	713
Summary	713
References	714
Explanation of photomicrographs	714
Explanation of text-figures	715

INTRODUCTION

Recent studies on the cytology of Peritrichous ciliates (Colwin, 1944; Dass, 1953, 1954; Finley, 1943, 1952; Seshachar, 1947, 1950; Seshachar and Dass, 1951, 1953*a* and 1953*b*; Seshachar and Srinath, 1947; and Willis, 1948) have revealed a number of interesting features in regard to the structure and behaviour of the nuclear apparatus in vegetative life and during conjugation. The present account is an extension of these studies and relates to an undescribed species of *Epistylis*. The cytological differences between this and *Epistylis articulata* described earlier (Dass, 1953) are so many and so significant that it was felt a complete account of them would not be without interest.

MATERIAL AND METHODS

The colonies of *Epistylis* sp. were collected in the first and second aeration tanks in the activated sludge plant in Madura Mills, Ambasamudram, South India. The colonies of this species are 3–4 mm. high. They are fixed to the substratum by a

Description	<i>Epistylis</i> sp.	<i>Epistylis articulata</i>	<i>Epistylis galea</i> *	<i>Epistylis anastatica</i> *	<i>Epistylis plicatilis</i> *
Habitat ..	Sewage water; attached to any available substratum.	Sewage water; attached to any substratum.	Fresh water; on aquatic plants.	Fresh water; on aquatic plants.	Fresh water; on aquatic plants.
Height of colony ..	3.0-4.0 mm.	1.5-2.0 mm.	1.0 mm.	1-6 mm.	3-0 mm.
Nature of holdfast and zooidendrium.	Disc-like holdfast about 50.0 μ in diameter. Zooidendrium stumpy and attenuate.	Disc-like holdfast about 35.0 μ in diameter. Zooidendrium slender and long.	Nature of holdfast not known. Zooidendrium relatively thick.
Mode of branching (Secondary branch)	Dichotomous ..	Dichotomous ..	Dichotomous ..	Dichotomous ..	Dichotomous ..
Number of individuals in colony	150-200	Many	Many	Many	Many
Dimensions of individuals:—					
Length ..	85-130 μ	60-80 μ	208 μ	89 μ	92-150 μ
Breadth ..	37-80 μ	40 μ
Nature of individuals	Cuticular surface smooth. On contraction does not show any transverse folds posteriorly.	Cuticular surface smooth. Folds appear in the posterior half on contraction.	Cuticular surface smooth. On contraction shows number of transverse folds.	Cuticular surface finely striate transversely. No folds on contraction.	Cuticular surface soft and flexible. Folds appear on contraction.
Special features ..	Microzooids present but there is no specificity in their distribution in colony.	Amaconucleate individuals in the colony. Branches articulate at the base. Bacterial growth on stalks.	Articulation at each bifurcation. Vestibular entrance prominent, projecting laterally in a spout-like manner.	Pedicle smooth. Non-articulate. Secondary branches alternate, equal to or exceeding the length of the zooids.	Body elongate and conical. 3-4 times longer than broad. Pedicle slender, finely striate longitudinally. Zooids of the colony all reach the same level.

* Based on descriptions given by Bhatia, B. L., in 'Fauna of British India, including Ceylon and Burma: Protozoa; Ciliophora', 1936.

disc-like holdfast. The main stalk is short and stumpy while the branches are slender. The branching is dichotomous, but the rhizoids occur at all levels in the colony. Usually 150–200 individuals are found in a colony. Individuals in a colony show variation in dimensions; they are 85.0–130.0 μ in length and 37.0–80.0 μ in breadth. In most cases binary fission is normal and the daughter individuals are similar. Quite frequently, however, the division is unequal and the result is a microzooid which is about a quarter the size of normal individual.

The Table on page 704 gives the major differences between the species of *Epistylis* found in India.

Decaying leaves and other debris bearing the colonies were fixed in bulk in hot Carnoy's fluid (3 parts absolute alcohol and 1 part glacial acetic acid). Colonies were later carefully separated from the leaves and stained in Feulgen and counter-stained in light-green. Some were also stained in haematoxylin, methyl green-pyronin and toluidine blue.

OBSERVATIONS

The Vegetative Individual

The vegetative individual possesses a large cylindrical macronucleus and a small spherical micronucleus. The macronucleus shows a great degree of variation in volume, ranging from 2963 μ^3 to 8820 μ^3 . The volume was calculated by employing the formula $\pi r^2 l$. On the other hand the micronucleus shows hardly any variation in size, the diameter varying from 2.5–3.0 μ . Of the two nuclei, the macronucleus is intensely stained with Feulgen, the micronucleus less so.

There seems to be a tendency for variation in the number of micronuclei in the species. While generally a single micronucleus is present, animals with two, three and four micronuclei were common in many colonies (Pl. XXXI, figs. 3 and 4). Often a whole colony exhibited individuals with multiple micronuclei. Instances where the micronucleus was entirely wanting, were also abundant.

Binary fission

Two types of binary fission are met with. In the first (Pl. XXXI, fig. 5) the macronucleus remains unchanged till the completion of micronuclear division. When the two daughter micronuclei move apart and reach the far sides of the body, the macronucleus orientates across the division plane which starts at the oral end and moves towards the base. The division furrow cuts it into two almost equal halves.

In the second type of binary fission (Pl. XXXI, fig. 6) the macronucleus loses its characteristic form and becomes a dense polymorphic body and by the time the micronuclear division is complete, the macronucleus, caught in the deepening cleavage furrow, becomes cut into two smaller polymorphic bodies. Later, each is drawn out into the cylindrical macronucleus characteristic of the vegetative animal.

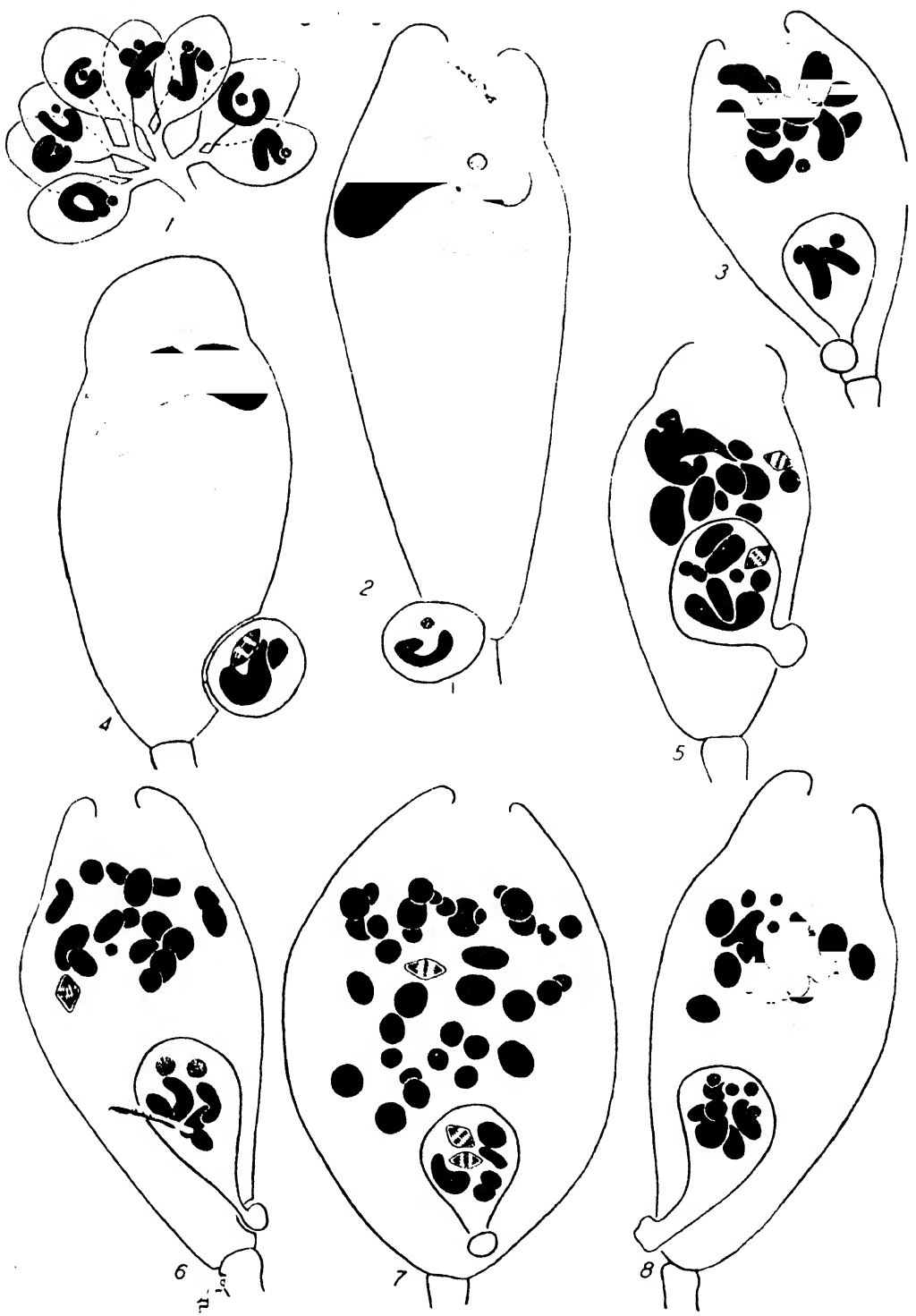
The division of the micronucleus is by mitosis. The different stages are clearly marked out, but as the number of chromosomes is high, a count of them could not be made. The nuclear membrane remains intact throughout division and an intranuclear spindle is formed.

In some instances during binary fission, the division of the cytosome is unequal producing two unequal daughters,—one very large and the other very small (Pl. XXXI, fig. 2). The small one is the microzooid.

Conjugation

(a) *Formation and fusion of conjugants.*

As in all Peritricha, the conjugating animals are of two types—the large attached macroconjugant and the small free-swimming microconjugant. Morphologically,



the macroconjugant resembles the vegetative individual of the colony, and can be distinguished from it only when the microconjugant becomes attached to it.

The microconjugant, however, is strikingly different. It is much smaller in size and is a product of three quick successive divisions of a vegetative animal. Eight such individuals are produced (Text-fig. 1). Each is a microconjugant; it soon acquires a ciliary girdle and moves away in search of a macroconjugant.

The microconjugant, on contact with a macroconjugant, spins on its surface for a while and becomes attached to it. The point of attachment on the macroconjugant is not fixed. In most cases, however, it is at the base of the macroconjugant near the stalk (Text-fig. 2). But there are instances where the microconjugant is found attached near the peristome.

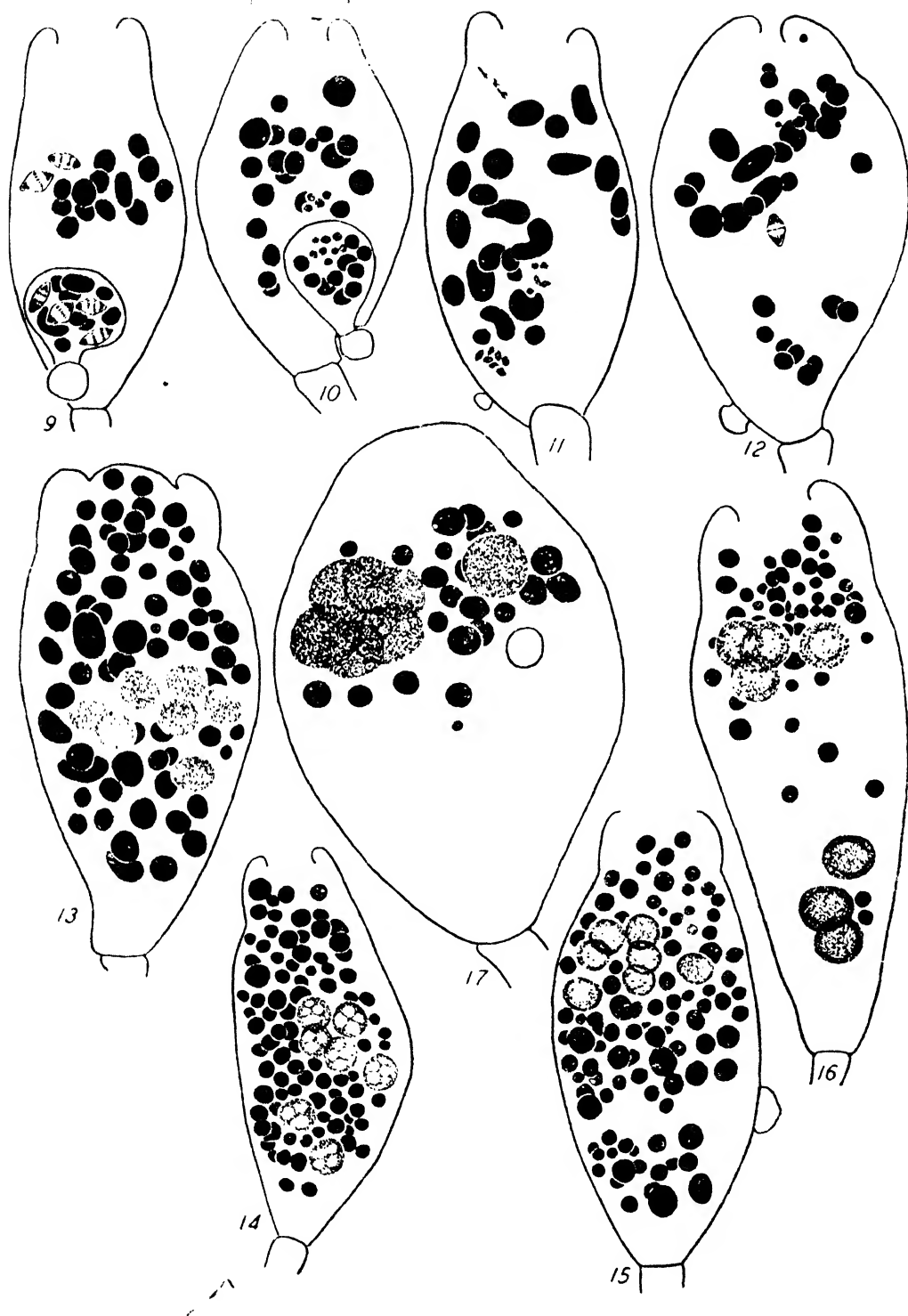
The mode of attachment of the microconjugant to the macroconjugant and the manner in which it obtains its relationship with the latter are of the greatest interest in this species and perhaps unique in the Peritricha. Soon after the microconjugant fixes on to the surface of the macroconjugant, a shallow depression is formed on the latter into which the microconjugant is received (Text-fig. 4). Gradually the depression deepens and the microconjugant is drawn into the body of the macroconjugant. Text-fig. 3 and Pl. XXXI, fig. 7, show this interesting phenomenon clearly. As the microconjugant continues to penetrate deeper, it becomes drawn out into a flask-shaped structure retaining its connection with the exterior by a long neck and terminating, outside at the point of penetration, in a button-like protuberance. For a considerable time, the identity of the two conjugants is clear and one can see the limiting membranes separating the two, but soon, with completion of the micronuclear divisions in the two conjugants, the boundary between them breaks down and all that marks the microconjugant is the button-like protuberance still evident at the point of its entry (Text-fig. 11). Long after the conjugants have fused together to form a synconjugant (Pl. XXXI, fig. 9), the protuberance is visible but in later stages it shrinks in size and drops off.

(b) *Micronuclear divisions.*

The micronuclei of the two conjugants, at the time they meet, are in the resting condition (Text-fig. 3). They start division only after the microconjugant has entered the macroconjugant. In a single instance, it was noticed, the first progamic division of the micronucleus of microconjugant had started and proceeded up to anaphase, even before the depression on the macroconjugant surface was formed (Text-fig. 4). The first division of the micronucleus in both conjugants starts simultaneously and proceeds up to metaphase (Text-fig. 5). At this stage, micronuclear division in the macroconjugant stops, while in the microconjugant it continues, to produce two daughter nuclei (Text-fig. 6). They immediately embark on a second division and when this reaches metaphase, the division process is resumed in the macroconjugant (Text-fig. 7). Thus the second progamic division of the micronucleus in the microconjugant and the first progamic division of the micronucleus of macroconjugant are completed simultaneously (Text-fig. 8). There are now four micronuclear products in the microconjugant and two in the macroconjugant. Another division is completed in both conjugants (Text-fig. 9), resulting in the production of eight progamic nuclei in the microconjugant and four in the macroconjugant (Text-fig. 10). Of the progamic nuclei only one in each conjugant differentiates into the pronucleus. At this stage the boundary between the two conjugants is lost and the protoplasts of the two conjugants merge into each other (Text-fig. 11).

(c) *Macronucleus.*

As in other Peritricha, the macronucleus of both conjugants breaks up during conjugation. The relatively smaller macronucleus of the microconjugant fragments



earlier to give rise to a number of spherical bodies. That of the macroconjugant is thrown into a long and complicated skein (Text-fig. 8) before it breaks up into fragments.

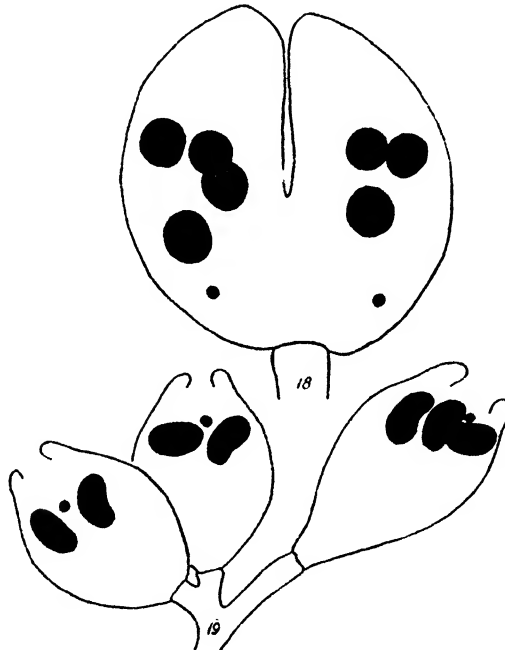
(d) *Formation of nuclear anlagen.*

With dissolution of the membranes separating the conjugants, the cytoplasm as well as the nuclear components merge. The fused body is referred to as synconjugant. The pronuclei of the two conjugants now fuse and form the synkaryon. The residual progamic nuclei of both conjugants are absorbed in the cytoplasm.

The synkaryon migrates towards the centre of the synconjugant and immediately starts dividing (Text-fig. 12). It divides thrice successively to give rise to eight metagamic nuclei. One of these remains small; this is the future micronucleus. The other seven metagamic nuclei gradually increase in size; these are the macronuclear anlagen. At first the macronuclear anlagen are faintly stained (Text-fig. 13). Soon they acquire basophilia and stain deeply in all nuclear stains. Meanwhile a number of Feulgen negative areas appear in each anlage (Text-fig. 14). These later coalesce to form a central faintly stained zone and a peripheral deeply stained region (Text-fig. 15). The macronuclear anlagen progressively increase in size and become uniformly deeply stained (Text-figs. 16 and 17).

(e) *Reorganization fissions.*

At the first reorganization fission of the synconjugant the macronuclear anlagen are intensely stained bodies (Text-fig. 17). The first fission separates the seven anlagen into two groups of four and three (Pl. XXXI, fig. 11; Text-fig. 18). Thus the two F1 individuals have four and three anlagen respectively. Each passes through two more fissions; thus at the end of three divisions all daughters possess the normal complement of the nuclear apparatus, a macronucleus and a micronucleus. At the end of reorganization fissions, the macronucleus becomes drawn out into the characteristic cylindrical form.



(f) *Macronuclear fragments.*

With fusion of the two conjugants, the cytosome of the synconjugant is filled with fragments of the old macronucleus of both conjugants (Pl. XXXI, fig. 8; Text-fig. 13). They vary from $2\ \mu$ to $5\ \mu$ in diameter.

As the macronuclear anlagen become differentiated, a gradual diminution in the number of macronuclear fragments is noticed (Pl. XXXI, figs. 9 and 10; Text-figs. 16 and 17). At first the smaller fragments are absorbed in the cytoplasm. Gradually however, as nucleination of the anlagen progresses, absorption of the fragments also becomes more rapid. By the first reorganization fission, the cytosome is practically free from macronuclear fragments (Text-fig. 18). During reorganization fissions, no macronuclear fragments occur in the cytosome.

DISCUSSION

Nuclear apparatus

The nuclear apparatus of *Epistylis* sp. generally resembles that of other Peritricha in the possession of a macronucleus which is cylindrical and bent, and a micronucleus which is spherical. The macronucleus in this species is uniformly stained at all stages unlike other forms, viz. *Zoothamnium alternans* (Fauré-Fremiet, 1930), *Vorticella microstoma* (Finley, 1943), *Epistylis articulata* (Dass, 1953) and *Carchesium spectabile* (Dass, 1954), where during certain phases of life-history a number of Foulgon negative spaces, considered equivalent to metazoan nucleoli, are seen. Another striking feature of the macronucleus in vegetative state is the great variation in its volume. In many species of Peritricha, a certain amount of variation has been noticed but it is in *Epistylis* sp. that I have found this variation highest. As observed earlier, in some instances the macronucleus is so small that its volume is about $2963\ \mu^3$ while in others it is nearly thrice as much, i.e., $8820\ \mu^3$. It has also been noticed that the macronucleus has a minimum volume immediately after binary fission and continues to grow during vegetative life. Apart from the actual mode of increase in size, which is itself a phenomenon of great interest, the origin of the most important constituent of the macronucleus, i.e., desoxyribose nucleic acid (DNA), requires an explanation. It is not clear what this origin is. It must come from two sources: (a) from the cytoplasm by a conversion of its ribose nucleotides into those of the desoxyribose type, (b) a *de novo* synthesis of DNA in the nucleus. Only future work on the biosynthesis of the nucleic acids would help determine this origin.

Multimicronucleate individuals occur so frequently in this species that a possible explanation of their origin would not be out of place. Whole colonies of bi-, tri- and tetra-micronucleate animals would probably result from the initial swarmer (which originates the new colony) being also in this condition. But the origin of such a swarmer would itself be interesting. My observations of large numbers of colonies indicate that an upset of binary fission during swarmer formation is responsible for the multimicronucleate condition, though it may also happen during reorganization fissions. It was noticed in *E. articulata* that sometimes, instead of one out of eight metagamic nuclei, two become the micronuclei, so that the race of animals produced from such stocks displays a bimicronucleate condition. However, this occurs so rarely in *E. articulata* that it is not considered as the possible cause of bimicronucleate condition. On the other hand, in *Epistylis* sp. it seems more likely that an upset of binary fission is the cause. I have noticed a number of instances where the two division products of the micronucleus are included, during binary fission, in one daughter cell so that it becomes bimicronucleate, while its sister lacks the micronucleus altogether. Curiously, in my material, amicronucleate animals also are quite plentiful and it seems this explanation would fit the observed facts.



Amicronucleate animals do not seem to show any abnormalities and obviously are none the worse for their deficiency; they appear to carry on their vegetative activities normally, an observation which is in consonance with that of Sonnerborn (1947) in *Paramecium*.

Binary fission

The two types of binary fission observed in this form have also been recorded in two other peritrichous ciliates, viz., *E. articulata* (Dass, 1953) and *Carchesium spectabile* (Dass, 1954). In *E. articulata* the macronucleus becomes condensed into a deeply staining polymorphic mass which puts out a number of filamentar processes into the cytoplasm. Such an observation has not been made in any other peritrichous ciliate. The filamentar processes given off from the macronuclear mass seem to indicate an intimate relationship between the macronucleus and the cytoplasm, especially during binary fission.

Conjugation

An analysis of the methods of production of conjugants in the order Peritricha is interesting. It is seen that in all solitary forms like *Vorticella*, *Lagenophrys*, *Trichodina* and *Urceolaria*, etc., the conjugants are produced by unequal fission of a vegetative individual, resulting in two dissimilar cells; the smaller is the microconjugant, the larger is the macroconjugant. On the other hand, in colonial forms like *Epistylis*, *Carchesium* and *Zoothamnium*, the microconjugants are produced by three rapid successive divisions of a vegetative individual, while the macroconjugant is a vegetative individual which has perhaps undergone a physiological transformation. The significance of this difference in microconjugant formation seems difficult to determine at present, but that it is in some manner related to colonial organization in the group, seems possible.

Perhaps the most interesting feature of conjugation in *Epistylis* sp. a feature in which it differs from other Peritricha refers to the behaviour of the microconjugant during the process. In most Peritricha, the microconjugant, which is always small and free-swimming, fixes itself to the body of the macroconjugant. At first the boundary line between the two conjugants is clear but with the progress of conjugation, this boundary is lost and the two conjugants merge into each other as a synconjugant. In *Epistylis* sp., however, the microconjugant, soon after its attachment to the macroconjugant, sends into the latter a tubular prolongation carrying the nuclear elements. This projection is often quite deep and penetrates into the cytoplasm of the macroconjugant to a considerable extent. All the while it retains its individuality and its connection with the exterior by a small button-like plug, which marks the point of entry of the microconjugant. It is only much later that the boundary line between the two conjugants breaks down and the two merge into each other. Such a behaviour of the microconjugant is unknown in any peritrichous ciliate and perhaps marks a highly specialized condition.

The behaviour of the two parts of the nuclear apparatus during conjugation is full of interest. It is profitable to discuss the entities,—the micronucleus and macronucleus—separately.

(a) Micronucleus.

With the first descriptions of micronuclear divisions in the two conjugants by Maupas (1888) and Popoff (1908) the interest in these divisions has accumulated and now it has been established that in all the Peritricha, so far examined, the number of micronuclear divisions differs between the two conjugants, being three in the micro-conjugant and two in the macro-conjugant (Finley, 1943; Dass, 1953, 1954). The homology between these divisions in the two conjugants on the one hand, and,

between them and the meiotic divisions in the higher animals on the other, is a subject of great interest and efforts have been directed towards determining it. I have discussed this subject at some length in an earlier paper (Dass, 1953) but it might not be out of place to mention here that the disparity in the number of divisions of the two conjugants is due essentially to their duration. The first division in the macroconjugant is particularly long drawn out and takes nearly as much time as is required for first two divisions in the micro-conjugant. Why it should be so, I am unable to explain at present.

(b) *Macronucleus.*

Till recently, the macronucleus was regarded as a body with no special rôle to play during conjugation and destined to degenerate during the process. With recognition of the fact that it contains large amounts of DNA, it became necessary to account for the absorption of this material and also assess the significance of such absorption. It did not appear that the older views, which regarded the phenomenon as equivalent to throwing off into the cytoplasm of waste products which had accumulated in the nucleus during vegetative life, explained the significance of the process adequately. Instances of the nucleus accumulating waste and effete substances have never been reported in any animal. Content with the observation that the macronucleus 'degenerated' and its products were 'absorbed' in the cytoplasm, no further attention was paid to it. Turner (1941) says, 'Until recently the behaviour of the macronucleus in conjugation has been given scant attention. The disintegration of the old macronucleus and the differentiation, number and distribution of a new macronuclear anlagen have been noted, but no great significance has been attached to these processes. It seems probable that more intensive investigation of the rôle of macronucleus in conjugation will be extremely profitable.' It seems possible to examine, in the light of more recent advances in our knowledge of cell structure, the significance of this breaking up of the macronucleus and its absorption. It is well known that the macronucleus of all ciliates contains large amounts of DNA. The work of Roskin and Ginsberg (1944*a* and *b*), Moses (1950) and more recently of Seshachar (1953) has shown that there is probably some RNA also in it. The dissolution of this body in the cytoplasm at every conjugation must involve far-reaching changes in cytoplasmic nucleotides. It has been noticed that the method of this dissolution offers a clue to the process. In *E. articulata* Seshachar and Dass (1953) have noticed that the macronucleus breaks up into a number of spherical fragments in each of which, later, a conversion of DNA into RNA appears to take place. The view was therefore developed that in this ciliate the dissolution of macronucleus was a process by which its DNA was converted first into RNA and was later distributed in the cytoplasm. More recently additional evidence for the same phenomenon has been provided in another ciliate, *Chilodonella*, by Seshachar (1953) who, examining the macronucleus in different stages of the life-history, by the application of metachromatic dyes, has found a gradual accumulation, in the degenerating macronucleus, of metachromatic material, which has been identified as RNA, and a later release of this RNA into the cytoplasm. While it is not claimed that the last word on this subject has been said, it seems highly possible that the degeneration of the macronucleus during conjugation involves essentially a conversion of DNA into RNA in it, and its breaking up, a distribution of the accumulated RNA in the cytoplasm. In *Epistylis* sp. evidence of such a conversion of DNA to RNA in the macronuclear fragments are not as striking as in *E. articulata* or in the degenerating macronucleus of *Chilodonella uncinatus*, but the gradual reduction in numbers of the macronuclear fragments would lead me to believe that an essentially similar change is taking place here also.

There is an interesting relationship, too, between the dissolution of fragments of the old macronucleus and the development of new macronuclear anlagen after

Conjugation. It is well known that both the micronucleus and the macronucleus are developed in the exconjugant from the synkaryon and its products and while the micronuclear anlage remains as a small body, the macronuclear rudiment enlarges in size and synthesizes the DNA so characteristic of it. The origin of this large amount of DNA, especially in *Epistylis* sp. where the macronucleus is large and subject to considerable variation, remains to be determined. In this connection there is an interesting and undeniable correlation between the development and nucleination of macronuclear anlagen and the absorption of fragments of the old macronucleus. Previous work by Seshachar and Dass (1951) in *Vorticella convallaria*, by Dass (1953, 1954) in *E. articulata* and *C. spectabile* and Seshachar (1950, 1953) in *Chilodonella uncinatus* has shown indications of an association between the two phenomena. As the old macronucleus and its fragments are absorbed, the new macronuclear anlagen appear to acquire DNA. This was especially striking in *C. spectabile* where a very close and unmistakable co-ordination existed between the two phenomena. Where the rate of nucleination of the anlagen was rapid, the dissolution and absorption of the fragments were also rapid; where it was slow or delayed, the absorption of the fragments was also delayed. Clearly there seemed support for the idea developed by Seshachar (1947) that the DNA of the old macronucleus was reinstated and restored on a new frame-work (see Glass, 1949).

ACKNOWLEDGEMENTS

My grateful thanks are due to Dr. B. R. Seshachar for guidance and encouragement. I am deeply thankful to the National Institute of Sciences of India for the award of I.C.I. (India) Research Fellowship which provided me the opportunity for this study. I am also thankful to the management of the Madura Mills, Ambasamudram, for kindly permitting me to collect material from their factory premises and to Mr. M. M. Veerabhadraiah who helped me in the preparation of the photomicrographs.

SUMMARY

The nuclear apparatus of *Epistylis* sp. consists of a cylindrical macronucleus and a spherical micronucleus.

The macronucleus exhibits a considerable variation in volume during vegetative life.

During binary fission generally, the macronucleus does not lose its form. It just stretches across the division plane and becomes cut into two. But in some instances the macronucleus becomes consolidated into a polymorphic mass often sending out into the cytoplasm filamentary processes. In either case the micronuclear division is by mitosis.

Normally a single micronucleus is found in each individual. But in some individuals in a colony or in whole colonies, two, three and four micronuclei are found.

Conjugation is between dissimilar organisms,—a small microconjugant which is free-swimming, and a large fixed macroconjugant.

The microconjugant becomes attached to the macroconjugant and makes its way into the macroconjugant, the point of entry being marked by a small plug, which however, drops off later.

For a considerable time after its entry into the macroconjugant, the microconjugant appears discrete but soon after the formation of pronuclei the boundary between the two conjugants is lost and the two merge to produce a synconjugant.

The micronucleus of microconjugant undergoes three divisions while that of macroconjugant passes through only two divisions. A single progame nucleus in each conjugant becomes the pronucleus and the two fuse to form synkaryon.

The synkaryon divides thrice to form eight metagamic nuclei. Of these, seven differentiate as macronuclear anlagen and the eighth is the micronuclear anlage.

The macronucleus of both conjugants fragments during conjugation. The cytosome of synconjugant becomes filled with these fragments.

The macronuclear fragments are absorbed slowly at first and more rapidly later. There seems to be a distinct correlation between the nucleination of the macronuclear anlagen and the absorption of macronuclear fragments. By the first reorganization fission the cytosome of synconjugant is free from macronuclear fragments. The nucleination of the anlagen also appears complete.

After three reorganization fissions each daughter individual possesses the normal complement of nuclear apparatus—a macronucleus and a micronucleus.

REFERENCES

- Colwin, L. H. (1944). Binary fission and conjugation in *Urceolaria synaptae* (?) Type II (Protozoa, Ciliata) with special reference to the nuclear phenomena. *J. Morph.*, **75**, 203-249.
- Dass, C. M. S. (1953). Studies on the nuclear apparatus of Peritrichous ciliates. Part I. The Nuclear apparatus of *Epistylis articulata* (From.). *Proc. Nat. Inst. Sci.*, **19**, 389-404.
- (1954). Studies on the nuclear apparatus of Peritrichous ciliates. Part II. The Nuclear apparatus of *Carchesium spectabile* Ehrbg. *Proc. Nat. Inst. Sci.*, **20**, 174-186.
- Fauré-Fremiet, E. (1930). Growth and differentiation of the colonies of *Zoothamnium arbuscula* (Clap. and Lachm.). *Biol. Bull.*, **58**, 28-51.
- Finley, H. E. (1943). The conjugation of *Vorticella microstoma*. *Trans. Amer. Micro. Soc.*, **52**, 97-121.
- (1952). Sexual differentiation in Peritrichous ciliates. *J. Morph.*, **91**, 569-605.
- Glass, B. (1949). Survey of Biological Progress. 15-37, Academic Press Inc., New York, N.Y.
- Maupas, E. (1888). Recherches experimentales sur la multiplication des Infusoires cilies. *Arch. zool. exp. et gen.*, **6**, 165-277.
- Moses, M. J. (1950). Nucleic acids and proteins of the nuclei of *Paramecium*. *J. Morph.*, **87**, 493-536.
- Popoff, M. (1908). Die Gametenbildung und die Conjugation von *Carchesium polypinum* L. *Zeitschr. f. Wiss. Zool.*, **89**, 478-524.
- Roskin, G. I. and Ginsberg, A. S. (1914a). Zymonucleic acid of the Protozoic cell. *Comp. Rend. de l'Acad. Sci., U.R.S.S.*, **42**, 348-351.
- (1944b). Basophilic protoplasm in Protozoa as connected with the occurrence in the cell of Zymonucleic acid. *Ibid.*, **43**, 122-125.
- Seshachar, B. R. (1947). Chromatin elimination and the ciliate macronucleus. *Amer. Nat.*, **81**, 316-319.
- (1950). The nucleus and nucleic acids of *Chilodonella uncinatus* Ehrbg. *J. Exp. Zool.*, **114**, 517-544.
- (1953). Metachromasy of the ciliate macronucleus. *Ibid.*, **124**, 117-130.
- Seshachar, B. R. and Dass, C. M. S. (1951). The macronucleus of *Vorticella convallaria* Linn. during conjugation. *J. Morph.*, **89**, 187-198.
- (1953a). Macronuclear regeneration in *Epistylis articulata*. *Q.J.M.S.*, **94**, 185-192.
- (1953b). Evidence for the conversion of Desoxyribonucleic acid (DNA) to Ribonucleic acid (RNA) in *Epistylis articulata* From. (Ciliata: Peritricha). *Expt. Cell Res.*, **5**, 248-250.
- Seshachar, B. R. and Srinath, K. V. (1947). The ciliate macronucleus. *Curr. Sci.*, **16**, 83-84.
- Willis, A. G. (1948). Studies on *Lagenophrys tattersalli* (Ciliata, Peritricha, Vorticellinae). Part II. Observations on bionomics, conjugation and apparent endomixis. *Q.J.M.S.*, **89**, 385-400.

EXPLANATION OF PHOTOMICROGRAPHS

Key to lettering:—

M Macronucleus; *m* Micronucleus; *Mc* Macroconjugant; *mc* = Microconjugant; *Rmc* = Residual microconjugant; *M.4* = Macronuclear anlagen; *Mf* = Macronuclear fragments.

PLATE XXXI

- FIG. 1. General picture of the colony. $\times 48$. Feulgen-light green.
- FIG. 2. Individuals of the colony enlarged, showing a large individual and its small sister produced as a result of unequal division of cytosome. $\times 560$. Feulgen-light green.
- FIG. 3. Individual with two micronuclei. $\times 625$. Feulgen-light green.
- FIG. 4. Individual with four micronuclei. $\times 625$. Feulgen-light green.
- FIG. 5. Binary fission Type I. $\times 560$. Feulgen-light green.
- FIG. 6. Binary fission Type II. $\times 560$. Feulgen-light green.
- FIG. 7. Conjugation. The microconjugant is lodged in the macroconjugant. The microconjugant plug is clearly seen. The macronucleus of macroconjugant fragmenting. $\times 560$. Feulgen-light green.
- FIG. 8. Early syncyconjugant. The macronuclear anlagen not yet differentiated. $\times 560$. Feulgen-light green.
- FIG. 9. Late syncyconjugant. Persistent microconjugant plug is seen. $\times 560$. Feulgen-light green.
- FIG. 10. Late syncyconjugant. The macronuclear anlagen have reached maximum size and nucleination is in progress. Note the smaller number of macronuclear fragments. $\times 560$. Feulgen-light green.
- FIG. 11. Individual of F_1 generation showing three macronuclear anlagen. Note the complete absence of macronuclear fragments. $\times 560$. Feulgen-light green.

EXPLANATION OF TEXT-FIGURES

1. Bunch of microconjugants. $\times 1750$. Feulgen-light green.
2. Conjugation. The microconjugant has just come in contact with the macroconjugant. $\times 1750$. Feulgen-light green.
3. Conjugation. The microconjugant has penetrated deeply into the body of the macroconjugant. The microconjugant plug is seen near the stalk. The micronucleus in both conjugants is in resting stage. $\times 1750$. Feulgen-light green.
4. Conjugation. The microconjugant lodged in depression on the macroconjugant. The micronucleus of microconjugant in late anaphase of first progamic division. $\times 1750$. Feulgen-light green.
5. Conjugation. The micronucleus of both conjugants in first progamic metaphase. The macronucleus in both conjugants is fragmenting. $\times 1750$. Feulgen-light green.
6. Conjugation. The micronucleus of microconjugant has completed the first progamic division, while that in macroconjugant is still in metaphase. $\times 1750$. Feulgen-light green.
7. Conjugation. The micronucleus of microconjugant is in second progamic division metaphase, while the micronucleus of macroconjugant is still in first progamic division metaphase. $\times 1750$. Feulgen-light green.
8. Conjugation. The micronucleus of microconjugant has completed second progamic division, while that in macroconjugant has completed first progamic division. $\times 1750$. Feulgen-light green.
9. Conjugation. The third progamic division is in progress in microconjugant, while the second progamic division is in progress in macroconjugant. $\times 1750$. Feulgen-light green.
10. Conjugation. Progamic divisions are complete in both conjugants. Four progamic nuclei are seen in macroconjugant and eight progamic nuclei in microconjugant. $\times 1750$. Feulgen-light green.
11. Synconjugant. The two conjugants have completely merged with each other. The two pronuclei are about to fuse. The residual progamic nuclei of microconjugant are all in one group. The microconjugant plug is still seen on the surface. $\times 1750$. Feulgen-light green.
12. Synconjugant. First metagamic division of synkaryon in progress. The residual progamic nuclei are already absorbed in cytoplasm. $\times 1750$. Feulgen-light green.
13. Synconjugant. The metagamic divisions are complete. The seven macronuclear anlagen are differentiated and are faintly stained. The micronucleus stippled. The cytosome is filled with macronuclear fragments. Microconjugant plug has dropped out. $\times 1750$. Feulgen-light green.
14. Synconjugant. The macronuclear anlagen increasing in size. Nucleination of anlagen has started. Note the Feulgen negative spaces in the anlagen. $\times 1750$. Feulgen-light green.
15. Synconjugant. The Feulgen negative spaces in each macronuclear anlage have merged to form a single central area with a Feulgen positive rim. Microconjugant plug persistent. $\times 1750$. Feulgen-light green.
16. Synconjugant. The macronuclear anlagen have increased in size. With the centripetal nucleination of each anlage, the central Feulgen negative zone has become smaller. The number of macronuclear fragments is greatly reduced. $\times 1750$. Feulgen-light green.
17. Synconjugant. The macronuclear anlagen have reached maximum size. The nucleination is almost complete. Feulgen negative spaces are no longer seen. A few macronuclear fragments present in cytosome. Microconjugant plug persistent. $\times 1750$. Feulgen-light green.
18. First reorganization fission in progress. Four macronuclear anlagen in one daughter and the other three in the other daughter. No macronuclear fragments in the cytosome. $\times 1750$. Feulgen-light green.
19. Second reorganization fission complete in one cell while the other is still in F_1 condition. $\times 1750$. Feulgen-light green.

